BRISBANE, AUSTRALIA
AND ONLINE
23 – 25 JUNE 2021

# MILL OPERATORS CONFERENCE 2021

## Conference Proceedings

Sponsored By

MAGOTTEAUX

# 15TH AUSTRALASIAN MILL OPERATORS CONFERENCE 2021

**23–25 JUNE 2021**
**BRISBANE, AUSTRALIA AND ONLINE**

The Australasian Institute of Mining and Metallurgy
Publication Series No 3/2021

Published by:
The Australasian Institute of Mining and Metallurgy
Ground Floor, 204 Lygon Street, Carlton Victoria 3053, Australia

All papers published in this volume were peer reviewed before publication.



ISBN 978-1-925100-98-3

# ORGANISING COMMITTEE

Katie Barns MAusIMM
*Conference Organising Committee Co-Chair*

David Seaman MAusIMM
*Conference Organising Committee Co-Chair*

Rob Coleman MAusIMM

Diana Drinkwater FAusIMM

Stuart Emery MAusIMM

Aidan Giblett FAusIMM(CP)

Bianca Newcombe MAusIMM

Andrew Newell MAusIMM(CP)

# AUSIMM

Kirsty Grimwade
*Head of Events, Industry Relationships and Operational Projects*

Kate Haralam
*Manager, Events*

Amelia Lundstrom
*Coordinator, Events*

# REVIEWERS

We would like to thank the following people for their contribution towards enhancing the quality of the papers included in this volume:

Sibasis Acharya FAusIMM

Peter Allen MAusIMM(CP)

Katie Barns MAusIMM

Duncan Bennett FAusIMM

Rob Coleman MAusIMM

Peter Colvin MAusIMM(CP)

Adrian Dance FAusIMM

Diana Drinkwater FAusIMM

Stuart Emery MAusIMM

Dieter Engelhardt MAusIMM

Aidan Giblett FAusIMM(CP)

Paul Griffin FAusIMM

Steven Hart FAusIMM

Bill Johnson

Fred Kock FAusIMM

Ray Koenig FAusIMM(CP)

Mike Larson

Virginia Lawson FAusIMM

Vanessa Liebezeit

Suzy Lynch-Watson

Karen McCaffery FAusIMM(CP)

Andrew Millar MAusIMM(CP)

Ben Murphy MAusIMM(CP)

Bianca Newcombe MAusIMM

Andrew Newell MAusIMM(CP)

Mark O'Dwyer

Joe Pease FAusIMM

Kym Runge

David Seaman MAusIMM

Bill Staunton FAusIMM

Maedeh Tayebi MAusIMM

Francois Vos

# FOREWORD

On behalf of the AusIMM, the Metallurgical Society of the AusIMM (MetSoc), and this year's organising committee, we have great pleasure in welcoming our delegates, sponsors, exhibitors, presenters and supporters to, this, the slightly delayed 15th Mill Operators Conference. Inaugurated in Mt Isa in 1978, the Mill Operators Conference aims to once again promote the sharing of knowledge in operating practices for mineral processing plants, including extractive metallurgy, process control and environmental issues.

When the organising committee started planning this conference shortly after the conclusion of the conference series' 40-year celebrations in 2018, none of us could have imagined how the next three years would unfold. Apart from the obvious postponement of the Mill Operators Conference, originally due to be held in September 2020, the arrival of Covid-19 into our lives has fundamentally changed the way we live, work, and operate on many levels. We have not only been separated from family and friends but also from colleagues and mentors. Companies and individuals have had to suddenly find new ways to work and connect while safe-guarding and ensuring the viability of their businesses and livelihoods. Many of us have been stuck in remote locations, experienced vastly changed working conditions and spent long periods in quarantine and isolation. While in Australia we have been largely insulated from many of the devastating effects of this global pandemic, our industry is not defined by geographical boundaries and so globally it has affected us all.

This conference, like so many aspects of our industry, has had to constantly evolve. So, while we expect that the 'in-person' attendees to this conference will be limited to those from Australia and, at this stage, New Zealand, the continued closure of international and intermittent closures of state borders has seen this AusIMM conference series move to a hybrid format. As we write this foreword three weeks out from our opening remarks, Melbourne remains in lock down and we wait to see if our Victorian colleagues will join us at the end of June.

Some reports have compared our current feelings of isolation as grief for our loss of connection to our communities. We hope this conference will help us overcome this by providing in person and online opportunities for plant operators, metallurgists, engineers, and suppliers to learn, share and network with others in the minerals industry. The technology advances over the decades have changed the way our industry operates, and it is some of these changes that now give us the opportunity to interact in new ways where we otherwise couldn't. We challenge you to find and take these opportunities, whether through conferences such as Mill Operators 2021 or other development opportunities.

In these unprecedented times we cannot begin to thank our sponsors and exhibitors enough for the support they have given the conference. The faith you have put in the conference is always appreciated and it is your support that has made this conference possible. Collaboration, now as much as ever, is fundamental to our industry and we would encourage you to take the time to visit booths, physical and virtual, talk with our exhibitors, and find out about changes in technology, what is available in our industry and what they can do for your operation.

In contrast to previous years, the committee decided that it was unnecessary to specify a theme for this conference. As we all know, the Mill Operators Conference is a place where the latest technologies, best practices, and plant updates are shared by and amongst those that operate minerals processing plants. The term 'Mill Operators' includes the many non-site or mining company employees that all play a part in contributing to the success of our minerals industry (vendors, technology providers, universities, and engineering firms to name a few).

For the preparation of this conference in 2020 we received close to 100 abstract submissions. With the conference postponement we gave our presenters the opportunity to withdraw their papers, however, not only did they all stick with us, but many updated their data and fine-tuned their papers to ensure that what you will experience during the conference is the very latest in developments. While not all of the proposed papers could be included in the program, we are confident that with the assistance and generous support of many peer reviewers the committee has been able to deliver a program that, over the next three days, captures the best of our industry. Our thanks also go to J-P Franzidis who ran our inaugural paper writing program for this conference.

Thank you to all the committee members who have each taken on their share of responsibility to make this event what it is. Thank you also to the AusIMM staff whose professional expertise and hard work is unfailing, especially given the challenges of operating in a global pandemic. It is this group of professionals who pull the conference together and make it the success that it has become. Without their expertise the Mill Operators conferences could never exist.

With the assistance of so many, the committee has pulled together a program that we hope inspires, educates and assists in the development of our industry. We commend this volume to your bookshelf and digital storage and trust it will become a valuable resource for years to come.

Yours faithfully,

Katie Barns MAusIMM and David Seaman MAusIMM

Mill Operators Conference 2021 Organising Committee Co-Chairs

# SPONSORS

## Platinum Sponsors

## Gold Sponsors

## Premier Content Sponsor

## Conference App Sponsor

## Conference Proceedings Sponsor

## Name Badge and Lanyards Sponsor

## Technical Session Sponsors

**Conference Dinner Sponsor**

**Welcome Reception Sponsor**

**Networking Hour Sponsor**

**Coffee Cart Sponsor**

**Lunch Sponsors**

**Note Pads and Pens Sponsor**

# CONTENTS

## Comminution



## Flotation

## Plant operations



## Process automation



## Process modelling and improvement

# Comminution

# Coarse vertical stirred mill applications

*G R Ballantyne[1], B Foggiatto[2], P Staples[3] and G Lane[4]*

1. Director Technical Solutions, Ausenco, Brisbane. Email: grant.ballantyne@ausenco.com
2. Senior Process Engineering Specialist, Ausenco, Vancouver.
3. VP and Global Practice Lead, Minerals and Metals, Ausenco, Vancouver.
4. Chief Technical Officer, Ausenco, Brisbane.

## ABSTRACT

Vertical stirred mills are more frequently being applied at coarser grinding duties as a replacement for ball milling. This trend is being driven by reductions in footprint and operating costs such as power and media consumption that counter the increased capital cost. Vertical stirred mills have been reported to use up to 40 per cent less energy (decreasing to 20 per cent for coarser applications $P_{80}$>200 µm) and 20 per cent less media than equivalent ball mills. However, this reduction is difficult to validate in operations as there is a tendency for these circuits to create a sharper product size distribution, and the evaluation techniques typically use $P_{80}$ figures. Although benefits are well established in regrind and tertiary duties, they have not been clearly proven in coarser applications following autogenous (AG) or semi-autogenous (SAG) mills and high-pressure grinding rolls (HPGR). This paper brings together data from three operating sites to better evaluate the performance of vertical stirred mills in coarse duties.

There are many applications where vertical stirred mills have been installed in coarse duties. Morenci conducted a long-term trial of a VertiMill™ (VTM) in secondary duty following an HPGR closed with an 8 mm wet screen. Boungou has recently commissioned a milling circuit with VTM following a SAG mill closed with a 6 mm scalping screen. Tambomayo has an open circuit VTM following a single stage SAG circuit closed with hydrocyclones. Cannington has employed a VTM in closed circuit following a single stage AG mill circuit. Finally, Cadia, New Afton, Chino and Raglan have employed VTMs in a tertiary application to debottleneck the ball mills and stabilise the float feed by providing a dampening effect to process variability. The efficiencies of these plants are evaluated to better define when and where VTMs are best employed.

## INTRODUCTION

Vertical stirred media mills were first introduced to the mining industry in the 1950s (Lynch and Rowland, 2005). They use a low-speed helical screw to agitate the media, which together with the compression caused by the weight of the media above induces particle breakage. There are two main suppliers of low speed vertical stirred mills: Eirich which produces the TowerMill® and Metso:Outotec which produces the VertiMill™ (VTM). This paper will focus predominately on the VTM but the conclusions should be the same, independent of the vendor, so both designs are illustrated in Figure 1.

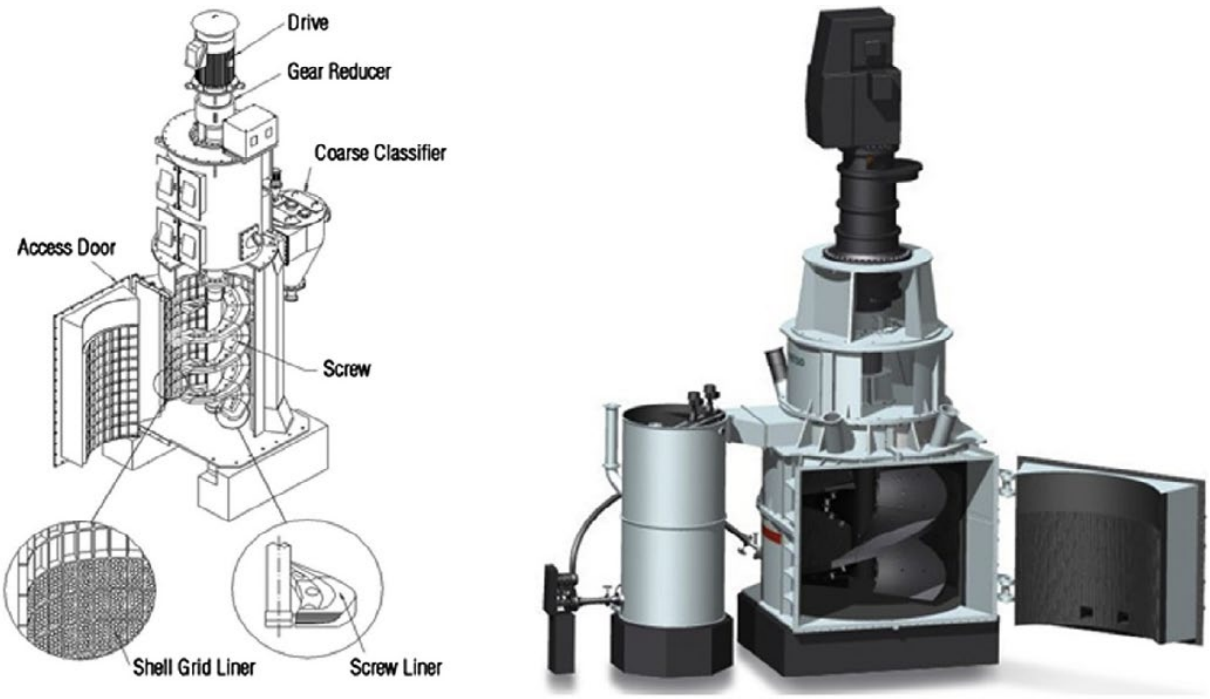


TowerMill®                Vertimill™

**FIG 1** – TowerMill® (courtesy of Eirich) and Vertimill™ (courtesy of Metso:Outotec) (Mazzinghy *et al,* 2015).

Huang *et al* (2019) collated the performance of many industrial and pilot-scale VTMs to assess the efficiency of these mills in comparison to the Bond ball milling work index (BBWi). The specific power draw of the VTMs were found to be higher than that calculated using the Bond method resulting in a efficiency factors below 100 per cent (Figure 2). The efficiency factor reduces linearly with the mill feed size $F_{80}$, which was be attributed to increased grinding efficiency of the small media used in a vertical stirred mill when processing finer feed size distributions.

Arguably, comparison between a ball mill and a VTM is only valid when the media size distributions are similar, and the ball mill lifters are removed. Two of the issues with using a Bond mill as a benchmark is that the media is not selected for regrind duties and the Bond mill has lifters installed (Levin, 1992; Tian *et al*, 2018).

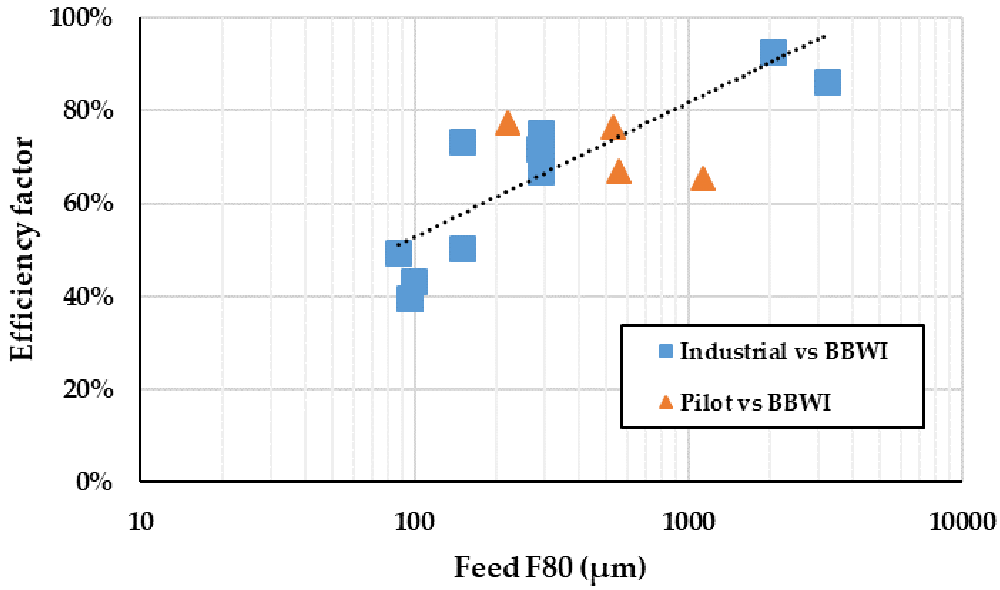


**FIG 2** – Relationship between feed size ($F_{80}$) and Bond efficiency factor (Huang *et al*, 2019).

Mazzinghy *et al* (2015) used breakage parameters from a conventional batch ball mill to develop a population balance model of a pilot scale VTM in closed circuit with a high frequency screen. The batch ball milling tests were conducted using the same ball size distribution as the pilot scale VTM. However, it was not clear whether the lifters were removed which may be responsible for a change in efficiency. The sample feed sizes ranged from an $F_{80}$ of 2 mm down to 80 μm. The media size distributions in the pilot mill were chosen based on Metso:Outotec's experience to ensure larger balls (35 mm) were available to break the coarser particles in the feed (6 mm). The result of the investigation was that breakage rate in the VTM was consistently 1.35 times higher than the bench scale ball mill (Mazzinghy *et al*, 2015). This equates to an effective efficiency factor of 74 per cent, but this was found to be feed size independent when the media size was correspondingly altered. The paper also indicated that the breakage mechanism was similar in both the VTM and the ball mill and predominately body breakage. This is in opposition to other publications that assume surface breakage to be dominant in the form of attrition and abrasion.

The energy efficiency of vertical stirred mills in comparison to ball milling has long been used as a selling point in trade-off studies. This paper will investigate data sets from three processing plants and highlight the pitfalls of calculating the efficiency of operating vertical stirred mills with coarser feed size distributions.

## HPGR/VTM CIRCUIT

Rocha (2019) surveyed a coarse-fed Vertimill following an HPGR to validate a population balance model of the VTM (Figure 3).

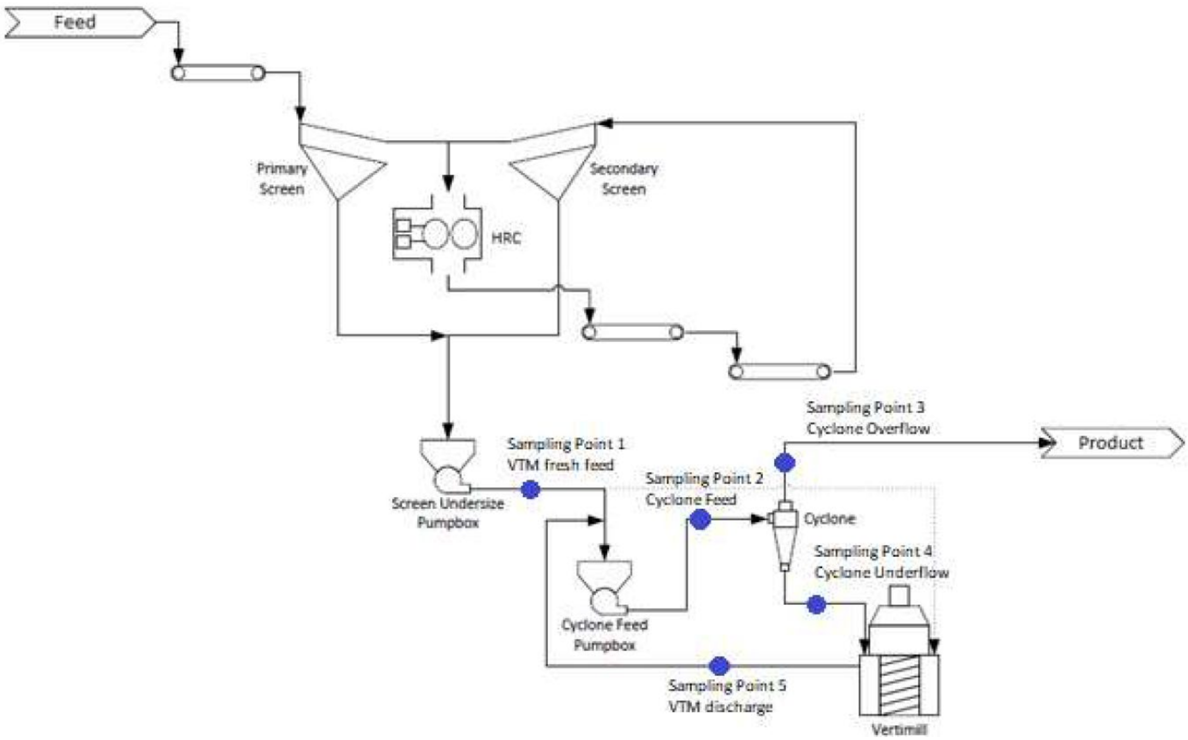


**FIG 3** – Flow sheet of surveyed plant (Rocha, 2019).

Rocha (2019) performed a laboratory ball milling test on the VTM feed and fitted a population balance model to the operating mill ignoring the classification. The breakage rates in the VTM were found to be 1.25 times higher than the Bond ball mill (with the liner and ball size issues highlighted above). However, when a simple Bond efficiency factor was calculated on the same results, the VTM appeared more efficient with a factor of 68 per cent (Table 1). Further explanation of this is provided in the analysis below.

**TABLE 1**

Bond efficiency factor calculated from the raw survey results in Rocha (2019).

| **Parameter** | **Units** | **Survey results** |
|---|---|---|
| Power | kW | 403 |
| Throughput | t/h | 81.4 |
| Specific energy | kWh/t | 4.95 |
| $F_{80}$ | µm | 2830 |
| $P_{80}$ | µm | 193 |
| Operating work index (OWi) | kWh/t | 9.3 |
| Bond work index (BWi) | kWh/t | 13.6 |
| Bond efficiency factor | | 68% |

The Bond approach requires parallel size distributions in log-log space to achieve realistic results. However, when evaluating the circuit feed and product size distributions measured in this survey, it was noted that the slope of the cyclone overflow particle size distribution (0.61) was sharper than the feed (0.50). Therefore, to evaluate the circuit fairly, an apparent $P_{80}$ was calculated by fixing the slope of the cyclone overflow at 0.50 and coarsening the size until the per cent passing 38 µm was equal to that obtained in the survey. This resulted in an effective coarsening of the $P_{80}$ by 43 µm and consequently the efficiency of the circuit reduced to 78 per cent which is comparable to the efficiency calculated through the population balance technique.

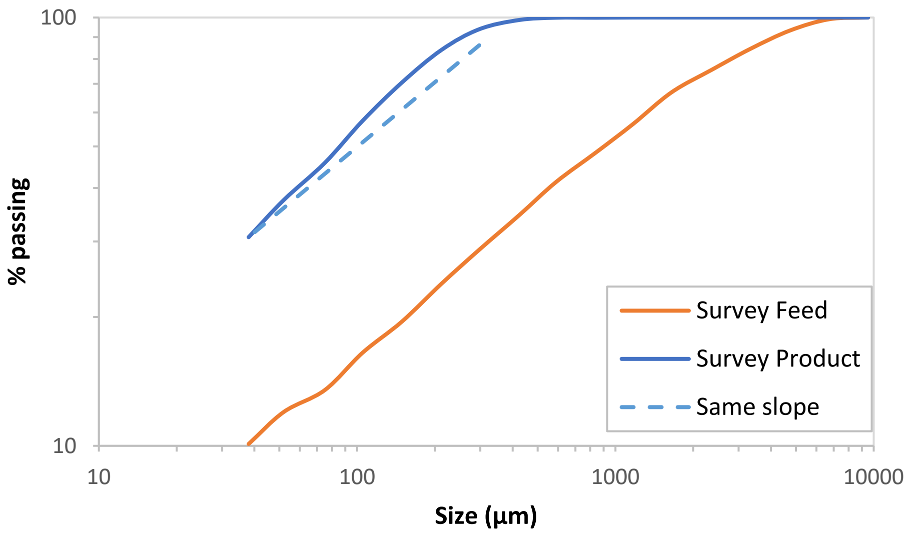


**FIG 4** – Feed and product size distributions for the VTM circuit with the modified slope-constrained product size distribution (after Rocha, 2019).

## BOUNGOU

SEMAFO's Boungou mine is a remote operation in the west African nation of Burkina Faso with a 1.34 Mt/a nameplate capacity and target grind size of 63 µm. Operating costs are high as electricity is generated locally and all consumables (fuel, reagents and media) are trucked in from neighbouring countries (Houde and Boylston, 2019). This motivated the exploration of energy efficient comminution circuit designs. A SAG-VTM-pebble crusher (SA-TM-C) circuit (Figure 5) was constructed to obtain the highest net present value (NPV) out of the eight alternatives evaluated (Table 2). The increased capital cost of this circuit was offset by the reduced operating costs.

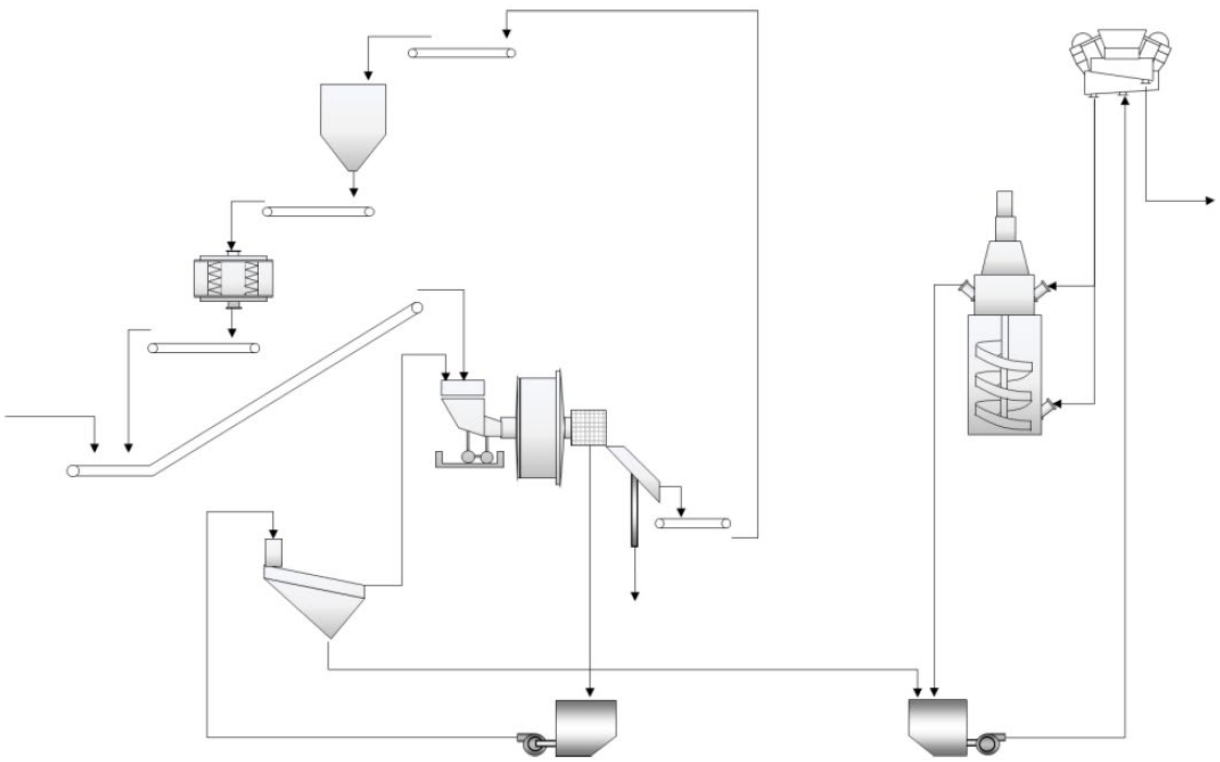

**FIG 5** – The Boungou SAG-Tower Mill-Pebble Crusher (SA-TM-C) comminution circuit (Houde and Boylston, 2019).

**TABLE 2**

Boungou concentrator value engineering summary (Houde and Boylston, 2019).

| Element | Unit | SAB | SA-TM | SABC | SA-TM-C | SSSAG-TM2 | 3C-BM | 3C-BM2 | 2C-RM-BM |
|---|---|---|---|---|---|---|---|---|---|
| Operating Cost | (USD/t) | -- | -$1.9 | $0.1 | -$2.0 | -$0.6 | $-0.3 | -$0.1 | -$0.2 |
| Capital Cost | (MUSD) | -- | $4.9 | $0.3 | $4.3 | $11.7 | -$0.2 | $1.4 | $1.4 |
| NPV | (MUSD) | -- | $8.2 | -$1.2 | $9.5 | -$5.6 | $2.7 | -$0.2 | $0.1 |

This circuit configuration is unique because the SAG mill is closed with a 6 mm screen rather than a cyclone, providing a coarser transfer size to the VTM than other SAG-VTM circuits, but similar to the HPGR-VTM circuit. The NPV benefit of the SAG-VTM circuits were based solely on the increase energy efficiency assumed for the VTM as the energy intensity was also used to calculate the media consumption. For the trade-off, the VTM was assumed to consume 15 per cent less power when compared with a ball mill. This was considered to be a relatively conservative figure. With the high electricity price (US $0.25/kWh) and media price, this resulted in a reduction in operating costs of US $2.0/t.

An independent retrospective sensitivity analysis was conducted for this case to test the minimum reduction in operating costs that was required to find a positive NPV benefit for the chosen circuit. It was found that a 50 per cent reduction in operating costs would result in the NPV of the VTM circuit being equivalent to the presented NPV of the three-stage crush and ball mill (3C-BM) circuit. Therefore, if the VTM efficiency improvement was halved, the VTM circuit would not be the preferred circuit option. This result highlights the importance of the efficiency factor in assessing the value of VTM circuits.

Houde and Boylston (2019) conducted two surveys of the comminution circuit that allowed performing an assessment of the efficiency of the operating circuit. The Bond (1952) formula and characterisation data was used with the Rowland and Kjos (1980) efficiency factors to calculate the equivalent ball milling requirements to reduce the VTM circuit feed $F_{80}$ to the circuit $P_{80}$. Using this analysis, the VTM consumed 89 per cent of the calculated ball milling power requirement.

This analysis failed to account for the increased fines typically measured in the product of SAG mills closed with screens (Ballantyne, 2019; Morrell, 2009). Because of this well-known phenomenon, the transfer size from the SAG mill ($T_{80}$) does not adequately reflect the work required by the secondary mill. To avoid this limitation, modern specific energy calculations require the secondary mill specific energy to be calculated by subtracting the SAG specific energy from the total circuit specific energy (Lane *et al*, 2013; Morrell, 2008). The survey data was analysed using this method and the results are shown in Table 3 alongside the design parameters. The total circuit power was calculated using Ausenco's in-house comminution design tool – Ausgrind, fitted to the design case (Lane *et al*, 2013). Unfortunately, the SAG mill power draw during the survey was not published and severe liner packing was identified. Therefore, the survey SAG mill power draw was calculated using a 10 per cent power reduction to account for slurry pooling. The VTM efficiency factor was calculated as the percentage power draw of the VTM in comparison to the equivalent ball mill.

**TABLE 3**

Design parameters and survey conditions from Houde and Boylston (2019). The values with an asterix (*) were calculated to assess the efficiency of the VTM during the survey.

| Parameter | Unit | Design SA-TM-C | Survey 1 SA-TM-C |
|---|---|---|---|
| Throughput | t/h | 167 | 140 |
| SG | $g/cm^3$ | 3.00 | 2.87 |
| A*b | - | 32.2 | 26.0 |
| Bond rod work index | kWh/t | 20.2 | 19.7 |
| Bond ball work index (106 μm) | kWh/t | 17.8 | 18.0 |
| Feed $F_{80}$ | μm | 133 | N/A |
| Grind $P_{80}$ | μm | 63 | 63 |
| SABC tumbling mill power requirement | MW | 4.8 | 4.4* |
| SAG mill pinion power | MW | 2.2 | 2.0* |
| Required ball mill pinion power | MW | 2.6 | 2.4* |
| VTM shaft power | MW | 2.2 | 2.4 |
| VTM efficiency factor | % | 84 | 100 |

For the design case, the VTM efficiency factor was 84 per cent which is comparable to the factor used in the trade-off study. However, using this updated approach, the VTM efficiency factor was calculated as 100 per cent during the survey, effectively the VTM used the same power as the equivalent ball mill. In comparison with Houde and Boylston (2019) the equivalent ball mill power was found to be 11 per cent lower using this approach. This difference can be attributed to the increased fines in the SAG mill product that are not reflected in the $T_{80}$.

At the time of the survey the circuit was constrained by the SAG mill, therefore the transfer size to the VTM was at the coarse end of the design (measured $T_{80}$ = 2.6 mm, design $T_{80}$ = 1 to 3 mm). Additionally, Houde and Boylston (2019) expected the efficiency of VTM to improve at the design throughput and at higher recirculating loads. Therefore, this case study proves that the VTM can perform this secondary milling duty from an $F_{100}$ of 6 mm down to a $P_{80}$ of 63 μm. However, the design of the VTM may require an efficiency factor closer to 100 per cent, especially if the circuit is SAG mill constrained and a coarser SAG mill circuit $P_{80}$ is required to de-constrain the circuit.

## TERTIARY MILLING

Increasingly, vertical stirred mills have been incorporated into brownfield expansions as tertiary mills following SAB or SABC circuits. Cadia, New Afton, Raglan and Chino are all good examples of this application. Vertical stirred mills have also been included in a tertiary-style duty following single-stage SAG and single-stage AG milling circuits, where the AG/SAG mill is closed with cyclones.

Examples of this style of application include Cannington and Tambomayo. These applications are coarser than the regrind application for which the vertical stirred mills were originally designed. However, in these applications, the efficiency factor can still be influenced by the slope of the particle size distributions.

The tertiary mill at Cadia was surveyed by Palaniandy *et al* (2015) and the results demonstrate the effect of the change in the shape of the particle size distribution. Palaniandy *et al* (2015) stated that this steepening of the product size distribution was likely to be beneficial for downstream flotation and was 'being observed in all Vertimill circuit operations'. The reduction ratio was small in this operation (typical of a tertiary duty), therefore the benefit of the change in particle size distribution slope was large in terms of the operating work index calculation. In this case, the survey operating work index was 13 kWh/t, whereas if the product slope was the same as the feed this increased to 24 kWh/t. Therefore, in this case, the steepening of the product size distribution was responsible for a 45 per cent reduction in operating work index.

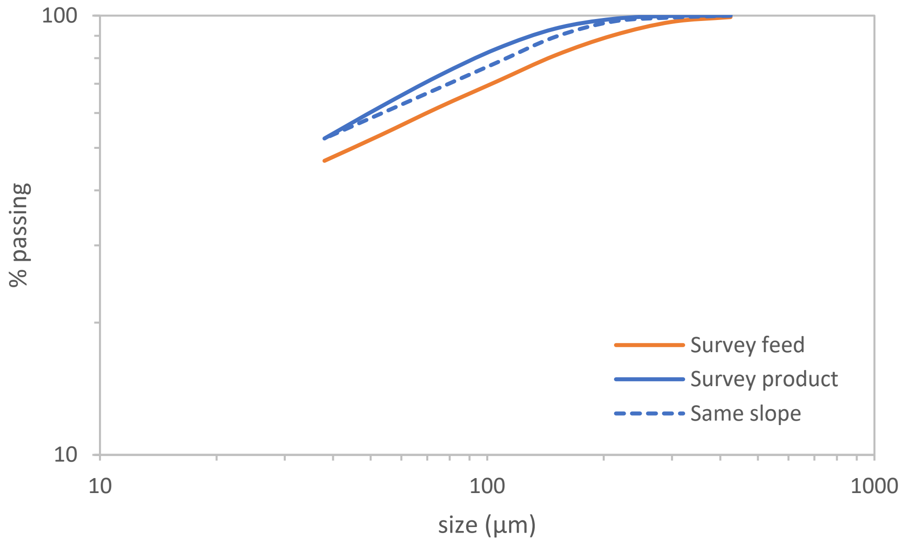


**FIG 6** – Feed and product size distributions from Cadia's tertiary VTM (Palaniandy *et al*, 2015) with the equivalent product size distribution with the same slope as the feed.

# CONCLUSION

Vertical stirred mills are being installed in increasingly coarser milling duties attempting to reduce operating costs, particularly power. Operating data from three VTMs installed in coarse duties have been explored in this paper. The efficiency factors used for design have been discussed and the operating data has been used to assess these assumptions. In all these cases, an efficiency factor was applied to the Bond work index to evaluate the mill installations. However, the validation of the operating efficiency was hampered by the sharper product particle size distributions from the VTM circuits.

The increase in the slope in the product size distributions resulted in an increase in the effective efficiency calculated for the VTM. For HPGR/VTM circuit, the feed to the VTM had increased fines due to the preceding HPGR and the sharper product size distribution was responsible for a 13 per cent reduction in the effective operating work index. At Boungou, the SAG mill provided a typically flatter size distribution that resulted in an estimated 11 per cent reduction in the predicted equivalent ball milling power. Finally, the sharpening of the product size distribution by the Cadia VTM was responsible for a 45 per cent reduction in the calculated operating work index.

The use of a Bond ball milling work index test to assess the grindability of the ore is likely to increase the calculated efficiency of the vertical stirred mills. The standard Bond ball mill test is inherently less efficient than an equivalent stirred milling. Smooth liners and smaller balls should be employed to better design or predict the performance of vertical stirred mills.

The intent of this paper is to highlight the limitation of assessing the efficiency of vertical stirred milling circuits using $P_{80}$ when the feed and product particle size distributions are not parallel. In cases such as these, the efficiency of the operating mills should be measured in the generation of new fine material rather than $P_{80}$ reduction. The authors intend to provide a clear methodology for vertical stirred mill sizing for coarse duties in a later publication.

## ACKNOWLEDGEMENTS

The authors would like to thank those who collected and published the data used in this analysis. Conversations with Martin Houde, Douglas Mazzinghy and Malcolm Powell were integral in the development of some of the ideas expressed in this paper. Finally, thanks to Ausenco for providing the impetus and opportunity to publish this paper.

## REFERENCES

Ballantyne, G., 2019. Assessing comminution energy efficiency with the Size Specific Energy (SSE) approach In *European Symposium on Comminution & Classification (submitted)*, Leeds, UK.

Bond, F.C., The third theory of comminution. Transactions AIME, 1952, 484–494.

Houde, M., Boylston, A., 2019. Design, Construction and Operating Experience of the SAG-Tower Mill Circuit at SEMAFO's Boungou Mine in Burkina Faso, In *SAG conference*, Vancouver, Canada.

Huang, M., Chandramohan, R., Foggiatto, B., Lane, G., 2019. Review of Comminution Testwork Requirements for Fine Grinding Mill Sizing and Selection, In *Procemin, Geomet 2019*, Santiago, Chile.

Knorr, B., Herman, V., Whalen, D., 2015. A Closer Look at Increasing HPGR Efficiency via Reductions in Edge Effect, In *SME*, Denver, USA.

Lane, G., Foggiatto, B., Bueno, M.P., 2013. Power-based Comminution calculations using Ausgrind, In *International Mineral Processing Conference – Procemin*, Santiago, Chile.

Levin, J., Indicators of grindability and grinding efficiency. Jounal of South African Institute of Mining and Metallurgy, 1992, **92(10)**, 283–290.

Lynch, A.J., Rowland, C.A., *The History of Grinding*. 2005, Society for Mining, Metallurgy and Exploration, Inc. (SME) Littleton, Colorado.

Mazzinghy, D.B., Schneider, C.L., Alves, V.K., Galéry, R., Vertical Agitated Media Mill scale-up and simulation. Minerals Engineering, 2015, **73**, 69–76.

Morrell, S., A method for predicting the specific energy requirement of comminution circuits and assessing their energy utilisation efficiency. Minerals Engineering, 2008, **21(3)**, 224–233.

Morrell, S., Predicting the overall specific energy requirement of crushing, high pressure grinding roll and tumbling mill circuits. Minerals Engineering, 2009, **22(6)**, 544–549.

Palaniandy, S., Powell, M.S., Seppelt, J., Griffin, P., Moore, A., Kermanshahi, K., 2015. Utilising a tertiary stirred mill to recover grind size after expansion of an SABC circuit, In *SAG 2015*, Vancouver, Canada.

Rocha, D.C., 2019. Predicting the product particle size distribution from a vertical stirred mill (PhD thesis). Colorado School of Mines.

Rowland, C.A., Kjos, D.M., 1980. Rod and ball mills, In *Mineral Processing Plant Design, AIME*, eds. Mular, A.L., Bhuppa, R.B., pp. 239–278.

Tian, J., Yang, Y., Morrell, S., 2018. Development of a laboratory test for regrinding ball mill or stirred mill circuits, In *Comminution*, Cape Town.

# Automated mill relining – current progress and future

*D Brander[1], J Bohorquez[2], S Gwynn-Jones[3] and M Turner[4]*

1. Chief Technology Officer, Russell Mineral Equipment, Toowoomba Qld 4350. Email: david.brander@rmeglobal.com
2. MRD Engineering Team Leader, Russell Mineral Equipment, Toowoomba Qld 4350. Email: joel.bohorquez@rmeglobal.com
3. Applications Engineering Manager, Russell Mineral Equipment, Toowoomba Qld 4350. Email: stephen.gwynn-jones@rmeglobal.com
4. MRD Analyst, Russell Mineral Equipment, Toowoomba Qld 4350. Email: melinda.turner@rmeglobal.com

## ABSTRACT

Grinding mill relining remains a major source of plant downtime in many mineral processing plants. Conventional relining activities accommodate hazards such as manual handling, working near suspended loads, the risk of falling from heights and working in confined spaces. Additionally, the time it takes to complete a mill reline varies significantly between sites. It is also difficult for any site or crew to build expertise, as the relines typically only occur every five to six months, and there are limited opportunities to practise the work. This makes it challenging to develop the site-specific expertise necessary to complete the relining activities in ways that are fast, safe and consistent.

Automation technology is often used industry wide to improve safety and reduce variability of repetitive and/or dangerous tasks. Automating the relining process enables autonomous placement and removal of liners with better speed and predictability than most human operators can achieve.

Every mill, liner set, mill relining machine and plant layout is different, so achieving automated mill relining requires a customised solution for each site. Achieving automated mill relining also requires close collaboration between site personnel, Russell Mineral Equipment (RME) engineers, relining crews and liner and bolt suppliers. An example of this collaboration has allowed RME to deliver the first implementation of automation technology (RME AutoMotion) that will enable the site to complete liner placement and removal without any personnel inside the mill, creating an unparalleled safety standard for mill relining.

This paper presents the results of recent automated relines on customer sites, and provides an analysis of the data collected, in order to generate insights into the future potential of automated relining.

## INTRODUCTION

Automating a complex process such as mill relining, or metallurgical circuits is best approached using a staged implementation. Incremental changes to a process to fully automate it, poses a lower risk of failure and reduces the resistances from both human and technical perspectives. It also facilitates the learning curve for the operators to increase the chances of successful adoption. Examples of an incremental approach to automation in previous Mill Operator's conferences include: the development of a flotation circuit control and automation for the Phu Kham Copper-Gold Operation concentrator (Baas and Mikhael Gurieff, 2018) and the implementation of model predictive control at Mount Isa lead zinc flotation circuit (Price *et al,* 2018).

A number of leading mineral processing plants are committed to automating their mill relining activities (Ikaheimonen *et al,* 2019). Some of them have made significant steps along this path, as is shown in Figure 1.


**FIG 1** – System for automating mill relining activities outside of the mill installed at two customer mine sites (RME's THUNDERBOLT SKYWAY).

There are three main motivators energising the drive towards relining the automation. These are:

1. Improved safety (elimination of hazards).
2. Increased production (increased mill availability).
3. Ensuring the planned shut duration finishes on time (reduced variability and therefore increased predictability).

These drivers are not unique to relining. In underground mining, these same drivers motivate a push towards automation of Longwall techniques (Ralston *et al*, 2017).

This paper is organised as follows:

- Methods of objectively measuring the three automation drivers (safety, productivity, and variability) are presented.
- A conventional (non-automated) reline is used as a case study to demonstrate the detailed application of these methods.
- Data from recent (partially) automated relines is then presented using this methodology, and experiences and results from these implementations are shared.

# METHODOLOGY

## The need for a common language

There are no agreed-upon industry standard metrics for defining mill relining performance. Conversations about mill relining performance are typically centred around the time spent relining, and the number of liner pieces moved during that time. However, even these (apparently) simple concepts can be manipulated to obscure performance.

Mill relining is a sequence of activities that are individually simple, but complex when considered as a whole. Activities are interrelated and can be completed in series or in parallel, having many factors that affect performance. It is also difficult to attribute performance changes to specific contributing factors. At a high level, factors that are considered to affect mill relining performance can include: liner and fastener design, crew skill, relining equipment and site level constraints such as the forklift availability or supply chain management issues.

Standard metrics for relining would ideally provide a common language between site owners, reline contractors and equipment suppliers for understanding and justifying the benefits of moving to automated mill relining systems. This section proposes relining metrics for productivity, safety and variability.

## Productivity metrics for relining speed

### *High level productivity metrics*

Automated mill relining is predicted to be faster than conventional methods (Ikaheimonen *et al*, 2019). It is necessary to outline the basis on which 'faster' is calculated to ensure that predictions can be easily related to conventional methods.

A common metric used to measure relining is reline shut duration (RSD). RSD is defined as the entire period of time from the when the mill shuts down to when the mill starts up again. When calculating the annual mill relining availability impact ($A_{RI}$), RSD is the appropriate value to use if the mill reline is on the critical path. $A_{RI}$ can be calculated as follows:

$$A_{RI} = \frac{downtime\ hours\ for\ relining}{hours\ in\ a\ year} = \frac{\sum_{i=1}^{s} RSD_i}{365\times24} \tag{1}$$

where s is the total number of relines each year.

Reline activities include all activities which are required to complete the relining of the mill while non-reline activities include any activities or breaks in time that are not necessary to complete the mill relining under expected conditions. Examples of each are provided in Table 1.

**TABLE 1**

Activities considered as reline time (RT) and non-reline time (NRT).

| **Period** | **Examples of Reline Activities (RT)** | **Examples of Non-reline Activities (NRT)** |
|---|---|---|
| From mill shutdown to first liner nut loosened | | Mill grind out<br>Feed chute removal<br>Liner handler installation<br>Mill isolation permits/protocol<br>Liner wear inspections<br>Other maintenance activities |
| From first liner nut loosened to last liner nut tightened | Bolt knock-in activities<br>Worn liner removal activities<br>New liner placement activities<br>Mill inching | Power outages<br>Safety incidents<br>Equipment breakdown<br>Other maintenance activities |
| From last liner nut tightened to mill start-up | | Liner handler removal<br>Feed chute installation<br>Mill de-isolation permits/protocol<br>Other maintenance activities |

Reline time (RT) can therefore be calculated by splitting the RSD time into RT and NRT using the definitions in Table 1 (Equation 2).

$$RT = RSD - NRT \tag{2}$$

RT has limitations as a comparative measure because the reline scope (the number and type of liners replaced) is usually different between relines. To create a comparative measure, we introduce the concept of liners per unit time, or 'liner rates'. This can be done by calculating the total number of liner movements in the reline ($N_{mov}$).

$$N_{mov} = N_{removed} + N_{installed} \tag{3}$$

In the situation that the liner design is not being changed during a reline, then the:

$N_{removed}$ = $N_{installed}$, and then Equation 4 also holds:

$$N_{mov} = 2.N_{pieces} \tag{4}$$

where $N_{pieces}$ is the number of liners in the mill that are to be replaced. Another way of saying this is that each piece has a movement in and out. As the liner design does frequently change during a reline, Equation 4 does not always hold and there is no simple way to calculate $N_{pieces}$. Therefore, it is generally preferable to use $N_{mov}$ instead of $N_{pieces}$ for the purposes of calculating the 'liner rate'.

Now that a method of calculating the number of pieces has been established, liner piece rates and liner movement rates can be calculated as follows:

$$R_{piece} = \frac{RT}{N_{pieces}} \tag{5}$$

$$R_{mov} = \frac{RT}{N_{mov}} \tag{6}$$

While $R_{mov}$ is the preferred comparative measure over $R_{piece}$, it still has limitations. In many relines, the reline crew is not responsible for inching (turning) the mill, and does not want measurements of the reline time to consider the inching time. Often this results in a modification to the rate $R_{mov,exc.inch}$ calculation as is shown in Equation 7. This modified rate is then no longer directly comparable to the $R_{mov}$ being reported by other sites where the reline crew is responsible for inching the mill.

$$R_{mov,exc.inch} = \frac{RT - Inching\ time}{N_{mov}} \tag{7}$$

A further limitation of $R_{mov}$ is that it does not provide a good relative measure when a site has optimised the liner design to have fewer, larger pieces. This liner optimisation method is being adopted widely within the industry to improve mill availability (Ikaheimonen *et al*, 2019). When there are fewer, larger liners, there are some activity times that are not reduced (eg there are often the same number of liner nuts, bolts and mill inches). This means the $N_{pieces}$ is reduced but the $RT$ has not necessarily decreased by a proportional amount, which leads to an increase in $R_{mov}$ even though there has been a significant reduction in RT.

To isolate the impact of the quantity of liners and provide a metric for sites changing liner designs, it is proposed that the mill shell area per unit of time could be used. This is called the 'relining area rate' ($R_{area}$).

$$R_{area} = \frac{RT}{A_{shell}} \tag{8}$$

where $A_{shell}$ is calculated as the area of the shell cylinder plus the area of the two truncated cones (the feed and discharge ends of the mill):

$$A_{shell} = \pi(2RL + l_{feed}(R + r_{feed}) + l_{dis}(R + r_{dis})) \tag{9}$$

where:

$$l_x = \sqrt{h_x^2 + (R - r_x)^2}$$

| | | |
|---|---|---|
| $R$ | = | inside diameter of the mill shell |
| $L$ | = | flange to flange length of the mill |
| $r_{feed}$ | = | internal diameter of the feed trunnion |
| $r_{dis}$ | = | internal diameter of the discharge trunnion |
| $l_{feed}$ | = | the axial length of the feed end |
| $l_{dis}$ | = | the axial length of the discharge end |
| $h$ | = | the length of the feed/discharge |

### *Detailed productivity metrics*

More detailed productivity metrics can also be useful in certain circumstances. These are often used to determine the strongest contributing factors to a specific reline's performance and construct discrete event simulations of relining.

The RT can be broken down into four distinct phases: knock-in, liner removal, liner placement and inching. Each phase can then be broken down into a number of relining activities. Examples of activities in the placement phase could include 'liner pickup', 'machine travel' and 'liner positioning and securing'. The cycle times for each activity must be measured by developing detailed definitions to describe the start and end of each activity.

Once a data set of cycle times ($C_i$) has been obtained, the median ($\tilde{X}$) and the mean ($\mu$) of the activities can be calculated. This data is best collected by the filming of reline activities for reduction into individual activity times. The approach described above has recently been used by RME for one site to identify and achieve a 30-hour saving in discharge end relines on a large SAG mill (Martinez *et al*, 2019). An example of calculating the mean shell liner placement activity time ($\mu_{shell\ liner\ placement}$) is provided in Equation 10:

$$\mu_{shell\ liner\ placement} = \frac{\sum_{i=1}^{s} C_i}{s} \tag{10}$$

where s is the total number of shell liner placements.

## Variability metrics for relining consistency

From a site perspective, it is desirable for mill relines to be predicable and to finish at the planned time. Relines are often the longest shutdowns in the annual maintenance plan, and many other critical maintenance activities are planned within the reline time frame. Relines that finish early can result in other planned maintenance activities being cut short if site management decides to prioritise the extra production. Automation of reline activities is predicted to significantly reduce variability and help to ensure relines finish at the predicted times.

Collecting detailed cycle times for individual relining activities for productivity metrics also provides the required data for studying the variability of the same activities.

One method that can be applied to studying variability in mill relining can be borrowed from Lean manufacturing methods (Deif, 2012). The concepts of Reline Time and Non-Reline Time can be used in place of the Lean concepts 'Value added' and 'Non-value added'. Using this approach, a process map of mill relining has previously been developed, including in a virtual model of a mill reline (Rubie *et al*, 2015).

The Variability Source Mapping tool (VSMII) described by Deif (2012) introduces the concept of a variability index (VI). VI can be used to quantify how important a single activity's variance is to the overall reline duration.

To calculate VI, it is first necessary to calculate the coefficient of variation (CV) of an activity as follows:

$$CV = \frac{\sigma}{\mu} \tag{11}$$

where $\mu$ denotes the activity duration and $\sigma$ denotes the standard deviation of a relining activity. It is then possible to calculate VI of a reline phase (eg liner placement) as follows:

$$VI = \left(\frac{\sum_{i=1}^{s} CV_i}{s}\right) \tag{12}$$

where s = the total number of unique activities within the phase (eg pick up, travel), and $CV_i$ has been calculated separately for each activity within that phase.

## Safety metrics for hazard exposure

Relining involves a number of activities both inside and outside of the mill that have associated safety risks to be managed. Most organisations use qualitative or semi-quantitative approaches to risk assessment that involve consideration of both exposure and consequences for various hazards.

Ideally, the metric for comparing the difference between conventional and automated relining would be objective.

To develop an objective measure of safety for comparing conventional and automated relining, RME has created a program using computer vision and deep learning. The program analyses video footage from a reline and quantifies when there is 'exposure' (measured by man-hours) to normal reline hazards in a simple and easily comparable way. Figure 2 provides examples of how this detector identifies the number of people in the mill during a reline, and also identifies pieces of relining equipment.

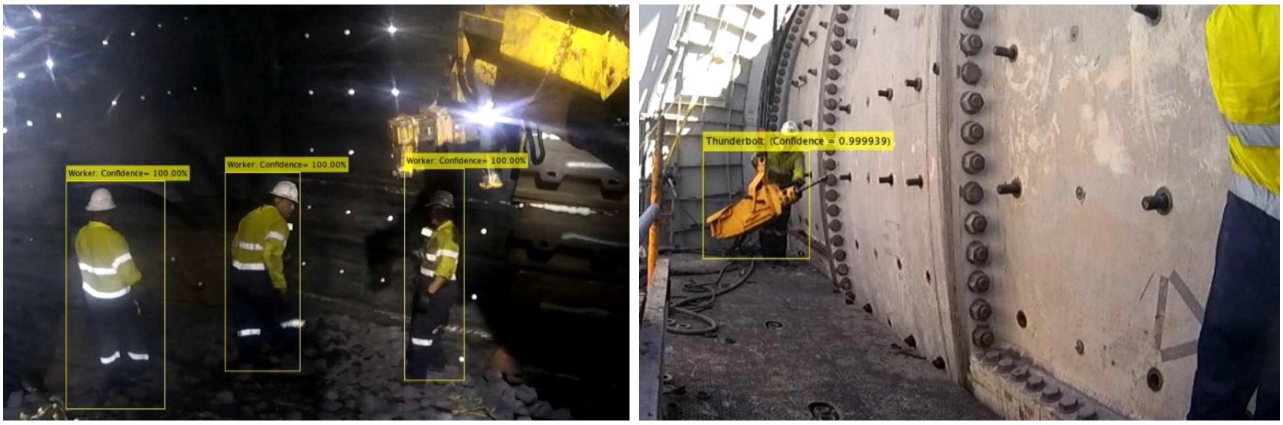


**FIG 2** – Example of detection of workers exposed to typical reline hazards inside of the mill (left) and knock-in equipment outside of the mill (right).

The outputs of this program are $n_{people}$ (number of people) in a specific zone (eg inside of the mill) at a given time. The program can then calculate the total man-hours of exposure to associated hazards (MHE) as follows:

$$MHE_{in\ mill} = \int_{t=0}^{t_{max}} n_{people,in\ mill}\,(t) \tag{13a}$$

$$MHE_{outside\ mill} = \int_{t=0}^{t_{max}} n_{people,outside\ mill}\,(t) \tag{13b}$$

where t is the time during the reline. MHE directly depends on the length of the reline, and the length of the reline also depends on the size of the scope of work, or in other words, the number of liner movements.

The number of liner movements can be used to calculate the exposure time per liner movement ($E_{mov}$), by dividing the total MHE by the number of liner movements:

$$E_{mov} = \frac{MHE_{in\ mill}}{N_{mov}} \tag{14}$$

## CONVENTIONAL RELINING CASE STUDY

This section uses a conventional SAG mill reline as a case study to apply the proposed analysis tools to provide a comparison point for automated relines. This reline will be referred to as the 'SAG mill A' reline throughout this work. Video footage was collected by RME at this reline. This reline was selected for this analysis for a number of reasons. The video footage obtained is comprehensive and of good quality, making calculations and conclusions both clear and accurate. Additionally, the crew performance is considered above average with efficient liner movement rates, making it a reasonable reline for comparison to automation data.

### Relining speed/productivity analysis

Table 2 shows performance metrics for the SAG mill A reline calculated in accordance with the methodology section. This reline involved a 'typical high-wear' scope, where only outer feed liners, outer discharge grates and shell liners were replaced. In this reline, the number of pieces removed were replaced by an equal number of pieces.

**TABLE 2**

Absolute metrics for SAG mill A reline.

| **Description** | **Value** | **Units** |
|---|---|---|
| Reline shut duration (RSD) | 45.1 | hours |
| This reline's availability impact (A_RI) | 0.2 | % |
| Reline time (RT) | 33.2 | hours |
| Non-reline Time (NRT) | 11.9 | hours |
| Number of inches | 14 | Inching events |
| | 13 | Turns |
| Number of pieces (liners) replaced | 137 | pieces |
| Number of movements (in + out) | 274 | movements |

The time spent in each of the reline phases was measured from the video footage and is summarised in Figure 3.

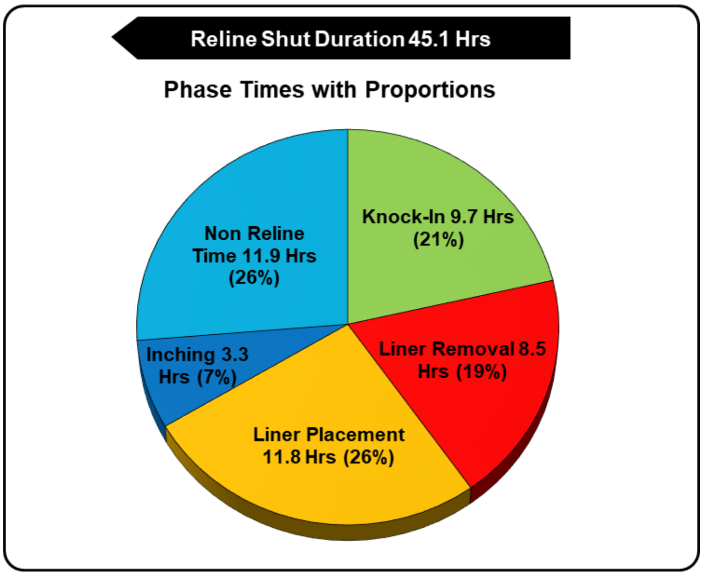


**FIG 3** – Phase times and proportions for the SAG mill A reline. Liner placement is the longest phase of the reline, accounting for 29 per cent of the reline duration.

Table 3 shows the rate-based metrics for the SAG mill A reline. These metrics indicate that it is considered to be a relatively fast reline based on RME's experience, where a typical industry value for $R_{mov,exc.inch}$ for this size mill is approximately 8.8 min/mov.

**TABLE 3**

Relative metrics for SAG mill A reline.

| | **Piece** | **Movement** | **Area** |
|---|---|---|---|
| Rate | 14.5 min/piece | 7.3 min/mov | 10.1 min/m$^2$ |
| Rate (excluding inching) | 13.1 min/piece | 6.5 min/mov | 9.1 min/m$^2$ |

## Speed of individual activity execution and human limitations

Automated mill relining is predicted to reduce the time it takes to complete specific activities when compared to manual methods. To illustrate this concept, the shell liner MRM travel activity within the placement phase from the SAG mill A reline is used as an example.

During shell liner placement, a key step is the movement of the liner from the liner cart to its final position on the mill wall using the RUSSELL Mill Relining Machine (MRM). This task requires the collaboration between the RUSSELL MRM driver and the crew members standing on the charge inside of the mill. It depends on the RUSSELL MRM driver's skills to manoeuvre the (typically) seven axes of the RUSSELL MRM to place the liner in close alignment between liner bolt holes and mill shell holes. It also relies on good communication between the crew members on the charge and the MRM driver for the final alignment so that the bolts can be inserted through both the liner and shell.

Figure 4 shows measured cycle times for the activity of transporting shell liners from the linercart to the mill wall using the RUSSELL MRM. The samples have been ordered from the slowest to the fastest sample and a theoretical 'best' speed has been calculated using the machine hydraulic specifications, liner mass and RUSSELL MRM layout inside of the mill (considering the typical travel paths of the liner). This theoretical speed represents the maximum practical human speed (and therefore the minimum time required) to complete this activity phase if optimal speed is always used without any delays, variations or inconsistencies caused by humans or other interferences. In calculating this theoretical 'best' speed it has also been considered that up to two axes can be moved simultaneously by a human. Acceleration and deceleration speeds have been taken into account.

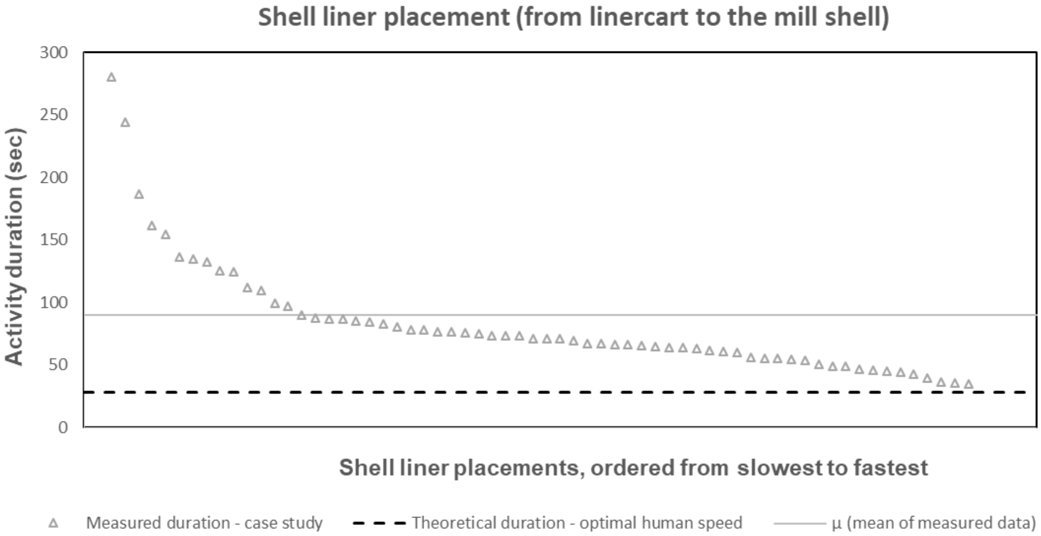


**FIG 4** – Shell liner movement duration measured in the SAG mill A reline. This activity measures the time taken to transport a shell liner from the liner cart to its final location on the mill wall. Samples have been ordered from slowest to fastest.

Figure 4 shows how the RUSSELL MRM drivers, on a few occasions, performed this activity very close to the theoretically best possible time; however, it is also evident how this level of performance cannot be maintained throughout whole relines as many issues arise such as driver fatigue (shifts are 12 hours long), communication issues (between driver and crew member on charge), and human errors (lack of training or error in spatial perception). All these issues cause inconsistent performance, and also lead to occasions where the activity takes a very long time.

### *Individual activity variability*

As shown in the previous section, even skilled human operators have a high degree of variability in the time it takes to complete individual activities. This variability in activity times contributes to unpredictable reline durations.

Figure 5 shows statistical distributions of four key activity cycle times, measured from the SAG mill A reline, that together describe the placement of one shell liner. These activities are described in more detail in the following paragraphs.

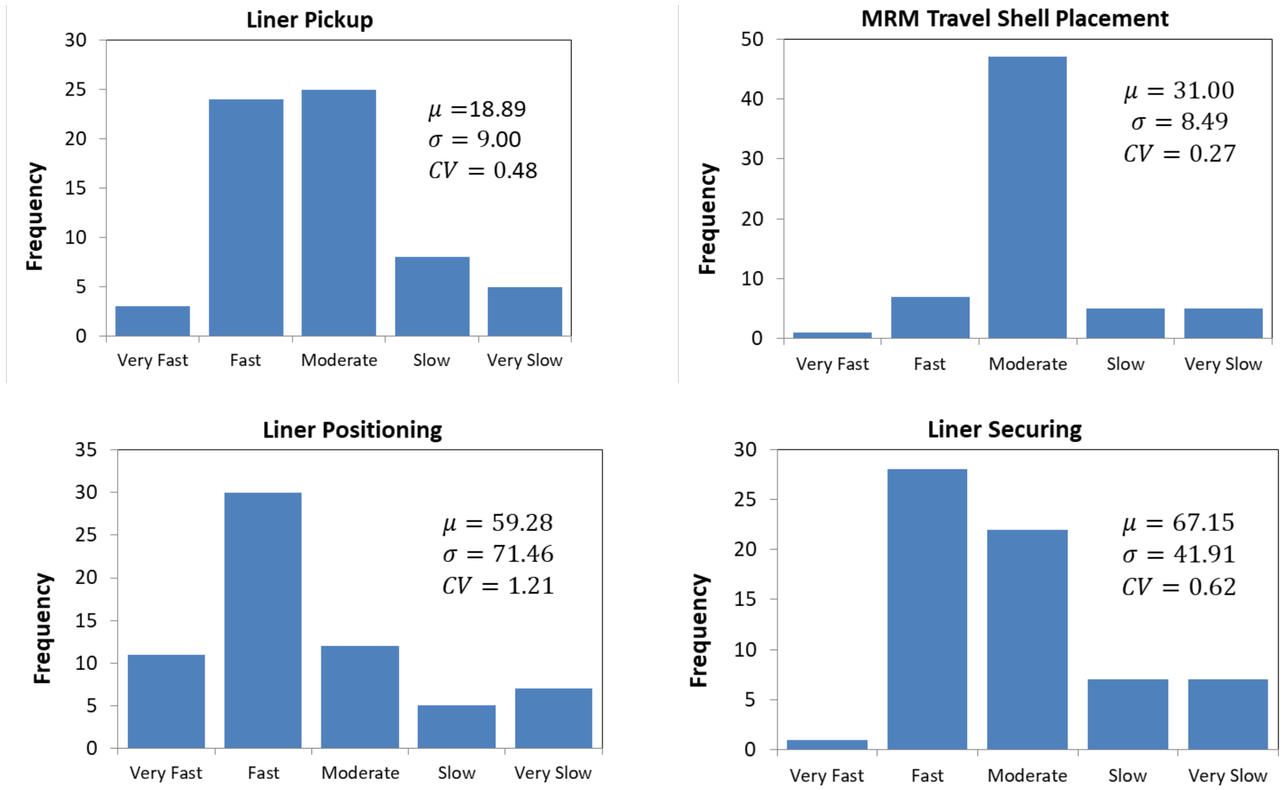


**FIG 5** – Cycle time distributions for selected activities during the liner placement phase.

**Liner pickup** is the action of using the RUSSELL MRM's grapple to attach the liner to the RUSSELL MRM by inserting two grapple pins into the liner lugs. This action requires collaboration between the RUSSELL MRM driver and the liner cart operator. The liner cart operator guides the RUSSELL MRM driver to align the grapple pins with the liner lugs. The cycle times of this activity depend on the skills of these two crew members and their communication.

**RUSSELL MRM travel (shell placement)** indicates the transport of new a liner to its final location in the shell part of the mill, using the RUSSELL MRM. It requires the use of large movements in most of the MRM axes. Cycle times for this activity depend on the RUSSELL MRM driver's skills in operating the machine and his/her spatial perception accuracy.

**Liner position** refers to the task of completing the alignment between the liner bolt holes and shell holes in order to allow securing bolts to pass through the mill shell. Cycle times of this activity depend on the skills of the RUSSELL MRM driver in getting an accurate first approximation so that only minute movement corrections are then required. They also rely on good guidance, communication and coordination from the crew members on the charge to allow the alignment of multiple bolt holes.

**Liner securing** is the final task in installing a new liner. This activity is executed by the crew members on the charge inside of the mill and also on the outside of the mill. The workers inside of the mill insert bolts through the liner and shell holes that the outside crew members secure using washers and nuts. Good communication, clear workflow and a clear plan of action are critical for these crew members to execute this activity as fast as possible.

The data sets summarised in Figure 5 are used to calculate the VI for shell liner placement for this single reline. This VI value is compared to other equivalent filmed relines in Figure 6. The results in Figure 6 show that even the fastest crews have high levels of variability in this particular activity type. It also shows that there is no correlation between speed and variability.

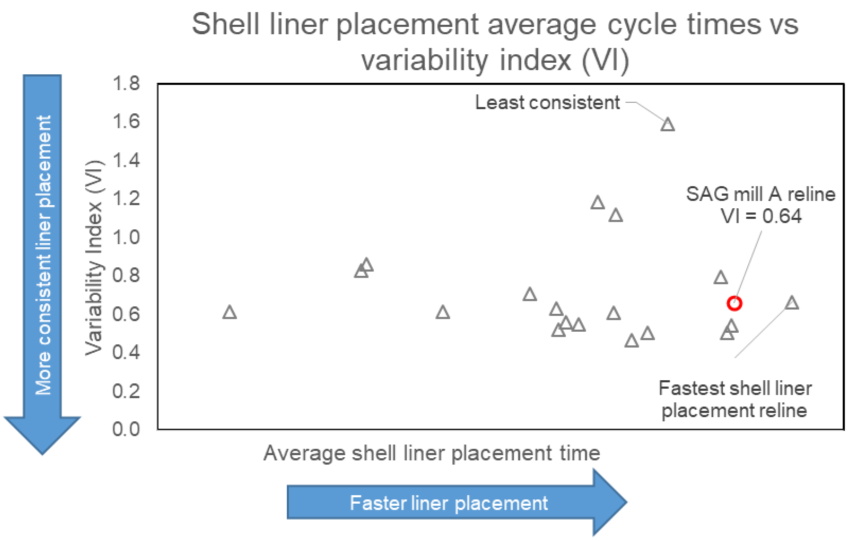


**FIG 6** – Average cycle time versus variability index of shell liner placement. SAG mill A reline is highlighted as a red circle with a VI that is common among many other SAG mill relines.

Figure 7 contains the same data as in Figure 4 (shell liner placement travel times) but ordered chronologically. It illustrates how cycle times exhibit no trend throughout the reline. The overall duration of this activity can therefore also be very inconsistent.

The split between RUSSELL MRM travel and liner positioning is marked by the point when the liner has arrived at its location (travel), but forward movements and small adjustments are needed to align it with the bolt holes in the shell wall before it can be secured (positioning).

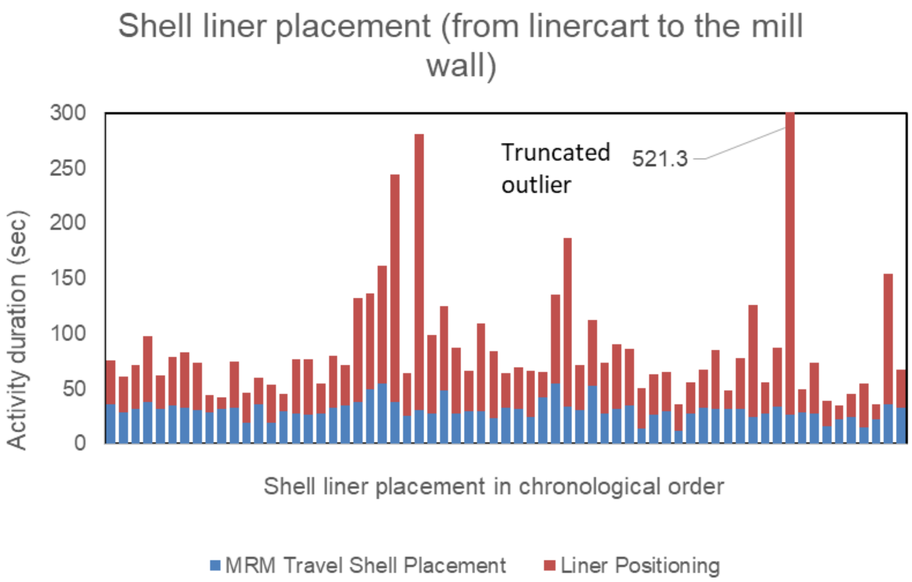


**FIG 7** – Shell line movement cycle times measured in the SAG mill A reline in chronological order.

## Hazard exposure analysis

The computer vision and deep learning tool was used with the video captured from the SAG mill A reline to measure the total exposure time for two areas: inside and outside the mill. The total MHEs for hazards in both of these areas were calculated using Equations 13a and 13b.

Figures 8 and 9 summarises the relining safety metrics from the SAG mill A reline footage. Three different camera positions were used by the computer vision tool for this analysis. One camera was inside of the mill and two cameras outside of the mill. One of the outside cameras recorded activities around the feed end and shell of the mill, while the other recorded activities around the discharge end of the mill. Activities occurred in these outside zones during the knock-in and liner placement phases. These results show that there are relatively more man-hours spent working in in the zones outside of the mill than inside of the mill for the case study reline, and that both exposure values exceed the actual reline shut duration (RSD).

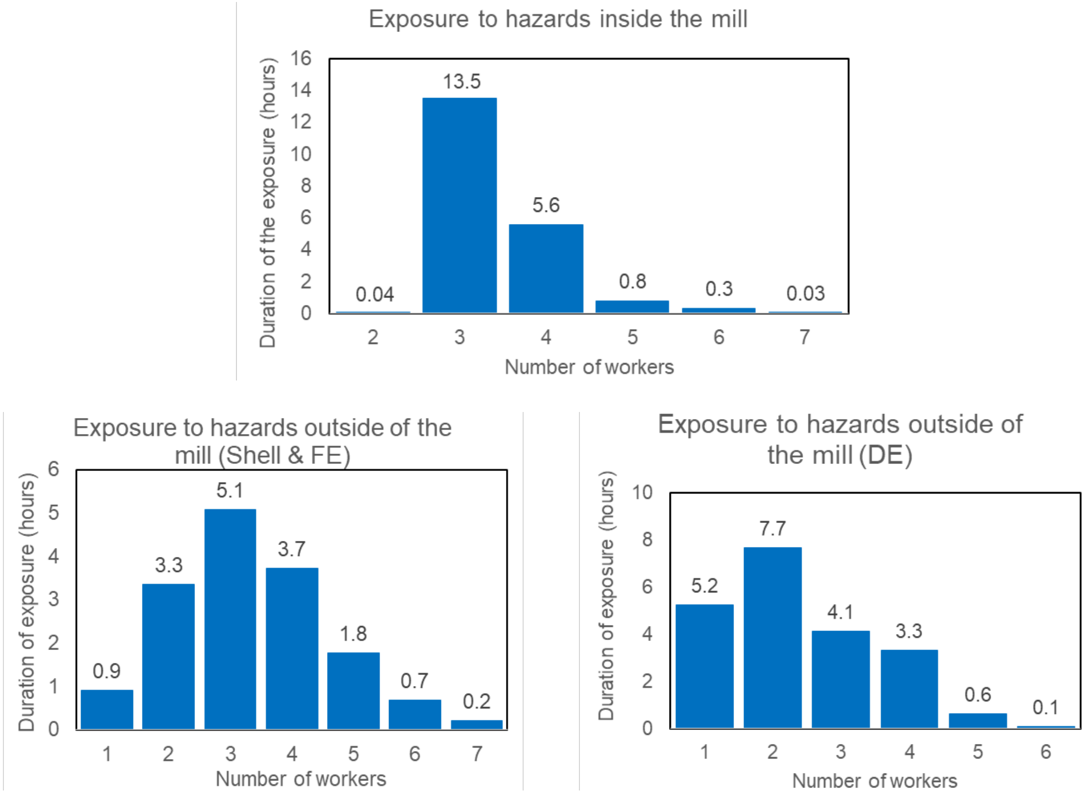


**FIG 8** – Exposure to normal relining hazards inside ($MHE_{in\ mill}$) and outside of the mill ($MHE_{outside\ mill}$) calculated using SAG mill A reline footage and computer vision and deep learning techniques for the various work areas.

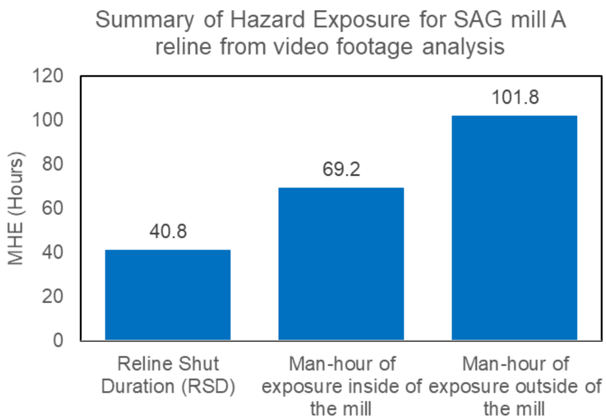


**FIG 9** – Summary of hazard exposure metrics ($MHE$) for SAG mill A reline, calculated from outputs of deep learning software applied to camera footage from reline.

MHE is quantified separately inside ($MHE_{in}$) and outside of the mill ($MHE_{out}$) as the severity of the hazards are different and therefore so are the risks.

The risk exposure duration inside and outside of the mill, per liner movement, are calculated for comparison to other relines later in this paper.

$$RE_{mov,in} = \frac{MHE_{in}}{N_{mov}} = \frac{69.2\ x\ 60}{274} = 15.2\ min/mov$$

$$RE_{mov,out} = \frac{MHE_{out}}{N_{mov}} = \frac{101.8\ x\ 60}{274} = 22.3\ min/mov$$

## AUTOMATED MILL RELINING

Automated relining technologies are being introduced in a multi-staged approach to several mineral processing plant.

This section summarises the current results of implementing different stages of automation at three different sites. One filmed reline per processing plant is analysed in this section and compared to the SAG mill A reline (conventional reline). Detailed analysis is conducted on those activities that are modified by the implementation of new technology in the mill relining automation process and compared to conventional reline data. SAG mills A to D are different sizes but are equipped with suitable mill relining machines for their respective mill sizes and liners.

The three filmed relines that are analysed in this section are named: SAG mill B, SAG mill C and SAG mill D. SAG mill B and C implemented a new set of RME technologies called 'RME INSIDEOUT liner placement' to install new liners without people on the charge inside of the mill. INSIDEOUT Technologies are an enabling technology to permit automated movements of an MRM by allowing relining to occur with no personnel inside of the mill. A summary of the new technology from each reline is included below:

1. The SAG mill B reline implemented the first step of seven to automate reline activities inside of the mill (see Figure 10), which is the installation of shell liners using RME INSIDEOUT liner placement technology.
2. SAG mill C reline implemented the second step of seven to automate reline activities, which uses RME INSIDEOUT liner placement technology to install feed and shell liners.
3. Lastly, SAG mill D reline implemented automatic bolt and liner knock-in. This was achieved by automating the use of the liner removal tools using the Thunderbolt Skyway.

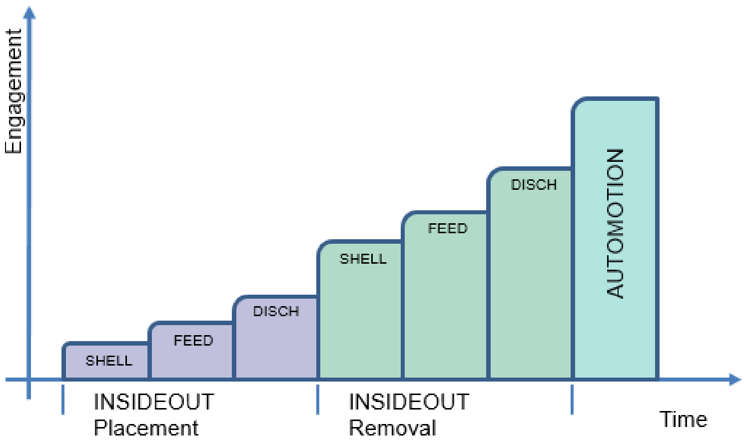


**FIG 10** – Seven steps to automate reline activities inside the mill using RME advanced technologies. Thunderbolt Skyway is not included as a final step in the figure as this system facilitates relining from the outside the mill.

### Impact of automated liner removal tool movement on bolt and liner knock-in

#### *Speed and variability analysis*

SAG mill D implemented automated bolt and liner knock-in using THUNDERBOLT SKYWAY, which resulted in a reduction in the time required to knock-in bolts and liners compared to conventional methods.

Figure 11 shows the following data to illustrate the impact of automating liner removal tool movement:

- Duration for knock-in of bolts from recent relines. Bolt knock-in time after installation of the Skyway system is compared to manual methods (using sledge hammers) on prior relines of the same mill. It is also compared to using Thunderbolt hammers suspended on monorails on a different mill of the same size and relined by the same crew.

- Duration for knock-in of liners from recent relines. The SKYWAY system data is compared to using a simple Jib crane for suspension of the THUNDERBOLT Hammer on the previous reline on the same mill. It is also compared to using Twin-Tube monorails for suspension of hammer on a different mill of the same size relined by the same crew.

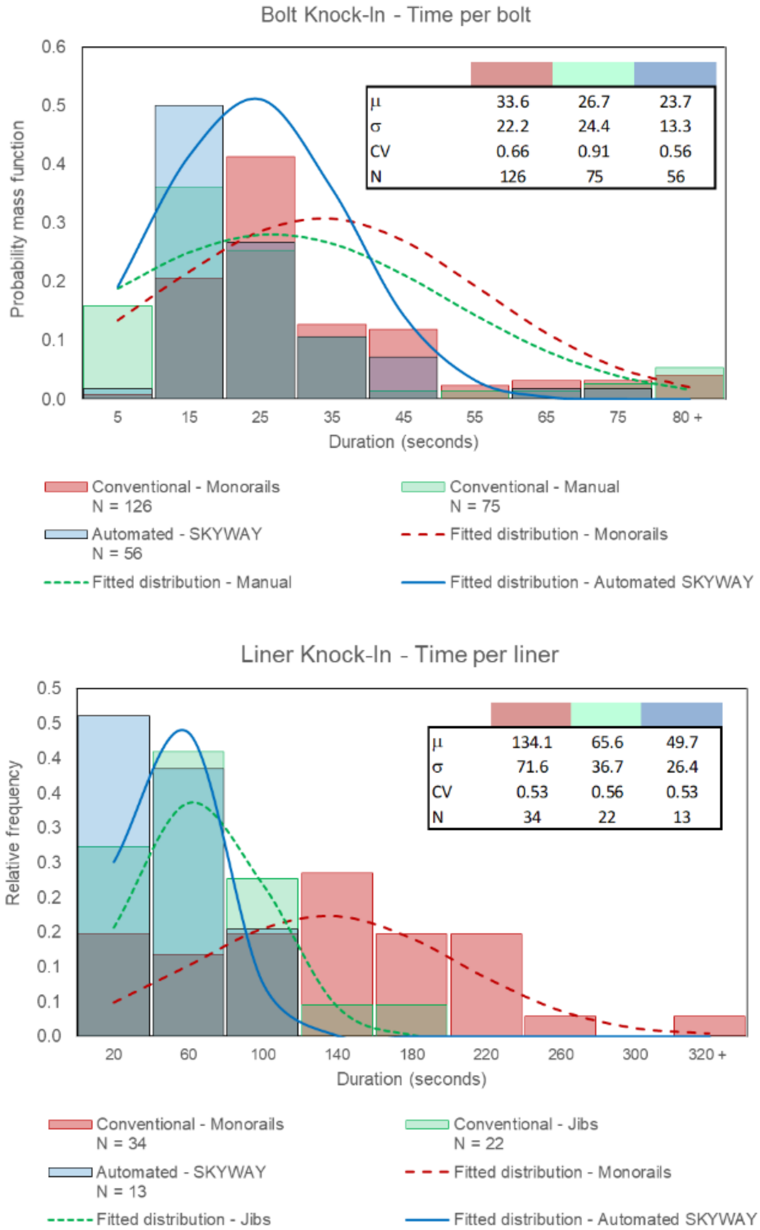


**FIG 11** – Comparisons of traditional methods and automated methods for bolt and liner knock-in from the SAG mill D reline.

The results in Figure 11 show that both bolt and liner knock-in are performed faster on average by the automated knock-in system when compared to conventional methods. Bolt knock in is performed three seconds faster when compared to manual knock-in and 9.9 seconds faster when compared to using the Thunderbolt hammer on monorails. Liner knock-in is performed 15.9 and 84.4 seconds faster using the automated system compared to using the Thunderbolt hammer on Jibs and monorails, respectively. More importantly than the average speed however, is the improvement in consistency. The standard deviation for the automated knock-in is nearly half the equivalent value for conventional methods.

Another method of studying the impact of automating the knock-in system is to analyse the individual activities that are independent of the liner design. Figure 12 shows cycle times of key individual activities that were automated with the new knock-in systems. These are:

- movement of the hammer between bolts
- time spent maintaining alignment of the hammer to the bolts and liner knock-in holes.

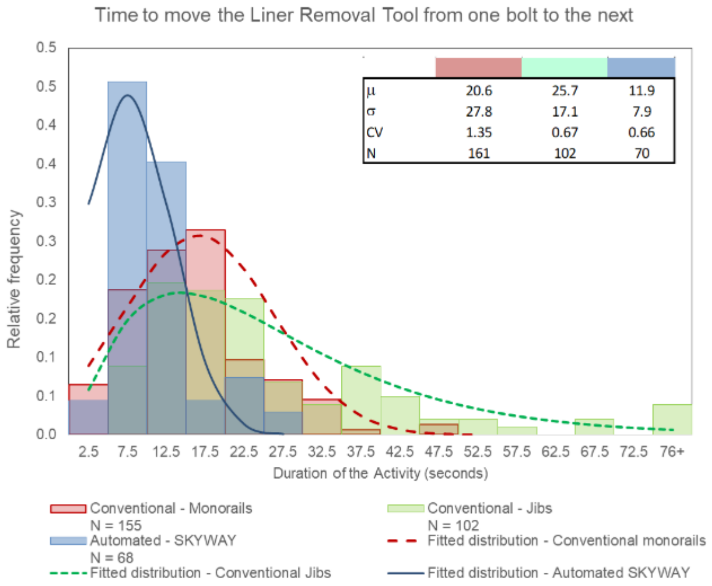


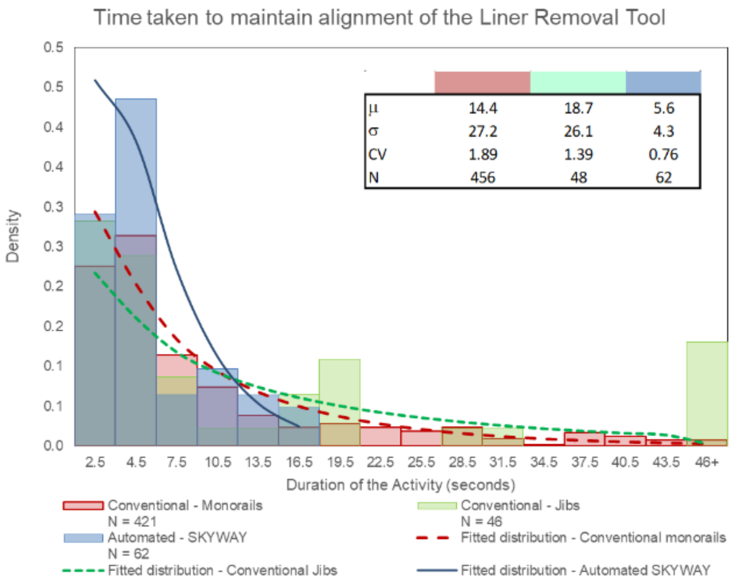


**FIG 12** – Comparisons of traditional methods and automated methods for liner removal tool movement and hammer alignment from the SAG mill D reline.

The bottom two histograms graphs in Figure 12 showed comparison among these same relines for the specific activities that have been automated. It is observed how activities were performed faster and more consistently using the automated equipment than using conventional methods. It is also observed how these two graphs shows how monorails facilitates the hammer movement when compared to using a Jib and alignment is also performed quicker when using monorails compared to Jibs.

### *Hazard exposure analysis on recent automated relines*

Automating the movements of liner removal tools improves safety. It eliminates the need for up to three people to manually handle and move liner removal tools around the mill deck where they are exposed to hazards such as suspended loads, slips, trips and falls. Instead, an operator pilots the liner removal tool remotely using a remote control.

Table 4 shows some of the safety metrics for the SAG mill D reline that implemented automated knock-in. There is still some exposure to hazards during the SAG mill D reline for rattle gun use (177.5 hours), however the exposure from handling the liner removal tool is eliminated. Reduction in exposure to hazards (MHE) has been estimated by multiplying the total time spent using the automated liner removal tool by three people, which is typical for conventional relining methods, assuming that additional people (typical number of person) had to operation a conventional knock-in system throughout the same duration of reline activities (RT – Inching). A reduction of 140.9 man-hours of exposure has been calculated as the benefit of implementing Thunderbolt Skyway in this reline. This results in the man-hours of exposure to hazards outside of the mill per hour of relining to be roughly half what is normal in conventional relining (1.7 versus 3.4).

**TABLE 4**

Comparing hazard exposure between a conventional reline (SAG mill A) and a reline that used automated bolt and liner knock-in (SAG mill D).

| **Metric** | **SAG mill A Conventional reline** | **SAG mill D Skyway** | **Units** |
|---|---|---|---|
| Reline time RT – Inching | 29.9 | 105.4 | hours |
| Hazard exposure outside of the mill operating liner removal tools MHEout,exc.inch | 101.8 | 177.5 | hours |
| Hazard exposure rate (REmov,out) | 22.3 | 13.6 | min/movement |
| Reduction in exposure outside of the mill from Skyway (ΔMHEout) | 0.0 | -140.9 | hours |
| Man-hours of exposure outside per hours relining (MHEout,exc.inch/RT – Inching) | 3.4 | 1.7 | hours/hours |

Figure 13 shows the reduction in relative man-hour of exposure to hazards outside of the mill in the SAG mill D reline. The introduction of the Skyway system to automate liner removal tool movements resulted in a 43 per cent reduction is exposure to hazards found in conventional relining.

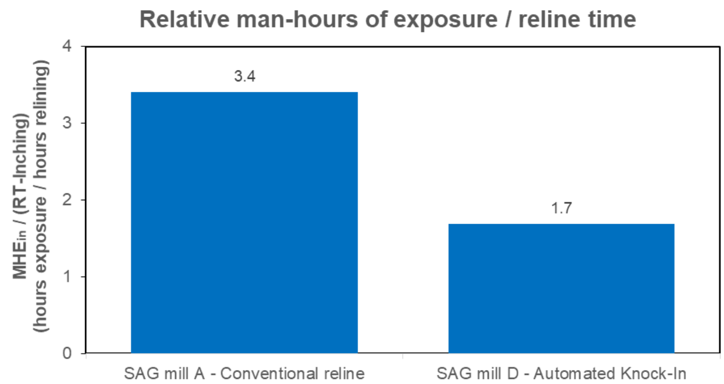


**FIG 13** – Reduction in exposure to hazards outside of the mill by automating the movement of liner removal tools (Thunderbolt Skyway).

## Impact of new technologies to remove people from the mill

SAG mill B and C relines involved different stages of implementation of a new technology (RME INSIDEOUT) to remove people from the mill to enable the RUSSELL MRM automation and complete automated liner removal and placement.

### *Speed and variability analysis*

Many variables affect the speed at which new liners are installed on the mill wall. Some of these variables are: reline crew skills, size of the liners, available space to manoeuvre the RUSSELL MRM and place liners, margin of error for adequate alignment between liner bolt holes and mill shell holes, among others.

The SAG mill C reline provided the best conditions to make a direct comparison of speed in liner placement using RME INSIDEOUT liner placement and conventional methods, as it involved a partial trial of these technologies on both feed and shell liners. This eliminated most of the variables affecting liner placement and provides ideal conditions for comparing both methods of new liner placement.

Figure 14 shows that liner placement times using conventional methods and RME INSIDEOUT liner placement were on average almost identical in the SAG Mill C reline. This means that the man-hours of exposure to conventional relining hazards inside the mill was reduced, without impact on reline time.

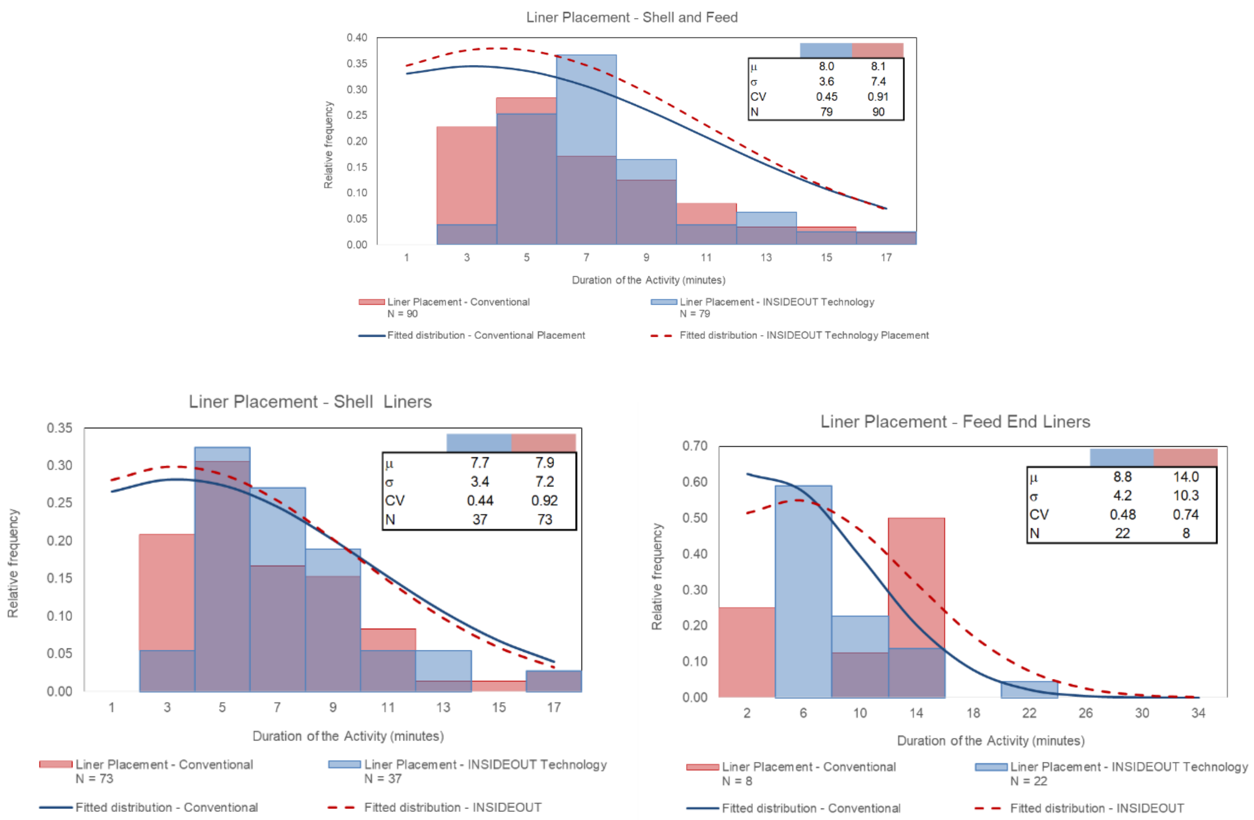


**FIG 14** – Time comparisons between traditional liner placement methods and automated methods. Cycle times are shown in minutes.

Comparison of the speed of shell liner placement using RME INSIDEOUT liner placement to conventional methods is not possible for the SAG mill B reline as no footage was captured prior to the new technology being implemented. However, the variability index (VI) is calculated for shell liner placement for this site and also for SAG mill C and plotted against the global MRD database in Figure 15. These results show that relines with RME INSIDEOUT liner placement present lower variability than many relines using conventional methods.

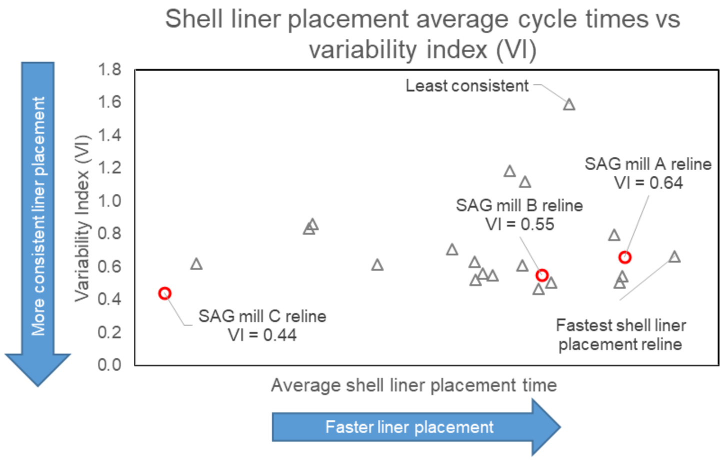


**FIG 15** – Shell liner placement speed versus VI.

### *Hazard exposure analysis*

Eliminating relining hazards by removing people from the mill is the main goal of implementing RME INSIDEOUT Technology. The sixth step of the automation journey is using RME INSIDEOUT Technology for removal and placement of all liners. This would eliminate the need for reliners to enter them mill for up to 95 per cent of activities in conventional relining.

Table 5 shows some of the hazard exposure metrics for SAG mill B and SAG mill C relines that implemented RME INSIDEOUT liner placement. Reduction in MHE has been calculated by estimating the typical number of workers used for placement during conventional relining compared to the MHE calculated from the computer vision analysis of actual reline footage from these two relines. A reduction of 6.3 and 22.4 man-hours of exposure has been estimated as the benefit of implementing RME INSIDEOUT liner placement in the SAG mill B and SAG mill C.

**TABLE 5**

Hazard exposure summary for two recent relines where INSIDEOUT Technology was implemented to reduce the exposure to hazards inside of the mill.

| **Metric** | **SAG mill B RME INSIDEOUT liner placement** | **SAG mill C RME INSIDEOUT liner placement** | **Units** |
|---|---|---|---|
| Step along Automation Journey (Step number) | 1 | 2 | - |
| Reline time RT – Inching | 27.5 | 106.8 | hours |
| Reduction in hazard exposure inside of the mill from INSIDEOUT (ΔMHEin) | -6.3* | -22.4 | hours |
| Man-hours of exposure inside per hours relining (MHEin,exc.inch/RT – Inching) | 2.1* | 2.5 | hours/ hours |

* when this technology was being used during the SAG mill B reline the reline crew members did not exit the mill, but instead took a rest break in an area of the mill away from the relining activities.

Figure 16 shows the reduction in man-hours of exposure inside of the mill on SAG mill B and C relines compared to equivalent conventional relines.

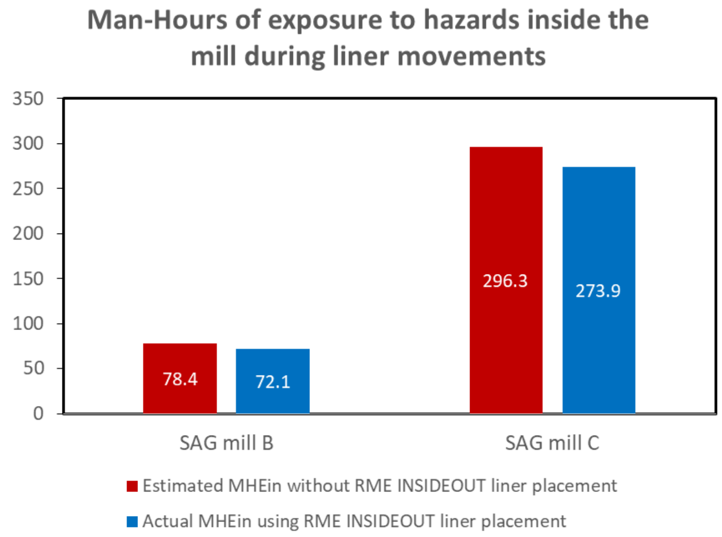


**FIG 16** – Man-hours of exposure to hazard reduction inside the mill during liner movements by using RME INSIDEOUT liner placement in SAG mill B and C.

Figure 17 shows the reduction in man-hours of exposure inside of the mill per hour of relining compared to equivalent conventional relines. These improvements to relining safety on SAG mill relines were achieved without negative impact on relining performance.

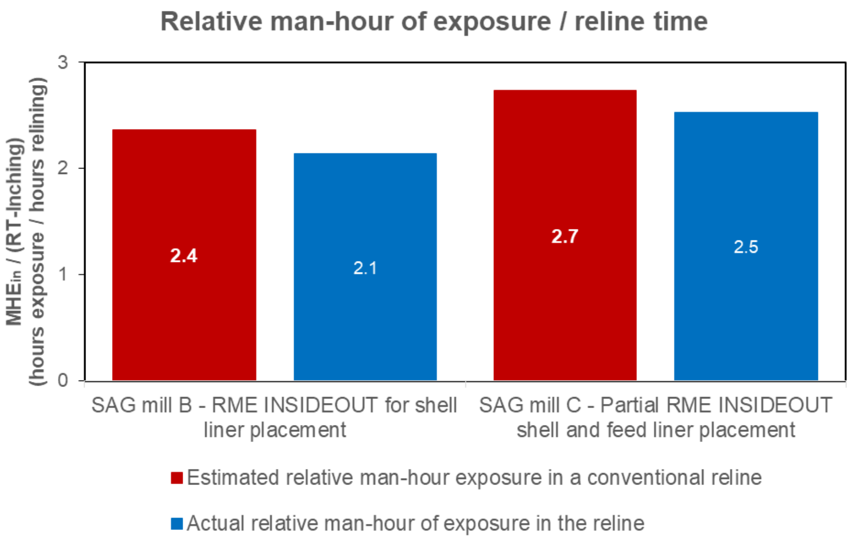


**FIG 17** – Safety risk reduction by using RME INSIDEOUT liner placement in SAG mill B and C.

## CONCLUSIONS

This paper has presented results from recent relines using technologies to automate the relining process. The data collected from these relines using new technologies was compared to a conventional reline. Automating reline activities shows improvements in the following areas:

- Safety is improved by reducing exposure to hazards using new semi-automated technologies both inside (RME INSIDEOUT Technology) and outside of the mill (THUNDERBOLT SKYWAY).
- Speed of knock-in activities is shown to be improved with the use of an automated system for movement of liner removal tools (THUNDERBOLT SKYWAY).
- Consistency of activity times is shown to be also improved by the new technologies. Improving consistency in individual relining activities is key to ensuring relines are finished on time.

A methodology for comparing relines with different reline durations and characteristics has been presented. This methodology relies on calculating relative metrics that can be used to compare relines and being able to recognise improvements in relining practices.


## ACKNOWLEDGEMENTS

As authors we acknowledge Dr John Russell and Dr Peter Rubie who have envisaged mill relining automation and facilitated its development and the associated investment, contributing thought leadership and mentorship to RME's technical personnel, product developers and engineers. We also note the strong collaborative relationship enjoyed with several RME colleagues and customers who have played significant roles in these technological developments, as early adopters.


## REFERENCES


Baas, D., & Mikhael Gurieff, L. (2018). Developing flotation circuit control and automation for the Phu Kham Copper-Gold peration concentrator. 14th AusIMM Mill Operators' Conference, Brisbane, Qld.

Deif, A. (2012). Assessing Lean Systems Using Variability Mapping. Procedia CIRP, 3, 2–7. https://doi.org/https://doi.org/10.1016/j.procir.2012.07.002

Ikaheimonen, T., Rubie, P., Gwynn-Jones, S., & Bohorquez, J. (2019). Implementing the first THUNDERBOLT SKYWAY with INSIDEOUT Technology at Cobre Panama. SAG 2019, Vancouver.

Ikaheimonen, T., Rubie, P., Gwynn-Jones, S., & Bohorquez, J. (2019). Implementing the first THUNDERBOLT SKYWAY with INSIDEOUT Technology at Cobre Panama SAG 2019, Vancouver, Canada.

Martinez, R., Rubie, P., Bohorquez, J., & Gwynn-Jones, S. (2019). Continuous Improvements in Mill Relining at Escondida SAG Conference, Vancouver.

Price, A., Okle, D., & Brooks, K. (2018). Glencore Mount Isa Lead Zinc Flotation Circuit – Experiences from the Implementation of Model Predictive Control. 14th AusIMM Mill Operators' Conference, Brisbane, Qld.

Ralston, J. C., Hargrave, C. O., & Dunn, M. T. (2017). Longwall automation: trends, challenges and opportunities. International Journal of Mining Science and Technology, 27(5), 733–739. https://doi.org/https://doi.org/10.1016/j.ijmst.2017.07.027

Rubie, P., Russell, J., O'Shannassy, G., & Yap, F. (2015). Simulation as a tool to enable world's best mill relining practice – a sense-making tool for decision makers SAG Conference 2015, Vancouver.

# Coarse particle retention testing on a ball mill at Lundin's Eagle Mine Humboldt concentrator

*R E McIvor[1], K M Bartholomew[2], O Arafat[3], S Daavettila[4] and E Savola[5]*

1. Chief Metallurgist, Metcom Technologies Inc, Grand Rapids, Minnesota, USA 55744. Email: rob@metcomtech.com
2. Senior Metallurgist, Metcom Technologies Inc, Grand Rapids, Minnesota, USA 55744. Email: kyle@metcomtech.com
3. Project Metallurgist and Business Development Manager, Metcom Technologies Inc, Grand Rapids, Minnesota, USA 55744. Email: omar@metcomtech.com
4. Mill Metallurgist, Eagle Mine, Champion, Michigan, USA 49814. Email: steve.daavettila@lundinmining.com
5. Lead Metallurgical Technician, Eagle Mine, Champion, Michigan, USA 49814. Email: elton.savola@lundinmining.com

## ABSTRACT

Ball mill media sizing investigations were carried out for the ball mill circuits grinding minus 12.5 mm crushing plant product at Lundin's Eagle Mine base metal concentrator in Humboldt, Michigan, USA. Batch grinding tests were carried out on mill feed with a torque-metered pilot mill with the same ball charge sizing (76 mm top size) as used in the plant. Calculated grinding rates of the coarsest particles were approximately four times higher for the plant mill than the pilot mill. One explanation is that coarser particles are retained in the continuous plant mill longer and thus exposed to more energy. This challenged the assumption used in population balance modelling that particles of all sizes, as well as the liquid, have the same residence time, as characterised by liquid tracer tests. A literature review revealed that this assumption is false, and that residence time as a function of particle size is not able to be determined precisely. To explore this further, a plant test was carried out by dosing a mill with 16–22 mm particles, coarser than any in the normal circuit feed, in conjunction with liquid residence tracing using salt and a conductivity probe. The test showed that the coarse particles were retained approximately twice as long as the liquid. It also showed that abrasion of these particles is contributing significantly to their size reduction.

## INTRODUCTION

As part of a ball size optimisation study for Lundin's Eagle Mine concentrator, located in Humbolt, Michigan, USA, a baseline comparison of plant versus pilot-scale torque mill cumulative grinding rates was conducted. These rates were approximately the same at fine sizes (less than 106 microns), but at coarsest particle sizes the rates were up to three to four times higher as measured in the plant versus the torque mill. These rates are shown in Figure 1.

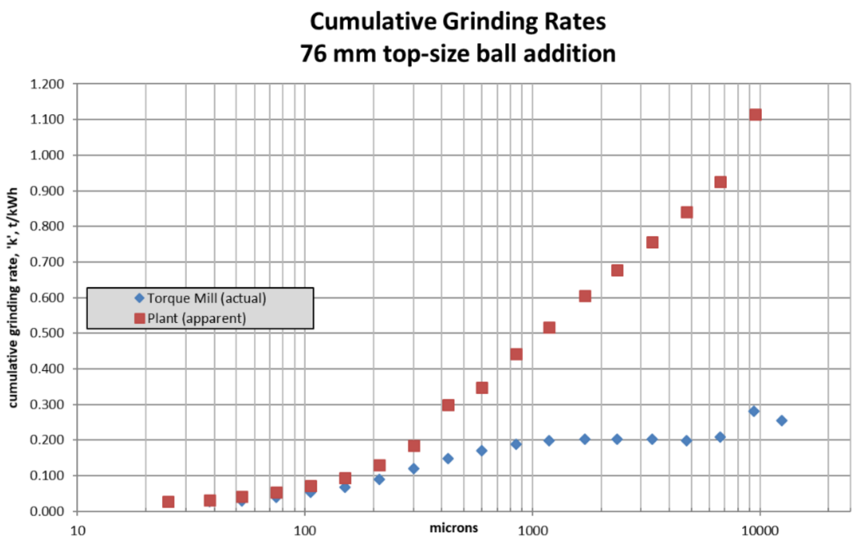


**FIG 1** – Plant versus torque mill grinding rates.

This was a curious result and prompted further investigation. The cumulative grinding rates, explained in more detail in the methodology section, are calculated from the mill feed size distribution, mill discharge size distribution, mill power draw, and residence time. One of the possible sources of the difference in the measured grinding rates is the retention time of particles in plant mill (unknown, and possibly size dependent) versus the torque mill (known, and size independent due to being a batch test). The plant mill retention time, as was investigated in a plant trial, is the focus of this paper.

# LITERATURE REVIEW

McIvor (2020) conducted an extensive literature review in relation to the historical development of population balance modelling. This review revealed a number of ball mill residence time studies in the literature including Davis (1945, 1946) and Hogg (1984). The Davis paper showed that the ball mill per cent solids, internally, did not match the per cent solids of the feed and discharge. This demonstrates a preferential retention of solids in the mill; ie solids retention time does not equal liquid tracer retention time. The Hogg paper, in a similar manner to Davis, states: 'essentially all reported investigations of transport in mills… reveal some evidence for the existence of internal classification effects.' From this review McIvor concludes, 'It is not possible, even with tracer particles, to decouple breakage and mill residence time as a function of particle size.' With understanding of this limitation, and with the previous literature findings in mind, an experiment to attempt to quantify the relative retention times of coarse particles versus liquid tracers was formulated and executed at the Eagle Mine.

# METHODOLOGY

The residence time plant experiment was initiated as part of the media size optimisation program for the Eagle Mine. A brief explanation of the media size optimisation methods is given below for context, particularly in regard to the calculation of the apparent cumulative grinding rate (ACGR). The liquid tracer test conducted in the plant, and the coarse particle retention time plant test details are also described in this section.

## Media size optimisation

Metcom Technologies Acerta™ ball mill media sizing test program is described in the literature (Conger, 2018; Bartholomew, 2019). The protocol utilises a torque-instrumented pilot-scale ball mill as shown in Figure 2.

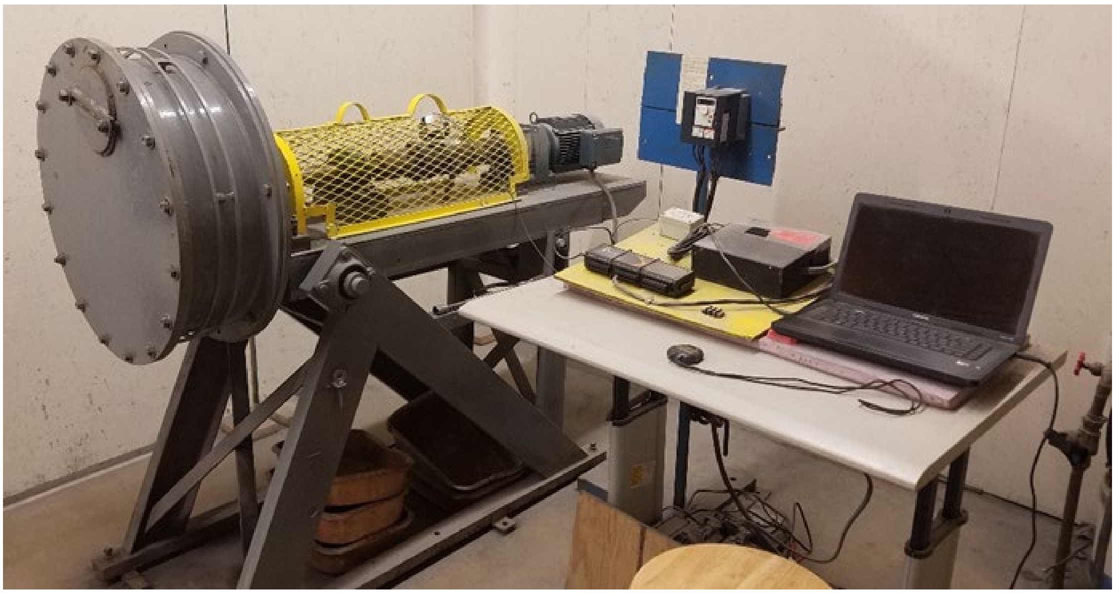

**FIG 2** – Acerta™ media size test apparatus.

The pilot mill is 0.6 m in diameter and 0.2 m long; normally operated at 65 per cent of critical speed. Over 30 graded ball charges, and mixes of ball sizes, have been constructed. A stage-gate approach starting with batch testing of plant ball mill feed samples, and concluding with locked-cycle testing of ball mill circuit feed samples is used to identify and confirm the best candidate ball charging practice for the particular ore and grind size objective of the plant.

The metric used to evaluate the performance of a given ball charge is the Functional Performance Mill Grinding Rate; McIvor (1988, 1991). The Functional Performance Equation is shown below with the Mill Grinding Rate in bold.

$$Q = MP \times CSE \times \underbrace{G \times MG_{eff}}_{\boldsymbol{MG_{rate}}}$$

where:

| | | |
|---|---|---|
| *Q* | = | metric tonnes per hour of new fines (<$P_{80}$) produced by the circuit |
| *MP* | = | mill power draw (kW, measured at pinion) |
| *CSE* | = | Classification System Efficiency (%) |
| *G* | = | ore grindability (grams per revolution) |
| $MG_{eff}$ | = | Mill Grinding Efficiency [(metric tonnes of new fines per kWh) / (g/rev)] |
| $\boldsymbol{MG_{rate}}$ | = | Mill Grinding Rate [(metric tonnes of new fines per kWh)] |

The mill grinding rate in plants is measured by populating the Functional Performance Equation using plant survey data (McIvor, 2006). Additionally, and of particular use in the case of batch torque mill tests, the same mill grinding rate can be calculated from a first-order rate equation as such (McIvor, 2020):

$$D_i = F_i \times e^{-k_i t}$$

where:

| | |
|---|---|
| $D_i$ | is the cumulative wt. % retained at size 'i' after grinding |
| $F_i$ | is the cumulative wt. % retained at size 'i' before grinding |
| $t$ | is the specific energy (kWh/t) |
| $k_i$ | is the cumulative grinding rate, at size class 'i' |

when 'i' is the size of interest (typically the ball mill circuit product $P_{80}$).

By measuring the feed and product size distributions, and the specific energy of the test or plant, the cumulative grinding rates can be calculated and plotted as was shown in Figure 1. In the case of the torque mill, where the exact residence time of all particles is known, the cumulative grinding rates are called 'actual', whereas in the plant mill, with unknown solids residence time, the rates are calculated with a plug-flow assumption, but are called 'apparent'. As was shown in Figure 1, a large difference in torque mill versus plant mill grinding rates was shown at the coarsest particle sizes. While there may be a number of factors contributing to the difference in grinding rates, this paper focuses on preferential coarse particle retention in the plant mill. If true, this would lead to a higher 'apparent' cumulative grinding rate because the coarse particles, in reality, spent more time in the mill which increases the specific energy (kWh/t) applied to them, as compared to the plug flow assumption. Properly accounted-for, this higher kWh/t would reduce the grinding rate closer to that measured in the torque mill. To explore this possibility of preferential coarse particle retention in a ball mill, two tests were planned and conducted at the Eagle Mine concentrator.

## Liquid tracer plant test

To represent what is expected to be the most mobile, and least retention time, material in the ball mill, a liquid tracer (conductivity) test was conducted. It is also presumed that as solid material is ground finer and finer that its retention time characteristics will become closer to that of the liquid. In the plant, salt was dosed into the mill feed while a conductivity probe inserted into the mill discharge stream was used to trace liquid movement through the mill. Since soda ash is used in the mill feed at this plant, an on/off trial was performed prior to the actual test to confirm there was no interference with the conductivity measurement; there was none.

During the actual test, salt was added to the mill feed at the exact same time as the coarse particles (described in next section). Conductivity was continuously measured and recorded at the mill discharge. It was expected to see a plot similar in shape to that shown in Figure 3 (Austin, 1984).

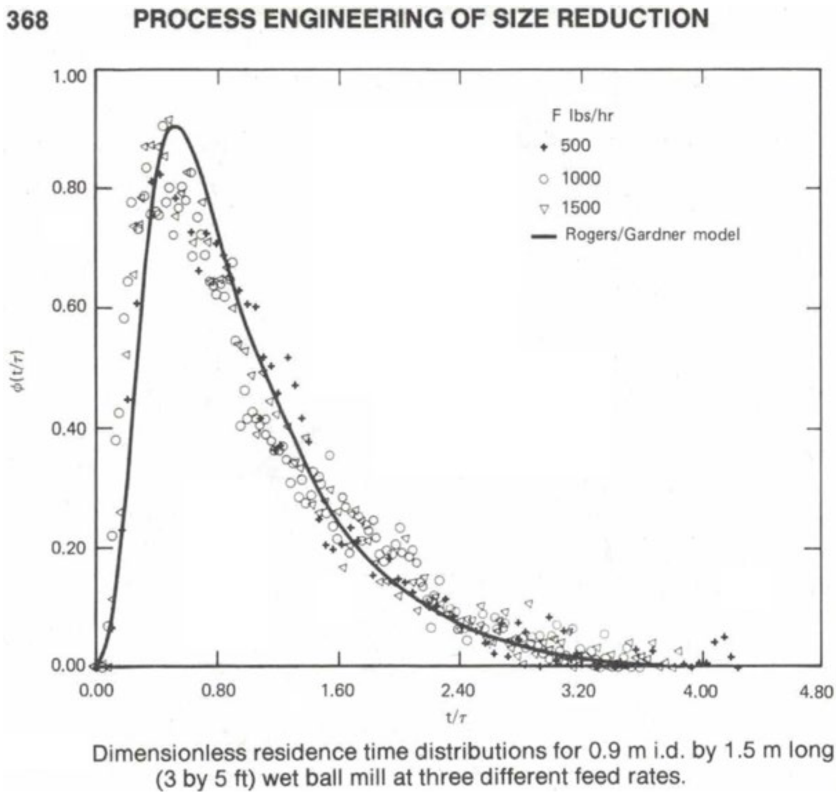


**FIG 3** – Published example of ball mill liquid tracer test results.

## Coarse particle retention time plant test

Ore fed to the Eagle ball milling circuit first passes through a crushing plant with a final closing screen having 12.7 mm (square) aperture. Plant sampling further confirmed that ball mill feed and discharge contain negligible +12.7 mm material.

Six 20 L pails of +16/-22 mm ore were prepared, slightly larger than the plant feed of -12.7 mm, in the laboratory from material collected in the crushing plant. These particles were also painted yellow as shown in Figure 4. It was hoped that these particles would be recoverable in the mill discharge by inserting a 16 mm screen into the mill discharge flow. The collection screen was 305 mm diameter, mounted on the end of a pole, and designed to be inserted a consistent distance and location into the middle of the mill discharge steam by sliding it along the grizzly screen bars, which are parallel to the discharge flow. Each cut was taken for an estimated ten seconds, by a 'one thousand and one; one thousand and two…' to ten count. The entire process was video recorded, allowing the timing of every step to be checked.


**FIG 4** – Sample of -16/+22 mm feed particles, painted yellow.

A pre-test trial was conducted with the discharge screen apparatus to evaluate performance. Large mill scats (20–40 mm) were dosed into the mill feed, and were detected by the screen device in the mill discharge approximately three minutes after the approximately 10 L of scats were dumped into the mill feed. This allowed for refinement of the sample collection technique and estimation of the quantity of close-sized (-16/+22 mm) that needed to be prepared for the actual trial.

## PLANT TEST OBSERVATIONS AND RESULTS

The test was conducted on August 1, 2018. Tonnage was 45 t/h (moist), and mill power draw was 709 kW. Approximate circulating load (by instruments) was 550 per cent. The ball mill is 3.20 m diameter and 4.88 m long.

Before the test, at approximately 9:30 am, 12 test cuts were taken with the coarse particle sampling screen at the mill discharge. Timing was ten seconds in the mill discharge stream, ten seconds out of stream to clear the screen into the collection bucket, for an overall cycle time of 20 seconds.

At 10:30 am, the salt and six pails of the prepared coarse particles were simultaneously dosed into the ball mill feed. This took 38 seconds to complete. From the dump point, onto the feed conveyor, to the mill feed is a transit time of ten seconds. Total weight of coarse particles dosed was 186 kg (dry) and the SG of the material was 3.4. Twenty kilograms of dry salt were added to the mill feed with the coarse rock. Conductivity measurements and coarse particle sampling at the mill discharge were started before material entered the mill.

The conductivity measurements display typical ball mill liquid tracer results. Allowing the ten seconds for conveying, the initial jump, from approximately 50 to over 3000 μS/cm, in the measurement took place at 1:44 into the test, 1 minute and 34 seconds from when the salt first entered the mill. It initially peaked at 3:48 into the test, dropped slightly until 3:56, and then started increasing again until 4:13, and then started falling off again. This indicates the return of salt laden recycle (cyclone underflow) water at 3:56 into the test. This is plausible, since it is close to the total elapse time it would take from the initial mill discharge (1:44), plus the time to pass through the sump and piping and cyclone (underflow) back to the mill (roughly, under one minute), plus another 1:34 to pass through the mill again. Data is shown in Figure 5.

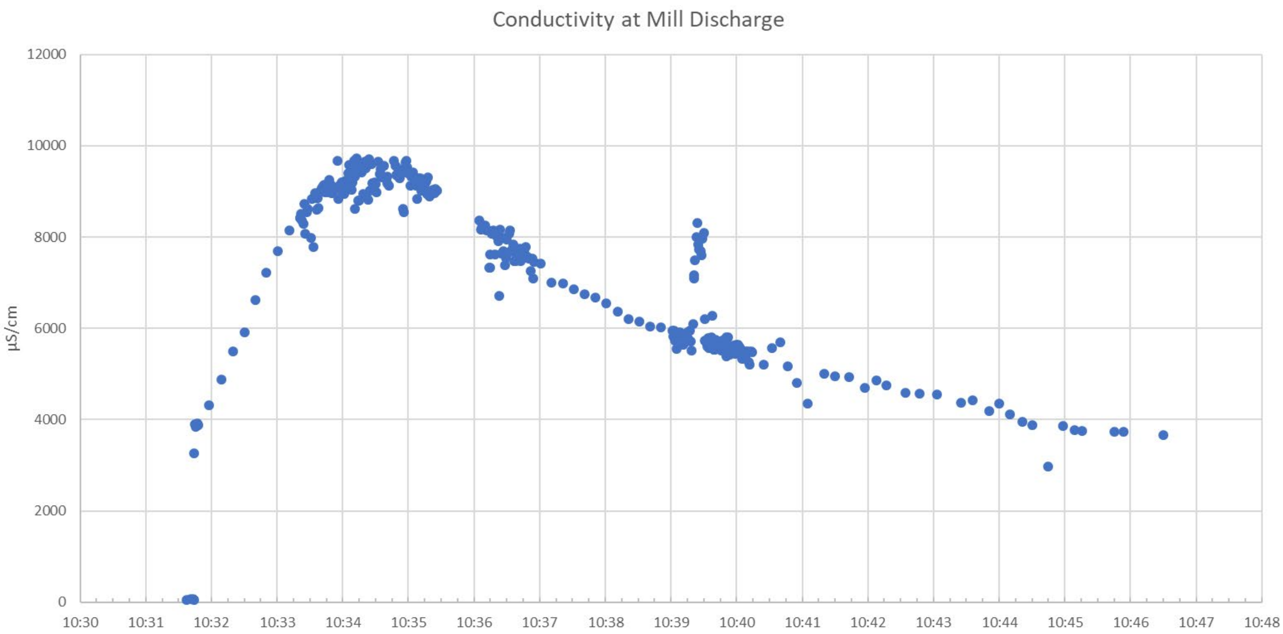


**FIG 5** – Conductivity probe results.

A total of 78 rocks were collected on the 16 mm screen during the sampling period with a total weight of 722 g, average 9.3 g per coarse particle. Much of the yellow paint was still visible on these rocks. The collected particles are shown in Figure 6.

**FIG 6** – Coarse particles collected at mill discharge.

As can be observed in Figure 6 the particles collected appear to be more rounded than the particles fed indicating abrasion (see feed particles in Figure 4). A group of 78 feed particles were weighed to characterise the weight lost due to abrasion. The total weight of 78 feed particles was 1055 g, or 13.5 g per particle. This indicates a weight loss of 30 per cent for the coarse particles collected, on average. Intuitively, this is a significant loss, and statistical tests confirmed. As shown in Figure 7, an F-test was conducted on the two sample populations to determine if the variances were unequal; which was true. Hence, a t-Test for two samples assuming unequal variances was conducted. This t-Test showed the mean weights of the feed and discharge sample populations to be different statistically.

Null hypothesis: no difference in variance

F-Test Two-Sample for Variances

| | *Variable 1* | *Variable 2* |
|---|---|---|
| Mean | 13.52 | 9.26 |
| Variance | 19.37 | 11.18 |
| Observations | 78 | 78 |
| df | 77 | 77 |
| F | 1.733 | |
| P(F<=f) one-tail | 0.008 | |
| F Critical one-tail | 1.458 | |

F > Fcrit so variances are unequal
Reject null hypothesis.
Use t-Test w/unequal variance.

Null hypothesis: no difference in means

t-Test: Two-Sample Assuming Unequal Variances

| | *Variable 1* | *Variable 2* |
|---|---|---|
| Mean | 13.52 | 9.26 |
| Variance | 19.37 | 11.18 |
| Observations | 78 | 78 |
| Hypothesized Mean Difference | 0 | |
| df | 144 | |
| t Stat | 6.821 | |
| P(T<=t) one-tail | 0.000 | |
| t Critical one-tail | 1.656 | |
| P(T<=t) two-tail | 0.000 | |
| t Critical two-tail | 1.977 | |

t Stat > t Crit (two tail), so means are statistically different.
Reject null hypothesis.

Conclusion: With very high statistical confidence, the average weight of a feed particle (-22 x +16 mm) was higher than the mill discharge coarse particles (+16 mm).

**FIG 7** – Statistical analysis of feed and discharge sample population weights.

The timing of the coarse particles was recorded and is plotted in Figure 8.

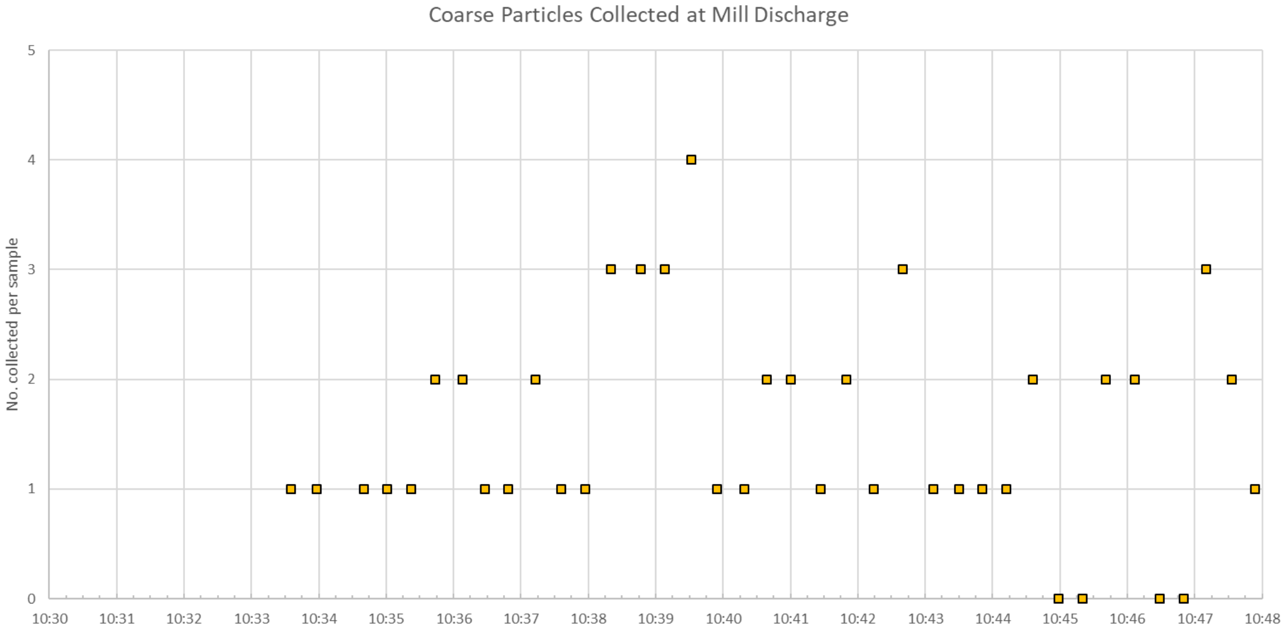


**FIG 8** – Coarse particles collected versus time.

The first particle collected was during the 10:33:25 to 10:33:35 time period, or about 3.5 minutes after the start of the test. This is approximately twice as long as it took to measure the first indication of liquid tracer by conductivity. This can be seen in Figure 9 where both liquid tracer and coarse particle collections are superimposed versus time.

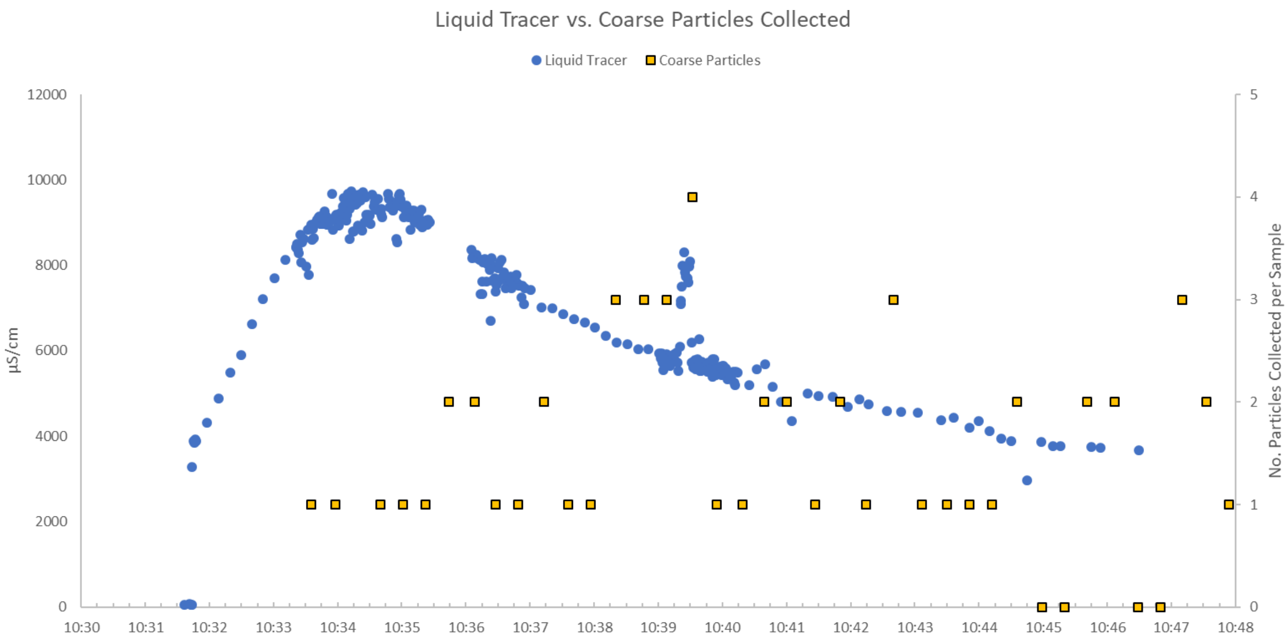


**FIG 9** – Liquid tracer and coarse particle collection versus time.

Based on the low number of particles collected, it is quite possible particles were present, but missed in the previous cut taken at 10:33.05 to 10:33.15, or close to 3.0 minutes from the time they first entered the mill. Also, since it took 38 seconds to empty the solids into the mill, the 'start' time could be extended by the time it took a substantial quantity of particles to enter the mill, say, the average time of 19 seconds. Both these adjustments would reduce the measured initial residence time of the coarsest particles to (no less than) approximately 2 minutes and 40 seconds. This does not change the conclusion that the coarse particles have a significantly longer residence time than the liquid.

There was a slight 'surge' in coarse particle count from 10:38.20 to 10:39.31. A second slight 'surge' may have occurred again from 10:47.10 to 10:49.27. This second 'surge' might be attributed to recycle of the first 'surge'. However, based on the low number of particles collected, the recycle probably had little effect on the number of particles collected. Based on the size (diameter of 305 mm) of the screen versus the discharge stream, roughly ¼ of the stream was cut. Since the screen was in the discharge stream close to 50 per cent of the time, a rough estimate would be that 10–15 per cent of all the particles in the discharge were collected. The count was close to 80. Therefore, there were roughly 550 to 800 total in the discharge during the collection period. This compares to the number initially dosed of approximately (155 kg × 1000/13.2 g each =) 12 000 rocks, for a survival rate of, say, (700/12 000 =) 6 per cent. Then, 6 per cent of 700 equals 40 likely survivors of a second trip through the mill. Collection of 10–15 per cent of these results in about five total. So, it is likely that very few recycled rocks were collected.

If we accept there was indeed an initial 'surge' (or peak) in the discharge rate of the particles, it occurred at close to 9 minutes into the test (10:39). Comparison with the initial peak in the conductivity measurements (at 10:33.48) puts the particle residence at just over two times that of the liquid.

## CONCLUSIONS

The plant test successfully demonstrated a measurable difference between the liquid tracer residence time in the ball mill versus the coarse particles charged to the mill. The approximate difference in residence time is a factor of two with the coarse particles taking twice as long as the liquid tracer to appear in the mill discharge. However, the small number of coarse particles collected makes the analysis of the full residence time curve difficult. A test with a larger amount of coarse particles dosed, and perhaps a larger sampling screen could help improve the measurement in the future.

The results of this test show that it is incorrect to assume, for modelling and calculation purposes, that the residence time of coarse solids in a ball mill is the same as, or close to, the residence time of liquids.


## ACKNOWLEDGEMENTS

The authors would like to acknowledge Lundin Mining for allowing them to conduct and publish the results of this test. The authors would also like to acknowledge the support of ME Elecmetal in the general development of the media size improvement program which prompted this study.


## REFERENCES


Austin, L.G., 1984. Process Engineering of Size Reduction: Ball Milling. Society of Mining Engineers of the AIME.

Bartholomew, K.M., 2019. A Method for Ball Mill Media Sizing for Different Upstream Processes. SAG Conference Proceedings.

Conger, W., Dupont, J.F., McIvor, R.E., Weldum, T.P., 2018. Advances in Industrial Ball Mill Media Sizing. Proceedings of the 2018 Annual Meeting of the Society of Mining, Metallurgy, and Extraction Engineers.

Davis, E.W., 1945/46. Pulp Densities within Operating Ball Mills, T.P. 1843, Min. Tech., May; and AIME Trans., V. 169, Richards Memorial Volume on Milling and Concentration, pp. 155–159.

Hogg, R., 1984. Mass Transport Models for Tumbling Ball Mills. Control'84, AIME, pp. 55–61.

McIvor, R.E., 1988. Technoeconomic Analysis of Plant Grinding Operations, Ph.D. Thesis, 1988, McGill University.

McIvor, R.E., 1991. The use of functional performance analysis for plant grinding media testing and selection. Proceedings of The Copper Conference, 1991.

McIvor, R.E., 2006. Industrial validation of the functional performance equation, Mining Engineering, November 2006, pp. 47–51, (The Society for Mining, Metallurgy, and Exploration, Inc: Englewood, CO)

McIvor, R.E., 2020. The Truth About Population Balance Modelling. CMP Proceedings.

# Continuous improvement at Edikan (with MillROC support)

*O Oblokulov[1], S Green[2], D Van Der Spuy[3] and M Becker[4]*

1. Processing Manager, Perseus Mining Limited, Accra Ghana.
   Email: oblokul.oblokulov@perseusmining.com
2. Group Operations Metallurgist, Perseus Mining Limited, Subiaco WA 6008.
   Email: stephen.green@perseusmining.com
3. MAusIMM, Technical Director, Process IQ Pty Ltd, Balcatta WA 6021.
   Email: daniel@processiq.com.au
4. MAusIMM, Senior Metallurgist, Orway Mineral Consultants, East Perth WA 6004.
   Email: michael.becker@orway.com.au

## ABSTRACT

One of the blessings associated with operating a modern metallurgical facility is the multitude of technologies, techniques and processes available to improve and optimise circuits. Circuit optimisation is typically an important KPI (key performance indicator) for many metallurgical operations and its staff. Diverse process teams, often consisting of different disciplines ranging from operations experts to off-site consultants, working together to enact positive change. Underpinning this effort is the culture cultivated by management to unify the ideas and focusing the efforts toward a common goal of system improvement.

This paper provides background on the different aspects of the project, the challenges faced, the changes made and the results achieved. Specific focus is given to upgrades made to instrumentation (ie installation of MillSlicer), implementation of advanced process control (MillStar) and providing real time consultation and coaching (via MillROC).

The results of the project include better insights into what's happening inside the mill, improved process stability, consistency of operation and better utilisation of mill power. Optimisation of the ball charge and steel-to-rock ratio also resulted in more efficient milling and greater throughput.

Based on the actual circuit throughput trajectory before circuit optimisations, the net circuit benefit in terms of fresh feed processed was initially estimated at +8.5 per cent in actual terms. It is interesting to note that the circuit bottleneck then moved to the stockpile vibrating feeders, which were operating at maximum output, requiring physical upgrades to further debottleneck circuit throughput. After removal of these bottlenecks and further optimisation the circuit throughput increased to 950 t/h (January 2020 average) from the 814 t/h average in April 2019, a further +15.8 per cent benefit in average instantaneous throughput. This further benefit is attributable to a combination of MillROC consultation, improved process control, Mine-to-Mill optimisation, softer feed blends (from November 2019 onwards) and plant modifications.

All up from implementation this team ethos of optimisation in combination with state-of-the-art technology and specialist consultants has resulted in a sustainable increase of 27 per cent in 8 months which will result in tens of millions of dollars in increased revenue a year at reduced operating costs, significantly improving the project economics.

Long-term benefits to liner life and media consumption are currently under investigation.

Optimisation cannot be a once-off exercise; if not continuous, the results deteriorate quickly over time. The optimisation at Edikan is therefore an ongoing team effort, supported by remote data access, analysis, modelling and consultation.

## INTRODUCTION

The Edikan Gold Mine is 90 per cent owned by Perseus Mining Limited and located in Ghana, in the Ashanti Gold belt known for a number of high-profile gold projects. Production commenced in 2011 with gold production over 1.58 Moz to date. Ore is supplied from multiple deposits, with mineralisation occurring in two principal modes: disseminated pyrite-arsenopyrite mineralisation associated with quartz veining and sericite alteration hosted by granitoids and shear-zone hosted mineralisation associated with pyrite-arsenopyrite mineralisation in and adjacent to quartz veins in deformed, fine-grained metasedimentary rocks. The yearly production target was set at 6.7 Mtpa of ore to produce approximately 180 000 to 200 000 ounces of gold per annum.

Orway Mineral Consultants (OMC) provided circuit design reviews during the original project inception and design as well as follow-up up circuit surveys and operational reviews. Although these evaluations are exceptionally useful from a value-add perspective, they evaluate specific periods only and are not frequent enough to cater for the dynamic changing operation of the circuit. In most cases, the lack of continual evaluation and implementation of change result in lost revenue, ie opportunity cost losses due to optimisations that could have been implemented sooner.

A period of declining throughput prompted site to pursue various optimisation projects, consisting of Mine to Mill optimisation, advanced instrumentation (MillSlicer), advanced process control (MillStar) and ongoing, real time consulting services (MillROC). MillROC (Milling Remote Optimisation Consulting) is provided by OrwayIQ and consists of frequent and real time feedback to the operations based on live data. Orway IQ is a JV company, harnessing the modelling and consulting expertise of OMC and the control and cloud-based platform of ProcessIQ, to deliver real time consultation and coaching.

The initial installation and set-up of MillSlicer, MillStar and MillROC was completed by April 2019. The rapid and frequent feedback enabled significant optimisation through the ongoing MillROC service during a period where changes to the feed blend resulted in challenging operating conditions.

## CIRCUIT DESIGN

The Edikan comminution circuit consists of a primary crusher feeding a single stage semi-autogenous grinding mill (1C SS SAG) operating in conjunction with a pebble crusher. The simplified flow sheet is shown in Figure 1 and a photograph of the comminution circuit in Figure 2.

The circuit design criteria are summarised in Table 1, with Tables 2 and 3 summarising the crushing and milling equipment specifications.

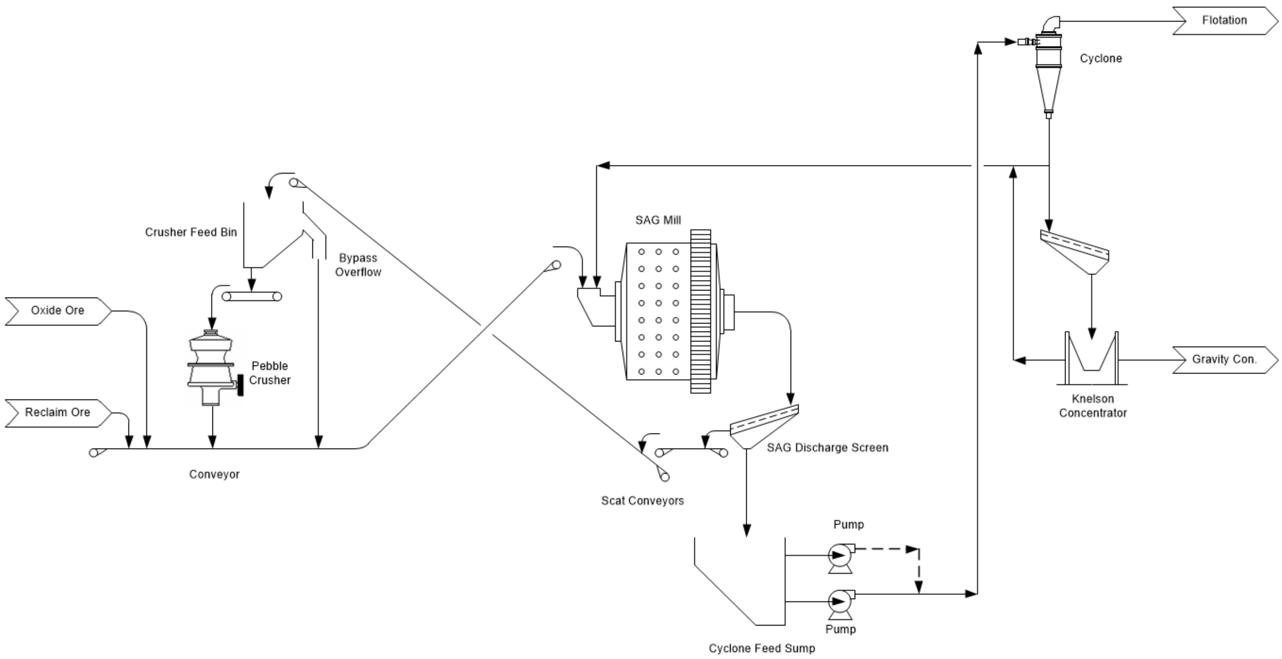


**FIG 1** – Simplified flow sheet.

**FIG 2** – The Edikan SS SAG mill.

**TABLE 1**
Design criteria.

| **Parameter** | **Units** | **Design** |
|---|---|---|
| Plant throughput | Million t/annum | 6.5 |
| Head grade | g/t Au | 1.0 |
| Recovery | % | 87 |
| Crushing | | |
| Availability | % | 75 |
| Throughput | t/h | 989 |
| Milling | | |
| Availability | % | 91.3 |
| Throughput | t/h | 813 |
| Grind size $P_{80}$ | µm | 212 |
| Ore characteristics | | |
| UCS | MPa | 76–165 |
| Abrasion index | g | 0.20–0.45 |
| Bond rod work index | kWh/t | 12.1–19.1 |
| Bond ball work index | kWh/t | 11.6–17.1 |
| JK drop weight parameters (Axb) | - | 28.0–80.7 |

**TABLE 2**

Major comminution equipment – crushing.

| Parameter | Units | Value |
|---|---|---|
| Primary crusher | | |
| Make | - | FLSmidth |
| Model | - | 1400 × 2100 TS |
| Number installed | - | 1 |
| Installed power | kW | 600 |
| Pebble crusher | | |
| Make | - | Sandvik |
| Model | - | CH660 |
| Number installed | - | 1 |
| Installed power | kW | 315 |

**TABLE 3**

Major comminution equipment – milling.

| Parameter | Units | Value |
|---|---|---|
| SS SAG mill | | |
| Make | - | FLSmidth |
| Inside shell diameter | m | 10.36 |
| Effective grinding length | m | 6.10 |
| Imperial measurements (flange to flange) | ft × ft | 34.0 × 22.0 |
| Installed power | kW | 14 000 |

## OPERATIONAL DATA

To effectively quantify the before and after effect of the continual improvement initiatives (Blasting pattern, MillROC, MillSlicer, MillStar etc), a review of operational data in relation to the various implementation dates of ongoing projects are required. Thereby accounting for external factors that may already be influencing the circuit, prior to, or at the same time as other modifications or circuit changes (Napier-Munn, 2014).

Major circuit changes were recorded, reflective of operating personnel feedback and observations made during the various evaluation periods. This gives a firsthand account of factors which influenced the Edikan circuit performance, such as when the MillSlicer data came online and the initial feedback was given from 06 April 2019.

Where changes to the operational data is noted, the preceding corresponding cause is highlighted (where known). This will be discussed in relation to the relevant circuit changes put forward to counteract negative circuit trends and improve the overall circuit efficiency.

A review of the long-term throughput data, contributing feed blend, received $F_{80}$ feed size and achieved $P_{80}$ product size was analysed to account for uncontrolled circuit inputs (ore hardness and feed size) and control targets (throughput and grind). A circuit power efficiency evaluation is therefore useful to normalise these factors and achieve a like-for-like comparison (Putland, 2019).

## Long-term throughput data

Figure 3 depicts the long-term daily dry throughput achieved in the circuit, with specific reference to the period leading up to the implementation of the MillROC system and associated circuit optimisation. When considering the increased ore hardness, it is safe to assume that the declining throughput would have continued if intervention was not initialised by plant personnel.

Key observations include the cyclical nature of the SAG power draw (as shown by the bright blue line) increasing as the liner mass loss is offset by a higher overall SAG total charge (as the same weight set point). The recorded throughput (dark blue circles) has a high degree of variability, and changes depending on the feed blend ore characteristics.

Similarly, as shown by the black line, the amount of oxide decreased which contributes to the throughput. Two key events to note is shown by the red line (when MillSlicer was implemented) and the light grey line indicating when the mining powder factor was increased. Considering the feed blend change for the period and associated increase to ore hardness, it is expected that the downward throughput trajectory would have continued if intervention was not implemented.

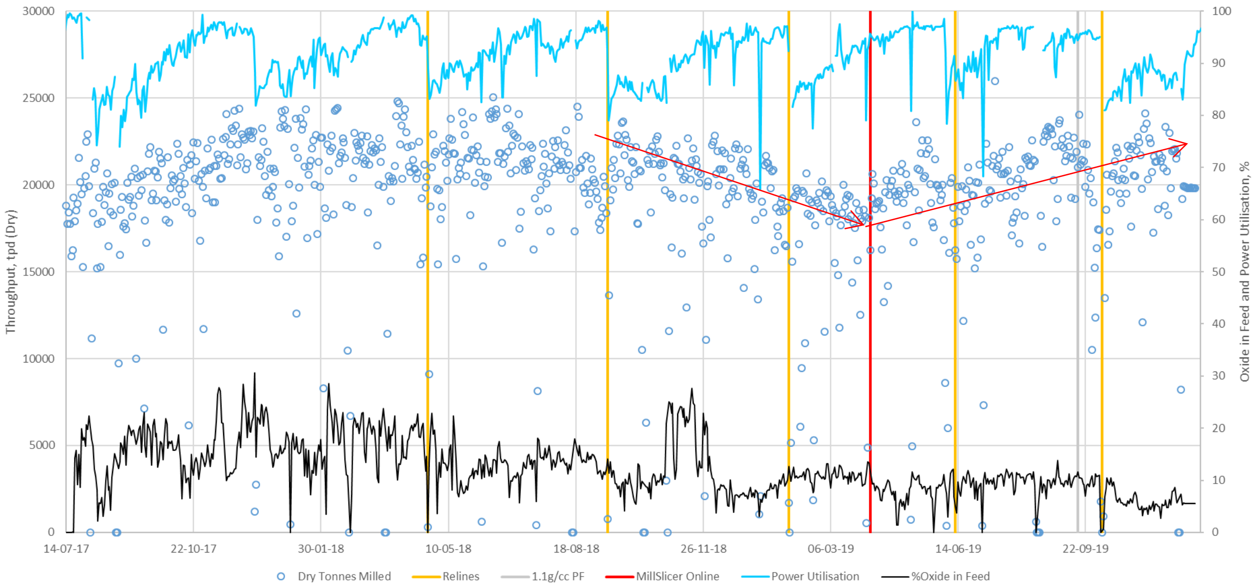


**FIG 3** – Long-term throughput data.

Figure 4 illustrates the recorded feed blend to the Edikan circuit which corresponds to the long-term throughput data with Table 4 summarises the associated comminution characteristics. It is important to note that the feed blend corresponds to increasing quantities of harder ore material. This is especially noticeable from December 2018, where Esuajah North material became the predominant fresh feed component, while the oxide component remained fairly well regulated, although at slightly reduced levels. From November 2019 onwards a small component of Bokitsi (softer) ore has formed part of the feed blend.

It should be noted that Run-of-mine (ROM) denoted material stockpiled prior to crushing with untracked blend, and Coarse Ore Stockpile (COS) material denoted stockpiled feed prior to milling with untracked blend.

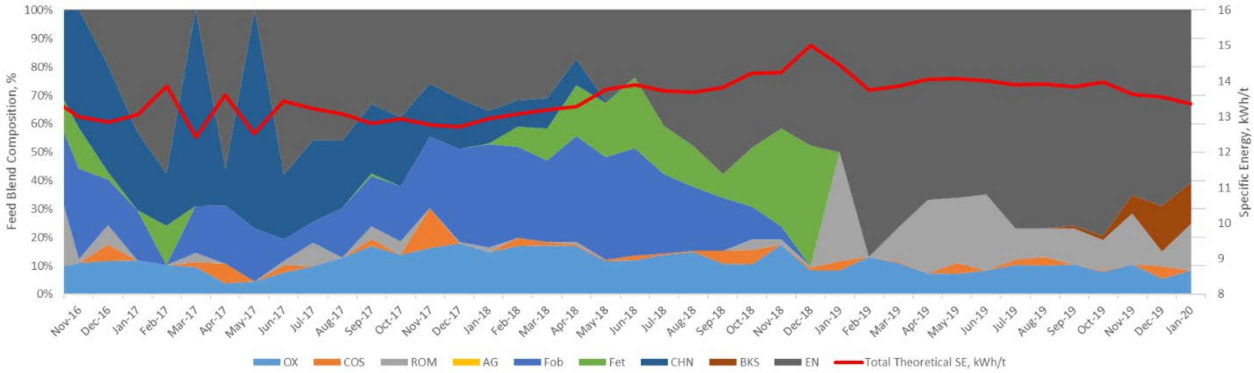


**FIG 4** – Long-term feed blend and theoretical SE.

**TABLE 4**

Feed sources and comminution characteristics.

| Feed source | Abbreviation | BWi, kWh/t | Axb |
|---|---|---|---|
| Abnabna Gap | AG | 13.8 | 49.1 |
| Bokisti | BKS | 14.3 | 68.4 |
| Chirawewa | CHN | 13.4 | 48.4 |
| Esuajah North | EN | 15.9 | 41.6 |
| Fetish | FET | 16.8 | 32.2 |
| Fobinso | FOB | 14.9 | 47.9 |

The total theoretical specific energy (SE) highlights the expected grinding energy required to achieve the grind target. The theoretical energy calculations are based on the 85th percentile BWi and 15th percentile Axb design values where available.

## Power efficiency evaluation

As part of OMC's standard procedure to evaluate circuit efficiency, the Operating Work index is used as defined in Equation 1, which accounts for circuit variability typically associated with changes in the mill power draw, feed/product size distribution variations and circuit inefficiencies.

Operating Work Index, kWh/t:

$$W_{io} = \frac{SE}{10\left(\frac{1}{\sqrt{P_{80}}} - \frac{1}{\sqrt{F_{80}}}\right)} \tag{1}$$

Where, SE, kWh/t:

$$SE = \frac{(SAG\ Power\ ) * Eff_{DriveTrain}}{Throughput} \tag{2}$$

The feed size ($F_{80}$) is based on the average of the measured fresh mill feed, as a combination of both physically sampled (belt cut) and digitally estimated (WipFrag) data. The product size ($P_{80}$) is taken as the average of the shift samples used to monitor the daily circuit performance.

It should be noted that the drive train efficiency ($Eff_{DriveTrain}$) was assumed to remain constant for the evaluation period, as this relates to the energy losses from where the power consumption is measured (incomers) to where the power is utilised (pinion power).

Another evaluation matrix typically considered is the circuit $f_{SAG}$, which denotes the circuit efficiency of a single stage SAG milling configuration when evaluated against a typical SABC circuit receiving a 150 mm feed $F_{80}$ and grinding down to a product $P_{80}$ of 75 µm and using the laboratory Bond Ball mill work index (BWi) as typically used by OMC (Siddall, 1996).

The $f_{SAG}$ therefore takes into account the breakage inefficiency typically not correctly represented by the Bond equation. Equation 3 defines the $f_{SAG}$ calculation, with Edikan having an averaging $f_{SAG}$ of 1.3.

SAG Circuit Efficiency Factor:

$$f_{SAG} = \frac{(Total\ SE) + \left(10*\mathrm{BWi}*\left(\frac{1}{\sqrt{\mathrm{F}_{80}}} - \frac{1}{\sqrt{150000}}\right)\right) + \left(10*\mathrm{BWi}*\left(\frac{1}{\sqrt{75}} - \frac{1}{\sqrt{\mathrm{P}_{80}}}\right)\right)}{10*\mathrm{BWi}*\left(\frac{1}{\sqrt{75}} - \frac{1}{\sqrt{150000}}\right)} \tag{3}$$

Figure 5 shows the mill power utilisation (as a percentage of the installed power) and the calculated operating work index as normalised data points on a time relationship basis. As shown by the operating work index, when accounting for changes in the circuit power draw and grind target, the inferred ore hardness has been increasing steadily, typically associated with increased quantities of fresh material as mining advances progressively deeper into the pit.

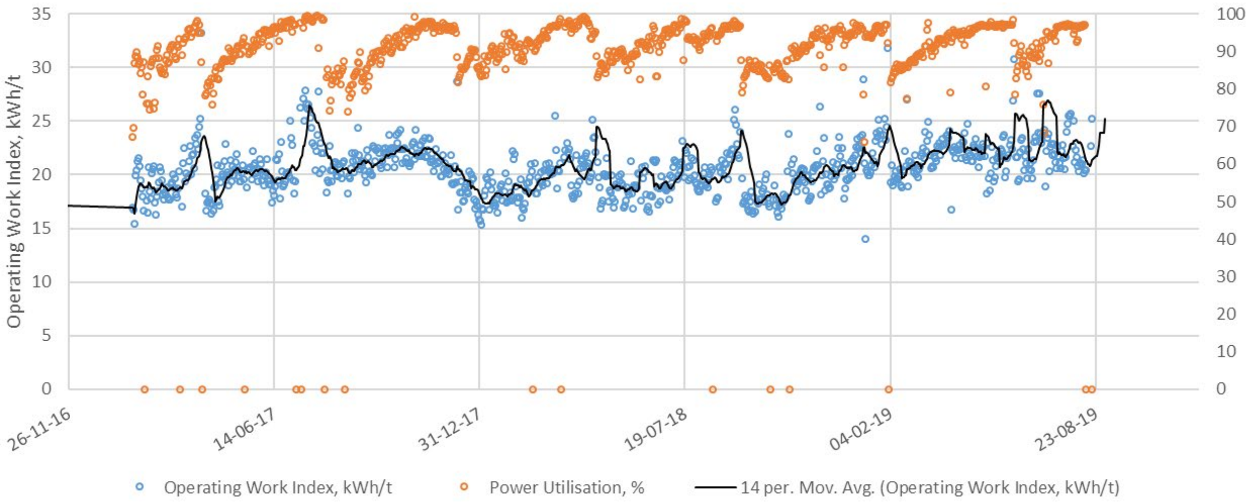


**FIG 5** – Operating Work Index (Wio) versus Time relationship.

It is interesting to note how the utilisation of installed power (ie operating power as a per cent of installed power) is affected by relining periods, typically occurring every 4.0 to 4.5 months as the historic baseline.

It should be noted that the SAG mill effectively operates at maximum output as a fixed speed mill, despite having a VSD drive installed. This is due to higher than tolerable vibrations being encountered within the drive train when transitioning through the lower speed range spectrum. Fluctuations to the mill power draw is therefore mainly a function of the SAG operating volume and steel charge.

Relining typically results in a drop to the SAG mill power draw, due to lower operating mill volume when operating at the pre-reline SAG weight (or bearing pressure) set point. This effect is counteracted by the fresh (unworn) lifter angle having a fairly aggressive ball trajectory which emphasises breakage in the SAG mill. The operational risk is therefore having a too low SAG operating volume for the aggressive ball trajectory, which increases the likelihood for steel ball to steel liner impacts. Optimisation of the pebble port fraction of total grate open area is used to further manage this risk (Putland, 2018).

Figure 6 depicts the Cumulative Sum (CUSUM) analysis of the SAG mill specific grinding energy (SGE) for the circuit. As shown, compared against a constant SGE of 13.5 kWh/t, the inferred ore hardness was softer than average leading up to January 2019. The SGE inverted post January 2019, indicating significantly harder than average ore characteristics were being processed during the optimisation period.

The Operating work index and SGE recorded is expected to follow each other closely, as no ball mill is available to influence the power split. The pebble crusher is therefore used to coarsen the circuit grind target.

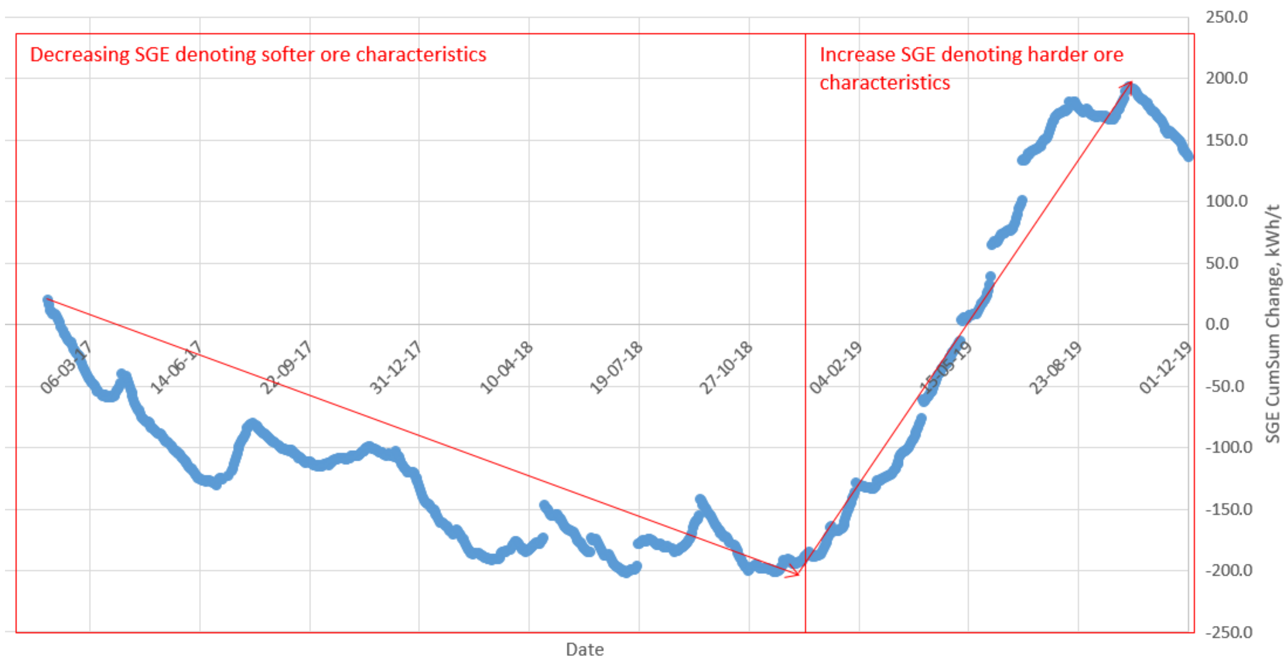


**FIG 6** – SAG mill specific grinding energy cumulative sum.

## Comparative throughput and grind analysis

Since long-term data obscures numerous smaller effects influencing circuit operability, it is useful to evaluate more detailed operational data directly before and after circuit changes, to better establish a like-for-like comparison.

For the comparison, an evaluation period of 128 days (64 before and 64 after the MillROC implementation period) was considered. It is important to note that this is associated with the initial optimisation and operational changes, namely setting the optimal operating mill weight set point and accompanying ball addition rate.

In the case of the Edikan data, there were a number of fortuitous factors occurring which greatly simplified such an evaluation. Most notably, Figure 7 gives a higher resolution view of the feed blend to the circuit directly before and after April 2019 implementation data. As shown, the primary feed source did not change significantly, with an actual reduction to the oxide proportion fed to the mill.

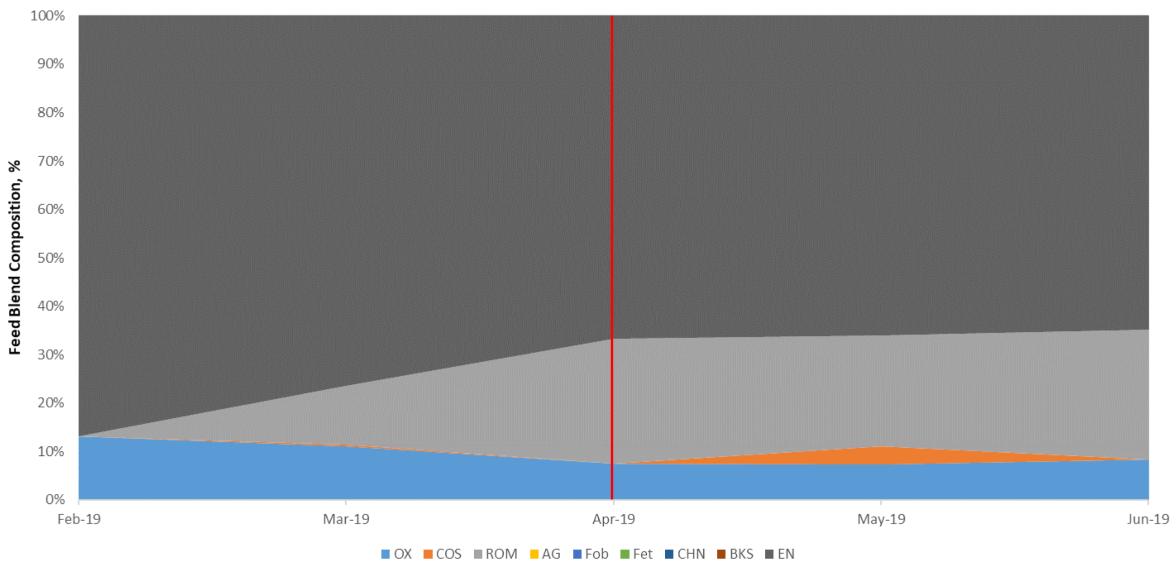


**FIG 7** – Comparative period feed blend.

Figure 8 depicts the near instantaneous throughput improvement by operating the SAG mill at an improved breakage state, while the circuit grind improvement was being maintained at constant levels. Figure 9 shows the corresponding mill feed PSD data as recorded. Throughput benefits were therefore achieved despite the mill feed size ($F_{80}$) and fines content (%Passing 50 mm sieve) not changing significantly either before or after optimisation and without compromising the circuit grind target.

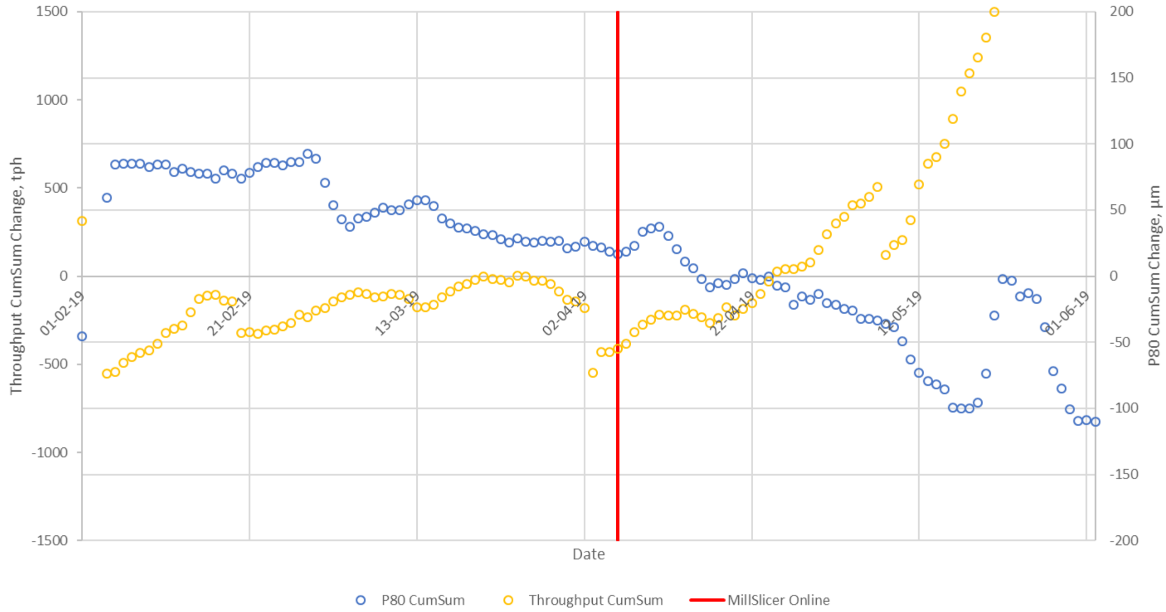


**FIG 8** – Comparative throughput rate and circuit grind $P_{80}$.

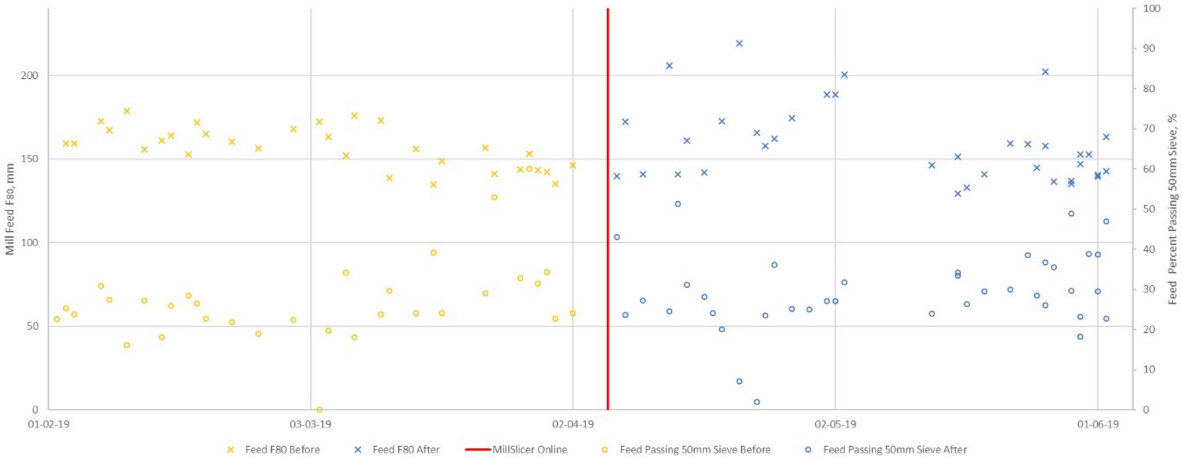


**FIG 9** – Comparative feed PSD change.

Before implementing changes, the mill feed PSD was shown to improve, but despite this, throughput rates continued to decline. Conversely, after implementing optimisation changes, throughput continued to improve, despite coarsening of the mill feed PSD. This is pertinent as deviating from typical SAG mill considerations (Putland, 2011) requires specific control philosophy considerations to maintain optimal performance.

Since the daily data points tend to obscure frequent circuit changes associated with the overall stability and control of the circuit, the average five minute data for the before and after period is compared in the histogram format, to indicate the relative shift in overall accuracy and precision. Figure 10 depicts the change in SAG mill Power draw, where Figure 11 shows the reclaim feed rate. Similarly, Figure 12 depicts the cyclone pressure control and Figure 13 the circuit grind $P_{80}$.

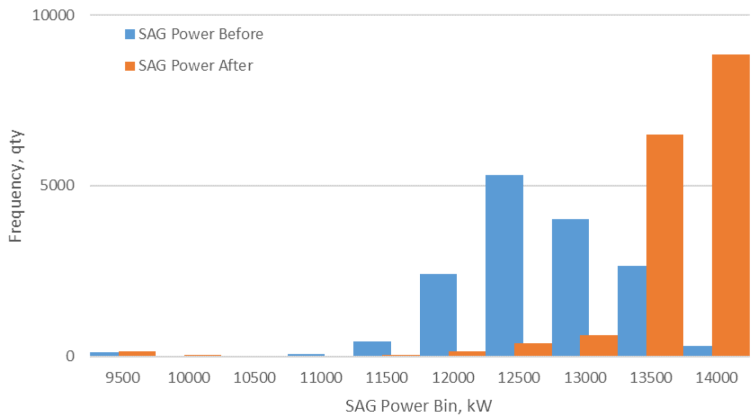


**FIG 10** – SAG power bin.

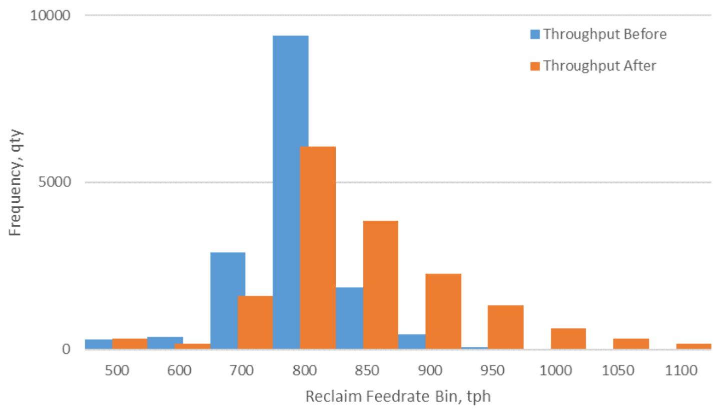


**FIG 11** – Reclaim feed rate bin.

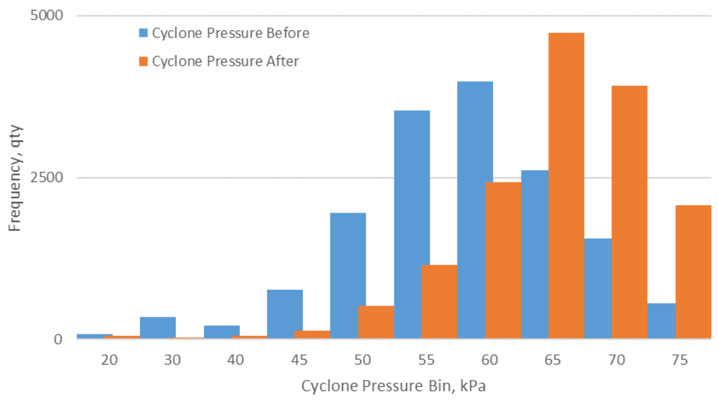


**FIG 12** – Cyclone pressure bin.

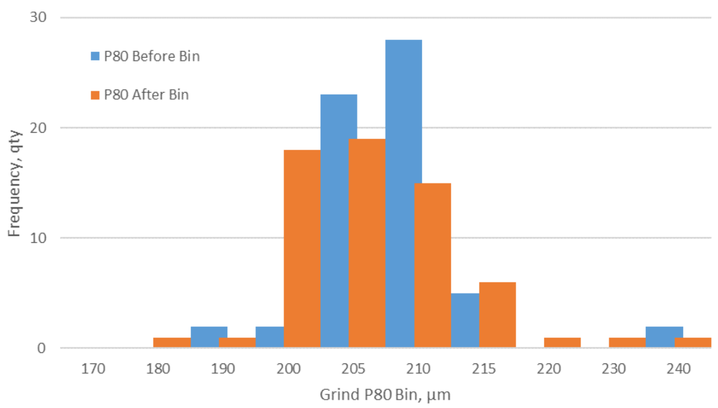


**FIG 13** – Circuit grind $P_{80}$.

One of the future optimisation targets under consideration is relaxing the circuit grind to a $P_{80}$ of 280 µm, at which point throughput can be further maximised. Downstream recovery past this point requires careful consideration, as it can impact the overall profitability.

## Mill control

To visualise the operating conditions within the SAG mill, Figures 14 and 15 depict the MillSlicer data interpretation as recorded before (when brought online 6 April 2019) and after the SAG weight setpoint has been adjusted and allowed to stabilise (25 April 2019).

It is important to note the ‘sawtooth’ pattern as recorded in the impact intensity graph, signifying significant ball on liner impacts, with reverberations recorded throughout the mill shell. After appropriate adjustments to the SAG weight (volume), a notable drop to the maximum impact intensity was recorded. This signifies reduced liner damage and optimised breakage by aligning the estimated toe of the charge to the maximum recorded intensity angle within the SAG mill.

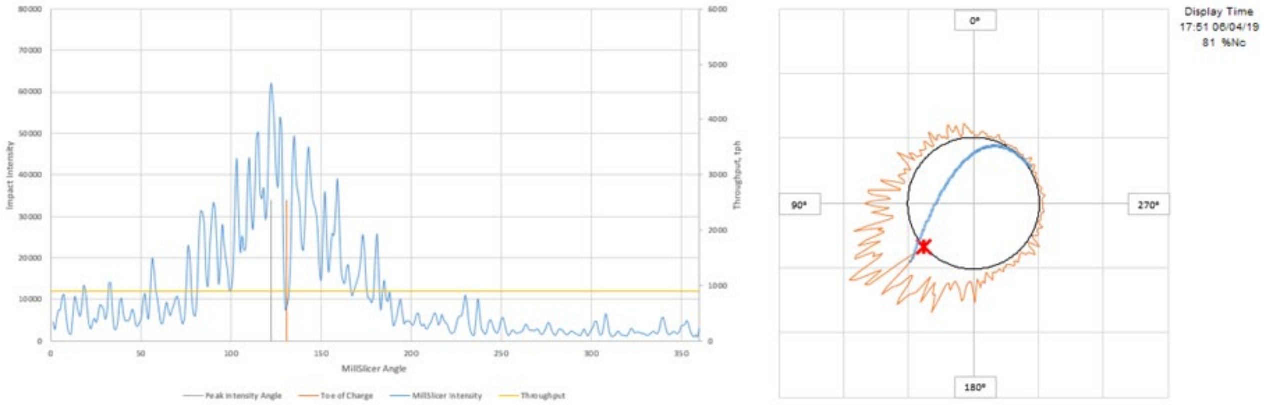


**FIG 14** – MillSlicer impact intensity before (06 April 2019).

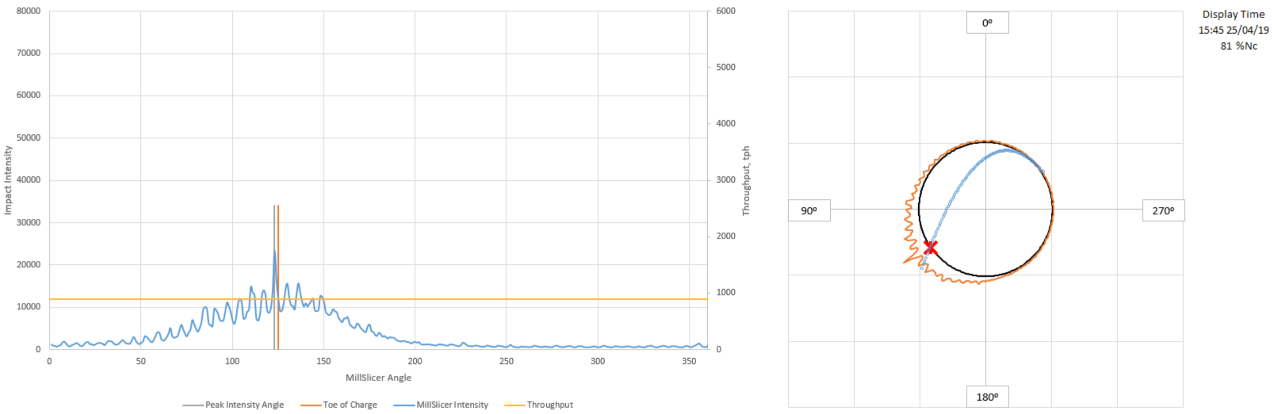


**FIG 15** – MillSlicer impact intensity after (25 April 2019).

Figure 16 illustrates the effect of improved operating milling conditions, where the throughput to mill power draw relationship indicates how quickly the MillStar control system is able to rectify circuit upsets. Due to the rapid power draw fluctuation encountered due to changes in the mill weight, the average instantaneous 5 min data-points were used for the comparative periods.

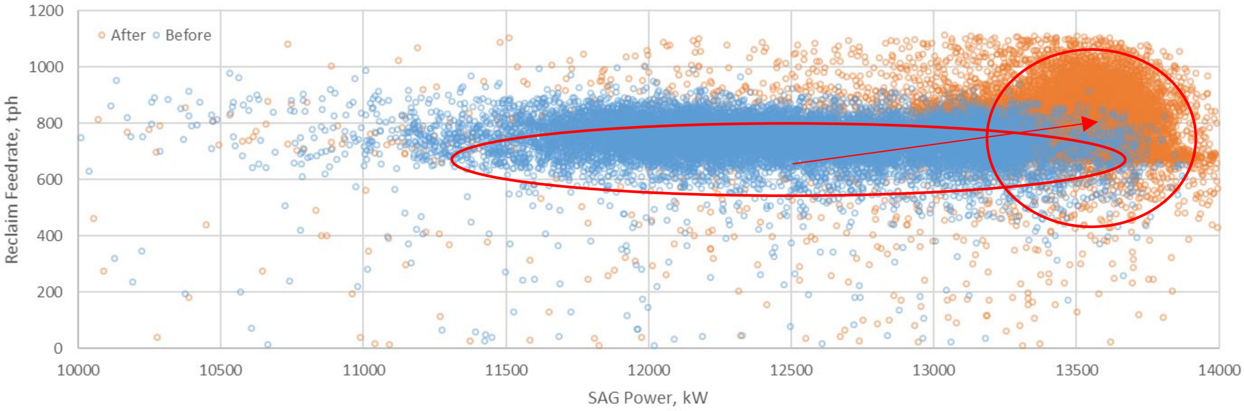


**FIG 16** – Circuit reclaim throughput versus SAG power (5 min instantaneous average).

As shown by the accuracy and precision of the SAG power draw at variable feed rates, after the implementation was significantly improved, with less energy wasted by under-filling the mill and even potentially damaging the liners. This was achieved by understanding the mill power draw in conjunction with the likely impact trajectory, mill load, impact intensity and more precise control.

Table 5 summarises the statistics for this comparison period as a like-for-like evaluation, as well as the most recent production data (for equal periods of time).

**TABLE 5**

Comparative circuit data.

| Parameter | Unit | Before implementation | After implementation | Before/after difference % |
|---|---|---|---|---|
| Start date | - | 1 February 2019 | 6 April 2019 | - |
| End date | - | 5 April 2019 | 8 June 2019 | - |
| Total fresh tonnes | t | 910 245 | 1 075 094 | **+18.1%** |
| Total oxide tonnes | t | 111 695 | 92 341 | -17.3% |
| Total tonnes milled | t | 1 021 941 | 1 167 435 | +14.2% |
| Mill feed rate, total | tph | 779 | 818 | +5.0% |
| Mill feed rate, fresh | tph | 694 | 753 | **+8.5%** |
| Mill feed rate, oxide | tph | 85 | 65 | -24.0% |
| SAG power | kW | 12 430 | 13 334 | +7.3% |
| Mill availability | % | 83.0 | 91.0 | **+9.6%** |
| Primary grind | % passing 212 µm | 80 | 82 | +2.3% |

The key takeaway for operating the milling circuit at optimised conditions is not only to stabilise reducing throughput rate but increase the circuit performance in terms of efficiency when considering both higher proportions of fresh feed and harder ore characteristics than what was historically processed in the circuit.

## Continual improvement

After the initial circuit optimisation, additional targets were set to further maximise the circuit operating parameters. The net effect of which was achieving maximum throughput, with higher proportions of fresh material, while maintaining the circuit grind. The circuit bottleneck moved to the vibrating feeders that required upgrading, as they could not keep up with mill demands.

The following subsections highlights the various continual improvement initiatives implemented and the corresponding effect to the circuit associated circuit said changes made.

### *Blasting practice*

Blasting optimisation was completed, with specific focus on delivering both a more consistent top size to the primary crusher and a higher proportion of fines to improve throughput (McKee, 2013). Table 6 summarises the changes made during 2019 to the powder factor (PF). Changes in blast practice post May 2019 were made in consultation between site and an external specialist consultant (Hatch).

**TABLE 6**

2019 blasting practice changes.

| Change description | Date |
|---|---|
| Higher PF in ore (0.7 g/cm³ to 0.8 g/cm³)/lower in waste | 15 March 2019 |
| Improved QAQC | 11 July 2019 |
| Focused blast evaluation and monitoring | 15 July 2019 |
| Explosive density review (1.1 g/cm³) | 16 September 2019 |

Figure 17 depicts the primary crushed product $P_{80}$ and fines component reporting as mill feed.

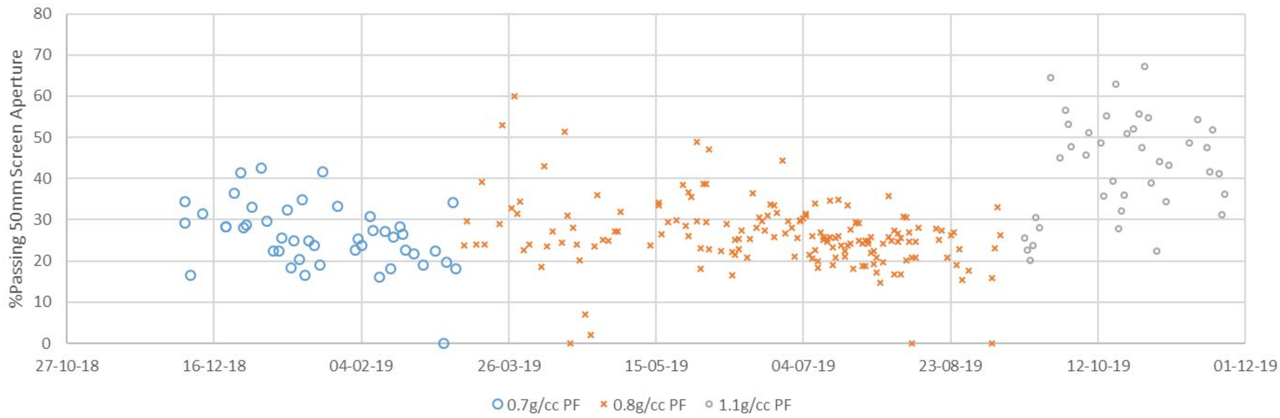


**FIG 17** – Primary crusher product fines content.

Prior to March 2019, the amount of fines being generated per blast was starting to decline in line with an increasing trend to the primary crusher product size. Therefore, the updated blasting pattern notably assisted in maintaining feed conditions to the milling circuit as the ore hardness is increased by mining depth. It is interesting to note that average fines generation gives a convenient indication of excessive SAG grate wear when the pebble extraction rate increases (Putland, 2019).

### *Mill weight set points*

One of the techniques utilised in the process of maximising throughput is optimisation of both the SAG weight control (to accurately manage weight via feed rate) and ball charge (Kock, 2019). The optimal mill weight, to account for the ore breakage characteristics, state of liner wear, ball charge and trajectory is selected and adjusted regularly. Figure 18 depicts the SAG weight set point changes and how the actual mill weight control is achieved in relationship with the feeder output.

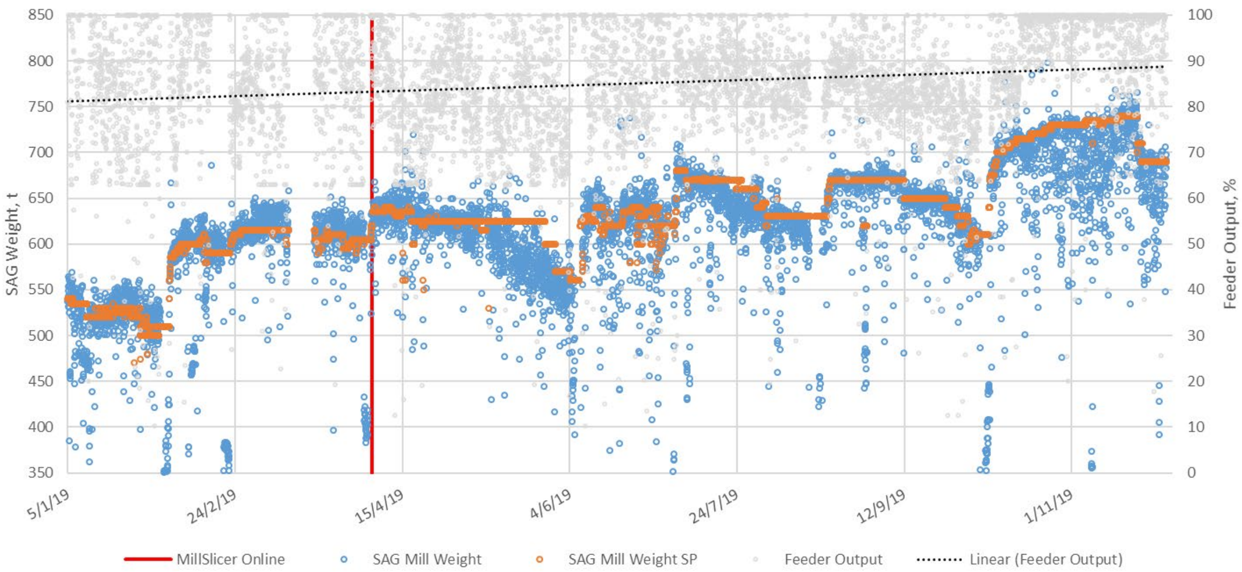


**FIG 18** – SAG weight control and feeder output.

The most recent challenge to the circuit is the physical limitation of the feeder system, as shown by the upward trending average output required to achieve the weight set point, which operates at near maximal output from mid-October 2019.

Since the physical feeder limitations have been debottlenecked in early January 2020, it is intended to further fine tune the SAG weight set point to allow for optimal control of the ball trajectory in relationship with the charge load within the SAG mill (Giblett, 2019).

### *Liner wear rates*

Consideration is given to the change in relining schedule, which is a function of the ore abrasion index, mill specific energy consumption and operating practices (such as liner impacts) which influence the overall wear life of the liner set. Table 7 depicts the five most recent periods preceding a mill reline. Key observations include reduced operating life and effective tonnes treated as the ore abrasiveness increased.

**TABLE 7**

Liner performance on daily COS tonnes treated.

| Liner set | Average abrasiveness, g | Operating life, d | COS tonnes treated, t | Effective treatment rate, t/d |
|---|---|---|---|---|
| Before optimisation | | | | |
| A | 0.248 | 141 | 2 506 938 | 17 780 |
| B | 0.288 | 142 | 2 418 079 | 17 029 |
| C | 0.301 | 131 | 2 098 579 | 16 020 |
| After optimisation | | | | |
| D | 0.299 | 115 | 1 978 297 | 17 203 |
| E | 0.283 | 62 | 1 160 847 | 18 723 |

The liner life started to decline in line with the reduced throughput rate discussed above, which corresponds with the expected ore hardness increase. By adjusting the optimal SAG weight set point, and by proxy the interface between the maximum impact angle and the toe of the charge, the liner impacts have been reduced to maximise throughput and liner life.

By continually operating at the optimal conditions, the liner wear profile can be reviewed to identify areas in the liner design where excess liner weight can be shaved, to save cost and reduce wastage.

### *Culmination of effort*

Based on the various circuit improvements and optimisation outlined, the progressive circuit throughput for the remainder of 2019 is outlined in Table 8 with Figure 19 depicting time normalised reclaim throughput rates extracted from the online system. As shown over a two-month period the throughput increase is sustained without excessive high and/or low values artificially impacting the average data summarised below.

**TABLE 8**

Summarised operating data (Kock, 2020).

| Parameters | Units | Mar-19* | Apr-19 | Nov-19 | Dec-19 | Overall % change April versus December |
|---|---|---|---|---|---|---|
| **Production statistics** | | | | | | |
| Reclaim feed rate | tph | 710 | 749 | 913 | 943 | +19.1 % |
| Oxide feed rate | tph | 87 | 65 | 56 | 51 | -21.9 % |
| Scats production | tph | 231 | 267 | 254 | 156 | -41.6 % |
| | % New Fd | 29 | 33 | 28 | 17 | - |
| Total feed | tph | 798 | 814 | 969 | 943 | +15.8 % |
| Circuit product $P_{80}$ | μm | 250 | 245 | 237 | 240 | -2.0 % |
| Oxide in feed blend | % | 11 | 8 | 6 | 6 | -25.0% |
| **Power utilisation** | | | | | | |
| SAG mill measured power | kW | 12 676 | 13 242 | 12 290 | 12 884 | -2.7 % |
| SAG mill specific energy | kWh/t | 14.1 | 14.4 | 11.7 | 12.0 | -16.7 % |
| Operating work index (WiO) | kWh/t | 23.2 | 23.5 | 18.8 | 19.4 | -17.4 % |
| **Operating parameters** | | | | | | |
| MillSlicer – delta intensity | Deg | - | - | 11 | 9 | - |
| Mill speed | rpm | - | 10.3 | 10.7 | 10.6 | +2.9 % |
| SAG milling density | % solids | - | 71.3 | 73.4 | 75.6 | +6.0 % |
| Cyclone feed density | $t/m^3$ | - | - | 2.07 | 1.97 | - |
| Cyclone pressure | kPa | 61 | 63 | 67 | 64 | +1.6 % |
| No. cyclones | | 6 | 6 | 6 | 5 | -16.7 % |
| Circulating load | % | - | 319 | 259 | 203 | -36.4 % |

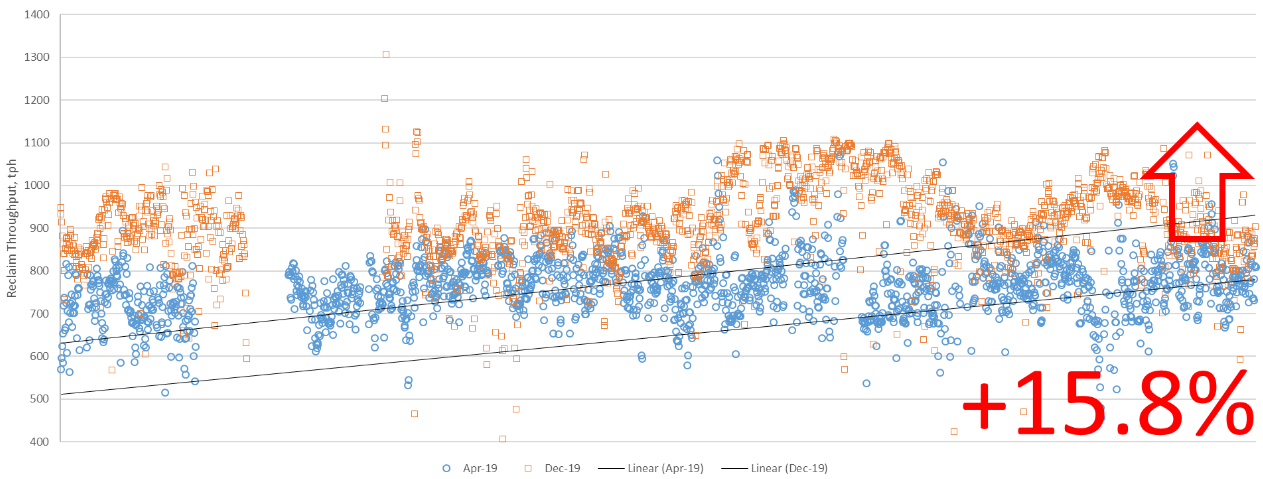


**FIG 19** – Relative reclaim feed rate for April and December 2019.

## CONCLUSIONS

As shown by the supporting data, continual effort by all personnel involved, Perseus staff and consultants on and off-site, managed to achieve a notable shift in circuit throughput. This effort is enabling the circuit to operate near or at the optimal throughput and grind range of the circuit for extended periods of time.

The main areas of optimisation to achieve this included:

- Optimal set point management.
- Improved control and measurement.
- Improved maintenance and equipment operability/stability.
- Improved blasting practices.

Based on the actual circuit throughput trajectory before circuit optimisations, the net circuit benefit in terms of fresh feed processed was initially estimated at +8.5 per cent in actual terms. It is interesting to note that the circuit bottleneck then moved to the stockpile vibrating feeders, which were operating at maximum output, requiring physical upgrades to further debottleneck circuit throughput. After removal of these bottlenecks and further optimisation the circuit throughput increased to a constant 950 t/h (January 2019 average) from the 814 t/h average in April 2019, a further +15.8 per cent benefit in average instantaneous throughput while the average ore hardness for the comparison period being within three per cent of each other.

The benefit of this optimisation strategy is that it identifies and actions most of the low capital-intensive circuit changes. This translates into an approximate monthly net cash flow benefit of A$6.3 million (per month), when considering the difference in tonnes treated (Apr 2019 versus Dec 2019) and assuming similar recovery and feed grades. Further circuit throughput increases are likely to required major modifications, signifying that utilisation the existing capital has been optimised.

All up from implementation this team ethos of optimisation in combination with state-of-the-art technology and specialist consultants has resulted in a sustainable increase in throughput of 27 per cent in 8 months which will result in tens of millions of dollars of increased revenue a year at reduced operating costs, significantly improving the project economics.

Once the maximum operating limits of the existing equipment has been achieved, physical upgrades will be required to further improve throughput. It is therefore useful to complete bottleneck evaluations to proactively identify where engineering consideration has to be focused, to minimise future time required to enact circuit upgrades.

Similarly, by applying the knowledge gained in a single circuits' optimisation to the other assets in the mining company's portfolio, the benefit gained can be multiplied through various sites.

## ACKNOWLEDGEMENTS

The authors would like to acknowledge the operational and management team of Perseus Mining Limited in providing critical feedback, implementing recommendations, driving on-site improvements (the hard bits) and permission to publish this paper.

## REFERENCES

Giblett, A. & Putland, B. 2018. The basics of grinding circuit optimisation. Proceedings of the 14th AusIMM Mill Operators conference, pp. 146–156.

Kock, F W & Becker, M, 2020. MillROC Reports No. 1 to No. 27. (Internal). Perth, Australia.

Kock, F W, Butar, R, Becker, M, Putland, B P, and Lovatt, I A, 2019. Continuous Improvement at Sentinel (With Remote Grinding Support). SAG 2019

McKee, D J, 2013. Understanding Mine to Mill. The Cooperative Research Centre for Optimising Resource Extraction (CRC ORE).

Mular, A L, & Jergensen, G V II, eds. 1982. Design and Installation of Comminution Circuits. Society of Mining Engineers of the American Institute of Mining, Metallurgical, and Petroleum Engineers. New York. p. 248–274

Napier-Munn, T J, 2014. Statistical Methods for Mineral Engineers – how to design experiments and analyse data. Julius Kruttschnitt Mineral Research Centre. Queensland, Australia.

Putland, B P, Kock, F and Siddall, L, 2011. Single Stage SAG/AG Milling Design. SAG 2011

Putland, B P, Lovatt, I A, Cervellin, A and Schwann, D, 2018. Mount Carlton Comminution Circuit Design, Start-up and Optimisation. Proceedings of the 14th AusIMM Mill Operators conference, pp. 517–528.

Putland, B P, and Sciberras, R, 2019. Hard Rock – Crush it or let it break itself?. SAG 2019

# Installation, commissioning, operation and performance review of TowerMill at OceanaGold Haile Gold Mine, South Carolina


*S Palaniandy[1], D Carr[2], J Johns[3] and N Williams[4]*

1. Process Manager, Nippon Eirich Co. Ltd., Willawong Qld 4110.
   Email: samayamutthirian@nippon-eirich.com
2. Chief Metallurgist, OceanaGold Corporation, South Brisbane Qld 4101.
   Email: david.carr@oceanagold.com
3. Processing Manager, Haile Gold Mine, Kershaw South Carolina 29067 USA.
   Email: justin.johns@oceanagold.com
4. Metallurgist, Haile Gold Mine, Kershaw South Carolina 29067 USA.
   Email: nathannael.williams@oceanagold.com



## ABSTRACT

Haile Gold Mine is an open pit gold mine located in the state of South Carolina, USA. The concentrator consists of a semi-autogenous mill–ball mill–pebble crusher (SABC) circuit, flash flotation, rougher flotation, concentrate regrind mills, leaching electrowinning and refinery. This paper focuses on the regrinding section. The original regrind circuit consists of six units of stirred media detritor that receives a combined flash and rougher flotation concentrates feed. The circuit could not cope with the coarser pyrite from the flash flotation concentrate stream that has resulted in a lower mass pull from the flash flotation and coarser product size distribution compared to the design. In 2019, Haile Gold Mine modified the circuit by introducing two stages of regrinding. One unit of ETM 1500 (1300 kW) TowerMill and an M10000 (3000 kW) IsaMill were installed for regrinding duties. This paper focuses on the TowerMill circuit. The TowerMill circuit was designed to reduce the particle size from 150 µm to 22–42 µm. The mill was successfully installed in five days and commissioned within six days in November 2018 and January 2019. For the first three months, the TowerMill was operated in open circuit configuration. In April 2019, the TowerMill circuit was closed with a cluster of 10” hydrocyclones. The leach circuit’s feed was reduced from 23 µm to 17 µm when the TowerMill was brought online. A recent TowerMill circuit performance review indicated that the circuit performs within the design specifications to produce a circuit product of 22 µm at a specific energy consumption of 16.4 kWh/t. The first set of the tip and flight liners’ wear rate was 0.1 and 0.05 g/kWh, respectively. This paper discusses the installation, commissioning and operational experience of the TowerMill circuit plus its process performances.


## INTRODUCTION

Haile Gold Mine is an open pit gold mine located in Kershaw, South Carolina, USA. Gold was discovered at this site in 1827, and the property has been through several operating periods. Wickens *et al* (2013) explained the history of the Haile Gold Mine. Romarco Minerals acquired this property in 2007 and began an exploration program that delineated 2.02 Moz of gold in reserve at an overall grade of 2.06 g/t (Wickens *et al*, 2007). OceanaGold acquires Romarco Minerals and Haile Gold operation in October 2015. Since then, OceanaGold has implemented numerous process changes to eliminate or mitigate risks identified in the processing circuit’s initial design (Larson *et al*, 2017). This paper focuses on the initiative and implementation to improve the concentrate regrinding section.

## REVIEW OF COMMINUTION TEST WORK AND PROCESSING CIRCUIT DESIGN

Romarco Minerals undertook an extensive metallurgical test work program at the initial design phase. The test program includes ore characterisation for comminution, gravity separation, whole ore leaching, flotation, ultrafine grinding, concentrate leaching, flotation tailings leaching and gold deportment. The metallurgical test work data and initial activities of circuit design de-risking have been reported extensively by Wickens *et al* (2013) and Larson *et al* (2017). This section focuses on the comminution-related test work and its effect on flotation and leaching. Metallurgical test work was carried out using the representative core samples from 23 drill holes within the Haile Gold orebodies – Mill Zone, Haile, Red Hill, Ledbetter and Snake.

The comminution test work includes crushing work index, abrasion index, rod mill work index and Bond ball mill work index. The abrasion and Bond ball mill work indices are within the interest and scope of this paper. Table 1 shows the summary of the abrasion and Bond ball mill work indices from different ore zones. The ores were categorised as moderately high abrasiveness based on the abrasion index values. A higher liners wear rate and grinding media consumption were anticipated. Meanwhile, the Bond ball mill work indices indicated that these are soft to medium hardness ores. The Mill Zone and Haile ore zones are not sensitive to the hardness as the Bond ball mill work index values at 74, and 150 μm closing screen were similar.

**TABLE 1**

Summary of Abrasion index and Bond ball mill indices (Wickens *et al*, 2013).

| **Ore zone** | **Abrasion index** | **Bond ball mill work index @ 150 μm (kwh/t)** | **Bond ball mill work index @ 74 μm (kwh/t)** |
|---|---|---|---|
| Mill Zone | 0.2785 | 8.87 | 8.77 |
| Haile | 0.3239 | 10.08 | 9.81 |
| Ledbetter | 0.1360 | 8.24 | 10.36 |
| Snake | - | 9.47 | - |
| Red Hill | - | - | 10.43 |

The leaching test was carried out in two different feed, ie leaching of the whole ore and flotation concentrate. The whole ore leaching was carried out at three different particle sizes, ie 150, 74 and 45 μm. The average gold extraction for all three particle sizes were 64.7, 69.3 and 72.1 per cent, respectively. Alternatively, the flotation test was carried out on the whole ore to obtain the concentrate for the leaching test. The flotation recovery ranged between 87–93 per cent.

The flotation test outcomes also indicated that the ores were not sensitive to the grind size as similar recovery was obtained at the P80 of 45 and 74 μm that warrants a coarser flotation feed (74 μm). The flotation concentrate was subjected to ultrafine grinding to prepare a leach feed of 7, 15, 22 and 55 μm. Higher gold extraction was observed during the leaching of flotation concentrate (between 85–87 per cent) compared to whole feed (69–81 per cent). This observation permits the whole ore flotation and concentrates regrinding. The ultrafine grinding test work was carried out on the composites from the rougher flotation concentrates. Three different stirred milling technologies were compared, and the specific energies required to produce a leach feed of 15 μm (80 per cent passing) were reported. The specific energy requirement for IsaMill, VertiMill and Stirred Media Detritor were 58.4, 52.1 and 45.9 kWh/t, respectively (Wickens *et al*, 2013). In addition, the flash flotation tests were confirmed to be a viable solution as the majority of the gold (62–66 per cent) floats quickly, recovering 5–7 per cent of its weight.

The Haile process flow sheet was designed to treat 6350 t/day ore based on the test work outcomes. Figure 1 shows the simplified process flow sheet. The ore from the pit is crushed in a primary crusher. The crushed product is transferred to a coarse ore stockpile that has 6350 t live capacity. The grinding circuit consists of a semi-autogenous mill and ball mill that grinds the coarse ore to 74 μm (P80). The grinding circuit product undergoes rougher flotation to separate the gold-bearing pyrite.

Meanwhile, 50 per cent of the hydrocyclone underflow stream is diverted to the flash flotation cell. The flash flotation tailings and the remaining 50 per cent of the hydrocyclone underflow stream are fed to the ball mill. The flash and rougher flotation concentrates are ground in six units of stirred media detritor to produce a leach feed of 13 μm (80 per cent passing). The ground product is pre-aerated before being pump into the carbon-in-leach (CIL) circuit (Tank 1). The rougher flotation tail is pumped into the CIL circuit (Tank 2–8). The following process includes carbon stripping, electrowinning and refining in the induction furnace. The CIL tailings pass through the cyanide recovery thickeners and are pumped into the tailings storage facility (TSF).

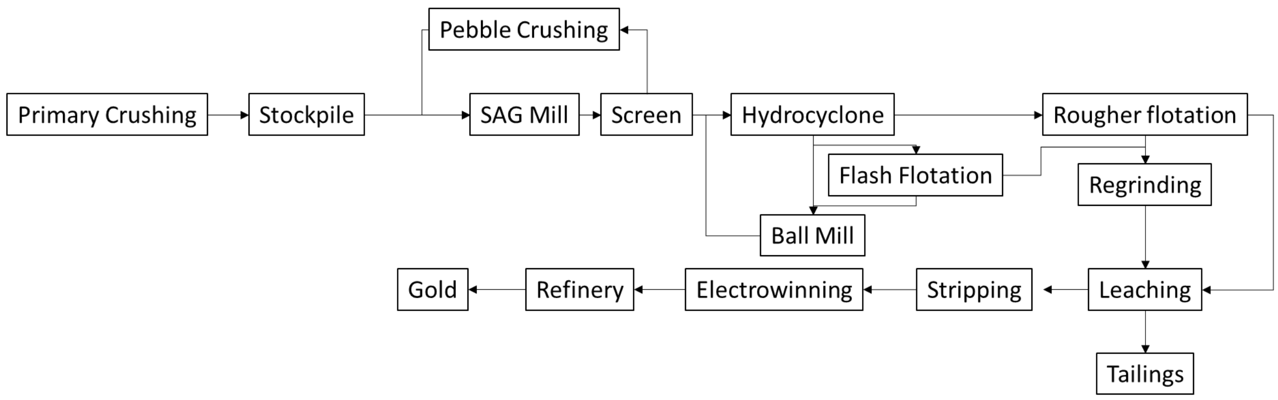


**FIG** 1 – Haile Gold Mine simplified process flow sheet (Larson *et al*, 2017).

Since acquiring the Haile Gold Mine property, OceanaGold has carried out a series of optimisation activities to improve the overall plant performance. The optimisation and de-risking activities were well documented in a technical paper presented by the Haile Gold Mine team at the 2017 SME Annual Meeting in Denver, Colorado (Larson *et al*, 2017). There were nine initiatives to improve plant performances that include improving the flash flotation cell and regrind circuit. The original 30 $m^3$ cell was too small with limited flexibility that leads to losses of recovery. The cell was upgraded to 50 $m^3$ as the steel structure was capable of supporting a larger cell.

The 50 $m^3$ cell has considerably more mass pull compared to the smaller cell. In this case, the regrind circuit receiving a higher ratio of coarse feed that coarsens the overall feed size distribution. The question is if the selected regrind mill technology would cope with the coarse feed size distribution. As mentioned in the previous section, the regrind mill test work was carried out using the rougher flotation concentrate. Based on the test outcome, the 2 mm ceramic media was proposed for the regrind mill. The harder and coarser feed from the flash flotation concentrate stream that was not considered for the regrind mill test work poses a risk of grinding efficiency. The top particle size can be as coarse as 1 mm, although the P80 of the flash flotation concentrate may range between 140–180 µm. Based on this scenario, Haile Gold Mine has decided to charge the first two mills with 6 mm ceramic media while the other four mills were charged with 3 mm grinding media. The following section will discuss the operational and performances of the stirred media detritor circuit.

## PERFORMANCE OF THE ORIGINAL REGRIND CIRCUIT

Based on the feasibility test work and laboratory scale-up factors, six stirred media detritor with 375 kW motors were installed in the regrind circuit. The total installed power in this circuit was 2250 kW with a power safety margin of 1.61. The additional power was expected to allow for variations in feed size, throughput, mill utilisation, and specific energy. The targeted grind size was not achieved after the circuit commissioning, and the total imparted power of the mills were averaged around 1200–1300 kW that reduced the circuit utilisation factor. A maximum and stable power draw of 300 kW per mill were achieved after a rebuild. The stirrer arm wear had a noticeable impact on drawn power (abrasive feed) for the mill's targeted media filling volume. The power draw of 300 kW can be maintained with new stirrer arms, but as the arms' tips started to wear, the mill's imparted power would drop noticeably. The top and bottom arms were changed every 750 hours, which would bring the power drawback from 150 kW to 300 kW; meanwhile, the screens were replaced at 1500 hours.

The flotation and regrind circuit operation with six mills, transfer pumps, media charging systems, and ancillary equipment required two plant operators' assistance. In addition, with a 750-hour cycle between arm changes, a mill would need to be taken off-line approximately every five days for maintenance, requiring three to four personnel for a shift for overhaul. This created a considerable burden for the maintenance staff and careful scheduling with other plant requirements. Besides power draw constraints, the circuit's ability to handle coarse pyrite from the flash flotation circuit limits the flash flotation's mass pull and affects overall flotation recovery of gold-bearing pyrite even with the use of coarser 6 mm media in the first mill in each train. Figure 2 shows the average utilisation of the regrind mills with greater than 90 per cent circuit availability was achieved after 18 months of operation. Meanwhile, the power draw ranges between 1000–1200 kW.

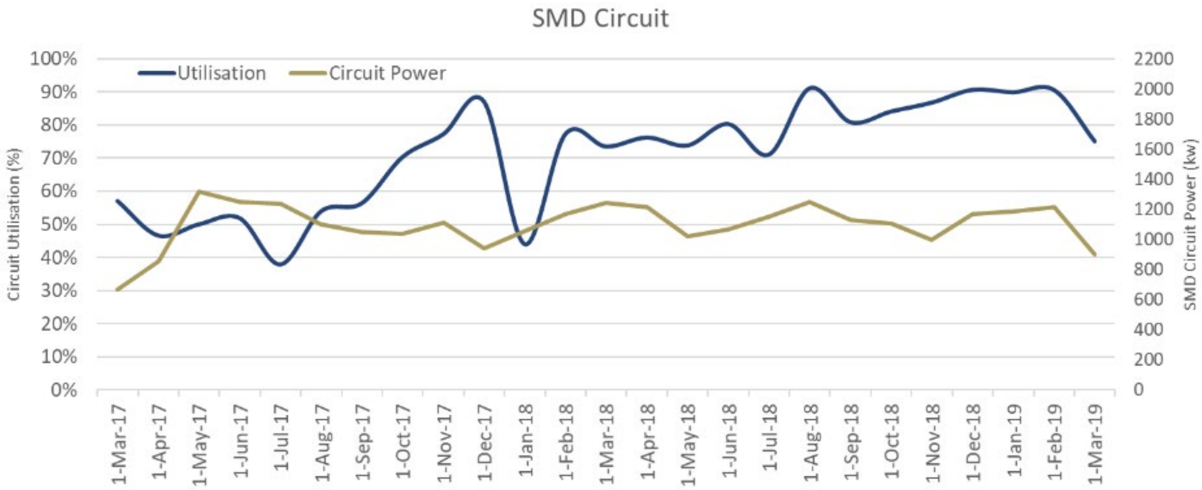


**FIG 2 –** Regrind circuit utilisation and power.

The concentrate production rate varies with the sulphur feed grade of the ore, mill throughput and flotation recovery. Figure 3 shows the circuit-specific energy and concentrate productivity. By 2018 the results of the site optimisation study were completed and being implemented with a steady increase in throughput from the 2.38 Mt/a towards 4 Mt/a with the regrind circuit duty increasing from 30 t/h to a maximum of 55 t/h requiring a significant increase in required power and the ability to handle a coarser circuit feed.

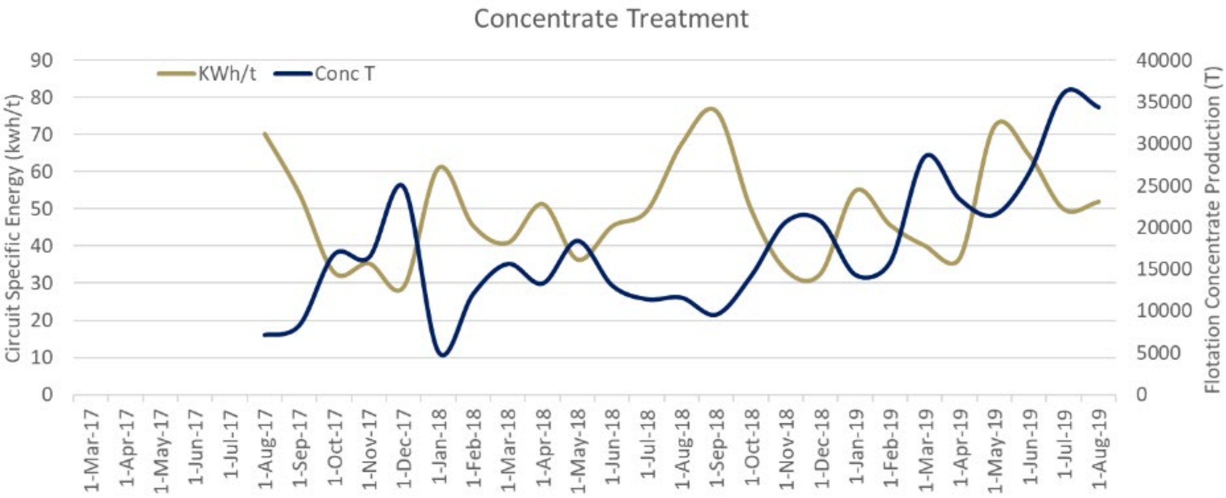


**FIG 3 –** Regrind circuit specific energy and flotation concentrate production.

## CAPITAL IMPROVEMENT OF THE REGRINDING CIRCUIT

Haile Gold Mine has decided to improve and upgrade the regrind circuit to overcome the challenges mentioned above and prepare the circuit for the increase in annual plant throughput circuit from 2.38 to 4.0 Mt/a. A solution with two regrinding stages was chosen to prepare the leach feed of 13 µm (80 per cent passing). An ETM 1500 (1300 kW) TowerMill circuit in closed circuit configuration was chosen for the primary regrinding circuit. An M10000 (3000 kW) IsaMill was chosen for the secondary regrinding circuit. The TowerMill circuit receives a combined bi-modal feed from the flash and rougher flotation concentrate streams. The circuit product gravitates to the IsaMill circuit and further reduces to 13 µm and feeds the first CIL tank.

Figure 4 shows the Haile Gold Mine comminution circuit after upgrading the regrinding circuit. During the design stage, the project team has considered operational flexibility to operate the TowerMill and IsaMill circuits in series or independently through the additional slurry piping arrangements.

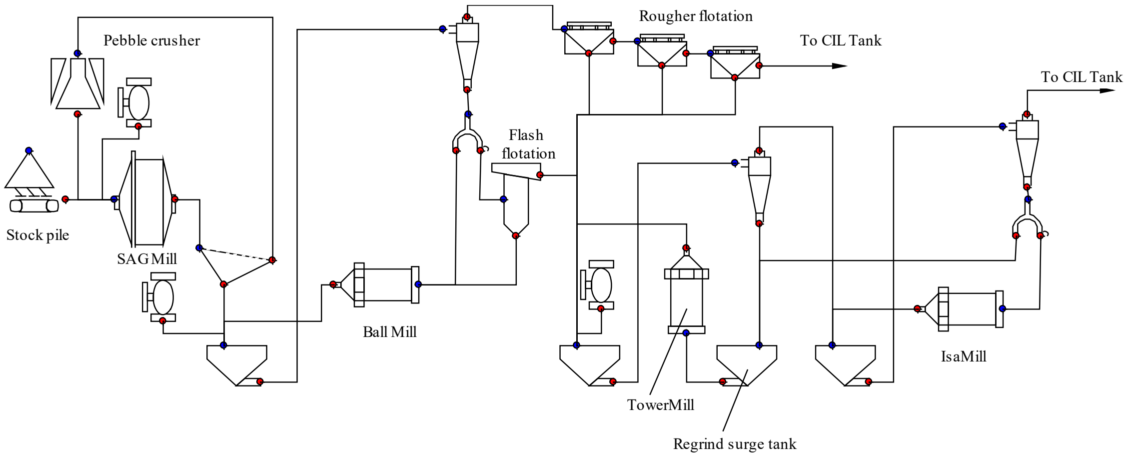


**FIG 4** – Haile Gold Mine comminution circuit after upgrading the regrind circuit.

There are three operational strategies for these regrind circuits. They are:

- Strategy 1 is when both regrind circuits are in operation. This strategy is the typical operational condition to produce the leach feed of 13 μm.
- Strategy 2 is when the TowerMill circuit is off-line. In this case, the flash flotation operation is shut off, and the whole primary hydrocyclone underflow stream is ground in the ball mill. The IsaMill circuit grinds the rougher concentrate stream only to feed the leach tank.
- Strategy 3 is when the IsaMill circuit is off-line. The TowerMill circuit operates in the normal mode receiving a feed from the flash, and rougher flotation concentrates. The TowerMill circuit hydrocyclone overflow stream gravitates to the IsaMill hydrocyclone feed tank. The IsaMill circuit hydrocyclone underflow stream is pumped back to the regrind surge tank (combined hydrocyclone underflow streams) to feed the TowerMill. In this configuration, the TowerMill circuit operates with two stages classification system.

The following sections focus on the primary regrinding TowerMill circuit.

## PRIMARY REGRINDING CIRCUIT

The TowerMill is closed with a cluster of 10” hydrocyclone, as shown in Figure 4. The regrind surge tank was available from the previous regrind circuit and reused in a similar configuration where the hydrocyclone underflow streamflows into this tank and feeds the TowerMill at a constant feed rate and slurry density, ensuring optimal grinding efficiency. The mill discharge flows into the hydrocyclone feed sump to combine with the circuit feed. Table 2 shows the design criteria of the primary regrind circuit.

**TABLE 2**

Design criteria for the primary regrinding circuit.

| | |
|---|---|
| **Circuit feed rate (t/h)** | 42–57 |
| **F98 (μm) – estimated** | 2000 |
| **F80 (μm)** | 150–300 |
| **P80 (μm)** | 22–45 |
| **Targeted operating work index (kWh/t)** | 20 |

OceanaGold placed an order to supply one unit of ETM 1500 with a 1300 kW motor in January 2018. This order was a fast-track project where the lead time to deliver the mill (FOB, Port of Busan) was seven months. The timeline was to install the TowerMill at the site in October 2018, followed by structural and piping work until December 2019. The cold and hot commissioning was scheduled just after the New Year of 2019. The timeline from the purchase order to production was 12 months.

OceanaGold and Nippon Eirich teams underwent good cooperation and teamwork throughout this project and finally achieved the targeted milestone of 12 months to production. Besides the normal manufacturing, this ETM 1500 TowerMill has undergone several product developments such as the variable speed drive, magnetic mill shell liner (supplied by Eriez Magnetics), 150 mm thickness tip liner and fan-cooled gear reducer lubrication unit.

## INSTALLATION AND COMMISSIONING OF TOWERMILL

The TowerMill was installed in October 2018. The foundation was prepared as per the specification from Nippon Eirich before the mill body installation. The magnetic liner was installed in the mill shell after the erection, followed by installing the screw and upper housing (including the drive shaft assembly). The platforms around the mill were constructed after the installation of the upper housing. Other parts such as the mill discharge launder, media hopper, media discharge chute, water pipes were installed along with the platform. Finally, the gear reducer, lubrication unit and drive motor were installed, and the mill was ready for commissioning. Gear reducer, bearing box, high and low-speed couplings were lubricated. In general, the circuit's construction was smooth based on detailed planning and risk analysis done by the project team. All electrical and instrumentation connection was made after the mechanical installation completed.

The commissioning exercise started in early January 2019 in two stages, ie cold and hot commissioning. The cold commissioning activities include checking all electrical and instrumentation connections and their responses. The alarm and trips were checked by simulating the condition by adjusting the current values from the sensors. Once the electrical and instrumentation check was completed, the mill was filled with water and checked for any leaks. No water leaks were observed. A cold run with water was carried out for eight hours, and the mill's operational condition was checked. The operational condition monitoring during the cold run is shown in Table 3. Figure 5 shows the example of the PI vision interface for conditioning monitoring during the cold commissioning.

**TABLE 3**

Operational conditional monitoring during commissioning.

| **Parts** | **Operational condition monitoring** |
|---|---|
| Drive motor | Motor bearings temperature (drive end and non-drive end<br>Motor winding temperature |
| Gear reduces | Lubrication oil level<br>Temperature<br>Vibration |
| Lubrication unit | Oil temperatures (in and out)<br>Duplex filter differential pressure<br>Oil flow rate |
| Bearing box | Oil level<br>Temperature<br>Vibration |

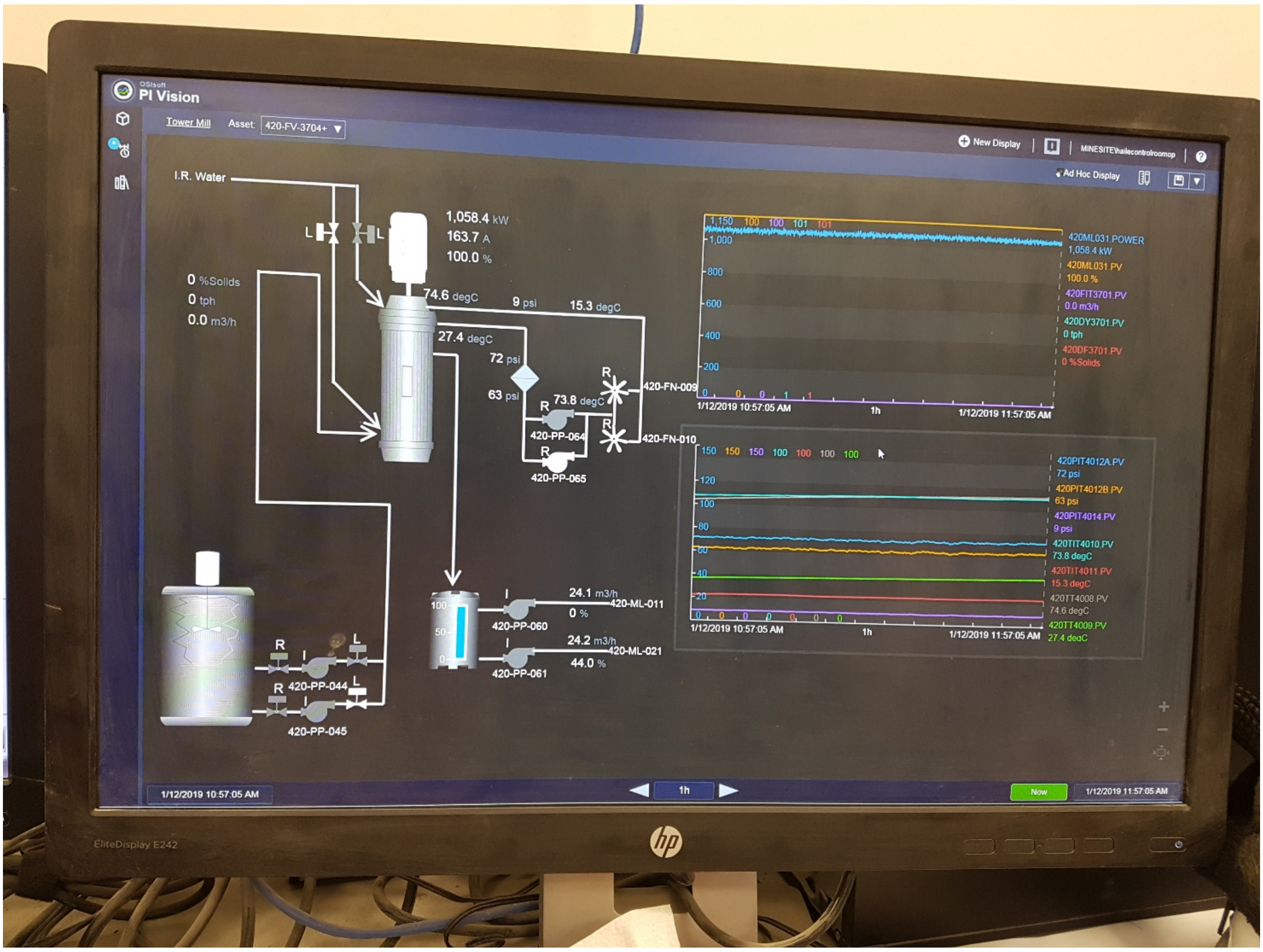


**FIG 5 –** PI Vision Interface for condition monitoring during the commissioning.

After the water-only run, grinding media was added into the mill. The variable frequency drive has created an opportunity to record the power draw at three different screw rotational speeds for a given grinding media loading in the mill. This exercise's outcome was mapped in a power draw-amount of grinding media-screw rotational speed plots (as shown in Figure 6). An empirical model that can determine the power draw for a given amount of grinding media and screw rotational speed was developed. The model can determine the amount of grinding media in the mill provided the screw liner in new or near new conditions.

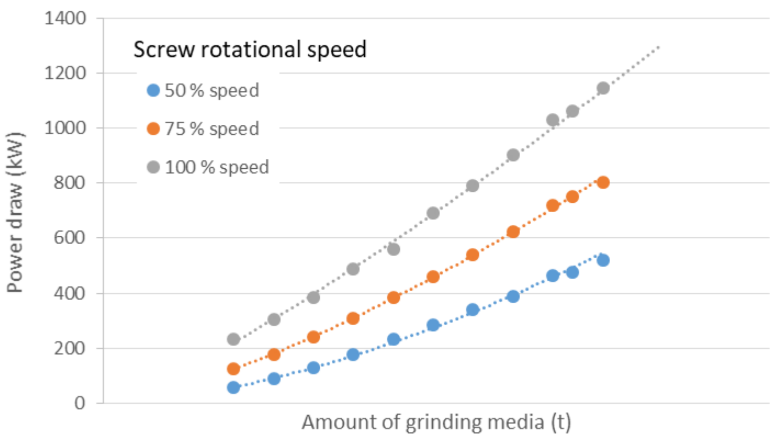


**FIG 6 –** Power draw at different media loading and screw rotational speed.

Further investigation will be carried out to determine the amount of media in the mill when the screw liner is in worn condition. The grinding media addition was stopped when the power draw reached

98 per cent of the installed power. The run with grinding media and water was carried out for 12 hours, and the operational condition (as shown in Table 3) was monitored. In general, the mill was operating within the specifications recommended by Nippon Eirich.

After completing the 12 hours grinding media-water only run, the slurry (combined flash and rougher flotation concentrate) was introduced to the mill. The mill discharge per cent solids were checked. At this stage, the TowerMill was operating in an open circuit to prepare the stirred media detritor circuit's feed. The following section discusses the initial operation of the TowerMill and its performances.

## PERFORMANCES OF TOWERMILL CIRCUIT

The TowerMill was handed over from the project team to the production team immediately after the hot commissioning to maximise its utilisation. The mill was operated in open circuit configuration for the first three months while waiting to install the new hydrocyclone feed sump and hydrocyclone cluster. The flash and rougher concentrate streams were ground in a single pass and fed to the stirred media detritor circuit. During this period, the IsaMill circuit was under construction. Following the commissioning of the TowerMill, the flash flotation circuit was able to be pulled harder, increasing flotation recovery without causing an overload of the first stirred media detritor mill in each train, as shown in Figure 3. Very high sulphur feed grades in Q3 2019 led to treatment rates of concentrate in excess of the circuit design criteria. Figure 7 shows the P80 of the leach feed for the first 24 hours after the TowerMill came online. An immediate drop in the leach feed particle size from 24 μm was observed when the TowerMill came online. The average leach feed P80 for the first 24 hours was 17 μm which is lower compared to when the regrinding circuit was operated with stirred media detritor only. This preliminary observation indicated the positive outcome of two stages regrinding and the TowerMill circuit's success reducing the coarse particles from the flash flotation concentrate stream. Figure 8 shows a long-term leach feed P80 from 17 January – 5 March 2019, the average P80 reduced from 25 μm (before TowerMill installation) to 17 μm, increase in throughput and reduction in specific energy.

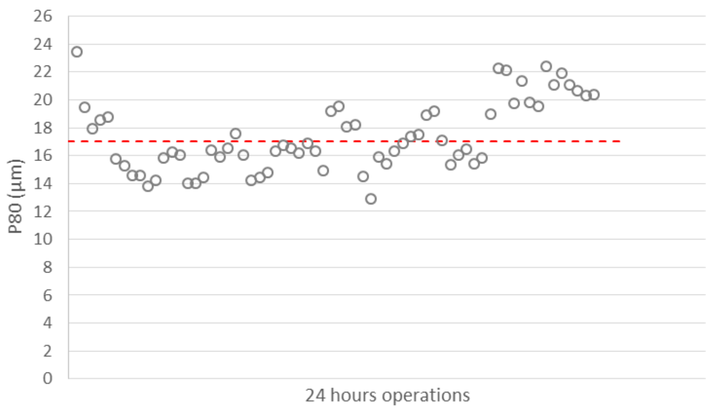


**FIG 7** – The leach feed P80 during the first 24 hours of TowerMill operation.

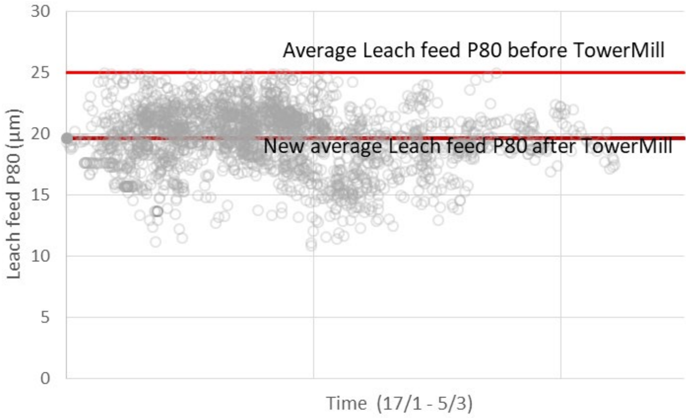


**FIG 8** – The leach feed P80 from 17 January – 5 March 2019.

## Open circuit survey and performances evaluation

The Haile Gold metallurgists carried a series of open circuit surveys at two different screw rotational speeds (75 per cent and 100 per cent rev/min). The mill was fed at a constant slurry flow rate and density. The mill feed and discharge streams were sampled to evaluate the circuit performances. The samples were characterised for particle size distribution and slurry densities. This survey exercise was the first published data where TowerMill performances were evaluated at different screw rotational speeds. Equations 1 and 2 show were used to calculate the circuit's performances – operating work index and size-specific energy at 20 µm marker size, respectively (Palaniandy *et al*, 2018). Table 4 shows the operating condition and performances of the circuit.

$$OWi\ \left(\frac{kWh}{t}\right) = \frac{SE\ (\frac{kWh}{t})}{\frac{10}{\sqrt{P_{80}}} - \frac{10}{\sqrt{F_{80}}}} * EF_5 \tag{1}$$

$$SSE_{20\ \mu m}(\frac{kWh}{t}) = \frac{SE\left(\frac{kWh}{t}\right)*100}{\%P_{20\ \mu m} - \%F_{20\ \mu m}} \tag{2}$$

Where:

$OWi$ – operating work index

$SE$ – Specific energy

$F_{80}$ – feed size at 80 per cent passing

$P_{80}$ – product size at 80 per cent passing

$\%F_{20\ \mu m}$ – per cent passing at 20 µm (Circuit feed)

$\%P_{20\ \mu m}$ – per cent passing at 20 µm (Circuit product)

$EF_5$ = efficiency factors 5 (fineness of grind factor)

The feed rate and F80 in Survey 2 were higher than Survey 1, and the mill was able to maintain the product size by increasing the power draw (higher screw rotational speed). This exercise shows the operational flexibility offered by the variable frequency drive to maintain the product size.

**TABLE 4**

TowerMill open circuit performances.

| **Survey** | 1 | 2 |
|---|---|---|
| **Circuit feed rate (t/h)** | 38.4 | 42.1 |
| **Power draw (kW)** | 705 | 1022 |
| **Screw rotational speed (%)** | 75 | 100 |
| **F80 (µm)** | 149 | 166 |
| **P80 (µm)** | 37.3 | 39.9 |
| **SE (kWh/t)** | 18.4 | 24.3 |
| **Operating work index (kWh/t)** | 22.4 | 30.0 |
| **SSE @ 20 µm (kWh/t)** | 47.5 | 58.2 |
| **Leach feed P80 (µm)** | 18.6 | 16.8 |

Screw rotational speed and amount of grinding media in the mill are the two variables that influence the power draw in the TowerMill. Most of the TowerMill were installed with a direct online fixed speed motor. In this type of mill, the amount of grinding media was adjusted to achieve the targeted power draw. For example, the amount of grinding media is reduced to turn down the power in the mill. During the commissioning phase, Nippon Eirich develops the grinding media mass versus power draw curves. The plant operators can use this curve to guide media addition or turn down the mill. The power draw of the TowerMills with variable frequency drive can be turned down by reducing the screw rotational speed. The survey results show the advantages of the variable speed drive, and further research is needed to understand the turndown strategies for the TowerMill.

A population balance model for the TowerMill was developed to predict the mill discharge particle size distribution for given operating conditions and ore characteristics. The model can be used to back-calculate the breakage rate values. The breakage rate was calculated at two different screw rotational speeds based on the survey data, as shown in Figure 9. The breakage rate values drop as the screw rotational speed reduces. In stirred mills where abrasion/attrition grinding mechanisms are predominant, the grinding media stress intensity plays an important role. The grinding media should impart enough stress intensity to the particles for successful breakage. Jankovic (2001) mentioned that the stress intensities are the combined stress intensities of the grinding media and gravitational stress intensity for the TowerMill. Equations 3 and 4 show the grinding media and gravitational stress intensities formulas, respectively. The tip speed influences the grinding media stress intensity. In this case, turning down the TowerMill screw rotational speed (lower screw tip speed) reduces the grinding media stress intensity. Jankovic's (2001) data shows that reducing the tip speed from 0.74 to 0.37 m/s reduced the stress intensities by 28 per cent. Additional work is being scheduled to understand the effect of screw rotational speed on grinding efficiency.

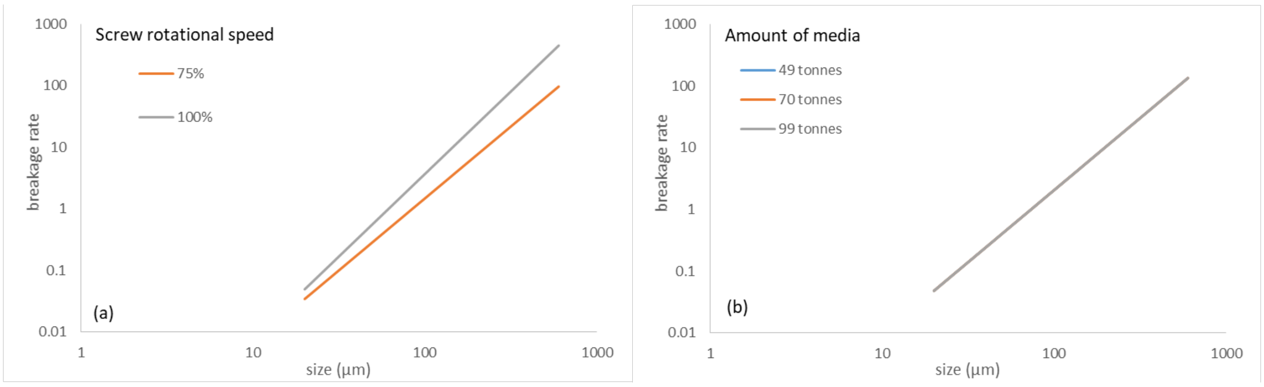


(a) (b)

**FIG 9** – Breakage rate at: (a) different screw rotational speed; (b) different media loading.

$$SI_m = D_m^3 \cdot (\rho_m - \rho) \cdot v_t^2 \tag{3}$$

$$SI_{gm} = k \cdot D_m^2 \cdot \frac{(D - D_s) \cdot (\rho_m - \rho)}{4 \cdot \mu} \tag{4}$$

Based on experiences from other installations, a reduction in the amount of grinding media maintains the grinding efficiency when the specific energy is maintained at a constant value. A survey data set was simulated at different media loading in the mill. The mill-specific energy was maintained by adjusting the feed rate and power draw (amount of grinding media). Figure 9b shows that the breakage rate values were maintained. This exercise has indicated a band or range where the screw tip speed can be adjusted to turn down the mill. A combination of grinding media and screw rotational speed reduction may help to maintain the grinding efficiency in the case of high-power turndown is required. The learning from this exercise can be used for future circuit design and operations. For example, the mill can be turned down when power is not required. This action has a positive impact on operating costs through a reduction in wear part consumption and electricity.

## Closed-circuit survey and performance evaluation

The TowerMill was converted to a closed-circuit configuration in April 2019 when the new hydrocyclone feed sump and 10" hydrocyclone cluster were installed. The circuit configuration is shown in Figure 4. The circuit product (hydrocyclone overflow stream) feeds the IsaMill circuit. The conversion from open to closed-circuit was smooth without much interruption to the production. The set-up of the circuit is relatively advanced compared to other TowerMill installations. The OceanaGold project and metallurgy teams and Ausenco engineers underwent a thorough exercise in designing the circuit based on the site's experience and the objective that the circuit should be achieving. There are multiple flow rate and slurry density measurements in the circuits. The TowerMill and hydrocyclone feed pumps were installed with a variable frequency drive for operational flexibility. Two online sampling points (TowerMill discharge and hydrocyclone overflow streams) were installed and connected to the online particle size analyser. This set-up enables operational flexibility (adjusting mill power draw through screw rotational speed and hydrocyclone pressure through hydrocyclone feed pump) to achieve a consistent targeted grind size. In May 2019, Nippon Eirich and Haile Gold Mine personnel conducted joint TowerMill circuit audits to evaluate the circuit performances. Similar to the open circuit audits, the circuit was surveyed at three different screw rotational speeds – 50 per cent, 75 per cent and 100 per cent. Figure 10 shows the TowerMill circuit sampling points. Seven samples were collected during the survey. The samples were flash flotation concentrate, rougher flotation concentrate, hydrocyclone feed, hydrocyclone overflow, hydrocyclone underflow, mill feed and mill discharge. The sampling exercise was carried out in a steady-state condition for one hour with 20 minutes of interval sampling (four cuts). All samples were subjected to particle size distribution and per cent solids determination.

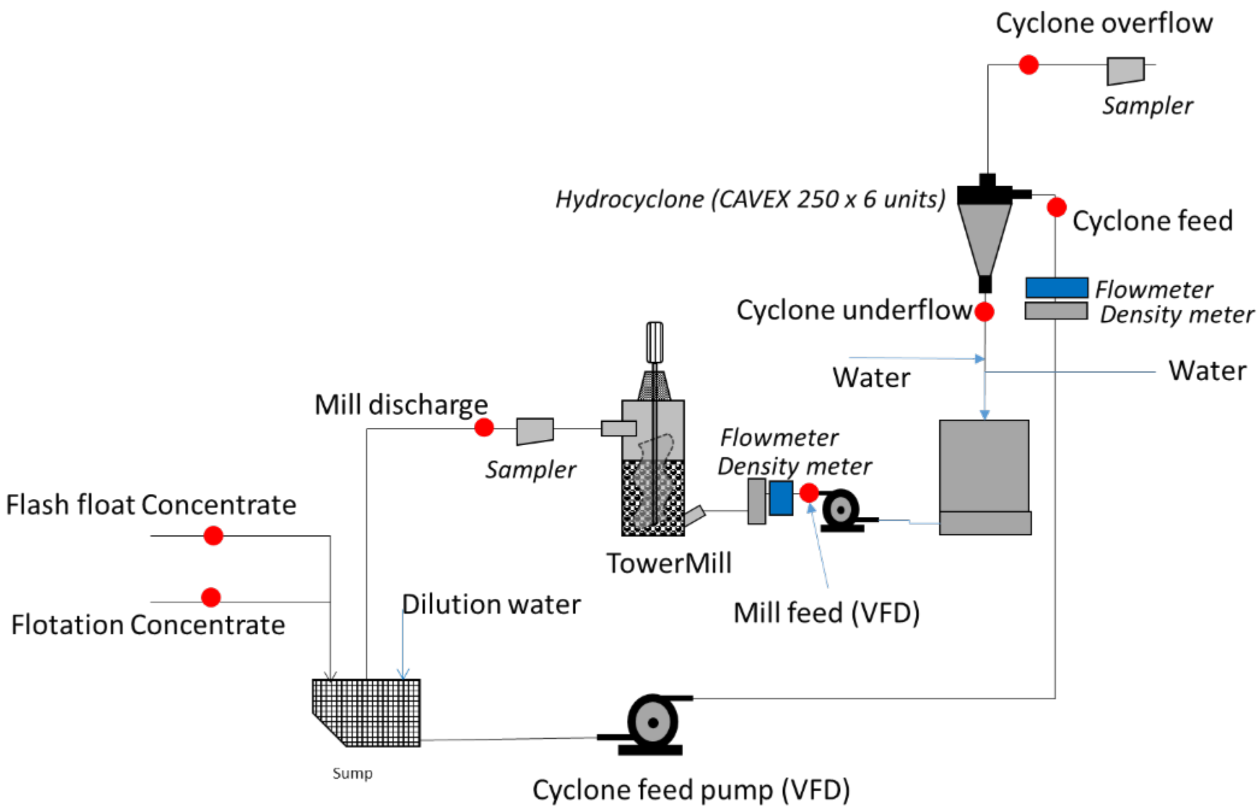


**FIG 10** – TowerMill circuit flow sheet and its sampling points.

One of the new circuit challenges is determining the circuit feed rate (flash and rougher concentrate mass flow rate). Flow rate measurements were not available in these two streams. During the open circuit survey, a combined mill feed (flash and rougher concentrate) was considered for evaluation as both streams were mixed and the stream has a flow metre.

A methodology was developed to determine the flash and rougher flotation concentrate feed rate. Manual time-cut sampling was performed at two locations of the flash flotation concentrate, ie inner and outer. Figure 11 shows the inner and outer launder sampling points at the flash flotation cell. Figure 12 shows the schematic diagram of the sample cutter. The 70 mm lip was used for sampling. The sampling period for each cut is 20 s. Sampling was carried out at three different spots around the circumferences of the inner and outer launder. Table 5 shows the flash flotation concentrate mass flow rate for all four surveys.

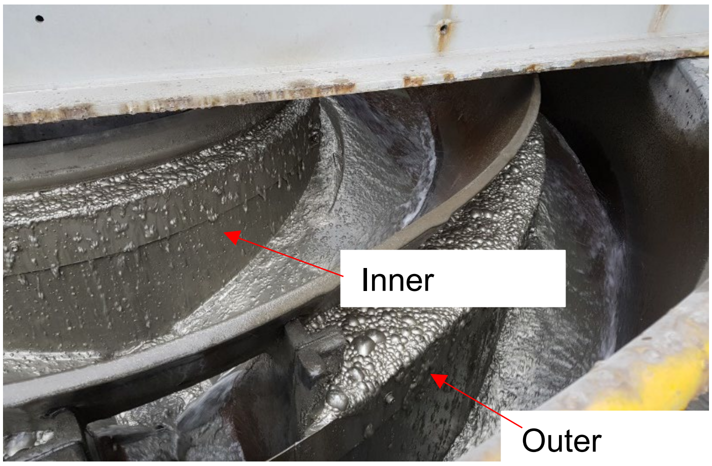


**FIG 11** – Flash flotation concentrate launder.

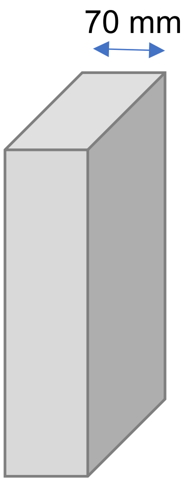


**FIG 12** – Sample cutter.

**TABLE 5**

Flash flotation sampling detail for mass flow rate determination.

| **Survey** | 1 | 2 | 3 | 4 |
|---|---|---|---|---|
| **Flash float concentrate feed rate (t/h)** | 12.6 | 17.3 | 19.6 | 19.7 |

The mass balancing exercise was carried out to check the stream's data quality and obtain unknown data based on the stream data (mass flow rate, per cent solids and particle size distribution). The circuit was mass balanced using the mass balance module in the JKSimMet mineral processing software. The mass flow rate of the rougher flotation concentrate stream was determined through the mass balancing exercise. The combination of flash and rougher flotation stream mass flow rate is the circuit feed rate.

Table 6 and Figure 13 shows the measured and balanced data and particle size distribution from Survey 1. In general, both measured and balanced data show a good agreement indicating good sampling practices. A similar trend was observed for all the surveys – good agreement between measured and balanced. The measured and balanced data for Survey 2, 3 and 4 are not shown in the paper as the trend is similar to Survey 1. The data shows discrepancy at the hydrocyclone underflow and mill feed P80. During the mass balance, a small discrepancy between hydrocyclone underflow stream and mill feed stream was observed due to slurry residence time in the regrind surge tank. In general, all survey data shows good agreement between measured and balanced. The balanced data was used for performance evaluation.

**TABLE 6**
Measured and balance stream data – Survey 1.

| | Flash float conc. | | Rougher conc. | | Circuit feed | | Hydrocyclone feed | |
|---|---|---|---|---|---|---|---|---|
| | Measured | Balanced | Measured | Balanced | Measured | Balanced | Measured | Balanced |
| Feed rate (t/h) | 12.6 | 12.6 | | 33.6 | | 46.2 | 106.1 | 106.1 |
| % solids | 35.0 | 35.1 | 25.6 | 26.0 | 28.2 | 28.5 | 38.9 | 37.6 |
| P80 (µm) | 171 | 173 | 49 | 49 | 77 | 79 | 59 | 49 |
| | **Hydrocyclone OF** | | **Hydrocyclone UF** | | **Mill feed** | | **Mill discharge** | |
| | Measured | Balanced | Measured | Balanced | Measured | Balanced | Measured | Balanced |
| Feed rate (t/h) | | 46.2 | | 59.9 | 59.9 | 59.9 | | 59.9 |
| % solids | 23.8 | 24.1 | 65.9 | 66.1 | 59.9 | 59.7 | 59.2 | 59.7 |
| P80 (µm) | 24 | 22 | 63 | 50 | 92 | 71 | 35 | 34 |

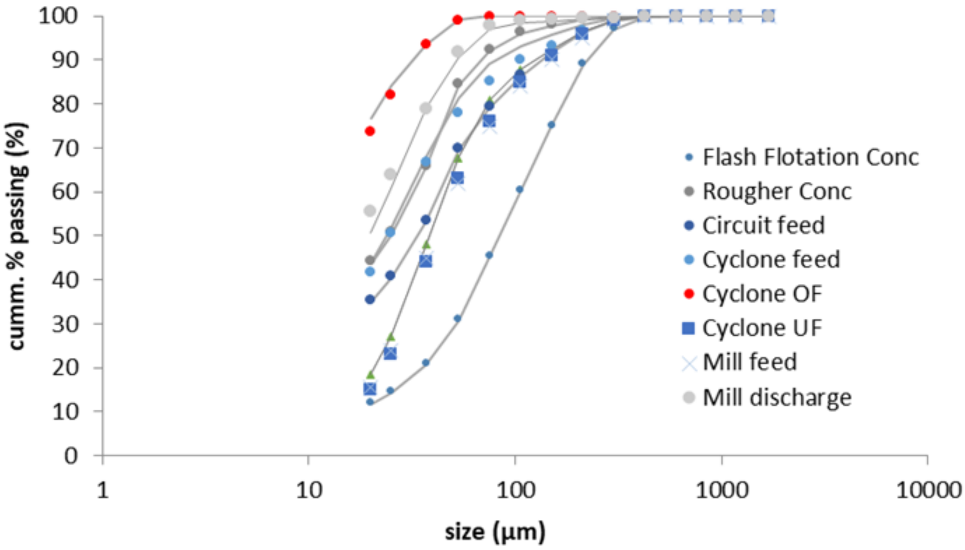


**FIG 13** – TowerMill circuit stream particle size distribution – Survey 1 (Measured: dot, balanced: solid line).

## CIRCUIT PERFORMANCE EVALUATION

Table 7 shows a summary of the circuit operational data and performance indicators. The sulphur grade influenced the TowerMill circuit feed rate in the feed. The data from Survey 2, 3 and 4 show a good relationship between the sulphur grade and regrind circuit feed rate ratio to SAG feed rate (as shown in Figure 14). The orange data point shows the data collected in Survey 1. It is worth collecting more data to build a robust model that predicts the regrind circuit feed rate for a given SAG mill feed rate and sulphur feed grade.

**TABLE 7**

Summary of TowerMill circuit operational data and performance indicator.

| Survey | 1 | 2 | 3 | 4 |
|---|---|---|---|---|
| **Screw Speed (%)** | 100 | 100 | 75 | 50 |
| **Circuit feed rate (t/h)** | 46.2 | 42.0 | 45.3 | 66.1 |
| **Power (kW)** | 1008 | 1066 | 734 | 451 |
| **F80 (μm)** | 79 | 99 | 106 | 75 |
| **P80 (μm)** | 22.2 | 22.5 | 25.2 | 33.8 |
| **SE (kWh/t)** | 21.8 | 25.4 | 16.2 | 6.83 |
| **SSE at 20 μm (kWh/t)** | 52.2 | 57.2 | 41.0 | 41.4 |
| **Bond Operating work index (kWh/t)** | 17.1 | 18.1 | 12.9 | 10.6 |

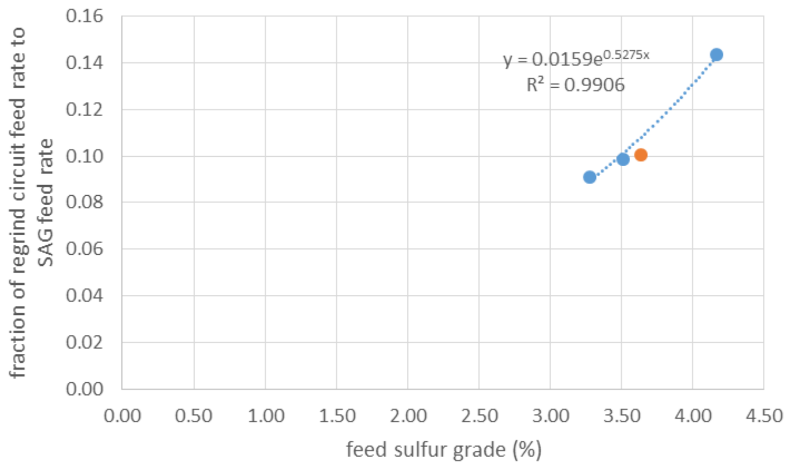


**FIG 14** – Fraction of regrind circuit feed rate to SAG feed rate as a function of feed sulphur grade.

Survey data shows that the circuit feed size ranged from 75 to 106 μm (F80) while the circuit product was ranged from 22–34 μm. A circuit product of 22 μm (P80) was achieved in Survey 1 and 2 when the screw rotational speed was 100 per cent. The operating work index ranges from 17.1 to 18.1 kWh/t, which are lower than the design operating work index value shown in Table 2.

Reduction in the screw rotational speed to 75 per cent has resulted in a lower circuit specific energy value of 16.2 kWh/t, which led to a slightly coarser circuit product size of 25.2 μm, which is within the design value.

Based on these findings, there is an opportunity to operate the TowerMill at a lower rotational speed, ie 75 per cent for OPEX savings (savings in energy, media consumption, and wear parts – screw liners).

Figure 15 shows the signature plot based on the survey data. A good correlation between P80 and specific energy was established to be used as a guide to determine the transfer size from the TowerMill circuit to the IsaMill circuit. Figure 16 shows the new generation of fines (-20 μm) as a function of specific energy for mill and circuit. Theoretically, the amount of fines generation should increase linearly as the specific energy increases. The linear trend lines were plotted using the efficient operation in fines production at 20 μm.

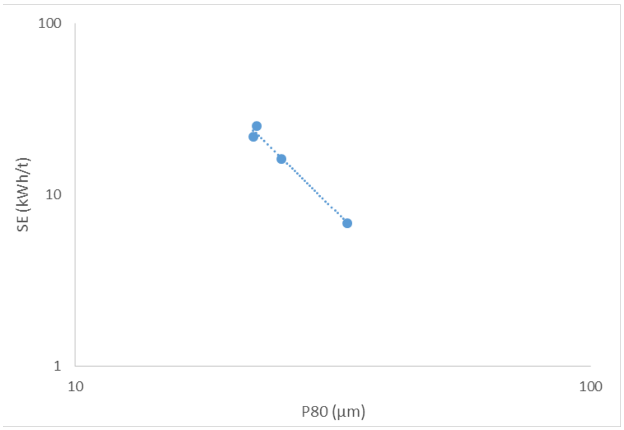


**FIG 15** – Signature plot based on survey data.

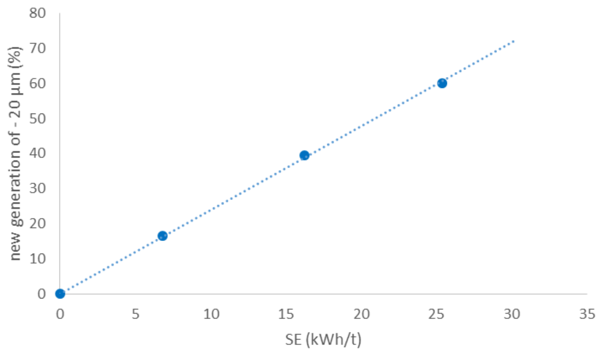


**FIG 16** – New generation of fines as a function of specific energy.

Table 8 shows the hydrocyclone operating data and its performances. Figure 17 shows the hydrocyclone efficiency curves. The hydrocyclone feed per cent solids range between 37–44 per cent. The sharpness of cut (α value) ranged from 0.96 to 1.68. Moreover, Figure 17d shows coarse end deflection indicating coarse low-density material bypass to the hydrocyclone OF stream. Typically, this phenomenon occurs when there are density differences in the particles. The low-density coarse particles flow into the overflow stream while the high-density fine particles flow to the underflow stream. Based on these observations, it is worth conducting assay/mineral by size analysis and evaluating the classification performances by considering the density effect. This analysis provides a better understanding of hydrocyclone behaviours. Plitt roping model was predicting the hydrocyclone is in spraying condition.

**TABLE 8**

Hydrocyclone operational data and its performances.

| **Survey** | 1 | 2 | 3 | 4 |
|---|---|---|---|---|
| **Hydrocyclone feed mass flow rate (t/h)** | 106 | 115 | 119 | 126 |
| **Hydrocyclone feed % solids (%)** | 37.6 | 43.1 | 44.0 | 39.7 |
| **Hydrocyclone pressure (psi/kPa)** | 12.5/86.2 | 12.5/86.2 | 12.5/86.3 | 12.5/86.2 |
| **Number of operating cyclone** | 4 | 3 | 3 | 3 |
| **d50c (mm)** | 21.5 | 22.8 | 22.7 | 33.2 |
| **α (sharpness of cut)** | 1.15 | 1.68 | 1.38 | 0.96 |
| **Fraction water to UF** | 0.17 | 0.25 | 0.20 | 0.13 |
| **P50 (mm)** | 23.5 | 24.2 | 28.7 | 28.7 |
| **Plitt Roping** | 20.2 | 20.7 | 23.7 | 23.7 |
| **Plitt Roping Condition** | Spray | Spray | Spray | Spray |

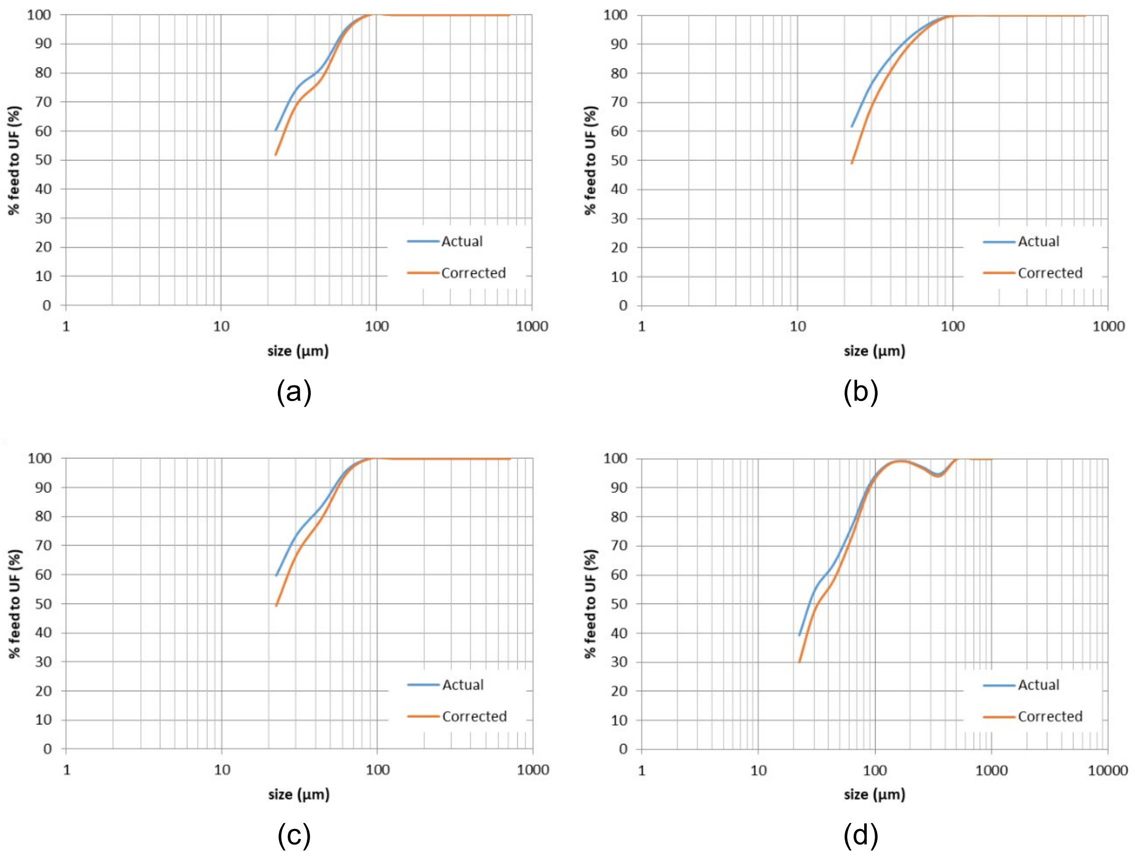


**FIG 17** – Hydrocyclone efficiency curve.

## WEAR PARTS LIFETIME – SCREW LINERS

The TowerMill screw liners consist of tip liner, flight liner, end cap and endplate. The liner wear was calculated based on the first-year operational data. The wear rate for tip liner, flight liners and the end cap is shown in Table 9. In general, the tip liner can last for five months based on the current operational condition considering the feed's abrasive nature. Typically, two units of tip liners and 12 units of flight liners were changed after five months of operation. Meanwhile, the end cap and endplate lasted for a year. Nippon Eirich is developing a new generation high-performance screw liner with longer wear life for abrasive ores.

**TABLE 9**

Wear rate of liners.

| Parts | Wear rate (g/kWh) |
|---|---|
| Tip liner | 0.10 |
| Flight liner | 0.05 |

Consequently, decommissioning the six stirred media detritor mills and replacing the TowerMill and IsaMill operating labour requirements have dropped to a single operator significantly more time dedicated to the flotation circuit operation. Maintenance requirements have been significantly reduced with the first internal inspection of the TowerMill conducted in April 2019 during the final circuit cutover and the first tip liner change at the end of May with the same labour requirements as a single stirred media detritor refurbishment.

## RECOMMENDATION AND IMPLEMENTATION

Based on the survey outcome, several recommendations were made to improve the performance of the circuit. They were:

- Reduce the screw rotational speed to 75 per cent when the mass pull of flotation cells is low.
- Multicomponent analysis – around hydrocyclone streams.
- To determine the appropriate transfer size to IsaMill size that improves the quality of leach feed and reduces the overall OPEX.

The first recommendations were implemented immediately as it is easy to implement and has operating cost benefits, ie savings in energy, grinding media and wear parts consumption.

## CONCLUSION

OceanaGold Haile Gold Mine started its operation in 2015 after acquiring Romarco Minerals and the Haile operation. Since the acquisition, OceanaGold has carried out plant optimisation and de-risking activities. Improvement in the concentrates regrind circuit was identified as an essential activity to improve the leach feed quality, improving the overall gold recovery. Two stages of regrind circuits were chosen based on the feed characteristics (a bi-modal distribution with coarse top size) and high reduction ratio requirement to prepare the leach feed. OceanaGold has chosen to proceed with capital investment to improve the regrinding circuit by installing a TowerMill and an IsaMill for the first and second stage regrinding, respectively. This paper focused on the installation, commissioning and performances of the first stage TowerMill regrind circuit. Good cooperation between OceanaGold and Nippon Eirich teams has resulted in a smooth installation and commissioning.

Moreover, the regrind circuit achieved the design specifications and enhanced productivity. Labour requirement for maintenance has reduced. The TowerMill circuit audit outcomes have indicated an opportunity to reduce the specific energy in the circuit by 25 per cent by reducing the screw rotational speed. At present, the screw rotational speed was reduced to 75 per cent rev/min, which positively impacted operating cost, ie energy, grinding media, and wear part consumption. Further investigation will be carried out around the hydrocyclone to improve the classification. In general, this is a successful capital improvement that has led to a profitable operation.


## ACKNOWLEDGEMENT

The authors would like to thank OceanaGold and Haile Gold Mine for giving their permission to publish this collaborative study's outcomes. The authors would like to thank the Haile Gold metallurgist team for their assistance during the survey and data collection.


## REFERENCE


Larson, C. Anderson, C. Deal, M. Carr D. and Johnston Q. (2017). OceanaGold Haile: Concept to reality. Proceedings of SME Annual Meeting 2017. Denver CO. 1–5.

Wickens, J. Deal, M. Spicher, M. Tittes P. and McDaniel S. (2013). Haile gold mine metallurgy and flowsheet review. Proceedings of SME Annual Meeting 2013. Denver, CO. 1–7.

Jankovic, A. (2001). Medis stress intensity analysis for vertical stirred mills. Minerals Engineering. 14. 1177 – 1186

# The application of ultra-fine grinding for Sunrise Dam Gold Mine

*A Paz[1], C Ypelaan[2], T Ryan[3] and M McInnes[4]*

1. Senior Process Engineer, Metso Outotec, Perth WA 6005. Email: andres.paz@mogroup.com
2. Metallurgical Superintendent, AngloGold Ashanti Australia Ltd, Sunrise Dam, Laverton WA 6440. Email: cypelaan@anglogoldashanti.com.au
3. Manager – Engineering Support, AngloGold Ashanti Australia Ltd, Sunrise Dam, Laverton WA 6440. Email: tryan@anglogoldashanti.com
4. Director Service Technical Support, Metso Outotec, Perth WA 6005. Email: michael.mcinnes@mogroup.com

## ABSTRACT

The AngloGold Ashanti (AGA) Sunrise Dam Gold Recovery Enhancement Project (REP) was an upgrade project to the existing process plant to increase gold recovery. The project required the existing screened cyclone overflow to be redirected into a new flotation and ultra-fine grinding circuit, producing concentrate up to a rate of 400 000 t/a. Metso Outotec supplied six TC200 TankCell® flotation units, one 14 m High Rate Thickener and one HIGmill® HIG3500/23000. At this point in time the HIGmill is the world's largest stirred mill supplied into a pyrite concentrate regrind duty.

This paper discusses the HIGmill test work and sizing, the challenges of commissioning and ramp-up and subsequent design optimisations. The energy efficiency and operational performance is also discussed.

## INTRODUCTION

The Sunrise Dam Gold Mine processing facility commenced operation in 1997 as a two-stage crushing, single-stage grinding plant, treating predominantly oxide material from the Cleo open pit with a capacity of 1 Mt/a. A second ball mill was added in 1999 to increase capacity to 1.5 Mt/a. In 2001 a major upgrade to the plant was completed. This consisted of a three-stage crushing circuit, two-stage grinding and a second parallel leach circuit. This upgrade increased throughput to 2.5 Mt/a and enabled treatment of harder material mined from the deeper levels of the open pit and from the new underground mine. De-bottlenecking projects have incrementally increased throughput to 4 Mt/a. Ore processed is predominantly fresh material sourced from underground mining activities.

As the amount of sulphide material treated increased, gold recovery decreased in response to the refractory nature of the ore. Flotation and fine grinding to treat refractory ore had been periodically explored since 2005. In 2012 as open pit mining was coming to a conclusion and underground material was to be the major mill feed source, the impact of the sulphide material was fully realised. A feasibility study was conducted to design and construct a flotation and ultra-fine grinding circuit.

Test work indicated that a ~6 per cent increase in recoverable gold could be obtained by grinding the sulphide material to 10 μm and leaching combined with the flotation tails in the existing carbon-in leach (CIL) circuit.

## LOCATION AND MINERALOGY

The Sunrise Dam Gold Mine is located 55 km south of Laverton, Western Australia. The regional geology of Sunrise Dam is well documented but understanding continues to evolve. Sunrise Dam Gold Mine is contained within a regional structural domain known as the Laverton Tectonic Zone, which hosts in excess of 20 individual gold deposits, totalling in excess of 27 Moz Au. Of these deposits, only five contain in excess of 1 Moz of gold. The two largest deposits lie within 35 km of each other and Sunrise Dam is the largest deposit in the Laverton Tectonic Zone with at least 11 Moz (AGA, 2014).

The Sunrise Dam deposit contains a structurally complex series of gold-rich orebodies with a variety of ductile and brittle deformation fabrics that influence the nature, geometry and distribution of the mineralisation. At Sunrise Dam, gold mineralisation is structurally controlled and vein hosted. The style of mineralisation can be differentiated depending on the structure or environment in which it is hosted. There are three dominant domains that are now recognised (AGA, 2014):

1. Shear-related and high ductile strain – eg Sunrise Shear Zone.
2. Stockwork development in planar faults with high strain brittle characteristics.
3. Placer-style mineralisation hosted within the fluvial sediments.

Broadly the ore types can be subdivided into pyritic and arsenical types. Sunrise Dam falls into the latter category where the ore types are dominated by arsenopyrite and arsenian pyrite. Arsenical ores vary in terms of processing from being free-milling to highly refractory depending on grain size. Fine grained arsenopyrite (sub mm) is typically highly refractory because there is a high concentration of submicroscopic gold which is structurally locked up in the crystal lattice. Gold recoveries for these refractory ores in the Yilgarn Craton are typically in the range of 30–80 per cent. As a consequence, several operations in the region have adapted their processing plants to treat the refractory ore by roasting (SuperPit), bacterial oxidation (Wiluna) or finer milling.

## PLANT DESCRIPTION

The Sunrise Dam plant has been running since Feb 1997. Ore is treated in a conventional gravity and CIL processing plant. The original design capacity at start-up was 1 Mt/a and as of 2018 throughput was 4 Mpta. Over the years Sunrise Dam has added extra crushing and ball milling capacity.

In 2017 AngloGold Ashanti (AGA) embarked on a Recovery Enhancement Project to increase gold recovery by ~6 per cent. A flotation cell bank was installed to recover the refractory pyrite, followed by a thickener and a HIGmill to provide fine grinding and liberation before the CIL circuit. Metso Outotec supplied the six TC200 TankCell® flotation units, one 14 m High-Rate Thickener and one HIGmill® HIG3500/23000 (Figure 1).

**FIG 1** – HIGmill, thickener, flotation circuit.

The flow sheet comprises three-stage crushing and two-stage grind, to flotation concentrate, to thickener, to HIGmill. Flotation tailings are combined with HIGMill product and sent to CIL.

The HIGmill is in open circuit with all concentrate reporting to the HIGmill for a single pass (Figure 2). Depending on throughput and slurry density, a grind P80 of between 9–12 µm is achieved. Metallurgical test work identified that grinding to 10 µm would deliver additional recovery in the 6 per cent to 8 per cent range. Since the commissioning of the ultra-fine grind circuit, a total of 7.7 Mt was processed at an average feed grade of 2.15 g/t and 82.1 per cent recovery.

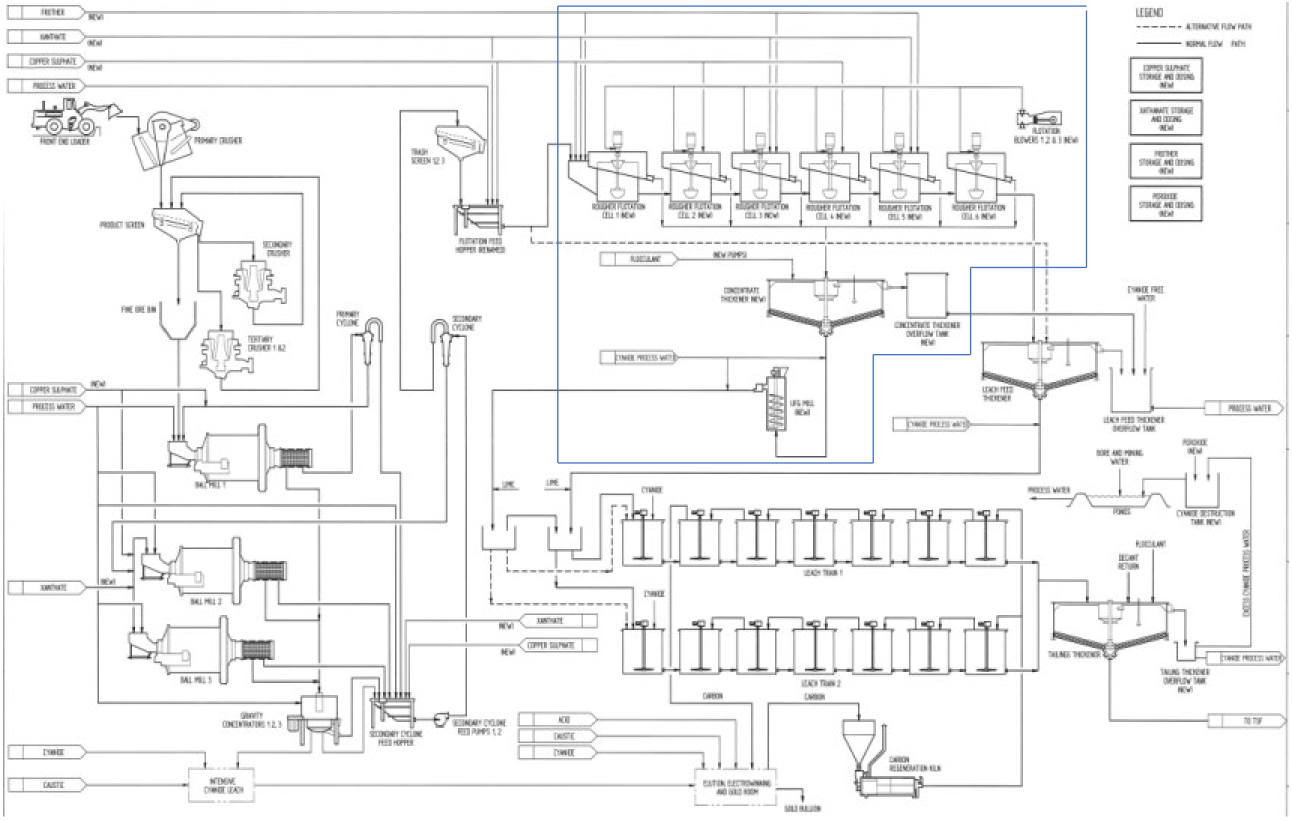

**FIG 2** – Process flow diagram (AGA, 2017).

The HIGmill grinds pyrite/arsenopyrite concentrate to 10 µm in order to release refractory gold for leaching. A single operator is required for the flotation, thickener and HIGmill area.

## HIGMILL SIZING

### Test work

Metso Outotec conducted HIGmill® grindability test work on a pyrite concentrate sample in 2016. Due to the limited sample size available the Small Sample Test (SST) method was conducted using 5 kg of solids. The feed F80 measured was 182 µm.

The SST was conducted in a HIG5 unit in closed circuit, with the mill speed and flow rate fixed. 4 mm media top size was selected based on previous experience of feed and product grind size. In the test procedure slurry is mixed to a target density of 45%w/w. The test slurry is pumped continuously through the mill and the mill is turned on for a certain amount of time to input power, then the mill is turned off and the sample is allowed to homogenise before taking a product sample. The mill is turned on again and the process is repeated.

The test results are presented as a performance graph (Figure 3) and are used for mill sizing. For the design F80 of 175 µm, the required specific grinding energy (SGE) was found to be 56 kWh/t for 10 µm.

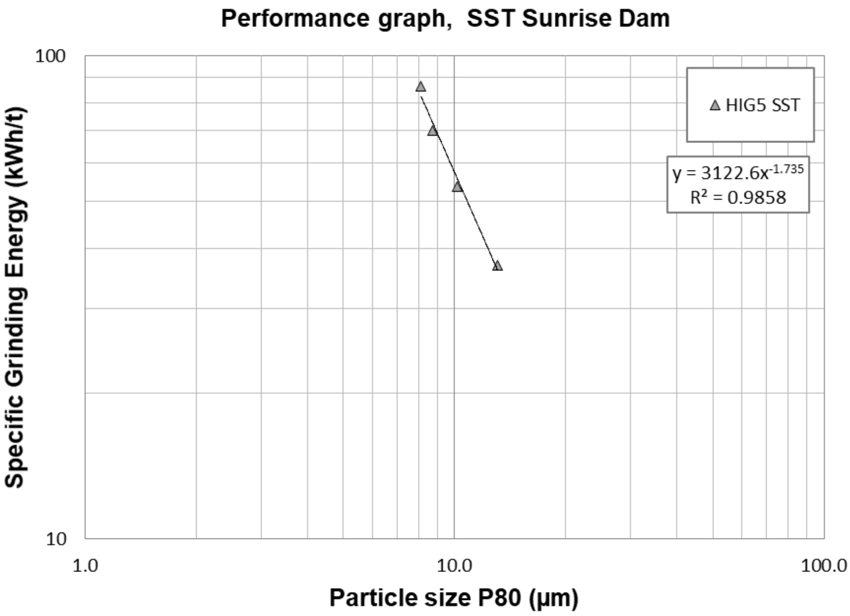


**FIG 3** – Performance graph for SST.

## Design

A HIGmill size of 3500 kW with 23 000 L body was selected based on the test work and design criteria. The process design criteria are outlined in Table 1.

**TABLE 1**

Process design criteria.

| Description | | Design Nominal | Design Maximum |
|---|---|---|---|
| Throughput | tph | 33.1 | 47.3 |
| Milling density | %w/w | 45 | 45 |
| Flowrate | $m^3/h$ | 48 | 53 |
| Solids SG | $t/m^3$ | 3.31 | 3.31 |
| Liquid SG | $t/m^3$ | 1.1 | 1.1 |
| Slurry SG | $t/m^3$ | 1.57 | 1.57 |
| Feed Size F80 | µm | 175 | 175 |
| Product Size P80 | µm | 10 | 10 |
| Reduction Ratio F80/P80 | # | 17.5 | 17.5 |
| Net Specific Grinding Energy | kWh/t | 56.0 | 60.0 |
| Power Draw (Motor Output) | kW | 1912 | 2926 |
| Installed Power (Motor Output) | kW | 3500 | 3500 |

Although the secondary grinding P80 was 175 µm, the P80 of the concentrate was expected to be 135 µm due to sulphide preferential grinding in the closed-circuit configuration. The design SGE was not reduced and instead this was considered design contingency.

The design power draw was 2923 kW and was checked against power models to ensure that the mill would operate in a suitable speed range across the lifetime of the internal wear parts.

Due to the target fine grind size, other design considerations were based on residence time and media retention requirements. The fine grind size required media retention in the mill of a 2 to 3 mm size range and media specific gravity (SG) range of 3.8 to 4.1. Media is retained in the HIGmill due to media fluidisation conditions relating to the settling velocity and flow rate. Media is also held within the chambers (stator compartments) by the centrifugal force generated by the rotors.

An energy balance confirmed that the exit temperature for the design was suitable for the materials of construction. The design inlet temperature of 30°C, 60 kWh/t, 45%w/w yielded an exit temperature of 66°C. The HIGmill was designed with a high alarm temperature limit of 70°C and a trip limit of 85°C.

## PROJECT

AGA worked closely with the engineers to ensure decisions were made during the EPC phase. They reviewed the specifications and mill selection.

The Recovery Enhancement Project was delivered very quickly; installation time for the complete upgrade project was approximately six months, and commissioning was four weeks. The HIGmill delivery time was 30 weeks ex-works.

Once the civil foundations were ready, the HIGmill installation took four weeks. Cold and wet commissioning took one week. Process Commissioning lasted one week, occurring in the last week of May 2018. The Recovery Enhancement Project was completed two weeks earlier than expected and under budget.

## COMMISSIONING

The mill was commissioned in May 2018 and has been operating since June 2018. Wet commissioning requires the checking and implementation of control logic and fine tuning is carried out during ore commissioning. Survey data was collected during ore commissioning to track the performance of the equipment and optimise the mill performance.

### Wet commissioning

The water calibration curve conducted during wet commissioning, as shown in Figure 4, was performed with 19 t of media, a media size range of 2–4 mm and a media specific gravity (SG) of 3.9 t/m$^3$. The mill may draw 30 per cent to 40 per cent less power with slurry compared to water due to the media fluidisation conditions such as buoyancy and viscosity. It is important to measure the speed/power/mill load/flow rate relationship during commissioning for both water and slurry, as the relationship is different for each application. These values are used to assess the mill's capability and are used for future operational guidance. These results can also be put into power models, for prediction of the operation and (if required) assist with future optimisation of the rotor design.

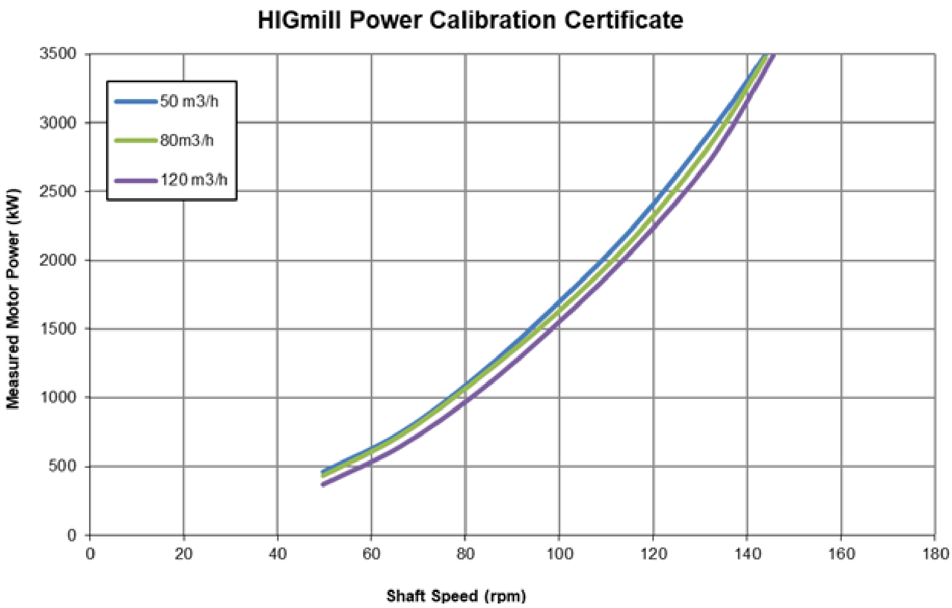


**FIG 4** – HIGmill power calibration certificate.

## Ore commissioning

During ore commissioning, the slurry density was optimised to account for the slurry viscosity effect on energy efficiency. A marsh funnel test (Fann, 2017) was conducted on several samples with varying feed densities. The optimum feed density generally corresponds to a marsh funnel time of 36 seconds. As detailed by Larson (2011), the Marsh Funnel is not a comprehensive measurement of rheology but serves as a quick and easy test. The current rule of thumb for this site recommends marsh times less than 36 sec. The marsh time limit typically comes from a plot of marsh time versus density, where it identifies the limit as the point at which marsh time rapidly increases with increasing density. If the time is greater, then the media movement and energy transfer is restricted, resulting in reduced energy efficiency. For the grind size of 10 µm, the optimum slurry density was found to be 37–38%w/w (Figure 5), which is considerably lower than the 45%w/w design density. It was observed during commissioning that operating above 38%w/w the media bed location is altered due to buoyancy.

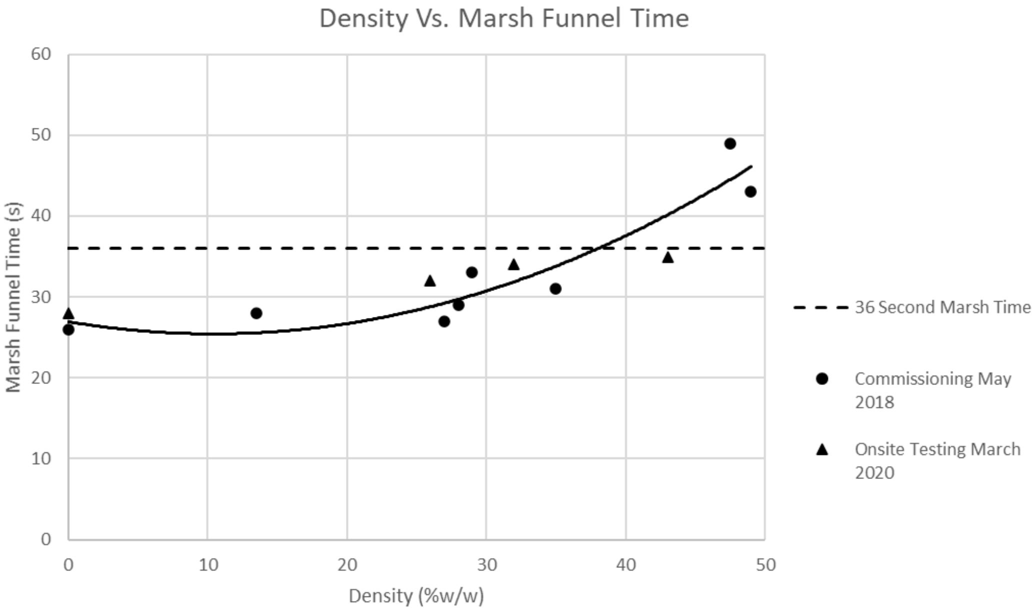


**FIG 5** – Marsh funnel test.

Subsequent Marsh Funnel testing in March 2020 (Figure 6) indicates that increasing the operational density to 43%w/w might be possible and is currently the subject of further optimisation.

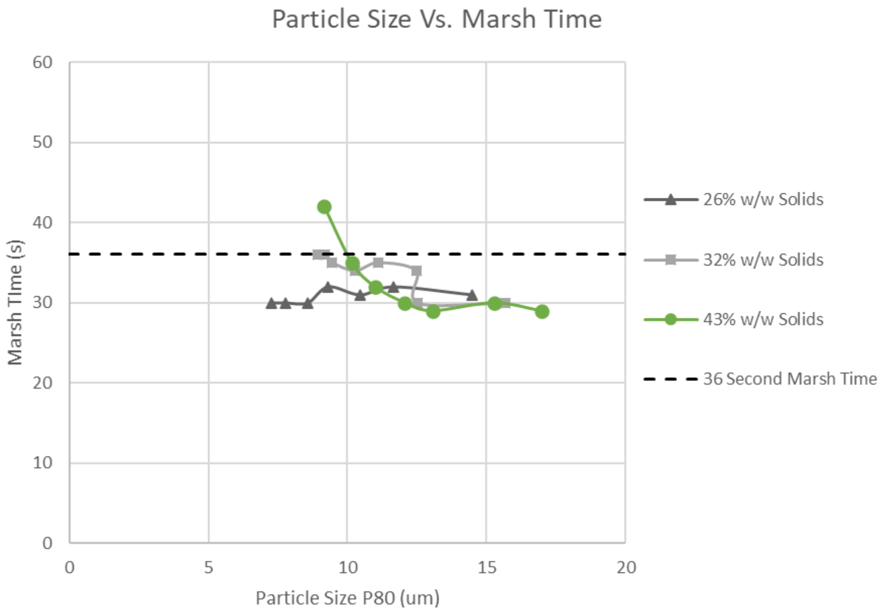


**FIG 6** – Marsh funnel test March 2020.

During ore commissioning the mill was filled with 2–4 mm ceramic media with an SG of 3.9 t/m$^3$. The process performance was tracked to target the P80 = 10 μm. It was observed that operating the mill with greater than 50%v/v media filling, combined with longer run time for media wear in, improved the energy efficiency. It is believed that this is due to the near plug-flow conditions experience at these filling levels, and the graded charge containing finer 2–3 mm media better suited to the feed size and target product size. A signature plot was generated for the first week of operation (Figure 7) and indicates the SGE required to achieve 10 μm was 59 kWh/t. During commissioning the feed size F80 was in the 30 to 60 μm range (laser measurement). This range, combined with the improved energy efficiency from media charge wear-in, lead to future media charges being 2–3 mm in top size.

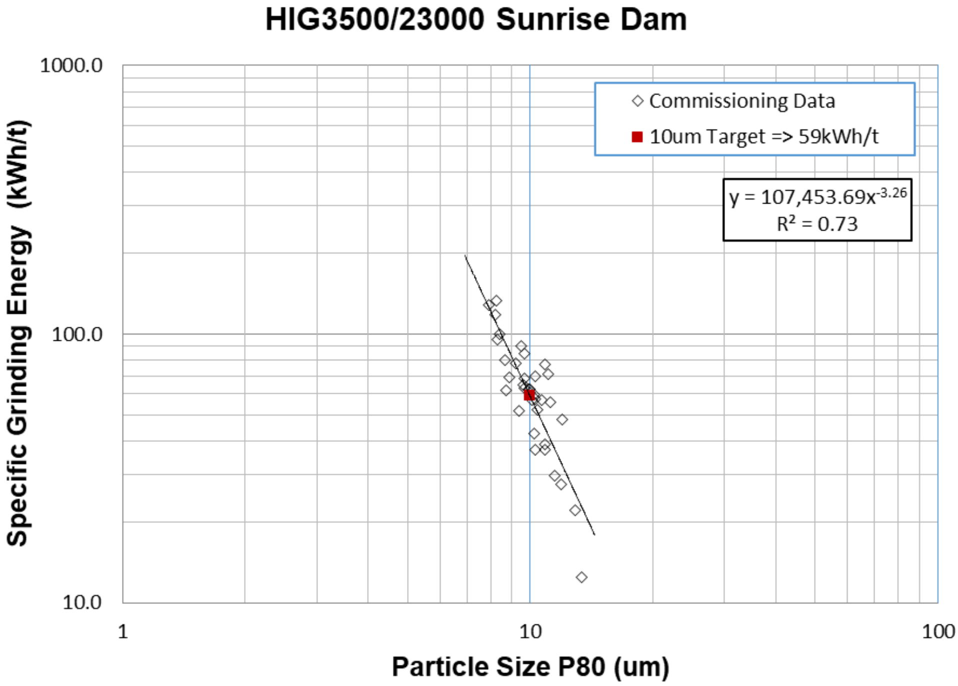


**FIG 7** – Commissioning survey data: 2–4 mm media.

One of the main challenges associated with obtaining the target grind size was the accurate measurement of P80 at the 8–12 μm grind size. P80 variances depended on: the operator experience from shift to shift; the average P80 of three tests versus the maximum P80 of one test; and the laser machine type and model. It should be noted that an online particle size analyser was not purchased for this plant expansion due to the reasonably stable feed size and concentrate mass flow rate. Automatic samplers are used, and the product size is verified manually in the laboratory's laser size machine.

The HIGmill feed pipe velocity is designed for 0.75 to 1.1 m/s for nominal and design flow rates. During commissioning, it was noticed that on start-up, when the pipe velocity reached 0.7 m/s, the 2–4 mm SG 3.9 t/m$^3$ media quickly cleared and the flow was unrestricted.

During the first week of ore commissioning, the mill was tested to obtain P80 in the 7 to 8 μm range inputting up to 110 kWh/t energy. The mill discharge temperature reached 80°C at one stage, which is less than the HIGmill trip limit of 85°C.

## RAMP UP PHASE (6 MONTHS POST COMMISSIONING)

The Sunrise Dam HIGmill achieved the design grind size and desired throughput quickly after commissioning. The key development area during the ramp up period was optimisation of wear component life and design to prevent component failure. During this ramp up period three failures occurred over the first five months, requiring unplanned shutdowns. These events, in order of occurrence, are listed below:

- The bottom cover plate polyurethane liner lifted from its backing plate the day after commissioning, due to a bonding issue, and damaged the bottom rotor. This required rebuilding the shaft (replacement of the broken rotor in position one) and exchange of the bottom plate liner with a rubber lined unit.

The decision to change to rubber wear material was due to a delay in the spare parts package and a quick turn-around was required. As of 2021 the same rubber wear material bottom cover plate liners are operating with change out cycles of 26+ weeks.

- After approximately seven weeks of continuous operation, one of the shell liners in the middle section of the mill failed and caused a subsequent rotor failure. The root cause analysis found the cast stator ring eroded away at the shell wall, which exposed the liner carrier steel structure to media and slurry ingress. Rubber on the liner carrier lifted and impacted on the rotor, causing the failure.

  As a result of this failure, Metso Outotec and AGA implemented a development program to design, trial and refine different stator ring materials and manufacturing techniques. Further details of this are found later in this paper.

- Approximately five months into the ramp up period, and after the failure in item two above, another unplanned shutdown occurred, and a solution was developed to rubber line hard cast stator rings. Errors in the surface preparation by a third-party contractor led to stator bonding failure and required another unplanned shutdown.

  This failure led to the development of new stator ring construction methods and rubber destructive testing techniques to verify bonding strength.

## OPTIMISING SHUTDOWN INTERVALS

Post commissioning, AGA advised that a key expectation was for the HIGmill to meet a minimum plant shutdown interval of 17 weeks. Total plant shutdown durations of approximately three to four days were available if required. Within 18 months, post commissioning, the HIGmill service interval between shutdowns was ramped up progressively to 23 weeks and effectively met AGA's target. Current operating campaigns are approximately 26+ weeks, with the aim to extend where feasible and attempt to phase into normal plant shutdowns. By matching the HIGmill shutdown timing to normal plant shutdowns, the annual HIGmill availability is improved, in addition to machine utilisation and gold recovery. When the HIGmill maintenance cycles do not match the plant shutdown schedules, the flotation and HIGmill is simply bypassed and selective ROM feed is processed based on expected ore grade and Mine to Mill planning.

Since commissioning, the HIGmill reline times have been optimised to approximately 36 hours, whilst maintaining safety expectations. This period captures machine shutdown through to handover back to the plant operations for re-start. This timing is achieved using rotable shell and shaft assemblies, specific tooling to match the works, various lifting equipment and Metso Outotec service technicians.

The two major components, which were the focus of wear life optimisation post ramp up, were the castellated grinding rotors and shell liner stator rings. The original designs and geometries were satisfactory, but the material selection did not meet AGA's wear life/shutdown schedule expectation. The grinding rotors were a cast material, which worked well in light duties or in smaller HIGmills, but were not fulfilling the expectations for this larger diameter, high tip tangential velocity, power-intensive fine grinding application.

## CASTELLATED ROTOR DEVELOPMENT

The development of the castellated rotor is detailed in various papers with reference to the Kevista site (Heath *et al,* 2017; Nielsen *et al,* 2016; Keikkala *et al,* 2018) where rotors with castellations were first designed and installed. The next evolution for the castellated rotor was a change in construction material and was implemented at Cracow (Paz *et al,* 2019). At Cracow, the rotor wear material was changed to rubber. Based on the feedback from this first trial at Cracow, AGA and Metso Outotec agreed to implement rubber castellated rotors in the Sunrise Dam HIGmill in December 2018. As this was a staggered approach, the initial quantity of rotors was four units mounted from the bottom of the shaft (rotor position one through four), as this location is exposed to the highest pressure and wear. This orientation is illustrated in Figure 8. As illustrated in Figure 8 the reduction in cast rotor diameter led to increase in media and slurry packing between the grinding chamber stator rings. The packing protected the shell carrier lining but led to increase in wear on the rotors' outside diameters and stator ring internal diameters/surfaces.

**FIG 8** – First use of flat rubber castellated rotors at Sunrise Dam (rotor position 1 through 4). Note the worn/reduced diameter of the cast rotors in position 5 through 12.

The improvement in wear life observed with these four rubber rotors led to the decision to ramp up the installed quantity from four to eight units in the next cycle and eight to eleven in the subsequent cycle. The latest shaft operating designs have eleven flat rubber castellated rotors in addition to two cranked cast castellated units. The cast units are from the original stock holding and are part of the phase-out consumption plan. The wear life on these cast units in rotor position 12 and 13 is sufficient to match the current operating cycles as shown in Figure 9. The cast non-castellated rotors, in position 14 through 18, are not always consumed per operating run and can be reused when assessed fit for operation. When the stock of the cast rotors is depleted, the plan is to replace with rubber lined units.

**FIG 9** – Rotor assembly with flat rubber castellated rotors prior to despatch from MO workshop.

The original castellated rubber rotors were flat in orientation. This flat definition means the rotor hub is in the same plane as the rotor ring. The cranked definition relates to the rotor hub being offset to the rotor ring via the use of spokes (Figure 10). Cranked rotors have the benefit of rotor spokes engaging the media zone between grinding chambers and ensuring the media is continuously stirred.

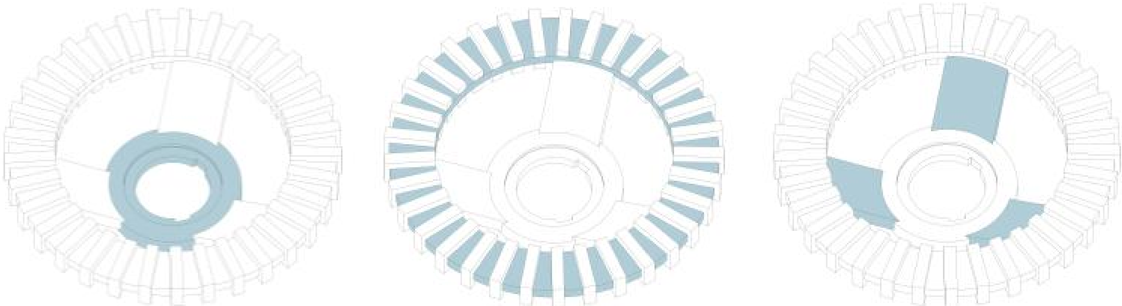

**FIG 10** – Castellated grinding rotor terminology (LHS – hub, Middle – rotor ring, RHS – spokes).

In addition to the previous developments in the castellated rubber rotors, a recent development is a moulded cranked design. The moulded rubber cranked rotors were previously field tested and three units were trialled for Sunrise Dam. These three units have been used in two operating cycles over 50 weeks. The assembly as shown in Figure 11 was installed during April 2021 and will have ten cranked rubber castellated rotors installed plus one flat unit. Operating power draw will be monitored and measured to observe possible process improvements.

**FIG 11** – Rotor assembly installed April 2021 prior to despatch from MO workshop.

## STATOR RING DEVELOPMENT

Following the failure of a cast stator ring seven weeks post commissioning, an intensive product development period started. Various materials and structures were trialled. In the initial period protective coatings, such as spray urea and hand laid poly urethanes, were applied on-site to existing cast units, with no success. Special plastic material was also used with some novel designs, but the product erosion resistance was not satisfactory. Whilst these smaller trials were underway, other designs, with longer manufacturing requirements, were also being investigated.

After resolving the bonding issues, rubber lined cast units were installed and have been successfully operating for long 20–26-week shutdown cycles. These rubber-lined cast units are deemed too expensive but were part of a stock phase out plan.

The two best performing stator ring materials at Sunrise Dam have been cast polyurethane (PU) stators and pressure moulded rubber stators, both with mild steel skeleton cores. Various grades of PU and rubbers have been trialled as shown in Figure 12. Metso Outotec and AGA have selected one of the cast PU designs as the machine standard due to optimised lead times, cost and wear life performance.

**FIG 12** – Shell with assembled shell liners and stator rings. Note different grade PU (red/yellow) mounted from the bottom/feed end of the mill shell through to rubber lined cast and cast only stator rings positioned higher up in the shell arrangement, above the media transition zone.

## WEAR LIFE OPTIMISATION SUMMARY

As the operating/shutdown cycles increase for the Sunrise HIGmill, new wear challenges arise and the critical components driving shutdown timing are shifting. Sunrise Dam's optimisation journey continues with a joint AGA and Metso Outotec effort, intent on reducing the total cost of ownership whilst maintaining safety, machine availability and key performance parameters.

## PLANT AND MACHINE AVAILABILITY

The HIGmill overall utilisation is 97 per cent and has an availability of 98.6 per cent. The availability is governed by the shell liner wear life interval of approximately 26 weeks, harmonising with other general plant shutdowns, and allows for a further two inspections per annum.

The HIGmill reline periods run for 36 hours each, excluding operator shutdown and start-up time. The main plant shutdown period is generally between 36–48 hours, governed by the primary milling circuit relines.

## SCALEUP AND OPTIMISATION TEST WORK

Metso Outotec conducted on-site scaleup pilot test work in 2020 to study the effect of residence time and operational density on the energy efficiency. A full scale HIGmill survey was conducted over a three-hour period where feed sample was collected for further HIG5 test work.

It was shown that residence time of 2 and 3 mins in the HIG5 unit didn't affect the energy efficiency significantly compared to the full scale (Figure 13 and Table 2). The results indicate that the full-scale operation is slightly more energy efficient than the HIG5 pilot test work. Please note the full-scale power measured was the VSD output, and a system efficiency of 92.63 per cent was used to compare the data against the HIG5 test work. The system efficiency allows for the gearbox efficiency, motor under partial load and motor cable transmission.

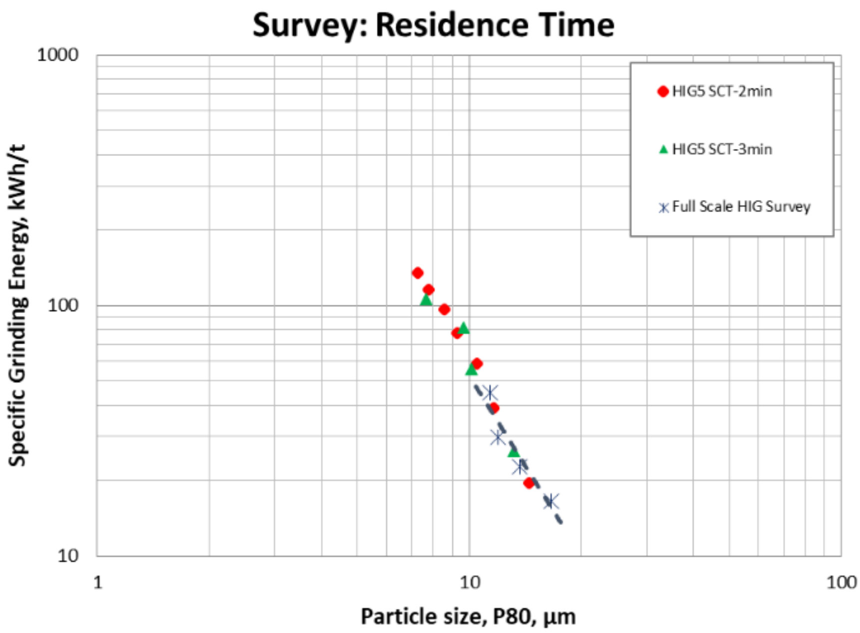


**FIG 13** – Scaleup test work – residence time.

**TABLE 2**

Scaleup test work – residence time.

| Test Description | Density %w/w | Time | P80 | A (Power Model - exponent factor) | B (Power Model - coefficient) | Specific Grinding Energy for P80 | $R^2$ coefficient of determination |
|---|---|---|---|---|---|---|---|
| Full Scale HIG Survey | 35.7 | 612.3 | 10.0 | -2.4 | 12722.3 | 52.4 | 0.894 |
| HIG5 SCT-3min | 27.5 | 181.0 | 10.0 | -2.6 | 25162.3 | 59.1 | 0.935 |
| HIG5 SCT-2min | 26.5 | 129.3 | 10.0 | -3.1 | 71961.2 | 62.5 | 0.996 |

Note: The line of best fit is based on a power model, where A is the exponent and B is the coefficient.

It was shown that a slurry density of 43%w/w was more energy efficient than the 26.5 per cent and 32%w/w tested in the HIG5 unit. However, this was counter to expectations with regard to slurry viscosity measured in the Marsh Funnel indicating a 37–38%w/w density limit. The full-scale survey was conducted at a density of 35.7%w/w and coincidently lies between the 43%w/w and 32%w/w density lines for the HIG5 (Figure 14 and Table 3). Considering the Marsh Funnel time, it was realised that the full-scale HIGmill was running at the optimum slurry density. Furthermore, the lower slurry density supports a reduced exit slurry temperature from the mill and therefore doesn't soften or weaken the wear part materials inside the HIGmill.

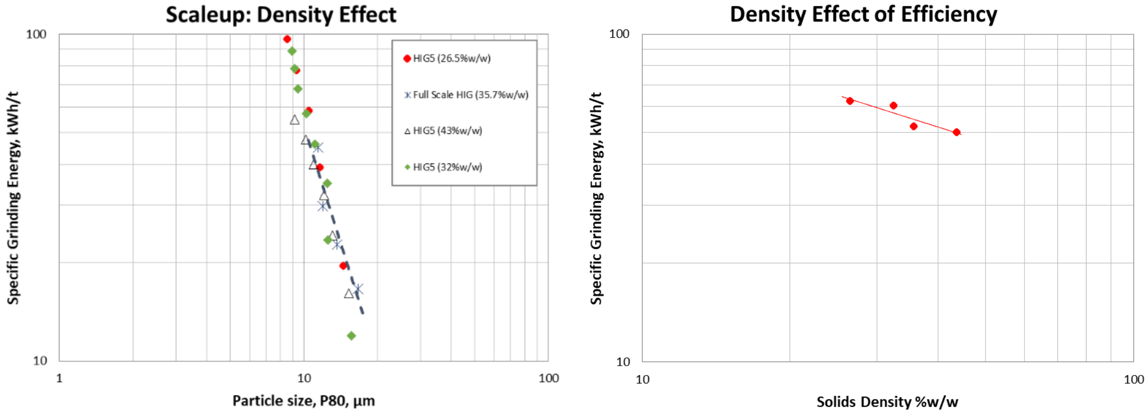


**FIG 14** – Scaleup test work – slurry density.

**TABLE 3**

Scaleup test work – slurry density.

| Test Description | Density %w/w | Time | P80 | A (Power Model - exponent factor) | B (Power Model - coefficient) | Specific Grinding Energy for P80 | $R^2$ coefficient of determination |
|---|---|---|---|---|---|---|---|
| HIG5 (26.5%w/w) | 26.5 | 129.3 | 10 | -3.1 | 71961.2 | 62.5 | 0.996 |
| HIG5 (32%w/w) | 32.5 | 133.6 | 10 | -3.5 | 179091.1 | 60.6 | 0.971 |
| Full Scale HIG (35.7%w/w) | 35.7 | 612.3 | 10 | -2.4 | 12722.3 | 52.4 | 0.894 |
| HIG5 (43%w/w) | 43.6 | 129.3 | 10 | -3.1 | 58731.1 | 50.2 | 0.947 |

The daily averages of the operational data have been plotted against the signature plots obtained from site scaleup HIG5 and its full-scale survey (Figure 15). The scaleup test work and survey is aligned with the bulk of the operating data. We can see that the operational data varies with respect to P80 and SGE, and we believe this is due to the following main reasons:

- The mine operates with open pit ore and underground ore and has a wide range in mineralogy.
- The HIGmill was run at a fixed speed.
- The operational density is operating in a range from 30%w/w to 38%w/w.
- Natural variability due to 12 hr testing frequency is observed in the daily operating data. Sampling frequency is a 12-hr shift composite.
- With SGE control it is much easier to target a P80 product size with variations in throughput. There is no online Particle Size Analyser (PSA) installed in the circuit, and as such no P80 control loop was implemented to account for natural variations in mineralogy.

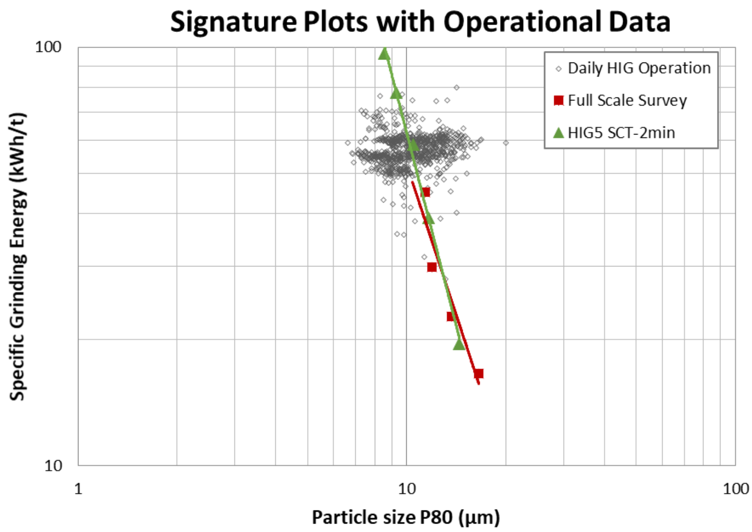


**FIG 15** – Signature plots with operational data.

## PROCESS AND OPERATIONAL PERFORMANCE

In the first 18 months of operation the HIGmill has obtained an average product size P80 = 9.4 µm. The corresponding gold recovery for the period was 81.5 per cent. For the 12 months after, the HIGmill grind size was 12.5 µm with a corresponding gold recovery of 82.6 per cent.

Gold recovery is impacted by grind size above 12.5 µm. This increased grind size is attributed to a number of factors including highly variable mineralogy of the feed ore and high talc concentrations. Overall recovery improvement of ~6 per cent has resulted from the installation of the fine grind circuit, with further optimisation of the circuit continuing.

Historically, the CIL recovery can be correlated accurately with the As/Au ratio, which formed the theoretical recovery for the plant prior to the fine grinding recovery upgrade and is currently used to demonstrate recovery improvement attributed to the Recovery Enhancement Project (REP).

The key HIGmill operating results are presented in Table 2. The highest average throughput achieved was 46.2 t/h with a power draw of 2571 kW and a product size P80 of 10.1 µm. This scenario is close the design throughput requirement of 47.1 t/h in Table 1, however the specific grinding energy of 52.6 kWh/t to achieve 10 µm is much lower than design.

The mill is achieving the product size (P80) design expectation of 10 µm. The mill has not processed the feed size (F80) design parameter of 175 µm. The coarsest feed size processed in the mill was an F80 of 101.3 µm with high reduction ratio 10.55, which achieved a product size P80 of 9.6 µm with an SGE input of 47.1 kWh/t (Table 4).

In Figure 16, the operational data exhibited a consistent trend for a five-month period, where we can see that most variables, such as P80 and SGE, are steady with the exception of F80. F80 varied significantly, however this didn't affect the P80 as much. The P80 was below 10 µm up until the September quarter 2019, when there was an increase in ore hardness (due to more silica in the above ground ore) and SGE set point not being increased.

**TABLE 4**

Operational results.

| | Operational | | | | |
|---|---|---|---|---|---|
| | Ave first 18 months | 12 months later | Highest Daily Ave. Throughput | Highest Daily Ave. Flowrate | Highest Daily Ave. F80 |
| Date (from) | 20/05/18 | 12/11/19 | 17/12/19 | 9/03/20 | 27/09/20 |
| Date (To) | 11/11/19 | 9/11/20 | 17/12/19 | 9/03/20 | 27/09/20 |
| Throughput | 35.1 | 37.8 | 46.2 | 35.8 | 28.3 |
| Milling density | 35.9 | 35.2 | 38 | 30.8 | 27.7 |
| Flowrate | 69.2 | 75.6 | 85.5 | 87.7 | 75.3 |
| Solids SG | 3.31 | 3.31 | 3.31 | 3.31 | 3.31 |
| Liquid SG | 1.065 | 1.065 | 1.065 | 1.065 | 1.065 |
| Slurry SG | 1.41 | 1.40 | 1.43 | 1.35 | 1.31 |
| Feed Size F80 | 31.0 | 38.8 | 21.1 | 47.1 | 101.3 |
| Product Size P80 | 9.4 | 11.9 | 10.1 | 11.6 | 9.6 |
| Reduction Ratio F80/P80 | 3.31 | 3.26 | 2.09 | 4.06 | 10.55 |
| Net Specific Grinding Energy | 51.9 | 54.0 | 52.6 | 42.8 | 46.0 |
| Power Draw (VSD Output) | 1963 | 2196 | 2571 | 1703 | 1511 |

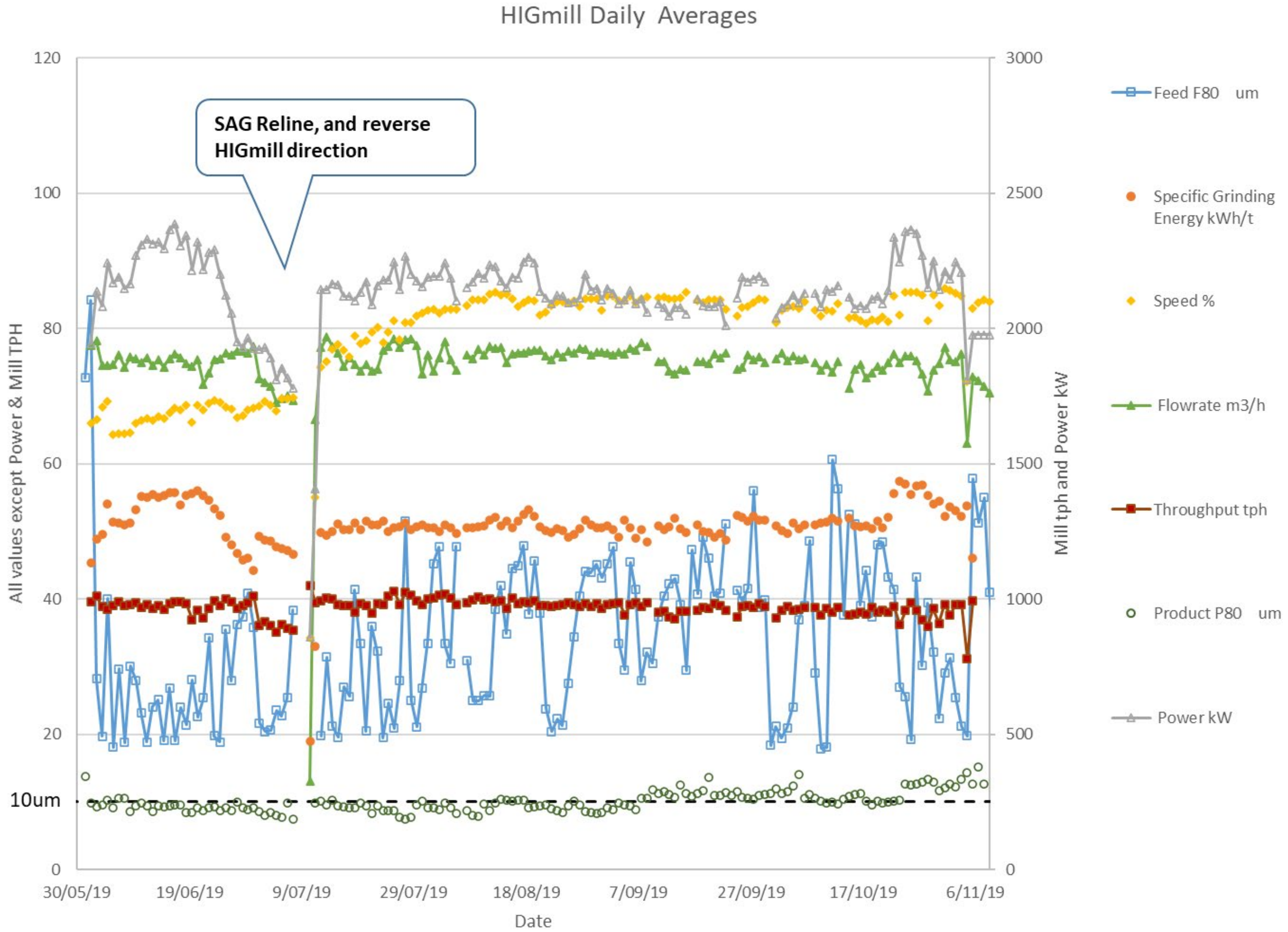


**FIG 16** – HIGmill operation – daily averages for a 20-week period.

The flotation circuit is operating well, and to ensure that pyrite is not depressed, there is a need to keep the Weak Acid Dissociable cyanide level in the process water below 20 ppm via cyanide detox.

There were some challenges during commissioning with lower adsorption kinetics observed due to the flotation reagent Potassium Amyl Xanthate (PAX), which resulted in the requirement for more carbon loading in CIL. A new kiln to allow for higher carbon regeneration rates has been installed to manage xanthate fouling of the carbon. The pre-oxidation tank in the existing CIL circuit was contributing to reduced recovery as the fine grind product, which had a high oxygen demand, was introduced and passivation of the surfaces resulted. This was overcome by converting the pre-oxidation tank to a leach tank through the addition of cyanide. Further test work and trials are continuing to identify the optimal leaching conditions and further increase recovery.

## Operator feedback

According to operators, the HIGmill is running well. It is very easy to change the mill speed, adjust the energy input and change the P80 during operation. As the thickener has been installed prior to the HIGmill, with large ~45 min mass inventory, a steady state process is easily achieved, delivering consistent throughput, flow rate and density.

In theory the rotor life can be maximised by increasing the media load in the mill and slowing the rotor speed down. Wear rate is proportional to the rotor speed to the power of a factor. Once the maximum media fill level or an upper torque limit is reached, the mill speed can be increased as the rotors wear to maintain the required power draw.

Media level measurements needed to be taken frequently during the first three months, as the media wear rate was unknown. There are various methods to measure the media level, including vibration (or acoustic) measurements between each shell segment, a special strain gauge, or a Boroscope camera. A Boroscope camera with light is used at Sunrise Dam to inspect the wear components or media fill level. The time it takes to conduct a Boroscope mill inspection is 10 hours: one hour grind out, four hours media dump, one hour inspection, and four hours to return media to mill. The current method of monitoring media fill level is to stop the mill, drop a weighted rope with measurement markers to the charge level and calculate the percentage of mill filled. This process takes less than an hour to complete and is performed weekly. This frequency is due to the highly variable viscosity of the mill feed and allows for accurate monitoring of the media wear and ejection from the mill.

The media charging mechanism is a six-tonne capacity davit crane, loading media into a charging hopper mounted over the mill. The ceramic media is loaded into the mill using a 4.5 t kibble. The current media charge is about 30 t with new rotors, and the aim is to maintain this level during operation. The removal of 30 t of media from this sized mill is labour intensive due to the use of the kibble and bags to remove media, therefore for future optimisation projects a media handling system would be reviewed.

The mill scats 1 to 1.5 mm media due to various factors, including the media vortex in the mill, buoyancy of the media size, combined with the media sphericity and slurry viscosity. AGA has re-directed HIGmill discharge slurry to an existing trash screen arrangement which is scalping this extremely small size media from the CIL feed. This arrangement is working successfully, and operators have monitored a steady state of media scat generation. Media loss from the mill can wear out the CIL pumps prematurely. Media can also become entrained in the carbon and downstream ball valves in the elution circuit.

In terms of the shutdown time for the flotation, thickener and HIGmill, once the fresh feed is cut from the primary ball mill, it takes six hours for the shutdown sequence to be completed: two hours for feed off, two hours for the concentrate thickener to empty, and 50 minutes to flush the HIGmill. The reason for these large flush times is the residence time in the flotation cells and HIGmill, where the HIGmill requires two volume changes to ensure slurry is cleaned from the media. It is not possible to shut down the HIGmill on its own, so future consideration of a bypass line around the HIGmill or a thickener closed recirculation line is required.

The HIGmill is achieving consistent and continuous operation. The mill can be run for the life of the wear components and does not need to be stopped and opened for regular wear inspections, resulting in high availability.

## CONCLUSIONS

The regrind project at Sunrise Dam has achieved an estimated average increase in gold recovery of ~6 per cent from commissioning to April 2021.

This HIGmill has achieved its required performance and continues to be operated with minimal operator input. After a challenging commissioning and wear part optimisation process, the HIGmill has exceeded operating and maintenance expectations. The HIGmill overall utilisation is 97 per cent and has an availability of 98.6 per cent. The mill currently targets P80s of 10–12 μm, while achieving a rotor wear life of up to 45 weeks and a shell liner component life of minimum 26 weeks.

According to operators, the HIGmill is running well. The mill can be run for the life of the wear components and does not need to be stopped and opened for regular wear inspections, resulting in high availability. It is very easy to change the mill speed, which adjusts the energy input and change the P80 during operation. With regards to maintenance, the HIGmill reline periods run for 36 hours, excluding operator shutdown and start-up time, with the main plant shutdown period generally between 36–48 hours.

There are various areas where the HIGmill could be further optimised, which include:

- A specialised media handling system, where media can be pumped from and to the mill. Metso Outotec now has various Media Handling Systems for this purpose.
- An external trash screen to capture media and prevent it from entering the CIL circuit.
- Consideration of a bypass line around the HIGmill or a thickener closed recirculation.
- Online PSA to enable accurate P80 control.

Closing comment from Tony Ryan, Manager: Engineering Support at AngloGold Ashanti Australia Ltd

*‘The HIGmill is still on a continuous improvement journey. Both the OEM and customer have an obligation to work together to get the continuous improvement benefits for both parties. As an industry we need to strive for wider participation with end users where we can all benefit from the larger knowledge base.’*

## ACKNOWLEDGEMENT

The authors would like to thank AngloGold Ashanti Australia Ltd and Metso Outotec for permission to publish this work.

## REFERENCES

AGA 2014, AngloGold Ashanti Australia Ltd, Sunrise Dam Gold Mine Recovery Enhancement Project PFS, Internal document.

AGA 2017, AngloGold Ashanti Australia Ltd, Sunrise Dam Gold Mine Recovery Enhancement Project, Process Flow Diagram, SDGM300F701 rev0, 18th August 2017

Fann, 2017, Marsh Funnel Viscometer Instructions (for Fann No. 201), online

https://www.fann.com/content/dam/fann/Manuals/Marsh_Funnel_Instruction.pdf, accessed 12/12/2015.

Heath, A., Belke, J., Lehto, H., and Orser, T. (2017). Fine grinding rotors with improved service life by DEM modelling, Procemin-Geomet 2017, Chile, Chapter 4.

Keikkala V., Paz A., Komminaho T., Lehto H., Loucas J., 2018, Energy Efficient Rotor Design for HIGmills, 2018 Minerals Engineering, Volume 128, November 2018, Pages 266–274

Larson, M., Anderson, G., Morrison, R., Young, M., 2011, Regrind Mills Challenges of Scaleup, page 13, SME Annual Meeting, Feb 27/3/2011, Denver, Colorado, USA.

Nielsen, B., Lehto, H., Musuku, B., (2016) Design, Installation, Comissioning and Operation of Fine Grinding Technology at the Kevitsa Mine, In: 13th AUSIMM mill operators’ conference, Perth WA 10–12 Oct., 2016.

Paz A., Ghattas, R., Loro, S., Belke, J., 2019, Fine Grinding Implementation at The Cracow Gold Processing Plant, MetPlant 2019, Perth WA, 9 – 10th September 2019.

# The endemic issue of ball mill overload in SABC circuits

*M S Powell[1,2], M Yahyaei[3], A N Mainza[4] and L M Tavares[5]*

1. FAusIMM, Comminution Reimagined, Brisbane Qld 4069.
2. Emeritus Professor, JKMRC, Sustainable Minerals Institute, University of Queensland, St Lucia Qld 4068. Email: malcolm.powell@uq.edu.au
3. Associate Professor, SMI-JKMRC, University of Queensland, Indooroopilly Qld 4068. Email: m.yahyaei@uq.edu.au
4. Head of Department, Professor, CMR – Department of Chemical Engineering, University of Cape Town, Rondebosch 7700, South Africa. Email: aubrey.mainza@uct.edu.za
5. Professor, Department of Metallurgical and Materials Engineering, Universidade Federal do Rio de Janeiro, COPPE-UFRJ, Rio de Janeiro RJ, Brazil. Email: tavares@metalmat.ufrj.br

## ABSTRACT

Maintaining the work balance between the primary SAG mill and secondary ball mill(s) is an overlooked bottleneck, and thus opportunity, in an increasing number of circuits worldwide. As circuit capacities are expanded by 'releasing' the SAG mill bottleneck, the work is progressively passed on to the downstream ball mills. This tends to be absorbed as a coarser grind and usually the consequential reduction in recovery, until it is dealt with through addition of extra milling capacity. However, there is abundant opportunity to rebalance the circuit in advance to recover recovery and open up additional grinding capacity across the circuit.

Common causes of loss of milling efficiency are addressed, along with practical techniques to identify mill overload, supported by plant data showing capacity gains in excess of ten per cent. Routes to redressing the ball mill overload are provided.

## INTRODUCTION

A SAG mill followed by one or two ball mills has become the standard circuit option for grinding ore to product sizes below 300 µm in mineral processing. In the inevitable push to increase production over the life-of-mine, in order to increase the mine profitability, or in dealing with the common issue of orebodies becoming more competent and lower grade with depth, the SAG mill becomes a bottleneck to circuit throughput. For a given mill power, the throughput can be increased by reducing residence time and passing a coarser product downstream to the ball mill(s). The common techniques to achieve this are closing the SAG mill with a recycle pebble crusher; passing the crushed pebbles forward to the ball mill; decreasing mill solids density; opening up the SAG transfer screen size; pre-crushing part or all of the run-of-mine (RoM) feed. These methods have met with considerable success in generally increasing throughputs by 10 per cent to 30 per cent (Lee *et al,* 2015). A separate method that is well-known and often claimed to be implemented is Mine to Mill; adjusting the blast size distribution to enhance SAG mill throughput (Kanchibotla *et al,* 1998). This is implemented to varying degrees, but by the authors' observation, often inconsistently and without a full appreciation of the circuit impact.

What appears to be poorly appreciated by mill operators, process engineering companies and even milling consultants, is that there is no free lunch. Pushing more feed through a circuit with no more, or only a few more per cent, of power must lead to a coarser product. Adding 1 MW of crushing power to a 40 MW milling circuit, ie 2.5 per cent more energy, cannot possibly result in the same grind size with the added 20 per cent of SAG mill throughput. In searching the literature and listening to many presentations on these expansions, the authors fail to find any coherent or consistent analysis of the impact on final product size. The papers tend to comment on the flotation or leach circuit 'not being negatively affected', or that 'recovery was maintained with a slight coarsening of grind'. It is also noted that the performance of the ball mills tends to be overlooked in production studies. In substantial plant expansions, it is usual to add an extra ball mill to the circuit, to the point where there can be three ball mills fed by a single SAG mill, a practice quite common in the Porphyry coppers of South America, such as the Los Bronces circuit (Powell *et al,* 2006).

The considerable coarsening of the SAG mill product resulting from these throughput increases, passes the work on to the ball mill(s), which generally become overloaded with the added grind duty.

The major work in milling is at the fine end, minus 100 µm, as captured so succinctly by the famous Hukki energy curve (Hukki, 1961). For a 20 per cent expansion, the ball mills land up with 20 per cent more feed with a coarser size distribution and often the ore is more competent for expansions or throughput maintenance projects that address increasing feed competence.

Any crushing of the feed to the SAG mill or of the pebbles results in a large portion of sub-grate size material (particles smaller than the discharge grate), which in essence is the purpose of this crushing. These particles add a considerable fraction to the coarse end that passes through the SAG mill classifying trommel or screen and on to the ball mill(s). Often, the screen or trommel aperture is increased to address overload issues arising from the increased mill feedrate, and from the (mis-understood) assertion that this will further increase SAG mill throughput. The increased top-size and fraction in the top-size has a marked negative impact on the ball mill, as these large particles tend to be in the region of decreasing milling efficiency. The resulting scatting of large particles out of the mill and dramatic rise in circulating load, is in turn addressed by coarsening up the ball size of the ball mill, often through a dual ball size addition, such as 2- and 3-inch balls. The coarser ball charge, in turn, reduces the milling rate at the fine end, exacerbating the coarsening of the grind.

The cyclone operation is used as the final tool to cope with the considerable coarsening of the grind and run-away circulating loads. Cyclones do not naturally cut at a coarse size, above 250 µm, so are operated at exceedingly high feed per cent solids of 65 per cent. This high feed solids has become an industry standard for large SAG-ball mill circuits, with little or no appreciation of the inefficiency of the classification process – with high bypass of final product to the underflow (30 per cent being common); overgrinding at the fine end (slimes production); loss of mill capacity due to the slimes production; carry-over of coarse material to the overflow due to the high density and increased turbulence in the cyclone; and the consequent negative impact on recovery.

The observation of the authors is that many SAG-ball mill circuits are in fact ball mill limited, with overloaded and inefficient ball mill operation, as a consequence of these overloading factors. This paper addresses causes, how to assess the severity in an operation, and methods to recover grind in circuits. Guidelines to avoiding these poor design outcomes are also presented.

## STATUS IN THE INDUSTRY

The mining industry is subject to ongoing pressures of cyclic metal demand and prices, decreasing ore grades as the better orebodies are mined out, more competent and complex ores as the mines become deeper and ore resources more difficult to access, as discussed in terms of complex orebodies by Valenta *et al* (2019). The resultant constant pressure to increase metal production, with minimal added capital investment is the primary driver of overloaded and inefficient ball mills.

The unappreciated prevalence of overloaded ball mills in the industry reflects poor or limited specialist process training of metallurgists; mill operators untrained in the science of the processes they control; mineral processing circuits being built without access to the samples required to properly, and regularly, assess circuit performance, design based on empirical database relationships rather than modern mechanistic process models.

This lack of knowledge has led to a creeping inefficiency that is not recognised and has become the ‘new norm’. Informal comparison of modern circuit performance relative to those of the 1970s and 1980s, indicates a reduction in process efficiency, that is in terms of energy to produce final product. It is the intention of the authors to gather more coherent information on this in the future, possibly via a collaborative Masters’ student project.

### Why this situation has arisen

Some clear indicators of why such a simple issue is almost overlooked in the industry include:

- Decreasing technical skills levels (not to be confused with the capability of our young engineers).
- Decreasing technical staff levels.
- Cyclic employment levels pushing out good and experienced staff.
- The conservative and risk averse industry falling back on the known.

- Cyclic accelerated expansion steps linked to metal prices leading to recycling off-the-shelf designs without any content of lessons learnt.
- Pressure to minimise capital investment.
- A conservative reliance on outdated tools and methods (many over 50 years old) because they are well-understood and link to large databases of process design groups.
- Low investment by the industry in progressing tools and techniques to the standards we are capable in the 21st century.

The list can continue, as is well presented by Munro and Tilyard (2009), but the point is that the industry has not adequately invested in the techniques and tools that can dramatically change processing efficiency and effectiveness. The unnoticed progressive overloading of ball mills and resulting reduction of overall circuit efficiency, ie underutilisation of capital investment, is but one example of the consequence of this.

## Shortfalls in modelling

Some of the modelling shortfalls are summarised as context to the issue of overloading and why it is allowed to arise in the design stage.

### *SAG mill*

The modelling of SAG mill transfer to ball mills that uses the Bond breakage relationship is flawed due to the non-parallel size distributions between the SAG and ball mill, illustrated by Powell *et al* (2014). A number of modelling and mill sizing techniques use a 'correction factor' to allow for this, Morrell (2008), however, this correction does not change as the SAG product size distribution changes at the fine end, being pegged at T80 values. With the majority of milling energy being required to produce the finer end, material below 400 µm, a shift in the mass fraction below that size is the major driver in the energy requirement of the ball mill. However, energy-based SAG mill models fail to capture the decrease in this finer size fraction.

SAG mill models that depend on breakage rate functions and impact breakage ore characterisation, lack the fidelity to simulate the changes in product at the finer end due to fixed rates functions based on the base case mill performance.

### *Crushers*

Power-based crusher models are useful for understanding the product size for a fixed crusher operation, but lack the ability to predict the influence of crusher speed, liner geometry, feed flow, volumetric constraints, total normal loading forces, and liner wear. More mechanistic models are required for this and applied to the control of crushing circuits, such as in the work of that of Hulthén and Evertsson (2009).

The issue of low-fidelity crusher models is that there is no opportunity to explore the limits of operation that will allow the crushed pebble size to be reduced, with positive knock-on to the ball mill performance.

### *Ball mill*

As already mentioned in the context of SAG milling, the basic requirement for using empirical energy-size reduction relationships such as Bond's is not met in the case of SAG milling, given the non-parallel size distributions of the feed and product. Methods that are based on the traditional population balance model have thrived in the last few decades in the context of simulating SAB and SABC circuits, but still face important challenges when applied in the context of these circuits. For instance, predicting the impact of oversized feed to the ball mill is not at all straightforward, in particular when using modelling/optimisation methods that rely on bench-scale ball mill tests, given the difficulty in obtaining reliable information on breakage behaviour of such material in laboratory mills due to their limited diameter and the difficulty associated to getting reliable results from the use of large ball sizes with them.

The sensitivity of the ball mill to the top size becomes even more significant when dealing with tough (hard) ores. Oversized feeds in ball mills are known to generate pebbles that do not break and only wear slowly as they move axially along the mill. There is also the issue of the natural variability in ore strengths in these coarser sizes and how this impacts the performance of the mill. Simulation shows that whereas at fine sizes a difference of on order of magnitude in strength of particles (which is quite common) typically results in changes in the order of 10–20 per cent in breakage rates, this same variability can translate to changes in breakage rates well above 100 per cent (Carvalho and Tavares, 2013). As such, relatively small proportions of tough and coarse particles, which do not readily break in the mill, will likely dramatically increase scats generation. This effect is regularly reported on in operations as an unexpected scatting problem from a small change in feed competence. Even when breakage of these particles finally occurs, they will concentrate in the top of the discharge size distribution, increasing the hardness of the circulating load to the ball mill.

In the case of multicomponent feeds, that is, feeds made up with ores with different competence classes, the effects described above can be exacerbated, with potential of accumulation of the tougher component in the circulating load, even when it represents a relatively small fraction of the feed (Tavares and Kallemback, 2013).

There is also the challenge in identifying when the ball mill becomes unable to transport slurry from the feed to the discharge. Such overloading would result in instability in operation and a drastic reduction in breakage rates. Arbiter (1991) has proposed the critical axial flow velocity of 0.072 m/s or the Arbiter flow number of 4.1, for identifying the onset of overloading, but experience over the last few decades has shown that ball mills with significantly higher axial velocities and Arbiter flow numbers as high as six performing in SABC circuits can still perform reasonably well, demonstrating that it is relatively tolerant in this extreme. The identification of this critical flow velocity remains to be relevant today and would be important to be identified, in particular in SAB and SABC circuits.

### *Process dynamics*

The use of steady-state models precludes prediction of realistic operating regimes as the feed size and competence varies. The reality is that these variations depress the overall operating performance, driving operators to pull back on process performance so as to accommodate the peaks and troughs in recycles, power, SAG screen loading, recycle pebble rate, etc.

A key aspect to realistic process modelling is the utilisation of each piece of equipment as feed varies and control systems or operators respond to the changes; maintenance downtime; unplanned downtime; drift in performance with wear; variable ball loading in mills between ball top-up; surges inflow and density to cyclones as sump level varies; and similar such disturbances. The industry is good at measuring downtime, but poor at measuring utilisation, or overall equipment effectiveness (OEE) as used in the manufacturing industry Dal, Tugwell and Greatbanks (2000). OEE utilises operating time, utilisation of available capacity (such as power) and product quality (such as percentage of product within the desired size range). Work by Powell, Evertsson and Mainza (2019) indicates that for crushing circuits in mineral processing, the OEE is in the range of 50 per cent to 60 per cent for the circuits they have reviewed. Unpublished data of the authors indicates OEE values of 80 per cent to 90 per cent for milling circuits – far below the industry perception of 95 per cent utilisation.

Capturing process dynamics in the modelling stage should highlight the actual utilisation, with pathways to improve this and at the least accommodate the predicted actual OEE in design.

### *Multicomponent ores*

The modelling techniques are established to deal with average ore feed, without ability to account for mixtures of ore competence within the feed. Considerable effort has been applied through the AMIRA P9 project to address this (Yahyaei *et al*, 2019), and these models are proving to add value to process design and optimisation. However, at this stage, the models remain steady state.

A marked issue of ores with a blend of competence is that the competent component is transported out the SAG mill through the coarse 12 to 18 mm SAG screens and on to the ball mills – which receive a disproportionate work-load. This disproportional distribution of the competent components in the feed to the ball mills further justifies describing them in the context of ball milling.

***Summary***

In summary, the limitations in models and the simplistic power-based approach to modelling and process design hides the consequence of design decisions, propagates design errors and maintains a status-quo of low circuit efficiency.

## SOME THEORY

Some key aspects of the theory of ball mill operation are presented to assist in understanding the underlying drivers.

### Mill power

Bulking out of the load of a ball mill with larger, competent rock particles, results in a reduction of mill power due to a lower density charge shifting the centre of mass towards the centre of the mill, thus reducing the torque arm, Govender and Powell (2006). Adding a considerable solids content to the slurry pool further reduces the mill power, Hilden and Powell (2018).

Quite simply, the amount of grinding work a mill can perform is a direct function of the power draw, as supported by all the power-based modelling. Thus, reducing the power draw of the mill, for any reason, reduces the grinding capacity of the mill. It is thus necessary to recover full power draw to maximise the grind from the ball mill.

### Energy spectra

It is well understood that ball mills do not deal well with oversize feed, and it is commonly observed that this problem worsens if the feed is highly competent. This is generally experienced on-site as excessive scatting from the ball mill trommel. This effect is captured in the population balance type models as a reduction of breakage rate at above a critical size, such as seen in the example of Figure 1.

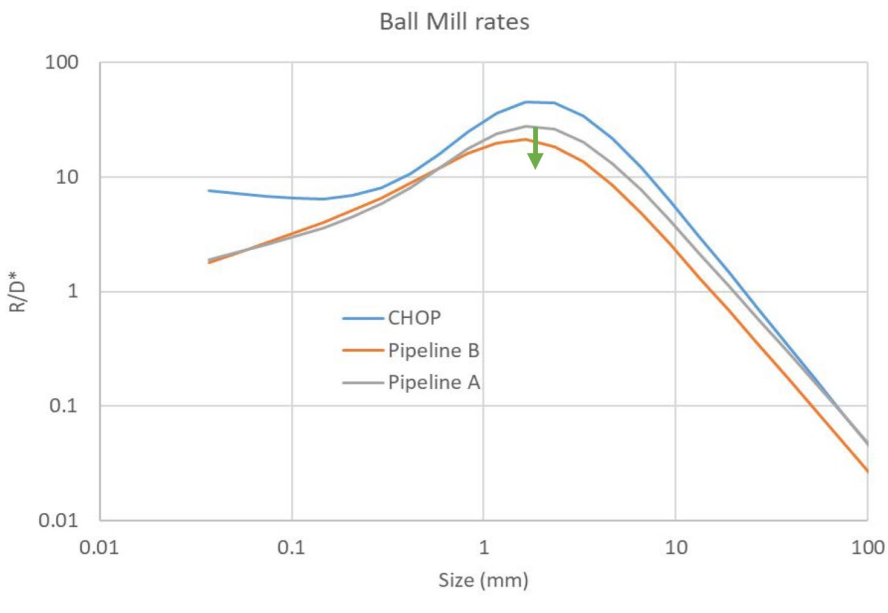


**FIG 1** – The typical reduction in breakage rates at larger sizes for a ball mill [data from surveys for three different ores at Barrick Cortez Mine].

The reduction in rates is now understood to be a consequence of limited compressive, or impact, force that can be applied by the balls on the particles. The probability of particle breakage and the resulting product size if it does break, is generally described in terms of applied specific energy, that is the energy density commonly given in kWh/t.

### Feed top-size to ball mills

The ball mill does not have sufficient impact energy to break oversize rocks in the feed. These particles are instead slowly worn down through abrasion. As a result, they build-up in the mill and in the circulating load, returning repeatedly to the mill until they are slowly worn out. Although they do produce a fine product, it is finer than required, so energy is wasted and excess slimes produced. The major inefficiency is from these rocks in the mill expanding the mill charge by building up between the balls. The expanded charge has a lower density, reducing the mill power draw for the same mass of balls in the mill. The rocks push the balls apart and reduce contact of the fine particles with the balls – thus reducing the milling rate. As noted, this is poorly understood in the industry, and there is little quantitative work on this effect. However, the author's measurements indicate that removal of the oversize top-size particles can increase the milling rate by up to 5 per cent. A reference to the impact of mill overload on circuit capacity and grind is provided in Powell *et al* (2018). The expression proposed by Fred Bond in which the feed size can increase with the square of the top ball size, the cubic root of the mill diameter, as well as the 0.7 power of the per cent of critical speed and inversely with this same power of the Bond work index and specific gravity contains some of the important drivers, but is oversimplistic and has often associated to significant deviations when applied to present-day ball mills.

# PRACTICAL MEASUREMENTS

There are a number of practical measurements that can be conducted by site metallurgists to assess the operating status and performance of their milling circuits. These are outlined ahead of the case studies, as the techniques are referred to in the studies.

## Measuring ball mill filling

It is rare for mine sites to measure the total filling in ball mills, as opposed to a level check after a partial grind-out. Knowing what the solids loading is in a ball mill is invaluable to diagnosing the status of the mill. The technique is to crash stop the ball mill in conjunction with a SAG mill crash stop. The cyclone pump is switched off and the mill stopped simultaneously, plus the pumps drained as required. The ball load is measured through the standard method of vertical height measures in four to five places along the mill. After inspection, the mill can be ground out and the ball load re-measured.

The crash stop provides a snapshot of the solids filling in the mill. Figure 2 shows the contents being assessed in a few ball mills. Dipping one's hand in down to the surface of the balls provides a measure of the depth of the solid. The clear water above this slurry layer is ignored. Solids depths of 100 to 150 mm are observed in three of the images, the extreme one has a depth of 700 mm. These are in contrast to the ideal of the solids loading being flush with the surface of the balls. Qualitatively, the authors have observed that providing the solids is within 50 mm of the ball surface, the ball mill performance does not seem to be compromised. If the solids loading is well below the ball surfaces, then the mill is being under-fed and can accept more feed. Alternatively, the ball load can be reduced to save on energy and media consumption. The change in ball load before and after grind out provides a further measure of mill overload. For a ball mill fed by a SAG mill, the ball load should not drop by more than 1 per cent of filling when ground out. If there is a greater reduction, this indicates that large, competent rock particles are bulking out the ball load.


**FIG 2** – Measuring solids overload in ball mills.

## Slurry flowability

The ability of slurry to move from the feed to the discharge end of ball mills can become a critical issue whenever more work is transferred from the SAG to the ball mill. Proper control of slurry density can contribute to minimising this issue. A simple, yet effective method to identify if the slurry is at the proper concentration is to conduct a slump test with a cut sample of the mill discharge. Another technique is to view the slurry as it flows out of the trunnion and note the height to which it is lifted. A high lift and laminar flow indicate that the viscosity is too high – add water; no lift and fast fluid flow indicate a low viscosity – reduce water. Reduce water addition until the flow is just laminar, then increase water to create a slightly steaming turbulent discharge.

## SSE – a practical measure of efficiency

Size specific energy (SSE) is a useful measure of ore competence for changing ores, or of circuit efficiency for a given ore. The theory and use of SSE is explained in the work of Ballantyne *et al* (2015a, 2015b, 2014). The concept is illustrated in Figure 3. As energy is cumulatively added to the circuit, the production of the fine final product, generally taken at 75 µm, is linear with the specific energy, in kWh/t. This is irrespective of the comminution equipment, as the efficiencies are closely similar. However, if one piece of equipment is operating at below the efficiency of the others in the circuit, it will fall below the line. Thus, a simple plot of per cent – 75 µm versus specific energy across the circuit, will highlight a poorly performing ball mill.

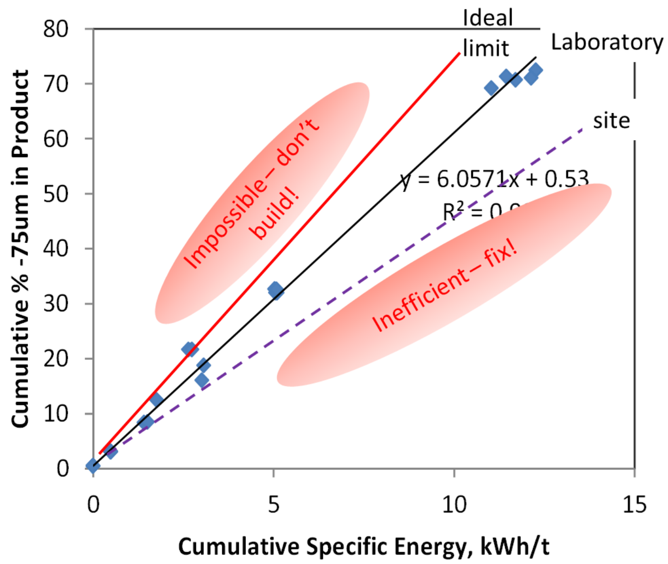


**FIG 3** – Illustration of SSE concept.

The methodology for calculating the SSE for individual comminution equipment within a circuit is described below to facilitate the use of this simple tool:

1. Segment circuit into individual components containing the minimum number of comminution devices either in parallel or series.
2. Record comminution equipment power consumption and the mass flow rate through the subcircuit.
3. Calculate the flow rate of 75 µm material for the feed and product of each comminution device within the subcircuit.
4. Calculate specific energy (kWh/t) and the per cent new 75 µm generated within the subcircuit by dividing the production rate (t/h) of 75 µm by the total circuit throughput.
5. The size specific energy (SSE) is the specific energy divided by the new 75 µm expressed as a proportion.

## Overall equipment effectiveness (OEE)

OEE gives a single-figure measure of the utilised versus available production capability in equipment, based on the following relationship (Dal, Tugwell and Greatbanks, 2000):

$$\text{OEE per cent} = \text{Availability} \times \text{Performance} \times \text{Quality} \times 100$$

- Availability = actual operating time/planned operating time
- Performance = actual rate of production/possible rate of production
- Quality = fraction of acceptable product

Performance – integral of the power draw over the operating time/peak practical capacity (the maximum continuous power that can be used, a reasonable value is 95 per cent of installed power).

Product quality – the percentage of product below desired top size is suitable.

# EXAMPLES OF OVERLOADING

A number of examples are provided from surveys and site measurements conducted by the authors. This both backs the claims of this paper and provides case studies for the industry to learn from.

## Cortez example

The comminution process of the Barrick Cortez mine in Nevada was studied in some detail by Powell *et al* (2018). This study is drawn from that work. The circuit has an SABC layout, with a single ball mill having the same installed power as the SAG mill, 3400 kW. The SAG mill was operating well below installed power, unable to build a load with the low competent CHOP ore. The short residence time and resultant coarse product led to overload of the single ball mill, with the circuit described as 'ball mill constrained'. The typical reduction in ball mill power is illustrated in the operating power of Figure 4, from 3400 kW down to 2900 kW, a 14 per cent loss in available grinding power. Upon crash-stopping the SAG mill and ball mill a massive overload of slurry and coarse stones even in the discharge was observed, clearly illustrated in Figure 5.

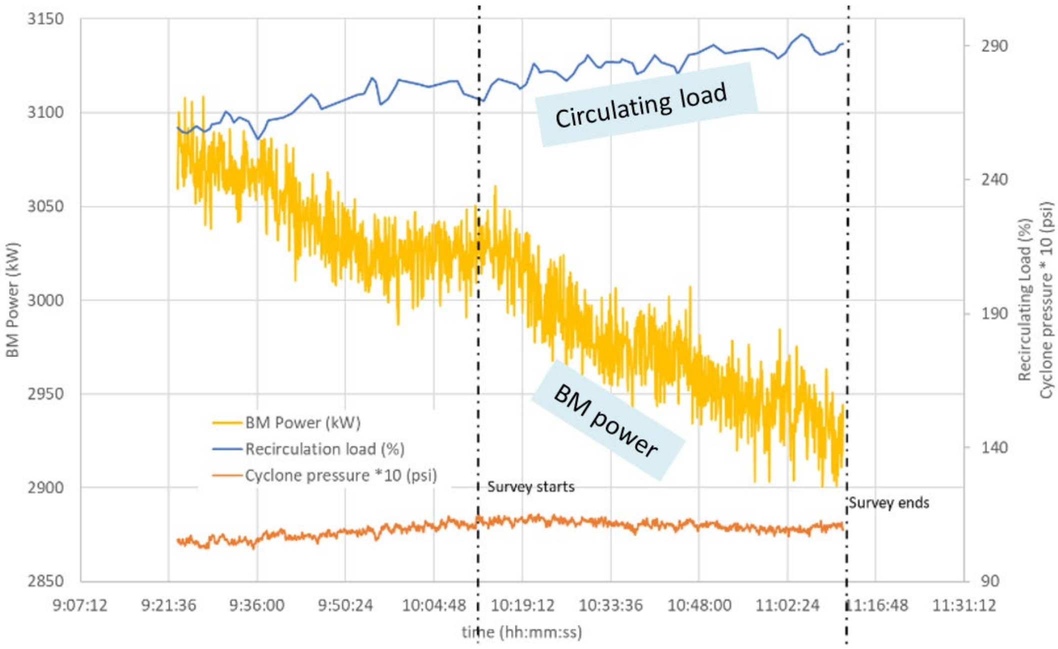


**FIG 4** – Drop in ball mill power with overloading at Cortez Mine.


**FIG 5** – Overloaded ball mill contents at Cortez Mine.

The research team blended competent rock in with the feed, opened up the crusher CSS, reduced the speed of the SAG mill and increased SAG mill slurry density in order to build-up a rock charge in the SAG mill. The attempts to obtain sufficient rock in the mill to improve the SAG mill power draw bore fruit, showing that the addition of coarser rock increases the SAG mill throughput and produces a finer grind for a soft ore. The impact on the ball mill, and circuit, was substantial, as shown in the plot of Figure 6, for the milling conditions at different SAG mill fillings, all for the same ore blend. The lowest filling gave the lowest throughput (525 stph). The highest and intermediate fillings gave the highest throughput (564 and 566 stph) despite the lowest mill speed and low power for the highest mill filling. Thus, the mill could have been sped up and processed a higher feedrate, while maintaining specific energy and thus grind size. What is particularly relevant to this study is that the ball mill power climbed as the SAG mill filling increased. This was because the transfer size to the ball mill was dropping with higher SAG mill fillings, so the ball mill unloaded and came onto grind, drawing full power of 3.4 MW. An outcome was that the grind becomes finer, shown by the circuit P80 dropping from 152 down to 124 µm as the SAG mill filled up.

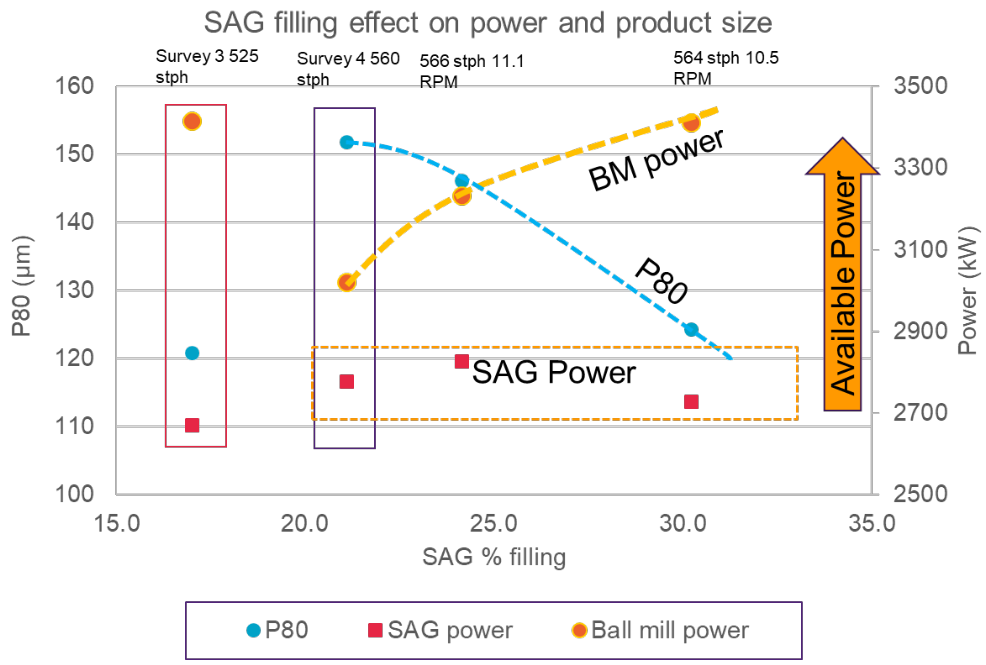


**FIG 6** – Effect of the SAG filling on the ball mill power and final product size, Cortez Surveys.

The survey outcomes are summarised in the plot of Figure 7, where the lines show the total circuit SSE for each survey. The SAG and ball mill individual points are for each equipment on its own. For a given ore blend, points above the line indicate equipment operating at a higher efficiency. In assessing different ores, the steeper the line, the softer the ore as it requires a lower specific energy to reach a given per cent passing 75 µm. For the range of SAG mill fillings, the low filling SAG test is less efficient than the medium and high SAG filling trials, validating the hypothesis that the ball mill efficiency reduces when it is overloaded. The difference in SSE from the low to high SAG filling represents an opportunity of 40 t/h, or 7 per cent, at the same grind size. Due to constraints around the pebble circuit, the throughput could not be further increased, but speeding up the SAG mill to draw full power at a higher feedrate, would allow a 16 per cent increase in throughput at the same grind.

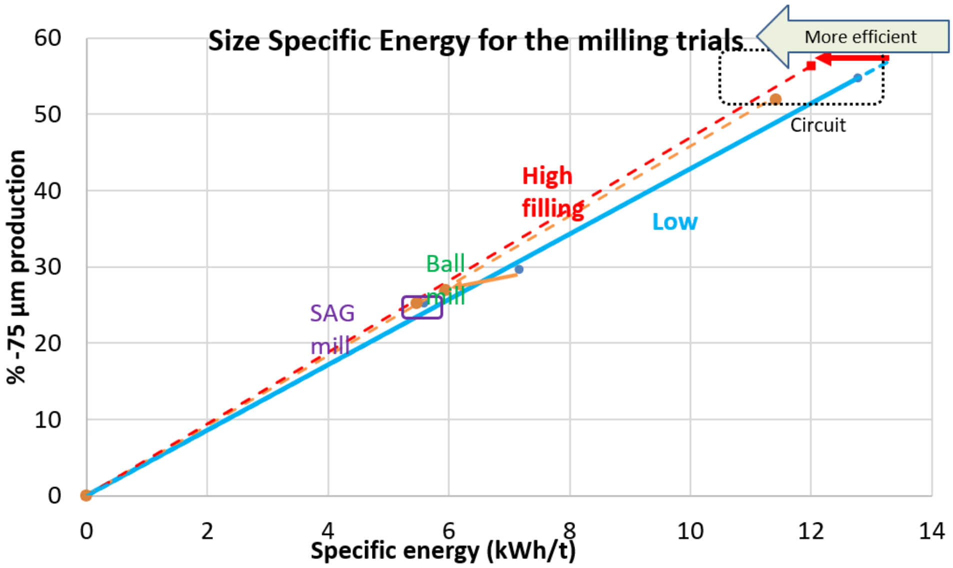


**FIG 7** – Size specific energy curves for the change in grinding distribution between SAG and ball mill, from Cortez surveys.

The site has since followed the advice of decreasing SAG transfer screen size from 14 to 7 mm, to dramatically reduce incidences of ball mill overloading. In a recent continuation of the ongoing project, the JKMRC research team again achieved higher feedrates by blending soft and harder ores from a new pit at Cortez.

## Newcrest's Cadia Mine Concentrator 1

Newcrest's Cadia Mine Concentrator 1 is a standard SABC circuit which is retrofitted with a 5.6 MW HPGR and Two MP1000 (750 kW) Cone crushers for pre-crushing the plus 45 mm feed ahead of the HPGR. A combination of run-of-mine ore and HPGR product is fed to the 40 ft, 20 MW SAG mill. SAG mill product is fed to two 22 ft, 10 MW ball mills closed with the SAG sump and a third 26 ft, 16 MW independent ball mill that was installed to expand the grinding capacity. A more detailed description of this circuit is provided in Engelhardt *et al* (2015). The 16 MW mill was fully surveyed in 2012, and also a grind-out was conducted in 2013 for a more detailed inspection. The ball filling was 31.4 per cent, which is at maximum on the discharge lip, as can be seen in Figure 8. The mill is known to have a high circulating load and coarse product.

**FIG 8** – Inspection of the Cadia 16 MW ball mill in 2013 and filling view from the discharge.

Mill scats had accumulated in the mill shutdown process, illustrated in Figure 9. The scatting rate during the operation was about 50 t/d which is relatively high for a secondary ball mill, especially considering that the trommel screen has large apertures for a secondary ball mill, at about 30 × 40 mm.

**FIG 9** – The Cadia 16 MW ball mill trommel panels and the resultant scats.

The presence of these scats is undesirable and a constraint on mill performance. Trommel aperture is exceptionally large, which introduces coarse scats to the cyclones. This has an adverse effect on cyclone efficiency and increases the wear of the cyclone feed pump. The aperture size of the trommel was increased in order to reduce the mill scats problem. However, this issue is introduced from the SAG mill trommel which has large apertures, 31 × 13 mm slots, wearing out to a markedly larger aperture, as presented in Figure 10.

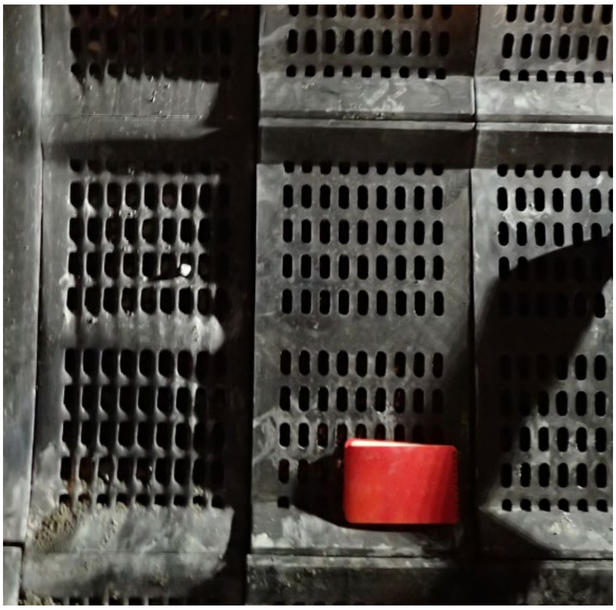

**FIG 10** – Partially worn and new SAG trommel screen panels on the Cadia ball mill.

Coarse particles passing through the trommel have multiple downstream consequences, including increased ball mill scats, reduced ball milling efficiency, as discussed earlier, and increased wear (including pumps and cyclones). SAG mill screen aperture is opened up on many sites to release trommel, and screen overload as the feedrate is increased through pre-crushing, however, this has a direct detrimental influence of ball milling capacity. If aperture size could be reduced or be made more consistent over trommel life, there would be substantial benefits to downstream grinding efficiency.

The $SSE_{75\mu m}$ for ball mill 1, 2 and 3 are 48, 35, and 37 kWh/t respectively, with the circuit SSE of 38. Due to a drive issue on ball mill 2, ball mill 1 was temporarily suffering from overload at the time of the survey, which is strongly reflected in its excessively high SSE.

## Anglo Gold Ashanti's Sunrise Dam Concentrator

The Anglo Gold Ashanti's Sunrise Dam Concentrator is a traditional three-stage crushing and grinding circuit. All four crushers discharge onto a single belt that feeds a double-deck screen. The coarse product (+45 mm) is recycled to the secondary crusher feed bin, the middle product (-45 mm +10 mm) is recycled to the two tertiary crusher feed bins, and the fine product (nominally -10 mm) proceeds to the milling circuit.

The observations presented here are based on the AMIRA P9 project circuit survey of 2014, as described by Ballantyne *et al* (2015c). Due to the large aperture of the screen closing the crushing circuit, delivering 25 per cent coarser than 7 mm; the abnormal drop in mill power as the feedrate increased; and the experience of the Operators that power reduces with a harder ore feed; it was deduced that the mill would be heavily overloaded. A proper crash stop procedure followed to ensure a snapshot of the load in the primary and secondary ball mills was captured. After inspection of the mills and completing the measurements, the mills were ground-out to measure the ball filling. Table 1 summarises the mill filling measurements. As can be seen from these calculations and the photos in Figures 11 and 12, the primary ball mill was considerably overloaded with slurry and packed solids after the crash stop. The solids load was 165 mm above the balls at the feed end and 115 mm above them at the discharge end of the mill. The ball load was also potentially higher than design because of the ball retention ring that can be seen in Figures 11 and 12. The mill overload and the high ball filling combined caused the mill to operate well beyond the peak of power. This hypothesis correlates to the reduction in power when the harder ore was fed into the mill (based on operator's experience) and the increase in power that was recorded during the grind out. When the mill operates over the peak of the power, increases in the mill load result in reduced power utilisation as the grinding toe rises and the centre of gravity of the charge shifts closer to the centre of the mill. It is generally more efficient to operate at a slightly reduced filling and utilise the maximum power for grinding.

**TABLE 1**

Sunrise Dam Mill filling measurements.

| | Crash stop | | Grind-out |
|---|---|---|---|
| **Mill** | **Balls** | **Solids level** | **Balls** |
| Primary | 37.7% | 41.2% | 37.7% |
| 2 | 44.5% | 45.4% | 43.2% |
| 3 | 46.7% | 46.7% | 45.0% |

**FIG 11** – The Sunrise Dam primary mill heavily overloaded with solids, observed at crash-stop.

**FIG 12** – Measuring slurry level above balls during the Sunrise Dam primary mill crash-stop.

Unexpectedly, the ball load in the primary mill did not reduce upon grind-out – which is expected as the coarser rocks that bulk out the ball charge are ground out. It was found that the standard ball addition had been implemented between the crash-stop and grind-out, resulting in a 1.3 per cent increase in ball load, based on the ball wear rate.

The secondary ball mills were both being operated with the slurry level almost equal to the ball level. Secondary ball mill 1 had a slightly higher slurry load (see Figure 13), but the total load in secondary ball mill 2 was higher than mill 1. The feed to the secondary ball mills were slightly different even though they were both fed from the secondary cyclone underflow. This is because the feed distributor had not been designed to allow an even split so the contents of the secondary mills are expected to be different.

Secondary ball mill 1 Secondary ball mill 2

**FIG 13** – Photo of mill charge inside Sunrise Dam secondary ball mills after crash-stop.

The SSE plot of Figure 14 shows that the primary circuit had a low efficiency and that moving it up to the same efficiency as the secondary mills, offered the potential of a 10 per cent increase in throughput. The low utilisation of the crushers, with an average OEE of 55 per cent, was identified as the issue, and a strategy provided to increase utilisation. With improved crushing capacity the aperture of the closing screen could be reduced to 7 mm, so as to better match the peak breakage rate of the mill of 5 mm, and thus unload the primary ball mill and allow it to operate at increased efficiency.

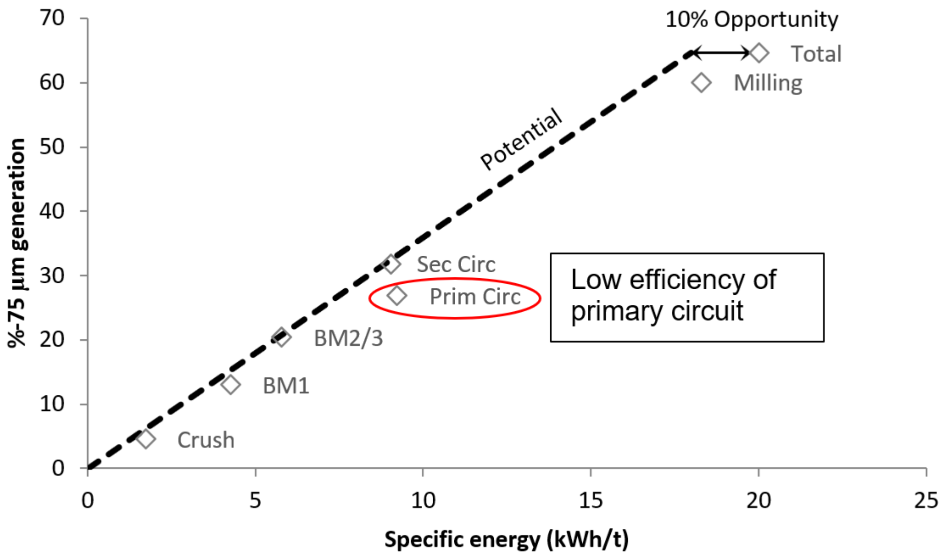


**FIG 14** – SSE plot for the Sunrise Dam circuit (Ballantyne *et al,* 2015).

## Altynalmas Pustynnoye processing plant

Altynalmas Pustynnoye processing plant, located in Kazakhstan, is an SABC circuit. The plant installed a pre-crushing circuit in 2016 to maintain the plant throughput when the ore competence increases at the greater depths in the open pit mine. The SAG mill and the two ball mills are all second hand and have similar shell dimensions (17 ft × 22 ft D×L). The SAG mill was originally operating in a ball mill duty and it has a low aspect ratio (diameter/length) which changes its operation relative to typical high aspect mills (Powell, Morrell and Latchireddi, 2001). The residence time is unavoidably longer and the product finer than for standard SAG mills. The work presented by Powell *et al* (2018) is the basis of this case study. The grinding circuit was surveyed in 2016. Following from a crash-stop, the SAG mill total filling at 112 t was 26.2 per cent. Plant metallurgists indicated that the total ball filling was 14 per cent. The mill operating condition is summarised in Table 2.

**TABLE 2**

Pustynnoye SAG mill condition at crash stop.

| Parameter | First crash-stop | Second crash-stop |
|---|---|---|
| Mill power (MW) | 2.5 | 2.8 |
| Mill load (tons) | 112 | 163 |
| Throughput (t/h) | 273 | 303 |
| Total filling (%) | 26.2 | 48 |
| Ball filling (%) | 14 | 15.5 |

A slurry pool was evident in the SAG mill upon mill entry which is presented in Figure 15. The average depth of the slurry was 8 cm. Mill filling at the second crash-stop at 303 t/h was 48 per cent. The average mill operating conditions for the second crash stop are summarised in Table 2. Inspection of ball mills during the crash stop indicated that both ball mills were overloaded with slurry and ore solids. There was 44 cm of sludge above the balls in both ball mills. Figure 16 shows the slurry level inside ball mill 2. The solids should be level with the balls when the mill is crash stopped, 44 cm is extremely high showing that the ball mills are not coping with the feedrate. Measurements indicated that the ball filling was 37.5 per cent and 35.5 per cent in ball mill 1 and ball mill 2 respectively. This was the measure from the top of the balls, excluding the slurry sludge on top.

**FIG 15** – SAG mill and slurry pool inside the Pustynnoye SAG mill.

**FIG 16** – Slurry level inside Pustynnoye ball mill 2.

Unusually, the site has the excellent facility of launders for the SAG and ball mill product as they flow into the common sump, plus an automated cross-cutter on the SAG stream, as illustrated in Figure 17. This is used to provide online data on the performance of the SAG mill. The impact of this overloading of the ball mills is quantified by the ball mills having a SSE over ⅔ higher than the SAG mill, as shown in Table 3. This is an excellent example of how inefficient an overloaded ball mill can be. The site was advised to improve the classification of the cyclones, increase ball load in the ball mills and to maximise the grinding work in the SAG mill through retaining a high mill filling.


**FIG 17** – Pustynnoye SAG mill discharge launder and sample cutter.

**TABLE 3**

SSE of the SAG and ball mills for Pustynnoye.

| | SAG mill | Ball mills |
|---|---|---|
| SSE, kWh/t -75 µm | 34.4 | 57.6 |
| Standard deviation | 3.8 | 8.4 |
| Increase in SSE, % | | 67% |

# ADDRESSING THE ISSUE IN INDUSTRY

Having discussed the reasons for ball mill overload occurring, the impact on milling efficiency and circuit throughput, and illustrated the issue through case studies, it remains to provide suggestions on how to address this issue. At the most basic level, the impact of expansions driving increased throughput with a coarser feed size to the ball mills, and of modifying SAG operation to recover throughput lost due to more competent feed, need to be understood and quantified in the studies.

There is a need to be able to predict the impact, design for this by rebalancing the circuit work load, measure the impact and mitigate through ongoing retuning of the circuit.

## Potential modelling approaches

As standard techniques tend to overlook the impact of overloading in ball mills, the following approach is needed to ensure that the knock-on to the ball mills is fully understood and quantified in expansion studies. Issues such as the impact of oversized feed to the ball mill, presence of coarse competent feed and of difficult to flow slurries, can be identified through the application of a new generation of ball mill models that explicitly and separately account for the contributions of machine and ore on the performance of the ball mill (Tavares, 2017). Proper ore testing coupled to these novel approaches can ensure that the knock-on to the ball mills is fully understood and quantified, so that expansions can be made to the circuit reducing undesirable negative impacts from the circuit to the ball mill performance.

## Online SSE

It has been shown in this paper how useful SSE is in identifying inefficiency of the ball mill, or anywhere in a circuit, and quantifying the potential gains of rectifying the lost efficiency. What is required is a valid representative sample of the SAG mill product that transfers to the ball mill(s). Usually, the process plant is designed to prevent access to the SAG mill product, rendering it challenging to even obtain a manual sample. Techniques to overcome this problem have been proposed by Powell and co-workers (Powell *et al*, 2006, 2018). Exceptionally, the Pustynnoye site has an automated cross-cutter on the transfer launder to the common sump, as illustrated in Figure 17. With such an installation, the SSE can be logged automatically. Without this luxury (essential?), manual samples can be used to conduct periodic checks on the relative efficiency of the SAG and ball mills.

## Acoustic monitoring

Monitoring of the slurry load and packing in the ball mill can be useful in identifying the build-up of a thick slurry pool and the bulking out of the load. Generally, in mineral processing such tools are only applied to SAG mills, however, there would be great value in their application to ball mills.

## Control signatures

The clearest indication of ball mill overload is the signature of increasing circulating load and the power reducing. The overload is reflected in high mill mass while the power reduces to well below the peak power draw. This issue is well illustrated by the Cortez example in Figure 4, while Figure 18 presents a 3-day period of ball mill operation on another site where the power and load trends move in opposite directions. The downward spike in load on the 24/12 is immediately reflected in an upward spike in power – classic of the mill overload signature. Additionally, the long-term decrease in power while load is held high, shows progressive worsening of overload over two days. With an installed power of 16 MW, the mill is losing 1 to 1.5 MW of useful grinding power, ie up to 10 per cent loss of grinding power.

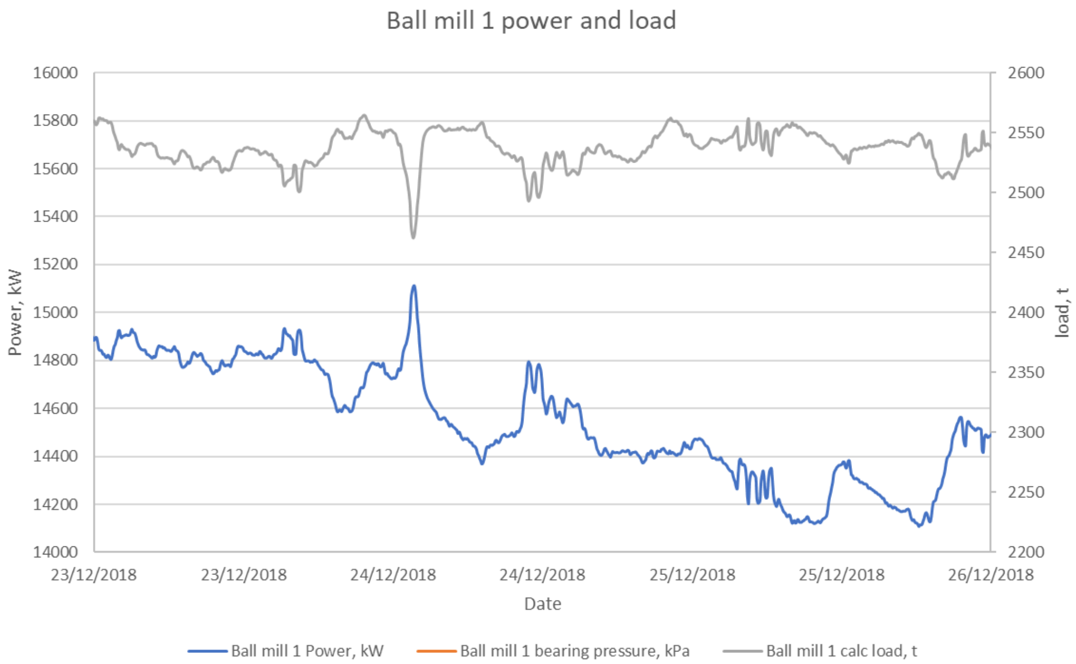


**FIG 18** – Ball mill overload power and load trends.

## OEE

The overall equipment effectiveness helps to highlight the loss of efficiency far more decisively than fluctuating operating trends. Figure 19 shows how two ball mills in parallel, had extra available capacity of 3 and 9 per cent against a target 95 per cent availability and operating at 0.5 MW below installed power.

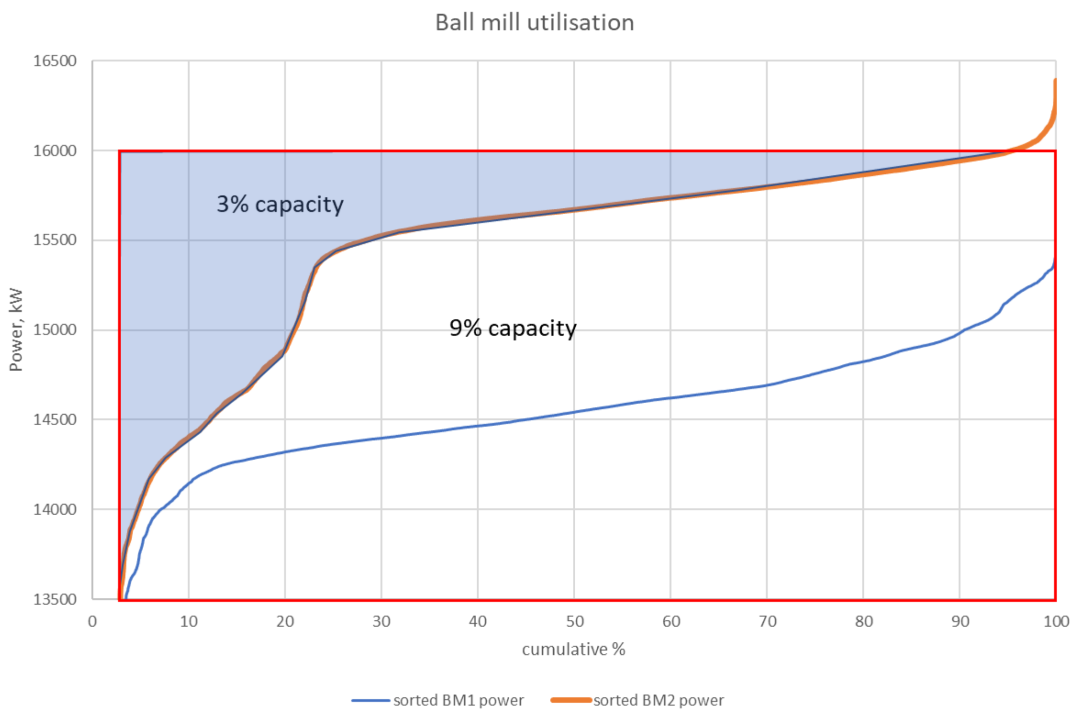


**FIG 19** – Ball mill utilisation distribution.

## Recycle crusher operation

It is generally not understood that improved operation of the recycle crusher increases SAG mill capacity and improves transfer size to the ball mill(s). Crushing the pebbles to a fine size, with a CSS of 10 mm or finer, boosts the SAG mill by feeding material into the fast-grinding size range. The more efficient recycle crushers also enables them to accept a finer size range, ie cope with a higher feed rate associated with a finer SAG screen. This is elucidated on in the work of Powell, Evertsson, and Mainza (2019).

## SAG discharge screen

Oversize transfer to the ball mills is a significant contributor to ball mill overload and reduction in milling efficiency. With increased throughput, the SAG mill trommel or screen tend to overload, so the aperture is opened up to ease operational issues, such as carry-over of slurry to the pebble recycle belt.

Improving feed distribution onto the screen and applying optimal screen wash water to both decks can go a long way to alleviating this issue on screens. This is illustrated in the excellent modification made to a screen treating over 3000 t/h illustrated in Figure 20, the best ever seen by the authors. Proper sprayers have been used and a rigorous system installed to feed both decks. Viewing the product on the top and bottom decks it can be seen that the rocks are clean with no fines carry-over.

**FIG 20** – Trommel screen spay water system. Standby screen showing the five rows of sprayers on the top deck, spray wash water in action, spray water delivery pipes to upper and lower decks, clean upper and lower deck products.

Trommel spray water is essential and should also be properly installed to cover the classification zone in the trommel with proper spray nozzles, not holes in pipes – as is so commonly the case. The nozzles should be protected from falling rocks and slurry. In addition, the practice of damming the trommel to increase residence time, works against screening efficiency – that is clearly understood to require a minimum bed thickness in order to maximise classification efficiency. This is an area requiring further research, as it is common practice in SAG mill trommels across the world.

The ball mill will be unloaded if the screen aperture is reduced to provide a top-size suited to an appropriate ball feed size to the ball mill. Note that the emphasis is on the top-size, not P80. For the Cortez example, the T80 measured at the SAG screen undersize was 1.8 mm with only 5 per cent coarser than 6 mm, yet this caused the massive overload of coarse material observed in the ball mill.

To prevent coarse particle overload in ball mills, the SAG screen aperture should be below 10 mm, preferably below 7 mm.

## Ball size

The ball top-up size is generally too coarse in ball mills, driven by the previous issue, of excessively coarse SAG transfer screens. It is common to use a dual addition size as a compromise, with the coarse size being anywhere from 70 to 90 mm diameter, which is far in excess of the optimal ball size for producing a product in the range of 200 to 100 μm, for which a 40–50 mm ball is more appropriate. To address this, it is first necessary to reduce the top-size of the feed to the ball mill, as described above.

## Cyclone classification

As noted in the theory, cyclone operation is pushed to high density in order to coarsen the product size, so as to compensate for the overloaded ball mills being unable to deliver the design product size. Reversing the trend to fewer, larger cyclones by maximising the number that can be accommodated in a cluster, will allow more stable control of cyclones. This is especially important for density, to prevent it drifting even higher than the target maximum of 65 per cent feed solids which causes dramatic coarsening of the product. Mainza (2016) presents case studies of increasing the throughput of SAG-ball mill circuits by up to 14 per cent, with a 9 per cent reduction in SSE energy, by changing only the cyclone configurations. He targeted sharper classification and lower feed per cent solids.

Cyclones are controlled by volumetric flow, the density and viscosity of the fluid. The number and size of the cyclones should be based on the ability to open and close cyclones to maintain a steady or consistent volumetric flow rate to each cyclone. A large and deep feed sump is the best route to achieve this. As this is often economised on at the time of construction, an alternate route is to install a separate feed transfer sump to achieve this. Once the size is chosen, there is flexibility to alter the performance of the hydrocyclone by adjusting the ratio of the vortex finder and spigot diameters and by changing the feed solids concentration. To maintain a consistent product from the cyclones within the same cluster it is important to keep the diameters of the vortex finder and spigot the same, which is achieved by ensuring that the wear is even during operation.

The issue with density control to ball mills, is that water addition is mostly controlled by the cyclone underflow density. Thus, is there is no inlet water addition. The route to density control, which is of central importance to ball mill efficiency, is to improve the operation of the cyclones. A common issue is flaring of cyclones – producing a low-density underflow feed to the ball mills. Correct feed pressure and density, plus stable control are used to produce a tight underflow flare – which indicates an efficient cyclone classification. In rare cases an ore that produces a high viscosity slurry can result in the ideal cyclone operation producing a higher viscosity than desired in the ball mill. In this instance mill inlet water is required.

For lower capacity circuits, up to 500 t/h is definitely feasible, fine screens can be used instead of cyclones. This is especially applicable to the coarser classification sizes of 200 μm. The ball mill unloads quite dramatically and the efficiency of grinding increases, as shown in work of Frausto *et al* (2017) where the operation of a ball mill with cyclones and screens was compared. A summary of conversion of small throughput circuits (up to 240 t/h) is provided in the work of Mainza (2016), showing substantial throughput gains for screen apertures in the 200–300 μm range.

## CONCLUSIONS

Ball mill overload is rather more common than perceived in the industry. It is driven by a few major factors:

- Too much feed.
- Target grind size too fine.
- Feed too coarse.
- Top-size of feed too large – critically the absolute top-size controlled by the SAG screen.

- Feed too competent – exceeding available power.
- Inefficient cyclone classification leading to large recirculating loads and overgrinding at the fine end (sliming).

Some theory behind the mill and classifier operation is presented, then simple methods to diagnose overloading are described, which followed by principal practical areas to tackle, provide an applied route to reducing the problem of ball mill overload and improving milling efficiency. A number of case studies are presented to illustrate these. There is abundant opportunity to rebalance the circuit, the work between the SAG mills, recycle crushers and ball mills to recover recovery and open up additional grinding capacity across the circuit. It is demonstrated that addressing the mill overload can provide 3–9 per cent more power plus improve milling efficiency by around 5 per cent, ie the mills could do an extra 8–12 per cent milling work.

## ACKNOWLEDGEMENTS

The tremendous support of our co-workers and the many sites where we have conducted survey and process improvement studies is sincerely acknowledged.

## REFERENCES

Arbiter, N., 1991. Dimensionality in ball mill dynamics, Mining, Metallurgy & Exploration volume 8, pages 77–81.

Ballantyne, G.R., Powell, M.S., Bonfils, B. and Yahyaei, M. 2015a. Simple energy measures for assessing total circuit efficiency. Proceedings International autogenous and semi-autogenous grinding and high pressure grinding roll technology 2015, Sep. 20–23, Ed. Klein et al, Published CIM.

Ballantyne, G.R., Mainza, A.N. and Powell, M.S., 2015b. Using comminution energy intensity curves to assess efficiency of gold processing circuits. Proceedings World Gold 2015, 29 Sep. to 1 Oct, Johannesburg, South Africa. Published SAIMM.

Ballantyne, G.R., Clarke, N., Elms, P., Anyimadu, A. and Powell, M.S. 2015c. Application of research principles to identify process improvement at Sunrise Dam Gold Mine. Proceedings Metplant 2015, published AusIMM, 7–8 September.

Ballantyne, G.R., Peukert, W. and Powell, M.S., 2014. Size Specific Energy (SSE) – Energy Required to Generate Minus 75 Micron Material. International J. Mineral Processing vol. 139, pp. 2–6.

de Carvalho, R.M. and Tavares, L.M., 2013. Predicting the effect of operating and design variables on breakage rates using the mechanistic ball mill model. Minerals Engineering, v. 43–44, p. 91–101.

Dal, B., Tugwell, P. and Greatbanks, R. (2000). Overall equipment effectiveness as a measure of perational improvement – A practical analysis. International Journal of Operations & Production Management, Volume 20 No. 12, pp. 1488–1502. https://doi.org/10.1108/01443570010355750

Engelhardt, D., Seppelt, J., Waters, T., Apfelt, A., Lane, G., Yahyaei, M. and Powell, M.S., 2015. The Cadia HPGR-SAG circuit – from design to operation – the commissioning challenge. Proceedings International autogenous and semi-autogenous grinding and high pressure grinding roll technology 2015, Sep. 20–23, Ed. Klein et al, Published CIM.

Frausto, J.J., Ballantyne, G.R., Runge, K., Powell, M.S. and Cruz, R. 2017. The Impact of Classification Efficiency on Comminution and Flotation Circuit Performance. In proceedings MetPlant 2017, published AusIMM.

Govender, I., and Powell, M.S. 2006. An empirical power model derived from 3D particle tracking experiments. Minerals Engineering, Special issue – computation 05. Vol. 19, No. 10, pp. 1005–1012.

Hilden M.M. and Powell, M.S. 2018. A model of SAG mill power incorporating slurry filling and its application to real-time mill performance analysis. Proc. Comminution 18, Cape Town, South Africa, April. Publ. MEI.

Hukki, R.T., 1961. Proposal for a Solomonic settlement between the theories of von Rittinger, Kick and Bond. AIME Trans. (mining) 220, 403–408.

Hulthén, E. and Evertsson, M. (2009). Algorithm for dynamic cone crusher control. Minerals Engineering, Volume 22, Issue 3, February 2009, Pages 296–303. https://doi.org/10.1016/j.mineng.2008.08.007.

Kanchibotla, S. S., Morrell, S., Valery, W., & O'Loughlin, P. 1998. Exploring the effect of blast design on SAG mill throughput at KCGM. Proceedings Mine to mill Conf., Brisbane. Publ AusIMM.

Lee, K., Rosario, P., Schwab, G. and Bogadi, A. 2015. An analysis on SAG pre-crush circuits. Proceedings International autogenous and semi-autogenous grinding and high pressure grinding roll technology 2015, Sep. 20–23, Ed. Klein et al, Published CIM

Mainza, A. N., 2016. The contribution of classifiers to comminution and separation processes in mineral processing. Proceedings of the XXVII International Mineral Processing Congress. October 2016, Quebec, Canada. ISBN: 978–1-926872–29–2

Morrell, S., 2008. A method for predicting the specific energy requirement of comminution circuits and assessing their energy utilisation efficiency. Minerals Engineering 21, pp. 224–233

Munro, P.D. and Tilyard, P.A., 2009. Back to the Future – Why Change Doesn't Necessarily Mean Progress. Proc. Tenth Mill Operators' Conference Adelaide, SA, 12 – 14 Oct. Publ AusIMM, pp 5–11.

Powell, M.S., Evertsson, C.M. and Mainza, A.N., 2019. Redesigning SAG mill recycle crusher operation. Proceedings International autogenous and semi-autogenous grinding and high pressure grinding roll technology 2019, Sep. 23–26, Ed. Staples et al, Published CIM.Powell, M.S., Kanchibotla, S.S, Jokovic, V., Hilden, M.H., Bonfils, B., Musunuri, A., Moyo, P., Yu, S., Young, J., Yaroshak, P., Yalcin, E. and Gorain, B., 2018. Advanced Mine to mill application at the Barrick Cortez mine. Proc. 14th Mill Operators conference, Brisbane, Australia, Aug. Publ. AusIMM.

Powell, M.S., Yahyaei, M., Geronimo, J., Yussupova, Z. and Kumar, P. 2018, The designed approach to Mill liner Optimisation – experience at Pustynnoye mine, Kazakhstan. Proc. 14th Mill Operators conference, Brisbane, Australia, Aug. Publ. AusIMM.

Powell, M.S., Hilden, M.M., Ballantyne, G., Liu, L. and Tavares, L.M. 2014. The appropriate, and inappropriate, application of the JKMRC t10 relationship. Proceedings XXVII IMPC, Santiago, Oct. paper 767.

Powell, M.S, Condori, P, Smit, I, and Valery, W., 2006. The value of rigorous surveys – the Los Bronces experience. Proceedings International autogenous and semiautogenous grinding technology 2006, Sep. 24–27, Ed. Mular et al, Published CIM. Vol. I, pp.233–248.

Powell, M.S. Morrell, S. and Latchireddi, S., 2001. Developments in the understanding of South African style SAG mills. Minerals Engineering. Vol. 14 No. 10, pp. 1143–1153.

Tavares, L.M. and Kallemback, R.D., 2013. Grindability of binary ore blends in ball mills. Minerals Engineering, v. 41, p. 115–120.

Tavares, L.M., 2017. A Review of Advanced Ball Mill Modelling. KONA Powder and Particle Journal, v. 34, p. 106–124

Valenta, R.K., Kemp, D., Owen, J.R., Corder, G.D. and Lebre, E., 2019. Re-thinking complex orebodies: Consequences for the future world supply of copper. Journal of Cleaner Production 220, pp. 816 – 826. https://doi.org/10.1016/j.jclepro.2019.02.146

Yahyaei, M., Hilden, M, Mainza, A., Tavares, L. M., Evertsson, M., Asbjornsson, G., Harris, M., Geldenhuys, S., Dundar, H., Benze, H., Runge, K., 2019, AMIRA P9Q: Translating research to industry tools, Developing validated multi-component mineral processing simulator, Technical report, August 2019.

# Investigating the size segregation of stockpile at MMG’s Las Bambas and its impact on performance of SAG mills

*M Yahyaei[1], Z Ye[2], M Hilden[3], E A Ruiz[4] and Z Gavelan[5]*

1. Associate Professor, Julius Kruttschnitt Research Centre, The University of Queensland, Brisbane Qld 4068. Email: m.yahyaei@uq.edu.au
2. PhD Candidate, Julius Kruttschnitt Research Centre, The University of Queensland, Brisbane Qld 4068. Email: ziming.ye@uq.edu.au
3. Senior Research Fellow, Julius Kruttschnitt Research Centre, The University of Queensland, Brisbane Qld 4068. Email: m.hilden@uq.edu.au
4. Metallurgy Superintendent, Minera Las Bambas, Jr. Cesar Vallejo J-3, Urb. Santa Mónica, Cusco, Peru. Email: erick.ruiz@mmg.com
5. Operations Vice President, Minera Las Bambas, Edificio Cronos, Torre 3, Piso 9, Av. El Derby 055, Santiago de Surco, Lima, Peru. Email: zetti.gavelan@mmg.com

## ABSTRACT

Stockpiles and bins are an integral part of every mineral processing plant, and their design and operation play a significant role in plant performance. Size segregation, which is a common phenomenon in most storage and materials handling facilities, could severely impact the performance of comminution and classification units downstream. Therefore, the ability to model the dynamic response of bins and stockpiles is important for enabling operators to enhance the operation and control of bins and stockpiles and minimise the impact of size segregation on downstream units’ performance.

MMG’s Las Bambas operation is a major copper mine worldwide placed between Grau and Cotabambas provinces, Apurímac region, Peru. The Las Bambas concentrator produces copper concentrate with gold, silver and molybdenum. The concentrator consists of two parallel SAG mills, each followed by a ball mill closed circuit with primary cyclones. Both lines are fed from coarse ore stockpile (COS) with 1 000 000 ton primary crushed ore capacity. The Las Bambas concentrator utilises Advanced Process Control (APC) along with a well-established quality control system to ensure high performance of each processing unit and consequently the overall process. One of the key challenges in maintaining the stability of the process is size segregation in the COS which causes instability in SAG mill’s performance. Therefore, the 3D dynamic model of stock which is developed in Julius Kruttschnitt Mineral Research Centre (JKMRC) is adapted to quantify the size segregation of the stockpile at Las Bambas and identify control strategies that suit the operation of SAG mills at various operating conditions. In this paper, the results of analysis conducted on Plant Information (PI) data and analysis of the behaviour of the stockpile at different operating regimes are presented.

## INTRODUCTION

Stockpiles and bins are common on mine sites, and their design can play a significant role in circuit performance (Wills and Napier-Munn, 2006). However, at both the plant design stage and during process optimisation, stockpiles and materials handling facilities do not receive as much attention as comminution and classification units. Segregation of coarse and fine particles, which is a common phenomenon in most storage and materials handling facilities, could severely impact the performance of both comminution and classification processes (Yahyaei and Powell, 2018). For example, segregation of coarse and fine particles in transfer points or on long conveyors due to stratification is a common phenomenon and can result in parallel units receiving materials with significantly different size distribution. Feeders placed at different locations beneath the stockpile can receive different size particles over time because of size segregated, which occurs during materials handling and stockpiles formation.

Consequently, the fluctuation in the size distribution of materials fed from stockpile will cause fluctuation in crushers’ operation or grinding mills downstream. Uneven distribution of feed affects the performance of comminution and classification units and increases the wear of equipment. Fluctuation in comminution and classification units’ performance will result in the final products not meeting the product quality required for optimum performance of separation units. Therefore, a better understanding of particle size segregation in materials handling facilities to develop a dynamic model for simulating size segregation in stockpiles and bins, conveyors and transfer points is an integral part of design and operation optimisation of comminution and classification circuits (Combarros *et al*, 2014; Yu *et al*, 2016).

## MMG'S LAS BAMBAS OPERATION

MMG's Las Bambas operation is a major copper mine worldwide placed between Grau and Cotabambas provinces, Apurímac region, Peru (Figure 1). The Las Bambas concentrator produces copper concentrate with gold, silver and molybdenum as a byproduct. The concentrator consists of two parallel SAG mills (40 ft × 22 ft, 24 MW) each followed by a ball mill (26 ft × 40 ft, 24 MW) closed circuit with primary cyclones. Both lines are fed from a coarse ore stockpile (COS) with the capacity of 1 000 000 ton of primary crushed ore. The plant is equipped with online size measurement cameras on each primary crusher product, feed to the stockpile at the point of discharge to stockpile (on CV0004), at the drawpoint of each feeder under the stockpile and on feed conveyor of each SAG mill.


**FIG 1** – MMG's Las Bambas operating plant layout.

The coarse ore stockpile is fed by a three-section conveyor belt that transfers material from two primary crushers in 5.2 km. The long transport distance and two transfer points introduce size segregation on the conveyor (CV004) feeding the stockpile and also the formation of the stockpile will result in size segregation of materials in the stockpile. Each grinding line has four feeders which drawing materials from the stockpile (Figure 2). The size segregation in the stockpile causes continuous fluctuation in the size distribution of feed of SAG mills, resulting in fluctuation in performance of ball mills, cyclones, and eventually flotation circuit. Because the level of material in the stockpile also has an effect on size segregation, it was proposed to conduct a study and collect data which are required for calibrating the Julius Kruttschnit Minerals Research Centre (JKMRC) dynamic model of stockpile with size segregation which then can be used for predicting fluctuations in size distribution of feed to each SAG mill.

The dynamic bin and stockpile model, which is developed at the JKMRC can simulate the materials flow and size segregation in bins and stockpiles and predict the size distribution of each drawpoint over time.


**FIG 2** – The layout of the feeders and the feed of stockpile.

This study's preliminary objective was to collect the operational data and conduct site trails for calibrating and validating the JKMRC's dynamic stockpile model. This paper focuses on the analysis of operational data to quantify size segregation in the stockpile and understand the behaviour of the stockpile as operating condition changes. This paper provides a guideline that plant metallurgists could use to analyse the plant information to diagnose the materials handling process and understand stockpiles' behaviour.

The application of the dynamic stockpile model in predicting size segregation is the focus of future papers which is under publication by the authors.

## Collecting the design data

Since the JKMRC dynamic stockpile model requires detailed design data, the first step in this study was collecting the design data from drawings and also direct measurements. There are eight feeders under the stockpile, which feed two parallel grinding circuits. Feeders 4, 5, 6, and 7 are feeding line 1 and feeders 8, 9, 10, and 11 are feeding line 2. The stockpile live capacity is 105 000 ton. The average plant throughput is 8000 t/h, and hence the average residence time of the stockpile is approximately 13 hours.

### *The angle between conveyor and feeders*

The conveyor CV0004, which feeds the stockpile, comes at 30° angle relative to feeders centreline as it is presented in Figures 2 and 4. The angle between the CV0004 conveyor and the feeders centreline aggravates the size segregation of stockpile.

### *The vertical angle of conveyor CV0004*

The vertical angle of CV0004 is also an important factor in the stockpile model, because this angle will impact the trajectory of material when it is fed to the stockpile. To confirm the angle acquired from the darwings, measurement of the angle was conducted on the structure of the conveyor CV0004. The conveyor's actual vertical angle was 14° which was slightly different from what acquired from the drawings. This angle is used in the stockpile modelling.

The key design factors for the stockpile and feeders are summarised in Table 1.

**TABLE 1**
Key design factors of the stockpile and the feeders.

| Design factor | Value |
|---|---|
| Stockpile diameter (m) | 137.2 |
| Stockpile live capacity (ton) | 105 000 |
| Stockpile height (m) | 58.5 |
| Maximum materials height (m) | 53.5 |
| CV0004 conveyor speed (m/s) | 4.5 |
| CV0004 vertical angle (°) | 14.25 |
| Angle between conveyor and feeders centreline (°) | 30 |
| Distance between two lines (m) | 48 |
| Distance of centreline of each line from the stockpile centre (m) | 24 |
| Width of each feeder (m) | 3.5 |
| Length of each feeder (m) | 9.1 |

### *The stockpile height sensor*

The position of the two ultrasonic hight sensors which measures and sends the height of material to the control room is presented in Figure 3. Height sensors are positioned at either side of the CV0004 conveyor on the structure of the conveyor. In Figure 3, only one of the sensors is visible. The limitation in the available position for installation of the hight sensors forced the site to install the sensor at a 15 m offset from the stockpile centre. Therefore, the sensor does not show the height of material at the centre of the stockpile and therefore, there is always an offset between the measured height and the actual height and plant operators are already aware of that. However, the hight data that are collected in the Plant Information historian can not be directly used in the analysis.

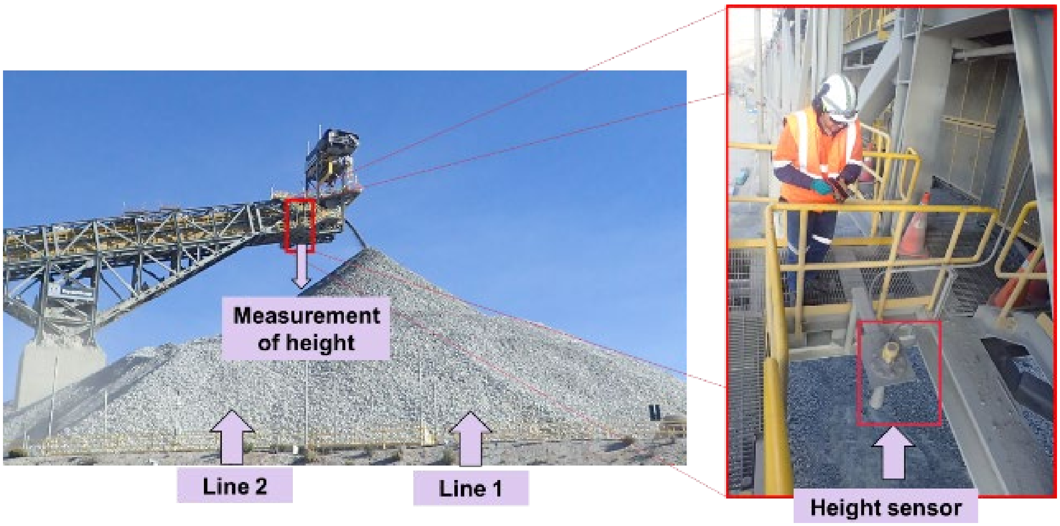


**FIG 3** – The position of the ultrasonic height sensors.

## Observations

### *Effect of stockpile height on the flow of materials*

Because of the feed conveyor's vertical angle and the velocity of material, material follows a parabolic trajectory when discharge from CV0004 conveyor. This phenomenon results in a different flow of material as the height of the stockpile changes over time as it is presented in Figure 4. Therefore, an accurate measurement of the height of the material is very important for operation.

The stockpile dynamic could be used as a soft sensor that provides the height of material at different location of the stockpile.

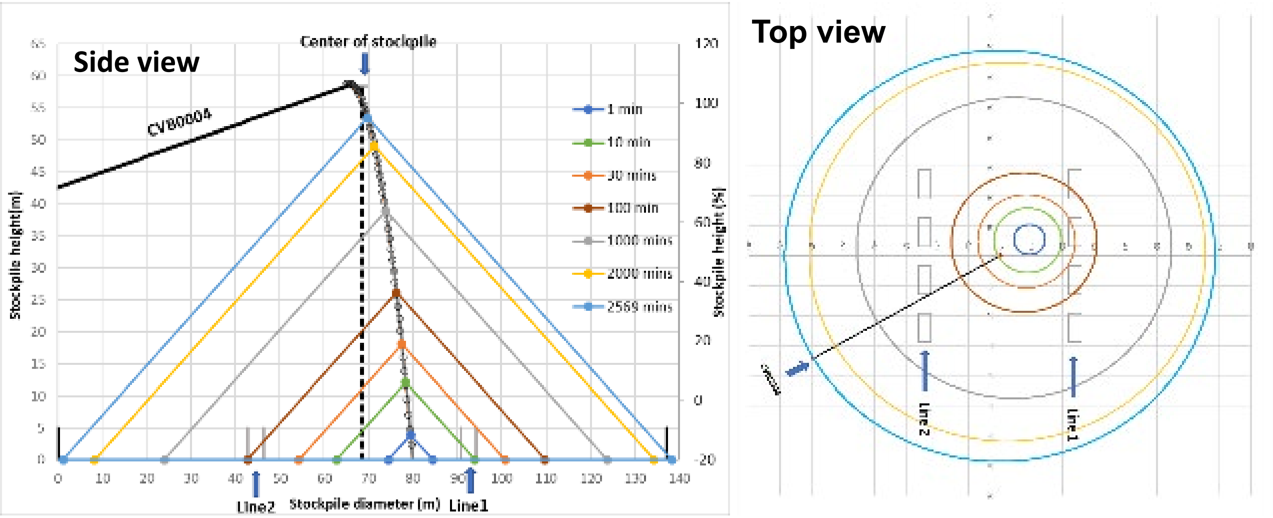


**FIG 4** – A simple representation of the trajectory of the material as the stockpile height changes.

### *Size segregation on feed conveyor*

The size segregation on the stockpile feed conveyor (CV0004) is another factor that contributes to the size segregation in the stockpile. Figure 5 shows a snapshot of materials captured by a high-speed camera that shows the size segregation of materials on the feed conveyor (CV0004) when discharged to the stockpile. The 5.2 km transport promotes stratification of materials, and it is an inevitable phenomenon that contributes to size segregation in the stockpile. The stratification of material is an aspect that should be incorporated in dynamic modelling of the stockpile to ensure simulation results are closer to reality.

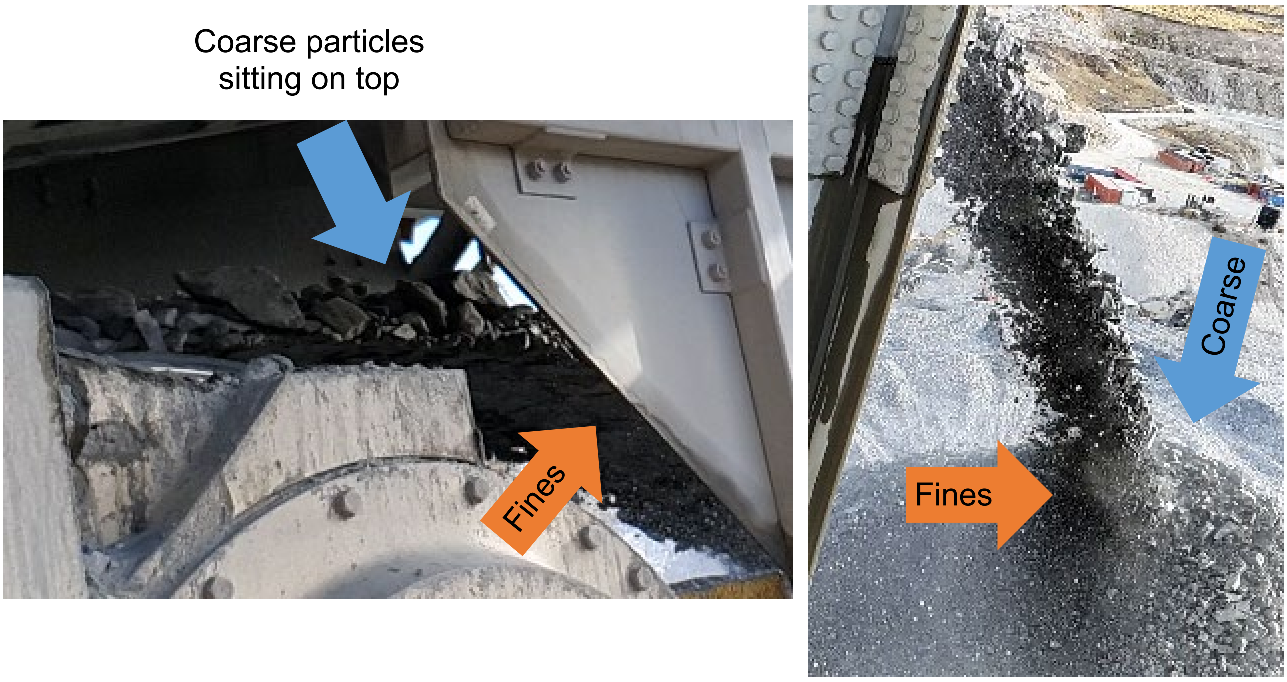


**FIG 5** – The size segregation on the feed conveyor due to stratification during transport.

## Analysis of plant information data

### *Calibration of online size distribution measurements*

The accuracy of the online size measurement is critical for the operation as well as for the validation of the dynamic model. Therefore, data collected from online size measurement for one hour before sampling the feed conveyor (CV0004) is analysed to identify the average size distribution measured by the online system and the actual size distribution measured from the 2.5 tons sample taken from the feed conveyor. The data presented in Figure 6a indicates that online system measurement for materials +10 mm is very close to the size distribution of belt-cut, but it underestimates the amount of -10 mm materials. This observation is expected due to the inaccuracy of online systems on measuring fines. The finding was consistent for the measurement conducted in early 2019, which confirms the online system's consistent bias in measuring fines.

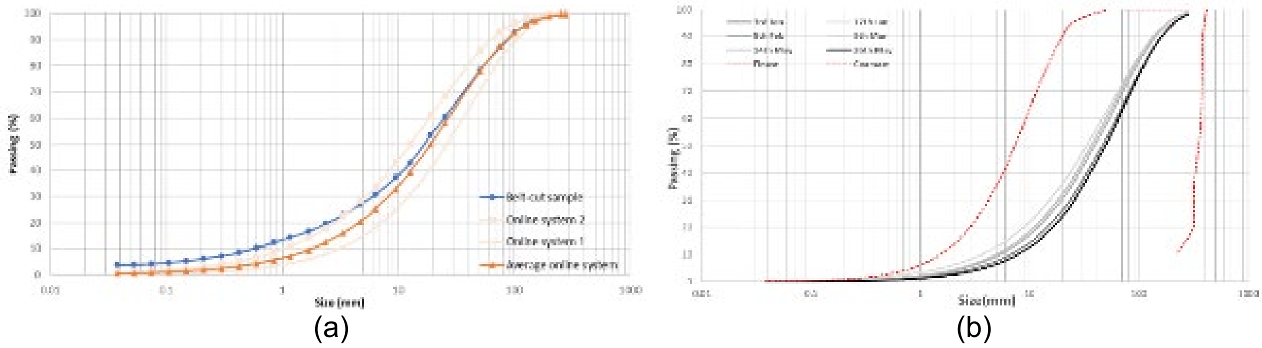


**FIG 6** – Online size distribution measurement: (a) comparison between online measurement and belt-cut; (b) variation in feed size distribution over the six months leading to June 2019 and daily average.

Data presented in Figure 6b demonstrates the variation in the feed's size distribution to stockpile over the six months leading to June 2019 based on the daily average of data from the online system. The daily average of the size distribution of feed in six days selected randomly between January and June 2019 are very close. However, the 95 per cent confidence interval of the size distribution covers a wide range between the coarsest and the finest lines in Figure 6b. The data indicates a wide range of fluctuation in the feed's size distribution to the coarse ore stockpile.

### *Comparison of the feed size distribution of SAG mill 1 and SAG mill 2*

Figure 7 shows the frequency analysis of P100, P80, P50 and P20 for the SAG mill feed for line 1 and line 2. As shown in Figure 7, line 1 SAG mill receives a more consistent feed with less variation regarding the feed top size (P100), and in general, line 1 SAG mill receives a coarser feed. Line 2 SAG mill receives more variable feed than the SAG mill in line 1.

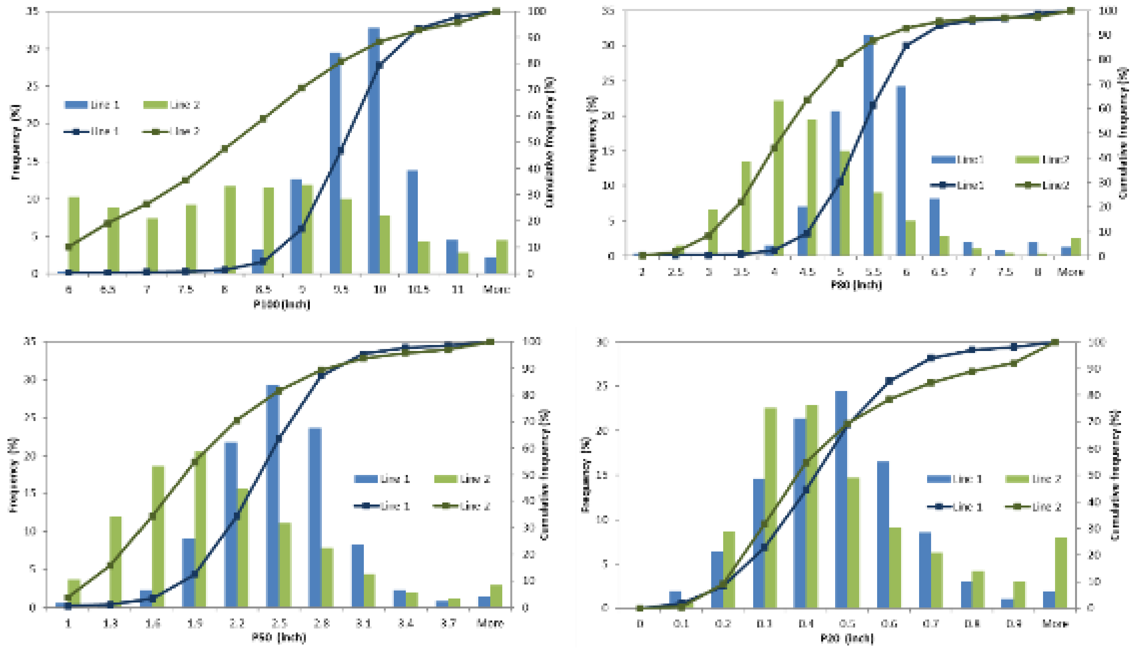


**FIG 7** – Frequency analysis of P100; P80, P50 and P20 of line 1 and line 2 over the six months leading to June 2019.

The insight gained from the PI data analysis regarding the size distribution of feed of the two SAG mills can be incorporated in the advanced control system, which is currently running in the control room. Both lines currently follow the same control strategy despite the fact that SAG mill in line one receives a coarser and more consistent feed.

### *Analysing operation of line 1 and line 2 feeders*

Figure 8 shows the frequency analysis of feeders speed for feeders of each line. Because the particle size measurement data for each feeder was available only from 1 May 2019, each feeder's frequency analysis is done for the two months leading to June 2019. Data in Figure 8 indicates that generally, operators run two middle feeders for each line (ie feeders 5 and 6 for line 1 and feeders 9 and 10 for line 2) and feeders 4, 7, 8 and 11 are usually off (Note that feeders are off, speed is recorded as 10 per cent). Also, feeders 5 and 10 typically are running at maximum speed. Therefore, feeders close to the edge of the stockpile are not used, and the feeders which are places close to the centre of the stockpile are usually operating at maximum speed. Operators implement this operation strategy to minimise the effect of size segregation in the stockpile. However, the particle size distribution of line 1 and line 2 are significantly different, as presented in Figure 7. Besides, this strategy will limit the stockpile's live capacity since four of the feeders are not utilised.

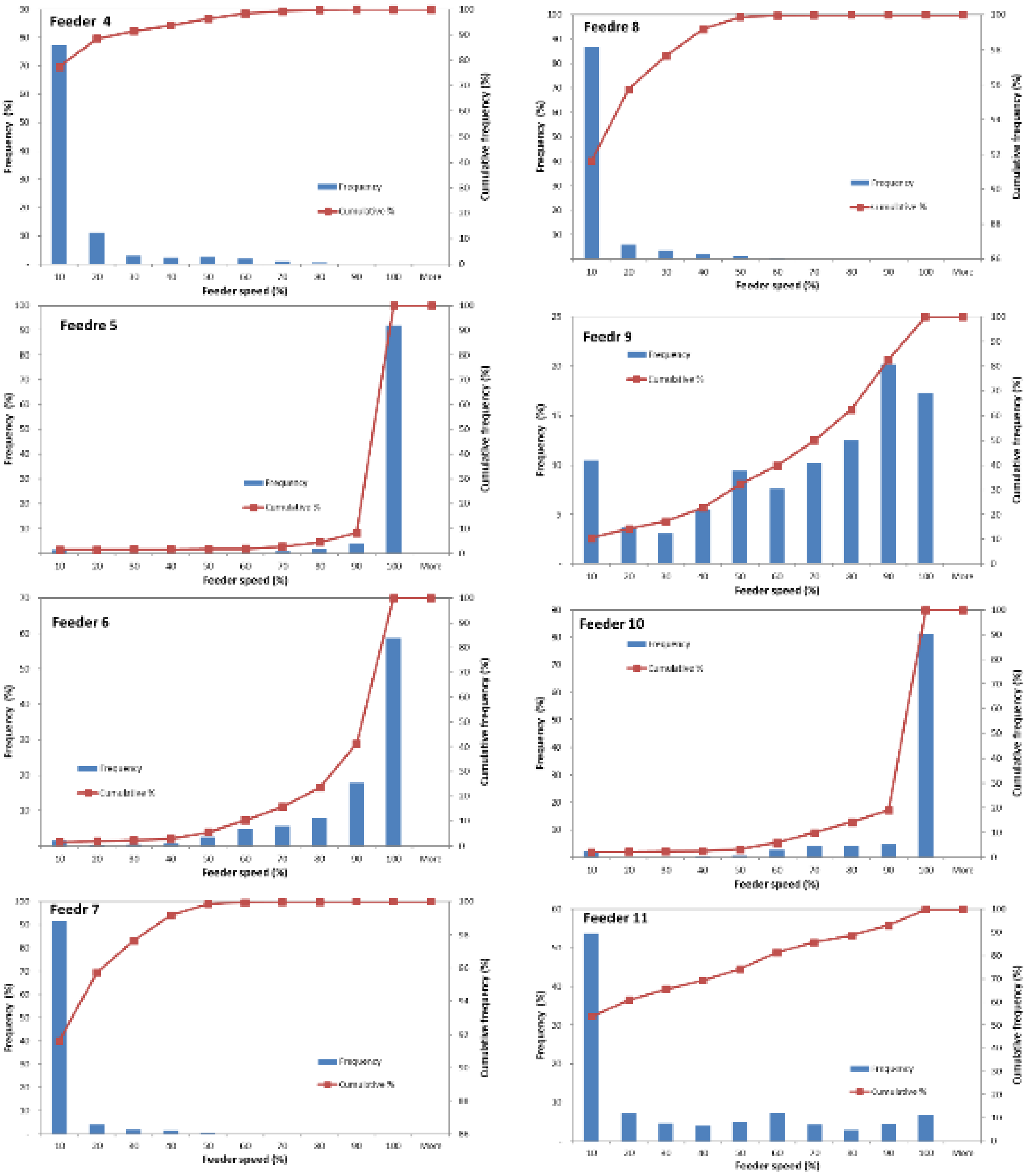


**FIG 8** – Frequency analysis of the feeders speed for each line for the two months leading to June 2019.

The frequency analysis for P80 of each feeder for line 1 and line 2 is presented in Figure 9 data for feeders 4, 7, 8, and 11 need to be cleaned before conducting the frequency analysis because those feeders are not operating most of the time. The data presented in Figure 9 shows that feeders 4, 7, 8, and 11 are on average coarser than feeders 5, 6, 9, and 10 as expected. Feeder 7 has the coarsest material, and feeders 5 and 10 contain the most fines which are expected given the arrangement of feeders in the stockpile relative to the feed to the stockpile.

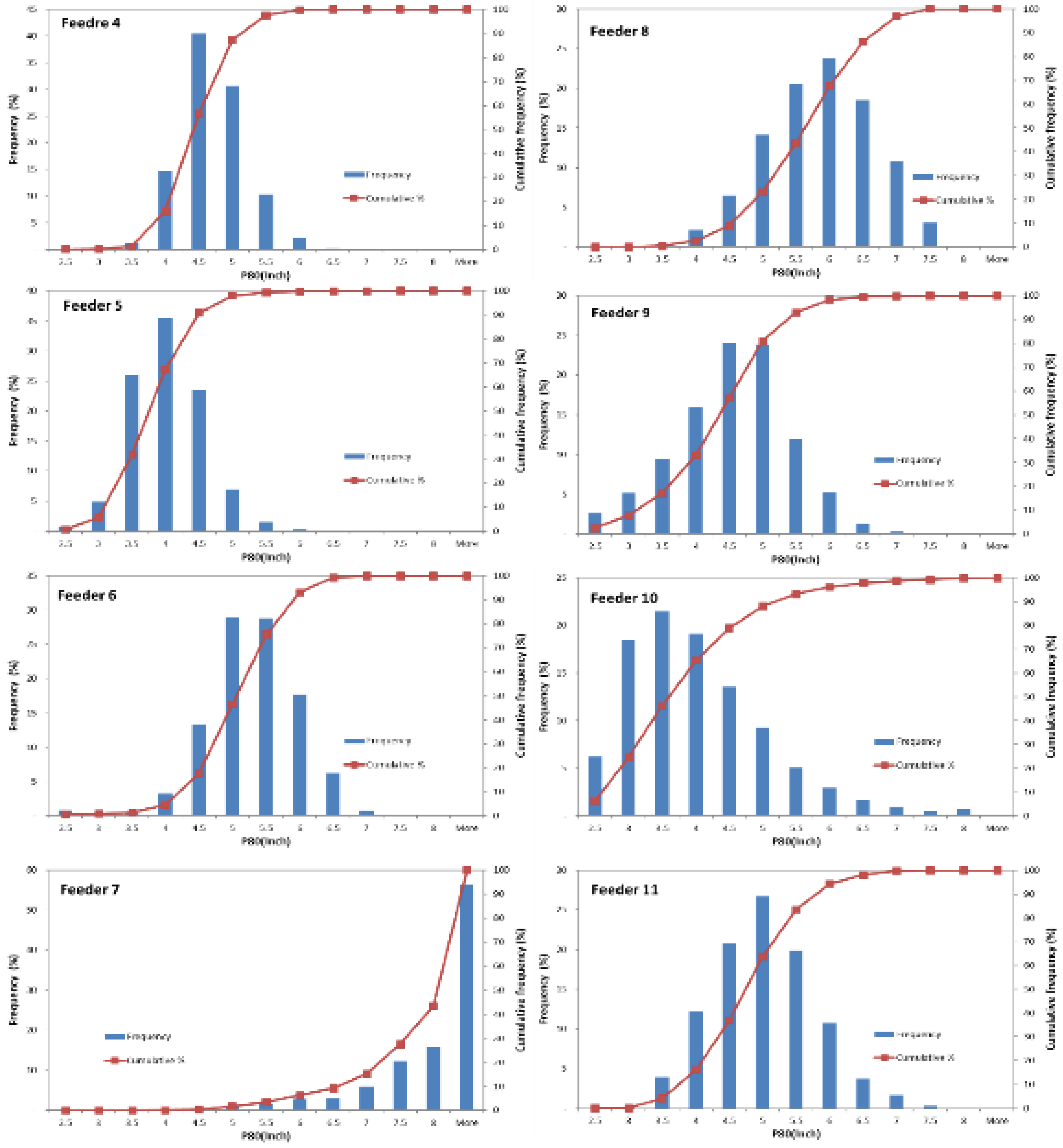


**FIG 9** – Frequency analysis of P80 of the feeders speed for each line for the two months leading to June 2019.

However, the stockpile size segregation pattern seems more complex since feeders pair 5 and 10 and feeders pair 6 and 9 show similar size distribution pattern. This phenomenon can be explained by considering the stockpile feeding arrangement with respect to feeders' position, as it is presented in Figure 10. Because of the direction of the flow of materials, the stockpile will form an ellipsoid shape, and therefore, feeders 9 and 6 will receive coarse material. In contrast, feeders 5 and 10 will receive fine materials as the stockpile fills.

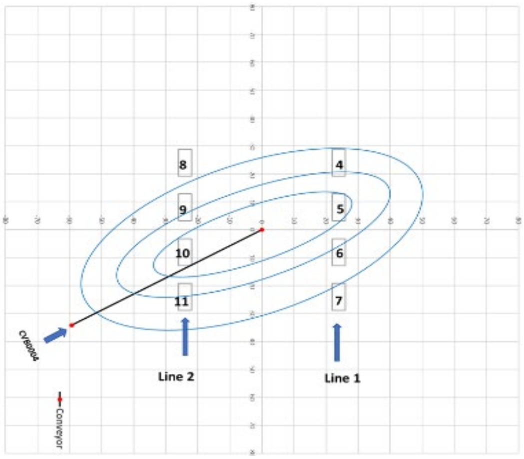


**FIG 10** – The model for the formation of the stockpile over time (each line represents the edge of the stockpile at a different time).

### *Analysis of SAG mills operation*

The plant data for the six months leading to June 2019 are analysed to assess the impact of the coarse ore stockpile's size segregation on the parallel SAG mills' operation. Figure 11 presents the frequency analysis of some of the key operating factors (ie throughput, mill weight, power draw, amount of pebble in SAG mill feed and pebble generated) for the SAG mills.

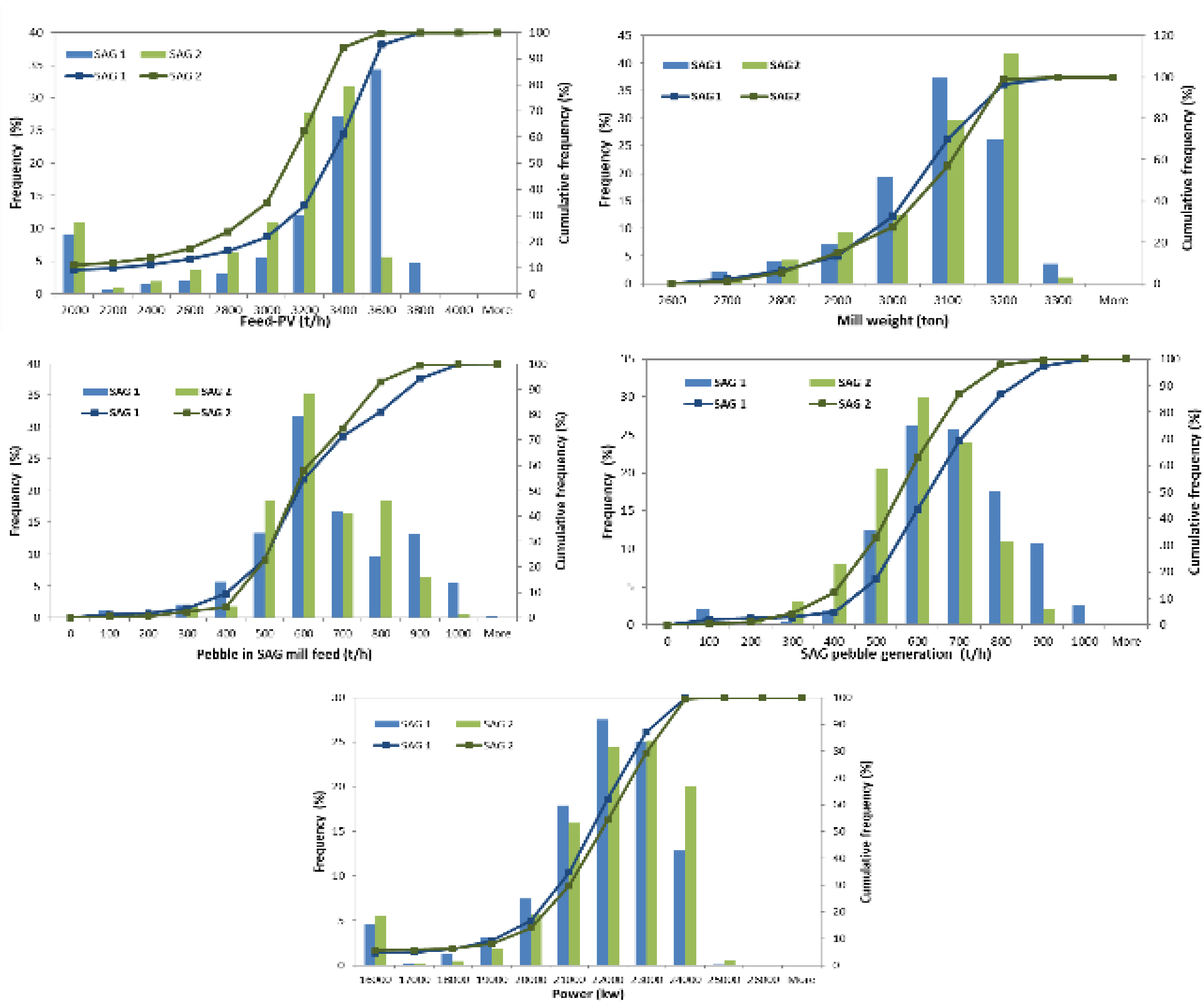


**FIG 11** – The frequency analysis of SAG mills key operation factors for the six months leading to June 2019.

As shown in Figure 11 and operators confirm it, the SAG mill in line 1 operates at a higher throughput than the SAG mill in line 2. Also, although both lines receive the same amount of crushed pebbles in feed to SAG mills, line 1 SAG mill generally produces more pebbles. This could be attributed to a coarser feed and higher throughput.

Analysing the mill power draw data indicates that line 2 SAG mill draws slightly more power since it is operating at a slightly higher mill load as well as it is presented in Figure 11.

The data presented in Figure 11 and analysis of other factors that are not shown in this paper due to space limitation indicates that the parallel SAG mills are performing different, which is primarily due to the size segregation in the coarse ore stockpile.

## CONCLUSION

This paper presented a case that size segregation in coarse ore stockpile due to number of factors such as stratification of materials during transport on conveyor belts, design of the stockpile and size segregation during the formation of the stockpile, causes variation in the size distribution of feed to parallel grinding lines.

The paper presented a simple method to benefit from the plant data available to understand and quantify the impact of size segregation on grinding efficiency. The paper demonstrates the importance of stockpiles and ore handling units that usually do not receive enough attention either during the process design or process optimisation initiatives. A better understanding of the behaviour of material handling and storage facilities and being able to model them can fill in gaps in the optimisation of mineral processing circuit and enhance the performance of advanced process control.

### Future plan for this research

The laboratory-scale experiment for size segregation of the stockpile that has developed in JKMRC will be conducted to collect calibration data for the JKMRC's dynamic model of the stockpile. The future work will specifically concern comparing the results between industrial trails that were conducted during the site visit and the dynamic model. After validation, the dynamic stockpile model can be used in operation to guide control of the stockpile level, feeders speed, and operation of SAG mills. After validation of the dynamic stockpile model, it could become an integral part of the concentrator's advanced control system at MMG's Las Bambas operation.

## REFERENCE


Combarros, M., et al. (2014). "Segregation of particulate solids: Experiments and DEM simulations." Particuology **12** (Supplement C): 25–32.

Wills, B. A. and T. J. Napier-Munn (2006). Will's mineral processing technology, Elsevier Science & Technology Books.

Yahyaei, M. and M. Powell (2018). Production improvement opportunities in comminution circuits. Mill Operators conference. Brisbane, Australia.

Yu, Y., et al. (2016). "DEM and experimental studies on pellet segregation in stockpile build-up." Ironmaking & Steelmaking: 1–8.

# Flotation

# Commissioning of the coarse ore flotation circuit at Cadia Valley Operations – challenges and successes

*E Jaques[1], L Vollert[2], B Akerstrom[3] and B A Seaman[4]*

1. Senior Plant Metallurgist, Newcrest Mining Limited, Orange NSW 2800.
   Email: emily.jaques@newcrest.com.au
2. Senior Metallurgist, Newcrest Mining Limited, Melbourne Vic 3004.
   Email: luke.vollert@newcrest.com.au
3. Manager – Ore Processing, Newcrest Mining Limited, Orange NSW 2800.
   Email: brandon.akerstrom@newcrest.com.au
4. Principal Metallurgist, Newcrest Mining Limited, Perth WA 6000.
   Email: brigitte.seaman@newcrest.com.au

## ABSTRACT

In August 2018 the first full-scale pneumatically assisted fluidised bed flotation cells for the recovery of coarse composited gold and copper were commissioned at Newcrest's Cadia Valley operation in New South Wales. The primary objective of the installation is to recover coarse value-bearing composites that are currently lost to conventional flotation tailings, without additional power input for particle size reduction to improve mineral liberation.

The Eriez HydroFloat™ separator is an aerated fluidised-bed (or teeter-bed) separator that has been demonstrated to increase the recovery of coarse, poorly liberated particles, compared to conventional flotation technology, by combining flotation fundamentals with hydraulically assisted separation. The technology was invented by Eriez in 1997.

At Cadia, composite particles are the principal carrier of gold and copper in the rougher tailings making up 50–60 per cent of the contained value in 2–5 per cent of the mass. Over 50 per cent of the composite particles in rougher scavenger tailings are in the lowest sulphide exposure range <10 per cent, where recovery via the existing conventional flotation circuit is poorest at only 30 per cent. This poor recovery of composite particles with low surface exposure presented a significant opportunity for the application of HydroFloat™ technology in a scavenging capacity.

The Cadia Coarse Ore Flotation Circuit is a novel application of aerated teeter-bed technology in sulphide flotation and presented many challenges during the commissioning and subsequent optimisation phases that needed to be solved to achieve successful delivery of the project. This paper gives an overview of the commissioning and ramp up journey, major operational challenges and solutions, high-level operational strategy and some analysis of the circuit performance to date.

## INTRODUCTION

In August 2018, the first full scale 3.4 m diameter Hydrofloat™ cells were commissioned at Newcrest's Cadia Valley Operation in New South Wales. The principal objective of the installation was to recover coarse, value-bearing composite particles that are lost to conventional flotation tailings without the need for additional upfront power input for particle size reduction to increase mineral liberation.

## CADIA VALLEY OPERATIONS – AN OVERVIEW

The Ore Treatment facility at Cadia Valley Operations (CVO) consists of two concentrators, Concentrator 1 and Concentrator 2, both of which process Cadia East ore to produce a copper-gold flotation concentrate and gold bullion. Concentrator 1, depicted in the simplified process flow diagram (Figure 1), employs secondary cone crushers followed by a HPGR to feed a single 40' SAG mill which then splits to three parallel ball mill circuits (referred to as Train 1, 2 and 3). Flash flotation cells treat primary cyclone underflow and centrifugal concentrators treat both flash flotation concentrate and a partial cyclone feed stream to target gravity gold. The three ball mill circuits each feed a dedicated rougher flotation train made up of Outotec tank cells. The rougher concentrate is sent to regrind prior to two stages of cleaning in both Outotec tank cells and Jameson cells to achieve the desired final concentrate grade (Akerstrom *et al*, 2018). The final concentrate product is dewatered at the Newcrest Blayney Dewatering Facility prior to being sent to Port Kembla for shipment. The rougher tailings are thickened and pumped to wet tailings storage facilities on-site.

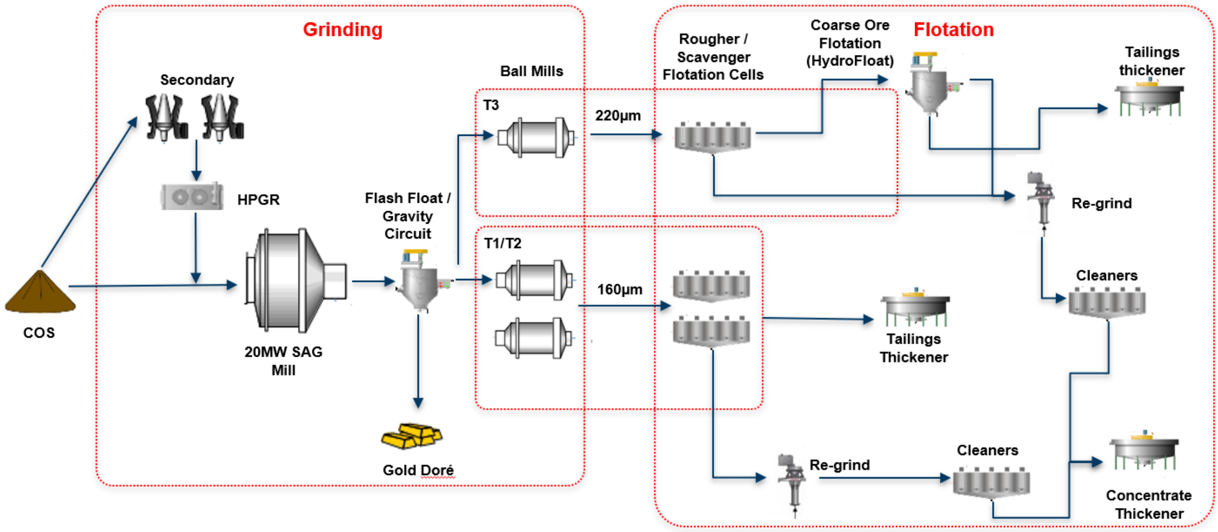


**FIG 1** – Simplified Concentrator 1 process flow diagram.

Due to a coarse bias in the split of SAG discharge material, the flotation feed grind size for Train 3 is nominally 220 µm while in Train 1 and Train 2 it is 160 µm. The Coarse Ore Flotation circuit (COF circuit) treats the Train 3 rougher tailings stream.

The Cadia East orebody is a low-grade porphyry style copper-gold-molybdenum deposit. Copper minerology is predominantly chalcopyrite and bornite with strong non-sulphide gangue mineral association. There are two primary geo-metallurgical domains:

1. Finely disseminated copper dominant mineralisation, which is predominant near the surface.
2. Sheeted veining which is localised around the core of steeply dipping sheeted quartz-calcite-bornite-chalcopyrite.

Gold from the Cadia East ore deposit exists primarily as native gold with some electrum. Due to the fine texture of the gold grains, recovery is sensitive to grind size and liberation in the flotation circuit.

The recovery opportunity at CVO, piloting and design of the COF circuit were discussed in-depth at Copper 2019 (Vollert *et al*, 2019).

## ERIEZ HYDROFLOAT™ TECHNOLOGY

The Eriez HydroFloat™ cell is an aerated fluidised bed which combines the principals of flotation and hindered settling. Eriez developed this technology in the early 2000s following research which showed that to float coarse particles effectively, a quiescent flotation environment and elimination of froth phase is required (Mankosa and Luttrell, 2002).

Deslimed, reagentised feed from the classification stage is presented to the top of the cell via a feedwell which distributes the solids evenly as they settle to create a bed. The bed is fluidised through the addition of the fluidisation (or teeter) water. Air and frother are also introduced into the fluidisation water distribution manifold prior to a cavitation tube which generates small bubbles. The water and bubbles move counter-current to the settling particles through the fluidised bed where the bubbles attach to the hydrophobic mineralised particles decreasing their density relative to the gangue particles and allowing them to rise to the top of the bed. These bubble particle aggregates either float immediately to the concentrate launder or are suspended on the top of the bed until sufficient bubbles attach to provide adequate buoyancy to float (Kohmuench *et al*, 2018). Figure 2 is a schematic of the HydroFloat™ cell with the bubble-particle aggregates sitting on the top of a fluidised bed shown in the photo.

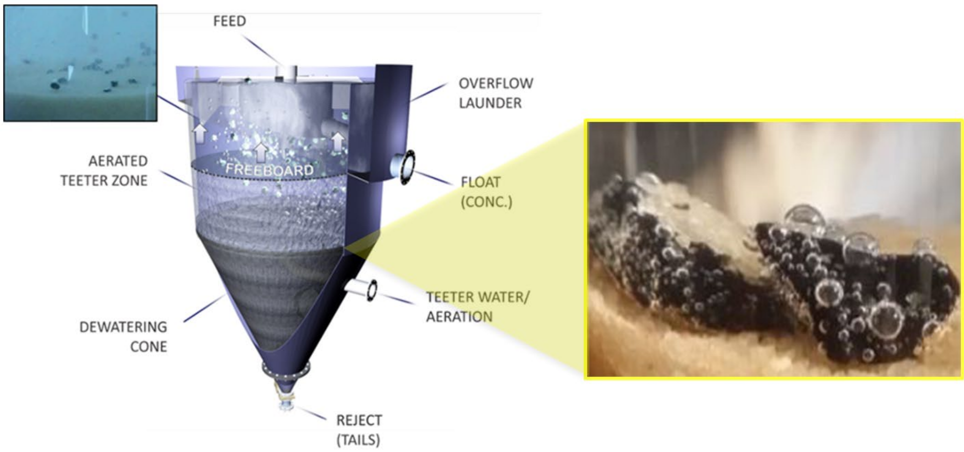


**FIG 2** – Simplified schematic of the Hydrofloat™ Separator with bubble particle aggregates (Kohmuench *et al*, 2018). NB: The bubble-particles are for illustration only and do not directly represent the Cadia ore.

## CADIA COARSE ORE FLOTATION CIRCUIT

Following pilot testing of the Eriez technology it was identified that the size distribution of the feed presenting to the HydroFloat™ cells can have a significant impact on their performance (Vollert *et al*, 2019). Therefore, a major focus at the study phase was determining an effective classification circuit upstream of the HydroFloat™ cells, the final design of the circuit is shown in Figure 3. The COF Circuit is comprised of 12 gMAX-26 cyclones as the initial classification stage to reject fines (<106 µm) to the overflow and to feed the four 3 × 3 m Cross Flow Classifiers with the underflow. The Cross Flow Classifiers are installed to ensure any remaining fines are not misreported to the HydroFloat™ cells as fines are ultimately entrained in the HydroFloat™ concentrate or can potentially cause settling issues in the HydroFloat™ cell leading to instability in the teeter bed. Potassium Amyl Xanthate (PAX) as a collector and Diesel as an extender, are added to the teeter water manifold of the Cross Flow Classifiers to create counter-current conditioning prior to the HydroFloat™. The overflow streams from both the cyclones and the Cross Flow Classifiers are directed to the final tailings thickener.

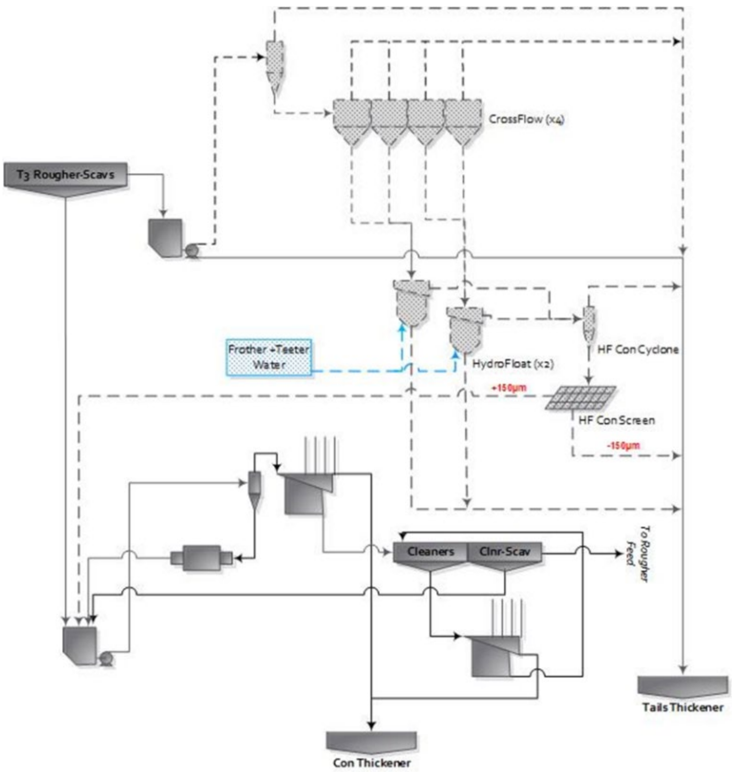


**FIG 3** – Cadia COF circuit.

Process water, frother and air are injected into the HydroFloat™ just above the dewatering cone to fluidise the particle bed and promote the flotation of particles up to 1 mm with surface liberation as low as five per cent. The HydroFloat™ cell tailings are directed to final tailings thickener with the concentrate sent to the dewatering circuit comprising of a dewatering cyclone fines and five deck Derrick StackSizer™ as a final stage to remove any entrained fines and increase the circuit gold and copper concentrate grade. The undersize from the StackSizer™ is pumped to the tailings thickener, the oversize is pumped to the existing Train 3 regrind circuit which was upgraded to a VTM800 from a VTM650 (~110 kW increase) to accommodate the coarser feed stream.

## COMMISSIONING CHALLENGES AND RECTIFICATIONS

The CVO Coarse Ore Flotation (COF) Circuit was commissioned in August 2018. As expected with the adoption of a new technology, an extended period of commissioning and ramp-up ensued during which several opportunities to improve the coarse particle flotation circuit operability and maintainability were identified.

### Increase in Train 3 grind size

During the design of the COF circuit, a primary grind size in Train 3 of 150 µm was used for all modelling and equipment sizing. However, following improvements in the Concentrator 1 crushing and grinding circuits, the throughput and subsequently primary grind size was increased to 220 µm in Train 3 as seen in Figure 4. This significantly increased the feed rate through the Cross Flow Classifier and HydroFloat™ cells by approximately 40 per cent.

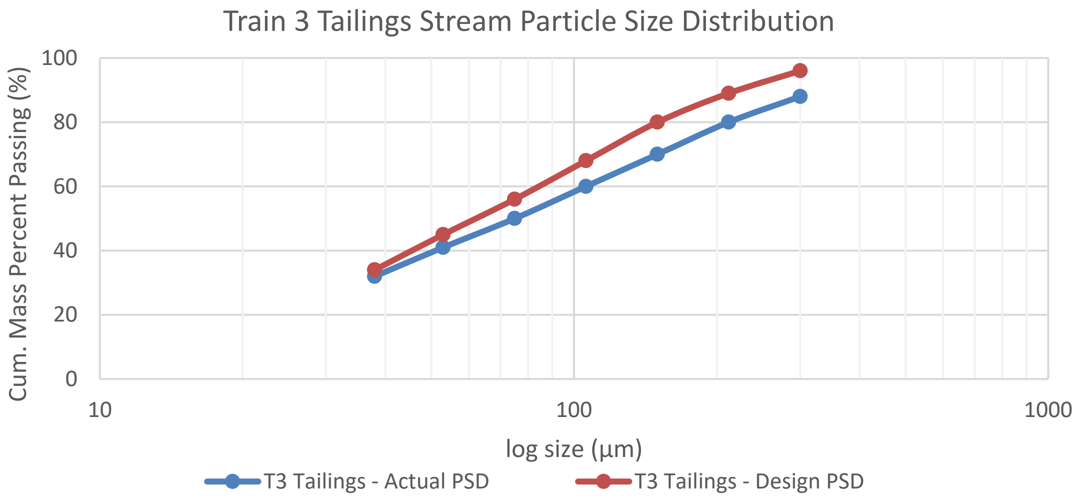


**FIG 4** – Effect of feed P80 on the feed tonnage rate to the Hydrofloat™ cells.

With the increase in feed presenting to the Cross Flow Classifier cells they became difficult to operate, regularly building up a load of solids, eventually causing the cells to become fully sanded. To reduce the total mass presenting to the Cross Flow Classifiers the spigot and lower cone section of one primary cyclone were temporarily removed and a blanking plate installed to bypass a portion of the circuit feed directly to tailings, whilst a circuit debottlenecking exercise was carried out.

The issues related to the increase in throughput to the Cross Flows was found to be exacerbated by the installed deflector plates. The deflector plates were intended to prevent instances of “ratholing”, a phenomenon whereby the teeter bed is disrupted and low-density material (including fines) preferentially flows to the underflow. The original deflector plates in Figure 5 had a flat top creating a ledge for solids to bridge across, significantly reducing the static head seen by the underflow valve and subsequently reducing throughout capacity relative to design.

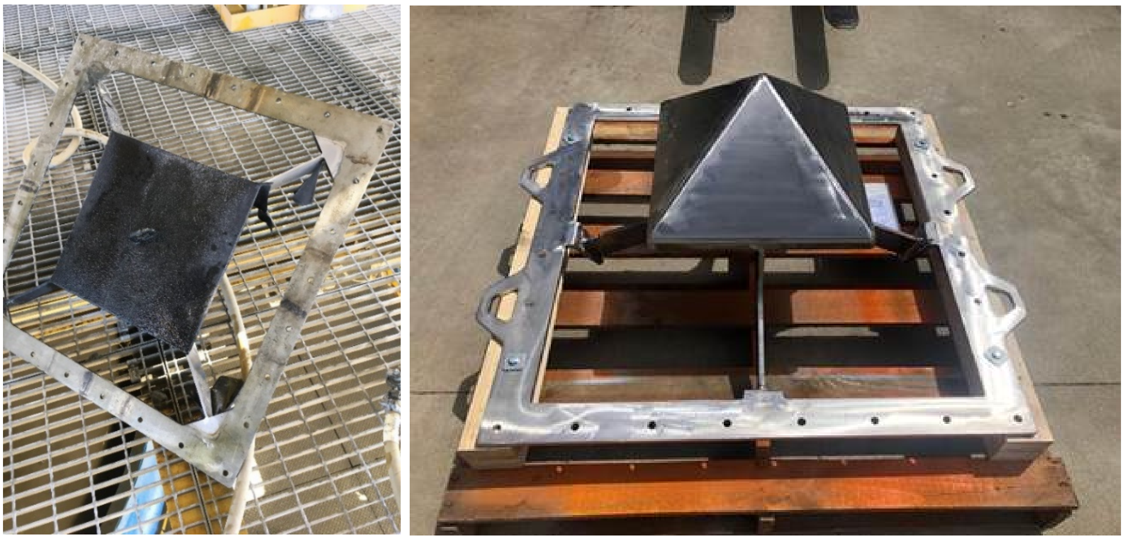

**FIG 5** – Original deflector plate (left); and new design for the Cross Flow Classifier deflector plates (right).

To handle the additional throughput, the Cross Flow Classifier SlurryFlo™ control valves were upgraded from 4” to 6” and from 4” to 8” for the HydroFloat™ cells. One major design lesson from this was that coarse (fines deficient) material can act as a self-supporting structure rather than true slurry at high per cent solids. This self-supporting structure absorbs a large portion of the available driving head, therefore when re-calculating the valve size required it was assumed the actual static head was only ~60 per cent of the total calculated head.

A new design Cross Flow Classifier deflector plate was also installed. The new design featured a raised and pointed section that eliminated sand build-up on the top of the deflector plate as slurry is diverted to the discharge valve whilst still achieving the design intent of minimising the occurrence of “ratholing” (Figure 5). Following these improvements, the bypass cyclone was closed to direct the full Train 3 rougher scavenger tailings to the circuit.

## Circuit size classification

As discussed above, there are two stages of size classification before the particles are presented to the Hydrofloat™, gMAX26 cyclones and Cross Flow Classifiers. Recent surveys showed the COF primary cyclone performance had drifted over time resulting in a significantly finer underflow compared to design and previous surveys due to misreporting fines (Figure 6). The decline in separation efficiency was due to worn rubber spigots and operational factors such as lower cyclone operating pressures and changes in Train 3 rougher scavenger tailings particle size distribution and slurry density.

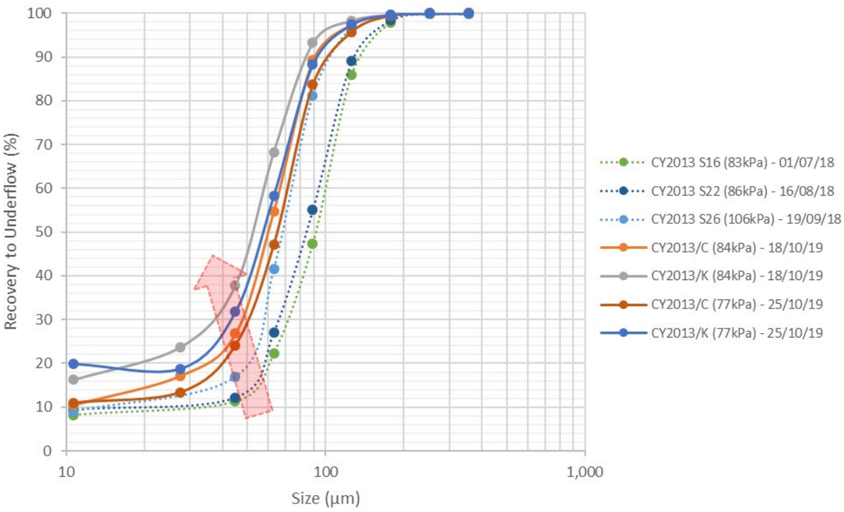


**FIG 6** – Fines distribution in the cyclone underflow of the COF primary cyclones.

The impact of this degradation in cyclone classification performance was a ~28 per cent increase in Cross Flow Classifier feed tonnage rates from a design of 136 t/h to 188 t/h. Consequently, most Cross Flow Classifiers were found to be operating at above the maximum flux of 16 t/m$^2$ (Figure 7). This presented operational challenges in the Cross Flow Classifiers where coarse material was unable to settle in the units driven by either; hindered settling due to increased viscosity, the higher velocity of the feed across the surface of the unit causing short circuiting, or a combination of both.

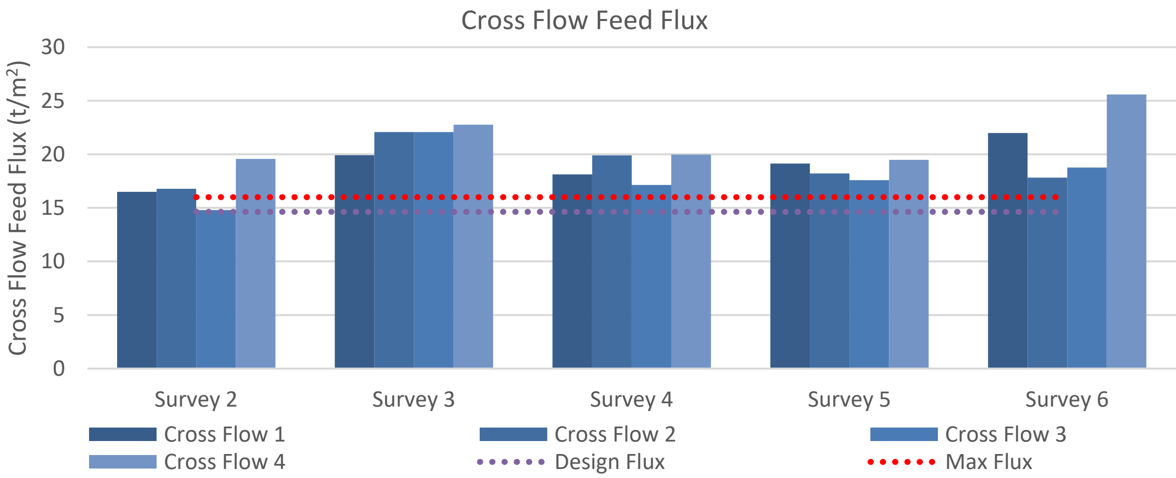


**FIG 7** – Cross flow feed flux with poor cyclone classification.

This indicates how crucial efficient classification at the primary cyclones is on the operability and performance of the Cross Flow Classifiers. This is unlike conventional flotation circuits where a shift in the particle size distribution presented to the circuit impacts metal recovery, but typically not the operability of the circuit. To ensure efficient classification in the primary cyclones, smaller spigots were trialled and proved successful, leading to improved operability of the Cross Flow Classifiers.

## Accelerated pipework and valve wear rates

Due to the coarse fines-deficient nature of the Cross Flow Classifier underflow stream, there was an unexpected acceleration in the wear of the valves and pipework. This was most evident in the Cross Flow Classifier discharge valves and spigots and the transfer lines to the HydroFloat™ feed as seen in Figure 8. The valve was comprised of an aluminium valve body and a tungsten carbide gate, while the spigot was rubber lined (6 mm) steel which wore through in approximately four weeks.

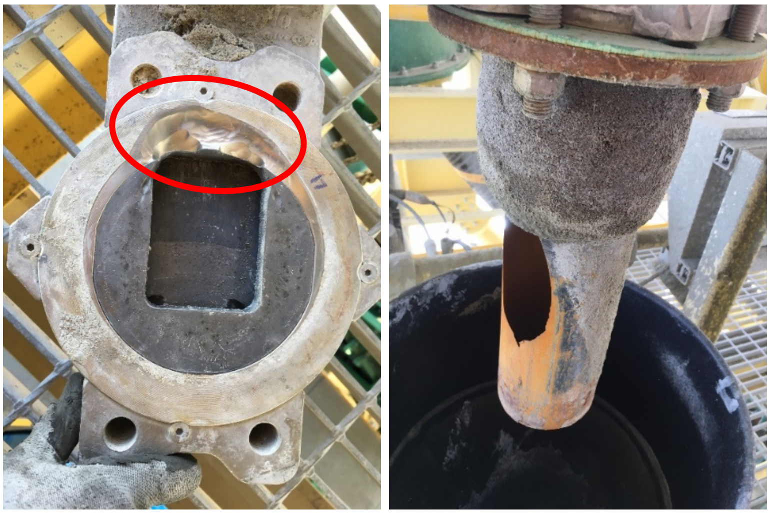

**FIG 8** – Coarse fines-deficient streams causing major wear of cross flow classifier valves and damage to the cross flow classifier discharge spigot.

To quantify the abrasiveness of key COF circuit streams, samples were sent to the CSIRO to determine the Miller Number. The Miller Number is a measure of slurry abrasivity as related to the instantaneous rate of mass loss of a standard metal wear block at a specific time on the cumulative abrasion-corrosion time curve. Figure 9 shows the Miller numbers for the Cadia COF circuit along with some generic mineral slurries for comparison. It is evident that the Train 3 rougher scavenger tailings had a lower Miller Number than all COF streams tested indicating it was less abrasive than those streams. It was suggested this was due to the larger proportion of fines creating a cushioning effect in the rougher scavenger tailings stream which is evident in Figure 10.

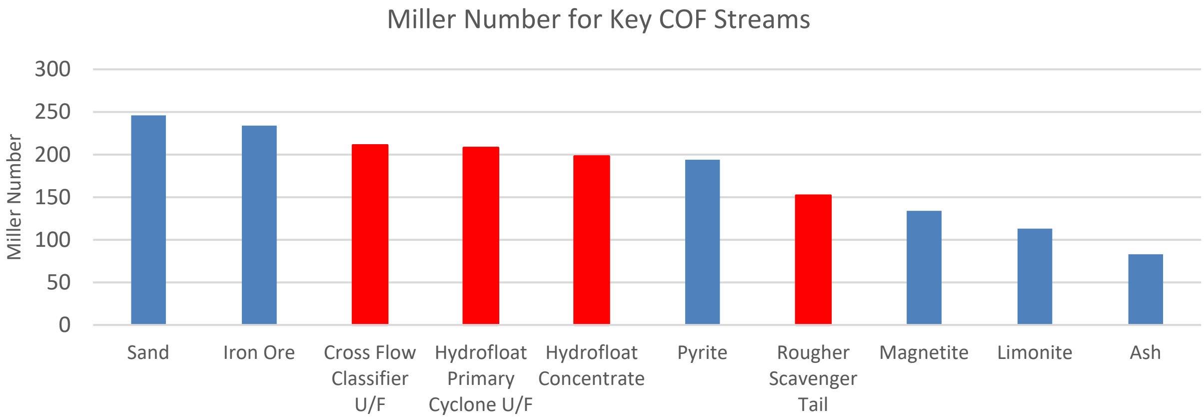


**FIG 9** – Miller number for key COF streams and generic mineral slurries for comparison.

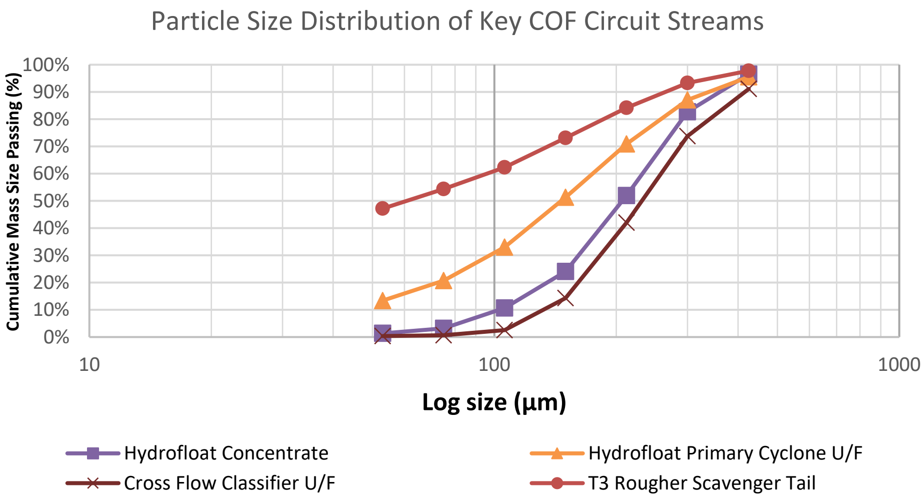


**FIG 10** – Particle size distribution of key COF circuit streams.

To rectify the issue of high wear, all SlurryFlo™ valves which were upgraded to the larger diameters were also upgraded to a cast stainless steel body with higher grade Sintered Tungsten Carbide gate, seat plate and bore liners to extend the valve life. These internals are rotable so can be replaced when worn without the need to change out the entire valve. To improve the longevity of pipework between the Cross Flow discharge and HydroFloat™ feed, all rubber lined steel was replaced with 20 mm cast Alumina ceramic lined pipework (Figure 11).

**FIG 11** – Ceramic lined pipework on the discharge of the cross-flow classifiers.

The operational strategy was also changed to limit the valve openings to 80 per cent of their full travel after consultation with the valve supplier. Flow modelling indicated that when the valves were open to 100 per cent slurry would be directed into the wall of the discharge pipework immediately after the valve body where most of the wear was observed. The new valves were sized accordingly so the normal operational range was between 50–70 per cent of the full valve travel distance.

There has been a significant improvement in the wear rate of these components following these improvements to the valve material of construction, the operational limits of the valve and the installation of ceramic lined pipework. This has decreased the maintenance frequency for this circuit to the required 13-week interval.

## SUCCESS AND A NEW LEVER TO PULL

With the design improvements having been successful in addressing issues with circuit operability and availability, the focus shifted to Metallurgical optimisation of the HydroFloat™ unit itself and a review of the overall plant operational strategy to realise the full potential of the installed COF circuit.

## HYDROFLOAT™ UNIT RECOVERY

To optimise Hydrofloat™ cell performance, a campaign of sized surveys was executed by sampling the feed, concentrate and tailings streams. A Box-Behnken experimental design was used to investigate the response to changes in teeter bed level, teeter water flow rate and air addition. The HydroFloat™ feed size distribution and grade were identified as uncontrolled variables which also affected unit recovery during the campaign. Figure 12 displays the spread of recovery by size data (relative to HydroFloat™ feed) collected, overall COF circuit recovery from the finer size fractions will be lower due to losses in upstream classification.

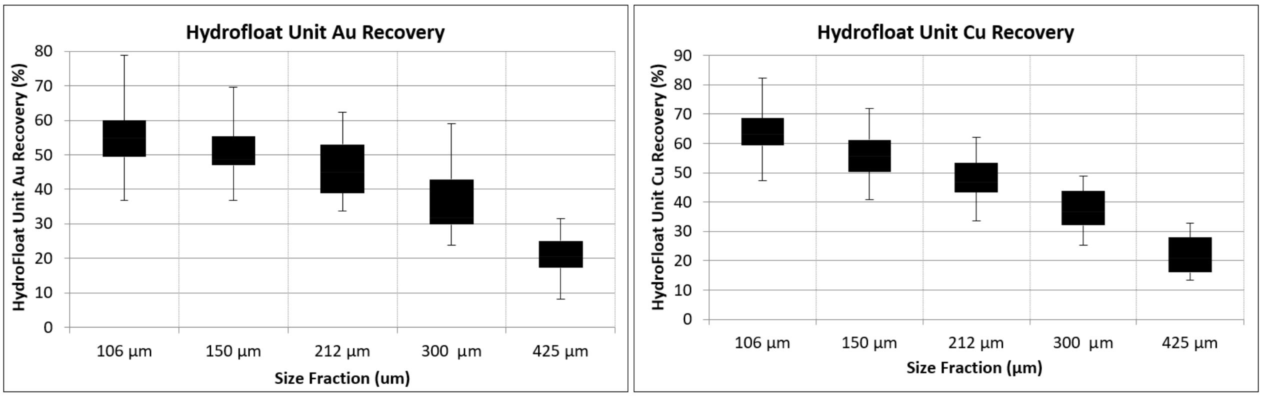


**FIG 12** – Hydrofloat™ Cu and Au unit recovery from 15 unit surveys.

Under all operational parameters tested the HydroFloat™ units were able to recover coarse copper and gold from tailings. It is worth noting that recovery in the 425 micron size fraction is impacted by the inclusion of any top size material (+600 micron) in tailings where majority of the copper and gold present is likely to be entirely encapsulated in gauge.

High level findings from the optimisation survey campaign were as follows:

- Teeter water rate, bed level and feed size distribution all influence the bed density.
- Increasing bed density increased concentrate grade.
- Increasing teeter water rate increased both copper and gold recovery up to the maximum tested flow rate of 200 $m^3/h$.
- Increasing bed level set point also increased copper and gold recovery.
- Both teeter water rate and bed level had a direct relationship with mass recovery to concentrate.

Figure 13 shows the liberation of copper sulphide particles in a sample of the COF concentrate, post dewatering and screening out of the fines. It clearly shows the particles which are floated by the Hydrofloat™ unit are not only coarse but also poorly liberated with >99 per cent of all particles in the concentrate having <50 per cent liberation by free surface area.

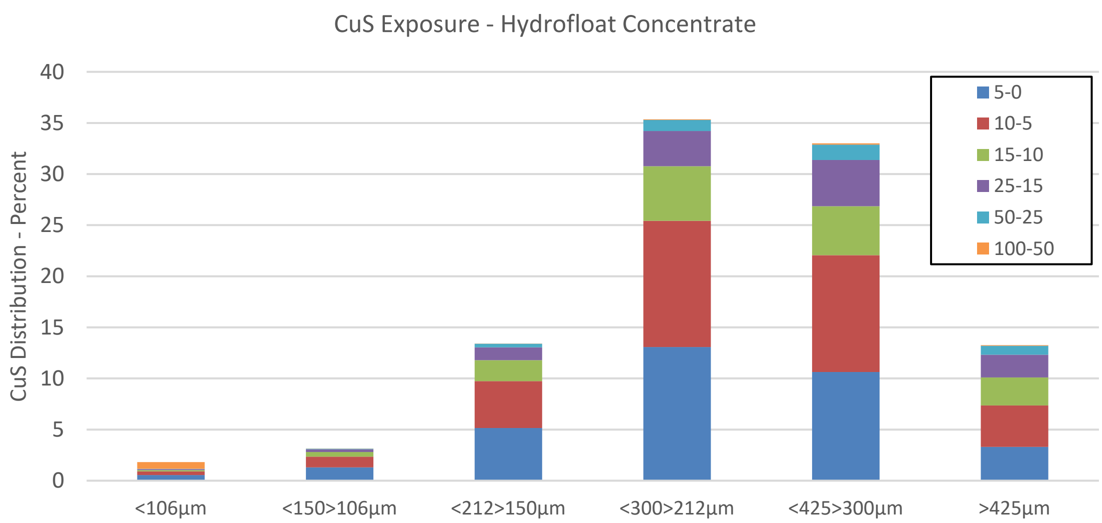


**FIG 13** – Liberation × Size of Hydrofloat™ concentrate.

## Shifting the economic optimum grind size

Using the survey data collected, total gold and coper recovery across the HydroFloat™ unit was modelled by applying a fixed recovery in each size fraction to the mass and metal deportment in

HydroFloat™ feed. The impact of coarsening concentrator primary grind size could then be investigated by employing the Bazin technique which assumes a constant relationship between the cumulative metal distribution and the cumulative solids distribution in the grinding circuit product, independent of grind size (Runge *et al*, 2014). This modelling exercise suggested that the primary grind size could be increased whilst maintaining the copper and gold recoveries.

Data presented in Figures 14 and 15 shows the copper and gold final tailings grades versus primary grind size for Trains 1&2 and 3 when the COF circuit was online. As these flotation circuits are both fed by Cadia East ore from a common stockpile, grind size versus tailings grade can be compared directly to highlight the impact that the COF circuit has had on the Train 3 tailings grade.

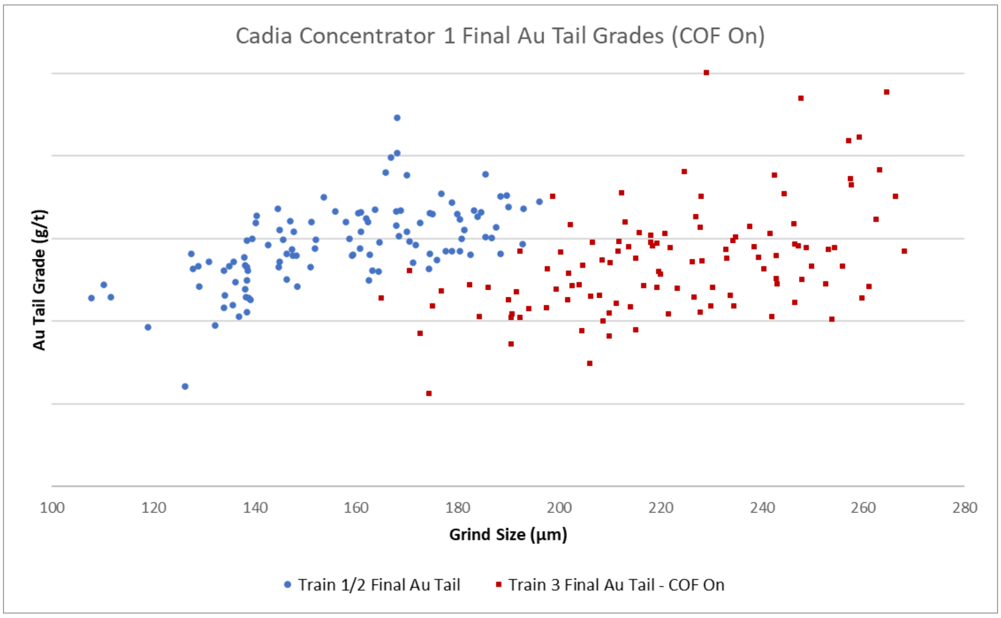


**FIG 14** – Comparison of the Train 1&2 and Train 3 Au tailings grades with the COF circuit on Train 3.

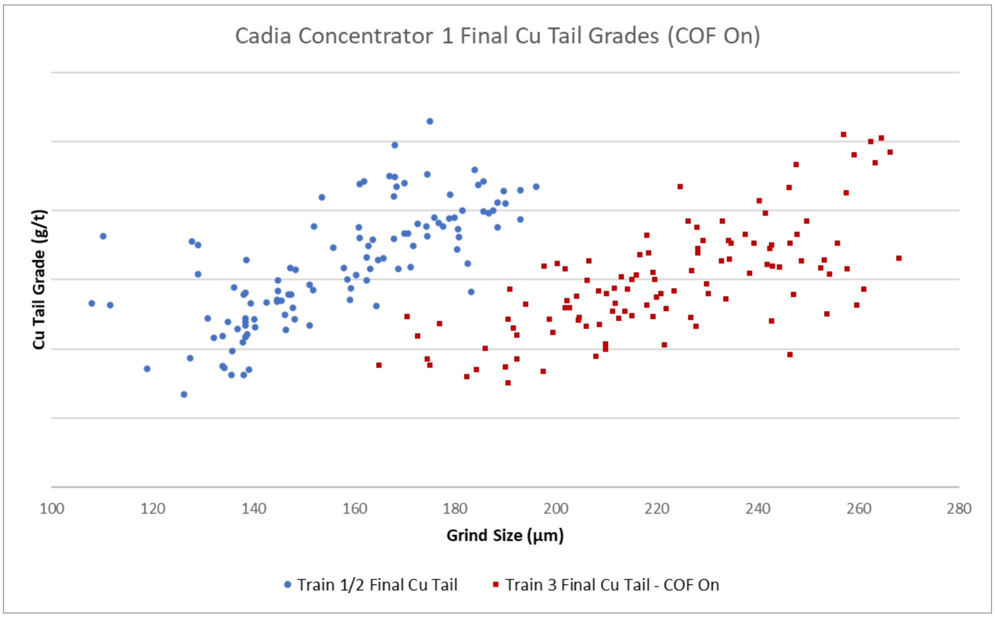


**FIG 15** – Comparison of the Train 1&2 and Train 3 Cu tailings grades with the COF circuit on Train 3.

There is a fundamental shift in the grind size versus final tailings grade relationship for Train 3 which has the COF treating the rougher scavenger tailings compared with the conventional Train 1&2 flotation circuit. Tailings grade in Train 3 is comparable to that of Train 1&2 despite the approximately 60 micron increase in primary grind size.

## Effect on Concentrator 1 recovery

The performance of the Train 3 flotation circuit was analysed for periods when the COF circuit was online and off-line. The average decrease in the Train 3 final tailings grade was used to calculate the improvement in Concentrator 1 overall recovery. Three different statistical methods were used for the exercise:

1. T-test.
2. Multivariable regression.
3. Comparison of regression lines (Napier-Munn, 1998).

For all data analysis a 95 per cent confidence interval was used.

To ensure the "COF On" and "COF Off" periods were comparable the data was filtered to ensure feed grades and grind sizes were statistically similar. The results of these tests showed a statistically significant reduction in the Train 3 final circuit tailings grade when the COF was online compared to when it was off-line. This was equivalent to an overall Concentrator 1 recovery improvement of ~2.12 per cent for gold and ~0.58 per cent copper.

Table 1 clearly indicates that the incremental gold recovery uplift with the COF circuit online was greater than for copper, although the expected recovery uplift for both gold and copper is the same based on the HydroFloat™ survey data and historically the recovery of gold and copper in the conventional circuit followed very similar trends. Focus therefore turned to the Train 3 cleaner circuit to determine possible causes for the disparity in recovery improvement.

**TABLE 1**

Analysis of Concentrator 1 recovery improvement with COF circuit online.

| | **Improvement in Concentrator 1 overall recovery** | |
|---|---|---|
| **Analysis method** | Gold | Copper |
| **COF On/Off t-test** | 2.00% | 0.42% |
| **COF On/Off regression** | 2.19% | 0.66% |
| **COF On/Off gradient of line** | 2.19% | 0.66% |
| **Average** | **2.12%** | **0.58%** |

## Effect on Train 3 cleaner circuit performance

A series of surveys in the Train 3 cleaner circuit were completed with the COF circuit online and off-line to quantify the cleaner block size × liberation × recovery to determine drivers of the poorer overall copper recovery relative to gold despite similar Hydrofloat™ unit recoveries. Results of these surveys were used to identify differences in the Train 3 cleaner circuit. From Table 2 it is evident that there was a 1 per cent reduction in Train 3 cleaner copper recovery when the COF circuit was online.

**TABLE 2**

Key circuit performance indicators for the Train 3 cleaner circuit.

| Key circuit performance indicators | COF Circuit Off | COF Circuit On | Difference |
|---|---|---|---|
| Train 3 regrind cyclone overflow P80 | 16 μm | 28 μm | +12 μm |
| Train 3 cleaner circuit Cu recovery | 94.4% | 93.3% | -1.1% |
| Train 3 regrind cyclone overflow CuS liberation | 85.7% | 65.5% | -20.2% |
| Train 3 cleaner circuit recovery losses in +53 μm fraction | 0.0% | 0.5% | +0.5% |
| Train 3 cleaner circuit recovery losses in liberated <C4>53 μm fractions | 0.1% | 0.5% | +0.4% |

The regrind cyclone overflow increased in grind size from a P80 of 16 μm when the COF was off-line to 28 μm when the COF was online. This corresponded to a distinct shift in the liberation characteristics of the regrind cyclone overflow. The proportion of copper sulphide minerals in the liberated fraction (50–100 per cent CuS exposure) was 85.7 per cent when the COF was off-line and reduced to 65.5 per cent when the COF circuit was online. This is illustrated in Table 2 and Figure 16.

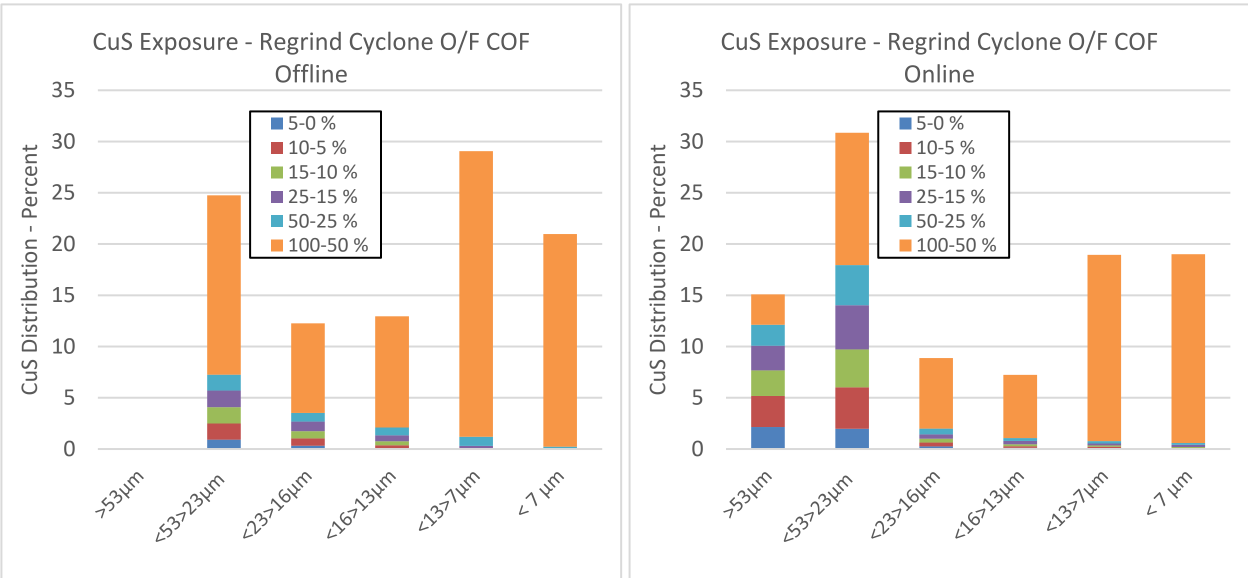


**FIG 16** – Copper Sulphide distribution of the Train 3 Regrind Cyclone Overflow with the COF Off-line (left); and Online (right).

The effect of the increase in coarser, poorly liberated particles feeding the cleaning circuit was also noticeable in the cleaner scavenger tail. There was an increase in grind size from 18 μm to 24 μm which resulted in an increase in the recovery losses of particles measuring greater than 38 micron with less than <50 per cent liberation from 1.2 per cent to 1.8 per cent supporting the hypothesis that one driver of poorer copper recovery was the increase in coarse particles in the cleaner circuit Figure 17.

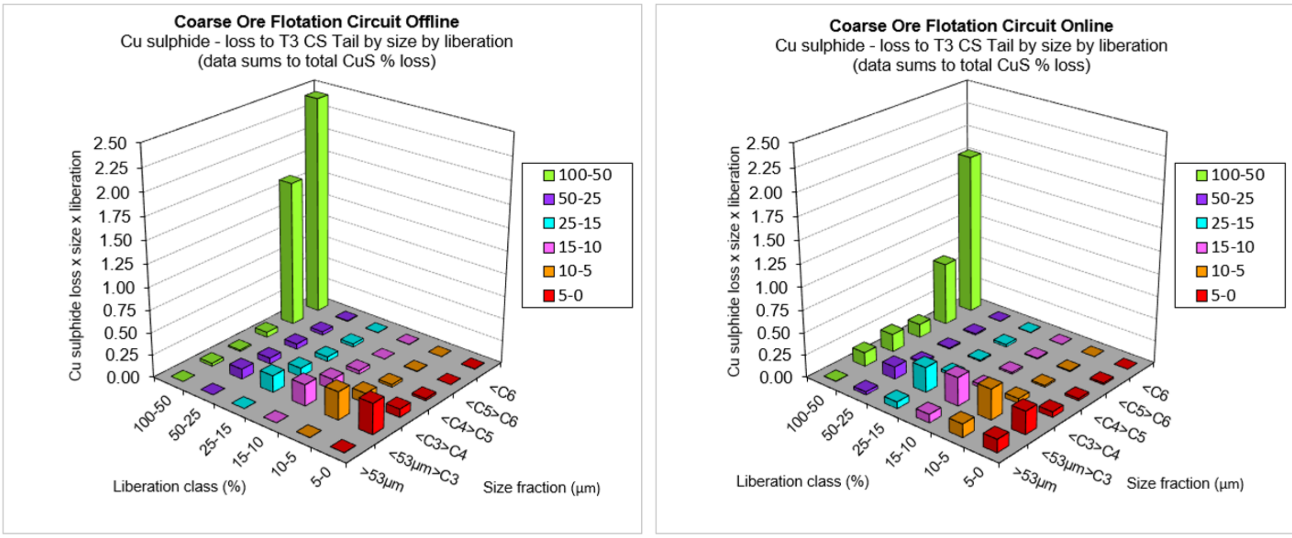


**FIG 17** – Size × liberation losses to the Train 3 cleaner scavenger tailings with COF off-line and online.

Additionally, the proportion of well liberated (100–50 per cent) in the size range of 20 to -53 µm suggests that although these particles are well liberated, they are still rejected to the cleaner scavenger tailings due to poorer cleaner kinetics or an insufficient residence time when the COF is online.

To confirm the grind sensitivity of the Hydrofloat™ concentrate stream, a series of bench scale laboratory flotation tests were completed at varied grind sizes. Figure 18 shows that, as the grind becomes finer, the recovery is significantly improved from 85.9 per cent to 96.9 per cent while maintaining similar concentrate grades.

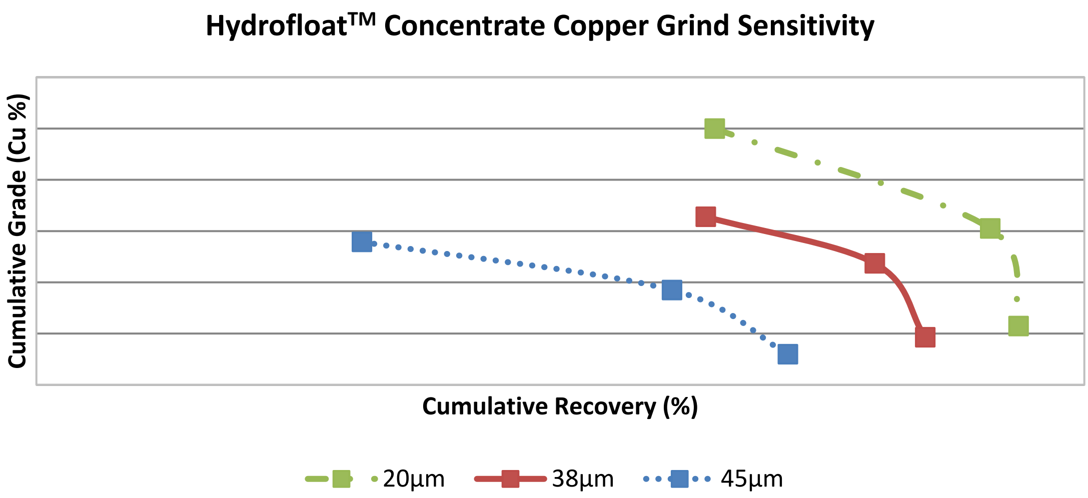


**FIG 18** – Grind Sensitivity of the Hydrofloat™ Concentrate.

To alleviate the identified constraint around regrind power, the site metallurgy team are progressing with capital projects to alter the cleaner circuit flow sheet and increase total regrind mill power to process the COF concentrate more effectively and thus optimise overall circuit recovery.

## THE FUTURE OF COARSE ORE FLOTATION

The Corse Ore Flotation circuit has increased the recovery of coarse, poorly liberated particles and allowed Cadia to coarsen the primary grind, improving energy efficiency and exceeding the benefit put forward in the original business case. Circuit data presented in this paper has successfully demonstrated the Hydrofloat™ technology can fundamentally shift the economic optimum grind size by extending the floatable size range relative to that of conventional flotation cells shown in the well-known graph in Figure 19.

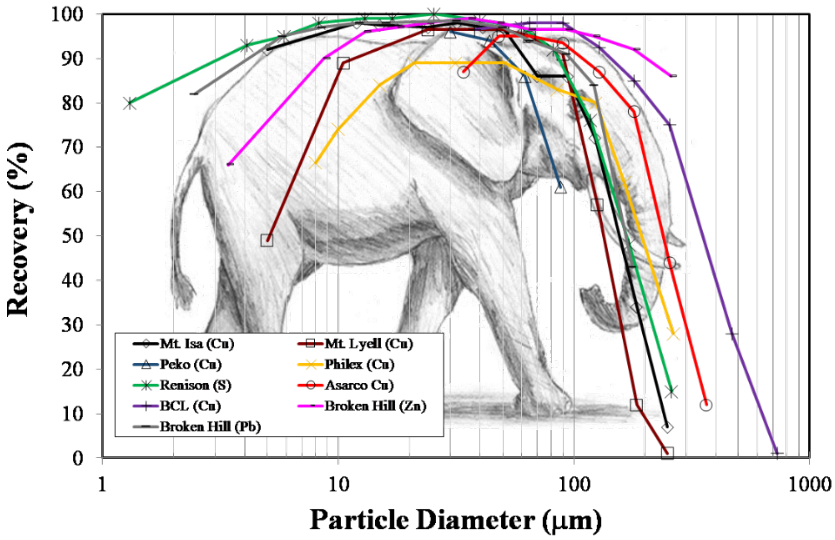


**FIG 19** – Conventional flotation recovery versus grind size for industrial sulphide flotation circuits (Lynch *et al*, 1981).

The Train 3 installation at Cadia has provided the business with confidence to proceed with additional installations like the recently announced Cadia Expansion Project which will extend the tailings scavenging approach to treat more than 70 per cent of the total site tailings stream. The updated design for the expansion circuit incorporates learnings from the first installation to improve operability and maintainability.

The next logical step is to review the design and operation of primary milling and classification circuits to further leverage coarse ore flotation. If the shape of the flotation feed particle size distribution can be changed to maximise material in the new floatable size range and reduce the generation of ultra-fines due to over grinding (Figure 20), additional recovery, throughput and energy efficiency could be achieved.

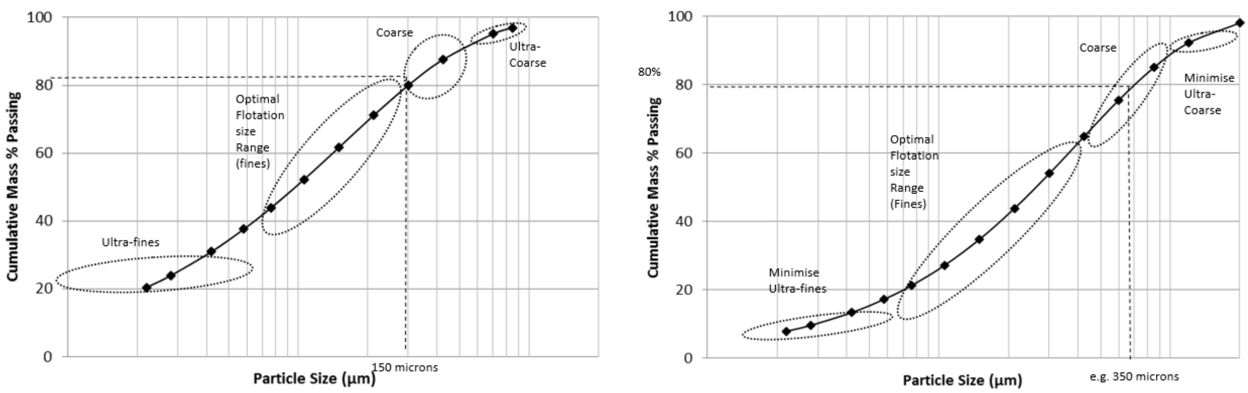


**FIG 20** – Potential to sharpen the PSD of primary cyclone overflow to minimise fines production.

For Greenfields projects, the ultimate goal is to achieve rejection of mass early in the flow sheet at the coarsest possible particle size. In addition to improved project economics, this style of flow sheet could also deliver a significant reduction concentrator footprint, power and water demand and enable the use of environmentally preferential tailings storage options like dry stacking or co-mingled deposition.

There are however, several challenges inherent with the HydroFloat™ technology to overcome in the design of a waste rejection flow sheet. Feed to the HydroFloat™ requires classification to remove fine particles which can hinder the formation of a stable teeter bed, the efficiency of fines removal is dictated by the ore properties. This deslimed, coarse material is both difficult to pump and highly abrasive. The overall water balance for the flow sheet also needs careful consideration as the fluidisation water requirement can be significant, generating a low-density product stream that then requires further treatment.

## CONCLUSIONS

Newcrest has successfully commissioned the first full-scale Hydrofloat™ cells for the recovery of sulphide and gold from the flotation tailings stream. Through the continuous problem solving of operational challenges and optimisation of operational strategies, recovery has not only increased for a given grind size, but also sustained at coarser grind sizes.

In conventional copper concentrators, there is always a trade-off between recovery and grind size. As primary grind size is decreased, more power is consumed per tonne of ore resulting in a lower throughput rate for a given installed power. It has been demonstrated that the application of coarse flotation technology such as the HydroFloat™ has the potential to shift the economic optimum grind size and increase cash flow. This success paves the way for significant changes in future plant design and provides operations with additional levers that can be pulled to economically recover low-grade orebodies.

## ACKNOWLEDGEMENTS

The authors would like to thank Newcrest Mining Limited for permission to publish this paper. A special acknowledgement is made to the many people who contributed to the successful commissioning and optimisation of the circuit including the Cadia site and corporate metallurgy teams, Ian Clatworthy, Andrew Thompson, David Buchanan and Eriez.

## REFERENCES

Akerstrom, B., Seppelt, J., Waters, T. & Seaman, J. B. a. D., 2018. Cleaner Circuit Optimisation as Cadia Operations. *Mill Operators Conference.*

Kohmuench, J., Mankosa, M., Thanasekaran, H. & Hobert, A., 2018. Improving coarse particle flotation using the HydroFloat™ (raising the trunk of the elephant curve). *Minerals Engineering*, pp. 137 – 145.

Lynch, A., Johnson, N., Manlapig, E. & Thorne, C., 1981. *Mineral and Coal Flotation Circuits: Their Simulation and Control.* Amsterdam: Elsevier Publishing.

Mankosa, M. & Luttrell, G., 2002. *Air-assisted density separator device and method*. s.l.:s.n.

Napier-Munn, T., 1998. Analyzing plant trials by comparing recovery grade regression lines. *Minerals Engineering*, pp. 949–958.

Runge, K., Tabosa, E. & Holtham, P., 2014. *Integrated Optimisation of Grinding and Flotation Circuits*. s.l., AusIMM.

Vollert, L., Akerstrom, B. & Seaman, B., 2019. Newcrest’s Industry First Application of Eries HydrofloatTM Technology for Copper Recovery From Tailings at Cadia Valley Operations. *Copper 2019*.

# Piloting study of the reflux flotation classifier (RFC) at a Queensland copper mine

*H Law[1], L Christodoulou[2], B Dabrowski[3] and A de Hesse[4]*

1. Regional Product Manager Flotation and Dewatering, FLSmidth, Brisbane Qld 4008.
   Email: harrison.law@flsmidth.com
2. Global Product Manager Flotation, FLSmidth, Salt Lake City Utah 84104.
   Email: lance.christodoulou@flsmidth.com
3. R&D Project Manager Flotation, FLSmidth, Salt Lake City Utah 84104.
   Email: bart.dabrowski@flsmidth.com
4. Process Engineer – Water Process and Systems, Brisbane Qld 4000.
   Email: annika.dehesse@ghd.com (previously: Plant Metallurgist, Glencore, Cloncurry Qld 4824)

## ABSTRACT

FLSmidth's new Reflux Flotation Cell (RFC) is an innovative flotation system that is proving to transform the hydrodynamics of traditional flotation. This novel flotation system has proven to reduce the flotation volume required by an order of magnitude when compared to traditional systems. Enhanced kinetics are achieved by increasing operating bubble surface area flux by as much as ten times more than is possible with existing technologies. The cell operates to maximise recovery while producing a high-grade flotation product. This is achieved by operating an effective sparging system, promoting bubble-particle attachment by producing optimum bubble sizes at high shear rates. The addition of wash water allows for grade control/rejection of slimes and ensures positive bias flow in the separator to maximise separation efficiency. FLSmidth has tested this technology on a pilot scale at a Queensland copper mine. A continuous sample in the form of slipstream from the feed to the existing rougher flotation circuit was tested. This paper aims to detail the testing campaign and relay the results achieved, comparing the RFC's performance to that of the existing plant rougher-scavenger flotation circuit. Copper recoveries and grades equivalent to that of the production circuit were readily achieved at retention times in the order of 10–15 per cent of the production circuit requirements. Direct comparison to plant performance as well as conventional laboratory flotation kinetic tests will be discussed along with the impact of these results and implementation of this technology on copper rougher flotation circuit design.

## INTRODUCTION

In the base metals industry, there is a continued trend of processing low-grade and often difficult to treat ores. In response to this, industry has developed larger flotation cells to treat ever-increasing tonnages. Commercially available cells are promising to increase in volume to over 600 $m^3$, as described by (Camomile and Lynch). This is likely to be approaching the upper limit of existing technology, with a significant reduction in footprint the only way industry can overcome this issue. This has led to the development the Reflux Flotation Cell (RFC). It has been developed from combining the Reflux™ Classifier and a novel approach to froth phase bubble recovery and washing.

The RFC is a fast flotation device, typically treating slurry in one tenth of the time of a conventional flotation device (Dickson, 2015). This means each stage will have under 30 sec residence time per cell at high mineral recovery rates. A key challenge in achieving such high rates is the treatment of ultrafine entrainment, which follows water in the froth phase. By applying an enclosed washing system, a significant reduction in the volume of entrained particles is possible at extremely high bubble surface area flux in comparison to conventional flotation. The application of lamella chambers on the underflow provides a highly efficient system for separating bubbles from the unattached particles and provides a path for loaded fine bubbles to return to the system to be recovered.

Previous testing on the RFC has primarily focused on the coal industry, with a full-scale unit being installed in the Hunter Valley in 2020. Initial research work at the laboratory scale has indicated a significant extension of recoverable size fractions along with increased recoveries for a typical copper ore. Due to considerable effort required and complexity to generate and prepare suitable flotation feeds, this testing program was limited. It was therefore essential for the technology to be tested on an existing continuous plant feed, to prove the technology against an existing flotation circuit and develop an operating strategy. This paper describes four test campaigns and over 100 individual tests of flotation conditions. It will discuss the performance, scale-up to the existing plant, and implications of future testing.

## PLANT DESCRIPTION

The copper concentrator is a single line plant with a nominal maximum throughput rate of 1200 t/h. The process flow diagram is depicted in Figure 1. The throughput rate averages 880 t/h. The grinding circuit comprises a SAG and ball mill in closed configuration, with cyclone overflow reporting to the flotation circuit, typically at a p80 of 105 μm.

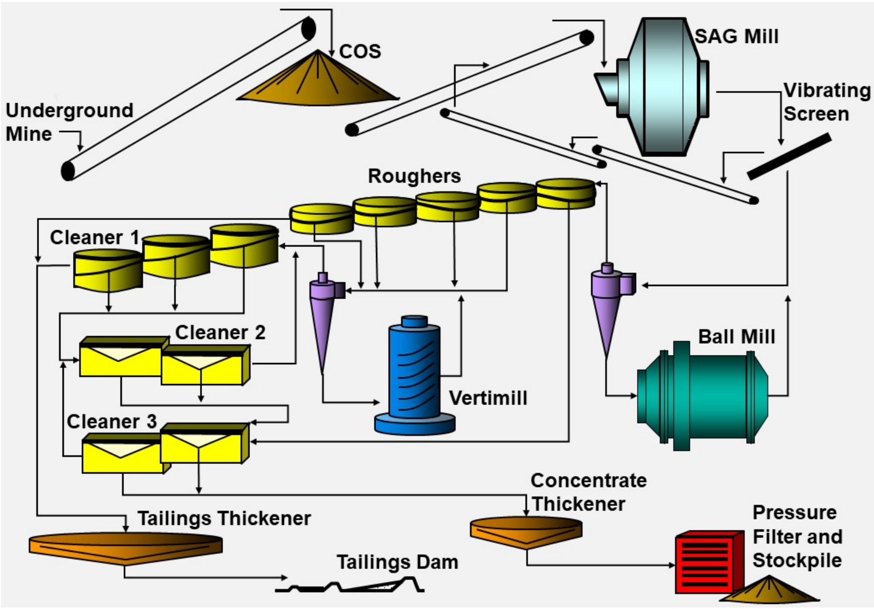


**FIG 1** – Copper concentrator flow sheet.

The flotation circuit is composed of a rougher train and three stages of cleaning. The concentrate from the first bank of two rougher cells is diverted to the third cleaner to capture liberated fast-floating copper bearing particles and reduce regrind duty. This is performed at pH of 7–8 with a highly selective collector DSP009 along with IF50 as frother. The remainder of the "scavenging" rougher train comprises seven Wemco 128 m$^3$ Smart Cells in four banks. This is performed unselectively to maximise copper composite recovery with the addition of a strong collector, PAX. The rougher tail combines with the cleaner tail and reports to the tailings thickener, while the rougher concentrate is reground in a vertical stirred mill prior to cleaning. Cleaner one comprises eight OK50 cells, while stages two and three contain eight and five OK16 cells respectively. The final concentrate reports to the concentrate thickener, then to a pressure filter for drying. The concentrate is subsequently hauled off-site by truck. Typical first-stage rougher recovery is 83 per cent, and typical overall recovery is 96 per cent. The high recovery is due to 90 per cent of the chalcopyrite particles being over 80 per cent liberated and very little associations with other sulphide minerals, as shown in Figure 2. This high degree of liberation does not vary from day-to-day and therefore the site is ideal for campaign-based piloting studies.

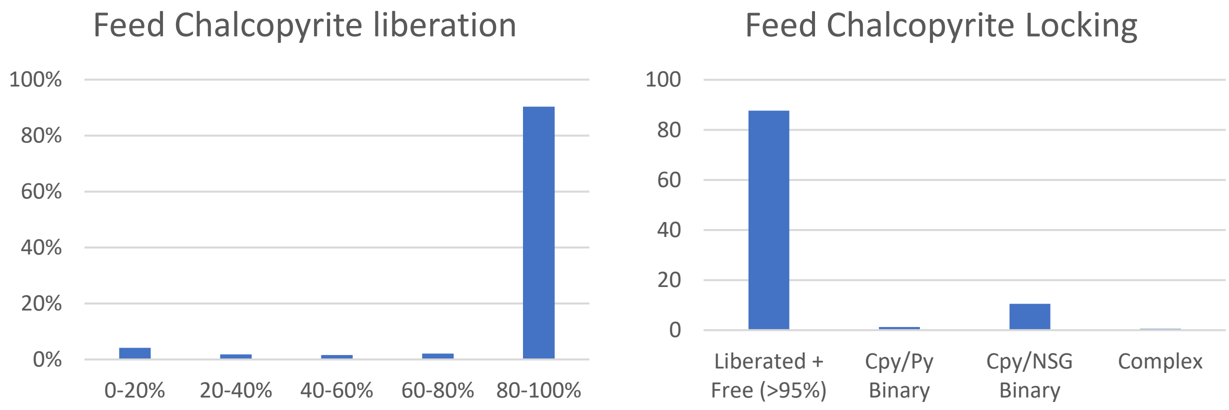


**FIG 2** – Feed Chalcopyrite liberation and locking.

## RFC TECHNOLOGY OVERVIEW

The Reflux Flotation Cell technology utilises several processing mechanisms to enhance flotation kinetics by altering or eliminating rate-limiting features of conventional open tank systems. Enhanced kinetics are achieved by:

- Increasing operating bubble surface area flux by as much as ten times that is possible with existing technologies (Dickinson, Cole and Galvin, 2019).
- Operating without a discernible froth/pulp interface effectively eliminating coalescence, with gas fraction in the order of 50 per cent, eliminating drop back of particles into the pulp phase.
- Generating a very fine bubble distribution and contacting these bubbles with floatable material in a high a shear environment at the inlet of the device.
- Applying wash/fluidisation water counter-current to bubbly flow of floatable material to enhance product quality and allow for bias flow control.
- Use of incline channels to quickly reject gangue out of system along with forcing mineral laden bubbles back into the system.

The cell operates to maximise recovery while producing a high-grade flotation product. Figure 3 shows a schematic depiction of the RFC cell, highlighting specific features enabling the high efficiency performance of the technology. An effective sparging system is utilised to promote bubble-particle attachment by producing optimum bubble sizes at high shear rates as feed enters the cell at the top of the machine.

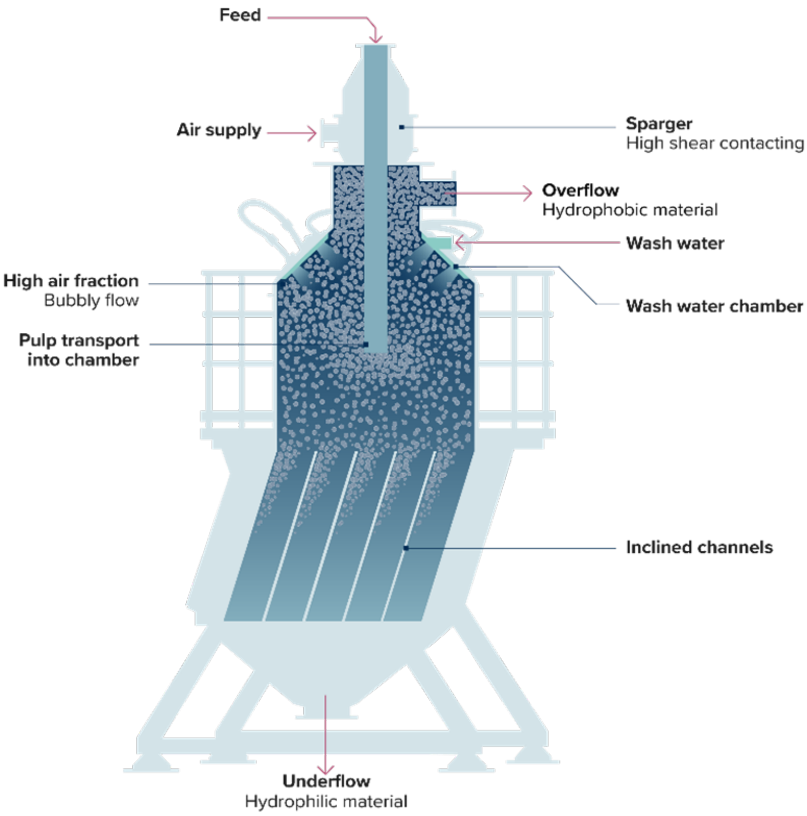


**FIG 3** – RFC schematic.

This bubbly mixture is transported into the main chamber of the machine, which allows further bubble-particle contact to occur in a fluidised bed of bubbles. Air fractions in the separation chamber are typically in excess of 50 per cent (v/v), which substantially increases the bubble surface area flux of the system. The inclined channels use a phenomenon commonly called the Boycott Effect which found that particles settle faster when on an incline (Boycott, 1920). Figure 4 shows the function of the inclined channels which results in:

- Immediate rejection of unattached gangue out of the system.
- Separation of mineral laden bubbles forced back into the flotation system.

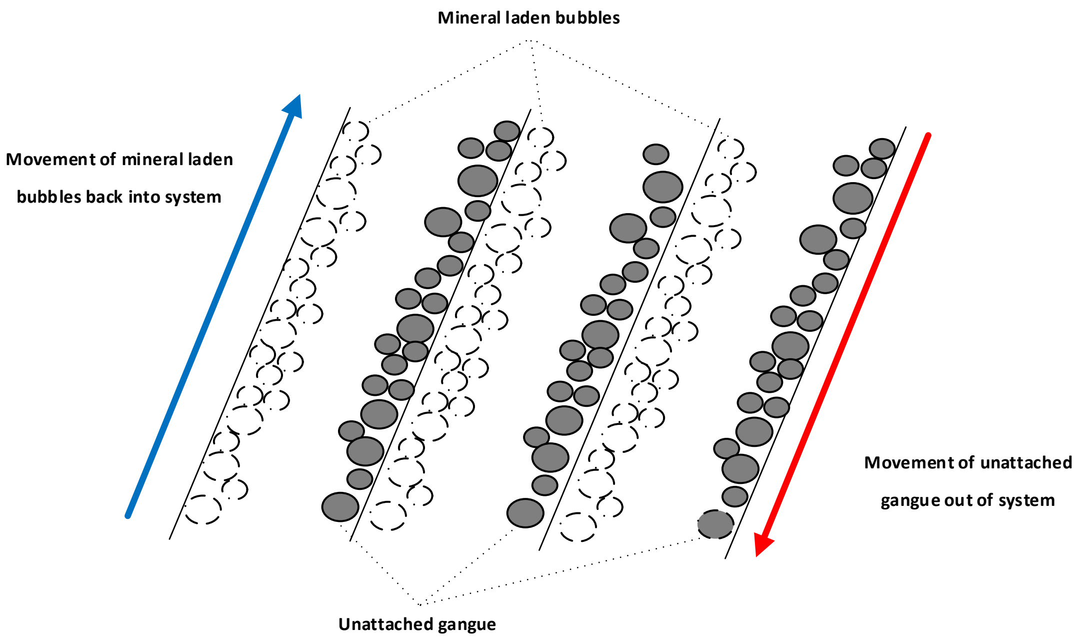


**FIG 4** – Function of the Inclined Channels.

This approach achieves segregation rates well beyond that is possible in open tank systems. This feature consequently allows for operation at much higher air fractions and bubble surface area fluxes than that is possible in traditional systems. Rapid unattached rejection reduces volumetric requirements along with the increased available bubble surface area further promotes kinetics. The increased available bubble surface area further promotes kinetics. Figure 5 shows the relationship between the achieved bubble surface area flux, bubble diameter and lamella chamber geometry.

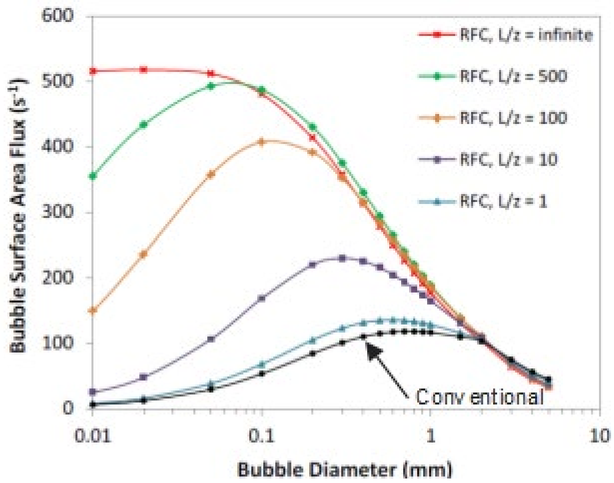


**FIG 5** – Bubble surface area flux achieved by RFC compared to conventional systems (Jiang, Dickinson and Galvin, 2014).

High fluidisation (wash water) fluxes are possible through a water distributor which encloses the free-surface of the cell. This allows for a strong positive bias flow which promotes enhanced froth washing and improved product grades. Figure 6 illustrates the operating range of the RFC when considering wash water and gas fluxes compared to conventional systems.

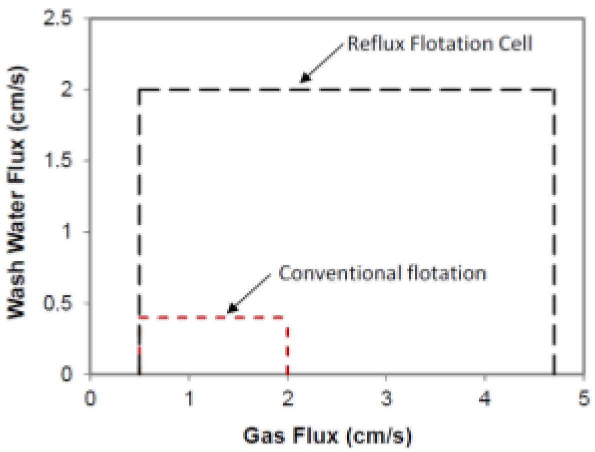


**FIG 6** – Wash and gas flux ranges (Dickinson and Galvin, 2015).

The wash system design allows for uniform distribution of wash water across the full cross-section of the vertical chamber. This design feature ensures that uniform washing is achieved. The addition of wash water or fluidisation water allows for grade control/rejection of slimes and ensures a positive bias flux to underflow in the separator to maximise separation efficiency.

The systems described above are controlled such that the bias flow (Jb) is maintained to be positive (net flow to underflow). The wash water flow is set to maintain a defined wash water flux (Jw) by controlling the wash water flow rate. Water flow rate control is achieved by utilising a flow metre in a PID control loop with a water flow control valve. Air rate/superficial gas velocity (Jg) is controlled in a similar fashion using a flow metre and control valve in a PID control loop configuration.

## RFC 100 pilot overview

The RFC 100 pilot is a skid-mounted unit that consists of two pilot units and fits into a conventional 20 ft container for ease of transport, the unit is shown in Figure 7. The 100 in the nomenclature represents the 100 mm × 100 mm chamber of the unit. It is essentially plug and play with the only requirements being: plant feed, air, clean wash water and electricity. The control system and PLC control panel are fully integrated into the unit. Both RFC units have mixing tanks that allow for up to three minutes of residence time, depending on feed flow rate, allowing for reagent addition if required. The unit can be operated in various modes including standalone, series and parallel, along with the ability to recycle the tails into the fresh feed line.


**FIG 7** – Mobile pilot plant.

The bubble-particle contact is performed by a single sintered tube sparger connected to a downcomer. The downcomer discharges to the upper fluidisation chamber, creating a froth column for enhanced washing of the froth zone. Utilisation of lamella plates in the lower chamber allows for high throughputs.

## Pilot test work overview

The piloting test work was completed in four campaigns over a period of approximately three months. Approximately 110 individual tests were completed over this time to generate the data presented in this paper. The mineralogy of this mine site is constant from day-to-day making tests comparable in performance between the campaigns. The objective of the testing was to replicate plant conditions of the first two cells in the roughing circuit along with identify the optimum condition for which the RFC operates. The test configuration is shown in Figure 8.

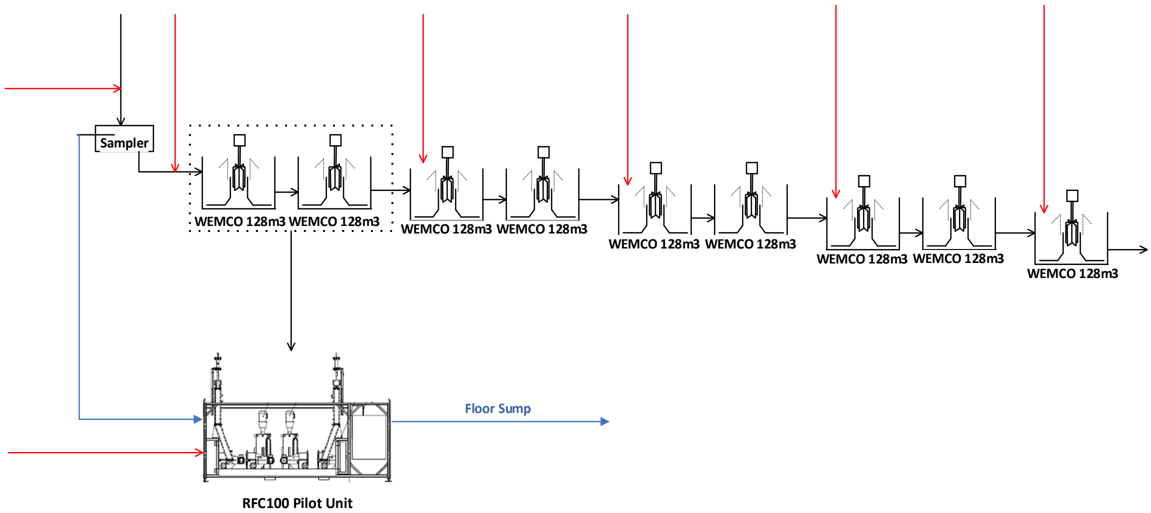


**FIG 8** – RFC100 Pilot Plant PFD.

Continuous feed was collected from the Rougher Feed spear sampler, which collects the representative sample used for metallurgical accounting. The feed was pre-conditioned with DSP009 based upon a g/tph Cu basis; throughout the test work program this was the only collector addition made, in comparison to the existing circuit with multistage Potassium Amyl Xanthate addition. The frother IF50 was added to the first RFC mixing tank by a small positive displacement pump. The existing rougher bank 1 cells have approximately 9 minutes residence time, or 4.5 minutes each. The existing cells consistently produce a concentrate grade of 28–30 per cent Cu at over 80 per cent recovery.

Due to the short residence time of the RFC (<30 sec per cell or 60 sec for the full system), sampling occurred over five-minute periods during each test. System stabilisation occurred for at least 15 minutes between tests. Laboratory kinetic flotation tests were performed to normalise any variation in mineralogy/grind size, and for scale-up purposes.

## Results

The biggest advantage of this technology is fast flotation kinetics, shown in the depiction of recovery versus residence time for all tests in Figure 9. Throughout the testing, this characteristic was exhibited regardless of the testing conditions. This included tests that were outside the expected normal operating conditions which were required to generate a model of the system. The minimum recovery observed for a single stage RFC was ~40 per cent, with a maximum of up to 80 per cent in a single stage in under 25 seconds. A two stage RFC further increased recovery to a minimum of ~70 per cent and a system maximum of 90 per cent in under 60 sec of residence time. Compared to the same flotation conditions at nine minutes residence time in conventional flotation cells, this improves flotation kinetics by up to 10 times.

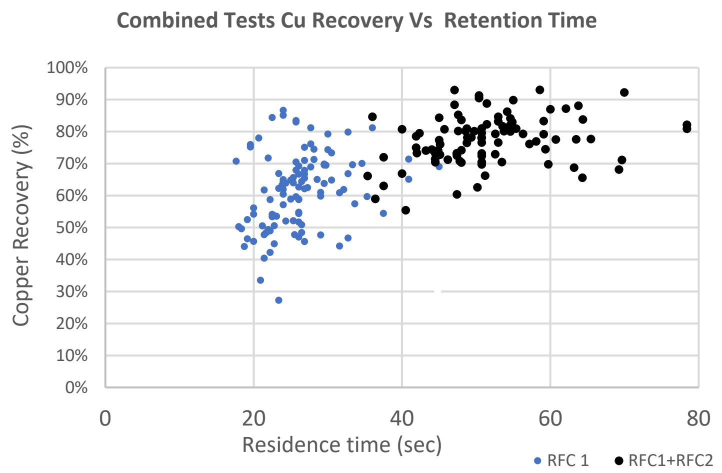


**FIG 9** – Combined tests Cu grade versus retention time.

The ability to achieve a suitable concentrate grade while also achieving fast kinetics has long been a challenge. Figure 10 shows the grade and recovery performance of all the tests with the plant performance of the first WEMCO bank represented also. It should be noted that scattering of data is primarily due to a wide range of operating conditions selected for testing for modelling purposes (ie conditions were selected outside of expected normal operating conditions). Although there is significant scatter in the data with regards to concentrate grade, it shows that under ideal conditions the plant performance can be met or exceeded for the liberation and reagent conditions of the flotation feed (ie high selectivity towards liberated chalcopyrite).

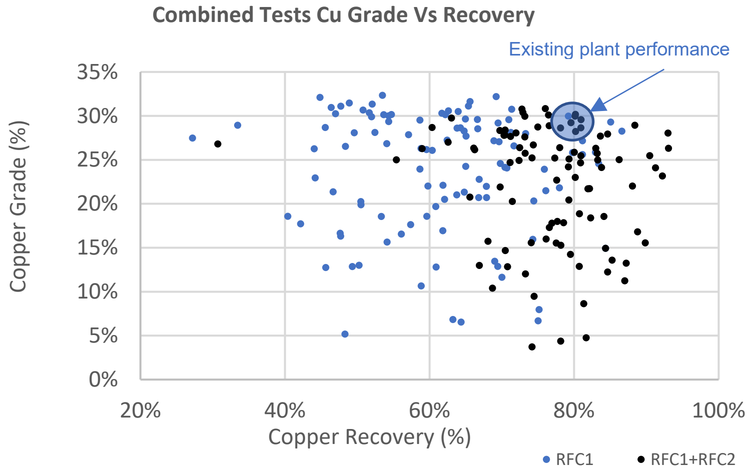


**FIG 10** – Combined tests Cu grade versus recovery.

To explore the scatter further both grade and recover has been plotted against the wash bias flux in Figures 11 and 12 respectively. The wash bias is the velocity at which fresh wash water to travelling through the bubbly column within the body of the cell; a positive bias means there is more wash water flowing through the cell than overflow. Unsurprisingly the higher the bias the higher the concentrate grade produced in the system, as entrained particles have a higher probability to be rejected. When considering recovery, it is far less sensitive to the wash bias than that of concentrate grade, meaning recovery can be maintained at higher washing rates if required.

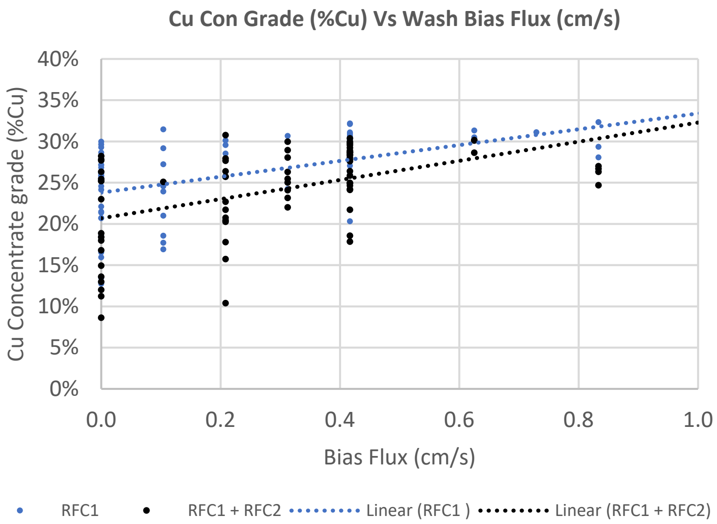


**FIG 11** – Copper concentrate grade versus wash bias flux.

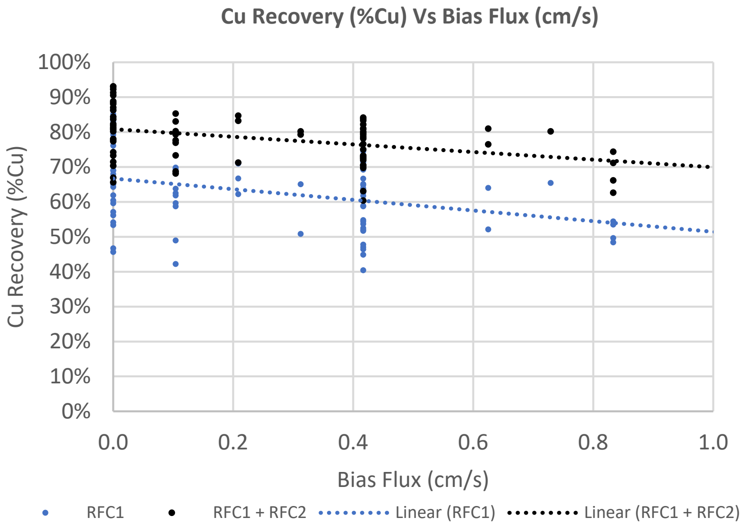


**FIG 12** – Copper recovery versus wash bias flux.

# FULL SCALE PLANT DESIGN IMPLICATIONS AND MODELLING

To illustrate the potential benefits of implementing the RFC into a full-scale circuit, a surface response statistical method was used to generate performance models. All data collected during the test campaign along with operating conditions were entered into the software which allowed generation of statistically significant models for single (rougher or scavenger) and two-stage (rougher-scavenger) flotation using RFC technology. Later, the models were used to identify optimum operating conditions for the RFC units, to simulate full scale circuit and compare with conventional flotation technology.

The RFC models (rougher and scavenger) were developed utilising a commercially available statistical software package which allows for investigation of vital factors and components to characterise interactions between system variables. Operating variables including feed rate, air rate, wash water rate and bias flux were adjusted to determine optimum performance levels, these variables were maintained to values within the original test matrix. Optimisation algorithms in the software were utilised to identify operating conditions leading to best performance at highest desirability.

The conventional flotation system was modelled utilising data from a set of 14 standard benchtop kinetics tests. These kinetics tests were performed over the period of the campaign utilising the same feed material as that presented to the RFC pilot equipment. Individual pilot test runs could be matched to corresponding benchtop tests. And an averaged kinetics response was generated to predict conventional flotation response. The recovery model utilised for this model is shown by Equation 1.

$$Rec = m_f\left[1 - e^{(-k_f t)}\right] + m_s\left[1 - e^{(-k_s t)}\right] \qquad (1)$$

Where

$m_f$ and $k_f$ = mass per cent and rate constant of fast floating species

$m_s$ and $k_s$ = mass per cent and rate constant of slow floating species

t = retention time

A grade versus recovery relationship was developed utilising statistical curve fitting software to predict product grade based on the recovery from the kinetics model above.

Models were reviewed to ensure validity based on the experimental data generated. Figures 13 and 14 show a summary of the averaged laboratory kinetics data, the RFC experimental data showing combined rougher scavenger performance as well as modelled RFC and full-scale conventional circuit performance. Circuit simulations shown utilise an averaged feed grade of 0.9 per cent copper, which is reflective of the average feed grade for the 14 kinetics tests performed. RFC circuit simulations show operating conditions to produce a set of data optimised to produce maximum grade and recovery values for various operational parameter values. Conventional simulation reflects plant conditions based on existing flotation cell configuration. It should be noted that the conventional circuit requires additional cleaning to meet product specification of copper grades in excess of 28 per cent copper.

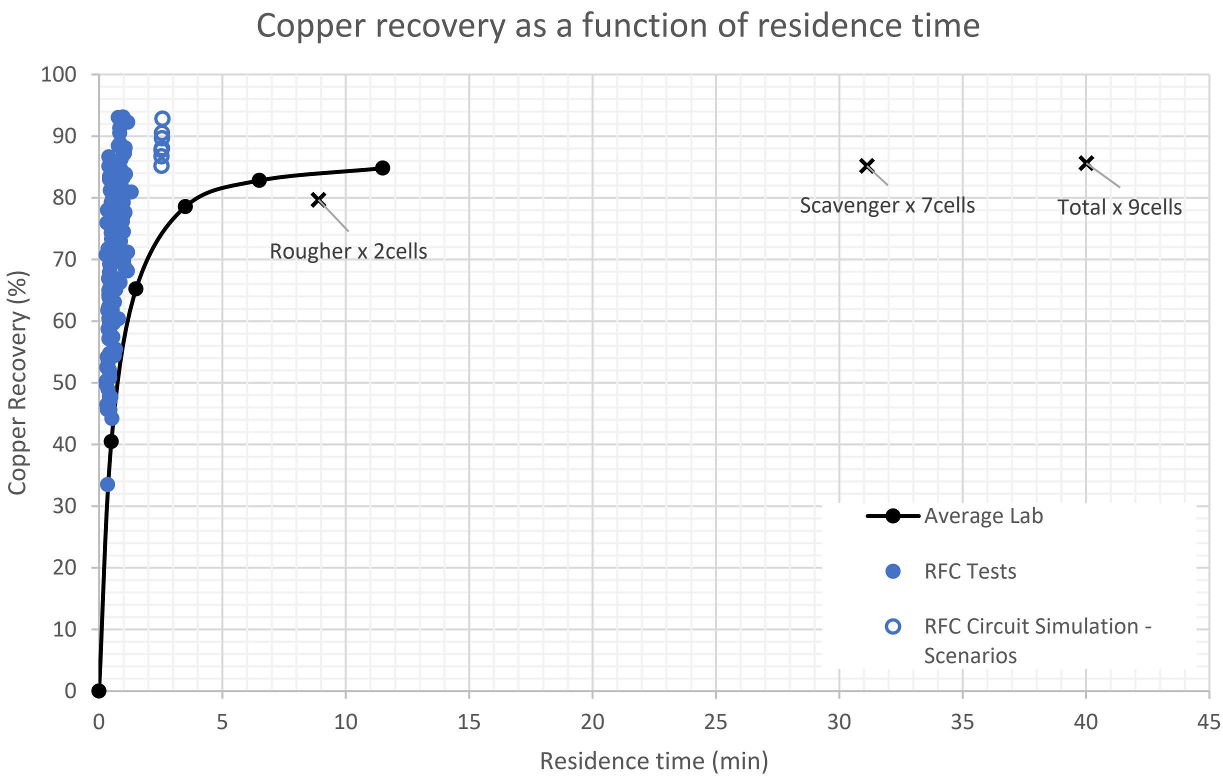


**FIG 13** – Copper recovery as a function of residence time.

Figure 13 shows that copper recovery equal to or greater than bench and production scale flotation systems are achieved in less than 3 minutes where industrial systems require in excess of 30 minutes residence time. This finding is not unique to this test campaign and study with similar results reported (Cole, 2020). It should be noted that the residence time achieved by the RFC circuit simulation is larger than the pilot testing due to the fact that the industrial system geometry is of such a nature that to maintain wash, feed and bias fluxes the effective circuit residence time is larger than pilot.

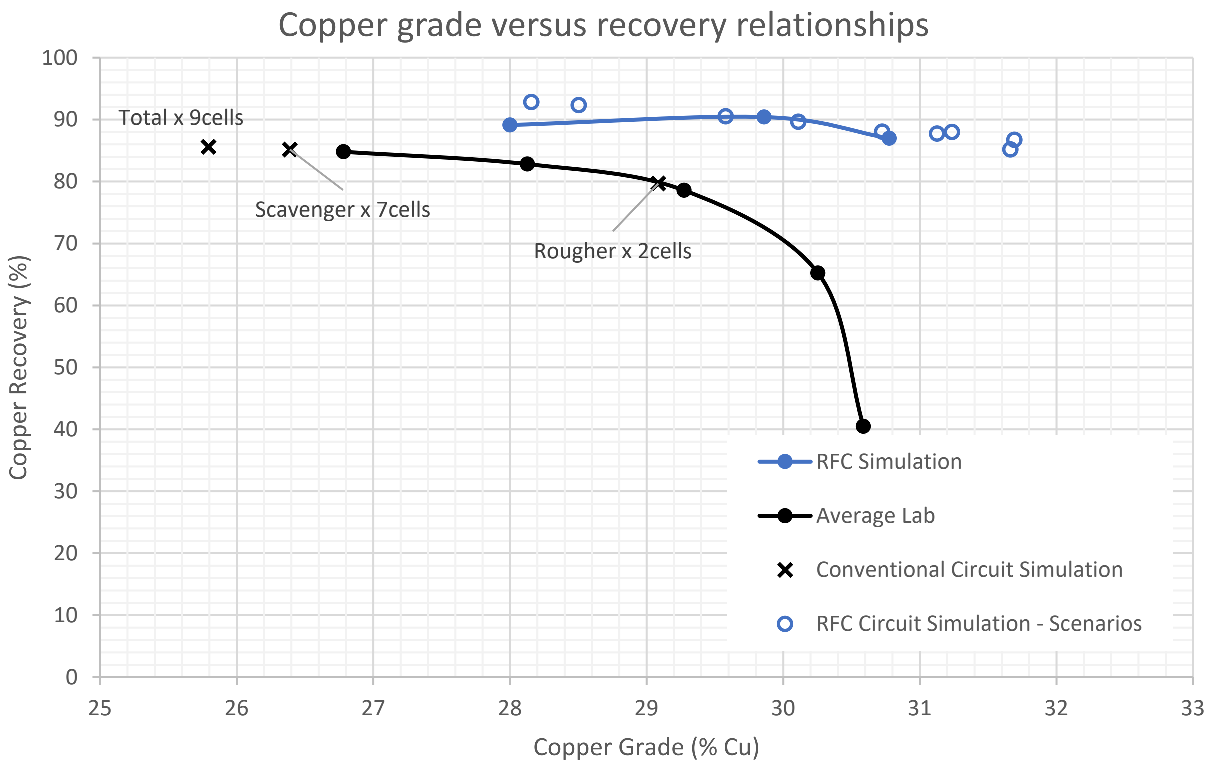


**FIG 14** – Copper grade versus recovery relationships.

In addition to achieving superior recovery the RFC circuit shows improved product quality when compared to rougher flotation. In this case, where the required product specification of 28 per cent copper is required, the RFC circuit will not require additional cleaner flotation.

When considering an alternative RFC circuit compared to the existing conventional circuit, the RFC circuit offers the following advantages:

- An approximate 5–8 per cent recovery improvement could be realised to produce on specification concentrate in excess of 28 per cent copper.
- The need to perform additional cleaning of the rougher flotation product is not required, negating the need for additional cleaning flotation capital equipment and associated flotation volume.
- Flotation volume is reduced up to ten-fold when considering the conventional rougher system only. This translates into reduced plant footprint and associated capital and installation cost savings.
- Reflux flotation machines do not require direct power input with power consumption limited to transfer pumping of slurry and wash water supply only. The comparative power value in Table 1 accounts for these in the power calculation.

Table 1 shows a summary of key areas where savings and performance improvements can be made when comparing the RFC and conventional rougher flotation bank.

**TABLE 1**
Comparison of key circuit variances.

| | Existing circuit | RFC circuit |
|---|---|---|
| **Flotation equipment** | 2 × WEMCO® 130 cells | 4 × RFC-2350 |
| **Configuration** | 2 × Rougher | 1 × Rougher, 1 × Scavenger |
| **Rows** | One | Two |
| **Power** | 100% | 60% |
| **Retention time** | 9 mins | 2.5 mins |
| **Flotation volume** | 100% | 30% |
| **Copper recovery** | 83% | 90% |
| **Copper con grade** | 29% | 30–31% |

## Further work

Although the pilot campaign showed that a significant reduction in residence time, footprint and power consumption is possible with RFC technology it was only compared to benchtop kinetic testing of the first two cells in the rougher bank. This is due to site employing a two-stage collector addition strategy, highly selective DSP009 in bank 1 and then unselective PAX addition down the banks starting at bank 2. This is performed at natural pH, meaning that unselective sulphide flotation is performed to recover poorly liberated chalcopyrite NSG composites along with pyrite increasing recovery of copper and gold. This piloting study did not study the scavenging stage with PAX addition, is so an alternative flotation configuration may have been recommended to meet full plant performance. There are other opportunity's around a conventional flotation circuit particularly around cleaning. It would be expected that with the high kinetics and superior washing ability of the RFC that this application would be best suited. It is likely a single RFC at the start of a cleaning circuit would be able to achieve concentrate grade at very high recoveries alleviating load on an existing circuit.

# CONCLUSIONS

The testing campaign produced a large volume of data over a range of operating conditions to enable generation of a statistically significant model of the system to allowing prediction of optimum performance.

It was shown that the system kinetics were between five to ten times faster than that of the comparable conventional equipment and that the metallurgical performance at optimum conditions exceeded traditional laboratory performance while remaining within experimental operating ranges.

It is expected that implementing the RFC in a rougher scavenger arrangement and operating within the optimum conditions it is possible to exceed operational recoveries by up 5–8 per cent while maintaining product quality, in turn eliminating the need for additional cleaning.

Further optimisation of the model is possible, however operating values outside that tested in this work would need to be utilised. Further testing is planned to explore these operating ranges.

Improved grade and high recoveries are possible due to the improved washing system and operating at high gas fluxes. This result is reflective of work completed by others.

# ACKNOWLEDGEMENTS

The first author would like to formally thank Annika de Hesse and Glencore Ernest Henry Mining for the continued support over the project. Without industry support on an industrial scale for testing development in minerals technology would not be possible.

# REFERENCES

Boycott, A E, 1920. Sedimentation of blood corpuscles. Nature 104, 532.

Camomile, A, Weber, A, Lelinski, D, Foreman, D, Traczyk, F, Baker, T, 2013. Development of the largest flotation machine: 600 series Supercell™ from FLSmidth, in Proceedings of 10th International Minerals Processing Conference, pp 233–233 (Procemin 2013).

Cole, M J, Dickinson, J E, Galvin, K P, 2020. Recovery and cleaning of fine hydrophobic particles using the Reflux™ Flotation Cell. Separation and Purification Technology 240, 2020

Dickinson, J E, Cole, M J, Galvin, KP, 2019. Chalcopyrite flotation using the Reflux™ Flotation Cell. Separation and Purification Technology 240, 2020.

Dickinson, J E, Cole, M J, Galvin, KP, 2013. Fluidized bed desliming in fine particle flotation, Chemical Engineering Science 108, 2014 pp283–298.

Dickinson, J E, Cole, M J, Galvin, KP, 2013b. Fluidized bed desliming in fine particle flotation – Part II: Flotation of a model feed, Chemical Engineering Science 108, 2014 pp299–309.

Galvin, KP, Harvey, N G, Dickinson, J E, 2014. Fluidized bed desliming in fine particle flotation – Part III: Flotation of difficult to clean coal. Minerals Engineering 66–68, 94–101.

Jiang, K, Dickinson, J E, Galvin, K P, 2014. Maximizing bubble segregation at high liquid fluxes, Advanced Powder Technology 25, pp 1205–1211.

Jiang, K, Dickinson, J E, Galvin, K P, 2015. Two-stage fast flotation of coal tailings using reflux flotation, Minerals Engineering 98, 2016 pp151–160.

Muerstenau, M C, Jameson, G J, Yoon, G J, 2007. Froth Flotation: A century of Innovation J, pp 65–91 (Society for Mining, Metallurgy, and Exploration).

# Nui Phao Mine – a study on the effect of flotation mechanism wear on metallurgical performance

*S Morgan[1], B Weekes[2], A Jakowetz[3], S Arnold[4], S Taylor[5], S Keokhounsy[6], J Lakanen[7] and J Tiitinen[8]*

1. Senior Technical Manager Flotation and Automation, Outotec Pty Ltd, Sydney NSW 2086. Email: sherwin.morgan@outotec.com
2. Processing Manager, Nui Phao Mining, Dai Tu Dist, Thai Nguyen, Viet Nam. Email: brenden.weekes@mr.masangroup.com
3. Metallurgy Superintendent, Nui Phao Mining, Dai Tu Dist, Thai Nguyen, Viet Nam. Email: anton.jakowetz@mr.masangroup.com
4. Senior Metallurgist, Nui Phao Mining, Dai Tu Dist, Thai Nguyen, Viet Nam. Email: stuart.arnold@mr.masangroup.com
5. Metallurgist/Trainer, Nui Phao Mining, Dai Tu Dist, Thai Nguyen, Viet Nam. Email: stephen.taylor@mr.masangroup.com
6. Metallurgist/Trainer, Nui Phao Mining, Dai Tu Dist, Thai Nguyen, Viet Nam. Email: sonethavy.keokhounsy@mr.masangroup.com
7. Service Product Manager, Outotec Oyj, 02230 Espoo, Finland. Email: jukka.lakanen@outotec.com
8. Product Engineer Flotation, Outotec Oyj, 02230 Espoo, Finland. Email: juha.tiitinen@outotec.com

## ABSTRACT

In most mining operations, achieving and/or exceeding plant production targets is an important measure of success. Equipment availability and efficiency greatly contributes to these targets and the best performance is obtained through routine preventative maintenance. For example, in comminution circuits, it is accepted that the SAG and Ball mill liners need to be replaced regularly to achieve the best grinding performance. However, for downstream equipment such as flotation cells, the effect of worn internal components on circuit performance is less understood. This can lead to flotation equipment being operated for longer periods 'as is' to reduce shutdown periods and spare part consumption. Thus, Outotec has partnered with Nui Phao Mining Company (NPMC) to study the effect of flotation mechanism wear (ie rotor and stator) on metallurgical performance. In addition, Outotec has conducted computational fluid dynamics (CFD) simulations to understand the effects of flotation mechanism wear on pumping and mixing within the flotation cell.

This paper will discuss the plant data collected at NPMC before and after the flotation mechanisms were replaced in the Fluorite circuit. Factors investigated were power consumption, float cell striation and Fluorite recovery and grade relationship. The findings of the CFD modelling simulations were also used to interpret the plant results.

## INTRODUCTION

In most mining operations, achieving and/or exceeding plant production targets is an important measure of success. Equipment availability and efficiency greatly contributes to these targets and the best performance is obtained through routine preventative maintenance. For example, in comminution circuits, it is accepted that the SAG and Ball mill liners need to be replaced regularly to achieve the best grinding performance. However, for downstream equipment such as flotation cells, the effect of worn internal components on circuit performance is less understood. This can lead to flotation equipment being operated for longer periods 'as is' to reduce shutdown periods and spare part consumption. Murphy *et al* (2014) explain this further, where the practice of running equipment to failure for short-term benefits, ignores the lost production associated with using worn flotation equipment.

The purpose of flotation equipment is to physically separate valuable minerals from gangue for further processing. Thus, all flotation equipment must provide certain conditions for mineral separation. These have been summarised by many authors and Murphy (2013):

- Ensure particles are kept in suspension and minimise sanding.
- Create conditions for bubble-particle collision and attachment.
- Provide good air dispersion into the slurry.
- Minimise short-circuiting and ensure all particles have an opportunity for recovery.
- Create two slurry regions, an intense mixing region and a quiescent region for bubble-particle aggregates to rise.
- Promote froth recovery.

The main type of flotation equipment used in industry is mechanical cells, where the slurry is agitated by a rotating rotor. Harris (1975) highlighted that the main difference between flotation equipment suppliers is in the design of the rotor. The rotor together with the stator form the flotation mechanism and create the intense mixing region that is responsible for pulp circulation, particle suspension and aeration. The flotation mechanism is also the internal component that wears most significantly and requires routine maintenance and replacement.

The flotation theory gives a general reasoning that on how flotation mechanism wear might affect metallurgical performance. However, it does not describe the phenomena in any detail. Murphy (2013) states that mechanism wear changes the geometric shape and clearances between rotor and stator components. This will result in a lower power draw and may coincide with a decrease in metallurgical performance.

To further understand the phenomena, Outotec decided to prepare a computational fluid dynamics (CFD) simulation with new and worn conditions of the FloatForce® mechanism. Coleman and Rinne, (2011) describe the development of the FloatForce® mechanism explain its benefits over previous Outotec designs. The FloatForce® mechanism components are described in Figure 1.

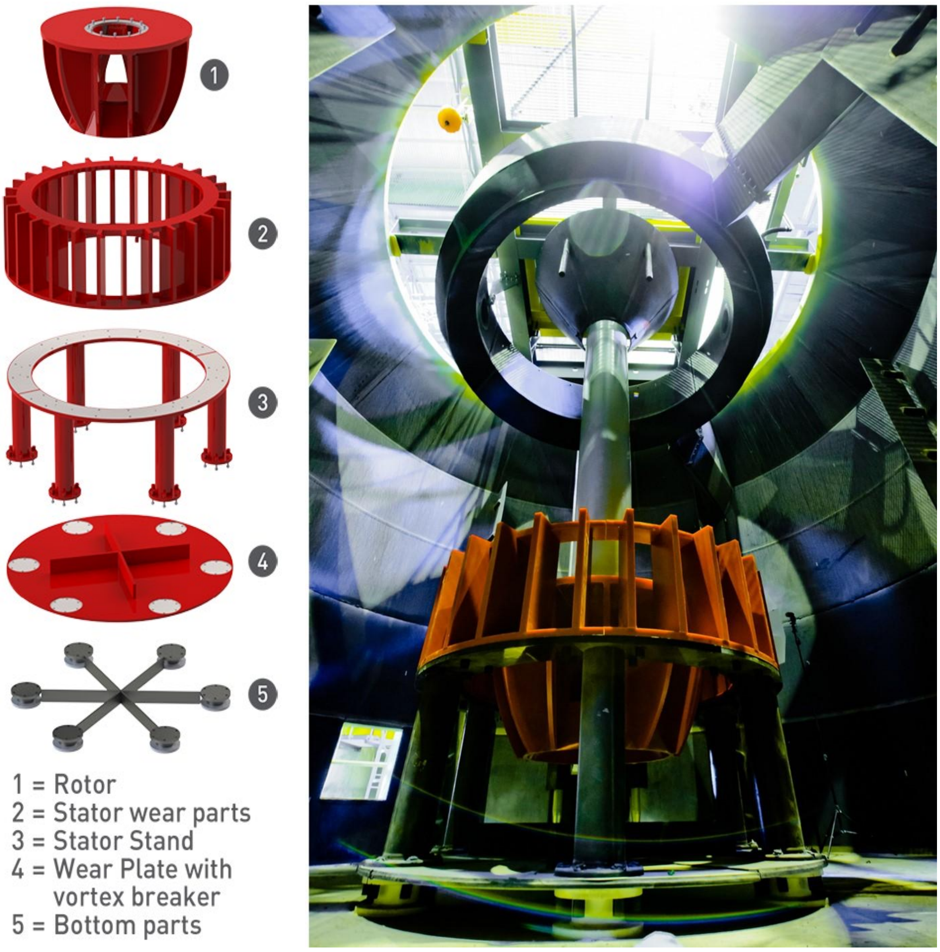


**FIG 1** – FloatForce® flotation mechanism components.

## CFD ANALYSIS FOR THE FLOATFORCE® MECHANISM DESIGN

The following section discusses the CFD analysis completed by Outotec on the FloatForce® mechanism design. The conditions selected for the investigation were:

- Cell volume – 333 $m^3$.
- Flotation mixing mechanism – FloatForce® rotor and stator.
    - FloatForce® rotor size: 1750 mm with 30 per cent bottom clearance.
    - FloatForce® rotor tip speed: 6.4 m/s (70 rev/min).
- Cell shape – Standard Tank Cell (cylindrical), with bottom slurry inlet and outlet.

The CFD analysis was for water and gas phases, no solid particles were modelled. The particles mentioned in the paper were 'simulated particles' with density equal to water density. This means that the particle path-lines are actually water path-lines.

The particle time part-lines are presented in Figure 2. The analysis indicated that for the 'new rotor and stator' condition, the flow path-lines entering the cell are mostly directed towards the flotation mechanism. Thus, there is a greater likelihood of bubble particle collision and attachment. Thus, the mixing conditions are optimum for target metallurgical performance.

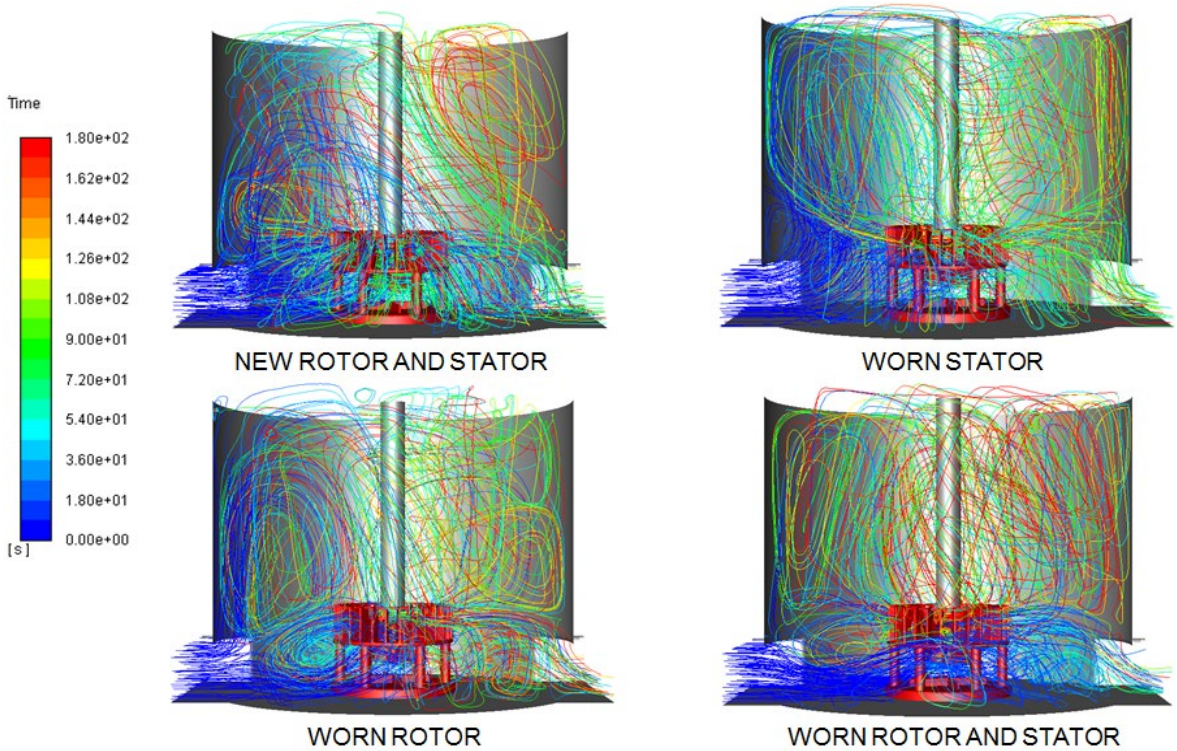


**FIG 2** – Particle time path-lines (side view).

When the stator wears, the analysis indicated that for the 'worn stator' condition, pumping is enhanced, and flows become stronger. This can be observed from path-lines being more straight up on the sides and rotating downwards around the shaft. The inlet flow is partially pushed up by the stream leaving the impeller. Thus, the mixing conditions are still for target metallurgical performance.

When rotor is worn, the analysis indicated that for the 'worn rotor' condition, the streams from the impeller become smoother when compared to the 'new rotor stator' condition. This suggests that there would be less turbulence and mixing in this region. Thus, the mixing conditions are not ideal for target metallurgical performance.

When both the rotor and stator are worn, the analysis indicated that for the 'worn rotor and stator' condition, a short-circuited flow can be observed at the bottom of the cell and under the impeller. A short-circuited flow is when the feed slurry enters and leaves the cell without circulating through the impeller. Thus, the mixing conditions are not recommended for target metallurgical performance.

In flotation cells, over 90 per cent of the total power input is consumed by the flotation mechanism. Thus, the CFD analysis also investigated the effect of flotation mechanism wear on power draw. The power draw equation is explained in Figure 3. Note, more efficient flotation mechanisms allow for intense mixing at lower rotor tip speeds (ie lower shaft rev/min or smaller rotor diameters) to promote longer mechanism wear life.

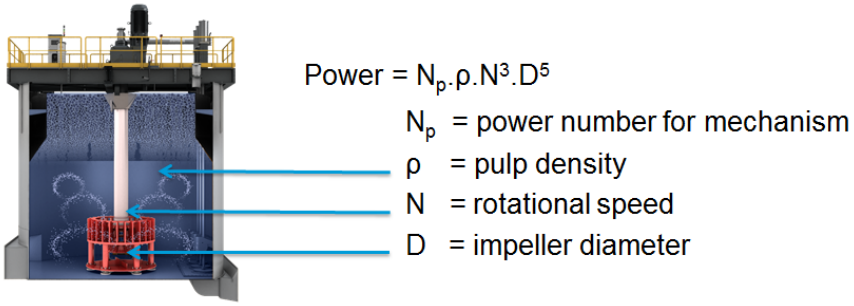


**FIG 3** – Power draw equation.

Power draw versus flotation mechanism condition is presented in Figure 4. The analysis indicated a power draw value of 136 kW for the 'new rotor and stator' condition, 133 kW for the 'worn stator' condition, 125 kW for the 'worn rotor' condition and 115 kW for the 'worn rotor and stator' condition. Thus, the analysis suggested that flotation mechanism wear resulted in a decline in power draw.

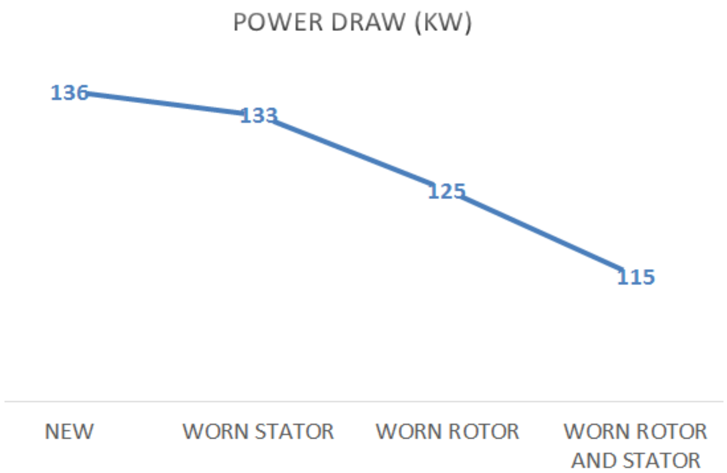


**FIG 4** – Power draw versus flotation mechanism condition.

The analysis suggested that rotor wear decreases the power number of the mechanism ie the rotor loses its capability to pump. Nelson and Lelinski (2000) describe the power number Np (a dimensionless number) relating resistance to inertial force which characterises the pulp/impeller interaction.

The analysis suggested that a stator wear results in an increase in the power number of the mechanism, letting the rotor pump more but there is less intense mixing. In both cases, there is less energy available for air dispersion and bubble-particle attachment. Key drivers for flotation performance.

It is also important to note that localised wear in the rotor or stator components can cause an imbalance between pumping and mixing in the cell. When both components wear simultaneously, the balance is less affected. Thus, it is preferred if both rotor and stator are replaced together.

In summary, the CFD analysis outcomes were:

- Wear on flotation mechanism components can have a negative effect on flotation performance.

- The main effects predicted are lower power draw and decreased capacity to disperse air.
- Impact of wear on flotation performance is most likely gradual and may occur before the mechanism wear approaches its structural limits.
- Periodical mechanism repair or replacement should be considered in order to maintain flotation performance.

Although the CFD analysis provided evidence of a relationship between flotation mechanism wear and flotation performance, it was felt that it may be difficult to observe in a full-scale flotation plant due to ore feed and process variations.

To investigate this further, Outotec partnered with Nui Phao Mining Company (NPMC) to study the effect of flotation mechanism component wear (ie rotor and stator) on metallurgical performance.

## NUI PHAO MINING COMPANY (NPMC)

Masan Resources is one of the largest private sector natural resources companies in Vietnam. It acquired a controlling interest in NPMC in 2010. Nui Phao Mine is a polymetallic project located in Northern Vietnam. The mine achieved commercial production in the first quarter of 2014, with steady state operation achieved in the end of 2014.

NPMC produces four products, tungsten, acid-grade fluorspar, bismuth and copper. It is now the largest producer of tungsten outside China, and amongst the largest producers of acid-grade fluorspar and bismuth in the world.

NPMC and Outotec have been in partnership since 2015 and Morgan *et al*, (2017) describes the circuit modifications completed on-site. For the flotation mechanism wear investigation, the Fluorite rougher circuit was selected for investigation. The Fluorite rougher circuit comprises of five 50 $m^3$ tank cells (FC-135 to FC-139) and was due for routine maintenance in the October 2019 plant shutdown. It was decided to conduct three surveys to investigate the float mechanism wear during this period. Survey 1 was conducted before the plant shutdown, whilst Survey 2 and 3 were completed after the plant shutdown, refer to Table 1.

**TABLE 1**

Fluorite circuit survey conditions.

| Survey | Date | Flotation mechanism condition | | | | |
|---|---|---|---|---|---|---|
| | | FC-135 | FC-136 | FC-137 | FC-138 | FC-139 |
| 1 | 14/09/2019 | FloatForce® 12-months | FloatForce ® 6-months | Competitor 12-months | Competitor 12-months | Competitor 12-months |
| | 02/10/2019 | Plant Shutdown | | | | |
| 2 | 12/10/2019 | FloatForce® New | Not changed | FloatForce® New | Competitor new | Competitor new |
| 3 | 30/10/2019 | FloatForce® New | Not changed | FloatForce® New | Competitor new | Competitor new |

Note, FC-135 had an old FloatForce ® mechanism replaced with a new FloatForce® mechanism. FC-136 was not changed and the same FloatForce ® mechanism was reused. The remaining three cells had competitor mechanisms. FC-137 was replaced with a FloatForce® mechanism and FC-138/139 were replaced with competitor mechanisms. Figures 5 to 9 present pictures of the float mechanisms during the plant shutdown.

**FIG 5** – FC-135 FloatForce® mechanism (after 12-months operation) – REPLACED with new FloatForce ® mechanism.

**FIG 6** – FC-136 FloatForce® mechanism (after 6-months operation) – UNCHANGED.

**FIG 7** – FC-137 Competitor mechanism (after 12-months operation) – REPLACED with new FloatForce® mechanism.

**FIG 8** – FC-138 Competitor mechanism (after 12-months operation) – REPLACED with new Competitor mechanism.

**FIG 9** – FC-139 Competitor mechanism (after 12-months operation) – REPLACED with new Competitor mechanism.

The process conditions for the Fluorite rougher feed stream are detailed in Table 2. The plant data indicates a similar dry solids feedrate, grind size and feed density for all three surveys. There was some variation in the ore feed grade. Survey 2 indicated the highest $CaF^2$ assay (17.1 per cent), followed by Survey 1 (15.5 per cent) and Survey 3 (14.4 per cent). However, the largest difference between the surveys was observed in the reagent addition.

**TABLE 2**

Fluorite rougher feed conditions.

| Survey | Feed rate (dry t/h) | Grind P80 (µm) | Feed density (% solids w/w) | Collector (g/t) | $CaF^2$ (%) | S (%) | $P^2O^5$ (%) | Fe (%) | $SiO^2$ (%) | $WO^3$ (%) |
|---|---|---|---|---|---|---|---|---|---|---|
| 1 | 291 | 190 | 54% | 467 | 15.47 | 1.36 | 0.06 | 13.00 | 43.03 | 0.13 |
| 2 | 301 | 195 | 54% | 456 | 17.06 | 1.31 | 0.09 | 12.85 | 40.04 | 0.16 |
| 3 | 303 | 191 | 55% | 645 | 14.42 | 0.90 | 0.06 | 12.13 | 45.38 | 0.14 |

When compared to Survey 1, the $CaF^2$ collector addition was 3 per cent lower in Survey 2 but 38 per cent higher in Survey 3. Thus, Survey 1 and Survey 2 had similar reagent conditions and are better suited for comparative purposes.

# RESULTS AND DISCUSSION

## Fluorite circuit metallurgical performance

For all three surveys, samples were taken down-the-bank of the Fluorite rougher circuit. These were analysed for $CaF^2$, and a summary of the results is presented in Table 3. For Survey 1, the results indicate a total cumulative $CaF^2$ recovery of 72 per cent at a grade of 43 per cent (per cent $CaF^2$). For Survey 2, both the $CaF^2$ recovery (77 per cent) and grade (63 per cent $CaF^2$) are higher. The same trend is observed for Survey 3. Both the $CaF^2$ recovery (84 per cent) and grade (53 per cent $CaF^2$) are higher, when compared to Survey 1.

As noted in Table 2, Survey 1 and Survey 2 have similar process feed conditions and are better suited for comparative analysis. Thus, the results suggest that the replacement of the worn flotation mechanisms improved the $CaF^2$ recovery by 5 per cent and grade by 20 per cent. In Survey 3, the results suggest that further improvements in metallurgical performance are possible with reagent optimisation.

The down-the-bank results indicate that in the first float cell (FC-135) the results are similar for all three surveys. However, in the second float cell (FC-136) there is a significant improvement in the metallurgical performance. In FC-136, the $CaF^2$ recovery is 5 per cent higher in Survey 2 and 10 per cent higher in Survey 3, when compared to Survey 1. The $CaF^2$ recovery in the remaining three cells FC-137,138 and 139 are consistent for all three surveys (~10 per cent).

**TABLE 3**

Fluorite circuit $CaF^2$ metallurgical results.

| | Survey 1 | | | Survey 2 | | | Survey 3 | | |
|---|---|---|---|---|---|---|---|---|---|
| | Cumulative results | | | Cumulative results | | | Cumulative results | | |
| | Mass pull | $CaF^2$ grade | $CaF^2$ recovery | Mass pull | $CaF^2$ grade | $CaF^2$ recovery | Mass pull | $CaF^2$ grade | $CaF^2$ recovery |
| FC-135 | 11.9% | 64.96 | 50% | 11.2% | 69.76 | 46% | 12.2% | 59.61 | 50% |
| FC-136 | 16.7% | 58.98 | 62% | 17.5% | 66.74 | 67% | 18.6% | 57.71 | 72% |
| FC-137 | 21.8% | 50.97 | 70% | 19.9% | 65.44 | 74% | 21.7% | 55.85 | 80% |
| FC-138 | 23.5% | 48.31 | 71% | 20.8% | 64.58 | 76% | 23.1% | 54.81 | 83% |
| FC-139 | 26.6% | 43.43 | 72% | 21.6% | 63.36 | 77% | 24.4% | 53.05 | 84% |

It is hypothesised that the new FloatForce® mechanism installed in FC-135 has produced more floatable minerals, however these were being recovered in the next cell FC-136. This can occur for two reasons:

- In the first cell (FC-135), the launder and crowding design does not have sufficient capacity to recover the additional floatable minerals.
- In the first cell (FC-135), the operational team has maintained the mass pull to stabilise the rest of the rougher circuit.

In the Fluorite rougher circuit, there is no operational strategy to control mass pull at the head of the circuit. Thus, it was decided to review the launder and crowder arrangement. Of interest were the froth transport parameters, froth carry rate (FCR) and lip loading (LL). Coleman and Wong (2018) define the FCR as the amount of concentrate (tonne) transported by the froth over a specific surface area ($m^2$) in a given time frame (hours), providing units of $t/m^2h$. They also define LL as the mass of solids passing over the launder lip per hour per unit length and is expressed in units of t/m/h.

To determine these froth parameters, the dimensions of the Fluorite rougher cells were measured. The results indicated as a froth surface area and lip length of 6.96 $m^2$ and 11.47 m respectively (refer to Figure 10). The concentrate mass recovery (tph) down the bank was also measured and the calculated FCR and LL for all three surveys are presented in Table 4.

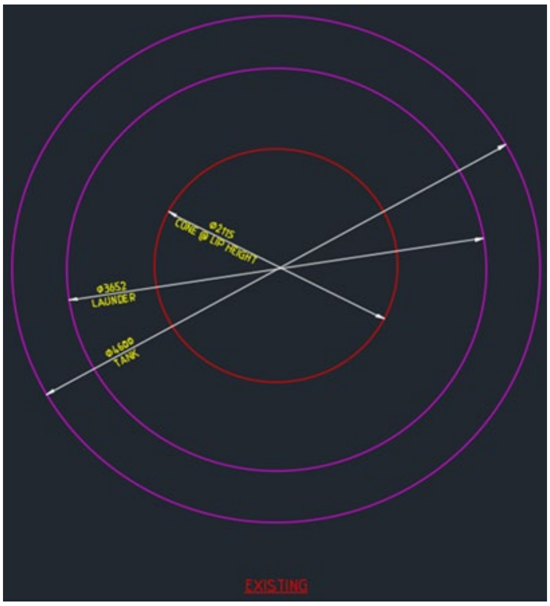


**FIG 10** – FC-135 Launder and crowder arrangement.

**TABLE 4**

Fluorite rougher circuit froth transport parameters.

| | Survey 1 | | | Survey 2 | | | Survey 3 | | |
|---|---|---|---|---|---|---|---|---|---|
| | Conc (tph) | FCR ($t/m^2/h$) | LL (t/m/h) | Conc (tph) | FCR ($t/m^2/h$) | LL (t/m/h) | Conc (tph) | FCR ($t/m^2/h$) | LL (t/m/h) |
| FC-135 | 34.50 | 4.96 | 3.02 | 33.60 | 4.83 | 2.94 | 36.97 | 5.31 | 3.23 |
| FC-136 | 12.27 | 1.76 | 1.07 | 16.93 | 2.43 | 1.48 | 17.05 | 2.45 | 1.49 |
| FC-137 | 12.61 | 1.81 | 1.10 | 5.97 | 0.86 | 0.52 | 7.79 | 1.12 | 0.68 |
| FC-138 | 3.77 | 0.54 | 0.33 | 2.30 | 0.33 | 0.20 | 3.95 | 0.57 | 0.35 |
| FC-139 | 7.05 | 1.01 | 0.62 | 1.77 | 0.25 | 0.15 | 3.68 | 0.53 | 0.32 |

Murphy and Heath (2013) present the FCR rules-of-thumb in Table 5 and indicate that the LL rule-of-thumb value is less than 1.5 t/m/h.

**TABLE 5**

Typical average froth carry rate ranges for banks of cells.

| Flotation duty | Rougher (ave) | Scavenger (ave) | Cleaner (ave) |
|---|---|---|---|
| Froth carry rate ($t/m^2/h$) | 0.8–1.5 | 0.3–0.8 | 1.0–2.0 |

The results indicate that majority of the total concentrate mass is recovered in the first cell, decreasing down the bank. For FC-135, the results indicate that the average FCR value (~5.0 $t/m^2/h$) is 350 per cent higher than the recommended value, whilst the average LL value (~2.0 t/m/h) is 200 per cent higher than recommended value. Thus, for FC-135 the results suggest that the launder and crowder arrangement is not ideal for the current duty and would struggle to accommodate even more concentrate. Thus, we can conclude that it is likely that limitations in the launder and crowder design have prevented metallurgical improvements in cell FC-135.

In summary, the survey results suggest that replacing the flotation mechanism in four of the rougher cells (ie FC-135, 137, 138 and 139) improved the grade/recovery relationship (refer to Figure 11). The major improvement was observed at the head of the rougher circuit in the first two cells (FC-135 and FC-136). The daily Fluorite recovery from August to November 2019 is presented in Figure 12. The results indicate a significant increase in Fluorite recovery after the plant shutdown and replacement of the flotation mechanism. Thus, the daily plant results confirm the findings of the survey results.

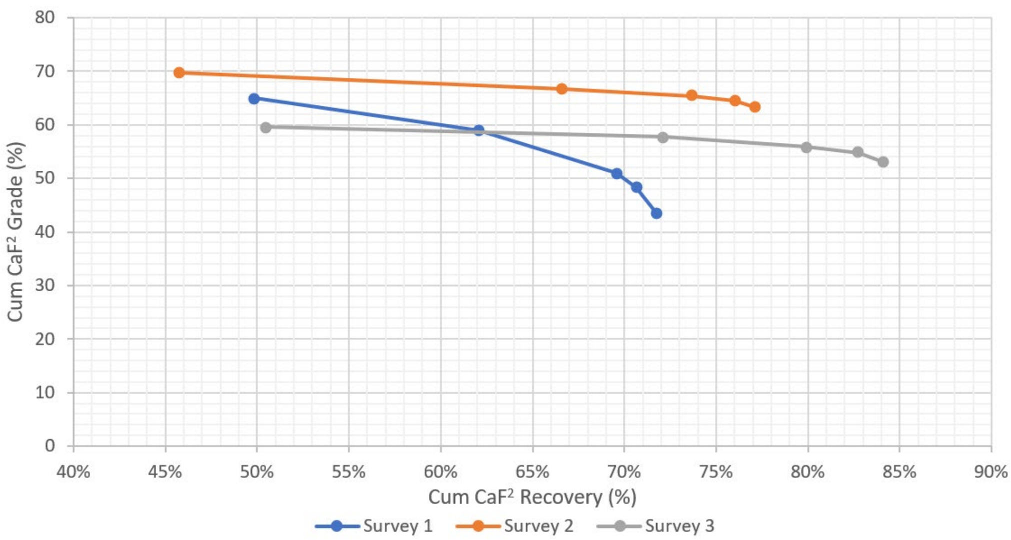


**FIG 11** – $CaF^2$ grade versus recovery for fluorite rougher circuit.

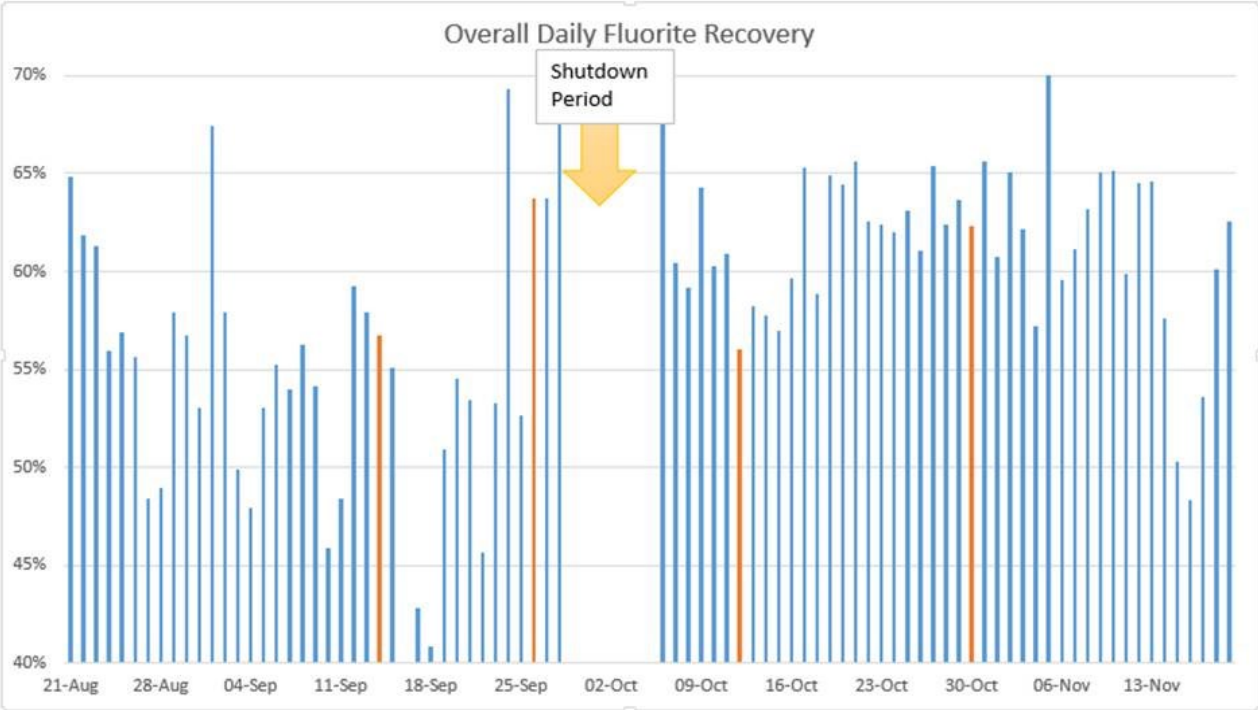


**FIG 12** – Daily fluorite recovery.

## Fluorite circuit concentrate recovery by size

To further understand the metallurgical performance, the concentrate streams down the Fluorite rougher circuit were sent for recovery-by-size analysis. The collected streams were screened at 212 µm, 150 µm, 106 µm, 75 µm, 53 µm, 38 µm size fractions.

The Fluorite rougher concentrate sizing results are presented in Figure 13. For all the rougher cells, the results indicate a significant increase in the P80 grind size for Survey 2 and Survey 3, when compared to Survey 1. For example, in FC-135 the P80 grind size was 87 µm for Survey 1, 117 µm for Survey 2 and 102 µm for Survey 3. A similar trend in observed for FC-136 and FC-137. FC-138 and FC-139 indicate more variation in the results but Survey 2 and Survey 3 are still coarser than Survey 1. It is important to note that for all three surveys, the flotation feed grind size was consistent at P80 ~192 µm as detailed in Table 2. Thus, the grinding circuit was not responsible for the change in the particle size recovery to the float concentrate.

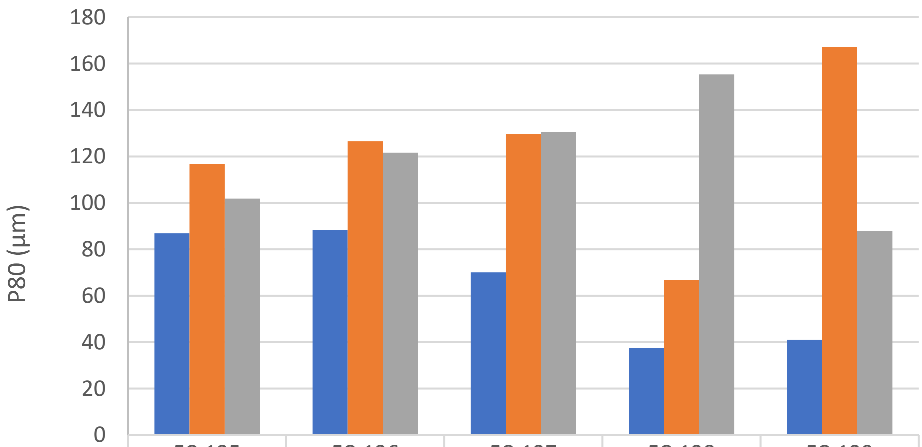


| | FC-135 | FC-136 | FC-137 | FC-138 | FC-139 |
|---|---|---|---|---|---|
| Survey 1 | 87 | 88 | 70 | 38 | 41 |
| Survey 2 | 117 | 127 | 130 | 67 | 167 |
| Survey 3 | 102 | 122 | 130 | 155 | 88 |

**FIG 13** – Fluorite rougher concentrate sizing.

To understand the $CaF^2$ distribution by size in the flotation rougher concentrate, the mass fractions were sent for $CaF^2$ chemical analysis. The results for all three surveys are presented in Tables 6 to 8. The results indicate an increase in the $CaF^2$ distribution in the coarser size fractions for Survey 2 and Survey 3, when compared to Survey 1. The most significant was observed in the 212 μm size fraction, followed by 150 μm, 106 μm and 75 μm size fractions. The coarse recovery improvement was distributed across all five rougher cells; however, the increase was higher in the last few rougher cells. Thus, the results suggest that increase in the P80 grind size to the flotation concentrates was due to selective flotation of $CaF^2$ minerals and not caused by slurry pulping and/or circuit instability.

**TABLE 6**

Cumulative $CaF^2$ Recovery to Concentrate (Survey 1).

| | Size Fraction | | | | | | | |
|---|---|---|---|---|---|---|---|---|
| | **212 μm** | **150 μm** | **106 μm** | **75 μm** | **53 μm** | **38 μm** | **-38 μm** | **Overall** |
| FC-135 | 13% | 26% | 39% | 52% | 70% | 80% | 66% | 50% |
| FC-136 | 18% | 34% | 54% | 71% | 84% | 88% | 79% | 62% |
| FC-137 | 23% | 42% | 65% | 81% | 90% | 93% | 89% | 70% |
| FC-138 | 24% | 43% | 66% | 83% | 91% | 93% | 90% | 71% |
| FC-139 | 24% | 43% | 67% | 84% | 91% | 94% | 92% | 72% |

**TABLE 7**

Cumulative $CaF^2$ Recovery to Concentrate (Survey 2).

| | Size Fraction | | | | | | | |
|---|---|---|---|---|---|---|---|---|
| | **212 μm** | **150 μm** | **106 μm** | **75 μm** | **53 μm** | **38 μm** | **-38 μm** | **Overall** |
| FC-135 | 21% | 31% | 41% | 67% | 66% | 43% | 53% | 46% |
| FC-136 | 35% | 48% | 65% | 83% | 88% | 82% | 81% | 67% |
| FC-137 | 42% | 55% | 72% | 90% | 93% | 89% | 88% | 74% |
| FC-138 | 44% | 58% | 75% | 92% | 94% | 91% | 90% | 76% |
| FC-139 | 45% | 60% | 76% | 92% | 95% | 91% | 91% | 77% |

**TABLE 8**

Cumulative $CaF^2$ Recovery to Concentrate (Survey 3).

| | Size Fraction | | | | | | | |
|---|---|---|---|---|---|---|---|---|
| | **212 μm** | **150 μm** | **106 μm** | **75 μm** | **53 μm** | **38 μm** | **-38 μm** | **Overall** |
| FC-135 | 22% | 33% | 48% | 73% | 59% | 56% | 59% | 50% |
| FC-136 | 41% | 57% | 72% | 89% | 87% | 78% | 80% | 72% |
| FC-137 | 50% | 67% | 80% | 93% | 92% | 90% | 89% | 80% |
| FC-138 | 55% | 72% | 83% | 94% | 93% | 91% | 91% | 83% |
| FC-139 | 57% | 74% | 85% | 95% | 94% | 91% | 93% | 84% |

In addition, in Table 3 the overall metallurgical results indicate an increase rougher concentrate $CaF^2$ grade for Survey 2 and Survey 3, when compared to Survey 1. Thus, the results suggest that the recovered coarse $CaF^2$ particles were relatively clean and rich in $CaF^2$. This can also be observed in Figure 11. For Survey 2 and Survey 3, the $CaF^2$ rougher recovery/grade relationship graph is flatter when compared to Survey 1. This suggests that the recovery of the coarse $CaF^2$ particles did not affect the $CaF^2$ concentrate grade.

In summary, the results suggest that replacing the flotation mechanism in four of the rougher cells has improved the transport of the coarse particles to the pulp-froth interface and increased their recovery to the concentrate. These coarse particles were rich in $CaF^2$ minerals and have contributed to the overall improvement in the metallurgical recovery and grade, as observed in Survey 2 and Survey 3.

It is hypothesised that the newer flotation mechanisms provide better hydrodynamic conditions for recovery of coarse valuable minerals when compared to worn flotation mechanisms close to replacement. As the flotation mechanisms wear the clearances between the rotor and stator components become less ideal and outside of design parameters. This can affect slurry pumping, bubble shearing, bubble-particle contact and cause short-circuiting.

## Power draw

CFD modelling predicts that as the flotation rotor and stator components wear, there will be a decrease in the measured power draw. The reasoning being the clearances between the components will increase resulting in less pumping intensity and efficiency. Although this has been simulated, it has not been validated with plant data. Thus, for the three surveys, the power draw measurements of the Fluorite rougher cells were recorded by the plant control system and the results are presented in Table 9. It should be noted that float cell power draw is also affected by the incoming slurry feed density and airflow rate into the cell. Generally, higher feed densities increase the power draw and higher air flow rates reduce the power draw. For the three surveys investigated, the feed density was relatively consistent at ~54 per cent solids (w/w), whilst the airflow rate varied. In most cases, the airflow rate was higher in Survey 2 and Survey 3 when compared to Survey 1, the results are presented in Table 9.

**TABLE 9**

Fluorite rougher circuit power draw results.

| | | FC-135 | | FC-136 | | FC-137 | | FC-138 | | FC-139 | |
|---|---|---|---|---|---|---|---|---|---|---|---|
| **Survey** | **Date** | **Power** | **Air flow** | **Power** | **Air flow** | **Power** | **Air flow** | **Power** | **Air flow** | **Power** | **Air flow** |
| | | **(amps)** | **($m^3$/h)** | **(amps)** | **($m^3$/h)** | **(amps)** | **($m^3$/h)** | **(amps)** | **($m^3$/h)** | **(amps)** | **($m^3$/h)** |
| 1 | 14/09/2019 | 148 | 575 | 138 | 500 | 139 | 219 | 163 | 460 | 139 | No record |
| 2 | 12/10/2019 | 167 | 660 | 132 | 600 | 134 | 400 | 167 | 294 | 158 | 165 |
| **% Change Survey 2 versus Survey 1** | | **12%** | **15%** | **-4%** | **20%** | **-4%** | **83%** | **2%** | **-36%** | **14%** | |
| 3 | 30/10/2019 | 170 | 590 | 136 | 556 | 135 | 403 | 182 | 348 | 149 | 350 |
| **% Change Survey 3 versus Survey 1** | | **15%** | **3%** | **-1%** | **11%** | **-3%** | **84%** | **12%** | **-24%** | **7%** | |

For the three cells *viz* FC-135, FC-138 and FC-139, the results indicate an increase in power draw from Survey 1 to Survey 2 and Survey 3. In these three cells, the worn flotation mechanism components were replaced with new components during the plant shutdown. For two cells, FC-136 and FC-137, the results indicate a decrease in power draw from Survey 1 to Survey 2 and Survey 3. In FC-136, the flotation mechanism was not replaced during the plant shutdown, and in FC-137 the air flow rate was increased significantly (>80 per cent) in Survey 2 and Survey 3. Thus, the lower power draw results were expected in both cases.

The survey results suggest that installing a new float mechanism will result in a higher power draw, provided the air flow rate is maintained at similar levels. This was observed in FC-135, FC-138 and FC-139, when old worn mechanisms were replaced with newer mechanisms. The $CaF^2$ rougher circuit power draw results from August to November 2019 are presented in Figure 14. The plant results indicate a significant increase in the float cell power draws after the plant shutdown. Thus, the plant results confirm the survey result findings.

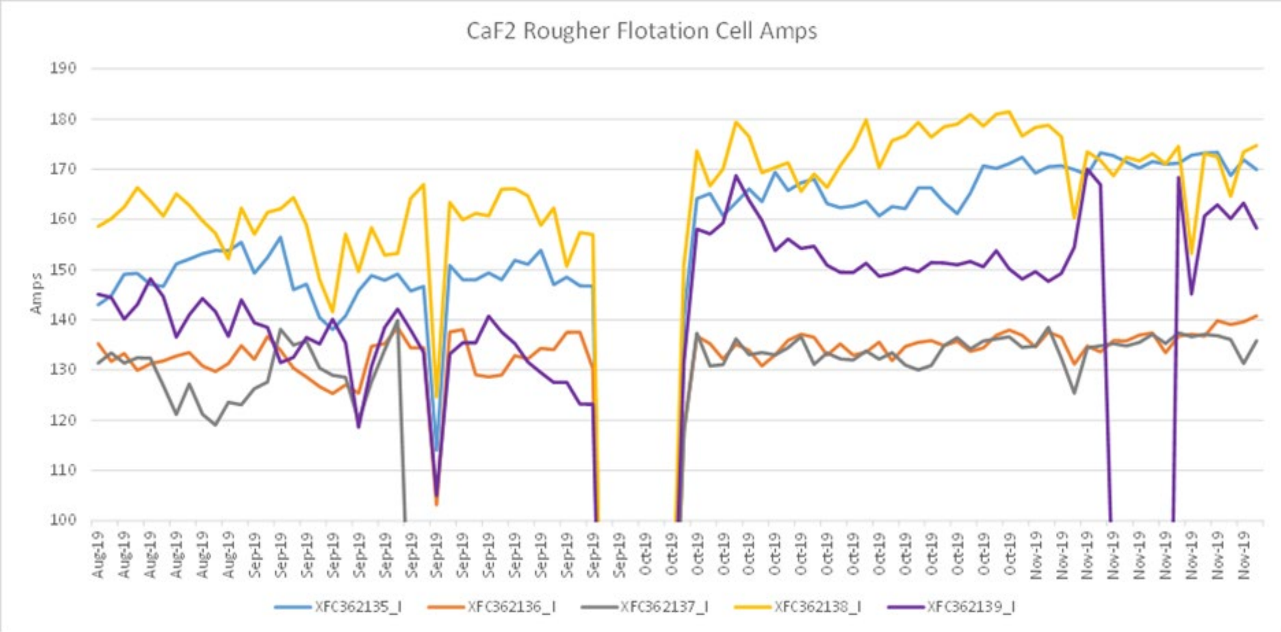


**FIG 14** – CaF[2] rougher circuit cell amps.

In summary, we can conclude that for similar air flow rates, the newer flotation mechanisms produce higher power draws and pumping efficiencies when compared to worn flotation mechanisms close to their replacement cycle.

## Particle suspension

An investigation was carried out to assess the impact of worn flotation mechanism on particle suspension. Samples were taken at three depth levels within the cell. The survey results for float cell FC-135 are presented in Figure 15.

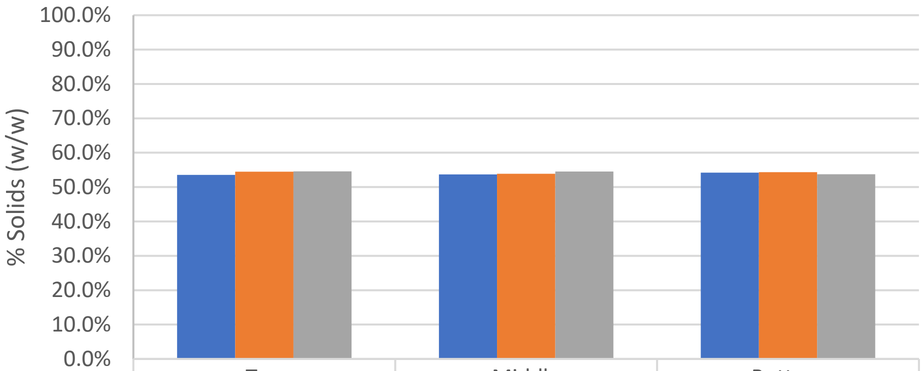


| | Top | Middle | Bottom |
|---|---|---|---|
| Survey 1 | 53.5% | 53.7% | 54.2% |
| Survey 2 | 54.5% | 53.9% | 54.3% |
| Survey 3 | 54.6% | 54.5% | 53.7% |

**FIG 15 –** Float cell FC-135 striation results.

Depths sampled:

- Top – 1.6 m below froth surface
- Middle – 2.7 m below froth surface
- Bottom – 3.4 m below froth surface.

The float cell height from the tank floor to the concentrate lip (froth surface) is 3.6 m and the solid specific gravity of Fluorite minerals is ~3.1 t/m$^3$.

For all three surveys, the FC-135 results indicate no significant difference in the solids density between the samples measured (refer to Figure 15). Thus, at the tank heights measured, the results suggest that there was sufficient particle suspension for both the worn (Survey 1) and new (Survey 2 and 3) FloatForce® mechanisms.

For future surveys, it is recommended that additional samples be taken closer to the froth surface, for example:

- Sample 1 – 0.5 m below froth surface
- Sample 2 – 1.0 m below froth surface.

This may better highlight the differences in particle suspension between worn and new flotation mechanisms.

## CONCLUSIONS

At NPMC, the flotation mechanism wear had a significant effect on metallurgical performance. Thus, the prediction that in full-scale plant conditions, ore feed and process variations would prevent any measurable relationships being discovered proved false. This may still hold true for some circuits, but at NPMC we can conclude that replacing the worn flotation mechanism in four of the rougher cells (ie FC-135, 137, 138 and 139) had the following process benefits:

- The $CaF^2$ rougher recovery/grade relationship improved significantly. The major improvement in recovery was observed in the first two rougher cells (FC-135 and FC-136).
- The improvement in metallurgical performance was due to the recovery of coarse $CaF^2$ rich minerals across the rougher circuit. These particles were recovered through selective flotation. The daily plant results confirmed these results and indicated an improvement Fluorite recovery.
- At similar air flow rates, the newer flotation mechanisms produce higher power draws and pumping efficiencies when compared to worn flotation mechanisms close to their replacement cycle. After the plant shutdown, the plant results indicated higher power draw measurements in the rougher circuit.
- There was no measurable difference in particle suspension at the sample depths measured. It is recommended that for future surveys, samples closer to the froth surface area are taken.

Based on the results, it is hypothesised that the new flotation mechanisms provided better hydrodynamic conditions for recovery of coarse valuable minerals when compared to worn flotation mechanisms close to replacement. This may be caused by changes in slurry pumping, bubble shearing, bubble-particle contact and/or combination of factors as the mechanism wear. Further work needs to be done, to better understand when the changes in clearances between wearing rotor and stator components start to affect metallurgical performance.

The next step would be to conduct recovery-by-size analysis on the cell concentrate streams over the duration of the flotation mechanism life (operational hours). It expected that a change in the recovery of the coarser valuable minerals would be observed as the components wear. Once enough data has been collected, a site-specific change-out schedule for the flotation components can be developed. The flotation components would then become process components, replaced based on metallurgical performance rather than on the likelihood of mechanical failure. This will result in flotation circuits being operated closer to optimum conditions for longer time periods and improve the overall profitability of operations.

Outotec is currently approaching customers to conduct this type of investigation.

## ACKNOWLEDGEMENTS

The authors would like to thank NPMC staff and management for their support and close collaboration during the flotation mechanism wear evaluation; this was a key factor in achieving the project outcomes.

# REFERENCES


Coleman, R and Rinne, A, 2011. Flotation mechanism design for improved metallurgical and energy performance, in Proceedings Metallurgical Plant Design and Optimisation (MetPlant11), pp 405–418

Coleman, R and Wong, B, (2018). Flotation Launder Design and the Measurement of Critical Froth Transport Parameters, in Proceedings 14th AusIMM Mill Operators Conference 2018

Harris, C C, 1975. Flotation Machines, in Flotation (ed M.C. Fuerstenau), ch27 pp 753–815 (AIME: New York).

Nelson, M G and Lelinski, D (2000). Hydrodynamic Design of Self-Aerating Flotation Machines, Minerals Engineering, Volume 13, Issue 13, November 2000, Pages 1429–1430

Murphy, B, 2013. Flotation energy consumption and opportunities for improvement, in Proceedings of MetPlant 2013: Plant Design and Operating Strategies – World's Best Practice, pp 399–412

Murphy, B, Heath, J L and O'Connell, S, (2014). Maximizing value through maintaining your flotation equipment, in Proceedings 12th AusIMM Mill Operators Conference 2014, pp 71–76

Morgan, S, Weekes B, Jakowetz A, Litson S, Taylor S, Do T L and Bourke P, (2017). Nui Phao Mine – Flotation Circuit Upgrade, in Proceedings Metallurgical Plant Design and Optimisation (MetPlant11)

Murphy, B and Heath J L, 2013. Selection of Mechanical Flotation Equipment, Presented at METCON 2013: Enhancing the resource value chain among ASEAN economies (Society of Metallurgical Engineers of the Philippines: Quezon City).

# Pressurised flotation for froth-free concentration

*G Rowe[1], A Luke[2], C de Leon[3] and G Dobby[4]*

1. Woodgrove Technologies, Toronto, Ontario, M3J 2P6. Email: gerardrowe@woodgrovetech.com
2. Woodgrove Technologies, Toronto, Ontario, M3J 2P6. Email: andrewluke@woodgrovetech.com
3. Woodgrove Technologies, Toronto, Ontario, M3J 2P6.
   Email: chesterdeleon@woodgrovetech.com
4. Woodgrove Technologies, Toronto, Ontario, M3J 2P6. Email: glenndobby@woodgrovetech.com

## ABSTRACT

The initial step in the flotation process is selective attachment of mineral particles to gas bubbles, which occurs rapidly under proper conditions. The subsequent transportation of bubble-particle aggregates to an external collection launder via the froth phase complicates the overall process, and is often a rate-limiting step and the bottleneck, ie a significant challenge in froth flotation is the froth itself. In other words, if the bubble-particle aggregates are collected without the formation of a froth phase, the flotation process will be much faster and efficient, and the residence time and footprint can be significantly reduced. This paper describes a novel flotation system developed by Woodgrove, which transports bubble-particle aggregates directly to a collection pipe via bubbly flow, and a conventional froth is not created. The separation system is pressurised, and product recovery is controlled through a control valve. Pressurisation is attained through a pump or a head tank, which allows for multiple separation stages in series that are constructed on a single elevation, with product pipes flowing into a common collection box. This design results in space savings and power savings over conventional mechanical cells. In addition, the low air rates of this system and multiple stages provide significant selectivity enhancement over flotation columns. The pilot plant testing of this froth-free equipment is described, and examples of industrial installations are provided.

## INTRODUCTION

The Woodgrove Technologies Staged Flotation Reactor (SFR) has been in use in the industry for almost a decade (Moore, 2014; Swedburg, 2016). During this period, it has been proven that SFR can achieve equivalent particle recovery with air consumption rates (expressed as $m^3/h$ air per $m^3/h$ feed slurry) 5 to 10 times lower than conventional mechanical flotation cells (Moore, 2014). The low air consumption of SFR is achieved through the unique design of the equipment such that the particle collection zone and froth recovery zone are separate and can be optimised independently, as shown in the photographs in Figure 1. The successful application of high-rate particle collection with very low air rates delivered through SFR operation has led to the opportunity to resolve the issue of recovery loss due to poor froth characteristics.


**FIG 1** – Two SFRs installed for copper cleaning on regrind cyclone overflow.

However, a froth zone is still created in SFR, and at times, especially for cleaning, it dictates the vessel size. In addition, to fully utilise the more optimised froth environment in the SFR, it must be a two-tank design, which despite being lower in footprint, power, and air consumption than conventional flotation machines, still requires a step height between cells as well as froth monitoring and froth control systems.

Building on the database of low air flotation, further research has allowed the elimination of step height between cells, reducing the process back to a single small vessel (resulting in a major reduction in footprint) and eliminating the need for froth control systems. This is achieved by eliminating the froth and replacing it with a 'bubble recovery' system, which is one of the critical elements of the Woodgrove Direct Flotation Reactor (DFR) described in this paper.

## THE CHALLENGE

The issues of particle froth drop-back, and variability in froth stability, are well recognised as significant challenges in flotation plants. Numerous academic and applied research works have been conducted to better understand flotation froths, and to better control the stability and movement of froths in the concentrator. However, these issues are still not fully understood and resolved, and often cause significant losses to the flotation plants.

In general, the mineral froth is a three-phase system comprising discrete mineral particles, a gas phase, and a contained slurry solution. The gas holdup in a mineral froth is typically higher than 90 per cent by the time the froth overflows the discharge lip. The gas phase in a mineral froth no longer exists as discrete spherical gas bubbles, but as a coalesced phase of three-dimensional polyhedral shapes with distinct borders between them, as shown in Figure 2. The mineral solids exist as hydrophobic particles attached to the surfaces of the polyhedral gas foam. The contained solution in the froth phase exists as a slurry liquid held up along the walls of the polyhedral gas foam. This slurry liquid comprises a solution medium, and gangue (solid) particles that are suspended in the froth phase not through attachment, but through entrainment.

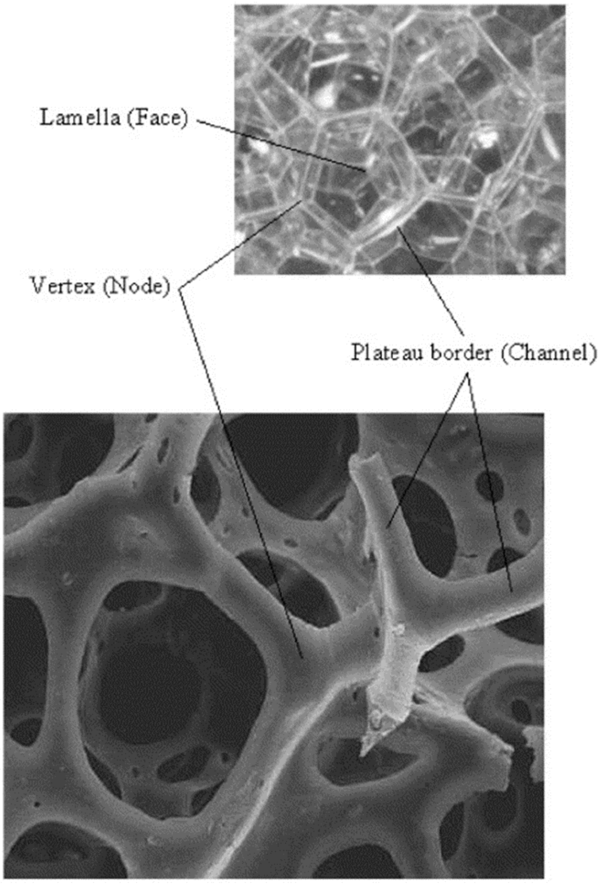


**FIG 2** – Structure of froth showing plateau borders, lamellae, and nodes (Ventura-Medina, 2002).

In mineral froths, there is a distinct interface between the slurry phase and the froth phase. The rise velocity of mineral-laden gas bubbles slows down dramatically as the bubbles travel over this phase boundary. The dramatic deceleration of the bubbles at or near the phase boundary initiates the coalescence of the discrete spherical bubbles and forms a mineral froth. Coalescence, with resultant reduction in bubble surface area, causes mineral particles to detach from the bubble surface and drop back into the slurry phase (a phenomenon known as froth drop-back). In the case of conventional flotation cells, these particles fall-back into the slurry and may be recollected within that vessel, or report to a subsequent collection stage for recovery. However, since the froth phase is eliminated in the DFR, there is minimal coalescence; and hence, no mineral particle drop-back due to an unstable froth.

## GLOSSARY

A glossary of the main terms associated with DFR is provided in this section.

- Gas holdup (Ɛg): Ratio of gas-phase volume to total slurry system volume, expressed as either a fraction or a percentage.
- Qc: Volumetric flow rate of the product stream (solids and water) exiting the system.
- Qcw: Volumetric flow rate of water contained in the product stream.
- Qg: Volumetric flow rate of gas delivered to the system.
- Qww: Volumetric flow rate of wash water delivered to the system.
- Mcs: Product stream solids mass flow.
- Rcg: Gas rate fraction → the ratio of Qg to (Qg + Qc).
- Flush efficiency: Ratio of water flow rate in the product stream with wash water flow rate delivered to the system, ie the ratio of Qww to Qcw.
- Froth phase: a distinct 3-phase system of solid particles, polyhedral gas foam and liquid slurry. There is a distinct interface between the slurry phase and the froth phase. In a froth phase, the typical Ɛg is above 90 per cent.
- Bubbly flow: a 3-phase system of the bubble-solids aggregate and the liquid slurry. There is no interface between the slurry phase and the bubbly flow phase.
- Froth recovery (%): Percentage of particles entering the froth phase, and attached to gas bubbles, that are recovered over the top lip of a flotation vessel as part of the coalesced froth.
- Bubble recovery: The recovery of mineral-laden bubbles into a distinct product from the flotation equipment, without coalescence of the spherical gas bubbles.
- Direct Flotation: The recovery of a product stream from the top of a flotation vessel in the form of a bubbly flow stream, with no bubble coalescence into a froth phase.

## DIRECT FLOTATION REACTOR (DFR)

### The key elements of the DFR

The schematic of a single DFR is shown in Figure 3. Feed slurry enters the bottom of the cell via a head tank, which provides sufficient head pressure to allow the product to exit at the top of the vessel (a sump and variable-speed pump can be used in lieu of a head tank). The top product is a concentrate for most applications and is referred to as such in this paper. An exception is the reverse flotation, such as the reverse flotation of coal, iron ore, and molybdenite (Araujo, 2005; Yuan, 2018, 2019), where the top product is the tailings. Air is piped into the tank near the bottom, usually near the feed slurry inlet, and is sheared into small bubbles by the impeller tip. The bubble-particle aggregates rise to the tapered top of the tank, and the reject stream ('tailings' for most flotation applications) discharges via a port on the side of the tank.

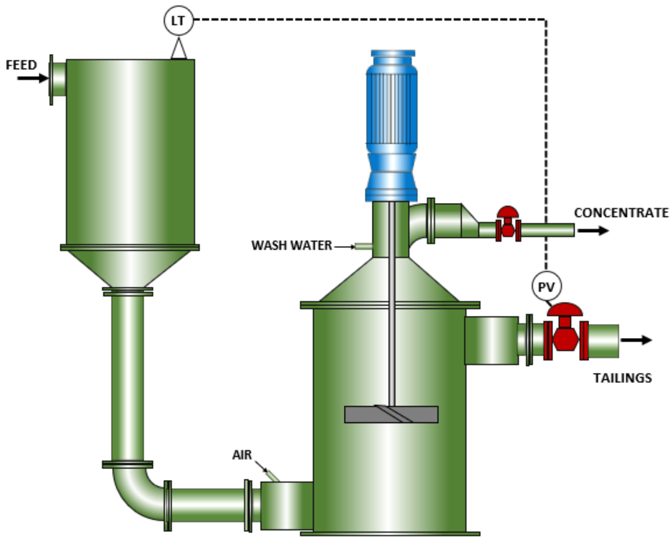


;

**FIG 3** – Schematic illustration of a single DFR installation, using a head tank to feed the cell.

The mineral-laden gas bubbles ('bubbly-flow') rise to the top of the tapered section of the tank and into a vertical 'bubble recovery' pipe. The pipe surrounds the rotating agitator shaft, which has a seal at the top. The three-phase bubble-mineral-water mixture at the top is withdrawn off a side port, with the product flow rate set by a control valve.

The head tank or feed pump is set to maintain a positive gauge pressure at the bubble recovery pipe. The desired pressure set point is controlled either with a tailings control valve, or with a direct-coupled variable speed pump.

A key improvement of the DFR is that no froth is formed at the top of the cell, which is achieved by the proper design of equipment dimensions and air rate. Bubble coalescence may be virtually eliminated, and a sufficiently high net rise velocity of bubbles and liquid in the pipe is maintained to prevent the formation of a froth-pulp interface. The gas holdup in the pipe is also an important control variable and is generally between 40 and 90 per cent; hence the concentrate is always in a bubbly-flow regime. This is clearly illustrated in Figure 4, which shows the bubbly-flow of concentrate in a copper cleaning application.

**FIG 4** – The bubbly-flow of concentrate in a copper cleaning application.

The water displacement of slurry that carries the bubbly-flow is achieved by injecting a wash water stream in or near the bubble recovery pipe. As with flotation columns, a common wash water displacement ratio is 1.0; however, this ratio can be as low as zero and as high as 1.5. The wash water ratio regulates the recovery of entrained particles, with a high wash water ratio acting to eliminate entrainment.

With this approach, concentrate flow is consistently regulated by the concentrate valve, where the target concentrate flow rate and the static pressure are used to set the valve opening.

## Multiple DFRs in series

The DFR can be directly connected one after another to form a train of flotation units in series; Figure 5 shows schematics of three DFRs in series. Figure 5a shows a DFR train fed by a head tank, while Figure 5b shows a train fed by a variable speed pump.

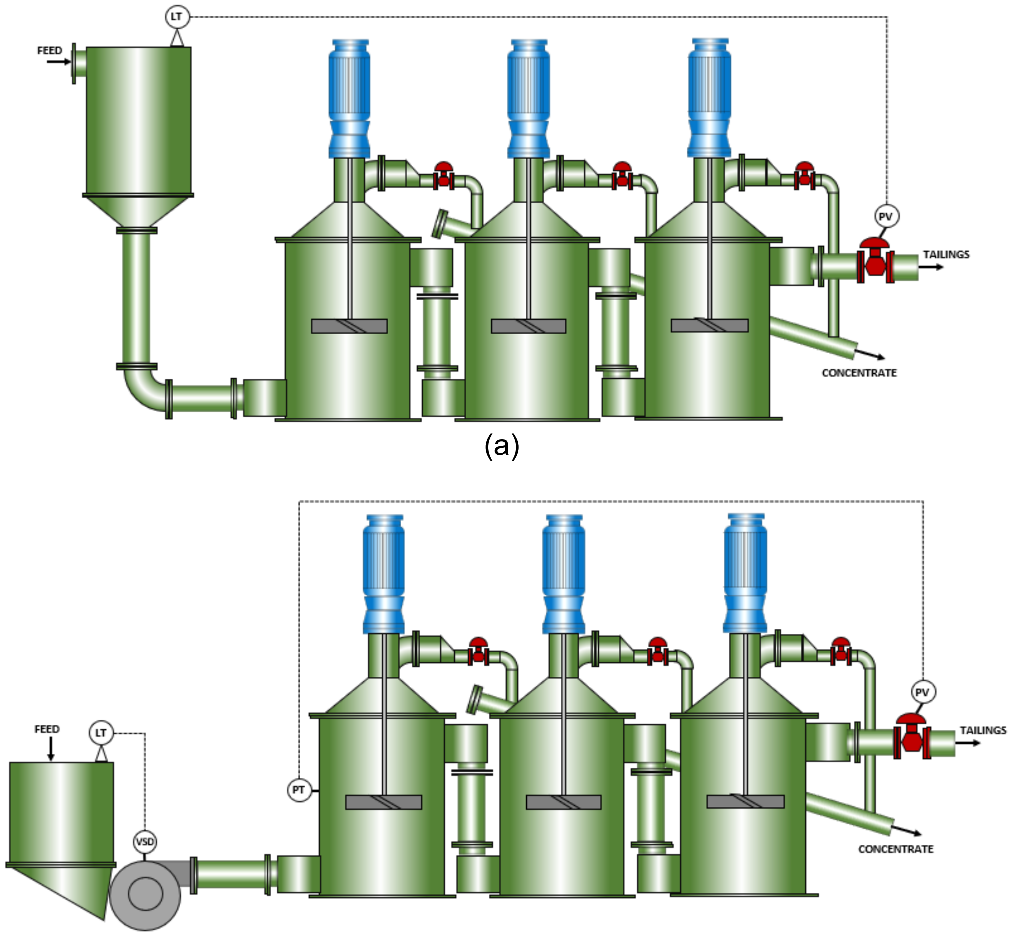


(a)

(b)

**FIG 5** – Schematic illustration of three DFRs connected in series, (a) using a head tank for DFR feed; (b) using a variable speed pump for DFR feed.

There are two important factors in the configuration of multiple DFRs that provide advantages over conventional flotation systems.

Firstly, only a single tailings control element is required for the whole train of DFR units. A head pressure is maintained on the system, and individual cells have small concentrate control valves to maintain target concentrate slurry flow. All cells are directly connected with each other, from tailings outlet to feed pipe, and it is only the last cell that has a level control element. This control element (control valve or pump) maintains a set point on the feed pressure. For a system fed via a head tank, this equates to maintaining the slurry level in the head tank to a set target. While for a system fed via a slurry pump, this equates to maintaining DFR tank pressure set point with the tailings valve, while regulating pump speed to maintain a target sump slurry level.

Secondly, the DFR cells can all be installed on the same elevation, unlike conventional froth flotation machines that typically require an elevation drop between cells (or between every second cell). Having the DFRs on one elevation simplifies layout issues and access, and reduces construction costs and building height. The reduced size, weight, power, and air requirements of DFR as compared to conventional flotation machines, reduces footprint and costs for civil, industrial, mechanical, and electrical infrastructure. In addition, reduced power and air requirements reduce operating costs.

## Concentrate flow control

The operation of conventional flotation machines with froths often struggles with a consistent pull rate on concentrate production. Froth mobility and stability may be altered with ore changes and feed grade variations, resulting in instability of concentrate production. This phenomenon is commonly observed in the scavenging stages of roughing, where the mass recovery requirement is low and the bubble surface area is high. Advanced Process Control (APC) has been applied successfully to mitigate these challenges; nevertheless, effects of ore changes can still dominate in extreme cases. With the DFRs, however, concentrate flow is reliably maintained through the use of head pressure and the flow control of the product concentrate valves.

When a flow surge occurs on a DFR stage, two complementary actions take place. First, the tailings valve at the end of the stage responds to the system pressure change (as any tailings valve on a conventional flotation machine would). Second, the concentrate flow control valve also responds to the system pressure change, opening for higher pressure and closing for lower pressure. The simultaneous actions of the tailings valve and multiple concentrate control valves result in a very steady concentrate production rate, largely independent of feed flow surges. The result is a much more stable control within the complete flotation circuit.

An extreme example is the handling of a massive flow surge from the grinding section into the rougher flotation stages, particularly for those high throughput circuits using a SAG/Ball mill combination. A great deal of work in the past decade has gone into the prevention and mitigation of large flow surges from these grinding circuits. However, extreme surges still periodically occur in many plants, typically resulting in flooding of the rougher flotation cells, floor spillage, and subsequent flooding of the regrind and cleaner circuits. With the DFR design, the system can prevent an extreme flow surge into the following cleaner circuit.

## Concentrate gas collection

The concentrate product of several cells in series can be discharged individually into an open-air launder, as with conventional flotation equipment. However, they also may be hard piped into a common collection pipe, offering the opportunity to collect an off-gas from the concentrate pipe, and process the gas as appropriate. For example, some molybdenite-copper flotation separation circuits may generate toxic hydrogen sulphide gas, and potentially at lethal dosages. These concentrators require extreme attention to personnel safety. The DFR offers the ability to reliably collect the flotation off-gases and remove them from the plant, preventing personnel harm.

A DFR flotation plant, with hard-piped concentrate collection lines, will provide an improved environment for plant operations and maintenance crews. In some cases, it could allow the use of collectors (such as some xanthates, with carbon disulphide decomposition product) that otherwise may not pass occupational hygiene standards).

## Reagents for DFRs

Flotation frothers have two primary functions: (i) allow sufficient change in the liquid surface tension to generates small gas bubbles, and (ii) assist with creating a froth with appropriate stability and mobility, while allowing the collected froth product to breakdown sufficiently for subsequent flow-through pipes and slurry pumps.

The ‘froth stability’ requirement of a frother disappears when the DFR is used. This opens the opportunity to investigate frothers that are excellent for particle collection, but could not provide the required froth stability. This aspect is typically evaluated on DFR pilot programs.

The lack of a froth in the DFR also opens the opportunity for the use of stronger collectors that otherwise may have caused froth immobility. The ability to use stronger collectors (and higher dosages) could improve coarse particle recovery in base metal rougher applications.

## Process control

The control variables in each DFR are air flow rate, wash water flow rate, and gas holdup of the bubble recovery section. The gas holdup of the bubble recovery section can be thought of as analogous to froth depth – deeper froth in conventional cells and higher gas holdup in DFR typically lead to higher concentrate grade.

As noted previously, concentrate flow normally will be very stable for each DFR cell. This suggests that the circulating loads in DFR circuits also should be more stable than in circuits operating with conventional equipment, such as tank cells and flotation columns.

# DFR PILOT TESTING

The DFR pilot plant is portable and can be fitted into an aluminium crate designed for truck or air travel. It can be set-up in half a day at a third-party testing facility, or in an operating concentrator.

A photograph of a DFR pilot plant unit is shown in Figure 6. This version of DFR pilot plant has a bottom entry agitator. Feed slurry is stored in an agitated tank and is fed to the DFR at a flow rate between 5 to 20 L/min, using a variable speed peristaltic pump. Pressure in the DFR is maintained through a manual control valve on the tailings port, which provides the head pressure for the up-flow of concentrate slurry. The concentrate flow is regulated with a small peristaltic pump.

Tailings from the DFR pilot are recirculated back to the agitated feed tank. Concentrate samples are continuously collected, with the collection bucket changed at periods that represent approximately one collection cycle, ie total system slurry volume divided by slurry flow rate. Tailings samples also are taken at the end of these cycles. In this manner, the pilot plant data approximates the sequential stages of DFRs.

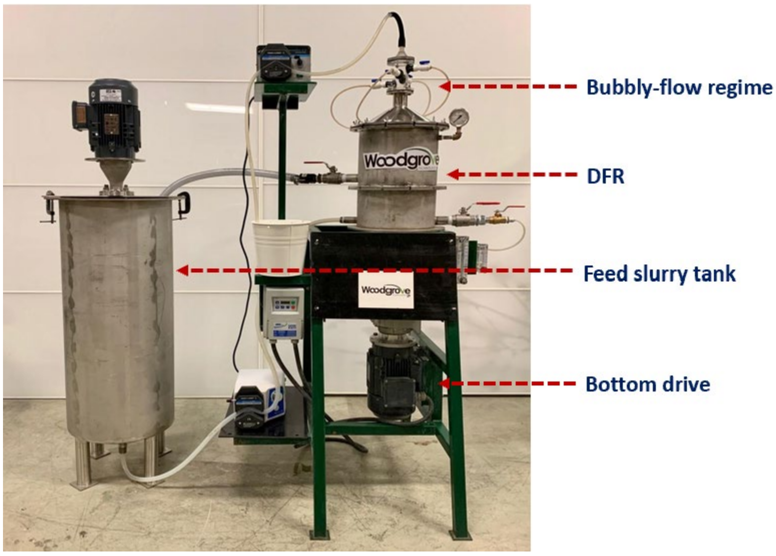


**FIG 6** – Photograph of a DFR pilot plant. The bottom-driven DFR unit is shown on the right, with a feed slurry tank on the left and feed and concentrate pumps in the middle.

# CASE STUDIES

## Case study 1 – DFRs versus flotation columns as final cleaner

A typical unit in the final stage of copper cleaning is the flotation column, a standard in the industry for the past 20 years. Woodgrove has recently conducted pilot tests with DFR equipment at several copper concentrators. In all cases, the DFR has achieved better selectivity over the flotation column(s), and significantly better in many cases. Two examples are summarised, and their grade-recovery curves are presented in Figures 7 and 8.

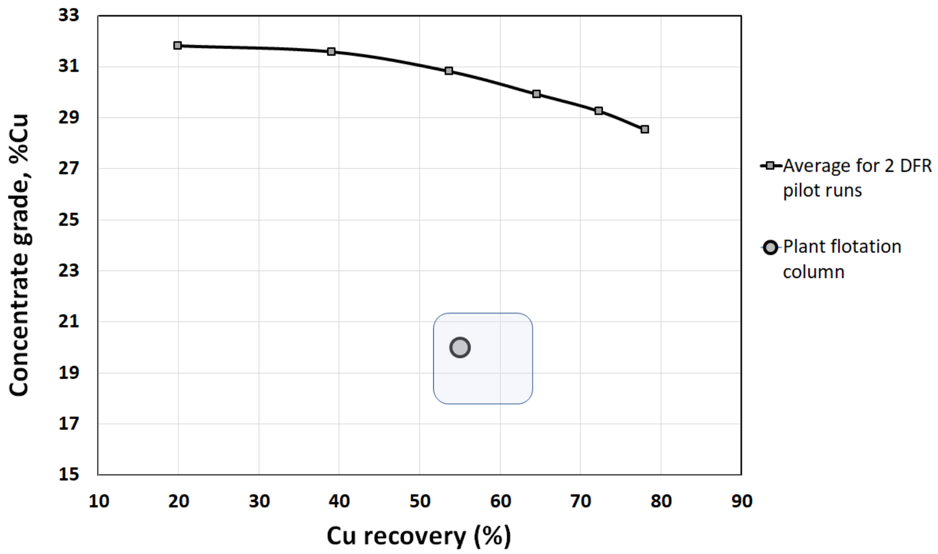


**FIG 7** – Grade-recovery curve for DFR pilot testing versus a single commercial flotation column at copper concentrator A, for copper cleaning (application is for production of a secondary concentrate).

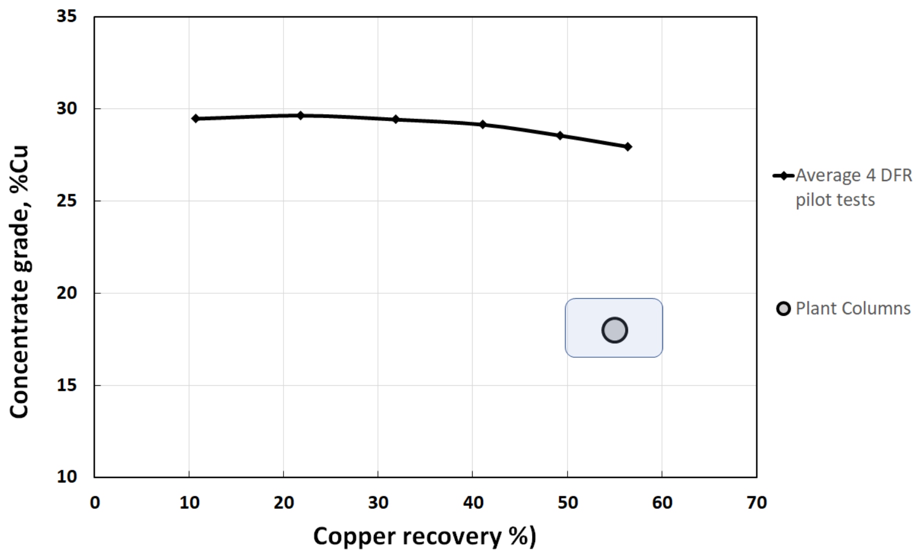


**FIG 8** – Grade-recovery curve for DFR pilot testing versus a single commercial flotation column at copper concentrator B, for copper cleaning (application is for production of a primary concentrate with significant talc contamination).

Figure 7 is a comparison of two DFR pilot tests against a commercial flotation column that produces a secondary stage final concentrate (after a higher-grade scalper concentrate has been produced). Copper occurs as chalcopyrite, and principal gangue minerals are pyrite and silicates. Feed grade averaged 9 per cent Cu and 25 per cent pyrite.

Figure 8 compares four DFR pilot tests against a flotation column that produces a final concentrate. Copper occurs as chalcopyrite, and principal gangue minerals are pyrite, talc, and silicates. Feed grade averaged 11 per cent Cu and 33 per cent pyrite.

Both applications show significant improvement in performance with the DFR. Note that both columns and DFRs have a system of water washing of the concentrate stream. Therefore, there are reasons other than wash water washing that cause the performance difference, and they are listed as follows.

The first reason is that the ratio of air flow rate to feed slurry flow rate in the DFR is dramatically lower than columns. For example, a common flotation column with a 10 m collection zone height operating with 30 minutes residence time (typical for copper cleaning) has a superficial slurry flow rate of 0.55 cm/s (or 0.55 $cm^3$/s of slurry moving downward per $cm^2$ of column surface area). A common superficial gas rate for copper flotation columns is 1.2 cm/s (often quite a bit higher). This yields a ratio of gas flow to slurry flow of 2.2; in other words, 2.2 $m^3$/h of gas flow per $m^3$/h of feed slurry flow.

In comparison, the DFR tests in Figure 7 had a gas to feed slurry flow ratio of 0.13 in each stage and the plant column recovery was matched with 3–4 DFR stages. The DFR tests in Figure 8 had a gas to feed slurry flow ratio of <0.10, and the plant column recovery was achieved by six DFR stages. In other words, each DFR stage operates at a ratio of air flow to slurry flow that is at least an order of magnitude lower than that in the flotation column. The reduced air rate of DFR reduces the bubble surface area available for pyrite and gangue minerals, lowers mechanical entrainment, and assists the selective recovery of chalcopyrite.

Secondly, the flotation column is a single-stage separation with a flow pattern similar to a single continuously stirred tank reactor (CSTR), while a row of five DFR's acts more like five CSTR's in series. Reactor theory shows that it is more efficient for recovery and selectivity to have several units in series instead of a single unit.

Thirdly, the mechanical impeller shear and agitation in the DFR promotes the bubble-particle collisions and attachments, leading to a significantly higher collection efficiency compared with the flotation columns (which usually lack of mechanical shear).

## Case study 2 – DFR for copper roughers

An example of the DFR pilot plant results on a copper rougher application is provided in Figure 9. In this example, four DFR pilot plant results are averaged and compared with the average of the four parallel bench kinetic tests. For each DFR pilot plant test, a standard bench float test is run in parallel using the same feed sample as the DFR. In this case, the pilot plant ran for ten stages, and the bench float ran for 15 minutes (as per design criteria). The tested ore has a naturally occurring hydrophobic gangue mineral that hinders upgrading in the cleaners. Figure 9 compares the average DFR rougher grade and recovery against the average of bench-scale tests.

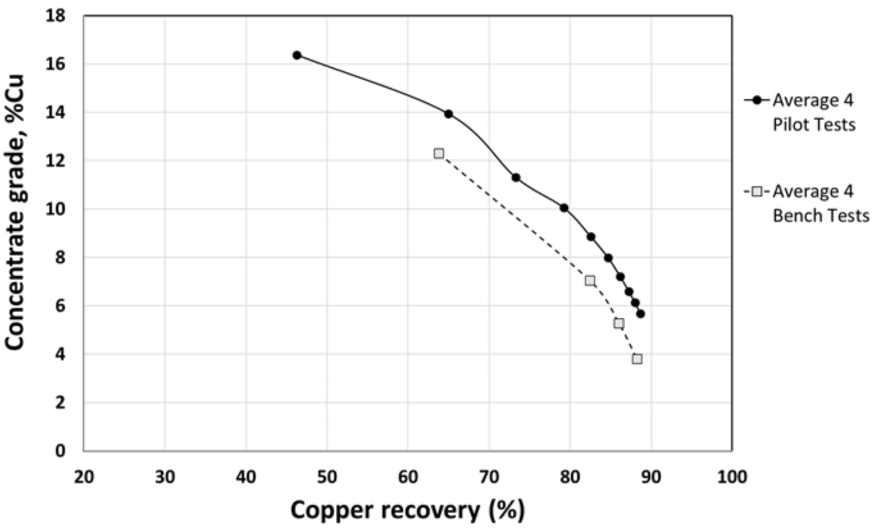


**FIG 9** – Grade-recovery curve for DFR pilot testing versus bench-scale testing in a copper rougher application.

The 15-minute bench float recovery is matched by the DFR, and the rougher concentrate grade is notably higher in the DFR, indicating a better rejection of hydrophobic gangue in the DFR. The mechanical shear in the collection zone of DFR enables it to achieve a similar collection efficiency and recovery to that of a conventional cell, while the wash water in the bubbly-flow zone of the DFR displaces entrained gangue, leading to enhanced grade at the same recovery target.

## Case study 3 – commercial design for copper cleaning

The objective of this section is to estimate the equipment sizes of flotation columns and DFRs at the same processing capacity.

Consider the final cleaner stage of a concentrator designed with the following criteria:

- Four flotation columns installed in parallel to process 1270 $m^3/h$ of feed slurry (ie 317.5 $m^3/h$ per column).
- The total copper concentrate production rate is 76 tph of solids or 19 tph of solids for each column. The optimal design of concentrate flux would be 1.2 tph/$m^2$ for a product P80 of 30–35 μm, which allows for an appropriate degree of water washing (Finch, 1990). Therefore, the required diameter of each column is 4.5 m. Consider a nominal residence time of 30 minutes and a feed slurry flow rate of 317.5 $m^3/h$ per column; the calculated column collection zone height would be 10 m. The actual column height should be around 13 m, which yields a total cell volume of 830 $m^3$ for four columns.
- Assuming a superficial gas velocity of 1.2 cm/s, the total air consumption would be 2750 $m^3/h$.

Based on the pilot test work to date at several copper concentrators, the DFR circuit selected for this application would be as follows:

- Five DFRs in series to process all 1270 $m^3/h$ of feed slurry.
- Each DFR would be roughly 20 $m^3$ in volume, for a total volume of 100 $m^3$ for the circuit.
- Total air consumption is 890 $m^3/h$, assuming a ratio of gas flow rate to feed slurry flow rate of 0.14 per cell (maximum expected, likely lower).

As summarised in Table 1, the four flotation columns would occupy a total cell volume of 830 $m^3$ and use 2750 $m^3/h$ of air. In comparison, the five DFRs would only occupy a total cell volume of 100 $m^3$ and consume 890 $m^3/h$ of air. In addition, an improved metallurgy performance can be expected from the DFR circuit as the DFRs are arranged in series (five stages) while the columns are installed in parallel (single stage).

**TABLE 1**

A comparison of flotation column and DFR in commercial design for copper cleaning.

| | **Column** | **DFR** |
|---|---|---|
| **Feed slurry flow rate, $m^3/h$** | 1270 | 1270 |
| **Throughput of each cell, $m^3/h$** | 318 | 1270 |
| **Required no of cells** | 4 | 5 |
| **Arrangement of cells** | In parallel | In series |
| **Total residence time, min** | 30 | 4.7 |
| **Total cell volume, $m^3$** | 830 | 100 |
| **Total air addition rate, $m^3/h$** | 2750 | 890 |

## CONCLUDING COMMENTS

The DFR has been installed and commissioned at three different mines as of July 2020, and more installations are under construction. The first DFR installation is a single unit acting as the first cell (of four) in a cleaner scavenger application at Lundin Mining's Chapada operation in Brazil. Thereafter, six DFRs have been installed at Chapada for additional flotation of rougher scavenger tailings. The second application is two stages of DFRs treating a copper cleaner circulating stream at Vale's Salobo1 concentrator. There are four DFRs in the first cleaner followed by three DFRs in the second cleaner, with the second cleaner tailings recycled to the first. The third industrial application is three DFRs operating as second cleaners in Copper Mountain Mining's cleaning circuit, which increased the copper concentrate grade from 25 per cent to 28 per cent Cu (Clausen, 2020).

The Salobo, Chapada, and Copper Mountain equipment are being optimised at the time of writing this technical paper, and future papers will provide more commercial results and scale-up assessments.

## ACKNOWLEDGEMENTS

The authors would like to acknowledge the diligence and contributions from the team of process engineers at Woodgrove who have all assisted in moving the DFR technology forward, through pilot testing, data analysis, and plant commissioning. As well, the Woodgrove design and engineering team have provided a consistent level of dedication to take the pilot plant results to operating commercial equipment. Last but not least, the collaborative support of our many clients is always critical to achieving successful technology transfer, and is recognised and most appreciated.

## REFERENCES

Araujo, A.C., Viana, P.R.M., Peres, A.E.C. (2005). Reagents in iron ores flotation. Minerals Engineering, 18, 219–224.

Clausen, G. (2020). Copper Mountain Mining Announces Commissioning of Direct Flotation Reactors at the Copper Mountain Mine. Canada NewsWire, July.

Finch, J.A., Dobby, G.S. (1990). Column Flotation, ISBN: 0–08–040186–4.

Moore, E. (2014). Underground achiever: Dundee Precious Metals took on a 50 year old mine. CIM Magazine, Sept.

Swedburg, K., Bennett, C., Samuels, M. (2016). Application of the Woodgrove Staged Flotation Reactor (SFR) Technology and the New Afton Concentrator. Proc. Canadian Mineral Processors Meeting, Ottawa, 214–223.

Swedburg, K., Bennett, C., Samuels, M., Wells, P.F. (2016). Application of the Woodgrove Staged Flotation Reactor (SFR) Technology and the New Afton Concentrator. 28th Inter. Mineral Processing Congress Proceedings, ISBN: 978–1–926872–29–2.

Ventura-Medina, E., Cilliers, J.J. (2002). A model to describe flotation performance based on physics of foams and froth image analysis. International Journal of Mineral Processing, 67, 79–99.

Yuan, D., Xie, L., Shi, X., Yi, L., Zhang, G., Zhang, H., Liu, Q., Zeng, H. (2018). Selective flotation separation of molybdenite and talc by humic substances. Minerals Engineering, 117, 34–41.

Yuan, D., Cadien, K., Liu, Q., Zeng, H. (2019). Separation of talc and molybdenite: Challenges and opportunities. Minerals Engineering, 143, 105923.

# Analysis of the Mount Isa Copper concentrate preflotation circuit using advanced diagnostic techniques

*K C Runge[1], S Brito e Abreu[2], C Evans[3] and R O'Donnell[4]*

1. Separation Group Leader, The University of Queensland, Sustainable Minerals Institute, Julius Kruttschnitt Mineral Research Centre, Indooroopilly Qld 4068. Email: k.runge@uq.edu.au
2. Research Fellow, The University of Queensland, Sustainable Minerals Institute, Julius Kruttschnitt Mineral Research Centre, Indooroopilly Qld 4068. Email: s.britoeabreu@uq.edu.au
3. Senior Research Fellow, The University of Queensland, Sustainable Minerals Institute, W.H. Bryan Mining and Geology Research Centre, Indooroopilly Qld 4068. Email: c.evans@uq.edu.au
4. Senior Metallurgist, Mount Isa Copper Concentrator, Mount Isa Mines, Mount Isa Qld 4825. Email: roxanne.odonnell@glencore.com.au

## ABSTRACT

The Mount Isa Copper concentrator employs a preflotation stage to remove naturally-floating talc prior to copper flotation. Julius Kruttschnitt Mineral Research Centre (JKMRC) researchers in collaboration with the Mount Isa metallurgical team performed a diagnostic study of this circuit with the aim of developing strategies to improve talc recovery to the preflotation concentrate while minimising copper losses. This study included a circuit survey, with samples assayed, sized and their liberation analysed using the Mineral Liberation Analyser (MLA). Batch laboratory flotation tests of key circuit streams were performed to enable development of a JKSimFloat flotation model. The surfaces of particles from the concentrate and tailings streams were analysed using Time-of-Flight Secondary Ion Mass Spectrometry (ToF-SIMS) to compare statistically the surface speciation of talc and chalcopyrite particles and determine the role of chemical speciation on flotation recovery.

The results of these various analyses indicated that talc recovery is incomplete in the circuit because talc, although liberated, is fine and floats very slowly. Copper recovered to the preflotation concentrate was primarily due to flotation (rather than entrainment) caused by residual collector in the process water attaching to chalcopyrite particle surfaces. Model simulations suggest that talc recovery could be improved by increasing preflotation roughing and cleaning capacity, but multiple stages of cleaning would be required to minimise copper recovery. Selective talc aggregation and process water modification were suggested as potential methods of improving talc recovery and talc/chalcopyrite selectivity.

This paper describes the experimental work performed and the results of sequentially applying analytical methods to diagnose circuit behaviour and demonstrates the power of combining mineralogical, modelling and surface chemical analysis to comprehensively study a flotation circuit. In this case, it enabled the particle recovery mechanisms to be determined and provided a diverse list of strategies for circuit improvement, many of which would not have been identified via a conventional circuit audit.

## INTRODUCTION

MgO is one of the major diluents in the final copper concentrate of the Mount Isa Mines copper concentrator and there is a limit to the amount of MgO that can be accepted in the concentrate due to its deleterious effect on the downstream smelter operations. Mount Isa Mines are, therefore, interested in the implementation of strategies to reduce MgO recovery in the copper concentrator. In doing so, however, it is desirable to minimise any copper lost to tailings. There are two major sources of MgO in the Mount Isa copper ores – dolomite ($CaMg(CO_3)_2$) and talc ($Mg_3Si_4O_{10}(OH)_2$) but talc is the most problematic because it floats readily without the aid of collector. Currently, MgO feeding the main copper flotation circuit is minimised through the use of a preflotation circuit where talc is recovered and removed from the flotation feed prior to the main copper rougher flotation.

JKMRC researchers in partnership with Mount Isa copper concentrator personnel conducted a circuit survey of the preflotation circuit in August 2017. The aim was to better understand the mechanisms of talc and copper recovery during preflotation so that strategies could be devised to improve performance in this section of the circuit.

This survey involved not just collection and assaying of circuit streams. Stream samples were also sized and the size fractions assayed and characterised using the Mineral Liberation Analyser (MLA) to determine modal mineralogy and particle liberation. Batch laboratory flotation tests were performed to help evaluate mechanisms of recovery and enable a JKSimFloat model to be developed of the circuit. Samples were also collected for Time-of-Flight Secondary Ion Mass Spectrometry (ToF-SIMS) analysis to compare statistically surface speciation of talc and chalcopyrite particles and determine the role of chemical speciation on flotation recovery.

This paper describes the experimental work performed and the results derived from sequentially applying analytical methods to diagnose circuit behaviour. The strategies developed to improve circuit performance will be outlined. The objective is to demonstrate the power of combining mineralogical, modelling and surface chemical analysis to comprehensively study a flotation circuit.

# EXPERIMENTAL

## Details of circuit survey

The Mount Isa preflotation circuit at the time of the audit consisted of two lines of 8 × 8.5 m$^3$ Agitair preflotation roughers and a preflotation Jameson cleaner (Figure 1). A semi-autogenous grinding (SAG) mill followed by a ball mill in closed circuit with cyclones is used to produce the feed to each flotation line. The concentrate from the two preflotation rougher lines is combined and sent to a Jameson cell for cleaner flotation. The particles which are not recovered in the Jameson cleaner are returned to the scavenger feed in the main flotation circuit. The aim is to maximise recovery of talc whilst returning what doesn't float in the Jameson cell to the main flotation circuit to minimise loss of copper to final tailings. No reagent other than MIBC and sodium cyanide is added to the preflotation rougher feed – ie no collector is added to the preflotation feed.

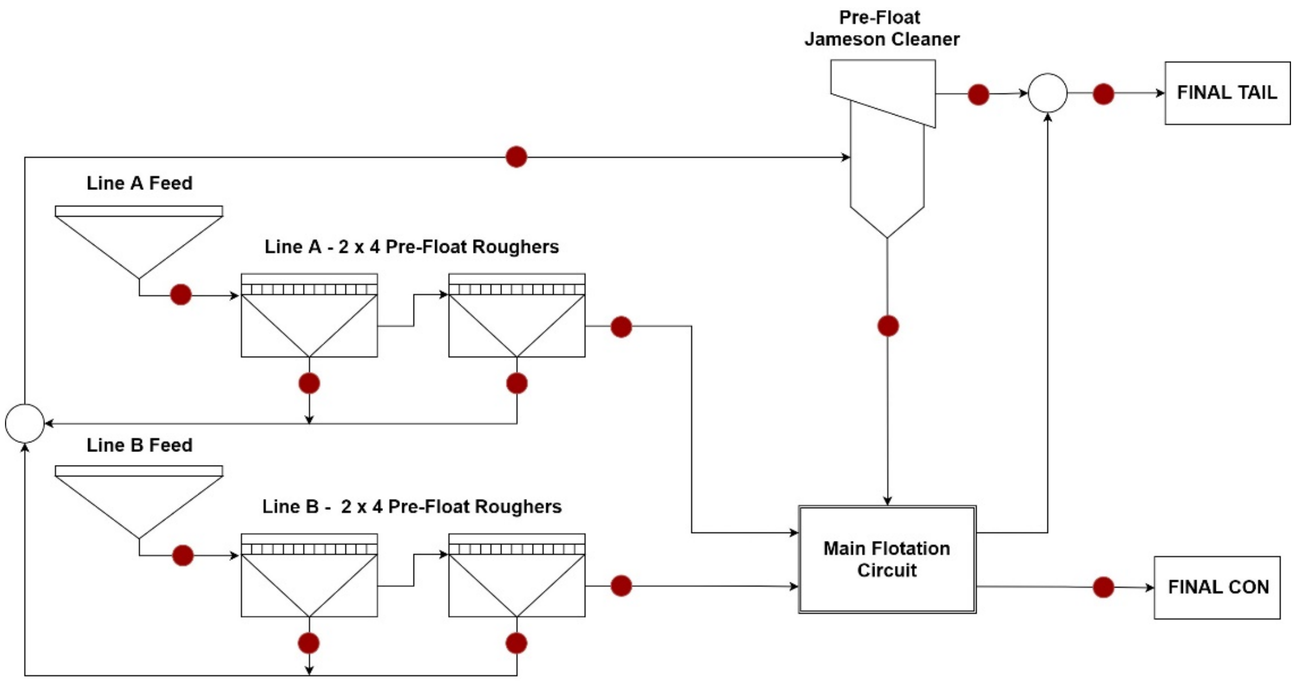


**FIG 1** – Mount Isa copper concentrator preflotation circuit denoting streams sampled during survey.

The full plant survey consisted of subsampling all the major streams from the circuit (denoted by circles on Figure 1) four times over the course of two hours. The preflotation line A and B feeds were collected by performing a manual cut using the inventory sampler. Timed concentrates were collected from the lips of the Agitair cells and combined to produce four preflotation rougher bank concentrate samples. Preflotation rougher tailings were collected using an in-pulp sampler inserted into the last cell of the 2nd preflotation rougher bank as close to the tailings plug as possible. A combined preflotation rougher concentrate was sampled from an OSA multiplexer along with the final concentrate and final tailings stream from the main flotation circuit. The concentrate from the preflotation Jameson cleaner was collected from the lip of the cell and the preflotation Jameson tailings using an in-pulp sample collected from the tailings box underneath the cell.

Samples from the circuit survey were weighed wet and dry to determine per cent solids and then rolled and divided into subsamples using a rotary sample divider. One sample was sent for head assay and another used for sizing. Sizing involved wet screening at 38 µm, with the +38 µm fraction dry screened on a √2 sieve series (from 38 to 600 µm) and the -38 µm fraction cyclosized. Size fractions were then sent for assay. All assaying was performed by Bureau Veritas in Canning Vale, Western Australia where XRF was used to determine the assay of the following elements: Cu, Fe, S, MgO, $Al_2O_3$, $SiO_2$, CaO.

Using all the information collected on the circuit survey streams (stream per cent solids, head assay and size by elemental assays) and relevant data from the Mount Isa concentrator PI data historian system (ie feed weightometer readings, water addition rates), a sized elemental based mass balance of the circuit was developed in an Excel spreadsheet.

The operating conditions at the time of the survey were representative of usual operation and all the experimental data were found to be consistent and easily mass balanced. It was concluded that the resulting data set provided an accurate representation of baseline concentrator operation. The overall circuit characteristics of the feed to the circuit, estimated by mass balancing, are outlined in Table 1.

**TABLE 1**

Summary of key mass balanced data for line 1 and line 2 flotation feed streams during baseline survey.

| Parameter | Line 1 flotation feed | Line 2 flotation feed |
|---|---|---|
| Solids feed rate (dry t/h) | 497 | 542 |
| P80 (µm) | 168 | 211 |
| Slurry density (weight % solids) | 48.6 | 54.0 |
| Copper head grade (%) | 1.85 | 1.89 |

## Mineralogical analysis

Mineralogical analysis for this study was conducted using MLA systems operated within JKMRC's Mineralogical Characterisation Research Facility. The MLA uses a unique method of combining BSE image analysis with X-ray mineral identification to provide automated quantitative mineral liberation characteristics (Gu, 2003). Information provided from a typical analysis of a size fraction includes the mineral and elemental assay, degree of mineral association and the proportion of minerals in different liberation classes. Images, which can be sorted according to mineral content, can also be viewed to enable the visual assessment of particle properties. The MLA, in summary, produces a rich source of information about the physical characteristics of the particles in the different streams of a circuit.

In the Mount Isa study, size fractions from the line 1 and 2 feed, the combined preflotation rougher concentrate, Line 1 and 2 preflotation tailings, the preflotation Jameson cell concentrate and the preflotation Jameson cell tailings were submitted for MLA analysis. To reduce the number of samples requiring mineralogical analysis in each stream some size fractions were combined, resulting in the following size fraction combinations: +425 µm, -425 +212 µm, -212 +106 µm, -106 +53 µm, -53 +38 µm, CS1 and CS2, CS3 to CS5 and -CS5. It should be noted that although the samples for MLA are not deslimed, a minimum grain size is set during measurement to ensure that only particles larger than the interaction volume of the beam are measured. Thus, particles smaller than about 2 microns do not get measured.

The information provided by MLA enabled the mineral assay by size to be determined in the streams analysed. Particles were also able to be binned to determine the proportion of a mineral in a stream in different mineralogical association classes (eg liberated chalcopyrite, liberated talc, liberated iron sulphides, liberated gangue, chalcopyrite/talc binaries, chalcopyrite/iron sulphide binaries, chalcopyrite/talc/iron sulphide ternaries etc). This liberation data exhibited sufficient consistency to be able to be mass balanced. What resulted was a comprehensive mineral by mineralogical class mass balance that could be interrogated to better understand the recovery mechanisms within the circuit.

## Batch laboratory flotation testing

JKMRC recommends that batch laboratory flotation tests of major streams in a circuit be performed during flotation surveys. These tests should be performed using the same operating conditions and no reagent addition so they can be directly compared to each other to enable an assessment of ore floatability, independently of cell operation. This batch test information complements the survey information by allowing:

- The development of floatability component circuit models where ore floatability is decoupled from cell operating variables. These models can be used to simulate alternative circuit flow sheets.
- Diagnosis of flotation mechanisms. It allows the degree to which a mineral in a concentrate has been recovered by entrainment or by natural floatability in the preceding banks of the circuit to be determined. It also provides an assessment of whether minerals in a feed or a tailings stream are floatable, and thus recoverable if provided additional residence time.
- A determination of the effectiveness of ore floatability modification strategies (eg regrinding, reagent addition) by enabling comparison of floatability before and after these processes (Runge *et al,* 2003).

For more details on how to perform and analyse information from these types of ore floatability characterisation tests, the reader is referred to Runge (2010).

During the Mount Isa preflotation circuit survey, samples of the combined preflotation rougher concentrate and preflotation rougher tailings were collected and subjected to a laboratory batch flotation test. These tests were performed in an Agitair 5L batch flotation cell operated at a high air rate, fixed scraping rate and minimal froth depth to minimise impact of the froth phase. No reagents were added to the cell during the test, other than frother which was dosed at 30 μL/litre in the process water added to maintain a constant froth level. Throughout each experiment, six concentrates were collected over designated time intervals. These concentrates and the tailings from each test were weighed wet and dry and submitted for assay.

Data from these tests were used to assess the copper and talc recovery mechanisms in the circuit. They were also used, in conjunction with the circuit survey information, to develop a floatability component model of the preflotation circuit using methods outlined by Harris *et al* (2002). This model was set-up in JKSimFloat and used to simulate alternative circuit flow sheet arrangements.

## Time-of-flight secondary ion mass spectrometry

Time-of-Flight Secondary Ion Mass Spectrometry (ToF-SIMS) is a surface sensitive analytical technique that uses a pulsed ion beam to remove ion species from the very outermost surface of a particle (secondary ions) which are subsequently analysed by a mass spectrometer, providing information about the chemical composition and its distribution on the particle surface (Vickerman, 2001). The University of South Australia has pioneered the use of this technique to characterise the surface speciation of mineral processing samples in Australia. Wet samples are loaded into the instrument under vacuum and spectral data from mineral particles are collected. Advanced statistical analysis (eg Principal Component Analysis) can then be applied to analyse the mass spectra and identify patterns in surface chemistry and reduce the data to a smaller number of key ToF-SIMS signals (Brito e Abreu *et al,* 2010). When applied to streams collected during a flotation circuit survey, this can be used to identify the major surface species (ie ToF-SIMS ion signals) differing between the concentrate and tailings streams, providing insights into what is promoting or inhibiting flotation.

To characterise the chemical speciation of the streams within the Mount Isa copper concentrator preflotation circuit, samples were collected from the preflotation rougher concentrate, preflotation rougher tailings, preflotation Jameson cleaner concentrate and preflotation Jameson cleaner tailings. These samples were placed in vials and immediately snap frozen using liquid nitrogen. They were transported to the University of South Australia where they were defrosted and deslimed prior to analysis to remove ultra-fine/colloidal particles from the pulp. The procedure involved diluting the slurry in Milli-Q water adjusted to pH 8 with NaOH (same pH as in the plant) and removing the fine material from the supernatant which could otherwise physically adsorb on the particle surfaces. A small subsample of the solids of each sample was then loaded into the ToF-SIMS instrument. In the order of 10 to 20 chalcopyrite and talc particles were then identified and ToF-SIMS individual spectral information collected. The spectra of the concentrate and tailings of the preflotation rougher and the Jameson cleaner were then statistically compared to determine the surface species primarily responsible for the observed flotation behaviour.

It should be noted that the stream samples collected for ToF-SIMS were not collected during the circuit surveying campaign described above but 11 months later. Circuit operation during the time of this subsequent sampling, however, had been set-up to be similar to the original survey and mineral recoveries were found to be similar, providing confidence that any conclusions drawn from this later survey would be applicable to interpreting the results from the earlier survey.

# RESULTS

## Talc metallurgical performance

The purpose of the preflotation circuit is to remove talc prior to copper flotation so that MgO recovery to the final concentrate can be minimised. Talc was only found to comprise 22.7 per cent of the MgO in the combined feed to the circuit but comprised 78 per cent of the MgO reporting to final concentrate (Figure 2). This highlights the importance of removing talc prior to copper flotation in order to minimise MgO final concentrate contamination.

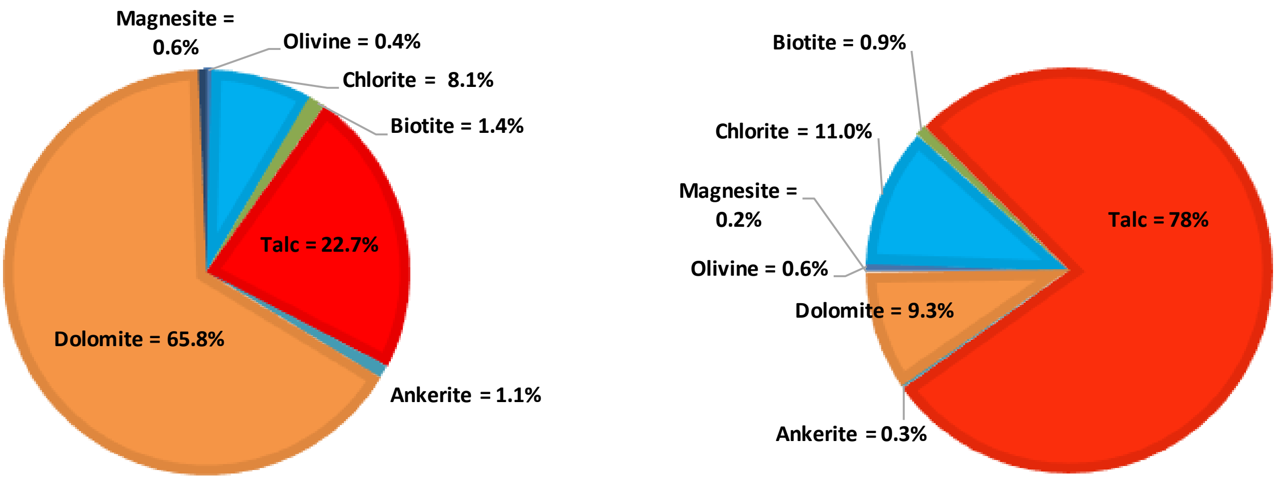


**FIG 2** – Distribution of MgO in the minerals of the combined feed and the final concentrate.

The mineral balance that was developed using the MLA data, enabled the talc to be tracked around the circuit, independently of other sources of MgO (eg dolomite). Figure 3 shows the talc distribution across the circuit estimated using mass balancing, based on 100 units in the feed. The preflotation rougher recovers 32.3 per cent of the talc in the feed but only half of this is recovered in the preflotation Jameson cleaner, with a significant proportion recycled back to copper flotation.

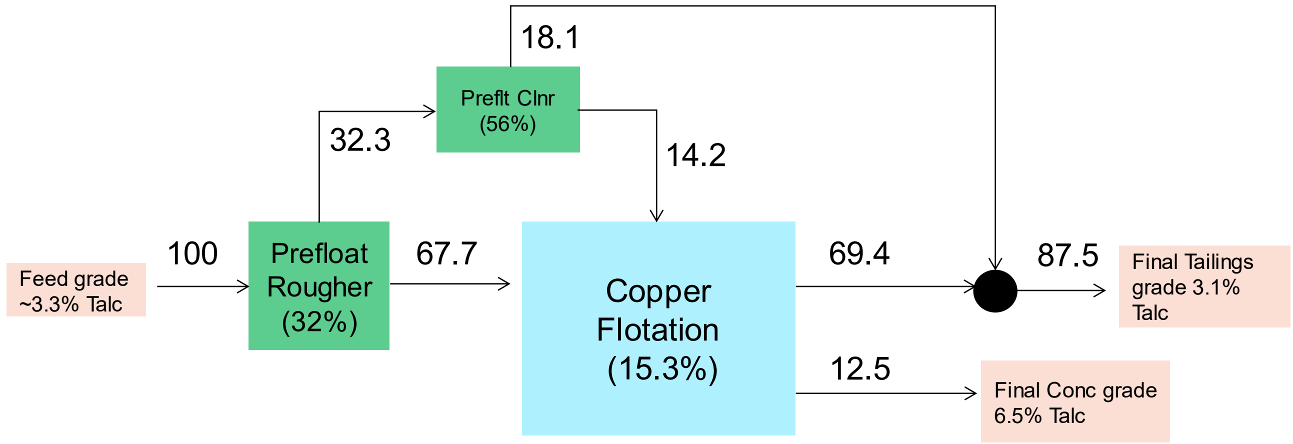


**FIG 3** – Distribution of talc in the key streams of the process based on 100 units in feed.

Talc is a naturally hydrophobic mineral and is therefore easily floatable. It was found to be largely very fine in nature, with over 50 per cent of the talc in the feed being less than 10 µm in size (ie -CS5 in Figure 4). Very fine particles will float slowly because of poor probabilities of collision with bubbles. Talc floats in the preflotation rougher with a size versus recovery profile indicative of a naturally floating mineral, with recovery optimal in the intermediate particle sizes (Figure 4). When refloated in the preflotation Jameson cleaner, the recovery of talc in all particle sizes is incomplete but increases with particle size. This suggests that the Jameson cell is undersized for this cleaning duty.

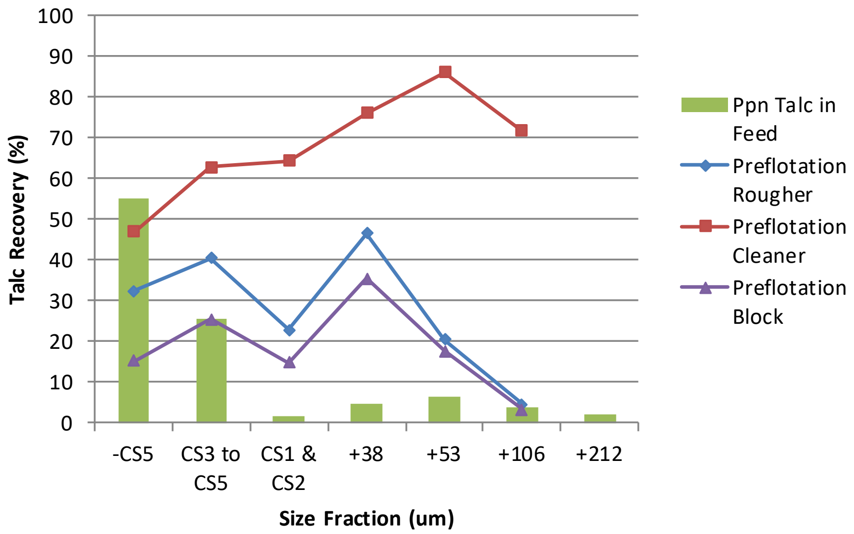


**FIG 4** – Proportion of talc in the circuit feed and talc recovery in the preflotation cells as a function of particle size.

The liberation characteristics of the talc reporting to the final concentrate are shown in Figure 5. This talc is largely liberated or locked in ternaries with other gangue minerals. The talc was also very fine in nature with over 80 per cent of the material finer than the CS3 size fraction (approximately 20 µm). This finding is expected because of the fine nature of the talc in the feed (Figure 4). An examination of the recovery of different mineralogical classes showed that an association with chalcopyrite does not enhance the floatability of talc. This is expected as the chalcopyrite in the preflotation rougher is largely not floatable. Interestingly, talc locked with gangue exhibited much lower recoveries than talc locked with chalcopyrite or iron sulphide minerals.

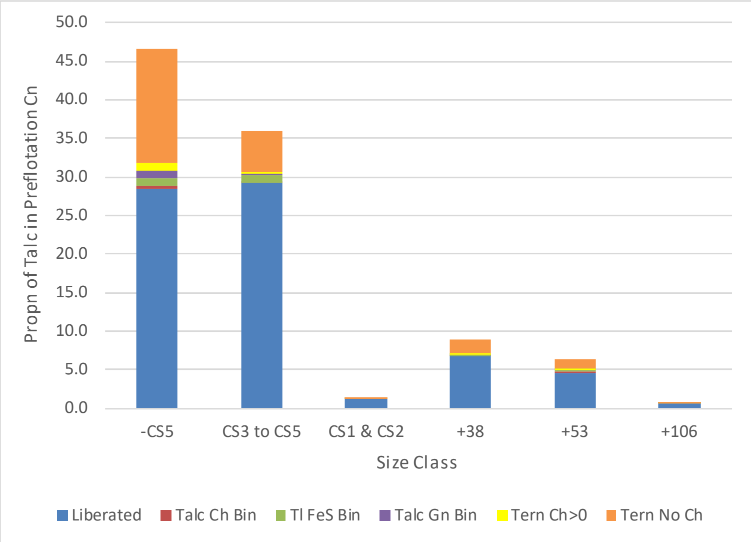


**FIG 5** – Liberation characteristics of talc in the Jameson preflotation cleaner concentrate.

The talc mineralogy results are consistent with that expected – talc is naturally floatable and is reporting primarily to the preflotation concentrate due to its natural floatability. It will, however, be floating slowly because it is very fine in size.

## Analysis of copper recovery during preflotation

It is important that copper recovery is minimised when removing talc in the preflotation stage in order to maximise copper recovery to final concentrate in the main flotation circuit. Copper is primarily present as chalcopyrite in the Mount Isa feed. On the day of the survey, the feed assayed 1.9 per cent copper which equates to 5.4 per cent chalcopyrite. Of this copper in the feed, 1.6 per cent was recovered into the Jameson preflotation rougher concentrate. This quantity of copper lost during preflotation would be unacceptable so, fortunately, copper recovery across the preflotation Jameson cell was only 25 per cent, resulting in overall copper loss across the entire preflotation block of 0.4 per cent.

The chalcopyrite recovered to the preflotation Jameson concentrate is very fine in nature with over 65 per cent in the -CS5 size fraction (<10 μm) and MLA analysis indicates that it is largely liberated (75 per cent), with the proportion locked with talc being very small (<10 per cent) (Figure 6). Therefore, it is concluded that chalcopyrite recovered in the Jameson cell is not a consequence of being in composite particles with a floatable species (talc) but rather reporting through a flotation mechanism.

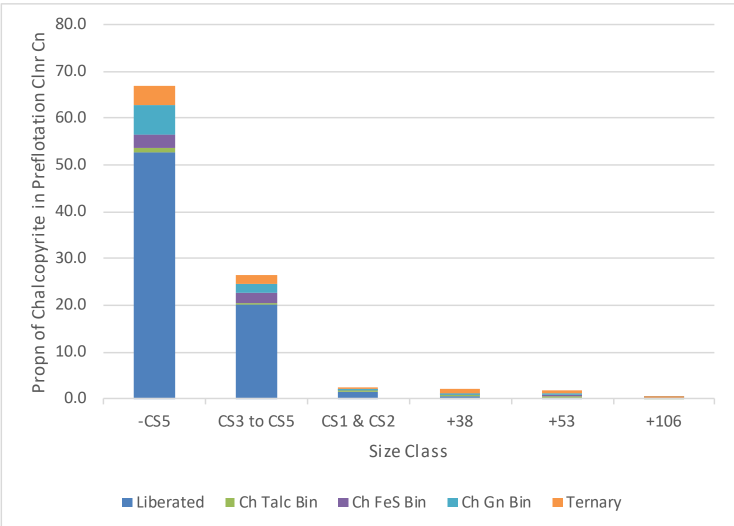


**FIG 6** – Characteristics of chalcopyrite in the Jameson preflotation cleaner concentrate estimated by mass balancing.

Chalcopyrite recovery in the preflotation rougher is optimal in the very finest size (-CS5) and it has been previously concluded in past surveys that chalcopyrite was being recovered predominantly by entrainment in this bank. The batch laboratory flotation test of the preflotation rougher concentrate would tend to dispute this assumption. Chalcopyrite (or the copper) present in this stream was found to float at a reasonable rate and was recovered to a much greater extent than the maximum it was expected to be recovered if carried over in the water phase by entrainment at the same concentration as in the pulp (Figure 7). The ToF-SIMS analysis to be presented below also suggests that the chalcopyrite recovered in the circuit has surface species that would render the surface floatable. It was, therefore, concluded that chalcopyrite lost in the preflotation circuit was recovered as a consequence of exhibiting natural flotation characteristics.

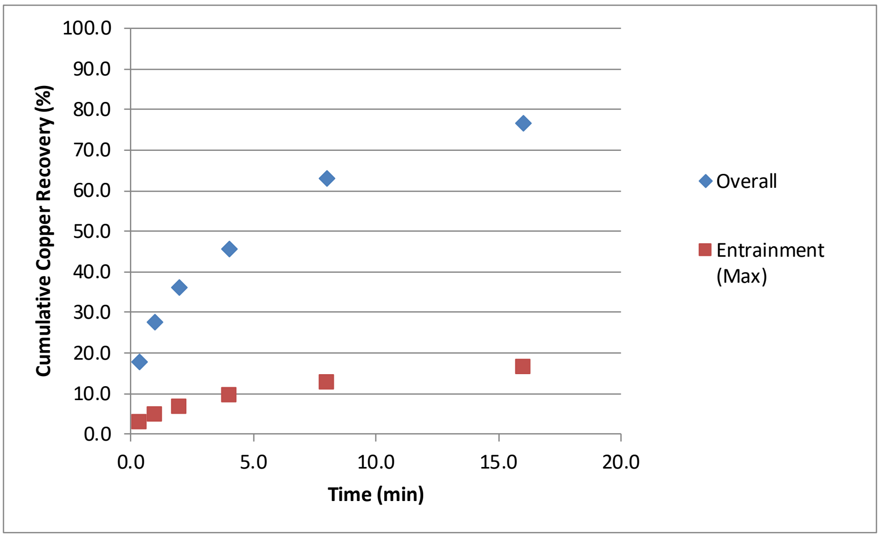


**FIG 7** – Copper recovery as a function of time achieved in a batch flotation test of the preflotation rougher concentrate (including an estimate of the maximum recovery by entrainment).

If chalcopyrite recovery was primarily by entrainment in the preflotation rougher, then preflotation in a Jameson cell (which operates with a deep froth depth and froth washing) should be sufficient to minimise copper recovery and maximise talc/chalcopyrite selectivity in the circuit. The fact that chalcopyrite is floating, makes separation more difficult and opens up the possibility of exploring alternative chemical regimes and/or circuit arrangements to achieve improved talc/chalcopyrite selectivity.

## Circuit simulation results

The preflotation circuit flotation model that was developed and set-up in JKSimFloat was capable of predicting the elemental grades and recoveries of copper, iron, sulphur, MgO and silica in the circuit with a change in feed flow rate, circuit configuration or circuit capacity. The cell recovery rate can also be varied, representing an operator changing the air rate or froth depth to increase or decrease the flow from a particular cell.

Simulations were performed in which additional rougher and cleaner capacity was added to the existing circuit configuration, as depicted in Figure 1. Two stages of cleaning were also simulated. In the two-stage circuit configuration, the preflotation cleaner Jameson concentrate was diverted to a 2nd preflotation Jameson cell, the concentrate of which was sent to final tailings and the tailings of which recycled back to the 1st preflotation cleaner feed (Figure 8). The MgO versus the copper recovery achieved in these various simulations is shown in Figure 9, with the baseline performance circled.

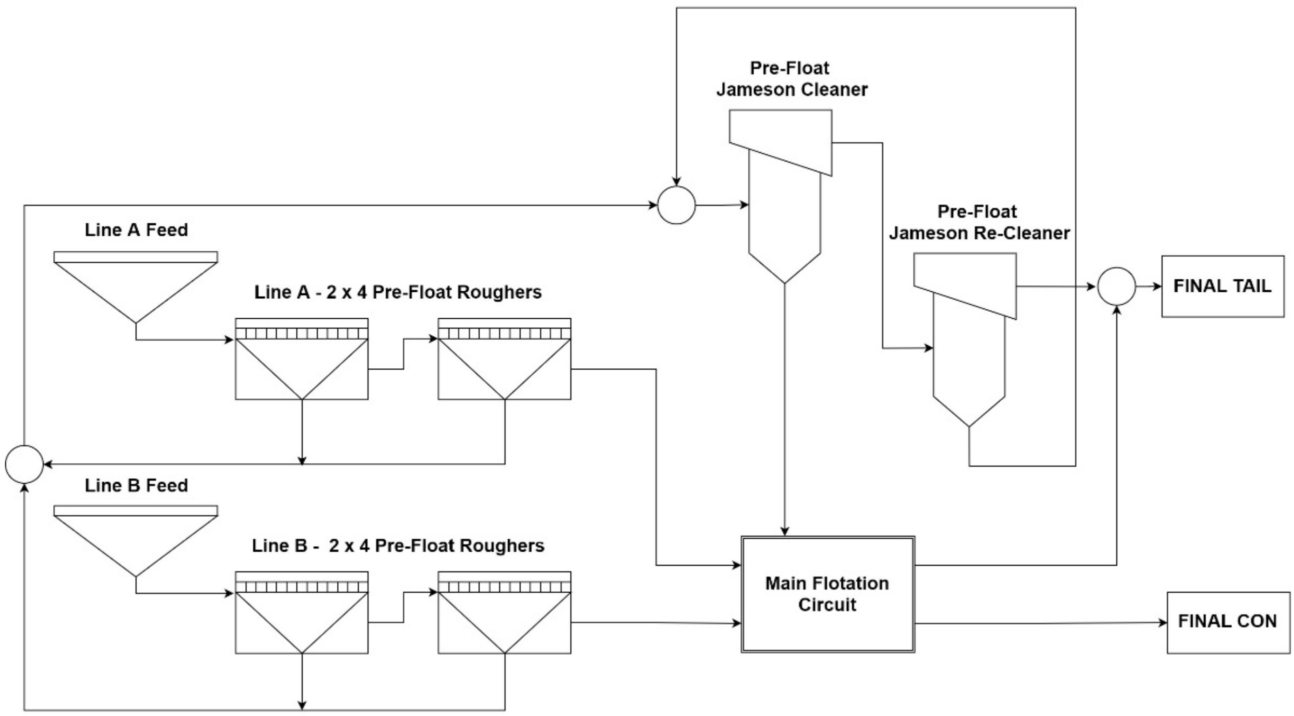


**FIG 8** – Mount Isa copper concentrator preflotation circuit incorporating two stages of cleaning which was simulated using JKSimFloat.

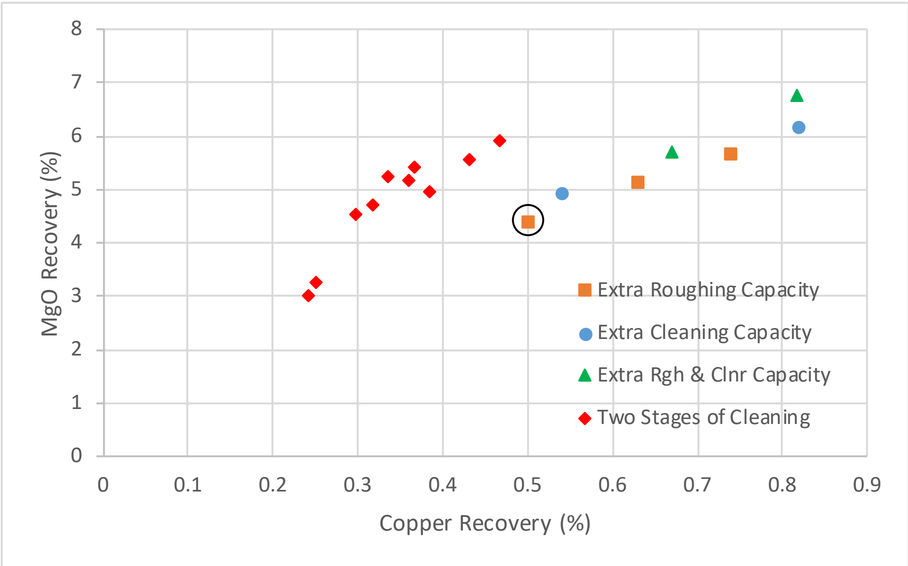


**FIG 9** – Copper versus MgO recovery achieved in circuit simulations performed using one or two stages of Jameson cleaning (baseline condition has been circled).

Increasing flotation capacity in either the preflotation rougher stage or the preflotation cleaners both indicate a potential to increase MgO recovery. The magnitude of additional MgO recovery achievable in the circuit seems relatively low but one should take into account that the 4.4 per cent MgO recovery measured in the baseline survey was equivalent to 18 per cent talc recovery. Assuming that this ratio remained relatively constant, it is concluded that there is the potential to remove 10 per cent more of the floatable talc prior to flotation during preflotation by adding capacity. A flotation capacity increase can be achieved either by the addition of new or bigger cells or through modification of cell operation to increase cell recovery rates. For example, Mount Isa mines have the ability to run a third line of roughers to increase preflotation rougher capacity under certain feed grade conditions.

Unfortunately, an increase in MgO recovery due to a capacity increase is predicted to be associated with an increase in copper recovery to the preflotation concentrate. It is predicted that for every

1 per cent increase in MgO recovery, the copper lost during preflotation would increase by 0.2 per cent.

Simulations suggest, however, that an improvement in talc/chalcopyrite selectivity is achievable if a two-stage preflotation cleaning arrangement is employed. By utilising this type of arrangement, copper recovery is halved at a particular MgO recovery. The improved selectivity is a consequence of less entrainment recovery in a two-stage flotation arrangement and because chalcopyrite floats more slowly than talc in the preflotation rougher concentrate (Figure 10). A two-stage cleaning arrangement enables a sharper separation efficiency to be achieved in the circuit and therefore better selectivity between fast and slow floating species.

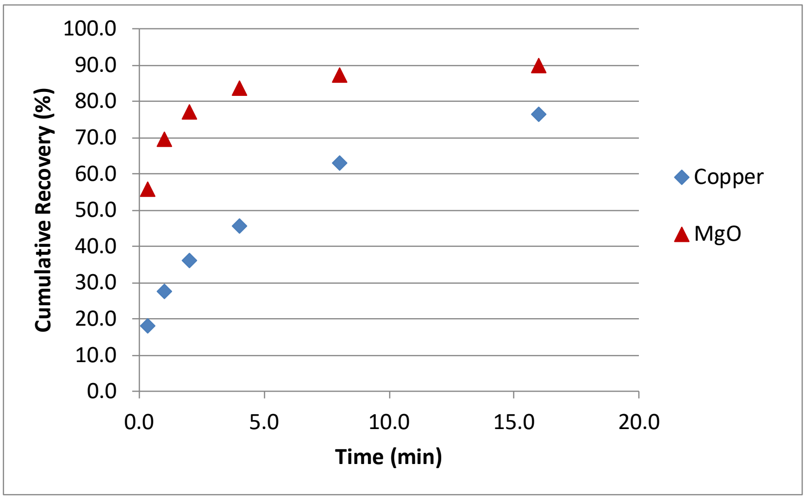


**FIG 10** – Copper and MgO recovery as a function of time achieved in a batch flotation test of the preflotation rougher concentrate.

## ToF-SIMS analysis

The ToF-SIMS spectral images collected from the preflotation rougher and preflotation Jameson cleaner streams were analysed using principal component analysis to identify differences, in surface chemistry, between the talc and chalcopyrite that were present in the concentrates and tailings of the preflotation cells.

In terms of the chalcopyrite, there were only subtle differences observed in surface speciation on these particles in the preflotation rougher concentrate and tailings. In contrast, there were two distinctly different populations identified for the chalcopyrite in the concentrate and tailings of the Jameson cleaner. The chalcopyrite that floated in the preflotation Jameson cleaner showed higher levels of collector, cyanide and dextrin adsorbed on the surface compared to the tailings. The signals of the chemical species associated with these reagents and their distribution across the concentrate and tailings samples are presented in Figure 11. More subtle differences were also detected in the Mg and Fe signals (higher intensities in the tailings), suggesting cleaner surfaces in the concentrate particles (ie less contamination from the gangue).

It was, therefore, concluded that it was reagent on the surfaces of the chalcopyrite that had rendered it sufficiently hydrophobic to be recovered by flotation. With these reagents not being added to the preflotation rougher feed, it was concluded that residual reagent in the recycled process water was likely responsible. The distinctly different surface chemistry between the concentrate and tailings was also further evidence that the copper recovered during preflotation is not due to entrainment but bubble-particle collection.

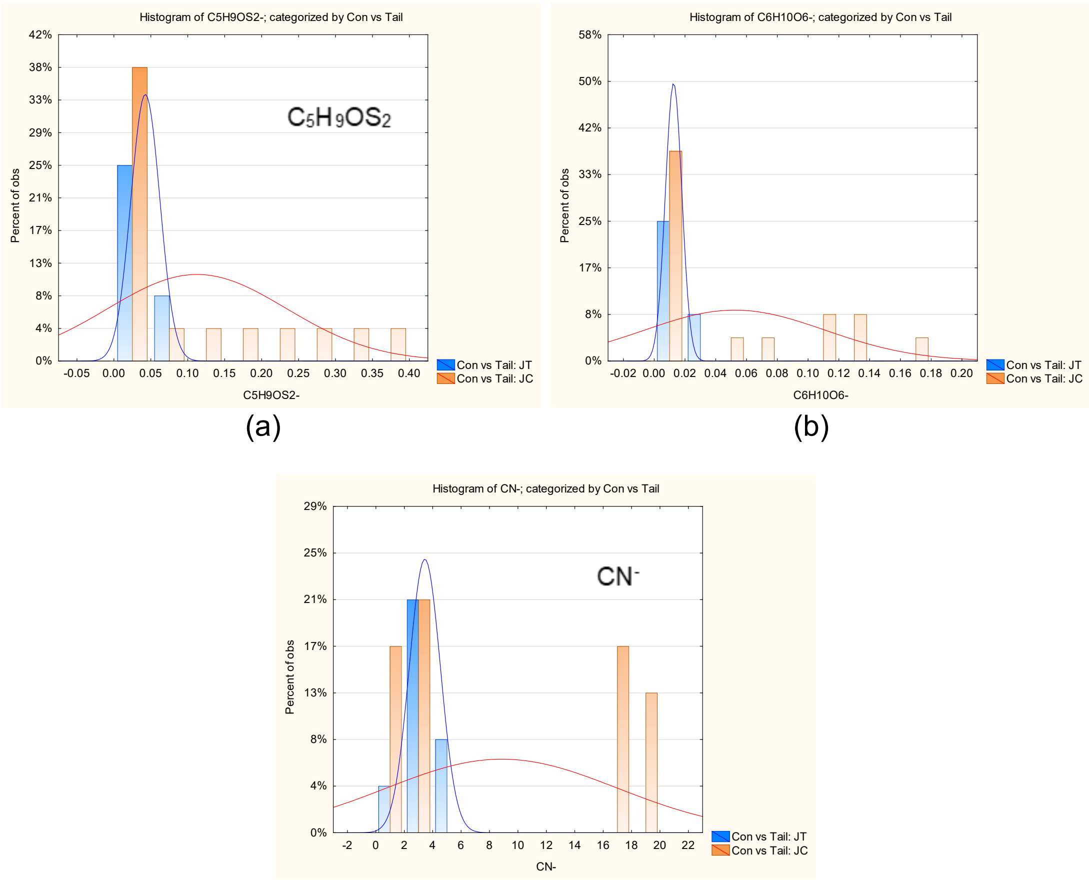


(a) (b)

(c)

**FIG 11** – Histogram of key ToF-SIMS signals differing between the chalcopyrite particles in the Jameson concentrate (JC) and tailings (JT) (a) $C_5H_9OS_2$ (SIBX Collector) (b) $C_6H_{10}O_6$ (Dextrin) and (c) CN (Cyanide).

A t-test was performed to determine whether differences in the chemical speciation between the concentrate and tailing could be proved statistically. Table 2 shows the results of this statistical analysis. Although the probability that the speciation is different is high (ie 88 to 93 per cent), it was not able to be proven at the usual benchmark of 95 per cent confidence. One of the potential reasons for this outcome is that the tailing stream results are not normally distributed and there may be two populations of particles within the tailing stream (Figure 11). This results in the variances within the groups not being of similar magnitudes (the tail has a much larger variance than the concentrate). These are assumptions required for the t-test which are not met. In future test work of this type, it is recommended that a larger number of particles be measured so that these statistical problems can be overcome.

**TABLE 2**

T-test for the difference between the mean ToF-SIMS signal intensities for the chalcopyrite particles in the preflotation Jameson concentrate (JC) and tail (JT) streams. T-value: the statistical value of the t-test for the difference between two groups; p: the probability that the two groups have the same mean.

| **ToF-SIMS signals** | **JT** | | **JC** | | **t-test statistics** | |
|---|---|---|---|---|---|---|
| | **Mean** | **Std Dev** | **Mean** | **Std Dev** | **t-value** | **p** |
| $C_5H_9OS_2^-$ | 0.042 | 0.020 | 0.112 | 0.120 | -1.610 | 0.1216 |
| $C_6H_{10}O_6^-$ | 0.012 | 0.005 | 0.052 | 0.058 | -1.887 | 0.0724 |
| $CN^-$ | 3.415 | 1.088 | 8.805 | 8.091 | -1.855 | 0.0770 |

The talc particles also showed distinctly different patterns of surface chemistry between the preflotation Jameson concentrate and tailings streams. The key surface species (ToF-SIMS signals) differentiating between these two groups of talc particles fall into two groups: (1) collector and cyanide species; and (2) hydrophilic/gangue coverage. The first group is an interesting observation, since it shows that the collector (present in the processing water) and cyanide (being added to the preflotation rougher) are interacting and forming an insoluble complex $(Cu\text{-}X)_2^+(CN^-)_2$ on the talc surface, increasing the natural hydrophobicity of talc, and hence, its floatability. This is evident by the higher intensities of these signals on the concentrate particles (Figure 12a–12c) compared to the tailings. The second type of species relate to the presence of hydrophilic gangue coverage on talc particles. It was found that the tailing particles have a higher intensity of $MgCO_2$, $MgOH_2$ and OH signals compared to the concentrate (Figure 12f–12h). The higher coverage of these hydrophilic species is likely causing a depressing effect. It was also found that the concentrate particles have a lower intensity of MgSiOH and a higher intensity of MgO (Figure 12d–12e). The t-test statistics for the differences in the surface species between the concentrate and tail are listed in Table 3. In this case, in contrast to the chalcopyrite results, the differences in the means are highly significant.

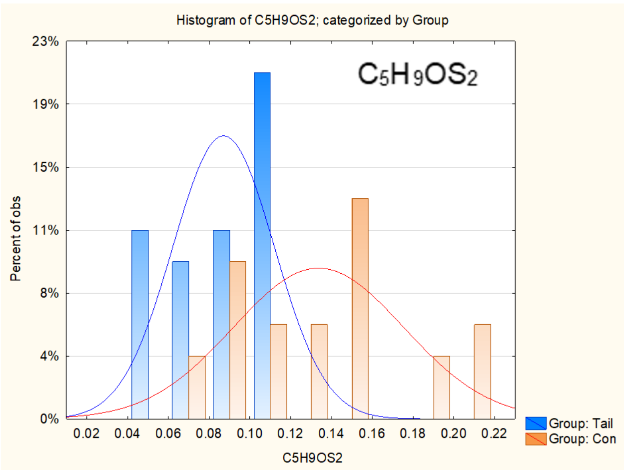


(a)

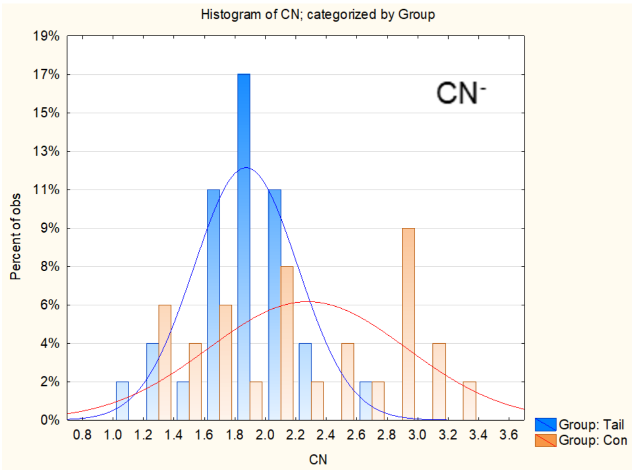


(b)

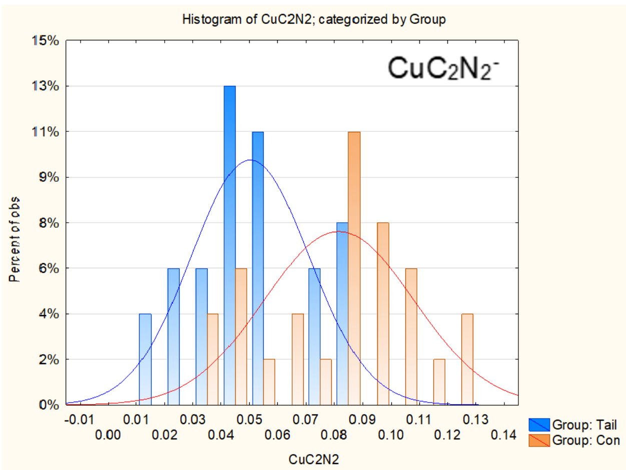


(c)

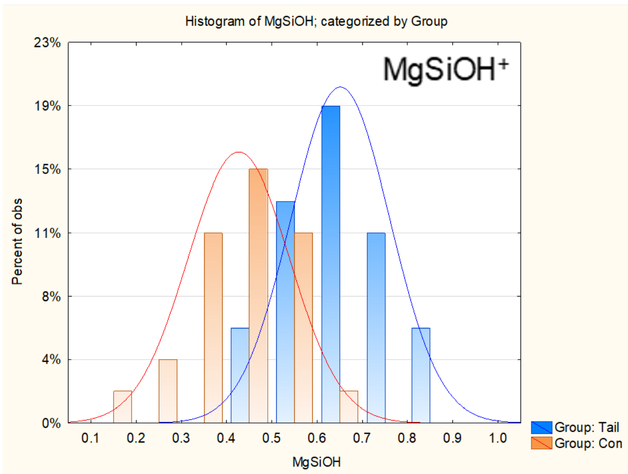


(d)

**FIG 12** – continued on next page…

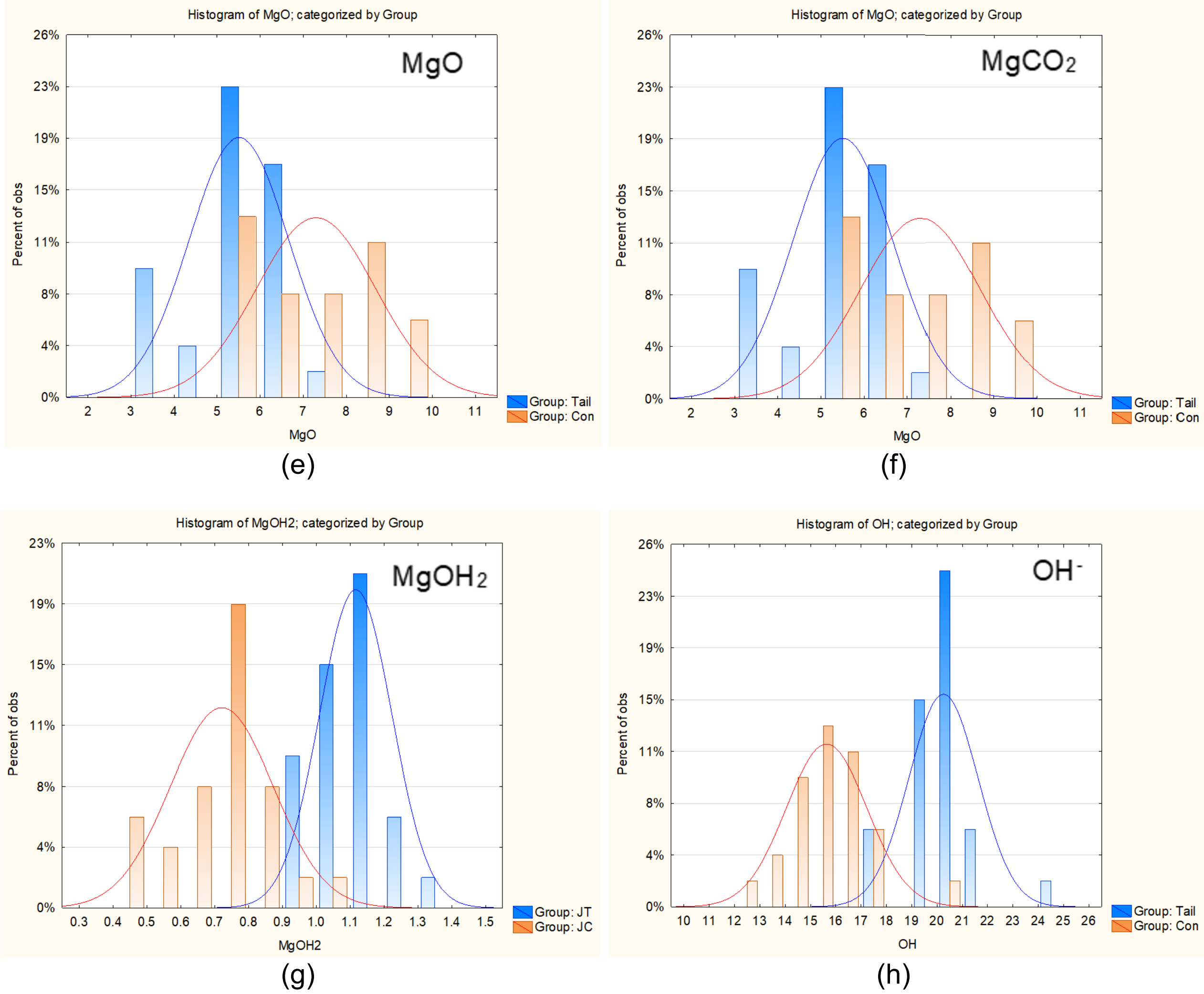


**FIG 12** – Histogram of key ToF-SIMS signals differing between the talc particles in the Jameson concentrate (JC) and tailings (JT): (a) $C_5H_9OS_2$, (b) CN, (c) $CuC_2N_2$, (d) MgSiOH, (e) MgO, (f) $MgCO_2$, (g) $MgOH_2$ and (h) OH.

**TABLE 3**

T-test for the difference between the mean ToF-SIMS signal intensities for the talc particles in the preflotation Jameson concentrate (JC) and tail (JT) streams. T-value: the statistical value of the t-test for the difference between two groups; p: the probability that the two groups have the same mean.

| ToF-SIMS signals | JT | | JC | | t-test statistics | |
|---|---|---|---|---|---|---|
| | Mean | Std dev | Mean | Std dev | t-value | p |
| MgO | 5.407 | 1.091 | 7.285 | 1.351 | -5.592 | 0.000001 |
| MgSiOH | 0.651 | 0.110 | 0.431 | 0.114 | 7.158 | 0.000000 |
| $MgCO_2$ | 0.283 | 0.046 | 0.189 | 0.037 | 8.214 | 0.000000 |
| OH | 20.201 | 1.360 | 15.606 | 1.585 | 11.359 | 0.000000 |
| $MgOH_2$ | 1.112 | 0.107 | 0.719 | 0.152 | 11.022 | 0.000000 |
| $C_5H_9OS_2$ | 0.087 | 0.025 | 0.133 | 0.042 | -4.980 | 0.000008 |
| $CuC_2N_2$ | 0.050 | 0.021 | 0.081 | 0.026 | -4.828 | 0.000013 |
| $CN^-$ | 1.867 | 0.340 | 2.269 | 0.647 | -2.874 | 0.005901 |

The conclusion from the TOF-SIMS analysis is that the presence of collector in the residual process water has increased the floatability of talc, but also enhanced the floatability of chalcopyrite, therefore, affecting the chalcopyrite/talc selectivity in the preflotation circuit.

## STRATEGIES FOR IMPROVING PERFORMANCE OF THE PREFLOTATION CIRCUIT

Talc recovery during preflotation prior to flotation is relatively modest (12 per cent). The analysis performed from data collected during the preflotation circuit survey outlined in this paper can be used to devise a number of avenues by which talc recovery might be increased. These include:

- Increasing preflotation circuit capacity. Simulations suggest that another 10 per cent of talc recovery may be possible during preflotation if additional capacity was installed or the recovery rates of the existing cells could be increased.
- Increasing talc recovery rates through agglomeration. Talc floats slowly because it is very fine in nature. There may be opportunities to agglomerate the fine talc by adjusting pH and/or using suitable agglomerating reagents. There is a risk of entrapment of chalcopyrite if performed in the preflotation rougher so it may be better to agglomerate the talc prior to preflotation cleaning.
- Increasing talc floatability by minimising surface contamination. Use of high chrome balls during grinding may result in less hydrophilic species on the talc surfaces which have been observed to preferentially be coating talc in the tailings of the Jameson preflotation cleaner.
- Higher Intensity Flotation. Talc is very fine and floats very slowly in conventional flotation cells. Due to its ability to create finer bubbles and high bubble particle contact in the downcomer, the Jameson cell technology may be better suited to recovering the fine talc particles in the circuit feed. Installation of a Jameson cell, prior to the Agitair roughers could increase talc preflotation rougher recovery rates.

Whilst there are many advantages to increasing talc recovery prior to flotation, the benefit is much reduced if it is also associated with unacceptable losses of chalcopyrite to the final tailings via the preflotation circuit concentrate. Strategies identified which might reduce chalcopyrite loss to preflotation concentrate include:

- Two stage cleaning of the preflotation rougher concentrate. It is estimated that chalcopyrite recovery can be halved (for a particular MgO recovery during preflotation) by utilising two stages of preflotation cleaning.
- Reduce the residual collector in the process water. Residual collector has been shown to be a mechanism by which chalcopyrite is rendered floatable and, thus, recovered during preflotation. There may be opportunities to minimise this residual collector by increasing the time for the residual reagent to breakdown before the process water is recycled back for use in the process. Heating of the process water (to temperatures exceeding 50°C) could be employed to accelerate this rate of reagent breakdown.
- Depress chalcopyrite in the preflotation Jameson cleaner by adding cyanide to the cell. Cyanide addition is expected to increase the solubility of the Cu-cyanide-collector complex and decrease chalcopyrite hydrophobicity. This may likely decrease the induced hydrophobicity of talc as well through the same mechanism; however, the selectivity may improve.

Since this preflotation audit has been completed, the Mount Isa Mines copper concentrator has increased both preflotation rougher and cleaner capacity and have also changed to using high chrome balls as a grinding media. Additional auditing is planned to evaluate the effectiveness of these circuit modifications. Laboratory testing is also planned to evaluate whether talc agglomeration or removal of residual collector from the process water are viable process strategies.

## CONCLUSIONS

A comprehensive circuit survey was performed of Mount Isa's talc preflotation circuit. This audit did not just involve collecting and assaying the process streams but also included detailed mineralogical characterisation, laboratory batch flotation of circuit streams and ToF-SIMS analysis to investigate talc and chalcopyrite surface chemistry. These measurements have enabled a detailed characterisation of circuit performance to be completed, allowing quantification of the talc and chalcopyrite floatability characteristics and the identification of a number of strategies that could be used to achieve circuit improvement. Many of these strategies would not have been identified via a conventional circuit audit.

What often prevents Metallurgists from undertaking such detailed analyses is the time that is required for all the test work to be completed and analysed. This can result in solutions being devised for problems that no longer exist because of changes in feed ore properties. There is also the lost opportunity for revenue during the time taken to devise the improvement strategies. Development of tools that can provide this kind of detailed analysis in a more timely fashion is a focus of future research at the JKMRC.


## ACKNOWLEDGEMENTS

The authors would like to acknowledge the large number of Mount Isa and JKMRC personnel that were involved in the circuit audit and subsequent sample processing. This includes JKMRC researchers and students and Mount Isa personnel involved in the circuit surveys and the JKMRC pilot plant staff and MLA mineralogical technicians who were involved in sample processing. Glencore's Mount Isa operation is also thanked for giving permission for publication of this study. Dr Alex Cavallaro (University of South Australia) is also thanked for helping with the ToF-SIMS analysis.


## REFERENCES


Brito e Abreu, S., Brien, C., Skinner, W., ToF-SIMS as a New Method to Determine the Contact Angle of Mineral Surfaces. Langmuir, 2010, *26*(11), 8122–8130.

Gu, Y., 2003. Automated Scanning Electron Microscope Based Mineral Liberation Analysis – An Introduction to JKMRC/FEI Mineral Liberation Analyser. Journal of Minerals & Materials Characterization & Engineering, 2 (1), 33–41.

Harris, M. C., Runge, K. C., Whiten, W. J. and Morrison, R. D. (2002). JKSimFloat as a practical tool for flotation process design and optimisation. In: Andrew L. Mular, Doug N. Halbe and Derek L. Barratt, Mineral Processing Plant Design Practice and Control: Proceedings. Mineral Processing Plant Design Practice and Control Conference, Vancouver, B.C., Canada, 20–24 October 2002, 461–478.

Runge, K.C., 2010. Laboratory flotation testing – An essential tool for ore characterisation. In: *Flotation Plant Optimisation: A Metallurgical Guide to Identifying and Solving Problems in Flotation Plants*. Edited by C.J. Greet. Melbourne, Victoria: Australasian Institute of Mining and Metallurgy, 155–173.

Runge, K. C., Manlapig, E. and Franzidis, J.-P. (2004). Optimisation of flotation pulp selectivity utilising nodal analysis. In: Steve Wilson (Conference Chairman), Proceedings of the 36th Annual Meeting of the Canadian Mineral Processors. 36th Annual Meeting of the CMP, Ottawa, Canada, (575–598). 20–22 January, 2004.

Vickerman, JC, 2001. ToF-SIMS: surface analysis by mass spectrometry, IM Publications and Surface Spectra Limited, Manchester, UK.

# Overcoming rougher residence time limitations in the rougher flotation bank at Red Chris Mine

*D R Seaman[1], K Li[2], G Lamson[3], B A Seaman[4] and M H Adams[5]*

1. Principal Metallurgist, Newcrest Mining Limited, Perth WA 6008.
   Email: david.seaman@newcrest.com.au
2. Senior Project and Tailings Metallurgist, Newcrest Red Chris JV, Canada.
   Email: kevin.li@newcrest.com.au
3. Senior Metallurgist, Newcrest Red Chris JV, Canada. Email: graeme.lamson@newcrest.com.au
4. Principal Metallurgist, Newcrest Mining Limited, Perth WA 6008.
   Email: brigitte.seaman@newcrest.com.au
5. General Manager Red Chris JV/Vice President Canadian Operations, Newcrest, Canada.

## ABSTRACT

Red Chis Mine, operated by Newcrest Mining Ltd, is a copper-gold mine located in Northern British Columbia, Canada. The process plant produces an auriferous-copper concentrate for sale to smelters and generates two tailings streams, a non-acid generating (NAG) stream and a potentially acid generating (PAG) stream. The PAG stream is disposed of sub-aqueously in the tailings impoundment area.

Rougher flotation performance was found to be poor in comparison to batch flotation tests conducted on ore samples during the feasibility study. Poor froth geometry in the rougher cells made it impossible to implement process control in the roughing circuit, and an inconsistent approach to operating these cells was identified as an opportunity for immediate improvement. Residence time limitations were found to be limiting rougher flotation performance.

This paper presents steps taken to optimise the existing rougher cells with the installation of concentric launders (donut launders) to reduce froth transportation distance followed by the implementation of a rougher flow controller to control the process and short interval control to align the focus and drive the operating philosophy towards improved recovery.

The paper also presents some brief results of a six-cell pilot campaign of the Eriez StackCell® technology planned to provide the next stage of rougher performance improvement.

## INTRODUCTION

The Red Chris Mine is in the Golden Triangle of Northern British Columbia, approximately 80 km south of Dease Lake and 18 km south-east of the community of Iskut. Newcrest Mining Ltd became the operator of the Red Chris Mine as of 15 August 2019 after purchasing a 70 per cent stake of the mine from Imperial Metals.

The concentrator processes a porphyry copper-gold ore from an open pit mine at a rate of approximately 10.5 Mtpa to produce an auriferous-copper concentrate that is trucked to the Port of Stewart where it is loaded on a ship for delivery to the point of sale.

The comminution circuit is comprised of a primary gyratory crusher, a SAG mill that is operated in closed circuit with a pebble crusher, and a ball mill that is operated in closed circuit with a cyclone pack.

Cyclone overflow is directed to the rougher circuit for the first stage of gold and copper recovery to concentrate. The rougher circuit is comprised of six 200 $m^3$ Outotec TankCells and one 160 $m^3$ Outotec TankCell that was retrofitted after commissioning to assist with managing the sulphur content in tailings to deliver non-acid generating tailings. To achieve compliance, the neutralisation potential ratio (NPR) of the tailings produced must exceed a value of two. Rougher cells 6 and 7 may be directed to this sulphide duty at any time to achieve this objective. Sacrificing these cells to sulphur recovery does have a negative impact on the overall copper recovery owing to a reduction in residence time of the copper rougher circuit.

Rougher concentrate is directed to the cleaner circuit via a two-stage regrind circuit. Several circuit configurations are possible in the regrind and cleaning circuit which has been modified post commissioning to address capacity deficiencies, especially when treating higher grade ores. The cleaning circuit operates with an open-circuit tailings which is disposed of sub-aqueously in the tailings impoundment area due to its higher sulphide content. The target final concentrate copper grade is 23 per cent.

The process utilises pH management via lime addition to the roughing and cleaning circuit to manage chalcopyrite-pyrite selectivity. A copper-selective collector, Solvay Aero 3477 (DTP, dithiophosphate) is used in the roughing and cleaning circuit for copper and gold recovery. Potassium Amyl Xanthate (KAX) is added to the rougher cells allocated to sulphur recovery. More recently, operations have successfully changed strategy with the KAX addition by moving the dosing point forward in the circuit. The concentrator utilises MIBC as needed in the circuit for froth stabilisation. The reagent selection and approach are considered typical of American (North and South) copper operations.

Trials utilising a synergistic (Lotter and Bradshaw, 2009) combination of IPETC (iso-propyl ethyl thiono-carbamate) and KAX in the copper circuit are underway as well as replacing the use of MIBC as the incumbent frother with a stronger alcohol/glycol alternative. These trials are also focused on moving the plant towards a more bulk-roughing condition to improve both recovery and sulphide removal from the rougher tailings.

Since commissioning of the process plant, performance has been lower than expectations from feasibility study test work. With Newcrest taking over operations at Red Chris, this presented an opportunity to transfer their proven experience at diagnosing and optimising flotation performance.

## ROUGHER CIRCUIT LIMITATIONS

The rougher circuit recovery was identified as the primary deficiency at Red Chris, with recoveries consistently below laboratory feasibility test work at equivalent head grade and grind-size conditions. While pulp and reagent chemistry are also a focus of ongoing circuit optimisation, this paper focuses on mechanical and kinetic implications.

### Residence time

Optimised laboratory test work conducted in the feasibility study resulted in a residence time of 9 minutes for the copper rougher stage. Typically, rougher tests are scaled to a plant requirement using a factor of 2.5 which translates to a required rougher residence time of 22.5 minutes for optimal recovery of gold and copper from this stage.

The rougher circuit was designed to have a residence time of 18 minutes (ie a scale-up factor of only two was applied in this case) for copper recovery and four minutes for sulphur recovery at a nominal feed rate of 1360 tonnes per operating hour (tpoh) and feed density of 38 per cent solids.

An analysis of residence time over financial year 2020 (FY202020, 1 July 2019 to 20 June 2020) was conducted to evaluate the actual plant residence time distribution relative to the process design criteria and lab-determined optimal residence time. Figure 1a shows the distribution of the number of cells utilised in a copper rougher duty as a fraction time in FY202020, and Figure 1b shows the resulting distribution of residence time on a shift basis over FY202020. Lines denoting the design residence time (18 min), desired residence time (22.5 min), and the resulting residence time if an additional 600 m$^3$ residence time were installed. Noting that, in the original plant, only six rougher cells were installed, the seventh cell was added later.

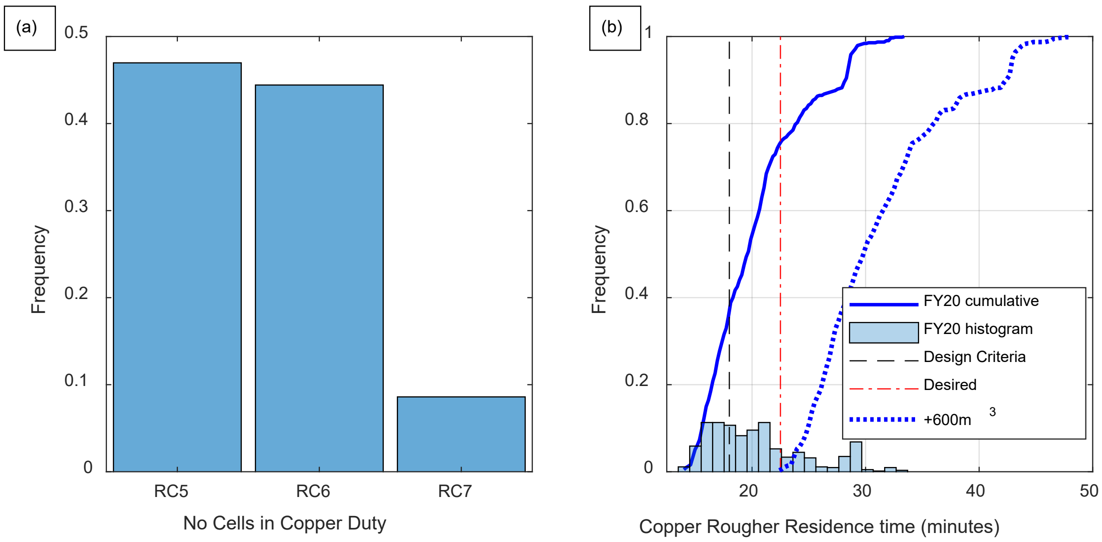


**FIG 1** – (a) Histogram showing the number of cells operating in copper rougher duty during FY202020; (b) Residence time distribution.

Based on the comparison it is evident that in FY2020 the actual residence time was lower than the design point for 35 per cent of the time, and the residence time was lower than the desired value of 22.5 minutes for 75 per cent of the time. Often, design criteria for flotation residence time uses the nominal or average throughput. In practice, however, the resulting throughput is distributed (often with a Weibull distribution). In addition, the plant is operated at a lower solids content than design, typically 32–34 per cent solids versus a design of 38 per cent. As flotation is a kinetic process, the gains at higher residence times do not offset the losses at lower residence times and thus one can expect the average recovery to be lower than expected if planning for the average.

The chart also shows that if an additional 600 $m^3$ of conventional tank cell volume was available in the copper rougher circuit, the expected distribution of residence time resulting from this increase in volume would be close to attaining the desired residence time under all conditions.

## Size based recovery performance

The comminution circuit was designed to produce a target flotation grind size of 150 microns at a throughput rate of approximately 30 000 tpd or approximately 1359 t per operating hour at 92 per cent runtime. A grind size of approximately 157 microns, nearly 10 microns higher, was achieved at a lower circuit throughput of 1324 tpoh for FY2020.

Monthly composite analysis is routinely conducted using a composite of metallurgical shift samples from the on-stream analyser. This analysis is summarised in Figure 2 and compared to benchmark copper performance provided by Munro (2015). The monthly size-by-recovery data shown in the figure covers a range of months when the plant was operated at significantly different throughput rates as a result of the implemented water conservation strategy during winter. As can be seen in the figure, the sized based performance of the Red Chris rougher circuit is well below other benchmarked copper operations. In addition, the performance decreases with increasing mill throughput. The cause of this decrease at higher throughputs can be attributed to a number of factors, including a reduction in rougher residence time, a causal increase in primary grind size, and a head grade impact (generally, the Newcrest strategy aims to process higher grade ore through the mill when throughput is limited by external factors such as water availability).

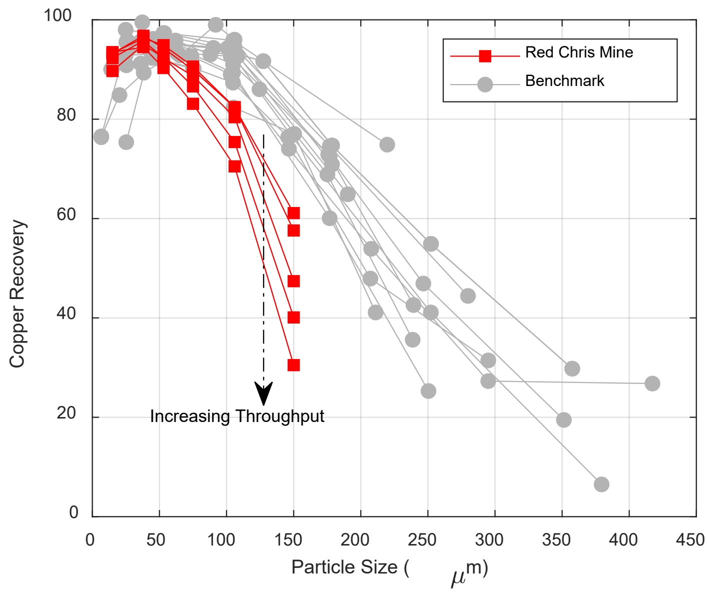


**FIG 2** – Size based recovery of copper, Red Chris Mine and benchmark (Munro, 2015).

## Froth geometry

Initially, the concentrate launders of the rougher cells were configured with only a single peripheral launder within the tank. Soon after commissioning, radial launders were added by the operation to improve froth transportation. Even with the radial launder addition, froth transportation was limited, with large stagnant zones of froth observed in all the cells. The practical operating range of the level and air in the cells was also limited and notably difficult to obtain any fine control over pull rate from the cells.

Froth geometry plays a critical role in determining the froth recovery achieved from a flotation cell. Several authors have reported froth recovery measurements in industrial flotation cells (Falutsu and Dobby, 1992; Savassi *et al*, 1997; Vera, Franzidis and Manlapig, 1999; Seaman, Manlapig and Franzidis, 2006; Ata, 2012). Seaman, Manlapig and Franzidis (2006) showed that froth recovery is a selective process with lower froth recoveries measured for coarse particles and particles with lower surface expression of valuable, hydrophobic minerals. Several authors have modelled froth recovery and froth transportation in two and three phase systems (Moys, 1984; Neethling, 1999; Ross, 1990; Zheng, Franzidis and Manlapig, 2004). Moys (1984) proposed a simplified froth model which breaks the froth phase of a flotation cell into three stages as shown in Figure 3.

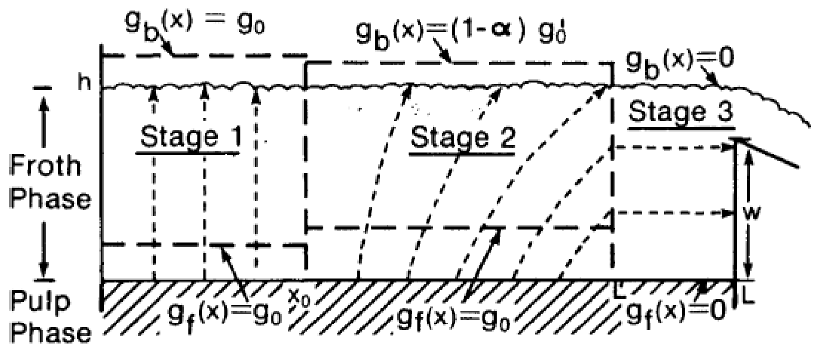


**FIG 3** – A three-stage froth model (after Moys, 1984).

From this description it can be easily observed that froth within Stage 1 has zero potential for froth recovery, while Stages 2 and 3 are together responsible for the successful collection of froth to the concentrate. A rule of thumb developed through the AMIRA P9 project for the scale of industrial flotation cell froth geometry is to limit the horizontal surface transportation distance of froth below 1 m. The installed transportation distance of the rougher cells at Red Chris had a maximum travel distance of 2.4 m, more than double this accepted minimum.

## FLOTATION OPTIMISATION EFFORTS PRIOR TO NEWCREST JV

Several recovery optimisation projects were completed post commissioning to improve plant recovery performance. Larger froth crowders were retrofitted on the last three rougher cells to improve froth mobility. Although the larger froth crowders reduced froth transportation distance (FTD), the preferential crowding in the central areas of the tank cells led to high gas velocities and caused slurry pulping near the froth crowders. This resulted in the shortening of radial launders to prevent excessive gangue recovery. Through operational observations, it was found that simply increasing the size of froth crowder did not improve froth mobility without detrimental impact to concentrate quality. The rougher cells were originally fitted with a peripheral launder only. The radial launders that were retrofitted to all cells were determined to be inadequate in addressing froth recovery limitations.

To alleviate downstream capacity limitations in achieving desired rougher mass pull, a series of piping modifications were completed allowing for flexibility in selection of circuit configurations. These reconfigurations included allowance for single stage cleaning by operating the two cleaner columns in parallel as opposed to in-series as per the original design. This configuration is used for treating higher grade ores (ie >0.4 per cent copper in feed) and takes advantage of ease of achieving concentrate grade at higher ore feed grades, using the additional capacity resulting from parallel operation to increase overall recovery. Other piping modifications also allowed options to handle a high cleaning circuit recirculating load at different feed grade ranges, and at the same time, to prevent overgrinding at different mill throughput ranges. Regrind pumping capacities were also upgraded through the installation of larger motors on the feed hopper pumps to handle higher mass and volumetric flows from the upstream rougher circuit.

Different regrinding configurations were also trialled, with coarser single-stage reground product cleaned in the larger column. Ultimately, two-stage regrinding offered the best result.

These projects provided more operational tools to optimise flotation performance especially in improving rougher mass pull. However, due to lack of operations buy-in and data driven guidance provided to operations at the time, these initiatives did not translate into consistently optimised mass pull and recovery performance. They did, however, provide a platform for future process improvements discussed in the following section of this paper.

## PROCESS IMPROVEMENTS – DPS

A series of process improvements have been made to the rougher circuit to improve performance and overcome the limitations described in the previous section. These improvements are referred to as DPS; namely Donut launders, Process control and Short-interval control.

### Froth geometry – donut launders

Upon assuming operational control of the Red Chris Mine, Newcrest acted to immediately address this froth geometry issue through the purchase and installation of internal concentric (donut) launders which are commonly in use in theirs and other Australian operations. A capital expenditure request for the installation was approved in the first week. It is noted that there is a distinct geographical preference for the radial-style launders in the Americas by way of comparison.

Figure 4 shows a three-dimensional representation of the modified launder design. The design incorporated a new concentric ring for concentrate collection with transfer chutes to main rougher concentrate launder. These launders as well as additional crowding were progressively installed in all six of the 200 $m^3$ cells.

Outotec (now Metso Outotec), designed and fabricated the retrofit launder and crowder components. The design incorporated a necessary breakdown of components that could be lifted and fitted to the cells without removal of the motor and gearbox assembly or bridge. The site maintenance department installed the launders over three planned shutdowns. The result of owner installation was a significant cost saving as well as a simplification of planning manpower requirements around the shutdowns.

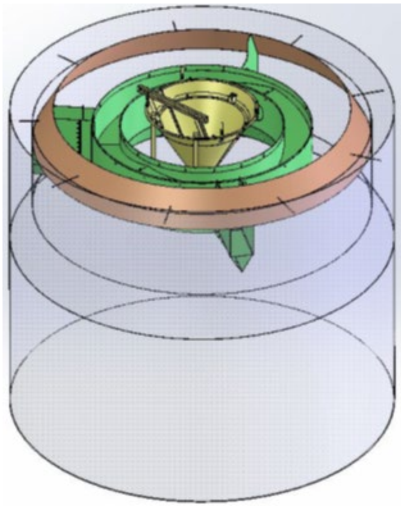

**FIG 4** – 3D view of the donut launder modification.

The modified design allowed for adjusting froth crowding at three settings, the froth crowders were installed to provide an increasing crowding profile down the bank. Table 1 shows a summary of the froth geometry before and after the modifications. The lip loading before and after is very similar, the major changes made were to the maximum travel distance (reduction from 2.4 m to below 1 m). Froth crowding also increased from 26 to 62 per cent.

**TABLE 1**

Froth geometry before and after modification.

| | Radial launder | Donut launder | Units |
|---|---|---|---|
| Launder lip length | 20.0 | 19.7 | m |
| Max travel distance | 2.4 | 0.9 | m |
| Froth surface area | 30.0 | 15.5 | $m^2$ |
| Crowding reduction | 26 | 62 | % |
| Average lip loading | 1.7 | 1.7 | tph/m |
| Average froth carry rate | 1.1 | 2.2 | tph/$m^2$ |

Coleman and Wong (2018) presented data on the industrial measurement of critical froth transport parameters. In rougher duties these authors reported froth carrying rates ranging from 0.01 to 4.3 with a median value of 0.9 tph/$m^2$ and a target design range of less than 0.8–1.5 tph/$m^2$ (Murphy and Heath, 2013). Similarly, the average lip loading of 1.7 tph/m is within typical ranges measured in industry with a median of 1.0 tph/m (Coleman and Wong, 2013) and a recommendation by Murphy and Heath to keep this value below 1.5 tph/m. While both froth transport design values fall slightly above the recommended ranges, it is the authors' experience that these values implemented at Red Chris are well within good operating practice.

Post installation of the launders it was readily observed that all the froth surface was mobile with the increased crowding and reduced travel distance, with no stagnant zones in any of the cells. Operationally, the cells have a larger operational range in terms of froth depth and air rate post modification, and it was found that the pull rate from the cells was more sensitive to changes in operating conditions than before the modifications. This allowed for the application of process control to target circuit mass pull, discussed further in the next section. The increased operating range of the cells also allow operation of the cells to maximise coarse particle recovery (lower air rates and shallower froth depths).

Figure 5 shows photographs before and after the donut launder installation.


**FIG 5** – Photographs of the launders before modification (left) and after installation of the donut launder (right).

Air rates in the cells reduced by approximately 25 per cent post donut launder installation, with similar froth depth ranges as a result of the increased crowding and reduced travel distance. Consequently, the froth retention time was reduced, and the achieved air recovery to concentrate increased. Improvements in air recovery are known to improve flotation bank performance as reported by Hadler and Cilliers (2009).

## Process control

Once the first four cells had been modified, a rougher concentrate flow controller was programmed in the distributed control system (DCS). The configuration was based on successful experience of similar configurations at other Newcrest operations. The controller configuration is shown in Figure 6. Rougher concentrate flow is measured with a magnetic flowmeter. The flow control loop takes a flow set point entered by the operator which controls the rougher concentrate pump speed. Rougher concentrate hopper level is maintained by a primary level controller which adjusts the froth depth of the rougher flotation cells, operators have access to adjust the ratio between the individual cells within allowable range. A secondary loop adjusts the air rates of the flotation cells to maintain the median froth depth within a controllable range. The secondary loop acts slower than the primary and acts to increase the dynamic range of the overall control system.

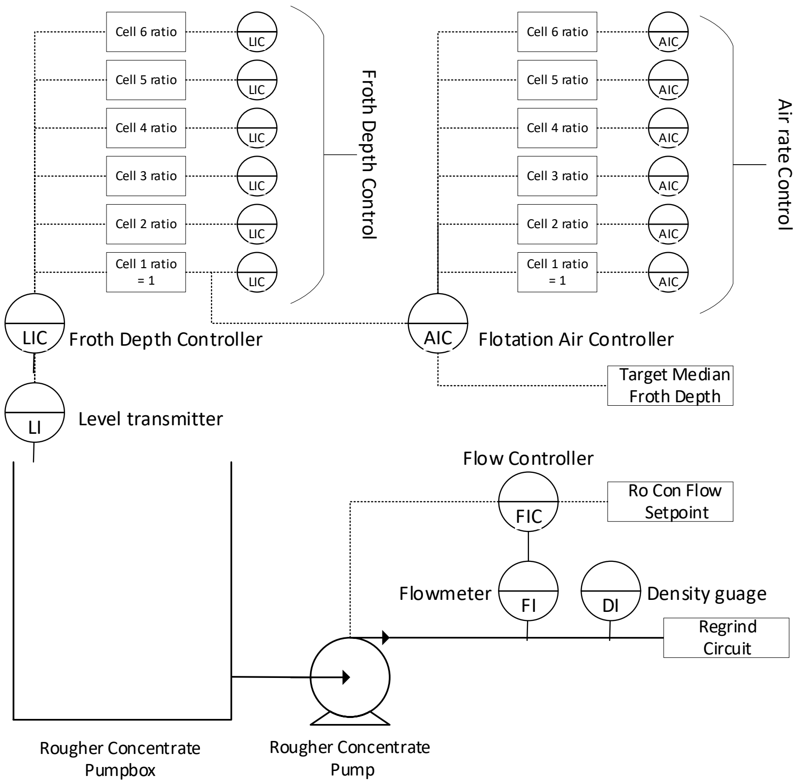


**FIG 6** – Rougher concentrate flow controller diagram.

Outotec FrothSense cameras were installed as part of the cell upgrades, the reported froth velocity profile is used by operators and metallurgists to tweak the ratios between cells to maintain a pull rate profile down the bank.

The controller has been operational for more than six months at the time of writing this paper. Over this period, utilisation of the controller has been close to 100 per cent. Operators have since had more time to focus on the metallurgical conditions of the roughers and downstream processing. The stabilised flow from the roughing circuit has also assisted in stabilising the regrind and cleaning circuit as well as achieving higher overall mass pull. Stabilisation of flow subsequently allowed greater average flow rates through the downstream constraints.

## Short interval control

Short Interval Control, as used in this paper, is defined as the establishment of an operational review practice that currently focuses on the use of interim online data during a shift and validated shift composite data to drive desired process outcomes. The desired objectives may be changed or fine-tuned over time, however, in this application the primary focus is on process recovery.

The primary objective of Short Interval Control as implemented at Red Chris is provision of a very few key factors that drive overall recovery, grind size to the flotation circuit, and rougher circuit mass recovery for continued focus.

The benefits of the process result from:

- Use of a common language when discussing opportunities for recovery improvement between operations crews and the metallurgical team.
- A unified approach to realising these opportunities.
- Identification of themes to be addressed beyond the scope of the day-to-day operation eg training, circuit bottlenecks, maintenance etc.

At this point in time, grind size to the flotation circuit is tracked, however, no direct action is currently being taken on a shift or daily basis to alter the resultant grind size. Grinding circuit efficiency has been the subject of a separate study.

Rougher circuit mass recovery, or mass pull from the rougher circuit, has formed the primary focus for recovery improvement. Evaluation of the rougher mass recovery has shown that it directly improves rougher recovery as is expected. Also as is expected, there is a point beyond which, cleaner recovery becomes adversely impacted. The increase in overall recovery has, however, outweighed the detriment in cleaner recovery within the upper bounds to which mass pull has been flexed.

Figure 7 presents the online dashboard that has been created in the plant's PARCView, real time data analysis and visualisation software and data historian. The PARCView software takes in measurements from the plant's OSA system coupled with flowmeter measurements and inputted metallurgical calculations to generate the observed data for decision-making during a shift. Target mass pull and stage recoveries were developed from multilinear regression of shift-based data, limited to variables that are measured online (mass flows and on-stream analyser data). The target mass pull is based on the historic 75th percentile performance curve in order to drive continuous improvement as well as the identification and eradication of bottlenecks preventing the continuous achievement of this target.

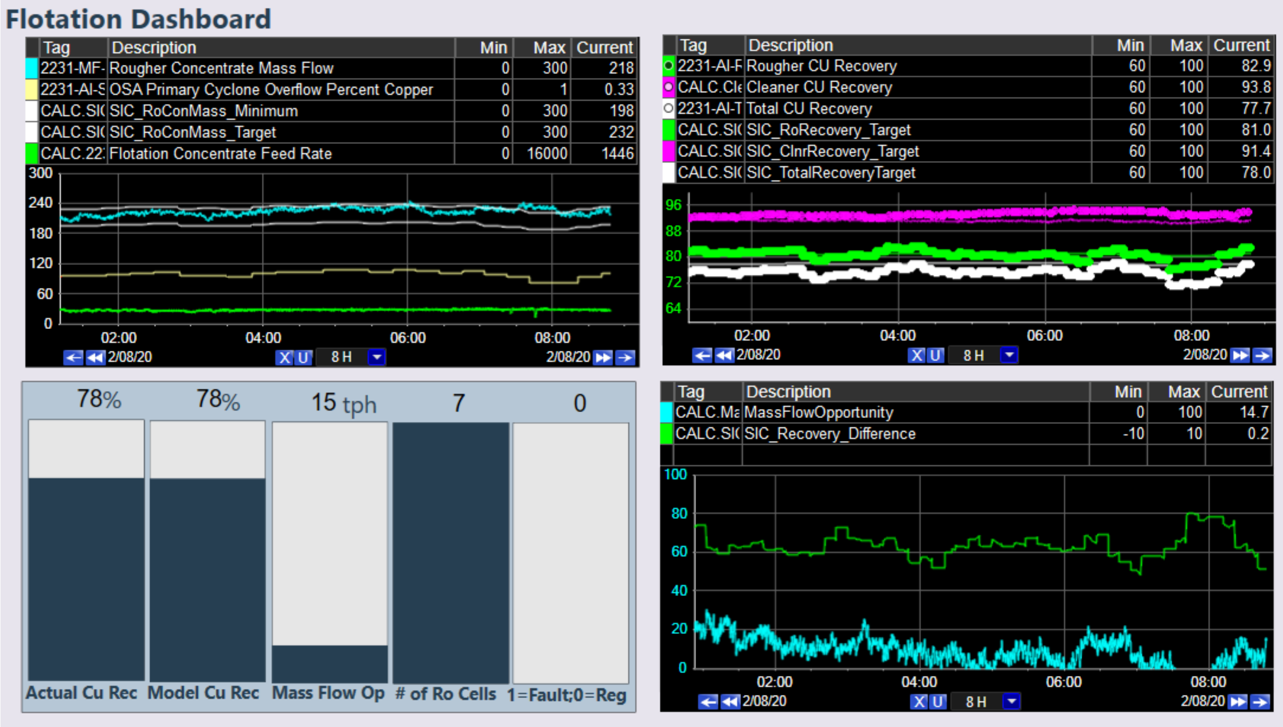


**FIG 7** – Flotation Short Interval Control dashboard.

Not shown here but included in Napier and Livingstone (2021) are examples of the shift Short Interval Control dashboards (specifically Figure 3 of their paper) that make use of the assayed shift composite data. These dashboards are then the subject of a more comprehensive metallurgical review with commentary assigned as to whether the opportunity for recovery improvement is related to:

- upstream operation
- rougher circuit operation
- downstream circuit operation.

The causes are further scrutinised to establish whether the limitations result from operational factors, process control and instrumentation, mechanical factors, or equipment limitations.

Through the process of drilling down to the root cause for each shift, it has been possible to identify that mass pull is primarily limited by the regrind pumps. The cause for the limitation requires further investigation as improved specificity is required in the current commentary to distinguish between pump capacity and pump maintenance.

The process has also identified that revision of the reagent dosing strategy was required and through this, benefit has been realised through improved mass pulls and reduced reagent dosing without substantial gangue dilution of the rougher concentrate.

Another benefit of this method of data interrogation is the assignment of value that is attributable to a root cause limitation on a shift basis, and this forms the basis of a value-based proposition for addressing the identified limitation.

## DPS OUTCOMES

The journey towards improving rougher flotation performance commenced in June 2019, when Newcrest representatives began their presence on-site. Newcrest officially took operational control of Red Chris Mine in August 2019. From June 2019, an operational focus of pushing the limits of rougher mass pull commenced, donut launder installation began with the first two rougher cells in December 2019 and all six were installed by April 2020. The Short Interval Control program was initiated in January 2020 with the assistance of Napier and Livingstone (2021), and soon after the flow controller was programmed.

As mentioned previously, gold and copper recovery are influenced positively by rougher mass pull. Due to downstream bottlenecks and variable mill throughput, the measure of mass pull used in the plant is rougher concentrate flow. Figure 8 shows a time series of rougher mass flow in dry tonnes per operating hour. The boxes in the boxplot show the variance in rougher concentrate flow (filled boxes representing the inner-quartile range of mass flow on a shift basis, and the horizontal red line indicates the median value per month).

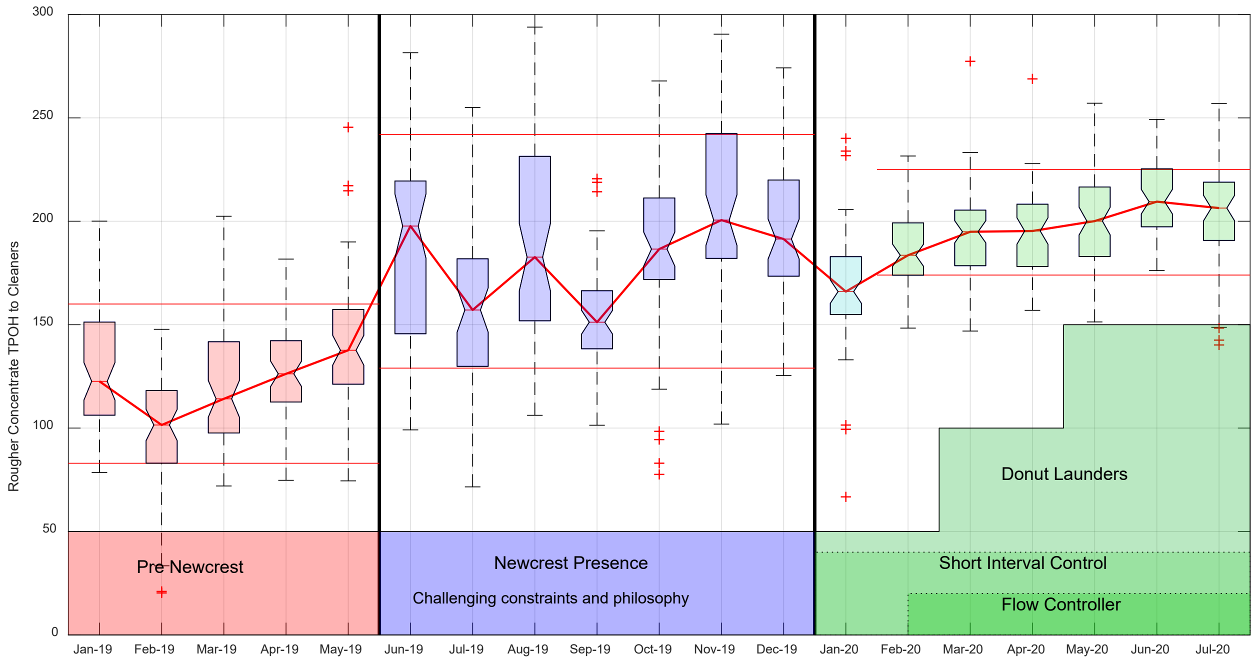


**FIG 8** – Rougher concentrate mass flow over time.

Figure 8 is broken up into three key regions:

1. Pre-Newcrest: An under-resourced and younger, less experienced, metallurgical team coupled with a more dominant operations team placed more attention on cleaner stability than rougher or overall recovery. The principle of higher mass pull driving improved recovery was known and discussed but never aggressively challenged. Prior to this period, several changes had already been made to the circuit to address shortcomings in the installed capacity of several pumps in the flotation and dewatering circuit as well as flow sheet changes in the cleaning circuit to allow processing of greater metal loads.
2. Newcrest Presence: Additional metallurgical support facilitating a behavioural change thus allowing for the adoption of an operating philosophy of maximising mass-pull in the plant. Prior conceptions of downstream constraints were continuously challenged, and with the support of additional resources and senior management buy-in, metallurgists influenced operators to target higher mass-pulls. As can be seen, this resulted in an increase in the median mass pulls achieved. Due to lack of stability and operationally inflexible rougher cells, the variance in mass pull significantly increased. Consistency between crews (day shift and night shift) was also found to be lacking.
3. Implementation of DPS: Over the period from January 2020, the modification of the rougher cells coupled with process and short interval control significantly reduced the variance in mass pull observed. The median has gradually increased over time. The operator buy-in to the new strategy dramatically increased as they now had the tools to achieve the requested outcome consistently and saw the benefits of this in their daily numbers. Consistency between crews (particularly day/night shift) has significantly improved as well.

## Tailings quality

The neutralising potential ratio (NPR) of the rougher, non-acid generating (NAG) tailings is an important criterion in terms of depositing material in the Tails Impoundment Area (TIA). A value greater than two is required to avoid sub-aqueous deposition of the NAG tailings. NPR is dependent on acid generating sulphides and neutralising carbonates (determined through carbon assay). Higher feed sulphur-to-carbon ratios (S/C) make achieving NPR compliance more challenging. A greater focus on rougher recovery through the systems described has provided an improved sulphide recovery in the copper roughers and subsequently resulted in more reliable production of NPR compliant NAG tailings. Figure 9 shows a boxplot of different time periods with the resulting NAG NPR achieved versus the feed S/C ratio. As with rougher concentrate flow, an improvement was observed when higher mass pulls were targeted by the operation and a further improvement was observed once the modifications to the circuit were made.

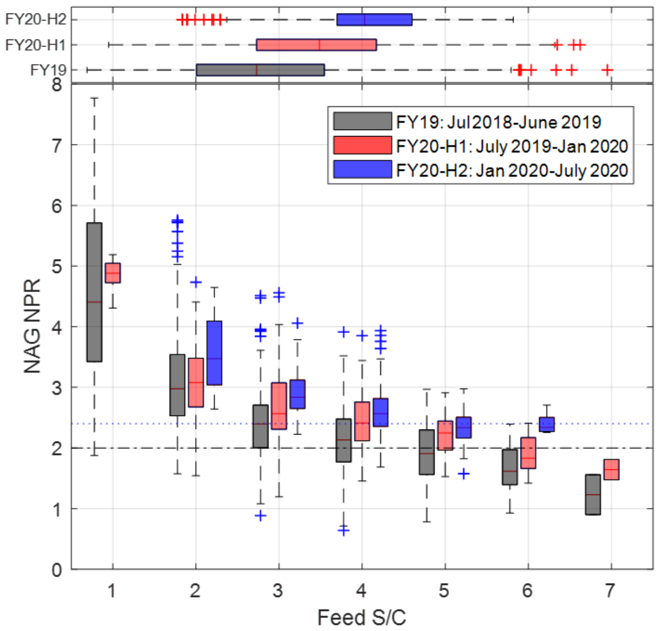


**FIG 9** – Non-Acid Generating tailings Neutralisation Potential Ratio versus Feed Sulphur to Carbon ratio boxplot over different time periods.

## Multivariate regression

In order to quantify the economic benefits of the changes described above, a multivariate linear regression was carried out over the second two periods shown in Figure 8. There was significant variance in many of the mill inputs, particularly mill throughput, head grade and the presence of fault (deleterious) ore.

Multilinear regressions were carried out with gold and copper recovery as the response variables. Input variables to the regression included, mill throughput, mill head grades (gold, copper, sulphur and carbon), rougher concentrate mass flow, presence of fault material (binary) and a binary variable describing the implementation of DPS (binary, with zero prior and one post January 1, 2020).

Only input variables showing a significant p-value of less than 0.05 were included in the final regression which was fitted stepwise to the shift data using Matlab®. Input variables were not normalised to allow direct comparison of the coefficients. Minor filtering was conducted on the input data to exclude shifts with a runtime of less than 10 (out of 12) hours. An adjusted R-squared value of 0.68 and 0.60 for gold and copper were achieved.

Importantly the changes implemented from January 1, 2020 were found to be significant at the 95 per cent confidence level with a magnitude of 1.6 per cent ± 0.5 per cent and 1.3 per cent ± 0.3 per cent gold and copper recovery improvement respectively which can be attributed to DPS. An overall improvement of 1.6 per cent in mass pull was also noted from a further regression.

Some co-linearity between input variables was observed in the regression which is often the case with minerals processing data. A bootstrap method was used to confirm the stability of the regression by randomly sampling shift data multiple times, the resulting improvement range was consistent with that quoted above.

## ROUGHER CAPACITY

As mentioned in the previous section, the installed residence time of the circuit is significantly lower than the desired capacity for optimal recovery. In addition to the improvements outlined above, there is still a need to increase the copper rougher circuit capacity. An analysis of plant data concerning the number of cells in copper rougher duty highlights that an additional 600 $m^3$ of rougher capacity is required to ensure there is always enough copper rougher capacity regardless of the sulphide removal requirement.

Red Chris is in a sub-arctic climate, it is therefore necessary to enclose process equipment in buildings to prevent freezing of slurry lines and allow safe operation and maintenance of equipment. With limited space in the existing concentrator, a smaller footprint solution to installing traditional flotation machines was sought to deliver the equivalent capacity of the traditional technologies and eliminate the need for constructing additional buildings to house new flotation equipment.

Two major mechanical cell technologies were considered for the Red Chris application: Woodgrove Stage/Direct Flotation Reactor (SFR/DFR) and Eriez StackCell®. Jameson cells were also considered for this duty. These technologies all provide a high intensity contained reactor zone where fine bubbles are generated and intensely mixed with feed pulp before discharging into a quiescent separation chamber.

Figure 10 shows a schematic drawing of the StackCell® technology (Wasmund *et al*, 2019). The Woodgrove equivalent has a separate reaction chamber while the Eriez unit is contained within a single unit, and the Jameson cell has a pump to generate the contact energy required.


**FIG 10** – Eriez StackCell® schematic.

Eriez provided six pilot size units to Red Chris for a collaborative evaluation of the units, which was conducted with technical personnel from both companies operating the units over a period of three months in parallel to the existing roughing circuit. Evaluations were conducted in different duties: rougher, scavenger and cleaning. Only roughing duty is reported here.

The cell volume of the pilot units is approximately 200 litres. A photograph of the pilot installation in the basement of the concentrator is shown in Figure 11.

**FIG 11** – StackCell® pilot set-up at Red Chris.

Down the bank plant rougher surveys were compared to the StackCell® bank performance on a residence time basis during the campaign. Flotation kinetics in the StackCell®s were found to be at least four times faster compared to the plant cells for copper and gold bearing minerals as depicted in Figure 12.

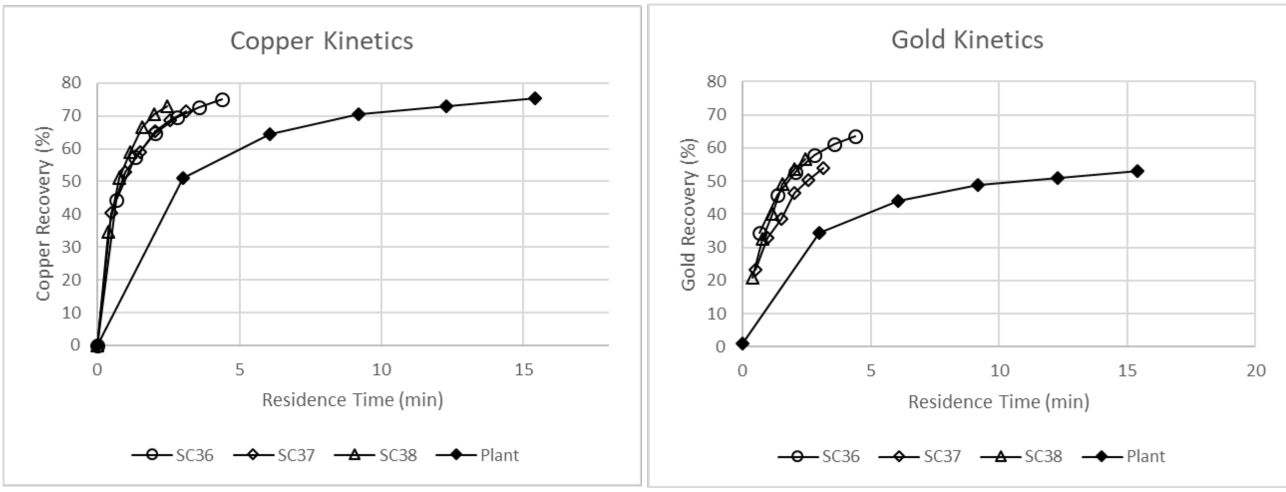


**FIG 12** – Stack Cell versus plant flotation kinetics (SC denotes StackCell ® surveys).

The significant increase in kinetics was observed across all StackCell® surveys conducted. A size analysis conducted on one of the StackCell® surveys is shown in Figure 13. It is evident that the pilot cells improved copper recovery in the mid-size fractions, but the very coarse recovery was lower. In the case of gold, a relatively larger increase in recovery of mid-size was observed. The fines performance of sulphides (predominantly pyrite) was dramatically improved in the StackCell®s, with the minus 20 micron increased from less than 20 per cent recovery to approximately 50 per cent.

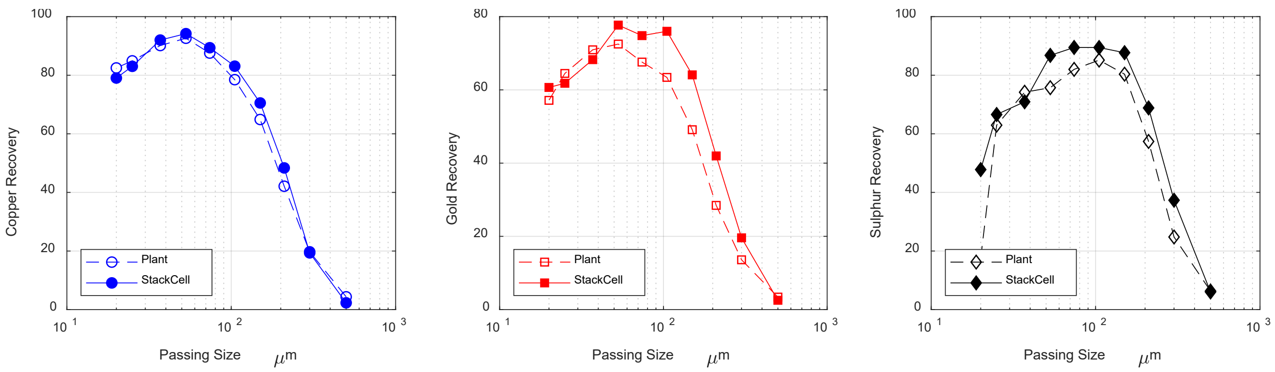


**FIG 13** – Size based recovery in the StackCell®s compared to plant.

An additional series of tests was conducted on the plant tailings. It was found that approximately 50 per cent of the pyrite in plant rougher tailings could be floated in the StackCell®s, with 30 per cent recovered in just two of the six pilot cells. This is equivalent to an increase in sulphide removal from the plant tailings of five per cent relative to plant feed which would substantially improve the ability of the plant to produce NPR compliant tailings.

It was notable that the ultimate copper recovery obtained from the StackCell®s was generally 1–2 per cent lower than that obtained in the plant cells despite the very fast kinetics, supported in part by the poor performance at the coarse end. The underlying hypothesis for this differential is related to froth recovery. In conventional flotation cells, particles detached within the froth phase and drop back into the cell where they recycle through the collection zone (Seaman, Manlapig and Fraznidis, 2006). Coarse and poorly liberated particles are particularly subject to detachment in the froth phase. In the case of StackCell® technology, any drop-back from the phase results in a likely loss to tailings as the slurry only has a single pass through the reaction chamber.

Based on the piloting results, an in-depth analysis of plant operating data and kinetic flotation modelling, a detailed design for the installation of two ~75 $m^3$ flotation cells are underway after confirming that these cells can fit within the existing process building. These cells are expected to provide the required additional rougher capacity required in the flotation circuit.

## CONCLUSIONS AND FUTURE WORK

Rougher flotation at Red Chris was improved through a systematic process of addressing the physical constraints in the existing flotation cells. Excessive froth transport distance was reduced from greater than two metres to below one metre. This modification provided a platform for implementing a flow controller to maintain mass pull from the roughers by manipulating the air rates and froth depths. The process control implementation was successful with virtually 100 per cent utilisation since commissioning.

A Short Interval Control process was also implemented around the same time as the completion of physical changes and process control. The system has provided supervisory management of the roughing circuit and has been a useful tool to modify the behaviour of plant operators and provide a systematic and consistent approach to operation of the circuit. All three systems combined have demonstrated a statistically significant improvement to plant recoveries of 1.6 per cent ± 0.5 per cent and 1.3 per cent ± 0.3 per cent for gold and copper recovery respectively.

Residence time of the copper roughers was found to be insufficient. A distribution analysis over FY2020 showed that 75 per cent of the time, the residence time was lower than the desired value of 22.5 minutes. An additional 600 $m^3$ of flotation capacity is required in the roughers to achieve the minimum desired residence time all the time. This analysis also demonstrates that expected variance in mill throughput should be considered in the design phase rather than designing for an average throughput.

Successful piloting of a new flotation technology, the Eriez StackCell®, demonstrated that this technology has greatly superior kinetic performance compared to conventional tank cells. The required volumetric increase of ~600 $m^3$ can be fulfilled by two 75 $m^3$ StackCell®s which were sized to be accommodated within the existing process building and are undergoing detailed design at time of writing this paper.

Ultimately the improvements presented in this paper are the result of successful technology and practice transfer between Newcrest operations.

## ACKNOWLEDGEMENTS

The authors would like to acknowledge the metallurgy, maintenance and operations teams involved in the successful implementation of the modifications made to the physical, and operational changes at Red Chris mine. Cross discipline support for this initiative as well as the gracious support of the Newcrest senior management team ensured the successful outcome presented herein.

The authors would also like to acknowledge the Telfer Operations management team for making, colleagues, Matt Livingstone and Lara Napier available to Red Chris for development, implementation and transfer of the short interval control approach adopted at Red Chris.

The Eriez flotation division provided valuable assistance and collaboration in the piloting program and provision of their technical specialists on the piloting and subsequent concept design for the next phase of improvement. Ray van Wagoner from Rio Tinto Kennecott Utah Copper graciously loaned Newcrest three of the pilot cells.

The authors would also like to acknowledge the Cadia Operations management team for making Emily Jacques available to support the Red Chris piloting team.

The authors would also like to thank Newcrest Mining Limited for the allowing the data to be presented and published.

## REFERENCES

Ata, S., 2012. Phenomena in the froth phase of flotation – A review. International Journal of Mineral Processing 102–103 pp 1—12.

Coleman, R and Wong, B, 2018. Flotation launder design and the measurement of critical froth transport parameters, in Proceedings: 14th AusIMM Mill Operators' Conference, Brisbane, 29–31 August 2018 (Australasian Institute of Mining and Metallurgy), pp 353--362.

Falutsu, M. and Dobby, G., 1992. Froth performance in commercial sized flotation columns. Minerals Engineering 5, pp 1207– 1223.

Hadler, K. and Cilliers, J.J., 2009. The relationship between the peak in air recovery and flotation bank performance. Minerals Engineering, 22 (2009), pp. 451–455

Lotter, N.O. and Bradshaw, D.J., 2009. The formulation and use of mixed collectors in sulphide flotation. In Proceedings: Flotation' 09, Cape Town, November 2009.

Moys, M.H., 1984. Residence time distributions and mass transport in the froth phase of the flotation process. International Journal of Minerals Processing. 13 (2), pp 117–142.

Munro, P. D and Munro, S.E, (2015). Observations on Cadia Valley concentrator operations (Newcrest internal report. Unpublished).

Murphy, B and Heath J L, 2013. Selection of Mechanical Flotation Equipment Presented at METCON 2013: Enhancing the resource value chain among ASEAN economies (Society of Metallurgical Engineers of the Philippines: Quezon City).

Napier, L. and Livingstone, M. 2021. Recovery opportunity models driving multi-disciplinary improvement. Submitted for publication in Proceedings: 15th AUSIMM Mill Operators' Conference 2021, Brisbane (Australasian Institute of Mining and Metallurgy).

Neethling, S.J., 1999. A mathematical model of flowing foams and froths. Ph.D. thesis, University of Manchester Institute of Science and Technology, UK.

Savassi, O., Alexander, D., Franzidis, J.-P., and Manlapig, E., 1998. An empirical model for entrainment in industrial flotation plants. Minerals Engineering 11 (3), pp 243– 256.

Seaman, D.R., Manlapig, E.V. and Franzidis, J.P., 2006. Selective transport of attached particles across the pulp–froth interface. Miner. Eng. 19 (6–8), pp 841–851.

Ross, V.E., 1990. Interpretation of froth data to study the detachment of floating particles in flotation froths. Miner. Eng. 3 (5), pp 525–531.

Vera, M., Franzidis, J.-P. and Manlapig, E., 1999. Simultaneous determination of collection zone rate constant and froth zone recovery in a mechanical flotation environment. Minerals Engineering 12 (10), pp 1163–1176.

Wasmund, E.B., Mankosa, M., Thanasekaran, H., Yap, NS, and Yan, E., 2019. A High Rate Mechanical Flotation Cell for Base Metal Applications. In Proceedings: 10th International Copper Conference, 58th Annual Conference of Metallurgists, Vancouver, August 18–21, 2019.

Zheng, X., Franzidis, J.-P. and Manlapig, E., 2004. Modelling of froth transportation in industrial flotation cells Part I. Development of froth transportation models for attached particles. Minerals Engineering 17 pp 981–988

# Improving Capricorn Copper concentrator process performance and the role of process mineralogy and surface chemistry

*M Tayebi-Khorami[1], M Muller[2], M Zanin[3] and T Do[4]*

1. Process Engineer/Project Metallurgist, Ausenco, South Brisbane Qld 4101. Email: maedeh.tayebi-khorami@ausenco.com
2. Concentrator Manager, Ausenco, Capricorn Copper Concentrator, Gunpowder Qld 4825. Email: mmuller@capricorncopper.com
3. Managing Director, MZ Minerals Pty Ltd, Prospect SA 5082. Email: max.zanin@mzminerals.com
4. Senior Metallurgist, Ausenco, Capricorn Copper Concentrator, Gunpowder Qld 4825. Email: tlong@capricorncopper.com

## ABSTRACT

Capricorn Copper Mine (CCM) is an underground copper mining operation located 125 km north-west of Mt Isa in North West Queensland, Australia. The plant restarted operations in late 2017 after being in care and maintenance for a number of years. After plant start-up in early 2018, copper recovery was well below the study expectation. Plant data confirms that the copper recovery is affected by the proportion of pyrite in the ore. This led to an investigation being carried out that found a significant amount of liberated ultrafine copper sulphides in the tailings and liberated pyrite in the final concentrate which called attention to a recovery improvement opportunity.

A comprehensive investigation was completed in 2019; it consisted of a full plant survey followed by ToF-SIMS, mineralogy and size-by-size analysis of key streams. In addition, batch flotation test work were carried out testing various assumptions for the mode of copper losses into tailings. Plant surveys of pH, pulp potential (Eh), Dissolved Oxygen (DO) and EDTA extraction were also performed investigating the effect of pulp chemistry on metallurgical performance. This paper demonstrates the power of combining process mineralogy and surface chemistry analysis to optimise and troubleshoot flotation circuit performance. The results are discussed in terms of improving the copper sulphides recovery and depressing pyrite flotation.

## INTRODUCTION

Capricorn Copper Mine (CCM), formerly Mt Gordon and Gunpowder mine, is an underground copper mining operation located 125 km north-west of Mount Isa in Queensland, Australia. The predominant feed source for the CCM concentrator comes from three underground copper mines: Esperanza South (ESS) at approximately 60 per cent, Mammoth (MAM) at approximately 28 per cent and Greenstone (GST) at approximately 12 per cent. Mine production is predominantly from the ESS, producing ~60 per cent of the ore tonnage. Esperanza South is considered to be predominantly shear-hosted mineralisation over a 50–75 m wide zone and comprises a high pyrite copper skarn ore with significant clay content. The ESS ore is relatively complex, with varying proportions of chalcocite, bornite, chalcopyrite, pyrite and clay minerals throughout the deposit. Batch treatment of ESS ore caused several plant events during 2018 thus copper concentrator achieved lower than expected copper grade and recovery, averaging 20 per cent Cu grade at copper recovery of 75 per cent.

In 2018, the CCM concentrator consisted of a grinding and flotation circuit (Figure 1). The comminution circuit comprised of a SAG mill followed by a ball mill in closed circuit with cyclones. SAG mill scats were recycled back uncrushed to the SAG mill feed, whilst the cyclone underflow reported to the ball mill. Cyclone overflow with a $P_{80}$ of 106 µm reported to the rougher flotation circuit. The rougher concentrates were not reground, instead each rougher concentrate individually reported to different stages of the cleaner flotation. The rougher 1 concentrate reported to the head of the cleaner 2, the rougher 2 and 3 concentrates diverted to head of cleaner 1 and the rougher 4 concentrate reported to the head of the cleaner scavenger. The cleaner concentrates were upgraded in a conventional circuit configuration to produce a final concentrate. The final concentrate and the flotation tailings were dewatered using thickeners, with the concentrate being further dewatered via a vertical plate filter for transport off-site. Collector FT1234 (thiocarbamate) was added to the head of SAG mill as well as rougher 2, and POLYFROTH W34 (polyglycol ether frother) was added to the conditioning tank. The pH target of 11 was achieved in the flotation conditioning tank by addition of milk of lime to the SAG mill. The regrind HIGmill® was turned off, as the copper recovery dropped sharply after regrinding and it was not possible to float it again efficiently despite trying various strategies.

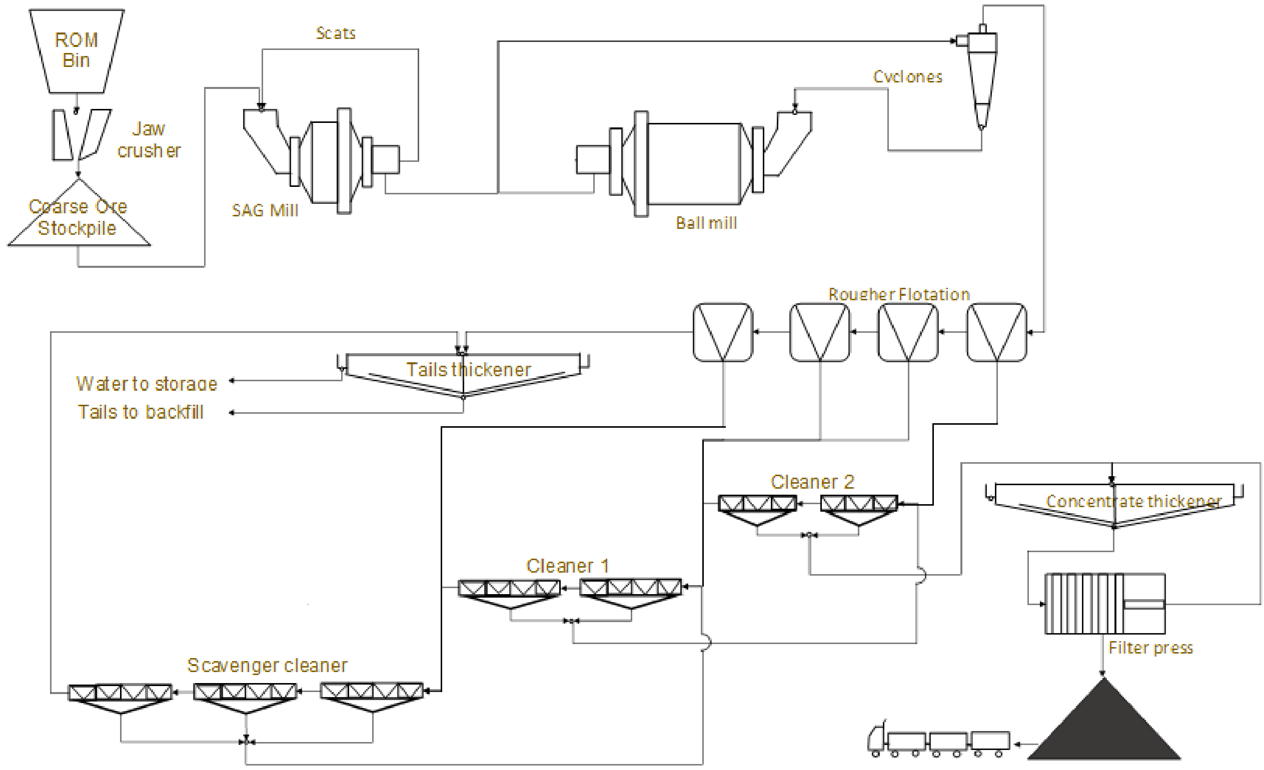


**FIG 1** – CCM Copper concentrator.

A comprehensive investigation was completed in 2019; consisted of a full plant survey followed by ToF-SIMS, mineralogy and size-by-size analysis of key streams. In addition, batch flotation test work was carried out testing various assumptions for the mode of copper losses into tailings. Plant surveys of pH, pulp potential (Eh), Dissolved Oxygen (DO) and EDTA extraction were also performed investigating the effect of pulp chemistry on metallurgical performance.

The objective of this paper is to demonstrate the power of combining mineralogical and surface analysis to comprehensively study a flotation circuit. This paper describes the experimental work performed and the results from mineralogy and surface chemistry when plant was feeding the ESS ore. The strategies developed to improve circuit performance will be outlined.

# EXPERIMENTAL

## Plant survey

A comprehensive plant survey was conducted in May 2019 when the plant was operating at ~270 tph on 100 per cent ESS ore. The survey included eight sampling rounds during a two-hour period. Timed concentrates were collected from the lips of the flotation cells and tailings were collected using an in-pulp sampler inserted into the cell as close to the tailings plug as possible. Combined concentrates were sampled from an OSA multiplexer along with the final concentrate and final tailings stream from the main flotation circuit.

All streams were weighed wet and dry to determine per cent solids. Dry samples were sent for head assay, size distribution using sieving and cyclosizing, size fractions assay for copper, iron, sulphur, and silicate. All sizing and assaying were performed in the CCM laboratory. The plant samples were sent to XPS in Canada for mineralogical analysis using QEMSCAN® to determine modal mineralogy and particle liberation. Electron Probe Microanalyser (EPMA) was completed on samples to determine mineral compositions. Specifically, this targeted Cu mineralogy and determined Cu in solid solution in pyrite and gangue.

Samples were also collected for Time-of-Flight Secondary Ion Mass Spectrometry (ToF-SIMS) analysis to examine the surface species on the pyrite particles that contribute to pyrite flotation to the final concentrate. The samples of rougher feed, rougher tailing, cleaner scavenger tailing, and final concentrate were sent to the University of South Australia for ToF-SIMS analysis.

## Batch flotation test work

Given the complexity of the ESS ore, multiple test work programs were conducted with different types of reagents and conditions. The aim of the test work programs were:

- Baseline modification test work: testing the effects of pH, $P_{80}$, plant process water, solid density.
- Copper grade-recovery improvement test work: testing different types of collector and frother dosing points and rates to improve the recovery of Cu minerals.
- Grinding media test work: testing different types of grinding media to manipulate the redox condition during grinding and find out the sensitivity of flotation to grinding media.
- Regrinding test work: testing the effect of regrinding stage on the cleaner performance.
- Pyrite depression test work: testing different types of depressant on pyrite recovery and (including sulphur-oxy reagents, cyanide, zinc sulphate, diethylenetriamine (DETA), aeration/prefloat, pH – Eh, EDTA etc).

The test work programs were completed in 2019 on the ESS ore samples in collaboration with CCM, AMML, UQ/Chemical school, JKMRC, MZ Minerals, and Interchem laboratories. The ESS ore sample was collected from the run-of-mine stockpile. The sample was stage crushed to 100 per cent passing 3.35 mm in a laboratory jaw crusher, before being thoroughly mixed and rotary split into 1 kg portions and were stored in a freezer to reduce further oxidation.

The grind determination was carried out in the laboratory stainless steel rod mill to determine the grind time required to obtain a mill discharge size distribution of $P_{80}$ of 106 μm to reflect the grind size of the plant. Grinding tests were completed at 60 per cent solids with a 1 kg charge.

Flotation tests were conducted in a 2.5 L laboratory flotation cell to give a pulp density around 35 per cent solids and conditioned with appropriate reagents prior to completing rougher flotation tests. Four flotation concentrates were collected after cumulative times of 1, 2, 7 and 12 min at an air flow rate of 6 $dm^3$/min to mimic the plant flotation conditions. The pH and Eh were measured after grinding using a TPS metre combined with a platinum electrode and expressed relative to the standard hydrogen electrode, SHE. The test products (four concentrates and a tail) were assayed for Cu, Fe, S. Selected tests had their concentrates and tailing sized, and the size fractions assayed to determine the flotation behaviour on a recovery-by-size basis.

Analytical-grade or equivalent chemicals were used throughout this investigation. The pH was adjusted by the addition lime or NaOH when necessary. A list of the pyrite depressant reagents that were used in this study is presented in Table 1.

**TABLE 1**

List of the inorganic and organic pyrite depressant reagents.

| | | |
|---|---|---|
| **Inorganic** | Cyanide | NaCN |
| | Sulphoxy Species | |
| | Sulphide ($S^{2-}$) | $Na_2S$ (Sodium sulfide) |
| | Sulphite ($SO_3^{2-}$) | $Na_2SO_3$ (Sodium sulphite) |
| | Metabisulfite ($S_2O_5^{2-}$) | $Na_2S_2O_5$ (Sodium metabisulphite) (SMBS) |
| | Sulphate | $ZnSO_4$ (Zinc sulphate) |
| | Hydroxyl ions (or pH) | Lime/NaOH |
| **Organic** | Polysaccharides polymer (Natural) | Starch/Dextrin/Guar Gum |
| | Monosaccharides polymer | CMC (carboxymethyl cellulose) |
| | Polyamine | DETA (diethylenetriamine) |
| | Ovalbumin (chicken egg albumin) | |

# RESULTS

## Pulp chemistry survey (pH, Eh, DO, EDTA extraction)

The pH was approximately 11 in the flotation feed, decreasing to approximately 10.2 at the end of the rougher 4. Due to the additional of lime to the head of cleaners 2, the pH increased to 11.6. The redox potential (Eh) was about +100 mV (SHE) in the rougher feed, increasing to +165 mV SHE in rougher 3 and 4, and in cleaner 1. Due to lime addition, the Eh decreased to +100 mV in cleaner 2.

Changes in pulp electrochemistry are due to oxidative reactions. Higher Eh enhances copper sulphides dissolution and, in turn, can promote pyrite activation. One other mechanism for pyrite flotation could be adsorption of collector on pyrite which is not Cu-activated. This mechanism is possible if the Eh is high (>160 mV SHE), particularly when xanthate or dithiophosphate collectors are used. In the case of the plant collector (dithionocarbamate), this should be more selective towards pyrite, and should not adsorb on the mineral unless Cu-activated.

The dissolved oxygen was about 90 per cent of saturation in rougher flotation, decreasing to 80 per cent in the cleaners and 60 per cent in the final concentrate. The DO was relatively high in flotation due to continuous aeration of the pulp. A rapid decrease of DO was observed with time as samples were left unaerated after collection. This indicates oxygen consumption and redox reactions in the pulp. Lower DO levels were measured in the mills, where fresh surfaces are produced and rapidly consume oxygen.

During the survey, some samples were also analysed by EDTA extraction technique. The method allows measuring the amount of surface oxidised metal species on minerals in the pulp. The results showed high EDTA extractable Cu at around 12 per cent in the flotation feed compared to around 2 per cent in the mill feed. This indicates that copper sulphides are oxidised in the grinding stage. Overall, the EDTA profile suggests high levels of oxide Cu on the mineral surfaces, which is highly soluble and can contribute to pyrite activation.

## ToF-SIMS analysis

Figure 2 presents the normalised positive ion signal intensities with 95 per cent confidence intervals, as measured by ToF-SIMS. The results showed that a statistically significant increase in copper was observed on the surfaces of pyrite in final concentrate, which confirms that pyrite is becoming copper activated. This is suspected to be caused by the galvanic interactions in the pulp between pyrite and copper sulphide minerals, causing the oxidisation of copper sulphides and the dissolution of copper into the pulp. Additionally, a high concentration of Mg was found on pyrite particles, suggesting attachment of ultra-fine talc particles to the pyrite surface causing unwanted flotation of pyrite.

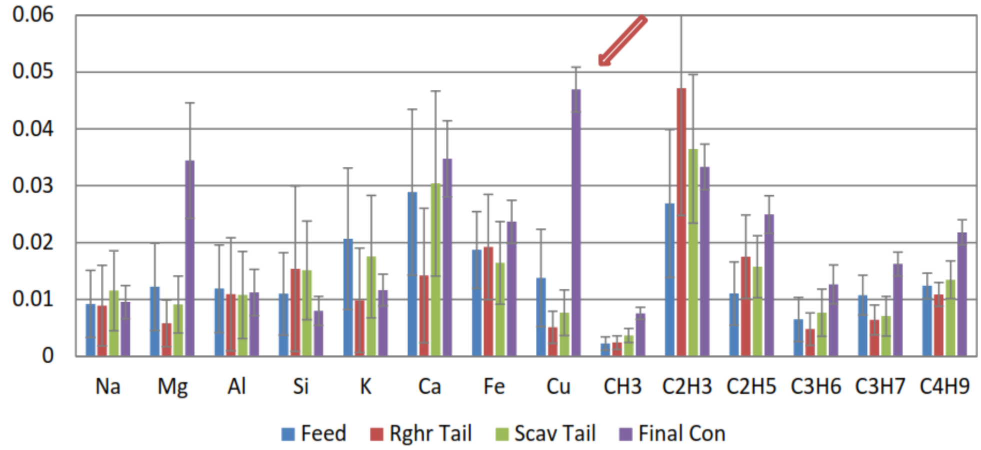


**FIG 2** – ToF-SIMS normalised peak intensities of positive ions with 95 per cent confidence intervals.

## QEMSCAN results

The ESS ore sample was classified as complex mineralogy. The silicate gangue mineralogy is dominated by quartz with muscovite, kaolinite, feldspar, chlorite. Magnetite and siderite (Fe-carbonate) present in minor amounts. The Fe oxide grouping contains trace amounts of Fe hydroxide. Alunite is present in trace amounts.

The Cu deportment is complex between various primary and secondary Cu sulphides (chalcopyrite, bornite, chalcocite), along with trace amounts of covellite, carrolite, enargite and native Cu. The ratio of chalcocite to chalcopyrite increases with reducing particle size and may indicate finer grinding of chalcocite (Figure 3).

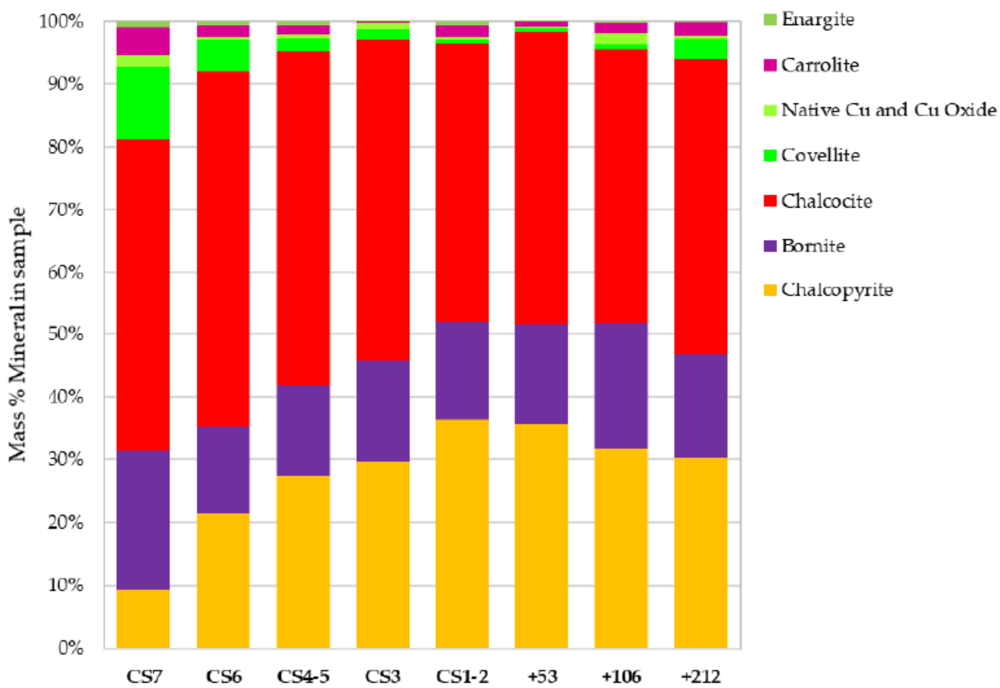


**FIG 3** – Size-by-size Cu mineralogy in float feed presented as mass per cent of minerals.

Liberation has been assessed for minerals of interest in the ore. The liberation and association of the Cu sulphides in the feed in size-by-size fractions are shown in Figure 4. Approximately 65 per cent of the mass of the combined Cu sulphides are liberated based on >80 per cent particle area. Around 16 per cent occurs as middlings (between 30–80 per cent of particle area) and

19 per cent are considered locked (<30 per cent of article area). The locked and middling material occurs either locked with pyrite or non-sulphide gangue minerals (quartz and clay minerals). The grain size distribution showed 80 per cent of the Cu sulphides passing 30 µm in size. This does correspond with an increase in the proportion of liberated Cu sulphides in the CS1–2 fraction (-53/+25 µm).

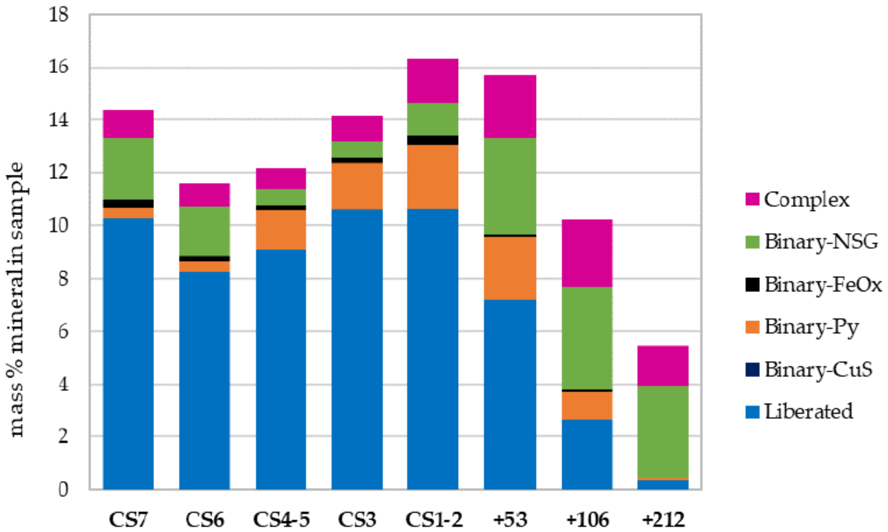


**FIG 4** – Combined Cu sulphide association in float feed.

Recovery of Cu sulphide minerals was assessed by particle size for the rougher concentrates. Approximately 80 per cent of the combined Cu sulphides are recovered and 90 per cent of Cu sulphides in particle sizes <30 µm recovered. Liberated Cu sulphides show higher recovery than the total of the Cu sulphides (Figure 5). The decrease in recovery observed in rougher concentrate is driven by Cu sulphides occurring as binary particles with gangue or pyrite particles. Cu sulphide binaries with pyrite float better than binaries with non-sulphide gangue.

It was observed that approximately 55 per cent of the Cu is recovered in the first stage of the roughing circuit. Rougher 1 recovered finer particle recovery (<30 µm and >5 µm), roughers 2 and 3 increased recovery in the mid particle size range 30–100 µm and the coarse size fractions (>150 µm) show significant recovery improvements in the last roughing stages. Recovery of liberated Cu sulphide drops from 90 per cent to 70 per cent for particles >150 µm.

Dilution to the rougher concentrates is dominated by pyrite at 30–50 per cent by mass (Figure 6). Pyrite in rougher concentrate is mostly associated with Cu sulphide and lesser liberated. Similar to the Cu sulphides, pyrite recovery is primarily in particle sizes <50 µm.

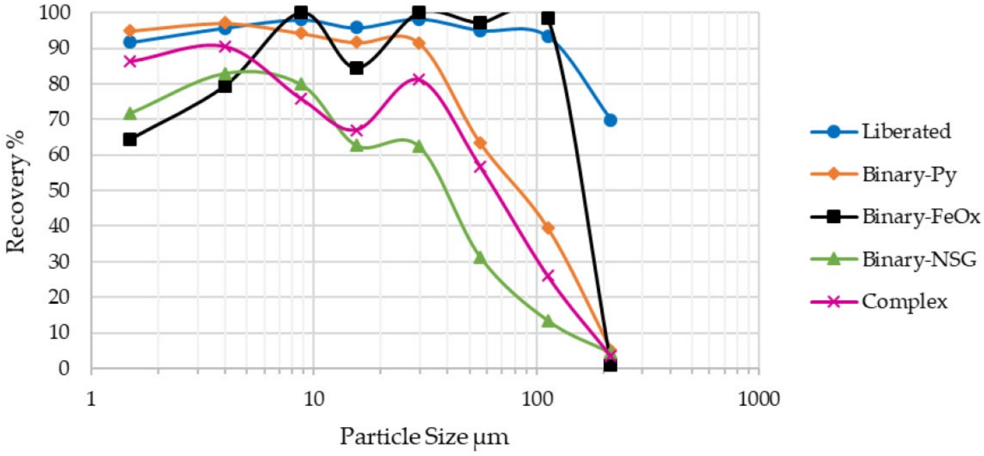


**FIG 5** – Rougher size-by-size recovery of Cu minerals by liberation classes.

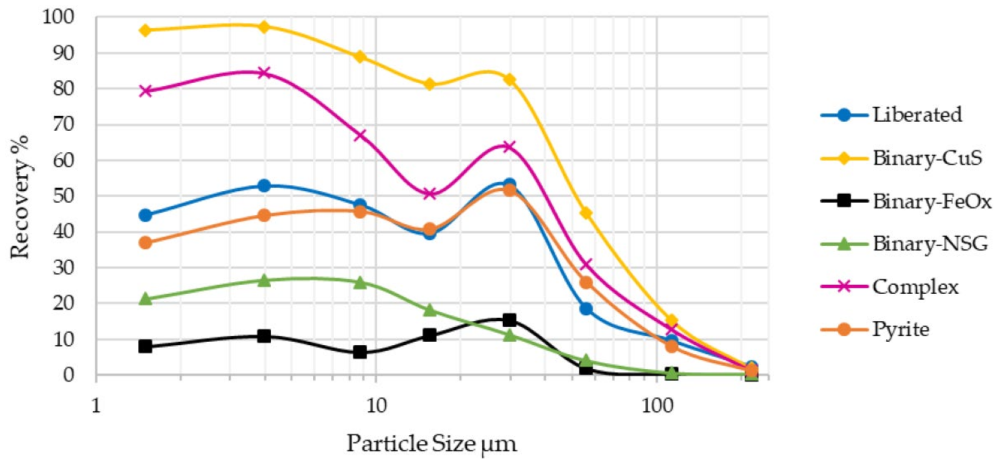


**FIG 6** – Rougher size-by-size recovery of pyrite by liberation classes.

The final concentrate has 40.4 wt% pyrite dilution and 11.1 wt% gangue dilution. Mica, kaolinite, and feldspar content increased in the ultrafine fraction (CS7). Pyrite liberation and association showed pyrite mostly recovered in the coarser fractions. Cleaner stage flotation with pH over 11 helped in reducing pyrite recovery by 4 per cent in fine fractions but was unable to depress the middle and coarse size fractions. 25 per cent of the pyrite is liberated while 54 per cent is associated with the Cu sulphides. 32 per cent of the gangue is liberated while 30 per cent is locked in binaries with Cu sulphides. It was observed that the cleaner circuit maintained the recovery of Cu sulphides collected to rougher concentrate below 100 μm. The cleaner circuit however did not maintain mass and Cu above this size.

The theoretical grade recovery was calculated based on the combined Cu sulphide liberation and Cu grade (Figure 7). Based on the mineralogical limits defined by the mineralogy in the float feed, there is potential for improving the concentrate grade and/or recovery. The mineralogy of the final concentrate was assessed to determine the mineralogical factor that limits the concentrate improvement. Two categories of particle types were determined to be diluting the concentrate: Free pyrite and non-sulphide gangue (NSG) and cu sulphides locked (<30 per cent by particle area) with pyrite or NSG. It would be expected that the locked grains are not considered a loss if liberation can be improved before reporting to the final concentrate. By removing all free gangue and pyrite, a maximum relative increase of 8.2 per cent in concentrate grade would be achieved. The removal of these grains indicates that maximum theoretical Cu concentrate grade can reach 48.6 per cent Cu with a 5.3 per cent Cu loss that can potentially be recovered within the cleaning circuit through regrinding.

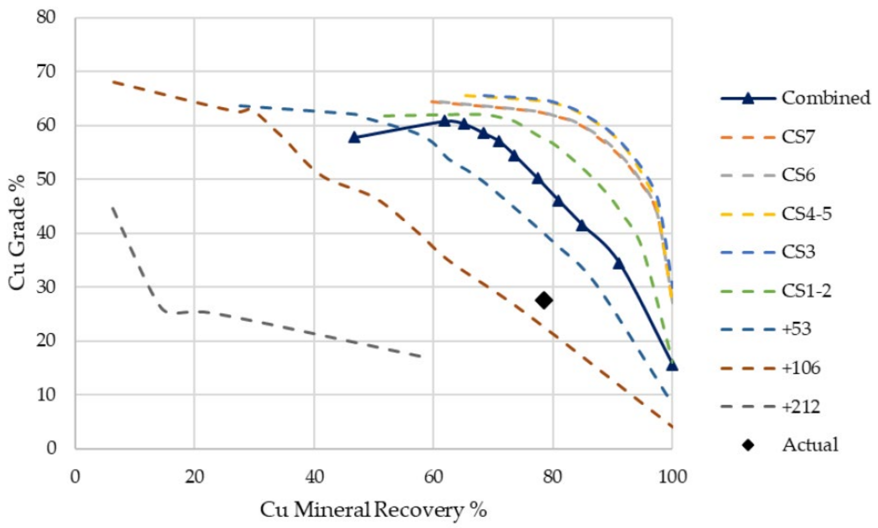


**FIG 7** – Theoretical grade and recovery curve for Cu minerals.

## Flotation test work

Approximately 200 flotation tests were performed during 2019. The key findings from the flotation test work includes:

- A moderate increase in copper recovery and reduction in grade was observed when reducing the grind size from $P_{80}$ of 106 to 75 µm due to copper sulphides reporting to the finer size fractions. However, it would cause a reduction in the plant throughput. It was therefore decided to fix the grind size $P_{80}$ to 106 µm for the plant and in all the tests.
- The adjustment of pH was found to be effective in improving the grade/recovery position. Optimum pH range was around 10.5 with minimal benefits seen when exceeding the pH to 11.5 with ~1.4 times the amount of lime required. Hence the pH target of 10.5 was set for the flotation conditioning tank and all the flotation tests.
- There was a tendency to increase the concentrate grade by decreasing per cent solids from the standard value of 35 per cent to 30 per cent. Recovery on the other hand remained relatively constant.
- Plant process water had a significant impact on flotation results, reducing the recovery by 8.5 per cent compared to fresh water. This is possibly due to the high levels of contaminations in process water that consumes the reagents before they have the chance of adsorbing onto the mineral surfaces. The lime demand to achieve the same starting pH of 10.5 for the process water test was considerably high at 4.5 g/t, against 2.5 g/t for the baseline test.
- Frother type, dosage and addition points were critical in the laboratory flotation test. A series of test work was conducted to benchmark a number of alternative frothers against the current W34 frother. Weaker frother provided better control of the froth phase and improved the copper grade without impacting recovery. The best results were achieved when frother was stage added. Based on the result, one IBC of a new frother trialled and has been added to the flotation conditioning tank since then.
- Of the various types of collectors tested, dithionocarbamate based collectors remained the best performing collector for the ESS ore; showing higher selectively against pyrite. The addition point of collector was an important factor; 5 per cent higher recovery was achieved when the collector was added in the conditioning stage instead of the grinding mill. The dosing point of collector in plant has therefore changed to condition tank.
- The high chrome media was found to produce a marginal improvement in grade/recovery position than stainless steel media, but the selectivity against pyrite remained the same. No change was made in the plant.
- The flotation test work was also conducted on the plant regrind product to assess the effect of peroxide, aeration, and low/high collector dosage on the copper recovery. Only marginal improvement was observed. The fresh feed sample was collected, and batch rougher/regrind/cleaner test work was performed. The copper recovery improved in the cleaner stage. It was found that the temperature of the slurry after regrinding had a significant effect on the copper recovery in the cleaner stage.
- A number of inorganic and organic depressants were tested including cyanide, zinc sulphate, sodium hydrosulphite, MBS, dextrin, CMC and starch to assess if the pyrite can be depressed effectively.
- Cyanide is often regarded as the strongest/most effective depressant for iron sulphide minerals. However, cyanide was found to be ineffective for the ESS ore, with detrimental effect on copper recovery seen when added in excess.
- Some depressions of pyrite were obtained with organic depressants, but organic depressants are not selective, and any depression of pyrite was also accompanied by some reduction in copper recovery, which is highly likely due to the close association between the pyrite and the Cu sulphide minerals.

- Inorganic depressants proved being less effective in depressing pyrite than what observed in the literature. It was presumed that the high solubility of copper sulphides and high levels of copper in solution would have caused the surface activation in pyrite. Thus, EDTA was added ahead of depressant to test out the effect of depressants on the inactivated pyrite particles. However, only marginal improvement in pyrite grade/recovery and the selectivity was observed and any depression of pyrite was also accompanied by some reduction in copper recovery.

None of these reagents yielded the desire results and the baseline condition test with no depressant continued to produce the highest copper grade/recovery. The extent of pyrite depression achieved was very limited and no improvement to the copper and pyrite selectivity was observed.

## EPMA analysis

The compositional analysis was completed using the microprobe. It was observed that pyrite contains variable Cu in solid solution with an average estimate of 0.34 per cent copper in pyrite. Cu in solid solution within the pyrite grains is not significant in terms of total copper in feed and only accounts for 2.5 per cent of Cu calculated for the flotation feed. However, it explains the poor performance observed from the depressant flotation test work.

# DISCUSSION

A comprehensive study was performed at Capricorn Copper Operation including plant survey, pulp chemistry survey, bench scale flotation test work, size-by-size mineralogical characterisation and surface chemistry analysis. These measurements provided a detailed characterisation of circuit performance.

The mineralogical data clearly demonstrated that the concentrate grades and recoveries achieved were not limited by Cu mineral liberation. Based on the theoretical grade and recovery curve defined by the mineralogy and liberation of Cu sulphides in the float feed, there is a potential for improved concentrate grade and/or recovery. Diluents in the concentrate occur as either free (no association with Cu sulphide) pyrite or non-sulphide gangue or Cu sulphides locked with pyrite or gangue. The removal of these grains indicates that maximum theoretical Cu concentrate grade can reach 48.6 per cent Cu with a 5.3 per cent Cu loss that can potentially be recovered within the cleaning circuit through regrinding.

It was observed that the pyrite reports to the final concentrate through three mechanisms:

1. Pulp chemistry survey confirmed the relatively high electrochemical reactivity of minerals in the pulp. It is therefore likely that copper sulphides oxidise due to galvanic interactions with pyrite in the mills. The reaction consumes oxygen and releases copper to solution. ToF-SIMS results showed that a statistically significant increase in copper was observed on the surfaces of pyrite in final concentrate, which confirmed that pyrite is activated by copper.
2. The extent of pyrite depression achieved was very limited in all tests using organic and inorganic depressants and any depression of pyrite was accompanied by equal depression of the copper minerals. Microprobe analysis proved that pyrite contains variable Cu in solid solution, which would cause unwanted flotation of pyrite. This is a separate/new issue to the Cu-activation issue caused by the galvanic reaction in the grinding circuit.
3. Mineralogy analysis confirmed that pyrite mostly recovered to the final concentrate in the middling and coarser fractions. Approximately 25 per cent of the pyrite was liberated while 54 per cent was associated with the Cu sulphides. The cleaner stage flotation was unable to depress the middle and coarse size fractions. The necessity of regrinding stage was concluded.

## Plant modification

Following the results of test work program and plant surveys, the following changes have been made to the plant:

- An option that was considered to improve Cu sulphide recovery in the rougher flotation was the addition point of collector. Approximately 5 per cent improvement in plant copper recovery was achieved when the primary collector addition point was changed to the conditioning tank instead of SAG mill in mid-2019.

- The CCM recovery model only had Fe, which did not correspond well to pyrite as some ore domains were elevated in hematite. As observed from the test work, pyrite content has a direct impact on copper recovery. Therefore, the CCM recovery model has been updated to include total S grade (pyrite content). S to Cu ratio also had a significant effect on the recovery, simply due to the crowding effect.
- Historical operations, prior to 2019, appear to have not focused on blending of ores on the ROM stockpile ahead of processing. The CCM blending strategy has been changed focusing on the ROM ore domains given the variable characteristics between the ore from the three mines.
- To reduce the losses of liberated fine copper sulphides to rougher tail, flotation needs to be more aggressive in the rougher circuit. This will increase the rougher mass pull which will ultimately affect concentrate grade without the regrind in operation. The coarser primary grind can be maintained, but not without the regrind.
- Although the circuit achieved reasonable concentrate grade and recovery with the regrind off, circulating rougher concentrate or scavenger cleaner concentrate to the regrind circuit can aid in improved liberation. Cleaner circuit was unable to depress the middle and coarse size fractions pyrite particles.
- The cleaner circuit is very efficient with cleaner scavenger tails accounting for 1.4 per cent Cu loss. Losses were primarily liberated copper minerals in particle sizes <10 μm. Additional retention time, smaller bubble size and reagent optimisation were trialled in the plant to improve copper recovery.
- The water retreatment plant has been upgraded with new air sparger to reduce $SO_4$ level in process water.
- Frother type, dosage and addition points was critical in the laboratory flotation test. Based on the result, one IBC of a new frother trialled and has been added to the flotation conditioning tank since then.

## CONCLUSIONS

Mineralogical analysis of composite sample indicated that a major source of copper loss was typically very fine (less than 10 μm) copper sulphide particles in rougher tailings that were significantly finer than the target flotation feed size distribution. These particles are easily oxidised and exhibited very slow flotation kinetics under the aggressively selective conditions employed in flotation for pyrite depression. The mineralogical data clearly demonstrated that the concentrate grades and recoveries achieved were not limited by copper mineral liberation.

Several inorganic and organic depressants were tested to assess if the pyrite can be depressed effectively. However, none of these reagents yielded the desire results. Pulp chemistry survey and mineralogical analysis confirmed that the deportment of pyrite to the final concentrate is a result of both mineralogy (insufficient liberation from the Cu sulphides and Cu in solid solution) and electrochemistry (Cu-activation of pyrite in the process).

## ACKNOWLEDGEMENTS

The authors would like to acknowledge the Capricorn Copper personnel that were involved in the survey audit and subsequent sample processing. Capricorn Copper Pty Ltd and Ausenco Ltd are also thanked for giving permission for publication of this study. The authors wish to acknowledge a large number of laboratories including CCM, AMML, UQ, JKMRC, MZ Minerals, and Interchem, XPS and ALS. They also gratefully acknowledge the ToF-SIMS analyses undertaken at the University of South Australia.

# Improving plant performance at the Endeavor Mine using Pionera F-250

*C Vanegas[1], M Sithole[2] and R A Lauten[3]*

1. Metallurgy Manager, CBH Resources Limited, Cobar NSW 2835.
   Email: vanegasc@endeavor.com.au
2. Senior Metallurgist, CBH Resources Limited, Cobar NSW 2835.
   Email: sitholem@endeavor.com.au
3. Senior Scientist, Pionera, Sarpsborg, Norway. Email: rolf.andreas.lauten@pionera.com

## ABSTRACT

Any processing plant dealing with sulphide minerals wants to control the amount of pyrite in their final concentrate. Depression of pyrite is complicated because the surface chemistry of pyrite is similar to that of valuable base metal sulphides. Additionally, galvanic interactions between pyrite and other sulphide minerals, combined with potential activation by ions present in the process water further complicates maintaining control over the amount pyrite reporting to the flotation concentrate.

At the Endeavor Mine in Cobar, NSW, production volumes suggest that the amount of pyrite in the final concentrate increases with the silver content in the ore. While there are several ways to deal with pyrite in concentrates, reduced production volumes of concentrates leave traditional ore blending techniques unavailable to the mine. Evaluation of different depressants revealed that Pionera F-250 adequately depressed pyrite demonstrated in both laboratory tests and in plant trials. F-250 was selected for use in the process as it efficiently reduced pyrite in the final concentrate and improved the grade of lead, silver and zinc concentrates produced.

## INTRODUCTION

Control of the amount of pyrite present in sulphide ore concentrates remains an important challenge at flotation plants. While it is a penalty element, pyrite has some value for its caloric value if concentrates are further refined in smelters. It is well established that the composition of an orebody varies within a deposit meaning that adjustment of operational variables in the flotation process are required for optimal recovery. On occasions it can be sufficient to adjust the dosage of flotation reagents, other times one may have to accept inferior recoveries or grades when processing material from specific parts of a deposit. Concentrates with composition outside budgetary production criteria may be blended with concentrates that comply, giving blended concentrates with composition that satisfy the requirements specified by smelters or leaching plants. Whichever strategy selected it is essential to maintain control of the flotation process and curb the amount of pyrite in the final concentrates while maintaining economically viable recoveries.

Galvanic interactions, either between sulphide minerals or between sulphide minerals and grinding media, are essential for understanding of the flotation recovery in processes where pyrite is depressed (Cruz *et al*, 2005; Peng *et al*, 2003; Qin *et al*, 2015). Essentially, pyrite in contact with less noble sulphide minerals will normally act as a cathode. This facilitates oxidation of the less noble sulphide minerals with an associated increase in hydrophilic oxidation products accumulating on the surface of the less noble sulphide mineral. This normally reduces the flotation recovery (Owusu *et al*, 2014a). Steel grinding media, depending upon the chrome content, can also become oxidised and the iron hydroxides produced may adsorb onto the surface of the desired sulphide minerals. It is essential to control the magnitude of these interactions to maintain control of the flotation process.

The Endeavor Mine is located in Cobar, New South Wales. Operation started in 1983, at that time it was called the Elura mine (Frew *et al*, 1993, 1988; Frew and Peck, 1991). Currently, the known resources are mostly extracted and the mine operates on a skeleton crew. The ore processed is part of a massive sulphide deposit consisting mostly of pyrite, galena and sphalerite along with some non-sulphide gangue (Leahey, 1990). Today, a lead concentrate with a tenor of silver along with a zinc concentrate are produced and sent off-site. Since the Endeavor Mine is reaching end-of-life the available variation in ore is limited and this effectively curtail possibilities for blending concentrates. The remaining resources are considered complex to process and typically only allow production of acceptable grades by sacrificing recovery, meaning that the existing flotation reagent suite was not selective enough. This situation motivated an evaluation of alternate pyrite depressants to improve both grade and recovery.

Laboratory flotation experiments indicated that higher lead recoveries were attainable with alternate pyrite depressants. Plant trials confirmed this and motivated a change of pyrite depressant from a naphthalene sulphonate to Pionera F-250 in production. Continuous use in production allowed better evaluation of how a change in pyrite depressant influenced the flotation process. Overall, more efficient pyrite depression in the lead circuit facilitated changing the collector from Aerophine 3418A to a less expensive dicresyl dithiophosphate (DSP 550). Changing the pyrite depressant also increased the recovery of lead, zinc and silver by at least 2 per cent. The additional improvements to the flotation process initiated by changing the pyrite depressant illustrate how important it is to always seek for ways to improve and/or optimise production parameters to maximise grade and recovery.

## THE ENDEAVOR MINE

Owned by CBH since 2003, the Endeavor Mine is located about 41 kilometres north-west of Cobar, New South Wales in Australia. Ore is mined underground and stockpiled on the surface before processing. Current production capacity is about 1.1 million tonnes per annum. Overall, the flow sheet is traditional with a two-stage grinding process using a SAG mill in the primary step. A vibrating screen return the oversize material to the SAG mill while the undersize enters the secondary step where a ball mill grinds the ore down to a $P_{80}$ about 40 μm. A battery of hydrocyclones return the oversize material to a sump that also contains the SAG mill discharge. Lead and zinc flotation are sequential and the overall layout of the two flotation circuits are similar, see Figures 1 and 2.

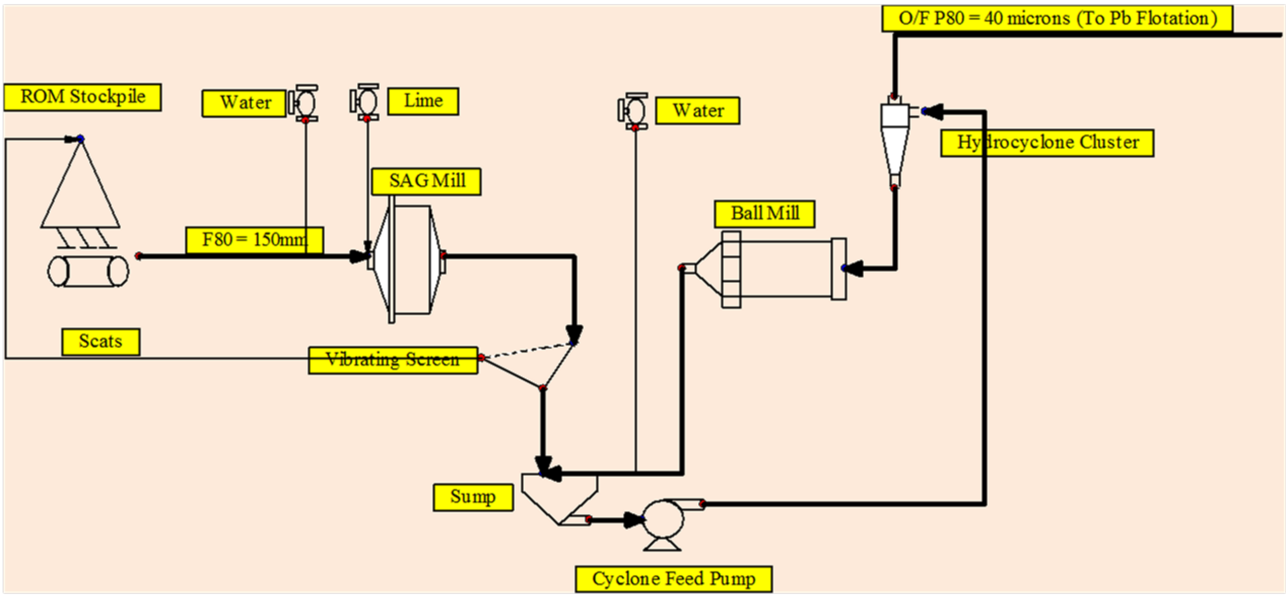


**FIG 1** – Schematic drawing of the grind circuit at the Endeavor Mine.

The lead circuit consists of two parallel lines of nine 8.5 m$^3$ Agitair flotation cells, the first six are used as roughers while the three last are scavengers. The rougher and scavenger concentrates are sent to a 185 kW Metso Stirred Media Detritor for ultrafine grinding before entering the lead cleaning circuit. There are in total three lead cleaning steps. The tails from the first lead cleaner is sent to the zinc flotation process together with the tails from the lead scavenger tails. Typically, large amounts of pyrite build-up in the circulating loads if the roughers are operated in closed circuit with the cleaners. As this is a non-desirable scenario, open circuit is the normal operational mode. An Outotec Courier 5SL on-stream analysis system provide live assays on five streams within the lead system every 10 minutes. This system facilitates constant monitoring of the performance of the flotation circuit. Reagent addition is handled using normal combinations of valves and flowmeters. The flotation cell levels are controlled by normal arrays of float level sensors and flow metres. Both addition of lime and flotation reagents is automated.

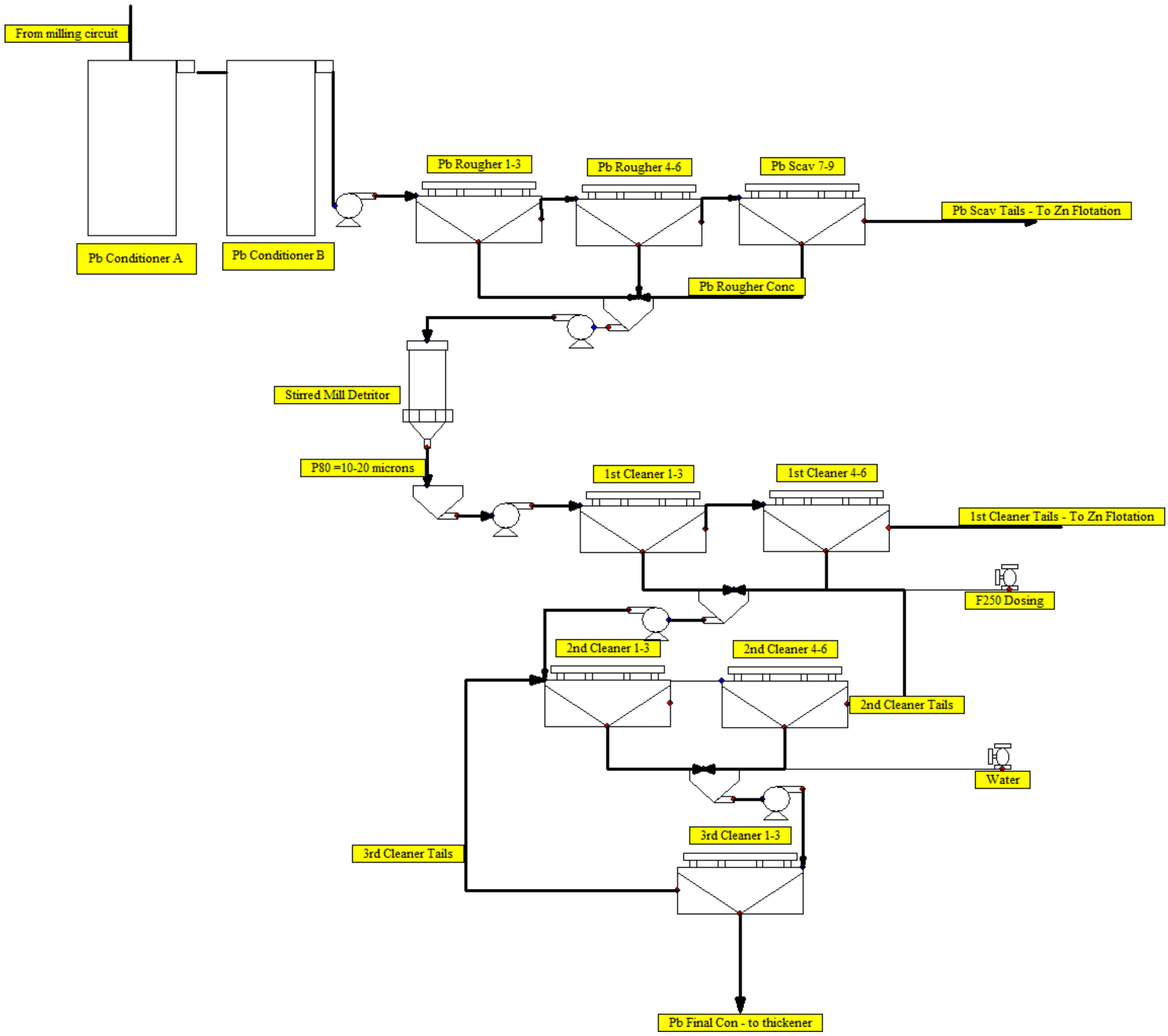


**FIG 2 –** Schematic description of the lead circuit at the Endeavor Mine.

Two conditioning tanks collect the feed to the zinc flotation circuit. Lime to maintain pH at pH 8.0–8.5 and copper sulphate to activate sphalerite is added in one while collector is added in the second tank. Open circuit roughing/scavenging is achieved in two parallel banks of nine 8.5 $m^3$ cells, the last three cells of each bank being the scavengers. The first cleaner is operated in closed circuit with the second cleaner which is also in closed circuit with the third cleaner. First cleaner tailings are further treated in four extension banks operated in a paired parallel configuration. An extension cleaning stage treats first cleaner tailings to recover composite particles (Figure 2). The extension cleaner concentrate combines with the rougher concentrate and get delivered for regrinding in 380 kW stirred media detritors from Metso. The regrind discharge at $P_{80}$ about 10–20 microns gets pumped to the first cleaner. Extension cleaner tailings together with zinc scavenger tailings combine to form the final tailings. The first, second and third cleaning stages take place in two parallel banks of six 5.7 $m^3$, five 5.7 $m^3$ and three 2.8 $m^3$ cells, respectively. The extension cleaners consist of four banks of three 2.8 $m^3$ cells run in a paired parallel configuration.

## PERFORMANCE – CALL FOR ACTION

The achieved degree of pyrite depression is unsatisfactory when processing ore from parts of the deposit, colloquially referred to as complex ore. The poor selectivity in the lead circuit causes production of lead concentrates below customer specification. Lead concentrates within customer requirements while processing the complex ore is possible by sacrificing lead recovery. Two short-term strategies have been utilised when processing the complex ore: maintain economic lead recovery while producing a concentrate outside customer specification. Another option is to direct lead cleaner tails directly to final tails. Directing the lead cleaner tails directly to final tails reduces the plant overall recovery in both the lead and zinc circuit and for that reason it is not a desirable strategy. Production of low-grade concentrates that can be blended with high-grade concentrate when available necessitates sufficient quantities of non-complex ore. This strategy ensures that most of the pyrite not depressed reports to the lead concentrate allowing production of zinc concentrates of acceptable quality. However, as the deposit is nearly exhausted, this is not a practical solution. It emerges that neither approach is satisfactory. Historically, pyrite depression was achieved using cyanide and oxygen (Frew *et al*, 1988; Pietrobon *et al*, 2002). At reduced production volumes the cost and safety measurements required to maintain this system becomes prohibitive. At some stage, cyanide and oxygen was replaced with naphthalene sulphonate as a pyrite depressant. Current evaluation of plant performance indicates the need for a stronger pyrite depressant to reach budgetary requirements since the opportunities for ore blending is limited.

Examination of plant performance using data from the last decade allows identification of conditions causing less than satisfactory plant performance. As illustrated in Figure 3 the lead and zinc recovery normally decrease as the lead, zinc, iron or silver grade in the ore feed increases. The current budgeted lead recovery is included in the figure and the trend clearly illustrate how the lead recovery falls below forecasted values as the silver feed grade increases above about 60 grams/ton. However, as seen in Figure 3 the data are scattered and a comparison of the slopes and correlation coefficients for a selection of dependencies between the ore composition and lead and zinc recoveries are shown in Table 1. Initially focusing on the fitted trend lines for the lead recovery the relation between lead recovery and silver feed grade stands out. The magnitude of the slope and correlation coefficient is larger for this trend line than the others. While none of the correlation coefficients indicate a strong correlation, it is important to notice the potential importance of the silver grade. The slope and correlation coefficient relating zinc recovery to the lead feed grade are largest suggesting that the lead feed grade is most important for the zinc recovery. This may simply reflect that zinc recovery suffers when large amounts of lead enter the zinc circuit. Lead floats first and it is important to depress pyrite to reach the targeted concentrate grade. In that sense, optimisation of the lead circuit is most important. On that basis, evaluation of alternate pyrite depressants should be conducted using ore with a high silver content since this appears to represent conditions where the plant performance is unsatisfactory.

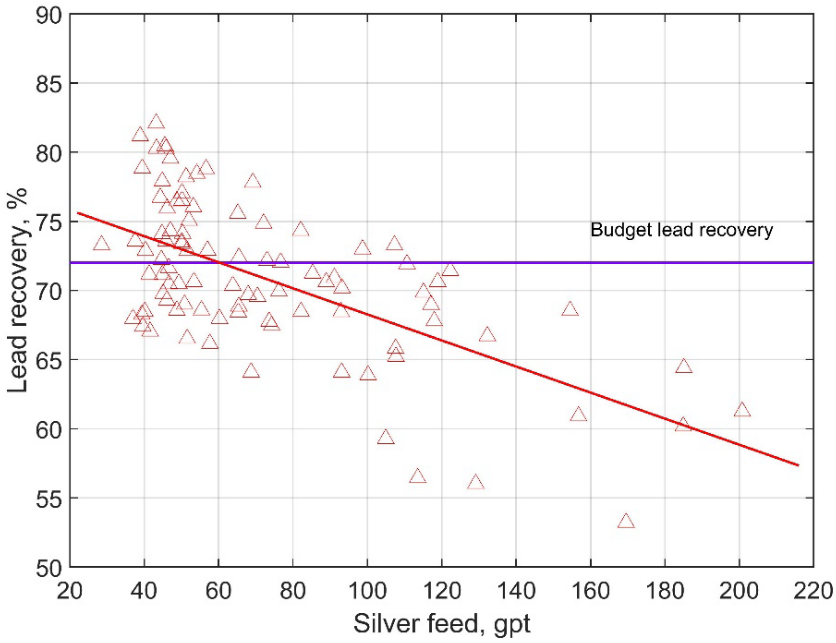


**FIG 3** – Lead recoveries versus silver feed grade at the Endeavor Mine over the last decade.

**TABLE 1**

Fitted slopes and correlation coefficients for trend lines describing the variation in lead and zinc recoveries versus different metal tenors in the feed ore.

| Dependency | Slope | $R^2$ |
|---|---|---|
| Pb recovery versus Fe feed grade | -0.53 | 0.32 |
| Pb recovery versus Pb feed grade | -2.41 | 0.21 |
| Pb recovery versus Zn feed grade | -2.44 | 0.28 |
| Pb recovery versus Ag feed grade | -3.39 | 0.48 |
| | | |
| Zn recovery versus Fe feed grade | -0.49 | 0.78 |
| Zn recovery versus Pb feed grade | -2.70 | 0.82 |
| Zn recovery versus Zn feed grade | -1.82 | 0.76 |
| Zn recovery versus Ag feed grade | -0.12 | 0.85 |

Notice the higher correlation coefficient and slope describing the variation in lead recovery versus silver feed grade. It emerges that the silver feed grade is presumably most important for the lead recovery. In the zinc flotation it appears that the lead feed grade is most detrimental to the zinc recovery, which may reflect contamination of the zinc circuit at high levels of galena in the feed.

## OPTIMISATION OF THE FLOTATION PROCESS

During processing of a complex ore a sample of the flotation slurry was collected from the lead regrind mill discharge, ie the feed to the lead cleaner circuit. Using this sample, laboratory floats evaluating alternate pyrite depressants were conducted. One sample of dextrin and three different biopolymers from Pionera were evaluated and the ability to depress pyrite was compared to that attained with the naphthalene sulphonate currently in use. Figure 4 displays results from the laboratory results. Compared to the naphthalene sulphonate in use, both dextrin and F-250 give higher lead recovery at comparable iron recovery. For instance, at 30 per cent iron recovery the lead recovery is about 76 per cent with the naphthalene sulphonate. At the same iron recovery, the lead recovery with dextrin is about 80 per cent and 82 per cent with F-250. Clearly, if similar results are attainable in production changing the pyrite depressant is an attractive prospect. It is common knowledge at the Endeavor Mine that the pyrite depressant is dosed based on the composition of the ore, generally higher dosages are required when processing complex ore. As the depressant dosage would have to further optimised in the plant, no dosage optimisation was done in the laboratory floats.

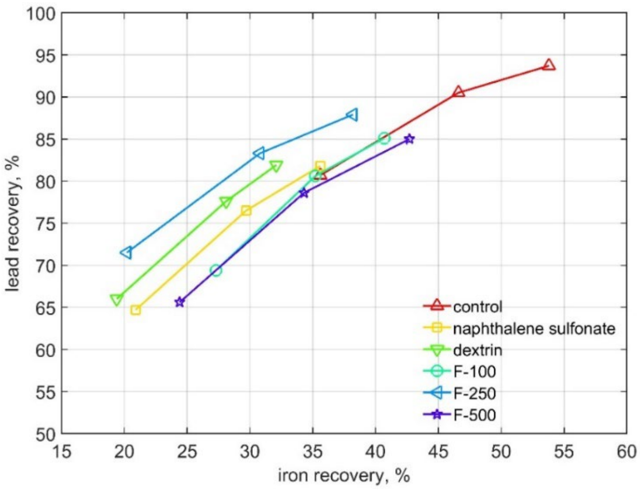


**FIG 4** – Results from laboratory floats using a sample from the lead regrind discharge.

Plant trials were scheduled using either dextrin or F-250. Since the plant essentially only had issues with the flotation recovery during processing of ore with high silver grade, plant trials were spread out in time and matched to the periods when complex ore was processed. In addition to standard metallurgical parameters, operational parameters like ease of handling, responsiveness of the circuit etc were considered as realistic criteria for comparison. As mentioned above, the Endeavor Mine is reaching end of mine and flotation is done in campaigns. Rather than evaluation of three different depressants during one campaign it was decided to use one depressant for the duration of one campaign. Similar to the addition of naphthalene sulphonate, dextrin and F-250 were added to the first lead cleaner feed conditioner. Results from seven different campaigns processing complex ore is shown in Figure 5 where the lead recovery is displayed as a function of the silver feed grade. In Figure 5 it is relevant to highlight overall less than budgeted lead recoveries in the campaign using naphthalene sulphonate in March 2018, while the budgetary demands were reached more often using F-250 in the April 2018 campaign. While only visual, the comparison emphasises the importance of the silver feed grade.

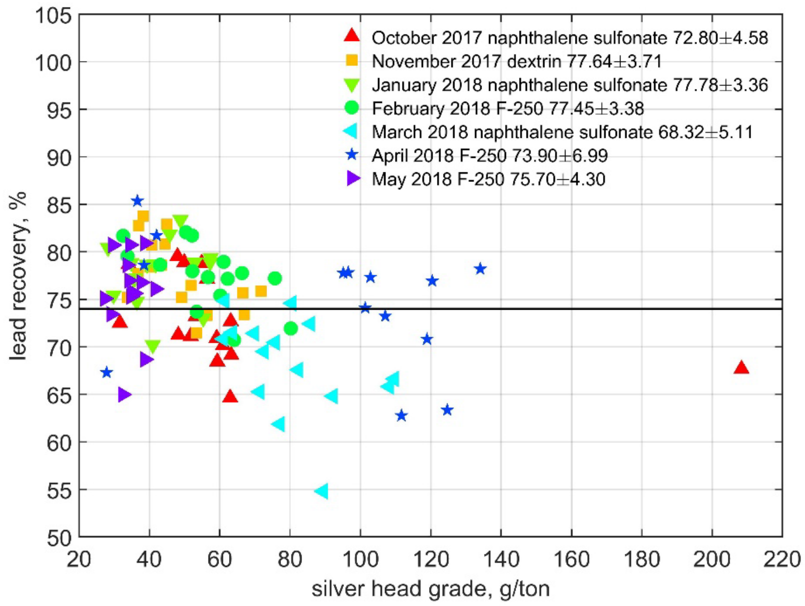


**FIG 5** – Variation in the lead recovery as a function of silver feed grade during several plant trials utilising different depressants.

The lead recovery in several plant trials is shown as a function of production day in each trial in Figure 6. Typically, a campaign lasted for about 20 days and data from the first three days and the last two are discarded since the process was judged to be unstable and not representative during plant start-up or shutdown. The budget lead recovery is marked by a horizontal line. As typical for plant trials the lead recovery fluctuates in each campaign and it is difficult to evaluate if one depressant gives better performance than the others. Using the data from Figure 6 as a basis one may use a null hypothesis and determine at what confidence level it is possible to claim a difference in the average lead recoveries. Such a comparison is included in Table 2 and examination of the results reveals that both dextrin and F-250 improve the lead recovery relative to that obtained using naphthalene sulphonate. There is no significant difference in the lead recoveries obtained with dextrin and F-250. However, the silver feed grade in the plant trial using dextrin averaged at 48 g/ton, while it was 56 g/ton during the plant trial in February 2018 and 92 g/ton in the plant trial in April 2018. Thus, the silver grades processed during the trial period when dextrin was evaluated as a pyrite depressant were not high enough for the ore to be considered complex (Figure 5), essentially indicating that F-250 was the only depressant that improved depression of pyrite in the plant at conditions associated with the processing of complex ore. The Pionera F-250 was selected as a new pyrite depressant because it was easier to handle than dextrin. In contrast, solutions of dextrin were viscous even at dosages around 5–10 mass%. Lumps of un-dissolved dextrin occasionally blocked pumps and valves.

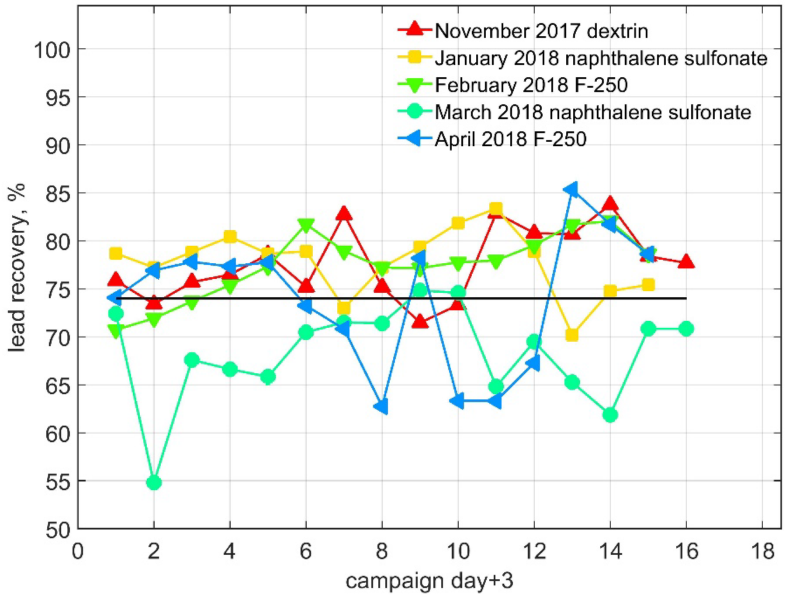


**FIG 6** – Variation in lead recovery as a function of campaign day (data from the three first days discarded due to plant disturbances during start-up) with the indicated depressants.

**TABLE 2**

Student t tests assuming equal variance of the lead recovery during plant trials with the indicated depressants.

| | **Dextrin versus naphthalene sulfonate** | | **Naphthalene sulfonate versus F-250** | | **Dextrin versus F-250** | |
|---|---|---|---|---|---|---|
| Lead recovery | 77.64% | 72.90% | 72.90% | 75.63% | 77.64% | 75.67% |
| Variance | 13.79 | 41.43 | 41.43 | 32.38 | 13.79 | 32.38 |
| Observations | 16 | 31 | 31 | 30 | 16 | 30 |
| Confidence level | 99.5% | | 96.0% | | 89.0% | |

In one of the plant trials (April 2018) the F-250 dosage was varied to gauge the effects on lead grade. It was realised that if overdosed, frothing was completely suppressed (this is apparent in the low recoveries at days 8, 10, 11 and 12 during the April 2018 plant trial in Figure 6). The suppression of lead flotation naturally leads to contamination of the zinc flotation circuit. To mitigate effects of over-dosage, the first lead cleaner tails were redirected to the lead rougher and blended with fresh feed. This strategy reduced the overall lead recovery. Considering the fine-grained nature of the ore it was assumed that reduced lead recovery in the rougher float was associated with the depression of lead-iron particles that otherwise would float (and later being separated in the lead cleaner). To create a buffer against F-250 over-dosage, the addition point was changed from the first to the second lead cleaner. It was later, during continuous use, realised that addition of F-250 led to some additional benefits.

Overall lower mass pull in the second lead cleaner reduced the dosage of F-250 added to the circuit. The typical mass pull in the second lead cleaner required addition of about 300–800 ml/min compared to dosages between 1200 ml/min to 2400 ml/min when added in the first lead cleaner. Lower dosage reduces the chance of over-dosage with potentially negative effects in other parts of the circuit. Further, lower reagent consumption reduces the cost.

The response time for plant operators is faster since only about 30 minutes is required to evaluate the effect of F-250 addition when added to the second lead cleaner, while around 70 minutes is required before the effect on the final product is observed in the final product. Essentially, it facilitates a faster detection of instances where F-250 is overdosed or pump failures occur.

More efficient use of the depressant since fast floating galena is collected in the first cleaner after regrinding. After collection of the easily floating galena, addition of depressant in the second cleaner allows F-250 to interact directly with the pyrite found difficult to depress without use of F-250.

An on/off trial to demonstrate how responsive the lead circuit became after implementation of all changes (reduced pH in the zinc circuit, F-250 rather than naphthalene sulphonate and DSM 550 instead of Aerophine 3418A) was completed and the results are illustrated in Figure 7. During a campaign, while maintaining similar pulp levels and air flow rates in the flotation circuit, the F-250 dosage was turned off after attainment of a steady state in the flotation process. After the dosing of F-250 was turned off 45 minutes was allowed to gradually wash residual F-250 out of the circuit, followed by one hour where the response of the lead flotation circuit was monitored closely before addition of F-250 commenced. The typical residence time in the second lead cleaner is about 20 minutes, meaning that the 45 minutes allows elimination of most F-250 present in process water.

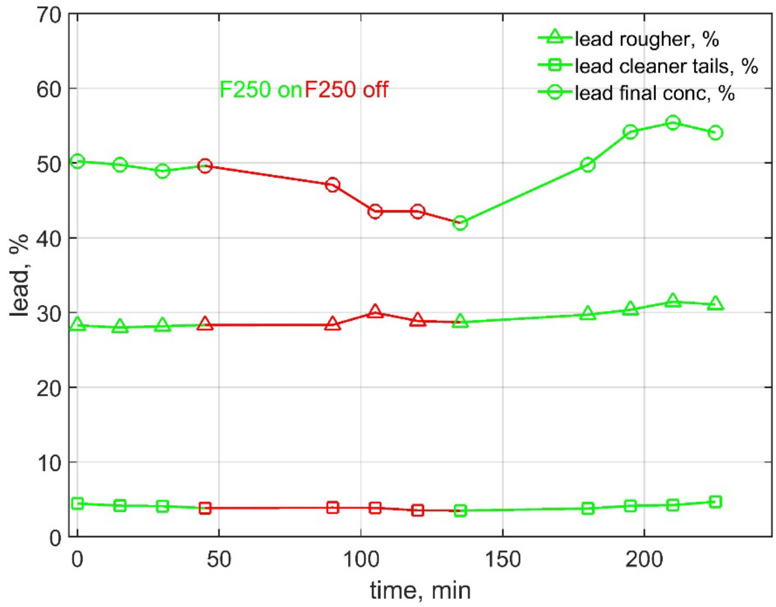


**FIG 7** – Results from an on/off trial.

In Figure 7, it is seen that the rougher lead grade is nearly constant at about 28 per cent during the on/off trial. Towards the end of the trial, an increase towards about 31 per cent lead can be observed. There is an almost immediate drop in the lead final concentrate grade after 45 minutes roughly representing the time when the F-250 is assumed washed out of the system. During the next hour the lead grade continuously decreases as the recirculating load of F-250 gradually decreases. Immediately upon addition of F-250, at around 135 minutes into the on/off trial, the lead final concentrate grade increases. A steady-state lead final concentrate grade establishes at a level somewhat higher than what it was prior to the off period. This likely reflects the modest increase in lead rougher concentrate grade. Also included in the Figure 7 is the variation in lead cleaner tails. The lead grade in the cleaner tails shows a corresponding variation, albeit corrected for a delayed response in this part of the circuit.

Everyday use of F-250 revealed additional benefits. As the F-250 acted as a competent pyrite depressant it was possible to increase the mass pull in the lead circuit, effectively increasing the recovery. The fact that less lead and iron report to the zinc circuit when using F-250 in the lead circuit meant that less lime was required to depress pyrite in the zinc circuit. Thus, the pH in the zinc circuit was gradually dropped from about 9.0–10.5 to between 8.0 and 8.5. Reduced pH in the zinc circuit combined with use of F-250 in the zinc circuit also gave increased recoveries in the zinc circuit also.

Finally, since F-250 acted as a more capable pyrite depressant than naphthalene sulphonate it was possible to replace Aerophine 3410A with a less selective collector (DSP-550). Replacement of the Aerophine 3410A with a less costly dithiophospate reduces overall operational expenses. Overall, the change of pyrite depressant increased the recoveries of lead, silver and zinc with 5 per cent without affecting the grade. In terms of cost, F-250 is more expensive than naphthalene sulphonate. The increased depressant cost is more than compensated by higher recoveries.

## DISCUSSION

From a practical point, the results speak for themselves: replacement of a naphthalene sulphonate with F-250 overall improve the recoveries of lead, zinc and silver while maintaining the grades in the concentrates produced at the Endeavor Mine. Further optimisation of the process after the initial successful plant trials demonstrates how changes in the reagent suite utilised in a plant normally allow additional fine tuning of operational parameters. Process optimisation requires desire to improve, a good understanding of how the flotation process responds to changes and patience.

Closely related to the need for an understanding of the sensitivity of the flotation process is its response to changes in the mineralogy. Analysis of the plant recovery revealed a correlation between the lead recovery and the silver grade in the flotation feed (Figure 3). Galvanic interactions between pyrite and valuable base metal sulphides are ubiquitous in base metal sulphide beneficiation. Pyrite, the most noble sulphide mineral, form galvanic elements with less noble minerals, here galena and sphalerite. Oxidation processes at the surface of galena or sphalerite lead to the formation of hydrophilic metal hydroxides which lower the flotation recovery. Lead ions released into the process water may attach to pyrite and in a process referred to as lead activation, increase the flotation recovery of pyrite. Yet, at Endeavor, the case is reduced flotation recoveries when the silver grade in the ore increases, suggesting more complex interactions between the constituents of the ore.

Sand is used as grind media in the lead and zinc regrind process prior to the respective cleaner circuits. This means that galvanic interactions take place between the sulphide minerals only, where pyrite is the dominant mineral. In the zinc circuit, copper sulphate is introduced to activate sphalerite. According to Zhang *et al* (1997) there is a preferential interaction between xanthate and copper-activated sphalerite effectively minimising the flotation recovery of pyrite, suggesting that depression of pyrite in the lead circuit is the main challenge. This is partially corroborated by Frew *et al* (1993) who stated that poor liberation was a significant cause of poor recoveries in the zinc circuit. Presumably, the detritor in the zinc regrind allows sufficient liberation. Disregarding silver, reduction of oxygen and formation of lead or zinc hydroxides on the surfaces of galena or sphalerite represents the expected outcome of galvanic interactions. Presumably, the solubility of these hydroxides in the process water determines how galvanic interactions reduces the flotation recovery of galena or sphalerite. Silver metal, on the other hand, is more noble than pyrite suggesting that in a galvanic element formed between silver and pyrite, pyrite will form the anode and contact with silver will promote anodic oxidation of pyrite. Oxidation of pyrite is a complex process with two well-defined oxidation products, ferrous hydroxide and sulphate ions, where the former normally takes place to a higher extent (Dos Santos *et al*, 2016; Owusu *et al*, 2014b). This allows for the presence of metal-deficient pyrite on the surface (Huai *et al*, 2017; Smart *et al*, 1999). Metal deficient pyrite has a higher hydrophobicity and is more likely to float. Thus, anodic oxidation of pyrite may increase the hydrophobicity of pyrite. A possible scenario in the flotation circuit at Endeavor is an increasing hydrophobic character of pyrite, due to galvanic interactions with silver present in the ore. It is possible that the magnitude of this pyrite surface modification scales with the relative proportions of the galvanically active constituents in the flotation slurry and thus only become apparent as reduced flotation recoveries above a minimum silver content in the ore.

The laboratory flotation experiments and results from plant trials indicate stronger pyrite depression when processing ores with high silver content in the presence of F-250 than naphthalene sulphonate. Assuming galvanic interactions between silver and pyrite indeed do increase the hydrophobic character of pyrite, and that use of F-250 yields more efficient pyrite depression may suggest that this depressant in addition to binding to hydrophilic patches on the pyrite surface also may interact with hydrophobic patches, as these are suspected to increase in number due to galvanic interactions.

Aerophine 3418A or sodium diisobutyl dithiophosphinate is an efficient collector in the flotation separation of galena from pyrite. According to Pecina-Treviño *et al* (2003a, 2003b) this collector adsorbs via chemical interactions to the surface of galena. It is suggested that the adsorbed layer of Aerophine 3418A inhibits further dissolution of galena, effectively reducing the amount of lead oxidation products that otherwise may lead to activation of pyrite (Peng *et al*, 2003) and associated higher flotation recoveries of pyrite. Piantadosi and Smart (2002) determined that Aerophine 3418A preferentially adsorbed onto galena rather than pyrite, accounting for its selectivity and popularity as a collector for complex sulphidic ores. As mentioned above, it was discovered that it was possible to replace Aerophine 3418A with a less selective dithiophosphate after switching from a naphthalene sulphonate depressant to F-250. Thus, the stronger pyrite depression obtained with F-250 allowed use of a less selective collector. In contrast to xanthates, both dithiophosphates and dithiophosphinates (also dithionocarbamates) are believed to chemisorb onto sulphide minerals. Holistically, one must assume that both will form a layer on the surface that inhibits galena dissolution and activation of pyrite. Thus, the difference in separation efficiency observed at the Endeavor Mine likely stems from stronger binding of F-250 onto pyrite, lead-activated or not, than naphthalene sulphonate. Disregarding differences in molecular weight, this conjecture demands that the variation in functional groups on the two polymers drives this difference in selective binding. Naphthalene sulphonate contains mainly hydroxyl and sulphonate groups while F-250 contains carboxylic acid groups in addition. In a comparison of biopolymers with composition similar to F-250, it was found that a higher content of sulphonic groups gave less efficient pyrite depression (Mu *et al*, 2016). In this context it is also relevant to consider dextrin, which also was evaluated as a pyrite depressant. Dextrin is a polysaccharide where the functional groups are hydroxyl groups (López Valdivieso *et al*, 2004). Judging from the results of the laboratory results (Figure 4) this depressant gave nearly similar depression of pyrite as F-250, and both gave substantially better pyrite depression than naphthalene sulphonate. Overall, a combination of functional groups, predominantly carboxylic acid and hydroxyl units appear to give stronger pyrite depression than either hydroxyl groups or sulphonic acid groups alone. A general observation is that rather than comparing the effect of collectors and depressants individually when optimising a flotation process, there is a need to consider the combined effect of both collector and depressant.

## CONCLUSION

Analysis of the ore composition and historical lead recoveries led to a proposed relation between the ore head silver grade and elevated amounts of pyrite in primarily the lead flotation concentrate at the Endeavor Mine. High pyrite contents in the final concentrates induces penalties when the concentrates are sold off-site and lower than budgeted recoveries at the mine. Substantial improvement in plant performance was achieved when the pyrite depressant was changed to Pionera F-250. This change led to improved pyrite depression independent of silver head grade. In addition, more efficient pyrite depression facilitated lower pH in the flotation circuit, essentially reducing the lime consumption and replacement of Aerophine 3148 to a less costly dithiophospate-based collector.

It is suggested that an increasing silver head grade enhances galvanic interactions between silver and pyrite in the flotation process. In the proposed galvanic element between silver and pyrite, pyrite is oxidised leading to the emergence of hydrophobic metal-deficient sulphide patches which readily reports to the flotation concentrate.

Comparison of different flotation depressants reveals that F-250 is a more efficient flotation depressant than a dextrin or the previously used naphthalene sulphonate. Assuming that an increasing silver grade in the ore increases the hydrophobic nature of pyrite via galvanic interactions, improved pyrite depression with F-250 may reflect improved binding to pyrite, independent of the presence of hydrophilic and hydrophobic surface sites, in contrast to naphthalene sulphonate or dextrin.

## REFERENCES


Cruz, R., Luna-Sánchez, R.M., Lapidus, G.T., González, I., Monroy, M., 2005. An experimental strategy to determine galvanic interactions affecting the reactivity of sulfide mineral concentrates. Hydrometallurgy 78, 198–208. https://doi.org/10.1016/j.hydromet.2005.03.006

Dos Santos, E.C., de Mendonça Silva, J.C., Duarte, H.A., 2016. Pyrite Oxidation Mechanism by Oxygen in Aqueous Medium. J. Phys. Chem. C 120, 2760–2768. https://doi.org/10.1021/acs.jpcc.5b10949

Frew, J.A., Davey, K.J., Glen, R.M., Orrock, G.I., 1993. Performance of the Pasminco Mining Elura Zinc Flotation Circuit, in: Flotation Plants: Are They Optimised? SME, Littleton, Colorado, pp. 95–193.

Frew, J.A., Heyes, G.W., Orrock, G.I., 1988. Defining Elura's Lead and Silver Flotation Problems, in: Third Mill Operators' Conference. AusIMM, Cobar, Australia, pp. 97–102.

Frew, J.A., Peck, R.C., 1991. The Effect of Liberation on Elura's Lead Flotation Performance, in: Fourth Mill Operators' Conference. AusIMM, Burnie, Tasmania, pp. 97–102.

Huai, Y., Plackowski, C., Peng, Y., 2017. The surface properties of pyrite coupled with gold in the presence of oxygen. Minerals Engineering 111, 131–139. https://doi.org/10.1016/j.mineng.2017.06.013

Leahey, T.A., 1990. Grade trends at the Elura mine, in: Mine Geologists' Conference. AusIMM, Mount Isa, Australia, pp. 99–112.

López Valdivieso, A., Celedón Cervantes, T., Song, S., Robledo Cabrera, A., Laskowski, J.S., 2004. Dextrin as a non-toxic depressant for pyrite in flotation with xanthates as collector. Minerals Engineering 17, 1001–1006. https://doi.org/10.1016/j.mineng.2004.04.003

Mu, Y., Peng, Y., Lauten, R.A., 2016. The depression of copper-activated pyrite in flotation by biopolymers with different compositions. Minerals Engineering, Special Issue: Froth Flotation 96–97, 113–122. https://doi.org/10.1016/j.mineng.2016.06.011

Owusu, C., Brito e Abreu, S., Skinner, W., Addai-Mensah, J., Zanin, M., 2014a. The influence of pyrite content on the flotation of chalcopyrite/pyrite mixtures. Minerals Engineering 55, 87–95. https://doi.org/10.1016/j.mineng.2013.09.018

Owusu, C., Fornasiero, D., Addai-Mensah, J., Zanin, M., 2014b. Effect of regrinding and pulp aeration on the flotation of chalcopyrite in chalcopyrite/pyrite mixtures. Powder Technology 267, 61–67. https://doi.org/10.1016/j.powtec.2014.06.026

Pecina-Treviño, E.T., Uribe-Salas, A., Nava-Alonso, F., 2003a. Effect of dissolved oxygen and galvanic contact on the floatability of galena and pyrite with Aerophine 3418A. Minerals Engineering 16, 359–367. https://doi.org/10.1016/S0892–6875(03)00022–0

Pecina-Treviño, E.T., Uribe-Salas, A., Nava-Alonso, F., Pérez-Garibay, R., 2003b. On the sodium-diisobutyl dithiophosphinate (Aerophine 3418A) interaction with activated and unactivated galena and pyrite. International Journal of Mineral Processing 71, 201–217. https://doi.org/10.1016/S0301–7516(03)00059–0

Peng, Y., Grano, S., Fornasiero, D., Ralston, J., 2003. Control of grinding conditions in the flotation of galena and its separation from pyrite. International Journal of Mineral Processing 70, 67–82. https://doi.org/10.1016/S0301–7516(02)00153–9

Piantadosi, C., Smart, R.S.C., 2002. Statistical comparison of hydrophobic and hydrophilic species on galena and pyrite particles in flotation concentrates and tails from TOF-SIMS evidence. International Journal of Mineral Processing 64, 43–54. https://doi.org/10.1016/S0301–7516(01)00075–8

Pietrobon, M.C., Grano, S.R., Greet, C. J., 2002. Matching laboratory and plant performance – a case study of the Elura lead circuit, Pasminco Australia Limited, in: Proceedings 34th Annual Meeting Canadian Mineral Processors. CIM, Ottowa, Canada.

Qin, W., Wang, X., Ma, L., Jiao, F., Liu, R., Gao, K., 2015. Effects of galvanic interaction between galena and pyrite on their flotation in the presence of butyl xanthate. Transactions of Nonferrous Metals Society of China 25, 3111–3118. https://doi.org/10.1016/S1003–6326(15)63940–1

Smart, R.S.C., Skinner, W.M., Gerson, A.R., 1999. XPS of Sulphide Minerals Surfaces: Metal-deficient, Polysulphides, Defects and Elemental Sulphur. Surface and Interface Analysis 28, 101–105.

Zhang, Q., Xu, Z., Bozkurt, V., Finch, J.A., 1997. Pyrite flotation in the presence of metal ions and sphalerite. International Journal of Mineral Processing 52, 187–201. https://doi.org/10.1016/S0301–7516(97)00064–1

# Advances in flotation froth pumping

*P Woodall[1], D Smith[2] and J Pease[3]*

1. Principal Engineer, Glencore, Mount Isa Qld 4825. Email: peter.woodall@glencore.com.au
2. Manager – Metallurgy and Port Operations, McArthur River Mining, Darwin NT 0820. Email: daniel.smith@glencore.com.au
3. Principal Consultant, Mineralis Consultants, Brisbane Qld 4006. Email: jpease@mineralis.com.au

## ABSTRACT

Handling of tenacious froths is a growing problem for the minerals industry. Increasingly it dominates plant performance, especially for operations that require finer grinding.

This paper investigates the pumping challenges faced at the McArthur River Mine from tenacious froths produced during the flotation of ultrafine mineral concentrates. It defines the development pathways followed to improve pump performance and the alternatives considered, many of which were failures. Finally, it provides an overview of the solution, its success at MRM and the implications of this work to the broader mineral processing industry.

## INTRODUCTION

It is not uncommon for the performance of mineral processing plants to be restricted by materials handling constraints. Some constraints (eg an undersized transfer chute) impact at a single 'point'. However, a constraint from 'difficult' froth, has wide-ranging consequences – including reduced plant throughput to limit spillage, poor process control due to inaccurate level control which leads to circuit instability, reagent dosing constraints and poor dewatering capabilities due to entrained air. A difficult-to-pump froth is a pervasive influence on a concentrator, adversely affecting throughput, recovery and concentrate grade, costs, and hygiene. A plant simply cannot meet design – let alone be optimised – while froth handling dominates operating decisions.

Flotation froth becomes much more stable for finer-sized solids, partly because higher reagent additions are needed, but mainly because the extremely high mineral surface area and homogeneous particle sizing affect water drainage and bubble breakage. At a $P_{80}$ of 7 μm there are no occasional coarse (eg 150 μm) particles to affect local water drainage and effectively 'prick' the bubbles. Designs of launders, sprays, sumps and pumps that are effective for concentrates with a $P_{80}$ of 35 μm will not be effective at 7 μm, where a given mass of solids has five times the surface area.

More operations will need to adopt fine grinding as future ores become more complex and as there are increased requirements to produce higher quality concentrates (eg to reduce arsenic) which necessitate finer regrinding. This will lead to an increased need to design for 'difficult' froth conditions. The warning signs of such problems are usually overlooked in laboratory and pilot test work – though the froth is tenacious, it is handled at small scale by oversized launders and pumps, high spray water additions, fresh water instead of recycled water, high technician attention and delays between steps. Most of this cannot be reproduced at full scale, so while serious froth handling constraints should usually be foreseen, they often are not.

## THE McARTHUR RIVER EXPERIENCE

The McArthur River (MRM) Zn/Pb operation in the Northern Territory of Australia was the first metals flotation plant to apply ultrafine grinding. It was commissioned in 1995, using the custom developed IsaMills to regrind all rougher concentrate to a $P_{80}$ of 7 μm before five stages of cleaning initially, with a sixth stage installed later. This ultrafine grind was required to achieve adequate liberation from gangue minerals to produce a saleable bulk concentrate. The design team expected difficult froth handling, and paid particular attention to over-size launders, sprays, sumps and pumps. However even this 'over-design' significantly underestimated the problem and handling of tenacious froth became a dominant issue for MRM over the next two decades. The best available technology was simply not good enough.

The inability to pump the tenacious froth hindered both operational and metallurgical performance, impacting zinc recovery due to the inability to increase flotation air rates or pulp levels without risking the overall stability of the flotation circuit. The plant bottleneck could move between any one of the six stages of cleaning when treating higher grade ore, or during ‘froth basher’ maintenance, requiring a whole flotation bank to be bypassed for periods of up to 72 hours. The poorly performing pumping infrastructure therefore contributed to poor upgrading within the cleaner circuit, and the resulting spillage limited plant throughput. On occasions the plant has had to shut down to get the froth spillage under control.

The ultrafine cleaner concentrates also contributed to downstream problems including difficult pumping of the flocculant-stabilised, but aerated thickener underflow stream. Pumping of this stream had historically been problematic with the pump components wearing rapidly due to excessive cavitation. Water injection points and air-breathers were used on the suction and discharge of the underflow pump to limit cavitation; however, this reduced plant filtering capacity by diluting the underflow.

To illustrate the problem with MRM’s $P_{80}$ 7 μm cleaner concentrates, even after the installation of a generously-sized continuous-air-releasing Weir 300LF pump in the final (sixth) cleaner stage, the pump could only develop a discharge pressure of between 60 and 70 kPa. This continued to be the plant’s throughput-limiting point with the sump regularly overflowing even with a ‘froth basher’ operating to ‘break’ froth before pumping (Figure 1). To achieve acceptable production rates, load had to be removed from this pump by bypassing some of the fifth cleaner concentrate away from the sixth cleaning stage and sending it directly to final concentrate, therefore compromising the cleaning circuit upgrade.

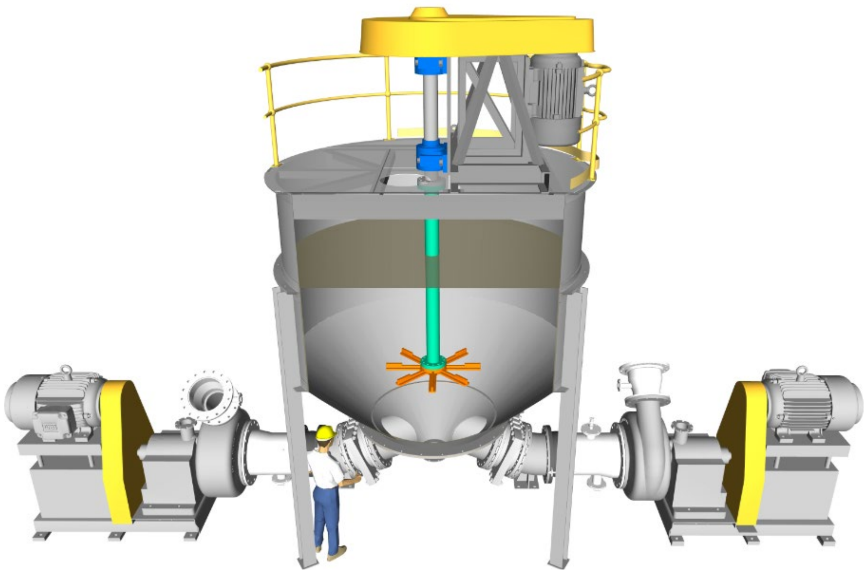

**FIG 1** – Typical ‘froth basher’ installation within the sump to assist froth breakage before the pump inlet. Note the high-volume sump and dual pumps often employed to assist froth pumping.

Successful pumping in the cleaner circuits has traditionally required the installation of tall sumps, multiple oversized pumps on each sump, and froth breakage devices in sumps including froth bashers and large water sprays. The froth bashers are typically driven by 55 kW motors and are therefore expensive to run. They are also difficult to maintain, requiring the sump to be isolated for access.

Manufacturers have continued to develop their pumps to improve handling of ultrafine froths. The key changes have included large-suction pumps, low net-positive-suction-head (NPSH), and flow-inducing impellers, together with the implementation of continuous air-releasing devices.

In this paper we review the pathway followed to improve MRM’s understanding of flotation froth pumping. The principles traditionally used to design cleaner circuit pumps were found to be inadequate for handling ultrafine concentrates. Even at a relatively modest froth volume factor (FVF) of 1.5 (33 per cent air by volume), performance does not conform to the pump characteristic. Further, while the traditional measure of froth volume factor is important, it is not insurmountable if the froth breaks (releases air) easily during handling and transport. More important is the *stability* of the froth – the bucket of MRM froth in Figure 2 would appear much the same if it was left for 24 hours. It does not 'collapse under its own weight' in a sump – or in the spillage pit or on the thickener surface. Application of some form of external mechanical energy is necessary to promote froth breakage.

**FIG 2** – Highly stable MRM final concentrate, which can appear more like 'whipped cream' than a typical froth.

Finally, this paper reviews the solution developed to significantly improve cleaner circuit pumping capacity and discusses the implications of the new designs for the broader mineral processing industry.

This paper reports insights gained and developments made from three decades of operating experience with highly tenacious froth. This is a difficult field and further understanding is still needed.

# THE PATH TO RECENT INSIGHTS

## Initial unsuccessful developments

After two decades of froth pumping constraints at MRM, in 2015 a Weir 300LF pump with continuous air release was installed in an attempt to meet the second cleaner concentrate pumping duty. The pump performance was however very poor. Glencore worked closely with Weir in an attempt to improve performance, including:

- Firstly, all the 'traditional' improvements were made to pumping infrastructure. Pump speed was increased, a large spray was installed at the top of the sump, the casing was rolled over to the 315° position, and a new high-capacity flow inducer was fitted behind the pump impeller. Unfortunately, no significant improvement in performance resulted from these modifications.
- The pump was then fitted with a new suction spool, which sloped up into the sump, and trials were conducted with radical screw and axial-flow feeders (Figure 3) fitted to the impeller assembly. A minimal improvement in performance was noted when the screw-flow feeder was fitted but the pump still could not handle the entire cleaner stream, even with the 'froth basher' in operation. The axial-flow feeder actually significantly impeded pump performance.

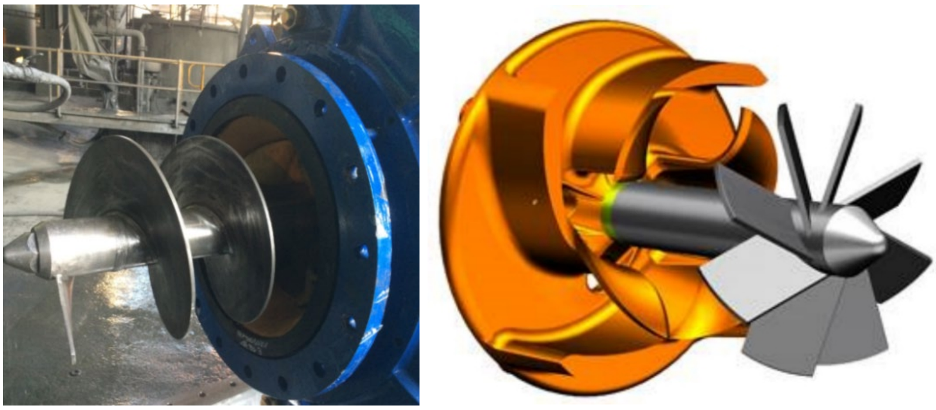

**FIG 3** – Screw-Flow (left) and Axial-Flow feeders.

After this close collaboration with Weir it was clear that these pumping problems could not be solved by traditional approaches and that advances in our understanding of flotation froth pumping were required.

## Advances through observation and test work

To develop our understanding of pumping tenacious ultrafine froths it was essential to work closely with the operations team and to conduct plant test work, sometimes sophisticated, sometimes necessarily crude. Some key learnings from prolonged observations and test work were:

- That a slurry pump handling an aerated stream performed better when running with a badly leaking gland – noted by an experienced operator.
- Clear evidence was found that the pump impeller liberated a portion of the air entrained in the slurry stream. As shown in Figure 4, some of this liberated air was driven into the suction spool where it could be identified by viewing intermittent discharge of air from the valve at the top of the suction spool adjacent to pump entry. Air could also be seen discharging within the sump, having travelled backup the pump suction pipework after being liberated from the froth.

  Air discharged from suction spool.mp4

  Air discharged from sump.mp4
- It was found that liberated air was centrifuged to the centre of the impeller and intermittently discharged from the 'pump vent' at the rear of an air-releasing pump. As air built up in the pump casing the discharge pressure also reduced. Note that a modest 20 kPa increase in pressure can represent a doubling of flow rate due to the low pipeline velocity.

  Air discharged from pump vent and influence of air-locking on pump discharge pressure.mp4
- Test work confirmed that the froth volume factor (FVF) at the wall of the suction spool was consistently lower than at the centre of the spool. This indicated the existence of pre-rotation as described by Breugelmans and Sen (1982). Pre-rotation of slurry in the suction spool drives air towards the centre of the spool. Pre-rotation usually reduces pumping efficiency and is avoided when designing for the 'best efficiency point' (BEP). As will be described later, the counterintuitive insight at MRM was that, for difficult froths, pre-rotation is an essential prerequisite to de-aerate the froth, and therefore it *improves* overall pumping efficiency for those froths.

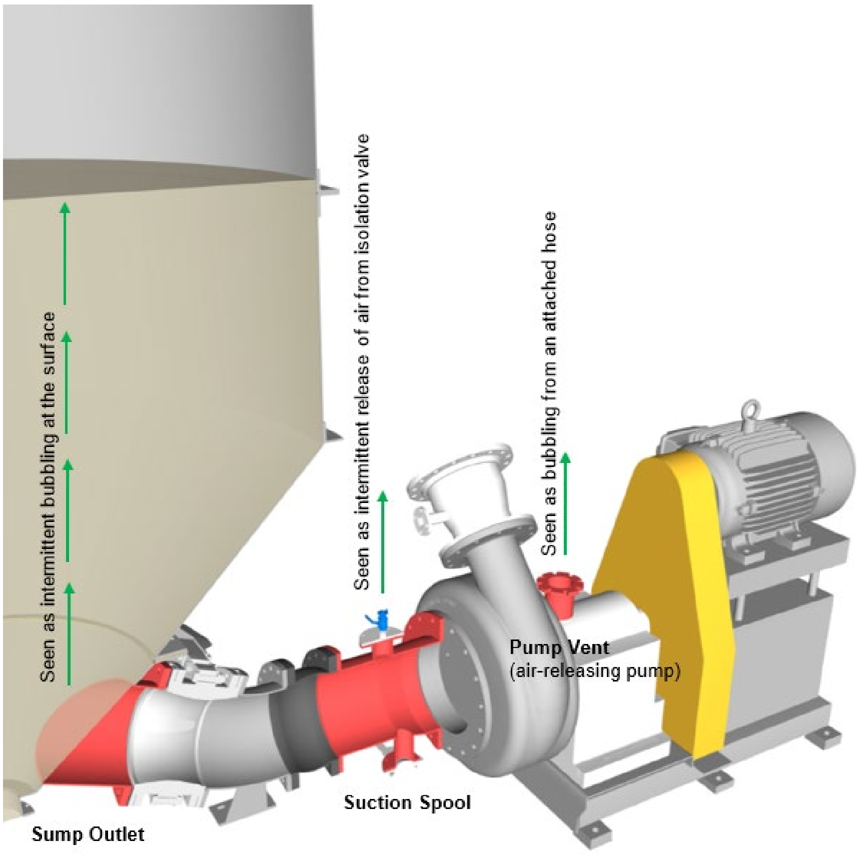


**FIG 4** – The arrows indicate the three 'air release' locations.

Finally, test work showed that the air liberated from the slurry needs to be removed from the pump at a sufficiently high rate. If not the rotation of the impeller induces pre-rotation of the slurry in the suction spool, with a velocity $V_t$ as shown in Figure 5. This causes build-up of high air content slurry at the centre of the suction spool and pump. Table 1 demonstrates the high froth volume factor at the centre of an operating pump. This impedes pump performance and is why, as operators understand, if you increase the speed of a froth pump its performance often becomes worse; but if the pump is stopped and restarted its performance temporarily improves.

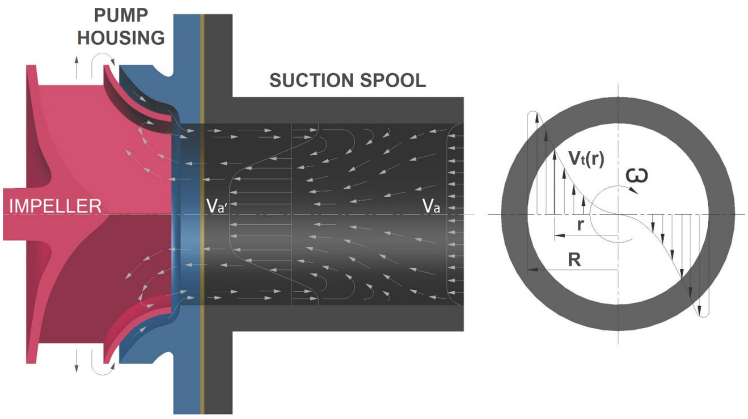


**FIG 5** – Pre-rotation and circulation within suction spool.

**TABLE 1**

Cleaner 1 variations in suction spool 'centre' (shown left) and 'wall' (right) FVF.

| Suction spool location | Froth volume factor, FVF |
|---|---|
| Wall | 1.11 |
| Centre | 2.86 |

A pump with reduced performance due to 'air-locking' is easy to detect by installing a valve positioned vertically at the top of the pump suction spool, adjacent to the pump flange as shown in Figure 4. If the pump becomes air-locked the valve discharges air when opened and the discharge pressure decreases and becomes unsteady.

## Confirmation of observations and understanding through literature study

While no relevant published information was found in the mineral processing industry, many water industry publications confirmed the presence of secondary pre-rotation, $V_t$, and axial back flow, $V_a$, in suction pipework. Because aerated slurry is not an issue in the water industry, practice has developed to maximise pumping efficiency by reducing pre-rotation, for example by installing inlet guide vanes.

The work done by Murakami and Heya (1966) is particularly useful to understanding the relationship between pre-rotation, $V_t$, and axial back flow, $V_a$, in relation to the actual flow rate with respect to the pump's best efficiency point flow rate, BEP. For the impeller tested in this paper (data replotted in Figure 6), at 86 per cent of the BEP flow rate no pre-rotation is induced in the suction spool, while at 70 per cent of BEP flow the pre-rotation is more than 60 per cent of impeller speed at the wall of the suction spool. This work also showed (not plotted in Figure 6) that at 70 per cent of BEP flow, the axial back flow is close to 20 per cent of the impeller speed.

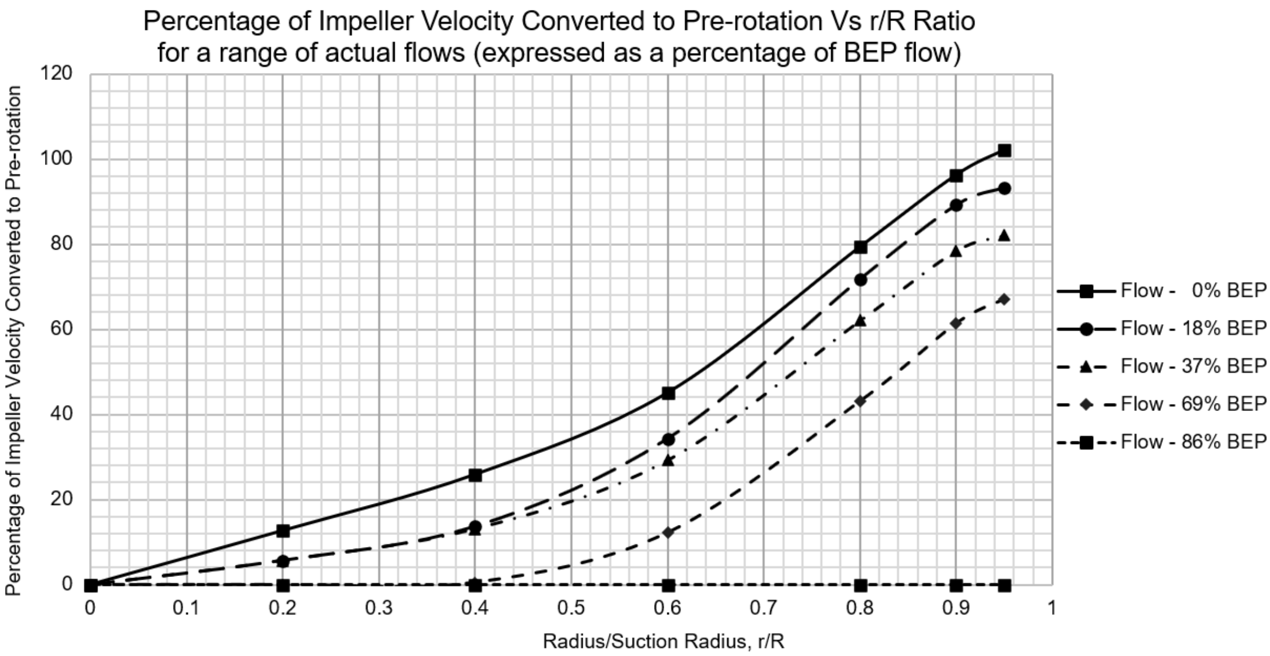


**FIG 6** – Relationship between the percentage of Impeller Velocity Converted to pre-rotation and the r/R ratio (see Figure 5) for a range of actual flows expressed as a percentage of the best efficiency point, BEP, flow.

As flotation froth pumps are often sized with duty points well below 70 per cent of BEP flow, pre-rotation and axial back flow can be expected to be induced deep within the suction spool. This amount of pre-rotation will centrifuge liberated air to the centre of the suction spool where it will reduce pump performance if it is not removed quickly enough.

# APPLYING THE NEW UNDERSTANDING TO DEVELOP SOLUTIONS

## Equipment development

The above observations, test work and literature showed that an opportunity existed to improve the performance of flotation froth pumps by:

- ***Firstly, separating the liberated air.*** Size the pump and suction spool to induce pre-rotation ahead of the pump to centrifuge the liberated air to the centre of the suction spool. The extent of this slurry pre-conditioning determines the extent of de-aeration. For example, increasing the impeller velocity from 13.8 to 18.8 m/s increased the volume percentage of air at the suction spool centre from 54 to 70 per cent. Though this would be a low efficiency point for a non-aerated feed, it allows higher efficiency for difficult froths – ***if*** the liberated air is removed quickly enough.
- ***Secondly, remove the liberated air.*** This required development of a device to remove the large volume of liberated air from the centre of the suction spool and impeller. This was achieved with a 'jet pump' powered by process water (Figure 7). There is an obvious maintenance advantage to such a device with no moving components; further the use of process water to drive air removal is sensible since cleaner feed streams are typically diluted to reduce entrainment anyway – at MRM they are diluted to around 10 to 15 per cent solids by weight, so part of the existing water addition can be redirected to this air-removal duty.

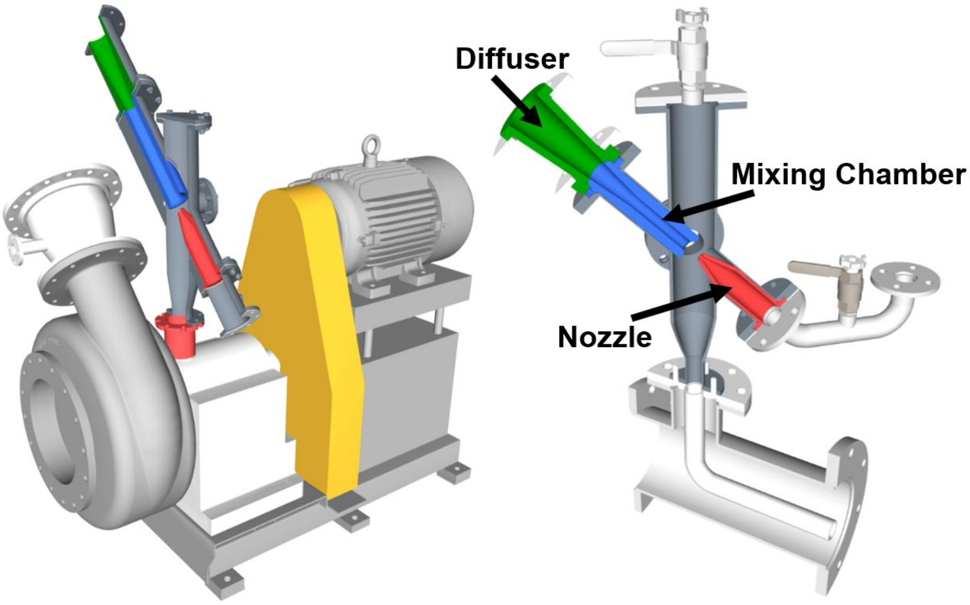


**FIG 7** – 200NB 'Pump Vent' mounted and 32NB 'Suction Spool' mounted vent (jet) pumps.

As seen in Figure 7, jet pumps are simple devices that consist of three components; the nozzle, mixing chamber, and diffuser. The *nozzle* is used to accelerate the process water stream and provide the energy to drive the 'pump'. The *mixing chamber* is where primary-secondary turbulent mixing occurs. The area ratio between the nozzle and the mixing chamber is critical to success because it determines the ratio between the driving and induced flows and the head which can be developed. The *diffuser* converts some of the stream's velocity to pressure head.

Glencore successfully patented these concepts and devices for froth handling, currently in Australia and the USA, with further patents pending.

## Froth pump performance

Before fitting air-removal devices to the final (sixth) cleaner at MRM, the pump could only develop a discharge pressure between 60 to 70 kPa even with a froth basher in operation. The de-aeration devices fitted to this circuit included:

- A froth basher to help break froth in the sump.
- A vent pump (Figure 8) – a jet pump mounted either to the 'pump vent' at the rear of the air-releasing pump or within the 'suction spool', to remove air from the centre of the suction spool and impeller. The discharge of the jet pump is sprayed back into the sump to help break froth before the pump inlet.
- A 'de-aerator' (Figure 9) – a very large jet pump to draw aerated flotation concentrates from the sump adjacent to the 'sump outlet', to de-aerate it before spraying it back into the sump to help break froth before the pump inlet.

**FIG 8** – 200NB vent pump circuit (jet pump on the 'pump vent').

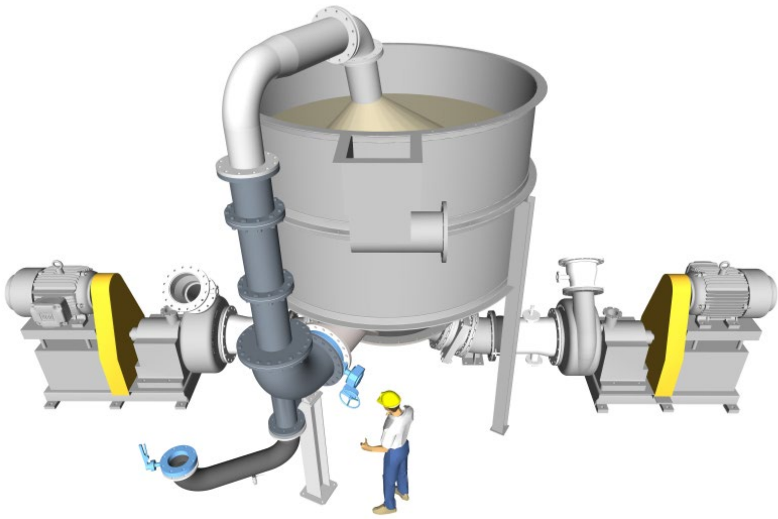

**FIG 9** – 500NB 'de-aerator' circuit (jet pump).

The performance of the combination of the vent pump (jet pump on the 'pump vent'), and the de-aerator jet pump adjacent to the suction inlet, is documented in Table 2. (Note that the operating pump was fitted with duplicate pipelines and therefore the documented flow represents only approximately 45 per cent of the total streamflow.)

**TABLE 2**

Froth pump performance data 'with' and 'without' vent pump in operation.

| **Sump level** | **Vent pump status** | **Pump performance** | |
|---|---|---|---|
| | | **Flow $m^3/hr$** | **Pressure kPa** |
| *At normal sump operating level* (2300 mm below overflow) | On | 561 | 130 |
| | Off | 453 | 100 |
| *At high sump level (overflow level)* | On | 622 | 135 |
| | Off | 465 | 110 |

The improvement in pumping flow rate ranged from 24 to 34 per cent prior to the upgrade of the vent pump capacity in early 2016.

The performance of a vent pump and therefore the cleaner pump depends on maintaining high enough process water pressure to the vent pump. In general, to achieve induction ratios in excess of 2.25 (induced to process water flow), the process water pressure should exceed 300 kPa and ideally be in the order of 350 to 400 kPa to remove sufficient air to allow good cleaner pump performance.

This development work also provided some useful understanding on the influence of sump height on pump performance (Table 2). The results indicated that when the vent pump was operating, pump flow rate increased in the order of five per cent per metre of sump level compared with an increase of only one per cent per metre when it was turned off.

## INDUSTRY LEARNINGS

It is now understood that air-locking within the impeller and suction spool is the principal cause of poor froth pump performance when pumping ultrafine cleaner concentrates at MRM. Air-locking, with its resulting effect on pump performance, also results from poor sump level control, a common concentrator issue, or slurry rotation (which promotes the formation of a vortex) within the sump.

Though the installed froth pumps had air removal systems they were unable to remove the large volume of air reporting to the centre of the pump impeller and suction spool at MRM. The installation of vent pumps, along with correctly sized pumps and suction spooling, improved pump flow rate by 24 to 34 per cent by efficiently removing the air from the pre-classified stream in the suction spool and impeller. The vent pumps were designed to remove between 10 and 250 $m^3$/hr of highly aerated slurry. To achieve this the process water supply pressure should ideally be around 350 to 400 kPa.

When a vent pump is designed with sufficient capacity to remove all the air from the suction spool and impeller eye, no liberated air can be seen collecting at the top of the suction spool and the pump discharge pressure both increases and becomes steady. Current test work suggests that the maximum extent of de-aeration is equal to the froth volume factor at the wall of the suction spool. This highlights the importance of optimising pre-rotation within the suction spool, to maximise the centrifuging of air from the froth. This is counter to normal pump design practice which aims to minimise pre-rotation to increase pump efficiency.

The addition of vent pumps to the froth handling circuits at MRM enabled the discharge pressure developed by these pumps to increase from typically 60 to 70 kPa to as high as 160 kPa.

Finally, reliable sump level control, especially when pumping final concentrate to a thickener, is critical. Plants often struggle to pump or more importantly dewater final concentrates simply because air is induced into the concentrate when a sump is operated with insufficient level, a pump is run in manual, or because of non-functioning level transmitters. This can significantly affect pumping of thickener underflow streams since viscosity increases exponentially with the air content.

## A GUIDE TO DESIGN FOR 'DIFFICULT FROTH' PUMPING

From experience with pumping highly stable tenacious froths at MRM over several decades, the following design approach is recommended for sites that expect difficult froth (as a guide, this includes – though is not limited to – any streams with $P_{80}$ below 20 µm):

### New installations

1. Employ flotation cells with launders which are both wide and deep.
2. Employ large diameter launder froth pipes with vents. Launder pipes should join the main line at a 'Y'. The main line should increase in area at each junction to keep constant froth velocity.
3. Use tangential entry of froth pipes into sumps or direct the stream into the wall. Do not allow the stream to 'jet' into the sump as this induces air into the stream.
4. Ensure sumps have well designed level transmitters. Pressure transmitters should be capable of being isolated online with mounting spools inclined 'downwards' to avoid or reduce the build-up of settled solids. The intent is to avoid operating froth pumps at 'snore' because of faulty level transmitters since this ingests further air into the stream.

5. Ensure the process water circuit is generously sized to distribute water at 500 kPa with the velocity in the pipework not exceeding 1.5 m/s. Process water circuits should always include a standby pump.
6. Install good pressure sprays on launders and sumps and ensure they can be easily and safely removed for cleaning. All spray offtakes should be taken vertically from the process water main and be sized to ensure that, where possible, only particles smaller than the spray orifice are drawn into the pipework. Large (minimum 50NB) full-cone sprays are ideal for sumps and are easy to design and cheaply manufactured.
7. Sumps with 6 m height from the centreline of the pump to the overflow are ideal as this provides approximately 4 m of usable suction head.
8. The suction spool should be run for a minimum length of twice the suction line diameter to encourage pre-rotation and therefore classification ahead of the pump. The suction spool should then angle up into the pump sump (with at least a 5D bend) to encourage the release of air pushed back into the suction spool by the induced axial backflow.
9. Specialist froth pumps should be selected preferably with air release mechanisms. These pumps should be sized to operate at not more than 70 per cent of BEP flow at maximum duty. At minimum duty the pump should operate at greater than 25 per cent of BEP flow.
10. Discharge pipework should be sized to limit the velocity of aerated slurry to 1.5 to 2 m/s.
11. Install a vent pump to draw either from the dedicated 'pump vent' (air-releasing froth pumps) or from the suction spool – see Figure 7. The process water pressure should exceed 300 kPa and ideally be around 350 to 400 kPa. The ratio between the extraction rate of highly aerated slurry and the process water flow rate will typically be between 2.25 and 2.5. Vent pump extraction rates currently range from 10 to 250 $m^3$/hr.
12. 6 mm pitot tube access points should be fitted at 45° off-centre and one pipe diameter (1D) from the pump suction and 10D after disturbances in the discharge pipework. 25NB ball valves should be positioned vertically in the 'suction spool' at approximately 150 mm from the pump inlet flange and also at 2D from the pump discharge flange (if accessible). These access points are required to analyse the 'froth' characteristics and pump performance because froth pumping is never quite as expected (it is usually worse) and it is variable with plant conditions, so information for troubleshooting and optimisation is essential.
13. Ensure the site has 6 mm OD pitot tubes to measure the FVF at the centreline and wall of the suction spool, and pressure gauges with protectors to measure the static pressure at both the pump suction and discharge.

## Existing installations

Existing installations are invariably constrained by space, access and by the cost of modifications. Each of the above design points should be considered to the extent practical, with focus on sequentially removing the obvious bottlenecks as they become apparent. It is often impractical to change existing layouts for launders, froth pipes and sumps, however the changes to pipework, pump type, vent pumps and measurement infrastructure are usually both possible and effective, and are almost certain to be necessary, and the cost justified, at a site constrained by froth handling.

If an upgrade is to be successful, reliable data must be gathered under varying operating conditions. To gather this data the suction and discharge spools must be fitted with 6 mm pitot tube access points and 25NB ball valves to allow fitting of pressure gauges.

# CONCLUSION

As required regrind sizes become finer, the handling of tenacious froths will become increasingly important to the minerals industry. Technology that is suitable for 'conventional' coarser, less stable froths is inadequate for fine-grained stable froths. When encountered, froth constraints become a dominant influence on operations, restricting the ability to achieve throughput, cost, metallurgical or hygiene targets. The developments presented here appear to offer a general solution.

## ACKNOWLEDGEMENTS

We wish to acknowledge the assistance and patience of the McArthur River Mining team, and in particularly S Strohmayr and J Andreatidis without whose assistance and support these developments would not have been realised.

Finally, we wish to acknowledge the unique tenacity, support and courage of the operations, metallurgical and maintenance personnel which is so characteristic of the MRM team.

## REFERENCES

Breugelmans and Sen, 1982. Prerotation and Fluid Recirculation in the Suction Pipe of Centrifugal Pumps, Proceedings of the Eleventh Turbomachinery Symposium, Texas A&M University.

Murakami and Heya, 1966. Swirling Flow in Suction Pipe of Centrifugal Pumps, Bulletin of JSME 621.67.01:532.542.

Engineering Sciences Data Unit, ESDU 85032, 2007. *Ejectors and jet pumps, Design and performance for incompressible liquid flow* (ESDU, London).

# Plant operations

# Debottlenecking of the Ridgeway Concentrator at Newcrest's Cadia Operation

*R Edmunds[1], M Wilkens[2], B Akerstrom[3] and C Haines[4]*

1. Specialist Performance – Processing, Newcrest Mining Limited, Orange NSW 2800. Email: robert.edmunds@newcrest.com.au
2. Senior Planning Metallurgist, Newcrest Mining Limited, Orange NSW 2800. Email: matthew.wilkens@newcrest.com.au
3. Manager – Ore Processing, Newcrest Mining Limited, Orange NSW 2800. Email: brandon.akerstrom@newcrest.com.au
4. Metallurgical Superintendent, Newcrest Mining Limited, Orange NSW 2800. Email: campbell.haines@newcrest.com.au

## ABSTRACT

The Ridgeway Concentrator at Newcrest Cadia was commissioned in 2002 as an ABC circuit to treat the ore from the Ridgeway sublevel cave (SLC) at around 5 MTPA. Consisting of a single pinion 32' autonomous grinding (AG) mill and a single pinion 7 MW ball mill, it was a much smaller plant than the adjacent Cadia Hill Concentrator. Subsequent expansion of the circuit saw additional infrastructure added as the ore source transitioned to Ridgeway Deeps, a block cave below the original Ridgeway SLC. The key additions were a secondary crusher to reduce the semi-autonomous grinding (SAG) mill feed size and tertiary grinding for reduction in flotation feed size to maintain recovery.

The Cadia East mine, which consists of two large block caves, became the sole feed source for the Ridgeway Concentrator in March 2016. The Cadia East ore has a higher Bond ball mill Work Index (BWi) and lower A*b than ore from the Ridgeway mine or Cadia Hill open cut. This paper details the debottlenecking improvements made to the plant to further increase grinding circuit throughput despite the harder ore, including installing new equipment to tertiary crush the SAG mill feed, optimisation of mill liner design, upgrades to grinding mill drive trains and numerous smaller optimisation activities.

## INTRODUCTION

Newcrest's Cadia Valley Operation is located approximately 25 km from the city of Orange in New South Wales. The operation comprises three copper/gold ore deposits: the Cadia Hill deposit, the Ridgeway deposit and the Cadia East deposit. Production of the first concentrate began in 1998 with the Cadia Hill processing plant and was followed by the Ridgeway processing plant in 2002, now known as Concentrator 1 and Concentrator 2 respectively. Both concentrators produce a gold doré and flotation concentrate of copper and gold. Initially Concentrator 2 was designed specifically to treat the Ridgeway sublevel cave ore deposit, the Ridgeway mine was then extended to Ridgeway Deeps block cave in 2008. The Ridgeway cave ceased production in 2016 and then concentrator capacity was used to treat Cadia East ore. This paper discusses key changes to the Concentrator 2 processing circuit over time with a focus on the comminution flow sheet and the major debottlenecking activities brought about by changing ore characteristics in the feed.

## RIDGEWAY ORE – 2002 TO 2014

### Ridgeway ore properties

Physical properties were determined from a combination of laboratory and pilot scale testing and coupled with actual plant performance data taken during the Cadia commissioning ramp up in 1998. This data was used to assist in determining the Ridgeway mill sizing and selection.

Ridgeway ore was determined to be softer than Cadia Hill ore, reflecting the increased level of quartz veining and sulphide mineralisation present in the Ridgeway deposit. At 16.0 kWh/t, the Bond ball mill Work index was 5–10 per cent lower than Cadia. Although the Ridgeway ore was softer, the abrasion index was notably higher than the majority of Cadia ores and appeared to increase with grade (Hart *et al,* 2003).

Of the five major rock types tested, monzodiorite intrusive (MDI) was significantly harder than the remaining components. This rock type comprised 15 per cent of the overall reserve tonnage and hence it was allowed for in mill sizing and selection but not a dominant factor. Table 1 compares key comminution properties from the dominant rock types in both the Cadia and Ridgeway deposits (Hart *et al,* 2003).

**TABLE 1**

Summary of Comminution Properties (Hart *et al,* 2003).

| **Rock type** | **Bond Crushing Work index CWi (kWh/t)** | **Bond rod mill Work index RWi (kWh/t)** | **Bond ball mill Work index BWi (kWh/t)** | **Abrasion index** | **JK A** | **JK B** | **JK Ta** |
|---|---|---|---|---|---|---|---|
| Cadia Monz | 16.7 | 19.9 | 18.0 | 0.35 | 65 | 0.6 | 0.3 |
| Cadia Volcs | 23.2 | 23.8 | 21.0 | 0.30 | - | - | - |
| R'Way HGV | 18.3 | 18.1 | 14.9 | 0.57 | 66 | 0.70 | 0.45 |
| R'Way LGV | 15.6 | 19.9 | 16.1 | 0.43 | 62 | 0.68 | 0.37 |
| R'Way MDI | 17 | 23.4 | 17.7 | 0.30 | 67 | 0.50 | 0.40 |

Note: HGV = High-grade Volcanoclasties. LGV = Low-grade Volcanoclasties. *A* and *B* are used to characterise the impact breakage of the ore. *Ta* is a measure of the resistance of the ore to abrasion as per the JK breakage test.

Gold mineralisation in the Ridgeway deposit occurred mainly as free grains in quartz or on the margins of sulphide grains. Visible gold was present in the ore with particle sizes ranging from a few microns up to 1 mm. Copper mineralisation occurred as chalcopyrite and bornite with the bornite content increasing towards the centre of the deposit, typical of a large porphyry system. Magnetite was present in significant quantities (between 10 and 20 per cent).

Notable changes to the Ridgeway Concentrator between prior to 2014 are detailed in previously published AusIMM papers (Hart *et al,* 2000, 2003, 2005).

## TRANSITION FROM RIDGEWAY DEEPS TO CADIA EAST – 2014 TO 2017

Ridgeway ore supply to the Ridgeway Concentrator transitioned to Cadia East ore due to declining grades from the Ridgeway deposit. Table 2 highlights the grade difference between the two ore deposits in the months leading towards the Ridgeway mine closure.

Note the naming convention for the concentrators changed following the closure of the Ridgeway mine. The Ridgeway Concentrator is now referred to as Concentrator 2 and this naming will be used throughout the remainder of the paper.

**TABLE 2**

Grade Comparison between Cadia East and Ridgeway Ore Deposits.

| Month | Ridgeway gold grade (g/t) | Ridgeway copper grade (%) | Cadia East gold grade (g/t) | Cadia East copper grade (%) |
|---|---|---|---|---|
| February 2016 | 0.43 | 0.28 | 1.24 | 0.34 |
| January 2016 | 0.55 | 0.31 | 1.26 | 0.35 |
| December 2015 | 0.47 | 0.26 | 1.21 | 0.34 |
| November 2015 | 0.46 | 0.26 | 1.23 | 0.35 |
| October 2015 | 0.50 | 0.29 | 1.22 | 0.35 |
| September 2015 | 0.42 | 0.24 | 1.14 | 0.33 |

## Cadia East ore properties

From earlier feasibility studies for the Cadia East deposit, the ore was known to be more competent and harder than the Ridgeway deposit. Table 3 summarises the ore hardness data that was available to design the plant upgrade of Concentrator 1, with the data indicating that the Cadia East deposit has a hardness profile classified as one of the hardest ores and is within the top 10 per cent of all ores measured in the Sag Mill Comminution (SMC) test database. In line with the transition from the Ridgeway deposit to Cadia East deposit, several plant trials of Cadia East ore through Concentrator 2 were executed and additional ore hardness obtained as per Table 3.

**TABLE 3**

Ridgeway and Cadia East ore properties.

| Ore property | Units | Concentrator 1 circuit design data | Ridgeway 2014 | Cadia East plant trial 2014 | Cadia East plant trial Mar 2015 |
|---|---|---|---|---|---|
| JK A | - | 90.2 | 66.2 | 66.2 | 66.5 |
| JK b | - | 0.3 | 0.58 | 0.53 | 0.53 |
| A*b | - | 27.1 | 38.4 | 35.1 | 35.2 |
| $DW_i$ (JK Drop-Weight index) | $kWh/m^3$ | 10.1 | 7.17 | 7.81 | 7.70 |
| SG (Specific Gravity) | $t/m^3$ | 2.75 | 2.77 | 2.72 | 2.70 |
| $BW_i$ | kWh/t | 21.7 | 21.7 | 19.7 | 22.6 |
| Mia (Work index for the grinding of coarser particles, >750 µm in tumbling mills) | kWh/t | | 20.1 | 21.9 | 21.8 |
| Mic (Size reduction in conventional crushers) | kWh/t | | 7.8 | 8.6 | 8.6 |
| JK $t_a$ | - | | 0.36 | 0.33 | 0.34 |

## Cadia East plant trial 1 (Nov 2014)

Plant surveys of the Cadia East ore trial through Concentrator 2 were carried out during 2014 and 2015. The objective was to assess the throughput impact of pre-crushing the Cadia East ore. As per Table 4 from the SMC Report, the Ridgeway ore was ranked as 'moderately hard' with 33.7 per cent of ores in the SMC database testing harder whereas the Cadia East ore from the plant trials was ranked as 'hard' with 26–27 per cent of ores in the SMC database testing harder.

**TABLE 4**

Ridgeway 2014 A*b and Ranking.

| | A*b | | | |
|---|---|---|---|---|
| **Sample designation** | **Value** | **Category** | **Rank** | **%** |
| Ridgeway 2014 | 38.4 | Moderately hard | 1479 | 33.7 |
| Cadia East Plant trial 2014 | 35.1 | Hard | 1172 | 26.4 |
| Cadia East Plant trial March 2015 | 35.2 | Hard | 1236 | 27.2 |

Therefore, it was expected that tertiary crushing would be required however the aim of the trial was to generate data to support this hypothesis and provide confidence to the Cadia Valley Operations management of the requirement to develop a business case to begin the tertiary crushing study phase and order the long lead items.

The secondary crushing circuit (pre-crushing) is shown in Figure 1, and it should be noted that the secondary crusher is in open circuit which was designed to keep the secondary crushing circuit as simple as possible. A separate closed circuit crushing option with a screen was investigated which produced a finer $P_{80}$ but resulted in a greater capital expense. The secondary crushing circuit utilised existing infrastructure; hence capital spend was reduced through integration into future plant design for Cadia East ore.

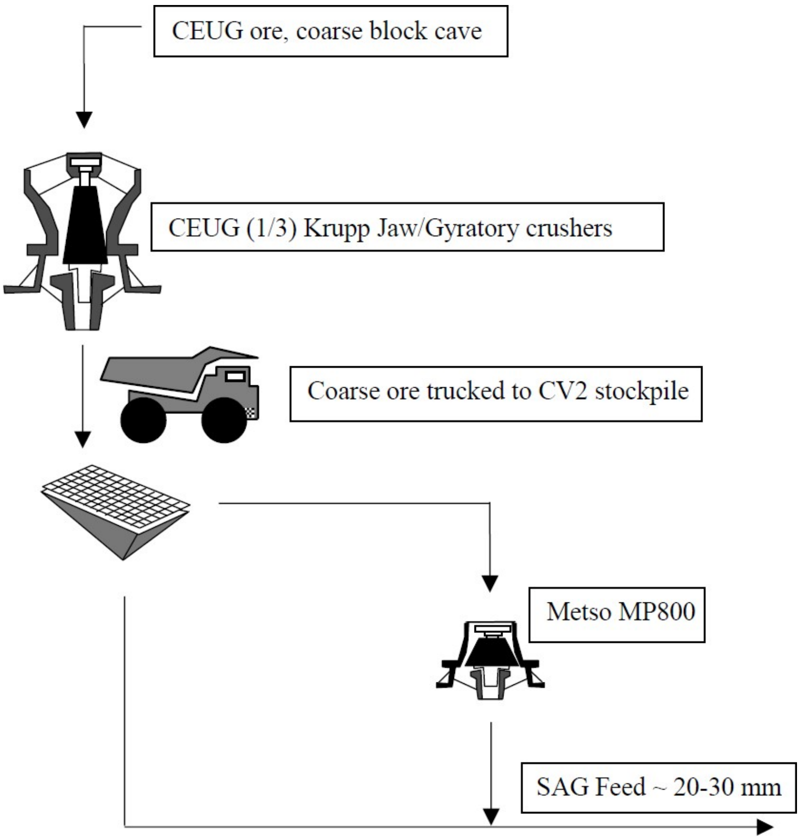


**FIG 1** – Flow sheet for Cadia East secondary crushing trials in Concentrator 2.

After the Cadia East ore had been primary crushed underground, it was trucked from the Concentrator 1 Coarse Ore Stockpile (COS) to the Concentrator 2 secondary cone crusher. Approximately 29 500 t of Cadia East ore was crushed from prior to start-up of the SAG Mill. Belt cuts of the crushing circuit feed and product were collected and then following start-up of the SAG mill a grinding survey was executed.

Upon presentation of the secondary crushed product to the SAG mill it quickly became evident that grinding circuit throughput was restricted by the SAG mill power of 7 MW at a much lower tonnage rate than when treating Ridgeway Deeps ore. The flotation feed rate averaged 525 t/h with low reclaim feed rates and pebble production below 50 t/h. The pebble crushers were not run during the trial due to the very low scatting rate and pebble stockpile. Other observations were that the mill scat discharge was more rounded than normal, indicating higher mill residence times.

This trial highlighted the hardness of Cadia East ore as detailed in Table 4 earlier, with a lower A*b value than Ridgeway Deeps. At a flotation feed rate of 525 t/h with Concentrator 2 historical availability of 95 per cent, annualised throughput was expected to be 4.37 Mt/a.

A 24-hour plant trial was undertaken, and surveys executed to gather survey data for evaluation of circuit performance, mass balancing, power modelling and JKSimMet simulations.

Several belt cuts were taken around the circuit with a comparison of the SAG mill feed during the Cadia East trial versus Ridgeway ore shown in Figure 2. The early stages of the Cadia East panel block cave ore delivered coarse, fines deficient feed to the SAG mill, with an $F_{80}$ of 44 mm and less than 10 per cent below 10 mm. In comparison, the Ridgeway Deeps had an $F_{80}$ of 27 mm.

These results confirmed known sensitivities of SAG throughput to feed size distribution, with Concentrator 2 regularly operating beyond 800 t/h when treating Ridgeway Deeps ore.

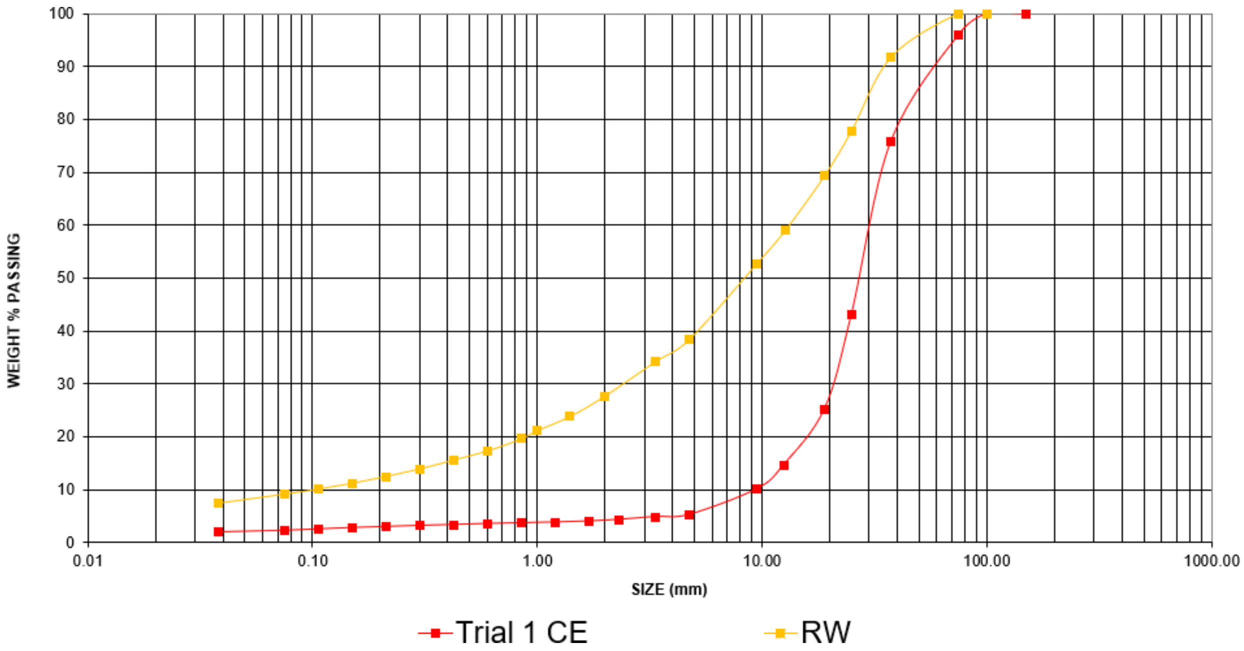


**FIG 2** – SAG mill feed PSD Cadia East ore trial 1 versus Ridgeway ore.

Once all belt cuts were complete, a grind out of the SAG mill was undertaken with the ball charge calculated to be 14.5 per cent.

## Cadia East plant trial 2 (Jan 2015)

Following the low plant throughput observed during Trial 1, a second trial (Trial 2) was scheduled in early January 2015, with a target $F_{80}$ of 20 mm for the Cadia East ore to determine whether throughput rates could be increased towards 800 t/h as had regularly been achieved when processing Ridgeway Deeps ore. The Cadia East primary crushed ore was processed through a mobile crushing plant and then fed through the existing secondary crushing circuit which was not used in a crushing capacity but as a transfer point to the Concentrator 2 circuit. The mobile crusher generated extremely fine material ($F_{80}$ of 9 mm) and there were concerns about maintaining charge level and damaging liners within the SAG mill, hence this material was blended with coarser high pressure grinding rolls (HPGR) feed material in Concentrator 1 to increase the $F_{80}$ towards the desired $F_{80}$ of 20 mm prior to transfer to Concentrator 2.

As expected with the targeted lower $F_{80}$ to the SAG mill, flotation feed rates of above 800 t/h were achieved, with SAG mill power constraint of 7 MW observed in Trial 1, not present during Trial 2. SAG mill power was approximately 6.6 MW during Trial 2 and there was no constraint present for additional float feed. In line with the increased flotation feed rates, pebble production increased to 10–25 per cent whereas pebble production was very low during Trial 1, ranging from 1–10 per cent. Prior to shut down, the grind size stabilised at 100 µm. Ore properties were not determined during Trial 2 however they were assumed to be the same as those determined from Trial 1.

As per Trial 1, a belt cut of SAG mill feed was taken with results shown in Figure 3. The PSD from Trial 2 is much finer, with an $F_{80}$ of 30 mm compared with an $F_{80}$ of 44 m from Trial 1. The quantity of material passing 10 mm in Trial 2 also increased significantly to approximately 40 per cent compared to Trial 1 where less than 10 per cent of the material is below 10 mm. The PSD of Trial 2 was most similar to the Ridgeway Deeps PSD and explains the higher float feed rates achieved during Trial 2.

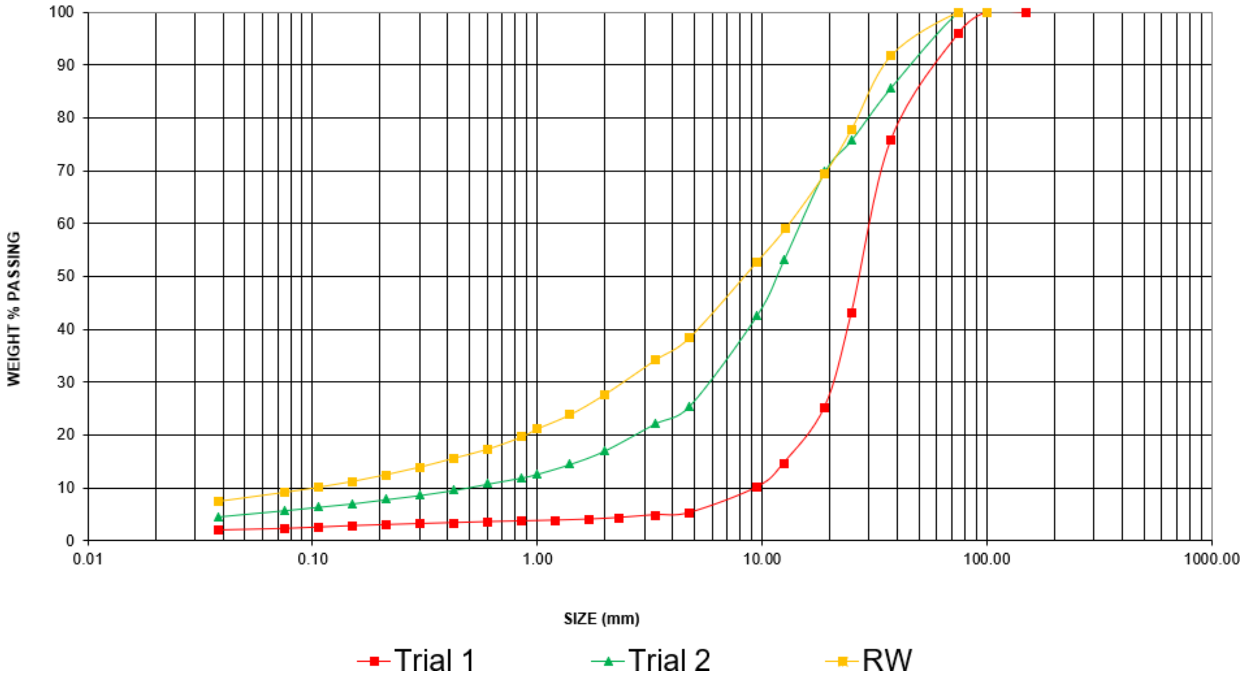


**FIG 3** – SAG mill Feed PSD Cadia East ore trial 2 versus Ridgeway ore.

Based on the results of Trial 2, Cadia Valley Operation had confidence that plant throughputs could be maintained after transitioning to Cadia East ore provided the feed was presented to the SAG mill at an $F_{80}$ of 20 mm. From the data in Trial 1, it was proven that the secondary crushing circuit was not capable of crushing the competent/fines deficient primary crushed Cadia East ore to the desired $F_{80}$ of 20 mm and hence a concept study commenced to investigate the option of an additional stage of crushing (tertiary crushing).

## Concentrator 1 to Concentrator 2 tertiary crushing upgrade

There was a need to tertiary crush the Cadia East ore but there was also a secondary requirement to transport the Cadia East ore from the existing Concentrator 1 crushed ore stockpile to the existing feeder to the Concentrator 2 crushing circuit. During the various Cadia East trials through Concentrator 2, the Cadia East ore was carted via truck from the Concentrator 1 stockpile to the Concentrator 2 COS. The ongoing operational cost required to truck the ore was very high given CVO's lengthy mine life and hence a pre-feasibility study was commenced to implement a conveying option.

As there was already an existing MP800 cone crusher in a secondary crushing duty, the conversion from secondary to tertiary crushing was somewhat simplified as existing infrastructure was in place that could be integrated into the final tertiary crushed solution. The modified flow sheet is shown in Figure 4 where a new conveying system was installed to deliver Cadia East primary crushed ore to a new secondary cone crushing circuit.

The screen undersize and the secondary crushing product from the new secondary crushing circuit is then conveyed through a new conveying system to the existing cone crushing circuit which is now converted to a tertiary crushing application.

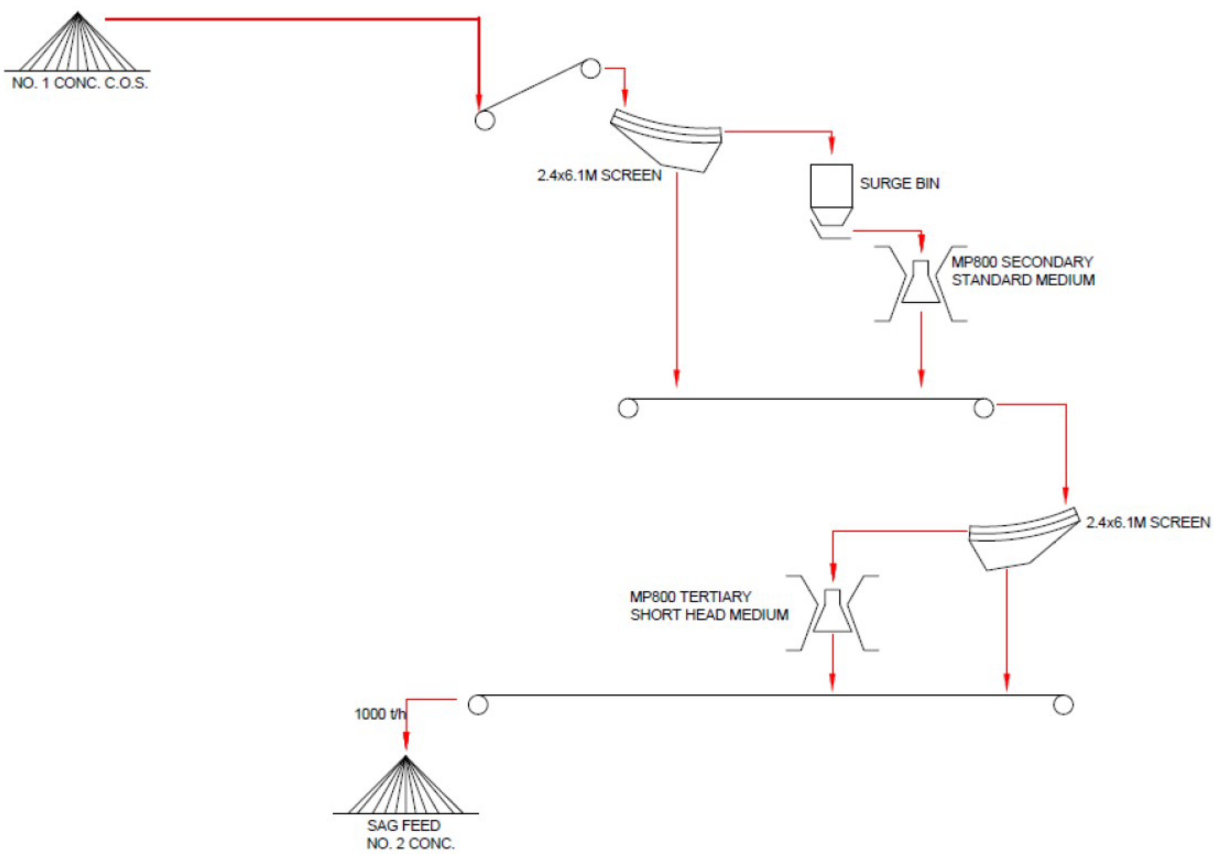


**FIG 4** – Modified Concentrator 2 crushing circuit incorporating tertiary crushing.

## Tertiary crushed readiness projects

As part of the preparation for the transition to tertiary crushed ore, the comminution circuit was reviewed to identify any potential bottlenecks that may impact on the ability to achieve maximum float feed rates. With the transition to the finer tertiary crushed feed, there was concern about the ability for the SAG mill to operate at low enough speeds to prevent liner damage given the limited speed range as a result of the Slip Energy Recovery (SER) drive. Furthermore, there is a need to operate in fixed speed (utilising the Liquid Resistance Starter or LRS) during start-up, resulting in the SAG mill turning at high speed for significant periods of time with high risk of liner damage.

Following mechanical investigation, it was determined that the most feasible option was to change the ratio of the gearbox enabling the minimum speed to be decreased from 66 per cent to 61 per cent critical speed. The entire speed range was lowered as a result of the gearbox modifications hence the LRS speed was also decreased from 74 per cent to 69 per cent critical speed. Another key advantage of the speed change meant that the mill would operate closer to synchronous speed when operating the SER drive. That is, when operating the SER drive the speed would be closer to the LRS mill speed leading to reduced slip ring and brush maintenance.

Another known bottleneck was the recirculating load in the ball mill circuit and an opportunity was identified to allow variable flow control functionality of the cyclone underflow between the SAG mill and the ball mill. The existing control was through use of an orifice plate, with the remaining cyclone underflow reporting to the ball mill. Further benefits could be attained through the variable flow control functionality. To enable further control of the cyclone underflow split between the SAG mill and the ball mill, a project was initiated to enable variable flow between the two mills via means of a chunk valve. After a short period of commissioning, it was identified that there was a limit on the amount of cyclone underflow that could be directed to the ball mill as indicated by a rapid decrease in ball mill power. When this event happened, it was determined that the ball mill was in a state of overload and the cyclone underflow needed to be re-directed to the SAG Mill until the ball mill power increased and stabilised. This overload observations are thought to be a consequence of approaching critical axial flow velocity for pulp (0.072 m/s) where all void space is filled, a pool is rapidly formed and all space is filled outside the ball load and up to the overflow level. Prior to this, pulp is discharged mainly along the ascending rim of the overflow (Arbiter, 1990).

## *Redesign of SAG mill liners for tertiary crushed feed*

In preparation for the transition from secondary crushed Ridgeway Deeps ore to tertiary crushed Cadia East ore, the existing SAG mill liner configuration was reviewed to determine what modifications would be required for processing of tertiary crushed feed. The original plan was to transition to a new shell and discharge grate design in November 2016 which was to align with completion of the tertiary crushing upgrade project.

With the decrease in feed size the optimal ball size for the SAG mill was reviewed. The existing 125 mm ball was found no longer suitable and risked causing damage to SAG mill liners. The optimal ball size was calculated using two different methods, the Ettore Azzaronis and Allis-Chalmers' formulae as shown below,

Ettore Azzaroni's formula: $d_B^* = 4.5\ F_{80}{}_{0.263}\ (r_s\ W_i)^{0.4} / (N\ D)^{0.25}$

Allis-Chalmers' formula: $d_B^* = 1.354\ (F_{80})^{0.5}\ [\ r_s\ W_i / (N_c\ D^{0.5})]^{1/3}$

where:

| | |
|---|---|
| $d_B^*$ | = ideal make-up ball size, mm |
| $F_{80}$ | = 80 per cent passing size in the fresh feed stream, microns |
| $r_s$ | = ore density, t/m$^3$ |
| $W_i$ | = Work index of the ore, kWh/ton (metric) |
| $N$ | = rotational mill speed, rev/min |
| $N_c$ | = rotational mill speed, as a percentage of the mill critical speed |
| $D$ | = effective mill diameter, feet |

Using an assumption of an $F_{80}$ of 20 mm, Ettore Azzaroni's formula determined the optimum ball size to be 99 mm and Allis-Chalmer's formula determined the optimal ball size to be 102 mm.

Cadia Valley Operations also made several requests to the liner supplier regarding specific requirements for the tertiary crushed liners including:

- Reduction in pebble port size from 55 mm to 40 mm.
- Reduction in grate size from 25 mm to 18 mm.
- Flexibility to easily remove grate/pebble ports by designing two types of outer grate pieces, one with pebble ports and one without. This was to provide the option to control the amount of pebble ports by varying the ratio between the two different grate pieces. It was thought at the time this may be required in the event of poor milling performance, eg high pebble production.
- Discharge liner configuration to change from the existing 25 mm grate/50 mm pebble port combination to alternating grate only (18 mm) and grate (18 mm)/pebble port (40 mm) to retain mill load with the finer SAG mill feed $F_{80}$.
- Reduction in shell lifter height with the ability to operate at high speed (LRS mode). LRS mode is 74 per cent of critical speed.
- Integration of filler rings with feed end outer liners and grates. This change was driven as a safety initiative to remove the existing risk of the standalone filler rings which are not supported by bolts and posed a risk to the reline team.
- Conversion from hockey stick to fully curved discharge end to increase discharge pumping efficiency.
- Modification of all existing liners as required to prevent liner damage and promote attrition grinding.

For the purpose of the mill liner design, three sets of particle size distributions were developed, as shown in Figure 5. Set 1 and Set 2 are the belt cuts taken during Trial 1 and Trial 2 as detailed above. Set 3 was taken from the tertiary crushing upgrade project design. As the estimates for the PSD to the SAG mill are based on simulations and plant trials, there was an element of uncertainty and likely variance in the size distribution of the SAG mill feed stream after the tertiary crushing facility is constructed hence an operating envelope was the best estimation that Cadia Valley Operations (CVO) could provide on this stream. One of the key components of the new mill liner design was that it needed to have the flexibility to be optimised for tertiary crushed Cadia East ore but capable of treating secondary crushed.

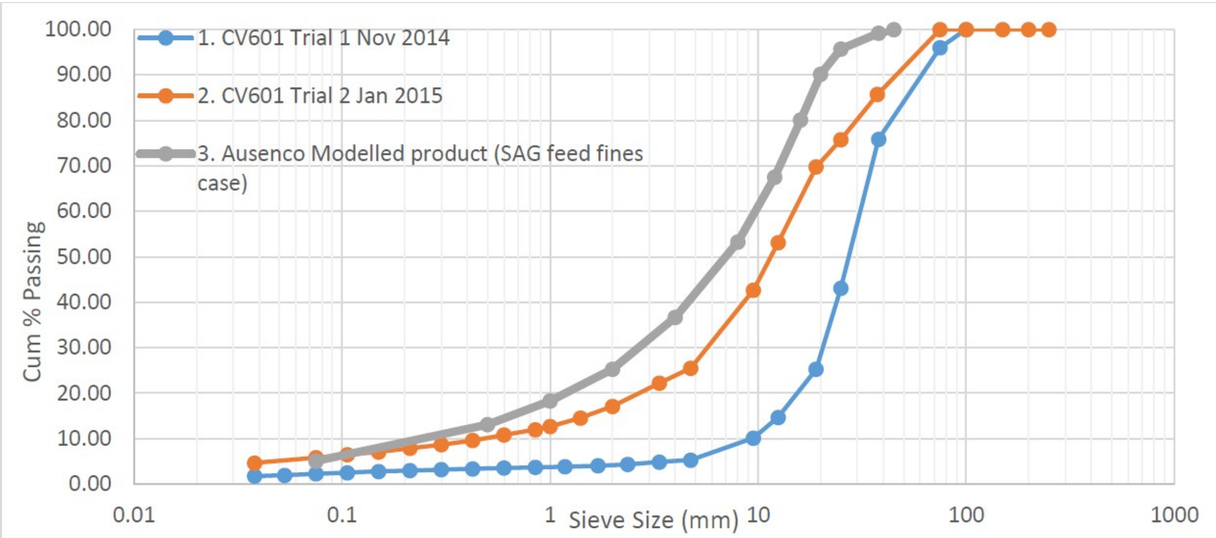


**FIG 5** – Design PSD SAG mill feed envelope for liner re-design.

As per the liner design criteria from CVO, the main lifter and small lifter heights were reduced by 50 mm and 40 mm respectively and the lifter face angles were increased to reduce overthrow and promote attrition grinding. The plate thickness through the middle section of the liner was reduced from 110 mm to 90 mm to provide a larger mill diameter and hence increased milling capacity whilst retaining a ‘choc-block’ above the plate which was an earlier design feature retained to prevent liner damage. The existing and modified shell liner design is shown in Figure 6.

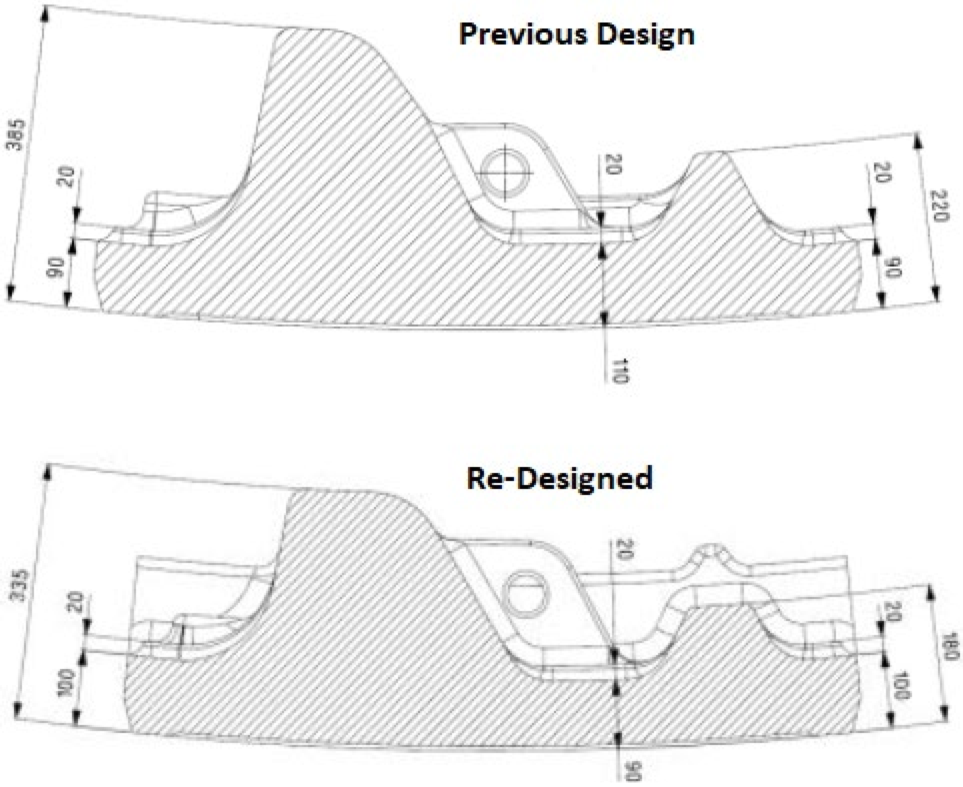


**FIG 6** – Existing and modified shell liner design.

As per CVO's request to move to a fully curved discharge end, the outer pulp lifter was extended to allow for a full curvature and longer grates to move away from the existing hockey stick design. The fully curved discharge end is designed to increase pumping efficiency. CVO had previously transitioned to fully curved pulp lifters in 2013 on the 40' SAG mill in Concentrator 1 which gave CVO the confidence to apply the same change on the 32' SAG Mill in Concentrator 2 (Waters *et al,* 2018).

### *Commissioning challenges*

One of the many challenges with the tertiary crushing upgrade was the requirement to construct the new reclaim tunnel/feeder for the new Concentrator 2 secondary crushing circuit underneath the live COS (crushed ore stockpile – Cadia East primary crushed). CVO chose to undertake this activity due to the significant downtime require to empty the COS and install the new tunnel/feeder from above. A tunnel contractor was engaged to bore the tunnel beneath the live COS.

As the CVO Projects team were focused on completion of the reclaim tunnel, the existing secondary crusher was not converted to tertiary crushing at this stage, hence the secondary crushed product and screen oversize from the new secondary crushing circuit was fed directly to the SAG mill. The delay in execution of the tunnel and tertiary crushing conversion also impacted the SAG mill liner configuration. The new design of liner was optimised for tertiary crushed feed, with an expectation of conversion during a planned outage in January 2017 however tertiary crushed feed was not expected until March-April 2017. As a result, the SAG mill discharge end configuration (ported versus non-ported grates) was reviewed to determine the optimum arrangement for secondary crushed Cadia East feed. As mentioned earlier, the design specification to the liner supplier was a requirement to be optimised for tertiary crushed Cadia East ore but capable of processing secondary crushed Cadia East ore. To prevent the SAG mill from overloading with coarse secondary crushed material, the number of pebble ports installed was matched to the number of pebble ports installed on the existing design for Ridgeway secondary crushed feed. This resulted in a combination of 20 ported liners and 12 grate only liners. The two different liner types are shown in Figure 7.

**FIG 7** – Tertiary crushed feed SAG mill grates – slot only versus pebble ported liners.

Following completion of the reclaim tunnel and new feeder, feeding of ore through the temporary feeder ceased and commissioning of the new feeder from underneath the Concentrator 1 COS commenced in March 2017. Almost immediately, there was evidence of coarse segregation of the ore reporting to the new feeder versus the ore reporting to the existing feeders to the Concentrator 1 circuit. The ore reporting to the new feeder was very slabby and fines deficient resulting in the new secondary crusher (CR2001) becoming power constrained. The positioning of the new feeder was thought to be contributing to the coarse segregation as the feeder was positioned towards the outside of the COS.

Following a commissioning period of a few weeks for the new feeder, the existing secondary cone crusher was commissioning to a tertiary crushing duty in early April 2017. A change in configuration of the SAG mill discharge grates back to 16 ported and 16 grate liners was undertaken at the same time. The change in grate configuration was to assist with maintaining volumetric charge in the SAG mill following transition to the finer feed and prevent liner damage.

After an extended period of limited ore supply, by October 2017, CVO's operating strategy focused on maximising feed rates to the Concentrator 2. This was an opportunity to complete commissioning and optimisation of the circuit while ore availability from the mine was the site constraint.

When operation in Concentrator 2 recommenced, it was evident that plant throughput was constrained by tertiary crushing performance with the tertiary crusher (CR603) averaging 300 kW and constrained by high crusher bowl level which restricted throughput. As mentioned earlier, due to the limited commissioning time in April 2017, this bottleneck was not identified initially and needed to be rectified with urgency to deliver the full value of the tertiary crushing upgrade. As the tertiary crusher is an MP800, the crusher should be able to operate at approximately 600 kW and hence it was concerning that only 50 per cent of available crusher power was being drawn.

In consultation with the crusher liner supplier and reviewed by external subject matter experts, modifications were made to the bowl liners as shown in Figure 8. On the original bowl liner design, the choke point in the crushing chamber was at the change in angle ahead of the parallel zone. The purpose of the bowl liner machining was to extend past the choke point and hence increase crusher throughput and downstream throughput through the SAG mill. Another benefit was as the crusher chamber opens, rocks fall further into the chamber before being gripped and broken resulting in increased crusher power draw.

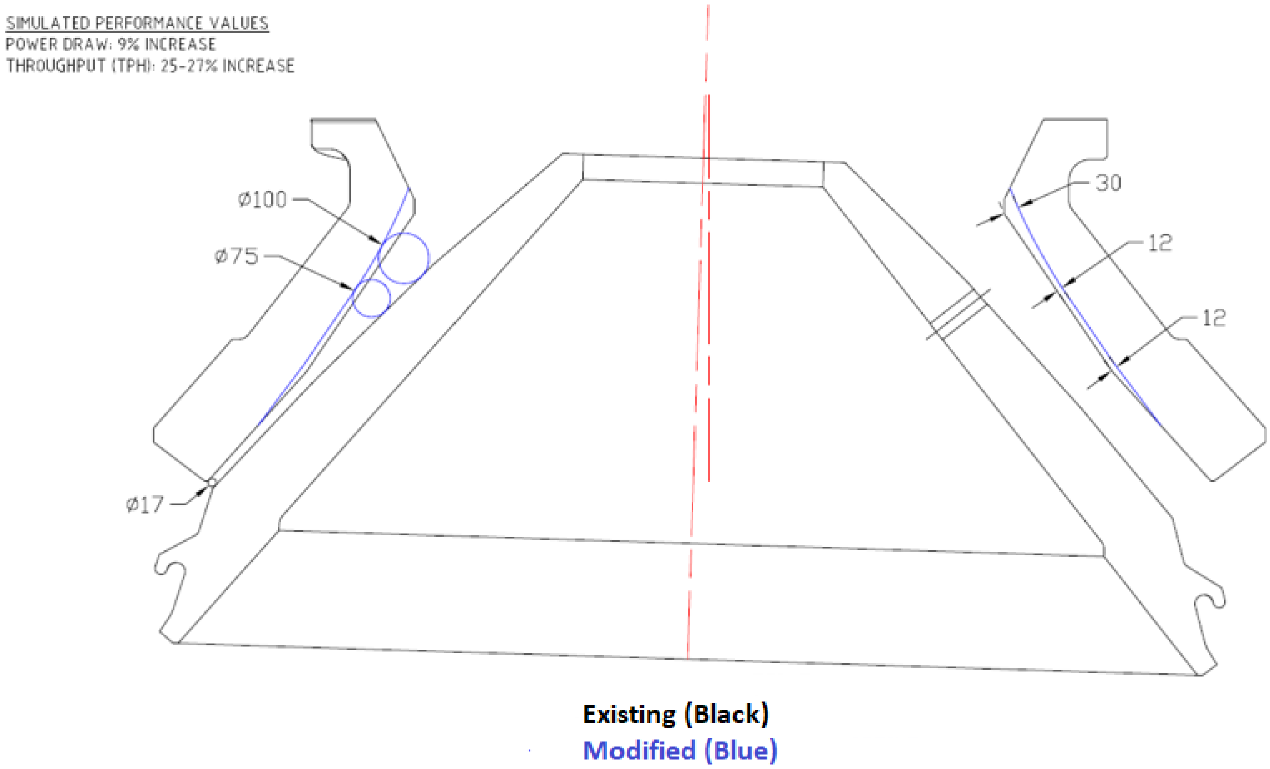


**FIG 8** – Existing tertiary crusher bowl liner profile versus modified bowl liner profile.

An uplift in crusher power draw and throughput was observed following the installation of the modified bowl liner above although the crusher was still not operating at maximum power. Several iterations of the above bowl liner machining took place with the third iteration resulting in average power of 570 kW and a corresponding increase in crusher throughput.

As the crushing circuit bottlenecks were removed, Concentrator 2 would regularly operate beyond 800 t/h and new constraints were identified within the ball milling circuit particularly with cyclone feed pumping.

### *Full plant survey – Dec 2017*

After a few months of operation on tertiary crushed feed, the CVO Metallurgical Team completed a full plant survey of both the comminution and flotation circuits to assess the performance of tertiary crushed feed and identify any new opportunities to further increase metal production from Concentrator 2. Of particular interest was the performance of the ore from Panel Cave 2 (PC2), as leading up to the survey, the recovery of this ore had been below expectations. To gather as much data as possible on the performance of the PC2 ore, the survey was scheduled to maximise PC2 ore feed (approximately 61–62 per cent of the feed during the survey), with the remainder of the feed being made up of Panel Cave 1 (PC1).

As per the earlier trials of Cadia East ore through Concentrator 2, belt cuts and slurry samples were taken around the comminution circuit for performance analysis with the SAG mill feed sizing shown in Figure 9. The $F_{80}$ of the material was 17 mm which is line with the design criteria for the tertiary crushing upgrade ($F_{80}$ of 20 mm) and SAG mill performance was good with float feed rates averaging 809 t/h.

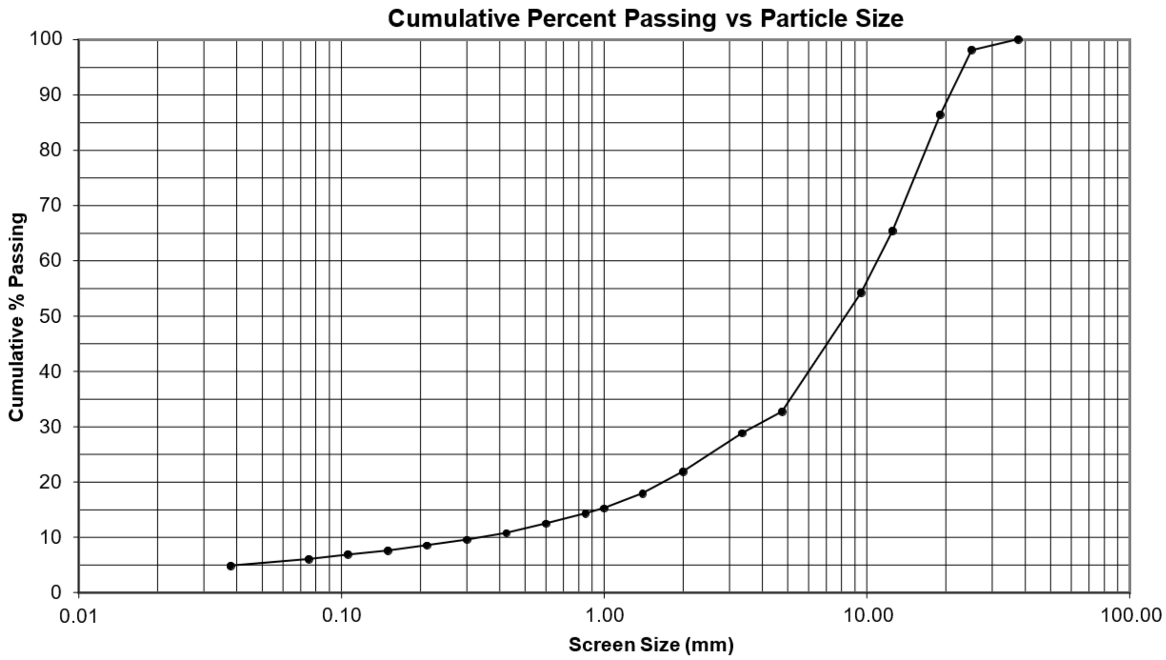


**FIG 9** – SAG mill feed sizing from full plant survey in Dec 2017 post tertiary crushing upgrade.

## SAG and ball mill motor upgrade – 2018

During the period 2015–2016, several motor failures occurred on the SAG mill which were attributed to poor quality motor windings and warm ambient temperatures. SAG throughput/volumetric load needed to be restricted to control winding temperatures and prevent premature failure of the motor. Both the SAG and ball mill motors suffered similar winding issues and so the decision was made to upgrade to a new style of winding which presented an opportunity to also increase the maximum available power to 7500 kW.

In March 2018, both motors and gear boxes were upgraded to 7500 kW and these changes unlocked additional float feed rates through increased ball charge in the SAG mill and reduction in ball mill re-circulating load through increased ball charge and increased speed. Concentrator 2 float feed rates were increased by 36 t/h (4.2 per cent throughput uplift) as a result of the motor upgrades.

## PLANT OPTIMISATION POST CADIA EAST TRANSITION – 2018 TO 2020

Figure 10 lays out the significant events from July 2018 to January 2020. Since July 2018 the main limit to maximum throughput of Concentrator 2 is the cyclone feed pump capacity, specifically the current limit on the motors. Opportunities were identified within this limit to improve circuit operability, reduce costs and increase the runtime operating at the cyclone feed pump limit.

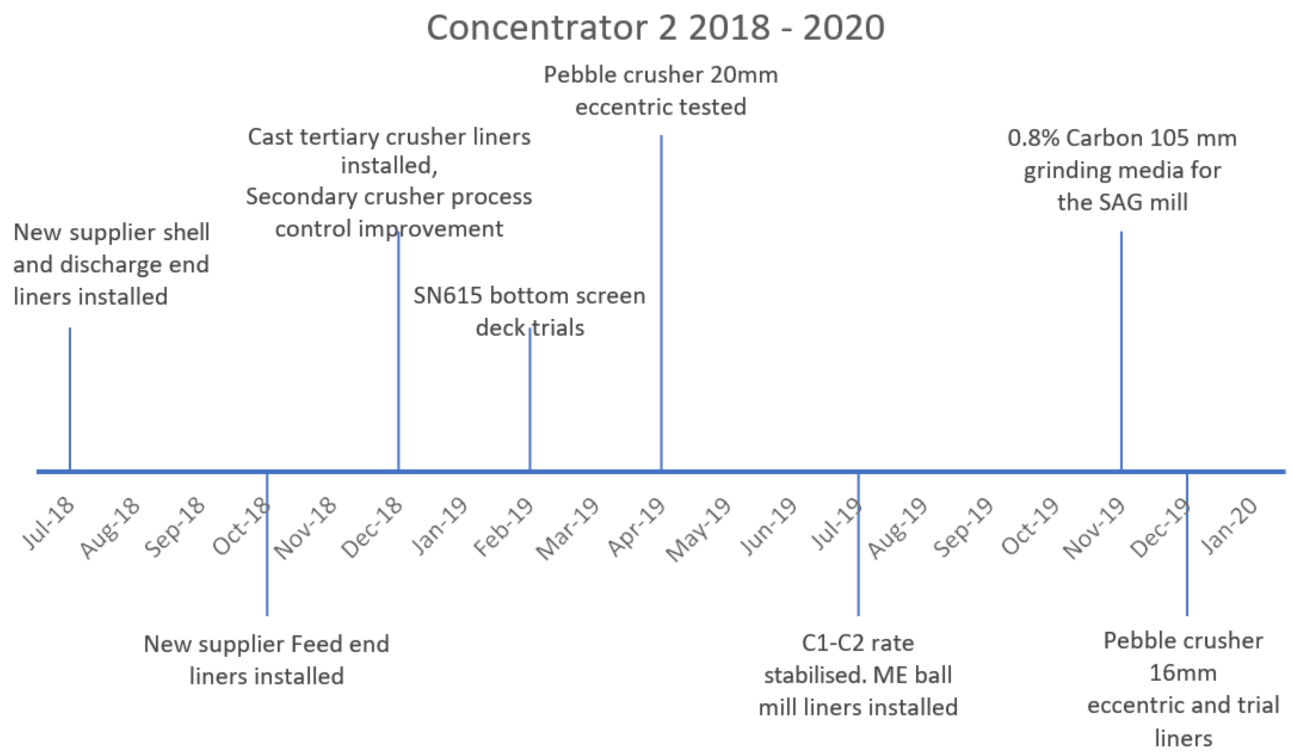


**FIG 10** – Concentrator 2 timeline 2018–2020.

## Liner development

Initial operation of the new SAG mill liners from July 2018 to the first inspection in October 2018 highlighted some areas of immediate improvement in mill performance. During the October 2018 reline, the new feed end outer design was installed, comprising a high/low arrangement, whereby the low lifters contained a cast white iron insert for extended wear life. Start-up of this new feed end required a significant reduction in mill speed to prevent overthrow of media onto the shell liners. A quickly executed change in feed end outer liner profile was initiated for the next reline to address this which included:

- Reduced feed end high lifter height reduced from 450 mm to 400 mm.
- Discharge grate lifter face angle relaxed from 20° to 30°.
- Feed end shell face angle from 33° to 35°.
- Discharge shell lifter face angle from 35° to 38°.

Each reline since has seen an iterative process of changes to almost all the parts in the mill. Each change aiming for higher start-up speeds, easier removal of worn liners (reduction in peening), reduction in part weight to allow more grinding media, reduced part cost and better alignment of the wear life to the re-line schedule. Note that the current shutdown schedule at CVO is time based as opposed to liner wear based, and as such it is desired that the liner wear is optimised to the routine shut schedule.

## Grinding media

Transition from secondary crusher SAG mill (ML601) feed to tertiary crushed SAG mill feed saw a move from a blend of 125 mm and 105 mm 0.6%C grinding media to straight 105 mm 0.6%C grinding media. Trials of 0.8%C grinding media had been conducted on-site previously, however the trials were deemed unsuccessful due to the safety risk introduced from a high degree of energetic grinding media failures in the scats ball bunkers and inside the mill during re-lines. Casting and heat treatment improvements in the grinding media supplier process led to a new trial of 105 mm 0.8%C grinding media. This trial was deemed successful due to the absence of energetic grinding media failures and a 12 per cent reduction in media consumption. SAG mill grinding media was transitioned to the new 105 mm 0.8%C specification in November 2019 and the trial consumption improvement has been exceeded in operation.

## C1-C2 crushing and screening

Feed presentation to the SAG mill is always a focus area, as one of the more significant operational levers to grinding performance. Changes described previously to SAG liners and discharge grates have enhanced the dependence on fine material in the mill feed. In order to achieve the finest $F_{80}$ to the mill without losing significant throughput rate the tertiary crusher liners were machined and the shut interval between planned relines was reduced to alleviate some of the C1-C2 throughput constraint. Further iterations to the previous liner design were completed with installation of the improved cast design in December 2018. This removed the crusher bowl level constraint previously mentioned entirely and presented the opportunity for further optimisation of the SAG mill feed presentation, as seen in Figure 11.

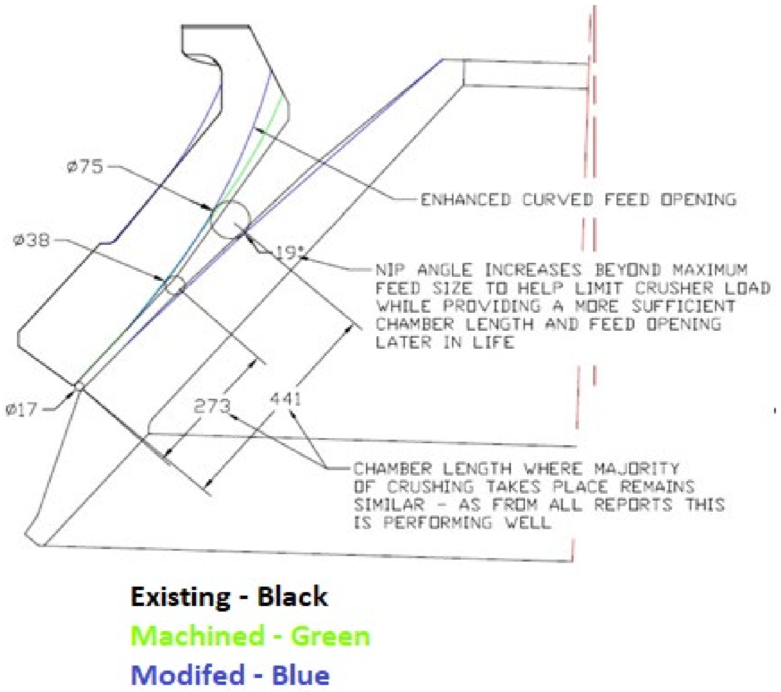


**FIG 11** – Tertiary liner development.

Process control optimisation at the same time changed the power and size reduction balance in the C1-C2 circuit through better utilisation of secondary crusher power. This instigated a series of reasonably rapid adjustments to the tertiary crusher feed screen (SN615) apertures between February 2019 and July 2019 as the extra power utilisation in the upstream secondary crusher (CR2001) resulted in a larger proportion of material bypassing tertiary crushing (CR603) through the bottom deck of the feed screen. With more material bypassing the tertiary crusher the overall feed to the SAG mill became coarser, thus limiting overall circuit performance. Surveys and step testing found a new balance in the circuit with installation of 23 mm bottom deck apertures down from the previous 30 mm apertures, tertiary gaps operating between 20 mm and 23 mm, maintaining a bowl choke level of 20 per cent at 1000–1100 t/h. Given the C1-C2 circuit availability of 83 per cent against the Concentrator 2 grinding circuit availability of 93 per cent the online rate of 1000–1100 t/h proved the optimum for the circuit configuration at the time. Feed size to the SAG mill was reduced from a $F_{80}$ of 19–21 mm to 16–18 mm as a result of this optimisation work, which resulted in a 12 t/h (1.4 per cent throughput uplift).

## Scats recycle crushing

During the transition from secondary crushed SAG mill feed to tertiary crushed feed, it was noted that the pebble crushers (Kawasaki KF1515Z, CR601 and CR602) would need to be modified to effectively crush a smaller scat size. Post the transition period to tertiary crushed feed there was an observed drop in throughput of approximately 50 t/h when the pebble crushers were in operation compared to when not in operation. This was due to the pebble crusher's poor ability to nip the finer scat material in the crushing chamber, essentially sending whole scats back to SAG mill. Breakage rates of the critically sized scat were extremely low in the SAG mill and hence the reduction in throughput when the pebble crushers were online.

Mechanical constraints on the crusher prevented closing the gap tighter than 10 mm, with an eccentric throw of 26 mm and the mill scats in a very tight size from 12.5 mm to 25 mm with a $P_{80}$ of 19 mm. This meant that the crusher could not be operated in a choke feed condition. Pebble crusher utilisation was a 50 per cent split of circuit runtime due to the high capacity of the pebble crushers and the presence of a scats stockpile between the mill discharge and the pebble crusher feed. An external subject matter expert was engaged to assist with improving the performance of the pebble crushers with the changed mill scats composition. Survey data provided a starting point for the required upgrades. Initially the eccentric throw was reduced from 26 mm to 20 mm, maintaining the existing liner profile. Observations during the first test period in April 2019 indicated that the throw could be further reduced to 16 mm and that a liner design change would also assist achieving a choke fed condition leading to a finer crusher product. In December 2019 the 16 mm eccentric and new profile liners were installed in CR601 with immediate success. The new liner profile and smaller throw enabled choke feeding with a large, closed side setting gap range (from the minimum tested 10 mm to 18 mm). Unit throughput reduced, allowing 74 per cent utilisation of the pebble crushers and an uplift in flotation feed throughput of 6 t/h while online, which is a total change of 56 t/h from the original condition where flotation feed used to decrease by 50 t/h when the pebble crushers were online.

## CONCLUSIONS

Over the years, the original Ridgeway flow sheet has continually evolved in line with changes in ore deposits. From the Ridgeway primary crushed ABC configuration at 5 Mt/a through to the current 7 Mt/a Cadia East tertiary crushed SABC configuration as described in this paper. Cadia Valley Operation's has implemented many debottlenecking exercises to exploit the orebody and maximise metal production Through constraint modelling and reiterative survey analysis, driven by site personnel, the following key changes were implemented in Concentrator 2:

- Change from secondary crushed to tertiary crushed sag feed.
- Grinding mill power upgrades.
- Mill liner redesign to accommodate the new feed size distribution.
- Crusher and screen optimisation including but not limited to liner design, eccentric throw, screen aperture and process control.

The future will be no different, with an expansion project currently in execution to debottleneck up to 9 Mt/a to exploit the increased ore production from the Cadia East mine.

## REFERENCES


Waters T, Rice A, Seppelt J, Bubnich J, Akerstrom B, 2018. The evolution of the Cadia 40-foot SAG mill to treat the Cadia East ore body: a case study of incremental change leading to operational stability in *The 14th AUSIMM Mill Operators' Conference 2018, pp 217–232.*

Hart S, Dioses J, Reed M, Gelfi P, Clements B, Valery W and Dunne R, 2000. Cadia Mines – Reflections After One Year's Operation, in *Proceedings of SME Conference* (SME / AIME).

Hart S, Griffin P, Cesnik F, Gordon D, Clements B, 2003. Design and Commissioning of the Ridgeway Concentrator, in *Eighth Mill Operators' Conference Proceedings 2003 – Evolution and Survival in the Minerals Industry*, (The Australasian Institute of Mining and Metallurgy (The AUSIMM).

Hart S, Green S, Cesnik F, Griffin P, 2005. Design, Construction and Commissioning of the Ridgeway Concentrator Regrind Circuit at Newcrest's Cadia Valley Operations, in *Centenary of Flotation 2005 Symposium*, (The Australasian Institute of Mining and Metallurgy (The AUSIMM).

Arbiter, N, 1990. Dimensionality in Ball Mill Dynamics, pp 77–81, (Society for Mining, Metallurgy & Exploration).

# Proving best practice gravity gold circuit design

*G Heard[1] and L D'Uva[2]*

1. Senior Metallurgist, Gold Fields Limited, Perth WA 6005. Email: goldie.heard@gruyerejv.com
2. Senior Metallurgist, Gekko Systems, Perth WA 6007. Email: lisal@gekkos.com

## ABSTRACT

The development of the three-stage gravity recoverable gold test work and modelling, by the late André Laplante and the AMIRA P420 Gold Technology group respectively provided tools that have become the foundation of best practice design and operation of gravity gold circuits using batch centrifugal concentrators. Test work and modelling have enabled the design of predictable, low risk gravity gold circuits and facilitate continuous improvement.

Gekko Systems in collaboration with Gold Fields Limited were involved in the design of the Granny Smith and Gruyere gravity circuits in 2014 and 2015 respectively, and the design of the Agnew gravity circuit upgrade in 2012 and again in 2016. Gold Fields carried out mill and gravity surveys at each of the respective sites post-commissioning to established baseline performance. Modelling of the survey data through the AMIRA P420 BCC Gravity Model generated recovery curves specific to the ore treated and the mill and gravity circuits being operated. This enabled both the variation in the recovery established during design, and opportunities to increase baseline recoveries to be verified.

Confirmed by surveying and modelling of the operating gravity circuits the AMIRA P420 BCC Gravity Model was a robust tool in establishing the optimal gravity circuit configuration and capacity. In each case study, modelling of the operational gravity circuits indicated a mill discharge fed gravity circuit was the optimal configuration to maximise gravity recovery. This aligned with the outcomes from the design stage of modelling.

The gravity recovery estimates attained from the design modelling, however, did not reflect the gravity recoveries achieved in the plant. The design modelling of the Brownfields Granny Smith gravity circuit underestimated gravity recovery by 11 per cent. Design modelling of the Greenfields Gruyere gravity circuit underestimated gravity recovery by 5.2 per cent. Remodelling of the GRG data applied during design with current mill operating data obtained from gravity circuit surveys identified that both the GRG data and the mill operating data can have a large influence on the position and shape of the modelled recovery curve. Given the accuracy of the model was validated repeatedly through modelling of surveyed data, where the Granny Smith, Agnew and Gruyere gravity circuit surveys resulted in a 3.2 per cent, 0.6 per cent and 1.0 per cent difference between the average plant gravity recovery and the modelled survey recovery, respectively; it was concluded that the gravity recovery discrepancies that exist between circuit design and real plant performance is a factor of the data that is applied during design.

This paper details the application of test work, modelling and performance monitoring of the Gold Fields Greenfield, retrofitted and existing gravity gold circuits. The Gold Fields case studies compare the BCC Gravity Model predicted gold recoveries to those being achieved in plant operation. The paper highlights the capability of modelling in best practice gravity gold circuit design, and demonstrates its benefits, reliability and shortfalls.

## INTRODUCTION

The accepted ideology of the 1990s was that a cyclone underflow fed gravity circuit was the optimal configuration because cyclones acted as pre-concentrators for gold in a milling circulating load (CL). Gravity circuits were commonly designed to be fed with one third of the cyclone underflow stream as this was known to correspond to a plateau in gold recovery with gravity effort. The grain size of the gravity recovery gold (GRG) in the ore was rarely considered. Despite the benefits of the AMIRA BCC Gravity Model being available since 2005, the cyclone underflow fed gravity circuit arrangement as an optimal configuration is still a preconceived design concept amongst gold processing metallurgists today.

Best practice gravity gold circuit design involves; liberation and recovery analysis of the GRG; modelling of the GRG test data using site specific milling and cyclone data where applicable; and the design of the circuit to fit with the plant and proprietor's design and operating constraints.

Gold Fields Australia (Gold Fields) in collaboration with Gekko Systems (Gekko) has been applying best practice gravity circuit design in the installation of new and upgraded gravity circuits since 2014. The upfront recovery of GRG at Granny Smith was reassessed in 2014 due to an increase in head grade overloading the downstream carbon-in-pulp (CIP) and elution circuit. In 2015, a gravity survey was carried out at the Agnew processing plant to identify opportunities to optimise the existing gravity circuit. The survey outcomes in conjunction with the associated costs of maintaining the two superseded KC-CD30 Knelson concentrators, identified an opportunity to increase the gravity effort. An increase in recovery capacity would also manage the frequent occurrence of head grade spikes. An upgrade to two KC-QS40 Knelson concentrators occurred in 2018. In 2015 GRG testing and modelling was carried out as part of the design for the Gruyere gravity circuit. The Gruyere gold processing plant was commissioned by Gold Fields and ACJV in 2019.

This paper aims to prove the reliability of best practice gravity gold circuit design. It details the application of modelling in both Greenfield and Brownfield gold processing plants, and plants with existing gravity circuits. Through the Granny Smith, Agnew and Gruyere case studies, the paper discusses the gravity surveys and analyses carried out post commissioning to justify best practice gravity gold circuit design.

## BEST PRACTICE GRAVITY GOLD CIRCUIT DESIGN

The first stage of any circuit design involves test work to quantify the target mineral, understand the mineralogy, and determine how the ore responds to the process in question. In gravity gold circuit design using a batch centrifugal concentrator (BCC), an ore sample undergoes three stage GRG testing. The three stage GRG test is an industry standard procedure developed at McGill University (Laplante, Woodcock and Huang, 2001) and simulates gravity recovery via a BCC in a milling CL at 100 per cent recovery efficiency. The test provides three stages of GRG liberation and recovery data and quantifies the GRG content of an ore sample. However, this test alone does not provide an estimate of the gold recoveries achievable on a plant scale; a concept that is still frequently misinterpreted. Modelling of the test work data using site specific milling and classification data simulates gold recoveries with gravity effort and provides a reliable estimate of the gold recoverable via a BCC on a plant. It is the outcomes from the modelling by which gravity circuit design is based.

The AMIRA P420 BCC Gravity Model simulates gravity circuit gold recoveries based on real milling circuit performance and is therefore a powerful tool for determining optimum circuit configuration and optimum gravity effort during the initial design process. The model, originally developed by André Laplante, became available online in 2005 to sponsors of the AMIRA P420 Gold Processing Technology Project and is maintained by the Curtin University Gold Technology Group (February 2020, personal communication).

## BROWNFIELD OPERATIONS – GRANNY SMITH

The gravity recovery of sulphides in the tailings stream has been the primary focus of gravity gold recovery at Granny Smith. Ultrafine gold associated with sulphides is recovered via spiral concentrators, subjected to ultrafine grinding and fed back into the head of the leach circuit. The recovery of gravity gold within the milling circuit was re-evaluated at Granny Smith in 2014 due to an increase in head grade. With promising test work and modelling outcomes, a gravity circuit was retrofitted in the Granny Smith processing plant and commissioned in 2015.

### Granny Smith design test work and modelling outcomes

Three stage GRG test work was carried out for amenability testing in 2014 by Gekko Systems Metallurgical Laboratory on a sample of Wallaby ore. The sample was obtained by cutting the SAG mill feed stream over one month to obtain a composite. The overall GRG content equated to 66 per cent and was classified as fine grained. To assess the effect of gravity feed configuration on gold recovery, the three stage GRG test results were modelled using the AMIRA P420 BCC Gravity Model. The BCC model was used to estimate gravity recoveries at increasing feed rate increments for various gravity circuit configurations. The 2014 modelling was carried out using the default cyclone partition data provided by the BCC model. The three main configurations considered included a gravity circuit fed from a split of: 1) cyclone feed; 2) cyclone underflow; and 3) mill discharge, with the gravity tails reporting back to the cyclone feed in each scenario. The modelled outcomes indicated at any given feed rate Figure 1 indicates a gravity circuit fed with mill discharge is capable of achieving the highest gold recovery. At 30 per cent to 50 per cent of the mill CL (280 to 470 t/h) a mill discharge fed configuration could recover 3.9 per cent to 5.3 per cent more gold than the preconceived optimal cyclone underflow fed configuration.

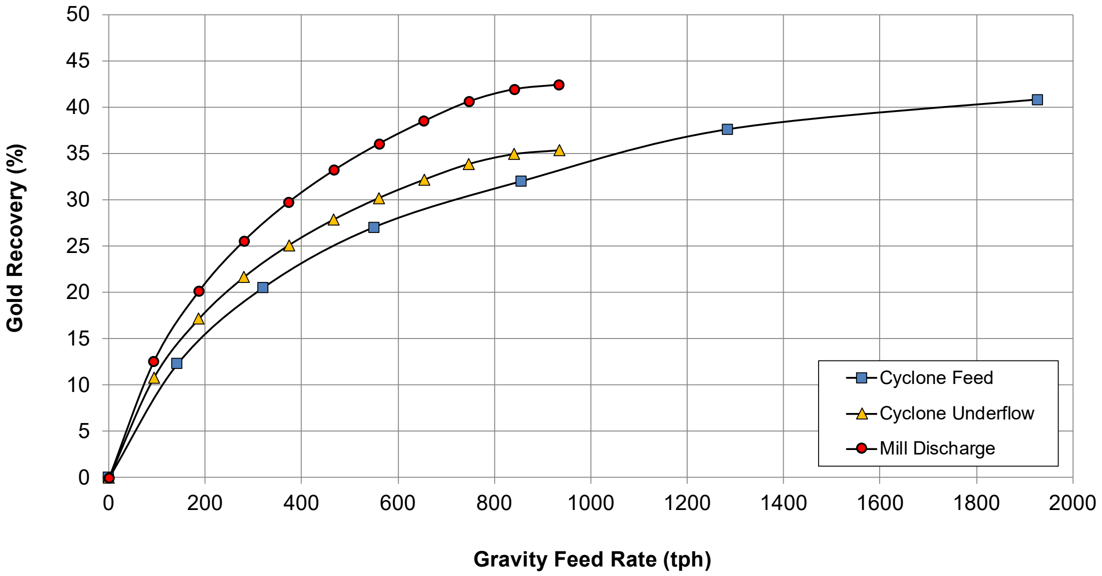


**FIG 1** – Granny Smith modelling outcomes comparing various gravity feed streams (2014).

The mill discharge stream has been found by Gekko Systems to be commonly modelled as the most optimal feed stream, particularly for operations treating ore containing fine grained GRG. In ores containing only very coarse GRG, which is a rare though fortunate occurrence, the variation in recoveries between each configuration is less pronounced. This effect is made evident in the following Agnew case study. The cyclone underflow stream despite being pre-concentrated via the cyclones, has the disadvantage of having lost fine GRG to the cyclone overflow stream. Thus, the gravity circuit is not even presented with the opportunity to recover this fine GRG which is an issue if the ore being treated contains predominantly fine GRG. Cyclone separation efficiency is critical for operations feeding their gravity circuits with cyclone underflow material to minimise fine GRG losses. The mill discharge stream alternatively has the benefit of containing freshly liberated and fine GRG. The cyclone feed stream is capable of exceeding gravity recoveries modelled for cyclone underflow as it contains the freshly liberated and fine GRG from mill discharge. However, the higher recoveries are only achieved at higher feed rates. This is due to the cyclone feed stream containing the highest solids flow rate and being diluted with gravity tails and incoming flows from various mill floor sumps.

## Granny Smith gravity circuit design

To pursue a mill discharge fed gravity circuit at Granny Smith either the redesign or relocation of the cyclone feed hopper would have been required, as well as the installation of a dedicated gravity feed pump. Despite the model indicating a mill discharge fed configuration was optimal, due to footprint and height restrictions of the existing grinding circuit at Granny Smith in conjunction with budget constraints the gravity circuit was designed with a cyclone feed fed configuration.

Utilising the capacity of the existing cyclone feed pump, a split of cyclone feed is obtained from one of the cyclone feed outlets on the cyclone distributor. Slurry flows into a gravity distribution box which splits the cyclone feed material between two gravity trains. Each train consists of a horizontal vibrating screen and KC-QS40 Knelson concentrator. The undersize from each gravity screen feeds its respective concentrator. The gravity gold concentrate produced from each concentrator discharges into the concentrate feed cone of a Gekko ILR. The gravity screen oversize and concentrator tails streams converge at a boiler box to discharge back into the cyclone feed hopper.

The design feed rate was established using the AMIRA P420 BCC Gravity Model to simulate gold recoveries at different gravity throughput rates. The mill water balance constrained the gravity circuit capacity to 500 t/h, and the capacity of the existing cyclone feed pump further restricted the gravity feed rate to 360 t/h. To facilitate opportunities for upgrade the circuit was ultimately sized with a 500 t/h capacity. With this design, the BCC model indicated an achievable gravity gold recovery of 26 per cent.

## Granny Smith gravity circuit performance

The Granny Smith gravity circuit was commissioned mid-2015 and was able to achieve a feed rate of 425 t/h on the existing cyclone feed pump. Operation of the gravity circuit resulted in the downstream CIP circuit being immediately alleviated. The average gold grade to leach feed decreased from 5.3 g/t (SD = 2.8 g/t), to 3.4 g/t (SD = 2.1 g/t), and the average plant recovery increased by 0.7 per cent (D'Uva, Robinson and Bell, 2016).

A gravity survey was carried out in 2016 to verify the expected recoveries determined from the 2014 design modelling. This survey was carried out prior to any gravity optimisation work being carried out, thus also serving to provide baseline performance data. Three stage GRG test work and modelling were carried out on the SAG discharge material obtained from the gravity survey, which was equivalent to fresh mill feed. The test work indicated the SAG discharge material had a GRG content of 62 per cent and was classified as medium grained. Modelling of the survey data to determine the optimal gravity circuit configuration aligned with the design modelling outcomes, with a mill discharge fed circuit being the optimal configuration. Although, there was less variation in the modelled recoveries at any given feed rate between each configuration compared to the design modelling. The recovery simulations for a cyclone feed fed configuration in Figure 2 indicated that the cyclone fed gravity circuit, given a feed rate of 425 t/h, could achieve a gold recovery of 38.2 per cent. The modelled recovery aligned with the 35 per cent average gravity gold recovery being achieved on-site at the time. The slightly higher modelled recovery is indicative of opportunities to increase gravity recovery through optimisation.

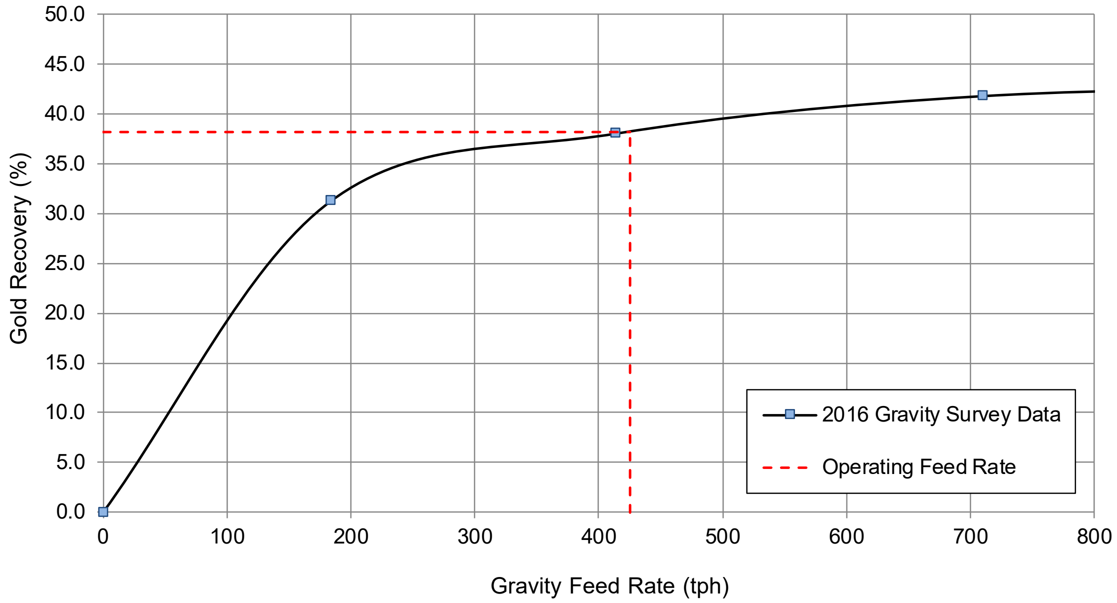


**FIG 2** – Granny Smith 2016 gravity survey modelled recovery curve.

## Granny Smith design validation

The 2014 design modelling did not accurately predict gravity gold recovery at Granny Smith, underestimating the achievable recovery by 11 per cent. At a gravity feed rate of 425 t/h, the 2014 modelled gravity recovery corresponded to 24 per cent. Given a consistent feed, the cyclone performance in a grinding circuit would be considered as having the most significant influence on gravity recovery (Grewel, Van Kleen and McAllister, 2009). Thus, it was initially assumed that the discrepancies between the 2014 and 2016 modelled recoveries may have been attributed to the use of default cyclone partition data being used during the design stage instead of real plant data (D'Uva, Robinson and Bell, 2016). However, further investigation identified that the default data used was coincidentally comparable to the performance of the cyclones at Granny Smith. The Plitt cyclone parameters calculated by the model using the input mill CL of 267 per cent resulted in a particle separation sharpness of 0.84 and a gold separation sharpness of 0.32. The 2016 cyclone survey data resulted in particle separation sharpness of 1.16 and gold separation sharpness of 0.43. Application of either of these cyclone partition parameters in modelling yielded comparable recovery curves.

A reassessment of the modelling identified the three stage GRG results from the 2014 design modelling and the 2016 gravity survey were inconsistent. The mill feed sample obtained from the gravity survey, despite having a comparable GRG content to the 2014 test work of 62 per cent, contained GRG that was classified as being medium grained. The circulating load of GRG increases with the grain size, thus the opportunity for gold to be recovered to gravity is also increased. Due to the discrepancy in the coarseness of the GRG, the 11 per cent underestimation in gravity gold recovery from the 2014 design modelling is now understood to be attributed to a difference in mill feed or unrepresentative sampling. To verify this the 2014 three stage GRG data was remodelled applying the mill and cyclone partition data derived from the 2016 Granny Smith gravity survey. The resulting recovery curve is compared to the recovery curves obtained from the 2014 design modelling and 2016 survey modelling in Figure 3. Modelling of a cyclone feed fed gravity circuit using the 2014 GRG data and 2016 operating data indicated an achievable gravity recovery of 26 per cent at a gravity feed rate of 425 t/h. This was comparable to the 24 per cent recovery estimate from the 2014 design modelling, indicating that the use of default mill and cyclone partition data was not a major contributing factor for the lower recovery estimate. The only variable between the 2016 survey modelling, and the remodelling of the 2014 design data was the three stage GRG results. This verifies that the apparent inaccuracy of the design modelling was due to either a change in mill feed or unrepresentative sampling.

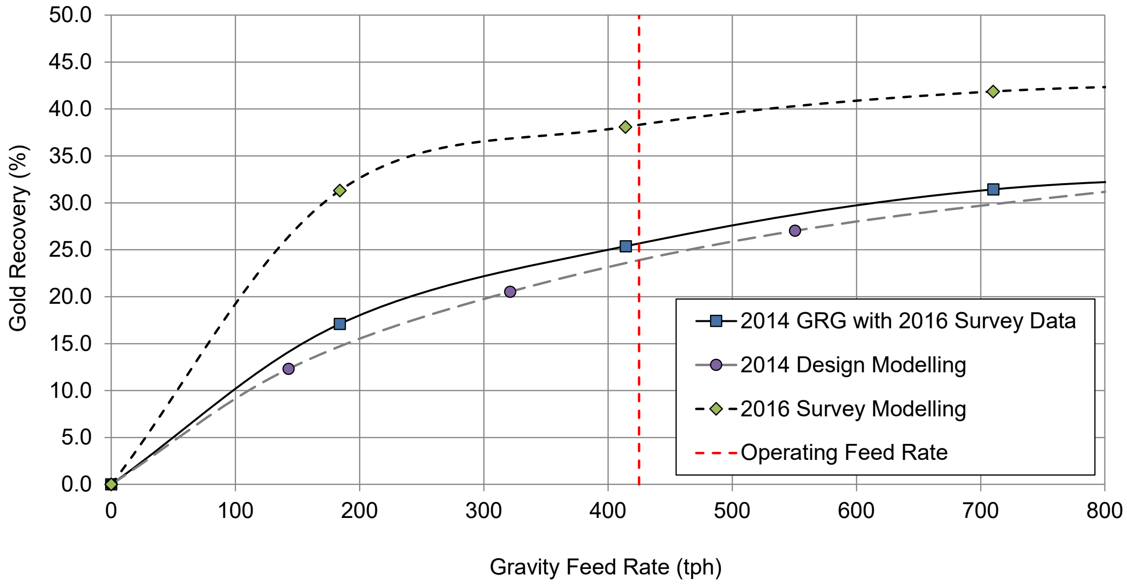


**FIG 3** – Remodel of 2014 three stage GRG results with 2016 survey plant data.

Overall, the gravity gold recovery at Granny Smith aligned with the modelling outcomes from the 2016 gravity survey, validating the accuracy of the BCC Gravity Model. Investigations into the apparent shortfalls from the design modelling highlighted that the BCC Model is only as accurate as the data used.

## UPGRADE OF AN EXISTING GRAVITY CIRCUIT – AGNEW

The existing Agnew gravity circuit has undergone two major upgrades in collaboration with Gekko Systems since its initial installation. The first upgrade was carried out in 2012 involving a change in the gravity feed configuration from cyclone underflow fed to mill discharge fed. This upgrade required a modified cyclone feed hopper and dedicated gravity feed pump. Mill discharge material discharges into a baffled cyclone feed hopper and is pumped via a dedicated gravity feed pump to a gravity feed distributor. Excess mill discharge material overflows into the cyclone feed side of the hopper which has its own dedicated cyclone feed pump. After the 2012 upgrade, the gravity circuit had an installed capacity of 200 t/h as dictated by the size of the Knelson KC-CD30 concentrators.

Design of the second gravity upgrade commenced in 2016, using the AMIRA BCC Gravity Model to understand potential increases in gold recovery with gravity throughput. The second upgrade was opportunistic due to the biannual replacement of the superseded KC-CD30 concentrators, as well as being driven by intermittent gold spikes exceeding the recovery capacity of the existing gravity and CIP circuits. An innovative design by Gold Fields involved modification of the gravity circuit configuration to a combination of mill discharge and cyclone feed, providing increased gravity effort without the need for any major capital. The circuit was commissioned in 2018 and is now operating with two KC-QS40 concentrators.

## Agnew test work and modelling outcomes

Three stage GRG test work was carried out on a mill feed sample as part of the Agnew gravity circuit performance assessment in 2015 by Gekko Systems. The GRG content of the blend being treated at the time of the survey equated to 77.6 per cent and was classified as coarse grained. Modelling of the GRG data with site specific mill and cyclone partition data obtained through the gravity survey, indicated that a feed rate of 200 t/h could achieve a gravity gold recovery of 47.6 per cent. This aligned with the 47 per cent average gold recovery being achieved on-site (Lim, 2015).

Demonstrating its ability to model gravity gold recovery representative to Agnew, the 2015 survey data and the AMIRA BCC Model was used in the design modelling for Agnew's second upgrade. Two gravity circuit configurations were considered in the feasibility study: (i) a standard mill discharge fed configuration; and (ii) a feed configuration consisting of a 50 per cent mill discharge and 50 per cent cyclone feed blend. The second configuration was a unique design proposed by Gold Fields to minimise capital requirements.

Limitations to the BCC model does not enable a combination of feed streams to be simulated. It was therefore assumed the predicted recovery for a gravity circuit fed by a 50/50 blend of mill discharge and cyclone feed would equal the average recovery between the two respective feed stream options at any given feed rate. This average recovery is represented by the dashed curve in Figure 4, positioned between the modelled cyclone feed and mill discharge fed configuration recovery trends.

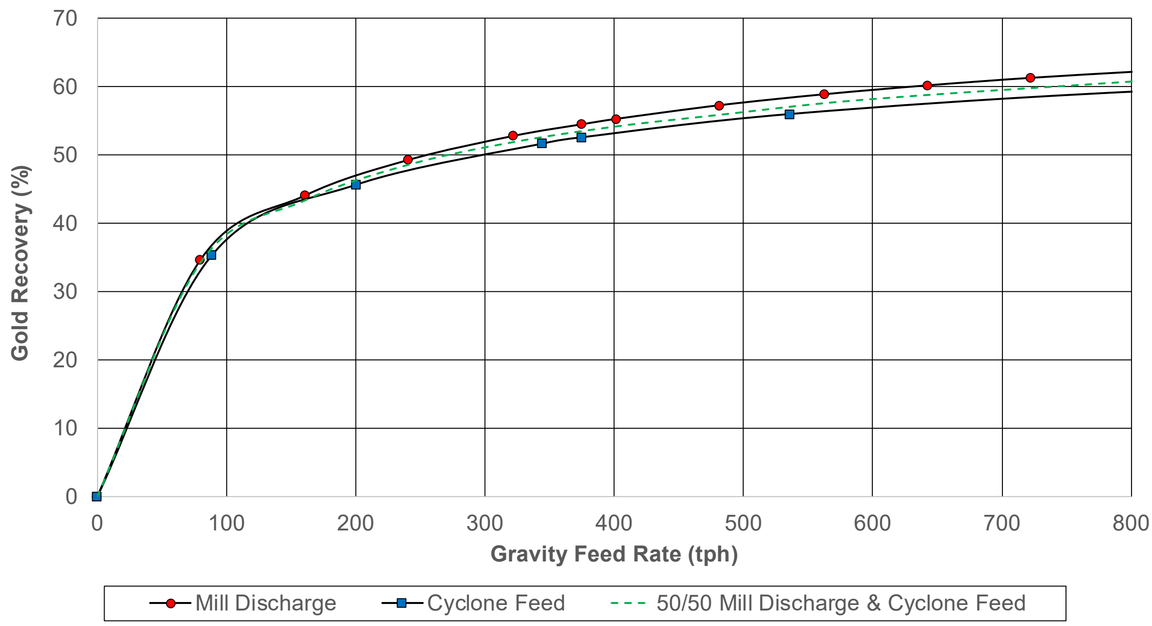


**FIG 4** – Agnew upgrade design modelling recovery curve (2016).

## Agnew gravity circuit design

To address the intermittent spikes in head grade the gravity circuit upgrade was designed with a 500 t/h circuit feed rate. The corresponding gravity gold recovery modelled for a mill discharge fed configuration equated to 57.7 per cent. The corresponding recovery for a 50/50 mill discharge and cyclone feed fed configuration was comparable at approximately 56.3 per cent (Figure 4).

Due to the modelled gravity recoveries indicating the circuit configurations being considered were in every practical sense as efficient as each other, the cost and operability of the potential circuits were considered. A mill discharge fed gravity circuit would have required an upgrade of the gravity feed pump to meet the increased flow demands. In addition to this, a mass balance around the milling circuit highlighted water constraints which could potentially result in operability issues. A combined mill discharge and cyclone feed arrangement however could utilise the capacity of the existing gravity feed and cyclone feed pumps to meet the target flow rates and enable flexibility around the mill water balance. Thus, the Agnew gravity upgrade was designed with a feed configuration consisting of 50 per cent mill discharge and 50 per cent cyclone feed. The corresponding increase in overall plant recovery from the upgrade was expected to be around 0.6 per cent. This was estimated based on the recovery benefit from the 2012 Agnew gravity circuit upgrade where a 1 per cent increase in overall gold recovery was achieved with every 14 per cent increase in gravity recovery (2015, personal communication).

An outlet from the cyclone distributor was used to direct cyclone feed material to the gravity circuit. To accommodate both the mill discharge and cyclone feed streams, as well the increase inflow rate, the old, pressurised gravity feed distributor was replaced with an open-air distribution box. Mill discharge and cyclone feed converge at the distribution box and is split to feed two KC-QS40 Knelson concentrators. Gravity concentrate is collected into the feed cone of an ILR2000BA, whilst Knelson tails is discharged into the cyclone feed hopper. A process flow diagram of the 2018 upgraded gravity circuit at Agnew is illustrated in Figure 5.

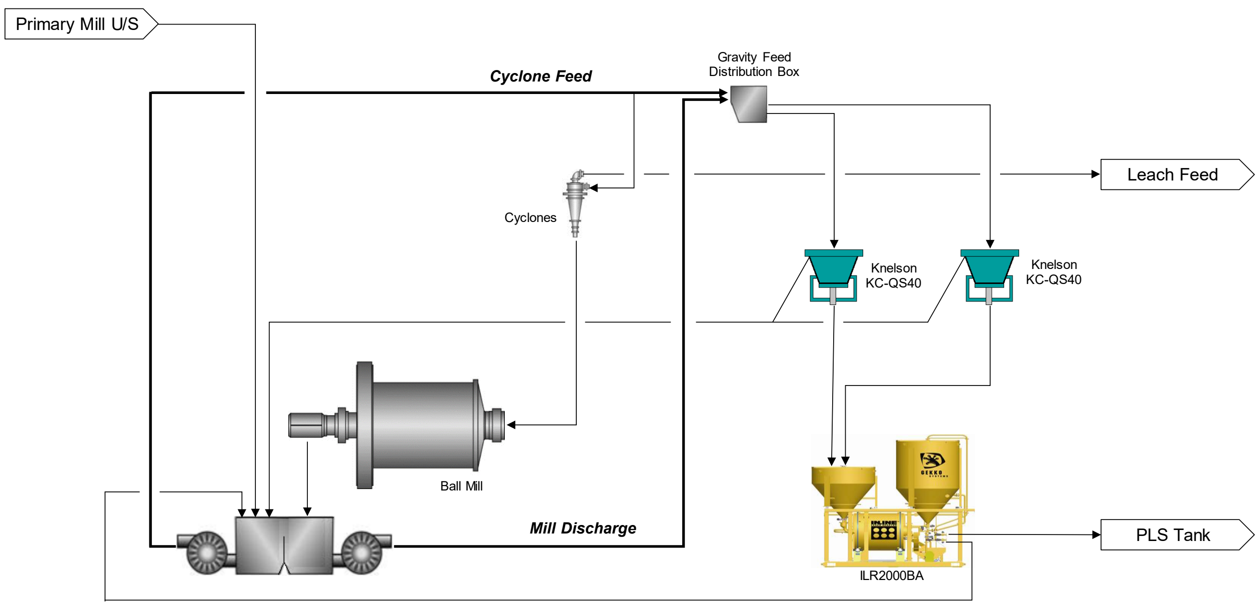


**FIG 5** – Agnew 2018 gravity circuit upgrade process flow diagram.

## Agnew gravity circuit performance

The upgraded gravity circuit was installed and operating within two weeks, with commissioning complete mid-2018. Enabling performance monitoring, flow metres were installed on both the mill discharge and cyclone feed lines discharging into the gravity feed distribution box. The gravity feed rate target of 500 t/h was achieved in excess from start-up of the circuit. The existing gravity feed pump was able to provide 290 t/h of mill discharge material.

The average gravity gold recovery prior to the upgrade at 57.1 per cent ± 2.04 per cent at 95 per cent confidence was comparable to what was achieved after the upgrade at 57.0 per cent ± 1.81 per cent, despite the increase in gravity feed rate from 200 t/h to 500 t/h. As a result, the average plant recoveries prior and post upgrade were comparable at 95.1 per cent ± 0.45 per cent and 93.7 per cent ± 0.41 per cent respectively. The average recoveries were assessed two months prior and two months after the upgrade due to consistent mill feed blends over these periods and comparable head grades averaging 6.19 g/t and 6.66 g/t respectively.

Although there was no apparent increase in gravity gold recovery after the upgrade, isolation of the occurrences of head grade spikes indicated the upgraded gravity circuit does provide an increase in recovery capacity. The gravity gold recovery when treating a mill feed grade in excess of 10 g/t increased from an average of 57.3 per cent prior to the upgrade, to 63.0 per cent. The high-grade occurrences and resulting gold recoveries to the gravity circuit pre- and post-upgrade are plotted in Figure 6. A linear regression of the recoveries with head grade indicated the recovery to gravity prior to upgrade decreased as the head grade increased, whereas recovery to the upgraded circuit increased.

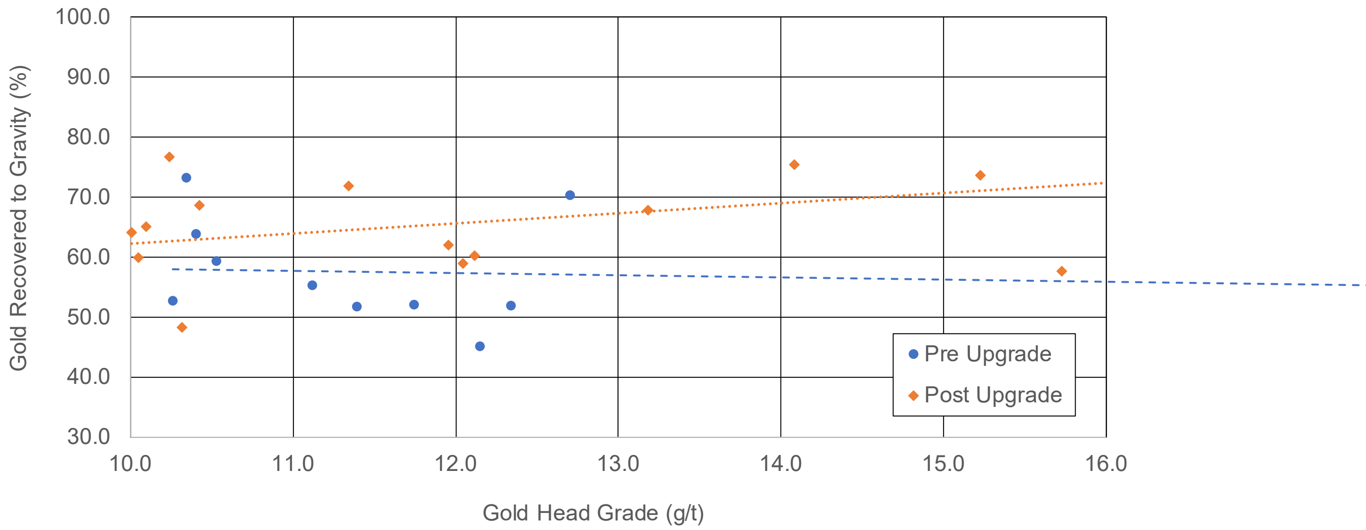


**FIG 6** – Agnew gravity gold recovery with head grade pre- and post-gravity circuit upgrade.

## Agnew design validation

The 2016 design modelling for the Agnew gravity circuit upgrade was based on data obtained from a survey carried out in 2015 where the average gravity recovery at the time was 47 per cent. However, prior to the upgrade the average gravity recovery had increased to 57 per cent. This indicates either the GRG component or the mill and cyclone performance had changed. Historical test work indicates the New Holland ore feeding the Agnew plant contains a high amount of GRG that has been classified as very coarse grained. This ore is known on-site to have a large influence on the gravity recovery (February 2020, personal communication). It is therefore more likely that the GRG component due to the blend influenced the gravity recovery between 2015 and 2018. Further investigation or an updated assessment of the gravity circuit at Agnew is required to validate this.

Overall, the ability for the AMIRA P420 BCC Gravity Model to accurately simulate gravity gold recovery was proven using the 2015 Agnew gravity survey data. Validation of the model through the 2018 gravity upgrade project was inconclusive due to the gravity circuit performance at the time of design no longer being representative of the gravity circuit performance at the time of the upgrade.

# GREENFIELD OPERATIONS – GRUYERE

The Gruyere deposit was discovered by Gold Road Resources in 2013, becoming a 50/50 joint venture with Gold Fields in 2016. Best practise gravity gold circuit design was implemented for the Gruyere project, with the outcomes from test work and modelling influencing the circuit configuration and sizing.

## Gruyere design test work and modelling outcomes

Amenability to gravity recovery via BCC was assessed on three composite ore samples from Gruyere in 2015. Test work was carried out at the Gekko Metallurgical Laboratory, Ballarat. Each of the three composites produced comparable gold recoveries. Between 28.9 per cent to 30.7 per cent of gold was recovered with the first pass, 53.4 per cent to 55.4 per cent was recovered with the second pass, and the overall resulting GRG content with the third pass was between 66.1 per cent and 67.7 per cent. The GRG in the Gruyere ore composites was classified as fine to very fine grained.

For each composite tested, the three stage GRG results were modelled using the AMIRA P420 BCC Gravity Model. Being a Greenfield project, no plant data was available for modelling. The designed mill CL of 300 per cent and default calculated Plitt cyclone parameters were applied. The modelled recovery curves for each of the three composites tested are compared in Figure 7. Modelling for each of the three composites again indicated a mill discharge fed gravity circuit configuration produced the highest gold recovery for any given feed rate. At a feed rate equal to 30 per cent to 50 per cent of the mill circulating load (1035 t/h to 1725 t/h) a mill discharge fed gravity circuit could recover 2 to 4 per cent more gold respectively than a circuit fed with cyclone underflow.

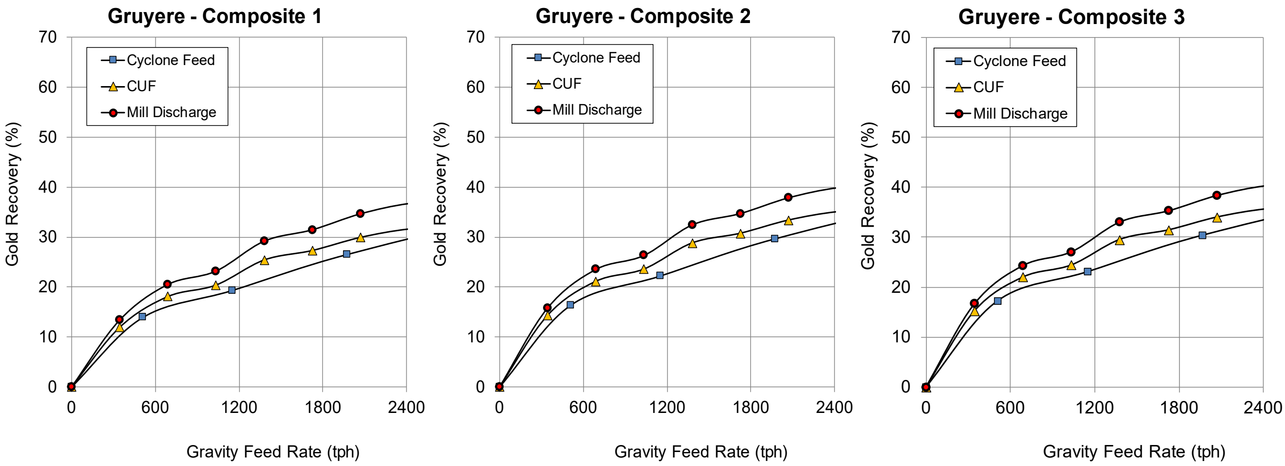


**FIG 7** – Gruyere composite 1 to 3 design modelling recovery curves.

## Gruyere gravity circuit design

Directly dictated by the modelling outcomes, the gravity circuit at Gruyere was designed to be fed with mill discharge. The hopper design was similar to that at Agnew, where the mill discharge hopper and cyclone feed hopper are combined. The mill discharge material is kept separate in the hopper via a baffle and pumped to the gravity circuit via a dedicated gravity feed pump. Excess mill discharge overflows the baffle to the cyclone feed size of the hopper. However, the hopper design at Gruyere enables minor bypassing of mill discharge to cyclone feed under the baffle and short-circuiting of cyclone feed to gravity feed. This was not accounted for in the modelling.

Mill discharge is pumped to a gravity feed distributor box which splits the gravity feed between two trains. Each train consists of a vibrating gravity screen and two KC-QS48 Knelson concentrators. The design target feed rate was 1200 t/h with the capacity to upgrade to 1600 t/h as dictated by the four KC-QS48 Knelson concentrators. The concentrate from each Knelson converges to discharge into the feed cone of a Gekko ILR4000BA. The gravity screen oversize and Knelson tails discharges into the cyclone feed hopper. The process flow diagram in Figure 8 details the streams around the Gruyere mill and gravity circuit.

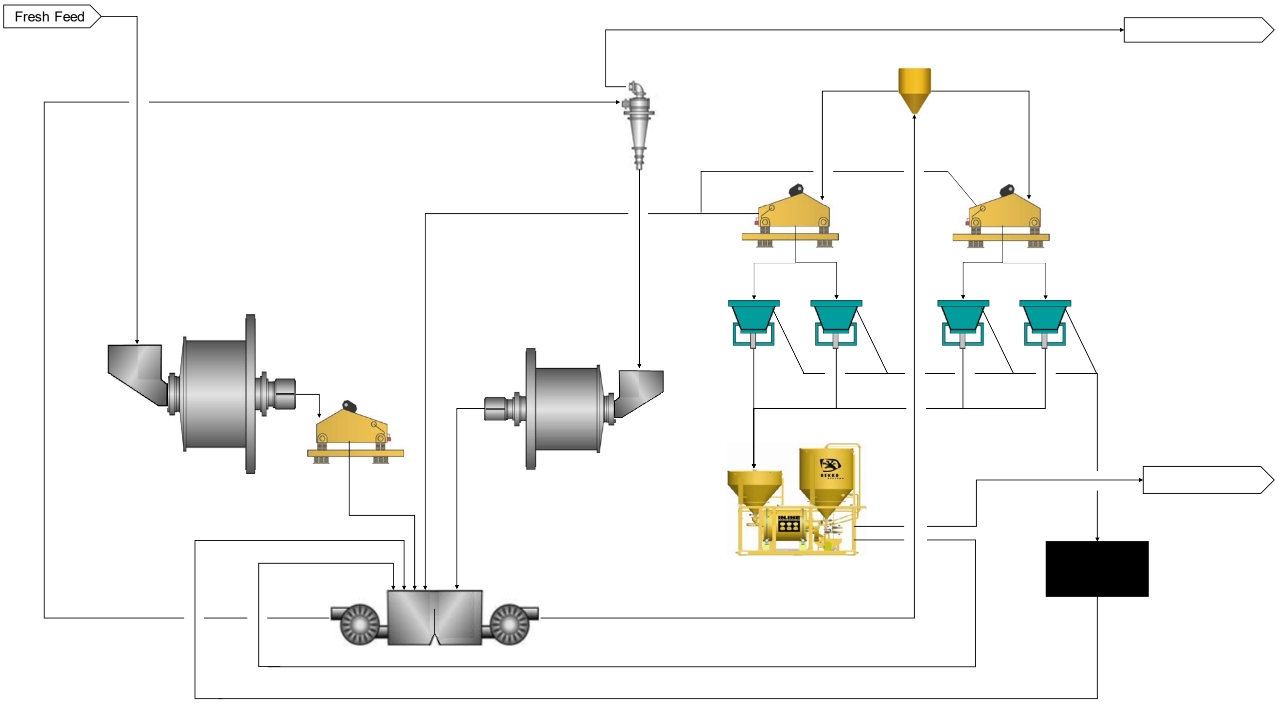


**FIG 8** – Gruyere mill and gravity circuit process flow diagram.

## Gravity gold circuit performance

Commissioning of the Gruyere process plant was completed in June 2019 with operation of the gravity gold circuit commencing in August 2019. Due to fluctuations in plant recovery due to the inherent issues and instabilities associated with concurrent plant commissioning, the leach feed grade was analysed to assess the performance of the gravity circuit. Prior to operation of the gravity circuit, the average leach feed grade, dictated by the plant head grade, was 0.91 g/t Au ± 0.10 g/t (SD = 0.32 g/t). However, since operation of the gravity circuit, the average leach feed grade decreased to 0.69 g/t Au ± 0.03 g/t with 95 per cent confidence, and the variability in leach feed grade decreased with a lower standard deviation of 0.18 g/t Au. The average head grade since operation of the gravity circuit was comparable to the head grade analysed pre-gravity recovery at 1.05 g/t Au (SD = 0.25 g/t). The effect of gravity recovery on the carbon-in-leach (CIL) feed grade is plotted in Figure 9. Not only does the feed grade to the downstream CIL circuit decrease as gravity recovery increases, but the CIL feed grade also becomes less variable.

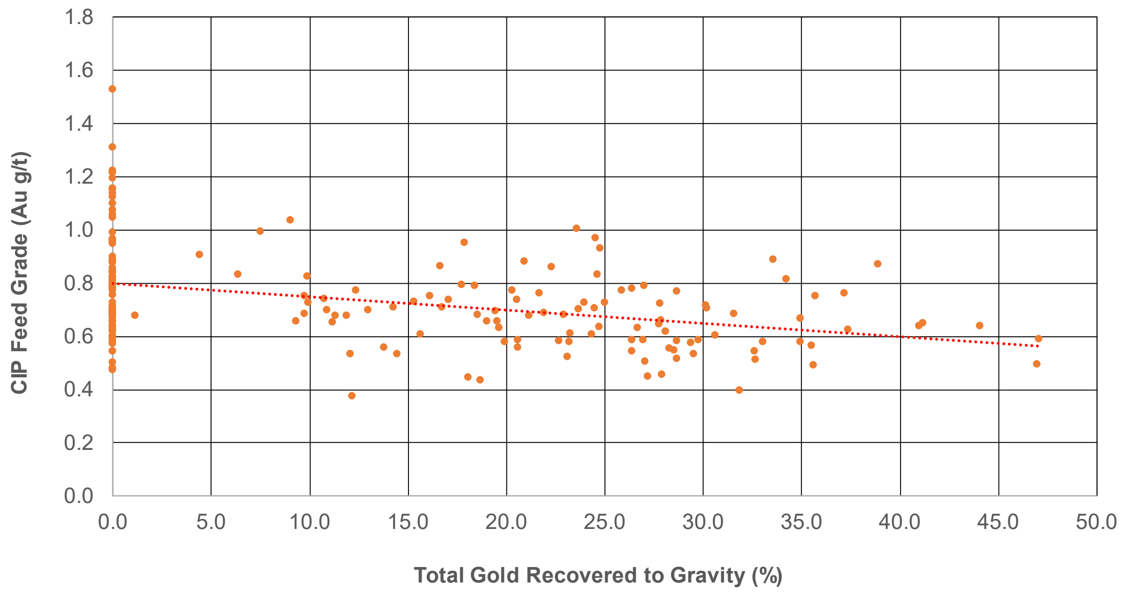


**FIG 9** – Effect of gravity recovery on CIL feed grade at Gruyere.

A gravity survey was carried out at Gruyere in March 2020 to obtain baseline performance data and identify opportunities for improvement. The survey data was also used to validate the modelling outcomes. Three stage GRG test work and modelling were carried out on the surveyed SAG feed material. The test work indicated the fresh mill feed material had a GRG content of 42.9 per cent and was classified as very fine grained.

Modelling of the GRG and survey data through the P420 BCC Gravity Model indicated a mill discharge fed gravity circuit configuration was optimal. This aligned with the outcomes from the design modelling. The resulting modelled recovery curve for the surveyed mill discharge fed gravity circuit is plotted in Figure 10. Determined from the survey mass balance, the Knelson concentrators at Gruyere are fed a combined feed rate of approximately 691 t/h. This corresponds to a gravity recovery of 22.3 per cent on the modelled recovery curve. This aligns with the reconciled gravity recovery of 21.3 per cent achieved for the month of March and validates the accuracy of the BCC gravity model.

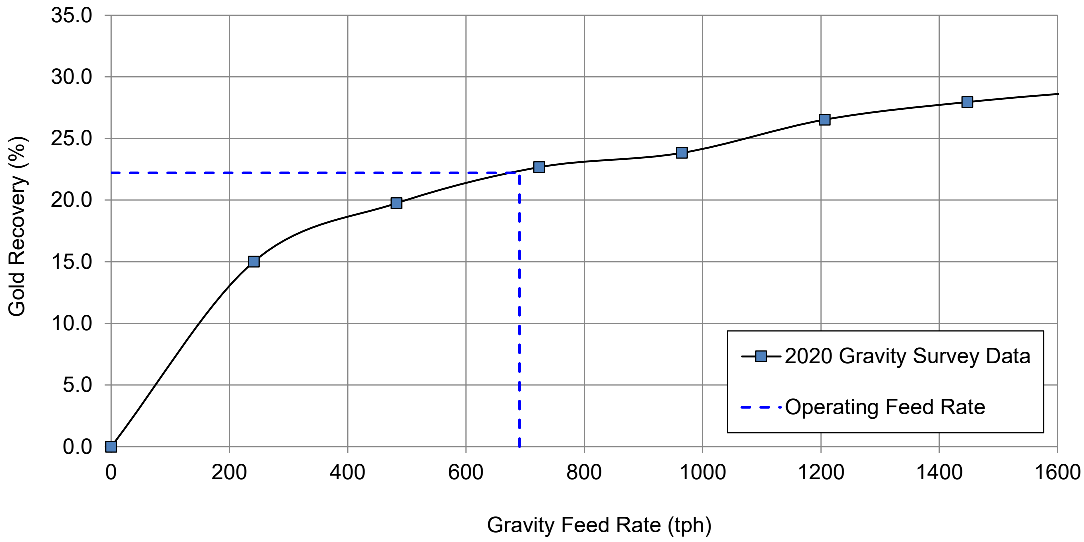


**FIG 10** – Gruyere 2020 gravity survey modelled recovery curve.

## Gruyere design validation

The GRG content and liberation size from each of the composites tested during circuit design in 2015 was not comparable to that of the SAG feed sample obtained from the 2020 survey. So, despite the application of inaccurate plant operating data, outcomes from the Granny Smith case study would support that with such variation in the three stage GRG data, it could not be expected for the Gruyere design modelling to reflect actual plant gravity recoveries. To validate this, an average of the GRG data from the three composites tested during design was remodelled using the surveyed plant data. The modelled recoveries are plotted alongside the 2015 design modelling curve and 2020 survey modelling curve in Figure 11. The 2015 GRG data remodelled with 2020 operating data indicated a mill discharge fed gravity circuit could recover 31.3 per cent of the gold at a gravity feed rate of 691 t/h. The use of default operating data, which was applied in the 2015 design modelling, resulted in a lower predicted recovery of 17.1 per cent for the same feed rate. This equates to a difference in predicted recovery of 14.2 per cent. A difference in the GRG data, where the 2020 surveyed SAG feed sample indicated a lesser GRG content and very fine GRG distribution, resulted in a difference in predicted recovery of 9.0 per cent. Due to the incomparable GRG and operating data between the design and survey modelling, the Gruyere design modelling could not have accurately predicted plant recoveries.

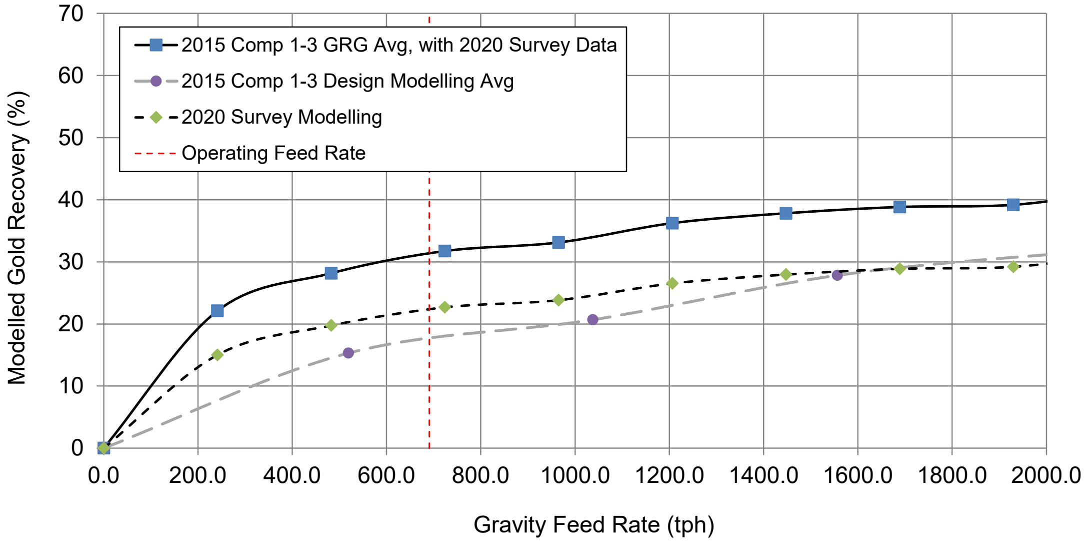


**FIG 11** – Remodel of 2015 three stage GRG results with 2020 survey plant data.

At the installed capacity of 1600 t/h, the design modelling curve does intercept the survey modelling curve. However, from the various GRG and operating data modelled through the Gruyere and Granny Smith case studies, it is apparent that the operating data influences the shape of the recovery curve, whilst the GRG data shifts the recoveries up or down for a given feed rate. Therefore, any apparent correlation in recovery at any given feed rate would be coincidental. Overall, the recovery curves in Figure 11 highlight the difficulties in obtaining representative samples and operating data to predict gravity recovery in Greenfield operations.

## SUMMARY OF FINDINGS

Each of the case studies validate the AMIRA P420 BCC Gravity Model as a reliable tool in gravity circuit design for determining the optimal circuit configuration. Aligning with the outcomes from the design stage of modelling, modelling of the operational gravity circuits using current GRG and milling data indicated a mill discharge fed gravity circuit was the optimal configuration to maximise gravity recovery. However, the discrepancy between the predicted gravity recovery during design and real plant gravity recovery was evident. The Granny Smith case study indicated a 11 per cent underestimation of gravity recovery from design. The Gruyere case study indicated a 5.2 per cent underestimation of gravity recovery from design. Yet modelling of site survey data validated the accuracy of the BCC model, where the Granny Smith, Agnew and Gruyere gravity circuit surveys resulted in a 3.2 per cent, 0.6 per cent and 1.0 per cent difference between the average plant gravity recovery and the modelled survey recovery, respectively. The accuracy of the gravity circuit upgrade design for Agnew was inconclusive due to the gravity recovery at the time of design no longer being representative of the gravity recovery at the time of the upgrade.

Comparing the effect of using GRG data obtained during design versus current GRG data from respective Granny Smith and Gruyere surveys as well as milling data applied in design versus accurate milling data from site surveys, has demonstrated how these variables change the shape and positioning of the modelled gravity recovery curve. Remodelling of the Granny Smith and Gruyere design GRG data with current operating data has emphasised the influence both the GRG data and operational data have on the accuracy of the modelled recovery.

Given the accuracy of the model in predicting plant recoveries when applying representative data has been repeatedly validated, it can be concluded that the gravity recovery discrepancies that exist between circuit design and real plant performance is a factor of the data that is applied during design. However, the author acknowledges that this data is inherently difficult to obtain during design as orebodies are often heterogenous and blending of ores will change. And the performance of various processes in the milling circuit will undergo changes with time such as changes in throughput and continuous optimisation. To ensure gravity recovery estimates through modelling during the design stage are as accurate as possible effort should be made to ensure representative samples are obtained for GRG testing and the most accurate or average operating data is available where applicable.

## CONCLUSIONS

Overall, the outcomes from the design of the; 2015 Granny Smith retrofitted gravity circuit; 2018 Agnew circuit upgrade; and the 2019 Gruyere greenfield gravity circuit, proved the AMIRA P420 BCC Gravity model was reliable in determining the optimal gravity circuit configuration for the ore sample tested. The model provided a good guide for establishing the circuit capacity in Brownfield and Greenfield installations. Whilst acknowledging the difficulties in obtaining data that is representative of the ore being treated and milling performance by the time the gravity circuit is built and operational; the discrepancies between design gravity recoveries and actual plant recoveries highlighted the significance of using representative mill and cyclone partition data during design and the influence of the GRG data.

## ACKNOWLEDGEMENTS

The authors wish to thank Gold Fields and Gekko Systems for their support and permission to publish this paper. Special mentioned to the metallurgical teams from the Granny Smith, Agnew and Gruyere process plants for providing the data for analysis. The invaluable contributions made by; the late Professor Andre' Laplante, and the AMIRA Curtin University Technology Group are also acknowledged, having provided the insight into gravity gold recovery that enabled the development of the AMIRA P420 BCC Gravity Model.

## REFERENCES

Laplante, A R, Woodcock, F., and Huang, L, 2001. Laboratory procedure to characterize gravity recoverable gold, Society for Mining, Metallurgy and Exploration, Inc. Transactions 2001, Volume 308, 53–59.

D'Uva, L, Robinson, J, Bell, T, 2006. Defying Gravity – Brownfield Continuous Improvement, *in13th AusIMM Mill Operators Conference 2016*, (The Australasian Institute of Mining and Metallurgy: Melbourne)

Grewel, I, Van Kleen, M, McAllister, S, 2009. Gravity Recovery of Gold from Within Grinding Circuits, in *Recent Advances in Mineral Processing Plant Design 2009*, (SME: Colarado USA)

Lim, L, 2015. Gold Fields Agnew Gravity Survey Testwork Report, Report SC0537.

# Tales of tails – values from liabilities?

*P D Munro[1], K E Barns[2] and D W Bennett[3]*

1. Principal Consultant, Mineralis Consultants Pty Ltd, Taringa Qld 4068.
2. Principal Consultant, Mineralis Consultants Pty Ltd, Waikouaiti 9471, New Zealand.
3. Principal Consultant, Mineralis Consultants Pty Ltd, Taringa Qld 4068.

## TALES OF TAILS – VALUES FROM LIABILITIES?

Processing of tailings has been a recurring theme throughout the modern history of mineral processing. There are various factors driving the reclamation and treatment of the tailings of previous operations. One can be the introduction of a new technology as was the case at the beginning of the 20th century when cyanidation rapidly replaced amalgamation as the predominant method of recovering gold. A second factor can be demand for an element or mineral in the tailings that was not previously targeted by the initial treatment process eg extraction of uranium from gold tailings. A sustained rise in a commodity price can also prompt the recovery of a mineral or element in tailings such as has been recently seen with the recovery of cobalt from copper tailings in Central Africa is a third reason driving tailings treatment. A final factor can be recognition of the environmental benefits of reprocessing and repurposing such as elimination of acid mine drainage issues.

This paper discusses aspects and presents case studies of the economic recovery values and environmental benefits that arise from tailings treatment. For beginners in the field it proposes several cautionary but important 'tests' to consider as a counter to the implicit hubris of 'we're smarter/we'll try harder and therefore do better than the previous operators' which is sometimes encountered. These tests are: (a) will the processing of tailings use a different mineral separation/extraction technology than the previous operation; (b) is the treatment of tailings making a different product; (c) is there an assured market for the product; and (d) is there an environmental benefit to treating the tailings?

## INTRODUCTION

A good question to continually ask during mineral processing plant operation is; 'What is in the tailings that should not be there?'. The answer to this question will have limitations based on the physical reality of the installed plant and process, for example if the grind for a gold leach plant feed is 106 µm, there is little point in pulverising daily tailings samples to 10 µm and re-leaching before claiming that the actual plant recovery shortfall is somehow the fault of the operators. The next question may not be asked as frequently but is worthwhile when significant values remain in the tailings; 'What is in the tailings that we could get if we did something different?'. The processing of tailings can be either an adjunct or an addendum improvement to an existing process, such as increasing flotation recovery with more stages and improving liberation from low quality composites through finer grinding. Or it can be reclamation of impounded tailings for retreatment enabled by new technology and perhaps making a different product, or targeting elements or minerals not previously extracted. Case studies and examples for both grade and recovery improvement and retreatment of impounded tailings are discussed in this paper.

The good news with tailings is that it is a known resource, but the bad news is that there are no hidden gems. Some common misconceptions about impounded tailings are that those who produced them weren't really trying, their economic motives were different, and they only cared about throughput rather than recovery, they were in financial difficulty so 'let the plant go', and that fine grained minerals sitting for a long time in a solution with occasional periods of drying out are exactly the same as the day they were deposited. There are many examples of successful tailings retreatment and recovery improvements, and with careful characterisation and process development treatment of tailings may provide both economic and environmental benefit.

## TALE OF TAILS 1 – RECOVERY AND GRADE IMPROVEMENTS

Seeking to improve recovery and grade is a normal part of operations. Study of the deportment of important minerals to tailings during operations should result in questioning whether 'retreatment' should take place <u>before</u> the material is deposited in a tailings dam. The installed process and the equipment in the existing plant will place constraints on achievable performance. For example, if examination of a gold leach plant tailings shows that doubling leach residence time or significantly reducing grind size will give a marked improvement in gold recovery, the existing process and equipment is unable to achieve the improvement – the process conditions must be changed to gain the benefit. The question then simply becomes whether it is economically beneficial to upgrade or expand the plant to achieve the recovery improvement.

The Phu Kham copper-gold operation in Laos PDR suffered from low copper and gold recovery from commissioning compared with operations treating similar deposits (Bennett *et al,* 2012). The causes of low recovery were predominantly related to a high pyrite content in ore which required selective flotation conditions in roughing, and very selective flotation conditions in cleaning. Combined with poor copper sulphide mineral liberation, and the major association of the gold with pyrite which would be rejected to achieve a saleable copper concentrate grade, recovery was well below benchmarked copper-gold deposits at approximately 70 per cent for copper and only 40 per cent for gold. Detailed mineralogy and characterisation data had been routinely collected soon after commissioning on monthly weighted composite samples, which gave information on the causes of copper sulphide mineral loss. The dominant cause of copper sulphide loss was in coarse (greater than 106 µm), poor quality binary non-sulphide gangue composite particles as presented in Figure 1.

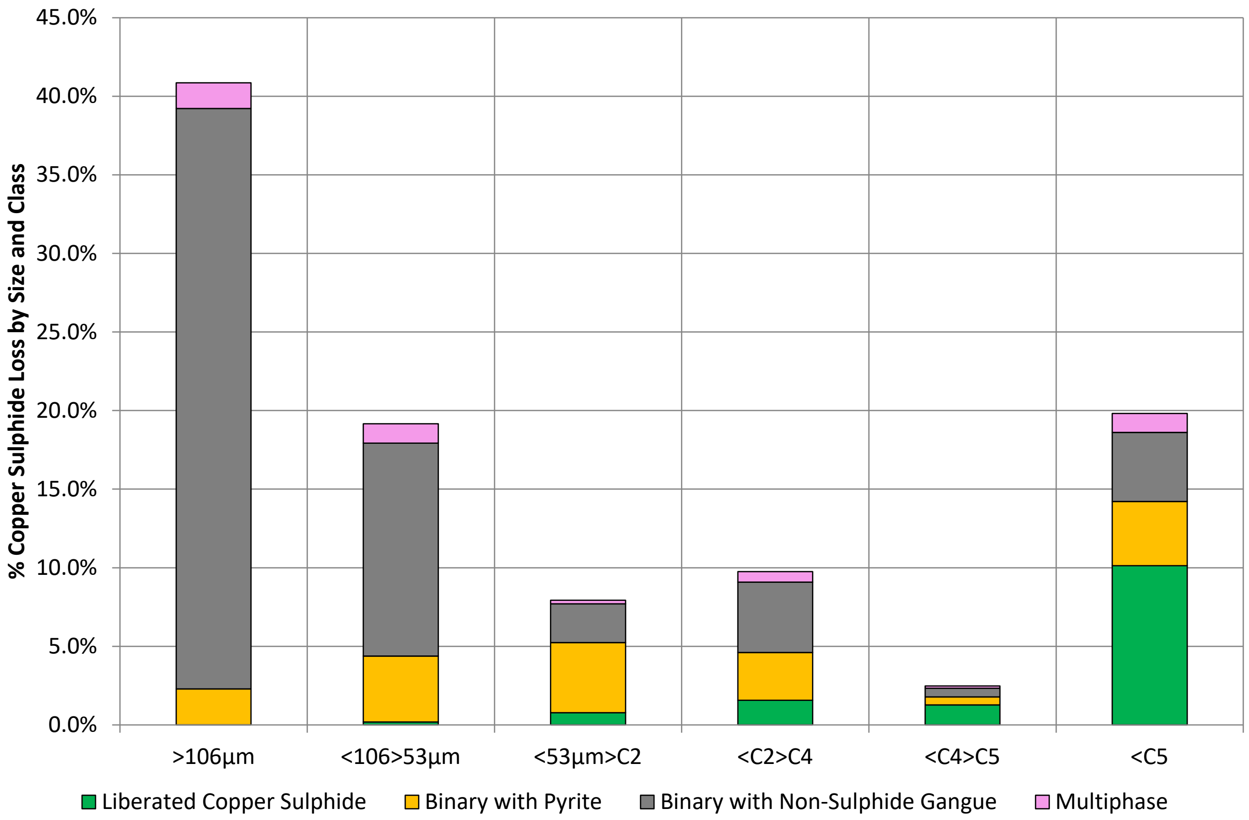


**FIG 1** – Copper sulphide deportment in Phu Kham flotation tailings.

A plant tailings retreatment project commenced in 2009 with the objective of producing a low-grade copper-gold concentrate for hydrometallurgical treatment. The test program initially focused on first cleaner tailings which contained fine and oxidised secondary copper minerals from the treatment of supergene ores, and could be up to five per cent copper grade based on shift assay data. As mining moved into areas with a higher primary copper sulphide mineral content, dominated by chalcopyrite, the test program focus shifted to aggressive bulk sulphide flotation of final combined rougher and first cleaner tailings as the majority of copper and gold loss was contained in the rougher tailings.

The results of the tailings retreatment program test work showed that bulk sulphide flotation of tailings using potassium amyl xanthate (PAX) collector, regrinding the bulk sulphide concentrate to approximately 80 per cent passing 15 µm, and cleaning to a final concentrate containing approximately 3 per cent copper and 3 g/t gold made a suitable product for leaching using the Albion Process™ followed by solvent extraction – electrowinning technology. The process would make copper cathode, and the leach residue would be neutralised and treated using conventional carbon-in-leach processing to produce gold Doré. Test work demonstrated that total Phu Kham copper recovery could be increased by over 15 per cent absolute, and gold recovery by over 25 per cent absolute.

The tailings retreatment program proceeded to a pre-feasibility level of study which included a pilot plant to produce low-grade concentrate for Albion Process™ feedstock. During the pilot plant run, capital and operating cost updates for the flotation, fine grinding, Albion and CIL process plants were received which rendered the process design concept less attractive; the focus was immediately switched to moving the aggressive bulk sulphide flotation concept into the existing plant and upgrading the poor-quality rougher concentrate by fine regrinding and increased cleaner flotation capacity. The pilot plant included flotation cells and an M20 IsaMill™ so was re-arranged to take a bleed of rougher flotation feed, maximise copper and gold recovery through aggressive unselective roughing conditions, regrinding to 20 μm, and cleaning flotation to make a 23 per cent copper concentrate.

The results of the pilot trials showed that over seven per cent absolute additional copper and gold recovery could be achieved by increasing existing plant rougher concentrate regrind and cleaning capacity, with only 20 per cent of the capital cost of the tailings retreatment process and minimal technical risk – all the required additional equipment was identical to the equipment already in use. The concept was confirmed by full-scale plant trials operating at half throughput rate and doubling rougher mass recovery as a percentage of feed mass while maintaining a regrind size below 25 μm. This achieved over seven per cent absolute increase in copper recovery and over 15 per cent absolute increase in gold recovery.

The study was changed to an 'increased recovery project' (IRP) with a focus on finalising design criteria, mainly to determine the rougher mass recovery requirement, and using mineral liberation data to determine the design regrind size to achieve 80 per cent copper sulphide mineral liberation. The resultant design included a doubling of rougher concentrate regrind and first cleaner capacity and concentrate filtration capacity. The extensive mineralogy, liberation, and test data accumulated rendered the design and operating outcomes virtually risk-free – the project achieved the target increase in copper and gold recovery of six per cent each within one month from commissioning.

Phu Bia Mining Limited's nearby 4 Mt/a Ban Houayxai in Laos PDR had conducted daily re-leach testing on shift composite samples using both extended leach time and additional cyanide concentration tests since commencement of operations in April 2012. The results of the re-leach tests were grinding product size and residence time (both related to throughput) dependent, showing an average gold and silver recovery benefit with either extended leach time and/or increased cyanide concentration at high throughput rates. Leach modelling work on plant data by Metifex Pty Ltd in 2015 highlighted the slow silver dissolution and adsorption kinetics in the air sparged leach/adsorption tanks and prompted operators to start focusing on silver recovery rather than gold recovery – conditions suited for increasing silver recovery would recover more gold anyway. The Metifex model also predicted approximately 4.3 per cent improvement in gold dissolution and 2.3 per cent improvement in silver dissolution could be achieved by increasing dissolved oxygen levels in the CIL to increase leach kinetics.

Gold leach test work in 2015 on future ore samples for the following three years of production were undertaken, using oxygen to vary the dissolved oxygen level in the leach from the plant normal level of 4–5 ppm provided by air injection. Although the results were variable based on the gold mineralogy and liberation, the increase in gold dissolution as presented in Figure 2 without having to increase cyanide concentration provided a compelling investment case.

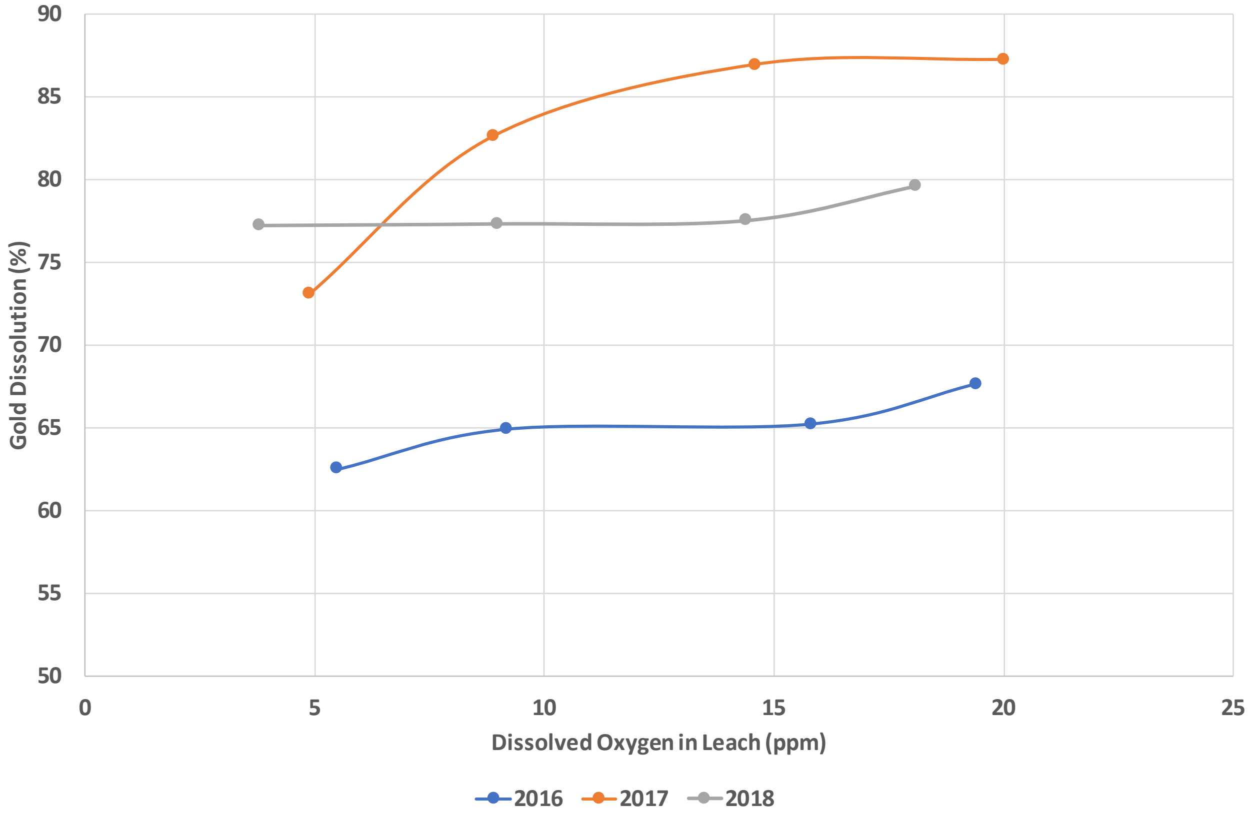


**FIG 2** – Average gold dissolution and dissolved oxygen levels for 2016 to 2018 test samples.

Installation of a Goldox™ system in 2016 for sparging oxygen to achieve greater than 15 ppm dissolved oxygen in the CIL tanks achieved a 4.4 per cent increase in gold recovery and 3 per cent increase in silver recovery, reducing the amount of gold and silver in tailings 'that should not be there'.

Probably the largest 'direct coupled' tailings retreatment operation in the non-ferrous mining sector is the Minera Valle Central plant of Amerigo Resources located 40 km south-west of the El Teniente copper mine in Chile. It processes 60 000 t/d of reclaimed historic tailings from the Cauquenes storage facility and 130 000 t/d of fresh tailings from current production at El Teniente. The simple flow sheet classifies the tailings using hydrocyclones with the coarse size fraction being reground before separate flotation of both size fractions. Recovery of contained copper in the fresh tailings has been a mean of 23 per cent from 2003 to 2018. The fact that a similar flow sheet was used in the former Bonneville Concentrator of Kennecott Copper in the USA (Jeppson and Ramsey, 1976) leads to the observation that the installation of appropriate equipment in the El Teniente Colon concentrator could be expected to render the downstream tailings retreatment plant uneconomic. The authors struggle to envision a scenario whereby the passage of the fresh tailings down the open launder to the Minera Valle plant can have somehow beneficially altered the surfaces of particles containing copper sulphide minerals facilitating subsequent recovery by flotation.

## TALE OF TAILS 2 – TAILINGS RETREATMENT

There can be multiple commercial 'drivers' for the reprocessing of tailings.

### Introduction of a new technology

- The best example of this is the retreatment of gold mine tailings from the amalgamation process where the recovery could be around 60–70 per cent for ores from the deeper unoxidised zone of the Witwatersrand deposits in South Africa. Cyanidation achieved gold recoveries well over 90 per cent. This went through several stages involving treatment of the separate sand and slime fractions which had accumulated before the 'all sliming' cyanidation process was introduced in 1918 (Bosch, 1987).

- At Broken Hill in Australia silver-lead-zinc tailings from the original gravity concentration process and the pioneering flotation plants have been reclaimed and retreated by 'modern' flotation processes (Mitchell and Bertrand, 1983; Seaborn, 1983; Hardy, 1998; Kleeman, 1998).
- From 1908 the Calumet and Hecla Consolidated Copper Company on the Keweenaw Peninsula, Michigan, USA reclaimed around 35 Mt of material in two tailings 'sandbanks' deposited in Lake Superior. The introduction of the ball mill at the beginning of the 20th century made it profitable to regrind copper-containing middlings particles in the sand size fraction of the tailings for subsequent treatment on Wilfley tables. The original estimate of recovering 30 per cent of the copper contained in the tailings by regrinding and gravity concentration was supplemented by another 45 per cent from ammonia leaching of the slime size fraction with a further 10 per cent by flotation for a total recovery of 85 per cent.
- The Rentails project at Renison in Tasmania proposes to treat low-grade concentrate from retreating tailings pyrometallurgically to fume off a tin-rich product (Metals X Limited, 2017).

## A sustained increase in price of the original target commodity

- The secular increase in the gold price since 1972 combined with the introduction of carbon-in-pulp technology made retreatment of tailings at grades hitherto regarded as uneconomic. In South Africa the economics of tailings retreatment operation in the Johannesburg area such as Ergo (Anon, 1988) were enhanced by the possibility of turning land previously occupied by tailings dams into commercial property. Australasian examples of gold tailings retreatment in this era are Kaltails (Finlay, 1992), Macraes and Mount Morgan (Parsons and Hampshire, 1986). Recent base metal tailings operations are New Century, Hellyer and Woodlawn.

## Increase in price of a previously neglected commodity

- Examples of this are the recovery of uranium from gold tailings in South Africa, cobalt from copper tailings in the Democratic Republic of the Congo, baryte from Mississippi Valley-type deposit lead-zinc tailings and magnetite from copper tailings at Ernest Henry in Australia (Siliézar, Stoll and Twomey, 2011) and La Candelaria in Chile.

## Partially defraying the costs of environmental remediation

- Reclaimed sulphidic tailings prior to storage in a properly engineered facility to eliminate acid mine drainage could be reprocessed to make saleable products.

Mineral processing engineers should approach the reprocessing of tailings with a degree of humility regarding the efforts of the people who made the original material. It is hubristic and probably delusional to believe that the tailings contain 'low hanging fruit' because of a lack of knowledge and/or insufficient application by their predecessors.

A relevant anecdote to this effect was an observation by the late Ian Chaston to one of the authors that no one ever made money out of reprocessing tailings from ancient mines in the Roman Empire. The Romans left virtually no residual value in the tailings and slags from their mineral workings because of the relatively high prices of precious and base metals in antiquity with economics enhanced by the use of slave labour.

An axiom is that the <u>reprocessing operation must do something different and/or produce something different</u> to the first time the ore was treated.

There is an important distinction between retreatment of gold tailings and base metals tailings; the former produces a Doré bullion which is virtually instant 'money' whereas latter makes concentrates that will almost inevitably be lower grade with higher levels of penalty elements and impurities than those from the previous operation. Downstream processors of these concentrates can be expected to take a higher share of the contained value than for a 'standard' concentrate. Marketing of such materials creates its own issues together with the higher working capital requirement compared with a gold operation selling Doré bullion.

Some cautionary observation for people considering reprocessing tailings follow:

Good news versus bad news:

- Good news is that you are dealing with a totally known 'resource' although with some local variation in head grade, particle size distribution etc.
- Bad news is that it will not get better!

While it might be a <u>tailing</u> it can be a <u>concentrate</u> of problems *viz*.

- Particles that didn't float because of surface impairment and/or very small size.
- Unliberated particles eg 'lean' binaries, complex ternaries etc.
- Unleached gold particles with altered surfaces eg iron stained, littered with 'debris'.
- Presence of concentrates from the previous operation's preflotation stage discarding naturally hydrophobic minerals such as talc, pyrophyllite, organic carbon and carbonaceous pyrite.
- Ratio of 'wanted' ie valuable mineral particles to 'unwanted' ie gangue mineral particles is very low. Iron sulphides in particular can be a problem ie the ratio of 'difficult' particles to 'target' particles is likely to be at least an order of magnitude higher than when the ore was first treated. Putting this in perspective if the original ore had an iron sulphide to copper sulphide ratio of 5:1 and made a copper concentrate at 90 per cent copper recovery containing 5 per cent w/w iron sulphides then the tailing will have an iron sulphide to copper sulphide ratio approaching 50:1.
- Even if the tailing has been stored for a long time there may be little oxidation of deeper, contained sulphides with respect to the *in situ* tailings because of the limited ingress of oxygen. However, subsequent oxidation of mineral surfaces may be extremely rapid when the tailings are exposed to air during reclamation as a slurry undergoing classification, comminution and flotation when reprocessed. The high rest potential of pyrite relative to other sulphide minerals causes galvanic corrosion resulting in 'shedding' of ion species and fouling of minerals surfaces: this will be exacerbated by the high pyrite: target mineral ratio and the fine particle sizing compared to run-of-mine ore. Flotation recovery and selectivity will be adversely affected.
- Other than what left with the concentrate, all the reagents (+ grinding media debris) added during processing will be present in the tailings solids + water.

Caution should be used when doing test work on reprocessing tailings. In addition to taking measures to minimise oxidation of sulphide mineral surfaces because of the reasons discussed above, sample history and preparation can significantly affect metallurgical outcomes. Two examples illustrate problems in this area:

1. Gold tailings were screened before flotation testing which rejected remnant abraded +300 µm carbon particles; carbon safety screens in the original carbon-in-pulp plant had an aperture of 300 µm to catch this abraded carbon. When the tailings were reprocessed, the coarse carbon particles were recovered to the flotation concentrate.
2. Oven drying of samples of zinc-lead-silver tailing before metallurgical testing was the most probable cause of subsequent galena depression in flotation. Zinc concentrate from the production plant reprocessing the tailing had a much higher lead content than that from the metallurgical test work as the flotation feed had not been exposed to high temperature passivation/oxidation of the galena surfaces.

Tailings reprocessing operation often take longer to ramp up to stable operation because of unrealistic expectations of feed system performance, usually caused by inadequate capital expenditure. Common problems are:

- Failure to understand that the tailings dam has been used as a rubbish dump for the life of the previous operation. Items encountered in reclamation can range from pipes and fittings, empty drums and drums containing toxic chemicals including polychlorinated biphenyl transformer oil, tyres, motor vehicle bodies and complete excavators! Consideration should be given to putting reclaimed tailings through a trommel or screen to reject trash.

- Insufficient working faces when using water monitors to reclaim tailings – original estimates on monitor performance tend to be wildly optimistic resulting in interrupted and erratic feeding of slurry to the process plant. Subsequent installation of additional monitors is often reported.
- Inadequate storage of slurry ahead of the process plant – best practice would be to thicken the reclaimed slurry with storage in a stock tank.

Process design criteria used for treating the original ore can be expected to be irrelevant eg flotation times are likely to be much higher and well out of the range of industry 'norms'.

## CONCLUSIONS

Reprocessing of tailings for an existing operation should lead to a close examination as to what caused values to be misplaced into the tailing. For flotation plants the usual culprits are misbehaving particles at the extreme end of the feed size distribution. The easiest fix is improved liberation of values from coarse particles through more efficient operation of existing classification and comminution equipment. This doesn't usually require the adoption of a new technology.

It is hubristic and probably delusional for mineral processing engineers to believe that the tailing contains 'low hanging fruit' recoverable by reprocessing because of a lack of knowledge and/or insufficient application by their predecessors.

A tailing reprocessing operation must do something different and/or produce something different to the first time the ore was treated – it is unrealistic to expect that 'more of the same' will produce a similar metallurgical result to that of the previous operation.

Unlike base metals operations, reprocessing gold tailings is not complicated by issues of product marketing and high working capital requirements.

While the material might be a <u>tailing</u> it can be a <u>concentrate</u> of problems for reprocessing for the reasons discussed above.

Tailings reprocessing operation often take longer to ramp up to stable operation because of unrealistic expectations of feed system performance, usually caused by inadequate capital expenditure.

## ACKNOWLEDGEMENTS

The authors thank colleagues who have generously shared their experiences over many years in the reprocessing tailings from laboratory investigations through to plant operations.

We thank Mineralis Consultants Pty Ltd for permission to publish this paper.

## REFERENCES

Anon, 1988, Ergo's new Daggafontein plant opened, Mining Magazine, January, pp6–7

C. Harry Benedict, 1952, Red Metal The Calumet and Hecla Story, University of Michigan Press, Ann Arbor

D. Bennett, I. Crnkovic, P. Walker, 2012, Recent Process Developments at the Phu Kham Copper-Gold Concentrator, Laos PDR, Proceedings 11th Mill Operators' Conference 2012, pp257–272. AusIMM Melbourne

D. Bosch, 1987, Retreatment of Residues and Waste Rock in The Extractive Metallurgy of Gold in South Africa, Vo. 2 G.G. Stanley (ed.), The South African Institute of Mining and Metallurgy. Johannesburg pp707–745

I.R.M. Chaston, 1982, personal communication

S.M. Finlay 1992, Kalgoorlie Tailings Retreatment – 'Kaltails' in International Conference on Extractive Metallurgy of Gold and Base Metals V.N. Misra, D. Halbe abd D.J. Spottiswood (eds), The Australasian Institute of Mining and Metallurgy, Parkville, pp73–78

E.L. Hardy, 1968, Treatment of De Bavay Slime Dump in Broken Hill Mines – 1968 Radmanovich, M. and Woodcock, J.T. (eds)., The Australasian Institute of Mining and Metallurgy, Melbourne pp459–464

R.D. Henderson, 2018, Minera Valle Central Operation Rancagua, Region VI, Chile, 43–101 Technical Report, prepared for Amerigo Resources Ltd.

R.D. Jeppson and R.J. Ramsey, 1976, The Kennecott Copper Corporation Bonneville Concentrator in Flotation A.M. Gaudin Memorial Volume, Vol. 2 Fuerstenau M.C. (ed.), American Institute of Mining, Metallurgical and Petroleum Engineers Inc pp 1055–1078

J.R. Kleeman 1968, Treatment of old tailings dumps at Broken Hill South Limited in Broken Hill Mines – 1968 Radmanovich, M. and Woodcock, J.T. (eds)., The Australasian Institute of Mining and Metallurgy, Melbourne pp437–457

Metals X Limited 2017, Renison Tailings Retreatment Project ("Rentails") Updated DFS Confirms High Margin Project. Australian Stock Exchange Release. 04 July

R.A. Mitchell and D.L. Bertrand, 1983, Development and operation of tailings dump retreatment facilities at ZC/NBHC, Limited in Broken Hill Conference 1983, The Australasian Institute of Mining and Metallurgy Parkville pp353–358

G.J. Parsons and M. Hampshire 1986 Process optimization of Mount Morgan gold tailings retreatment plant in Publications of the 13th CMMI Congress Volume 4 Metallurgy L.E. Fielding and A.R. Gordon (eds) 13th Congress of the Council of Mining and Metallurgical Institutions and Australasian Institute of Mining and Metallurgy Parkville pp205–214

C.J. Seaborn, 1983, The rise and fall of Mt Keast – Locating feed for current retreatment operations from a study of processing history at the Zinc Corporation Limited in Broken Hill Conference 1983, The Australasian Institute of Mining and Metallurgy Parkville pp359–364

J. Siliézar, D. Stoll and J. Twomey, 2011, Unlocking the value in waste and reducing tailings: Magnetite Production at Ernest Henry Mining in Iron Ore 2011, The Australasian Institute of Mining and Metallurgy, Carlton pp529–535.

# Fosterville Gold Mine – adapting to new challenges

*A Nash[1], R Symes[2], D Buchanan[3], J Van Niekerk[4] and C Van Buuren[5]*

1. Senior Metallurgist, Fosterville Gold Mine, Fosterville Vic 3557. Email: anash@kl.gold:
2. Development Metallurgist, Fosterville Gold Mine, Fosterville Vic 3557. Email: rsymes@kl.gold:
3. Technical Process Superintendent, Fosterville Gold Mine, Fosterville Vic 3557. Email: dbuchanan@kl.gold
4. Director Gold, Metso Outotec, Centurion South Africa 157. Email: jan.vanniekerk@mogroup.com:
5. Process Engineer, Metso Outotec, Centurion South Africa 157. Email: craig.vanbuuren@mogroup.com:

## ABSTRACT

The Fosterville operations of Kirkland Lake Gold are a high-grade, low-cost gold mine located 20 km east of the city of Bendigo in the state of Victoria, Australia. A feasibility study into a sulphide mining operation was completed in 2003 and the operation, commissioned in 2005, comprised of a crushing and grinding circuit followed by Flotation, Bacterial Oxidation (BIOX®) and CIL areas. In the past 15 years, the BIOX® process has demonstrated to be a reliable and effective pre-oxidative technology yielding in excess of 97 per cent sulphide oxidation (for a design of 95 per cent).

Sulphide gold mineralisation at Fosterville occurs in a solid solution within disseminated arsenopyrite and pyrite, and the challenging orebody contains varying amounts of native carbon (non-carbonate carbon (NCC)) in the form of black shale. This native carbon typically reports to the concentrate and can adversely impact leach performances through preg-robbing as the native carbon competes aggressively with the activated carbon in adsorbing solubilised gold-cyanide complexes. In 2008 Fosterville Gold Mine pioneered the development of a high temperature preg-robbing mitigation process called HiTECC™, with the first commercial installation commissioned on-site in 2009. This highly successful technology has been demonstrated to increase overall plant recoveries by up to 12 per cent.

With the discovery of the fabulously high-grade Swan orebody the increase in the presence of gravity recoverable gold (GRG) at depth, saw the complexities of the processing circuits grow with the installation of Knelson concentrators and shaking tables. This additional equipment assists in recovering up to 85 per cent of the GRG before it reports to the BIOX® circuit.

As a non-discharge site, Fosterville Gold Mine have maintained their commitment to strengthening the sustainability of the sites water balance through the application of innovative technologies among them, the Metso Outotec ASTER™ process. This technology can treat leach tailing solutions with concentrations of up to 5000 ppm of thiocyanate to concentrations as low as 0.1 mg/L. Globally, the facility at Fosterville is the fourth commercial application of the ASTER™ technology.

This paper further describes these innovative solutions which, in the third quarter of 2020, have assisted in establishing Fosterville Gold Mine as one of the largest and lowest cost gold-only producers in Australia.

## INTRODUCTION

Kirkland Lake Gold is a senior gold producer operating in Canada and Australia that produced 1 369 652 ounces in 2020, with target production for 2021 of 1 300 000 to 1 400 000 ounces. The production profile of the company is anchored by three high-grade, low-cost operations, the Macassa Mine and the Detour Lake Mine, both located in north-eastern Ontario, and the Fosterville Mine located in the state of Victoria, Australia. Kirkland Lake Gold's solid base of quality assets is complemented by district scale exploration potential, supported by a strong financial position with extensive management and operational expertise.

Kirkland Lake Gold acquired the Fosterville Gold Mine through the business combination with Newmarket Gold, which was completed on 30 November 2016. The Fosterville Gold Mine is located near the town of Bendigo in the state of Victoria, Australia. The Fosterville BIOX plant was commissioned in 2005 and has been in operation since. The Fosterville primary ore is highly refractory generally exhibiting less than 10 per cent cyanide leach extraction. The bio-oxidation of refractory sulphide ore concentrates results in the liberation of the occluded gold for recovery via cyanidation, and in the case of Fosterville, this pre-oxidative treatment route in combination with the other recovery processes results in overall gold recoveries up to 99 per cent.

The recovery of occluded gold from refractory sulphide orebodies is sometimes compounded by the presence of naturally occurring organic carbon in the ore. In extreme cases this naturally occurring carbon is preg-robbing. Refractory preg-robbing ores are generally referred to as double refractory. The native carbon reports to the carbon-in-leach (CIL) circuit and results in reduced gold recoveries. The hot caustic leaching process was developed, trialled, and implemented at Fosterville where significant amounts of naturally occurring organic carbon reporting to the flotation concentrate was impacting CIL recoveries, with recoveries as low as 35 per cent in CIL. Commissioning of the hot caustic leach circuit in 2009 resulted in an approximately 4–14 per cent recovery gains through the heated leach circuit.

The bio-oxidation of refractory sulphide ore concentrates results in the liberation of the occluded gold for recovery via cyanidation. It is predominantly the reaction between residual cyanide and reactive sulphur species which results in the formation of thiocyanate (SCN). The micro-organisms used in BIOX have a low tolerance to thiocyanate and cyanide species which renders the upstream recycling of this solution impractical. In addition, environmental legislation associated with the land disposal of cyanidation tailings and water discharge is becoming increasingly stringent, enforcing the need to treat or recycle cyanide contaminated water streams from mining operations. As a non-discharge site, Fosterville Gold Mine, in quarter one of 2021 has commissioned the ASTER process which has resulted in the degradation of SCN levels as high as 2500 ppm in leach tailings solutions to below 0.1 ppm. ASTER, an acronym Activated Sludge Tailings Effluent Remediation, is a biological process which has been successfully implemented on three metallurgical facilities. Globally, the facility at Fosterville is the fourth commercial application of the ASTER technology.

## BIOX AT FOSTERVILLE

The Fosterville Mine is a high-grade, low-cost underground gold mine, located 20 km from the town of Bendigo, Australia. It was the third largest Australian gold producer for the 2019–2020 financial year. The Fosterville Mine features extensive district scale exploration potential and low-cost production. The mine is located in an area with well-developed infrastructure and is accessible by paved roads. Fosterville's ore is processed at the mine's ~830 000 tonnes per annum mill. The Fosterville primary ore is highly refractory with less than 10 per cent gold dissolution achievable on the flotation concentrate without any pre-oxidation. The refractory nature of this orebody warranted an oxidative pre-treatment step to destroy the sulphide mineral lattices which has as its main constituents, pyrite, arsenopyrite and minor stibnite. As part of the project development and due diligence, various oxidative technologies were investigated (Whincup *et al*, 2004) *viz*:

- BIOX (bacterial oxidation) of the concentrate (Metso Outotec).
- BacTech (bacterial oxidation) of the flotation concentrate.
- Pressure oxidation of the flotation concentrate.
- Roasting.
- High Temperature Redox.
- Activox®.

Following the outcome of the test work results and selection criteria which ranked certain parameters such as safety, technical risk, operability, maintainability, economic risk etc, BIOX was selected as the preferred oxidative pre-treatment technology. The processing plant design basis in early 2003 therefore considered crushing and grinding followed by flotation, BIOX and finally the CIL circuit. The Fosterville design basis was perhaps unique as it was constructed by evaluating the BIOX response across a number of concentrates selected to describe the orebody variability and spanned varying grades of sulphide sulphur, arsenic and antimony. Moreover, the design basis was formulated only from the series of discrete batch test results and was not abstracted from a continuous pilot testing campaign on a single bulk concentrate. Table 1 shows some detail of the concentrates tested during the BIOX evaluation.

**TABLE 1**

Fosterville concentrates tested for variability in BIOX.

| Sample | Fe(T) % | S(T) % | $S^{2-}$ % | As % | Sb ppm | $CO_3^2$ %$^-$ |
|---|---|---|---|---|---|---|
| A | 22.1 | 20.2 | 19.2 | 8.7 | 160 | 0.5 |
| B | 21.5 | 19.1 | 18.3 | 8.1 | 89 | 0.9 |
| C | 21.3 | 20.9 | 18.8 | 7.0 | 270 | 0.9 |
| D | 19.7 | 18.6 | 18.2 | 6.0 | 6900 | 1.3 |
| E | 18.1 | 17.8 | 14.9 | 6.7 | 51 000 | 1.7 |
| F | 17.5 | 15.6 | 14.5 | 5.4 | 180 | 1.3 |
| G | 15.9 | 20.4 | 17.6 | 5.5 | 118 000 | 0.9 |
| H | 21.4 | 19.7 | 18.3 | 8.5 | 3900 | 1.7 |
| I | 16.1 | 14.1 | 13.2 | 7.0 | 22 000 | 2.1 |

While some variation in sulphur and arsenic is noted, the swings in antimony are more pronounced across the variability samples. Antimony is known to be inhibitory to bio-oxidation cultures but in the BIOX batch testing campaigns, no microbial inhibition was noted. Variability testing is quite important as it is conducted precisely to tease out the mineral and gangue nuances which may express themselves differently across an orebody. The batch BIOX concentrate testing was successful in attaining high sulphide oxidation and gold dissolution extents and the Fosterville basic design criteria for the circuit and flow sheet development is shown in Table 2.

**TABLE 2**

Basic BIOX Fosterville design criteria.

| Parameter | Units | Value |
|---|---|---|
| Nominal Feed Rate | t/h | 9 |
| BIOX Residence Time (Primary Reactors) | d | 2.5 |
| BIOX Residence Time (Secondary Reactors) | d | 2.5 |
| Total BIOX Residence Time | d | 5 |
| Reactor Configuration (Primaries in Parallel) | | 3 |
| Reactor Configuration (Secondaries in Series) | | 3 |
| BIOX Solids Concentration | % | 20 |
| Operating Temperature | °C | 42 |
| Sulphide Sulphur | | 20.5 |
| Arsenic | | 6.3 |
| Antimony | | 1.0 |
| Pyrite | % | 33.3 |
| Arsenopyrite | % | 13.7 |
| Stibnite | % | 1.4 |
| Target Sulphide Oxidation | % | 95 |

Based on the design criteria, it was therefore possible to develop the BIOX circuit design envelope and this is shown in Figure 1.

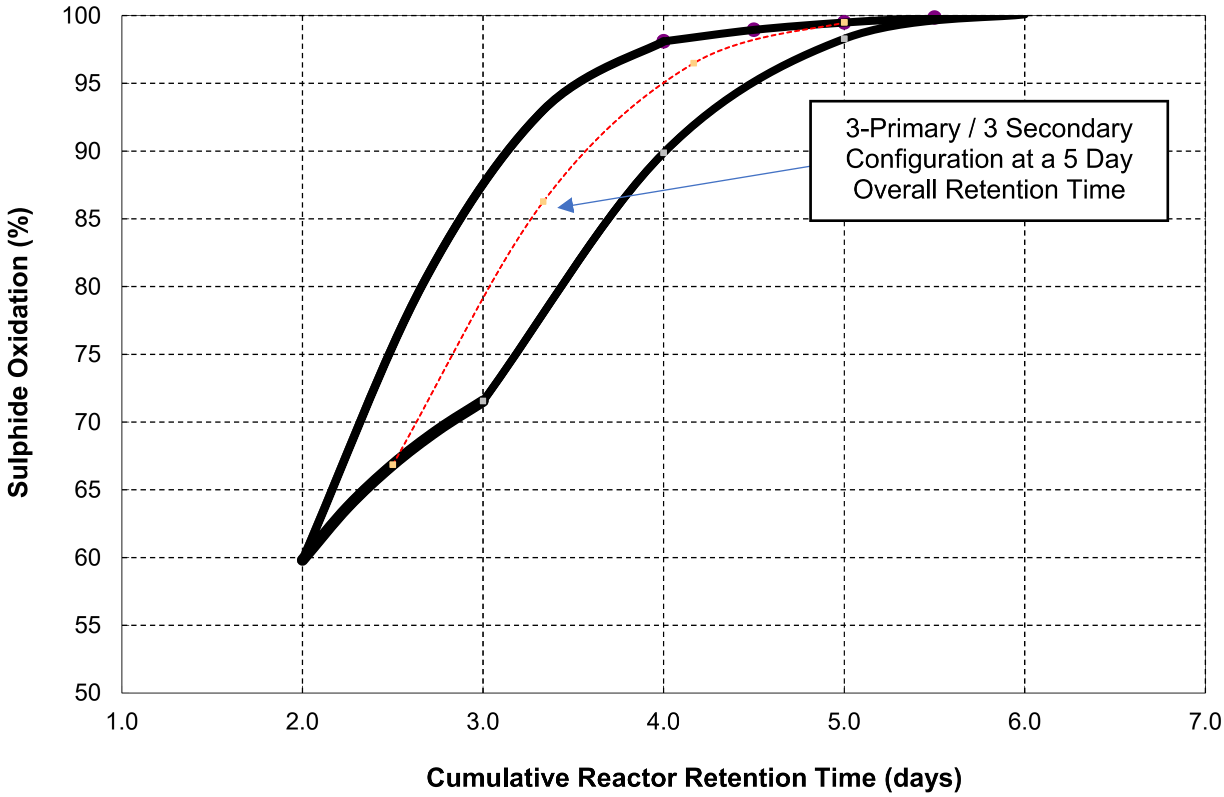


**FIG 1** – Fosterville BIOX circuit oxidation envelope showing installed design.

The Fosterville gangue–sulphide mineral composition results in nett acid production in BIOX and limestone is added to control the reactors in the selected pH range. Peripheral work on the oxidised BIOX slurry settling characteristics and neutralisation was also undertaken to inform the design of these corresponding circuits.

## Fosterville (Kirkland Lake) BIOX Plant

Construction of the Fosterville BIOX plant commenced in March 2004 and was completed the following year with the first gold bar produced in May 2005. The Fosterville BIOX plant consists of a feed surge tank, six BIOX reactors with live operating volumes of 900 $m^3$ followed by three 9 metre diameter counter current decantation thickeners which produce washed BIOX product solids for pH stabilisation prior to leaching with cyanide, and a diluted BIOX acidic ferric-arsenate liquor which is neutralised in six neutralisation reactors.

Owing to the background residual chloride values determined to be in excess of 250 mg/L in the recirculating process water, SAF 2205 was selected as the principal material of construction to withstand the BIOX temperature (42°C) and slurry acidity (pH 1.2). SAF 2205 is a duplex stainless and provides much higher tolerance to chloride corrosion than the typically utilised 316 L austenitic stainless steel.

Views of the Fosterville BIOX plant is provided in Figure 2.

**FIG 2** – Views of the Fosterville BIOX installation.

The BIOX plant has been operating since April 2005 and has proven to be reliable, achieving recoveries through the BIOX circuit consistently over 99 per cent.

The health of the BIOX circuit is monitored via four key metrics:

1. Dissolved oxygen levels.
2. Ferrous levels.
3. Temperature.
4. pH.

If any of these start to drift out of operational limits, then action is taken. Contaminants that can impact this circuit include step changes in minerals in the ore (for example stibnite), flow rate changes and external contaminates like hydrocarbons or chemicals.

## MITIGATING AN AGGRESSIVE PREG-ROBBING ORE WITH HITECC

Gold extraction from double refractory ores using conventional cyanidation can be challenging with considerable losses occurring owing to the presence of active carbon components in the ore. These carbon particles may re-adsorb the solubilised gold causing the gold to be lost to the tailings and this lost gold is commonly referred to as preg-robbed gold.

The Fosterville orebodies contain various amounts of native carbon in the form of bituminous coal (Binks *et al*, 2011) and this carbon (referred to as Non-Carbonate Carbon or NCC) occurs through hydrothermal alteration and as a significant sedimentary structure along the Fosterville fault line. These carbonaceous minerals in the ore have resulted in significant gold losses during conventional CIL recovery as a result of its aggressive preg-robbing characteristics. Figure 3 shows a trend derived from the plotting of the CIL residue gold grade and the NCC levels obtained from composite samples drawn over a period of two years. This general trend shows a reasonable correlation exists between the level of native carbon and the exiting CIL residue gold grade.

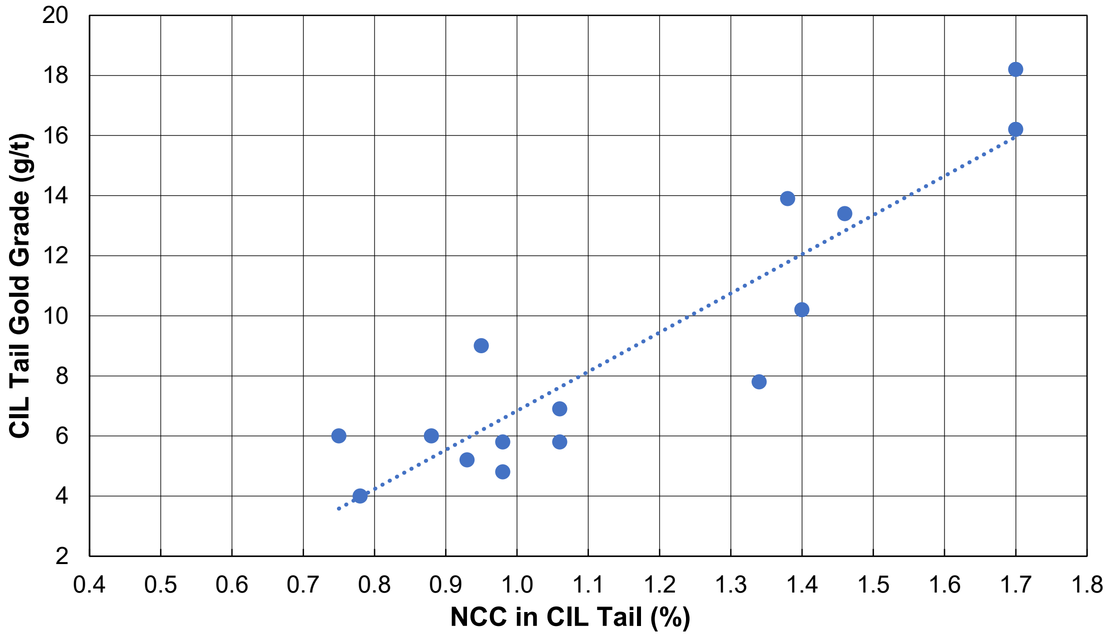


**FIG 3** – Relationship between the CIL tails grade and the NCC.

The determination of a material's ability to compete for solubilised gold is generally undertaken as a series of gold in solution adsorption tests. These techniques are commonly referred to as Preg-Robbing Index (PRI) tests and although the protocols do vary slightly in its application, they are useful in providing a sense of the aggressiveness of an ore to compete with activated carbon to adsorb solubilised gold. Figure 4 shows some responses and PRI determinations for previous subsamples of the Fosterville concentrate and BIOX product (or CIL leach feed).

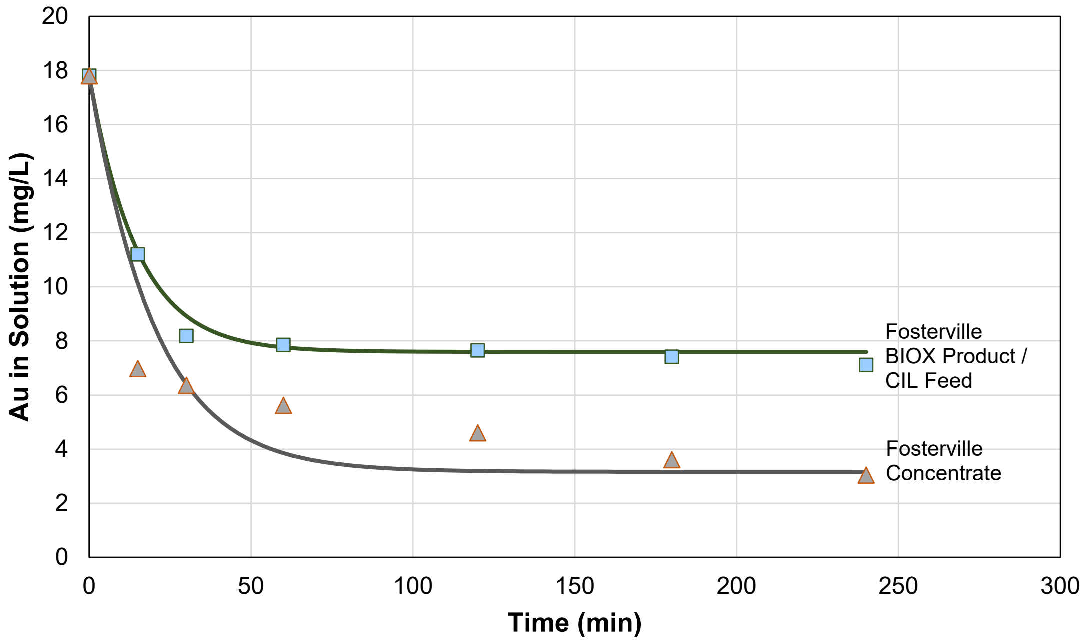


**FIG 4** – Adsorption or Preg-Robbing Index responses of Fosterville concentrate and BIOX product.

Interestingly, as shown in Figure 4 bio-oxidation does show a tendency to blind the carbon material, rendering it less of a preg-robber. While preg-robbing in gold processing may be controlled by inactivation of the carbonaceous material either through oxidation (high temperature) or saturation with strongly adsorbing organic compounds and competitive adsorption on activated carbon particles in a Carbon in Pulp (CIP) or CIL processes, in some cases the gold losses remain high. Attempts to remove the carbon are typically not effective as well as carbon is hydrophobic and high proportions report to the concentrate and subsequent cyanide leach. To mitigate the gold losses occurring at Fosterville, the team undertook various testing initiatives such as, but not restricted to:

- using high carbon concentrations
- ore blanking with kerosene
- thiosulphate leaching
- chlorination
- pressure oxidation
- thiourea leaching.

These tests yielded limited success and an avenue of batch testing relating to the application of heat and caustic to provide a mild elution environment was pursued and this testing yielded appreciable benefits. To further the development and extrapolate the learnings of the HiTeCC batch tests to an understanding of the process behaviour on a continuous scale for flow sheet development, a pilot plant consisting of two trains containing six vessels per train was constructed. Each train consisted of different reactor volumes to allow comparisons in residence time as well as different test conditions (temperature, carbon concentrations, reagent additions) to be studied simultaneously. Heating of the pulp was achieved by circulating hot water through heating jackets around the reactors and the reactors were fitted with baskets to retain carbon and allow for easy carbon transfer. The pilot plant is shown in Figure 5.


**FIG 5** – View of the Fosterville continuous rig for HiTeCC flow sheet development.

The development and trialling of the HiTeCC process at Fosterville to recover additional gold from the CIL tailings, as well as further batch test work and predictive modelling undertaken by Metso Outotec showed that indeed, the addition of sodium hydroxide facilitates the desorption of gold by exchanging calcium ions in the aurodicyanide complex pair with less strongly adsorbed sodium ions, and that increasing the temperature of the pulp would favour both the tendency and rate of gold desorption. Most of the gold released can then be recovered onto reactive granular activated carbon by favouring adsorption by providing adequate adsorption sites and by lowering the temperature again. By far, the most important parameter in recovering the preg-robbed gold was determined to be the temperature and this is depicted in Figure 6.

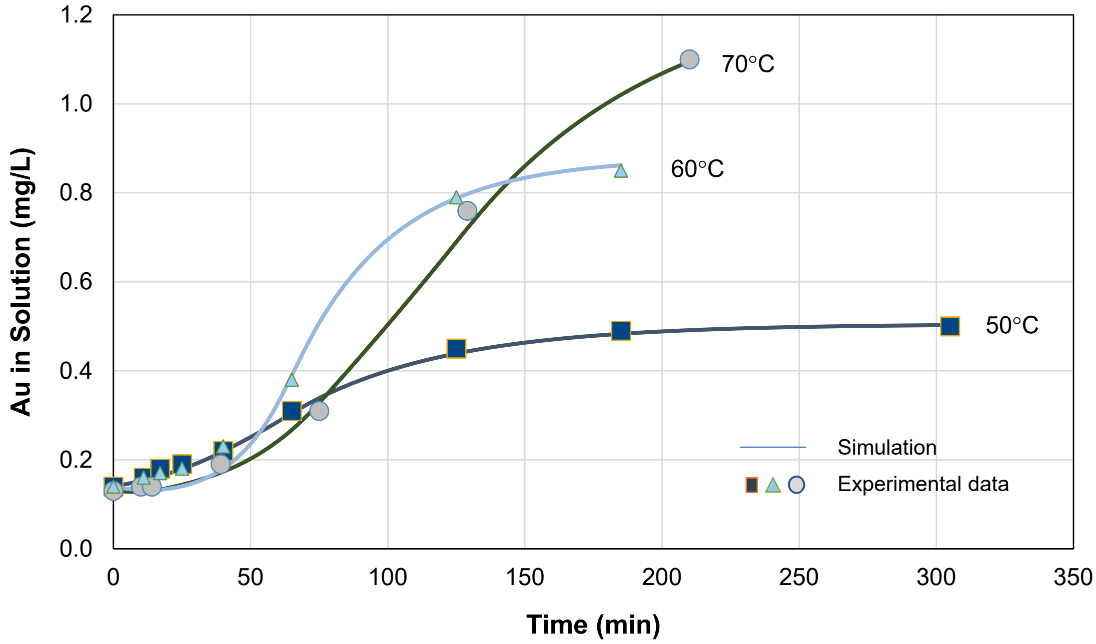


**FIG 6** – Influence of temperature on the batch scale desorption of gold from a Fosterville CIL residue subsample (Pieterse *et al*, 2020).

It is clear from Figure 6 that applying a temperature of 70°C in the batch desorption stage produced the highest extent of gold release. This was followed by 60°C while applying a desorption temperature of 50°C yielded the lowest gold release.

## Fosterville (Kirkland Lake) HiTeCC Plant

The pilot plant trialling showed that the HiTeCC treatment of the CIL plant residue was the best method for increasing the overall gold recovery from the ore with recovery increases over 10 per cent achieved. The pilot plant trialling was also extended to evaluate the ability of the process to recover gold from the historic leach tails and showed that gold in the old tailings residue could be recovered. It was therefore decided to design the HiTeCC treatment plant with additional capacity to allow reclaimed old tails to be processed concurrently with fresh CIL residue slurry.

Construction of the Fosterville HiTeCC plant commenced in January 2009 with plant commissioning underway in April 2009. The plant is configured as a cascade of six reactors with the counter-current flow of CIL tailings slurry and freshly added activated carbon. The tailings slurry is conditioned using sodium hydroxide and heated to temperatures between 70 and 80°C in the desorption stages (first three reactors). The slurry is then cooled to lower temperatures for the next three stages to promote the adsorption of desorbed gold onto the activated carbon.

Heating of the CIL tails slurry is achieved through inline injection of steam and the desorption reactors (first three reactors) are rubber lined and insulated to minimise heat loss. The first four reactors are fitted with lids to retain heat and reduce steam entering the operator working zone on the top of the reactors. The loaded carbon from the HiTeCC circuit is recovered to a carbon column, regenerated, and then returned to the CIL circuit. Figure 7 depicts the carbon movement at nominal rates and grades.

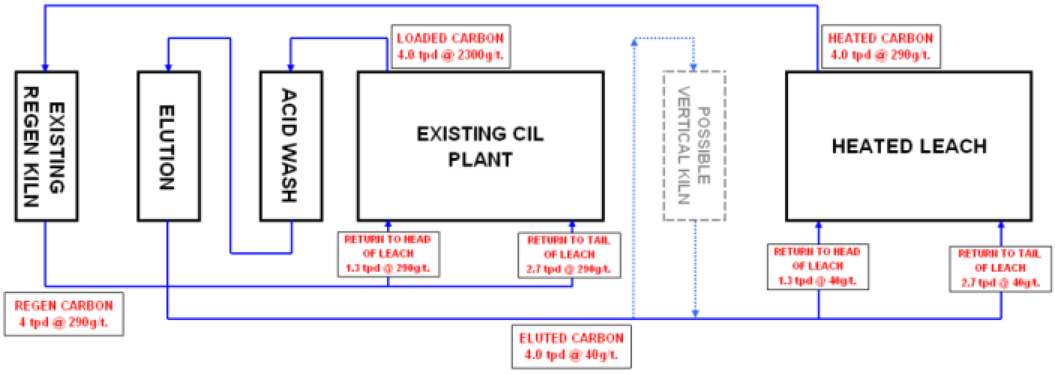


**FIG 7** – Carbon movement schematic for the Fosterville CIL and HiTeCC circuits.

Views of the Fosterville HiTeCC installation is provided in Figure 8.

**FIG 8** – Views of the Fosterville HiTeCC installation.

The HiTeCC plant has been operating for almost 12 years and has proven to be an effective technology for the recovery of preg-robbed gold.

## SUPPORTING AN INTEGRATED WATER BALANCE WITH THE ASTER PROCESS

During the cyanide leaching of bio-oxidation product solids, cyanide reacts with reduced sulphur species to form thiocyanate (SCN), with concentrations of up to 5000 mg/l recorded in cyanidation tailings effluent. Owing to its toxicity, the presence of residual cyanide, metal cyanide complexes and thiocyanate in the effluent streams has necessitated the development of specific treatment technologies for the remediation of these effluents. Some of the familiar and established chemical cyanide and thiocyanate destruction processes are summarised in Table 3.

**TABLE 3**

Summary of published cyanide destruction processes.

| Process | Description |
|---|---|
| Inco sulphur dioxide | High reagent consumption ($SO_2$, lime and Cu). pH Control required. Moderate SCN degradation efficiency. |
| Hydrogen peroxide | Relatively high reagent costs. Low SCN removal. |
| Caro's acid | Reactive and decomposes quickly and requires production on-site. SCN removal possible. |
| Alkaline chlorination | Very effective for CN removal. Oxidation of SCN is possible when excess chlorine present. |
| Ozonation | Ozone use is becoming more frequent as ozone generators become simpler. Ozone is a stronger oxidant than oxygen and removes CN effectively. The removal of SCN is also possible. |

Another class of treatment option are biological processes. These rely on the metabolic capability of certain micro-organisms which have enzymatic pathways capable of catalysing the metabolism of cyanide and thiocyanate. The primary reaction products are ammonia, sulphate and carbon dioxide/bicarbonate. Ammonia may be assimilated as the nitrogen source for the organism. Biological systems are advantageous from the perspective that the micro-organisms are able to adapt, within limits, to changes inflow rates and substrate concentrations in the short-term, providing robustness to the process. Metso Outotec's ASTER process was developed specifically to treat tailings effluent produced during the biological processing of refractory gold ores using the BIOX process where thiocyanate is the primary contaminant. The process configuration is modular, with a number of primary oxidation reactors in parallel, feeding a set of secondary reactors in series. Depending on the project specifics, the overflow from the final secondary can pass to a settler/clarifier which yields clarified effluent and settled sludge, a portion of which may then be recycled to the primaries to maintain high biomass concentrations. The reaction pathways as well as the overall reaction that is believed to occur are summarised as:

$$SCN + H_2O + \rightarrow HCNO + HS \tag{1}$$

$$HCNO + 2H_2O \rightarrow NH_4 + HCO_3^- \tag{2}$$

$$HS + 2O_2 \rightarrow SO_4^2 + H+ \tag{3}$$

$$SCN + 3H_2O + 2O_2 \rightarrow HCO_3 + NH_4 + SO_4^2 + H+ \tag{4}$$

As of today, three commercial ASTER plants have been installed across the globe and some process design information is shown in Table 4. A fourth ASTER installation, the Fosterville plant in Australia is currently being commissioned while a fifth ASTER plant is in the final design stage, *viz*: the CAM and Motor ASTER installation in Zimbabwe. Views of the Suzdal and Runruno ASTER installations follow in Figure 9.

**TABLE 4**
ASTER technology commercialisation.

| Mine | Year commissioned | Capacity ($m^3/d$) | Reactor size ($m^3$) | SCN level (mg/L) | Status |
|---|---|---|---|---|---|
| Consort, South Africa | 2010 | 320 | 20 | 150 | Operating |
| Suzdal, Kazakhstan | 2013 | 528 | 200 | 1200 | Operating |
| Runruno, Philippines | 2016 | 5000 | 600 | 350 | Operating |
| Fosterville, Australia | 2021 | 792 | 200 | 5000 | Commissioning |
| Cam & Motor, Zimbabwe | 2021 | 7800 | 400 | 300 | Design |

**FIG 9** – Views of the Suzdal (Kazakhstan) and Runruno (Philippines) ASTER plants.

## Fosterville (Kirkland Lake) ASTER Plant

The Fosterville ASTER plant currently under commissioning will be the fourth commercialised landing of the technology. This plant has been designed to treat a 792 $m^3/d$, 5000 mg/L SCN feed (Van Niekerk *et al*, 2020) and has the additional features noted as follows:

- It will be the first ASTER installation in Australia.
- The plant will treat the highest feed SCN level to date, ie 5000 mg/L.
- The processing will be solution based and thus the reactors have no installed agitators with solution homogenisation brought about by aeration only.

The Fosterville metallurgical team identified the ASTER process as a potential solution to treat tailings dam return water to reduce the thiocyanate concentrations to levels where the water can be circulated to the process plant and used upstream of the BIOX process. The team at Fosterville set-up a pilot plant facility and commenced an ASTER test work program in cooperation with the Metso Outotec BIOX team. The test work campaign focused on adapting locally sourced microbes to the Fosterville tailings solution, followed by optimising the performance of the culture through further adaptation to progressively higher duties and optimising the process parameters.

The test work was successful and confirmed the suitability of the ASTER process for the required application. The test work also generated the required destruction rates and other process design criteria required for the Metso Outotec BIOX team to develop an ASTER process design for the Fosterville ASTER plant. The process design was reviewed and optimised a number of times between the Fosterville and BIOX teams to select the optimum reactor configuration. Figure 10 shows the design basis for the Fosterville ASTER plant as well as that for the operating ASTER plants in Kazakhstan and the Philippines.

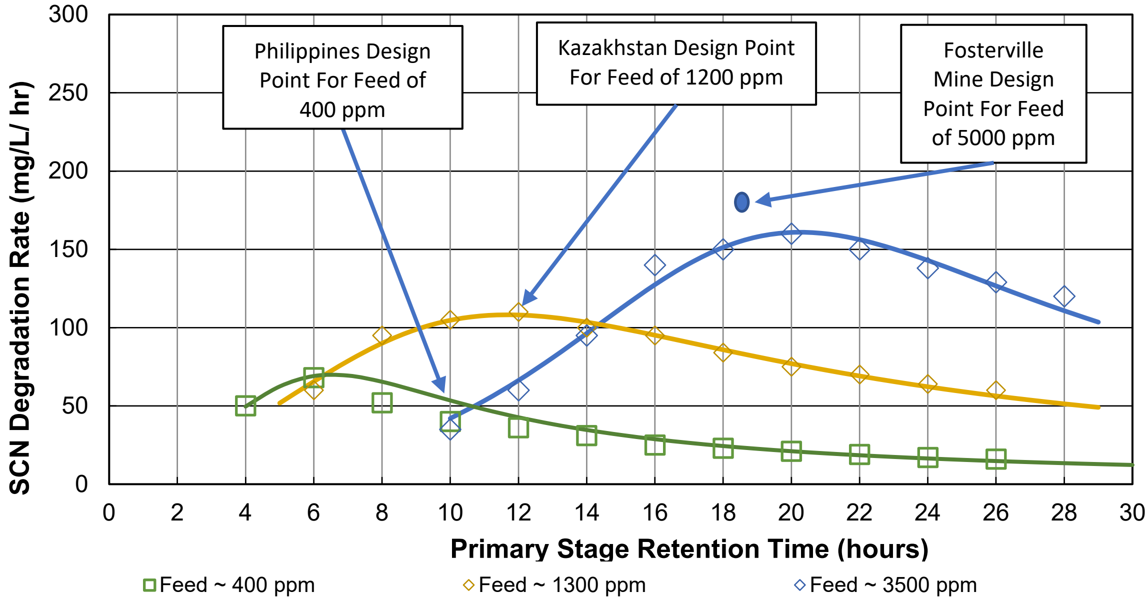


**FIG 10** – Comparison of ASTER SCN degradation rates.

The Fosterville plant will consist of six tanks with an operating volume of 180 $m^3$ each followed by a static settler. The static settler will enable recycling of thickened biomass to the ASTER primary tanks, thereby increasing the biomass concentration in the primary ASTER reactors and increasing the thiocyanate degradation rate. The feed to the ASTER reactors is heated to maintain the optimum temperature for the ASTER culture. The design specification of the Fosterville ASTER plant is summarised in Table 5.

**TABLE 5**

Summary of the Fosterville ASTER design specification.

| Parameter | Unit | Design |
|---|---|---|
| Plant design | $m^3/d$ | 792 |
| Primary reactor volume | $m^3$ | 200 |
| No of primaries | | 4 |
| Secondary reactor volume | $m^3$ | 200 |
| No of secondaries | | 1 |
| Tertiary reactor volume | $m^3$ | 200 |
| No of tertiaries | | 1 |
| Feed SCN- | mg/L | 5000 |
| Feed CN- | mg/L | <5 |
| Retention | hours | 27 |
| Effluent SCN- | mg/L | ≤0.1 |
| Effluent CN- | mg/L | ≤0.1 |
| Dissolved $O_2$ | mg/L | ≥4 |
| Temperature | °C | 25–27 |
| Nutrients: Molasses | $kg/m^3$ | 0.15 |
| Nutrients: Phosphorous | $kg/m^3$ | 0.15 |
| Sludge recycle | % $v/V_{Feed}$ | Variable |

Figure 11 shows a 3D rendering as well as a view of the installed Fosterville ASTER plant.

**FIG 11** – Views of the Fosterville ASTER plant, Australia.

Construction of the plant commenced in 2019 at the Fosterville site. Commissioning of the Fosterville ASTER circuit is currently underway.

## CONCLUSIONS

The Kirkland Lake Gold Fosterville operation treats a double refractory gold ore where the sulphide gold mineralisation occurs in solid solution within disseminated arsenopyrite and pyrite. The orebody contains varying amounts of native carbon (non-carbonate carbon (NCC)) in the form of black shale.

The Fosterville BIOX plant was commissioned in 2005. The primary ore is refractory generally exhibiting less than 10 per cent cyanide leach extraction. The bio-oxidation of refractory sulphide ore concentrates results in the liberation of the occluded gold for recovery via cyanidation, and in the case of Fosterville, this pre-oxidative treatment route in combination with the other recovery processes results in overall gold recoveries up to 99 per cent.

The hot caustic leaching process was developed, trialled, and implemented at Fosterville where significant amounts of naturally occurring organic carbon reporting to the flotation concentrate was impacting CIL recoveries, with recoveries as low as 35 per cent in CIL. Commissioning of the hot caustic leach circuit in 2009 resulted in an approximately 4–14 per cent recovery gains through the heated leach circuit.

Fosterville Gold Mine, in quarter one of 2021 commissioned the ASTER process which has resulted in the degradation of SCN levels as high as 2500 ppm in leach tailings solutions to below 0.1 ppm.

These innovative solutions have assisted in establishing Fosterville Gold Mine in quarter three as one of the largest and lowest cost gold-only producers in Australia in quarter three of 2020.


## ACKNOWLEDGEMENTS

The authors would like to thank Kirkland Lake Gold Fosterville Mine and Metso Outotec South Africa for allowing publication of the paper.


## REFERENCES


Binks, M, Wemyss, P, 2011. Fosterville Gold Mine Heated Leach Process. Metplant 2011.

Pieterse, P J, Sandenbergh, R F, Van Buuren C B, 2020. Characterization and optimization of the high temperature caustic conditioning (HiTeCC) activated carbon process for optimised gold recovery from double refractory ores. IMPC 2020.

Van Niekerk, J, Van Buuren, C B, 2020. Recent developments in the Metso Outotec BIOX® Process. ALTA 2020

Whincup, P, Binks, M, 2004. A case study of the development, engineering and construction of a biological oxidation plant for a refractory pyrite-arsenopyrite gold ore. Bac-Min 2004.

https://www.australianmining.com.au/news/australia-remains-worlds-second-largest-gold-producer.

# Newmont Boddington concentrate grade improvement project

*P Petrucci[1], S Hart[2], C Williams[3] and J Stewart[4]*

1. MAusIMM, Senior Metallurgist, Newmont Boddington, Boddington WA 6390.
   Email: paul.petrucci@newmont.com
2. FAusIMM, Director, Processing, Newmont Australia, Subiaco WA 6008.
3. Process Coordinator, Tianqi Lithium Australia Pty Ltd, Kwinana Beach WA 6167.
4. FAusIMM, Metallurgical Superintendent, Newmont Boddington, Boddington WA 6390.

## ABSTRACT

Newmont Boddington's ore may be described as a gold ore with a copper problem. The majority of revenue is derived from sale of gold contained in either a gold bearing copper concentrate or doré bars. The copper head grade is below what would typically be considered economic for a copper sulphide flotation circuit. Despite the low copper head grade, the sulphide flotation circuit contributes to increasing overall gold recovery (as some gold is encapsulated in sulphide minerals) and lowers the cyanide destruction costs following leaching by removing up to 80 per cent of the copper beforehand.

Producing a marketable gold bearing copper concentrate from copper head grades as low as 0.06 per cent Cu has necessitated a cleaner circuit, which includes concentrate regrinding and up to three stages of conventional cleaner flotation.

The levels of non-sulphide gangue in the copper concentrate needs to avoid exceedance of a concentration level at which penalties would apply to concentrate sales. The concentrate grade improvement project investigated a number of alternative methodologies to reduce the non-sulphide gangue entrainment. The project outcome was the installation of a cavitation tube flotation column with froth washing. The cavitation tube flotation column was installed in a cleaner scalper flotation duty with a number of alternative circuit configurations either retained or modified to maintain the flexibility of the circuit to treat a wide range of copper head grades. Reducing the non-sulphide gangue entrainment also reduced transportation and treatment costs through the lower mass of concentrate produced. This paper will outline the concentrate grade improvement project from identification through to benefits. The paper will also outline some unique design features that further improve the operability and maintainability of cavitation tube flotation columns with froth washing.

## INTRODUCTION

Newmont Boddington Gold Mine (NBG) is situated 12 km north-west of the town of Boddington and 130 km south-east of Perth in Western Australia. Gold was discovered at Boddington in 1980. Production from the oxide ores began in August 1987 at a throughput rate of 3.0 Mtpa. Oxide ore treatment continued with circuit expansions and the addition of a facility to treat supergene and high-grade basement ores until 2001, at which time the operation was placed under care and maintenance. The current mining operations at NBG commenced in 2008 and commissioning of the processing plant started in the latter half of 2009. The process flow sheet comprises primary crushing, closed circuit secondary and tertiary crushing (with high-pressure grinding rolls (HPGR) in the tertiary stage), ball milling and hydrocyclone classification to generate a milled product with a $P_{80}$ of 150 µm (Hart, 2011). The ground ore is then floated to produce a gold rich copper concentrate for filtration and sale to overseas smelters. Flotation tailings are then leached for further gold recovery. The processing plant achieved nameplate design of 35 Mtpa in 2014 and continued to increase throughput following a number of de-bottlenecking projects, achieving 39.8 Mtpa processed in 2019.

The low copper head grade of 0.06 per cent to 0.12 per cent Cu (mostly as chalcopyrite), significant iron sulphide content and the association of gold with sulphide minerals meant that Boddington would always be challenged to produce a high-grade copper concentrate. Project feasibility studies and pilot plant testing demonstrated that a copper concentrate grade ranging from 12 to 18 per cent Cu would be expected over the life-of-mine. Post commissioning the plant achieved slightly better concentrate grades, consistently averaging 17 per cent Cu over the first five years of operation. However, despite better than predicted concentrate grades, the level of non-sulphide gangue minerals in the copper concentrate contributed to penalty element deductions under some sales contracts (particularly alumina) that reduced returns from concentrate sales. Furthermore, the copper concentrate grades were expected to decline towards the low end of the feasibility study range as the mine developed further and copper head grades reduced in some areas of the pit. The concentrate was expected to become more difficult to sell and would incur higher selling costs for the operation. In order to increase the grade of concentrate produced, and maximise the return on sales, methods for reducing non-sulphide and sulphide gangue content in the copper concentrate were investigated, giving impetus to the concentrate grade improvement (CGI) project.

## Flotation circuits

The original NBG flotation circuit consisted of three parallel trains of rougher and scavenger cells and a cleaning circuit with regrinding and up to three stages of conventional cleaning. A selective collector (thionocarbamate-based) is used in the rougher circuit. The rougher concentrate reports to the cleaning circuit without regrinding. The scavenger circuit has xanthate added to recover composite particles. The scavenger concentrate is reground before reporting to the cleaning circuit. The cleaning circuit is operated at a higher pH than the rougher/scavenger trains in order to depress sulphide gangue such as pyrrhotite and pyrite. Prior to the project, all flotation cells were mechanical agitated forced-air tank or u-shape cells. A simplified representation of the former flotation circuit is shown in Figure 1.

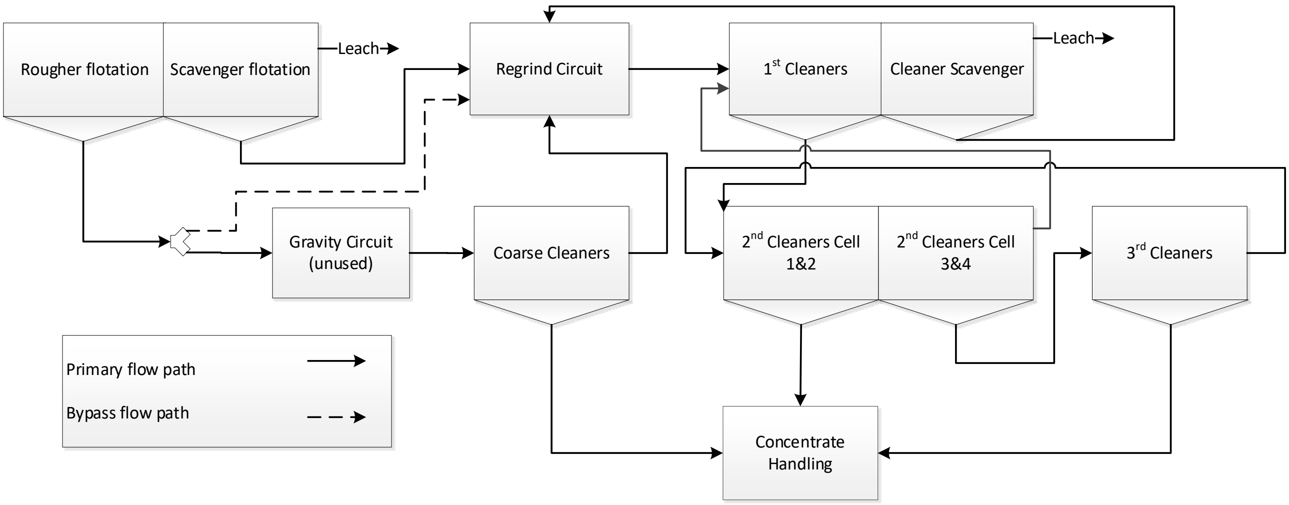


**FIG 1** – Pre-CGI project simplified flotation circuit process flow diagram.

# IDENTIFICATION AND EARLY RESPONSE

From commissioning onwards, monthly composite samples were prepared in order to evaluate key processing streams in detail and assist in the identification and development of improvement opportunities for the operation. Flotation feed, concentrates and tailings streams were analysed to determine the major mineral abundances, size-by-size assay and distribution as well as modal mineralogy. Quantitative mineralogical analysis of the final concentrate confirmed that chalcopyrite followed by non-sulphide gangue (NSG) and pyrrhotite made up 95 per cent of the concentrate mass (Table 1).

**TABLE 1**

Typical concentrate mineral analysis and detailed NSG composition.

| Mineral type | Mass % |
|---|---|
| Chalcopyrite | 50–55 |
| Non-sulphide gangue | 20–25 |
| Pyrrhotite | 15–20 |
| Pyrite + other iron sulphides | 3 |
| Cubanite | 2 |

| Mineral type | Mass % |
|---|---|
| Quartz | 7 |
| Albite (feldspar) | 6 |
| Mica | 6 |
| Clinochlore | 2 |
| Actinolite | 1 |
| Clays and Talc | <1 |

The presence of significant quantities of NSG in the concentrate stream was attributed to one or a combination of the following causes:

- True flotation: NSG particles are hydrophobic and selectively report to the concentrate stream.
- Composites: particles contain both hydrophobic sulphide mineral, (which is recovered to concentrate by flotation) and significant amounts of non-sulphide gangue.
- Entrainment: fine particles which are not recovered by true flotation but report to the concentrate non-selectively with the water in the froth product.

Size-by-size analysis of the final concentrate demonstrated that the 'coarser' fractions (+38 microns) were lower grade, probably not well liberated and would benefit from regrinding ahead of flotation (Figure 2). The mass distribution of copper in these fractions was typically less than 25 per cent, hence targeting this component of the concentrate stream (by regrinding) would not on its own result in a significant improvement in concentrate grade. Quantitative modal mineralogy identified the liberation and locking deportment of major sulphide and NSG species in the final concentrate stream. These analyses demonstrated that a significant proportion of NSG present in the final concentrate was well liberated (>90 per cent classification) and although present across all size fractions it was most prevalent in the –C5 ~8 µm fractions (Figure 3). The nature of the NSG minerals (Table 1) was such that the majority would not likely float due to natural hydrophobicity, and hence were more than likely entrained in the concentrate froth.

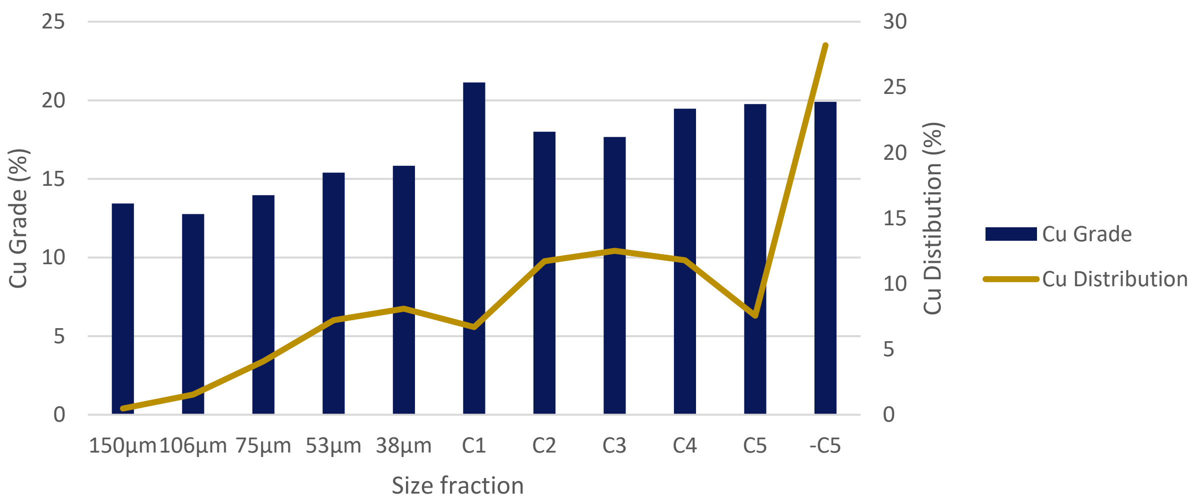


**FIG 2** – Typical final concentrate assay by size fraction for copper – Q4 2011.

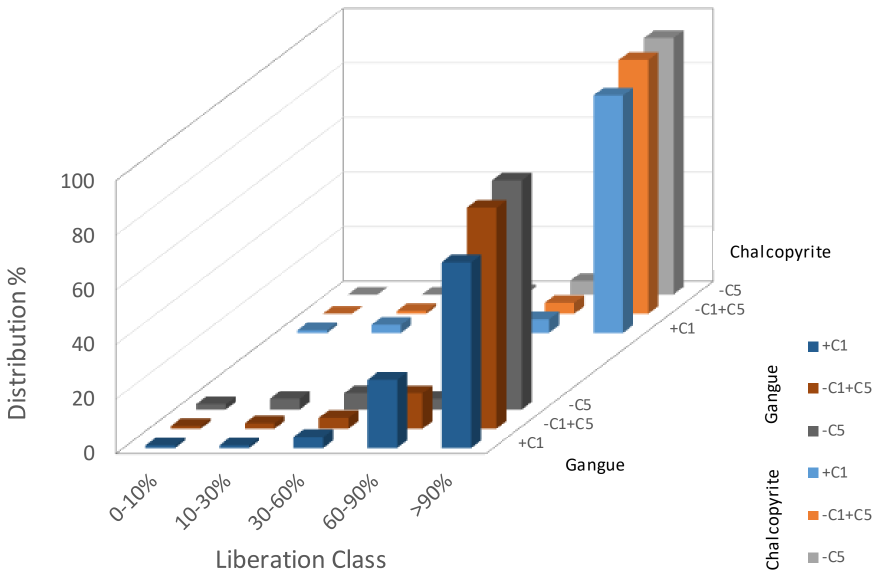


**FIG 3** – Typical final concentrate mineral distribution by size and liberation class – 2011.

It was concluded from these studies that there was a reasonable chance of improving concentrate grade further by rejecting entrained (well-liberated) NSG minerals. Focus therefore shifted to demonstrating various ways to achieve this.

Laboratory dilution and simplified kinetic flotation tests determined the liberated non-sulphide gangue was being entrained and could be washed out of the concentrates. However, greater than design rougher flotation mass pull rates and smaller than required capacity of the cleaner circuit to facilitate low pulp densities in the plant meant that options were limited. Dilution water was added in the cleaner circuit up to system capacity constraints in an attempt to reduce entrainment. Wash water trays were unsuccessfully trialled on the coarse cleaner flotation cells to further reduce entrainment. In addition, reagent trials using a number of silicate depressants were also conducted but while some improvements were seen in the laboratory, no improvement was observed during plant trials.

A large number of simple kinetic float tests were carried out during the early stages of the project to ensure the quantity and quality of data was available to generate a flotation kinetic model (the Aminpro$^{TM}$ Boddington flotation circuit model). This model was ultimately utilised to better understand and predict the benefits of installing alternative cleaning technologies in the circuit to reduce non-sulphide gangue contamination of the copper concentrate product.

## ALTERNATIVE CLEANING TECHNOLOGIES AND KEY FINDINGS

After identifying limitations with the capacity of the current cleaning circuit to reduce entrainment the focus shifted to introducing further cleaning circuit capacity. Both column and Jameson flotation cells were considered during the preliminary evaluation stage.

A pilot flotation column was sourced from Eriez in order to demonstrate the benefit of installing wash water cleaning of the rougher and cleaner flotation concentrates. The initial flotation column pilot test work was undertaken using a 150 mm diameter and 4200 mm tall column fed from a portion of the main process flow stream. This allowed direct comparison with the performance of the existing plant. During the first pilot program, the column was operated by an Eriez representative in several cleaner duties. These included as a cleaner scalper treating rougher concentrate and as a recleaner treating second cleaner feed.

The first round of testing on the coarse cleaner feed stream demonstrated a significant increase in concentrate grade compared to the conventional mechanically agitated cells with a 5 per cent increase in concentrate grade achieved at the same unit recovery. The concentrate grade increased from 16 per cent Cu to 21 per cent Cu, with over 97 per cent stage recovery achieved compared to the conventional cells. The importance of wash water addition was highlighted by turning the wash water off the column, which then reverted to producing a 17 per cent copper concentrate grade, very similar to the conventional cells at that time. The performance of a Jameson cell was tested using a laboratory batch dilution procedure as provided by Xstrata Technology (now Glencore Technology).

These tests again showed a higher-grade concentrate than could be produced in the existing plant however at a marginally lower copper recovery.

Although the pilot test work was successful and detailed engineering was completed on the preferred option a shift in focus of capital funding resulted in the project being deferred for a period, and the pilot plant test work repeated to confirm the previous results. The second program utilised a larger 500 mm diameter and 4500 mm tall column. The results from these programs were used in the flotation modelling undertaken to generate a mass balance to set the process design criteria for the project. The project objective was to reduce concentrate mass recovery by 11 per cent and increase copper recovery by 1 per cent. This would result in a 2 per cent increase in copper concentrate grade over the life-of-mine.

## DESIGN OPTIONS

Many options for reducing non-sulphide gangue entrainment were investigated before moving into detailed design. The lower capital cost options such as retrofitting froth trays to existing cleaner circuits cells, non-sulphide gangue depressants and regrinding the rougher concentrate in the existing regrind mills were ruled out due to either unsuccessful test work and/or plant trials. The successful option determined from pilot test work and flotation modelling was the addition of a cleaner scalper flotation column with froth washing. The location of the column was chosen so it was stand alone to the bulk of the plant to improve constructability in an operational plant.

The selected design option resulted in the flow paths shown in Figure 4.

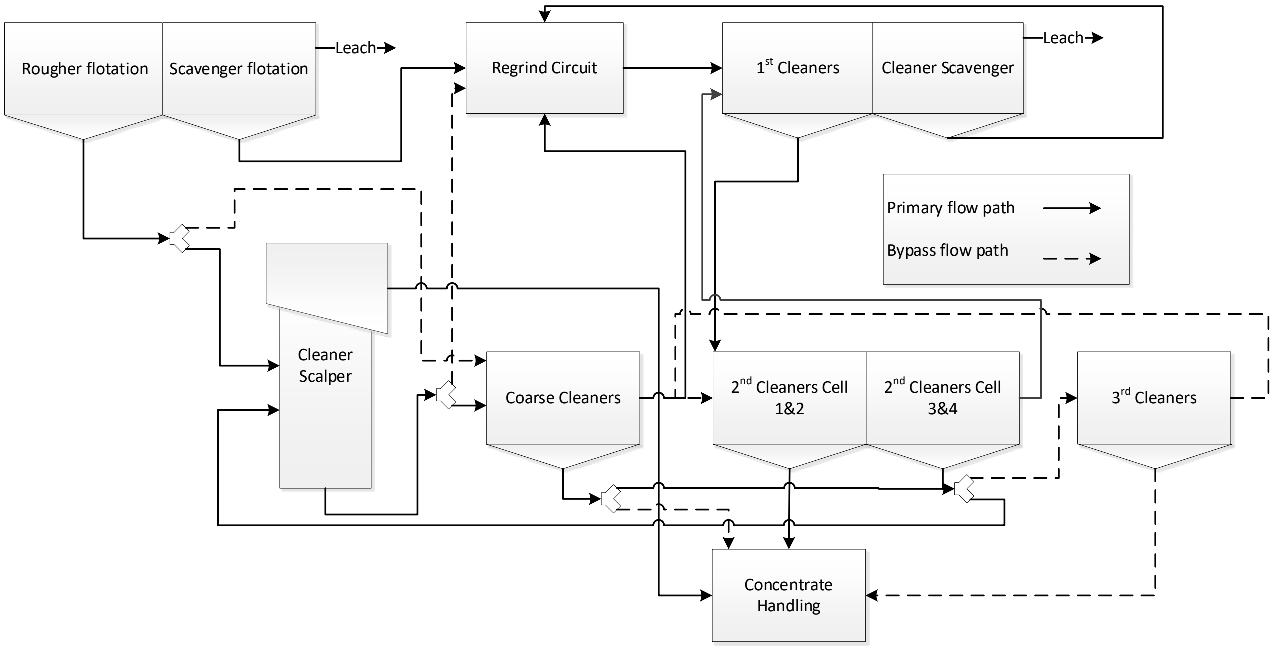


**FIG 4** – Post-CGI project simplified flotation circuit process flow diagram.

## DETAILED DESIGN

A number of benchmarking visits were undertaken early on during the detailed design stage of the project with specific focus on the cavitation tube columns, wash water addition and control as well as column tailings discharge arrangements.

Some of the key observations and the resultant design changes are listed in Table 2.

**TABLE 2**

Benchmarking observations and responses.

| Observation | Design change |
|---|---|
| Launder height should be around waist height to allow easy hosing of lips and launders | Launder height set at minimum level above grid mesh not requiring a handrail (900 mm) |
| Wash tray has to be removed with a crane each shutdown to allow launders to be cleaned | Split wash tray into two halves on rails to permit launder cleaning without a crane |
| Accessing launders for cleaning difficult due to distance to centre from the edge | Platform installed above wash tray such that when the wash tray is split and withdrawn the launders can be pressure cleaned from above |
| Steel ceramic lined slurry ring main is difficult to install | Mining hose used for slurry ring main |
| Ring main slurry feed pipe prevented continuous access around perimeter of column at cavitation tube height | Slurry ring main height increased |
| Stainless steel wash trays accumulated corrosion products in holes | High density polyethylene wash tray |

The design changes noted in Table 2 led to some unique features being included some of which are highlighted in Figure 5.

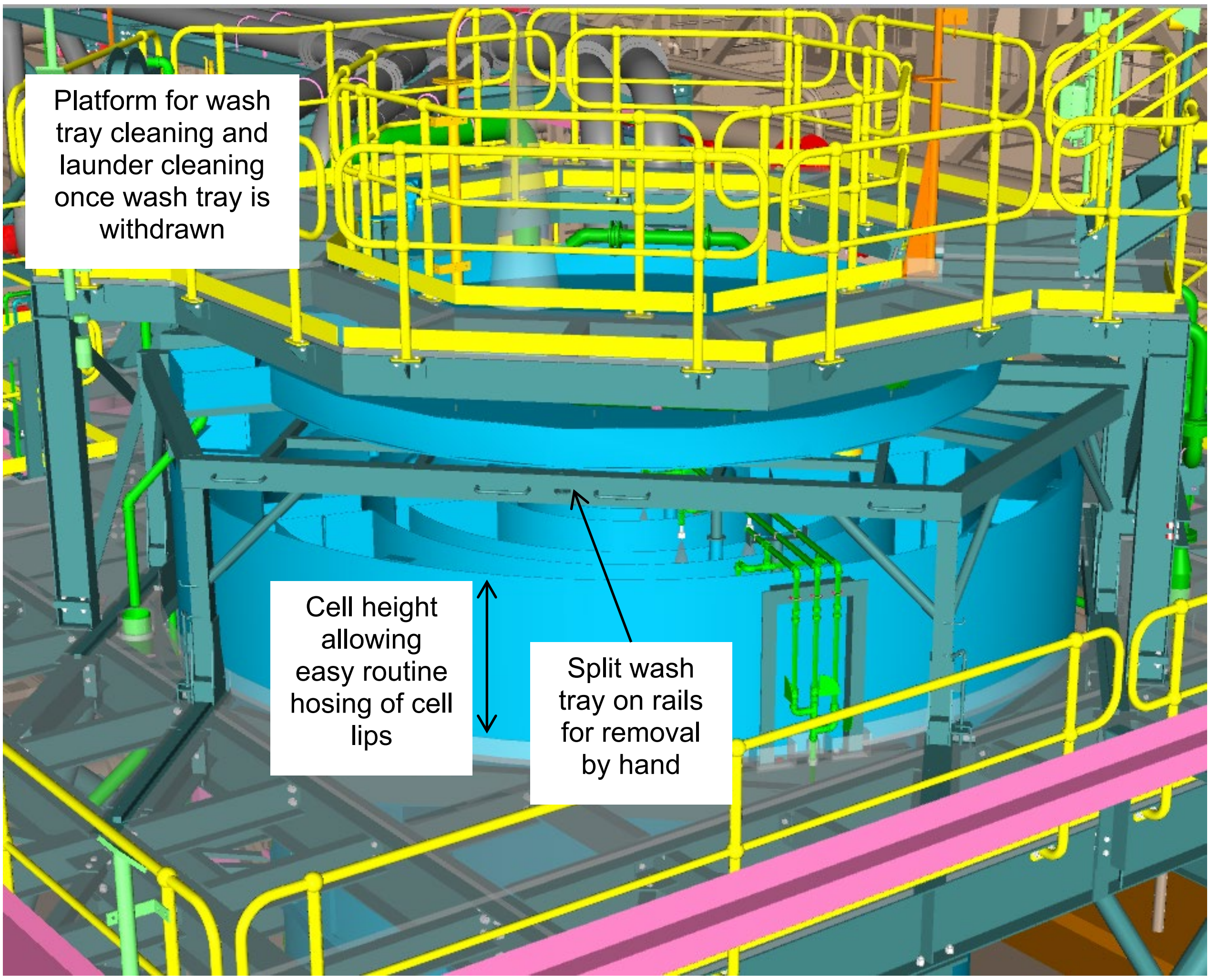


**FIG 5** – Top of column design features.

During detailed design, an investigation was undertaken to determine the preferred cleaner scalper tails-pumping configuration. Single or dual pumps were considered. The recommended and implemented option was dual pumps as this allowed the turndown determined by modelling from high to low sulphide head grade (which will be processed over the life-of-mine). It also had the added benefit of providing a duty/standby pump operation during periods of low sulphide head grade.

## CONSTRUCTION AND COMMISSIONING

Construction commenced with installation of plant tie-ins in July 2018 and was completed in February 2019. The Boddington plant has three full plant shutdowns per annum (March, July and November); hence these tie-ins were critical to the success of the installation and commissioning schedule.

The project included six major contracts that were scoped, tendered and awarded:

1. Engineering
2. Cleaner scalper column supply
3. Civil works
4. Structural steel
5. Structural, mechanical and piping
6. Electrical and instrumentation

Newmont staff managed the procurement and construction aspects of the project, with detailed engineering completed by DRA in Perth. The selected location of the column allowed for demarcation of the construction area from the existing operational plant. However, a large proportion of the required pipelines extended outside of this area into the operational plant. Significant effort was therefore required to ensure operations could intermittently undertake essential activities during construction breaks.

In order to expedite commissioning of the cleaner scalper column and the systems associated with it the construction contracts included milestone payments. Rather than percentage completion, the milestones were set for when systems were handed over to be commissioned. For example, the mechanical milestones were:

- Shutdown tie-ins:
  - install construction isolation points such that commissioning would only require de-isolation not further tie-ins.
- Cleaner scalper column and services:
  - install cleaner scalper column, associated equipment and all area services (raw water, gland water, process water, fire water and plant air) to permit water testing of the column.
- Cleaner scalper column operating on rougher concentrate:
  - install cleaner scalper column tails pumps and pipelines.
  - install modified rougher concentrate pump discharge piping to column feed box.
- Cleaner scalper column operating on second cleaner concentrate:
  - install modified second cleaner concentrate pump discharge piping to column feed box.
- Ancillary systems:
  - install cleaner scalper column sampling equipment.

This milestone process incentivised the construction contractor to provide equipment and systems in a manner which aligned to the order in which systems would be commissioned.

## PERFORMANCE TO DATE

Wet commissioning of the column commenced on 15 February and was completed by 27 February. An increase in final concentrate copper grade was immediately noted and accompanied by a corresponding reduction in the non-sulphide gangue levels determined by X-ray diffraction (XRD) analysis of daily composite samples. The average chalcopyrite (& cubanite) and non-sulphide gangue levels prior to and post commissioning are shown in Table 3.

**TABLE 3**

XRD non-sulphide gangue early performance.

| Period | Two weeks prior to commissioning | Two weeks post commissioning |
|---|---|---|
| Non-sulphide gangue (%) | 26 | 15 |
| Chalcopyrite and Cubanite (%) | 47 | 54 |

To further demonstrate the magnitude of change in the copper concentrate non-sulphide gangue content pre and post CGI commissioning, six months of semi-routine mineralogical analysis data was interrogated using a cumulative sum of deviations. Figure 6 shows a distinct change in the gradient corresponding to the commissioning of the cleaner scalper column in late February 2019.

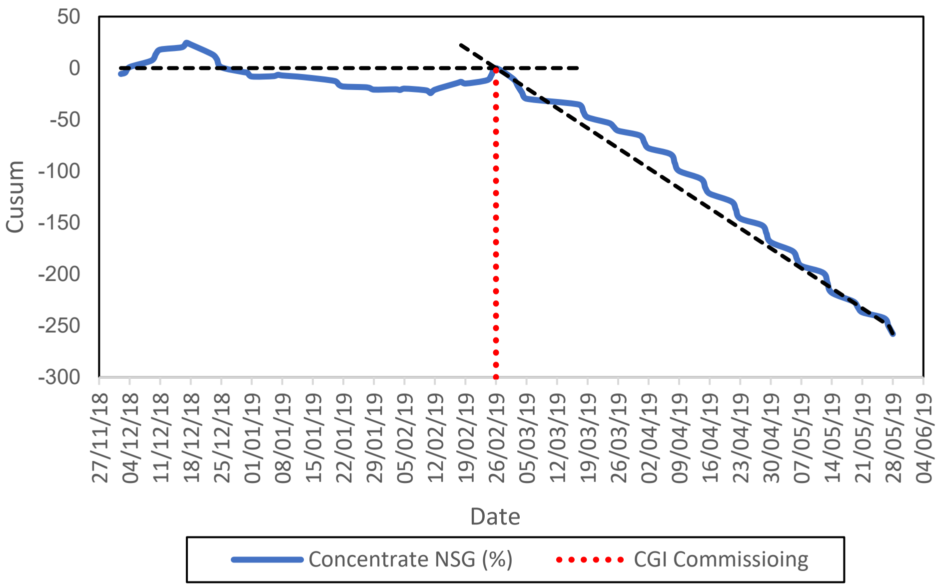


**FIG 6** – Six Month cusum of concentrate non-sulphide gangue.

The concentrate mass recovery at Boddington is modelled as a multiple linear regression with responses to copper head grade, sulphur head grade and daily throughput considered significant. In reviewing plant performance prior to the implementation of the CGI project, it was demonstrated that the strongest correlation was to the copper head grade, followed by sulphur head grade. As such the statistical analysis was simplified into comparisons of the linear regression of mass recovery to copper and sulphur head grade.

The pre-CGI and post-CGI data analysis used monthly-reconciled data. Table 4 shows some key performance parameters throughout the two periods compared, with March 2019 excluded as this was the month the column was commissioned. Figure 7 compares the copper upgrade ratio and the head grade and Figure 8 compares the concentrate mass recovery and the copper + sulphur head grade over the two periods.

**TABLE 4**
Data comparison information.

| | Pre-CGI | Post-CGI |
|---|---|---|
| Period | Jul 2017 – Feb 2019 | Apr 2019 – Jun 2020 |
| Average monthly copper head grade (%) | 0.116 | 0.092 |
| Average monthly sulphur head grade (%) | 0.227 | 0.235 |
| Average monthly copper + sulphur head grade (%) | 0.343 | 0.327 |
| Average monthly copper recovery (%) | 79.5 | 79.9 |
| Average monthly copper concentrate grade (%) | 15.9 | 17.4 |

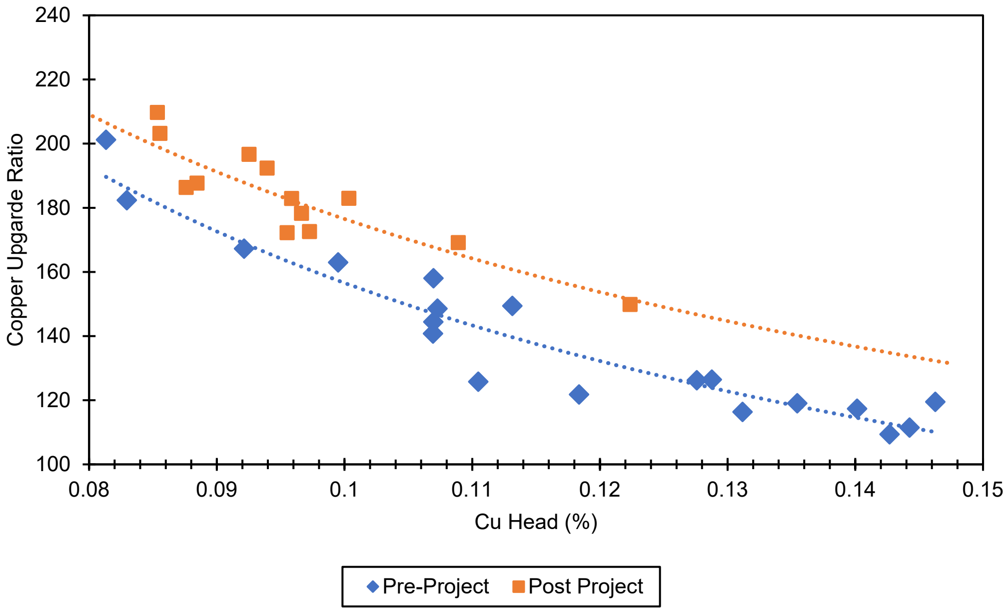


**FIG 7** – Copper upgrade ratio.

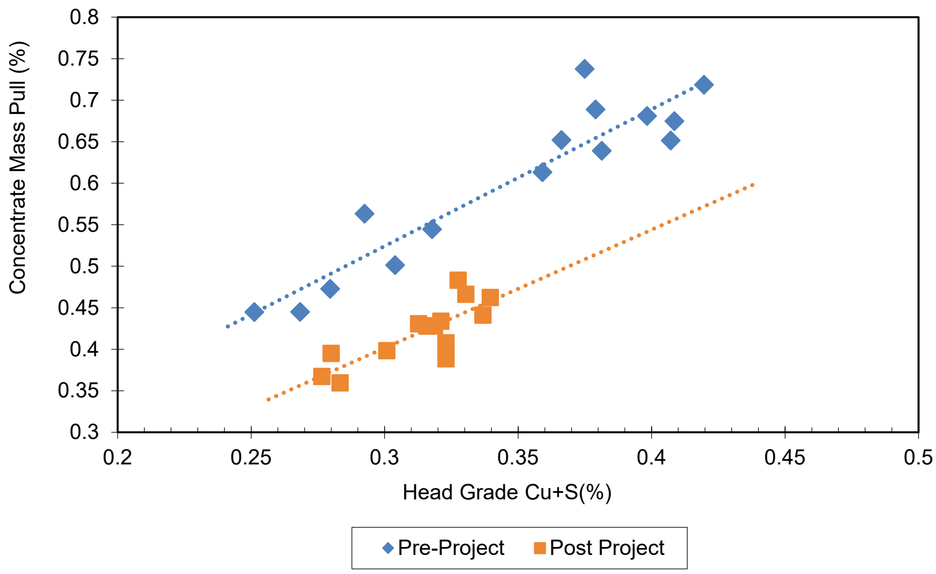


**FIG 8** – Comparison of regression line.

While the copper head grade reduced by 20 per cent (on average) over the two operating periods, making the direct comparison of results challenging, Figures 7 and 8 clearly show an uptick in the copper upgrade ratio for the same copper head grade, as well as a significant reduction in mass pull when the copper and overall sulphide content are considered.

The data was analysed as per the methodology outlined by Napier-Munn (2013). The analysis can be summarised follows:

1. The correlations are very strong (RPre = 0.93 and RPost = 0.80), and are therefore considered very significant.
2. The difference in residual mean squares is significant but is explainable due to the low head grade range since the project was commissioned.
3. The lines have similar slopes.
4. The intercepts are significantly different, $p<0.01$ or greater than 99 per cent confidence.
5. The separation of the lines is also significant, $p<0.01$, or greater than 99 per cent confidence. The value of the separation is 0.127 per cent with the post project implementation concentrate mass recovery being lower.

The conclusion is that the concentrate grade improvement project gives approximately a 0.127 per cent reduction (absolute) in concentrate mass recovered. At a typical copper head grade of 0.092 per cent and a sulphur head grade of 0.235 per cent this is a reduction in mass of 21 per cent.

In addition to the reduction in concentrate mass, there has been observed improvements in copper and gold recovery above that modelled for their respective head grades. As a number of other changes and trials were conducted in the plant, it cannot be concluded that all of the observed recovery increases can be attributed to this project. However, there is a case for attributing some of the benefit to the project. The addition of capacity to the cleaning circuit has enabled a significant change in rougher operating philosophy to increase the rougher concentrate mass recovery.

## CONCLUSIONS

The reduction in concentrate mass recovery achieved is equivalent to a reduction in concentrate production of approximately 51 000 tonnes per annum at an annual plant throughput rate of 40 MT. Combining the cost of transportation, storage and shipping as well as treatment charges and applying this to the concentrate mass reduction results in an expected saving of around AU$9.6M per annum. Coupled with recovery improvements seen to date the CGI project is expected to result in a capital payback of less than two years.

## ACKNOWLEDGEMENTS

The authors would like to thank (in alphabetical order) Ian Edwards, Tom Hamdorf, Ronel Kappes, Oliver Liebrich, Jim Orlich, Brendan Parker and Ben Richards for their support throughout the various phases of the project.

The authors would also like to thank Homie Thanasekaran and Nee San Yap of Eriez for assistance throughout pilot test programs and commissioning of the cleaner scalper flotation column.

## REFERENCES

Hart, S, Parker, B, Rees, T, Manesh, A, and Mcgaffin, I, 2011, Commissioning and Ramp Up of the HPGR Circuit at Newmont Boddington Gold in *Fifth Autogenous and Semi-Autogenous Grinding Technology Conference.* Westmount, QC: Canadian Institute of Mining, Metallurgy and Petroleum, pp1–23

Napier-Munn, T, 2013. *An Introduction to Comparative Statistics and Experimental Design for Mineral Engineers*, Course Notes, 2nd Edition, Version 4.14, Julius Kruttschnitt Mineral Research Centre, Indooroopilly Qld, Example 2.12

# Gruyere Gold Project Western Australia, part 1 – from design to commissioning

*R Radford[1], I Lovatt[2], B Putland[3] and M Becker[4]*

1. Metallurgy Manager, Gold Fields Australia, Perth WA 6005. Email: reg.radford@goldfields.com
2. Lead Metallurgist, Orway Mineral Consultants, Perth WA 6004.
   Email: ivka.lovatt@orway.com.au
3. Principal Metallurgist, Orway Mineral Consultants, Perth WA 6004.
   Email: brian.putland@orway.com.au
4. Senior Metallurgist, Orway Mineral Consultants, Perth WA 6004.
   Email: michael.becker@orway.com.au

## ABSTRACT

The Gruyere Gold Project was discovered by Gold Road Resources Limited in October 2013 on the Yamarna Belt 200 km east of Laverton in Western Australia. The Feasibility Study for Gruyere, which was completed in October 2016, envisaged a large-scale open pit mine feeding a 7.5 Mtpa processing plant and producing an average of 270 000 ounces of gold a year over an initial 13-year mine life.

A comminution circuit option study was conducted as part of the Feasibility Study, which examined four circuit options. The preliminary option study identified a primary crush SAG-ball circuit with recycle pebble crushing (SABC) and two-stage crush-HPGR-ball mill as the two options to evaluate in detail for the Gruyere Gold project. Ultimately, primary crush-SABC was selected due to its operational robustness and being the more cost-effect solution for the life of the project.

Gruyere Management Pty Ltd (GRM) – a wholly owned subsidiary of Gold Fields, has undertaken detailed reviews of Feasibility Study engineering, procurement and construction which has resulted in a number of improvements and enhancements to the Project. Gold Fields extensive operational experience has directly contributed to these improvements and enhancements, which aim to deliver:

- improved operational ergonomics and maintainability
- advanced process plant control
- increasing throughput beyond design
- more consistent metallurgical recovery.

An Engineering, Procurement and Construction (EPC) contract was executed in June 2017 with commissioning of the project commencing mid-2019.

This paper examines the comminution test work and the subsequent modelling completed during the feasibility study. It also discusses changes to the early design of the project and reasons for driving those improvements, as well as covering commissioning issues in the grinding circuit during the early stages of processing.

## INTRODUCTION

Gold Road Resources Limited discovered the Gruyere Gold orebody (the Project) in October 2013 on the Yamarna Belt 200 km east of Laverton in Western Australia. The Gruyere mineral resource has since grown to 148 Mt grading 1.3 g/t for 6.2 Moz of contained gold, making it one of the largest undeveloped gold deposits in Australia.

The Gruyere feasibility study was completed in October 2016. The study envisaged a large-scale open pit mine feeding a 7.5 Mtpa processing plant producing an average of 270 000 oz of gold a year over an initial 13-year mine life.

The gold mineralisation is hosted within a medium-grained quartz monzonite porphyry rock that exhibits moderate to hard competency. A comminution circuit option study was conducted as part of the feasibility study, which examined four circuit options. The preliminary option study identified a primary crush SABC and two-stage crush-HPGR-ball milling as the two options to evaluate in detail.

Ultimately, the primary crush SABC was selected due to its operational robustness and being the more cost-effective solution for the life of the Project. Further consideration was given to the final mill selection in order to maximise operational flexibility while reducing operating costs.

In November 2016, Gold Road entered into a 50:50 Joint Venture with Gold Fields Ltd (Gold Fields), to form the Gruyere Joint Venture (Gruyere JV), managed by Gruyere Management Pty Ltd (GRM) – a wholly owned subsidiary of Gold Fields. GRM has undertaken detailed reviews of feasibility study engineering, procurement, and construction, which has resulted in a number of improvements and enhancements to the Project. Gold Fields' extensive operational experience has directly contributed to these improvements and enhancements, which aim to deliver:

- Improved operational ergonomics and maintainability.
- Advanced process plant control.
- Increasing throughput beyond design.
- More consistent metallurgical recovery.

An engineering, procurement, and construction (EPC) contract was executed in June 2017 with construction and commissioning of the Project planned for early 2019.

In this paper, the authors examine the comminution test work and the subsequent modelling completed during the feasibility study. The authors also discuss changes to the early design of the Project and reasons for driving those improvements, as well as covering commissioning issues in the grinding circuit during the early stages of processing.

## ORE CHARACTERISTICS

The Gruyere deposit is located within the Yamarna Terrane of the eastern Yilgarn, Western Australia (200 km east of Laverton and 1000 km north-east of Perth). The deposit occurs on a flexure point of the regional-scale Dorothy Hills shear zone within the Dorothy Hills greenstone belt. Orogenic gold mineralisation is hosted within the steep easterly dipping Gruyere porphyry, a medium-grained quartz monzonite porphyry. The entire Gruyere porphyry is variably altered and gold grade is related to variations in style and intensity of the alteration, structure, veining, and sulphide species. Zones containing higher-grade gold mineralisation above 1.2 g/t gold generally have strong albite, sericite, chlorite, and biotite alteration and are associated with a sulphide assemblage of pyrrhotite, pyrite, arsenopyrite, weak to moderate foliation, common micro-fracturing, and steeply dipping quartz veining.

Ore from two smaller open pit deposits (Attila and Alaric) within trucking distance from the Gruyere plant is planned to be blended with the Gruyere ore. Gold mineralisation at Attila and Alaric comprises steeply dipping shear hosted gold in volcaniclastic sequences, with gold associated with zones of albite, sericite, chlorite, and pyrite mineralisation.

Samples from the mineralised zones were classified into weathered states, Oxide, Transition, Saprock, and Primary ore. From the Gruyere deposit, comminution test work was conducted on 19 Fresh samples, 5 Transition samples, 7 Saprock samples, and 1 Oxide (saprolite) sample. Comminution tests were also undertaken on the 12 Attila and 2 Alaric Fresh samples, as well as a single Oxide sample from Attila.

The plant was designed to treat 100 per cent Gruyere Fresh ore. A summary of the design (85th percentile) and average comminution test work parameters for the Gruyere Fresh ore is given in Table 1.

**TABLE 1**

Summary of Gruyere Fresh ore comminution test work parameters.

| Parameter | Units | Design | Average | St. dev. |
|---|---|---|---|---|
| Crushing work index (CWi) | kWh/t | 21.0 | 6.0 | 57.0 |
| Bond rod work index (RWi) | kWh/t | 22.0 | 20.8 | 0.7 |
| Bond ball work index (BWi) | kWh/t | 18.3 | 17.6 | 1.3 |
| Abrasion index (Ai) | g | 0.53 | 0.49 | 0.07 |
| SMC Test work | | | | |
| ta | | 0.3 | 0.36 | 0.1 |
| A×b | | 31.5 | 35.6 | 5.2 |
| DWi | kWh/m$^3$ | 8.5 | 7.4 | 1.2 |

## FLOW SHEET SELECTION

A percentile ranking of the Gruyere Fresh ore characteristics against the Orway Mineral Consultants (OMC) test work database (over 9000 samples) is given in Table 2.

**TABLE 2**

Gruyere Fresh ore ranking against OMC database (percentile).

| Parameter | Units | Gruyere design | Gruyere average |
|---|---|---|---|
| Ai | % | 84.0 | 84.9 |
| RWi | % | 77.9 | 75.8 |
| BWi | % | 74.0 | 68.3 |
| A×b | % | 11.6 | 19.4 |
| Uniaxial compressive strength | % | 97.9 | 95.0 |

The value of A×b is a measure of resistance to impact breakage, in contrast to the DWi, a high value of A×b indicates that an ore is soft whilst a low value means that it is hard. The comparison shows that both the A×b and BWi values for the Gruyere ore are harder than the database average. The BWi is moderate when compared to the A×b, which indicates that SAG milling of this particular ore will not be the most energy efficient comminution circuit option (Scinto, 2015). Ores that exhibit this type of relationship between the A×b and BWi values have higher $f_{SAG}$ values (Siddall, 1996). These ores typically benefit from multistage crush-ball milling circuits to reduce the overall comminution energy consumption (Scinto, 2015). For a project of this size and location, finding the most cost-effective flow sheet typically depends on the magnitude of the difference between the A×b and BWi, and the cost of power over the life of the project (Putland, 2006). Options initially considered for Gruyere were primary crush-SABC, full secondary crush-SABC, secondary crush-HPGR-ball milling, and conventional three stage crush-ball milling. The preliminary studies indicated that the SABC and HPGR-ball milling options should be investigated further.

A summary of the predicted power utilisation for the SABC and HPGR ball milling options at the original design grind $P_{80}$ of 106 µm is compared in Table 3.

**TABLE 3**

Comparative specific energy used in the study phase, kWh/t

| Equipment | SABC | HPGR-Ball mill |
|---|---|---|
| Primary crushing | 0.1 | 0.1 |
| Secondary crushing | - | 0.4 |
| HPGR | - | 4.0 |
| SAG mill | 11.6 | - |
| Recycle crusher | 0.2 | - |
| Ball mill | 12.3 | 13.7 |
| Auxiliary equipment* | 2.0 | 3.7 |
| Total | 26.2 | 21.9 |

Note: *Conveyors, screens, lube packs etc.

The SABC option had an $f_{SAG}$ value of 1.32. It was accepted during the Pre-Feasibility Study (PFS) stage that a total energy consumption saving of around 16 per cent could be expected for the HPGR option when compared to SABC. When considering maintenance, power, reagents and other operating costs, the SABC option was also higher at A$17.60/t compared to the HPGR option at $17.05/t. The SABC comminution circuit had the lowest predicted project development capital cost at A$313M when compared to the HPGR option at A$363M. Ultimately the overall project economics determined that the operating cost saving was not significant enough to justify the additional capital cost of the HPGR option. It is acknowledged that the HPGR design was conservative as there was no HPGR test work conducted at the time of the study, and there was no additional HPGR benefit was applied to the ball mill specific energy as the supporting data was scarce at the time of the study. The PFS risk assessment indicated that a robust SABC circuit design with low complexity and proven comminution configuration was favoured over the HPGR option. At the time, the HPGR option was seen as complex less mature technology that required higher upfront capital. In the authors opinion, the primary crush-SABC option better suited the junior gold miner's appetite for risk at the time of the study (before the Gruyere JV was formed).

This result is an interesting contrast to the nearby Tropicana Project, also modelled by OMC, which has similar design ore characteristics (A×b of 33.1 and BWi of 18.2 kWh/t) and subsequently has comparable $f_{SAG}$ values (1.3 to 1.4). In that case, the preliminary option study identified the same two comminution circuit options for further analysis; however, the final selection was the HPGR ball circuit (Kock, 2015). A future comparison of the actual operating data from the two projects will give a relatively good energy efficiency comparison between a conventional primary crush SABC circuit and HPGR ball mill circuit. This should ideally occur once the operating data is available from the Gruyere Project when treating fresh ore at design operating conditions.

## PROCESS FLOW DESCRIPTION

The circuit is a conventional primary crush – SABC circuit that includes a pre-leach and tailings thickener. A stand-alone gravity circuit is fed from dedicated pumps at the mill discharge hopper. Gravity concentrate is treated via an Inline Leach Reactor (ILR). The elution circuit is a split AARL with acid wash and an optional cold cyanide wash step. A cyanide DETOX circuit was not included.

The Gruyere comminution flow sheet includes primary crushing followed by a coarse ore stockpile (COS). The primary crusher is an FLSmidth TSU 1400 × 2100 gyratory crusher fitted with 600 kW motor. The crusher is designed to achieve a $P_{80}$ of 150 mm to 170 mm and treat 1550 t/h. The coarse ore is reclaimed from the stockpile via three reclaim apron feeders and conveyed to the SAG mill.

The primary crushed feed reports to the SAG mill feed chute. Lime is dosed onto the SAG mill feed conveyor from two lime silos. The SAG mill is a single Outotec 10.97 m (36') diameter × 5.79 m (19') effective grinding length (EGL) mill equipped with a 15 MW dual pinion drive. The SAG mill discharges onto a single 3.6 m × 8.5 m vibrating screen fitted with 8.5 mm aperture screen panels. The screen oversize is conveyed to the pebble crusher storage bin. Pebbles are reclaimed from the bin via two belt feeders, each reporting to a pebble crusher. The pebble crushers are two parallel Metso HP4 cone crushers fitted with 315 kW drives. The pebble crushers are designed to treat 200 t/h each at a closed side setting (CSS) of 13 mm. Crushed pebbles are returned to the SAG mill feed conveyor.

The SAG mill discharge screen undersize reports to the common mill discharge hopper, along with the ball mill discharge and dilution water. This is pumped to the cyclone cluster for classification, which is fitted with 12 × 650 mm hydrocyclones. The cyclone overflow reports to the trash screens followed by the leach feed thickener, while the cyclone underflow reports to the 7.93 m (26') diameter × 10.82 m (35.4') EGL overflow discharge ball mill for further size reduction. The FLSmidth ball mill is equipped with twin 7.5 MW drives, common with the SAG mill drive. The flow sheet includes the ability to bleed part of the cyclone underflow to the SAG mill feed chute, if required. The cyclone overflow $P_{80}$ target is 125 µm.

A portion of the combined mill discharge is bled from the mill discharge hopper via a dedicated set of pumps to the gravity circuit. A baffle in the mill discharge hopper is designed to separate the SAG mill and ball mill discharge, with the gravity feed drawn from the ball mill side to assist in pre-concentration of the gravity feed. The gravity circuit comprises two vibrating screens and four 48" Knelson concentrators. Tailings from the gravity concentrators is combined with the gravity screen oversize and returned to the mill discharge hopper on the SAG mill discharge side of the baffle. The gravity concentrate reports to a Gekko ILR, with pregnant solution reporting to the gold room, and washed leach residue returned to the mill discharge hopper. A block flow diagram of the Gruyere comminution circuit is shown in Figure 1 and an aerial circuit layout in Figure 2.

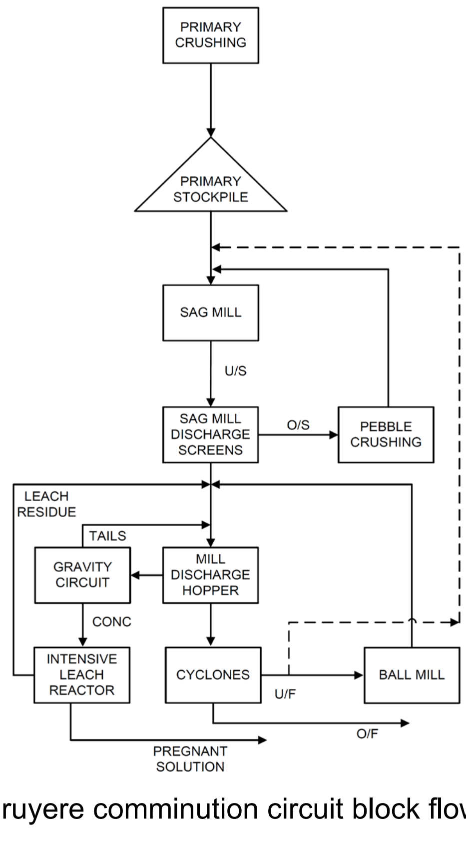


**FIG 1** – Gruyere comminution circuit block flow diagram.

**FIG 2** – Gruyere plant aerial photograph.

# FLOW SHEET DESIGN

## Mill selection

The predicted specific energy requirement to achieve the design grind $P_{80}$ of 125 μm was 11.4 kWh/t for the SAG mill and 11.3 kWh/t for the ball mill. Once contingency is added, this resulted in a minimum required installed power of 14.3 MW for the SAG mill and 12.9 MW for the ball mill. In the interest of commonality, 14.3 MW SAG and ball mills were initially selected for the Project.

At the time of the mill tender, a partially built 10.97 m (36') diameter × 5.79 m (19') 15.4 MW Outotec SAG mill became available. This mill was available for a comparable price to that offered for a new 14.3 MW by the same vendor, the additional civil and services upgrades required to accommodate the larger SAG mill was predicted to add approximately A$2M to the capital cost of the Project. Further complicating the decision was the ball mill selection, which following the formation of the joint venture with Gold Fields, resulted in an FLSmidth mill being reassigned from another Gold Fields Project. This ball mill has 15 MW of installed power. A cancelled 10.97 m (36') × 5.3 m (17.5') EGL 15 MW SAG mill order was also being considered from another vendor. All of the tendered mills were assessed, and it was found that the two-foot difference in the SAG mill EGL was significant. The key findings were as follows:

- The shorter EGL mill required operation at 13 per cent ball charge to achieve the design pinion power draw, while the longer mill achieve the same the same power draw at 9 per cent ball charge (assuming 25 per cent total load in both cases).
- While both mills had more than the estimated installed power requirement of 14.3 MW, the longer mill could draw the full installed power at a lower ball charge. This results in the additional contingency being available at more sustainable operating conditions.
- Operating the SAG mill at above 13 per cent ball charge may prove to be problematic from a load stability point of view, particularly for the harder ore types of the Gruyere deposit. Higher ball charge levels result in a flatter power curve, making the mill more susceptible to overloading. It is likely that operating at lower ball charges will be beneficial when treating harder ore.

- Operating at the lower ball charge also resulted in a reduced media consumption rate. It was estimated that a saving of A$1.15 million per annum could be expected from the longer EGL mill by operating at the lower ball charge.

Ultimately, the longer Outotec SAG mill was selected for the Project. The motor design was revised to match that of the FLSmidth ball mill, such that both mills have common twin 7.5 MW low-speed synchronous motors equipped with variable voltage variable frequency (VVVF) speed control drives.

## Main design changes

At the time the Gruyere joint venture was formed in November 2016, the Gruyere Project had already passed the feasibility study stage and was in the final stages tendering the EPC contract. The Gruyere Project team together with operation and mechanical leads from Gold Fields Australia carried out design reviews to improve the operability and enhance long-term success of the Project. These included:

- FLS crusher sizing and apron feeder capacity changes.
- Drive in cleanout for the ROM primary crusher pocket.
- Crusher and COS tunnel access for cleaning and maintenance.
- Grinding area layout – addition of mill ramp for access, Russell Mineral Equipment (RME) chute handlers replacing winch/cables.
- Additional reline space.
- Addition of cyclone underflow partial bypass line for SAG mill.
- Additional tramp metal removal on the recycle pebble crusher conveyor.
- Dual access around conveyor systems with dedicated maintenance and splicing bays.
- Additional standby equipment, trash and carbon safety screens, air compressors.
- Gravity area design with screens, batch concentrators, and leach reactor offset, preventing spillage on equipment at levels below.
- Fully decked leach and carbon-in-leach (CIL) circuit with dedicated central piping system.
- Additional instrumentation for thickener and leach systems control.

## Process control system

The Gruyere feasibility study included a review between a programmable logic controller/supervisory control and data acquisition (PLC/SCADA) process control system and a distributed control system (DCS). Due to the tight integration, reliability and its life cycle cost-effectiveness, the Yokogawa DCS was chosen. It would deliver a good and robust level of regulatory control of the plant and like any process control system would however require constant monitoring of control room operators to adjust the process parameters to maintain plant operations. Operator response to constantly varying process variables is commonly delayed and not consistent, resulting in underutilisation, downtime, and/or damage to equipment.

Gold Fields Limited has had a technical collaboration with Manta Controls since 2005 and uses the Manta Cube system under licence at several operations to provide throughput, recovery, and reagent optimisation. The Manta Cube system utilises advanced control fundamentals including constraint control, feed forward control, expert system control, gain scheduling, object-oriented control, model predictive, decoupling control, and new optimisation process control technology that has been developed by Manta Controls. As an example, the Gruyere SAG Cube utilises key drivers, such as feed rate, mill speed, feed density to control the SAG mill weight and other constraints such as mill power draw and impact sound.

The Manta Cube systems including the Feed Cube, SAG Cube, Ball Mill Cube, Cyclone Pressure Cube, the pre-Leach Thickener Cube with Manta Sub (Submarine), the Cyanide Leach Cube and the Tails Thickener Cube with Sub were seamlessly integrated into the plant Yokogawa DCS installed by Manta Controls and engineered during the design and construction phase so that they were available once care, custody, and control of the plant is transferred from the EPC contractor to the company. By fast tracking the historical method of justifying installation of advanced process control systems over a period of years after start-up, installing proven advanced process control technology enabled the Gruyere Project to achieve circuit stability and improve ramp-up rates from day one

## Debottleneck study

OMC was commissioned to assist with the identification of possible bottlenecks at the Gruyere plant based on the current design and equipment selection. The study assumed that there is sufficient ore delivery to the primary crusher to meet plant feed requirements. The original mill design was based on the 85th percentile ore characteristics to warrant that nameplate throughput can be consistently achieved. To evaluate potential restrictions throughout the rest of the plant, a review was conducted utilising the 25th percentile ore characteristics (providing higher throughputs for the milling circuit) on Fresh ore only (Table 4).

**TABLE 4**

Throughput modelling at 25th percentile ore parameters.

| Parameter | Unit | Design grind | Relaxed grind |
|---|---|---|---|
| **Ore parameters** | | | |
| BWi<br>A×b<br>Ore SG | kWh/t | 17.0<br>36.1<br>2.69 | 17.0<br>36.1<br>2.69 |
| Feed rate | t/h | 1222 | 1290 |
| Primary feed size, $F_{80}$ | mm | 124 | 124 |
| Product size, $P_{80}$ | µm | 125 | 140 |
| Pebble crushing | % feed<br>t/h | 14.3<br>175 | 15.2<br>196 |
| SAG mill specific energy<br>Ball mill specific energy<br>Total specific energy<br>$f_{SAG}$ | kWh/t<br>kWh/t<br>kWh/t<br>- | 10.50<br>9.76<br>20.30<br>1.28 | 10.23<br>9.25<br>19.53<br>1.28 |
| SAG mill pinion power required<br>BM pinion power required | kW<br>kW | 12 825<br>11 927 | 13 199<br>11 931 |

Under the modelled conditions, a throughput of 1222 t/h is anticipated while maintaining the grind size at a $P_{80}$ of 125 µm. With the softer ore, the ball mill becomes the limiting unit process. If the grind is allowed to coarsen to a $P_{80}$ of 140 µm, a throughput up to1290 t/h is possible, at which point the SAG mill becomes the limit. For this evaluation,1222 t/h was used as a sustainable basis with commentary on maximum capacity.

The review identified the maximum sustainable capacities of the mills by modelling under operating conditions considered sustainable under good supervision and control. While the equipment is not fully utilised, there is limited margin between nominal and maximum conditions. All major processing equipment (conveyors, screens, pumping and piping, tanks etc) were then evaluated based on these calculated throughputs to assess that there was sufficient capacity at each processing stage.

The key areas highlighted as potential capacity restrictions at higher throughput rates were:

- Primary and recycle crusher power draw operating at close to the installed power and instantaneous spikes could result in larger OSS/CSS or material bypassing the crusher.

- Both the leach feed and tailings thickeners are a limitation at the design flux rates of 1.0 t/m$^2$h. However, test work has confirmed flux rates of up to 1.5 t/m$^2$h on Fresh ore are achievable.
- Leach residence time reduced to about 18.5 hours and there was a predicted inability of the 6 t/d oxygen plant to supply at a rate of 0.22 kg/t of ore.
- Trash screen solids and flow rate capacity of the two duty units limit throughput; however, a third 'standby' unit has been included in design for ease of cleaning and maintenance while providing additional capacity when required.

The capacity limitations in these areas are expected to be overcome with relatively minor capital and operational adjustments, which leaves the mill as the true plant bottleneck. The OMC review confirmed that under the current Amec Foster Wheeler Civmec Joint Venture (ACJV) design and with the selected equipment, there were no foreseeable bottlenecks or risks to achieving the nameplate 7.5 Mtpa capacity. The review provided confidence in the ability of the circuit to increase annual throughput to 8.2 Mtpa capacity. An updated mine plan was announced in December 2018 increasing average annual production to 300 000 oz, up from 270 000 oz/a as per the 2016 feasibility study.

## CONSTRUCTION AND COMMISSIONING

The construction of the Gruyere processing plant commenced in the first quarter of 2018 with commissioning completed and handover to operations occurring in the third quarter of 2019. A timeline of key events for the project is presented in Figure 3.

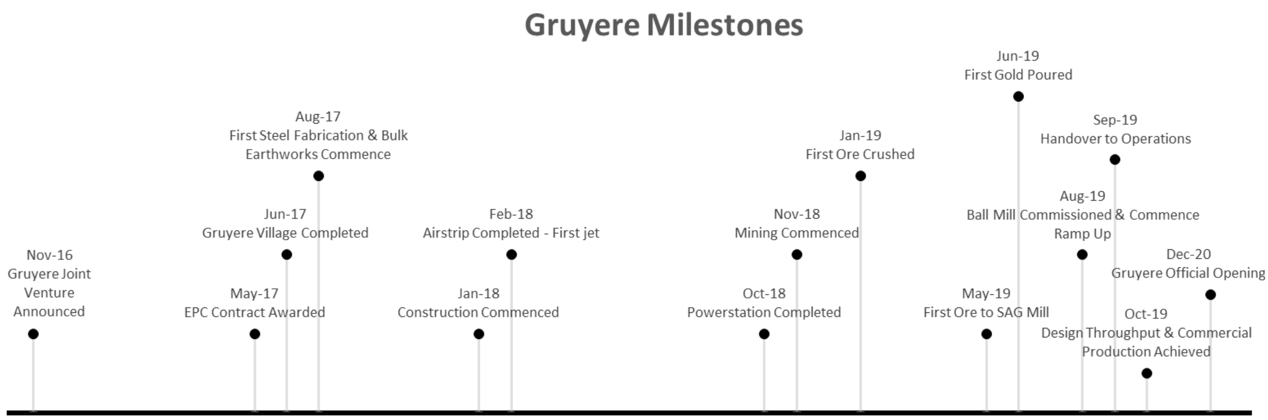


**FIG 3** – Gruyere project timeline.

## SAG mill grate apertures

During early stages of design, it was proposed that the SAG mill grates would have a 25 mm aperture; however, this was decreased to an 18 mm aperture during final engineering and purchasing. Initial start-up was based on 100 per cent Oxide ore feed and the SAG running without pebble crushing. Modelling conducted by Outotec indicated that:

- A full set of 32 × 18 mm grates provided 5.7 per cent open area, which was suitable for Oxide ore at 70 per cent solids w/w pulp density.
- Flow rates of 1354 m$^3$/h at 25 per cent mill load and 70 per cent of critical speed (Nc) is equivalent to 1600 t/h, far exceeding design of 1100 t/h.

It is expected that the circuit will operate at lower mill speeds to maintain sufficient mill load to prevent liner damage and grate peening from ball impacts. As the ore gets harder and the plant commences processing Transitional ore, it is expected that 7 per cent open area would be considered with 20 mm to 25 mm apertures. This can then be supplemented with pebble ports as the plant processes Fresh ore. To maintain flexibility and the ability to react to changing conditions, additional sets of 25 mm aperture and 45 mm aperture grates were ordered and mobilised to site prior to commissioning.

## Grinding media first fills

The SAG mill is designed to operate with a top ball size of 125 mm. The ball mill is designed to operate with a top ball size of 65 mm. Mill datasheets were provided to Moly-Cop to review the initial grinding media size recommendations, ball charge estimates, and wear rate estimates using the Moly-Cop Tools$^{TM}$ software.

The EPC requested an initial SAG charge of a 105 mm top size ball before transitioning to 125 mm as ore competency increases with higher proportions of Transitional and Fresh ore processed. The initial 63 t charge is approximately 2.5 per cent by volume and consists of 80 mm diameter balls to minimise the risk of liner damage by an operational mistake. The remainder of the first fill consists of 126 t of larger 94 mm and 105 mm balls was planned to be added as required for make-up to approximately 7.8 per cent by volume.

For Oxide ore, the review recommended a ball mill media top size of 55 mm increasing to 65 mm as the operation begins treating Fresh ore. The initial 441 t charge is approximately 20 per cent by volume, which is expected to be enough to allow the mill to grind reasonably efficiently. To improve the early grinding efficiency the initial charge was made by combining 25 mm, 38 mm, and 50 mm balls to emulate a seasoned charge, see Table 5. The remainder of the 378 t first fill 50 mm and 65 mm balls were stored in the grinding media bunkers and were planned to be added opportunistically over a span of two to three weeks after the introduction of ore.

Actual graded charge quantities differed from the supplier recommendations after taking into consideration standard bulk haulage quantities that could be delivered remotely to site. Table 5 details the recommended and actual graded charges for both mills.

**TABLE 5**

Initial charge recommendations.

| Ball size (mm) | SAG mill % | | | | Ball mill | | | |
|---|---|---|---|---|---|---|---|---|
| | Recommended | | Actual | | Recommended | | Actual | |
| | (%) | (t) | (%) | (t) | (%) | (t) | (%) | (t) |
| 125 | - | - | - | - | - | - | - | - |
| 105 | 27 | 54 | 33.3 | 63 | - | - | - | - |
| 94 | 41.5 | 83 | 33.3 | 63 | - | - | - | - |
| 80 | 31.5 | 63 | 33.3 | 63 | - | - | - | - |
| 65 | - | - | - | - | 41 | 336 | 23.1 | 189 |
| 50 | - | - | - | - | 44 | 360 | 30.7 | 252 |
| 38 | - | - | - | - | 15 | 123 | 30.7 | 252 |
| 25 | - | - | - | - | | - | 15.4 | 126 |

## Start-up strategy

During the design reviews, provision was made in the grinding circuit flow sheet to divert part of the cyclone underflow stream into the SAG mill via a bypass line, whilst operating the two mills at the same time. The bypass system exists as a variable knife gate valve and V-notch overflow weir built into the cyclone underflow launder with a 500 mm pipe returning to the SAG feed chute. The partial bypass was primarily included for future optimisation of the grinding circuit. To prepare for all eventualities and construction delays, two options were considered for initial commissioning of the grinding circuit:

1. Commissioning of the SAG and ball mills at the same time in semi-autogenous ball (SAB) mode.
2. Commissioning of the SAG mill ahead of the ball mill in single-stage (SS) SAG operation mode.

### *SAB mode advantages*

- No variations or modifications required to plant flow sheet (to bypass, isolate unused lines etc). For example, SS SAG operation requires return of the cyclone underflow to the SAG mill rather than to the ball mill, requiring installation of a blanking flange on the ball mill feed line.
- SAB operation is inherently easier to control and operate compared to SS SAG operation and produces a more consistent final product size ($P_{80}$).
- All equipment will be operated as per the original design intentions and specifications and a faster ramp-up to achieve full plant capacity is expected.

### *SAB mode disadvantages*

- If the SAG mill installation is completed ahead of the ball mill, commissioning of the grinding circuit will have to await completion of the ball mill.
- Commissioning and initial testing of the mill motors at the same time may be difficult in terms of specialist commissioning resources, specifically ABB personnel from Switzerland.

### *SS SAG mode advantages*

- More efficient allocation of specialist vendor commissioning resources (ABB).
- More focused team efforts (both commissioning and GRM operations personnel) on getting the SAG mill and its ancillaries commissioned and operational.
- Earlier commencement of ore through the plant with a gentler ramp up in filling CIL tanks and thickeners and establishment of production procedures.

### *SS SAG mode disadvantages*

- Lower than design throughput levels are expected through the SS SAG mill circuit.
- Settling of solid particles may occur downstream if the slurry flow rates are too low or grind size is too coarse.

For single stage operation on commissioning ore, the following conditions were considered likely:

- Milling speed of 60 per cent Nc
- Ball charge of 10 per cent volume
- Operating mill load of 25 per cent volume
- Pulp density of 65 per cent solids w/w
- Circulating load of 200 per cent to 300 per cent.

These conditions were modelled to establish the likely new feed solids rate that is possible when considering the grate flow restriction in single stage operation.

The power of the SAG mill indicated a capacity of 878 t/h; however, the grate geometry is predicted to restrict the expected throughput rate to between 428 t/h and 570 t/h depending on the circulating load. Key items that were considered during SS SAG operation included:

- Stability of the SAG mill charge weight, rock to ball ratio, power draw, and speed.
- Final product sizing without the ball mill to prevent downstream sanding in early commissioning stages.
- Reliable charge weight from the Outotec SAG mill hydrostatic bearing load measurement system.
- Capacity of the cyclone underflow bypass line to handle the SS SAG recirculation flow rates, which at a design rate of 2500 $m^3$/h was deemed sufficient.

Ultimately the process plant was commissioned on first ore operating in SS SAG configuration. The decision being driven by the requirement to ensure production targets were achieved and the advantage of a steady ramp up of the thickener and carbon-in-leach circuit. Of the key points identified during the risk assessment on operating in SS SAG mode, achieving the target grind size of 125 μm whilst processing oxide material with low ball and rock charge was most problematic.

Despite the graded charge loaded into the SAG mill and reduced top size ball of 105 mm, shift composites indicated a grind $P_{80}$ between 150 μm and 200 μm with the top size exceeding 600 μm. This led to grit and slurry spillage from the cyclone overflow trash screens at throughput rates over 500 t/h. Further optimisation of the SAG operating conditions utilising lower speeds, higher charge levels and bypassing the recycle pebble crushers aided in minimising the coarse grit until the Ball mill was commissioned. The hydrostatic bearing load measurement system proved reliable allowing charge weight to be controlled via mill speed and no noticeable downstream issues occurred in either the pre-leach or tails thickener and carbon-in-leach circuit related to the coarse particle sizing.

## CURRENT OPERATION

The average monthly throughput and grind size achieved since commissioning is presented in Figure 4. The mill utilisation, defined as the actual run time of the mill, is presented in Figure 5. Material processed during the ramp up period consisted of oxide and transitional ore from Run-of-mine (ROM) stockpiles and the design targets shown correspond to the transitional ore. Ramp up of the Gruyere processing plant commenced in the second quarter of 2019 in SS SAG mode and continued until the ball mill was brought online two months later. The circuit transitioned to SABC mode however the recycle crushers were not required due to the soft ore characteristics at the time. Throughput increased as availability and utilisation improved across the circuit with design tonnes being achieved in the first five months of operation.

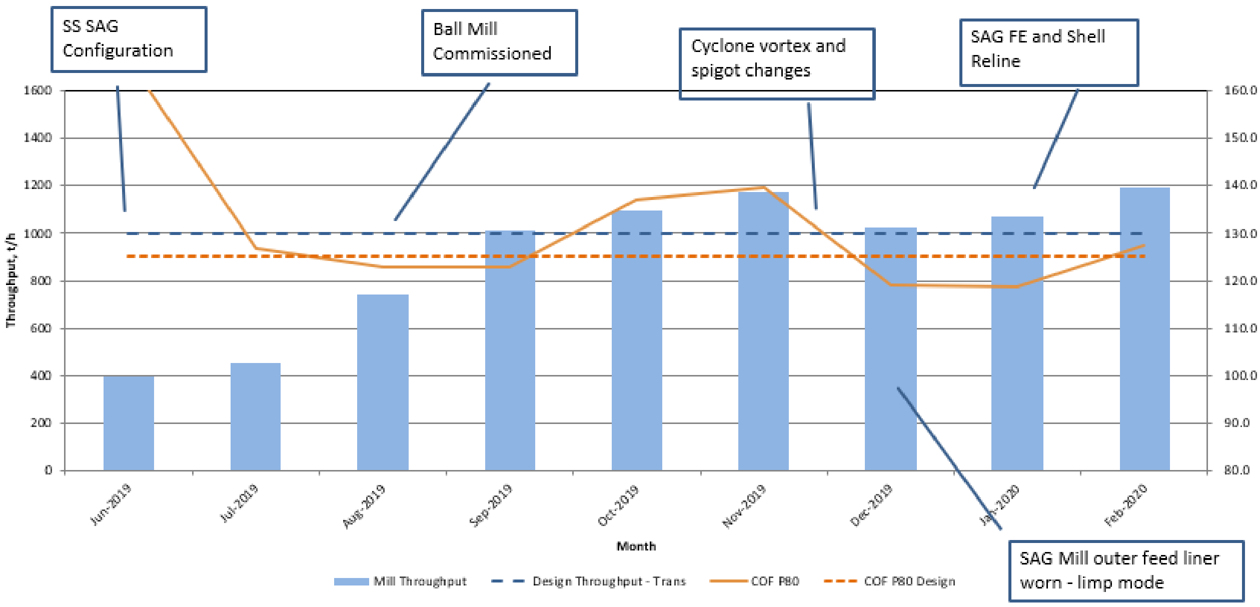


**FIG 4** – Mill throughput and cyclone overflow (COF) $P_{80}$.

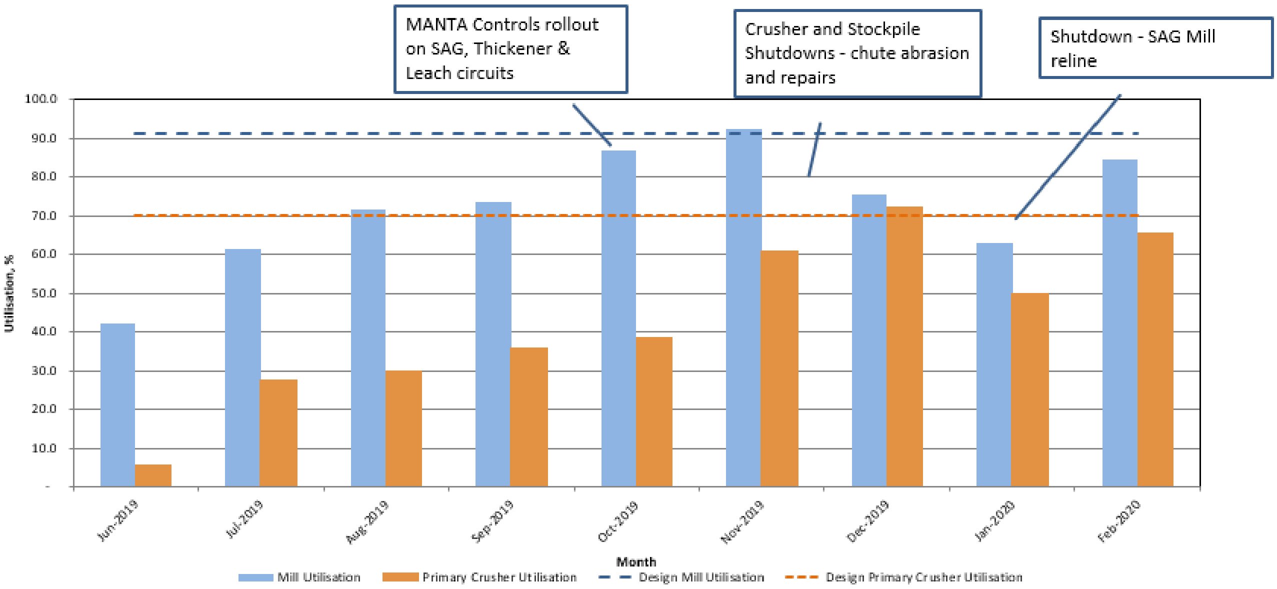


**FIG 5** – Circuit utilisation.

Circuit stability was affected by limited process control loops being in place at the time of commissioning. Key circuits that required monitoring and manual adjustment by the process technician included

- SAG feed tonnes to stockpile apron feeder control.
- SAG power and load to variable speed control.
- Cyclone feed pump to level, pressure or density control.
- Thickener bed level, pressure, underflow density and mass flow control.
- Tailings discharge hopper level and mass flow control.

In effect much of the plant was operated manually by the control room technician during an ongoing commissioning period with at times stressful background distractions and constant radio communications. Priority was placed on resolving this with the EPC contractor working closely with Gruyere's internal and external resources. The commitment from GJV to install the MANTA Controls system during the project stage allowed the project schedule for this work to be brought forward without the usual one to two year process of justifying and executing process control upgrades once the circuit was stable and operational. Within the first six months of commissioning the key SAG, Ball, Thickener and Leach circuits were all operating under the Manta Controls Cube system leading to immediate throughput benefits whilst meeting downstream operating targets for grind size, density and reagent control.

In the early stages of commissioning the ball mill, two main issues arose. Firstly, when throughput exceeded 1200 t/h cyclone overflow (COF) $P_{80}$ exceeded the design target of 125 µm with daily composites averaging 150 µm. The second issue involved low cyclone underflow/ball mill feed density (<55 per cent solids w/w) causing low power draw from the ball mill and excessive slurry spillage from the feed chute retainer ring as shown in Figure 6. While throughput was exceeding design, circuit stability and performance was suboptimal. A series of cyclone spigot and vortex finder trials were completed with the vortex finder being reduced from 320 mm to 280 mm and the spigots being progressively reduced from 190 mm to 180 mm, 170 mm and finally 160 mm. These changes increased the ball mill density to the target range >70 per cent solids w/w and as well as reducing the COF $P_{80}$ back to design of 125 µm and maximising gold recovery. The ability to quickly resolve the poor classification issue was assisted by purchasing alternate vortex and spigot sizes prior to commissioning for trialling as well expediting the desired size ranges from the supplier.

**FIG 6** – Excessive Ball mill feed spillage.

The initial 820 t graded charge loaded into the 7.92 m (26’) diameter × 10.79 m (35.4’) EGL ball mill equated to 33 per cent ball charge volume. The mill speed was progressively increased from 80 per cent to 95 per cent motor speed (where 100 per cent motor speed is 76 per cent Nc) whilst final commissioning of the ball mill motors was completed. Being a dual pinion drive, alignment and temperature monitoring of the geared mill was critical. In early October the ball mill achieved close to full power draw at 14 MW and 100 per cent $Nc_{80}$ with regular mill inspections and laser scans indicating a charge volume of 32 per cent and grinding media addition rate stabilising at 0.44 g/t. The 7.92 m (26’) diameter × 10.79 m (35.4’) EGL SAG mill grinding media top size was increased from 105 mm to 125 mm to coincide with the commissioned of the ball mill and the progression from oxide to transitional ore being treated. The ball charge was steadily increased from the initial charge of 8 per cent to a design target of 13 per cent ball load through regular inspections and laser scans. Power draw increased from a range of 5–7 MW during SS SAG mode to a maximum power draw of 11–13.5 MW in SABC mode. Media addition to the SAG mill has since stabilised at a rate of 0.26 g/t when processing transition ore.

Tables 6 and 7 present a summary of the key operating data from when the circuit was running in SABC mode and SS SAG mode respectively.

**TABLE 6**

Key operating parameters – SABC mode.

| Parameter | Units | SAB | Standard deviation |
|---|---|---|---|
| **Primary crushing** | | | |
| -Throughput | t/h | 1835 | 297 |
| -Power draw | kW | 259 | 28 |
| -Specific energy | kWh/t | 0.15 | 0.04 |
| -Auxiliary specific energy | kWh/t | | |
| -Overall utilisation | % | 62.5 | - |
| **SAG Mill** | | | |
| -Throughput | t/h | 1128 | 168 |
| -Power draw | kW | 10 181 | 1870 |
| -Specific energy | kWh/t | 8.8 | 0.9 |
| -Auxiliary specific energy | kWh/t | | |
| -Overall utilisation | % | 75.6 | - |
| **Ball mill** | | | |
| -Throughput | t/h | 1128 | 168 |
| -Power draw | kW | 13 762 | 607 |
| -Specific energy | kWh/t | 11.8 | 0.9 |
| -Auxiliary specific energy | kWh/t | | |
| -Overall utilisation | % | 75.6 | - |
| -Cyclone O/F $P_{80}$ | µm | 121 | 10 |
| **Total specific energy** | **kWh/t** | **20.6** | **1.4** |

**TABLE 7**

Key operating parameters – SS SAG mode.

| Parameter | Units | SS SAG | Standard deviation |
|---|---|---|---|
| **Primary crushing** | | | |
| -Throughput | t/h | 1579 | 256 |
| -Power draw | kW | 251 | 23 |
| -Specific energy | kWh/t | 0.16 | 0.05 |
| -Auxiliary specific energy | kWh/t | | |
| -Overall utilisation | % | 57.7 | - |
| **SAG Mill** | | | |
| -Throughput | t/h | 402 | 136 |
| -Power draw | kW | 5608 | 1623 |
| -Specific energy | kWh/t | 12.9 | 1.5 |
| -Auxiliary specific energy | kWh/t | | |
| -Overall utilisation | % | 51.8 | - |
| -Cyclone O/F $P_{80}$ | µm | 144 | 18.2 |
| **Total specific energy** | **kWh/t** | **13.1** | **1.5** |

The specific energy consumption was lower in SS SAG mode, however a higher fraction of the feed was Oxide during this period. A circuit survey was conducted in December 2019 as part of an optimisation study conducted by OMC. There were three main goals of the survey:

1. Provide a baseline set of operating conditions for the circuit.
2. Evaluate the efficiency of the circuit and identify opportunities for optimisation.
3. Begin the process of learning how to survey the circuit. Developing the survey plans, training the site metallurgists, modifying the sample points and purchasing required sampling equipment.

It is the opinion of the author that the third point is almost more important than the first two, no two comminution circuits are the same and every new operation must start somewhere.

Samples were tested for moisture content, percent solids and particle size distribution at the on-site Gold Fields laboratory. The SAG mill fresh feed sample was packaged and dispatched to ALS Metallurgy's Perth laboratory for testing of a suit of comminution tests including SG, RWi, BWi, Ai and SMC. The comminution test work results were still pending at the time of writing this paper. Historical test work results were used to produce a fitted model in JKSimMet and to determine the energy efficiency of the circuit. The fitted JK SimMet model output is presented in Figures 7 and 8. The energy comparison summary in Table 8.

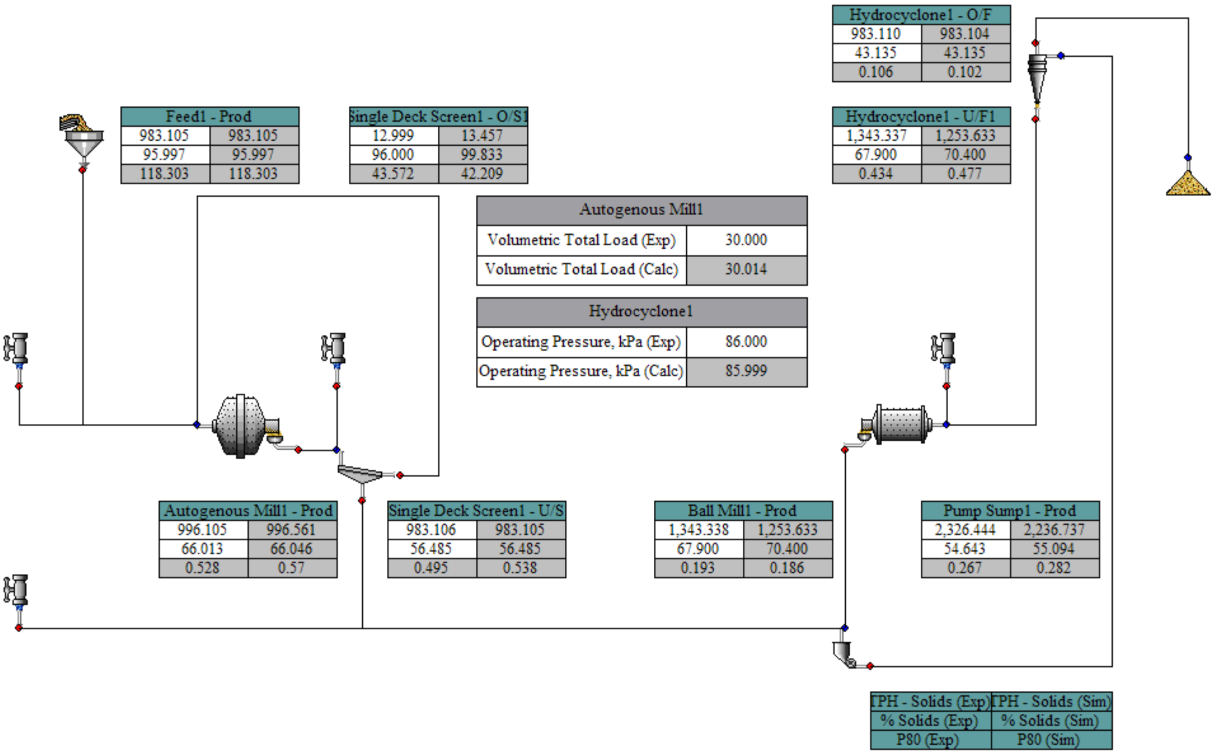


**FIG 7** – Fitted JKSimMet model – December 2019 survey.

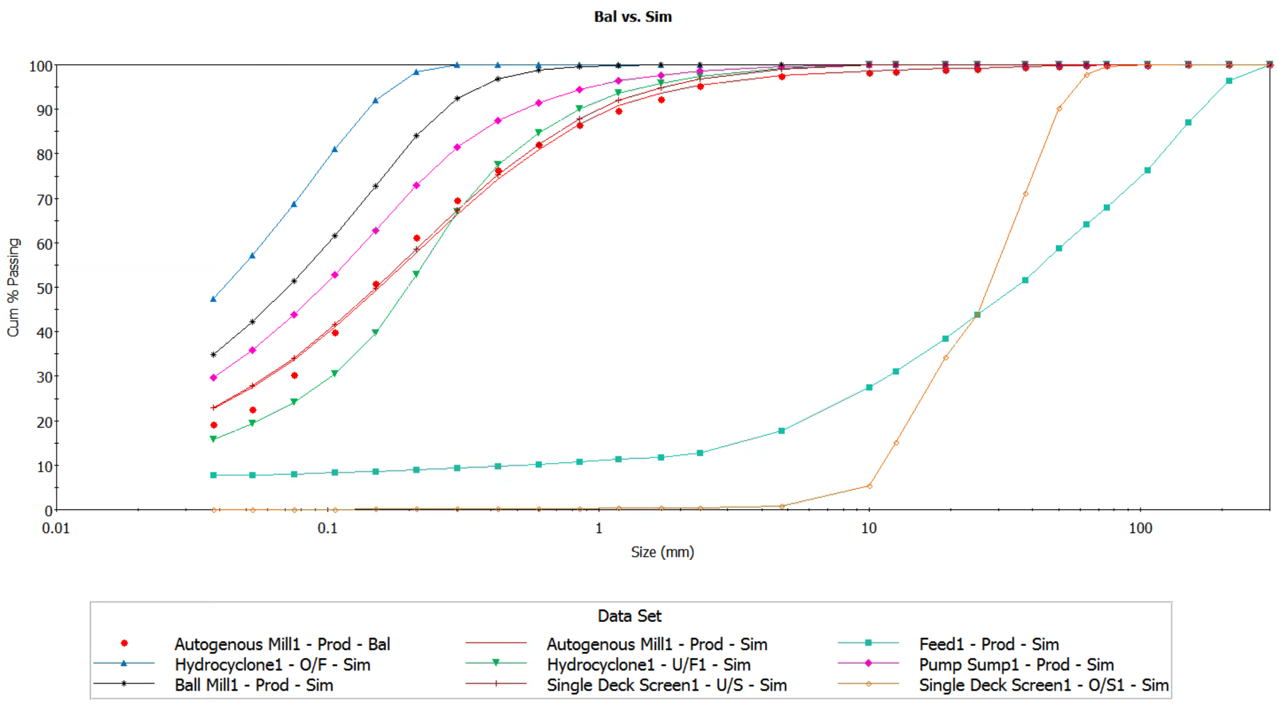


**FIG** 8 – Fitted particle size distributions – December 2019 survey.

**TABLE 8**

Power utilisation analysis – December 2019 survey.

| **Parameter** | **Unit** | **SAB survey 1** | **SABC design characteristics** |
|---|---|---|---|
| Feed rate | t/h | 984 | 1370 |
| Primary feed size, $F_{80}$ | mm | 121 | 121 |
| Product size, $P_{80}$ | µm | 113 | 113 |
| Pebble generation | % Feed | 1.1 | 7.9 |
| | t/h | 13 | 108 |
| SAG mill specific energy | kWh/t | 11.9 | 9.9 |
| Ball mill specific energy | kWh/t | 13.7 | 9.8 |
| Pebble crusher specific energy | kWh/t | 0.0 | 0.1 |
| Total specific energy | kWh/t | 25.7 | 19.8 |
| $f_{SAG}$ | | 1.07 | 1.22 |
| SAG mill pinion power | kW | 11 739 | 13 594 |
| BM pinion power | kW | 13 513 | 13 536 |

The key findings of the survey were as follows:

- The circuit is operating below expected efficiency for the given ore type and circuit configuration, (with pebble crushers off-line). The survey specific energy consumption was 25.7 kWh/t, compared to the design value of 19.8 kWh/t. The energy consumption has increased further from that shown in Table 6 for the two-stage circuit. This is unexpected given that the design ore is expected to be more competent than the ore treated at the time of the survey. This suggests that the circuit is performing inefficiently. The performance will be reviewed once the comminution test work results are received, however this only expected to make the outcome worse, given the feed is predicted to be softer than design.

- Based on the current circuit performance, pebble crushing is not recommended and should remain off-line. At the higher throughput rate, the pebble crushers will however be required to assist management of the SAG load.
- The main sources of inefficiency are believed to stem from operating at below optimal milling density, and poor operation of the classification circuit. The SAG mill was operating at 66 per cent solids w/w, while the ball mill was at 68 per cent solids w/w. It is recommended that a constant flow cyclone control philosophy is implemented to improve the stability of the circuit, giving better control over the water balance.
- The inferred ore characteristics indicate a much higher BWi than previously tested for either the Transitional or Oxide material. This may be indicating circuit inefficiencies associated with either over grinding, the low recirculating load, low ball milling densities or potential issues with the measured feed/product PSDs. Similarly, for the current softer feed blend, a ball mill ball top size of 50 mm may be beneficial.
- Modelling of the circuit found that by increasing the recirculating load to 250 per cent (from 137 per cent currently) is expected to yield a throughput increase and operation closer to the 1370 t/h, indicated from the original design test work data, at the current feed blend (from the current 984 t/h observed during the survey). It is recommended that the vortex finder size is reduced from 290 mm to 230 mm and operating pressure increased to 120 kPa to help facilitate this in conjunction with adopting the constant flow pressure control philosophy.

This first survey also gave an opportunity to assess and refine the survey procedure and cutter requirements for the Gruyere circuit. Another survey is proposed following the transition to more competent ore.

## LINER WEAR

As is the case with most commissioning exercises, extra attention is paid to monitoring the internal conditions of the respective SAG and ball mills checking for items such liner wear or damage, rock and ball charge conditions and conditions of grates. This was the case for the Gruyere circuit with internal mill inspection occurring during planned and opportune downtime events. Liner suppliers were requested to conduct full laser scans of the SAG and ball mill liners with inspections occurring in August, October (see Figure 9) and again in December (see Figure 10). These first surveys provided the critical liner wear profile information required to estimate the reline times. Initial reports from the August and October inspections indicated an expected reline would be required in March 2020 and a planned scan during a December shutdown expected to confirm this. Unfortunately, the December laser scan combined with visual inspections, indicated that the feed end outer lifters and feed end shell lifters had already progressed past the expected wear profile and were providing minimal lift or shell plate protection.

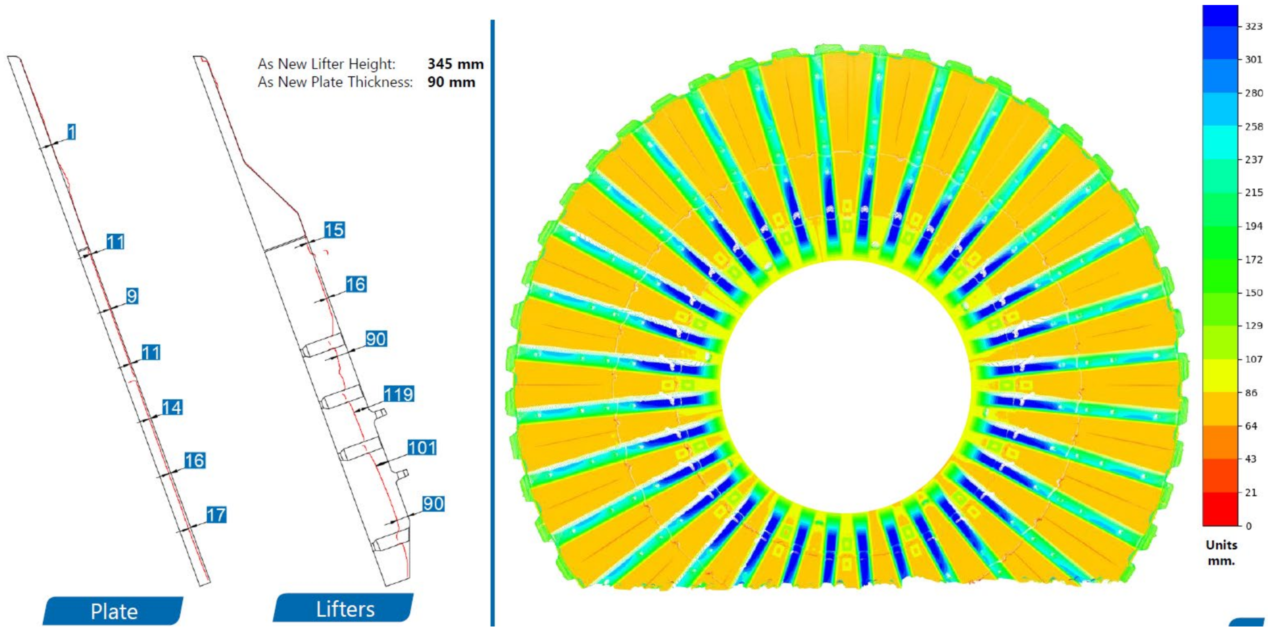


**FIG 9** – SAG feed end liners – October 2019 scan.

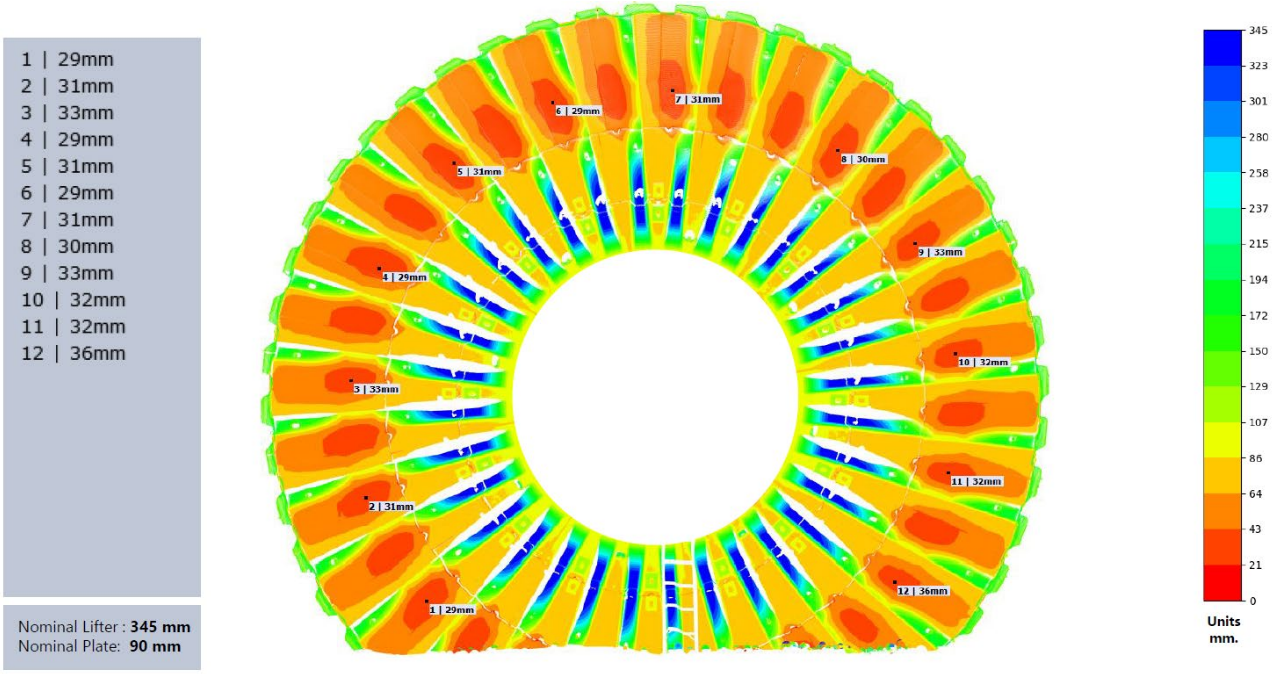


**FIG 10** – SAG feed end liners – December 2019 scan.

A SAG reline was unable to be organised until January and the decision was made to proceed at a reduced throughput rate until this time whilst monitoring closely for signs of liner wear such as leaking bolts. Fortunately, during the project construction and commissioning period a full set of SAG liners had already been purchased and stored on-site. This enabled the reline to occur at the earliest opportunity (within four weeks) and avoid being exposed to a typical supplier delivery time of 16–20 weeks for mill liners, thus minimising the impact on the business.

It was suspected that the liners may have worn prematurely due to a manufacturing fault and in January a selection of worn liners were dispatched for independent metallurgical examination to determine the failure mechanism and any contributing factors to the premature failure. Results from the testing concluded that the liners showed material properties consistent with that typically expected for such an operation, therefore the liners were satisfactory for their intended use. It was recommended that due to the satisfactory liner material and shorter predicted life, a review of the liner material specification and design for the SAG mill be undertaken. While the first set of spare liners were a like for like replication of the original profiles, liner design changes have already been implemented to reduce the likely hood of premature wear.

Using the existing Gold Fields St Ives SAG mill liner design as a starting point, the following short-term improvements are underway in time for the next reline expected in mid-2020:

- Feed end Outer and Middle Liners combined as one (saving 16 pcs to install and remove), plus the addition of White Iron Inserts into the Lifter section, to provide improved wear resistance, rather than increase the lifter height and therefore the amount of extra weight needed.
- Feed End and Middle Shelli Liners lifter height and plate thickness increased in the high wear zone, as shown in scan results.
- Rubber Filler Rings added for handling safety, plus provides weight savings over the steel items.

Improvements are being made to the next design iteration to assist in reducing relines times and further reduce overall set weight for the next shell liner change out expected in late 2020. This includes:

- Shell Liners have been changed to a single row to allow more lifter rows to be installed per inch (turn) of the mill. Refiners found that they could only install one row of the double chord shell liners as the reach was too high, whereas they can install three rows of the single chord liners which should save inching the mill eight times. The mill is currently inched 24 times per reline.
- Pulp Lifters converted to the traditional Single Direction Big Curve (Pump design), more suited to higher pebble extraction rates. Discrete Element Modelling (DEM) is underway for comparing the current Turbo Pulp Lifters to Big Curve.
- Centre Dischargers converted to a modular composite design, same as Gold Fields St Ives operation.

## CONCLUSIONS AND LESSONS LEARNT

Gruyere was discovered in October 2013 and six years later the project had been successfully designed, constructed and commissioned achieving commercial production in October 2019. Gruyere is currently operating at throughput rates significantly exceeding the design throughput and is at the beginning of the 13-year life-of-mine journey of continuous improvement. As the operation stabilises and the Gruyere open pit deepens into transitional and fresh ore types there will be an opportunity to review the mechanical and operational costs of the crushing and grinding circuits. This information will provide a unique opportunity to revisit the internal SABC versus HPGR trade-off study as well as an external comparison with the existing Tropicana operation.

Identifying during the project phase and implementing the MANTA Controls system in conjunction with the EPC has provided the operations with a seamless transition to supervisory control of the SAG and ball mills, cyclones, thickeners and leaching circuits within the first six months of operation. Conducting internal and external design reviews of the entire circuit identified potential bottlenecks early in the project life cycle and while not everything can be addressed, design changes that were implemented have assisted in improving the operability and reliability of the plant.

An important lesson that has been reinforced at the Gruyere operation is the ability of the site to react quickly during commissioning by being well prepared and utilising the operational experience of Gold Fields and Gruyere Project. Ensuring that critical spares have been purchased, ordered and mobilised to site prior to commissioning can mean the difference between a rapid ramp up or continuous delays. Purchase of a full spare set of liners for the SAG and ball mills prior to commissioning minimised the impact of accelerated wear on the SAG mill and alternate sets of discharge grates and cyclone parts enabled for quick optimisation of the circuit.

The Gold Fields St Ives comminution circuit consists of a 10.97 m (36’) SAG mill operating in closed circuit, this experience proved invaluable when commissioning the Gruyere project in SS SAG mode before transitioning to SABC which allowed for a smooth and controlled ramp up of the thickener and leaching circuits at lower volumetric flow rates. It is important to work closely with comminution consultants that have a broad knowledge across the industry and can provide guidance on various scenarios for the client. It is also important to have the confidence to decide what direction to take using the best information available at the time. Then act quickly on that decision. It is for these reasons that by utilising the existing operational and mechanical knowledge from the Gold Fields sites and personnel there has been a rapid ramp up of production at Gruyere.

At the time of this paper, preparations were already well underway to ensure there was a smooth transition to increasing quantities of fresh ore. We can now say after the 2020 COVID-19 delay to the release of the paper that the circuit is now processing up to 1400 t/h on transitional material after optimisation and removal of some downstream bottlenecks. Furthermore, it is averaging around 1080 t/h, on design hardness ore, comfortable exceeding the design capacity of 938 t/h. The grinding circuit was recently surveyed on the hard fresh material and this information will form the basis of a future paper covering the full ramp up and optimisation at Gruyere.

## ACKNOWLEDGEMENTS

The authors wish to acknowledge the support and contribution of the Gold Fields Gruyere operations and maintenance teams.

## REFERENCES

Kock, F. et al. (2015). Rapid Ramp-Up of the Tropicana HPGR Circuit. Proceedings of Advances in Autogenous and Semi-autogenous Grinding and High Pressure Grinding Roll Technology, SAG 2015.

Scinto, P., Festa, A., & Putland, B. (2015). OMC Power-Based Comminution Calculations for Design, Modelling and Circuit Optimization. Proceedings of 47th Annual Canadian Mineral Processors Operators Conference, 271–285.

Putland, B. (2006). Comminution Circuit Selection – Key Drivers and Circuit Limitations Proceedings of Advances in Autogenous and Semi-autogenous Grinding and High Pressure Grinding Roll Technology, SAG 2006.

Siddall, B, Henderson, G & Putland, B. (1996). Factors Influencing Sizing of SAG Mills from Drill Core Samples Proceedings of Advances in Autogenous and Semi-autogenous Grinding and High Pressure Grinding Roll Technology, SAG 1996.

# Development and application of an innovative approach to the beneficiation of serpentine ores for the Bozymchak Concentrator

*R Ventura*[1] *and K Mangulov*[2]

1. MAusIMM, Principal Metallurgist, Core Resources Pty Ltd, Brisbane Qld 4010.
   Email: rventura@coreresources.com.au
2. General Plant Director, KAZ Minerals Bozymchak Mine, Bishkek, Kyrgyz Republic, 720010.
   Email: kenzhitay.mangulov@kazminerals.com

## ABSTRACT

KAZ Minerals operate a copper-gold processing plant in the Kyrgyz Republic. The operation currently processes 1 Mt/a, and with future planned upgrades, intends to be a top ten global copper producer. The Bozymchak plant began operations in 2015. Feed to the plant from the orebody has proven to be different to that originally understood from the initial mine plan. Over the years the Bozymchak processing plant has been adapted to manage this ore variability, with a good degree of success – especially in managing the Talc and Pyrite components of the current ore being treated.

However, the global orebody is highly variable, with up to seven ore zones identified. In particular, Serpentine-containing ores have been identified as a significant issue for future mine planning/processing, with five ore zones containing the majority of Serpentine minerals. These minerals will have a significant impact on plant feed in the future. To help address these future ore issues, KAZ Minerals engaged Core Resources (Core) to assist with developing a revised process flow sheet that will be able to handle the impact of these Serpentine minerals.

This paper outlines the various stages in the development of the revised flow sheet starting from understanding the mineralogy, performing laboratory-scale metallurgical test work, conducting full-scale plant trials treating various proportions of the Serpentine ore to completing an engineering study to develop a suitable flow sheet for the Bozymchak future operations.

## INTRODUCTION

The KAZ Minerals Bozymchak copper-gold processing plant operations have been treating their Wollastonite ore deposits mined by open cut mining method since they started operations. The Wollastonite ore deposits are expected to be depleted in the near to medium term, hence the Serpentinite copper-gold bearing ores have to be mined and treated next into the processing plant. The proposed strategy in the transition stage of mining the Serpentinite ores while the Wollastonite ores are slowly being depleted would be to blend the Serpentinite ore deposits from the Central and Southwestern ore zones first before the other zones of Eastern, Davan and Deep ore deposits.

In this regard, KAZ Minerals requested Core to carry out beneficiation test work for their Serpentinite ores focusing first on the Central and Southwestern ore samples. Test results would then be applied to develop the proposed processing flow sheet option to treat their new Serpentinite ores. As a result, preliminary process engineering works are carried out for the proposed process flow sheet and technology upgrade to treat these new ores at their Bozymchak concentrator.

Extensive test work programs were carried out treating Serpentine ores from November 2018 to November 2019, along with preliminary process engineering works through to December 2019. In relation to this, plant trials were carried out in September 2019 at the KAZ Minerals Bozymchak copper-gold concentrator in Kyrgyzstan, Kyrgyz Republic. Hence, recommendations of practical strategies to treat these new ore deposits were made after applying laboratory test work results and outcomes of the plant trials at Bozymchak copper-gold concentrator.

The future ore reserves for the major five Serpentine ore zones of the Bozymchak copper-gold mine are presented and summarised in Table 1. Among the easily accessible and first to be developed and mined Serpentine ore zone deposits are the Central orebody, which has the largest copper, gold and silver reserves (at 31 per cent of total Serpentine ore reserve), and the Southwestern orebody (at 12 per cent of total Serpentine ore reserve).

**TABLE 1**

KAZ Minerals, Bozymchak Copper-Gold mine – New and future Serpentine ore reserves (Mangulov, 2019).

| Ore zones | Ore type | Ore reserve | Copper | Gold | Silver | Grade | | | Proportion of skarn and serpentinite in total ore | Proportion of each ore zone in total ore |
|---|---|---|---|---|---|---|---|---|---|---|
| | | kt | t | koz | koz | Cu, % | Au, g/t | Ag, g/t | % | % |
| Central | Skarn C1+C2 | 9 100 | 73 360 | 431 | 3 051 | 0.81 | 1.5 | 10.4 | 77 | 31 |
| | Serpentinite C1+C2 | 2 756 | 24 352 | 100 | 529 | 0.88 | 1.1 | 6.0 | 23 | |
| | **Total Skarn+Serpentinite C1+C2** | **11 856** | **97 712** | **531** | **3 580** | **0.82** | **1.4** | **9.4** | **100** | |
| Southwestern | Skarn C1+C2 | 3 205 | 17 093 | 100 | 678 | 0.53 | 1.0 | 6.6 | 67 | 12 |
| | Serpentinite C2 | 985 | 4 963 | 32 | 214 | 0.50 | 1.0 | 6.8 | 21 | |
| | Skarn P1 | 589 | 2 924 | 20 | 131 | 0.50 | 1.1 | 6.9 | 12 | |
| | **Total Skarn+Serpentinite C1+C2+P1** | **4 779** | **24 980** | **152** | **1 024** | **0.52** | **1.0** | **6.7** | **100** | |
| Eastern | Serpentinite C1+C2 | 2 949 | 17 307 | 96 | 354 | 0.59 | 1.0 | 3.7 | 75 | 10 |
| | Serpentinite P1 | 959 | 9 444 | 25 | 98 | 0.98 | 0.8 | 3.2 | 25 | |
| | **Total Skarn+Serpentinite C1+C2+P1** | **3 908** | **26 751** | **122** | **452** | **0.68** | **1.0** | **3.6** | **100** | |
| Davan | Serpentinite C2 | 2 817 | 11 609 | 115 | 248 | 0.41 | 1.3 | 2.7 | 61 | 12 |
| | Serpentinite P1 | 1 822 | 6 979 | 66 | 149 | 0.38 | 1.1 | 2.5 | 39 | |
| | **Total Skarn+Serpentinite C2+P1** | **4 639** | **18 588** | **180** | **397** | **0.40** | **1.2** | **2.7** | **100** | |
| Deep | **Serpentinite P1** | **13 582** | **141 932** | **612** | **4 193** | **1.05** | **1.4** | **9.6** | **100** | **35** |
| All ore zones | Skarn C1+C2 | 12 305 | 90 454 | 531 | 3 728 | **0.74** | **1.3** | **9.4** | 32 | 100 |
| | Serpentinite C1+C2 | 9 507 | 58 231 | 343 | 1 346 | **0.61** | **1.1** | **4.4** | 25 | |
| | Skarn P1 | 589 | 2 924 | 20 | 131 | **0.50** | **1.1** | **6.9** | 2 | |
| | Serpentinite P1 | 16 363 | 158 355 | 703 | 4 440 | **0.97** | **1.3** | **8.4** | 42 | |
| | **Total Skarn+Serpentinite C1+C2+P1** | **38 764** | **309 964** | **1 597** | **9 646** | **0.80** | **1.3** | **7.7** | **100** | |

The Eastern and Davan orebodies (10 per cent and 12 per cent of total Serpentine ore reserves, respectively) are next to be tested at Core, to be followed by plant trials later. The Deep ore zone is estimated to be the largest (but deepest in elevation) at 35 per cent of the total Serpentine ore reserve. However, its development as a reserve is still at the early stage, hence, likely to be developed and mined last due to its depth and accessibility only to underground mining.

A summary of results from both test work and plant trials are presented and discussed in the next sections.

# TEST WORK RESULTS

## Head characterisation and mineralogy

The characterisation results of the Central and Southwestern head samples are summarised in Table 2. Copper content of the Central ore sample is relatively higher, at 1 per cent, than Southwestern ore at 0.86 per cent. Gold contents are similar at 0.65 g/t and 0.64 g/t, respectively, while silver contents are relatively similar at respective levels of 5.80 g/t and 6.10 g/t.

Understanding the basics of minerals processing and its implications is very important in addressing beneficiation issues (Evans and Wightman, 2018), hence identifying the problematic minerals is vital. The magnesium level of the Central ore sample is very high at 20.9 per cent compared with 8.2 per cent on the Southwestern ore sample. This high magnesium content confirms the very high Serpentine mineral content of Central ore sample at 70.1 per cent, more than four times higher than Southwestern ore at 16.3 per cent. Likewise, high magnesium levels also confirm the appreciable amounts of Diopside minerals in both ore samples at 9.7 per cent (Central ore) and 5.5 per cent (Southwestern ore). It is important to note that high Calcite and Andradite minerals are present in the Southwestern ore sample but not in the Central ore sample.

**TABLE 2**

Ore characterisation – Central and Southwestern ores (Core Resources, 2019a).

| Element | Central | Southwestern |
|---|---|---|
| **Cu**, % w/w | 1.00 | 0.86 |
| **Au**, g/t | 0.65 | 0.64 |
| **Ag**, g/t | 5.80 | 6.10 |
| **S**, % w/w | 2.15 | 1.97 |
| **Fe**, % w/w | 5.89 | 10.40 |
| **Ca**, % w/w | 3.25 | 14.70 |
| **Mg**, % w/w | 20.90 | 8.24 |

| Mineral | Central % | Southwestern % |
|---|---|---|
| *Serpentine* | 70.1 | 16.3 |
| *Diopside* | 9.7 | 5.5 |
| *Phlogopite* | 2.4 | 0.8 |
| *Clinochlore* | 1.2 | 1.2 |
| *Calcite* | 1.8 | 16.4 |
| *Talc* | 1.5 | 8.1 |
| *Magnetite* | 2.9 | 4.2 |
| *Chalcopyrite* | 2.6 | 1.6 |
| *Pyrite* | 3.7 | 3.3 |
| *Fluorite* | 1.2 | |
| *Andradite* | | 15.3 |
| *Vesuvianite* | | 1.2 |
| *Quartz* | | 8.0 |
| *Dolomite* | | 6.8 |
| *Ankerite* | | 3.0 |
| *Biotite* | | 1.2 |
| *Wollastinite* | | 2.6 |
| *Iron Hydroxide* | | 1.1 |
| *Other* | 2.8 | 3.6 |
| **Mineral, Sum** | **100** | **100** |
| ***Chalcopyrite : Pyrite Ratio*** | **0.70** | **0.48** |

The Central ore sample also has higher chalcopyrite content than the Southwestern ore sample. Central ore has a chalcopyrite to pyrite ratio of 0.70, while Southwestern ore has a ratio of 0.48. Based on test work results, such lower ratio indicates a certain degree of difficulty in chalcopyrite selectivity against pyrite in the cleaning flotation stages, even with sufficient liberation by ultrafine grinding.

## Copper mineral liberation analysis

The two ore samples analysed were milled to 80 per cent passing 75 µm. Mineral liberation of copper sulphide minerals from the '-106 +53 µm' size fraction of Central ore sample is presented in Figure 1a. Copper sulphide particles are still partially liberated in this fraction. Most of these unliberated minerals are attached with Phyllosilicates and some Oxides-hydroxides, with other Sulphide mineral grain associations.

Similarly, the mineral liberation analysis of the Southwestern ore at the same size fraction as shown in Figure 1b clearly shows that there are roughly equal proportion of unliberated copper sulphide particles as in the Central ore sample. The unliberated copper sulphide particles are attached with Phyllosilicates, some Oxides-hydroxides, other Silicates and other Sulphide minerals.

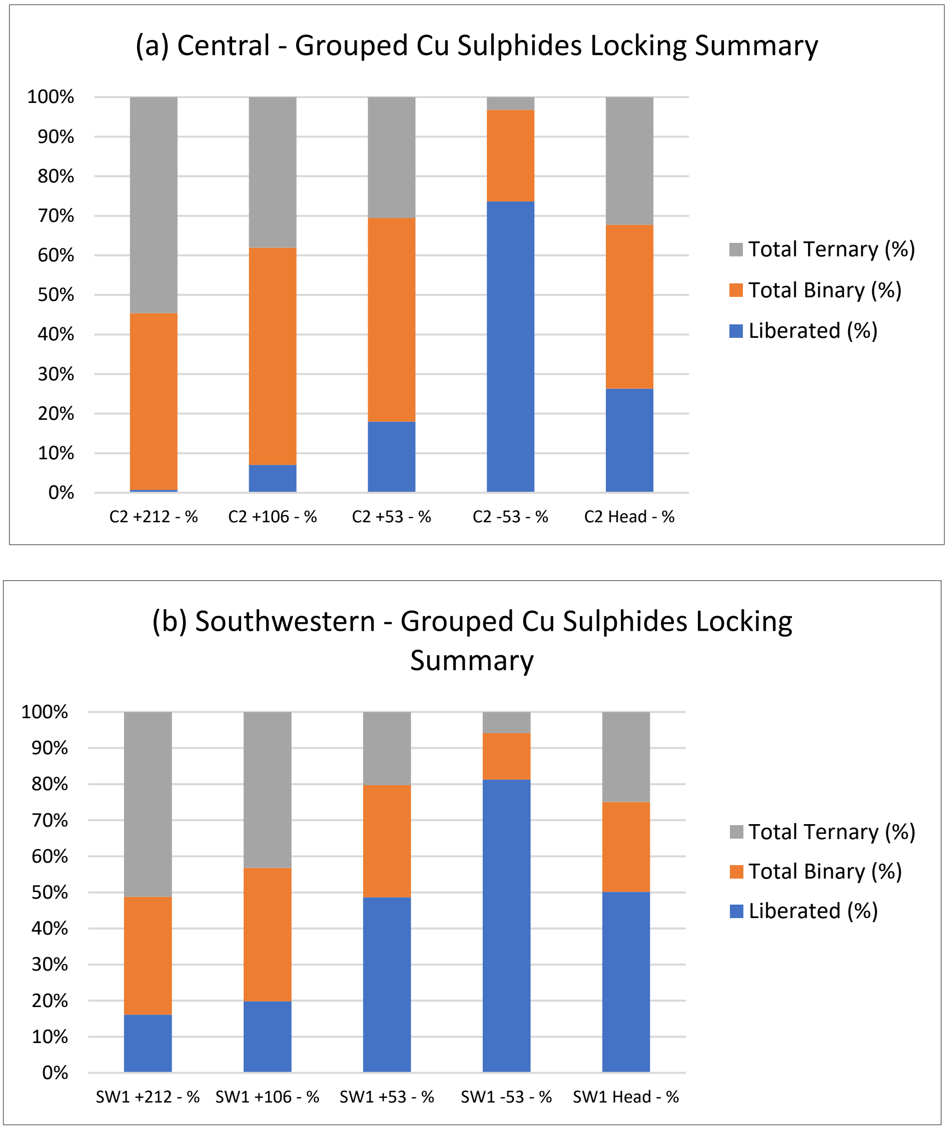


**FIG 1** – Quantitative liberation comparison on '-106 +53 µm' size fractions of (a) Central ore, and (b) Southwestern ore (Core Resources, 2019a).

Clearly, at such grind size, regrinding to a finer particle size range is mandatory in order to achieve better and more sufficient liberation of copper sulphide minerals from gangue minerals prior to cleaning flotation stages. Such liberation analysis guided the approach of improving flotation selectivity and recovery in all of the tests carried out for both Central and Southwestern ore samples.

The qualitative presentations of mineral liberation for both Central and Southwestern ores are shown in Figure 2. The apparent lack of chalcopyrite/pyrite mineral association is noteworthy for both ores. The unliberated copper sulphide mineral grains are mostly attached with non-sulphide minerals like Phyllosilicates and some Oxides-hydroxides, hence, the regrind size indications for cleaning are very fine at less than 20 µm.

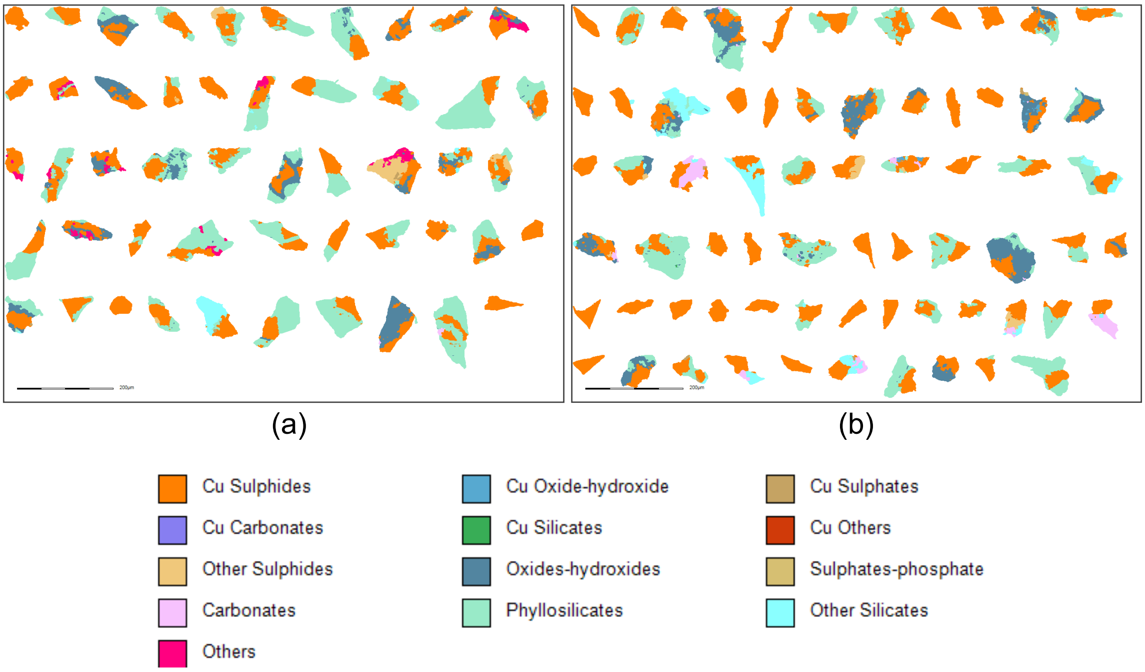


**FIG 2** – Qualitative copper mineral liberation on '-106 +53 µm' size fractions: (a) Central ore, copper sulphide mineral liberation; (b) Southwestern ore, copper sulphide mineral liberation (Core Resources, 2019a).

## Sulphide minerals characterisation and associations

Proper interpretation of mineral associations (as shown in Figure 2), and applying the knowledge of mineral behaviour during beneficiation processes provide good navigational tools to solve issues during processing (Schouwstra and Smith, 2011). For this, Table 3 presents the sulphide minerals characterisation of the Central and Southwestern ores. Mainly chalcopyrite minerals (at 31.4 per cent), with a minor trace of copper sulphate in the form of botryogen-copper mineral (at 0.3 per cent) are present in the Central ore sample. The majority of other sulphides are in the form of pyrite (at 68 per cent), which are likely the host mineral for gold and silver in the Central ore, with minor trace of other sulphides at 0.3 per cent.

On the other hand, the Southwestern ore contains 23.4 per cent chalcopyrite, 1.1 per cent bornite, 0.9 per cent chalcocite, and 0.4 per cent botryogen-copper sulphate. The corresponding amount of pyrite is 72.5 per cent, with 0.8 per cent arsenopyrite, 0.4 per cent sphalerite, and 0.4 per cent other sulphides. Gold-bearing sulphides are likely the pyrite and arsenopyrite minerals, in addition to chalcopyrite and chalcocite minerals.

With the Central ore, the bulk of the copper is chalcopyrite at 99 per cent, and 0.8 per cent as botryogen-copper sulphate, with the remainder of 0.2 per cent as traces of other copper minerals. Likewise, from the Southwestern ore, the majority of copper is chalcopyrite at 76.7 per cent, along with 11.9 per cent as chalcocite, 9.1 per cent as bornite, 0.6 per cent as copper (as native or oxide form), 0.7 per cent as botryogen-copper, with the remainder 1.0 per cent as traces of other copper minerals.

**TABLE 3**

Serpentine ores – Sulphide minerals and copper minerals characterisation (Core Resources, 2019a).

| Mineral group | Sulphide mineral | Central - Sulphur distribution, % | | | | | Southwestern - Sulphur distribution, % | | | | |
|---|---|---|---|---|---|---|---|---|---|---|---|
| | | +212 µm | +106 µm | +53 µm | -53 µm | Head (wt %) | +212 µm | +106 µm | +53 µm | -53 µm | Head (wt %) |
| Cu Sulphides | Chalcopyrite | 27.9 | 27.9 | 31.2 | 41 | 31.4 | 23.3 | 18.4 | 25.9 | 25.9 | 23.4 |
| | Bornite | - | - | - | - | - | 0.6 | 0.7 | 1.4 | 1.6 | 1.1 |
| | Chalcocite | - | - | - | - | - | 1.0 | 0.6 | 1.2 | 0.9 | 0.9 |
| Cu Sulphates | Botryogen Cu | 0.1 | 0.1 | 0.3 | 0.9 | 0.3 | 0.2 | 0.2 | 0.2 | 0.8 | 0.4 |
| Other Sulphides | Pyrite | 71.8 | 71.9 | 68.5 | 57.3 | 68.0 | 73.8 | 78.8 | 68.5 | 68.9 | 72.5 |
| | Arsenopyrite | - | - | - | - | - | 0.5 | 0.7 | 2.3 | 0.5 | 0.8 |
| | Sphalerite | - | - | - | - | - | 0.4 | 0.3 | 0.2 | 0.7 | 0.4 |
| | Others | 0.1 | 0.1 | 0.0 | 0.8 | 0.3 | 0.2 | 0.3 | 0.3 | 0.7 | 0.4 |
| **Total** | | **100** | **100** | **100** | **100** | **100** | **100** | **100** | **100** | **100** | **100** |

| Copper mineral | Central - Copper mineral distribution, % | | | | | Southwestern - Copper mineral distribution, % | | | | |
|---|---|---|---|---|---|---|---|---|---|---|
| | +212 µm | +106 µm | +53 µm | -53 µm | Head (wt %) | +212 µm | +106 µm | +53 µm | -53 µm | Head (wt %) |
| Chalcopyrite | 99.5 | 99.6 | 99.2 | 97.8 | 99.0 | 78.3 | 80.5 | 74.6 | 75.1 | 76.7 |
| Chalcocite | - | - | - | - | - | 13.3 | 11 | 13.8 | 10.9 | 11.9 |
| Bornite | - | - | - | - | - | 5.1 | 7.1 | 9.8 | 11.5 | 9.1 |
| Copper | - | - | - | - | - | 2.2 | 0 | 0.6 | 0 | 0.6 |
| Botryogen Cu | 0.5 | 0.3 | 0.4 | 1.8 | 0.8 | 0.3 | 0.5 | 0.3 | 1.1 | 0.7 |
| Others | - | 0.1 | 0.4 | 0.4 | 0.2 | 0.8 | 0.9 | 0.9 | 1.4 | 1.0 |
| **Total** | **100** | **100** | **100** | **100** | **100** | **100** | **100** | **100** | **100** | **100** |

| Copper content by size | Central - Copper by size distribution, % | | | | | Southwestern - Copper by size distribution, % | | | | |
|---|---|---|---|---|---|---|---|---|---|---|
| | +212 µm | +106 µm | +53 µm | -53 µm | Head (wt %) | +212 µm | +106 µm | +53 µm | -53 µm | Head (wt %) |
| Mass | 33.4 | 22.8 | 14.6 | 29.2 | 100 | 23.2 | 23.9 | 17.3 | 35.6 | 100 |
| Assay | 0.95 | 0.85 | 0.90 | 0.95 | **0.92** | 0.63 | 0.60 | 0.77 | 0.87 | **0.73** |
| **Distribution** | 34.5 | 21.1 | 14.3 | 30.2 | **100** | 20.0 | 19.6 | 18.2 | 42.3 | **100** |

With regards to copper distribution by size, the Central ore has most of its copper in the +212 µm and -53 µm sizes at 34.5 per cent and 30.2 per cent, respectively. The +106 µm size contains 21.1 per cent of the total copper while +53 µm has 14.3 per cent of the total copper. With the Southwestern ore, the -53 µm size has the highest distribution of copper at 42.3 per cent, while +212 µm size has 20 per cent, +106 µm has 19.6 per cent, and +53 µm has 18.2 per cent distribution of the total copper in the ore sample.

## Flotation test work

The locked cycle flotation performance of each ore is summarised in Table 4. The copper recovery and grade achieved for Central ore were 85 per cent and 24.6 per cent respectively, while Southwestern ore gave 83.7 per cent copper recovery and 23.5 per cent Cu grade. Overall, the Central and Southwestern ores displayed inferior flotation performance at the same grind, reagent scheme and flotation conditions employed in treating the current Wollastonite ores at Bozymchak concentrator.

In all test work, slurry viscosity even at lower pulp densities was an issue which resulted in poor selectivity of the copper-gold bearing minerals during flotation. An inferior flotation response is expected due to the presence of elevated Serpentine, Diopside, Calcite and Andradite minerals in the Central and Southwestern ore samples, as observed by Farrokhpay and Bradshaw (2012). The Southwestern ore was nine times higher in Calcite mineral content, and 15 times higher in Andradite mineral content than the Central ore sample (as presented in Table 2), and this appears to have contributed to its inferior and problematic flotation response.

**TABLE 4**

Locked Cycle Flotation performance of Central, Southwestern and Wollastonite ores (Core Resources, 2020).

| Parameter | Central Ore | | Southwestern Ore | | Wollastonite Ore | |
|---|---|---|---|---|---|---|
| Final concentrate | Grade % | Recovery % | Grade % | Recovery % | Grade % | Recovery % |
| Copper (%) – final con | 24.6 | 85.0 | 23.5 | 83.7 | ≥25 | ≥89 |
| Gold (g/t) – final con | | 73.7 | | 77.0 | | ≥80 |
| Silver (g/t) – final con | | 63.1 | | 69.0 | | ≥78 |
| Copper (%) – head | 1.0 | | 0.84 | | 0.52–0.82 | |
| Gold (g/t) – head | 0.65 | | 0.62 | | 1.00–1.40 | |
| Silver (g/t) – head | 5.70 | | 5.20 | | 6.70–9.40 | |

## Impact of two or three stage cleaner flotation

The impact of two or three stage cleaning on the flotation response of the Central and Southwestern ores was determined in a bench-scale rougher-scavenger flotation test, followed by two and three stage cleaner flotation. The plant's primary grind size of 80 per cent passing 75 µm was used for all bench-scale tests. Unground and reground rougher concentrates were tested to simulate current two stage plant cleaner conditions and estimate future fine grinding and three stage fines flotation cleaning circuit.

Figure 3a shows results of the multistage cleaner flotation of ultrafine-ground rougher concentrates derived from Central ore sample. Results indicate that the finer the regrind size (80 per cent passing 10 to 15 µm) with three stage cleaning instead of two, the better the selectivity of copper minerals, hence the higher the copper concentrate grades achieved. Figure 3b shows the results of multistage cleaning flotation of ultrafine-ground and unground rougher concentrates produced from the Southwestern ore sample. The test results clearly show that further ultrafine regrinding of the rougher concentrates prior to multistage cleaning flotation is required. Three stage cleaning flotation, with ultrafine grinding to 80 per cent passing 10 to 15 µm, should be employed in order to produce higher copper grade of final concentrates.

It is evident that producing higher copper grade concentrates from treating pure Central ore material is much harder due to the much higher serpentine content of 70 per cent, even with much higher chalcopyrite to pyrite ratio of 0.70. Liberation issues of copper sulphides and non-sulphide gangue minerals along with very high serpentine content of the Central ore, and the apparent flotation of pyrite minerals, interfere with good flotation selectivity and recovery of copper and gold bearing minerals in treating this ore.

Liberation issues of copper sulphides from non-sulphide gangue minerals along with its serpentine content are still problematic in treating Southwestern ores, but to a lesser degree. Compared with the Central ore cleaning flotation response, Southwestern ore displayed better cleaning flotation performance by producing higher copper concentrate grades with good recoveries, after ultrafine grinding to 10 µm and three stage cleaning. Such results may be due to its much lower serpentine content of 16.3 per cent, even with much lower chalcopyrite to pyrite ratio of 0.48.

Based on these test work results, fine grinding and fines flotation technologies to treat a particle size range of 80 per cent passing 10 to 15 µm are the recommended process upgrades to address the issues of very fine liberation of copper sulphides with non-sulphide gangue minerals. Such very fine regrind size along with depressing the liberated pyrite minerals will enable good copper selectivity to produce higher copper concentrate grades above 23 per cent, at an overall copper recovery above 86 per cent, with acceptable gold recoveries.

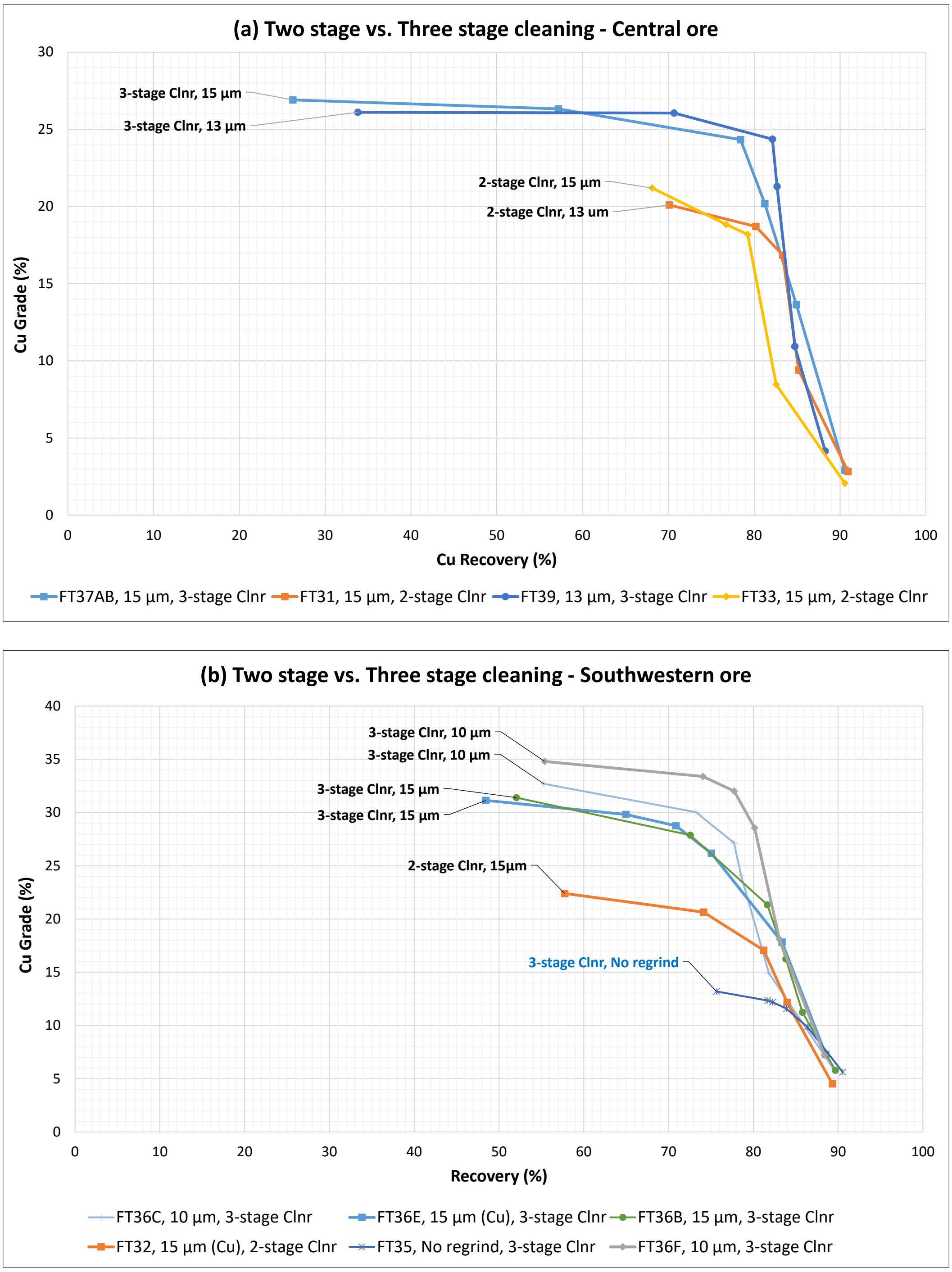


**FIG 3** – Two versus three stage cleaner flotation: (a) Central ore, (b) Southwestern ore (Core Resources, 2019a).

## Impact of Ultrafine Grinding (UFG)

Figure 4a shows the cleaner flotation performance of ultrafine-ground and unground rougher concentrates from the Central ore sample. Evident from the results is that cleaning without further regrinding will not work for the serpentine-rich Central ore deposit. Also, the finer the ultrafine grind size, the better selectivity of copper minerals – an obvious result of better liberation. Therefore, ultrafine grinding of rougher concentrates prior to three stage cleaning flotation is clearly necessary for processing the Central ore sample.

Figure 4b shows the effects of ultrafine-ground and unground Southwestern rougher concentrates in the cleaning flotation stage. Without further regrinding of rougher concentrates prior to cleaning flotation, limited selectivity is expected in treating the Southwestern rougher concentrate. Ultrafine grinding to very fine sizes of 80 per cent passing 10 to 15 µm would be necessary to achieve good selectivity of copper minerals in the cleaning stages of the Southwestern ore.

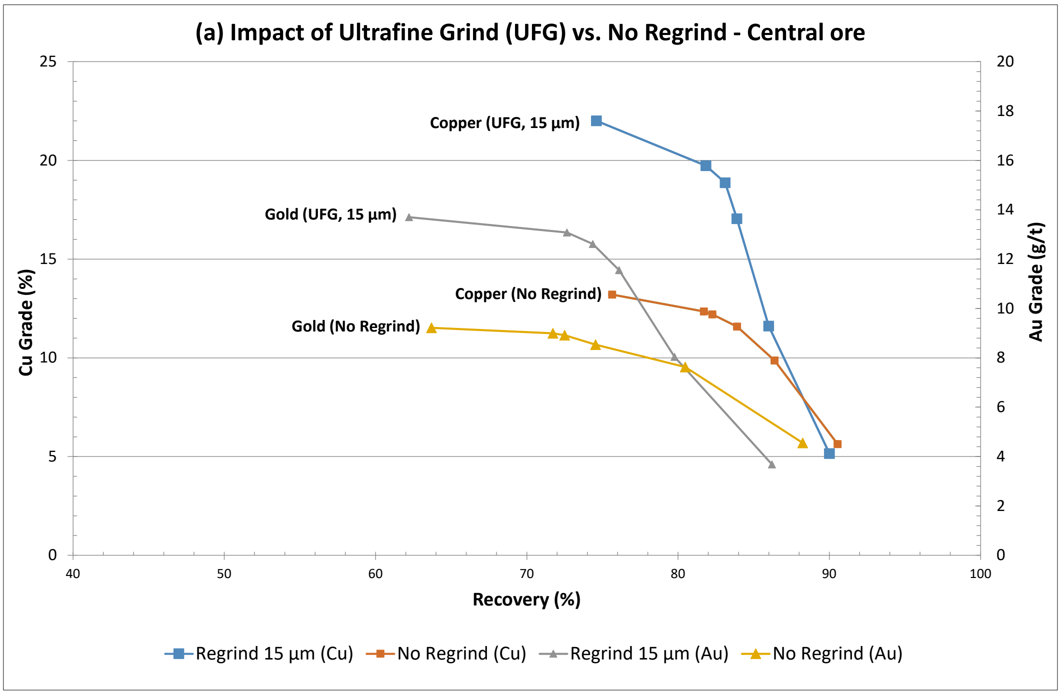


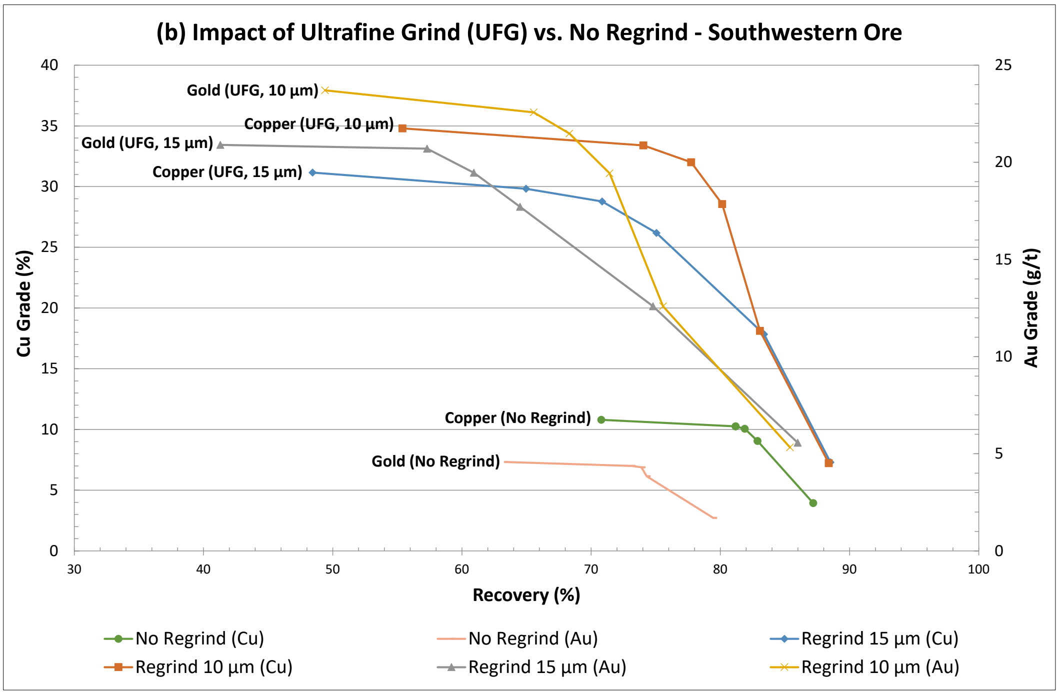


**FIG 4** – Impact of Ultrafine Grinding (UFG): (a) Central ore, (b) Southwestern ore (Core Resources, 2019a).

## PLANT TRIAL DATA AND RESULTS

The site management of KAZ Minerals Bozymchak copper-gold operations arranged a plant trial run at the Bozymchak concentrator soon after the laboratory test work program was completed at Core. The authors were both present in the supervision and execution of the successful plant trial run.

The planned mill feed ore blends for the plant trial were the following:

- Blend 1 – starting blend, current mill feed of 90 per cent Wollastonite ores, plus 10 per cent oxide ores.

- Blend 2 – first trial blend, 75 per cent Wollastonite ores, plus 25 per cent Serpentinite ores.
- Blend 3 – second trial blend, 50 per cent Wollastonite ores, plus 50 per cent Serpentinite ores.
- Blend 4 – final blend (similar to Blend 1), 90 per cent Wollastonite ores, plus 10 per cent oxide ores.

## Plant trial – comminution circuit performance

In the crushing section, the performance of the crushing facility stayed the same as the baseline of 185 t/h crushing rate while feeding all the Blends 1 to 3. However, the final crushed product size was finer by 3.2 per cent for Blend 2, and 0.8 per cent for Blend 3, relative to the baseline of 88 per cent passing 8 mm. This indicates that the introduction of Serpentinite ores with the current Wollastonite ores made the feed blend softer, producing finer crushed product at the same crusher feed rate.

On the milling stage, the Ball mill feed rate was higher at 137 t/h while feeding Blends 2 and 3, an increase of 5.8 per cent from the baseline of 129.4 t/h, confirming that Serpentinite ores blended with the Wollastonite ores made the overall feed blend softer to grind. Final milled product particle sizes were 79.8 per cent and 79.4 per cent passing 75 µm for Blends 2 and 3 respectively, a slightly coarser size than the baseline of 80 per cent passing 75 µm, mainly due to slightly higher feed rate.

In regard to water consumption for milling, Blend 2 consumed 0.96 $m^3$/t and Blend 3 consumed 0.99 $m^3$/t, 3.2 per cent and 6.1 per cent higher than baseline at 0.93 $m^3$/t, respectively. Hence, this suggests that as the proportion of Serpentinite ore increases, the water requirement for milling increases.

## Plant trial trends – mill feed grade, and tailings grade

Figure 5 shows the plant trial trends. From the period of 9 September (night shift), the Bozymchak plant started operating at a steady state, treating Blend 1. This was necessary to establish a baseline steady state operating condition prior to starting to feed Blend 2. The baseline steady state operating conditions lasted for more than five × 12-hour shifts until the midnight of 12 September, when Blend 2 started feeding the Ball mills.

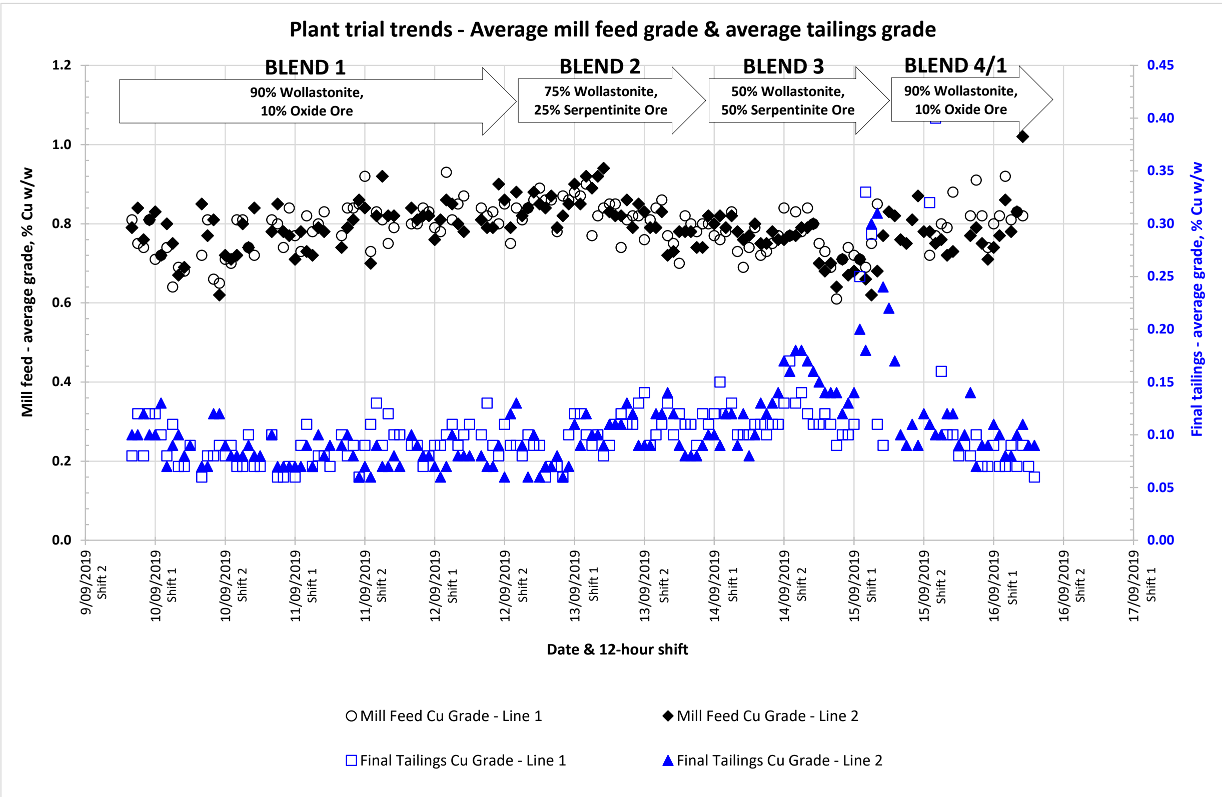


**FIG 5** – Average mill feed grade and average tailings grade – Plant trial trends (Core Resources, 2019b).

As soon as Blend 2 reached the two rougher flotation conditioning tanks, the roughing and scavenging conditions were closely monitored and adjusted to maintain good rougher-scavenger flotation conditions and responses. An almost immediate variation in flotation response was evident in the two split-parallel flotation banks (line 1 and line 2) of rougher-scavenger-cleaner flotation circuits. The froth bubbles became larger with evidence of talc and sulphide particles on the froth from the first and second rougher cells for both lines 1 and 2. This was due to the presence of high serpentine, calcite, talc and andradite minerals in Blend 2 with the increasing amount of Serpentinite ore. Hence, rougher-scavenger concentrates produced were relatively dirtier than in Blend 1. Flotation conditions obviously got worse on both lines when the plant started treating Blend 3.

Particle size distributions (PSD) of the cyclone overflow (or flotation feed) were closely monitored in order to stay within the range of target grind size similar to the current Blend 1 feed. Blend 2 mill feed grades were stable during the first 12-hour shift of operation, 13 September (until 12 midday), then gradually decreasing in copper head grades towards the middle of the second 12-hour shift through to third 12-hour shift in 14 September (until 12 midday). It is important to note, that the final tailings average hourly grades started increasing or trending up, at almost the same time, when the copper head grades started decreasing, or trending down.

## Plant trial trends – copper concentrate grades and recoveries

The trends of copper concentrate grades and recoveries during the Bozymchak plant trial run are presented in Figure 6. It is clear that treating the current mill feed ore represented by Blend 1 achieved and maintained a copper recovery range from 86 per cent to above 90 per cent, with copper grades from 23 per cent to above 30 per cent in most cases.

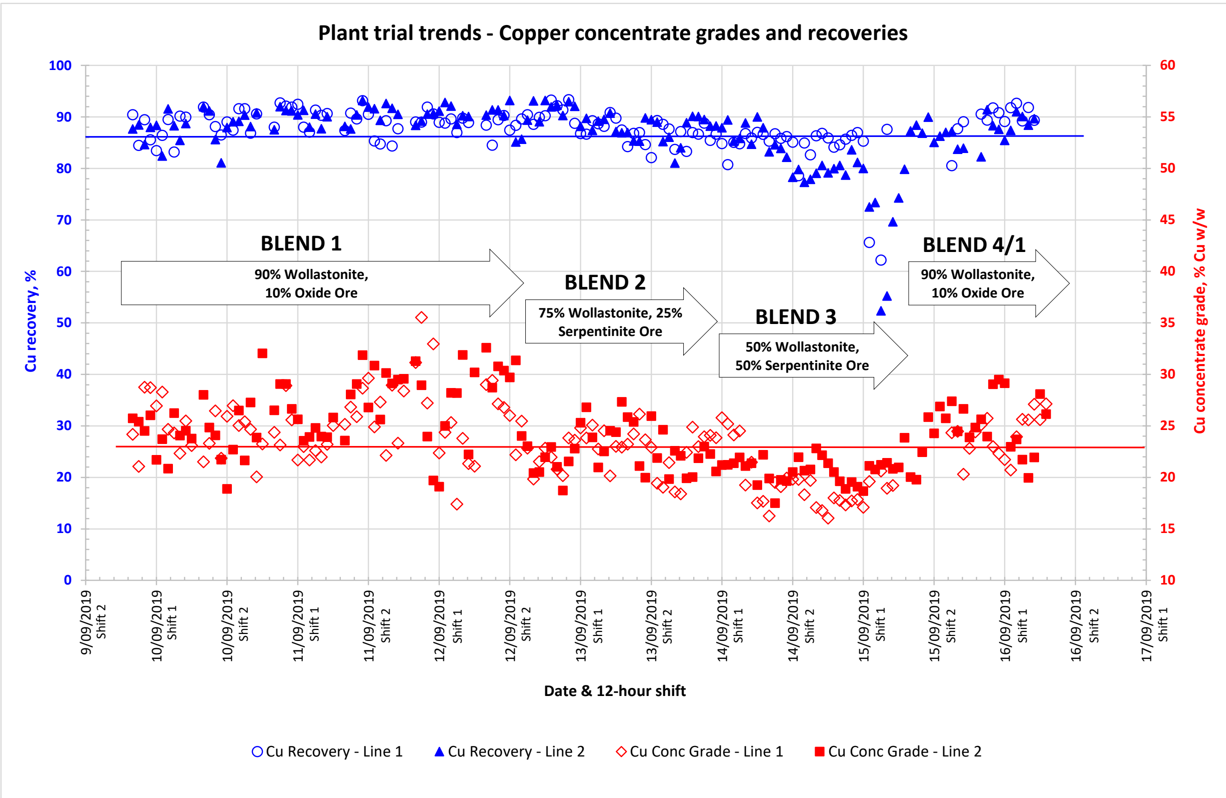


**FIG 6** – Copper concentrate grades and recoveries – Plant trial trends (Core Resources, 2019b).

However, the same trend of copper recoveries started to gradually decrease as soon as Blend 2 was added to the Ball mills and reached the flotation circuits. Correspondingly, the trend of copper concentrate grades started to hover around the target copper grade of 23 per cent, as soon as Blend 2 reached the flotation circuit. The following three 12-hour shifts treating Blend 2 resulted in the copper concentrate grades slowly dropping below the target 23 per cent. This was due to an increase in the circulating loads of pyrite and non-sulphide gangue minerals in rougher 1 and 2 cells, and the cleaner 1 stage.

## Plant trial trends – concentrate dewatering; tailings filtration operation

During the plant trial, the concentrate thickening and filtration were monitored closely especially the per cent moisture of the concentrates (as filter cakes) being produced and bagged for shipment. Due to the remoteness of the Bozymchak mine operations, in order to reduce transport costs it is very important to maintain low levels of moisture of the filtered concentrate cake (average range between 12.5 and 13.5 per cent moisture) before further drying and bagging for shipment. Figure 7 shows the plant trial trends for concentrate thickener underflow per cent solids, filtered cake per cent moisture, and tailings filtration rate along with the levels of tailings filter feed tanks serving the tailings filtration house for dry stacking of final tailings.

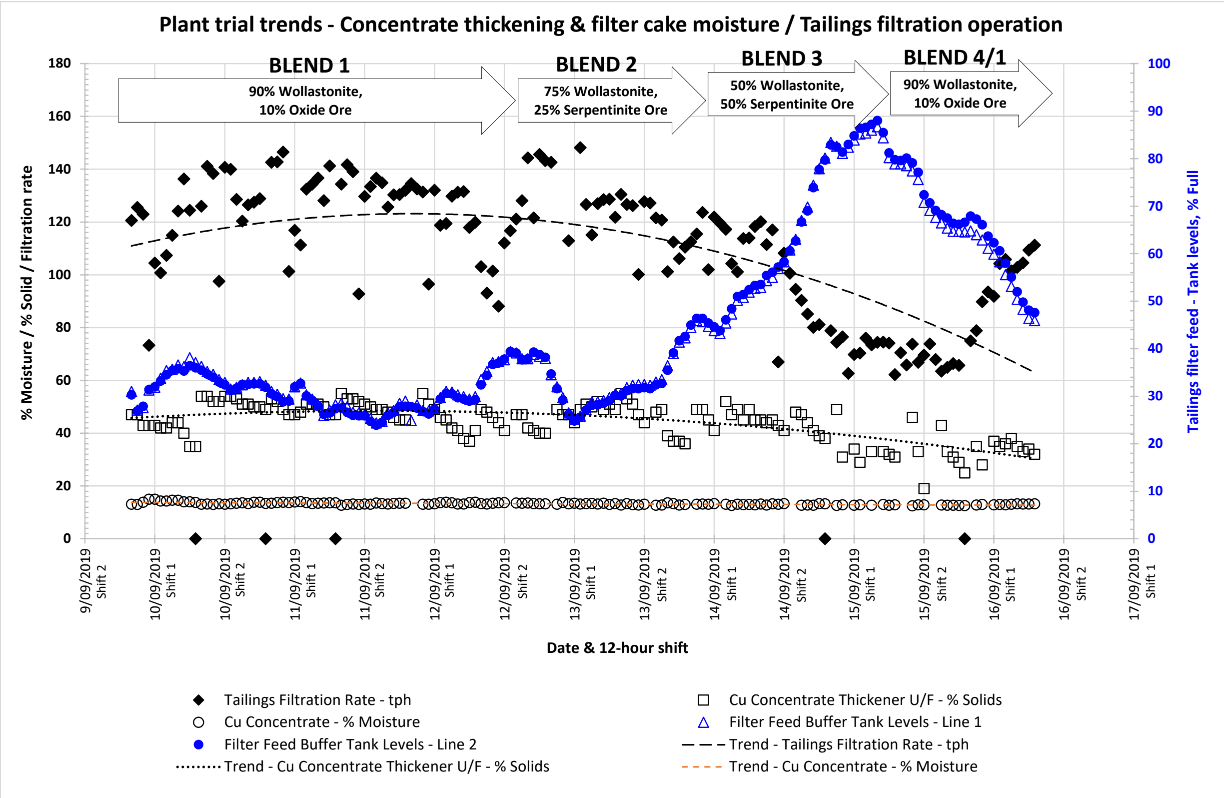


**FIG 7** – Concentrate thickening, filter cake moisture and Tailings filtration – Plant trial trends (Core Resources, 2019b).

Treating Blend 1 ores appeared to be all nice and easy on both flotation lines because treating Blend 1 is the norm for the whole concentrator circuit. As soon as Blend 2 started feeding the two parallel Ball mills, the flotation response on both flotation lines started behaving abnormally with too much frothing, causing froth bubbles to overflow out of the rougher cell launders. This appeared to be due to high levels of talc, calcite and other clay-rich minerals from the Blend 2 ores. Reagent addition levels from the prior Blend 1 feed had to be adjusted lower to suit normal frothing behaviour, while monitoring closely the final concentrate and tailings assays for the grade and recovery target levels.

In the background, the concentrate and tailings thickeners and filters were monitored closely in order to see any adverse effects of the new Blend 2 feed. Filtration rates immediately becoming erratic and then slowed down as evidenced by the decreasing trend in tailings filtration rates. Simultaneously, the trend of tailings thickener underflow slurry tank levels started to increase steadily towards the end of first shift treating Blend 2 feed. Treating Blend 3 next only worsened the situation.

Figure 7 clearly shows the increase in tailings slurry levels on the two filter feed tanks which indicate that tailings filtration rate for dry stacking has slowed down considerably, hence, tank levels start to rise and risk the chance of slurry overflowing. Such issues caused serious bottlenecks on the whole processing plant operation which caused panic with the site management because the plant cannot run with restricted backend filtration for the tailings dry stacking disposal system.

## Plant trial – flotation circuit performance

After the plant trial runs, the Bozymchak metallurgical operations team carried out plant production reconciliation and mass balances. The audited copper flotation recovery performance data is reported in the following Table 5.

**TABLE 5**

Bozymchak Copper Concentrator performance during plant trial runs.

| Flotation Stage | Target Recoveries & Grades | Baseline Target Performance (baseline for the project) | Blend 1 90% Wollastonite / 10% Oxide ore (deviation from the project) | Blend 2 75% Wollastonite / 25% Serpentinite (deviation from the project) | Blend 3 50% Wollastonite / 50% Serpentinite (deviation from the project) | Notes & Comments |
|---|---|---|---|---|---|---|
| Flotation Products | Cu Recovery, % | 86 | 89.5 (+4.0%) | 84.9 (-1.3%) | 75.3 (-12.4%) | Increase of serpentinite proportion in the blend considerably increased losses of metals in the tailings, which led to low recovery performance. Application of the second cleaner increased concentrate grade to 20 -22% but decreased recovery due to increased circulating loads. Lime addition to the cleaner circuit didn't give any improvement effect. |
| | Au Recovery, % | 80 | 80.6 (+0.8%) | 77.9 (-2.6%) | 62.6 (-21.8%) | |
| | Ag Recovery, % | 75 | 78.6 (+4.8%) | 76.8 (+2.4%) | 66.7 (-11.1%) | |
| | Cu Grade in Con, % | 23.2 | 24.4 (+5.1%) | 19.7 (-15.1%) | 22.6 (-2.6%) | |
| | Au Grade in Con, g/t | 38.6 | 37.7 (-2.3%) | 27.2 (-29.5%) | 27.0 (-30.1%) | |
| | Ag Grade in Con, g/t | 193.8 | 313.2 (+61.6%) | 216.5 (+11.7%) | 244.8 (+26.3%) | |
| | Cu Grade in Tails, % | 0.12 | 0.09 (-25.0%) | 0.12 (0%) | 0.17 (+41.7%) | |
| | Au Grade in Tails, g/t | 0.31 | 0.28 (-9.7%) | 0.31 (0%) | 0.38 (+22.6%) | |
| | Ag Grade in Tails, g/t | 1.52 | 1.96 (+28.9%) | 2.2 (+44.7%) | 2.7 (+77.6%) | |
| *Head Grade* | *Cu Grade, %* | *0.83* | *0.83* | *0.77* | *0.67* | Head Grades consistently decreased from Blend 1 to Blend 3. |
| | *Au Grade, g/t* | *1.50* | *1.40* | *1.35* | *1.00* | |
| | *Ag Grade, g/t* | *5.95* | *8.95* | *9.17* | *7.93* | |

The baseline copper, gold and silver recovery targets were 86, 80 and 75 per cent, respectively.

The current plant feed of Blend 1 achieved 89.5 per cent average copper recovery, at least 4 per cent higher than the baseline target. Gold recovery was 80.6 per cent and silver recovery was 78.6 per cent, an increase of 0.8 and 4.8 per cent from baseline target levels, respectively.

Blend 2 achieved 84.9 per cent average copper recovery, a decrease of 1.3 per cent lower than baseline target. Gold recovery was 77.9 per cent, a decrease of 2.6 per cent from baseline, while silver recovery was 76.8 per cent, an increase of 2.4 per cent above baseline target.

Blend 3 achieved only 75.3 per cent average copper recovery, a drop of 12.4 per cent from the baseline target. Gold recovery was only 62.6 per cent (drop of 21.8 per cent from baseline target), while silver recovery was only 66.7 per cent (an 11.1 per cent decrease from the target baseline).

With regards to the metal losses in the final tailings, the audited rejected metal values are as follows.

The baseline copper loss to the final tailings was 0.12 per cent, while baseline gold loss was 0.31 g/t Au, and baseline lost silver was 1.52 g/t Ag.

The performance of the current plant feed (Blend 1) rejected 0.09 per cent copper in the final tailings, a 25 per cent reduction in copper losses to final tailings. Gold lost to tailings was 0.28 g/t Au (a 9.7 per cent decrease in gold losses), while silver losses were 1.96 g/t Ag (an increase of 28.9 per cent in silver losses) to final tailings.

The treatment of Blend 2 saw 0.12 per cent copper losses into the final tailings, which matched the baseline target copper losses to tailings. Gold losses averaged at 0.31 g/t Au which is equivalent to the baseline target of gold losses to tailings. Silver losses, however, were 2.2 g/t Ag, a 44.7 per cent increase in silver losses to tailings from the baseline target level.

Additionally, the treatment of Blend 3 saw 0.17 per cent copper losses into the final tailings, a 41.7 per cent increase in copper losses to tailings from the baseline target. Gold losses were 0.38 g/t Au, a 22.6 per cent increase in gold losses to tailings relative to the baseline level. Silver losses were 2.7 g/t Ag, a significant 77.6 per cent increase in silver losses from the baseline level.

## Concentrate thickening and filtration performance

To fully evaluate the downstream effects of treating the new Serpentinite ores, the operating performance of both the concentrate thickener and the concentrate filters were monitored, recorded and analysed. The following data and information were gathered and recorded as summarised in the following Table 6.

**TABLE 6**

Summary of concentrate thickening and filtration plant performance during plant trials.

| Stage | Parameters | Baseline Target Performance | Blend 1 90% Wollastonite / 10% Oxide ore (deviation from the project) | Blend 2 75% Wollastonite / 25% Serpentinite (deviation from the project) | Blend 3 50% Wollastonite / 50% Serpentinite (deviation from the project) | Note & Comments |
|---|---|---|---|---|---|---|
| Concentrate Thickening | Density of thickened product, % | 55 | 47.8 (-13.0%) | 43.5 (-20.9%) | 32.9 (-40.1%) | Observed decrease of concentrate density due to the lack of material. Turbidity value for the thickener overflow according to the process-flow diagram - not more than 50 NTU |
| | Thickener overflow turbidity, NTU | ≤50 | 34.4 (-31.2%) | 31.2 (-37.6%) | 23.4 (-53.2%) | |
| Concentrate Filtration | Moisture of cake from filter press, % | 12 | 13.23 (+10.2%) | 13.02 (+8.5%) | 12.71 (+5.9%) | Changes in concentrate moisture are insignificant. |

The concentrate thickener underflow density baseline target level was 55 per cent solids. The current plant feed Blend 1 achieved 47.8 per cent solids underflow which is 13 per cent lower than baseline target. Blend 2 reported 43.5 per cent solids, a 20.9 per cent lower than baseline underflow target. Blend 3 achieved 32.9 per cent solids, a significant reduction of 40.1 per cent from the baseline underflow target.

Concentrate thickener overflow turbidity levels were recorded and referenced to the baseline level of 50. Blend 1 overflow gave an average turbidity reading of 34.4, 31.2 per cent lower than baseline of 50. Blend 2 showed an average turbidity reading of 31.2, 37.6 per cent lower than baseline level, while Blend 3 reported a very low average turbidity reading of 23.4; a 53.2 per cent lower than baseline target level.

With regards to concentrate filtration, the baseline moisture target level was 12.0 per cent. Current mill feed of Blend 1 produced an average per cent moisture of 13.2 per cent which is 10.2 per cent higher than baseline target. Blend 2 reported an average per cent moisture of 13.0 per cent which is 8.5 per cent higher than baseline target. Blend 3 produced an average moisture level of 12.7 per cent, only 5.9 per cent higher than target moisture level. It was evident that per cent moisture of final concentrates were slightly lower than the levels achieved by the current mill feed (Blend 1) of the plant.

## Tailings thickening and filtration (dry stacking) performance

To fully evaluate the downstream effects of treating the new Serpentinite ores, the operating performance of both the tailings thickener and tailings filters for dry stacking were monitored, recorded and analysed. The recorded data and information are summarised as follows in Table 7.

**TABLE 7**

Summary of tailings thickening and filtration for dry stacking performance during plant trials.

| Stage | Parameters | Baseline Target Performance | Blend 1 90% Wollastonite / 10% Oxide ore (deviation from the project) | Blend 2 75% Wollastonite / 25% Serpentinite (deviation from the project) | Blend 3 50% Wollastonite / 50% Serpentinite (deviation from the project) | Note & Comments |
|---|---|---|---|---|---|---|
| Tails Thickening | Density of thickened product, % | 50 | 61 (+22.0%) | 60 (+20.0%) | 60 (+20.0%) | Observed increase of % solids in the thickeners' overflows. Turbidity value for the thickener overflow according to the process-flow diagram - not more than 50 NTU |
| | Thickener overflow turbidity, NTU | ≤50 | 43.9 (-12.2%) | 42.2 (-15.6%) | 50.3 (+0.6%) | |
| Tails Filtration | Tailing Filtration Facility (TFF) performance, tph | 125.4 | 124.2 (-0.9%) | 103.3 (-17.6%) | 66.2 (-47.2%) | TFF performance drops by 17.6% at 25% serpentinite blend, and by 47.2% at 50% serpentinite blend. |
| | Cake moisture from Disc Filters, % | 14 | 11.7 (-16.4%) | 12.3 (--12.1%) | 13.7 (-2.1%) | |

The tailings thickener underflow density baseline target level was 50 per cent solids. The current plant feed Blend 1 delivered 61 per cent solids underflow which is 22 per cent higher than baseline target. Blend 2 produced 60 per cent solids, a 20 per cent higher than baseline underflow target. Blend 3 also achieved 60 per cent solids, a 20 per cent improvement from the baseline underflow target.

Tailings thickener overflow turbidity levels were recorded and referenced to the baseline level of 50. Blend 1 tailings thickener overflow produced an average turbidity reading of 43.9, 12.2 per cent lower than baseline of 50. Blend 2 produced an average turbidity of 42.2, a 15.6 per cent lower than baseline level, while Blend 3 achieved a higher average turbidity reading of 50.3 per cent which is 0.6 per cent higher than baseline level.

With regards to tailings filtration for dry stacking, the baseline moisture target level was 14.0 per cent. Current mill feed Blend 1 produced an average per cent moisture of 11.7 per cent which is 16.4 per cent lower than baseline target. Blend 2 produced an average per cent moisture of 12.3 which is 12.1 per cent lower than baseline target. For Blend 3 the average moisture level was 13.7 per cent, only 2.1 per cent lower than target moisture level. It is clear that per cent moisture of filtered tailings were lower than the target level of 14 per cent w/w for dry stacking of tailings solids on-site during the plant trials.

Finally, the rates of tailings dewatering for dry stacking were closely monitored and recorded because this is the most important backend unit operation for the whole Bozymchak operations. The baseline filtration rate is 125.4 t/h. The current mill feed Blend 1 produced an average filtration rate of 124.2 t/h (0.9 per cent lower than baseline target). Blend 2 produced an average of 103.3 t/h filtration rate (17.6 per cent lower than target level). Blend 3 produced a very slow filtration rate of 66.2 t/h (a 47.2 per cent lower than the baseline target level).

## CONCLUSIONS

The test data, results and technical conclusions presented in this paper have been used in real plant operation applications in Bozymchak copper-gold concentrator. The operational data gathered during the plant trials helped Core and the operating team at Bozymchak to determine the following.

With the current flow sheet, reagent scheme and plant conditions and configuration, the Serpentinite ore levels of 5.0 to 7.5 per cent mixed with 92.5 to 95.0 per cent Wollastonite ore appears to be the most optimum proportion of Serpentinite to Wollastonite ore blend to achieve good concentrator performance of mill throughput, concentrate grade, and metals recovery.

For a blend of up to 15 per cent Serpentinite ore and 85 per cent Wollastonite ore, good concentrator performance is possible with additional reagent scheme optimisation including the use of better copper-gold collector, and depressants for pyrite, talc and other non-sulphide gangue minerals.

With a blend up to 25 per cent Serpentinite ore and 75 per cent Wollastonite ore, it is only possible to achieve good copper-gold recoveries at saleable copper grades with more effective reagents (collector, frother and depressant), as well as an increase in tailings filtration rate of the ceramic disc filters by means of better flocculants and filter aides in the tailings filtration stage. Existing production rate capacities of units of equipment in crushing, milling, tailing and concentration thickening are sufficient. For this, regrind and cleaning circuit capabilities would need to be upgraded.

For a much higher blend of 50 per cent Serpentinite and 50 per cent Wollastonite, the following concentrator upgrades must be implemented before such a high proportion of Serpentinite ores can be successfully treated.

The use of more effective and selective flotation reagents including copper-gold collector, more selective frother, and more effective depressant for talc, calcite, pyrite and other non-sulphide minerals from the Serpentinite ores.

Expansion of the rougher circuit to handle lower per cent solids and slower flotation kinetics due to high levels of non-sulphide readily floatable fine gangue mineral particles.

Upgrade of the cleaner circuit by fine grinding of the cleaner flotation feed in order to increase liberation of the locked fine copper minerals, coupled with the installation of a high shear flotation cell (like a Jameson Cell™ for cleaning duties) which is known to be efficient in floating fine copper-gold bearing sulphide particles at grind size range of 80 per cent passing 10 to 15 μm.

A more effective flocculant should be employed in the tailings thickener to remove the bottleneck of tailings filtration to meet the dry stacking rate requirement.

Increase the filtration rate of thickened tailings material by means of filter upgrades via additional filter press units to supplement the existing ceramic filters.

Continue with laboratory test work and process engineering to better understand the impacts of treating the higher blend of Serpentinite ore on circuit performance.

Together the team from Core and KAZ Minerals successfully developed and applied an innovative approach to evaluate the effects of upcoming ore changes through the Bozymchak processing plant.

## ACKNOWLEDGEMENTS

The authors would like to acknowledge and thank the site management of KAZ Minerals Bozymchak copper-gold mine operations for giving consent and approval for presenting this paper. Furthermore, acknowledgement to all the members of the Bozymchak Process Plant operating team including their Technology Consultant, Mr Artyom Trokhimchuk, and his personal assistant Mr Roman Skvortsov for their full support, on and off-site, during the plant trial runs.

Acknowledgement and gratitude are also given to David Cavanagh, Cathy Mitchell, James Rowe and Rob Coleman of the Core Group for their input into the test work and report.

## REFERENCES

Core Resources, 2019a. Interim Report 1 – Determine optimum conditions for Locked Cycle Tests, Core Report No. CM1093C-002.

Core Resources, 2019b. KAZ Minerals – Bozymchak Cu-Au Mine, Site visit, Plant trial run, and other tests, Core Site Exit Presentation Report, September 2019.

Core Resources, 2020. KAZ Minerals – Bozymchak Operations, Engineering Study on Serpentinite Ore Processing, Core Report No. CM1093E-001.

Evans, C L and Wightman, E M, 2018. Understanding minerals in minerals processing – the basics and beyond, 14th AusIMM Mill Operators' Conference 2018/Brisbane, Qld, 29–31 August 2018.

Farrokhpay, S and Bradshaw, D, 2012. Effect of Clay Minerals on Froth Stability in Mineral Flotation: A Review, Paper No. 313, XXVI International Mineral Processing Congress (IMPC) Proceedings 2012, New Delhi, India, 24–28 September 2012.

Mangulov, K, 2019. KAZ Minerals – Aspects of development on concentration procedure for Serpentinite ores of Bozymchak mine, KAZ Minerals Management Presentation Report, September 2019.

Schouwstra, R P and Smith, A J, 2011. Developments in mineralogical techniques – What about mineralogists? Minerals Engineering, 24: 1224–1228.

# Recent improvements in ore sorting at the Renison Tin Concentrator – target 1 Mt/a

*B Wraith[1], J Resta[2] and J Welmans[3]*

1. Senior Metallurgist, Bluestone Mines Tasmania JV, Zeehan Tas 7469.
   Email: ben.wraith@bluestonetin.com.au
2. Technical Manager – Metallurgy, Bluestone Mines Tasmania JV, Zeehan Tas 7469.
   Email: justin.resta@bluestonetin.com.au
3. Processing Manager, Bluestone Mines Tasmania JV, Zeehan Tas 7469.
   Email: johan.welmans@bluestonetin.com.au

## ABSTRACT

Bluestone Mines Tasmania JV, Tasmania Tin Operations recognised value in mining at or near to 1 Mt/a. However, the Renison Tin concentrator is restricted at 750 kt/a. The solution chosen was to upgrade the Ore through XRT Ore Sorting via the removal of waste material within the Crushing Circuit. In 2018 a three-stage crushing circuit coupled with two XRT ore sorters were installed. The ore sorting circuit contains a triple deck dry screen for initial classification, a wet screen for secondary classification and feed preparation, two XRT ore sorters targeting different size fractions, and an EM sorter to separate waste into Non-Acid Forming (NAF) and Potentially Acid Forming (PAF) waste. Challenges such as processing multiple ore sources and variable operating conditions require agile planning and clear operating strategies. Tools utilised to achieve this are: plant surveys including mass balances and process modelling, monitoring of particle size delivered to the ROM and fed to the crushing circuit, ROM pad management and blending based on grade, particle size distribution and amenability to XRT sorting. This paper will explore these tools in conjunction with good Mine to Mill and Geo-metallurgy practices in order to overcome challenging conditions and deliver value and process successfully at 1 Mt/a rates.

## INTRODUCTION

The Renison ore sorting circuit was commissioned in July 2018 as part of a three-stage crushing and ore sorting installation. The circuit suffered an extended commissioning and ramp-up period due to a variety of mechanical, operational and machine related issues. These issues regularly severely impacted sorting performance for the initial seven months of operation. However, beyond mid-January 2019 metallurgical performance of the sorting circuit has been significantly more reliable despite various ongoing operational and maintenance challenges.

### Background

Pre-concentration of ore is used to remove waste minerals early in the mineral concentration process to minimise unnecessary higher cost downstream processing of this material, and effectively increase ROM throughput rate. It can also be used to improve resource utilisation and increase plant head grade, resulting in increased metal production.

The Project Manager (Robinson, 2019) states that pre-concentration of ore at Renison was previously undertaken through a Heavy Medium Separation (HMS) plant which operated from December 1974 until March 1993. The process involved separation of a -12.5 mm +1.7 mm feed material into a 'sinks' and 'floats' fraction at a heavy medium SG of around 2.8. On average 24 per cent of the original ROM ore was rejected to the 'floats' fraction for the loss of between 2.4–3.5 per cent of the tin contained in the ROM ore. The HMS plant historically achieved 'reject' (floats) grades of around 0.19 per cent Sn.

From the late 1980s there was a steady deterioration in the HMS section as resources became scarcer. The HMS section was eventually shutdown due to a combination of reduced mining rates and high operating costs; of which high ferrosilicon medium usage was a major contributor.

X-ray Transmission (XRT) ore sorting aims to separate gangue particles from particles containing valuable minerals by measuring differences in atomic density. Cassiterite has a high density. Particles of high density can be detected and accepted whilst low density particles are rejected, thereby concentrating the valuable cassiterite minerals. Solenoid operated air jets are used to blow either 'accepts' or 'rejects' into a different collection chute as they fall from the conveyor discharge.

In 2015/2016, the increased mining of bulk stopes at Renison and a reduction in mined head grade generated interest in ore pre-concentration using ore sorting.

## Renison Tin Concentrator flow sheet

The Renison flow sheet is complex and consists of crushing, grinding, sulphide flotation, gravity separation, desliming, oxide flotation and concentrate leaching. The plant generates four separate tailings streams. The inclusion of the ore sorting circuit in 2018 added a fifth tailings stream. At the simplest block flow level Figure 1 depicts the major changes to the overall flow sheet.

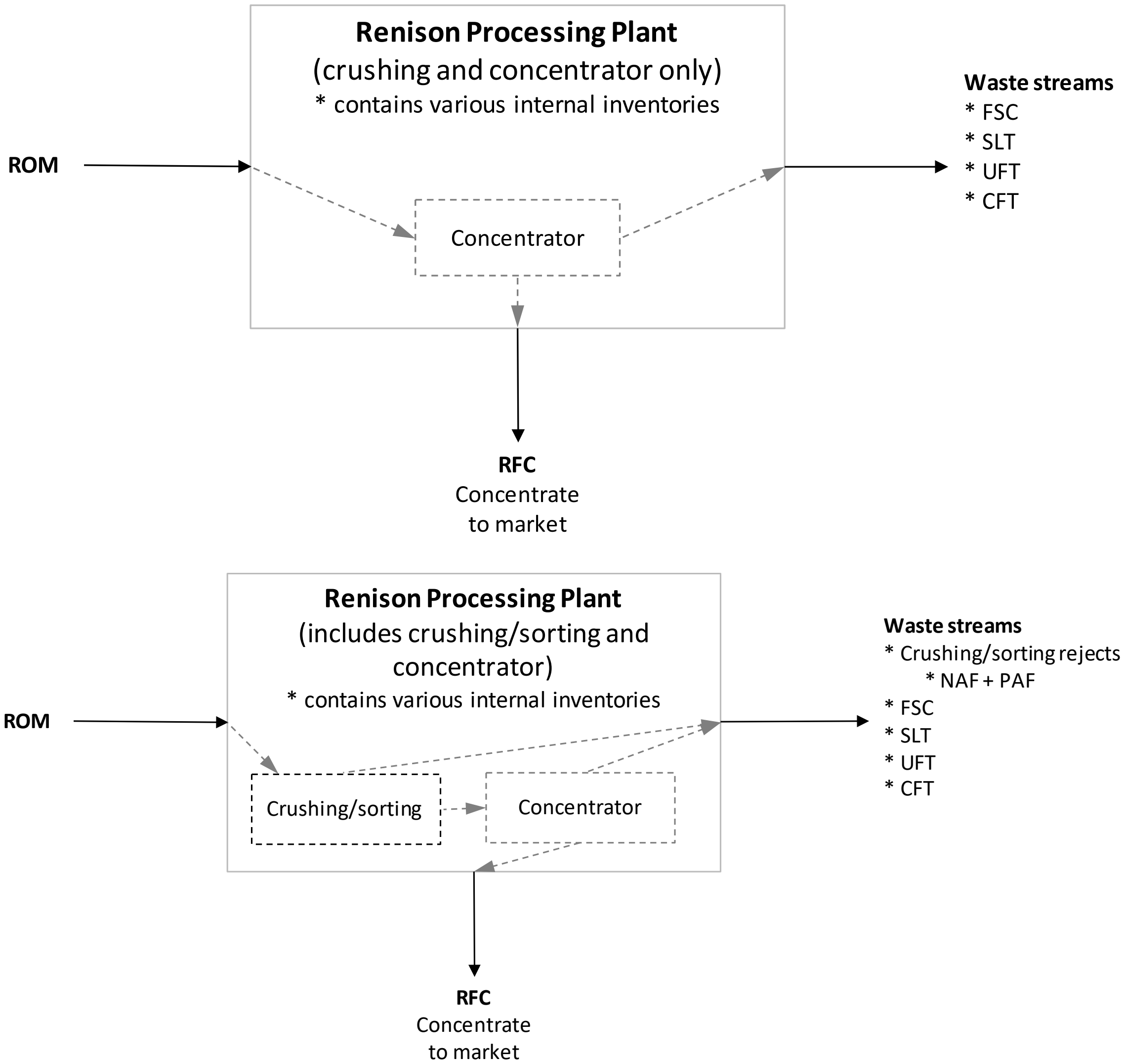


**FIG 1** – Basic block flow diagram.

## Sensor selection and circuit design

Ore sorting laboratory scale testing of 18 different rock domain types from Renison was undertaken in 2015–2016 by both Tomra and Steinert. The rock samples included different types of mineralised and un-mineralised samples from Crimson Creek Formation (CCF), Red Rock Member (RRM), Renison Bell Member (RBM), Dolomite No. 2, Dalcoath Member (DM) and Federal Bassett Fault (FED).

The Tomra results indicated that 37.4 per cent of the ore sorter feed mass could be rejected for the loss of 2.0 per cent of the tin metal. Steinert did not assay the rock samples but based upon hand sorting of mineralised rocks and waste rocks estimated that 45 per cent of the ore sorter feed mass could be rejected for the loss of 10 per cent of the mineralised rock. These results were achieved using an X-ray Transmission (XRT) ore sorting method.

Three bulk samples were then tested by Tomra and Steinert. The samples were obtained from the current main sources of ore: Lower Federal, Central Federal Bassett and Area 4. Samples were sized and the +20 mm -45 mm fractions were fed to an ore sorting unit having a 600 mm wide conveyor operating at 2.7 m/s. Sample fractions ranged from 250 kg to 560 kg. ROM ore screened finer than the minimum ore sorter feed size (<20 mm) bypasses the ore sorting system.

The Tomra results averaged rejection of 32.9 per cent of the ore sorter feed mass for the loss of 1.8 per cent of the tin. The Steinert results averaged rejection of 39.4 per cent of the ore sorter feed mass for the loss of 3.4 per cent of the tin. In operation, ore sorter settings can be adjusted to provide varying rejection/loss ratios.

### *Crushing circuit*

A 60 t live capacity ROM ore bin holds the crushing plant feed material. A Sandvik SW1052H vibrating grizzly feeder feeds material from the ROM ore bin to the jaw crusher. The jaw crusher is a Sandvik CJ409 single toggle jaw crusher and operates at a nominal CSS of 100 mm.

Jaw crusher product are transferred by a 1200 mm wide belt to the cone crusher discharge conveyor where it combines with cone crusher product before being fed to the primary control screen as shown in Figure 2.

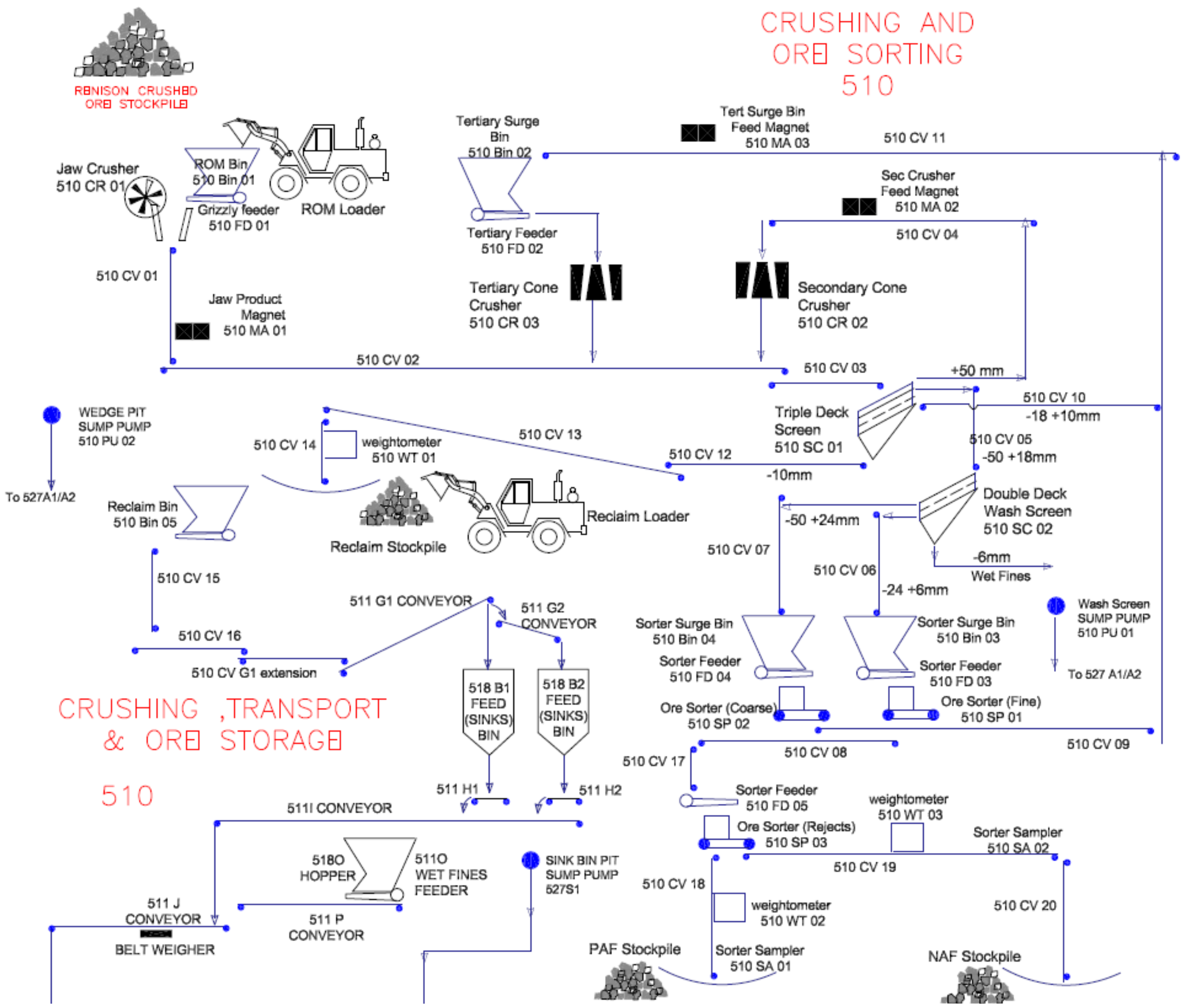


**FIG 2** – Crushing and sorting process flow diagram.

The primary crusher product is combined with secondary and tertiary crusher product and fed to a Sandvik SC2463 circular motion inclined, vibrating, triple deck screen. The primary screen has a mechanically operated discharge chute to facilitate chute inspection and maintenance.

The control screen top deck oversize (+60 mm) is fed to the secondary crusher, which is a Sandvik CS430 cone crusher with 160 kW motor. The CSS is controlled by a hydroset system and ASRi crusher control system. The crusher operates with a 30–38 mm CSS. The CS430 cone crusher was selected to minimise excessive size reduction and therefore maximise the amount of material available for ore sorting (-60 mm +18 mm).

The control screen bottom deck oversize (-18 mm +10 mm) is combined with ore sorter 'accepts' (-60 mm +18 mm) and fed via a 50 t live capacity surge bin and Sandvik SP0725 vibrating pan feeder to a Sandvik CH540 cone crusher with 250 kW motor. The CSS is nominally 11 mm CSS.

### *Sorting circuit*

The control screen intermediate deck oversize (-60 mm +18 mm) is wet screened on a Sandvik LF1230D linear/elliptical motion double deck horizontal screen. Both decks have water spray bar systems installed at the feed end. The wet screening of ore sorter feed prevents build-up of fines within the ore sorter, particularly around the discharge end where falling particle trajectories are altered by high pressure air blasts to separate 'accepts' from 'rejects'.

The double deck screen also separates the ore sorter feed into two streams, a -60 mm +24 mm coarse stream and a -24 mm +15 mm fine stream. The 7 mm bottom deck is to allow any fines adhered to the particles to be washed through to a collection sump and pump that transfers the fine washings to the mill discharge sump, whilst still retaining the +15 mm particles for feed to the fine ore sorter. Each stream feeds into a small surge bin ahead of each Tomra ore sorter.

Material passing through the control screen bottom deck is final crushed product has a P80 of 8 mm. Final crushed product conveyed via a luffing radial stacker either directly into a reclaim bin and then via transfer conveys downstream to the concentrator or is slewed to a fine ore stockpile effectively decoupling the crushing circuit from downstream processing.

Ore sorting is accomplished via two Tomra COM Tertiary XRT 1200 ore sorters operating in parallel. Each stream feeds into a small surge bin and feeder to provide even distribution of feed to the ore sorters. Feed is moved through each ore sorter via a 1200 mm wide conveyor belt at 3 m/s. One ore sorter processes the fine product and the other processes the coarse product from the double deck wet screen. Each ore sorter is fitted with dual energy X-ray generators to account for differences in X-ray attenuation caused by differences in particle thickness rather than atomic density. The sensors detect differences in X-ray transmission through each particle which enables particles separated based on their specific atomic density.

The mass of the 'rejects' stream is measured by weightometer and a shift composite sample obtained by automatic sampler for assay, metallurgical accounting and environmental monitoring purposes. This stream, having a particle size range of -60 mm +15 mm, was planned to be returned underground via a borehole.

During periods of high head grade or for ore sorter maintenance purposes, the ore sorters are bypassed by operating a pneumatic diverter gate within the primary control screen intermediate deck oversize chute. Product from this deck then reports to the tertiary crusher feed conveyor, rather than the wet screen and ore sorters.

The process mass flows were simulated using Sandvik's Plant Designer software and were similar to those estimated from existing crushing circuit survey.

During the preparation of the business case for the ore sorter, one risk that was identified was the proposed underground storage of the ~180 000 t/a rejects waste material expected to be generated by the ore sorter. Due to the potential acid forming nature of this material it was planned to be sent underground via a borehole. However, insufficient void underground was expected to become an issue.

Accordingly, further test work was completed by Tomra Engineers (Sandy, Rech) during 2017 using an electromagnetic (EM) sorter that successfully demonstrated the separation of Potential Acid

Forming (PAF) and Non-Acid Forming (NAF) ore. Rather than excavating a borehole, the purchase of a third ore sorter (EM) and associated conveyors, concrete, electrics and structures in replace of the ore sorter rejects hole was approved in January 2018.

The installation of the EM sorter allows the NAF material, estimated at 145 000 t/a or 80 per cent of waste generated, to be kept on surface where it will be utilised as road base or stored on the surface in an environmentally approved manner, with a much smaller proportion of the PAF material, estimated at 35 000 t/a or 20 per cent of ore sorter waste generated, being returned to the underground mine, mainly as road base and rock fill.

## Ore sorting business case

The sorting circuit offers significant additional upside in the future with ongoing optimisation, and increased in mining rates, with ROM throughput rates of approximately 1 Mt/a considered achievable. The business case in the CER stated that the objective of the Project was to increase net cash flow by approximately 20 per cent via increasing tin production by 1100 t tin per annum.

### *One Mt/a*

Subsequent to commissioning the opportunity to exceed the original performance objectives was identified. The opportunity was to increase ore treatment rates with ongoing optimisation of mass rejection across the circuit.

Notably, in January 2020 a record monthly ROM throughput of 84 881 t was achieved. Mass recovery of 74.3 per cent mass with 96.9 per cent tin recovery exceeded the performance for all months budgeted in CY2020 and was within 0.2 per cent of model. Equivalent to an annualised ROM throughput rate of 1.02 Mt/a.

The results from January were repeated in October 2020 when the record monthly ROM throughput of 85 185 t was achieved whilst operating at a mass recovery of 71.0 per cent and tin recovery of 96.9 per cent.

This opportunity provided a challenge to the entire operation to sustain the 1 Mt/a rate.

# CHALLENGES IN ORE SORTING AT RENISON

Challenges in project planning and implementation lead to the installation of a suboptimum circuit design and an extended commissioning/ramp-up period. Shortfalls arose in operability, maintainability and in the Mine to Mill process. The pre-December 2019 operating strategy focused on low reject grades rather than maximising tin production. The preoccupation on reject grades led to loss of focus on achieving the mass reject rate and overall process plant throughput.

A lack of operational readiness and commissioning documentation led to many lessons learned being forgotten. As issues repeated the investigations were repeated and without shared documentation and the lessons were lost again. Standard operating guidelines were only developed 12 months after commissioning. The guidelines were developed as an interim tool to assist in training the operations and metallurgical teams.

Resourcing sufficiently generated another challenge. During the difficult commissioning period and throughout 2019 the circuit did not have a dedicated operator. A select few became the only source of knowledge amongst the operations and metallurgy team. The lack of change logging extended troubleshooting timeliness and effectiveness. On multiple occasions operators from other sections in the plant were called away to troubleshoot, reset faults or clean up around the crushing circuit, often resulting in tin losses elsewhere in the plant.

As the proportion of material that is fed to the ore sorters is a key economic driver it was believed that maximising the material fed to the ore sorters maximises the revenue. The per cent screened to the sorters was optimised through aperture changes to the screen media on the control screen and process control loop tuning provided a relatively steady state of operation. This operating philosophy did not account for large variance in run-of-mine (ROM) particle size distribution frequently overloading the circuit. The overloading increased operational downtime and capability loss.

Failing to operate at steady state meant that the sorting parameters could not be changed with confidence. In order to sort more ore the circuit was unknowingly overloaded. The overloaded circuit cycled between filling one surge bin and then another all in a vain attempt to keep the ore sorters at maximum count levels. Each cycle was exacerbated by the lack of surge capacity. As these disturbances multiplied the control system could not respond effectively. The overloading of the sorters reduced both performance and total throughput. At times throughput reduced to the point at which the previously bottlenecked milling circuit could outpace the crusher. The disturbances lead to noise in the key metrics used to measure performance making any benefit achieved unclear.

Another key driver is sorter performance. Design test results indicated a base case of 60 per cent accepts and 40 per cent rejects. These targets were used in project design and subsequently guided the operating strategy upon start-up. Figure 3 shows the relationship between concentrate yield and tin recovery developed. The point of inflection on the curve at around 25 per cent concentrate yield is the point at which the maximum NPV is realised. Operating at this point was deemed risky because significant tin losses could occur if concentrate yield reduces below this optimum point or if this optimum point shifts for different ores. The project risk assessment noted that a reasonable operating safety margin was required to be maintained to avoid high tin losses. Ore sorter concentrate yield target was then set between 40 and 60 per cent. This stipulation generated a 'low reject grade' management paradigm which hindered realisation of mass recovery targets. All metrics were geared around the reject grades instead of performance versus model.

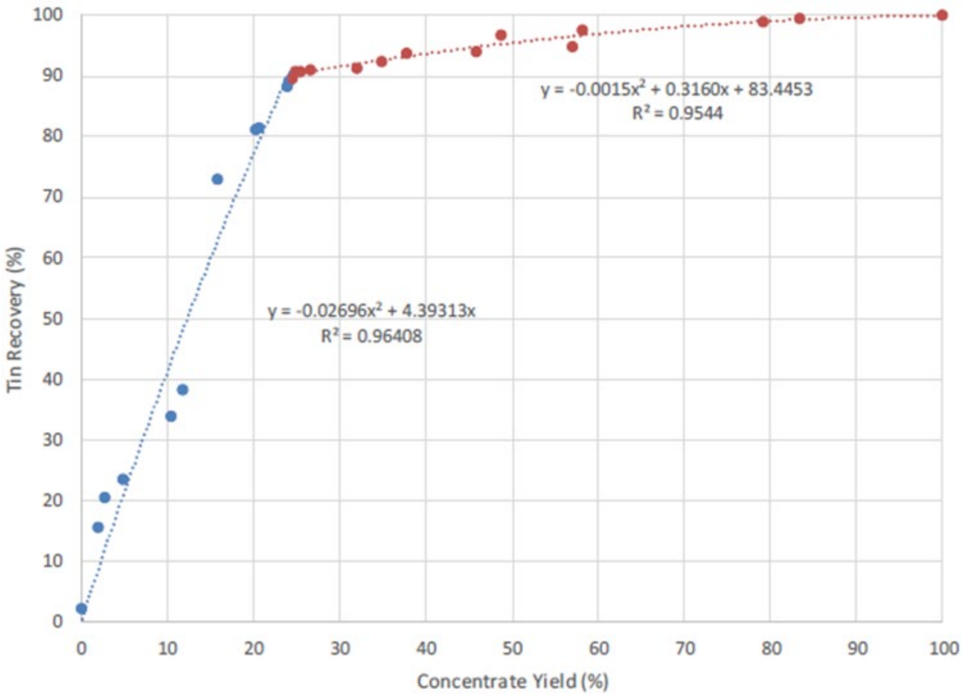


**FIG 3** – Example of a Tomra sorting performance curve.

During commissioning, it was found that a relationship between air supply pressure and eject performance existed. As shown in Figure 4 at air supply pressures between 700 and 750 kPa performance was negatively affected and when operating below 700 kPa the performance drops off rapidly. The operating pressure set point was recommended to be greater than 750 kPa and suitable alarm limits set. Causes for low air pressure included increased demand and supply failure via compressor faults. Demand is driven by both the number of objects fed to the sorters, the tin grade and the sorting parameters. As such poor performance was compounded by the pre-December 2019 operating strategy coupled with a fail to waste set-up. As the sorting parameters were targeted at tin recovery the number of objects required to be ejected increased and performance would reduce. The low air supply would be flagged as a result and the Tomra feed set points lowered reducing total circuit throughput.

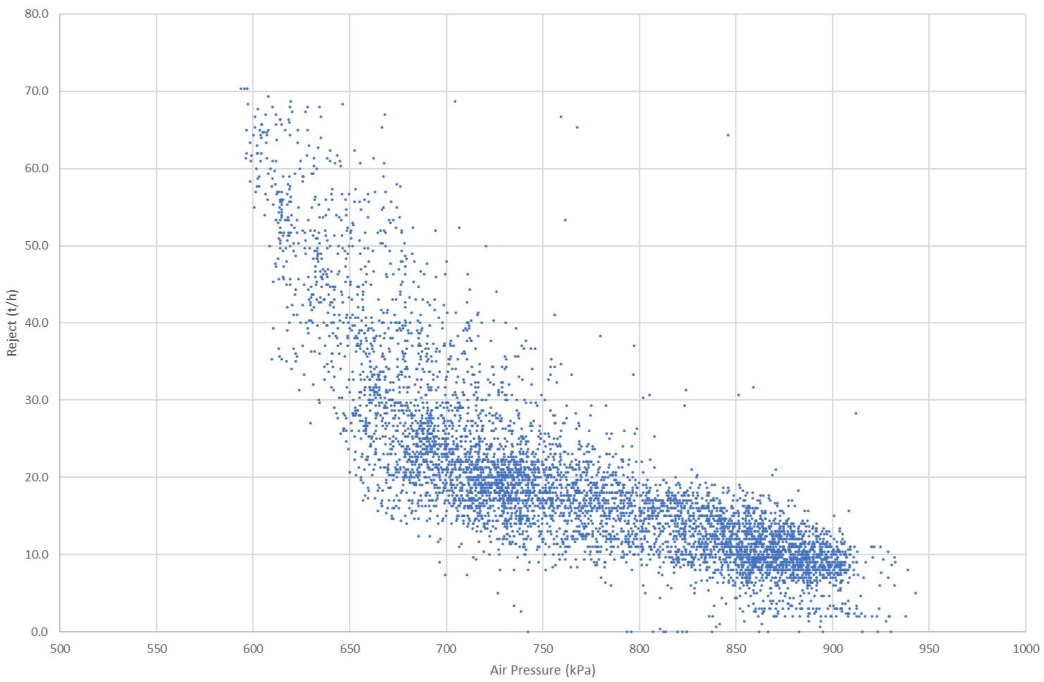


**FIG 4** – Impact of air supply pressure on miss reporting.

General environmental challenges exist. The West Tasmania wet combined with high moisture ore delivered from underground hindered steady state operating. Of particular note is the impact on sorting. As screen panels blind an increased proportion of fines reports to the sorting circuit, overloading the wet screen and blocking the surge bins. The disturbances reduced overall throughput and distracted from optimising metallurgical performance. High ambient moisture content resulted in multiple failures of the ejectors leading to poor sorting performance and extended ramp up.

Mechanical issues with the ore sorters have gradually been remedied as events arose. Opportunities to improve the sorters existed in materials of construction of the conveyor belt, the bed, the doors and hinges and ejector nozzles and the air supply system was completely re-engineered and replaced.

An opportunity arose whereby the overrun of the six-monthly planned maintenance shutdown led to an increased ore availability contained in surface stockpiles. Processing rates were ramped up and production-based evidence further highlighted the processing capacity made available through sorting. The demonstrated capacity has increased focus on mine sequencing, capital projects and providing supplementary ore sources.

Waste disposal issues required increased attention. The evaluation of the electromagnetic sorter failed to identify what mechanism determines the classification of non-acid forming waste and how this corresponds to mine sequencing and the LOM. A reduction in acid neutralising capacity has generated excess material requiring storage underground. Learnings from this include evaluating multiple methods of waste disposal and applying economic justification for the development of appropriate storage facilities.

## MASS RECOVERY OPERATING STRATEGY DEVELOPMENT

From October 2019 a new investigation was opened into ore sorting performance. An approved systematic derating of the circuit was undertaken. Metallurgist (Wraith, 2019) reduced total throughput of the circuit in a determined effort to gain control over mass recovery. Attainment of target mass recovery is critical to achieving targeted overall ROM treatment rates and realising an IRR in excess of 105 per cent. The approach has been to ensure the sorters are fed within their maximum count rate at all times to minimise miss-sorting whilst adjustments were made to screen panels to adjust the mass split to the two XRT sorters to allow utilisation of these to be simultaneously maximised, whilst also managing the total portion of crusher feed directed to the sorting circuit to allow overall mass recovery targets to be achieved. This has been highly successful, with month-on-month improvements in mass recovery achieved from October 2019 to January 2020. The end result is a paradigm shift away from targeting low reject grades and towards sorting as aggressively as possible whilst staying within tight tolerance limits of the model. Thus, moving from a tin recovery based operating strategy to a mass recovery one.

## Overview

A review of the circuit design criteria analysed against multiple circuit mass balances indicated parts of the circuit were overloaded. In order to identify sources of variance the following equation was interrogated. In order to achieve the required mass recovery, it was first necessary to determine what constituted the Waste tonnage. Disturbances to the circuit occurred both in a controlled and uncontrolled fashion. Examples of uncontrolled disturbances are run-of-mine (ROM) particle size distribution (PSD) and holed screen panels. Surges from blocked surge bins, blinded screen panels (miss classifying) and failure to intervene when the circuit is cycling between surges are considered controlled. Based on the following equation the only way to eliminate surges within the circuit was to reduce the '%toOreSorter' to a minimum leaving the only source of variance as the '%toProduct' or ejects.

$$CrusherFeed \times \%toOreSorter \times (1 - \%toProduct) = Waste$$

$$Mass\ Recovery = \frac{CrusherFeed - Waste}{CrusherFeed}$$

The sorting circuit was starved of fed by opening the apertures on the control screen. Once the throughput reduced sufficiently a disturbance elimination program occurred. Poorly behaving control loops were remedied, and the control philosophy was analysed. Learnings were communicated with the mill control operators and a set of operating guidelines were developed. The guidelines provided much needed troubleshooting tips to correct any disturbances before they compounded and began cycling the circuit. The de-rated circuit found a steady state of production and weekly performance modelling indicated a return to model. The per cent to product was found to be relatively stable regardless of feed blend. The sorting parameter of Darkbrightness was adjusted until it reached its minimum. The performance remained on model. The sorting parameter of Area was adjusted until it reached its maximum. The performance remained on model. The '%toProduct' or yield had stabilised between 30 and 40 per cent regardless of ore source treated. This exceeded the previously safe operating target of 60 per cent.

As one source of variance was controlled the focus shifted to per cent of ore diverted to the Ore sorters. The ROM PSD, fresh crusher feed rates, recirculating load and screen media selection all contribute to the '%toOreSorter'. Variance associated with the recirculating load was initially reduced through the optimisation of the '%toProduct' whereby increased waste production reduced tertiary crusher feed. Further reduction of recirculating load occurred by increasing the open area on the bottom deck of the control screen. A calculated crusher feed rate was required as the circuit has no online measurement. The operating guidelines were modified to include the maximum allowable feed tonnage based on the design criteria of 180 t/hr. With a reduced recirculating load and an instruction to cap throughput at nameplate the only remaining source of variance was the ROM PSD. As only the design criteria's size distribution was available WIPFrag IOS monitoring was instigated, and data collected on a routine basis for analysis. The proportions of ore found to exist within sorting size fraction varied greatly but once measured it could be managed. Changes were made both to the underground jaw crusher and the ROM blending strategy. Both resulted in more consistent operability of the circuit. Allowing for the controlled increase in '%toOresorter' until a safe maximum was set on the control screen and then fine-tuned via blending.

$$ControlScreenFeed \times \%OpenArea = \%toOreSorter$$

$$CrusherFeed + Recirculating\ Load = ControlScreenFeed$$

### *Influence of ROM particle size distribution*

As the crushing circuit stabilised the variance in sorting performance reduced. The residual variance was caused by each ore type's amenability to XRT sorting. As the blend varied the performance would follow suite. Results steadied at 30 to 40 per cent recovered to product. As the sorting parameters were set to as aggressive as possible the per cent to product driver was fully utilised.

No further work was required. The overall circuit performance was hence limited by the presentation of ore to the sorters which is largely driven by ROM particle size distribution.

Figure 5 compares the design ROM PSD and a band of operating data. A lack of adequate assessment of variability in ROM size distribution led to inappropriate expectations in the achievable presentation of ROM to the sorters and hence overall circuit mass rejection.

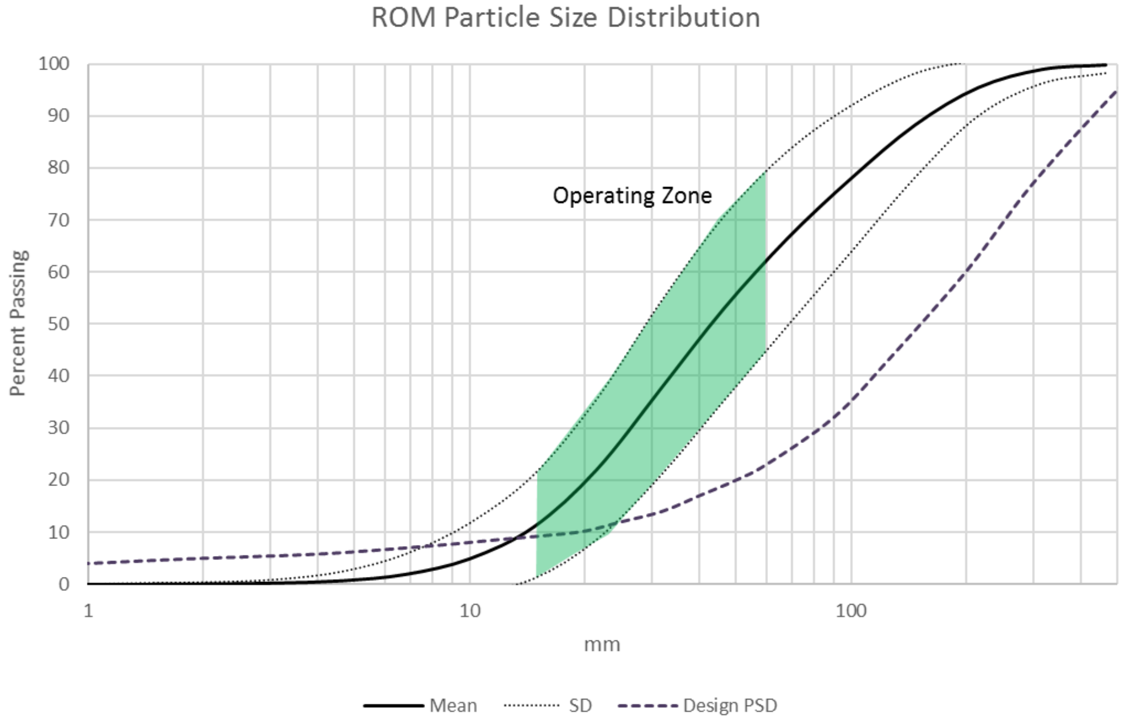


**FIG 5** – ROM particle size distribution (actual envelope versus design).

Crusher feed blend tracking was established to analyse ore sorting performance versus ore source. Challenges arose in identifying ore parcels through the materials handling process. Due to multiple ore sources and the mining sequence ore is often blended at the tipple, underground crusher and hoist. By the time the ore hits the ROM a mixture of unknown quantities results. Radio communication between the crusher operator and the mill control room aims to keep track of the ore source and where it has been hoisted. This is overcome via blending. To facilitate this a map of the ROM pad overlaid on a white board provides a visual aid to both mill control and the metallurgy team. A weekly hoist schedule provides a basis for the weekly blend and forecast production. Future work to utilise online particle size analysis and GPS geofencing of the ROM coupled with live slew location and hoisting data. This will enable automatically tracking of the ore on the ROM and its varying properties.

### *Reporting versus model*

Initial model development was based on sorter sensor design test work completed by Tomra. A revised operating based model was developed utilising crusher and sorter performance from the first five months of 2019 this included tolerance levels of 0.7 per cent based on operating experience as shown in Figure 6.

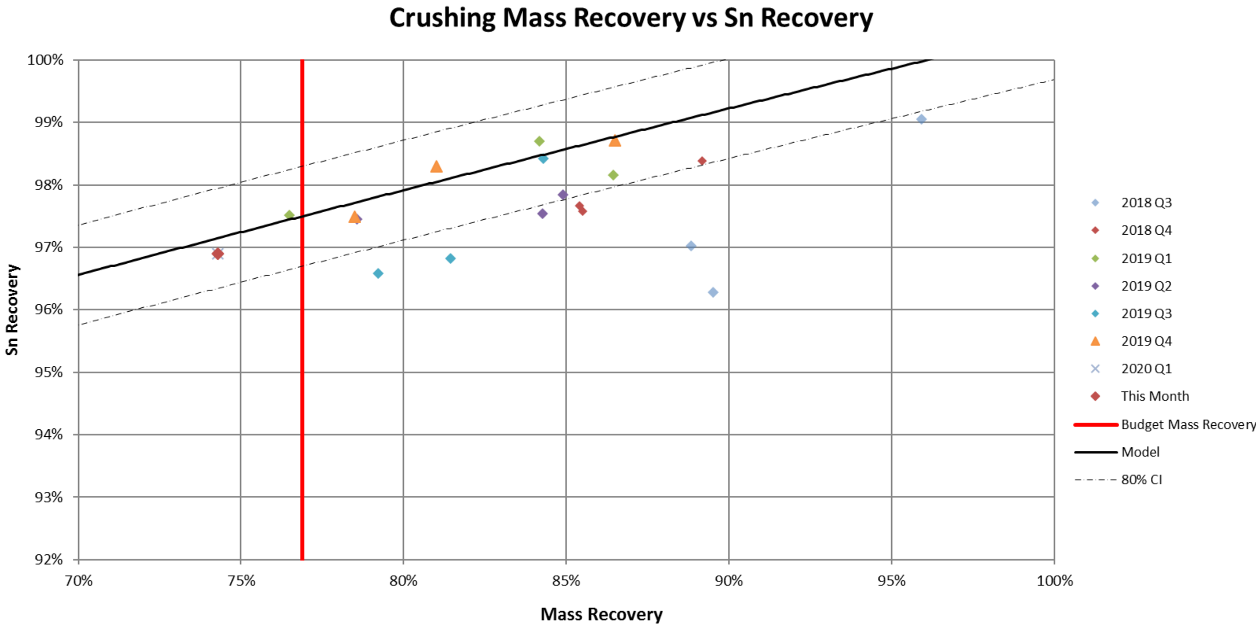


**FIG 6** – Example of model utilised to highlight quarterly optimisation.

The model is utilised to forecast circuit performance for budgeting and weekly schedules. The model is also utilised on a shift-by-shift basis to highlight performance excursions.

Confidence in the model was validated by Metallurgists' (Resta, 2020) when reviewing the previous 12 months operating data. As shown in Figure 7, 60 per cent of all shifts conformed to the model and 70 per cent of all shifts were within one per cent of the model. Conformance to model is expected to tighten through ongoing optimisation of the overall circuit.

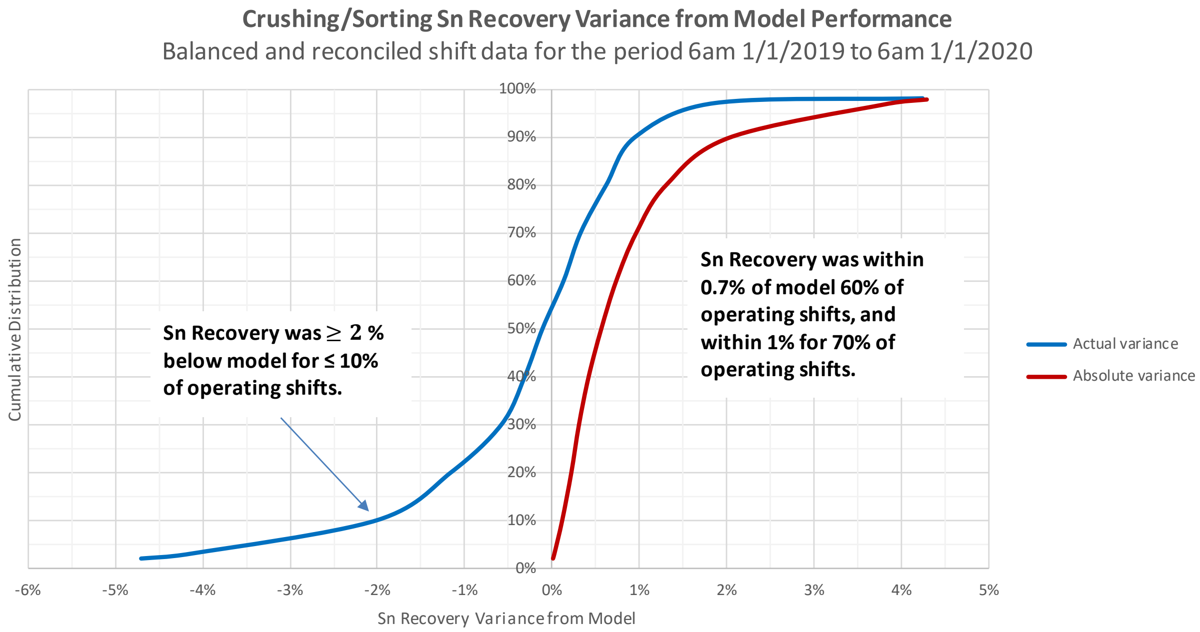


**FIG 7** – Variance in Sn recovery from the performance model. Shown are the actual positive and negative variances from the model (actual recovery – model prediction), and absolute variance from the model (√(actual recovery – model prediction)2) plotted as cum.

## *Paradigm shift*

Upon redefining the operating strategy, communication across the business of appropriate performance metrics was required to provide a clear perspective on the impact of sorter performance on ROM throughput capability, processing costs and overall tin recovery. Historically KPI's were geared towards obtaining low waste grades for fear of impacting overall tin recovery. This led to a paradigm shift, focusing on the key objective of maximising ROM throughput via targeting appropriate mass recovery targets which fundamentally drives the overall tin production rate.

Figure 8 highlights as crushing circuit mass recovery decreased the increased tin losses in sorting were offset by increasing concentrator performance. Figure 9 highlights the overall impact of varying mass recovery on tin production rate.

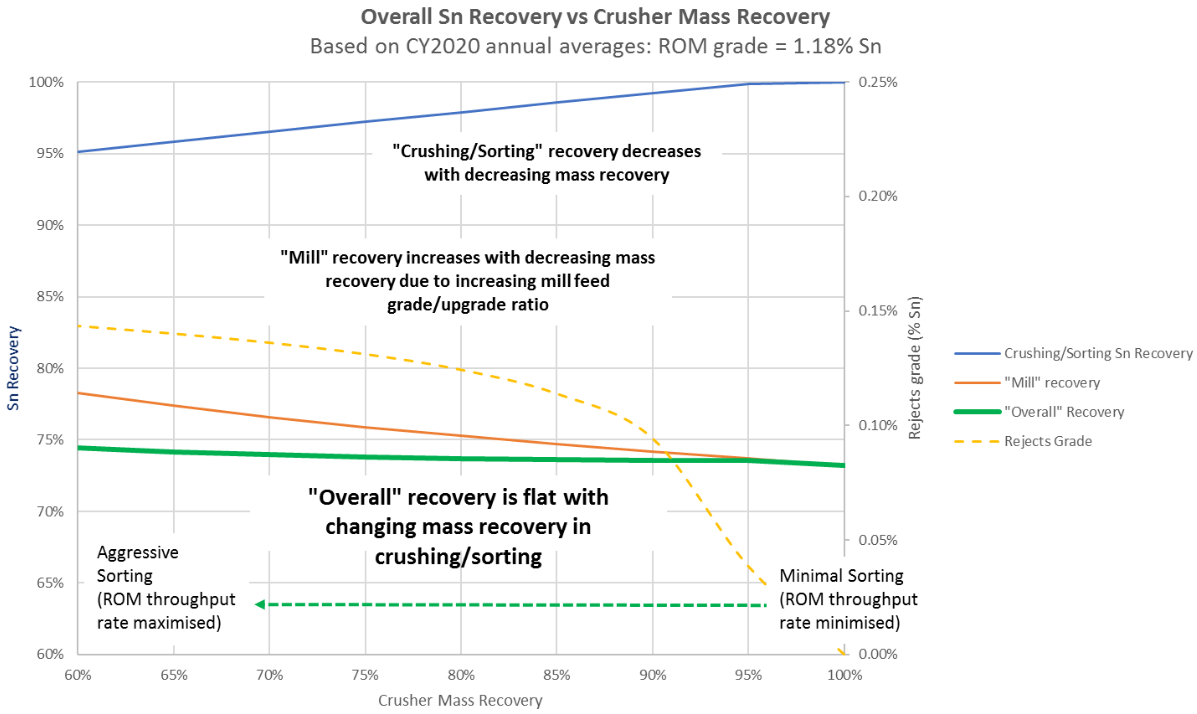


**FIG 8** – Key communication tool utilised when explaining changes in KPI's.

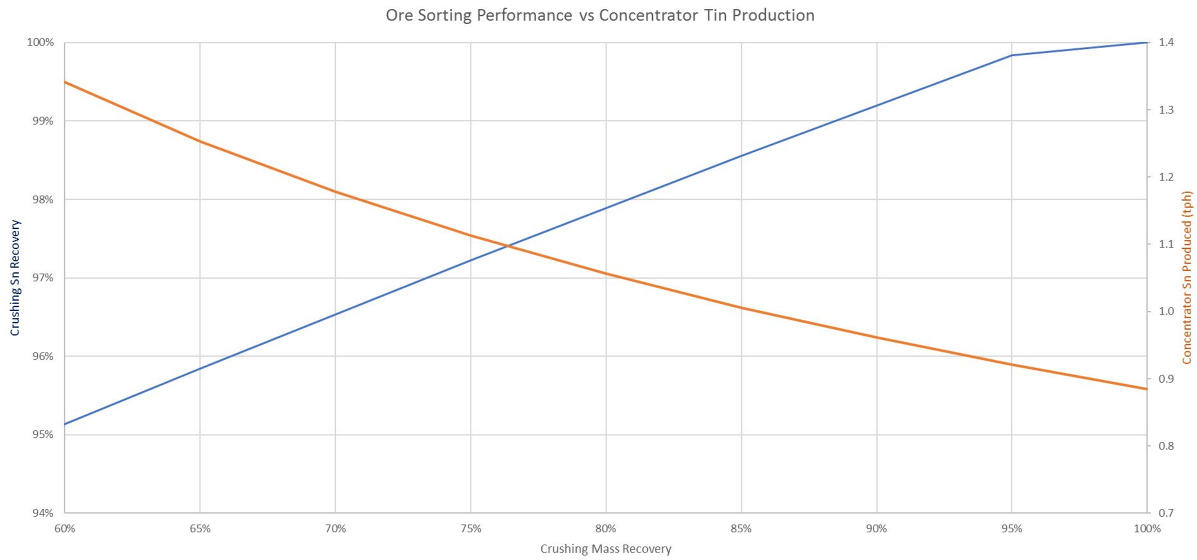


**FIG 9** – Tin production versus mass recovery (fixed milling rate).

## Renison operating strategy

The overall operating strategy is driven to achieve the key objectives of the crushing and sorting circuit summarised as:

1. Reduce the ROM particle size to a size suitable for milling.
2. Selectively reduce the mass of ROM to a mass with fits with the milling capability ie a targeted mass recovery.
3. Achieve points 1 and 2 at the required ROM treatment rate.

To achieve the objective the control strategy is focused on the management of ROM blend to manage particle size distribution inline within the constraints required to maximise the proportion of material presented to the sorters whilst managing the split to the fine and coarse sorters. Essentially the sorting circuit capacity is fully utilised. Sorter parameters are used to trim the mass recovery as required.

Recent experience has indicated there is further room for improvement. Aspects of sorting via tin and not objects are being explored to debottleneck the sorters. At the time of writing the paper a mass recovery process control loop is under development to control the mass recovery online via varying the sorting parameters to reduce excursions from targets. Mine to mill monitoring of fragmentation will fully integrate the ore sorter into the business and enable further revenue generation via increased presentation of ore to the sorting circuit.

### *Impact on costs*

At the time of writing this paper operating costs for the crushing/sorting were $4.80/t of ROM treated. Of this cost $1.80/t ROM is attributed directly to the sorters, and $3.04/t ROM to crushing (ie cost of crushing excluding sorting was $3.04/t ROM). Figure 10 shows a breakdown of costs attributed directly to sorting (costs for crushing without sorting excluded). Ore sorting costs are dominated by equipment maintenance costs, with 49 per cent of costs attributed to the sorting machines. Additionally, operation of the sorters led to increased costs for power, materials handling (of sorter rejects), and maintenance of screens, bins, conveyors and crushers due to increased throughput rates and recirculating loads.

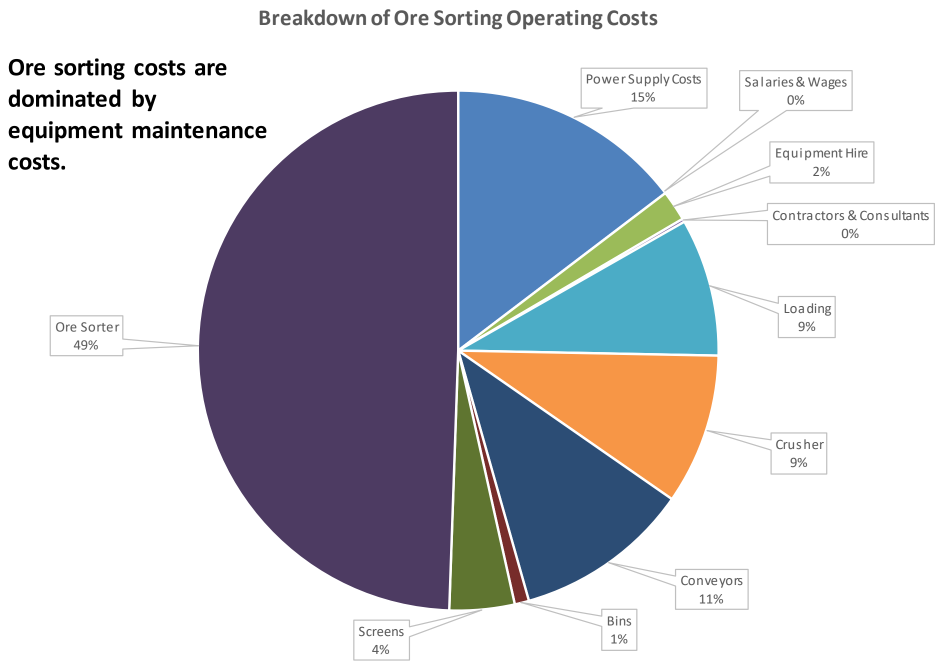


**FIG 10** – Ore sorting operating cost breakdown.

Flow on cost impacts of sorting included increased operating costs in concentrate leach and filtration due to increased tin production.

Operation of the ore sorting circuit increased overall processing operating costs. This was offset by the increased ROM throughput by 152 724 t and tin production 1305 t enabled by sorting. This led to a reduction of unit operating costs from ~$42/t ROM to ~$38/t ROM treated, equivalent to a reduction of approximately $500/t tin produced. Benefits of sorting are expected to increase in the future due to optimisation of the overall Renison Project.

## CONCLUSIONS

Overall the project has been extremely successful in providing a significant step change in ROM treatment and tin production capability, for similar overall processing cost, leading to a step change in the achievable economic outcome for Renison. It is recommended to develop a holistic project plan and objects which will require business wide acceptance and action to be fully successful.

## ACKNOWLEDGEMENTS

The authors wish to thank and acknowledge Bluestone Mines Tasmania Joint Venture for permission to publish this paper. We also wish to thank the Processing and Maintenance staff at Renison for their input and efforts throughout the optimisation program. Special thanks to Scott Gleeson (Shift Supervisor) for operational insights, Steve Robinson (Group Project Manager) for historical project notes and Johan Welmans and Justen Resta (Processing Manager and Group Metallurgist) for their support during plant trials and subsequent operational strategy development, communication and execution.

## REFERENCES

Jones, S, Rech, G, 2017. Bluestone Tin Sorting of Tin Ore (NAF Test Work) Performance Test Report, Tomra Ore Sorting Solutions

Resta, J, 2020. Memorandum Ore Sorter Performance Review: CY2019, Metals X Limited

Robinson, S, 2019. Surface Crushing, Screening and Ore Sorting Facility Project Close-Out Report, Bluestone Mines Tasmania JV

Wraith, B, 2019. Memorandum Crushing and Sorting Optimisation, Bluestone Mines Tasmania JV

# Operational improvements at FCF Minerals Runruno process plant

*X Zheng[1], A Crawford[2] and D Bowden[3]*

1. Technical Director, FCF Minerals Corporation, Manila, Philippines.
   Email: xiaofeng.zheng@metalsexploration.com
2. Operations Manager, FCF Minerals Corporation, Manila, Philippines.
   Email: andrew.crawford@fcfminerals.com
3. Chief Executive Officer, Metals Exploration Plc, London WC2R IDJ.
   Email: darren.bowden@metalsexploration.com

## ABSTRACT

FCF Minerals' Runruno is a sulphide gold operation. Most of the gold is finely grained and disseminated in pyrite hence refractory to direct cyanidation. The Runruno process plant uses single stage SAG milling, gravity separation followed by intensive cyanide leaching of the gravity concentrate, flotation followed by bio-oxidation of the concentrate and cyanide leaching to extract the gold.

Since the beginning of 2019, the mill throughput has gradually increased and reached 26 per cent above the design capacity. Meanwhile, the overall plant gold recovery has also improved significantly, ie from 61 per cent in January to 85 per cent in September, by optimising the flotation operating conditions and eliminating excessive froth in the BiOX circuit.

Further optimisation and improvement projects are currently being developed, including retreatment of the InLine Leach Reactor (ILR) solid residue, commissioning of a variable speed drive for the SAG mill, additional flash flotation and gravity separation inside the grinding circuit, additional pneumatic flotation ahead of the existing conventional flotation bank, and additional air supply for the bio-reactors. The aim is to increase Runruno gold production from 48.1 koz in 2018 and 68.6 koz in 2019, to 80 koz in 2020 and beyond.

## INTRODUCTION

FCF Minerals Corporation, a wholly owned subsidiary of Metals Exploration Plc., operates the Runruno gold mine, located 328 km north of Manila in the province of Nueva Vizcaya. Gold occurs as native and electrum and is mostly associated with finely disseminated pyrite thus refractory to direct cyanidation. The processing plant involves gravity concentration followed by intensive cyanide leaching and flotation followed by bio-oxidation and carbon-in-leach to recover the gold into dore. A simplified process flow sheet of the Runruno processing plant prior to 2019 is illustrated in Figure 1.

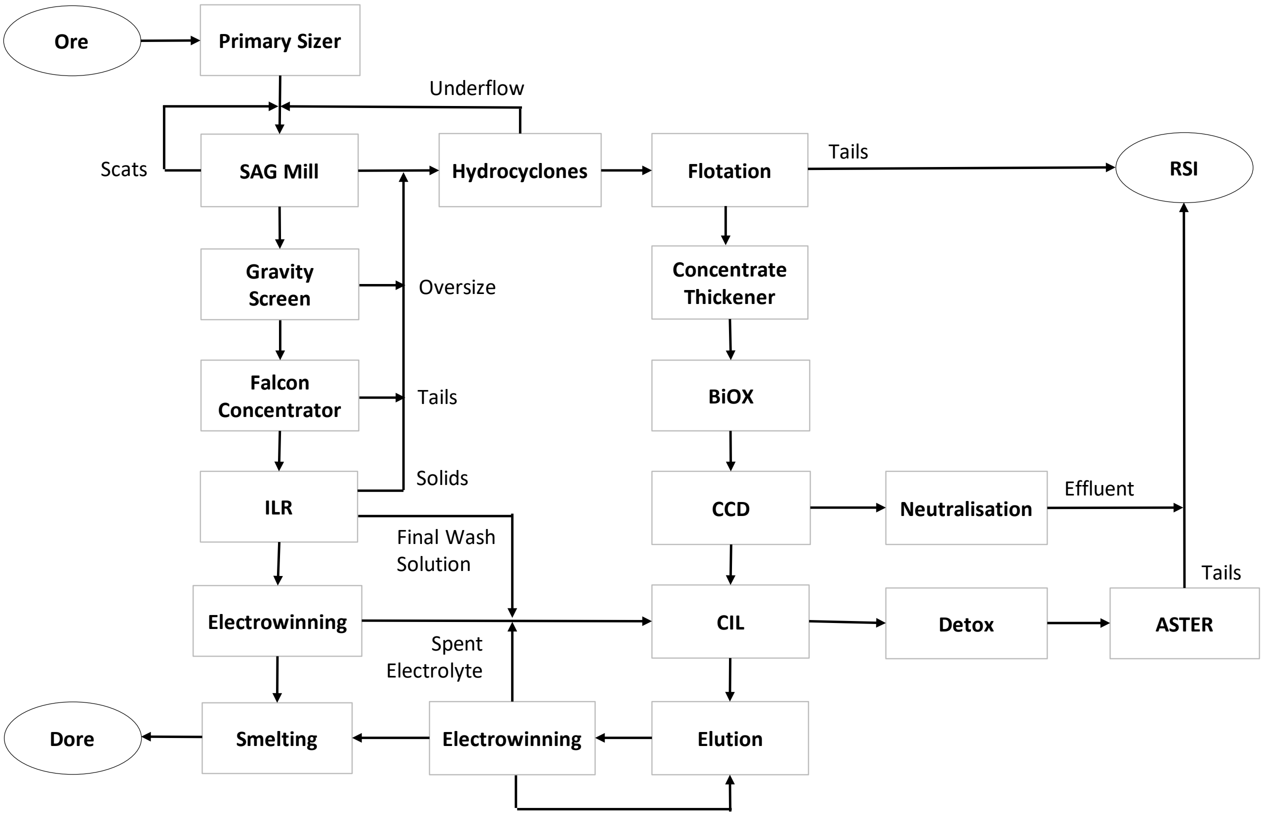


**FIG 1** – A schematic representation of Runruno process flow diagrams.

The plant was designed to treat 1.75 Mt of ore per annum at a feed grade of 1.89 g/t gold and 1.46 per cent sulphide sulphur and produce on average 96 700 ounces of gold per annum over ten years of mine life (van Niekerk, Olivier and Jardine, 2017). However, despite ramp-up to the design milling rate in six months after the commissioning in May 2016, the operation is yet to achieve the design gold production. The gold production was 36 006 ounces in 2017 and 48 373 ounces in 2018. Moreover, until December 2018, Runruno was operated at a financial loss. A change of operating strategy was initiated at the end of 2018. The new operating strategy and subsequent process optimisation improved the gold production in 2019 to 68 563 ounces in dore plus potentially an additional 2155 ounces in gravity concentrate. A number of projects are currently being studied or implemented to increase gold production further to achieve an ultimate goal of 80 000 ounces per annum in the remaining mine life.

## HISTORICAL PERFORMANCE AND MAIN CONSTRAINTS

The lower gold production than that anticipated in the initial design was mostly a result of lower feed grade and plant recovery. As shown in Figure 2, the average mill feed grade in the three years from 2017 to 2019 was 1.56 g/t Au, which is 17 per cent lower than 1.89 g/t estimated in the feasibility study due to the higher mine dilution than that assumed in the feasibility study. The mine dilution is not expected to improve in the remaining mine life.

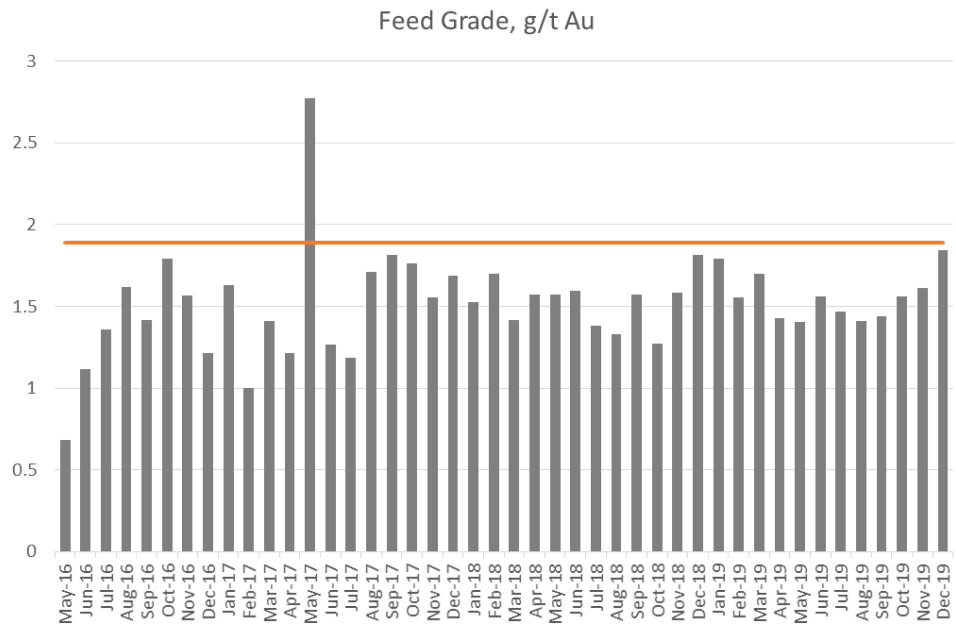


**FIG 2** – Historical monthly average mill feed grade of gold.

The flotation and CIL recoveries were both significantly below the initial projection in the feasibility study. Gold recovery in the flotation was 43.4 per cent in 2017 and 54.4 per cent in 2018, compared with the initial prediction of 92 per cent based on the test work conducted during the feasibility study. However, the samples used in the test work were not representative of the overall orebody. The test samples were taken from a few selective areas of the deposit, had a significantly higher grade and were less oxidised than the ore processed. The average grade of sulphide sulphur was 1.4 per cent in the test samples and assumed to be 1.46 per cent in the original process design criteria with no waste dilution while the average grade of the actual plant feed was 0.91 per cent between 2017 and 2019. Furthermore, over 95 per cent of the sulphur was present as sulphide in both the primary and the transitional ore samples while the average sulphide sulphur proportion of total sulphur in the actual plant feed was significantly lower at 82 per cent, especially in 2017 and 2019 as shown in Figure 3. The transitional ore received in the plant had a much lower sulphide sulphur to total sulphur ratio than the feasibility samples and made up a much greater proportion of the plant feed than expected. It was evident in the plant operation that the flotation recovery of gold decreased as the feed sulphide grade decreased (Figure 4) and the proportion of transitional ore in the feed increased.

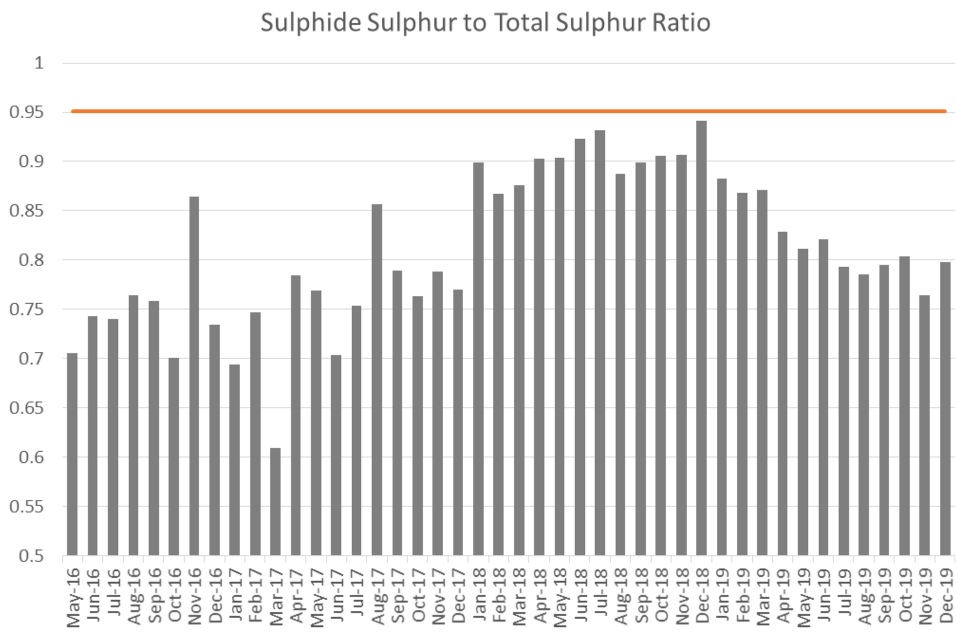


**FIG 3** – Historical monthly average of sulphide sulphur to total sulphur ratio in the mill feed.

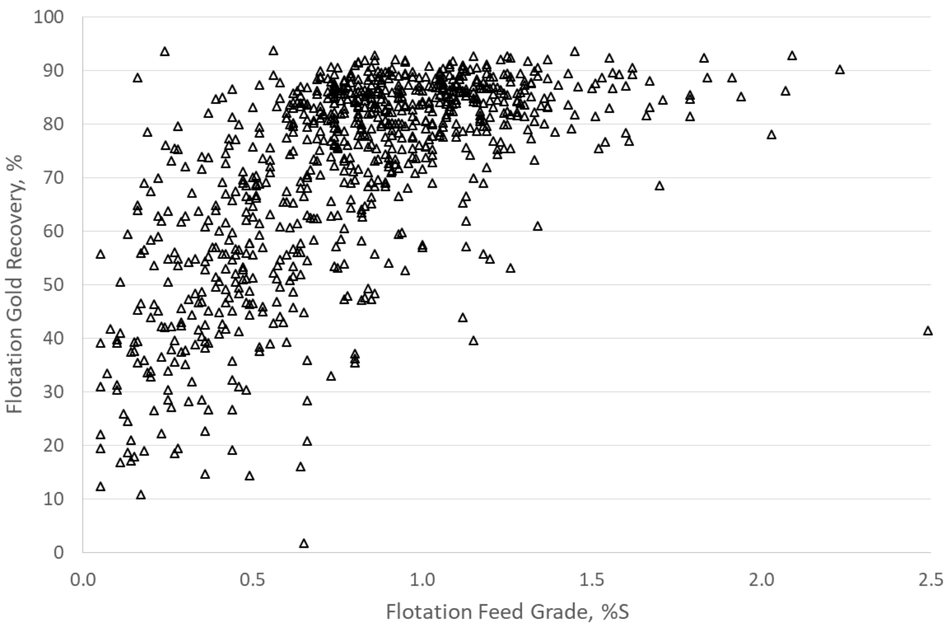


**FIG 4** – Monthly average flotation gold recovery versus feed grade of sulphide sulphur.

Flotation recovery was also affected by the poor performance in the upstream grinding circuit and the oxidation capacity constraint in the downstream BiOX circuit. The 24-foot SAG mill is operated at a fixed speed of 11.8 rev/min, or 75 per cent of the critical speed, in closed circuit with hydrocyclones. The mill power utilisation was low, typically below 4.5 MW of the installed 7.2 MW prior to 2019. The recirculating load in the grinding circuit is typically between 700 per cent and 1100 per cent. The recirculating load measured in one survey was 841 per cent for the solids, 2858 per cent for the pyrite and 4955 per cent for the gold even with approximately 31 per cent of the gold removed from the circulating load by a Falcon concentrator. Due to the high recirculating load, the cyclones usually operate with a feed density of above 65 per cent solids and can reach as high as 71 per cent solids in order to reduce the volumetric flow within the cyclone feed pump capacity. As a result of the high feed density, cyclone classification efficiency is poor with not only a significant number of coarse particles short-circuiting to the cyclone overflow but also a high proportion of fines reporting to the cyclone underflow. The final grinding product has a rather flat particle size distribution with high proportions of both coarse and fine particles, not ideal for flotation. Figure 5 shows the particle size distribution in the cyclone feed, overflow and underflow from the plant survey. The cyclone classification curve from the same survey is presented in Figure 6.

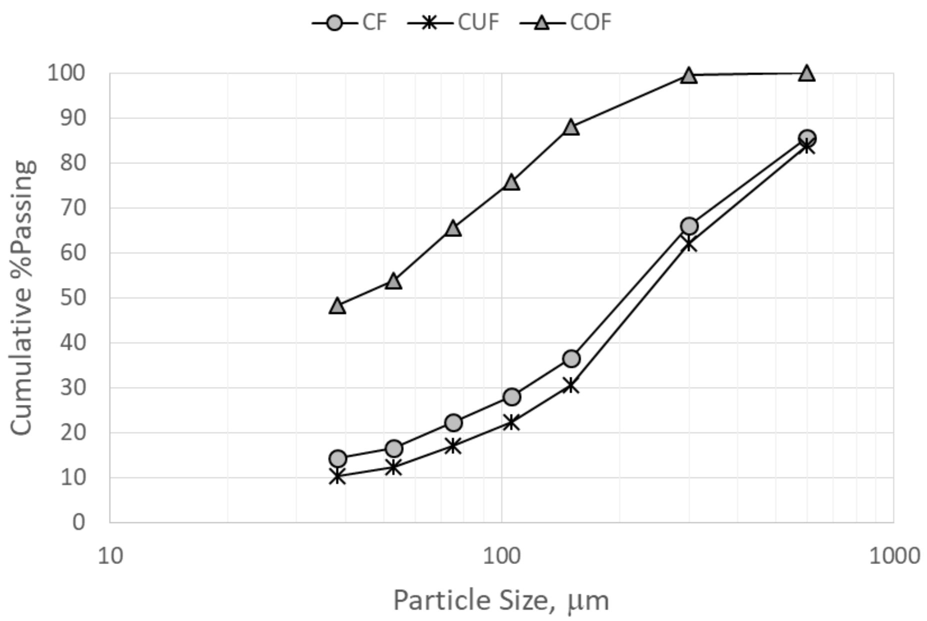


**FIG 5** – Particle size distribution of cyclone feed, overflow and underflow.

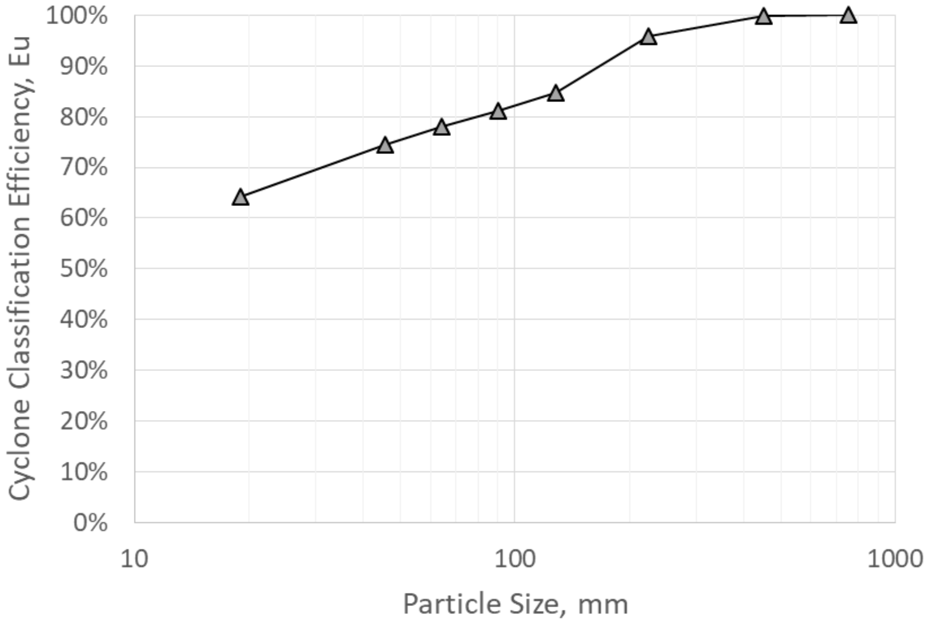


**FIG 6** – Cyclone classification curve.

Figure 7 shows the gold distribution between the individual particle size fractions in the flotation shift composite samples. Flotation recovery by particle size is shown in Figure 8. Gold was present predominantly in the minus 38 μm size fraction in the flotation feed and the fine gold remained as the main loss in the tailings. Meanwhile, despite a relatively small proportion of the gold in the particles coarser than 75 μm in the flotation feed, the loss of gold in the coarse size fraction made up nearly 20 per cent of the total losses in the tailings. It should be noted that the losses of gold in the coarse and fine size fractions could be attributed partially to the slow flotation of these particles relative to the residence time available in the flotation circuit. As can be seen in Figure 9, the down-the-bank recovery profile was yet to reach a plateau for either sulphide or gold in the survey. Mineralogical analysis revealed that only 52 per cent of the pyrite in the +53 μm size fraction was liberated and overall, 67 per cent liberated for all sizes in the concentrate sample taken from the last flotation cell. Meanwhile, over 90 per cent of the gold in the same concentrate sample was liberated, not associated with pyrite.

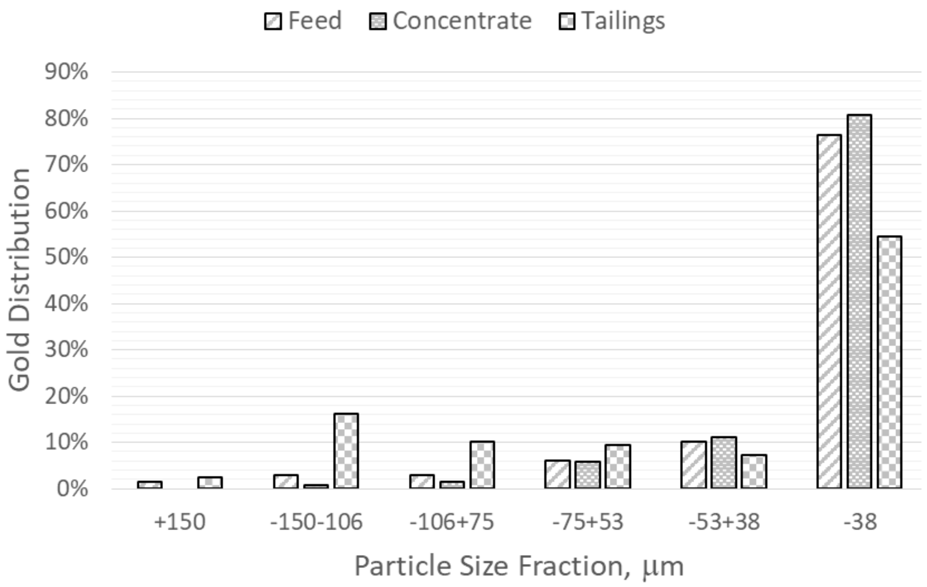


**FIG 7** – Gold distribution by particle size in flotation samples.

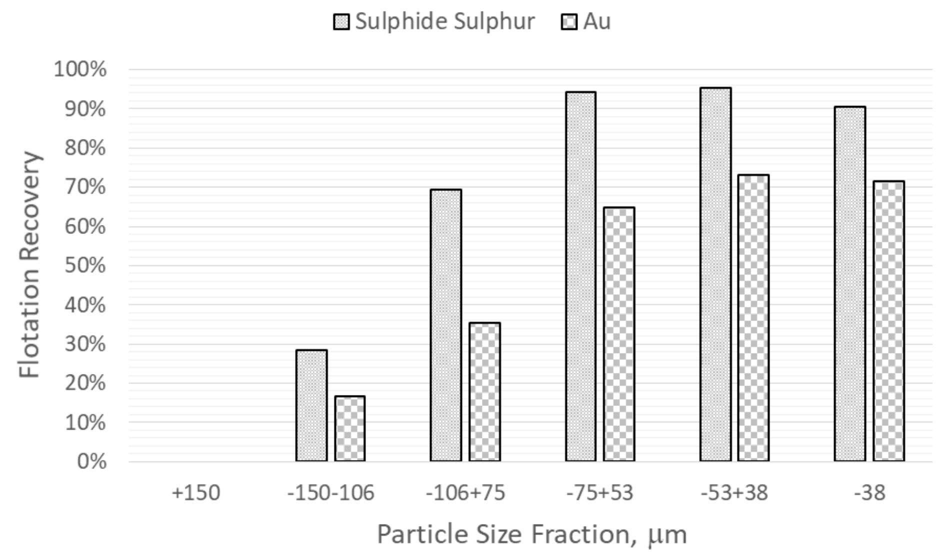


**FIG 8** – Flotation recovery by particle size.

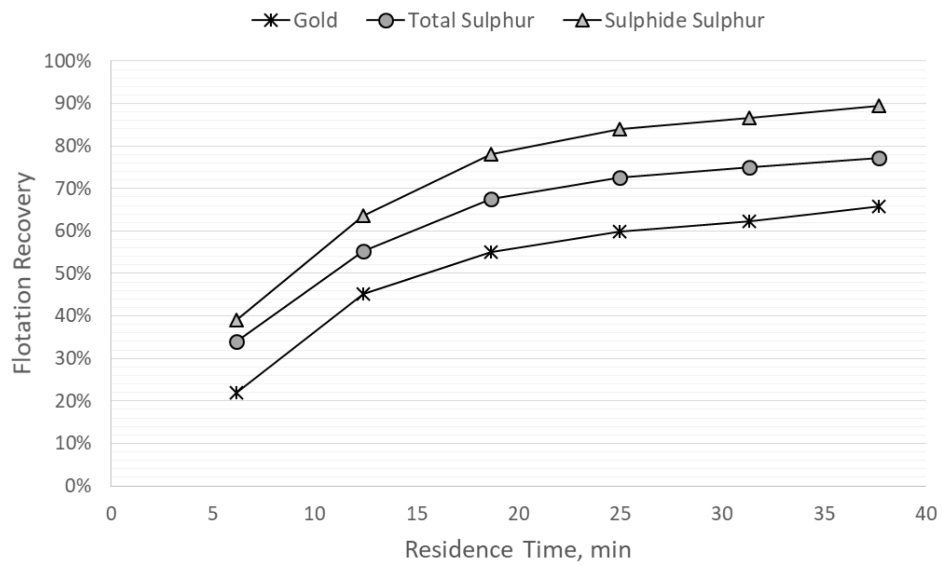


**FIG 9** – Flotation bank recovery profile.

The initial study expected the CIL circuit to recover 97 per cent of the gold in the flotation concentrate after 95 per cent of the sulphide oxidised in the BiOX circuit. The potential gold loss in the BiOX product CCD overflow and the carbon loss in the CIL circuit were not specifically mentioned in the feasibility study but assumed to be included in the 3 per cent loss. After the commissioning, the CIL circuit initially processed only the oxide ore and the recovery was mostly above 97 per cent in early 2017. When the sulphide flotation concentrate was fed directly to the CIL circuit later in 2017, the gold recovery decreased to as low as 40 per cent due to the refractory nature of the gold. It took significantly longer for the inoculum to build-up in the BiOX circuit. Not until April 2018 did the BiOX start to receive more consistent feed and CIL recovery start to increase. Figure 10 shows the historical gold recovery in the CIL circuit and the residual sulphide in the CIL tailings. Due to the delay in starting up the BiOX circuit operation and direct bypassing of the flotation concentrate fully or partially to the CIL circuit, the average CIL recovery was only 58 per cent in 2017 and 70 per cent in 2018.

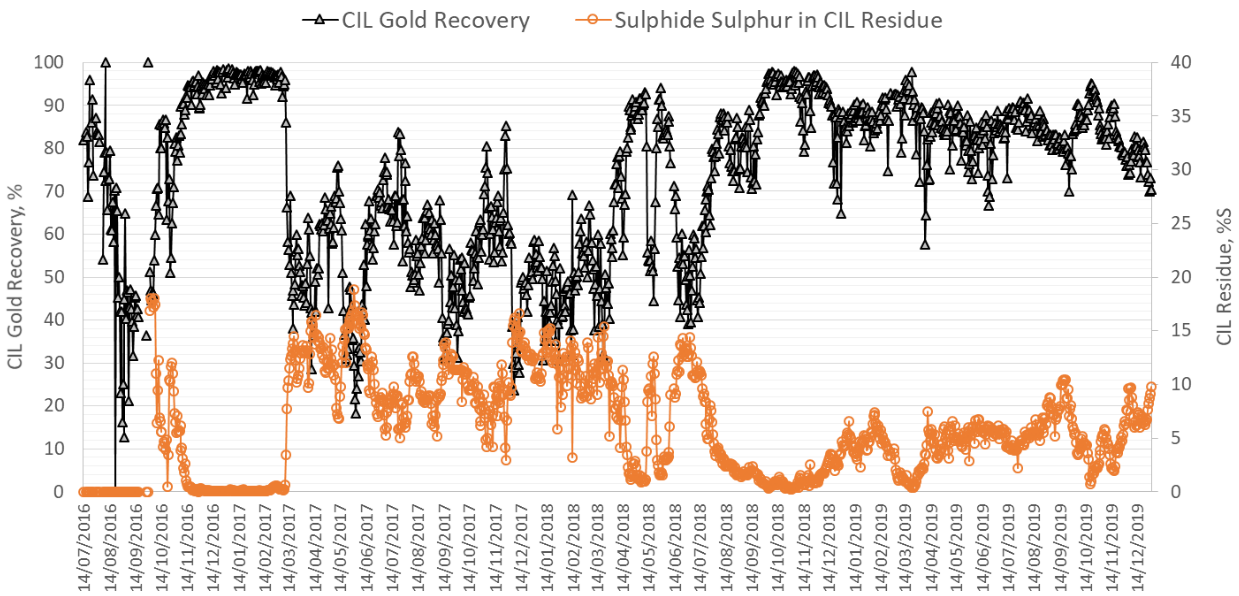


**FIG 10** – Historical CIL gold recovery.

The BiOX circuit was designed to treat 404 t of flotation concentrate at 17 per cent sulphide sulphur daily, or 69 t of sulphide sulphur per day. It was expected that 95 per cent of the sulphide would be oxidised, or 65 t of sulphide sulphur per day, to allow maximum CIL recovery. However, the circuit became a bottleneck of the processing plant ever since the commissioning and remains as the main bottleneck at the present due to lack of oxidation capacity. The first challenge encountered was excessive froth. The froth overflowed all the BiOX reactors continuously, carrying the high-grade sulphide with it. A large quantity of spray water was used to supress the froth, which diluted the pulp and reduced the circuit retention time significantly. Sometimes, the froth on the bunded floor was returned to the secondary reactors. In the process, additional hosing water was required and further reduced the retention time. Most of the time, the bund material was pumped directly to the CCD and onwards to the CIL circuit. Froth re-appeared in the CCD and CIL circuits, resulting in significant gold losses. Furthermore, the gold in the un-oxidised sulphide in the overflowing froth remained refractory, lowering the CIL recovery. The frothing issue was not resolved until the flotation reagent was changed from DSP007 to PAX in August 2019.

Another key factor affecting the BiOX performance is insufficient air. The initial design was to supply a total of 48 000 $Nm^3/h$ air to the BiOX reactors. However, only three of the four proposed air blowers were installed. Poor maintenance resulted in blower efficiency to decrease over time and delivering only approximately half of the required amount to the BiOX circuit in 2019. Before 2019, the operation capped the BiOX feed solids at 300 t per day and sulphide sulphur at 40 t per day to allow adequate sulphur oxidation in the BiOX circuit to ensure high recovery in the CIL circuit. Figure 11 shows the historical BiOX feed solids and sulphide sulphur tonnes. Capping the BiOX feed restricted the mill throughput and also the flotation concentrate mass pull.

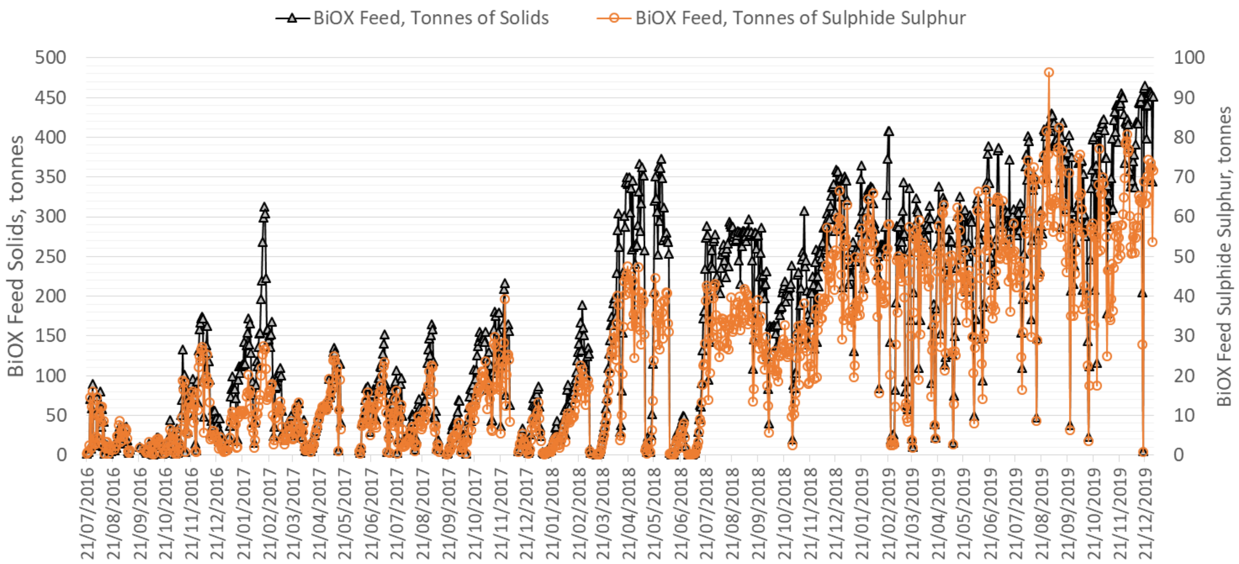


**FIG 11** – Historical BiOX circuit feed rate.

Until 2019, the combined effect of low-grade feed and low recovery inevitably led to low gold production and put the company under severe financial stress. The financial constraints prevented the company purchasing instruments and auto-samplers and installing proper process monitoring and control systems. Sampling, measurement, and process control are predominantly carried out manually. The financial constraints also held back replacing, upgrading, or servicing equipment. Many pumps had no standby, and critical spare parts missing or inadequately stocked on-site. Due to lack of preventative maintenance, equipment conditions deteriorated rapidly, and reliability increasingly became a major risk.

## IMPROVEMENTS

The new management team starting at the end of 2018 set increasing gold production to generate positive cash flow as the first priority. As additional transitional ore was scheduled for processing in 2019, having a lower grade and being more difficult to float, the operating strategy was to focus on maximum utilisation of the plant capacity while optimising individual circuit performance. A number of immediate actions were taken to:

- increase mill throughput
- discard low-grade scats, ie below the mine cut-off grade of 0.7 g/t Au
- increase cyanide concentration in the ILR and closely monitor dissolved oxygen level
- collect ILR solid residue for separate treatment, not returning directly to the mill
- increase flotation mass pull and feed to BiOX
- stop BiOX froth reporting to the CCD circuit.

Further optimisation was carried out in the grinding, flotation, BiOX, CCD and CIL circuits. The result was an increase in both mill throughput and gold recovery, and consequently gold production in 2019. Table 1 summarises the year-by-year process plant performance. Figure 12 shows the historical monthly gold production. Note that the 2019 data in Figure 12 excludes the gold contained in the ILR residue. At the end of 2019, the operation reached a gold production rate exceeding the target of 80 000 ounces per annum. It should be noted that the BiOX circuit was not in full operation until April 2018. Some of the flotation concentrate bypassed the BiOX circuit and was fed directly to the CIL circuit. Therefore, a higher sulphur oxidation in the BiOX circuit was reported but a lower CIL recovery was achieved in 2017 and 2018. It should also be noted that the 2017 and 2018 data were not properly reconciled. The overall plant recovery calculated from the reported stage recovery in the individual gravity, ILR, flotation and CIL circuits using the equation below was more than 10 per cent higher than the recovery based on the mill feed and the dore poured.

**TABLE 1**
Trade-off study between throughput and recovery.

| | | 2017 | 2018 | 2019 |
|---|---|---|---|---|
| Throughput | tpa | 1,687,811 | 1,655,368 | 1,950,641 |
| Runtime | h/y | 7,627 | 7,424 | 7,620 |
| Milling Rate | tph | 222 | 223 | 256 |
| Mill Feed - Au | g/t | 1.55 | 1.56 | 1.56 |
| Mill Feed - Sulphide Sulphur | % | 0.82 | 0.98 | 0.96 |
| Scats Loss | % | | | 1.63 |
| Falcon Recovery | % | | 43.7 | 34.4 |
| ILR Recovery | | | 73.2 | 90.3 |
| Gravity/ILR Recovery | | 23.5 | 32.0 | 31.0 |
| ILR Residue | % | | | 3.4 |
| Flotation Recovery - Au | % | 72.2 | 76.6 | 74.1 |
| Flotation Recovery - Sulphide | % | 85.6 | 90.1 | 87.0 |
| BiOX Feed - Sulphide Sulphur | tpa | 3,278 | 8,069 | 16,353 |
| BiOX Oxidation | % | 97.6 | 88.8 | 67.7 |
| CCD/Neutralisation Loss | % | | 0.5 | 1.2 |
| CIL Recovery | % | 58.1 | 70.1 | 83.9 |
| Overall Recovery | % | 42.8 | 57.9 | 70.0 |
| Au in Dore | oz | 36,006 | 48,081 | 68,563 |
| Au in Concentrate | oz | | | 2,155 |
| Total Contained Au | oz | 36,006 | 48,081 | 70,719 |

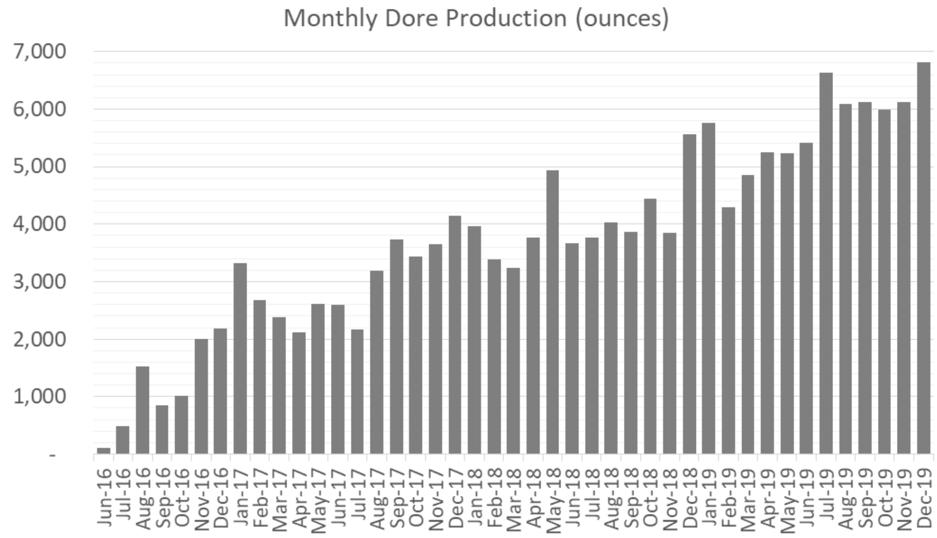


**FIG 12** – Historical monthly gold production.

For 2017 and 2018, the overall recovery should match the stage recoveries by:

$$R = R1 + ((100\% - R1) \times R2 - R3) \times R4$$

where R1 is the gravity/ILR recovery, R2 is the flotation recovery, R3 is the loss in the CCD/Neutralisation circuit, and R4 is the CIL recovery.

For 2019, the scat loss and the ILR solid residue are included in the mass balance. Hence, the overall recovery becomes:

$$R = R1 + ((100\% - R1 - R5 - R6) \times R2 - R3) \times R4$$

where R5 is the gold in the discarded scats and R6 is the contained gold in the ILR solid residue.

## Grinding and mill throughput

The design milling rate was 219 t/h based on an annual mill throughput of 1.75 Mt and 8000 operating hours in a year. After the commissioning, the mill throughput gradually increased and reached 250 t/h at the end of 2017. After the start-up of the bio-oxidation process in 2018, the mill throughput was largely capped to the design rate. This was to limit the amount of feed to the BiOX circuit to prevent excess froth overflowing the bio reactors and to allow maximum sulphur oxidation and CIL recovery. Figure 13 shows the historical daily mill throughput rate.

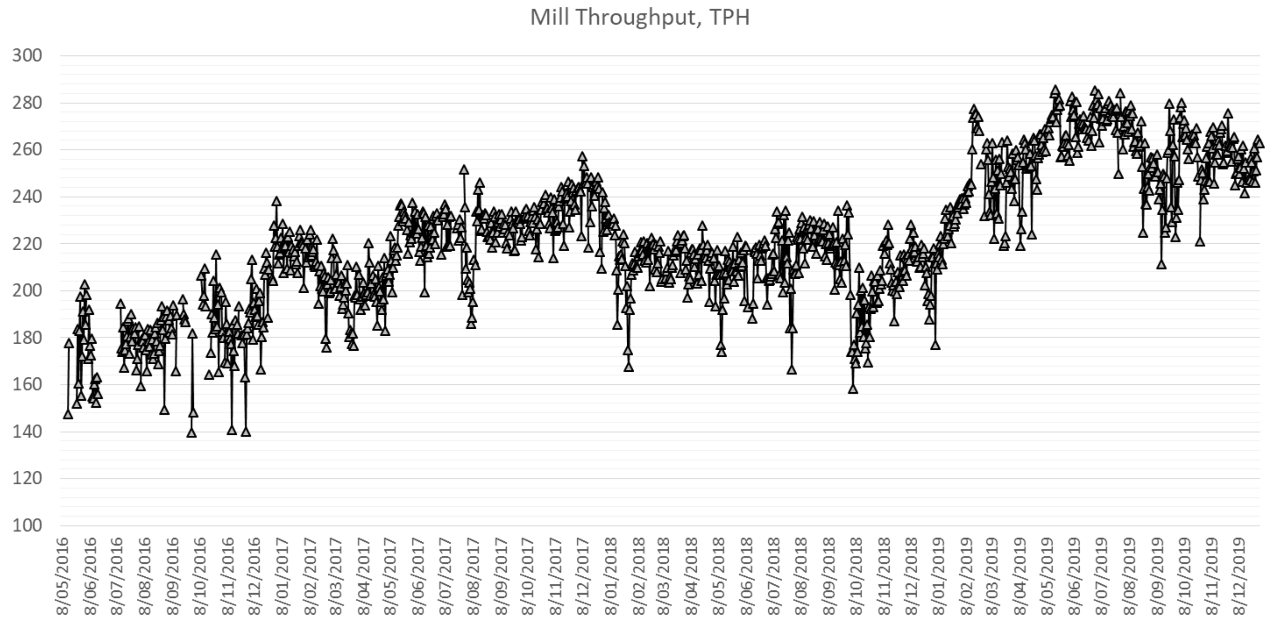


**FIG 13** – Historical mill throughput rate.

At the end of 2018, the SAG mill operated at close to the design throughput rate and drew approximately 4.3 MW of the installed 7.2 MW power. The mill feed was increased firstly gradually to 250 t/h in early 2019 and quickly to 280 t/h by mid-February. During this time period, no modification was made to the existing mill operating conditions. The power draw increased linearly proportionally to the mill feed rate and the grind size became coarser while the operating work index remained largely unchanged. Mill throughput rate and power draw in 2019 are given in Figure 14, and grind size and operating work index in Figure 15.

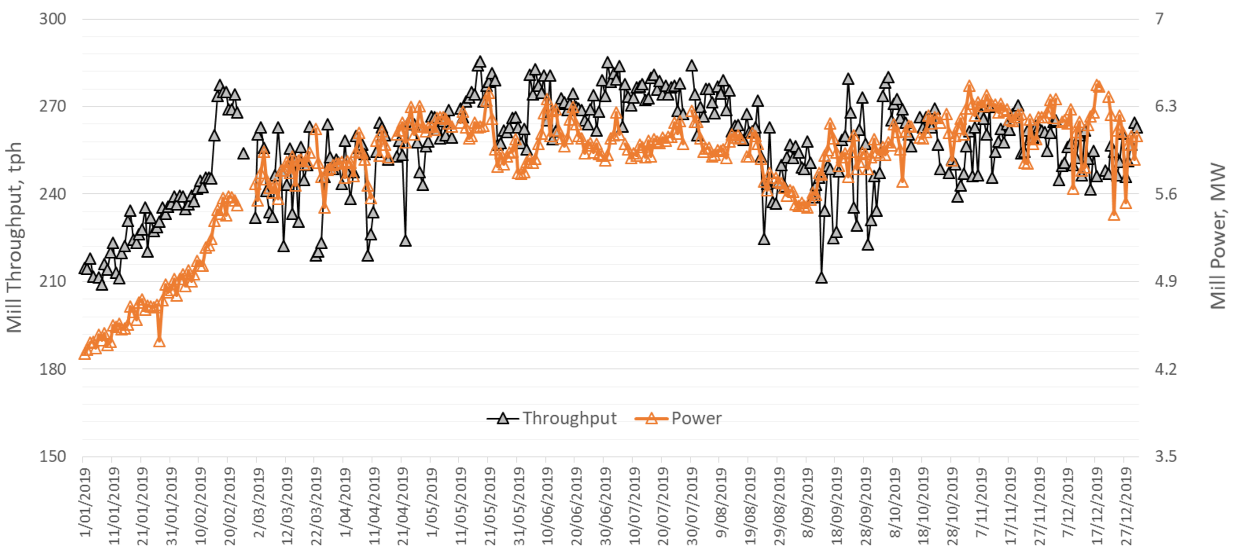


**FIG 14** – Mill throughput rate and power draw in 2019.

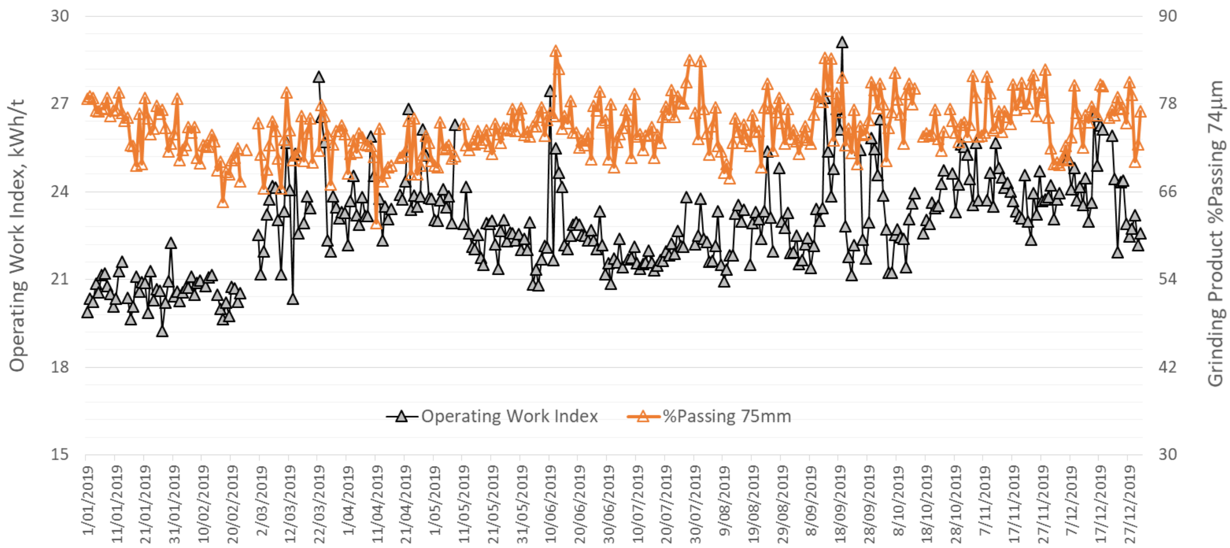


**FIG 15** – Mill product size and operating work index in 2019.

The mill could not sustain the new throughput rate between March and May 2019 due to tailings line restrictions. Once the tailings issue was resolved, an average of 278 t/h ore was milled in July 2019 which is 27 per cent above the design. The mill power consumption was 6 MW in July. After achieving a higher throughput rate, the next step was to improve power utilisation and grind size by increasing the ball charge from 18 per cent at the beginning of March to 24 per cent in May 2019. The grinding product size returned to almost the same level as before the throughput increase. In the last two months of 2019, pegging of the steel mill discharge grates became an issue. The milling rate dropped to 260 t/h then 250 t/h. Nevertheless, the pulp was retained inside the mill for longer and the power utilisation remained high resulting in a higher operating work index and a finer grinding product.

The SAG mill has been operating at a fixed speed of 11.8 rev/min, equivalent to 75 per cent of critical speed since commissioning. A Slip Power Recovery (SPR) system is scheduled for commissioning in February 2020 to allow the mill speed to be varied.

At the beginning of 2019, the scats grade was typically around the mine cut-off grade of 0.7 g/t Au. Figure 16 shows the scats grade and the scats production and contained gold as a proportion of the mill feed in 2019. It was observed that most of the scats returned to the mill would come out of the mill remaining as scats, as shown in the trial at the end of February 2019 in Figure 16. It would take a number of passes to sufficiently grind down the scats. Clearly, scats would not only displace the higher-grade fresh ore but were also uneconomic to process most of the time. With the increase in ball charge, the scats production gradually decreased, and the grade also decreased to below 0.6 g/t Au. Therefore, it was decided that the low-grade scats should be discarded. Removing the scats effectively increased both the mill throughput and the head grade to the flotation circuit.

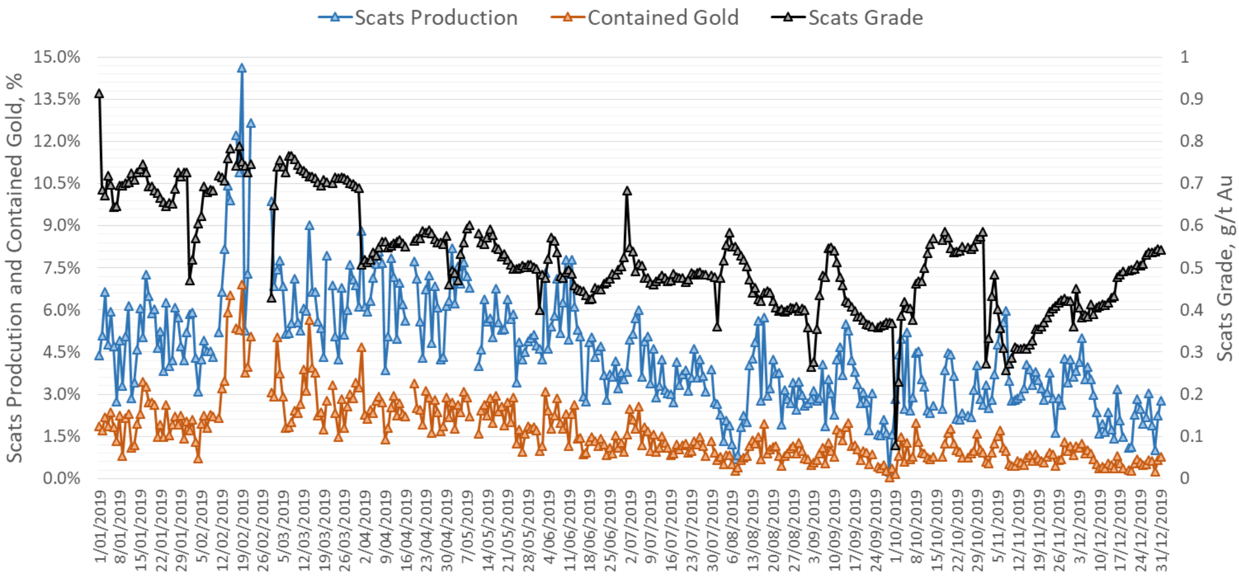


**FIG 16** – SAG mill scats production, grade and contained gold in 2019.

## Gravity and ILR

The average ILR gold extraction from the Falcon concentrate was 73 per cent in 2018 although improved to 88 per cent at the end of 2018 in comparison with 98 per cent expected in the initial design. Cyanide concentration was typically below 10 000 ppm but not accurately monitored, neither were the sodium hydroxide addition and dissolved oxygen level. The ILR solid residue was returned to the mill discharge hopper after washing twice. Occasionally when there were disruptions to the ILR operation, the ILR residue contained high cyanide was going to the milling circuit. From the beginning of 2019, the ILR solid residue was collected and stored in Intermediate Bulk Containers (IBC's). The final residue solution is decanted and pumped to the CIL circuit. No ILR residue, solids or solution, returns to the milling circuit to eliminate any potential impact of residual cyanide on flotation. At the end of February 2019, cyanide concentration was increased to 15 000 ppm, minimum 12 000 ppm. A DO probe was also installed to ensure the DO level is within the range of 10–12 ppm. Since March 2019, gold extraction in the ILR has been consistently above 93 per cent except August 2019 due to a faulty valve. Figure 17 shows the ILR leaching efficiency in 2018 and 2019. Figure 18 shows the ILR feed and residue grades. As the ILR leaching efficiency improved, the ILR solid residue grade decreased. The average ILR solid residue grade between March and December 2019 was 115 g/t Au, still sufficiently high to justify separate treatment.

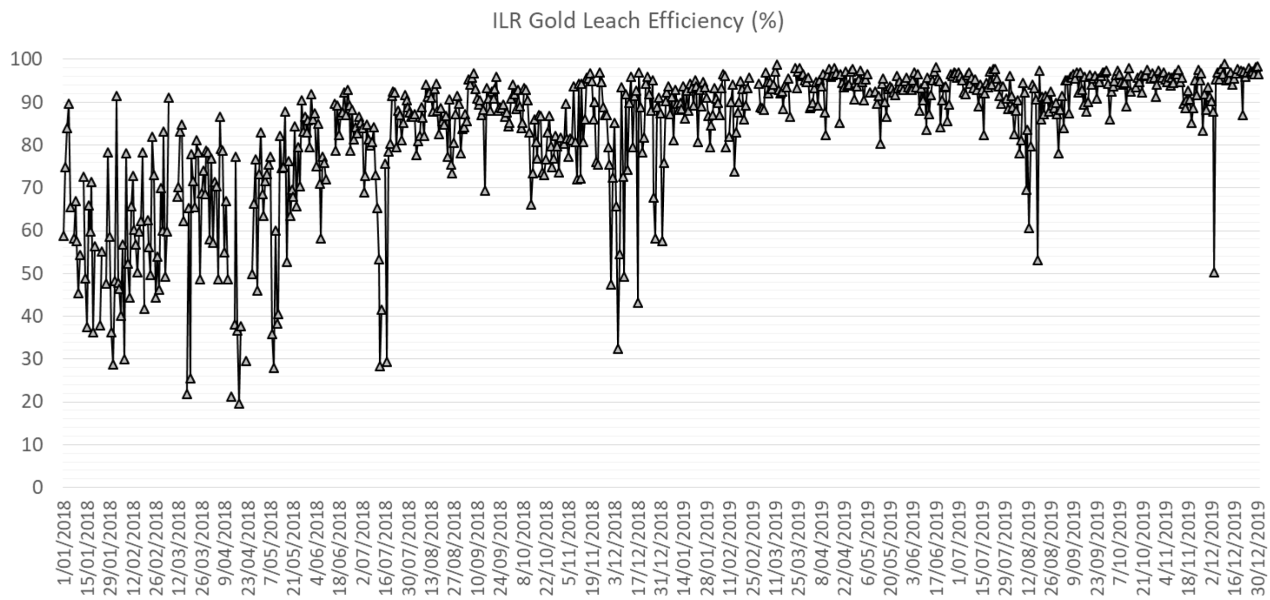


**FIG 17** – ILR gold leaching efficiency.

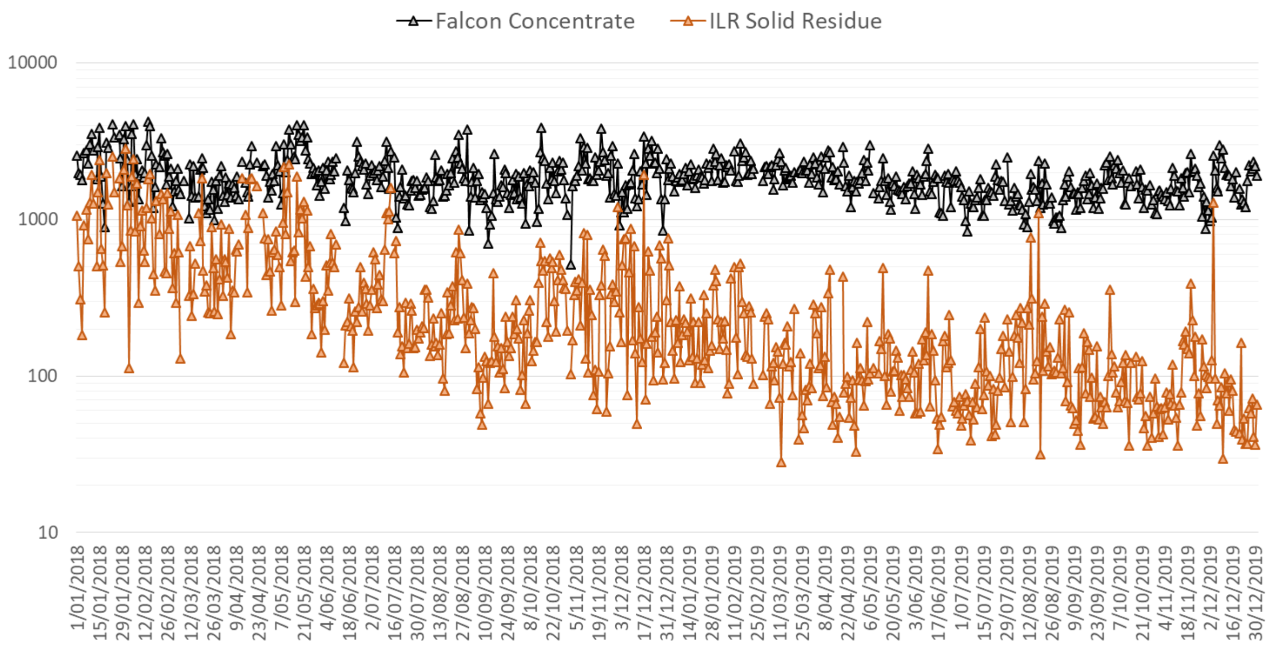


**FIG 18** – ILR feed and tailings grade.

With removal of the scats and storage of the ILR residue, the process flow sheet changed to Figure 19 as currently implemented.

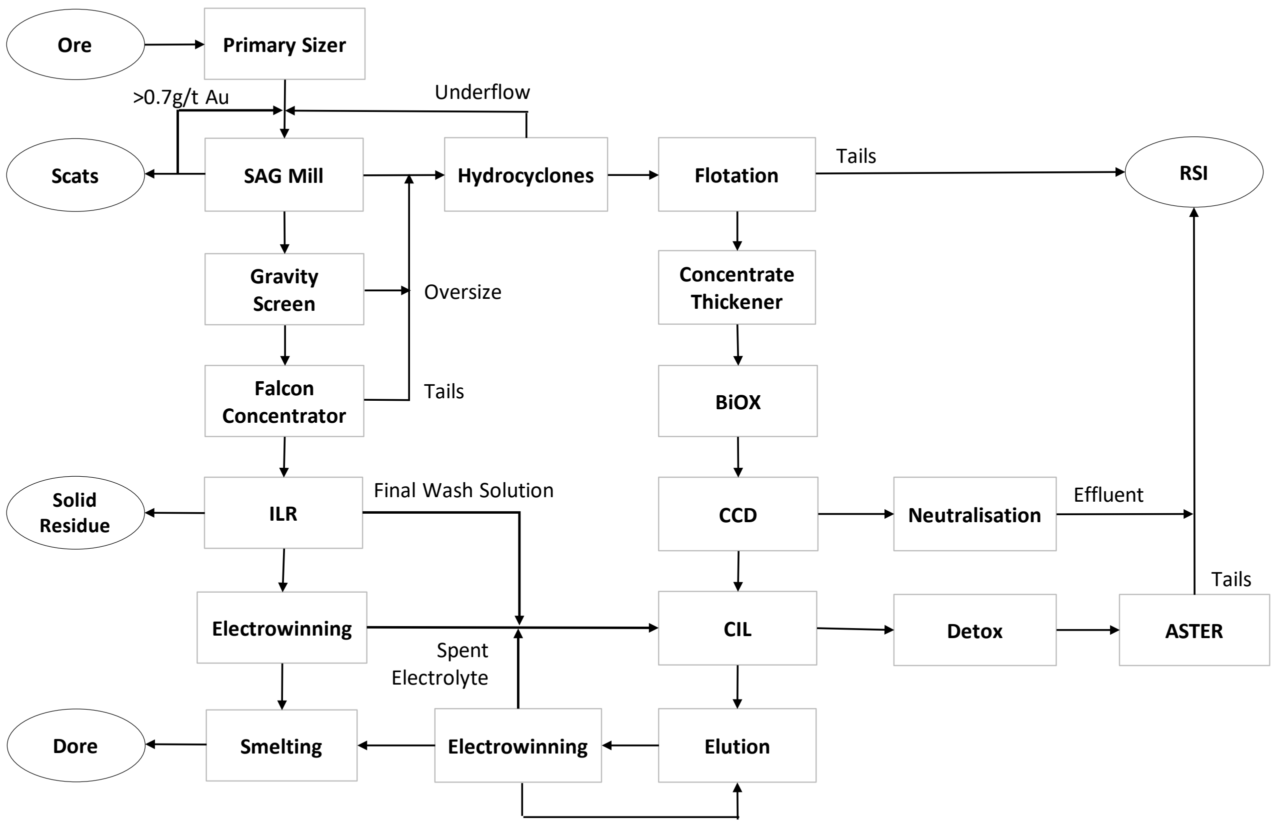


**FIG 19** – Current process flow diagrams.

## Flotation

Flotation was unable to achieve the design recovery due to the increased proportion of transitional ore in the feed, poor grinding circuit performance resulting in excess fines and coarse composite particles in the flotation feed, relatively short circuit residence time, and constraint on mass pull caused by the downstream BiOX circuit. With the increase in mill throughput in 2019, some of the limitations became even more pronounced. A number of changes were made to the flotation operation in 2019, including:

- Increase of flotation feed density from 33 per cent solids to 40 per cent solids to gain additional circuit residence time.
- Increase of BiOX feed to allow a greater mass pull in the flotation circuit.
- Development of a new control strategy based on mass pull and Peak Air Recovery (PAR), using more air at a deeper froth and using frother to control the froth stability and mobility.

The most significant improvement was observed in August 2019 when the pH was adjusted from natural 6.3–7.5 to 8.5 using hydrated lime and mixed Potassium Amyl Xanthate (PAX) and dithiophosphate (DSP007) were used as collector instead of just DSP007. The higher pH and introduction of PAX improved flotation kinetics significantly. In comparison with DSP007, PAX produced more mineralised and drier froths. Another important benefit of PAX replacing DSP007 is elimination of the frothing issue in the BiOX circuit as the residual PAX in the flotation concentrate fed to the BiOX circuit does not have the same frothing effect as DSP007. The flotation gold recovery increased to 74 per cent from 54 per cent in 2018. Meanwhile, the concentrate grade of sulphur was also higher in 2019 than 2018 even though the flotation feed grade was lower in 2019. Figure 20 shows the historical monthly average flotation gold recovery. Note that change in the circuit gold inventory was not accounted for in the monthly reconciliation in Figure 20. There was significant accumulation of concentrate in the BiOX bund area in May, June and July, which only returned to the circuit in August and September. Therefore, the flotation recovery in May to July 2019 was under-reported in Figure 20 and over-reported for August and September 2019.

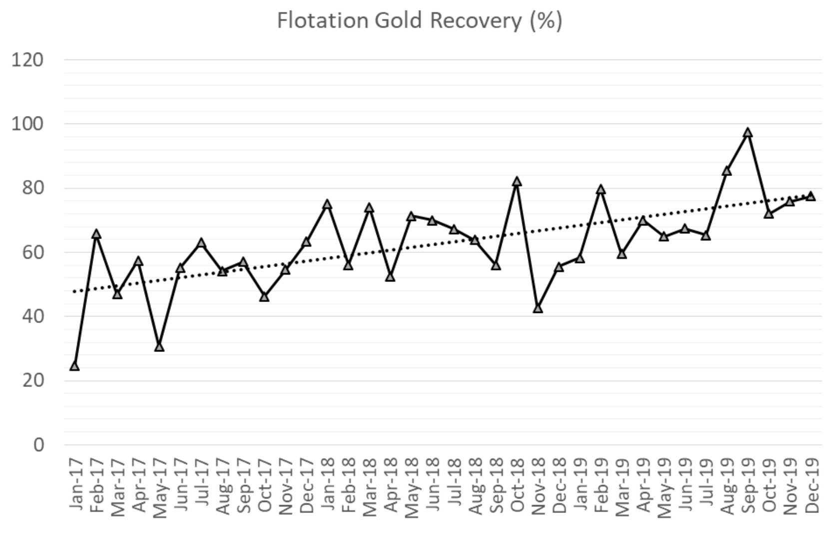


**FIG 20** – Historical monthly flotation gold recovery.

## BiOX and CCD

Frothing was a major issue in the BiOX circuit. With the change of flotation collector and pH in August 2019 and modification of defoamer distribution and spray system, this issue was finally resolved. Figure 21 shows the BiOX tank conditions before and after the change.

**FIG 21** – BiOX frothing issue before and after change of flotation collector.

The BiOX froth contained mostly sulphide with a gold grade higher than the fresh BiOX feed. When the BiOX froth entered the CCD via either the launder or the sump pump, some of the gold in the froth would be lost via the CCD overflow to the neutralisation effluent and final tailings. In 2019, transfer of the BiOX froth to the CCD via the sump pump was restricted to minimise the gold loss in the CCD overflow. Elimination of the frothing issue from August 2019 onwards resulted in reduction in the gold loss, as can be seen in Figure 22.

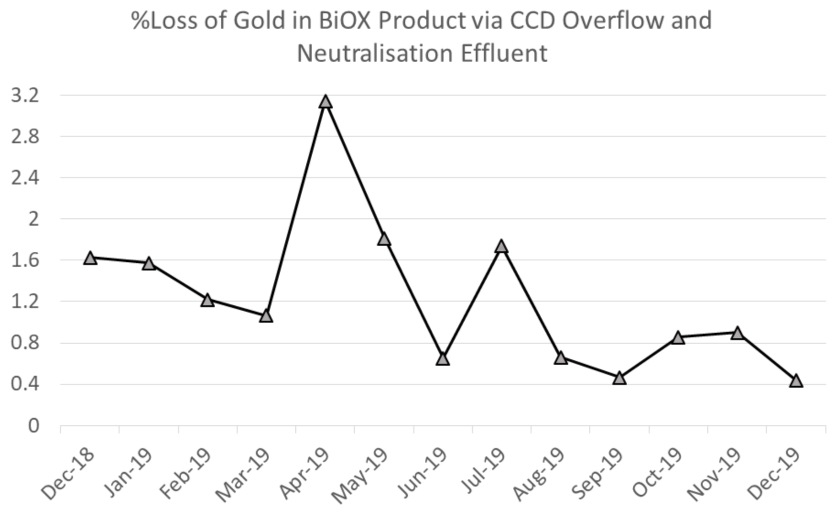


**FIG 22** – Gold loss in neutralisation effluent.

The artificial constraint on the BiOX feed rate was removed in 2019 even though a higher feed rate would result in a lower sulphur oxidation and consequently a lower CIL recovery. A trade-off study of increased mill throughput and BiOX feed versus higher sulphur oxidation and higher CIL recovery clearly indicated that the higher throughput would deliver greater gold production and a better financial return. As shown in Figure 11, the BiOX feed peaked at 461 t/d of solids and 82 t/d of sulphide sulphur in 2019, significantly higher than the 2018 data and the design values.

Since June 2019, nutrient addition doubled from 3 kg/t of BiOX feed to 6 kg/t. In September, operation of a third air blower started increasing the total air supply from an average 24 000 Nm³/h to 30 000 Nm³/h. Figure 23 shows the sulphur oxidation and the amount of sulphur oxidised. Despite the higher feed rate and consecutive failures of primary reactor agitator shafts from October onwards resulting in a lower degree of sulphur oxidation, the tonnes of sulphur oxidised per day increased slightly in the last quarter of 2019 compared with the first half of 2019. Not only the extra oxidised portion but also the extra un-oxidised portion would contribute to the gold production even though the CIL recovery would be lower.

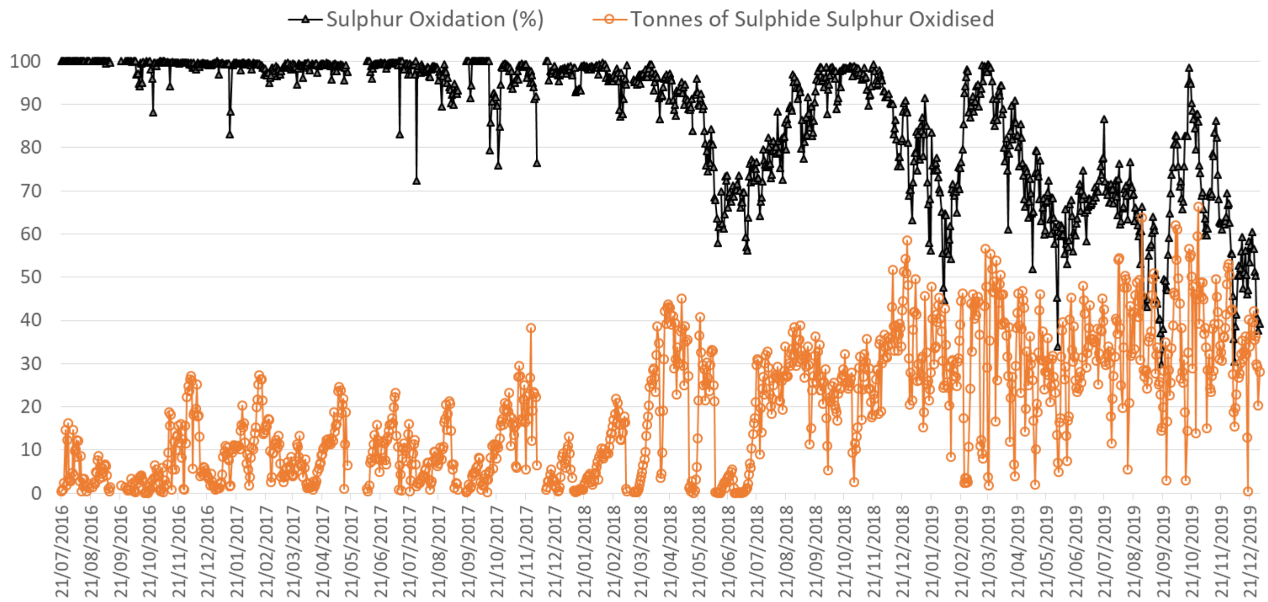


**FIG 23** – Historical sulphur oxidation in BiOX circuit.

## CIL

The CIL circuit provides over 35 hours of residence time at the maximum mill throughout. The leach kinetics are relatively fast, and leaching is generally complete by the time the slurry reaches the fourth tank. Figure 24 shows gold in solids profile down the bank surveyed at the end of each month in 2019. The carbon adsorption kinetics are also fast. All the gold leached can be adsorbed onto the carbon within each individual tank. The gold in carbon and gold in solution profiles follow the same trend as the gold in solids. The typical carbon loading is under 2000 g/t, while the laboratory test indicates maximum loading can be 50 000 g/t.

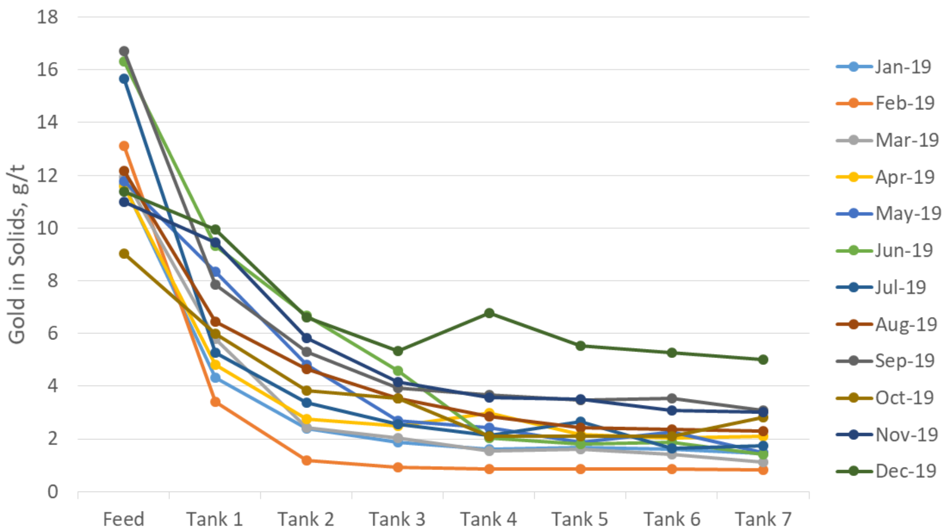


**FIG 24** – Down the CIL bank profile of gold in solids.

The CIL performance is largely dictated by the sulphur oxidation in the BiOX circuit. Once the sulphide is fully oxidised, the overall CIL recovery can generally reach 96 per cent. Although the CIL gold recovery in 2019 was lower than the last quarter 2018 due to the higher throughput and lower sulphur oxidation in the BiOX as shown in Figure 10, improvement has been observed in the CIL circuit. At a given sulphur grade or a gold to sulphur ratio in the CIL feed, the CIL recovery in 2019 was above the historical data. The comparison results are presented in Figures 25 and 26.

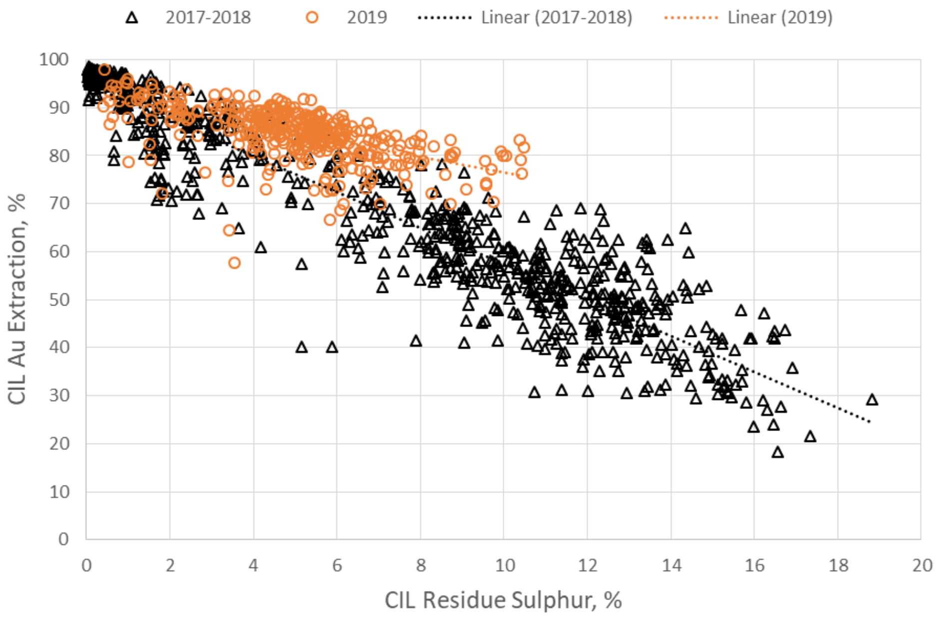


**FIG 25** – CIL gold extraction versus sulphur grade.

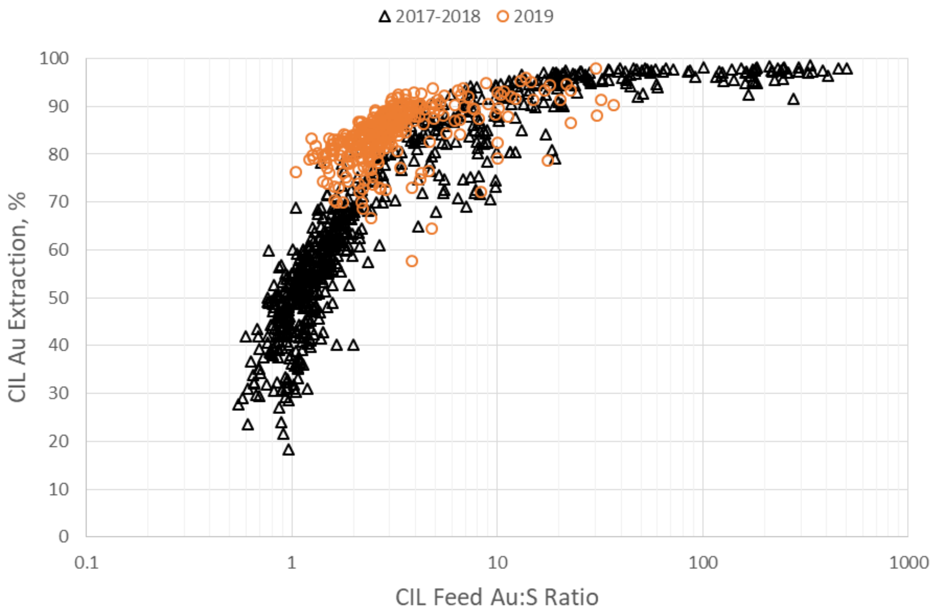


**FIG 26** – CIL gold extraction versus gold to sulphur ratio.

Previously, the DO level in the CIL pulp could be as low as 1–2 ppm in some of the tanks when the air sparger was blocked. To prevent the sparger blockages, a cylindrical cap was installed to shield the air sparger from the settling particles and create an air pocket above the sparger outlet, as shown in Figure 27. Now the DO can be maintained at approximately 6 ppm.

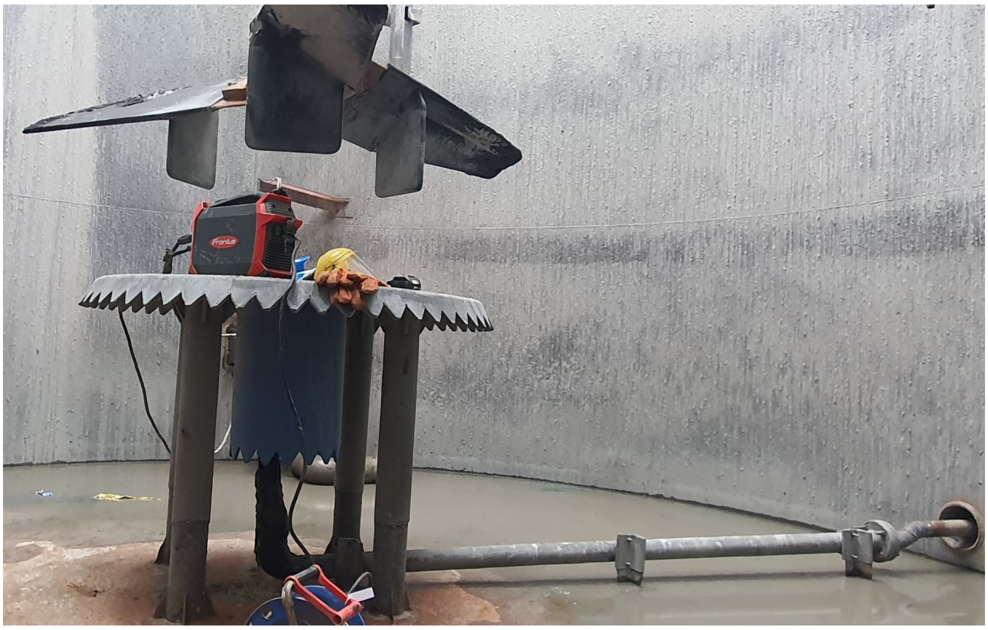

**FIG 27** – Cylindrical cap on CIL air sparger.

Figure 28 shows the effect of BiOX sulphur oxidation on the CIL gold recovery. The improved CIL recovery at a given degree of sulphur oxidation in the BiOX circuit in 2019 could possibly also be partially due to short-circuiting of the flotation concentrate to the CIL circuit. According to the mineralogical study, fine pyrite and arsenopyrite in the Runruno deposit tend to contain more gold. As the fine pyrite and arsenopyrite in the flotation concentrate are more likely to be oxidised than the coarse pyrite, the partially oxidised concentrate is likely to perform better in the CIL circuit if the whole concentrate has gone through the BiOX process rather than if only part of the concentrate has gone through the BiOX process, even though the two final BiOX products have the same degree of sulphur oxidation.

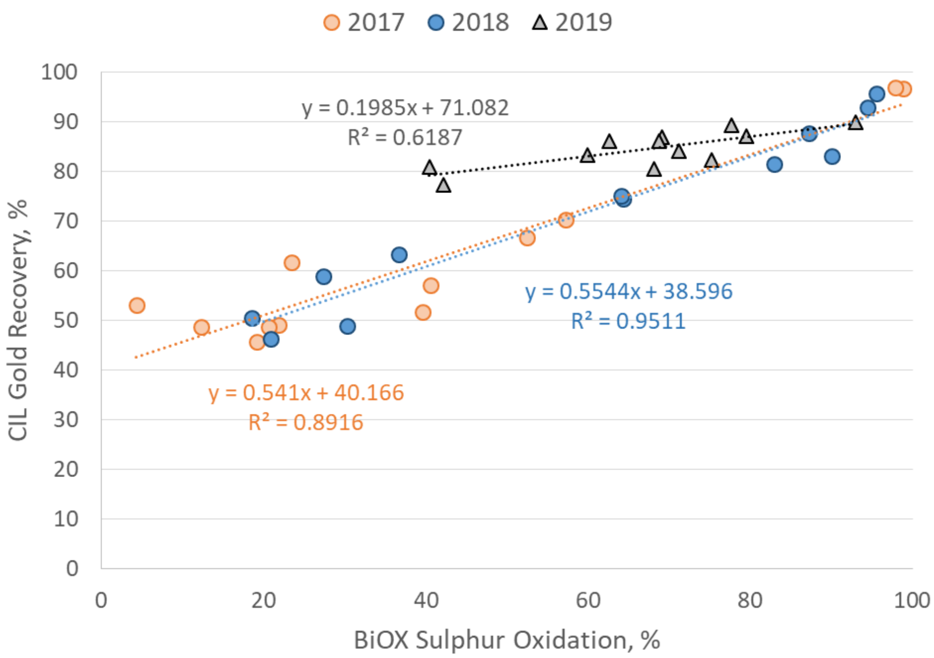


**FIG 28** – CIL gold recovery versus BiOX sulphur oxidation.

## ILR residue retreatment

Approximately 672 t of ILR residue was collected in 2019, containing 2694 ounces of gold. A small treatment plant was installed to process this material. The new plant consists of a screen, a Low Intensity Magnetic Separator (LIMS) and a shaking table to produce a gold concentrate for sale. The screen oversize (+1 mm particles), the magnetic faction (mostly steel from the grinding media) and the table tailings are sent back to the mill for reprocessing in the main plant. The table consistently recovers over 95 per cent of the gold. The table concentrate typically contains over 500 g/t of gold and over 90 per cent of the mass is pyrite. The gold concentrate will be sold to external smelters. The commercial terms are currently being negotiated and the payable gold in concentrate is expected to be significantly higher than the recovery in the existing flotation, BiOX and CIL circuits if the ILR residue were to return to the circuit directly.

## PROJECTS

A number of projects are currently under study or being implemented. The key ones are:

- Residue Storage Impoundment (RSI) discharge line (RDL) modification to reduce downtime.
- Commissioning of a Slip Power Recovery (SPR) drive system, re-design of mill liners and discharge grates, grinding circuit optimisation, and automatic process control to ensure high mill throughput and optimum grind size.
- Installation of pneumatic flotation to expand the flotation capacity.
- BiOX air blower services and installation of an additional air blower to improve sulphur oxidation and CIL recovery.

### RSI discharge line (RDL) modifications

The mill runtime was 87.2 per cent in 2019, lower than 89.4 per cent in 2018. Figure 29 shows the monthly mill runtime. Approximately half of the downtime in 2019 was caused by RSI discharge line failures. Breakdowns of the major downtime events are shown in Figure 30. Between February and May 2019, all three sections of 400 mm steel residue line failed due to wear on the bottom of the pipe.

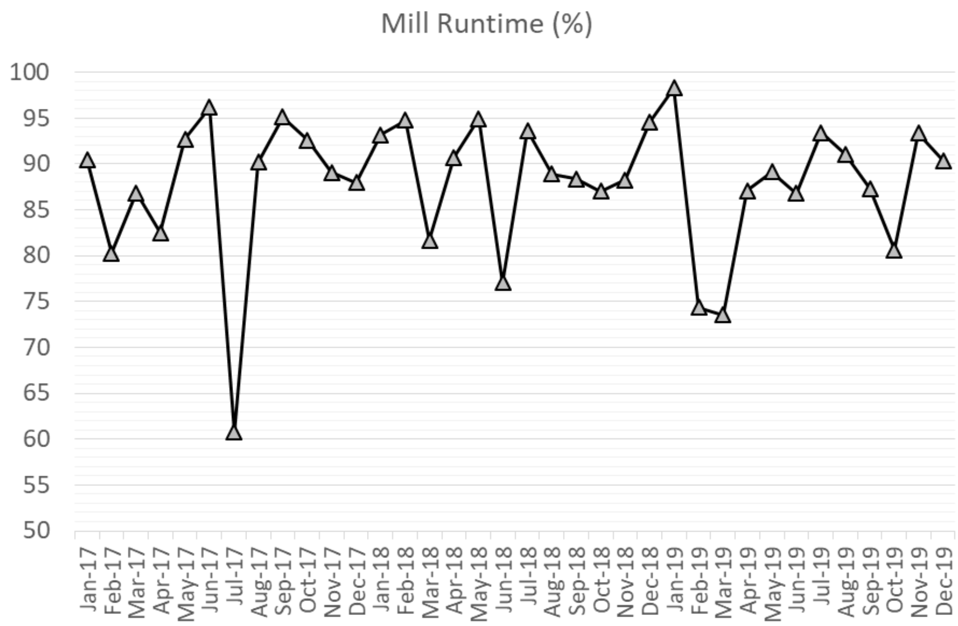


**FIG 29** – Monthly mill runtime.

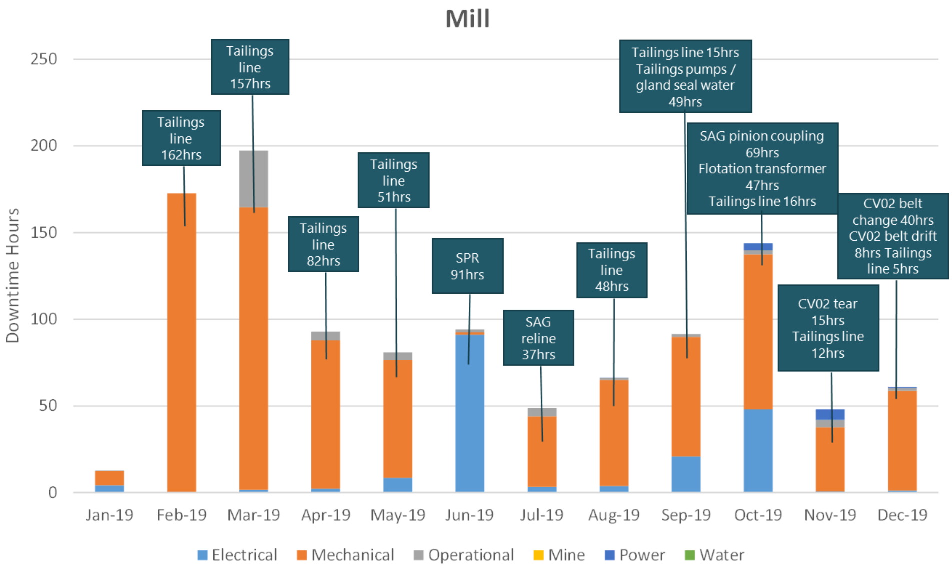


**FIG 30** – Breakdowns of mill downtime in 2019.

The total length of the RSI discharge line is approximately 2.3 km. Three stage pumping via 315 kW HP250 pumps is currently used and the pipeline pressure is typically around 1800 kPa. Pump discharge static head is currently 130 m at the present elevation of the RSI crest. Four stage pumping is scheduled for commissioning in February 2020. At final RSI crest height, tailings pump discharge static head will increase to 159 m. The bulk of the line consists of 450 mm HDPE PE100 PN25.

The corrective actions taken in 2019 included replacement of the worn sections of steel pipes, reducing the number of HDPE welded joints, installation of anchor blocks to reduce the pipe movement and installation of a check valve to reduce water hammer (Figure 31).


**FIG 31** – Corrective actions taken for RSI discharge line in 2019.

The remaining issues include:

- Insufficient HDPE line length in areas, resulting in insufficient ability to cope with line thermal expansion/contraction and other movement and creating localised excessive tension, potentially pulling the line apart.

- Insufficient anchoring of the line in places allowing downhill line movement and causing increased tension up gradient.
- Excessive HDPE welded joins in areas where additional pipe length has been inserted to reduce increasing line tension.

Some of these remaining issues are shown in Figure 32.


**FIG 32** – RSI discharge line remaining issues.

Additional measures to rectify some of these remaining issues are scheduled for completion in February 2020. Intermittent rotation of the steel pipeline sections has been scheduled to increase wear life.

## Grinding circuit optimisation

The SAG mill currently operates at a fixed speed of 11.8 rev/min, equivalent to 75 per cent of the critical speed. The pulp is discharged too quickly at this speed, and the rock/pulp level is low inside the mill. Ball to ball and ball to liner impact at times creates a significant amount of metal debris, as can be seen on the gravity feed screen (Figure 33). The inefficient grinding also results in a high recirculating load, which limits the amount of water that can be added to the mill discharge hopper. The high cyclone feed density then produces poor classification with a relatively large proportion of coarse composite particles short-circuiting to the flotation circuit via the cyclone overflow. Meanwhile, a large proportion of the fines are entrained in the cyclone underflow and return to the mill, potentially being over-ground.

**FIG 33** – Steel debris from grinding balls on gravity screen oversize.

The SAG mill SPR is scheduled to be commissioned in February 2020. This will allow the mill speed to vary. The plan is to slow down the mill and increase the ball and rock charge in the mill to improve grinding during each pass and reduce the recirculating load. Meanwhile, the cyclone feed will be diluted to improve classification efficiency and reduce fines returning to the mill and coarse composites misplaced in the cyclone overflow.

There are existing flowmeters and a density gauge to measure water addition to the mill and the mill discharge hopper as well as cyclone feed flow and density. There are also load cells available to measure the mill weight, noise monitors on both sides of the mill shell, a pressure gauge on the cyclone feed distributor and a level sensor on the mill discharge hopper. However, the mill feed rate is currently manually set by operators. All water additions are also set manually. After the SPR commissioning, the plan is to implement automatic process control for the grinding circuit. Mill feed rate will be allowed to vary by controlling to a set mill weight and cyclone control to a set pressure. Power utilisation will be maximised to produce a finer and narrower size product at the target throughput.

Figure 34 shows the pegged mill discharge grates observed in December 2019. It has been proposed to replace the existing steel grates with more flexible rubber panel grates. Another option is to change to angled slots design.

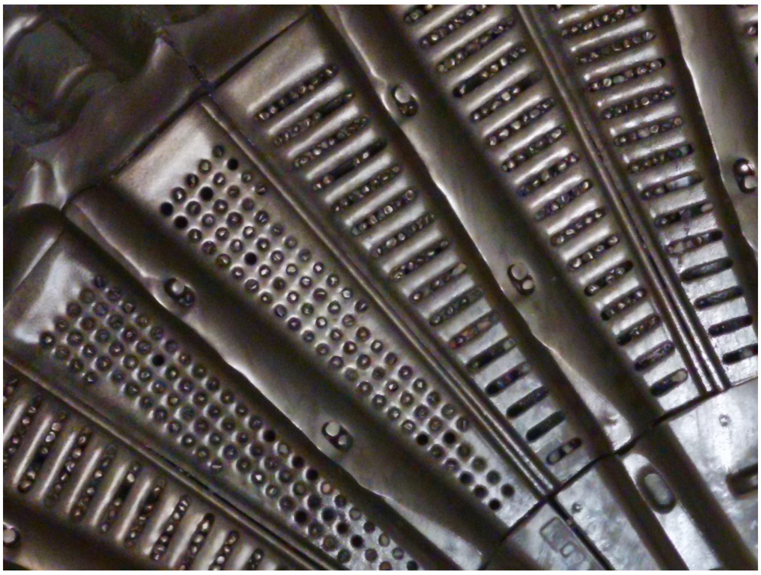

**FIG 34** – Mill discharge grate pegging with steel.

## Pneumatic flotation

The existing flotation circuit is a bank of six 70 $m^3$ tank cells, performing a bulk roughing duty. The limited capacity of the existing circuit is one of the main constraints for flotation to achieve the target recovery, especially at the increased throughput. It becomes even more challenging to achieve the recovery target when the mass pull is restricted by the downstream BiOX circuit capacity. A number of options have been considered to expand the circuit capacity and/or reduce the concentrate mass, including additional roughers/scavengers, a new cleaner bank, and a flash flotation cell in the grinding circuit. To minimise the capital requirement and time delay, it is proposed to install a pneumatic flotation device on the existing flotation feed tank. The device is similar to the Jameson cell's downcomer. This will not only add additional flotation capacity but also provide a higher turbulent environment for fines recovery. The device is currently being trialled in the plant (Figure 35).

**FIG 35** – Trial of pneumatic flotation device on feed conditioning tank.

## BiOX air supply

Shortage in air supply is the main cause for the lower-than-expected sulphur oxidation in the BiOX circuit. Figure 36 shows a strong correlation between air supply per tonne of BiOX feed and sulphur oxidation.

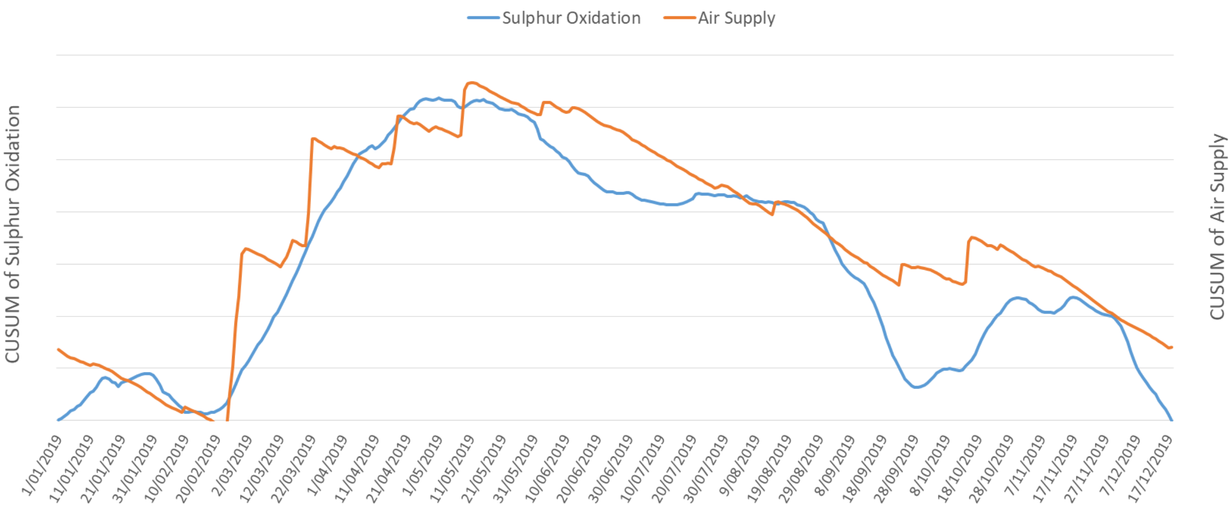


**FIG 36** – Cusum of air supply and sulphur oxidation in BiOX circuit.

There are currently three air blowers installed. However, until August 2019, only two blowers were in operation and delivered on average 24 000 $Nm^3/h$ of air. After continuous operation of the third blower commenced, the total air supply increased to approximately 30 000 $Nm^3/h$. In comparison, the initial design states 48 046 $Nm^3/h$ of air is required. With the dual blade Afromix agitators replacing the single blade agitators in the initial design, oxygen utilisation can be improved by 20 per cent. Still, 38 437 $Nm^3/h$ of air is required to achieve the target sulphur oxidation. The air blowers have not undergone a major OEM service since the commissioning in 2016. The amount of air they deliver is significantly less than the specification provided by the manufacturer. An on-site inspection was conducted by the original manufacturer in November 2019 and a full service is schedule in March 2020. Meanwhile, a fourth air blower has been ordered and is expected to be delivered in December 2020.

## CONCLUSIONS

Prior to 2019, Runruno was operated at a financial loss. Given the spare mill power available, a decision was made to increase the mill throughput even though there would potentially be a negative impact on the metallurgical performance. Meanwhile, a number of changes were also made to optimise the individual circuits. The main ones included:

- Discard the low-grade scats to allow additional fresh mill feed.
- Increase the ball charge in the SAG mill to reduce the product particle size.
- Collect the ILR solid residue for separate treatment to produce a gold concentrate for sale to external smelters.
- Increase the cyanide concentration and the DO level in the intensive leaching of the Falcon concentrate to improve the ILR extraction.
- Increase the flotation pH and change the flotation collector to PAX to improve the flotation recovery and concentrate grade and to eliminate the excessive froth in the BiOX circuit.
- Minimise short-circuiting of the flotation concentrate around the BiOX circuit to the CCD to allow all sulphide to undergo the bio-oxidation process to improve the CIL recovery.
- Start-up the third air blower to increase air supply in the BiOX circuit to improve the sulphide oxidation and CIL recovery.
- Improve air sparging and increase the DO level in the CIL tanks to improve the CIL recovery.

With the average milling rate being 17 per cent above the nameplate and the 12.1 per cent increase in gold recovery in 2019 from the previous year, Runruno produced 68 563 ounces of gold in dore and approximately 2155 ounces of gold in concentrate in 2019. The gold production in 2019 is 47 per cent more than the previous year and turned the company into a positive cash flow situation. A number of projects are currently underway to optimise the grinding product and further improve the flotation recovery, sulphur oxidation in the BiOX circuit and CIL recovery. It is anticipated that the mill throughput will increase to 2.1 Mtpa, overall gold recovery to 85 per cent and annual gold production to 80 000 ounces for the remaining life-of-mine at Runruno.


## ACKNOWLEDGEMENTS

The authors would like to acknowledge the permission of Metals Exploration Plc to publish this work. Many people at Runruno were involved in the test work, plant trial and project implementation. In particular, the authors would like to thank Adelaida Gayyed for performing the flotation and CIL test work, Gennad Comtiag for conducting the BiOX frothing study, Nick Holder for his work on BiOX, and Craig Jacobson for his work on gravity, ILR and elution and his assistance with project implementation.


## REFERENCES


van Niekerk, J A, Olivier, J W and Jardine, J G, 2017. Implementation of the BiOX® process at the Runruno Gold project, in Proceedings of MetPlant 2017, pp 218–228

# Process automation

# Online gold analysis at Evolution Mining Mt Carlton

*A Cervellin[1], J Robinson[2], A Sia[3], E Craig[4] and L Killer[5]*

1. Senior Metallurgist, Evolution Mining, Bogie Qld 4805. Email: andrew.cervellin@evolutionmining.com
2. Senior Metallurgist, Evolution Mining, Bogie Qld 4805. Email: james.robinson@evolutionmining.com
3. Head of Digital Solutions, Gekko Systems, Ballarat Vic 3350. Email: andrews@gekkos.com
4. Process Engineer, Gekko Systems, Ballarat Vic 3350. Email: elizac@gekkos.com
5. Graduate Metallurgist, Evolution Mining, Bogie Qld 4805. Email: lindsey.killer@evolutionmining.com

## ABSTRACT

Gekko Systems have collaborated with the CSIRO and Evolution Mining's Mt Carlton operation to complete the first successful site-based trial of an on-stream analyser capable of directly reading gold in slurries and solutions to sub-ppm levels. Developed by the CSIRO and commercialised by Gekko, the XRF-based analyser was installed in the flotation circuit at Mt Carlton and is the first of its type to be installed and trialled in an operating environment.

The collaboration has seen Gekko, CSIRO and Mt Carlton retrofit CSIROs lab analyser into a modular integrated solution. The analyser, known as the OLGA (OnLine Gold Analyser) delivers a real-time hourly rolling average of the gold grade in the targeted process stream, a measurement that is updated every ten minutes and is fed back directly into the plant DCS.

Before the installation of the OLGA, Mt Carlton operational staff used spot assays (taken every six hours) and shift composites to make decisions regarding day-to-day operation of the plant. The turnaround time of these assays was >six hours due to the requirement to dry and prep the samples.

The OLGA has now been successfully trialled on the flotation feed and flotation tails at Mt Carlton and has been providing real-time feedback to the operational staff since December 2018. Having access to real-time feedback of the grades in these streams in higher resolution data than previous sampling intervals has enabled Mt Carlton operational staff to make real-time decisions regarding the operation of the plant. The OLGA is capable of detecting short excursions (which were not visible in the existing assay regime) and also longer-term trends and significant deviations.

This paper discusses the motivations for the OLGA installation, the benefits of OLGA versus existing assay technology, the challenges associated with the trialling of new technology, the results of the trial and the ongoing utilisation/future possibilities of the data provided by the OLGA at Mt Carlton.

## INTRODUCTION

Since Mt Carlton started, the operations has been searching for an on-stream analysis system to effectively monitor and control it's flotation circuit. A number of traditional/existing technologies have been tested/evaluated since the design phase of the project and continued right through to the present. Unfortunately these have all been unsuccessful.

The Mt Carlton ore is a highly variable sulphide ore with heterogenous gold bearing mineralogy. Gold occurs in all of the sulphide minerals at variable and inconsistent proportions. The host rock contains variable levels of dominant sulphate minerals (Alunite) and sulphide sulphur levels that limit the reliability of XRF for the measurement of sulphides.

In December 2018, the world first Online Gold Analyser (OLGA) was installed at Evolution Mining's Mt Carlton Operation in North Queensland, Figure 1 shows the unit after installation. The OLGA technology was developed in the Commonwealth Scientific and Industrial Research Organisation's (CSIRO's) 'UltraGold' Project and has been substantially tested within a laboratory environment to detect low levels of gold contained in slurries and solutions.


**FIG 1** – OLGA installed within the flotation circuit at Mt Carlton Operation.

## LOCATION – EVOLUTION MINING, MT CARLTON GOLD OPERATION

The Mt Carlton operation is located 150 km south of Townsville, Queensland, on the traditional lands of the Birriah People. Local communities include are Gumlu, Home Hill, Bowen, Collinsville and Townsville. At Mt Carlton, Evolution developed the expertise to commercialise a refractory, non-oxidised, high-sulphidation epithermal deposit which is a great example of thinking differently to unlock a previously uneconomic deposit.

The deposit is a high sulphidation epithermal style with mineralisation occurring within felsic volcanic rocks on the northern margin of the Permian Bowen Basin.

The resource comprises gold, silver and copper primarily as copper arsenic sulphides (enargite) and silver arsenic sulphides (tetrahedrite/polybasite) and some native gold (within pyrite). Mineralisation is structurally controlled which is hosted within advanced argillic altered rhyodacite.

The operation was developed by Evolution and commissioned in 2013. Mt Carlton has been a core asset within the Evolution portfolio producing more than 100 koz of gold per annum in the period between FY2017 to FY2019. As one of the highest grade open pits in the world, the mine generated exceptional cash flow in these years averaging approximately A$100 million per annum.

## TECHNOLOGY DESCRIPTION

A process flow diagram for the OLGA module is displayed in Figure 2. A continuous slurry sample from the existing primary flotation feed sampler in the plant is directed via gravity to a header tank on the OLGA module, which controls the flow to the analysis tank. The excess sample is directed back to a return hopper.

The analysis hopper contains a small Poly-Ether Ether Ketone (PEEK) window through which targeted X-rays can be transmitted to and from the slurry. The OLGA is an X-ray Florescence (XRF) technology developed by the CSIRO called UltraGold that utilises focused X-rays to irradiate particles within the slurry, characteristic X-rays are then emitted from the particles and specialised detectors count the number of X-rays emitted for each wavelength, which are then converted to a concentration of each element.

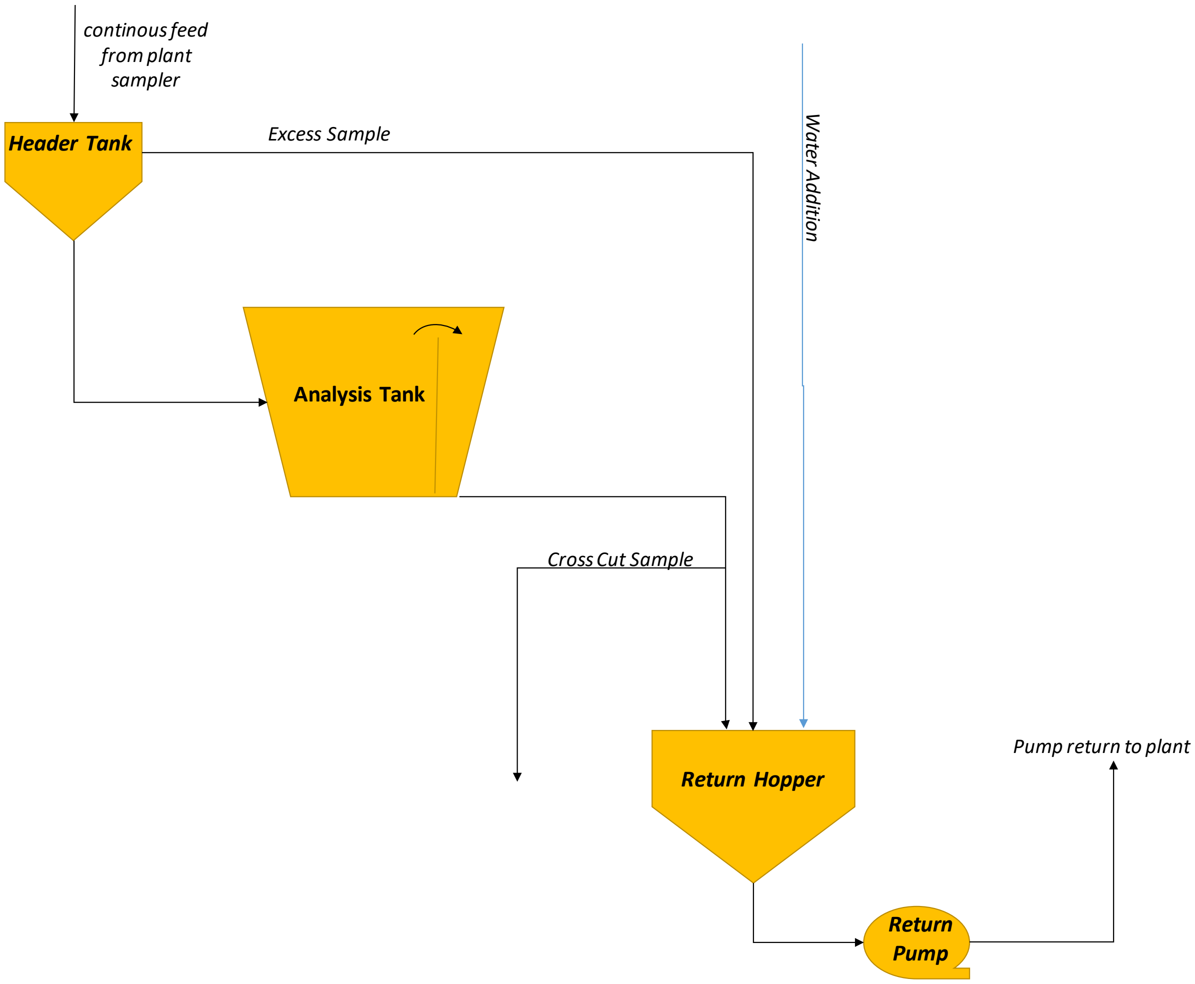


**FIG 2** – OLGA process flow diagram.

Additionally, the OLGA uses two of CSIRO's patented X-ray Optics 'lenses' which enable direct detection of the characteristic gold X-rays (Van Haarlem, 2017). Without the lens systems, the detectors would not be able to detect the characteristic X-rays emitted from the gold particles, which is the case for existing XRF analysers.

The slurry continuously overflows the analysis tank to the return hopper. A cross-cut sampler on the discharge of the overflow allows representative samples to taken for comparative assay and the slurry stream is pumped back to the plant. The OLGA produces an hourly moving average of the measured concentration/grade of a slurry stream, which is updated every 10 minutes.

# OLGA VERSUS OTHER TECHNOLOGY

## Elemental assays

All minerals processing plants require continuous feedback on the concentration of target elements within process streams in order to continuously optimise and report on the performance of the plant. At Mt Carlton, feedback to the metallurgical team is done through assays conducted in the on-site assay lab. The samples are analysed for gold using Aqua Regia extraction.

Two different types of samples are taken:

- Spot sample:
  - Grab sample taken by operators at an instantaneous point in time.
  - Taken approximately every six hours.
  - Reported approximately six hours after the sample is submitted to the assay lab.

- Composite sample:
  - Composited by operators over 12 hour shift period.
  - Submitted to assay lab at end of shift.
  - Results reported approximately 12 hours after the sample is submitted to the assay lab.

### On-stream analysers

On-stream analysers like the OUTOTEC Courier and the THERMOFISHER Multi Stream Analyser are common in base metal processing, however, are ineffective for gold applications as they cannot directly read gold at low concentrations such as those found in gold ore and tailings.

### Mt Carlton motivations to trial OLGA

The process plant has a current capacity of 840 ktpa, where primary curshed ore is milled in a single stage SAG milling circuit, with metal recovery via a gravity gold circuit and froth flotation. Approximately 15–20 per cent of gold feed is recovered through the gravity circuit producing dorē gold bars which are sold to the ABC Refinery in Sydney prior to the flotation circuit producing a pyrite gold concentrate which is sold to the Shandong Gouda Gold Company Refinery in China. After the installation of the gravity circuit in 2017, optimisiation of flotation recovery whilst maintaining concentrate grade became more crucial due to the lower grades in the circuit. A key project was undertaken to implement an online stream analyser for the processing team to effectively monitor and adjust operating parameters in real-time to minimise the effects of losses to tailings. Numerous technologies were investigated, before CSIRO and Gekko were approached to trial the UltraGold technology incorparated in the OLGA. Testing the OLGA in the Mt Carlton process plant was seen as benicfical for CSIRO, Gekko and Mt Carlton Gold Operation, to validate the technology, equipment and improve operational performance.

## EQUIPMENT TRIAL

The purpose of the trial was to install and trial the GEKKO OLGA on the flotation feed and flotation tailings at the Mt Carlton plant. The goal was to assess the mechanical availability and functionality of the OLGA module.

The OLGA was first installed on the flotation feed stream. After installation, GEKKO and CSIRO technical personnel travelled to complete the commissioning and calibration of the unit. A sampling methodology was established by programming the on-board cross-cut sampler to cut the analysis tank overflow for a one-hour period. The samples was prepped and assayed at Mt Carlton's on-site lab as per their normal production assay procedure. This sample then formed a matched pair with the corresponding one-hour OLGA measurement.

### Challenges

As this was the first installation of an OLGA in a production environment, several challenges had to be overcome before a large amount of valid data could be collected to validate the unit.

The first major challenge was to troubleshoot the continuous operating sequence and make the HMI more user friendly. As this unit was originally built and operated in the lab, it was never able to run in 'continuous' mode for extended periods. The sequencing and interlocks for the automatic subsampling and wash cycles needed trialling and troubleshooting to ensure the OLGA could run continuously for an indefinite period. The OLGA is now able to auto-initiate a wash cycle once per day and resume normal analysis without any interference from the operators. The OLGA is also able to take an automatic one-hour validation sample at a set time per day, with the option for the operators initiate a one-hour manual sample at other appropriate times. Establishing the ability to take representative validation samples and establish matched pairs of data was critical to validate the performance of the analyser.

Once troubleshooting of the programming sequence had been completed, it became clear that more work would be required to upgrade the calibration before validation could begin. The OLGA was originally calibrated by CSIRO in the lab, using a small number of feed samples.

With the complex mineralogy of the Mt Carlton ore and the recent development of the underground mine from within the open pit and the highly variable orebody feed to the processing plant, frequent calibration sampling campaigns were necessary for CSIRO to establish a refined and complex calibration.

Mechanical parts and electrical part availability on-site was an issue as wear increased with the continuous operation of OLGA. A revised critical parts list was drawn and furnished to have them in stocks on-site.

In addition to refinment of the calibration, the materials handling and transport of slurry to and from the analyser needed attention. Some modifications to the feed hopper were made to prevent excessive slurry splashing and froth generation, and a timed wash tap was installed to keep the level switches clean. Ongoing issues with the feed hopper design has resulted in GEKKO re-designing the feed system in an attempt to rectify these issues.

Water quality was also an issue for the chilling circuit during the early phase of the trial, however this was rectified by changes upstream of the OLGA. Available clean water was identified as a critical service needed to keep the analyser running smoothly.

## Methodology

Although the OLGA was pre-calibrated using a calibration database of 15 samples, the initial perceptions of the analyser performance was that it was not performing as well as the calibration would suggest. This was determined to be due to several factors, including the high variability of the Mt Carlton orebody. The original calibration database with a small number of samples did not cover the range of variations within the orebody. Additionally, the calibration was performed under laboratory conditions in a ‘batch’ environment. Consequently, the first 66 samples taken under normal ‘continuous’ operating conditions were added to the calibration database and CSIRO remotely recalibrated the analyser with the new sample set. The methodology for calibration falls under CSIRO’s intellectual property and will not be covered within this paper.

Once a more complex calibration was established by CSIRO, more samples were collected throughout January 2019 – May 2019. Each sample was assayed for gold via aqua regia extraction. Repeat assays for all samples were obtained, and the average of the assay and repeat was used in the analysis. These samples were known as the ‘validation’ data set ie a data set not already ‘seen’ by the analyser. This was the data set used for statistical analysis.

At the conclusion of the trial on the flotation feed, the analyser feed samples line was rerouted and a new sample line was run from the discharge of the flotation tails pump. This enabled a new data set of flotation tails samples to be analysed and collected, a new calibration to be established and validation of the analyser on the lower grade flotation tails to occur.

## Results

### *Flotation feed*

107 matched pairs were collected over the trial period. Three pairs were eliminated as outliers, due to the assay value being much greater than normal, while the analyser value was within the range of normal operation.

Table 1 shows the averages and spread of each of the remaining 104 matched pairs. The mean difference in the reading was 0.16 ppm Au and the standard deviation was 0.82 ppm Au.

**TABLE 1**

Flotation feed trial data summary.

| Measurement type | No. of measurements | Average (ppm) | Minimum (ppm) | Maximum (ppm) | Range (ppm) |
|---|---|---|---|---|---|
| Assay | 104 | 4.70 | 2.20 | 8.92 | 6.72 |
| OLGA | | 4.86 | 3.29 | 8.30 | 5.01 |

The data collected was plotted both as a time-series plot and a x-y plot to determine the relationship between the analyser readings and the assay data. A paired t-test between the analyser readings and assay values (Table 2) showed that we cannot reject the hypothesis that there is no statistical difference between the analyser and assay values suggesting no bias in the analyser readings. This is corroborated as a fitted trendline of the data (Figure 3) very closely follows the parity line.

**TABLE 2**

Paired T-test for flotation feed validation.

t-Test: Paired Two Sample for Means

| | *Database Au Reading (ppm)* | *Average Assay* |
|---|---|---|
| Mean | 4.855515 | 4.700096154 |
| Variance | 1.014449 | 1.862941253 |
| Observations | 104 | 104 |
| Pearson Correlation | 0.802486 | |
| Hypothesized Mean Difference | 0 | |
| df | 103 | |
| t Stat | 1.934908 | |
| P(T<=t) one-tail | 0.027872 | |
| t Critical one-tail | 1.659782 | |
| P(T<=t) two-tail | 0.055744 | >0.05 |
| t Critical two-tail | 1.983264 | |

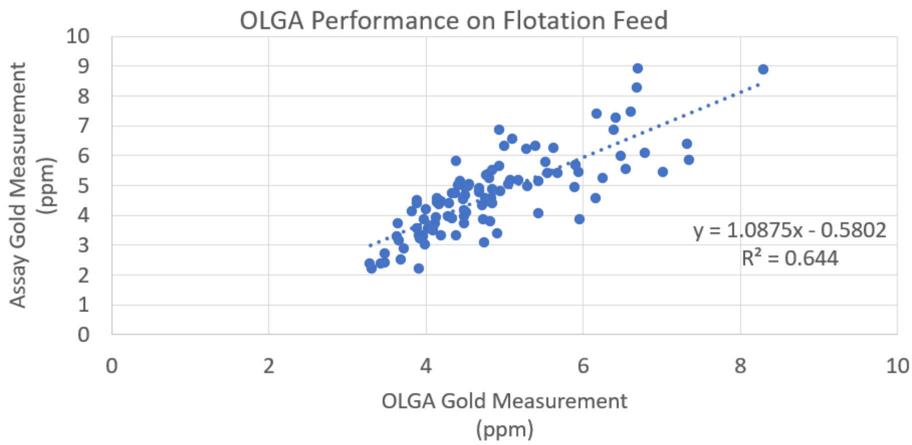


**FIG 3** – OLGA performance data, flotation feed (unseen validation samples).

A two one-sided t-test (TOST) (Napier-Munn, 2014) equivalence analysis (Table 3) shows that any bias in the results is unlikely to exceed 0.3 ppm, thus the analyser was determined to accurately measure the gold content in the slurry.

**TABLE 3**

Flotation feed TOST analysis.

t-Test: Paired Two Sample for Means

| | Database Au Reading (ppm) | Average Assay |
|---|---|---|
| Mean | 4.855515 | 4.700096154 |
| Variance | 1.014449 | 1.862941253 |
| Observations | 104 | 104 |
| Pearson Correlation | 0.802486 | |
| Hypothesized Mean Difference | 0.3 | |
| df | 103 | |
| t Stat | -1.79997 | |
| P(T<=t) one-tail | 0.037396 | |
| t Critical one-tail | 1.659782 | |
| P(T<=t) two-tail | 0.074793 | |
| t Critical two-tail | 1.983264 | |

t-Test: Paired Two Sample for Means

| | Average Assa | Database Au Reading (ppm) |
|---|---|---|
| Mean | 4.70009615 | 4.855515 |
| Variance | 1.86294125 | 1.014449 |
| Observations | 104 | 104 |
| Pearson Correlation | 0.80248622 | |
| Hypothesized Mean Difference | 0.3 | |
| df | 103 | |
| t Stat | -5.6697871 | |
| P(T<=t) one-tail | 6.5699E-08 | |
| t Critical one-tail | 1.65978227 | |
| P(T<=t) two-tail | 1.314E-07 | |
| t Critical two-tail | 1.98326414 | |

Using the standard deviation which is equal to the standard error of the least squares regression, it can be inferred that we are 95 per cent confident that an observation will be within ±1.96 × 0.82 = ±1.61 ppm Au. This is a measure of the precision/spread of the measurements generated by the experiment. Consultation with statistical expert Professor Tim Napier-Munn confirmed that the uncertainty within the readings includes sources of error from the process of conducting the field experiment and my not necessarily be attributed to the analyser itself. Sources of error which have been identified include:

- Sample error in the cross-cut sampler.
- Errors with sample timing and logging.
- Contamination of samples within the sample preparation area.
- Errors in the assay readings.
- Errors in the analyser readings.

Without further experiments, the error in the analyser readings cannot be determined separately, and so the calculated precision is not the true precision of the analyser. Additionally, the precision can be improved by increasing the number of measurements taken:

i.e. for 12 measurements, $95\%\ \mathrm{CI} = \frac{2.201 \times 0.81}{12} = \pm\, 0.52\ \mathrm{ppm\ Au}$ for a 12-hour shift.

On a qualitative level, the measurements obtained from the analyser tracked well with the normal production and metallurgical accounting samples. Figure 4 shows a seven-day timeline of the hourly moving average (data points are shown every 10 minutes) OLGA measurements, with shift composite assays and instant grab samples overlaid. From the graph, it is clear that there are discrepancies between the spot (grab) and shift composite samples, and that OLGA tracks small changes in the flotation feed grade with better resolution than the spot samples while remaining consistent with the shift composite samples. Additionally, as the analyser produces measurements in real-time (ie the measurements are not retrospective assays) this information is conveyed to the metallurgical team in a much more timely manner.

It is the combination of statistical analysis and qualitative observation that enabled the project team to conclude that for the period of the trial on the flotation feed at Mt Carlton, the Online Gold Analyser was successful in achieving the required outcomes.

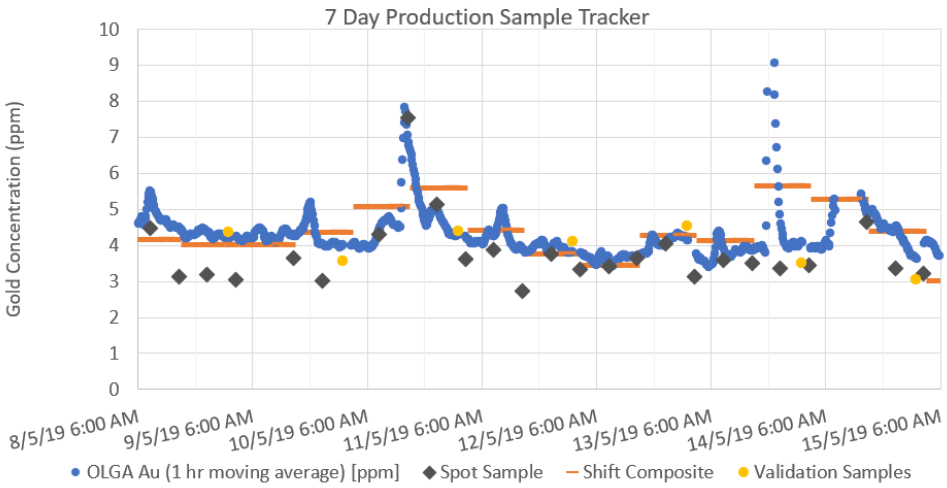


**FIG 4** – 7 day production sample tracker.

## Flotation tails

For validation of the flotation tails, a completed calibration was established in August 2018 and 88 matched pairs were collected. Two outliers were eliminated, and the analysis was conducted on 86 matched pairs, a summary of which is in Table 4.

**TABLE 4**

Flotation tails trial data summary.

| Measurement type | No. of measurements | Average (ppm) | Minimum (ppm) | Maximum (ppm) | Range (ppm) |
|---|---|---|---|---|---|
| Assay | 86 | 0.46 | 0.23 | 0.98 | 0.76 |
| OLGA | | 0.48 | 0.30 | 0.88 | 0.58 |

An analysis of the data yielded similar results to those obtained on the flotation feed; the mean difference was 0.02 ppm, the trendline of the scatter plot is very close to the parity line, as shown in Figure 5, a paired t-test shows a two-sided P-value of >0.05 (thus there is no systematic difference in the readings) and TOST analysis showed that the difference between the two values is not greater than 0.06 ppm. However, the standard deviation of the differences is 0.13 ppm Au, which translates to the 95 per cent confidence interval of ±0.26 ppm Au, which is quite high (nearly 50 per cent of the mean). It is also worth noting that there are very few points collected which are greater than 0.6 ppm. The trendline obtained is very dependant on the few higher-grade samples, thus it was established the while the performance of the OLGA on the tails looks promising, more data is needed to validation the analyser. Due to operational requirements within the processing plant, the OLGA was required to be re-deployed on flotation feed and more data could not be obtained for flotation tails.

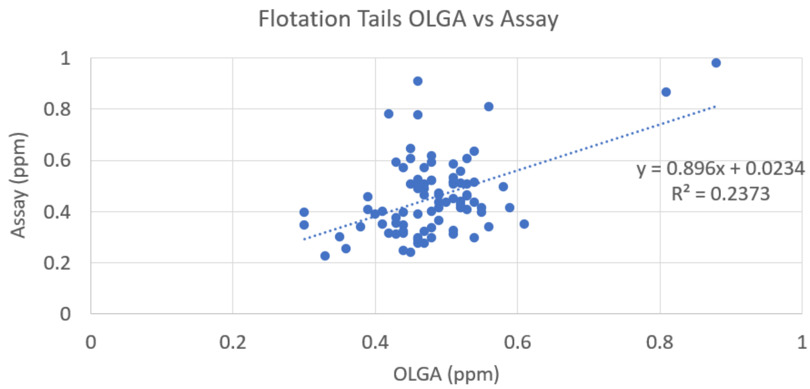


**FIG 5** – Flotation tails OLGA versus assay.

## RECENT ACTIVITIES AND MOVING FORWARD

Continuous operation and monitoring of the OLGA is ongoing with daily validation samples collected and assayed to building an ongoing database. Open communication between Gekko, CSIRO and Mt Carlton is very crucial for further information and fine-tuning and development of OLGA. Additionally, further testing is underway to validate the simultaneous measurement of copper and arsenic in the targeted streams.

Critical parts stock on-site list reviewed and finalised to have stocks to prevent delays due to non-availability of critical stock item.

## CONCLUSIONS

In conclusion, the trial of the OLGA on the flotation feed was seen as a success, with the OLGA providing accurate, real-time readings of the gold in the streams. This represents a significant milestone in the ability to read gold grades in real-time and unlocks significant potential for real-time control and automation of gold plants.

The OLGA also showed promising results when reading flotation tailings, however, more validation testing is required.

The next phase of the unit deployment will be to test and validate the simultaneous readings of copper and arsenic (as well as gold) and to put into place an action plan to ensure the data being provided by the OLGA is utilised in its fullest.

## ACKNOWLEDGEMENTS

The authors would like to acknowledge Evolution Mining and the Mt Carlton Operation for conducting the trial and continuing to support the development of the Online Gold Analyser, including allowing the publishing of this paper.

Additional acknowledgement to the CSIRO for their continued support, expertise and development of the analyser, and to Emeritus Professor Tim Napier-Munn for his consultation on statistical analysis.

## REFERENCES

Napier-Munn, T., 2014. *Statistical methods for mineral engineers; how to design experiments and analyse data*. Brisbane: JKMRC (University of Queensland).

Van Haarlem, Y., 2017. *Ultragold: Real-Time Gold-In-Slurry Analysis With 100 ppb Accuracy*. Vancouver, Canadian Institute of Mining, Metallurgy and Petroleum.

# Application of the pulp chemistry monitor at Prominent Hill

*D Holden[1], C Greet[2], A L Randriamanjatosoa[3] and M Myllynen[4]*

1. Metallurgical Superintendent, OZ Minerals Prominent Hill, South Australia.
   Email: damien.holden@ozminerals.com
2. Manager Minerals Processing Research, Magotteaux Australia Pty Ltd, South Australia.
   Email: christopher.greet@magotteaux.com
3. Senior Metallurgist, Magotteaux Australia Pty Ltd, South Australia.
   Email: andry.lazamanana@magotteaux.com
4. Senior Metallurgist, Magotteaux Australia Pty Ltd South Australia.
   Email: michael.myllynen@magotteaux.com

## ABSTRACT

It has long been observed in the laboratory that the pulp chemistry (ie pH, pulp potential (Eh), dissolved oxygen and oxygen demand) vary with changes in mineralogy, reagent additions and grinding environment. In the case of grinding environment, Magotteaux has extensive experience in making pulp chemistry measurements within a plant before and after a change in grinding media, and associating these differences with variations in metallurgical performance.

These measurements are collected using handheld laboratory instruments and are collected in short campaigns before and after the change in media. This technique, while valid, has limitations, and the question was asked: can this data be collected online and in real time? This led to the development of the Pulp Chemistry Monitor (PCM®). However, it quickly became apparent that measuring these parameters is only part of the story.

Measuring is NOT enough! The data must be processed into a form that provides value to the plant by either improved reagent utilisation and/or delivering better metallurgical performance. To this end, a PCM® was installed on the Jameson Cell feed at Prominent Hill in December 2018. The pulp chemical data generated was married together with other plant parameters to build algorithms for concentrate grade and recovery control. Subsequent step testing of the Jameson Cell collector, air and pulp level showed that the algorithms were able to predict changes to the Jameson Cell copper concentrate grade and recovery as these parameters were varied. This suggests that it would be possible to employ the algorithms to control the Jameson Cell flotation behaviour dynamically. This hypothesis was tested in a short ON/OFF trial. The paper discusses the results of the step testing and trial using the algorithms to control Jameson Cell flotation.

## INTRODUCTION

It has long been observed in the laboratory that the pulp chemistry (ie pH, pulp potential (Eh), dissolved oxygen and oxygen demand) vary with changes in mineralogy, reagent additions and grinding environment, and have a marked effect on the flotation of sulphide minerals (Hu, Sun and Wang, 2009). Magotteaux has extensive experience in making pulp chemistry measurements within a plant before and after a change in grinding media, as well as associating these differences with variations in metallurgical performance (Greet, 2019). However, we know that the feed to a plant is heterogeneous with the mineralogy changing constantly, which means the pulp chemistry will also continuously vary. So, the question is: Can we measure the pulp chemistry online, in real time and use the data to improve process performance?

Greet and Selga (2016) showed some trends relating the ore to pulp chemistry measured by the PCM® at an Australasian concentrator. While that study was able to identify some relationships between chemistry and the plant's metallurgical performance, it was often difficult to quantify such relationships due to the complex interplay of the many parameters involved; some measured but many not. For example, an increase in recovery is not always guaranteed when the feed grade increases particularly if the liberation, pulp chemistry and plant operating conditions are not ideal.

There is an abundance of data collected in the modern flotation concentrator measuring many parameters (eg throughput, particle size, pulp density, reagent additions, air and level in flotation cells, feed, concentrate and tailing grades (using in-stream analysis techniques) etc), but very limited data outside of pH when it comes to chemistry. Further, the interplay between these variables and how they influence concentrate grade and recovery is often complex and not well understood.

While recent progress in data science and computing power have helped many industries, their applications to mineral processing plants are limited (Jovanovic and Miljanovic, 2015). A major limitation to utilise data analytics to improve mineral separations is that many of the important parameters that affect flotation (eg mineral liberation and pulp/surface chemistry) are not currently measured online or in real time. Further, the raw data must be cleansed and processed into a form that produces meaningful relationships that can be employed to provide value to the plant by either improved reagent utilisation and/or better metallurgical performance.

Therefore, the first step to applying big data principles to mineral processing is to develop sensors that adequately measure parameters that influence the separation process. Based on years of measurement and observation, Magotteaux developed the Pulp Chemistry Monitor (PCM®) which measures pH, pulp potential, dissolved oxygen, temperature and oxygen demand online and in real time. However, just measuring stuff, while interesting, brings very little value so the data must be used in some way for better reagent utilisation and/or improved concentrate grades and recoveries.

## PULP CHEMISTRY MONITOR (PCM®) AND PLANT MODELLING

The first PCM® was built and installed at Perilya Broken Hill on the primary ball mill discharge in 2009 to test the concept (Figure 1). This unit was only able to sample one process stream and while proving that it was possible to measure the pulp chemistry online and in real time, there were some obvious deficiencies to the design. The Mark II PCM® design was able to sample from two-process streams alternately and had improved guarding (Figure 2). Greet and Selga (2016) provide a description of its operation. This design was installed at a number of mines in Australasia, with the unit operating at Phu Kham (Laos) for nominally two years with few operational issues. However, it was apparent from this and other experiences the design required a radical overhaul to reduce the number of moving parts to make the unit more robust and increase reliability.


**FIG 1** – PCM® installation at Perilya Broken Hill.

**FIG 2** – PCM® Mark II installation at Phu Kham, Laos.

In late 2018 a comprehensive review of the mechanical design of PCM® facilitated by Hydrix Pty Limited was completed. This study altered the way the measuring chamber was fed and emptied thereby significantly reducing the number of moving parts. This meant that the size of the measuring chamber could be reduced considerably. A prototype of this design was constructed and tested in Magotteaux's Adelaide facility for six months. The unit worked faultlessly, and this design was retrofitted to an existing PCM®, which was dispatched to Prominent Hill for installation on the primary Jameson Cell feed to test at industrial scale.

Concurrently, a successful application for funding through METS Ignited Australia Limited was made to complete a critical review of the instrumentation and control, then construct and test the resulting new PCM® design in the field. With these moneys secured, the use of digital probes was investigated. It was found that their response time, reliability and accuracy were superior to analogue probes, so they were included on PCM® Mark III (Figure 3).


**FIG 3** – PCM® Mark III installation.

All through this development, data was being collected and analysed. Broadly, it was apparent that the pulp chemistry did move around frequently, and that these changes tended to correspond to changes in mineralogy. For example, as the pyrite content of the pulp increased it was not unusual to see the pH become more acidic, the Eh shift to more reducing values, the dissolved oxygen concentration decrease and the oxygen demand (or reactivity) increase. Generally, these changes were associated with a decrease in concentrate grade and/or recovery. However, making these observations is 'nice' but if this information cannot be used to adapt and improve the process these measurements are of little value.

## Data collection and modelling

OZ Minerals agreed to have PCM® installed at Prominent Hill to determine if the data generated provided any insights into plant operation, and if this information could be readily adapted into their control system for flotation.

In the current study, PCM® was installed on the primary Jameson Cell feed. As shown in the flow sheet in Figure 4, the combined rougher concentrate is cycloned with the cyclone underflow reground in an IsaMill®. The IsaMill® discharge and the cyclone overflow combine to feed the primary Jameson Cell, which produces final concentrate. The Jameson Cell tailing is the feed to three stages of conventional cleaning, with the third cleaner concentrate cleaned in a second Jameson Cell. The concentrate from the two Jameson Cells is combined to make final product.

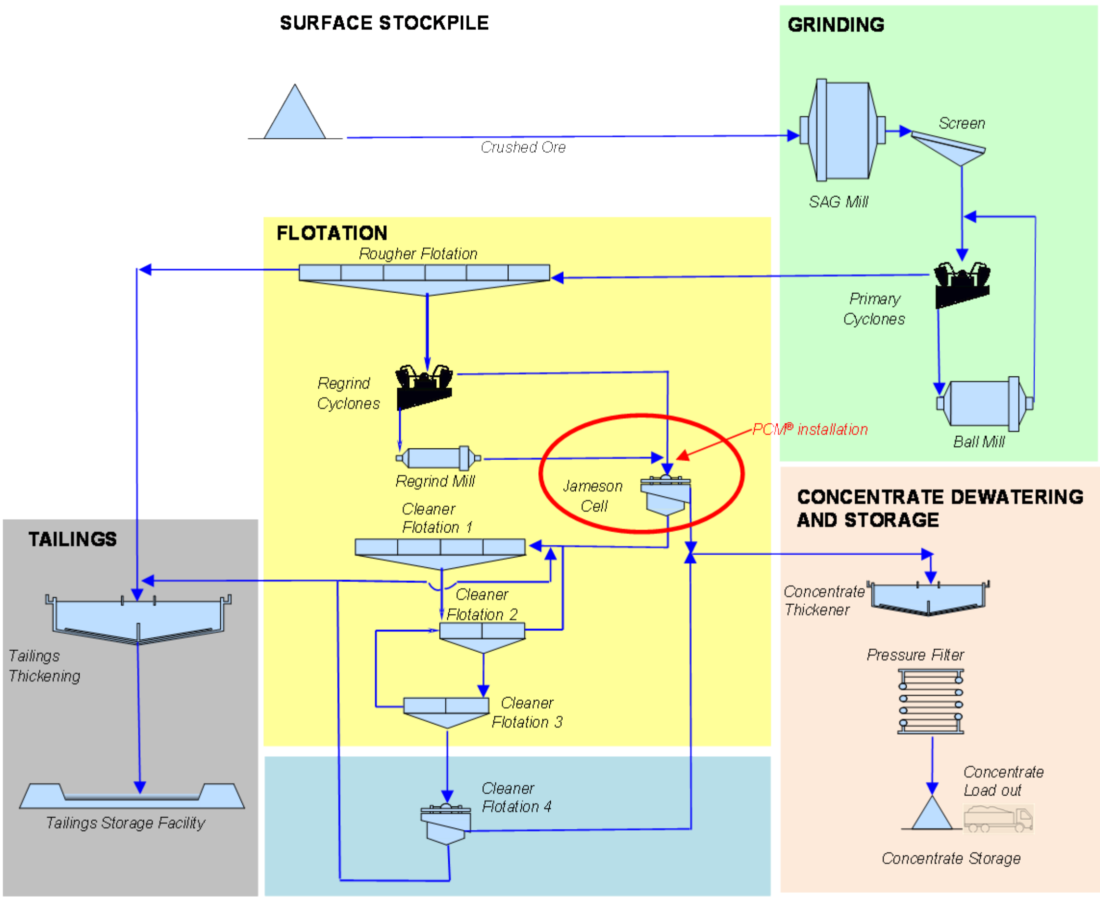


**FIG 4** – Prominent Hill flow sheet showing the location of the PCM® installation.

The pulp chemistry (pH, pulp potential (Eh), dissolved oxygen, oxygen demand and pulp temperature) of the primary Jameson Cell feed stream was measured and the data used to understand and learn how the Jameson cell can be optimised. The chemistry data are stored on both PCM® and the plant historians.

In the first instance, the historical plant sensor data (throughput, particle size, pulp density, reagent additions, air and level in flotation cells, feed, concentrate and tailing grades (from the on-stream Courier system)) were imported from the PI servers for analyses. It is important to ensure the available data were of good quality prior to any model development and plant optimisation (Oliver and Willingham, 2016). The data cleaning process was completed by Magotteaux with the help of a purpose built, in house, software application.

During the data exploration phase, it was observed that an increase in Jameson feed grade was not always associated with an improvement in recovery or concentrate grade. There were also times when the same feed grade produced lower recovery and concentrate grade. For example, for the same Jameson feed grade of 18.4 per cent copper (Figure 5), it was observed that a combination of higher collector dosage (2 g/t) and changes to less oxidising pulp chemical conditions resulted in a significantly lower copper recovery and copper concentrate grade. The inferior metallurgical performances in that example were associated with a decrease in pH of 0.6 pH units, a more reducing Eh (by 55 mV) and a lower dissolved oxygen concentration (ie 1.4 ppm lower).

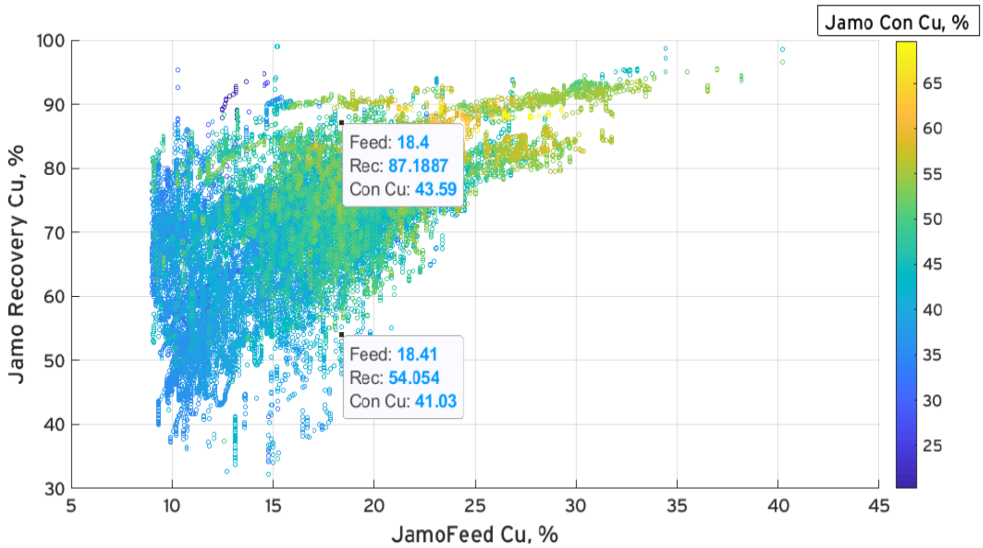


**FIG 5** – Jameson copper recovery and concentrate grade as a function of feed grade.

While the negative impact of overdosed collector or less oxidising chemistry conditions can be graphically visualised in some cases, quantifying their individual effects on metallurgy is a lot more complicated. Machine learning techniques were used to quantify their effects. This was completed with the MATLAB® software by MathWorks®. Once the data integrity was checked, supervised algorithms were chosen to train the data set. Stepwise regression was selected to remove input parameters that were not statistically significant. Among all the investigated learners (linear regression, regression trees, support vector machines, Gaussian process regression and ensemble of trees), multivariate second order polynomial regression was found to reasonably fit the training data and better predict new data sets as described in Randriamanjatosoa, Greet and Small (2018). The resulting Jameson Cell concentrate grade and recovery models were assessed. For example, sensitivity analyses showed that under given constant conditions, adding more collector increased the recovery up to a maximum. Beyond that, the model suggested that further collector addition would result in lower recovery. In addition, the collector dosage that corresponds to the maximum recovery changes with the chemistry of the slurry.

The effect of chemistry alone on copper metallurgy under specific operating conditions was investigated during the model sensitivity analyses. If all parameters except the dissolved oxygen concentration and oxygen demand were held constant (for example, 16.4 per cent copper feed grade, 654 $m^3$ air per hour, 801 mm level, same wash water, throughput, mill power and collector), the changes in copper recovery and concentrate grade were evaluated (Table 1). In this example, a change to more oxidising conditions improved the copper metallurgy. The effect of chemistry is discussed further below with the step testing data.

**TABLE 1**

Effect of dissolved oxygen and oxygen demand if all other parameters were kept constant.

| | DO (ppm) | OD (min$^{-1}$) | DO (ppm) | OD (min$^{-1}$) |
|---|---|---|---|---|
| | **0.01** | **1.11** | **0.04** | **0.50** |
| Modelled Jameson Cell Cu concentrate grade, % | 40.49 | | 40.58 | |
| Modelled Jameson Cell Cu recovery, % | 80.6 | | 81.4 | |

## Step testing

Step testing of collector dosage, air and froth level were conducted separately to confirm the findings from the models' sensitivity analyses. The collector step testing results are presented here (Figures 6 and 7). During the collector step tests, the plant conditions (ie throughput, air and level) were kept constant with only the collector addition adjusted from 7.0 g/t down to 4.0 then back up again. Unfortunately, the feed grade did change during the test.

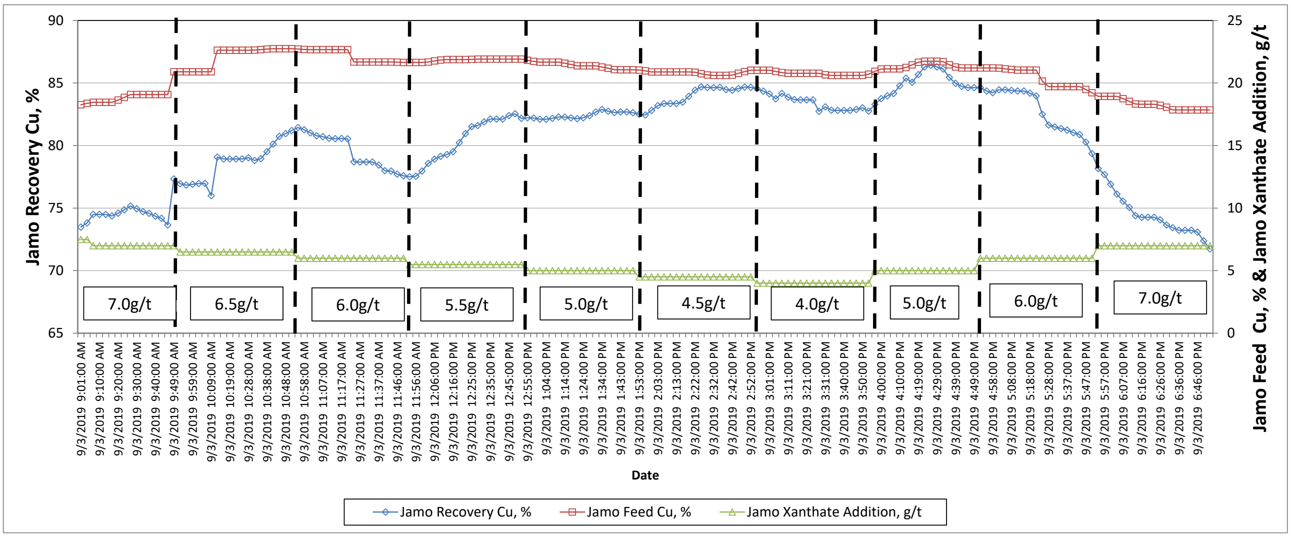


**FIG 6** – Effect of collector dosage on Jameson Cell recovery.

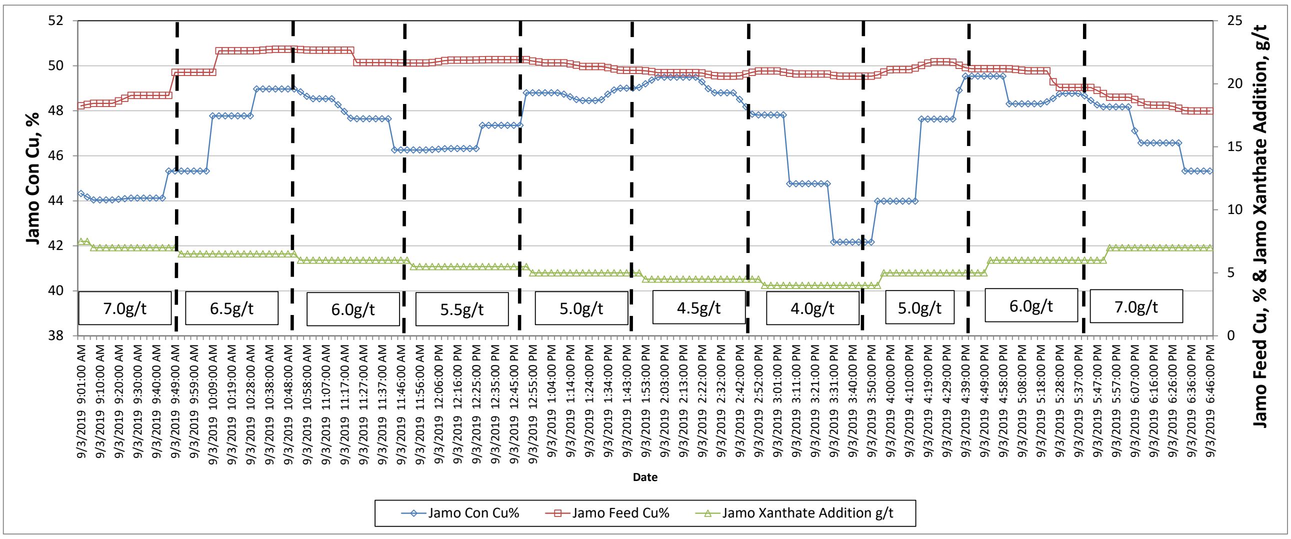


**FIG 7** – Effect of collector dosage on Jameson Cell concentrate grade.

The results showed that for a reasonably constant or slightly low feed grade, reducing the collector addition from 6.0 to 4.5 g/t increased the recovery from 78 to 84 per cent (Figure 6) without negatively affecting the concentrate grade (Figure 7). A further decrease to 4.0 g/t saw the concentrate grade decrease from 49 to 42 per cent (Figure 7). When collector dosage was returned to 6 g/t, the recovery dropped again while the concentrate grade went backup (Figures 6 and 7). The trends observed during step testing mirrored those predicted during data exploration and model sensitivity analyses.

For a better picture of the effect chemistry had on the process, time series and cusum plots showing the effects of oxygen demand on recovery are given in Figure 8. It is noted that the chemistry of the feed sample was measured prior to collector addition. From these results, the copper recovery was inversely proportional to the oxygen demand. That is, as the oxygen demand increased the copper recovery decreased, and vice versa. This observation mirrors that noted in Table 1, in that a more oxidising system tended to produce a higher copper concentrate grade and recovery.

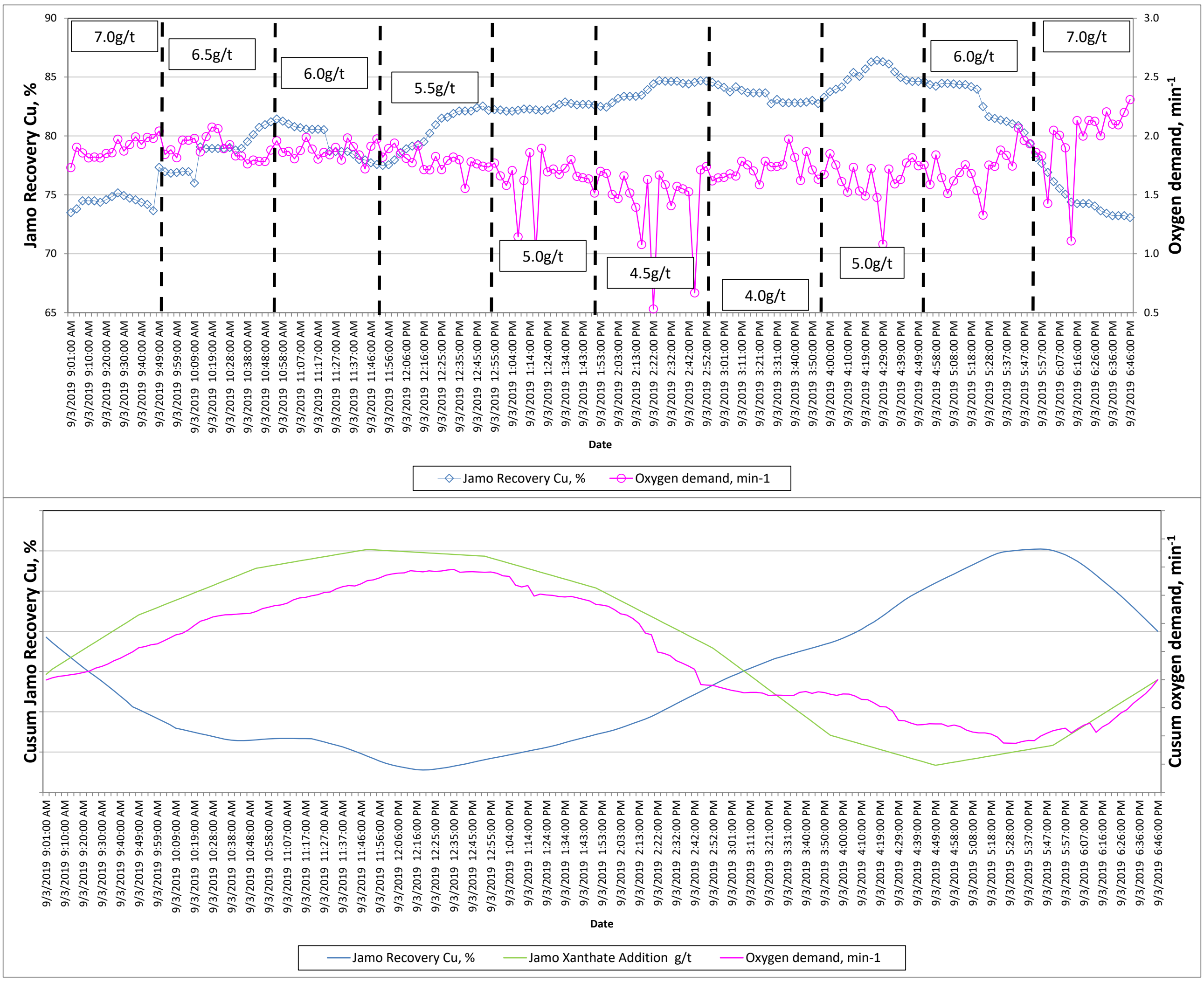


**FIG 8** – Time series and cusum plots showing the effect of oxygen demand and collector dosage on Jameson cell copper recovery.

The air and level step testings were harder to interpret as the step changes coincidentally occurred at the same time as the copper feed grade increased or decreased. Thus, the resulting changes in metallurgy can be partially attributed to the feed grade and not due to change in the air or level only.

## Plant optimisation

Since the trends were consistent from data exploration, model sensitivity analyses and step testing, the models were compiled into a computer application with a graphical user interface that facilitates interaction with the user. The final goal was to help the operators optimise the metallurgical performance of the Jameson cell.

The PCM® App continuously collected new sets of data from the site historian as they were made available. It then assessed the integrity of the data and only worked on clean data sets. Optimisation algorithms were performed to optimise the metallurgical response of the Jameson cell and the results stored on the plant historian. Anticipating some improvements and thus changes in future, data transfer between the PCM® App and the site historian is currently done through PI Datalink functions for simplicity. At this stage of the study, the App's outputs were displayed on a dashboard in the form of advice for the operators. The PCM® App's settings also allow the user to select the frequency at which the model is retrained (eg every day, every week). If the retrained models were not robust enough because of some new condition(s) in the plant, the PCM® App continued to use the previously retrained models.

The Jameson cell optimisation by the PCM® App was focused on concentrate grade and recovery. They were achieved by simultaneously adjusting the collector addition, air and level. The user may choose whether to maximise recovery while maintaining a target concentrate grade; or maximise the concentrate grade without allowing the recovery to drop below a minimum value. It is important to note that the PCM® App's optimisation objective can be customised to suit the concentrator's requirements and constraints.

In the present study, the Jameson Cell concentrate grade was maximised without letting the recovery fall below 70 per cent. The objective was to produce high-grade concentrate knowing that copper loss could be recovered in subsequent cleaner stages. The PCM® App was implemented at site and trialled for a number of days. The trial was completed between 6:00 am and 4:00 pm in nominally three hours blocks of 'OFF' and 'ON' periods each day (Figure 9). In total, 15 'OFF' and 15 'ON' periods were retained after discounting some partial plant shutdown times and equipment failures. During the 'OFF' periods, the operators disregarded the advice from the App, whereas the App's recommendations were implemented during the 'ON' periods. The optimisation frequency was set to every 20 minutes. This choice was made to fit the Courier measurement cycle. As the plant was treating a different ore from available historical data, the learner retrain frequency was set to every day. An example of time series plots of the Jameson Cell final concentrate grades and recoveries shows that the final concentrate grade increased with an increase in Jameson cell concentrate grade when the PCM® App's advice was implemented (Figure 9). This was accompanied by an apparent reduction in Jameson cell recovery but without affecting the final copper recovery (Figure 9).

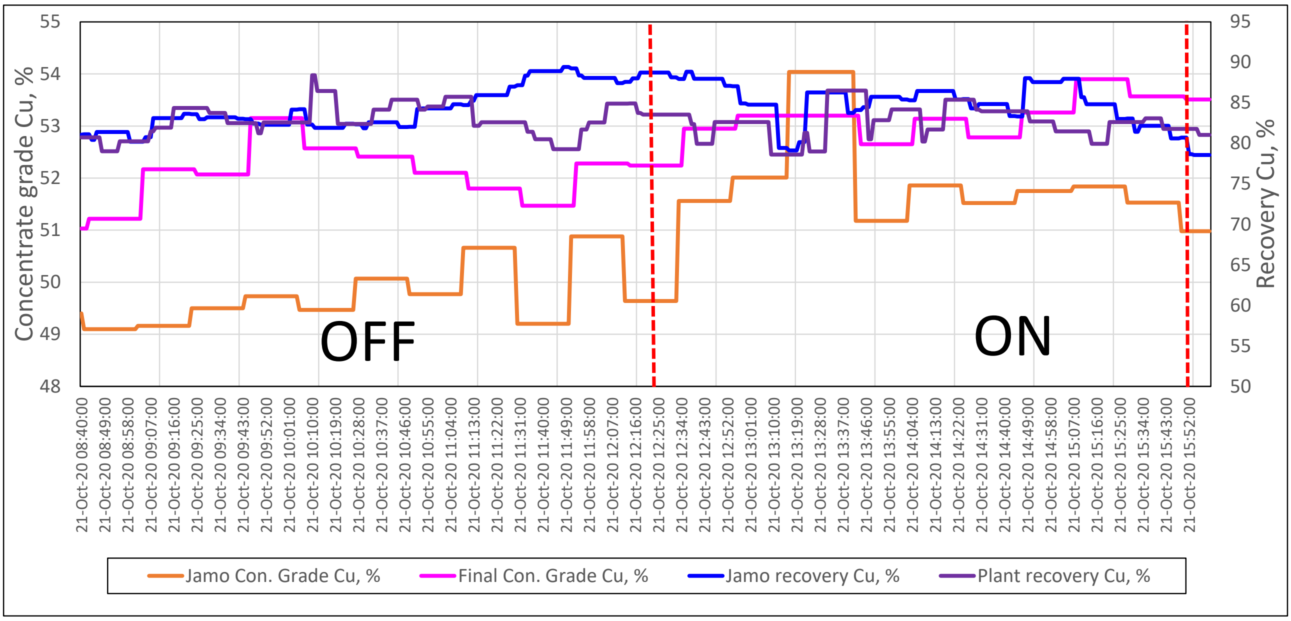


**FIG 9** – PCM® App trial optimising the concentrate grade.

The time series trends do not necessarily imply that using the PCM® App's advice was the only cause for the improved concentrate grade. In order to isolate the effect of using the App, multiple linear regression analyses were conducted. The results of the statistical analysis are presented in Table 2. The results show that despite the reduction in Jameson cell recovery, the final copper recovery remained statistically the same. This was attributed to copper lost from the Jameson Cell being recovered during subsequent cleaning stages as predicted. In contrast however, the Jameson Cell and final copper concentrate grades increased by approximately 0.8 per cent (Table 2).

**TABLE 2**

Effect of using the PCM® optimisation App on plant performance.

| | Change due to PCM® App | 90% confidence interval |
|---|---|---|
| Jameson Cell Cu concentrate grade, % | 0.78 | ±0.50 |
| Jameson Cell Cu recovery, % | -5.06 | ±0.93 |
| Final Cu concentrate grade, % | 0.85 | ±0.41 |
| Final Cu recovery, % | - (*) | - (*) |

(*) no statistically significant change.

## ONGOING WORKS

The present study showed that the application of pulp chemistry with relevant plant control parameters it was possible to optimise the Jameson Cell at Prominent Hill. The observed changes in metallurgy from the data as a result of variations in chemistry and other parameters such as collector dosage were consistent with the models' sensitivity analyses, step testing and 'ON/OFF' trials. Since the optimisation can be customised to meet the plant's requirements, it is important to understand the plant's specific needs and underlying constraints. For instance, a plant trial optimising the Jameson Cell recovery without compromising the target concentrate grade is recommended. This is currently simulated using historical data (Figure 10), but an extended randomised block ON/OFF trial, where the block are a number of days, would give a clearer picture. Such an extended trial would have the luxury of using the shift composite assays rather than the online OSA assays in the analysis.

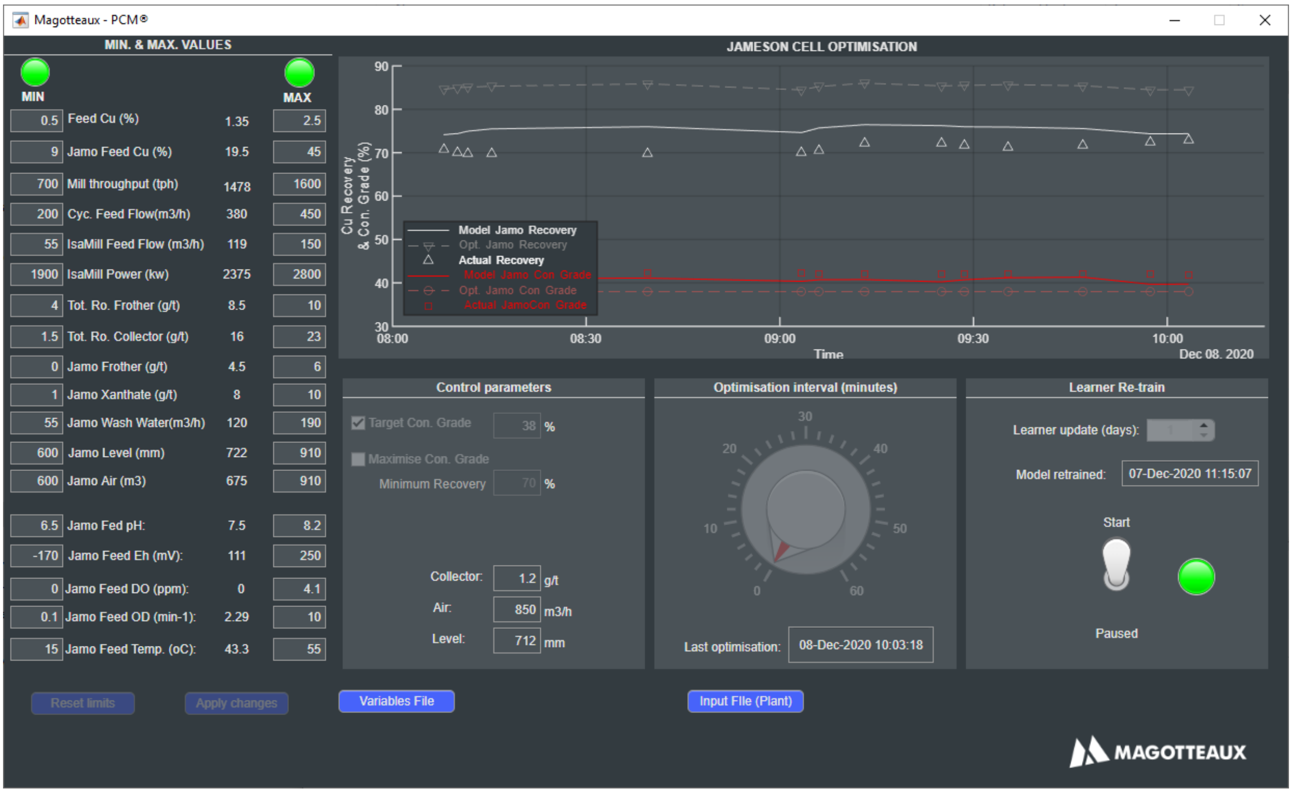


**FIG 10** – PCM® App simulation using historical data.

## CONCLUSIONS

Magotteaux's online pulp chemistry monitor (PCM®) was installed at Prominent Hill to measure the Jameson Cell feed's chemical characteristics. These data were used with other sensors' data to model its behaviour. The PCM® App was developed using supervised machine learning algorithms and trialled in three-hour blocks of 'ON/OFF' to maximise the Jameson cell concentrate grade while keeping the recovery above a minimum value. The results showed an improved Jameson Cell and final concentrate grade without negatively affecting the final recovery. An extended trial will be conducted in early 2021.


## ACKNOWLEDGEMENTS

The authors would like to acknowledge OZ Minerals Prominent Hill staff for their invaluable help during the course of this study. They would also like to thank Magotteaux International for funding this work.


## REFERENCES


Greet, C J, 2019. Grinding chemistry and its impact on copper flotation, in the Proceedings of the Copper 2019 conference, Mineral Processing (The Metallurgy and Materials Society of the Canadian Institute of Mining, Metallurgy and Petroleum of Canada, Toronto).

Greet, C and Selga, K, 2016. Continuous, Real time pulp chemistry measurements and what they tell us about metallurgical performance, in 12th International Mineral Processing Conference, 2016.

Hu Y, Sun W & Wang, D, 2009. Electrochemistry of Flotation of Sulphide Minerals, Tsinghua University Press, Beijing.

Jovanovic, I and Miljanovic, I, 2015. Contemporary advanced control techniques for flotation plants with mechanical flotation cells – A Review, Minerals Engineering, Volume 70, pp 228–249.Oliver, S, J and Tooher, R, 2018. Optimising flotation plant operation by using a digital twin in the control room, in fourteenth Mill Operator's Conference 2018, pp 93–101.

Oliver, S and Willingham, D, 2016. Maximise orebody value through the automation of resource model development using machine learning, in third International Geometallurgy Conference, 2016.

Randriamanjatosoa A L, Greet C and Small G, 2018. Effects of pulp chemistry on plant and laboratory flotation modelling, in 14th Mill Operators' Conference 2018, pp 423–433.

# Metallurgical testing – the pain continues

*A J H Newell[1], P D Munro[2] and K Fiedler[3]*

1. MAusIMM(CP), Executive Consultant Processing, RPMGlobal, Brisbane Qld 4000.
   Email: anewell@rpmglobal.com
2. FAusIMM, Principal Consultant, Mineralis Consultants Pty Ltd, Taringa Qld 4068.
   Email: pmunro@mineralis.com.au
3. MAusIMM, Director, Mineral Processing Consultants Pty Ltd, Flaxton Qld 4560.
   Email: kelvinfiedler@mineralprocessing.com.au

## ABSTRACT

This is the second in a planned series of three papers reviewing metallurgical test work practices and outcomes. The first paper focused on the 'before phase' and was presented to the *14th Mill Operators' Conference* in Brisbane, (Newell, Munro and Fiedler, 2018). This paper covers the issues that are commonly encountered 'during' a metallurgical test work program.

Test work is the foundation upon which the success of projects and subsequent operations is laid, reflected in Arthur Taggart's pithy observation: 'Make your mistakes on the small scale and your profits on the larger scale'. Indeed, Allen Trench has succinctly noted that 'Get the metallurgical characteristics wrong and you don't have a project'.

This paper provides some observations and guidelines for the period when metallurgical testing is being conducted, noting preferred practices as well as precautions and mitigations. This includes the key characteristics of metallurgical test work programs, such as quality control and associated outcome drivers, and most importantly, managing test work facilities.

## INTRODUCTION

Managing a test work program and a test work facility requires preparation and a proactive and interactive approach, even with an experienced, professional and reputable test work facility. Ideally, it is a partnership of equals, with both parties bringing knowledge, experience, skillsets and insight to generating meaningful outcomes.

The skill is to cultivate and harness this synergy by deeply understanding the test work program requirements and outcomes as well as the personnel, the 'modus operandi' and the limitations of the test work facility. While it is important to be vigilant by recognising and mitigating potential issues, things will occur on a day-to-day basis that require thoughtful and timely solutions and directions.

Test work providers typically appreciate the interaction and hands-on/real time direction, and assuming that a good relationship has been developed, common sense and reasonableness is in the ascendency and that matters have not descended to pettiness. Based on trust and respect by both parties, this is unquestionably the best approach to get the most from test work programs and not waste time, samples or money.

The paper outlines the preparation requirements, that are key to successfully completing a test work program, and includes re-familiarising yourself with the scope of work, sample and assaying details, establishing the relationship with the test work facility, confirming the equipment, procedures and the standards that will be applied as well as insights into some of the issues that may arise.

As well as providing commentary on overseeing a test work program and providing direction to ensure that the program basically run to plan, recommendations are provided on managing the budget, test work program duration and the expectations of your management.

In the first paper of this three-part series (Newell, Munro and Fiedler, 2018), the authors provided an overview of the test work requirements as well as the basis for selecting test work facilities, which are summarised in Appendices 1, 2 and 3. Examples of typical test work approaches for various commodities are provided in Appendices 4 to 10 and include some key references to support the testing of these commodities. Note that for some more complex ores, multiple separation methods may need to be employed and the test work program would need to reflect these requirements.

## PRIOR TO INITIATING TEST WORK

### Preparation

Before confirming that the appointed test work facility has received all of the samples, it is important to re-acquaint yourself with the purpose and requirements of the test work program. Re-familiarise yourself with the Scope of Work, including the metallurgical objectives (grade/recovery), drill core/samples, the test work plan including sample and compositing requirements, characterisation test work, the order of testing, the nature and priority of the assaying requirements.

Review what needs to be conducted prior to launching into the main test work program (typically sample preparation, head assays, mineralogy and other characterisation tests) and what test work can proceed in parallel (such as comminution testing, pre-concentration, size by size assays) (refer to Appendices 4 to 10).

Finalise a single spreadsheet with all the planned tests and required sample masses for each test. Recheck the plan for anything that might have been missed, including samples for bulk materials handling, equipment vendor test work, rheology, Transportable Moisture Limit, and Safety Data Sheet preparation.

Generally, a specialist comminution consultant would be engaged to assess the comminution test work results. Different comminution specialists can differ as to the preferred comminution tests to be conducted, depending on how they approach their modelling. If using a comminution consultant and sample is limited, reconfirm and prioritise the type of tests required if there is limited sample.

If the test work is for a Feasibility Study/detailed design, prior to finalising the directions for compositing of any samples, detailed discussion in consultation with the geologist who is responsible for the resource model, and the mining engineer should be undertaken. If flow sheet/grind size/reagent optimisation is to be performed on composites, then the mine and process plant production schedules should be reviewed and confirmed that they are 'frozen' and will not change prior to release of the Feasibility Study (FS). This is important to maintain the validity of the composites tested when reported in the FS.

### Day one – meet, greet and set the rules

When you feel confident that you have a good handle on things, prepare a checklist and arrange to meet the test work facility Project Manager. The Project Manager is naturally the key point of contact and a good working relationship needs to be cultivated. While being thorough and addressing the subjects outlined in this section, some balance is required going forward so that you aren't considered 'a high maintenance client'.

Establish the methods and frequency of communication, such as updates, for example, after key stages/'milestones' have been achieved. Ensure that all test work results be sent through as a 'live' spreadsheet, not a pdf file, as this allows easy assessment of the data in addition to any plots provided by the laboratory, and also makes it much easier to perform check calculations for recovery and cumulative grade/recovery. Besides progress and success, the most important communication concerns issues and problems, which need to be brought to your attention in a timely and appropriate manner. Bringing to bear the combined experience and knowledge of the test work team, namely the technicians, metallurgists and the management as well as your technical resources, are key to conducting a successful test work program in a timely fashion.

Discuss your approach to supervision, what you expect to see and be told (eg the Project Manager to report early any unexpected delays or unforeseen issues), when and how often you will be present at the test work facility and what your expectations and standards are.

Understand how busy the test work facility is and will be (future work), and how this will impact the availability of technicians and services and thus the timing and delivery of your project. Understand how your test work program sits in the test work facility's overall program and how the test work facility prioritises current and future clients. It can be disappointing to see your test work program slow down or grind to a halt due to previous commitments of which you were not advised, poor organisation or getting 'bumped' by the test work facility taking on and prioritising new work over your test work. It happens either for business reasons or when there is a commodity 'bubble' and junior mining companies are desperate to get a processing announcement out there.

Extract a commitment that your test work is important and will not be sidelined and that key technicians from the test work team will be available for the duration of the test work program and if annual leave would be taken the subsequent duration. The impact of key personnel, including technicians, leaving the test provider can impact not only the schedule but also the budget, where additional costs may be incurred to get the program back on track through longer hours and getting replacement personnel up to speed. This possibility needs to be discussed prior to commencement of the test work program, including what approach would be adopted and who would be responsible for the additional costs.

In terms of understanding the potential test work program duration issues, it is also important to 'touch base' with other test work facility managers, such as the assaying and mineralogical facilities.

This includes assay turn-around time, which can really slow down a test work program, especially in the early stages. Several flotation tests can be conducted in a day, though sometimes it may take a week to receive the assays, resulting in assay turnaround time being the largest time input into the schedule – make sure you are aware of the expected turn-around time! This aspect needs to be discussed with the test work facility Project Manager and obtain a clear commitment to duration and what would be unacceptable. Often this commitment cannot be reliably given by the test work Project Manager, since the operation of the assay facility is typically not totally dependent upon the test work facility and often has independent sources of work.

Review the sample assaying requirements as well as the likely sample assaying schedule prior to investigating the assay facility and meeting the manager. Discuss the sample preparation methodology, assaying procedure, availability and quality of equipment and confirm the typical time taken between receipt and assaying (confirm, where possible, a maximum 24-hour turnaround time).

Understand the current and forecast workload and the likely schedule over the test work program period, being mindful of the assay facility taking on assaying for drilling programs. In any event, request the nature of a 'Plan B' should any delays be experienced or expected with regard to assay turnaround time. This may require prioritising the samples to be assayed as well as limiting the assaying requirements (eg key elements, noting that the most reliable assays for elements like sulphur and carbon are obtained from dedicated procedures). Plan B may require assaying being conducted externally and the high-level details presented by the test work facility.

Confirm the nature of the assay standards, if they are suitable and when they are used as well as 'blanks'. Confirm the detection limits of the assay methodology to be used and check that is well below the expected tailing grades that will be produced.

Some programs can be accelerated by paying the laboratory higher rates for assays for additional overtime or developing a 'modified' assay method for a faster turnaround. These approaches can distort the routine structure of an analytical laboratory and can end up with monumental re-assay consequences.

Similarly, the availability and workload of the mineralogical facility (internal or external) needs to be confirmed. As noted for the assaying facility, a similar situation often arises for mineralogical determinations, particularly with automated processes such as QEMScan as well as more specific determinations (eg quantitative XRD). Confirm the likely schedule of the mineralogical facility over the test work program duration. Familiarise yourself with the equipment and techniques, sample preparation and scanning times as well as the overall turnaround time. Ensure you convey to the mineralogist any specific minerals of interest if in low concentrations as more sample mounts may have to be prepared to allow for scanning of a larger number of particles eg cobalt or molybdenum minerals in head samples. The mineralogical facility should employ an experienced mineralogist who reviews the automated output and provides interpretation and commentary. Discuss what you expect to see in the mineralogical report and likely delivery period. Request progressive reports as work is completed, and that data is provided in spreadsheet format so you can plot data based on your interpretation. The progress of the test work program can be dependent on the mineralogical report, and if the mineralogical facility has become overloaded, request a high-level summary report with the delivery of a more detailed report at a later stage. Check if optical mineralogy is also available (becoming quite rare these days) in addition to SEM work, as sometimes separate mounts and optical work could be required.

Ensure a systematic and reliable sample naming and storage methodology is in place so that samples that are stored post assaying can be easily retrieved for mineralogy if required.

Confirm the availability and turn-around times for potential vendors who may be used to conduct specialised testing (typically dewatering as well as ore sorting, larger scale gravity testing), and that the laboratory can provide bench space if it is possible for the equipment vendor to perform test work in the metallurgical laboratory. This approach minimises the risks related to sample transportation and sample ageing.

Rheology testing of thickener underflow slurries can be problematic and may have to be undertaken by a specific laboratory. Depending upon the company/person that undertakes the pump and pipeline calculations (eg a long tailing run or long concentrate pipeline), there may be some very specific requests for the type of rheometer and spindle used, and as with other test work, the results can be dismissed as 'the right viscometer wasn't used'. For long pipe runs, the production of large amounts of sample would be required for pump loop testing to be supervised by the pump/pipeline designers.

Develop an understanding of how the laboratory will approach and conducts the test work program, noting potential limitations or bottlenecks. Discuss and correct as required.

Confirm the working hours of the various facilities and whether that includes the weekends, or the sentiment for working overtime if required. Make allowances for public holidays. If the laboratory is offshore, ensure you have a very good understanding of country specific public holidays and annual vacation times as people do take holidays!

Meet the technicians who will be involved, confirm their credentials, availability and that they have been made aware of your test work program and the associated requirements. The Project Manager should provide a commitment that the test work team, particularly the technicians, would be available for the duration of the proposed test work program.

Check where the test work will be conducted and whether a separate area has been set-up to cater for your test work needs.

Observe the layout of the test work area, noting instrumentation, probes and their condition, test work recording sheet and watch a test being performed to ensure that you are comfortable with the test work practice – for example, considering flotation, air flow rates and scraping technique and rates at different stages, addition of reagents (very small additions of immiscible reagents can present issues), washing down, addition of make-up water, flotation times, instrumentation measurements and recording of observations. Discuss the test conditions for each test with the laboratory Project Manager and have the laboratory work sheet forwarded to you for review prior to approval and commencement of the test. This will confirm alignment on every aspect of the test and ensure that valuable samples are not consumed in a test that used conditions not agreed upon. When you are comfortable with the test work procedure and technician, insist, for example, in the case of flotation separations, that the same technician(s) does all of the flotation test work. This ensures that the results would be comparable and the same techniques (eg froth removal) have been consistently applied.

Some of these aspects would be discussed and settled upon as a standard procedure. Ensure that you are comfortable with what pulp chemistry measurements would be taken as well as the nature of instrumentation calibration procedure, frequency and whether instrumentation probes are correctly stored between tests (ie 3M KCl solution).

Confirm the nature of the equipment such as make/type (for example, regrind and attrition mills and media type and sizing), size (for example, a range of flotation cell sizes for cleaning duties) and condition (maintenance).

Determine where your samples are kept and confirm the requirements, future availability and costs for storage and disposal.

Think about whether you will store any products and for how long (and how much it will cost). Don't forget to budget for either the return of samples to the project owner, or associated costs if the laboratory is asked to dispose of samples/tailings.

## Complete the sample chain of custody

Confirm that the drill core/samples have arrived (including the manifest) and inspect the packaging and sample condition.

If you didn't oversee the packing of drill core/samples, confirm that the correct drill core/samples were packed and sent.

Check that drill core samples to be used in comminution testing are intact (eg drop weight testing, unconfined compressive strength) and haven't degraded in transit.

Most test work facilities are diligent with the receipt and handling of drill core/samples, duly recording the description (usually a drill core collar and interval) and weighing them. Photographic record of the sample before they leave site and samples received at the laboratory is recommended practice.

When reviewing the sample quantities that have been delivered to the test work facility, confirm that they are sufficient to conduct the proposed test work program, which has previously considered the other sample demands from marketing (eg concentrates), geotechnical testings (eg tailings), environmental testing (eg feed and tailings as well as waste rock) and equipment vendor (eg HPGR, regrind mills, thickeners, filters).

If site water is proposed to be used, confirmed that it has arrived and fully assayed. Conversely, check that a suitable 'recipe' has been prepared for the preparation of a synthetic equivalent.

# DURING TEST WORK

## Sample preparation

Test work should not proceed until you are comfortable with the prepared test work sample head assays, particularly when these assays of the prepared samples do not meet expectations. A cross-check should be performed of existing assays from the geological database versus the head assays from the metallurgical laboratory. The issue is whether to continue and use the sample in the test work program or consider preparing another sample from available drill core or 'adjust' the sample feed grade by blending with other drill core.

The blending recipes for preparing the drill core/samples as the test work samples are usually based on the 'geological' drill core assays when half-core or quarter core drill holes are involved. Where a full drill core is available for test work, the 'geological' assays for the same interval from a twinned drill holes is typically used.

If the orebody is homogenous, then there would be no difference in assay values between the arithmetically calculated values for the blended composite and the actual assay. However, orebodies are rarely homogeneous, and it is not unusual for there to be a difference, particularly for minor elements such as gold and silver, or where sulphide occurrence is vein-like or 'blebby'. This also occurs because the 'geological' assays are only a proxy for the drill cores and mineralogical variation can occur across and within a drill core sample.

Caution must be exercised on blending and compositing samples. This automatically assumes that this is how the material be mined and presented to the processing plant ie imposes a mine production schedule. This it introduces the dimension of 'time' into what has been purely a spatial context. Wherever possible, test individual samples and domains and composite the metallurgical results arithmetically.

Subsequently, the test work sample head assays need to be confirmed before progressing the test work program. Should a 'significant' variation (>25 per cent or <25 per cent) in the principal element (eg Cu, Pb, Zn, Au) head assays be found, then some decisions need to be made about what to do with this sample, such as appropriately blending or diluting this composite, assigning it to the feed-grade-recovery sample suite or calling it a variability sample.

Initial test work is based on ore types with life-of-mine (LOM) feed grades. While blending to achieve this LOM feed grade, it is important to confirm that the lithology and mineralogy is typical of the LOM material. It is possible that the LOM feed grades reflect a modelled grade from intervals that have been subjected to a grade 'top cut' by the geologists, though individual samples may indeed contain some very high-grade intervals. While blending high-grade samples with low-grade samples to achieve the desired feed grade is not ideal practice, unless the mineralogy is very similar, it can bias the metallurgy. For example, if the sample is a gold ore and nuggetty, there may be over representation of the lower grade material when blending with high-grade samples. For some ores, the mineralogy of lower grade samples can be finer grained and not readily amenable at the proposed grind size. However, it is useful and realistic to dilute the sample with gangue, particularly for potential open cut operations.

If the metallurgical behaviour an ore type is found to 'problematic' (eg a supergene contamination that, if included in a composite with primary ore types, would most likely either cause some degree of depression or 'complete' flotation due to activation), then a composite based on the mine schedule needs to be prepared and tested for confirmation.

## Sample reserve

The amount of drill core to be kept as a reserve depends upon the nature of the test work program. Additional test work may be required depending on the extent of optimisation test work, achieving the desired test work sample head grade and how the sample 'ages'.

Samples stored in a refrigerator can still undergo 'aging' and replication of previous test work may not be achievable (eg lower flotation recoveries). How soon any follow-up test work would occur is a factor in this decision-making, as well as the likelihood that test work may need to be repeated or that a new flow sheet may need to be pursued.

## Sample characterisation

While the primary characterisation tests include head assays and mineralogy, it is worth considering some simple tests, such as checking the exposure of 'oxide' or transitional ore samples to water (Newell, Munro and Fiedler, 2018).

EDTA analysis (Rumball and Richmond, 1996) can be used to check the degree of oxidation of sulphide mineral samples. It is problematic for the project when metallurgical results bring into question the geometallurgical model. For example, Armstrong *et al* (2011) report a test work program that produced unexpected results resulting in the re-mapping of an orebody in terms of ore types due to the unexpected presence of lead ions on sulphide ore test samples.

Check that the proposed head assay is conducted for each test work composite does include all of the 'penalty' elements (eg Hg, Sb, F, Cl). Note that the geological database of the drill core assays can be useful in identifying penalty elements and their frequency distribution of concentration. While low level concentrations for penalty elements may appear benign, if these elements can 'follow' the primary elements, then the separation process will naturally concentrate these elements into the final product, possibly resulting in an unmarketable product. This situation is exacerbated for by-products, such as molybdenum concentrates prepared from copper-molybdenum ores, where the concentration upgrade ratio can be as much as 5000.

For composite samples, it is worth cross-checking the assayed head versus the calculated head of the drill core interval assays used to prepare the composite. Differences may be found, especially if different assaying methods were employed, requiring a re-think of the 'recipe' used to prepare the composite.

If there is some uncertainty about the mineral species present and the associations, mineralogical tests should be performed prior to the separation test work and repeated at the selected primary grind size.

## Test work

As previously noted, it is important to cultivate patience and an air of calmness during the test work program.

It is very desirable to be present when test work is being conducted, however not all tests need to be observed. You definitely need to be available for scoping or sighter tests (where on-the-run decisions need to be made during a test if it 'doesn't look right'), key optimisation tests, the Locked Cycle Tests (for flotation) as well as when issues occur to provide guidance and advice.

It is also useful to consider a few 'practice' tests to allow the technician to develop familiarity with the sample flotation behaviour as well as the test work requirements and procedures. This may fine-tune the test with some changes in the scraping rate, the flotation residence times and the need for changes in frother additions.

Elicit feedback from the technician conducting the testing, what do they see and think. Metallurgical technicians typically have a keen sense of colour and froth characteristics that can't be conveyed through analytical assays – actively seek their observations and opinions for due consideration!

Encourage the use of photographs and video; digital storage is cheap and permits the test to be revisited in the decision-making process. It also is useful to capture 'oddities' such as precipitates, residues or molybdenite sticking to a diesel layer on the side of a perspex flotation cell. If the laboratory doesn't have a stereomicroscope, purchase a USB connectable microscope for your laptop, or purchase a handheld pocket microscope with a graticule.

When metallurgical issues occur, it is important to take time out, carefully analyse the results (ensure that there are no basic errors such as unexpected conditions or calculations ie it is a 'real' result) and employ diagnostic tests, conduct trial mass, mineralogical and elemental balances and look at size-assays analyses.

However, if you have any doubts, don't be afraid to conduct a repeat test or use third party experts to peer review the results. Note that the testing facility can often offer good advice. As a last resort, replicate the test at another test work facility.

Given the increasing importance of solid-liquid separation such as dry stacking of tailings (eg paste thickening and filtration of tailings), try to avoid the re-pulping of 'aged' samples for tailings dewatering test work. If samples do need to be sent to vendors for testing as a slurry, send as wet filter cakes or as a slurry. Drying samples particularly with high 'clay' contents which are repulped for thickening test work can seriously understate the thickener area required. If samples are to be subjected to flocculation/thickening test work, ensure that the test work pH and chemical environment is aligned with the expected chemistry of the processing plant when in operation. Laboratory tap water used can be significantly superior to site water speciation, particularly compared to proposed bore water sources.

## Ongoing result analysis

Results need to be scrutinised and interpreted prior to conducting the next stages of test work. This is where time is required to consider the results and how to move forward, which may result in some changes to procedure, conditions or even approach. When key decision points are reached (particularly for programs with limited sample), ensure that you accurately record the rationale for such decisions, as it will be an important component of the final reporting, particularly if the direction of the test work, or test work objectives change during the test work program.

If a result is in doubt, repeat the assay. If matters remain unsatisfactory, repeat the test. It is important to understand anomalous results or 'outliers' and why they are occurred. Be very, very careful of deleting an outlier as an aberration or an anomaly, particularly in variability testing.

Carefully check the calculations on the test work reporting spreadsheet; sometimes it may be based on a reporting sheet that was used for another project and the calculations are not correct.

## Result reproducibility/accuracy

The relative errors in testing and assaying need to be understood, in order to make meaningful decisions when the results start becoming available. Small distinctions in metallurgical test results are not meaningful when they are within experimental error. All things being equal, a good laboratory should be able replicate flotation tests with the grade-recovery curves lying on top of each other. Be careful of seemingly significant differences in recovery between tests with very low tailings grades, as sometimes a very small change of one unit of the assay accuracy can drive a recovery difference of several percent, even though the tails assays are essentially the same.

It is important to make sure the data is worthy of interpretation and repetition of key tests and assays is an important tool. The 'gold standard' established a baseline with six repetitions and then three repeat tests for each variable condition (Greet *et al*, 2019).

Plot results in a form that you are familiar with on axes that are realistic. If necessary, plot the results in a number of different ways as it can be surprising what insights can materialise from the data by looking at it differently.

Use statistics where possible to analyse test work; Napier-Munn (2014), Corby (2006) and Bazin *et al* (1996) provide examples of the application of these techniques to design and analyse test work results.

## Managing the budget

Using the quotation as a checklist, you can monitor the cost of the test work program based on the work that you are aware of and check against the test work facility invoice, typically monthly for larger test work programs.

Ideally a contingency (at least 10 per cent and preferably 30 per cent) has been built into the test work program budget to allow for unexpected requirements, such as repeat tests or further investigations to resolve matters. Test work requiring regrind optimisation with alternative regrind mill methods (ball mill, stirred mill, attritioner etc) can sometimes exceed the planned test work program due to the number of grind time calibration tests.

However, when additional test work and associated characterisations are required, in spite of the size of the budget and the associated contingency, it is important to distinguish between 'must do'/'must resolve' and 'nice to' requirements and prioritise accordingly. This can sometimes be reduced to optimising grind size to give a capital cost benefit, or optimising a high consumption/cost reagent that will provide an operating cost benefit.

When such situations arise, as they often do, it is important to understand the impact on the laboratory in terms of availability (space, technicians, assay facility) as well as the length of the test work program, amount of sample and naturally the budget.

## Management feedback

Be cautious and indeed conservative when reporting results back to your management. Ideally, provide feedback at key junctures in the test work program when you are comfortable with the results.

Avoid being influenced by management pressure and be careful about offering optimistic timetables and forecasting metallurgical outcomes.

Typically, the main enquiry concerns the schedule; test work is a linear business, events outside your control impact the progress of test work and occasionally substantial changes need to be made to the program.

An example is continued exploration or in-filling drilling where additional ore and ore types are discovered, potentially resulting in a review of the scope of the test work program and the need for additional test work.

# PILOT PLANTS

## Preparation

Preparing for a pilot or demonstration plant requires considerably more planning and checking. It is important to remember that a pilot plant should be a confirmation of a treatment scheme/flow sheet that has been rigorously/exhaustively tested at the bench scale.

Ensure that a suitable bulk sample is selected: a key failing in pilot plant programs that 'accessible' material, bearing little resemblance to the likely plant feed, is tested.

Conduct mineralogical studies on the bulk sample, since the appearance of an element/mineral fundamentally affecting metallurgical performance can occur that was not detected in the bench scale samples. The classic intruders are 'clays' and naturally floating minerals (eg carbon, talc, some 'clay like' minerals), which may impact concentrate grades, slurry rheology and well as affecting solid-liquid separations.

Confirm whether the pilot plant has been set-up to test the whole flow sheet is being tested or just parts of it. This is an important consideration where the flow sheet has recycling streams and water circulating such as in many hydrometallurgical and some flotation cleaning flow sheets.

Hopefully the key equipment sizing and selection would have been identified in the test work facility response when the Request for Quotation (RFQ) was submitted. Nonetheless, the actual equipment sizing and selection as well as the flow sheet configuration that would be used needs to be confirmed based on the proposed throughput and residence times.

This can be facilitated by preparing a mass and water balance based on bench scale test work results and the proposed head grade, specifically Locked Cycle Tests in the case of flotation projects and applying appropriate scale-up factors for residence times.

Historically, the bane of many an unsatisfactory pilot plant program has been incorrectly sized slurry pumps, pump failures and the inability to pump tenacious froths. Slurry pumps not only need to satisfactorily accommodate the proposed range of flow rates, but they also need to have been recently serviced. And if there is some doubt, incorporate a standby pump in key flow sheet locations.

While reagent additions are generally less of an issue, the reagent system does need to be examined, from source and 'freshness' of reagent to mixing and dosing practices. For soluble reagents, there are a wide range of dosing pumps that can accommodate calculated reagent solution flow rates based on an agreed solution strength. Similarly, for immiscible reagents that are typically added 'neat', there has to be certainty that any immiscible reagents are well mixed into the slurry and don't accumulate on the surface. Dosing very small flows, sometimes dropwise, will require specialist dosing equipment with high reproducibility. In the case of insoluble reagents (eg lime), matters become more difficult and can create or be prone to potential problems. In order to maintain a consistent density of the reagent slurry at the operating flow rates and minimise sanding of the reagent lines, a plant scale application would be employed, such as a ring main and a solenoid controlled by a pH metre.

It is important to identify the nature of the lime, *viz* quicklime, slaked lime or 'commercial lime', the available CaO and diluents, which may have, for example, a content of 20 per cent silica. While the pH would be achieved, the 'lime' consumption may be misleading.

Depending upon the commodity, processing requirements and availability of sample, a pilot/demonstration plant throughput of at least 100 kg/h is desirable while it is considered good practice to apply full scale residence times.

In the case of flotation pilot plants, the flotation residence time scale-up factor from the bench scale residence time is influenced by equipment (eg intensity of mechanical agitation), the flotation stage (eg cleaning) and the degree of risk adverseness and can vary from 1.5 to 4.0 (fine grained refractory ores, platinum ores, or where high depressant regimes are required).

Care needs to be taken in flotation circuit regarding froth launder spray water additions, as cell per cent solids can end up unrealistically low if all water additions are not tightly controlled, resulting in low flotation residence times.

You need to be comfortable with the sampling procedures, the streams to be sampled and the frequency of sampling (in terms of impact on operational stability – three residence periods). This includes the types of sampling and their purpose: grab (whole stream sample, assay – operational check), timed sample (flow rate, SG and assay – control, stability and mass balance) and survey sample (timed, multiple cuts, assay – metallurgical performance). Attention also needs to be paid to the reagents, namely, type/brand, quality as well as the mixing and addition systems, and the planned regularity of reagent flow checks.

Logistical matters such as the receipt, storage and handling of the sample, which may be several tonnes, can be significant.

The hours and days of operation of the test work facility are an important consideration in planning; confirm what is standard practice (eg 12 hour days, only week days, no weekends or public holidays) and understand what would be required in terms of resources and costs to operate the pilot plant outside the standard operating hours.

If continuity is desired or indeed a necessity (eg 'novel' processes or some hydrometallurgical processes), which should be the preferred approach, then this needed to be identified as a key criterion in the test work facility selection stage.

In the case of a pilot plant, shift updates are mandatory. Besides progress and success updates, any issues and problems need to be brought to your attention as soon as possible.

The availability of the assaying facility is important, which typically has independent sources of work to that of the test work facility, as well as other test work providers that have input to the test work program, such as mineralogical studies as well as vendor testing (typically dewatering as well as ore sorting, larger scale gravity testing).

It is important that process operators are experienced in pilot operations that have employed a similar flow sheet and particularly for hydrometallurgical pilot plants where some uncommon unit operations may be required. This needs to be confirmed and commitment by the Pilot Plant Manager a sufficiently sized cohort the process operators (backup for sickness or absenteeism) would be available for the duration of the proposed pilot plant operation.

Confirm what measurements would be taken around the pilot plant and their frequency. Ensure that you are comfortable with the nature of the instrumentation as well as calibration procedure and frequency and whether the instrumentation probes are correctly stored between runs.

Products will need to be packaged, labelled and stored. In some cases, the dewatered tailings are transported back to site or sent for further test work. In this case, the logistics need to be in place prior to the commencement of the pilot plant operation.

## During operation

It is important to be present at all stages of a pilot plant operation although, unless a number of metallurgists are available, it is difficult to fully monitor a continuous operation. In these cases, attend selected day 'shifts' particularly during the initial periods, then random appearances on 'night' shift are suggested to ensure that the same operational and sampling standards are being maintained around the clock.

Photographs and video are particularly useful for pilot plants. For flotation operations, for example, where the nature of the froth is important, it is useful for training the production plant operators as well as recording unexpected events such as precipitates and residues that may occur during a hydrometallurgical pilot plant. Froth factors should be determined where possible for use in concentrate launder and pump hopper design and for froth pump calculations.

Carefully observe the start-up and how quickly stable conditions are achieved. This includes slurry flow rates, reagent additions and the initial sampling campaign.

Should major issues be encountered during operating a pilot plant, then the program should be halted until the issue/s are resolved. The nature of the problem may include sample quality (eg not representative and merely 'accessible', previously unidentified mineralogy, contamination etc), operational matters (eg equipment availability or suitability (froth pumping), external services turn-around times, sampling and staffing problems) or metallurgy.

Like a full-scale operation, most issues tend to be associated with equipment and instrumentation failures although occasionally sample and metallurgical issues do rear their ugly head.

Establishing the mill type, media and operating conditions for regrinding can sometimes be a challenge, particularly for some industrial minerals.

Slurry temperatures should be monitored through the circuit, particularly post regrinding, as slurry temperature can have a significant effect on collector and frother degradation, and hence the required dosage rates required in subsequent processing.

While equipment and instrumentation issues should be readily resolved, sample and metallurgical issues are far more challenging and may seriously impact the program timetable. A more representative bulk sample may need to be sourced while a bench scale program may be required to address the unexpected metallurgical problems.

Pilot plants can generate a large amount of data in a very short period of time. If the results are not aligned with expectations, then the pilot plant testing may have to be paused to provide time for detailed evaluation of the data available or some parallel bench scale work may need to be undertaken. Pausing a pilot plant program can have major ramifications as to personnel availability (time over-run conflict with planned work for other clients) and tightly managing the overall program. Most battles are won or lost in the planning.

## CONCLUSIONS

Conducting a successful test work program, whether at the bench scale or pilot plant scale, is based on a suitable scope of work, carefully selected samples and a capable test work facility. This needs to be supported by timely feedback from the test work facility as well as timely and effective directions to the test work facility.

Preparation prior to conducting the test work program is the key to ensuring that the program successfully achieves the proposed aims in a timely and cost-effective manner. Developing a constructive relationship with the test work facility based on agreed procedures, standards and frequency of communications is critical while recognising potential bottlenecks, such as assaying turnaround time and mineralogical studies.

During the test work program, it is important to keep focused, provide guidance and be present for as many test work stages as possible, while drawing upon diagnostic tools as well as leveraging external knowledge to resolve unexpected problems.

## ACKNOWLEDGEMENTS

The authors thank colleagues and collaborators throughout the years who have freely shared their experiences of the joys, frustrations and disappointments that come with any program of metallurgical testing.

## REFERENCES

Anderson, C.G., 2006. *The Use of Design of Experimentation Software in Laboratory Testing and Plant Optimisation*, Paper 35, 38th Annual Meeting of the Canadian Mineral Processors, Ottawa.

Armstrong, B., Czerw, A, Glen, J., Johnston, N. W. and Munro, P. D., 2011. *Realisation of Value through Identification of Various Oxidation Fronts and Mineralisation Styles at Trilogy Cu-Au-Ag-Pb-Zn Deposit*, in the Proceedings of the AusIMM International Geometallury Conference (GeoMet 2011), pp. 47–51, editor Dominy, S.

Bazin, C., Hodouin, D. and Grant, R., 1996. *Semi-Batch Flotation Tests: Reliability of Performance Indices*, Canadian Metallurgical Quarterly, The Canadian Journal of Metallurgy and Materials Science, Volume 35, Issue 4, pp. 321–327.

Greet, C.J., Morgan, D., Davis, J., G Small, G. and X du Toit, X., 2019. *Metallurgical Improvements at Northparkes Concentrator through the Application of High Chrome Grinding Media,* in the Proceedings of the AusIMM Metallurgical Plant Design and Operating Strategies Conference (MetPlant 2019), pp. 150–162.

Molnar, R., 2006. *Hydromet Piloting: What can the Mineral Processor Expect*, Paper 36, 38th Annual Meeting of the Canadian Mineral Processors, Ottawa.

Napier-Munn, T.J., 2014. *Statistical Methods for Mineral Engineers: How to Design Experiments and Analyse Data*, Monograph 5, Julius Kruttschnitt Research Centre, Indooroopilly, Queensland.

Newell, A., Munro P.D. and Fiedler K., 2018. *Metallurgical Test Work – Between a Rock and Hard Place*, in Proceedings of the 14th AusIMM Mill Operator's Conference, pp. 15 – 35.

Rumball, J.A. and Richmond, G.D., 1996. *Measurement of Oxidation in Base Metal Flotation Circuits by Selective Leaching with EDTA*, International Mineral of Mineral Processing, 48 (1–2), pp. 1–20.

# APPENDIX 1

## MINIMUM TEST WORK REQUIREMENTS

### Generic test work requirements

The typical generic test work requirements are listed below and are summarised for a number of commodities in the following Appendices. While the actual test work requirements depend upon several aspects, including the mineralogy, test work aims, sample availability and the budget, these generic requirements need to be satisfactorily addressed. Note that test work conducted for bulk minerals, smelting and hydrometallurgical flow sheets may have additional requirements.

### Reference


Guresin, N., Lorenzen, L., Dominy, S. C., Muller, H. and Cooper, A., 2012. *Importance of effective sampling and test work protocols for process plant design*, In Proceedings Sampling 2012, The Australasian Institute of Mining and Metallurgy, Melbourne, pp 95–108.


- Sample
  - Ore types – classification basis
  - Life-of-mine and Mine Schedule
  - Representative of the sample type, *viz* feed grade and mineralogy
  - How were they obtained and from where
  - Sufficient quantity available
  - Appropriate type: Bulk, RC chips, diamond drill core
- Mineralogical studies
  - Determines the grind size, separation route and thus the flow sheet
- Pre-concentration
  - Establish potential: size-assay studies at selected crush sizes
- Comminution
  - Dedicated samples
  - Milling parameters
    - Crushing, primary milling and regrind
    - Bond Mill Work Indices
    - Drop weight and JK
- Materials handling studies
  - Ore recovery from bins and stockpiles (eg TUNRA, Jenike and Johansen)
  - Presence of clay
- Separation
  - Method
    - Gravity (eg coarse gold, minerals sands, hematite etc)
    - Magnetic (eg magnetite, wolframite, ilmenite etc)
    - Flotation (eg copper, molybdenum, nickel, lead, zinc, graphite etc)
    - Leaching (eg gold, copper, cobalt, nickel, uranium)
    - Electrostatic (eg zircon)
  - Benchscale: continuous (Locked Cycle Tests [LCT] for flotation or pilot plant) where required
    - Kinetic test work – modelling and vendor process guarantees
    - Equipment vendor test work
  - Reproducibility studies – particularly when results are variable
  - ‘Site’ water

- Sample ageing
- Establish feed grade-recovery relationships
  - Need to understand metal recoveries and product grades – as a function of ore type and head grade
  - Important for production schedule and financial evaluation
- Understand metallurgical losses
- Understand ore variability: within ore types, between ore types and the effect of grade
- Sufficient amount of test work to support flow sheet interpretation and metallurgical response
  - Test Work
    - Comminution – crushing, milling
    - Materials handling
    - Pre-concentration
    - Dewatering (thickening and filtration)
  - Ore variability
  - Metal recoveries and product grades – as function of ore type and head grade

- Product characterisation
  - Full assay (penalty and credit elements)
  - Sizing
  - Samples for marketing/further value adding test work (eg graphite flotation concentrate for spheroidisation test work)
  - Dangerous Goods Certification to support a Materials Safety Data Sheet (MSDS) and International Maritime Dangerous Goods (IMDG) (the latter if it is proposed to export product by ship)
  - International Maritime Solid Bulk Code (IMBSC Code) classification (if it is proposed to export product by ship)
  - Flammability and combustibility (mainly sulphide concentrates)
  - Self-heating (mainly sulphide concentrates)
  - Corrosivity (mainly sulphide concentrates)
  - Other characteristics: eg friability
- Dewatering
  - Concentrates and tailings – rheology, settling and filtration properties
  - Concentrates – Transportable Moisture Limit (TML)
  - 'Dry stacking' of tailings, ensure appropriate range of separation tailings samples are tested
    - Typical range of 'fines' (<10 microns) proportions
- Samples for test work by others eg tailings, geotechnical and geochemical test work (eg ARD tailings classification)

## Study minimum test work requirements

### *Scoping study/preliminary evaluation assessment (PEA)*

- Sample: representative, at least dominant ore types (*cf* oxidised, primary) and primary diluent, possibly LOM
  - Quantity: ~50 kg with ~20 kg/ore type for separation and characterisation; >30 kg for comminution
- Head assay, moisture, ore, bulk density
- Mineralogy: Optical, MLA/QEMScan on separation feed (degree of liberation), diagnostic leach (gold ores)

- Size fraction-assay for two crush sizes
- Grinding studies: Bond Mill work indices and/or SMC tests (DWi, SAG Mill Amenability)
- Separation studies
  - Rougher-scavenger sighter tests at least two grind sizes, reagent type/addition rate studies, pH, per cent solids, concentrate regrind
  - Cleaner studies
  - Gravity
  - Leaching: grind size, bottle roll, leaching time, pH, cyanide concentration, oxygen demand
- Dewatering studies: settling and filtration, concentrates and tailings
- Concentrates: full assay and size fraction-assay

### *Pre-feasibility study*

- Sample: representative: LOM, ore types, mining samples (based on mine schedule), head grade, variability and diluent material
  - Quantity: ~400 kg with ~60 kg/ore type for separation, characterisation and materials handling; >80 kg variability; >200 kg for comminution
- Head assay, moisture, bulk density
- Mineralogy: Optical, MLA/QEMScan on separation feed (degree of liberation), diagnostic leach (copper and gold ores)
  - If pyrite present, need to determine acid forming potential
- Crushing studies: Crushing Work Indices, Unconfined Compressive Strength, Point Load – also consider the primary gangue dilutent
- Test pre-concentration options if appropriate– more than classification – magnetic, colour, SG, X-ray
- Grinding studies: Bond Mill work indices, SMC tests (DWi, SAG Amenability), Abrasion Index, size-assay (pre-concentration), regrinding
  - Suitable range of samples
  - Modelling/simulation of comminution circuit: higher throughputs and/or very hard ores: SAG mills, ball mills, pebble crushers, crush sizes, recycle streams
- Gravity studies
- Materials handling studies: angle of repose, bin and stockpile drawdown ('live' capacities), effect of moisture content
- Separation studies
  - Use site water if appropriate
  - Rougher-scavenger tests: rheology, per cent solids, optimising primary grind size and concentrate regrind, reagent type/addition rate studies, kinetic studies
  - Cleaner studies – circuit configuration, cleaner scavengers
  - Locked Cycle Tests (LCT), duplication of LCT under best conditions
  - Leaching: optimising studies, oxygen demand, rheology (gold ores); ferric leaching (biological oxidation), fine grind/oxidative leach (sulphide ores)
  - Size-assay/mineralogy on tailings
  - Effect of oxidation (sulphide ores)
- Dewatering studies: concentrates and tailings – settling, paste thickener; concentrates – filtration as well as tailings for 'dry' stacking
- Concentrates: full assay, size fraction-assay and Transportable Moisture Limit (TML)

### *Feasibility study*

- Similar range to PFS but more extensive and more detailed particularly comminution

- Samples: representative: LOM, ore types, mining samples (based on mine schedule), head grade, variability and diluent material
- May involve a pilot plant

### *Other testing requirements/considerations*

- Friability/degradation: Drop/Tower tests: hematite ores (lump/fines ratio)
- Product testing: Decrepitation Index (DI), Tumble Index, Sintering properties, Loss on Ignition (LOI): hematite ores. Concentrate bulk density per size fraction and flow characteristics for bagging (eg graphite)
- Testing for MSDS/SDS preparation
- Spontaneous combustion (eg pyrrhotite rich concentrates)
  - Flammability and combustibility
  - Self-heating
- Concentrate transportation by pipeline
  - Rheological studies (viscosity – per cent solids)
    - Note that the thickener underflow rheology can be very sensitive to flocculant type and addition rate
  - Abrasion
  - Corrosion
  - Freezing

## Key test work issues

- Selecting samples: metallurgists must take ownership (ie experience, competency and decisiveness) involving geologists to the spatial context and mining engineers to understand the time context ie when it will be treated in the processing facility
- Identifying ore types: another metallurgist ownership issue is to understand ore types, proportions (geologists) and the likely blends, including dilution, that will be presented to the plant (ie the Mine Schedule, which must identify ore types and grades, and unless the deposit exhibits some unusual mineralogical and ore type features, on monthly basis for Years 1 and 2, quarterly for Years 3 to 5, and annually thereafter (mining engineers)
- Internal and external dilution: understand the lithology/mineralogy of dilution, and how much is expected
- Understanding mineralogy and variability: implications for the flow sheet and testing
- Properly identifying ore types: metallurgists need to spend time with the geologist and the resource estimator
- Establishing an appropriate test work plan, which is dependent upon the purpose and the Study stage, which is systematic, incorporates flexibility and has contingencies with regard to sample quantities, time and budget
- Properly determining comminution properties for the optimum separation conditions by ore type and proposed feed type blends, as revealed by the mine schedule; note that more ore types and gangue types maybe identified with increased drilling
- Selecting appropriate separation methods and optimising the separation conditions for each ore type and the proposed feed type blends, as revealed by the mine schedule
- Understanding the nature of errors and taking them into account (not making decisions based on one test result, especially in flotation): test work: duplicate optimised test (eg for flotation the best LCT result; assays: check/repeat assays; mill modelling: range of throughput estimates
- Use of site water if >6,000 TDS
- Identifying metal recovery as a function of head grade and ore type, at least three feed grades
- Understanding where and why the process losses occur

- Fully characterise dewatering properties for the separation tailings over a range of feed blends; note that these samples are often useful for environmental characterisation studies
- Characterising concentrate/product properties
  - Full assay – identify penalty (eg Hg, Cl, F, As, Sb etc) and credit (eg Ag, Au etc) elements
  - Sizing
  - Bulk density
  - Dewatering properties; note that filtration determinations should reflect the likely filter that would be selected eg vacuum or pressure filtration
  - Moisture
  - Transportable Moisture Limit (TML) for each concentrate (typically at the PFS or FS phase)

# APPENDIX 2

# TEST WORK CHECKLIST

## Preface

The following test work checklist is a high-level guide to confirm that you have most of the bases covered with regard to initiating a test work program.

Some references are provided as a guide to planning in terms of the possible test work approach and strategies that may be applied as well as the considerations as well as potential detail that may be required for the ores that you plan to test.

## References


Anderson, W., 2000. *The Scheduling, Costing and Importance of Metallurgical Testwork Programs in Process Feasibility Studies*, in the Proceedings of the International Congress on Mineral Processing and Extractive Metallurgy (Minprex 2000), Melbourne, pp. 79–89, editor D.R. Swinbourne.

Doll, A. and Barratt, D., 2011. *Grinding: Why So Many Tests?* In Proceedings of the 43rd Annual Canadian Mineral Processors Conference, Paper 34, Ottawa, pp. 537–556.

Pocock, B.J., Smith, C.B. and Welch, G.D., 2002, *Bench-Scale and Pilot Plant Tests for Thickening and Clarification Circuit Design*, in Mineral Processing Plant Design, Practice and Control, Volume 1, Mular A.L., Halbe D.N. and Barratt D.J. (editors), Society for Mining, Metallurgy and Exploration, Littleton, CO, USA, pp. 201–206.

*Sampling and Testing*, in SME Mineral Processing Handbook, Volume 2, Weiss N.R. (editor-in-chief), Society of Mining Engineers of American Institute of Mining, Metallurgical and Petroleum Engineers, New York, NY, USA, pp. 30–1 to 30–129.
*Spedden H.R., 1985. Introduction, pp. 30–1 to 30–4.*
*Spedden H.R., 1985. Quantitative Mineragraphy, pp. 30–60 to 30–65.*
*Bergstrom, B.H., 1985. Crushability and Grindability, pp. 30–65 to 30–68.*
*Bergstrom, B.H., 1985. Abrasiveness, pp. 30–68 to 30–72.*
*Macdonald, R.D., Brison, R.J. and Hellyer, W.C., Flotation Testing Procedures, pp. 30–96 to 30–104.*
*Wesely, R.J.,1985. Laboratory Methods in Solid-Liquid Separation, pp. 30–104 to 30–108.*
*Macdonald, R.D., Hellyer, W.C. and Harper, R.W., 1985. Process Development Testing, pp. 30–116 to 30–120.*


## Test work checklist

- Test work objectives
  - Defined
- Test work program
  - Scope of Work
    - Based on likely flow sheet as inferred by likely mineralogy
    - Allow for variations, additional work
  - Duration: allowance for additional time to complete the test work program that may arise due to delays in assay turnaround, requirement for repeat or additional test work, unexpected problems or events
- Test work facility
  - Requirements defined
  - Due diligence conducted
  - Requests for Quotation (RFQs) submitted
  - Accreditation eg ISO 9001, ISO/EC 17025
  - Selection (refer to Appendix 3)
- Test work budget
  - Internal
  - Quotations
  - Contingency
- Ore types

  - Defined – discuss with geologist
  - Proportions – based on resource model: discuss with geologist
- Samples
  - Types
  - Quantity
  - Availability
    - Diamond Drill Core
      - Full core (comminution – UCS)
      - Half/quarter core (comminution, mineralogy and separation)
    - Rotary Percussion
  - Mine schedule – discuss with mining engineer: feed blends that would be presented to processing plant over LOM
  - Characterisation
    - Head assays
    - Mineralogy
    - Moisture
    - Specific Gravity
    - Bulk density
  - Logistics
    - Local
      - Getting samples from site to test work facility
      - Packaging – needs to be good to minimise drill core breakage for certain comminution tests (eg UCS, Drop Weight)
      - Paperwork
        - Sample Packing List
        - Address Label
        - Declaration of Origin of Material Samples
      - Alert test work facility – consignment notes
    - Overseas
      - Complete paperwork (importation and clearance)
        - Pro forma Commercial Invoice
        - Customs Declaration
        - Quarantine requirements (eg gamma irradiation)
        - LCL Packing Declaration (sea freight)
        - Address Label (nearest port to test work facility)
        - Sample Packing List
      - Packaging
        - No wooden crates – quarantine hazard
        - Needs to be good to minimise drill core breakage for certain comminution tests (eg UCS, Drop Weight) – use bubble wrap
        - Careful labelling of all samples – labelling can get abraded off if containers rub against each other in transit
      - Track sample transit location daily if possible
      - Alert test work facility well ahead of time – likely flight and arrival time, consignment notes
- Comminution
  - UCS

    - Crushing Work Index
    - Bond Rod and Ball Work Indices
    - Drop Weight Index
    - SMC parameters
    - Bond Abrasion Index
- Pre-concentration: potential, size-assays by crush size
- Separation
    - Gravity; Heavy Liquid, Centrifugal, upflow classifier
    - Flotation
        - Bench scale: sighter, optimisation, Locked Cycle
        - Pilot Plant: required?
- Leaching
    - Gold: columns (heap), bottle roll, oxidation required, preg-robbing, cyanicides, oxygen demand (high – passivate, aeration (pyrrhotite)/lead nitrate [pyrite]), slurry rheology
        - Initial assessment: LeachWELL™
    - Copper: columns (heap), agitated tank, autoclave or high temperature atmospheric leach
        - Initial assessment: bottle roll
    - Nickel: columns (heap), atmospheric or pressure leaching (HPAL)
- Magnetic: dry/wet, intensity (*cf* LIMS and WHIMS), number of stages
- Dewatering
    - Concentrates
        - Settling: flocculent type and addition rate
        - Filtration, cake moisture, thickness, cycle time, TML
    - Tailings
        - Variability – ranges of fine content, sulphur grade, residual reagent
        - Settling – conventional, paste
        - Filtration – dry stacking

# APPENDIX 3

## TEST WORK FACILITY SELECTION CRITERIA

Important criteria for ranking and selecting a laboratory are:

- Demonstrated experience and competency at that test work facility
  - Comminution
  - Gravity
  - Flotation
  - Leaching/hydrometallurgy
  - Pyrometallurgy
- Quality and reputation
  - The 'A' team particularly the technicians
  - Accreditation: eg ISO 9001, ISO/EC 17025
- Management and supervision
  - Managing in your interest – not defending laboratory's behaviour or deficiencies
  - Dedicated competent staff
    - To your project – not several
    - Not just recently hired off the street – have performed this type of work previously
- Current and future workload – availability of equipment, personal and where your project sits in 'the pecking order'
  - This includes the assaying facility as well as the mineralogical services, who often operate independently
- Quality of facilities – equipment, drying procedures, internal sample tracking and storage
- Availability
  - When they can they undertake your program?
  - Are other services (mineralogy, assaying) also available at the same time?
- Degree of outsourcing
  - Assaying (see below)
  - Mineralogy
  - Vendor equipment testing (typically specialised equipment (eg HPGR), thickeners, filters etc)
- Assaying
  - In-house or sent to another analytical laboratory (can significantly increase turn-around time)
  - Equipment and methodology
    - Checks and balances (QA/QC)
    - Turn-around time – negotiate maximum 24 hours
- Availability of other services, such as mineralogy
- Progressive reporting, all data in spreadsheets, not pdf files
- Quality of the report – does it provide opinions and recommendations?
- Selection of test work facilities based on cost (ie avoid cheapest quotation)
  - For a test work program supporting a Feasibility Study, the laboratory has to bring something more to the table other than bottle rolls or a flotation machine and manual manipulation of a froth scraper
- Set-up a checklist of selection attributes

- Rank the test work facilities: using a weighting system (eg 1 to 5) for each selection attribute, which is then rated (eg 1 to 10) for each test work facility with ranking determined based on the sum of the weighted ratings

## Due diligence

Conduct a due diligence on the proposed laboratory with the following focusing questions:

- Discuss the laboratory with colleagues and mentors
  - Previous experiences
  - Has the test work facility recently been upsized or down sized?
- Note location and ease of getting samples to the laboratory
  - Can they handle overseas samples (quarantine certification) – procedures, importation paperwork?
- Laboratory capabilities – what can they do, have done and what they can't do
  - Clarity required on work that will be outsourced eg mineralogy, solid-liquid separation, geochemical characterisation tailings, transport properties of concentrates
- Laboratory experience (at that site) with the commodity and separation
- Examples of previous programs successfully conducted at that facility, and that the relevant personnel are still employed
  - Provision of references
- Key personnel and experience
  - Particularly technician(s) who will be conducting the separation work
  - Any proposed leave during the test work program?
- Amount of your time required to manage the laboratory
  - This does not mean a 'stream of consciousness' emails to the laboratory on your daily thoughts!
- Availability of facilities ie current work schedule
- Schedule of rates; most laboratories quote a flotation test inclusive of assay cost for a given number of products. Confirm assay costs independent of the test for the selected assay suite and methodologies
- Can they contribute to the program?
  - The best laboratories will identify and resolve processing problems of their own volition
- Do they produce a final report?
  - What is the nature of the final report? Be prepared to pay for a good one
  - Does it just collate results or provide opinions and guidance?
  - Timing for final report post completion of the test work program?

## Pilot plant

Although most aspects are similar to the bench scale test work facility due diligence, there are additional requirements that need to be closely investigated, including, if possible, inspecting the more promising test work facility/facilities:

- Experience
  - Facility – have they undertaken this before, at this location, especially with this commodity and style of flow sheet?
    - Examples of previous pilot plant programs successfully conducted at that facility
    - Provision of references
  - Personnel – have they worked on a pilot plant with this commodity and style of flow sheet?
- Pilot plant management
  - Who would be responsible and your point of contact?

- Safety
- Management of personnel
  - Shift meetings, updates
- Operations reporting frequency
- Metallurgical results – frequency of reporting

- Hours of operation
  - If continuous operation is required, need 24/7
- Availability of facilities ie current work schedule
- Schedule of rates
- Availability of equipment and range of equipment sizes
  - Would the preferred equipment available?
  - Equipment size: based on proposed treatment rates and residences times, would all the key pieces of equipment be correctly sized, including conditioning and storage tanks as well as reagent and slurry pumps?
  - Milling and classification circuits reflect the likely plant scale equipment
    - Mode of operation: batch or continuous
  - Product dewatering and drying facilities
    - Capable of handling the proposed volumes
  - Reagent storage, mixing and distribution systems
  - Instrumentation capability
    - What needs to be measured and how often?
      - Milling: power draw, feed and product sizing, feed and product moistures, circulating load etc
      - Separation: feed and selected separation stage per cent solids, assays, slurry flow rates, airflow rates, slurry chemical parameters (pH, Eh/Es, Temperature, Dissolved Oxygen)
      - On-stream analysis or bench XRF
      - Particle sizing methodology and turnaround time
    - Calibration – method and frequency
    - Recording, collation and reporting
- Ability to close the water circuit with tails settling/thickening
- Capacity to store and handle the pilot plant sample(s) and site water
  - Fully characterise pilot plant sample
    - Size range, head assays and mineralogy
  - If proposing to conduct pilot plant using site water or synthetic equivalent, check that sufficient storage capability exists, or in the case of synthetic water, ability to prepare and store on a daily basis
- Assaying facilities
  - Ideally dedicated or there is preferential treatment for pilot plant samples (no queues or delays)
  - Confirm likely assay turnaround time and the backup plan to ensure acceptable assay turnaround on metallurgical results
- Confirm sampling procedures
  - Control – often spot samples, frequency, basis for taking samples
  - Metallurgical – survey, conducting metallurgical mass balances, performance
    - Ideally three residence time periods, which should include the whole processing (eg flotation circuit including cleaners, leaching circuit including recycling streams)

- Capability for undertaking bench scale test work as required to cross-check against pilot plant
  - Potential availability of equipment and personnel
- Carefully consider your schedule and amount required to manage and check the pilot plant operation
  - Test work objectives clearly relayed to all personnel
  - Walk the circuit and check all equipment is per flow sheet, water and reagent addition points and proposed sample points
  - Commissioning plan, time required to obtain required grind size
  - Who to call in the middle of the night if things go sideways
  - Always good to observe the start-up and how quickly stability is achieved
  - Important to observe the sampling procedures
  - And if a 24/7 operation, appearing unannounced on a night shift or three is always recommended

# APPENDIX 4

# TESTING BASE METAL ORES

## Preface

As usual, the test work approach is dependent on mineralogy, the base metal, gangue associations and grade eg common base metals (copper, nickel, lead, zinc): sulphides (pre-concentration, flotation) and oxides (leaching, sulphidisation/flotation). Although a base metal, test work approaches for iron have been addressed separately (refer to Appendix 6). For less commonly encountered base metals such as tungsten, mineral type is critical eg wolframite/ferberite (pre-concentration, gravity, magnetic separation), scheelite (pre-concentration, gravity, flotation) and hűbnerite (pre-concentration, gravity, flotation).

As background, references to some relevant test work papers have been provided.

## References

Dunne, R.C., Lane G.S., Richmond G.D. and Dioses J., 2010. *Flotation Data for the Design of Process Plants: Part 1 – Testing and Design Procedures*, Transactions of the Institutions of Mining and Metallurgy, Section C, Mineral Processing and Extraction Metallurgy, 119:4, pp. 199–204.

Ounpuu, M., 2001. *Was that Locked Cycle Test Any Good?* In: Proceeding of 33rd Annual Meeting of the Canadian Mineral Processors, Canadian Institute of Mining, Metallurgy and Petroleum, Montreal, Quebec, Canada, pp. 389–404.

Thompson, P., 2016. *Laboratory Testing for Sulfide Flotation Process Development.* Transactions of the Institutions of Mining and Metallurgy, Section C, Mineral Processing and Extraction Metallurgy, 33:4, pp. 200–213.

Williams, S.R., Ounpuu, M.O. and Sarbutt, K.W., 2002. *Bench and Pilot Plant Programs for Flotation Circuit Design*, in Mineral Processing Plant Design, Practice and Control Volume 1, Mular A.L., Halbe D.N. and Barratt D.J. (eds), Society for Mining, Metallurgy and Exploration, Littleton, CO, USA, pp. 145–159.

## Test work approach

### *Sulphide minerals*

- For representative sample and each ore type
  - Mineralogy
  - Head assay including S, Fe, Hg, Bi, As, Sb, Cd, V, Pb, Zn, Cu, Co, U, Th, Au, Ag, MgO, $SiO_2$, F, Cl
  - Mineral speciation: Diagnostic leach
    - eg Cu: Hot Acid Soluble, Weak Acid Soluble, Cyanide Soluble, etc
  - Moisture
  - Bulk density
- Understand mineralogy, petrology and alteration: implications for testing and flow sheet
- Determine comminution parameters (CWi, Ai, UCS, DWi, a, b, BBMWi, BRMWi)
- Materials handling characteristics
- Determine grind size for optimum separation performance
- Pre-concentration: size fraction-assays by crush
  - If potential, examine classification, gravity, X-ray sorting, optical sorting, gravity, optical sorting
- Gravity: liberated gold
- Flotation: sighter tests, bulk flotation, differential flotation, effect of oxidation, rougher concentrate regrind, number of cleaning stages, reagent suites, optimisation, kinetic, variability, Locked Cycle Tests
  - Effect of site water
  - Effect of sample ageing
- Product

- Full assay suite including S, Fe, Hg, Bi, As, Sb, Cd, V, Pb, Zn, Cu, Co, U, Th, Au, Ag, MgO, $SiO_2$, F, Cl
    - Size fraction assays
    - Specific Gravity
    - Bulk density
    - Materials handling characteristics for products that will be bagged and shipped eg graphite, molybdenum, tin, etc
- Dewatering
    - Concentrates
        - Thickening: flocculent type and addition rate, rise rate, unit settling rate ($t/m^2h$), underflow per cent solids/rheology, overflow clarity
        - Filtration: effect of feed solids concentration, cake moisture, thickness, cycle time, washing (high chloride levels)
        - Transportable Moisture Limit
        - Dangerous Goods Certification to support a Materials Safety Data Sheet (MSDS) and International Maritime Dangerous Goods (IMDG) (the latter if it is proposed to export product by ship)
        - Dangerous Goods Certification to support a Materials Safety Data Sheet (MSDS) and International Maritime Dangerous Goods (IMDG) (the latter if it is proposed to export product by ship)
        - International Maritime Solid Bulk Code (IMBSC Code) classification (if it is proposed to export product by ship)
        - Flammability and combustibility
        - Self-heating
        - Corrosivity
    - Tailings
        - Thickening: conventional, paste: flocculent type and addition rate, rise rate, unit settling rate ($t/m^2h$), underflow per cent solids, overflow clarity
        - Filtration (dry stacking): cake moisture, thickness, cycle time
        - Samples to be sent for tailings geotechnical and geochemical studies supervised by specialist consultants

### *'Oxide' minerals (generic term for oxides, carbonates, sulphates, phosphates)*

- For representative sample and each ore type
    - Mineralogy, 'clay' content (effect on slurry rheology)
    - Head assay including S, Fe, Hg, Bi, As, Cd, V, Pb, Zn, Cu, Co, U, Th, Au, Ag, MgO, $SiO_2$, F, Cl
    - Mineral speciation: Diagnostic leach
        - eg Cu: Hot Acid Soluble, Weak Acid Soluble, Cyanide Soluble, etc
    - Moisture
    - Bulk density
- Understand mineralogy: implications for testing and flow sheet
- Determine comminution parameters (CWi, Ai, UCS, DWi, a, b, BBMWi, BRMWi)
- Materials handling characteristics
- Determine crush/grind size for optimum separation performance
- Pre-concentration: size fraction-assays by crush; if potential examine classification, gravity, X-ray sorting, optical sorting
    - For lateritic ores eg limonite and some saprolites: scrubbing, attrition, screening, classification (hydrocyclone, screw classifier)

    - Measure – mass and metal recoveries, impurity (Mg, Ca etc) rejection
- Sulphidisation flotation: sighter tests, Es potential (sulphide ion concentration), pH, collector type (usually strong eg PAX), number of cleaning stages, recycle streams, optimisation, kinetic, variability, Locked Cycle Tests
- Leaching: heap – column testing, crush size; agitated – grind/beneficiated size; pressure – grind/beneficiated size
    - Leach time, acid addition rate, pH, temperature, water type etc
    - High acid consumption: alternative approach eg another lixivant; eg soda ash or sulphidisation/flotation (*cf* cobalt, heterogenite)
- Purification: solvent extraction, precipitation
- Product
    - Full assay suite including S, C, P, Fe, Hg, Cd, V, Pb, Zn, Cu, Co, Mn, U, Th, Au, Ag, MgO, $SiO_2$
- Dewatering
    - Concentrates
        - Thickening: flocculent type and addition rate, rheology, unit settling rate ($t/m^2h$), underflow per cent solids, overflow clarity
        - Filtration: cake moisture, thickness, cycle time, washing (high chloride levels)
        - Transportable Moisture Limit
    - Tailings
        - Thickening: conventional, paste: flocculant type and addition rate, rheology, unit settling rate ($t/m^2h$), underflow per cent solids, overflow clarity
            - Counter Current Decantation (CCD)
                - For ores that contain clays eg limonite ores, test feed samples with a range of clay contents
        - Filtration (dry stacking): cake moisture, thickness, cycle time
        - Samples to be sent for tailings geotechnical and geochemical studies supervised by specialist consultants

# APPENDIX 5

# TESTING GOLD ORES

## Preface

An oft repeated theme in test work and the development of a suitable flow sheet is the role that mineralogical properties play however gold ores epitomise this theme in abundance and a wide range of techniques are subsequently employed. This includes the nature and size of the gold occurrence (eg free gold, gold tellurides, gold bearing pyrite and arsenopyrite) – gravity, cyanide leaching, flotation, oxidation, gangue associations (eg pre-robbing, oxidation required to release gold [roasting, pressure, ferric leaching [bacterial, Albion process,]) as well as grade (heap leaching).

Marsden and House (1992) provide descriptions of the mineralogies of various gold ores as well as the process flow sheets that have been developed to recover gold from these gold ores.

The following references are provided to assist in the formulation of suitable test work programs.

## References


Dominy, S.C., O'Connor, L., Glass, H.J., Purevgerel, S. and Xie, Y., 2018. *Towards Representative Metallurgical Sampling and Gold Recovery Testwork Programmes*, MDPI, Minerals, 8 (5), 193, pp.1–47.

Dunne, R., Buda, K., Hill, M., Staunton, W., Wardell-Johnson, G. and Tjandrawan,V., 2012. *Assessment of Options for Economic Processing of Preg-robbing Gold Ores*, Transactions of the Institutions of Mining and Metallurgy, Section C, Mineral Processing and Extractive Metallurgy, 121:4, 217–223.

Lunt D., Richie I., and Fleay, J., 1997. *Metallurgical Process Development for Plant Design*, in Proceedings of the International Conference on Mine Project Development (Mindev 97), Paper 10, editor E. Barnes.

Marsden, J. and House, I., 1992. *Section 3.13, Metallurgical*, The Chemistry of Gold Extraction, Ellis Horwood Limited, Chichester, England, pp. 98–104.


## Test work strategy

Marsden and House (1992) recommend the following test work strategies for Free Milling, Preg-robbing and Refractory gold ores as shown respectively in Figures 5–1 to 5–3.

Needless to say, a good mineralogical study and particularly a diagnostic leach of the samples can quickly align the test work strategy and subsequently the best test work approach.

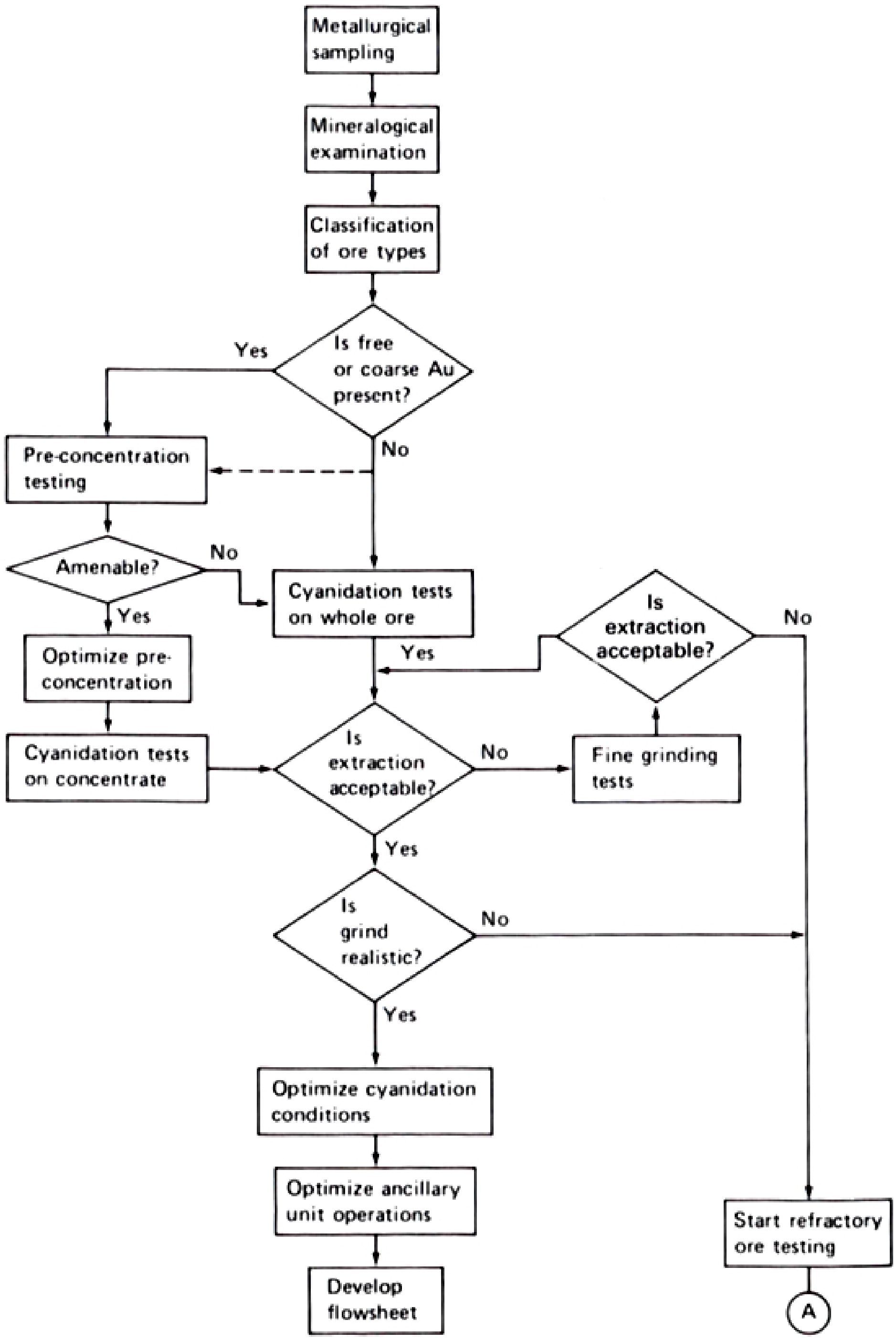


**FIG 5–1** – Free milling gold ores (after Marsden and House, 1992).

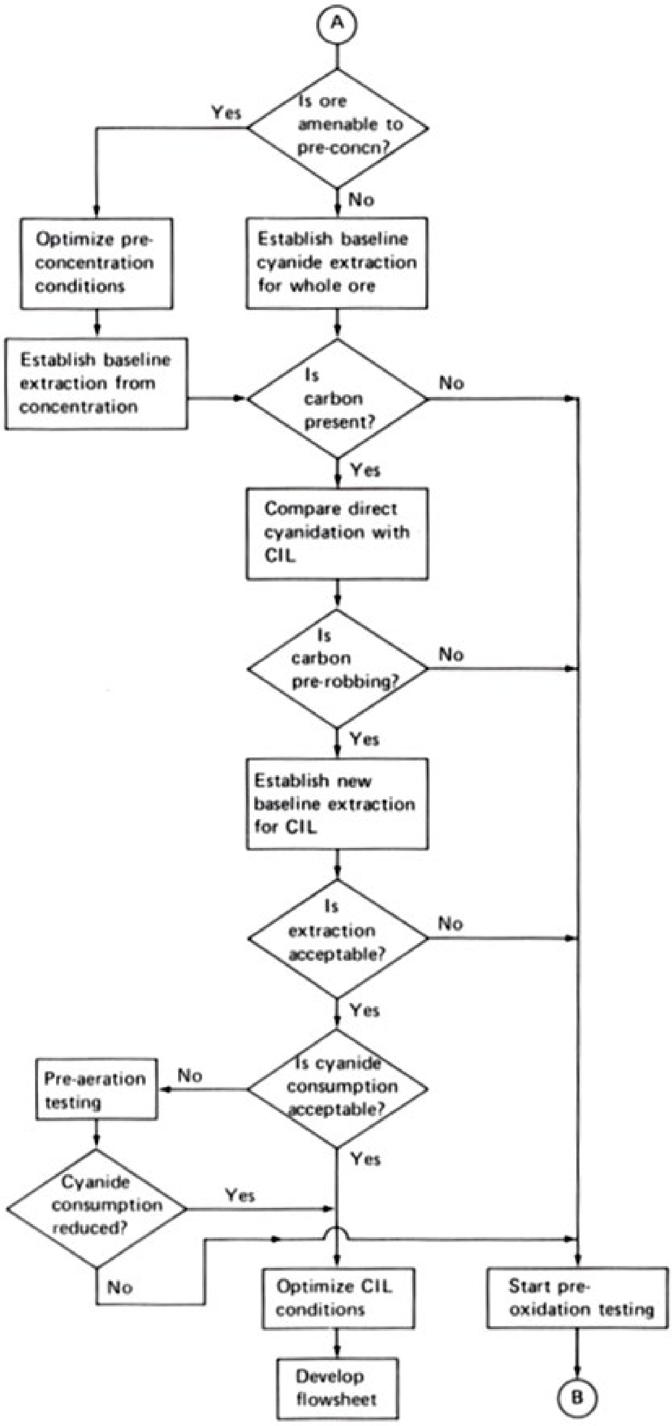


**FIG 5–2** – Pre-robbing gold ores (after Marsden and House, 1992).

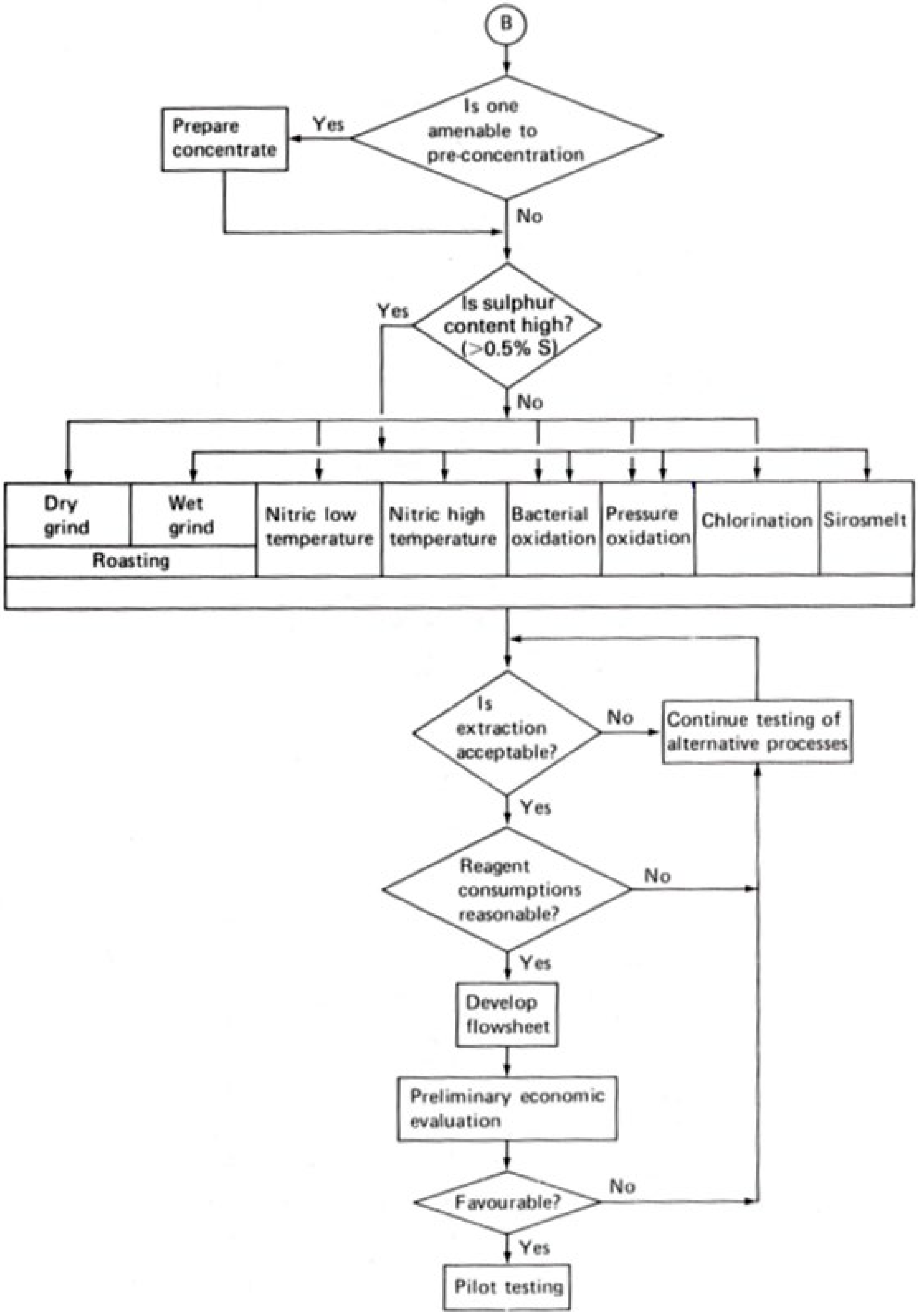


**FIG 5–3** – Refractory gold ores (after Marsden and House, 1992).

## Test work approach

- For representative sample and each ore type
  - Mineralogy
  - Head assay including Au, Ag, Cu, Pb, Zn, Ni, Sb, Cd, Fe, S, As, C, Te, Hg, P, Mn, MgO, $SiO_2$
    - Presence of cyanicides
    - Assay potential problems: coarse or 'spotty' gold – 'screen fire assay'
  - If refractory or partially refractory, diagnostic leach tests
    - Free gold, silica (gangue) hosted, pyrite hosted, arsenopyrite hosted, carbonate hosted
  - Moisture
  - Bulk density

- Understand mineralogy and/or the diagnostic leach results: implications for testing and flow sheet
- Pre-concentration: size fraction-assays by crush size
  - If there is potential, examine classification, gravity, X-ray sorting, optical sorting, gravity, optical sorting
- Determine comminution parameters (CWi, Ai, UCS, DWi, a, b, BBMWi, BRMWi)
- Materials handling characteristics including slurry agitation/solids re-suspension testing
- Slurry rheology
- Gravity gold potential: Heavy Liquid Separation, jigging/tabling, Nelson/Falcon
  - Gravity concentrate
    - Direct smelt
    - Intensive leaching: cyanide solution strength, oxidant, temperature, residence time
- 'Free milling' gold ore: cyanide leaching
  - Low-grade – heap leaching, determine crush size, set-up columns (>150 mm diameter), duration, monitor temperature
  - Higher grades
    - Determine gravity gold potential
    - Cyanide leaching tests (bottle roll, agitated vessel), oxygen uptake rate, residence times, pH, cyanide concentration, cyanide addition rate compare to consumption, carbon adsorption parameters (Fleming k,n)
    - Presence of base metal minerals
      - Sulphides (increased cyanide consumption and high $CN_{wad}$)
        - Passivation with lead nitrate (pyrite)
        - Pre-aeration (pyrrhotite)
      - 'Oxides' (significant impact on cyanide consumption and very high $CN_{wad}$)
        - Need to be totally removed before leaching
        - Test work program to develop a suitable flow sheet
          - Gravity, flotation, leaching
- High silver ore: slow leaching requiring long leach time, possible requirement for a CCD circuit with Merrill Crowe precious metal recovery circuit
- Refractory gold ores
  - Sulphides (eg arsenopyrite, pyrite, pyrrhotite, stibnite – often with aurostibnite)
    - Grind determination
    - Confirm direct leaching
      - Passivation with lead nitrate (pyrite)
      - Pre-aeration (pyrrhotite)
    - Whole ore oxidation
      - Dry/wet milling
    - Flotation
      - Pyrite/arsenopyrite/stibnite concentrates
        - Sighter tests, bulk flotation, differential flotation, effect of oxidation, rougher concentrate regrind, number of cleaning stages, reagent suites, optimisation, kinetic, variability, Locked Cycle Tests
      - Regrind/leaching
      - If not sufficiently successful, conduct oxidation studies *viz* ferric leach [e.g. Biox™, Albion process – both lock up arsenic] autoclave [Pressure Oxidation, POX], roasting
  - Carbon/montmorillonitic clay: 'preg-robbing'

- Presence of clays: rheology (for CIP/CIL greater interstage screen area)
  - Use of sodium hydroxide instead of lime
  - Viscosity modifiers
  - Lower per cent solids; CIL/CIP not suitable; use of carbon adsorption columns?
  - De-sliming
    - Track gold losses; decide upon what would be acceptable
- Water quality: if saline/hypersaline, test selected flow sheet using site water, titration curve – lime consumption versus pH (Mg buffering)
- Products: full assay suite including Au, Ag, Cu, Pb, Zn, Fe, S, Te, As, Hg, Sb
- Tailings
  - Dewatering properties
    - Thickening: conventional, paste: flocculent type and addition rate, unit settling rate ($t/m^2h$), underflow per cent solids, overflow clarity
    - Filtration (dry stacking): cake moisture, thickness, cycle time
  - Detoxification studies for thickener underflow
  - Samples to be sent for tailings geotechnical and geochemical studies supervised by specialist consultants

# APPENDIX 6

# TESTING IRON ORES

## Preface

The test work approach is dependent primarily on the iron mineral which is dictated by the deposit type. Iron ores are considered bulk commodities and minimal processing is preferred. Generally, for hematite ores, a minimum product of 62 per cent Fe is targeted and in the case of magnetite ores, 66 per cent Fe is a common target.

Hematite ores are generally quite rich (>58 per cent Fe) and typically removal of the fine size fractions (where the impurities tend to reside) is all of the processing that is required.

On the other hand, magnetite ores have lower grades (circa 30 per cent Fe) and are often quite competent, requiring milling to moderately fine sizes to recover the magnetite.

Occasionally other iron minerals are mined (eg limonite, goethite, siderites etc) and generally require upgrading.

## Test work approach

- Samples
  - Like other commodities, products are tested by prospective buyers however the volumes are naturally significantly larger, typically minimum parcel range of 1 to 10 t
  - Subsequently, test work samples often need to be very large (tonnes rather than kilograms), particularly to support Pre-Feasibility and Feasibility Studies; sample collection is a dedicated exercise, for softer ores, often employing Bauer rigs which can extract cores with diameters in excess of 1 m
  - Ore types as well as samples based on the Mine Schedule need to be taken
  - Later Study stages of separation test work are pilot plant scale and will require substantial quantities of sample
- Hematitic ores including itabirites (hematite, martite, limonite, goethite, mag-hematite)
  - For representative sample and each ore type
    - Mineralogy
    - Head assay including Fe, V, Mn, Cr, Ti, $SiO_2$, P, S, $Al_2O_3$, K, Ca, Na
    - Bulk density, porosity
    - Moisture
    - Crushing parameters (CWi, Ai, UCS)
    - If required – grinding parameters (DWi, a, b, BBMWi, BRMWi) and grind size determination
    - Materials handling characteristics
  - Understand mineralogy and fragmentation properties: implications for testing and flow sheet
    - Proportion of lump and fines (sinter and pellet feed)
    - Wet or dry processing
    - Crush size(s)
    - Scrubbing
    - Coarse upgrading: screening, gravity: HLS at the Scoping Study stage, jigs and DMS at larger scales; by size fraction
    - Fines upgrading: classification (including up-current), gravity: HLS at the Scoping Study stage, spirals at larger scales (by size fraction), magnetic separation (WHIMS)
    - Flotation: grind establishment, de-sliming, collector type and quantity, number of cleaning stages, silica/phosphate removal, iron losses, kinetic, variability, Locked Cycle Tests

    - Dewatering: thickening, filtration, TML
    - Product
        - Size range
        - Moisture
        - Full assay including Fe, V, Mn, Cr, Ti, $SiO_2$, P, S, $Al_2O_3$, K, Ca, Na
        - Loss on Ignition (LOI)
        - Other properties such as degradation studies, Decrepitation Index (DI), Tumble Index, sintering properties (fines)
- Magnetic ores including taconites (magnetite)
    - For representative sample and each ore type
        - Mineralogy
        - Head assay including Fe, $Fe_{mag}$, V, Mn, Cr, Ti, $SiO_2$, P, S, $Al_2O_3$, K, Ca, Na
        - Bulk density, porosity
        - Moisture
        - Comminution parameters (CWi, Ai, UCS, DWi, a, b, BBMWi, BRMWi) and grind size determination
            - Feed
            - Intermediate concentrates
        - Materials handling characteristics
        - Pre-concentration: dry magnetic separation at a coarse size
    - Understand mineralogy: implications for testing and flow sheet
        - Davis Tube: crush/grind size
        - Magnetic separation: LIMS, dry/wet, number of stages, grind size for each magnetic separation stage
        - Size fraction by size fraction assays: understand location of impurities
            - Remove by classification
                - Hydrocyclones
                - Elutriation
        - Flotation: grind establishment, de-sliming, collector type and quantity, silica/phosphate removal, iron losses
        - Selective flocculation (silica removal, taconite ores)
        - Dewatering
            - Concentrates
                - Thickening: flocculant type and addition rate, rheology, upflow rate, unit settling rate ($t/m^2h$), underflow per cent solids, overflow clarity
                - Filtration: cake moisture, thickness, cycle time, washing (high chloride levels)
                - Transportable Moisture Limit
            - Tailings
                - Thickening: conventional, paste: flocculant type and addition rate, rheology, upflow rate, unit settling rate ($t/m^2h$), underflow per cent solids, overflow clarity
                - Filtration (dry stacking): cake moisture, thickness, cycle time
                - Samples to be sent for tailings geotechnical and geochemical studies supervised by specialist consultants
        - Product
            - Size range
            - Moisture
            - Full assay including Fe, FeO, V, Mn, Cr, Ti, $SiO_2$, P, S, $Al_2O_3$, K, Ca, Na

        - Loss on Ignition (LOI)
        - Sintering and pelletising properties
- Mixed ores (mag-hematite, martite, limonite, goethite, hematite, magnetite): as above
    - Require a number of techniques to separate the iron minerals from the gangue and often to separate products
    - Gravity step to recover coarse non-magnetics
    - Grinding and magnetic separation to recover magnetics – multiple stages
        - LIMS (magnetite)
        - WHIMS (hematite/martite)

# APPENDIX 7

# TESTING GRAPHITIC ORES

## Preface

It goes without saying the test work approach is strongly dependent upon the proposed products and market.

This guideline is based on the mineral processing aspects of graphite production which is generally for the anode and lithium-ion battery market. The test work approach for the downstream processes required to produce suitable product for the battery market are not only specialised but often proprietary and include spheroidising, purification and coating, and are typically available from dedicated test work facilities.

In the current market, flake graphite is keenly sought, and the flake size and purity affect the received price. While these two aspects principally drive the approach of the test work program, mineralogy continues to play an overarching role.

## Reference

Jara, A.D, Betemariam, A., Woldetinsae, G. and Kim, J.Y., 2019. *Purification, application and current market trend of natural graphite: A review,* International Journal of Mining Science and Technology, 29, pp. 671–689.

## Test work approach

- For representative sample and each ore type
  - Mineralogy
  - Flake size determination: MLA often used
    - Jumbo (+300 µm), Large (-300 µm/+180 µm), Medium (-180 µm/+150 µm) Small (-150 µm/+74 µm) and Fine (-74 µm)
  - Head assay including C [Total Carbon ($T_c$), Graphitic Carbon ($C_g$), Organic Carbon ($C_{org}$)], Fe, S, As, Cl, F, Hg, P, Mn, V, Mg, K, Na, $SiO_2$
    - Need to distinguish between graphitic carbon, organic carbon and carbon as carbonates ($T_c$-$C_{org}$-$C_g$). Be careful as to the assay methodology, as different laboratories can use different methods for determination of graphitic carbon
  - Moisture
  - Bulk density
- Understand the mineralogy: implications for testing and flow sheet
- Pre-concentration: size fraction-assays by crush
  - eg if potential examine classification, gravity, optical sorting
- Determine comminution parameters (CWi, Ai, UCS, DWi, a, b, BBMWi, BRMWi)
  - Drum scrubbing/attrition for weathered/low hardness feed
  - Preference for staged crushing and rod mills
  - Determine optimum separation feed size
- Materials handling characteristics
  - Flotation: sighter, per cent solids, flotation time, reagent suite (kerosene, diesel, coal collectors, frothers, modifiers (eg lime for pyrite depression), depressants (eg for sodium silicate for silica depression – best for last stages of cleaning), per cent solids, flotation time, number of cleaning stages, rougher and other selected cleaner concentrate 'regrinding' (attritioning – equipment [attritor, bead mill] and conditions [energy input, regrind feed density, time, bead charge, SG, shape and size], optimisation, kinetic, variability testing, Locked Cycle Tests Target concentrate grade (at maximum flake size): better than 92 per cent $T_c$, preferably at least 94–95 per cent $T_{c.}$ Can vary for different size fractions, marketing feedback is very important
- Efficiency of slurry wet screening and product dry screening

- Froth factors for pump calculations
- Water quality: if saline, test selected flow sheet using site water
- Product
  - Sizing: screening: Jumbo (+300 µm), Large (-300 µm/+180 µm), Medium (-180 µm/ +150 µm) Small (-150 µm/+74 µm) and Fine (-74 µm)
  - Full assay of each sized product including C, $SiO_2$, Cu, Pb, Zn, Fe, S, As, Hg, Mg, K, Na, V
  - Consolidated and unconsolidated bulk density for different size fractions
  - Dewatering properties
    - Thickening: flocculant type and addition rate, rheology, upflow rate, unit settling rate ($t/m^2h$), underflow per cent solids, overflow clarity
    - Filtration: Some plants do not thicken the final concentrate due to excessive graphite loss to the thickener overflow and filter unthickened feed. Test filtration for thickened and unthickened feed. Difficult to satisfactorily filter to low moisture content. Drying studies: Materials handling properties for successfully feed a dryer. Thermal requirements for selecting and scaling equipment. Very low moisture content required. Smaller plants typically use indirect drying
- Tailings
  - Thickening: conventional, paste: flocculent type and addition rate, rheology, upflow rate, unit settling rate ($t/m^2h$), underflow per cent solids, overflow clarity
  - Filtration (dry stacking): cake moisture, thickness, cycle time
  - Samples to be sent for tailings geotechnical and geochemical studies supervised by specialist consultants

# APPENDIX 8

# TESTING LITHIUM BEARING ORES

## Preface

The test work approach outlined in this section is based on hard rock lithium sources, such as spodumene and lepodilite. Like many commodities, there are two stages, namely a mineral processing stage and the downstream lithium extraction process.

Spodumene occurs in coarse grained pegmatites and is often associated with other minerals, such as tantalite, which is recovered by gravity techniques (spirals). Spodumene often occurs as both coarse and fine grained which influences the flow sheet development.

Test work required to establish a flow sheet for the recovery of lithium salts from spodumene and salar (eg soluble lithium chloride) sources is not presented, since they are quite specialised and test work expertise is restricted to a few test work facilities. Once the lithium has been extracted from the spodumene (through pyrometallurgical and hydrometallurgical means), the solution purification process shows some similarities to that employed for 'salar' lithium (magnesium contents are substantially higher) where a number of precipitation processes and liquid/solid separations are used.

The final product from these hydrometallurgical processes is either lithium hydroxide or lithium carbonate for the lithium-ion battery market although the bulk of spodumene production is used in the glass market [100–300 microns] and the ceramics market [20–100 microns].

## Test work approach

- For representative sample and each ore type
    - Mineralogy
    - Head assay including Li, Mg, $SiO_2$, Fe, S, P, Ca, C, F, Cl, $Al_2O_3$, K, Na, Ta, Sn
    - Moisture
    - Bulk density
- Understand mineralogy: implications for testing and flow sheet
- Pre-concentration: size fraction-assays for a few crush sizes; if potential, consider ore sorting (optical), gravity, classification

## Coarse spodumene

Typically recovered by classification and gravity:

- Comminution properties: Abrasion index, UCS, CWi, HPGR Index
- Materials handling characteristics
- Crush size determination: size-assay at a number of crush sizes
- Classification: size-assays
    - Remove minerals like mica before gravity
    - Up current/reflux classifier
- Gravity: Heavy Liquid Separation at different size fractions; larger scale Dense Media Separation
    - Reject gangue – quartz, feldspar, some mica
    - Product concentrate grade
        - Chemical grade lithium (various chemicals including metal): 4–6 per cent $Li_2O$ (no firm ranges on impurities, *viz* feldspar, iron and mica)
        - Technical grade lithium (glass and ceramics): 4.1 per cent to 7.5 per cent $Li_2O$ *cf* 6 per cent $Li_2O$ (SC6.0)
            - Low impurity content required

    - Iron: 0.06 per cent to 0.17 per cent $Fe_2O_3$
    - Mica: <1 per cent
    - Alkaline ($K_2O$+$Na_2O$): <1 per cent
- Dewatering: product coarse enough to naturally drain to a low moisture content
- Tailings
  - Potential for fine spodumene recovery
- Suitable for dry stacking
- Product
  - Full chemical assay, including Li, Mg, $SiO_2$, Fe, S, P, Ca, C, F, Cl, $Al_2O_3$, K, Na, Ta, Sn
  - Sizing

## Fine spodumene

Typically recovered by flotation and gravity:

- Comminution properties: Abrasion index, UCS, CWi, HPGR Index, DWi, a, b, BBMWi, BRMWi
- Materials handling characteristics
- Grinding size determination: size-assay at a number of grind sizes; can be quite coarse (eg $P_{100}$ = 300 microns)
- Classification: size-assays
  - Remove minerals like mica before flotation (Up current/reflux classifier)
- Gravity: Heavy Liquid Separation at different size fractions; larger scale spirals
- Flotation: Conditioning requirements (~70 per cent solids) eg pre-treatment ('cleaning' agents) for weathered ores, de-slime (10–20 microns), per cent solids (15–25 per cent), pH, reagents (modifiers [NaOH, $Na_2CO_3$], depressants [$CaCl_2$], collector type [fatty acid (oleic acid) amines]), conditioning and flotation residence times, number of cleaning stages
  - Reject gangue – quartz, feldspar, carbonates (acid consuming), some mica
  - Product concentrate grades: target at least 5.5 per cent $Li_2O$ or better (eg 6 per cent $Li_2O$)
  - Low impurity content
    - Iron: 0.06 per cent to 0.17 per cent $Fe_2O_3$
    - Mica: <2 per cent preferably 1 per cent
    - Others: feldspar, petalite
- Magnetic separation
  - Remove iron (including iron bearing micas eg biotite)
  - LIMS and WHIMS: magnetic intensity, number of passes, drum speed
    - After de-sliming
    - Flotation concentrate
- Dewatering
  - Concentrates
    - Thickening: flocculant type and addition rate, rheology, upflow rate, unit settling rate ($t/m^2h$), underflow per cent solids, overflow clarity
    - Filtration: cake moisture, thickness, cycle time, washing (high chloride levels)
    - Transportable Moisture Limit
  - Tailings
    - Thickening: conventional, paste: flocculant type and addition rate, rheology, upflow rate, unit settling rate ($t/m^2h$), underflow per cent solids, overflow clarity
    - Filtration (dry stacking): cake moisture, thickness, cycle time
    - Samples to be sent for tailings geotechnical and geochemical studies supervised by specialist consultants

- Product
  - Full chemical assay, including Li, Mg, $SiO_2$, Fe, S, P, Ca, C, F, Cl, $Al_2O_3$, K, Na, Ta
  - Sizing
  - Moisture

## By-product (eg Tantalum)

- Usually a 'tailings' product from gravity separation
  - Mineralogy
  - Head assay including Ta, Li, Mg, $SiO_2$, Fe, S, Ca, $Al_2O_3$, K, Na
- Understand mineralogy: implications for testing and flow sheet
- Grinding size determination: may requires further grinding: size-assay at a number of grind sizes
- Classification: size-assays – may be able to discard some size fractions
- Gravity: Heavy Liquid Separation at different size fractions
  - Number of stages
  - Larger scale spirals
- Magnetic separation: may be required to remove iron/iron bearing minerals
- Dewatering
  - Concentrates: thickening, filtration, Transportable Moisture Limit
  - Tailings: thickening, paste, possibly filtration (dry stacking)
- Product
  - Full chemical assay, including Ta, Li, Mg, $SiO_2$, Fe, S, P, F, Ca, C, F, Cl, $Al_2O_3$, K, Na
  - Sizing
  - Moisture
  - Specific Gravity

# APPENDIX 9

# TESTING MINERAL SAND ORES

## Preface

The test work approach outlined in this section is based on alluvial sources rather than hard rock, which often require comminution. Alluvial deposits, typically current or fossil beach and river accumulates, are generally relatively straightforward to mine and process. Like all industrial commodities, product specifications can be demanding, with premiums paid for high quality products, and may influence the test work program.

Mineral sand products, such as ilmenite, can be upgraded using processes like the Becher process to remove lattice bound iron by atmospheric oxidation to produce the higher value product 'synthetic' rutile.

## Reference


Boschoff, L.I. and Gracie, S., 2007. *A Metallurgical Evaluation of a Heavy Mineral Sand Deposit based on Stratigraphic Unit Classifications*, In Proceedings of The 6th International Heavy Minerals Conference 'Back to Basics', The Southern African Institute of Mining and Metallurgy, pp. 139–150.

Macdonald, E.H., 1973. *Sections III, IV, V, VI and VII*, *Manual of Beach Mining Practice – Exploration and Evaluation*, Depart of Foreign Affairs, Australian Government Publishing Service, Canberra, pp.22–73.


## Test work approach

### *Overview*

The test work for ores from alluvial source is based on gravity separation to remove the bulk of the silica followed by magnetic separation to produce a range of intermediate products based on the magnetic response. Subsequent separation uses differences in electrical conductivity properties.

- For representative sample and each ore type
  - Mineralogy
  - Head assay including Ti, Fe, Mg, Zr, Hf, $SiO_2$, Cr, P, Ce, La, Ca, Sn, S, F, Cl, $Al_2O_3$, K, Na
  - Moisture
  - Bulk density
- Understand mineralogy: implications for testing and flow sheet
  - Note amount of slimes (eg clays) present
  - Not all mineral particles are fully liberated and may contain inclusions
  - Mineral surfaces may have coatings, and require treatment (eg attritioning or acid cleaning of zircon rich streams prior to electrostatic separation)
- Materials handling characteristics
- Scrubbing – clay bearing ores
  - De-sliming
  - Impact on mineral sands losses
- Classification: discard material above 2 mm; size-assays – some size fractions may be enriched in mineral sands
- Gravity separation: Heavy Liquid; larger scale may examine spirals, jigs
- Magnetic separation (wet): range of magnetic intensities (0.05 to 1.5 T), number of stages, drum speed, gap size, configuration
  - Strongly magnetic: Magnetite
  - Moderately magnetic: Ilmenite
  - Weakly magnetic: Monazite
  - Non-magnetic: Rutile, zircon

- Electrostatic (high tension) separation (both material and environment need to be dry): two streams – weakly and non-magnetic: feed rate, voltage, electrode configuration, number of stages
    - Effective particle size range (80 µm to 3 mm)
    - Conductors: Rutile, ilmenite, chromite
    - Non-conducting: Zircon, monazite, xenotime, magnetite (high iron ilmenite)
- Products
    - Full chemical assay for each product such as including Ti, Fe, Mg, Zr, Hf, $SiO_2$, Cr, P, Ce, La, Ca, S, P, F, Cl, $Al_2O_3$, K, Na
    - Sizing
- Tailings
    - Typically returned to mining area for deposition
    - De-slime stream
        - Test potential blending ratios with gravity tailings and suitability for mining area deposition
        - Otherwise, conventional dewatering testing before blending thickened product with gravity tailings for mining area deposition, *viz*
            - Thickening: conventional, paste: flocculant type and addition rate, rheology, upflow rate, unit settling rate ($t/m^2h$), underflow per cent solids, overflow clarity

# APPENDIX 10

# TESTING URANIUM ORES

## Preface

As for all ores to be tested, the approach is highly dependent on mineralogy and gangue type as well as association however it is primarily based on hydrometallurgy. Needless to say, characterising comminution properties is generally a pre-requisite (exceptions may include heap leaching and *in situ* leaching [ISL]). It is noted that with favourable mineralogy, ores can be amenable to pre-concentration such as X-ray ore sorting and flotation (eg removal of carbonate gangue).

The extent of the test work program depends upon a number of factors, including the purpose of the test work, the study stage, availability of samples, the mineralogy, the size of the deposit and the amount of funding. Preliminary test work is typically conducted for Scoping Study, with more detailed test work required for a Pre-Feasibility Study and particularly a Feasibility study.

This Appendix provides some guidelines mainly for preliminary test work. Note that *In situ* Leaching projects rarely undergo benchscale test work; once the likely acid consumption properties are known (ie acid or akaline leaching based on gangue content), a trial leach is typically conducted to establish the metallurgical metrics.

To assist in the design of suitable test work program, it is worth reviewing the referenced articles.

## References


Abzalov, M.Z. and Allaboun, H.,2015. Bulk Sample Testing for Metallurgical Characterisation of Surficial Uranium Mineralisation at the Central Jordan Uranium Project, Transactions of the Institutions of Mining and Metallurgy, Section B, Applied Earth Science, 124:2, 129–134.

Brough, C.P, Bowell, R.J., Grogan, J.M., Randabel, J. and Woolrich, P., 2013. Letlhakane project: case study in complex uranium mineralogy and its geometallurgical implications, Transactions of the Institutions of Mining and Metallurgy, Section A, Mining Technology, 122:1, 53–61.

Lanshiedel, K. and Schröer, K., 1987. Test Procedures for the Metallurgical Evaluation of Uranium Ores, In: Proceedings of a Technical Committee Meeting, Vienna, 25–28 November, 1985, International Atomic Energy Agency, Vienna, Austria, pp.101–111.

Manual on Laboratory Testing for Uranium Ore Processing, 1990. Technical Reports Series No. 313, International Atomic Energy Agency, Vienna, Austria.

McCabe, W.L., and Thiele, E.W., 1925. *Graphical Design Of Fractionating Columns.* Industrial and Engineering Chemistry, 17, pp. 605–611.

Significance of Mineralogy in the Development of Flow sheets for Processing of Uranium Ores, 1980. Technical Reports Series No. 196, International Atomic Energy Agency, Vienna, Austria.

Uranium Extraction Technology, Technical Reports Series No. 359, 1993, International Atomic Energy Agency, Vienna, Austria.


## Test work approach

Uranium test work needs to satisfactorily characterise the handling and processing behaviour of the ore for the six key processing stages, namely:

- Size reduction: crushing and grinding
- Leaching: lixivant (acid [sulphuric] or alkaline [carbonate]), oxidant, temperature and pressure
- Solid-liquid separation and washing
- Purification and concentration
- Precipitation and solid-liquid separation
- Drying or calcining the product

A generic processing flow sheet is shown in Figure 10.1.

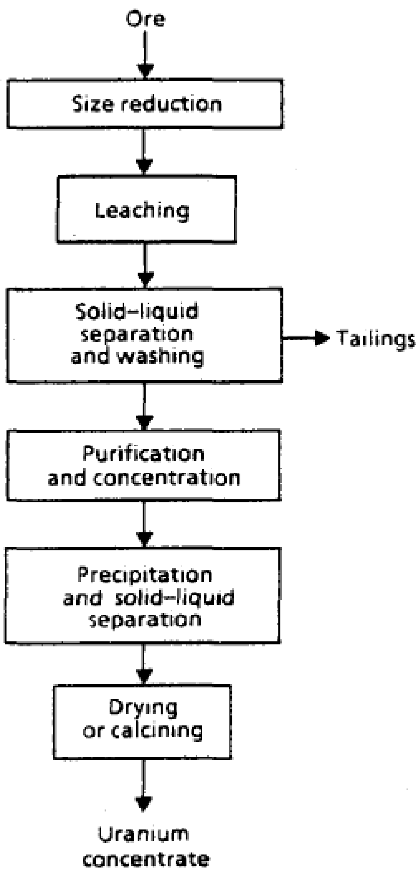


**FIG 10.1** – Generic uranium processing flow sheet (after IAEA, 1990).

The most common 'front end' flow sheets employed in practice are:

- Acid/alkaline leaching in mechanically agitated, purification and concentration by solvent extraction (acid) or ion exchange (alkaline)
- Highly refractory minerals (eg brannerite): acid leaching at pressure and temperature (autoclaves)
- Acid/alkaline heap leaching, purification and concentration by solvent extraction (acid) or ion exchange (alkaline)
- Acid/alkaline *in situ* leaching (ISL), purification and concentration by ion exchange (occasionally solvent extraction for acidic solutions)

They share a common 'backend' flow sheet, namely precipitation, solid-liquid separation and drying/calcining of the uranium product ($U_3O_8$).

The typical flow sheets and the various processing techniques are discussed in more detail in Uranium Extraction Technology (1993) which provides insight into the likely range of test work requirements.

## Test work approach

- For representative sample and each ore type
  - Mineralogy (see comments below)
  - Head assay including the following elements/species: U [$U_3O_8$], $CO_3^{2-}$, $SO_4^{2-}$, $S^{2-}$, $Mo^{2+}$, $V_2O_5$, $PO_4^{2-}$, $SiO_2$, Cu, $Fe^{2+}$ and $Fe^{3+}$
  - Moisture
  - Bulk density, porosity
- Understand mineralogy: implications for testing and flow sheet
- Pre-concentration: size fraction-assays for a few crush sizes; if potential, consider ore sorting radiometric, XRD, optical, gravity, classification

- Comminution parameters (CWi, Ai, UCS, DWi, a, b, BBMWi, BRMWi) and grind size determination
- Materials handling characteristics

### *Mineralogical studies*

Once samples have been selected, typically based on ore type and LOM, and head assays conducted, mineralogical analysis is strongly recommended.

Most importantly, mineralogy will inform on the nature of the uranium mineralisation: some uranium minerals (eg uraninite and coffinite) are readily leached, occasionally without the requirement of an oxidant, while others are more refractory (eg brannerite and davidite) and require very aggressive acidic leaching conditions. In addition, mineralogy will provide an insight into the size reduction requirements for satisfactory leaching, noting that substantial liberation is not required for leaching to be effective.

It will also identify the lixiviant; when more than 10 per cent carbonate mineralisation is present, the alkaline leaching method is preferred based on economics, however it is not unusual to test both acidic and alkaline leaching routes, carefully monitoring the lixiviant consumption and uranium recovery over the proposed leaching period.

Preliminary testing typically establishes the requirements for the first three key processing stages, namely size reduction, leaching and solid-liquid requirements. If high uranium recoveries are readily obtained, then some purification and concentration test work may be considered.

As with all test work program, the potential for pre-concentration needs to be determined, typically by a size-assay program at various crush sizes.

### *Leaching studies*

Like many leaching programs, the key parameters are explored as shown in Table 10.1. For acidic leaching, depending upon the uranium mineralogy, feed grade and leach recovery, less than 200 kg/t acid consumption is considered acceptable.

**TABLE 10.1**

Key preliminary test work parameters (after Lanshiedel and Schröer, 1987).

| Test Work Parameter | Units | Acid Leaching | Alkaline Leaching |
|---|---|---|---|
| Temperature | °C | 40-60 | 80-120 |
| Retention | h | 4-16 h | 24-96 |
| Consumption | kg/t | 40-200 | 30 (Na as soda ash) |
| Recovery | % | 95-97 | 85-90 |
| Pressure | kPa | 100-400 | 200-800 |
| Grind size (minimum) | µm | 500 | 63 |

The next test work phase is solid-liquid separation, which in the case of an acid leaching system, has been historically accomplished with typically six stages of counter-current decantation.

This is relatively straightforward and identical to test work used to support the sizing of thickeners for tailings and concentrates, where settling rates are determined as a function of flocculent type and addition rates.

Where poor settling characteristics are encountered, Resin-In-Pulp (RIP) has been used, after the coarser size fractions have been removed (minimise attrition of the resin).

In this situation, the optimum cut-size needs to be established (‘fine’ as possible) prior to embarking upon RIP studies.

In the case of alkaline leaching systems, filtration is typically required to satisfactorily separate solids from the liquid, noting that filter cake washing would be required to minimise uranium losses.

## *Purification studies*

Three methods are available, namely Ion Exchange (IX), RIP and Solvent Extraction (SX).

### Ion exchange

This method can be applied to both acidic and alkaline uranium bearing solutions, based on resins with good adsorption properties over the desired pH range.

A number of resins (0.25–1 L) in columns are tested for adsorption and elution properties, with optimised flow rate, loading capacity and 'breakthrough' time (when the solution concentration has fallen to 5 per cent of the initial concentration) investigated for adsorption, and in the case of elution, the type of eluant (eg NaCl, $NH_3(NO_3)_2$, 10 per cent $H_2SO_4/(NH_4)_2SO_4$,) and concentration need to be determined (refer to Table 10.2).

**TABLE 10.2**

Key preliminary ion exchange test work parameters (after Lanshiedel and Schröer, 1987).

| Test Work Parameter | Units | Adsorption | Elution |
|---|---|---|---|
| Solution Flow | Bed volumes/h | 10-30 | 10 |
| Loading Capacity | g/L | 20-60 | - |
| Stripping Capacity (after 10 BVs) | % | - | 95 |

Note that in the case of the alkaline leaching system, direct precipitation is possible, however does not appear to have been applied commercially. Nonetheless, it may warrant further investigation and testing to avoid the purification step.

### Resin-in-pulp

This test procedure has similarities with Carbon-In-Pulp/Carbon-In-Leach for cyanide leach solutions from gold bearing ores. As noted earlier, it is important that the coarser size fractions have been removed before testing uranium bearing solution with RIP. Columns or multistage agitated tanks (0.2–1 L) are used with similar measures to Ion Exchange (refer to Table 10.2).

After the resin has been rinsed, the elution procedure is the same as that for Ion Exchange.

### Solvent extraction

This is the most common method used for the extraction of uranium from acidic solutions and for detailed testing, requires several litres of solution.

'Shake-out' tests are used to select a suitable solvent dissolved in kerosene (eg amines, tributyl phosphate – organic phase) where the uranium bearing solution is shaken vigorously with the selected solvent for a minute or so in a separatory funnel. The subsequent separation is closely observed for speed of phase separation, interfacial scum, insoluble compounds.

The next step, using the selected solvent, along the addition of a modifier such as isodecanole, is to establish the extraction equilibrium curve by testing different ratios of the organic phase and the uranium solution (aqueous phase). The number of extractions is subsequently determined using the McCabe-Thiele method.

Stripping of the loaded or pregnant organic phase is investigated by the same method employing solutions such as ammonium sulphate. Key stripping parameters are pH and ion concentration.

For the final design, a pilot plant is often undertaken with multiple stages as determined from bench scale testing. At least 250 to 1000 L would be required.

A full assay of the 'purified' solution is required, mainly to identify other metallic species that may be present in solution. The presence of these species may influence the selection of the precipitating agent that would be used to produce the final product.

### *Precipitation studies*

This test work is relatively straightforward and can be conducted in a stirred beaker. A precipitating agent is added to the uranium bearing solution.

The parameters that are investigated include temperature, retention time, precipitating agent and final pH, as well as the consumption rate of the precipitating agent.

The type of precipitating agent depends on the solution chemistry; for acidic solutions hydrogen peroxide and ammonia are commonly used, while alkaline solutions employ magnesium or sodium hydroxide.

When other metals are present in solution and co-precipitation is likely, the use of hydrogen peroxide is necessary. In the case of alkaline solutions, acidification is required.

While settling properties are determined for the final product, filtration properties are typically not determined due to the fineness of the precipitated product. Specialised equipment like tube pressures can be used, however in practice, the thickened final product is commonly dried using indirect heat exchangers such as an internally heated screw conveyor.

The need for test work to support the selection and sizing of these pieces of equipment would be undertaken by approaching the equipment vendor.

After washing the final product precipitate, a full assay is conducted and compared to the typical product specifications.

### *Dewatering*

- Product
  - Thickening: conventional, paste: flocculant type and addition rate, rheology, upflow rate, unit settling rate ($t/m^2h$), underflow per cent solids, overflow clarity
  - Filtration studies are rarely undertaken due to the very fine nature of the precipitated product. While specialised batch pressure filters can be used, in practice, the thickened product is often dried through indirect means, such as internally heated screw conveyors
- Tailings
  - Thickening: conventional, paste: flocculant type and addition rate, rheology, upflow rate, unit settling rate ($t/m^2h$), underflow per cent solids, overflow clarity
  - Filtration (dry stacking): cake moisture, thickness, cycle time
  - Samples to be sent for tailings geotechnical and geochemical studies supervised by specialist consultants

# Process modelling and improvement

# Multi-component Mine-to-Mill optimisation applied to iron and gold ores

*B Bonfils[1], W Valery[2], A Jankovic[3], K Duffy[4], E Tabosa[5] and P Holtham[6]*

1. Senior Process Engineer, Hatch, Brisbane, Qld. Email: benjamin.bonfils@hatch.com
2. Global Director – Consulting and Technology, Hatch, Brisbane, Qld.
   Email: walter.valery@hatch.com
3. Principal Consultant, Hatch, Brisbane, Qld. Email: alex.jankovic@hatch.com
4. Senior Process Engineer, Hatch, Brisbane, Qld. Email: kristy.duffy@hatch.com
5. Senior Process Engineer, Hatch, Brisbane, Qld. Email: erico.tabosa@hatch.com
6. Senior Consultant, Hatch, Brisbane, Qld. Email: peter.holtham@hatch.com

## ABSTRACT

The benefits of Mine-to-Mill optimisation have been understood by the industry for many years. If well executed, with a structured methodology, the overall operation throughput (mine and plant) can be maximised using the existing equipment, while minimising the unit operating costs. This has been accomplished by integrating blast fragmentation and comminution modelling, simulation and analysis. To take the process a step further and optimise the process from mine to concentrator (in terms of recovery, concentrate grade and throughput), it is necessary to track minerals or elements through the process using multi-component modelling.

In the traditional Mine-to-Mill approach, blasting and *JKSimMet* models are used to predict throughput and size distributions for comminution and classification. However, these models cannot track minerals or elements that are used in the recovery models. To optimise the process from mine to concentrator, the processing flow sheet is created in *Limn* software and integrated with the *JKSimMet* models. This takes into account recovery, concentrate grade and plant throughput.

*Limn* is an add-on in Microsoft Excel software. *Limn* allows the user to duplicate the process flow sheet and specify size fractions and mineral components. Models for each process (eg classification, gravity, magnetic and flotation) are developed based on recovery-by-size data obtained from plant surveys. When a comminution stage is integrated into the recovery circuit, *JKSimMet* is used to develop component specific breakage rates which are then incorporated into the *Limn* model.

This paper describes the application of integrated *JKSimMet* and *Limn* simulations for Mine-to-Process optimisation of two mining operations:

- The first operation, where gold ore is treated by a gravity concentration process.
- The second operation, where iron ore is treated by magnetic separation and flotation processes.

For example, in the gold operation, integrated simulations allow evaluation of the impact of different potential locations of the flash flotation circuit on gold circulating load on a size-by-size basis.

## INTRODUCTION

The Hatch Mine-to-Process methodology takes the Mine-to-Mill approach a step further and integrates multi-component modelling of the comminution, classification and beneficiation stages such that concentrate production and concentrate quality can be modelled and simulated. This is illustrated in Figure 1. The simulation study is combined with historical data analysis, energy-based calculations, capacity calculations, industrial experience and benchmarking using an extensive database of operational data. These are used to develop integrated strategies from the mine to the plant. These strategies are used to maximise recovery and throughput, while minimising unit costs and ensuring all product quality specifications are met.

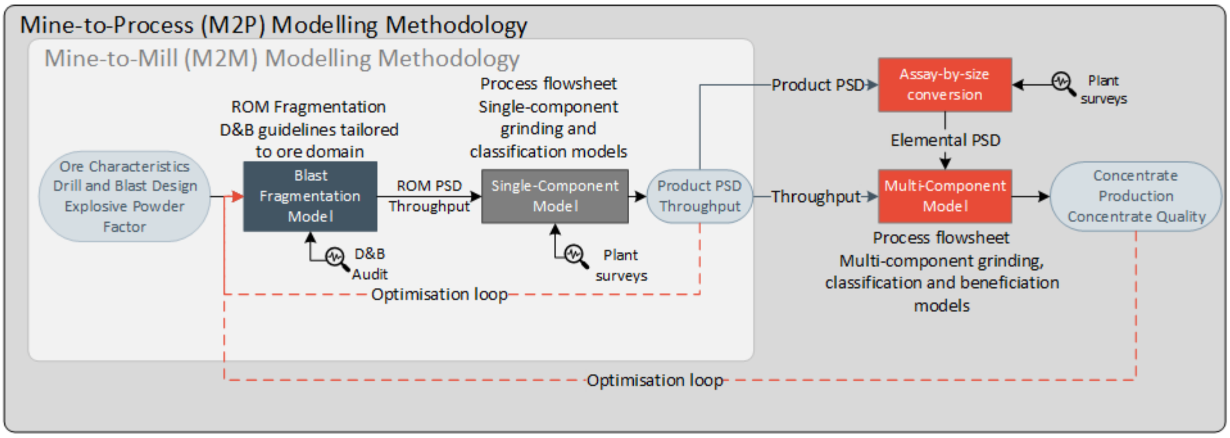


**FIG 1** – Flow sheet showing integrated multi-component Mine-to-Process modelling and simulation.

This paper describes the application of this integrated multi-component simulation approach to the Mine-to-Process optimisation of two operations:

- The first operation, where gold ore is treated using a gravity concentration process.
- The second operation, where iron ore is treated by magnetic separation and flotation processes.

In the gold operation, two components were tracked: gold and gangue. In the iron ore case there were four components: iron (Fe), iron oxide (FeO), phosphorous (P) and gangue.

## METHODOLOGY

Blast fragmentation modelling, simulation and analysis is used to optimise the blast designs and practices for the different ore types present in the deposit. These models demonstrate the impact of blasting on downstream comminution processes. The Hatch Blast Fragmentation model is a modified version of the two-component crushed-zone model, which has been validated at numerous sites around the world. The model accounts for the major parameters known to affect blasting performance including rock mass properties (such as structure and strength), blast design and explosive properties. The model is calibrated for each operation (using ore characterisation and blast audit data) and predicts the Run-of-Mine (ROM) particle size distribution (PSD) which forms the inputs to the comminution circuit models.

Comminution circuit models are calibrated using plant surveys, which are typically conducted while treating ore from the audited blasts. *JKSimMet* is used for comminution modelling and simulation. It incorporates empirical models of all the major process equipment such as crushers, mills and cyclones, and is widely used in the industry. The blast fragmentation and comminution circuit models are used together to maximise throughput whilst achieving the required final grind size. These models consider the different ore types and properties. However, it is also important to determine the optimum final grind size, which is completed using a trade-off study. This trade-off study typically compares the higher throughput and lower cost of a coarser grind size, versus improved recovery and concentrate grade in the downstream separation processes of a finer grind size.

To optimise the process from mine to concentrator (in terms of recovery, concentrate grade and throughput), it is necessary to track minerals or elements through the process. *JKSimMet* is suitable for predicting throughput and size distributions for comminution and classification; however, it cannot track different minerals or elements. *Limn*, which is an add-on for Microsoft Excel software, can be used for this purpose. It allows the user to complete multi-component modelling by duplicating the process flow sheet and specifying size fractions and mineral species (which are defined as components).

Valuable minerals typically behave very differently to gangue minerals in ball mill circuits which are closed circuit with cyclones, due to the density differential amongst different minerals. Therefore, it is essential to include these density effects in the *Limn* multi-component models. The ball mill and cyclone models are first fitted in *JKSimMet*, and the fitted parameters are then used to develop the multi-component models in *Limn*. Component grade-by-size data is obtained from balanced plant survey data. Multi-component models are then developed for each process (eg ball mill, cyclone, gravity separation, magnetic separation or flotation) and then combined into an overall process model. *Limn* then calculates stream head assays, total solids flow rates and water flow rates. Limn also calculates the flow rate of each component in each size fraction. This allows grades of each stream and recoveries to be calculated.

## CASE STUDY 1 – GOLD ORE

A Mine-to-Process optimisation project was completed at a gold mine. At the mine, the process plant was treating 1600 t/h of ore with an average head grade of around 1.2 g/t Au. The flow sheet is shown in Figure 2.

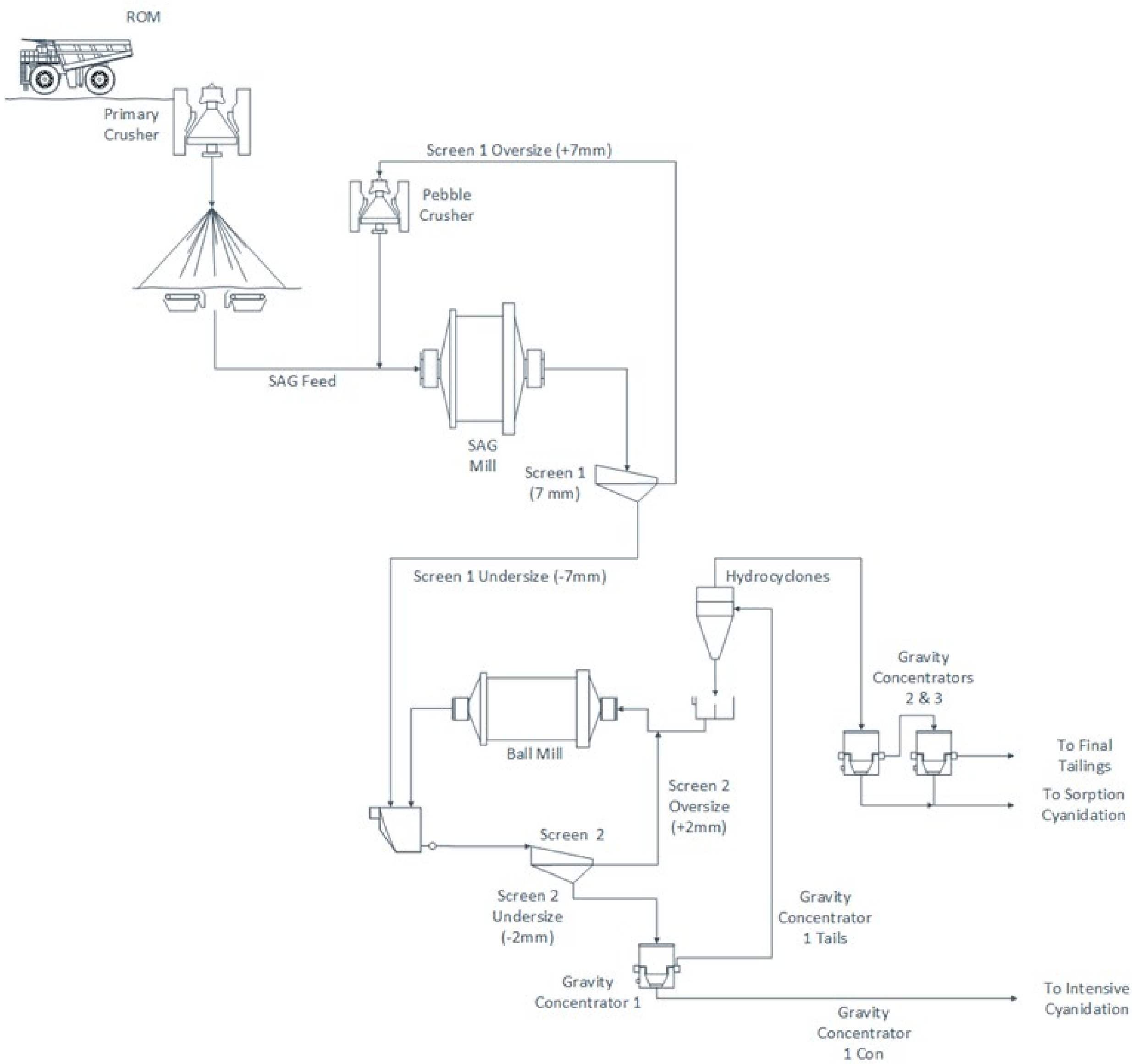


**FIG 2** – Simplified flow sheet of gold plant.

In the process flow sheet, ROM ore is crushed in gyratory crusher and then stockpiled. The crushed ore reports to a grinding circuit consisting of a SAG mill in closed circuit with a screen and pebble crusher, and a ball mill in closed circuit with a screen. The ground product reports to a primary gravity concentration circuit using Knelson centrifugal concentrators. Primary gravity tailings are pumped to a bank of cyclones. The cyclone underflow returns to the ball mill, whilst cyclone overflow is pumped to a secondary gravity concentration circuit which also contains Knelson concentrators. Secondary gravity tailings form the final plant tailings. Gold is recovered from the primary and secondary gravity concentrates by cyanidation processes.

All crushing, grinding, and gravity concentration circuits were surveyed. The surveyed samples were sized and assayed. The data was mass balanced for gangue and gold using *JKSimMet* and *Limn*. Gold assay-by-size data was only available for streams from the Screen 1 (SAG screen) undersize onwards.

Site-specific models, including crusher, SAG mill, ball mill, screen and cyclone models were developed by fitting the survey data in *JKSimMet*. The behaviour of gold in the ball mill circuit is of particular interest, as it is very different to the behaviour of gangue. This is due to the density and malleability of gold which affects breakage, classification and liberation characteristics (Banisi *et al*, 1991). Therefore, the ball mill breakage rates for gold and gangue were fitted separately based on the assay-by-size data, as shown in Figure 3. Gold grinds slower than other minerals (as noted previously by Laplante *et al*, 1991), with the breakage rates noticeably reducing for the coarsest fractions.

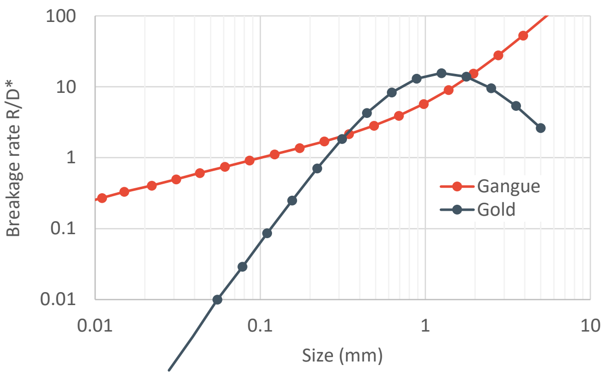


**FIG 3** – Fitted ball mill breakage rates for gold and gangue.

Figure 4 shows the modelled feed and product size distributions for gangue and gold. Figure 4 shows that the model fitted the experimental data well for both components. Hence, the model is considered suitable for multi-component simulations (gold and gangue) of the ball mill in closed circuit with the gravity concentrators and cyclones.

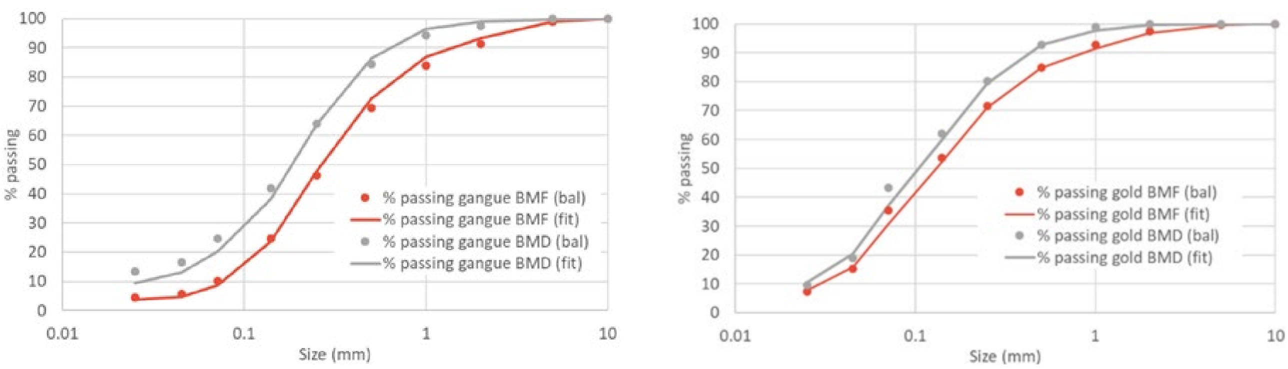


**FIG 4** – Feed and product size distributions for gangue (left) and gold (right).

For multi-component modelling, the circuit from Screen 1 undersize onwards was re-drawn in *Limn*. The flow sheet was configured to have 21 size fractions (which ranged from 10 mm to 10 µm) and the two components – gold and gangue. The fitted parameters from *JKSimMet* were copied into the *Limn* ball mill model. The screen d50c and sharpness of separation ($\alpha$) values were also copied across from the *JKSimMet* model and applied to both components.

There is a significant difference in classification for the two components in the cyclones. Due to its density, gold has a finer cutpoint than the gangue, and this is reflected with the *Limn* cyclone model. The size-by-size mass balance data was used to generate the partition curves for both gold and gangue which is shown in Figure 5, and the fitted d50c and alpha values were used in the *Limn* model. The d50c for gangue was 101 µm and 38 µm for gold. The $\alpha$ was 1.1 for both components, although often with cyclones the sharpness of the partition curve is poorer for gold.

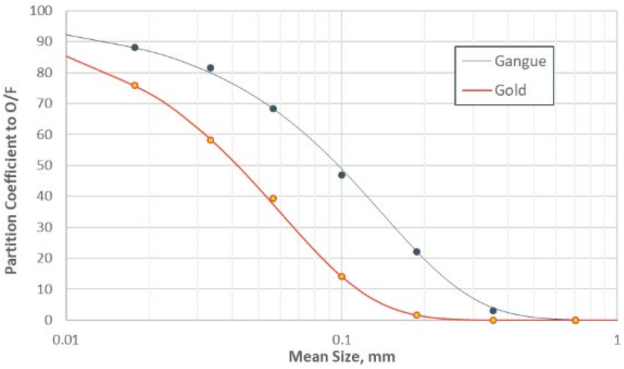


**FIG 5** – Gold and gangue cyclone partition curves.

The gold recovery-by-size showed considerable variation in both the primary and secondary Knelson concentrators. This was probably due to the difficulty of accurately sampling and assaying gold bearing streams on a size-by-size basis. Historical data from other surveys was also used to compute average recoveries-by-size. The smoothed recovery-by-size curves were derived for the *Limn* model, as shown in Figure 6.

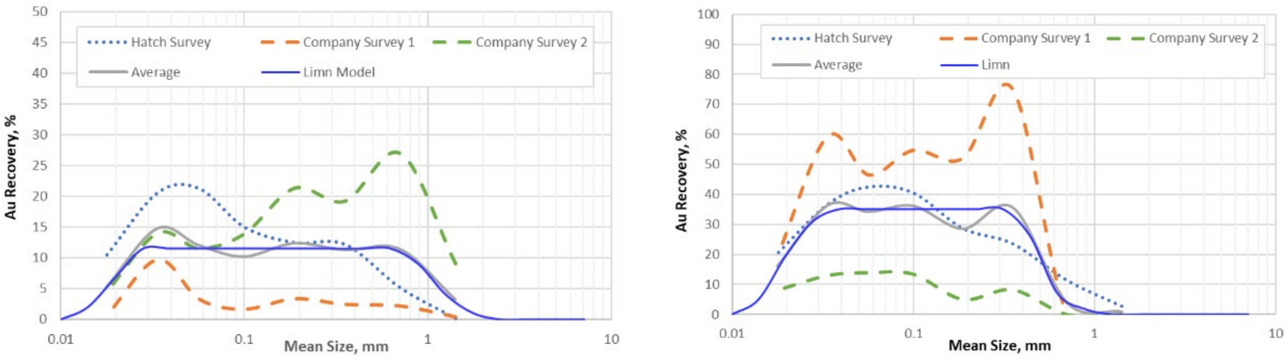


**FIG 6** – Gold recovery-by-size for primary gravity stage (left) and secondary gravity stage (right).

These recovery-by-size gravity stage models do not account for any changes to feed flow rate or to the number of separators in use. More complex models would need to be developed for this purpose, which was beyond the scope of the project. However, the absolute maximum flow rates specified by the manufacturer were included in the *Limn* spreadsheet, along with a user adjustable de-rating factor. The number of separators used is entered by the user. For example in Figure 7, 18 separators in the primary gravity stage were entered by the user (highlighted in grey). If the simulated flow to any gravity stage (either mass or volumetric flow rate) exceeds the de-rated capacity of the stage, an ‘Overload’ warning appeared below the number of separators on the flow sheet page.

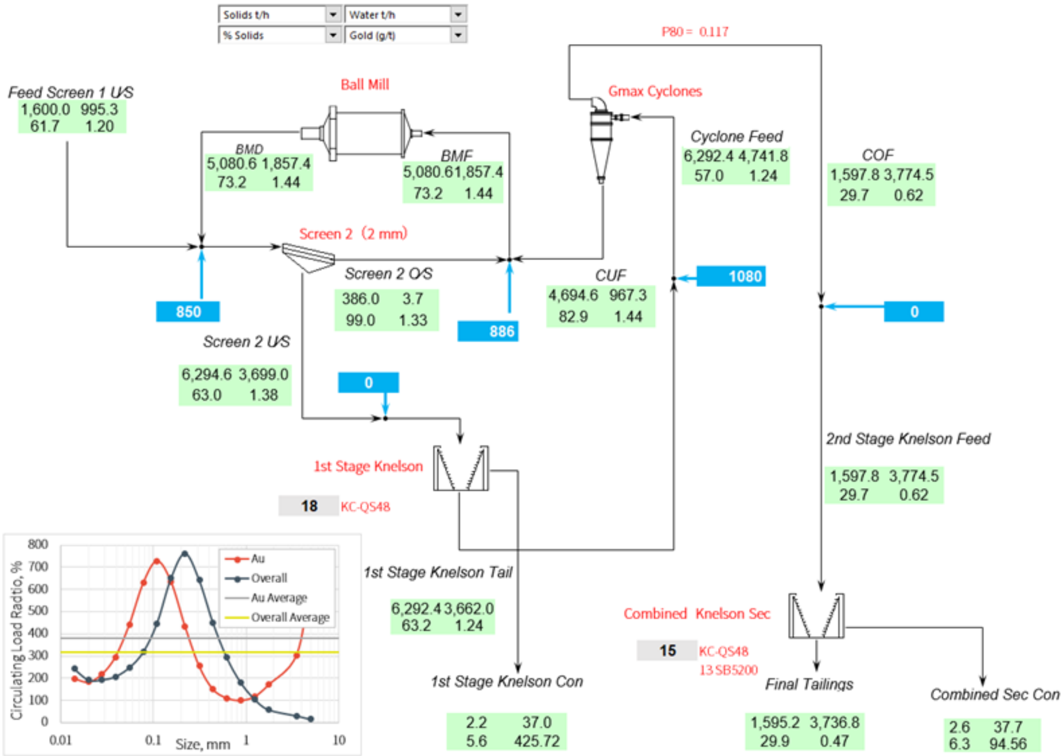


**FIG 7** – *Limn* flow sheet of gold plant.

To combine the *JKSimMet* and *Limn* simulations together; the *JKSimMet* predicted Screen 1 (SAG Screen) undersize PSD and solids and water flow rates were used as the inputs to the *Limn* simulation. The balanced gold assay (in g/t) in each size fraction in the undersize was used as the basis for all simulations. If the Screen 1 undersize PSD changed as a result of blast or comminution optimisation, the size-by-size gold assays were adjusted using the Bazin technique (Bazin *et al*, 1994) to maintain a constant gold head assay of 1.2 g/t.

Simulations demonstrated that throughput could be increased by over 20 per cent. This was achieved by tailoring the blast design according to ore characteristics (rock structure and strength) and improving the utilisation of available SAG mill power, by adjusting media size and charge and pebble production (port size). Some of these recommendations have already been implemented in the plant with great success. Expansion options were also investigated to increase throughput even further. In each case, the simulations were carried through the multi-component *Limn* model to understand the impact on downstream processes and potential recovery losses. Simulations were also conducted to evaluate various options to increase gold recovery and examine the effect on gold recirculating load.

One of the advantages of *Limn* as a process simulation platform, is that normal Excel functions can be used. For example, the circulating load ratio (CLR) can be calculated for both gangue and gold based on the flow rates by size and plotted on the flow sheet. This is shown in Figure 7. The gold deportment in the circuit for all size fractions is shown in Figure 8. This highlights the high overall CLR of gold.

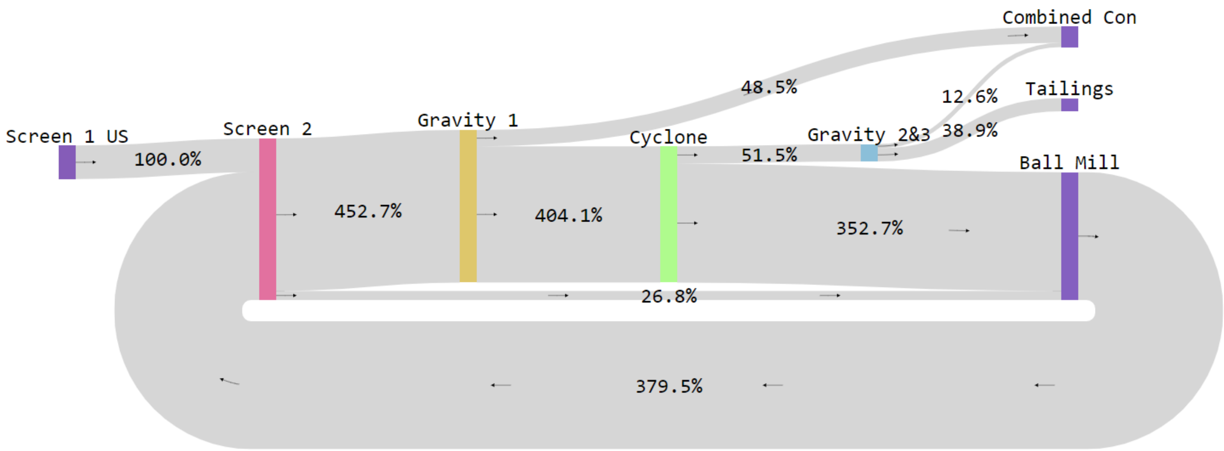


**FIG 8** – Gold deportment of *Limn* gold plant flow sheet.

Much of the gold lost to final tailings is ultrafine and microscopic gold, which is not amenable to recovery by gravity processes. Therefore, the operation is considering incorporating flash flotation technology. Flash flotation test work has been conducted. The test work data was used to generate a simple recovery-by-size model of the flash flotation cell. Modified *Limn* flow sheets were created to evaluate three potential locations or streams. The flash cell would treat a portion of these streams:

- primary gravity feed
- primary gravity tails
- cyclone underflow.

The simulations showed that the highest gold recovery was achieved when the flash flotation circuit treated 20 per cent of the primary gravity tailings stream. This case was recommended by the supplier. The improvement in recovery was achieved in the finest sizes (-30 µm), with the flash cell recovery dropping off rapidly at coarser sizes.

In a separate initiative, plant metallurgists moved two of the primary Knelson concentrators so they treated a fraction of cyclone underflow. An increase in gold recovery was observed. Simulations predicted the observed increase in recovery which validated the multi-component modelling approach. The simulations showed that the overall gold CLR decreased substantially and the CLR for each size fraction were also lower.

## CASE STUDY 2 – IRON ORE

A mine to process optimisation project was completed at an iron ore plant. This plant treated magnetite, hematite and apatite in a complex circuit involving magnetic separation and flotation processes. The plant processes up to 2000 t/h through five similar processing lines. A simplified flow sheet is shown in Figure 9.

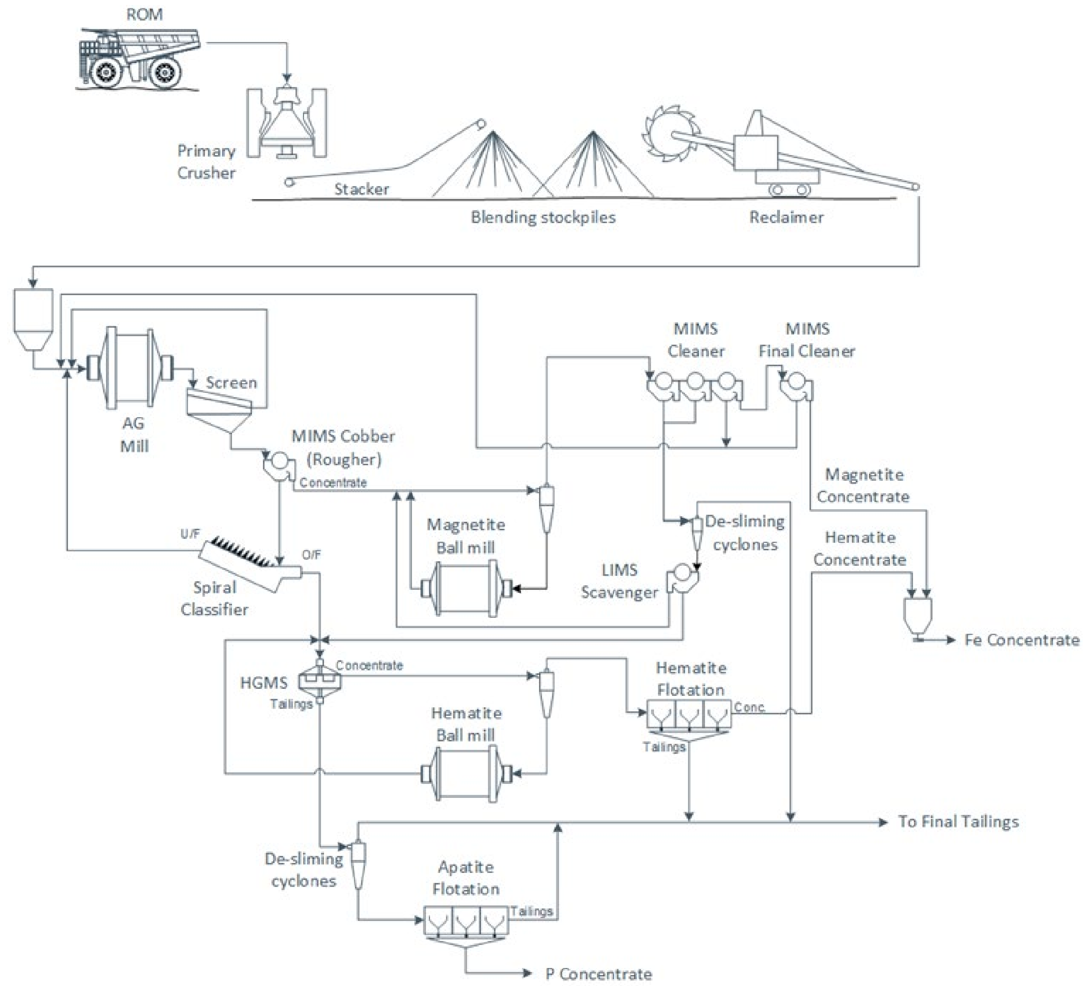


**FIG 9** – Simplified flow sheet of iron ore processing plant.

In the plant, ROM ore is crushed in a gyratory crusher and stockpiled on two blending beds. The blended ore is processed in a fully autogenous (AG) mill operating in closed circuit with double deck screens. AG mill undersize is sent to the magnetite cobbing circuit. The cobbing stage employs medium intensity magnetic separation (MIMS) using three concurrent drum separators in parallel to recover magnetite. The Cobber concentrate is ground in a closed magnetite ball mill circuit to a $P_{80}$ of around 45 µm. The ground material reports to a cleaner magnetic separator circuit.

The cleaner magnetic separator stage consists of three groups of concurrent drum MIMS units operating in parallel. Each group consists of four separators in series. The concentrate from the final separator reports to a dewatering stage to form the magnetite component of the final plant Fe concentrate.

Cobber tailings feed the hematite recovery circuit. The tailings are sized in a spiral classifier. The classifier fines are combined with the scavenger magnetite separator tailings and report to a wet high gradient magnetic separator (HGMS) to recover hematite. The hematite concentrate is subject to further regrinding in a ball mill in a closed circuit with cyclones to a $P_{80}$ of 45 µm. Cyclone product is then upgraded in the hematite reverse flotation circuit.

The hematite reverse flotation circuit comprises of rougher/scavenger stages, followed by three cleaning stages. The third cleaner stage tailings form the final hematite circuit product and join other streams to become the final tailings.

The high intensity magnetic separation (HGMS) tailings are sent to a cyclone cluster. Cyclone overflow reports to final tailings, and the cyclone underflow feeds the apatite flotation circuit. The apatite flotation circuits consist of rougher and cleaner stages. The tailings from the last rougher bank report to the final circuit tailings. The final cleaner concentrate forms the final apatite concentrate.

Comprehensive surveys of the comminution, magnetic separation and flotation circuits from Processing Line 2 were conducted. The survey was conducted whilst treating material from a single blending bed. The primary crushing and AG mill circuit mass balance data were fitted to the semi-empirical models in *JKSimMet*. These models have predictive capabilities for throughput and product size distributions. The drill and blast models were used to estimate the ROM size distributions expected from the proposed changes to blasting practices. The *JKSimMet* models were then used to evaluate the impacts these ROM size distributions had on crushing and AG milling throughput.

*Limn* was used to create an overall simulation for one processing line for all circuits after the AG mill. This is shown in Figure 10. The simulation included solids flow rates, water additions, per cent solids, size distributions and assay-by-size data for each stream for iron (Fe), iron oxide (FeO) and phosphorus (P). The models used for each process unit differ in complexity. For example, the magnetite and hematite ball mills use the Whiten perfect mixing model but with the multi-component model structure. This is shown in Figure 11 for each component (Fe, FeO, P and the remainder). The surveyed mass balance data was used to calculate individual component size distributions for the ball mill feed and product streams. The component size distributions were then used to fit the ball mills to obtain breakage rates for each component.

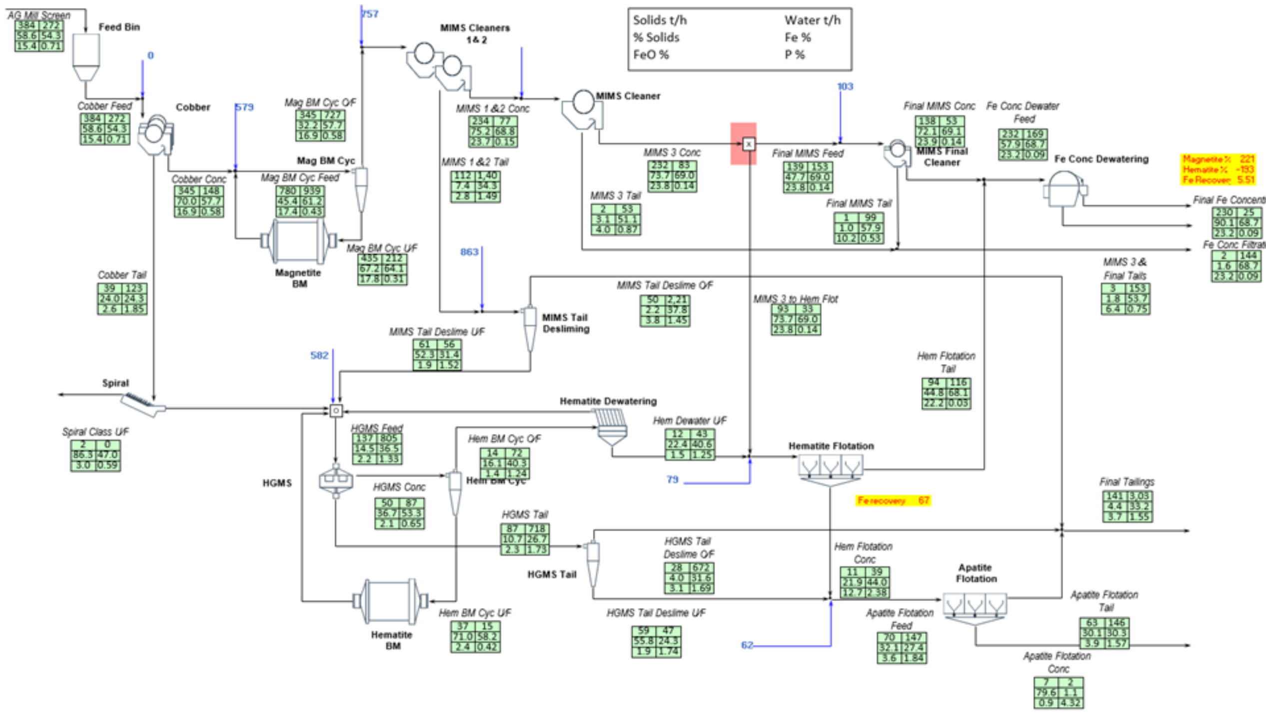


**FIG 10** – *Limn* flow sheet iron ore plant.

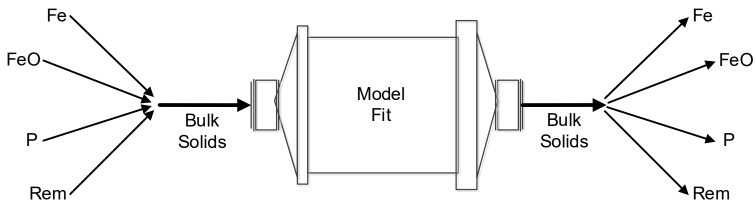


**FIG 11** – Schematic of multi-component ball mill model fit.

The cyclones and spiral classifier were modelled using efficiency curves described by a sharpness of separation ($\alpha$) and d50c for each component. These were derived by fitting the Whiten equation to the mass balanced data. The magnetic separators, hematite flotation and apatite flotation were modelled in terms of a recovery-by-size vector for each component and a water split. The partition curves for the magnetite ball mill cyclones are shown in Figure 12 (left), and the recovery curves for the cobber magnetic separator are shown in Figure 12 (right) as examples.

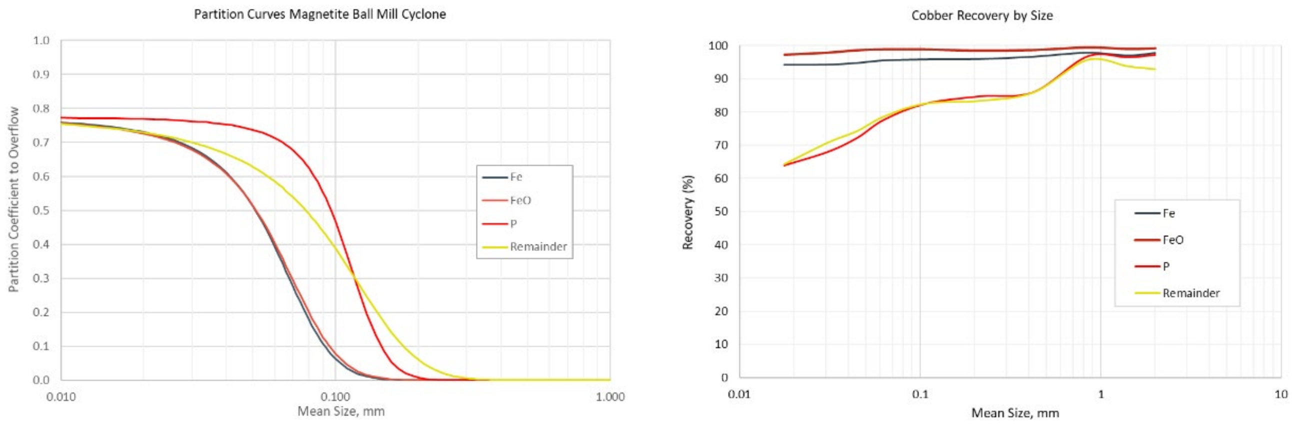


**FIG 12** – Examples of classifier and separator models used in *Limn* flow sheet.

The *JKSimMet* and *Limn* flow sheets were linked through the AG Mill screen undersize stream. Changes in the size distribution or flow rate of this stream, following changes in ROM fragmentation or increased AG mill throughput, formed the input to the *Limn* simulation. Head grades of the stream were maintained at the balanced values using the Bazin method to adjust the size-by-size assays for each component.

Mine production was considered the constraint and not processing. Therefore, there was ample comminution circuit capacity available. So, it may be possible to reduce mining costs and increase productivity by decreasing blast intensity and making use of the available comminution circuit capacity. However, if blast intensity were simply reduced for all ore blasts using a single blast design, the resulting fragmentation may be too coarse in areas where the ore is harder and less jointed. Therefore, the calibrated site-specific blast fragmentation model was used to optimise the blast design according to the rock structure and strength. In the softer and more fragmented ore domains, it was possible to expand the drill and blast pattern and reduce blasting intensity to reduce costs and increase productivity. Sufficient fragmentation for excavation, hauling and downstream comminution was still achieved. Using this approach, the ROM fragmentation would be marginally coarser overall but more consistent, so there is less variability.

One of the concerns of the site was maintaining the final iron concentrate phosphorus grade below the 0.07 per cent specification. The advantage of the multi-component *Limn* simulation is that factors that affect the final concentrate phosphorus grade can be investigated. The plant metallurgists can control the concentrate phosphorus grade to some extent by changing the amount that is split from the MIMs Cleaner 3 concentrate to the hematite flotation circuit. The splitter is highlighted in pink in Figure 11. In the base case, the split was 0.4 to hematite flotation, which corresponded to the balanced survey of the processing line. Simulations were conducted where the split to the hematite flotation circuit was increased, as shown in Figure 13. Increasing the split to hematite flotation reduces the final concentrate phosphorous grade, while having only a very minor effect on the final concentrate iron grade. The hematite reverse flotation circuit floats fine phosphorus bearing minerals into the concentrate, reducing the phosphorus grade in the hematite tails which report to final concentrate. Increasing the split substantially increases the volumetric flow rate to hematite flotation. However, evidence from the plant survey suggests there is some spare capacity in the hematite flotation circuit.

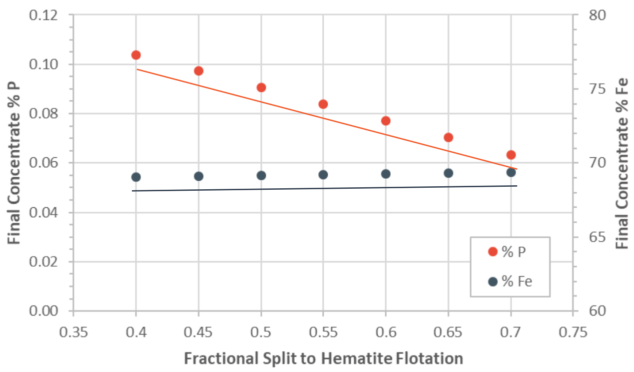


**FIG 13** – Effect of magnetite concentrate split to hematite flotation on final concentrate grades.

The trend in Figure 13, together with the lack of selectivity seen in the MIMS Cleaner 3 survey data, suggested that sending the entire MIMS Cleaner 3 concentrate to hematite flotation, (bypassing the final MIMs cleaner circuit), might be an option. This assumes that the hematite circuit be upgraded to deal with the increased flow rate. Increasing the fractional split to hematite flotation in the simulation decreases the phosphorus grade, whilst iron grades are still within specification. The phosphorous grade could be well below the specification value, but this may provide the site with additional flexibility in feed blending. This conclusion should be treated with caution given the very simple models used but does suggest a more detailed investigation is warranted.

## CONCLUSIONS

The integrated multi-component blasting/comminution/separation simulation procedure described in this paper provides several advantages for overall mine-to-process optimisation. Valuable minerals often behave quite differently to gangue during grinding and classification due to the density differential. For example, between gold and gangue; and magnetite/hematite and gangue. Separation processes such as magnetic separation, flotation or gravity concentration are most effective within certain size ranges.

Integrated multi-component modelling and simulation of grinding and separation processes provides a more complete understanding of the distribution of minerals and gangue in different size fractions. Thus, opportunities to increase concentrate production and improve product quality can be identified.

Multi-component modelling provides a greater understanding of the impact of increased throughput and changes in blasting, comminution and classification on the final grind size. In particular, the size distribution of the valuable mineral, not just total ore. All processing streams including recirculating loads are defined in terms of components within size fractions. Thus, it is possible to identify if minerals are retained in certain size fractions that are not efficiently recovered by the current process. The models can be adapted to simulate and evaluate alternative flow sheets, and the gold case study presented here demonstrated this was well validated by actual plant data. Furthermore, tracking of penalty and other undesirable elements through the process and by size fraction can be used to identify effective removal or management strategies.

Incorporating multi-component modelling in mine-to-process optimisation allows another level of optimisation, considering concentrate production and quality, in addition to throughput. This is combined with historical data analysis, energy-based calculations, capacity calculations, industrial experience and benchmarking with an extensive database of operational data to develop integrated strategies from mine to plant. These strategies maximise throughput and recovery; whilst minimising unit costs and ensuring all product quality specifications are met.

## REFERENCES

Banisi, S., Laplante, A. R., Marois, J., 1991. *The Behaviour of Gold in Hemlo Mines Ltd Grinding Circuit*, CIM Bull. 84, pp 72–78

Laplante, A., Woodcock, F., Noaparast, M., 1994. *Predicting Gold Recovery by Gravity*, SME Preprint 94–158, SME Annual Meeting, Albuquerque, New Mexico, Feb 14–18, 1994

Bazin, C., Grant, R., Cooper, M. Tessier, R., 1994. *Prediction of Metallurgical Performance as a Function of Fineness of Grind*, in Proc. 26th AGM of Canadian Mineral Processors, Ottawa, Paper # 8.

# Back to basics – a practical approach to troubleshooting plant grade/recovery issues in the Mt Isa Copper Concentrator

*C Evans[1] and R O'Donnell[2]*

1. Senior Research Fellow, The University of Queensland, Sustainable Minerals Institute, W H Bryan Mining and Geology Research Centre, Indooroopilly Qld 4068.
   Email: c.evans@uq.edu.au
2. Senior Process Engineer, Copper Concentrator, Mount Isa Mines, Mt Isa Qld 4825.
   Email: roxanne.odonnell@glencore.com.au

## ABSTRACT

Like many operations, the Mt Isa Copper Concentrator occasionally has operational periods when it is difficult to achieve target grade and/or recovery, often due to feed ore type changes as mine production is drawn from different stopes in the underground mine. At times like these it is useful for metallurgists to have a suite of tools that they can use to quickly diagnose the problem or at least eliminate some potential causes. This paper describes an investigation in the Mt Isa Copper Concentrator to identify the potential cause of periods where grade or recovery was below target values. The strategy used applied a sequence of steps, starting with fast turnaround analyses that could be done on-site and only moving to more intensive analyses with longer turnaround times if these were needed to identify the cause. The analyses used shift samples from the inventory samplers – flotation feed, final concentrate and final tail – as the basis for the investigation as these were readily available and represented known periods of operational performance. The samples were sized, the size fractions assayed and the elemental compositions converted to mineral content (chalcopyrite, iron sulphides, non-sulphide gangue) using a standard element-to-mineral conversion method.

Comparing the mineral recovery by size performance of the plant with baseline data from a previous plant survey identified much higher recovery of fine iron sulphides as the major difference. The assumption that these fine iron sulphides were liberated was confirmed by MLA analysis. The reason for higher recoveries of the fine liberated iron sulphides was identified using a simple laboratory batch flotation test which showed that the problematic ores have a high proportion of naturally-floating iron sulphides which, once recovered in the roughers, would be difficult to depress from Final Concentrate. The main steps of the diagnostic approach can be performed on-site, providing metallurgists with fast turnaround options to troubleshoot future problems.

## INTRODUCTION

During 2018–2019, Glencore's Mt Isa Copper Concentrator operations saw periods of time when it was difficult to achieve the target concentrate grade or recovery and the project described here was established to investigate the cause of this so that a solution to the problem could be identified. Metallurgists from the Julius Kruttschnitt Mineral Research Centre (JKMRC) at the University of Queensland's Sustainable Minerals Institute had previously collaborated with the Copper Concentrator operations team in August 2017 to complete a detailed survey of the concentrator performance, with data analysis to the level of size by assay by mineralogy. The full plant survey was a major investment in time and effort but the value of having this data has been underlined on several occasions when it has provided a baseline measure of plant performance for comparison when the plant is not operating optimally.

The project described in this paper provided an opportunity to leverage the detailed knowledge that had been gained from the earlier survey, by comparing the baseline measure of plant performance with the period of poor performance to identify potential sources of the low final concentrate grade problem. While the main objective of the work was to identify the reasons for the operational periods of low-grade (or low recovery at acceptable grade), a secondary objective was to develop an initial circuit diagnosis method using tools and techniques that could be applied on-site by the metallurgical team using resources available on-site. This was important since the intermittent nature of the problem would require a fast response to be able to diagnose what was happening in the concentrator. The subsequent project is a case study in forensic metallurgy!

## DIAGNOSING THE CAUSE OF LOW COPPER CONCENTRATE GRADE

During February 2019 the copper concentrator was achieving lower than expected copper grade in the final copper concentrate, averaging 23.6 per cent Cu grade over the month (at copper recovery of 91.4 per cent). This followed an earlier period where the operators could only achieve acceptable copper grade of 26.3 per cent Cu at a lower than expected 89.4 per cent copper recovery. This is in comparison to the 26.4 per cent Cu grade achieved during a full plant survey in August 2017 (at copper recovery of 90.3 per cent). It appears that during the period of challenging performance the plant was trading off grade to achieve recovery and vice versa but could not achieve both targets at the same time. MIM metallurgists wanted to identify the potential causes of this problem and submitted samples of flotation feed, final concentrate and final tail streams from the February 2019 monthly composite for analyses aimed at providing this information. The use of good sampling practice in this type of investigation is critically important as a considerable investment of time and money may be made in analysing the samples and operational decisions may be made based on the results. For this reason, the monthly composite samples which come from inventory samplers were used in this investigation. The stream samples were submitted for a series of analyses including unsized assay, size analysis, assay of size fractions, MLA analysis of size fractions.

The size analysis consisted of wet screening at 38 μm, dry screening of the +38 μm material and Cyclosizing of the -38 μm material. The sieve sizes were chosen to align with the size fractions analysed in a previous August 2017 baseline survey to allow comparison of the size and assay data across the two time periods. Each size fraction was representatively split into two subsamples and one subsample of each size fraction submitted for assay for Cu, Fe, S, MgO, $SiO_2$, CaO and $Al_2O_3$ at the Mt Isa Mines (MIM) assay laboratory in Mt Isa.

The mineralogy of the Mt Isa copper ore is relatively simple, with the copper present as chalcopyrite, the only other major sulphide minerals being iron sulphides (mainly pyrite and pyrrhotite) and the major gangue minerals being dolomite and quartz. This mineralogy means that elemental assays can be used to estimate the proportions of these valuable and gangue sulphide minerals in the process streams via a simple element to mineral conversion calculation (Johnson, 2016).

The MLA analyses to measure mineralogy and the liberation of the key minerals were performed on the same set of size fractions as used in the previous baseline survey to allow direct comparison of the two sets of results. These size fractions were:

-425 +212 μm, -212 +106 μm, -106 +53 μm, -53 +38 μm, -38 +C2, -C2 +C5

The analyses were performed in sequence with cross-checks of data quality at each stage before moving to the next.

## RESULTS

### Identifying the cause of low final concentrate grade

The initial analyses of unsized assay of each of the flotation feed, final concentrate and final tail streams shown in Table 1 were used to calculate the overall copper recovery for the concentrator. The objective here was to check that the stream samples represented the low recovery behaviour that was the subject of the investigation. Comparison with the shift data corresponding to the stream samples showed that the copper recovery of 89.4 per cent was similar to the shift copper recovery of 89.7 per cent and so the samples were sufficiently representative of the plant performance to move on to the next stage of analysis – size by assay.

**TABLE 1**

Assays of concentrator feed and products from February 2019.

| Stream | Flotation feed | Final concentrate | Final tail |
|---|---|---|---|
| Distribution of solids | 100 | 8.04 | 91.96 |
| Assay – Cu | 2.08 | 23.65 | 0.19 |
| Recovery of Cu | 100 | 91.4 | 8.6 |
| Assay – Fe | 8.22 | 28.48 | 6.44 |
| Assay – S | 5.6 | 29.7 | 3.5 |
| Assay – MgO | 7.66 | 1.32 | 8.19 |
| Assay – $SiO_2$ | 46.73 | 9.49 | 49.99 |
| Assay – $Al_2O_3$ | 2.44 | 0.32 | 2.62 |
| Assay – CaO | 9.69 | 1.38 | 10.41 |

Size analysis showed that the flotation feed of February 2019 is slightly finer than the August 2017 data, with a $P_{80}$ of 170 µm compared to the $P_{80}$ value of 190 µm on 6 August 2017. The final tail size distribution (not shown) follows the same trend. The final concentrate size distributions are similar, with the February 2019 concentrate being slightly coarser with a $P_{80}$ of 75 µm compared to the $P_{80}$ of 65 µm observed in the baseline survey of August 2017.

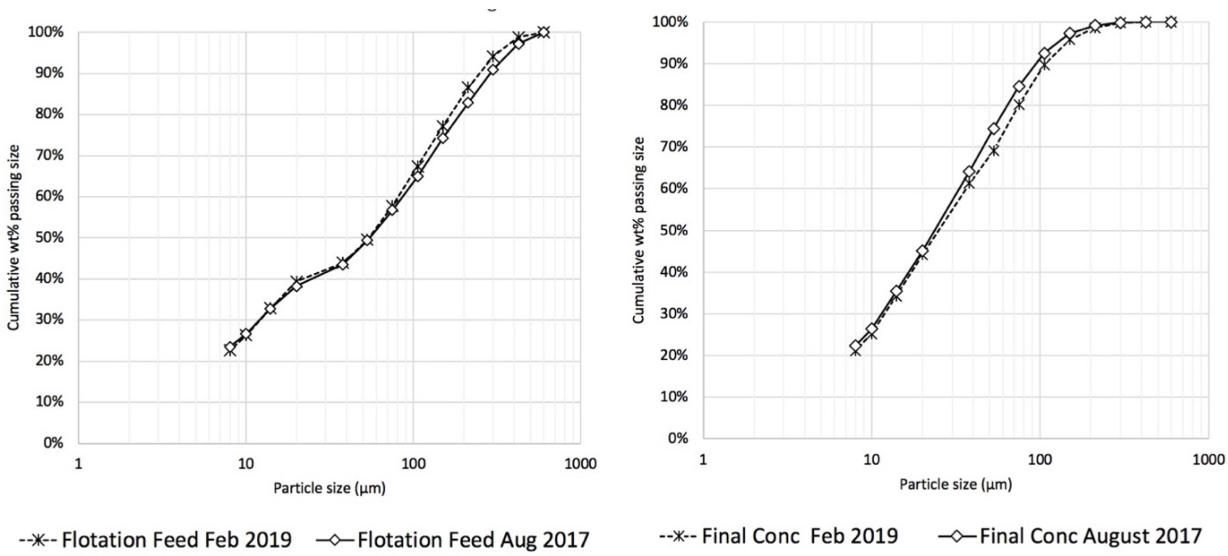


**FIG 1** – Comparing particle size distributions from February 2019 with baseline survey data.

Since the main focus of the project was to identify the reason for the difficulty in maintaining concentrate grade at the required recovery the logical first step in the data analysis was to identify what is diluting the concentrate grade. The unsized assay data for the final concentrate were used to estimate the mineral content of the final concentrate and the results summarised in Figure 2 show that chalcopyrite forms 68.1 per cent of the mass of the final concentrate with 11.0 per cent iron sulphides and the remainder comprising 20.1 per cent non-sulphide gangue. The comparison of the mineral composition estimated from assays for the February 2019 final concentrate with the baseline data from the August 2017 survey in Figure 2 shows that the dilution of the grade in February 2019 was caused by both a doubling in iron sulphides content and a 50 per cent increase in non-sulphide gangue. In the project the reasons for both the increased amounts of non-sulphide gangue and iron sulphides in the final concentrate were investigated, however the investigations relating to the iron sulphides are the focus of this paper.

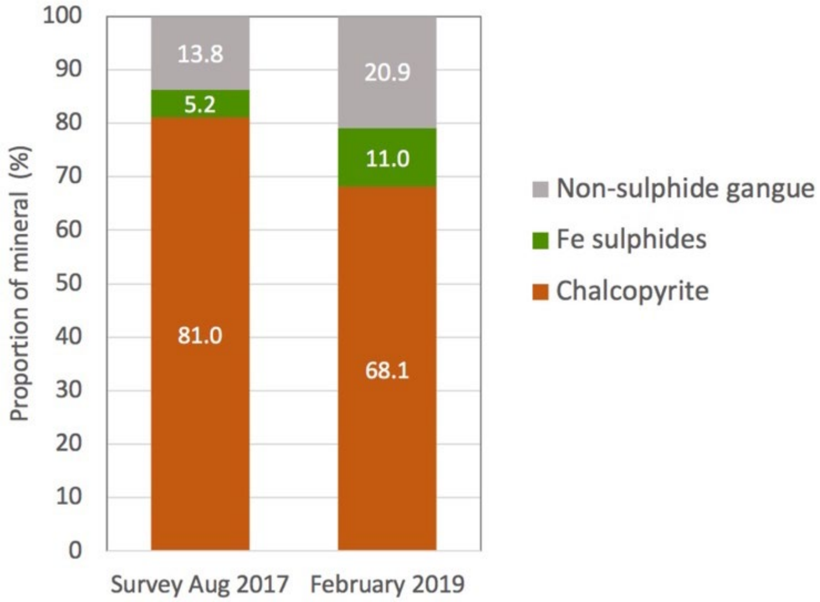


**FIG 2** – Comparison of final concentrate mineralogy estimated from assays showing increased gangue mineral content in February 2019.

The next step in the analysis used the size by assay data to provide some clues as to whether the gangue being recovered into the final concentrate is there through lack of liberation or through other mechanisms such as entrainment. As with the unsized assays, the elemental assay data of the size fractions can be converted to minerals and the recovery by size behaviour of chalcopyrite and iron sulphides across the entire concentrator as a block plotted as shown in Figure 3. The data for CaO (mainly present in dolomite) and MgO (present in both talc and dolomite) are also shown. The CaO data indicate the response of non-floating components of the ore, particularly at finer sizes.


**FIG 3** – Recovery as a function of size for the entire copper concentrator for February 2019 data.

The chalcopyrite data shows the classic recovery versus size curve with maximum recovery occurring over the particle size range 8 to 106 µm and recovery decreasing slightly below 8 µm and decreasing rapidly with increasing particle size above 106 µm.

To assess what might have changed since the 2017 baseline survey the recovery by size data for chalcopyrite and iron sulphides in February 2019 are compared with the baseline survey data in

Figure 4. The comparison shows that the recovery of chalcopyrite has not changed significantly between the two time periods. However, from the results shown in Figure 4, it is clear that the recovery of iron sulphides in February 2019 was higher than was observed in the August 2017 survey for almost all size fractions. This increase in iron sulphide recovery is particularly pronounced at the finer particle sizes below 38 µm. On an overall, unsized basis, the overall recovery of iron sulphides increased from 3.1 per cent in August 2017 to 13.6 per cent in February 2019.

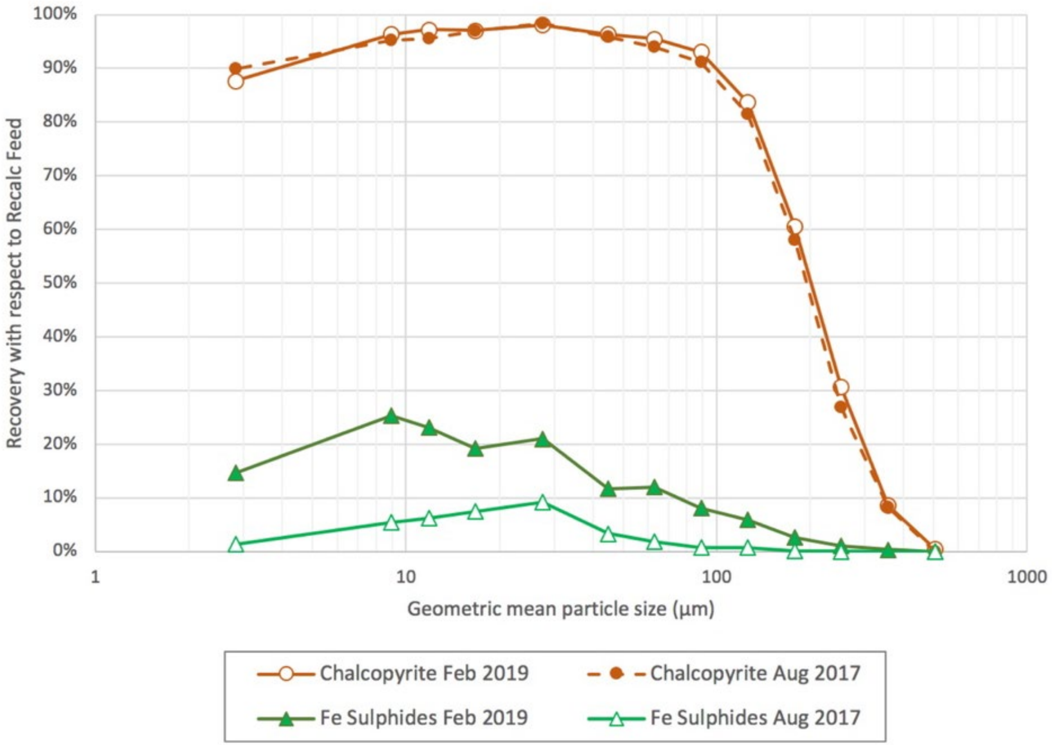


**FIG 4** – Comparing recovery as a function of size for the entire copper concentrator for February 2019 and baseline survey data from August 2017.

Alongside the recovery by size data, it is important to also consider what proportion of the minerals in the flotation feed are located in each of the size fractions in that stream. Figure 5 shows that the distribution of the iron sulphide minerals across the size fractions in the flotation feed is similar for the August 2017 and February 2019 time periods, with a slight shift of iron sulphides from the particle size classes above 106 µm into the intermediate sizes in February 2019. Figure 5 also shows that the fine fractions below 38 µm (which show the highest recovery of iron sulphides to final concentrate) contain 48 per cent of the total iron sulphides in the flotation feed.

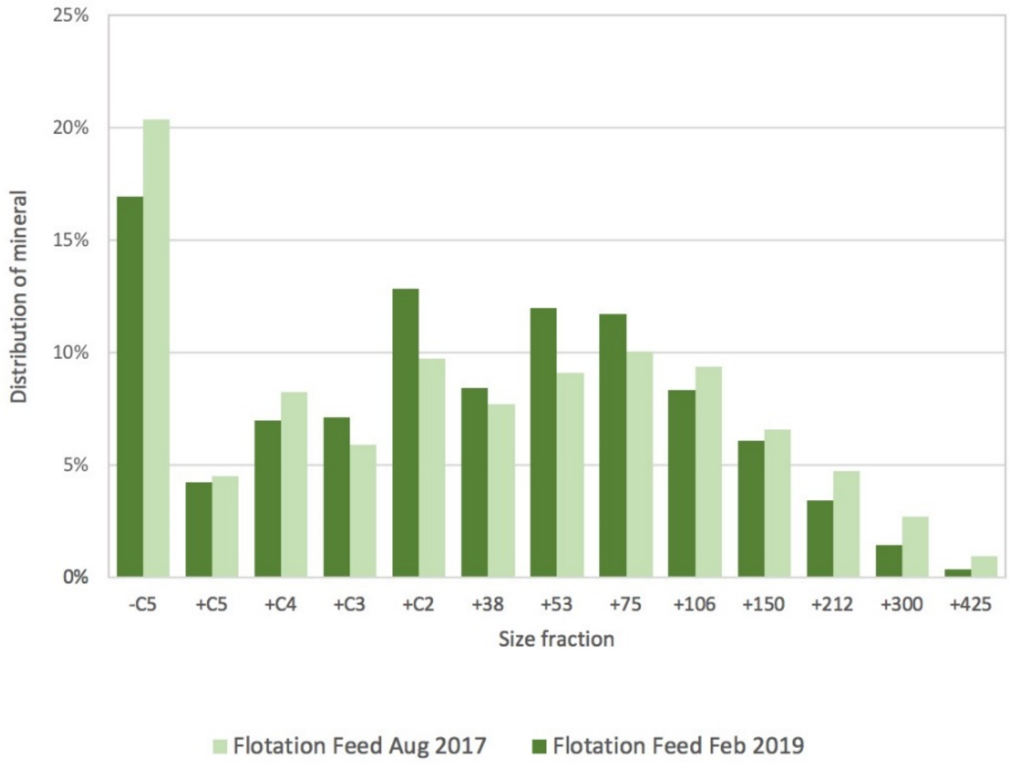


**FIG 5** – Distribution of iron sulphides by size in the flotation feed from February 2019 and August 2017 survey.

The evidence from the size by assay data indicates that the iron sulphides diluting the final concentrate grade are present due to the increased recovery from fine size fractions below 38 µm. It is more likely that the iron sulphides in these fine particles are liberated, particularly in the finest size fractions and therefore have not been recovered locked in particles with chalcopyrite but through flotation of the iron sulphides. This can only be confirmed by mineralogical analysis and it is at this point in the data analysis that MLA analyses were deployed to measure the mineralogical and mineral liberation data that provide an extra level of detail which complements the assay by size data.

The MLA liberation data for iron sulphides in the final concentrate presented in Figure 6 confirmed that the majority of the iron sulphides in the final concentrate are liberated particles (ie particle composition is 100 per cent iron sulphides) which are finer than 38 µm. This confirmed that their dilution of the final concentrate is due to the recovery in flotation of the iron sulphide particles rather than poor liberation of iron sulphides from chalcopyrite.

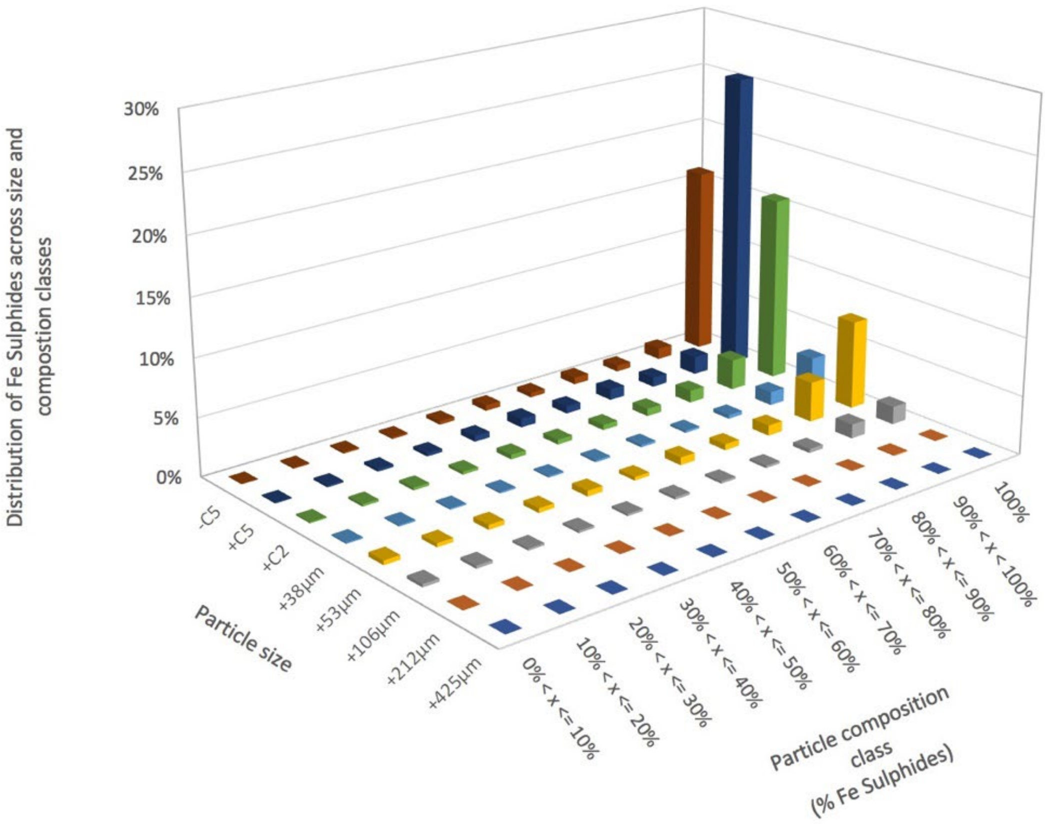


**FIG 6** – Distribution of iron sulphides by size and liberation class in the February 2019 final concentrate.

There is a type of pyrite in the Mt Isa copper ore (also present in the Mt Isa Zn/Pb ores) known as carbonaceous pyrite and this form of fine-grained pyrite has natural flotation behaviours – that is it floats in the absence of collector. The different recovery behaviours of the iron sulphides in February 2019 and August 2017 may be a result of different ore types being present in the feed, with the February 2019 ores containing more of this naturally hydrophobic pyrite.

Examination of the flotation feed mineralogy data obtained from the MLA analyses indicates that the ores did indeed show different proportions of some minerals. While the mineral contents in terms of chalcopyrite and iron sulphides are not significantly different between the two time periods, the ores fed to the plant in February 2019 and August 2017 did contain different proportions of the major gangue minerals, with the February 2019 ore containing a lower proportion of quartz and more dolomite and other carbonates. Unfortunately, the carbonaceous pyrite cannot be distinguished from ordinary pyrite using SEM-based mineralogy systems such as the MLA. The February 2019 ore also contained lower amounts of talc – a naturally floating silicate mineral which, being a carrier of MgO, is problematic in the smelter.

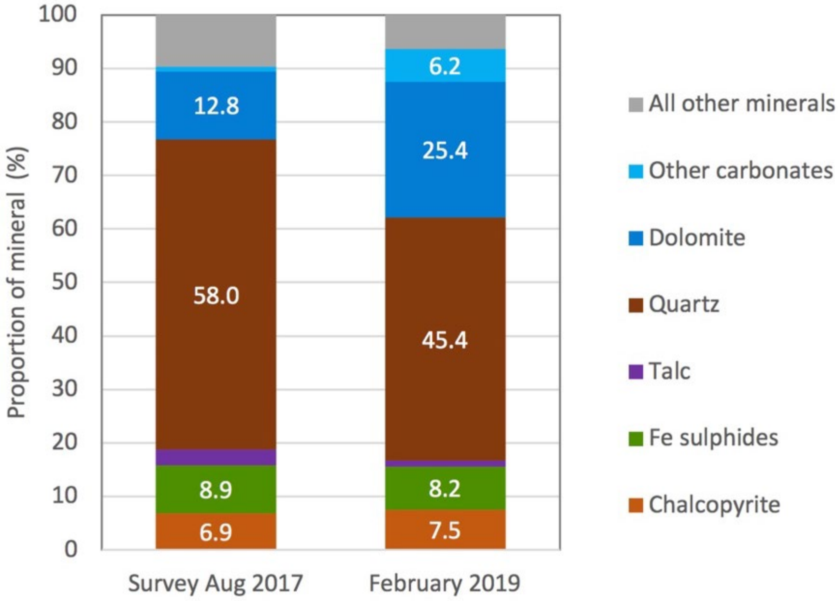


**FIG 7** – Comparing flotation feed mineralogy for February 2019 and baseline survey.

The chemical assays of the flotation feed reflect the change in gangue mineralogy as the comparison of the assays in Table 2 with the $SiO_2$ (mainly present in quartz) decreasing from 61.6 per cent in the baseline survey to 46.7 per cent in February 2019 and CaO assay (mainly present in dolomite ($CaMg(CO_3)_2$) and other carbonates) increasing from 4.41 per cent to 9.69 per cent.

**TABLE 2**

Comparing chemical assays of flotation feeds from February 2019 and the August 2017 baseline survey.

| **Assay of flotation feed** | **August 2017 survey** | **February 2019** |
|---|---|---|
| Assay – Cu (%) | 1.87 | 2.08 |
| Assay – Fe (%) | 7.18 | 8.22 |
| Assay – MgO (%) | 6.18 | 7.66 |
| Assay – $SiO_2$ (%) | 61.6 | 46.7 |
| Assay – $Al_2O_3$ (%) | 2.67 | 2.44 |
| Assay – CaO (%) | 4.41 | 9.69 |

If a link could be identified between the change in gangue mineralogy and the increased presence of naturally floating iron sulphides to the final concentrate, then assays may be a useful indicator of the ore changing to this problematic type and one which is fast enough and low-cost enough to be used in practice on-site.

The assay and mineralogy data alone do not provide enough information to determine whether the recovery of liberated iron sulphides is caused by insufficient depression of iron sulphides or whether the presence of some carbonaceous pyrite (naturally floating pyrite which was not recovered along with the naturally floating talc in the preflotation section) is responsible. At this point in the investigation there are a number of potential approaches to identifying the presence of naturally hydrophobic pyrite. Surface analysis using X-ray photoelectron spectroscopy (XPS) or Time of Flight Secondary Ion Mass Spectroscopy (ToF-SIMS) would be one option to provide a detailed analysis of the particle surfaces to identify hydrophobic species. However, these techniques require special sample handling and are performed in specialist centres typically in major cities. While these techniques provide detailed surface analysis which can be useful in identifying the most appropriate solutions to the problem, the extended turnaround times for these techniques make them impractical for rapid plant diagnostics. An alternative approach, based on basic metallurgical tools and skills, which can easily be applied on-site as a diagnostic test to detect naturally floating iron sulphides is described below.

## A simple diagnostic test for naturally floating iron sulphides

For a diagnostic test to be useful in a plant operational context the results of the test must be available in time to be used in optimising the plant. To achieve this, the test needs to use the resources (people, equipment, analytical services) that are available on-site. The diagnostic test applied to identify the amount of naturally floating iron sulphides present in the plant feed is a simple batch flotation test which floats the flotation feed without collector. This will quantify the flotation behaviour of the minerals without addition of collector and will identify the presence of naturally hydrophobic minerals which will be recovered into the concentrate.

In the context of the project described in this paper the diagnostic batch flotation tests were applied to four individual ores sampled from the operating stopes that formed the blend being fed to the plant in February 2019. The objective of these tests was to determine whether the diagnostic test would show the presence of naturally floating iron sulphides in the ore, and if so, to identify which stopes may be the sources of this problematic feed material.

The batch flotation test could equally be applied to a sample of flotation feed slurry collected in the plant and although the presence of residual collector in the process water may mean that the test is not strictly collectorless flotation, the relative responses of the minerals will provide an indication of how the ore will behave in the preflotation and copper roughers.

The head assays of the four ore samples in Table 3 show that the four stopes have similar Cu assays, ranging from 2.3 per cent to 3.0 per cent. The iron, total sulphur, and MgO contents also do not vary greatly across the four stopes. There is a slight variation in the calculated values of sulphur in iron sulphides, ranging from 2.9 per cent for J691, to 4.5 per cent for X620 (which equates to 5.4 per cent and 8.4 per cent pyrite respectively, assuming that all of the iron sulphides are pyrite). However, differences in the CaO, $SiO_2$ and $Al_2O_3$ assays indicate that the ores have different gangue mineralogy. The pair of stopes J691 and V582 have similar gangue mineralogy to one another, as do the pair of Q364-Q361 and X620, but the differences between these pairs are significant, with J691/V582 having more $SiO_2$ and less CaO than Q364-Q361/X620. In terms of mineral content of the ores these assays may indicate that J691/V582 contain more quartz and less dolomite than Q364-Q361/X620. Given that the MgO contents are similar for the four ores, the reduced amount of dolomite (which contains MgO) in J691/V582 may indicate that these ores contain more talc (which is also a source of MgO) than Q364-Q361/X620. However, this inferred mineralogy would need to be confirmed through mineralogical analysis.

**TABLE 3**

Summary of head assays of ore samples from operating stopes from February 2019.

| Ore source ID | Cu (%) | Fe (%) | CaO (%) | S (%) | S in Fe Sulphides (calculated*) (%) | $SiO_2$ (%) | $Al_2O_3$ (%) | MgO (%) |
|---|---|---|---|---|---|---|---|---|
| J691 DPT1 | 2.3 | 8.9 | 4.5 | 5.2 | 2.9 | 53.4 | 4.7 | 8.9 |
| V582 DPT1 | 3.0 | 9.0 | 5.1 | 6.1 | 3.1 | 54.1 | 3.4 | 7.7 |
| Q364-Q361 | 2.6 | 8.7 | 11.8 | 6.7 | 4.1 | 40.3 | 1.6 | 8.9 |
| X620 DPT1 | 3.0 | 9.1 | 10.4 | 7.4 | 4.5 | 44.0 | 1.6 | 7.9 |

* Assumes all S not accounted for in chalcopyrite is present in iron sulphides.

For the diagnostic tests on ore samples the rock was crushed and then ground to flotation feed size ($P_{80}$ 170 µm) in a laboratory batch mill prior to flotation of the slurry in a 5L batch flotation cell at natural pH with frother only (no collector added). In this project, timed concentrates were collected to assess the flotation kinetics, but a single concentrate would be equally valid as a measure of natural flotation behaviour. For each test the flotation concentrates and tails were filtered, dried and submitted to the Mt Isa assay laboratory for elemental assays of Cu, Fe, S, MgO, $SiO_2$, CaO and $Al_2O_3$. The calculated recoveries for the four flotation tests are shown in Figure 8.

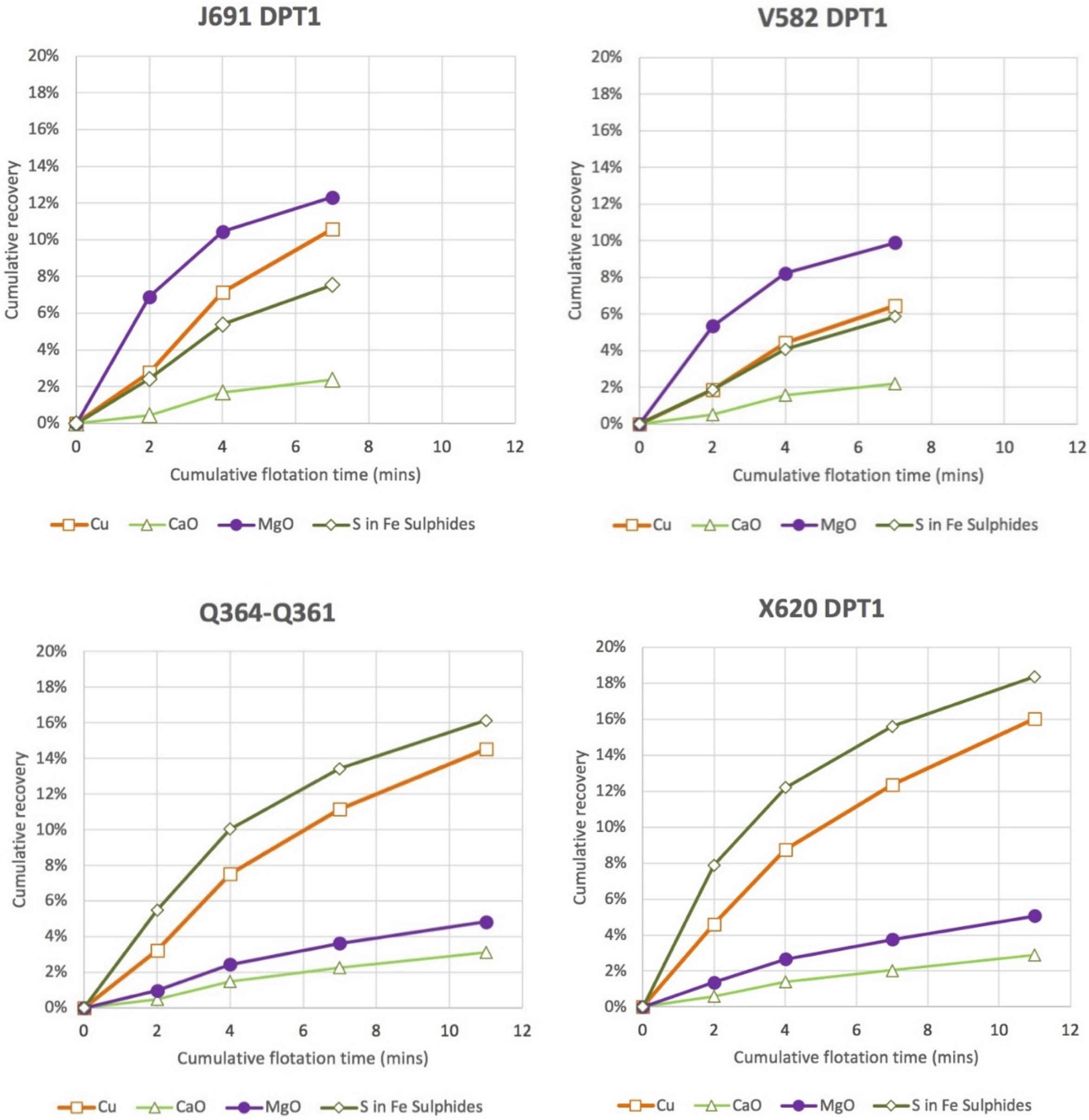


**FIG 8** – Comparison of collectorless flotation recovery as a function of time for four production stopes from February 2019.

The flotation responses are presented in terms of the elemental recoveries since elemental data is what is available in short turnaround times. The Cu assay represents chalcopyrite recovery, while CaO is used to represent the non-floating minerals in the ore. Based on the mineralogy measured for the February 2019 flotation feed (shown earlier in Figure 7) the CaO is mainly (80 per cent) present in dolomite ($CaMg(CO_3)_2$) and ankerite ($Ca(Fe,Mg,Mn)(CO_3)_2$) and so can be used to represent the non-floating minerals in the ore. The MLA results showed that the dolomite in the plant flotation feed is highly liberated (87 per cent in particles >95 per cent dolomite content) and it is likely that recovery of CaO is predominantly due to entrainment rather than flotation in composite particles. Silica ($SiO_2$) is present in multiple gangue minerals in the ore, mainly as quartz but also in talc ($Mg_3Si_4O_{10}(OH)_2$) which is known to show natural flotation behaviour in Mt Isa copper ores. Therefore, in this analysis $SiO_2$ is less useful as a representative of the non-floating gangue behaviour and is not shown in the graphs.

The flotation results show that in all four ores the chalcopyrite (represented by the Cu assay) is showing natural flotation (ie floating in the absence of collector), with three of the ores showing similar Cu recovery in the range 10 per cent to 12 per cent after 7 minutes of flotation, and stope V582 showing slightly slower chalcopyrite kinetics.

When the flotation behaviours of the floatable gangue minerals, (talc and iron sulphides) shown in Figure 8 are considered it is clear that the four ores fall into two categories. Two stopes, J691 and V582, show flotation recovery of MgO which is higher than chalcopyrite and iron sulphides, which in turn are higher than the CaO. Observations of the froth collected during the flotation of J691 and V582 showed the matt grey colour typical of talc in the froth. Based on the assay data and the froth colour it is likely that these ores showed the typical natural flotation of talc which the copper concentrator circuit and operating strategy are designed to deal with. The other two stopes, Q364-Q361 and X620, show high flotation recoveries of iron sulphides (higher than the chalcopyrite recovery in both cases) and low recovery of MgO. In both of these latter two cases the froth was dark, almost black, with a metallic sheen. From the mineralogy inferred from assay discussed above it is likely that the MgO in stopes Q364-Q361 and X620 is present mainly as dolomite rather than the naturally floating talc and so the recovery of MgO is lower, closer to that of the non-floating gangue represented by the CaO assay.

The high recoveries of iron sulphides in stopes Q364-Q361 and X620 indicates that the iron sulphide minerals in these zones of the orebody are being recovered by flotation. After 7 minutes of flotation the iron sulphide recovery in Q364-Q361 and X620 is almost double that observed in stopes J691 and V582. No mineralogy data are available for the batch flotation samples and so the liberation status of the chalcopyrite and iron sulphides has not been quantified. However, the MLA analysis of the plant flotation feed from February 2019 which was produced from the four stopes, indicated that both the chalcopyrite and iron sulphides were highly liberated and so it is likely that the source ores from the individual stopes also contain mainly liberated chalcopyrite and iron sulphides. On this basis it is probable that the observed flotation behaviour reflects the responses of the individual minerals as liberated particles rather than a response due to the presence of locked particles of chalcopyrite/iron sulphide and that the iron sulphides and chalcopyrite have some natural flotation response, presumably due to natural hydrophobicity. These naturally floating iron sulphides from the Q364-Q361 and X620 stopes are almost certainly the cause of the higher levels of iron sulphides diluting the final copper concentrate in February 2019.

The head assays of the four ore samples follow the same pattern identified in the comparison of baseline feed and February 2019 feed, in that the ores showing the problematic collectorless flotation of iron sulphides have less $SiO_2$ (quartz) and more CaO (dolomite and other carbonates) than the ores which have low levels of naturally floating iron sulphides. This may mean that head assays are a useful indicator of these problematic ores but more extensive analyses of a wider range of ores needs to be done to confirm this. This could be determined as part of a geometallurgical program to quantify the extent to which future ore sources in the Mt Isa copper orebodies contain the problematic naturally floating iron sulphides.

## CONCLUSIONS

Applying basic metallurgical knowledge and skills in a logical sequence allowed metallurgists to identify the cause of lower copper grades in the final concentrate. The existence of a baseline survey of the concentrator which quantified the plant performance in normal operation was an important part of the analysis, since it provided reference data against which the lower grade operating conditions could be compared. By using a sequence of basic analyses that are readily implemented on an operating site – good sampling, unsized assays, sizing, assay of size fractions – the flotation performance of the ore through the copper concentrator was characterised and the likely causes of poor performance identified. MLA analyses were used to quantify mineralogical data (in this case ore mineralogy and mineral liberation data) for the size fractions of the key streams to provide confirmation of the causes identified in the previous steps of the analysis.

A simple laboratory batch flotation test was tested as a potential diagnostic test for the presence of problematic naturally floating iron sulphides in the Mt Isa copper ores. The results of the diagnostic batch flotation tests indicate this is a useful method to identify the presence of naturally floating iron sulphides in the ore being fed to the copper concentrator. Since the test can be applied using the resources available on-site, it is a practical tool for providing a rapid identification of whether naturally floating iron sulphides in the feed are the cause of operational difficulties in achieving concentrate grade or recovery. This type of test is useful in a geometallurgical program to identify potentially problematic ore sources across the orebodies. Having such information would support business decision-making on the best way to deal with these problematic ores, including determining whether ore from specific stopes or regions of the orebodies can be mined and processed economically and if so, developing strategies in mining and processing to minimise their impact on copper grade and recovery in the final concentrate.

## ACKNOWLEDGEMENTS

The authors would like to thank Mt Isa Mines Ltd for permission to publish this paper. The technical support provided by the Mineralogy Services group at JKMRC is acknowledged, with special recognition to Kellie Teale for her high-quality technical work.

## REFERENCES

Johnson, N.W., 2016. Using mineralogical data in mineral processing in *Process Mineralogy* (eds M. Becker, E. Wightman and C. Evans), pp189–203 (Julius Kruttschnitt Mineral Research Centre: Brisbane)

# Predicting mill feed specific energy from Bond ball mill Work index tests at Olympic Dam

*Y Li[1], V Liebezeit[2], K Ehrig[3], M Smith[4], B Pewkliang[5] and E Macmillan[6]*

1. AAusIMM, Senior Geometallurgist, BHP Olympic Dam, Adelaide SA 5000. Email: yan.li@bhp.com
2. Principal Geometallurgist, BHP Olympic Dam, Adelaide SA 5000. Email: vanessa.liebezeit@bhp.com
3. FAusIMM(CP), Superintendent Geometallurgy, BHP Olympic Dam, Adelaide SA 5000. Email: kathy.ehrig@bhp.com
4. Lead Geoscience Data Management, BHP Olympic Dam, Adelaide SA 5000. Email: michelle.smith@bhp.com
5. MAusIMM, Senior Geometallurgist, BHP Olympic Dam, Adelaide SA 5000. Email: benjamath.pewkliang@bhp.com
6. MAusIMM(CP), Senior Geometallurgist, BHP Olympic Dam, Adelaide SA 5000. Email: edeltraud.macmillan@bhp.com

## ABSTRACT

Ore hardness, like many other intrinsic ore properties, varies across a deposit, hence will also vary in ore delivered to the mill throughout the life-of-mine. There are a variety of laboratory-scale tests which assess comminution breakage properties, such as Bond ball mill Work index (BWi), JK Drop Weight Index (DWi) and SMC Test®. The test outputs can be used to predict specific energy. During the early days of the Olympic Dam Geometallurgy program, results from BWi, DWi and SMC Test® tests were used to develop predictive relationships for BWi and DWi as functions of ore characteristics. There are now more than 1700 samples with BWi measurements. Regression models were developed based on sample bulk dry density and chemical composition, which predict BWi at the sample scale. The stope BWi and specific energy are then predicted from the block model estimates of stope density and chemical composition.

Even though the processing plant does not see the full range of ore hardness displayed by the individual samples or stopes due to blending of stope ore during production, the specific energy at the mill does fluctuate according to the composition of ore feed to plant. The regression model effectively reflects this fluctuation which is evidenced by the correlation between actual mill feed specific energy and tonnes weighted stope average BWi of the ore feed over the same period. Currently the milling circuit is not the constraint at Olympic Dam. However, the ability to predict stope average BWi, carry it into the block model and hence into the mine plan can enable material blending among ‘hard’ and ‘soft’ ores to maintain plant feed hardness within the optimum range.

## INTRODUCTION

Olympic Dam is a uranium-bearing, iron oxide copper gold (IOCG) deposit. Disseminated copper sulphide, uranium oxide and gold mineralisation occur within the Olympic Dam Breccia Complex which is hosted within the 1.59 billion year old Roxby Downs Granite. Breccia clasts and matrix span the entire spectrum from granite to hematite-rich endmembers. Minor clast types also include lithologically diverse bedded sedimentary facies and felsic and mafic-ultramafic volcanics and dykes. Hematite alteration is the dominant alteration style within the breccia complex. Even though there are over 100 minerals that occur within the deposit, only 15 minerals (ie hematite, quartz, sericite, chlorite, feldspars, fluorite, barite, siderite, chalcocite, bornite, chalcopyrite, pyrite, sphalerite, molybdenite, galena) are process critical minerals and they account for greater than 99.5 per cent of the deposit mass (Ehrig, McPhie and Kamenetsky, 2012).

The mineralogical and chemical composition of breccia clasts and matrix are often similar, or not. The particle size difference between clasts and matrix can also be similar, or not. Individual breccia zones are typically not mappable. Significant meso-scale textural heterogeneity can occur down to the one-metre scale. Hence, classic domaining based on relatively large volumes of rock containing similar features pertinent to ore hardness is not practical. Ore hardness domains are classified on a drill core sample-by-sample or resource estimate block basis.

Underground mining is undertaken using a sublevel open stoping method with cemented aggregate fill. Ore is crushed underground to a nominal product size of 80 per cent passing 145 mm before hoisted to the surface where an over-land conveyor sends the material to a run-of-mine (ROM) stockpile. Ore delivered to the ROM stockpiles is sourced from ~5 stopes per day (equivalent to ~60 stopes on an annual basis) with approximately 10–20 per cent of the tonnage derived from lateral development (Ehrig *et al*, 2019).

The fully integrated processing plant includes unit operations of grinding, flotation, leaching, solvent extraction, smelting and refining. There are two autogenous mills with independent pebble crusher at the front of the plant. The Svedala and Fuller mills have capacities of 900 t/h and 500 t/h, respectively. ROM ore is ground to 80 per cent passing 75 microns by either one of the two autogenous grinding mills before the sulphide flotation circuit separates copper concentrate from flotation tailings. The $P_{80}$ size was selected during the design phases to maximise sulphide mineral liberation while minimising slimes generation and power wastage. Copper sulphide concentrate is leached to prepare the material for smelting by removing the majority of fluorine and uranium. The leach process has the effect of increasing the copper concentration by removing a portion of hematite gangue. The resultant copper concentrate is smelted in the copper smelter and then electro-refined to produce copper cathode and anode slimes, which are treated in the gold room to recover gold and silver bullion. Flotation tailings containing the majority of the uranium is leached in the hydrometallurgical plant before being concentrated by solvent extraction. The final uranium product is calcined uranium oxide.

## Geometallurgy

The Olympic Dam geometallurgy program officially started in 2006. The program was purposefully designed to mimic the plant flow sheet at that time and focus specifically on processes where metallurgical performance is influenced by mineralogy ie grinding, flotation and leaching. The primary objective of Olympic Dam geometallurgy is to develop metallurgical performance predictors that reliably describe the process performance of different ore types and spatially distribute these into the resource block model for use as a fundamental input into mine planning (Ehrig, 2013; Liebezeit *et al*, 2016). Apart from the recovery of payable metals, there are a wide range of variables that influence processing performance. Table 1 lists the main processes that are influenced by mineralogy. This paper will discuss how we predict ore hardness at the stope level based on existing measured BWi results and compare the model prediction with plant performance.

**TABLE 1**

How minerals affect process performance at Olympic Dam.

| Plant process | Critical minerals | Effect on performance metrics |
|---|---|---|
| Grinding | hematite, quartz | mill throughput and energy consumption |
| Sulphide flotation | chalcocite, bornite, chalcopyrite, pyrite | concentrate copper grade, flotation rate, flotation recovery |
| Tails leach | uraninite, coffinite, brannerite | uranium recovery |
| | chlorite, siderite | acid consumption |
| | chlorite | gelling |

## Test program

The geometallurgy team selects diamond drill core samples (BQTK or NQ2 diameter) from the resource delineation program based on their locality and mine plan in order to maintain a certain level of geometallurgy coverage for the next five years' production stopes. Each sample is a composite of approximately 20 m continuous interval of the half core (the other half is used for resource estimation purposes). Hence, each sample is related back to its original spatial location in the deposit and this information is stored in the database. Samples are initially crushed to 3.35 mm at which stage BWi charges are taken out; the balance will be further crushed to 1.7 mm and split into charges for extensive metallurgical tests. The head sample is analysed for over 30 elements including a wide range of minor elements such as rare earth elements (REE) and potentially deleterious elements. Modal mineralogy, liberation and association within the head sample are measured via various techniques including X-ray Diffraction (XRD) and Mineral Liberation Analyzer (MLA).

The BWi measurement is acquired via the industry standard Bond ball mill test, ie a locked-cycle grinding test that measures the input energy required to grind the material to a specified size at certain throughput. A higher BWi value means harder ore, which requires more energy to grind. So far, over 1700 samples from various locations in the Olympic Dam orebody have undergone a BWi test and Figure 1 shows the distribution of those samples in the deposit. Although this is a data-rich set from the metallurgical viewpoint, the sample support is far too low (by at least 2–3 orders of magnitude) to allow the use of traditional geostatistical estimation techniques in Olympic Dam's 20-million block resource block model. Therefore, a block calculation approach is used. The purpose of the block model calculation is to determine the metallurgical performance of the ore in each block and thus estimate the recoverable products from each block (variable size, 5 × 10 × 5 up to 30 × 30 × 15 m).

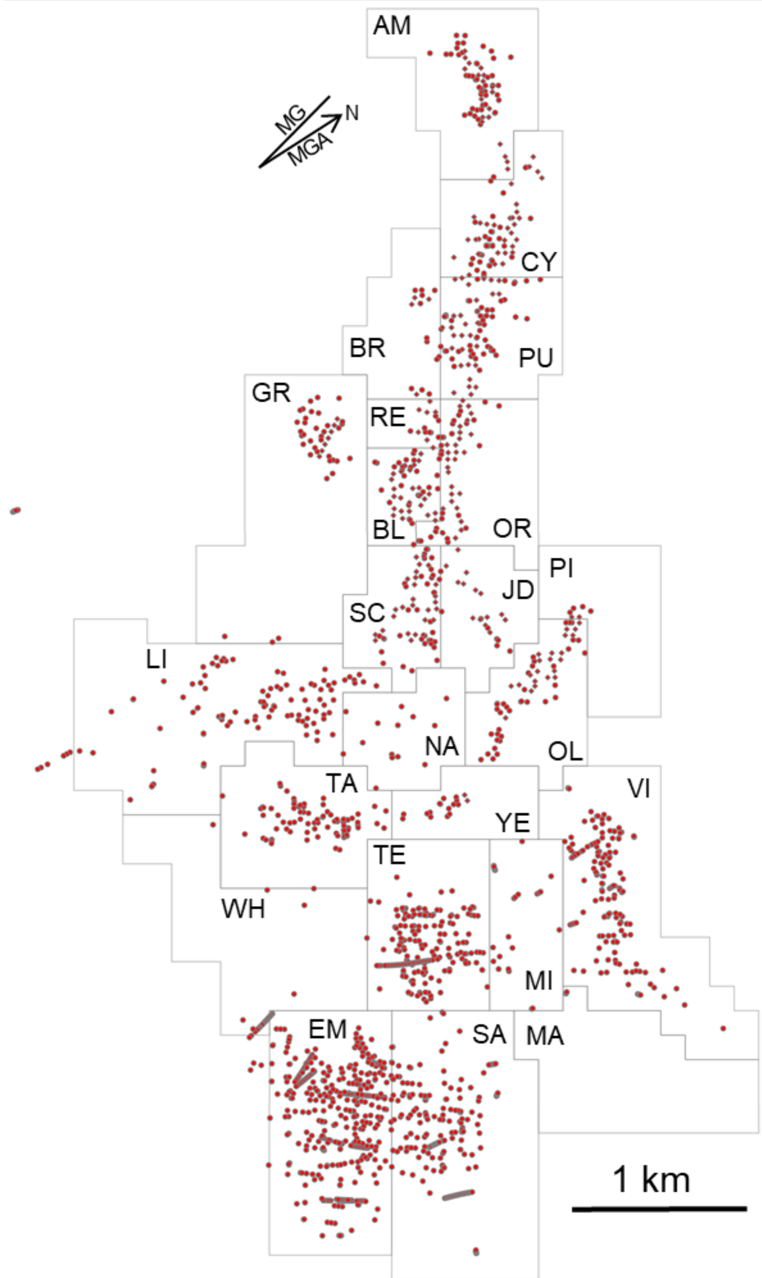


**FIG 1** – Plan view of samples with measured BWi across the Olympic Dam deposit. The abbreviations and boundaries represent different stope/mining areas.

Comminution models determine the throughput rate and therefore the processing time, energy and cost required to achieve the recovered metal. For Olympic Dam, Steve Morrell (SMCC) developed the specific energy model to predict specific power, power consumption and mill throughput (Morrell, 2006). This is in the generic form of Equation 1.

$$\text{Specific energy (kWh/t)} = a \times (DWi^{\,b}) \times (BWi^{\,c}) \times (F_{80}{}^{d}) \times (P_{80}{}^{e}) \qquad (1)$$

a, b, c, d, e are parameters specific for Olympic Dam.

As one of the specific energy model inputs, a geometallurgical model describing the relationship between BWi value and variables which exist in the block model (elements, minerals and density) must be developed in order to calculate BWi on a block level. The BWi model used in the block calculation is the focus of this paper.

## Model development

### *Global model*

As discussed by Ehrig *et al* (2019), concentrator metallurgists at Olympic Dam recognised the relationship between iron to silica ratio (proxy for the relative abundances of hematite, quartz and sericite) of plant feed and mill throughput shortly after plant commissioning in 1988. Of the 15 process critical minerals, hematite and quartz have the major impact on mill throughput and energy consumption. Hematite-rich material consumes less power to break in the autogenous mill, while quartz-rich ore needs more power. Figure 2 shows the relationship between BWi and iron, silicon or density for all available samples with BWI, head assay and density available. These charts demonstrate that the BWi value decreases with increasing iron content and increases with rising silicon. Low density materials have higher BWi compared with higher density material because low-density ore are normally high in quartz, which are harder to grind and low in hematite. Table 2 lists the formula and density for some of the common minerals in Olympic Dam.

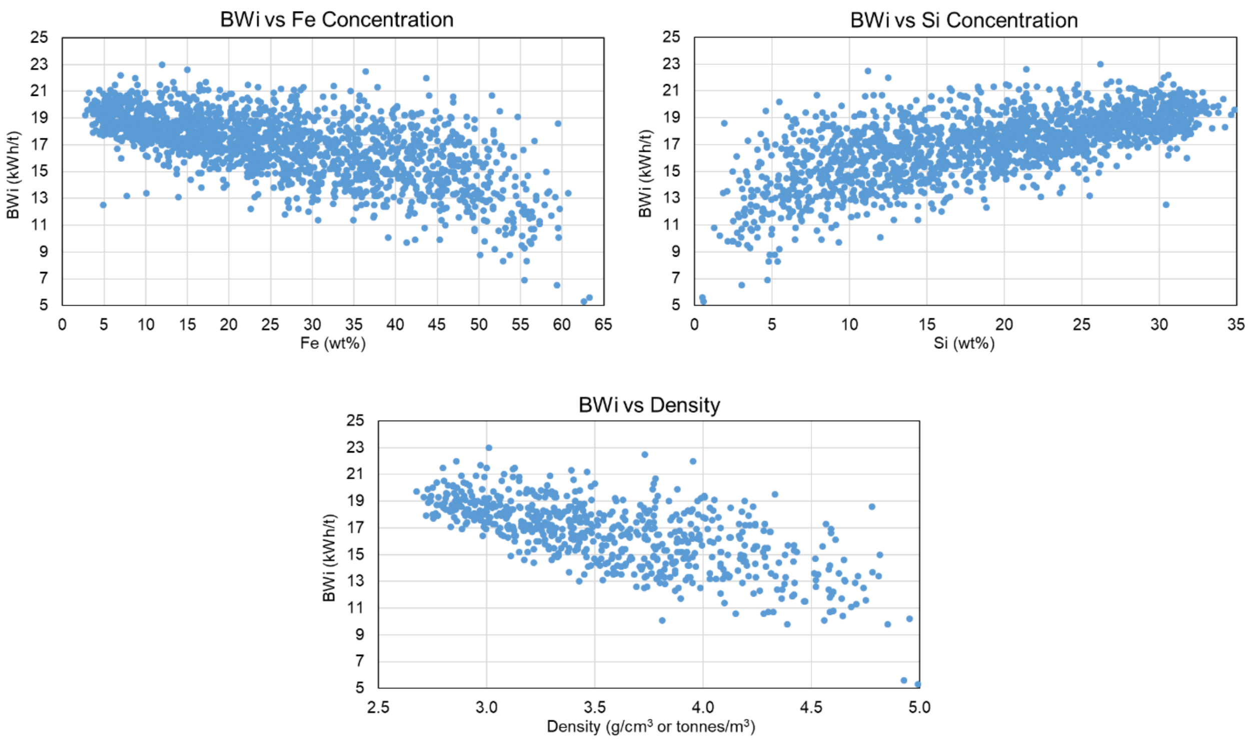


**FIG 2** – Relationship between BWi and head Fe% (top left graph) head Si% (top right graph) and density (bottom graph).

**TABLE 2**

Formula and density for major Olympic Dam gangue minerals.

| Mineral | Formula | Density (g/cc) |
|---|---|---|
| hematite | $Fe_2O_3$ | 5.28 |
| quartz | $SiO_2$ | 2.65 |
| sericite | $KAl_2(Si_3Al)O_{10}(OH,F)_2$ | 2.82 |
| chlorite | $(Fe,Mg)_5Al(Si_3Al)O_{10}(OH,O)_8$ | 3.20 |
| siderite | $FeCO_3$ | 3.96 |
| fluorite | $CaF_2$ | 3.13 |
| barite | $BaSO_4$ | 4.48 |
| K-feldspar | $KAlSi_3O_8$ | 2.56 |

Figure 2 shows the clear correlation between BWi and Fe%, Si% and density but all three sets of data exhibit a large scatter and clearly a single parameter relationship is not sufficient to describe the BWI. Data were grouped by density then binned by 0.5 per cent Si intervals. Figure 3 shows the effect of Si on BWi results varies for different density groups. At high density, Si has a greater effect on BWi than lower density samples. Initially an individual BWi versus Si% model was developed for each density group, but the correlations were not statistically significant, and the model fit was not satisfactory. However, it was identified that both density and Si% could be potential variables in the model. Density alone is not adequate to explain hardness of the ore because one density can be from a wide range of multiple minerals, which all have different hardness characteristics.

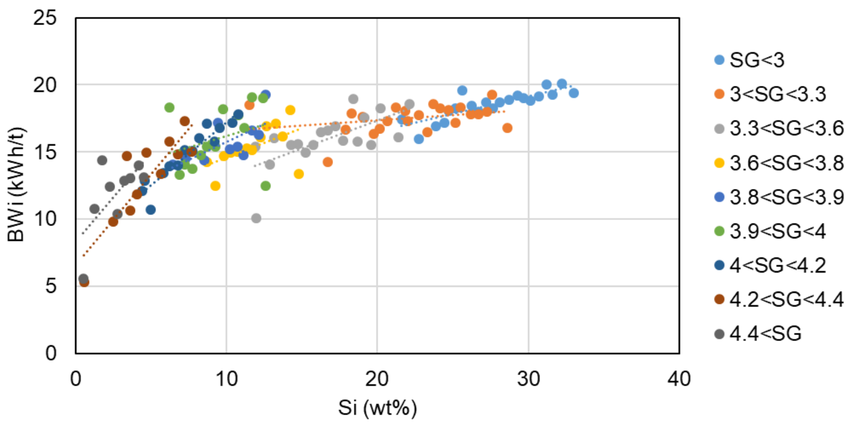


**FIG 3** – BWi versus Si% for different density groups and binned by 0.5 per cent Si.

At the time of the initial global model development, there were 970 data points with enough information (BWi, head assay, mineralogy and density) of which 80 per cent (770) were randomly selected to develop the model and 20 per cent were used to test the validity of the model ('hold-out' data set). Potential models were developed with various head assay, modal mineralogy and density as model inputs. Model selection criteria included best fit (as measured by standard error) and the simplest form. The final global model from this analysis is described in Equation 2.

$$BWi = 0.279 \times Si \times density^{2} - 1.552 \times density \times Si + 2.494 \times Si + 8.769 \quad (2)$$

### *Area-specific model*

The possibility of creating mine area-specific models was also considered. Figure 4 groups existing BWi results by mine area and it shows ore hardness can be quite different for different areas. Some adjacent areas were combined to make sure each group has at least 30 BWi test results so they are a good representation of the area. Note that these mine areas are not based on geological domains or necessarily similar geology, they are more aligned with mineable blocks (ie ventilation and development). However, as shown in Table 3, there are some significant differences in mineralogy and density between areas. This reflects the stope scale mineralogy and breccia textural heterogeneity within the deposit. During the OD open pit expansion study (from 2006 to 2008), deposit scale geomet testing was conducted on samples from the Southern Mine Area. As shown in Figure 1, the number of samples from the Emerald (EM) mine area of is much higher than other areas of the deposit because ore from the Emerald mine area was planned to be the location of the starter pit for the open pit expansion.

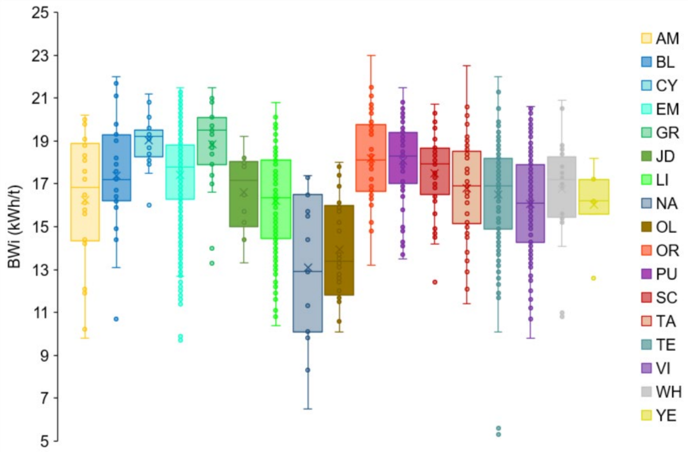


**FIG 4** – Box plots for BWi values of geomet samples grouped by mine area.

**TABLE 3**

Hematite and quartz content for each mine area.

| Area colour | Average hematite % | Average quartz % | Average sericite % | Average density t/m$^3$ |
|---|---|---|---|---|
| AM | 37 | 20 | 16 | 3.7 |
| BL | 28 | 12 | 8 | 3.7 |
| CY | 25 | 22 | 21 | 3.5 |
| EM | 20 | 30 | 16 | 3.15 |
| GR | 22 | 40 | 21 | 3.1 |
| JD | 39 | 14 | 9 | 4.3 |
| LI | 51 | 24 | 14 | 4.1 |
| NA | 68 | 13 | 6 | 4.2 |
| OL | 55 | 12 | 6 | 4.4 |
| OR | 33 | 20 | 17 | 3.9 |
| PU | 30 | 24 | 20 | 3.4 |
| SC | 43 | 19 | 11 | 3.9 |
| TA | 41 | 29 | 20 | 3.6 |
| TE | 41 | 22 | 13 | 3.7 |
| VI | 29 | 26 | 14 | 3.7 |
| WH | 21 | 17 | 9 | 3.5 |
| YE | 30 | 37 | 25 | 3.4 |

Figure 5 shows the key minerals (hematite, quartz, K-feldspar) and density for the Emerald and all other samples in box and whisker charts. It demonstrates Emerald material is high in K-feldspar and quartz but low in hematite when compared with all other samples. With abundant test results available, an area-specific BWi model was developed for Emerald to investigate if the fit is better than the global model. Data excluding Emerald (all other samples) are analysed as well.

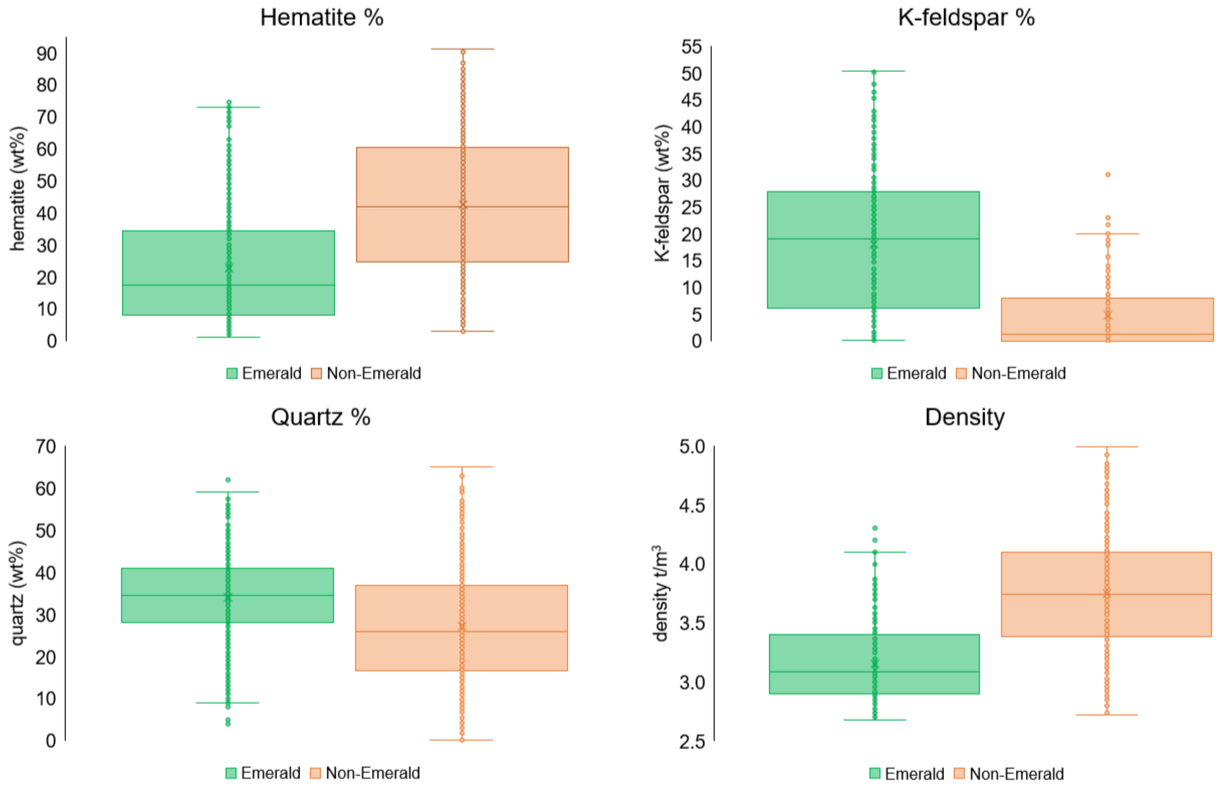


**FIG 5** – Box and Whisker plots comparing Emeralds with all other samples.

For non-Emerald data, the deposit-wide model as described in Equation 2 has the best fit and for Emerald, the area specific model has a slightly improved performance based on standard error. However, the improvement is not sufficient to justify area specific models at this time.

### *Mineralogy model*

Even though the purpose of the predictive geometallurgical models is to populate the block model with estimates of metallurgical performance based on variables that exist in the block model (ie assays, density and modal mineralogy), exploring variables outside the block model improves our understanding of ore hardness behaviour. Detailed mineralogy data acquired via MLA on a coarse size fraction of the head sample are available for the geometallurgy samples. Mineral association data for hematite and quartz were analysed against BWi value but only end up with an over-fitted model with 20 inputs that do not predict any better than the original model. The author also studied the liberation data for hematite and quartz but again failed to develop a better model. Unlike other metallurgical processes such as flotation and leaching, macro-scale breccia textures influence grindability as well as the microscale modal mineralogy. Part of the scatter in our predictive BWi models is likely due to the impact of macro-scale breccia texture variability.

### *BWi test precision*

Initially, it was somewhat surprising that even inclusion of the best available mineralogy data did not produce a substantially better model than the deposit-wide model using density and %Si. Therefore, the limiting precision of the model was examined by considering the inherent errors generated from BWi tests.

The Olympic Dam geometallurgy program includes tests on reference samples on a regular basis including the BWi test. GR001 to GR004 are bulk samples (300–500 kg) collected from various sources such as underground drawpoint sampling or surface stockpile sampling. Ehrig, Liebezeit and Macmillan (2017) summarised the BWi results for Olympic Dam reference samples GR001, GR002 and GR003. Since then, BWi testing on GR002 and GR003 was completed and testing of GR004 commenced. Table 4 shows the results of these four reference samples. The standard deviation of the BWi test ranges between 0.3 and 0.4 kWh/t. The low standard deviation for GR004 is most likely caused by the low number of test results available so far. This result is comparable with Angove and Dunne (1997) published result of 0.34–0.82 kWh/t standard deviation for average BWi value of 15.8–18.0 kWh/t. The slightly higher standard deviation is expected by varying the laboratory, where there may be slight variations in test procedures (Ehrig, Liebezeit and Macmillan, 2017). This means the best a metallurgical model can predict will be ±0.6–0.8 kWh/t around the true BWi value (two standard deviations) and this uncertainty is due to the test itself.

**TABLE 4**

Summary of BWi results for OD reference samples.

| Sample | Number of tests | Mean BWi (kWh/t) | Standard deviation (kWh/t) | Relative standard deviation (%) |
|---|---|---|---|---|
| GR001 | 19 | 17.1 | 0.32 | 2 |
| GR002 | 21 | 16.4 | 0.27 | 2 |
| GR003 | 13 | 16.8 | 0.39 | 2 |
| GR004 | 5 | 16.5 | 0.08 | 1 |

## MODEL PREDICTION VERSUS PLANT PERFORMANCE COMPARISON

Figure 6 displays the predicted BWi in the block model at -400 m RL by applying the BWi model (Equation 2) at the individual resource block scale. The bar chart in Figure 7 presents the distribution of existing BWi test results from the tested samples. The values have a very wide range from 5 kWh/t as the minimum to 23 kWh/t with majority of the data sitting between 16 and 20 kWh/t. However, owing to the intrinsic blending that occurs as a result of extracting ore from multiple stopes during production, material processed in the metallurgical plant has relatively consistent specific energy as shown in Figure 8.

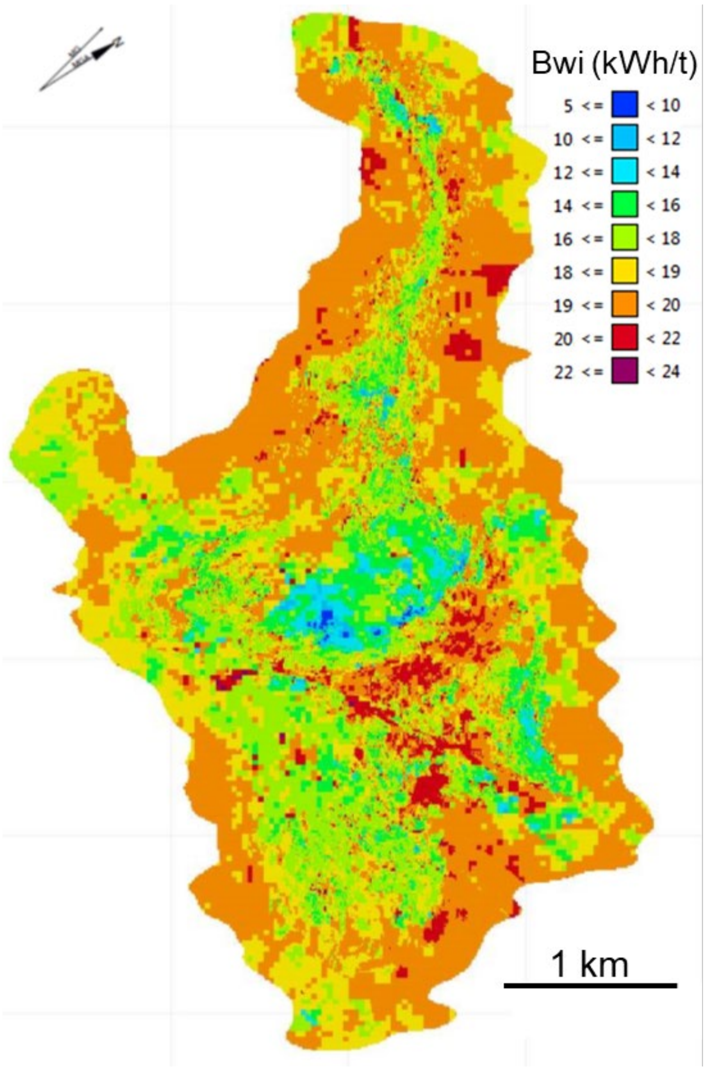


**FIG 6** – Block model predicted BWi at the -400 m RL level.

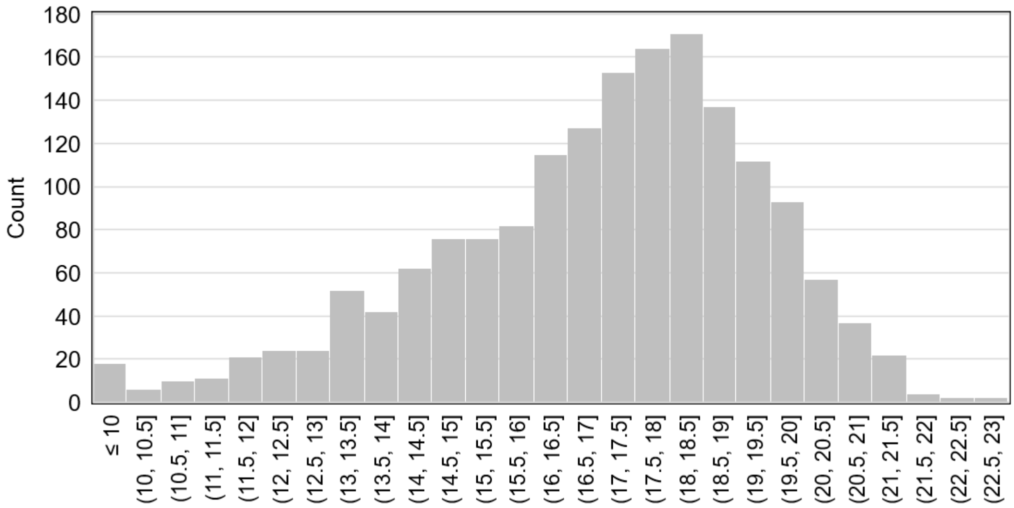


**FIG 7** – Histogram of BWi values for the Geometallurgy samples.

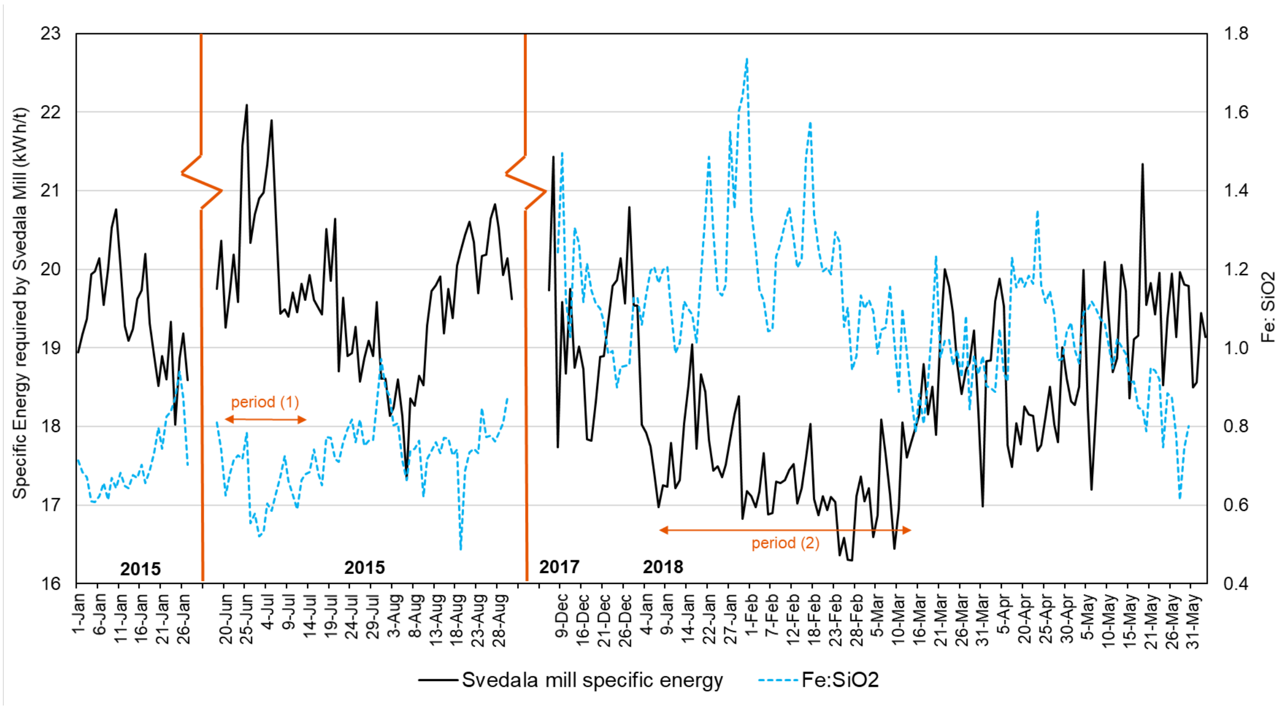


**FIG 8** – Daily variation in specific energy for Svedala mill for periods from 01-Jan-2015 to 27-Jan-2015, 18-Jun-2015 to 31-Aug-2015, 08-Dec-2017 to 03-Jun-2018. Refer to Figure 9 for discussion about period (1) and period (2).

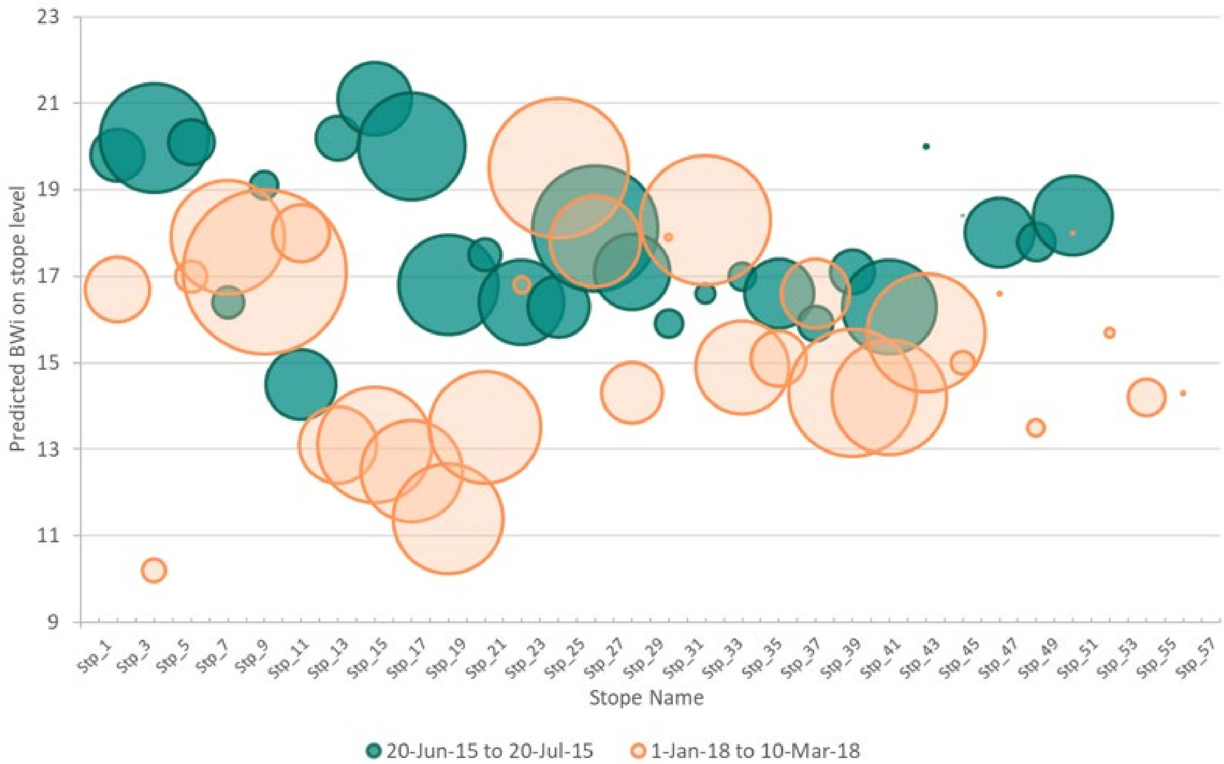


**FIG 9** – Bubble chart showing predicted stope level BWi and tonnages fed to plant for two periods: (1) 20-Jun-15 to 20-Jul-15 and (2) 1-Jan-18 to 10-Mar-18 with each bubble representing a production stope and bubble size indicating the relative tonnage.

The plant daily average specific energy for the Svedala mill was calculated by dividing average mill power consumption by average mill throughput, which were obtained from the plant production database. Figure 8 graphs the daily specific energy of three separate periods because they were relatively free of major outages and able to demonstrate a reasonable historical range along with plant feed Fe:$SiO_2$. Plant specific energy for the selected periods fluctuates between 16 and

23 kWh/t, which has an expected narrower range than the stope-based samples. Plant specific energy of two periods were investigated here: (1) 20-Jun-2015 to 20-Jul-2015 with specific energy hovering between 19 and 22 kWh/t and (2) 1-Jan-2018 to 10-Mar-2018 with specific energy on the low side between 16 and 19 kWh/t. This chart also confirmed the inverse correlation between $Fe:SiO_2$ and specific energy. Feed $Fe:SiO_2$ were trending low (around 0.8) for period (1) then rose to about 1.2 for period (2).

In order to identify the cause of high/low specific energy for above specified time frames, ore source (ie stope source) and corresponding tonnages fed to the processing plant for those two periods were retrieved from the mine production management system. Predicted BWi on the stope level is determined by applying the BWi model on stope average chemistry and density then reviewing the results for samples in the local region of the stope and modifying if appropriate. The review is performed for stopes about to enter production, while stopes in longer-term plans have the block modelled BWi applied.

Weighted average BWi for those two-time frames was calculated and exhibits similar patterns where period (1) has a higher value than (2). Individual contributing stopes for those two periods were analysed and predicted BWi and tonnages fed to processing plant were presented in Figure 9. There are more stopes/tonnages with low BWi values processed in the plant during period (2) compared with period (1). This demonstrates that the model reflects the plant behaviour, although the nature of the underground mine (multiple stope areas open at any time) means that the mill feed will always be less variable than the range shown for the geometallurgy samples.

Currently mill throughput is not a constraint for Olympic Dam and specific energy is not one of the parameters that is considered in the mine plan, although BWi can be analysed and reported for any schedule (as can DWi, the modelling of which is not discussed here). However, having it in the block model gives us the ability to plan around mill throughput and energy consumption if the need arises in the future.

## CONCLUSION

At Olympic Dam, the geometallurgical BWi model is an input to the specific energy model which is used to predict mill throughput, energy and cost required to achieve a specified product size. Variation in gangue mineralogy (proxy from ore density) at the micro-scale and breccia texture on the meso-scale impacts on ore hardness, hence BWi. The predictive error of the current BWi model is partially from the BWi test itself and partially from variation in gangue mineralogy and breccia texture. Our BWi model development certainly supports the axiom “rock type controls throughput and mineralogy controls metallurgy” (Bill Johnson and Peter Munro, personal communication).

Modelling of one mine area with the greatest number of samples showed an improved prediction over the global model based on standard error. There is insufficient data for each of the other areas for specific models although this remains a focus of further work.

The mill has rarely been the bottleneck for Olympic Dam owing to both upstream and downstream constraints. The current BWi model based on dry bulk density and %Si is fit-for-purpose. If the mill becomes the plant constraint, modelling using breccia texture classification, for instance based on image classification, could be an option in further BWi model development. It is likely that closer space sampling for BWi measurements will also be required. However, at the moment and into the foreseeable future, this is not necessary.

## ACKNOWLEDGEMENTS

The authors thank BHP Olympic Dam for permission to publish this paper.

## REFERENCES

Angove, J E, Dunne, R C, 1997. A review of standard physical ore property determinations, in *Proceedings World Gold’97 Conference,* pp 139–144 (The Australasian Institute of Mining and Metallurgy: Melbourne).

Ehrig, K, 2013. Geometallurgy – what do you really need to know from exploration through to production? in *Proceedings MetPlant 2013*, pp 28–33 (The Australasian Institute of Mining and Metallurgy: Melbourne).

Ehrig, K, Liebezeit, V, Macmillan E, 2017. Metallurgical QA/QC – Who needs it? The Olympic Dam Experience, in *Proceedings MetPlant 2017*, pp 31–44 (The Australasian Institute of Mining and Metallurgy: Melbourne).

Ehrig, K, Liebezeit, V, Smith, M, Pewkliang, B, Li, Y and Macmillan, E, 2019. Effect of gangue mineralogy on flow sheet design and plant operation – Olympic Dam, in *Proceedings MetPlant 2019*, pp 15–28 (Australasian Institute of Mining and Metallurgy: Melbourne).

Ehrig, K, McPhie, J and Kamenetsky, V S, 2012. Geology and Mineralogical Zonation of the Olympic Dam Iron Oxide Cu-U-Au-Ag Deposit, South Australia, in *Geology and Genesis of Major Copper Deposits and Districts of the World: A Tribute to Richard H. Sillitoe* (eds: Hedenquist, J W, Harris, M and Camus, F), Society of Economic Geologists Special Publication 16, pp 237–268.

Liebezeit, V, Ehrig, K, Robertson, A, Grant, D, Smith, M and Bruyn, H, 2016. Embedding geometallurgy into mine planning practices – practical examples at Olympic Dam, in *Proceedings The Third AusIMM International Geometallurgy Conference 2016*, pp 135–143 (The Australasian Institute of Mining and Metallurgy: Melbourne).

Morrell, S, SMCC, 2006. Throughput modelling using drill core data, internal report to Olympic Dam.

# Recovery opportunity models driving multi-disciplinary improvement

*L Napier[1] and M Livingstone[2]*

1. Senior Metallurgist, Newcrest Mining Limited, Telfer Operations, Telfer WA 6762. Email: lara.napier@newcrest.com.au
2. MAusIMM, Metallurgy Superintendent, Newcrest Mining Limited, Telfer Operations, Telfer WA 6762. Email: matthew.livingstone@newcrest.com.au

## ABSTRACT

An understanding of target mineral recovery is vital in the development of operational philosophy, control system design, and maintenance allocation for optimal processing plant performance. As ore feed and conditions within the plant change, missed recovery opportunities move between unit processes and quick identification of these areas can be used as a short interval control tool to maximise the recovery within the process plant.

Daily mineral recovery is calculated with the return of assay results; however, this data is only available two days post the recovery opportunity being missed.

This paper presents the development of a recovery opportunity tool implemented to create a zero financial spend, collaborative approach aimed at improving operational discipline and subsequent mineral recovery. Factors influencing mineral recovery were identified, their optimal values determined, and a short interval control model created to provide near real time information about when a factor has deviated from optimal operation. The model consists of operational variables measured online, combined with regression coefficients to determine the recovery opportunity currently available, as well as opportunity missed in the previous day to encourage maintenance focus on influential areas.

This approach has been implemented successfully at the Telfer Gold Mine with significant gold and copper recovery improvements seen as a result. The model proves valuable for not only operational discipline, but has resulted in a single focus between maintenance, operations, and process control. Missed recovery opportunity is used as a tool to enable the maintenance emphasis on identified areas within the plant, as well as providing financial justification for process control initiatives. The model is regularly updated to ensure that focus areas are still relevant and have not been surpassed by different unit operations within the plant.

## GLOSSARY

| Term | Definition |
|---|---|
| Random forest | A random forest model is a based on typical regression trees and uses the concepts of bagging to generate a forest of decision trees, each with equal weight to calculate the prediction. |
| Principal component analysis | Method to reduce the dimensionality of data set by representing correlated variables via a reduced set of uncorrelated variables, known as principal components. |
| Out-of-bag observations | As each tree in a random forest model is generated, the observations not used in its development become part of the out-of-bag set. |
| Bootstrap aggregating (bagging) | Method of subsampling from a large set of data whereby a specified number of training sets are created from the full data set each with ⅓ the number of predictor variables and ⅔ the number of observations. |

# INTRODUCTION

Telfer is a gold-copper dual train concentrator operation in the Pilbara region of Western Australia. Ore is mined from the Main Dome and West Dome open pits, along with an underground mining operation. West Dome is a low-grade auriferous pyrite orebody and is the predominant ore source for future processing. As of December 2017, West Dome has a mining inventory of 200 MT 0.62 g/t gold, and 0.06 per cent copper with appreciable pyrite (Newcrest, 2018).

Large geometallurgical disparities are seen throughout the orebody including variations in head grade, copper and gold mineralisation, subsequent Cu:S ratio, and physical properties including hardness and competence. Consistent production of a saleable copper concentrate grade, whilst maintaining gold/copper recovery, is a key issue complicated by the low copper head grades in West Dome ranging from nuance copper levels of 0.05 per cent up to readily floatable material of 0.11 per cent.

The processing plant at Newcrest's Telfer Operation consists of gravity gold concentration, production of a copper concentrate via sequential copper-pyrite flotation, and cyanide leaching of gold from pyrite concentrate as shown in Figure 1. Grinding unit operations are fed by ore from a primary gyratory crusher and consist of one 15 MW SAG mill and 13 MW ball mill in closed circuit with primary classifying cyclones per grinding train (two of). Typical plant throughputs range between 2600–3400 t/h.

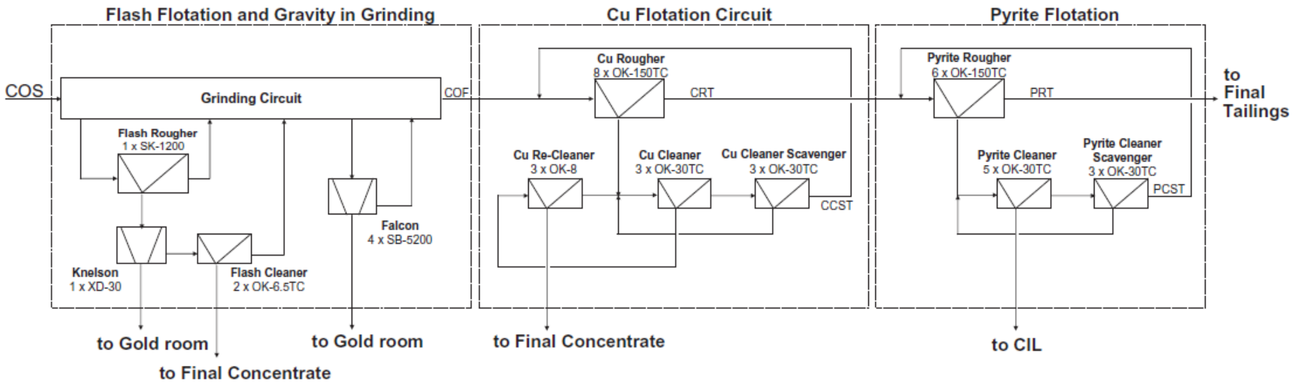


**FIG 1** – Telfer circuit flow sheet (Zheng *et al,* 2010).

A nominal portion of primary cyclone feed is split off, screened, and then processed through four parallel SB5200 Falcon gravity concentrators, with recovery ranging between 15–20 per cent, to produce a gravity gold concentrate for further refining in the Gold Room. Gravity gold catchments are predominantly liberated gold with a typical grade range between 60–90 per cent Au.

Primary cyclone underflow material is split between ball mill feed and a flash flotation circuit. Cyclone overflow reports to copper flotation from which the concentrate (10–14 per cent Cu) is pressure filtered and trucked to Port Hedland for ship loading. Copper flotation tail reports to a pyrite flotation circuit. The plant can run in Bulk Flotation (BF) mode, whereby the pyrite concentrate reports to the copper concentrate, however it is preferential to run in Sequential Flotation (SF) mode whereby the pyrite concentrate is reground and treated through cyanidation leaching circuit. Auriferous pyrite is the primary gold bearing mineral in the feed resulting in the pyrite circuit accounting for approximately 10 per cent gold recovery.

# PROJECT SCOPE AND OBJECTIVE

High annual material treatment targets at Telfer meant that throughput often took priority over recovery. This mindset facilitated decision-making that did not necessarily deliver the most value for the operation in terms of total gold and copper production. In lieu of this, the problem definition is defined as:

- No multi-disciplinary focus on key recovery drivers causing an inconsistent and reactive approach to maintenance and operations practices.

Although daily gold and copper recovery is calculated with the return of assay results, at Telfer this data is only available two days post the recovery opportunity being missed. This lack of granularity in recovery results creates a disconnect between daily performance and suggested operational strategies. Further to this, different teams within the workspace operated under different recovery assumptions leading to instabilities within the processing plant.

Creation of a near-real time gold recovery model built on feed material and operational conditions provides an opportunity for more timely gold recovery results and the use of short interval control tools.

The following scope of work is presented in this paper to address the issues identified.

1. Creation of a Daily Recovery Opportunity report each morning outlining the recovery opportunities missed in the previous 24 hours.
   - Distribution of the report to plant operational crews and metallurgy team.
   - Presentation of the report at the daily morning meeting involving mechanical, electrical, process control, metallurgy, and production to allow recovery driven decision-making.
2. Creation of near real time short interval control dashboards.
   - Quantification of the impact of key gold recovery levers identified during model building shown in near real time to operations teams.

# APPROACH AND IMPLEMENTATION

## Recovery model generation

The purpose of the gold recovery model is to provide recovery performance information in a timely manner to assist in recovery driven decision-making. Both operationally non-controllable and controllable variables were used in model generation to account for variations in feed grades, while still capturing key operationally controllable recovery levers. Key variables used are shown in Table 1.

**TABLE 1**

Model variables.

| **Predictor variable** | **Non-controllable** | **Controllable** |
|---|---|---|
| Feed grade gold | ● | |
| Feed grade copper | ● | |
| Feed grade sulphur | ● | |
| Mill throughput | | ● |
| SAG mill feed stability | | ● |
| Gravity circuit utilisation | | ● |
| Copper flotation mass pull | | ● |
| Copper/pyrite flotation operation mode | | ● |

Daily predictor and response data were filtered for SAG mill runtime <50 per cent and to remove non-complete observation sets leaving ~300 records for model prediction.

Principal component analysis (PCA) and correlation coefficients were investigated before any recovery modelling to look for collinearity within the data set and to determine variable importance. Although a portion of collinearity is almost inevitable when including multiple operational variables in a data set, care was taken to minimise the effect of exaggerated variable influence as a result.

Regression analysis was completed to determine how the total gold recovery depended on one or more of the identified recovery levers. An iterative approach was used during the analysis to filter out variables with P-values greater than 0.05 and to ensure the significance F is less than 0.05 (as

5 per cent significance level was used in evaluating the model). The resultant linear regression could explain 59 per cent of variance in the response variable ($R^2$ of 0.59).

Non-linear models including random forests were also built to explain a larger portion of the variance in the gold recovery values. Although a slightly greater parity plot $R^2$ of 0.64 was achieved, the black box nature of the model inhibits the direct translation to daily reporting based in Excel. The linear regression model was selected for further development as it stops the issue of time lagged data and is easily updated with recent records as variable influences change.

## Model limitations

In this project, the response variable was artificially upsampled by averaging the real-time plant data (mass pull, mill stability) over a 12-hour period to align with gold recovery calculated through shift-wise composite assays. This is likely to be an oversimplified approximation of the variation in the actual predictor variable influence on gold recovery but was necessary in the absence of more information. The alternative approach of downsampling the operational variables was not applicable due to the nature of concentrator feed sampling.

Another model limitation is the manual model updating procedure. Model validation is currently done based on tracking variable influence and time since last update. Although retraining the model on recent observations is necessary, this approach neglects the concept that a deviation of model behaviour can be simplified to two issues:

1. Operational behaviours, control instrument failure, or mechanical limitations in the processing plant causing erroneous model predictor measurements.
2. Process drift and distribution of model predictor data shift causing the model input data to differ from the distribution of the training data.

If the distribution of the model predictor changes, then retraining on a new observation set is required; however, if it is an operational reason causing the deviation of model behaviour then retraining the model can simply mask an underlying issue.

Recalibration of the sensor using principal component analysis (PCA) and autoencoder feature space is discussed in the future recommendations section.

## Daily reporting

Target values were assigned to each of the key operationally controllable variables shown in Table 1 which had a p-value less than 0.05 during the regression analysis. Daily recovery model reporting was created using the target values and model coefficients to determine the recovery opportunity for the previous day's operation. Equation 1 shows the generalised recovery opportunity formula for operationally controllable 'Variable A'. Model coefficients also allow a baseline understanding of the impact that a step change in the nominated variable has on overall gold recovery.

$$Recovery\ opportunity_{(VarA)} = Coefficient_{(VarA)} \left[Target_{(VarA)} - Measurement_{(VarA)}\right] \quad (1)$$

The daily reporting tool shows the recovery opportunity missed for the previous 24 hours of operation and encourages commentary and investigations to outline causes of missed opportunities (Figure 2).

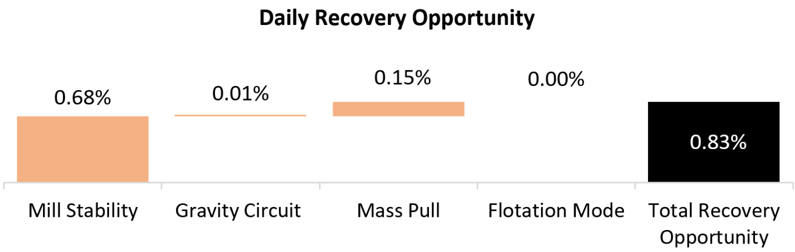


| | | |
|---|---|---|
| **Mill stability** | 0.68% | SAG trip due to blocked chute, ramp up after restart, throughput capped for flotation restrictions. |
| **Gravity circuit utilisation** | 0.01% | Falcon 1 VSD trip (2.5hrs). |
| **Copper rougher mass pull** | 0.15% | Air for three copper roughers greater than 90% indicating inability to meet controller SV and potential loss of pullrates – may need additional blower to meet SV. |
| **Flotation mode** | 0.00% | |
| **Other recovery impacts** | High froth in copper cleaning circuit limiting cleaning capacity, level control issues rectified by calibration and mechanical adjustments. | |

**FIG 2** – Recovery opportunity waterfall chart and commentary.

Commentary on the daily opportunity is aimed to at classifying the issues in direct causation trees with specific information given regarding equipment malfunctions or deviations from operational philosophy. This opportunity report is presented each morning at a meeting involving key stakeholders in operations, maintenance, control, and metallurgy teams. The benefit of the discussion at this daily meeting is to align multidisciplinary focus on the key variables identified as having a negative influence on gold recovery.

An additional benefit from daily reporting is the greater understanding of recovery levers by planners and maintenance teams. Appropriately timed planned maintenance works can then be given to equipment and unit operations shown to have the most influence on overall plant gold recovery. Subjectivity and speculation are reduced in priority work allocation in both day-to-day and long-term planning as a result.

Comparison between actual and model plant gold recovery is also shown in the report to prompt discussions outlining other possible recovery levers which are not explicitly identified in the model. An example is shown in Figure 3. Understanding the causes of high and low model predictions helps narrow the scope of non-considered factors which caused performance to exceed/fall below model prediction.

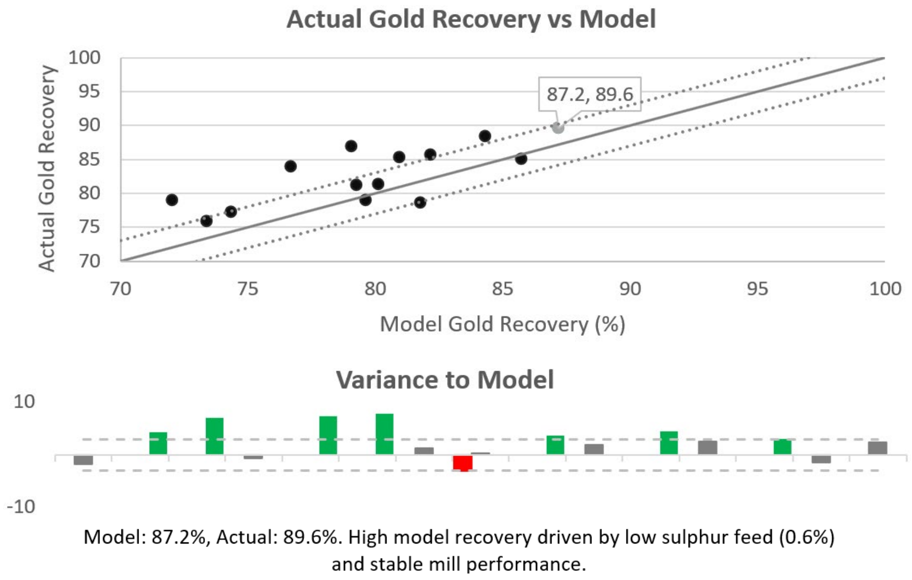


**FIG 3** – Actual versus model gold recovery.

## Short interval control

Short interval control dashboards were created using the operationally controllable recovery opportunity coefficients with real-time plant data. Recovery opportunity is displayed in a waterfall chart of the levers which were negatively impacting gold recovery at that point in time. Example shown in Figure 4.

Dashboards were built in Excel to stop clunky data pull requirements or specific applications being needed on each computer in which they are used. Operations crews in the plant routinely use the dashboards to ensure that factors directly in their control are running optimally with regards to gold recovery, while still meeting concentrate grade requirements.

A problem identified during dashboard roll out was the differing way each crew made process changes to reduce the recovery opportunity. Large discrepancies in operational methodology between crews was found and prompted the creation of trigger action response plans. Theoretically, and practicably achievable, targets for each influential area were documented and embedded in reinvigorated operational philosophies. Initially, the philosophies were organic in nature while being refined in conjunction with the operational teams. This unified approach to ensuring gold recovery between operations teams increased circuit stability, otherwise disrupted by inherently unsteady constant parameter changes.

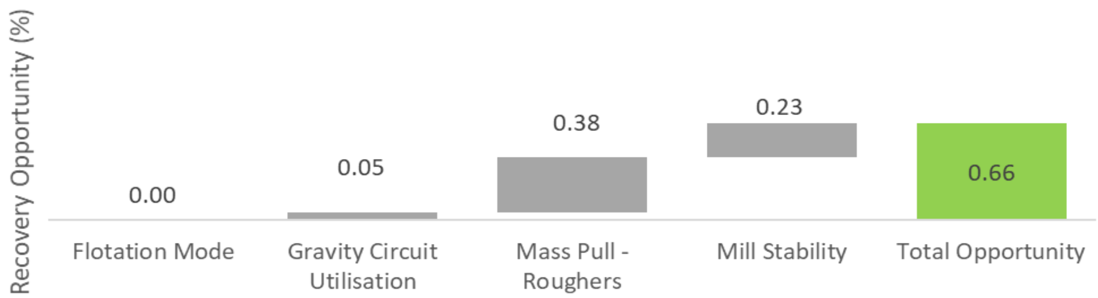


**FIG 4** – Recovery opportunity short interval control dashboard.

# BENEFIT

There has been a significant improvement to both gold and copper recovery since the implementation of the opportunity model. The implementation and benefit observed was in two stages:

- Phase 1 – identification and focus on key areas at a technical and leadership level.

- Phase 2 – implementation of the live short interval control being managed live by the operations and maintenance teams.

The benefit from the reduction in opportunity is displayed in Figure 5.

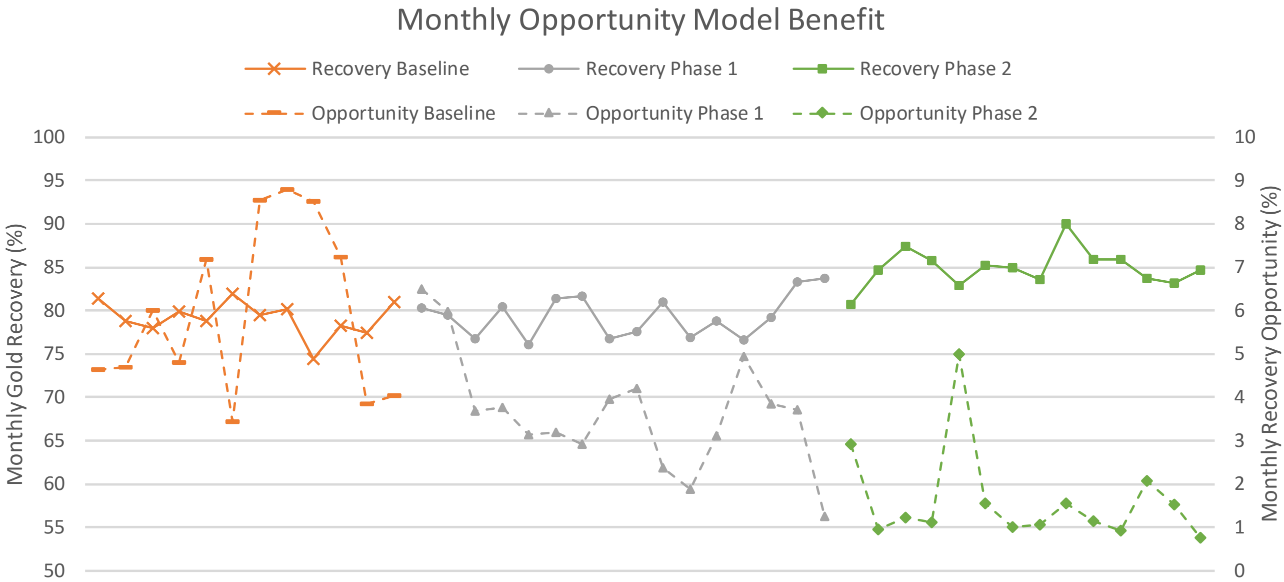


**FIG 5** – Plant recovery and recovery opportunity (July 2016 to December 2019).

A portion of the 5.4 per cent recovery uplift from the baseline to the end of Phase 2 can be associated with a change in feed mineralogy, however a significant amount (4.1 per cent) is associated with the reduction in recovery opportunity through the single, cross-collaboration focus. The impact on total recovery started to be observed through Phase 1 of the implementation, however a step change improvement in total recovery was only seen upon the implementation of Phase 2. This highlights the importance of short interval control, with the live management of the key recovery impacts being a critical part.

Another key indication of the success in the implementation of the recovery opportunity model is the reduction in variation of recovery (Figure 6). The standard deviation of daily recovery data reduced from 6.3 per cent in the baseline period to 5.6 per cent in the Phase 2 implementation. Along with the reduction in standard deviation, the reduction of low recovery outlier days played a major part. Noting that the maximum recovery did not change significantly through the implementation period, however the minimum recovery achieved shifted from 65 per cent to 72 per cent upon implementation of Phase 2.

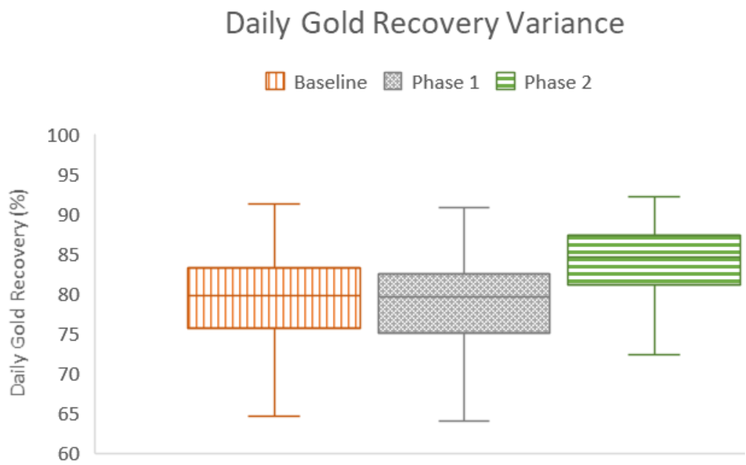


**FIG 6** – Recovery variation reduction.

Improvement actions undertaken as part of Phase 1 included, but was not limited to:

- Planned maintenance strategies optimisation:
  - Copper rougher concentrate pumps – PM modified from 8 monthly to 4 monthly early 2019 after identifying importance of performance on recovery.
- Increasing stock holdings of key parts:
  - Falcon rotables – several changes with Falcon rotable parts, changing from 1-piece to 2-piece baskets, more economical for repairs; changed liner material for the lids, eliminates wear issues, improved lid design, new serial number system initiated for all rotables, used to track condition and eliminate and replace poor quality units, which is currently difficult due to lack of oversight data.
- Prioritisation of key operations and maintenance tasks.

These key steps resulted in a significant improvement to the gravity circuit utilisation resulting in the recovery opportunity decrease (Figure 7) and operation in the correct flotation mode (Figure 8).

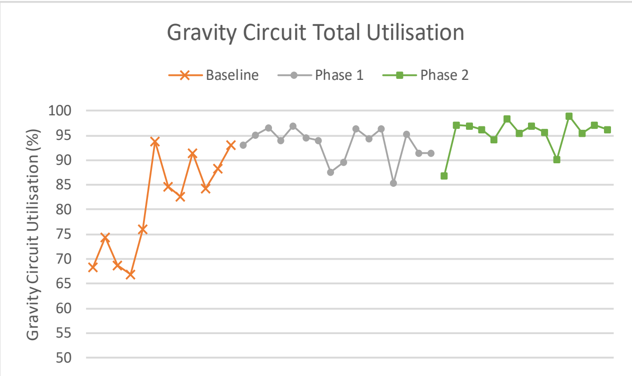


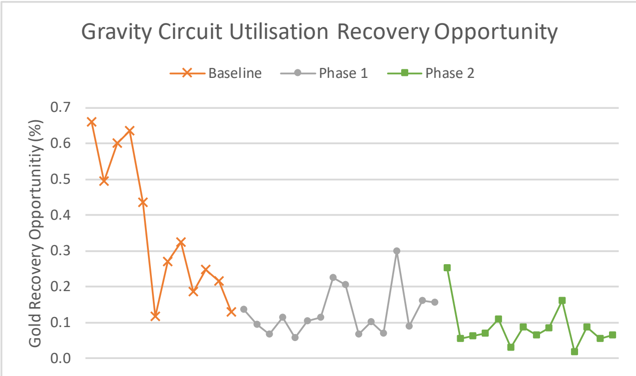


**FIG 7** – Gravity circuit utilisation increase and recovery opportunity (July 2016 to December 2019).

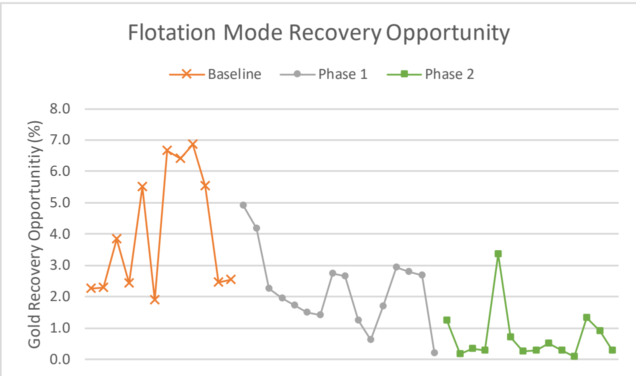


**FIG 8** – Flotation mode recovery opportunity reduction (July 2016 to December 2019).

Further work was undertaken as part of Phase 2, with the key improvement actions undertaken included, but were not limited to:

- daily reporting
- short interval control.

As discussed above these were key in embedding the improvements seen in the gravity circuit utilisation and operation in the correct flotation mode, but they also resulted in a significant improvement to copper rougher mass pull (Figure 9).

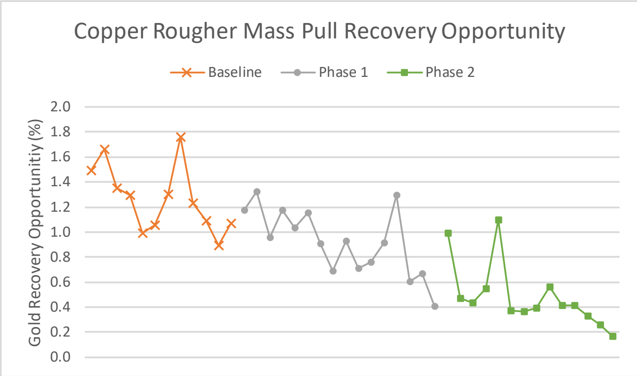


**FIG 9** – Copper rougher mass pull recovery opportunity reduction (July 2016 to December 2019).

Further work is still underway to continuously improve, with the current major focus being mill throughput stability (Figure 10). This is yet to see the same benefit as the other key levers identified, however the continual focus will ensure the best chance of success in reducing the recovery opportunity associated with it.

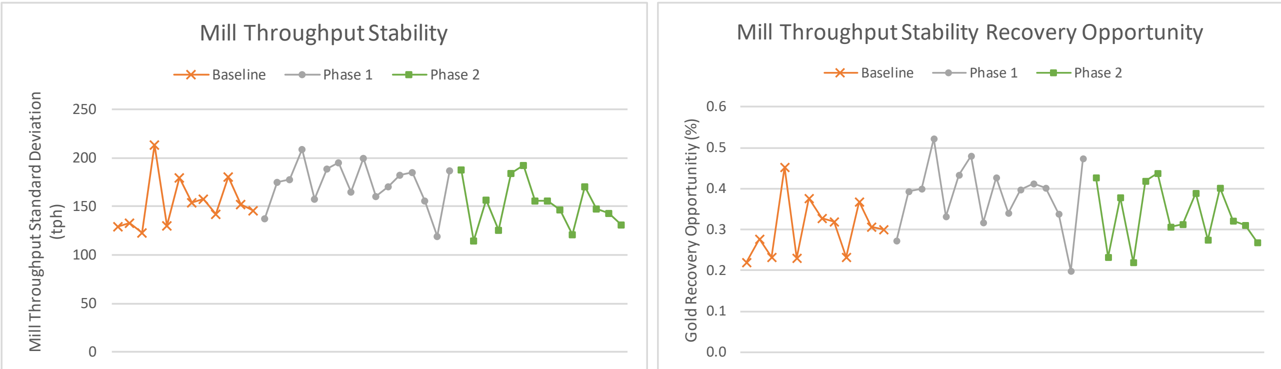


**FIG 10** – Mill throughput stability and recovery opportunity (July 2016 to December 2019).

## PROPOSED IMPROVEMENTS

As previously noted, upsampling of the data was necessary due to the lack of concentrator feed information needed to downsample accurately. Considering this, methods of feed material sampling have been corrected in the plant to allow an even greater understanding of feed material influence on operational conditions and recovery. As the measurement is online, future iterations of the model can be more discrete with sample intervals and better capture variable influence on the recovery response variable.

Another limitation of the current model iteration is the non-quantitative governing as to when the model requires retraining. Tracking of variable influence on recovery through linear coefficient magnitude is done regularly to monitor if the impact has reduced to a point at which daily recovery opportunity is negligible. As the model assumes linearity within the data, the coefficients and regression statistics are the primary method of determining variable importance, yet do not consider purely operational factors such as equipment malfunctions in the plant. Proposed options to validate model performance are variable importance through random forests out of bag prediction error and principal component coefficients, with process shift seen through autoencoders and principal components in the feature space (Napier and Aldrich, 2017).

### Variable importance

Random forest variable importance is either completed using random variable permutation or out of bag prediction error. A variable in the out of bag data is permuted, substituted back into the out of bag set and run through the tree constructed using the bootstrap sample. Each variable is treated in the same method with the error incurred due to each variable being saved for each tree. Intermittent checking of variable importance in this manner can be used as a tool in the recovery opportunity model to select which variables should be a dominant focus in the daily reporting.

Another linear method to determine variable importance is by looking at the principal component variable coefficients. PCA aims to reduce the dimensionality of large data sets by representing correlated variables manipulated by the same driving force into a reduced set of uncorrelated variables. If the sum of the variances in the first components accounts for a significant portion of total variance in the data set, then the remaining components can be disregarded; hence a reduction in dimensionality. Although dimension reduction is not required in this application, the coefficients applied to each variable in the first few components can be used as an indicator of influence on overall data set variance. Again, checking variable importance in this manner could assist with determining which variables to include and not include in model training and short interval control creation.

Dimensionality reduction through autoencoders can often account for a greater portion of variance in the input data compared to PCA. This suggests that there is an element of underlying non-linear structure and correlation between predictor variables and can be used for greater understanding of predictor variable behaviour.

## Model retraining

A self-diagnostic model can track the degradation of model quality and indicate when the model needs to be recalibrated with more recent process data. Variable importance can be used as an indication that recovery levers within the plant are shifting but may not capture when there is a process shift away from the data distribution the model was trained on. A process shift can be detected in complex mineral processing applications by comparing recent measurements to those within historical data sets. This however is not a trivial task. Subtle changes are not easily detected with linear methods such as PCA and may require non-linear feature extraction methods such as auto-associative neural networks (auto-encoders).

Projecting the new data onto the phase space defined by the first three principal components can be used for model validation by generating a visual representation of whether the apparent shift in the system is due to movement in the data distribution. Decision boundaries are then formed using the representation and used as a tool to indicate model updating is required.

Auto-encoders follow the same principal of dimensionality reduction but are non-linear. Features of the data can also be extracted using auto-encoders and be used in the same fashion as PCA to analyse process shift.

# CONCLUSIONS

The recovery opportunity model implemented at Telfer has proven valuable in improving operational discipline across a range of working groups. Despite some limitations of the model, its consistent application has provided a single and consistent focus for these groups. Ultimately, a significant improvement in gold recovery has been observed over a consistent 2.5-year implementation period.

# ACKNOWLEDGEMENTS

The authors would like to acknowledge the metallurgy and operations teams involved in the successful implementation of the recovery project initiative. Collective knowledge and combined dedication from everyone involved made the recovery project execution a success. The authors would also like to thank Newcrest Mining Limited for the allowing the data to be presented and published.

# REFERENCES

Napier, L.F.A., Aldrich, C., 2017. An IsaMillTM Soft Sensor based on Random Forests and Principal Component Analysis. IFAC-PapersOnLine 50, 1175–1180. doi:10.1016/j.ifacol.2017.08.270

Newcrest Mining Ltd. (2018). Annual Report 2018. Available at: https://www.newcrest.com/investor-centre/reports (Accessed: 12 February 2020).

Zheng, X., Manton, P., Griffin, P., 2010. Operating strategies to maximise gold recovery at Telfer. Minerals Engineering 23, 1159–1166. doi:10.1016/j.mineng.2010.03.014

# Application of process data to identify process improvement opportunities – case study: Antofagasta Mineral S.A.'s Los Pelambres

*M Yahyaei[1], D Silva[2], N Manzanares Morales[3], I Yutronic Nunez[4], N Aguila[5] and J Ojeda[6]*

1. Associate Professor, Julius Kruttschnitt Mineral Research Centre, The University of Queensland, Brisbane Qld 4068. Email: m.yahyaei@uq.edu.au
2. Process Control Superintendent, Teck Chile, Santiago, Chile. Email: daniel.silva@teck.com
3. Process Management Superintendent, Minera Los Pelambres, Santiago, Chile. Email: nmanzanare@pelambres.cl
4. Sulphide Process Expert, Antofagasta plc, Santiago, Chile. Email: iyutronic@aminerals.cl
5. Associate Professor, Department of Electricity, Universidad Tecnológica Metropolitana, Santiago, Chile. Email: norelys.aguila@utem.cl.
6. Research Engineer, SMI-International Centre of Excellence, Santiago, Chile. Email: j.ojeda@smiicechile.cl

## ABSTRACT

Advances in sensors and digital technologies enable operations, collecting a vast amount of data from the operation. The real-time Plant Information (PI) data which are continuously being collected and stored, is a valuable source of information for assessing the performance of the process control and identifying opportunities for improvement. In recent years with Artificial Intelligent (AI) becoming popular and easy to utilise, there is a strong push for applying AI to analyse the PI data. Although this approach is proven to be powerful and beneficial, it has a major shortcoming which is incorporating the domain knowledge. Nevertheless, the powerful statistical analysis, which inherently incorporates the domain knowledge, must not be neglected. This paper presents the statistical data analysis, which was implemented to benchmark the advanced process control performance (APC) in Antofagasta Minerals – Los Pelambres Mine Site operations.

Los Pelambres concentrator is a copper-molybdenum processing plant treating 175 000 tons ore daily. Los Pelambres is one of Chile's most advanced operations, which has implemented APC through the development of Model Predictive Control (MPC) for their processing units (ie SAG mills, ball mills, cyclones, flotation and regrind) of its three parallel lines. An overall analysis of data indicates the application of MPC resulted in process stability and 2.8 times more throughput on average. Although SAG mills MPC is utilised above 90 per cent of the time, the ball mills and flotation MPC utilisation can be enhanced further by improving maintenance of mechanical parts and calibration and maintenance of sensors. There are opportunities to boost the performance of MPC for each unit through the implementation of semi-empirical models for SAG mills, cyclones and gravity-induced stirred media mills developed in Julius Kruttschnitt Mineral Research Centre (JKMRC).

## INTRODUCTION

The third industrial revolution, which is characterised by the industry's digital revolution, started in the 1960s or 1970s (Humphreys, 2019). The third industrial revolution transitioned the industry from analogue, electrical and mechanical technologies to digital technologies which are associated with computers and internet-based tools and advanced information technologies. Over the recent years, significant discussion and development are occurring to bring the fourth industrial revolution to the mining industry (Group, 2019).

The advances in the industry following from the fourth industrial revolution resulted in more data than ever before (roughly 2.5 quintillion bytes globally each day in 2017) (Cloud, 2017). The rapid increase in data generation along with advances in data analytics tools and technology, creates the opportunity for the mining industry to benefit for those advances to transform and enhance productivity (Lala *et al*, 2016).

For decades, data was assumed as an asset in particular when the data is readily available for business analysis and for providing actionable insight (Lampshire, 2016; Berlioz, 2015; Isson, 2012). In the mining industry, most of the data are machine-generated data which are characterised as 'Big

Data' based on Ohlhorst's for V's concept, namely Volume, Velocity, Variety and Veracity (Ohlhorst, 2012). Most data in mining comes from operation technologies. Generally, the data in mining operations are structured data in logged data or time-series data, which is often generated by various sensors and managed by data historians such as OSIsoft PI systems (O'Neill, 2019).

## Importance of knowledge-based data analytics

Gathering large amounts of data will not necessarily enhance productivity or transform the business unless proper analysis are conducted to generate insight that can inform decisions at relevant levels (Rogers *et al*, 2019). Besides, one source of information often is not adequate. Data collected from multiple sources and covers different aspects of the process are essential for generating useful insight for decision-making (Broekhuizen *et al*, 2018). Therefore, it is not important if a large amount of data is stored somewhere in business servers unless it turns into actionable knowledge (Isson, 2012). The data only is valuable for businesses because it will give them the power to act.

Data analytics is defined as any data-driven process that generates actionable insight (Stubbs, 2011). Nowadays, there are a variety of large, medium and small companies and numerous start-ups who are offering different approaches and tools to mining companies to perform data analytics. This is in addition to the in-house capability that most of the medium to large sized mining companies have developed over the past few years, particularly for using Artificial Intelligent (AI) and Machine Learning (ML) tools for analysing data generating insight. Today, decision-making based solely on experience is not acceptable. On the other hand, mining companies have begun to realise that analysis based only on data analytics also does not deliver value and often provides insight that is not actionable.

As a result, more companies choose the hybrid approach, which takes advantage of the knowledge of domain experts and the power of data analytics tools. The hybrid approach process the 'Big Data' and generate knowledge and insight that can inform decision-making at various mining business levels.

This paper presents simple data analytics tools implemented in Antofagasta Minerals S.A. (AMSA) Los Pelambres concentrator to provide insight into the performance of the advanced process control and identify opportunities for enhancing the performance of the process control.

# BACKGROUND

The project's main objective was to conduct a benchmarking study of the current state of automation and process control in Los Pelambres concentrator. The project also aimed to deliver a quantification of the benefit that could be achieved if AMSA enhances the control system's performance in Los Pelambres.

## AMSA's Los Pelambres operation

AMSA's Los Pelambres operation is 200 km north of Santiago in Coquimbo region in El Choapa Valley. Mine pit is positioned at 3600 m above sea level, and processing plant is at 1600 m above sea level. The mine is a porphyry copper (Cu-Mo) deposit in sedimentary-volcanic rocks with 2100 Mt of reserves. The mine production began in late 1999 with the estimated mine life of at least 30 years (Bechtel Chile, MLP Design criteria, 2008). The processing plant consists of three parallel standard SAG mill, Ball Mill, Pebble crushing (ASBC) circuits followed by flotation circuit, including roughers, cleaners, and cleaner's scavengers flotation cells for collective flotation (Figure 1).


**FIG 1** – Overview of AMSA's Los Pelambres operation (adapted from Google Maps).

The plant initially commissioned with two parallel SABC lines. After expansion in 2008, the third SABC is added to the grinding circuit along with new flotation circuits to expand the plant capacity.

## APC in AMSA's Los Pelambres concentrator

Los Pelambers is one the most advanced operation in Chile and benefits from APC in its control system for controlling SAG mills, ball mills and cyclones, and flotation and regrinding. The plant has developed a dashboard for presenting real-time operation metrics in plant offices which is based on advanced data analytics. A snapshot of one of the dashboards is shown in Figure 2.

**FIG 2** – Application of APC and digitisation to calculate real-time operation metrics for presentation in plant offices.

## SAG mill APC

APC implemented in the SAG mill circuit is divided into two main parts, regulatory control and Model Predictive Control (MPC). Regulatory control is in charge of controlling process variables and stabilising the process, while MPC is in charge of selecting the optimal set point values for the controlled variables of the regulatory control loop.

There are three MPC for each SAG mill which includes MPC for predicting the mill load and setting the throughput set point, MPC for predicting the throughput based on available feeders and setting feeders speed and MPC for protecting the mill shell liners based on mill sound. Details of the SAG mill MPC can be found in Misle and Silva (2014).

### Ball mills and cyclones APC

In secondary grinding (ie ball mills and cyclones circuit) the MPC is utilised to calculate the set points for the hydrocyclones operating pressure and the hydrocyclones feed density. The MPC uses a fuzzy logic model based on a set of rules (Misle and Silva, 2014). This set of rules gives the optimal values for the set points taking into account:

- Keeping a safe sump level (priority situation).
- Avoiding the overload of the ball mill (priority situation).
- Improve the classification through the increasing of cyclones feed pressure and decreasing per cent solids (optimising situation).
- Increasing the grinding efficiency through the control of the ball mill power consumption, related to the circulating load (optimising situation).

### Cyclones rotation control

There is also an APC to control the rotation of cyclones to ensure even wear of cyclones to maintain consistent performance. The main goal of the cyclone rotation control is to optimise the use of cyclones. To that extent, a control strategy is implemented, which states which cyclone will be operated, based on its availability and the number of hours in operation. Cyclones which will be opened or closed will be the one with less or more operating hours, respectively.

### Flotation MPC

In the flotation circuit, The MPC is implemented for each cell as well as each flotation bank. The MPC in flotation circuit calculates the set points for each cell's froth depth and calculates the set point for the position of discharge valve of each cell based on the inlet flow and the froth depth set point (Misle and Silva, 2014).

All flotation cells are equipped with froth vision camera to measure the froth velocity to calculate the mass pool. However, at the time of this study, the froth vision cameras were only used by operators as a tool to identify overflow from cells, although the froth velocity calculations were recorded in the PI system.

## METHODS AND TOOLS

### Project approach

The project's work plan included the collection of Plant Information (PI) data for one year (2018) of the operation for the preliminary analysis to asses the process stability and performance. A site visit was conducted following from initial data analysis with the following objectives:

- Presenting and discussing findings from PI data analysis.
- Technology and Knowledge transfer to use the tools and indices developed for regular analysis of PI data.
- Discussion with personnel of each processing unit to collect more detail information and receive their feedback on analysis.
- Observing the operation and discussion with operators to identify practical constraints.
- Reviewing the control logic for each section of the circuit.

After the site visit, essential modifications were applied to analysis to incorporate comments from the site personnel and the site visit findings.

## Analysis of data

The first step in the analysis of data includes cleaning the data by removing 'missing' or 'bad' data and identifying unstable periods that will not be included in some of the performance assessment analysis.

The initial analysis was carried out, making a frequency analysis of the main variables in the process. This analysis's main goal is to conclude how frequently the main variables stay within the correct operational ranges. These ranges were defined by plant design specifications together with information from plant specialists. PI data used for the analysis corresponds to a 1-year data (2018) with a sampling rate of 1 minute for grinding circuit and 5 minutes for the flotation circuit.

## Plant audit

Plant audit was conducted after the presentation of the results of the preliminary analysis of PI data to process and control engineers. Over three days, data analysis results presented to operators, process engineers and plant manager and their feedback were collected. Also, through interviews with operators, their comments on our findings and process constraints in their view were collected (Figure 3).


**FIG 3** – Interview with operators in the: (a) grinding control room, (b) flotation control room.

# RESULTS AND DISCUSSIONS

## Plant throughput

It is clear from Figure 4 that when the MPC for SAG mills are On, the plant throughput in all three lines is significantly higher than when the MPC is Off (on average 2.8 times). It is clear that MPC is contributing significantly to plant throughput, which can be attributed to the process's stability. However, by enhancing the SAG mills MPC, there is an opportunity to increase the plant throughput further to achieve the 3000 t/h which the target plant throughput. Also, there is an opportunity to increase annual throughput further by increasing the portion of MPC's time. This could be achieved by identifying the underlying reasons for turning the MPC Off.

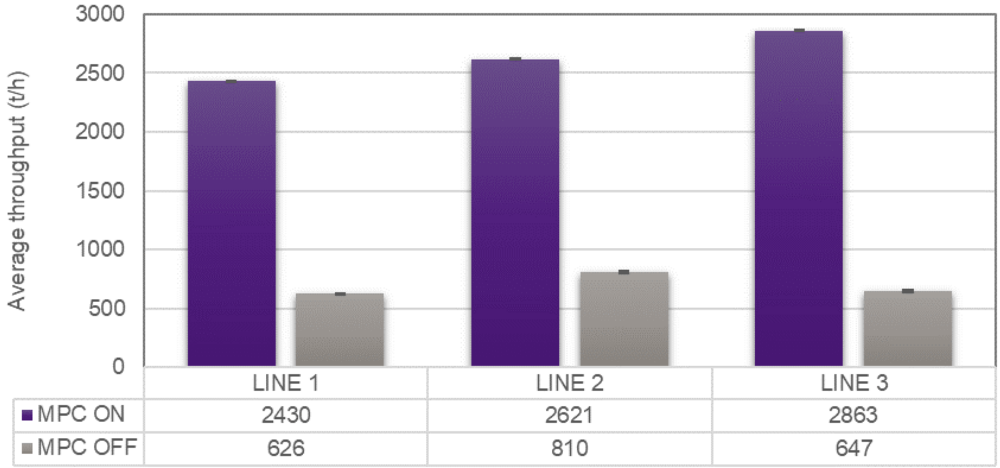


**FIG 4** – Comparison of average plant throughput when MPC is On with when MPC is Off.

The data in Figure 4 also indicates that when MPC is On, on average SAG mill three operates at a higher throughput compared to SAG mill 1 and 2 and SAG mill one has the lower throughput among the three mills.

## Utilisation of MPC

Figure 5, shows the utilisation of MPC in SAG mills over 2018, based on the processed data, the MPC utilisation on Line 1, Line 2 and Line 3 were 89 per cent, 92 per cent and 92 per cent, respectively.

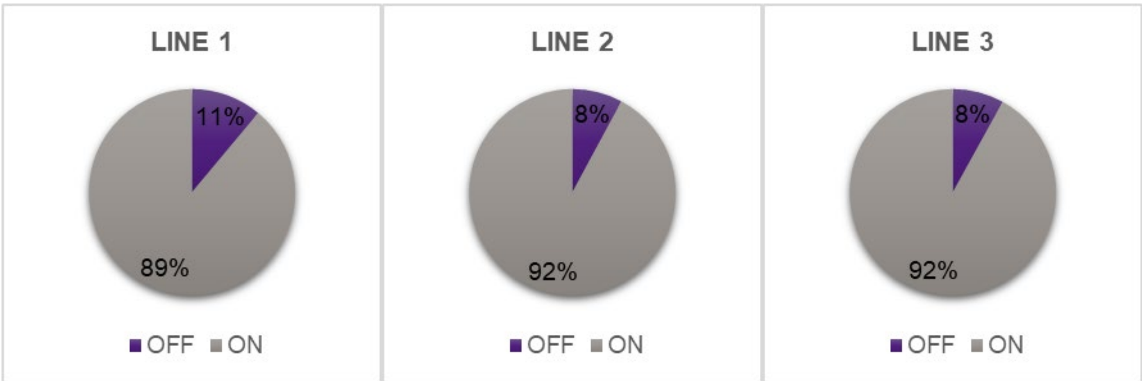


**FIG 5** – Utilisation of SAG mills MPC in 2018.

Comparative studies were conducted on several operating variables, including the feed size distribution, mill load, mill speed, operating per cent solids and mill power draw to understand the underpinning reasons for lower utilisation of MPC in line 1. Due to constrain in space for this paper, few of the analysis are presented in Figure 6.

The ideal range for each operating parameter in Figure 6 is defined through consultation with operators, process engineers and control engineers and reviewing the process design documents and plant control strategy documents.

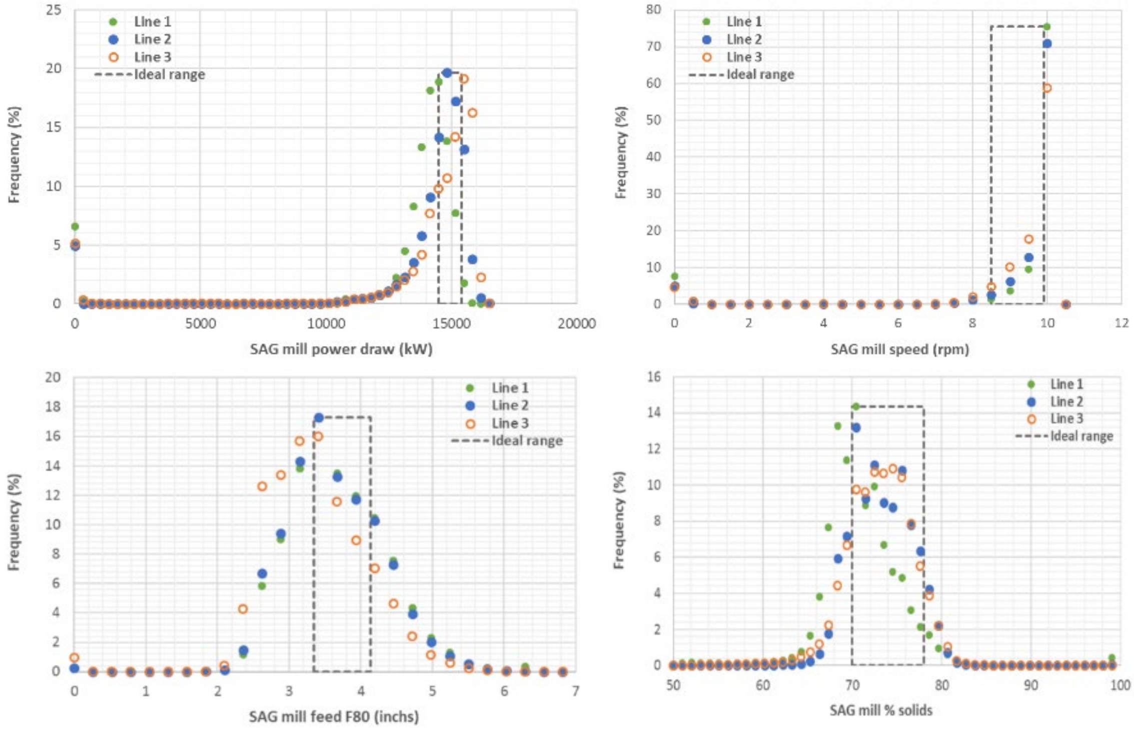


**FIG 6** – Frequency analysis of some of the key operating factors of Line 1 to 3 SAG mills.

The detailed analysis of operating parameters and interview with plant personnel indicated that Line 3 due to size segregation in Coarse ore stockpile receives a finer feed which allows operating the mill at higher throughput. Also, since the ball mill in Line 3 is larger, the secondary grinding usually is not a constraint for higher throughput. On the other hand, SAG mill one due to a longer ramp-up time after each reline overall has lower throughput among the three SAG mills. One of the reasons for lower utilisation of the MPC for SAG mill one is related to the ram up after each reline because operators prefer operating the SAG mill one without MPC during the ramp-up to prevent damage the shell liners.

Unlike the utilisation of MPC in SAG mill circuit, which is above 90 per cent on average, utilisation of MPC for the secondary grinding and flotation is significantly lower, and it can be enhanced. For example, utilisation of MPC for secondary grinding on Line 3 is presented in Figure 7.

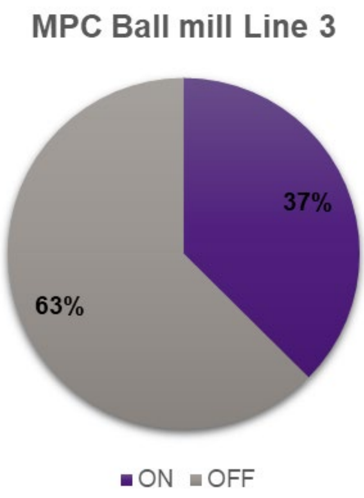


**FIG 7** – Utilisation of MPC of secondary grinding Line 3 in 2018.

Analysing ball mills' critical operational parameters (eg power draw, mill load and operating per cent solids) and cyclones (eg feed per cent solids, operating pressure, overflow $P_{80}$) indicates that when MPC is On, those operating parameters improve.

The main barrier to increasing the utilisation of MPC in secondary grinding and flotation circuit was the availability of equipment and maintenance of mechanical parts such as valves and calibration of instrumentation such as flow metres and gauges. Therefore, opportunities were identified to enhance the utilisation of MPC in secondary grinding and flotation by addressing equipment maintenance and instrumentation issues.

## Further development of MPC

The semi-empirical models which are developed in Julius Kruttschnitt Mineral Research Centre (JKMRC) can be implemented to increase the performance of MPC for each section of the process. For example, models developed for SAG mills, ball mills, pumps and pipes, cyclones, and gravity-induced stirred media mills model which can be simplified for application in MPC.

Also, JKMRC has developed several soft sensors such as mill filling prediction tools that can be used to advance MPC's capability. The JKMRC soft sensors are based on simplified semi-empirical models calibrated using regular measurements of design details and linked to live operational data to predict parameters that are hard to measure those using hard sensors accurately.

# CONCLUSIONS

This paper presents the opportunities available in analysing plant information data through the application of data analytics tools directed by domain experts' knowledge. Simple data analytics tools and methods implemented for benchmarking the performance of APC in AMSA's Los Pelambres operation demonstrated the power and value of conducting such studies. This study identified opportunities for further improvements of APC in Los Pelambres, translating into higher plant throughput while maintaining the plant performance.

# ACKNOWLEDGEMENTS

The authors would like to acknowledge the support of AMSA for funding this study and extend their gratitude to Los Pelambres personnel who contributed to this work with their support and invaluable comments and insight provided by them throughout the process.

# REFERENCES

Berlioz, C. A., (2015). The convergence of data analysts and business analysts, SparklingLogic.

Broekhuizen, T. L. J., Bakker, T., and Postma, T. M., (2018). Implementing new business models: what challenges lie ahead?, Business Horizons, Vol. 61:4, pp. 555–566.

Cloud, I.M., (2017). 10 key marketing trends for 2017 and ideas for exceeding customer expectations. [cited 2020 22/01/2020]; Available from: https://bizibl.com/marketing/download/10-key-marketing-trends-2017-and-ideas-exceeding-customer-expectations.

Bechtel Chile LTDA, (2008). MLP Design criteria, 25351–220–3DR-V01L-00002 for process, proyecto repotenciamiento II No. MLP 25351–000-B-CD-002, Bechtel Chile, 24 March 2008.

Fekete, J., (2015). Big data in mining operations. Masters thesis, Copenhagen Business School, University of Copenhagen,

Denmark.

Group, L., (2019). The first digital decade begins – defining the DNA of digital business transformation. [cited 2019 22/10/2019]; Available from: https://www.uk.logicalis.com/news/2016-thefirst-digital-decade-begins/.

Humphreys, D., (2019). Mining productivity and the fourth industrial revolution. Mineral Economy. https://doi.org/10.1007/s13563–019–00172–9.

Isson, J. P., (2012). Win with advanced business analytics: creating business value from your data, 1st edition, ed. J. Harriott, 2012: Somerset: John Wiley & Sons, Incorporated.

Lala, A., Moyo, M., Rehbach, S., and Sellschop, R., (2016). Productivity in mining operations: reversing the downward trend. AusIMM Bulletin, August 2016, pp 46.

Lampshire, G., (2016). In: Meers D (ed) The data and analytics playbook: proven methods for governed data and analytic quality, Elsevier Science, Saint Louis.

Misle, J., Silva, D., (2014). Innovation in advanced control at Minera Los Pelambres, XXVII International Mineral Processing Congress, Santiago, Chile.

Ohlhorst, F. J., (2012). Big data analytics: turning big data into big money, John Wiley & Sons

O'Neill, K., (2019). Advantages of Deploying PI for the Collection of Discrete Data from an Automated Bioreactor Sampling System (Merck), [cited 2020 18/02/2020]; Available from: https://www.osisoft.com/Presentations/Advantages-of-Deploying-PI-for-the-Collection-of-Discrete-Data-from-an-Automated-Bioreactor-Sampling-System--Merckx/.

Rogers, W. P., Kahraman, M. M., and Dessureault, S., (2019). Exploring the value of using data: a case study of continuous improvement through data warehousing, International Journal of Mining, Reclamation and Environment, Vol. 33:4, pp. 286–296, DOI: 10.1080/17480930.2017.1405473.

Stubbs, E., (2011). The value of business analytics: identifying the path to profitability, Wiley and SAS Business Series Vol. 43, John Wiley & Sons

# AUTHOR INDEX